VOLUME 27 / NUMBER 22
NOVEMBER 23, 1989
ACC. NOS. N89-27632 TO N89-28484

STAR

AN ABSTRACT JOURNAL

Scientific and Technical Aerospace Reports

PRODUCED BY THE
SCIENTIFIC AND TECHNICAL
INFORMATION
DIVISION

NASA

NATIONAL AERONAUTICS AND SPACE ADMINISTRATION

WHAT YOU CAN DO FOR *STAR*

All users of this abstract service are urged to forward reports to be considered for announcement in *STAR*. This will aid NASA in its efforts to provide the fullest possible coverage of all scientific and technical publications that might support aeronautics and space research and development. If you have prepared relevant reports (other than those that you will transmit to NASA, DoD, or DOE through the usual contract- or grant-reporting channels), please send them for consideration to the NASA Scientific and Technical Information Facility, P.O. Box 8757, BWI Airport, Maryland 21240.

Reprints of journal articles, book chapters, and conference papers are also welcome. These will be considered for announcement in *STAR's* companion journal, *International Aerospace Abstracts*.

You may specify a particular source to be included in a report announcement if you wish; otherwise the report will be placed on public sale at the National Technical Information Service. Copyrighted publications will be announced but not distributed or sold.

PURCHASE OF *STAR*

The semimonthly issues are available to registered users on annual subscription for $99.00 from the NASA Scientific and Technical Information Facility, ATTN: Registration Services, P.O. Box 8757, BWI Airport, MD 21240. *STAR* is publically available on annual subscription for $99.00 from the Superintendent of Documents, U.S. Government Printing Office, Washington, DC 20402.

PUBLISHED BY:

UNITED STATES GOVERNMENT
NATIONAL AERONAUTICS AND SPACE ADMINISTRATION
SCIENTIFIC AND TECHNICAL INFORMATION DIVISION
Scientific and Technical Aerospace Reports, Volume 27, is prepared by the NASA Scientific and Technical Information Facility operated for the National Aeronautics and Space Administration by RMS Associates.

The Administrator of the National Aeronautics and Space Administration has determined that the publication of this periodical is necessary in the transaction of the public business required by law of this Agency. Use of funds for printing this periodical has been approved by the Director of the Office of Management and Budget through March 22, 1990.

US ISSN 0036-8741

INTRODUCTION

Scientific and Technical Aerospace Reports (STAR) is a major component of a comprehensive National Aeronautics and Space Administration information system covering aeronautics, space, and supporting disciplines. *STAR* is issued on the 8th and 23rd of each month and announces current publications of the following types:

- NASA, NASA contractor, and NASA grantee reports
- Reports issued by other U.S. Government Agencies, domestic and foreign institutions, universities, and private firms
- Translations in report form
- NASA-owned patents and patent applications
- Other U.S. Government Agency and foreign patents and patent applications
- Domestic and foreign dissertations and theses

Journal, book, and conference literature, cover-to-cover journal translations, and certain foreign dissertations are announced in a companion journal, *International Aerospace Abstracts (IAA),* available on subscription from the American Institute of Aeronautics and Astronautics, Technical Information Service, 555 West 57th Street, 12th Floor, New York, New York 10019.

SUBJECT SCOPE

Subject scope of *STAR,* and *IAA* includes all aspects of aeronautics and space research and development, supporting basic and applied research, and applications. Aerospace aspects of earth resources, energy development, conservation, oceanography, environmental protection, urban transportation, and other topics of high national priority are also covered.

OTHER NASA PUBLICATIONS

Other NASA publications and information services are described in the publication, *The NASA Scientific and Technical Information System ... and How to Use It,* available without charge from the NASA Scientific and Technical Information Facility, P.O. Box 8757, BWI Airport, Maryland 21240.

HOW TO USE *STAR* SUBJECT CATEGORIES

STAR is categorized by 10 major subject divisions divided into 76 specific subject categories and one general category/division. The major subject divisions are listed in the Table of Contents, together with a note for each that defines its scope and provides any cross-references. For example:

AERONAUTICS

Includes aeronautics (general); aerodynamics; air transportation and safety; aircraft communications and navigation; aircraft design, testing and performance; aircraft instrumentation; aircraft propulsion and power; aircraft stability and control; and research and support facilities (air).

For related information see also *Astronautics.*

Each major division is further divided into as many as nine specific categories, which are identified by category numbers.

Abstracts in *STAR* are grouped by specific category, the categories appearing in sequential order. Category breaks in the abstract section are identified by the category number and title, and a scope note. Cross-references to other categories are provided as appropriate. For example:

02 AERODYNAMICS

Includes aerodynamics of bodies, combinations, wings, rotors, and control surfaces; and internal flow in ducts and turbomachinery.

For related information see also *34 Fluid Mechanics and Heat Transfer.*

CROSS-REFERENCES

Individual *STAR* abstracts are not ordinarily cross-referenced, except for certain conference reports or book translations that have had separate abstracts written for their component papers or chapters. Citations and abstracts of the components follow immediately after those of the parent document. When the subject content of a component differs sufficiently from the general content of the parent, a cross-reference citation also is printed at the end of the category to which it normally would have been assigned if it were independent.

DOCUMENTS ON MICROFICHE

Documents on microfiche[1] are designated by a pound sign (#) following the accession number. The pound sign is used without regard to the source or quality of the microfiche.

AVAILABILITIES

One or more sources from which a document announced in *STAR* is available to the public is given in each citation. The most commonly indicated sources and their acronyms or abbreviations are listed below. If the publication is available from a source other than those listed, the publisher and his address will be displayed on the availability line or in combination with the corporate source line.

Avail: NTIS. Sold by the National Technical Information Service. Prices for hard copy (HC) and microfiche (MF) are indicated by a price code following the letters HC or MF in the *STAR* citation. Current values for the price codes are given in the tables on page vii.

Initially distributed microfiche under the NTIS SRIM (Selected Research in Microfiche) is available at greatly reduced unit prices. For this service and for information concerning subscription to NASA printed reports, consult the NTIS Subscription Section, Springfield, Va. 22161.

NOTE ON ORDERING DOCUMENTS: When ordering NASA publications (those followed by the * symbol), use the N accession number. NASA patent applications (only the specifications are offered) should be ordered by the US-Patent-Appl-SN number. Non-NASA publications (no asterisk) should be ordered by the AD, PB, or other *report number* shown on the last line of the citation, not by the N accession number. It is also advisable to cite the title and other bibliographic identification.

Avail: SOD (or GPO). Sold by the Superintendent of Documents, U.S. Government Printing Office, in hard copy. The current price and order number are given following the availability line. (NTIS will fill microfiche requests, as indicated above, for those documents identified by a # symbol.)

(1) A microfiche is a transparent sheet of film, 105 by 148 mm in size, containing as many as 60 to 98 pages of information reduced to micro images (not to exceed 26:1 reduction).

Avail: BLL (formerly NLL): British Library Lending Division, Boston Spa, Wetherby, Yorkshire, England. Photocopies available from this organization at the price shown. (If none is given, inquiry should be addressed to the BLL.)

Avail: DOE Depository Libraries. Organizations in U.S. cities and abroad that maintain collections of Department of Energy reports, usually in microfiche form, are listed in *Energy Research Abstracts.* Services available from the DOE and its depositories are described in a booklet, *DOE Technical Information Center - Its Functions and Services* (TID-4660), which may be obtained without charge from the DOE Technical Information Center.

Avail: ESDU. Pricing information on specific data, computer programs, and details on ESDU topic categories can be obtained from ESDU International Ltd. Requesters in North America should use the Virginia address while all other requesters should use the London address, both of which are on page vi.

Avail: Fachinformationszentrum, Karlsruhe. Sold by the Fachinformationszentrum Energie, Physik, Mathematik GMBH, Eggenstein Leopoldshafen, Federal Republic of Germany, at the price shown in deutschmarks (DM).

Avail: HMSO. Publications of Her Majesty's Stationery Office are sold in the U.S. by Pendragon House, Inc. (PHI), Redwood City, California. The U.S. price (including a service and mailing charge) is given, or a conversion table may be obtained from PHI.

Avail: NASA Public Document Rooms. Documents so indicated may be examined at or purchased from the National Aeronautics and Space Administration, Public Documents Room (Room 126), 600 Independence Ave., S.W., Washington, D.C. 20546, or public document rooms located at each of the NASA research centers, the NASA Space Technology Laboratories, and the NASA Pasadena Office at the Jet Propulsion Laboratory.

Avail: Univ. Microfilms. Documents so indicated are dissertations selected from *Dissertation Abstracts* and are sold by University Microfilms as xerographic copy (HC) and microfilm. All requests should cite the author and the Order Number as they appear in the citation.

Avail: US Patent and Trademark Office. Sold by Commissioner of Patents and Trademarks, U.S. Patent and Trademark Office, at the standard price of $1.50 each, postage free. (See discussion of NASA patents and patent applications below.)

Avail: (US Sales Only). These foreign documents are available to users within the United States from the National Technical Information Service (NTIS). They are available to users outside the United States through the International Nuclear Information Service (INIS) representative in their country, or by applying directly to the issuing organization.

Avail: USGS. Originals of many reports from the U.S. Geological Survey, which may contain color illustrations, or otherwise may not have the quality of illustrations preserved in the microfiche or facsimile reproduction, may be examined by the public at the libraries of the USGS field offices whose addresses are listed in this Introduction. The libraries may be queried concerning the availability of specific documents and the possible utilization of local copying services, such as color reproduction.

Avail: Issuing Activity, or Corporate Author, or no indication of availability. Inquiries as to the availability of these documents should be addressed to the organization shown in the citation as the corporate author of the document.

NASA PATENTS AND PATENT APPLICATIONS

Patents and patent applications owned by NASA are announced in *STAR* under appropriate subject categories and are referenced in the *STAR* indexes. In the Report/Accession Number Index, patents are indexed by the NASA Case Number (which appears in lieu of the report number in other indexes), the U.S. Patent Number, the U.S. Patent Application Serial Number, and the U.S. Patent Class. Patent applications for which patents have not yet been issued are indexed by the NASA Case Number and the U.S. Patent Application Serial Number.

NASA *patent application specifications* are sold in paper copy by the National Technical Information Service at price code A02. Microfiche are sold at price code A01. The US-Patent-Appl-SN- number should be used in ordering either paper copy or microfiche from NTIS. Printed copies of *patents* (which are not microfiched) are available for purchase at $1.50 per copy from:

Commissioner of Patents and Trademarks
U.S. Patent and Trademark Office
Washington, D.C. 20231

When ordering patents, the U.S. Patent Number should be used, and payment must be remitted in advance, preferably by money order or check payable to the Commissioner of Patents and Trademarks. Prepaid purchase coupons for ordering are also available from the Patent and Trademark Office. The patents and patent applications announced in *STAR* are owned by NASA and are available for royalty-free licensing. Requests for licensing terms and further information should be addressed to:

Associate General Counsel for Intellectual Property/Code GP
National Aeronautics and Space Administration
Washington, D.C. 20546

ELIGIBILITY AND REGISTRATION FOR NASA INFORMATION PRODUCTS AND SERVICES

A variety of services is available to organizations of the following types that have registered with NASA to receive specific services or products:

1. NASA offices, research centers, contractors, subcontractors, grantees, and consultants;
2. Other U.S. Government agencies and their contractors;
3. Libraries in the United States that have arrangements with NASA to maintain collections of NASA documents for public reference;
4. Other organizations in the United States having a need for NASA documents in work related to aeronautics and space research;
5. Organizations abroad that have established reciprocal document exchange arrangements with NASA.

Only the central service points or central points of document acquisition and control within qualified organizations are eligible to register for NASA products and services. Domestic organizations that may be eligible to receive various classes of NASA publications and services should address their requests for registration or for further information to:

NASA Scientific and Technical Information Facility
ATTN: Registration Services
Post Office Box 8757
BWI Airport, Maryland 21240

Organizations abroad should direct requests to Manager, International STI Activities, NTT, NASA Headquarters, Washington, D.C. 20546.

AVAILABILITY OF *STAR* ABSTRACTS ON MICROFICHE

Microfiche of the abstract sections of this issue and other issues of *STAR* are available on annual subscription from NTIS as PB89-911300, Attn: Subscriptions, 5285 Port Royal Road, Springfield, Virginia 22161. Annual subscription rates are $70.00 North America; $140.00 foreign. Abstract sections for previous years retroactive to 1964 are available at the current rates. Microfiche for individual *STAR* issue abstract sections are not available.

PUBLIC COLLECTIONS OF NASA DOCUMENTS

DOMESTIC: NASA and NASA-sponsored documents and a large number of aerospace publications are available to the public for reference purposes at the library maintained by the American Institute of Aeronautics and Astronautics, Technical Information Service, 555 West 57th Street, 12th Floor, New York, New York 10019

EUROPEAN: An extensive collection of NASA and NASA-sponsored publications is maintained by the British Library Lending Division, Boston Spa, Wetherby, Yorkshire, England for public access. The British Library Lending Division also has available many of the non-NASA publications cited in *STAR*. European requesters may purchase facsimile copy or microfiche of NASA and NASA-sponsored documents, those identified by both the symbols # and * from ESA - Information Retrieval Service European Space Agency, 8-10 rue Mario-Nikis, 75738 Paris CEDEX 15, France.

FEDERAL DEPOSITORY LIBRARY PROGRAM

In order to provide the general public with greater access to U.S. Government publications, Congress established the Federal Depository Library Program under the Government Printing Office (GPO), with 50 regional depositories responsible for permanent retention of material, inter-library loan, and reference services. At least one copy of nearly every NASA and NASA-sponsored publication, either in printed or microfiche format, is received and retained by the 50 regional depositories. A list of the regional GPO libraries, arranged alphabetically by state, appears on the inside back cover. These libraries are *not* sales outlets. A local library can contact a Regional Depository to help locate specific reports, or direct contact may be made by an individual.

ADDRESSES OF ORGANIZATIONS

American Institute of Aeronautics and Astronautics
Technical Information Service
555 West 57th Street, 12th Floor
New York, New York 10019

British Library Lending Division,
Boston Spa, Wetherby, Yorkshire,
England

Commissioner of Patents and Trademarks
U.S. Patent and Trademark Office
Washington, D.C. 20231

Department of Energy
Technical Information Center
P.O. Box 62
Oak Ridge, Tennessee 37830

ESA-Information Retrieval Service
ESRIN
Via Galileo Galilei
00044 Frascati (Rome) Italy

ESDU International
P.O. Box 1633
Manassas, Virginia 22110

ESDU International, Ltd.
251-259 Regent Street
London, W1R 7AD, England

Fachinformationszentrum Energie, Physik, Mathematik GMBH
7514 Eggenstein Leopoldshafen
Federal Republic of Germany

Her Majesty's Stationery Office
P.O. Box 569, S.E. 1
London, England

NASA Scientific and Technical Information Facility
P.O. Box 8757
B.W.I. Airport, Maryland 21240

National Aeronautics and Space Administration
Scientific and Technical Information Division (NTT)
Washington, D.C. 20546

National Technical Information Service
5285 Port Royal Road
Springfield, Virginia 22161

Pendragon House, Inc.
899 Broadway Avenue
Redwood City, California 94063

Superintendent of Documents
U.S. Government Printing Office
Washington, D.C. 20402

University Microfilms
A Xerox Company
300 North Zeeb Road
Ann Arbor, Michigan 48106

University Microfilms, Ltd.
Tylers Green
London, England

U.S. Geological Survey Library
National Center - MS 950
12201 Sunrise Valley Drive
Reston, Virginia 22092

U.S. Geological Survey Library
2255 North Gemini Drive
Flagstaff, Arizona 86001

U.S. Geological Survey
345 Middlefield Road
Menlo Park, California 94025

U.S. Geological Survey Library
Box 25046
Denver Federal Center, MS914
Denver, Colorado 80225

NTIS PRICE SCHEDULES

(Effective January 1, 1989)

Schedule A
STANDARD PRICE DOCUMENTS AND MICROFICHE

PRICE CODE	NORTH AMERICAN PRICE	FOREIGN PRICE
A01	$ 6.95	$13.90
A02	10.95	21.90
A03	13.95	27.90
A04-A05	15.95	31.90
A06-A09	21.95	43.90
A10-A13	28.95	57.90
A14-A17	36.95	73.90
A18-A21	42.95	85.90
A22-A25	49.95	99.90
A99	*	*
NO1	55.00	70.00
NO2	55.00	80.00

Schedule E
EXCEPTION PRICE DOCUMENTS AND MICROFICHE

PRICE CODE	NORTH AMERICAN PRICE	FOREIGN PRICE
E01	$ 9.00	18.00
E02	11.50	23.00
E03	13.00	26.00
E04	15.50	31.00
E05	17.50	35.00
E06	20.50	41.00
E07	23.00	46.00
E08	25.50	51.00
E09	28.00	56.00
E10	31.00	62.00
E11	33.50	67.00
E12	36.50	73.00
E13	39.00	78.00
E14	42.50	85.00
E15	46.00	92.00
E16	50.50	101.00
E17	54.50	109.00
E18	59.00	118.00
E19	65.50	131.00
E20	76.00	152.00
E99	*	*

*Contact NTIS for price quote.

IMPORTANT NOTICE

NTIS Shipping and Handling Charges

U.S., Canada, Mexico — ADD $3.00 per TOTAL ORDER

All Other Countries — ADD $4.00 per TOTAL ORDER

Exceptions — Does NOT apply to:

ORDERS REQUESTING NTIS RUSH HANDLING

ORDERS FOR SUBSCRIPTION OR STANDING ORDER PRODUCTS *ONLY*

NOTE: Each additional delivery address on an order requires a separate shipping and handling charge.

VOLUME 27 NUMBER 22 / NOVEMBER 23, 1989

TABLE OF CONTENTS

AERONAUTICS

Includes aeronautics (general); aerodynamics; air transportation and safety; aircraft communications and navigation; aircraft design, testing and performance; aircraft instrumentation; aircraft propulsion and power; aircraft stability and control; and research and support facilities (air).

For related information see also *Astronautics.*

01 AERONAUTICS (GENERAL) 3091

02 AERODYNAMICS 3091

Includes aerodynamics of bodies, combinations, wings, rotors, and control surfaces; and internal flow in ducts and turbomachinery.

For related information see also *34 Fluid Mechanics and Heat Transfer*

03 AIR TRANSPORTATION AND SAFETY 3092

Includes passenger and cargo air transport operations; and aircraft accidents.

For related information see also *16 Space Transportation* and *85 Urban Technology and Transportation.*

04 AIRCRAFT COMMUNICATIONS AND NAVIGATION 3093

Includes digital and voice communication with aircraft; air navigation systems (satellite and ground based); and air traffic control.

For related information see also *17 Space Communications, Spacecraft Communications, Command and Tracking* and *32 Communications and Radar.*

05 AIRCRAFT DESIGN, TESTING AND PERFORMANCE 3093

Includes aircraft simulation technology.

For related information see also *18 Spacecraft Design, Testing and Performance* and *39 Structural Mechanics.* For land transportation vehicles see *85 Urban Technology and Transportation.*

06 AIRCRAFT INSTRUMENTATION 3094

Includes cockpit and cabin display devices; and flight instruments.

For related information see also *19 Spacecraft Instrumentation* and *35 Instrumentation and Photography.*

07 AIRCRAFT PROPULSION AND POWER 3096

Includes prime propulsion systems and systems components, e.g., gas turbine engines and compressors; and onboard auxiliary power plants for aircraft.

For related information see also *20 Spacecraft Propulsion and Power, 28 Propellants and Fuels,* and *44 Energy Production and Conversion.*

08 AIRCRAFT STABILITY AND CONTROL 3098

Includes aircraft handling qualities; piloting; flight controls; and autopilots.

For related information see also *05 Aircraft Design, Testing and Performance.*

09 RESEARCH AND SUPPORT FACILITIES (AIR) 3098

Includes airports, hangars and runways; aircraft repair and overhaul facilities; wind tunnels; shock tubes; and aircraft engine test stands.

For related information see also *14 Ground Support Systems and Facilities (Space).*

ASTRONAUTICS

Includes astronautics (general); astrodynamics; ground support systems and facilities (space); launch vehicles and space vehicles; space transportation; space communications, spacecraft communications, command and tracking; spacecraft design, testing and performance; spacecraft instrumentation; and spacecraft propulsion and power.

For related information see also *Aeronautics*

12 ASTRONAUTICS (GENERAL) N.A.

For extraterrestrial exploration see *91 Lunar and Planetary Exploration.*

13 ASTRODYNAMICS 3100

Includes powered and free-flight trajectories; and orbital and launching dynamics.

14 GROUND SUPPORT SYSTEMS AND FACILITIES (SPACE) 3100

Includes launch complexes, research and production facilities; ground support equipment, e.g., mobile transporters; and simulators.

For related information see also *09 Research and Support Facilities (Air).*

15 LAUNCH VEHICLES AND SPACE VEHICLES 3101

Includes boosters; operating problems of launch/space vehicle systems; and reusable vehicles.

For related information see also *20 Spacecraft Propulsion and Power.*

16 SPACE TRANSPORTATION 3101

Includes passenger and cargo space transportation, e.g., shuttle operations; and space rescue techniques.

For related information see also *03 Air Transportation and Safety* and *18 Spacecraft Design, Testing and Performance.* For space suits see *54 Man/System Technology and Life Support.*

17 SPACE COMMUNICATIONS, SPACECRAFT COMMUNICATIONS, COMMAND AND TRACKING N.A.

Includes telemetry; space communications networks; astronavigation and guidance; and radio blackout.

For related information see also *04 Aircraft Communications and Navigation* and *32 Communications and Radar.*

18 SPACECRAFT DESIGN, TESTING AND PERFORMANCE 3101

Includes satellites; space platforms; space stations; spacecraft systems and components such as thermal and environmental controls; and attitude controls.

For life support systems see *54 Man/System Technology and Life Support.* For related information see also *05 Aircraft Design, Testing and Performance, 39 Structural Mechanics,* and *16 Space Transportation.*

19 SPACECRAFT INSTRUMENTATION N.A.

For related information see also *06 Aircraft Instrumentation* and *35 Instrumentation and Photography.*

20 SPACECRAFT PROPULSION AND POWER 3106

Includes main propulsion systems and components, e.g. rocket engines; and spacecraft auxiliary power sources.

For related information see also *07 Aircraft Propulsion and Power, 28 Propellants and Fuels, 44 Energy Production and Conversion,* and *15 Launch Vehicles and Space Vehicles.*

CHEMISTRY AND MATERIALS

Includes chemistry and materials (general); composite materials; inorganic and physical chemistry; metallic materials; nonmetallic materials; propellants and fuels; and materials processing.

23 CHEMISTRY AND MATERIALS (GENERAL) N.A.

24 COMPOSITE MATERIALS 3122

Includes physical, chemical, and mechanical properties of laminates and other composite materials.

For ceramic materials see *27 Nonmetallic Materials.*

25 INORGANIC AND PHYSICAL CHEMISTRY 3124

Includes chemical analysis, e.g., chromatography; combustion theory; electrochemistry; and photochemistry.

For related information see also *77 Thermodynamics and Statistical Physics.*

26 METALLIC MATERIALS 3126

Includes physical, chemical, and mechanical properties of metals, e.g., corrosion; and metallurgy.

27 NONMETALLIC MATERIALS 3129

Includes physical, chemical, and mechanical properties of plastics, elastomers, lubricants, polymers, textiles, adhesives, and ceramic materials.

For composite materials see *24 Composite Materials.*

28 PROPELLANTS AND FUELS 3134

Includes rocket propellants, igniters and oxidizers; their storage and handling procedures; and aircraft fuels.

For related information see also *07 Aircraft Propulsion and Power, 20 Spacecraft Propulsion and Power,* and *44 Energy Production and Conversion.*

29 MATERIALS PROCESSING N.A.

Includes space-based development of products and processes for commercial application.

For biological materials see *55 Space Biology.*

ENGINEERING

Includes engineering (general); communications and radar; electronics and electrical engineering; fluid mechanics and heat transfer; instrumentation and photography; lasers and masers; mechanical engineering; quality assurance and reliability; and structural mechanics.

For related information see also *Physics.*

31 ENGINEERING (GENERAL) 3135

Includes vacuum technology; control engineering; display engineering; cryogenics; and fire prevention.

32 COMMUNICATIONS AND RADAR 3136

Includes radar; land and global communications; communications theory; and optical communications.

For related information see also *04 Aircraft Communications and Navigation* and *17 Space Communications, Spacecraft Communications, Command and Tracking.* For search and rescue see *03 Air Transportation and Safety,* and *16 Space Transportation.*

33 ELECTRONICS AND ELECTRICAL ENGINEERING 3148

Includes test equipment and maintainability; components, e.g., tunnel diodes and transistors; microminiaturization; and integrated circuitry.

For related information see also *60 Computer Operations and Hardware* and *76 Solid-State Physics.*

34 FLUID MECHANICS AND HEAT TRANSFER 3153

Includes boundary layers; hydrodynamics; fluidics; mass transfer and ablation cooling.

For related information see also *02 Aerodynamics* and *77 Thermodynamics and Statistical Physics.*

35 INSTRUMENTATION AND PHOTOGRAPHY 3156

Includes remote sensors; measuring instruments and gages; detectors; cameras and photographic supplies; and holography.

For aerial photography see *43 Earth Resources and Remote Sensing.* For related information see also *06 Aircraft Instrumentation* and *19 Spacecraft Instrumentation.*

36 LASERS AND MASERS 3158

Includes parametric amplifiers.

For related information see also *76 Solid-State Physics.*

37 MECHANICAL ENGINEERING 3160

Includes auxiliary systems (nonpower); machine elements and processes; and mechanical equipment.

38 QUALITY ASSURANCE AND RELIABILITY 3162

Includes product sampling procedures and techniques; and quality control.

39 STRUCTURAL MECHANICS 3162

Includes structural element design and weight analysis; fatigue; and thermal stress.

For applications see *05 Aircraft Design, Testing and Performance* and *18 Spacecraft Design, Testing and Performance.*

GEOSCIENCES

Includes geosciences (general); earth resources and remote sensing; energy production and conversion; environment pollution; geophysics; meteorology and climatology; and oceanography.

For related information see also *Space Sciences.*

42 GEOSCIENCES (GENERAL) N.A.

43 EARTH RESOURCES AND REMOTE SENSING 3165

Includes remote sensing of earth resources by aircraft and spacecraft; photogrammetry; and aerial photography.

For instrumentation see *35 Instrumentation and Photography.*

44 ENERGY PRODUCTION AND CONVERSION 3174

Includes specific energy conversion systems, e.g., fuel cells; global sources of energy; geophysical conversion; and windpower.

For related information see also *07 Aircraft Propulsion and Power, 20 Spacecraft Propulsion and Power,* and *28 Propellants and Fuels.*

45 ENVIRONMENT POLLUTION 3174

Includes atmospheric, noise, thermal, and water pollution.

46 GEOPHYSICS 3175

Includes aeronomy; upper and lower atmosphere studies; ionospheric and magnetospheric physics; and geomagnetism.

For space radiation see *93 Space Radiation.*

47 METEOROLOGY AND CLIMATOLOGY 3177

Includes weather forecasting and modification.

48 OCEANOGRAPHY 3178

Includes biological, dynamic, and physical oceanography; and marine resources.

For related information see also *43 Earth Resources and Remote Sensing.*

LIFE SCIENCES

Includes life sciences (general); aerospace medicine; behavioral sciences; man/system technology and life support; and space biology.

51 LIFE SCIENCES (GENERAL) 3192

52 AEROSPACE MEDICINE 3192

Includes physiological factors; biological effects of radiation; and effects of weightlessness on man and animals.

53 BEHAVIORAL SCIENCES N.A.

Includes psychological factors; individual and group behavior; crew training and evaluation; and psychiatric research.

54 MAN/SYSTEM TECHNOLOGY AND LIFE SUPPORT 3194

Includes human engineering; biotechnology; and space suits and protective clothing.

For related information see also *16 Space Transportation.*

55 SPACE BIOLOGY 3209

Includes exobiology; planetary biology; and extraterrestrial life.

MATHEMATICAL AND COMPUTER SCIENCES

Includes mathematical and computer sciences (general); computer operations and hardware; computer programming and software; computer systems; cybernetics; numerical analysis; statistics and probability; systems analysis; and theoretical mathematics.

59 MATHEMATICAL AND COMPUTER SCIENCES (GENERAL) N.A.

60 COMPUTER OPERATIONS AND HARDWARE 3210

Includes hardware for computer graphics, firmware, and data processing.

For components see *33 Electronics and Electrical Engineering.*

61 COMPUTER PROGRAMMING AND SOFTWARE 3210

Includes computer programs, routines, algorithms, and specific applications, e.g., CAD/CAM.

62 COMPUTER SYSTEMS 3214

Includes computer networks and special application computer systems.

63 CYBERNETICS 3215

Includes feedback and control theory, artificial intelligence, robotics and expert systems.

For related information see also *54 Man/System Technology and Life Support.*

64 NUMERICAL ANALYSIS 3216

Includes iteration, difference equations, and numerical approximation.

65 STATISTICS AND PROBABILITY 3219

Includes data sampling and smoothing; Monte Carlo method; and stochastic processes.

66 SYSTEMS ANALYSIS 3219

Includes mathematical modeling; network analysis; and operations research.

67 THEORETICAL MATHEMATICS 3220

Includes topology and number theory.

PHYSICS

Includes physics (general); acoustics; atomic and molecular physics; nuclear and high-energy physics; optics; plasma physics; solid-state physics; and thermodynamics and statistical physics.

For related information see also *Engineering.*

70 PHYSICS (GENERAL) N.A.

For precision time and time interval (PTTI) see *35 Instrumentation and Photography;* for geophysics, astrophysics or solar physics see *46 Geophysics, 90 Astrophysics,* or *92 Solar Physics.*

71 ACOUSTICS 3220
Includes sound generation, transmission, and attenuation.
For noise pollution see *45 Environment Pollution.*

72 ATOMIC AND MOLECULAR PHYSICS 3221
Includes atomic structure, electron properties, and molecular spectra.

73 NUCLEAR AND HIGH-ENERGY PHYSICS N.A.
Includes elementary and nuclear particles; and reactor theory.
For space radiation see *93 Space Radiation.*

74 OPTICS 3224
Includes light phenomena and optical devices.
For lasers see *36 Lasers and Masers.*

75 PLASMA PHYSICS 3226
Includes magnetohydrodynamics and plasma fusion.
For ionospheric plasmas see *46 Geophysics.* For space plasmas see *90 Astrophysics.*

76 SOLID-STATE PHYSICS 3227
Includes superconductivity.
For related information see also *33 Electronics and Electrical Engineering* and *36 Lasers and Masers.*

77 THERMODYNAMICS AND STATISTICAL PHYSICS 3231
Includes quantum mechanics; theoretical physics; and Bose and Fermi statistics.
For related information see also *25 Inorganic and Physical Chemistry* and *34 Fluid Mechanics and Heat Transfer.*

SOCIAL SCIENCES

Includes social sciences (general); administration and management; documentation and information science; economics and cost analysis; law, political science, and space policy; and urban technology and transportation.

80 SOCIAL SCIENCES (GENERAL) N.A.
Includes educational matters.

81 ADMINISTRATION AND MANAGEMENT 3232
Includes management planning and research.

82 DOCUMENTATION AND INFORMATION SCIENCE 3233
Includes information management; information storage and retrieval technology; technical writing; graphic arts; and micrography.
For computer documentation see *61 Computer Programming and Software.*

83 ECONOMICS AND COST ANALYSIS 3234
Includes cost effectiveness studies.

84 LAW, POLITICAL SCIENCE AND SPACE POLICY 3234
Includes NASA appropriation hearings; aviation law; space law and policy; international law; international cooperation; and patent policy.

85 URBAN TECHNOLOGY AND TRANSPORTATION 3235
Includes applications of space technology to urban problems; technology transfer; technology assessment; and surface and mass transportation.
For related information see *03 Air Transportation and Safety, 16 Space Transportation,* and *44 Energy Production and Conversion.*

SPACE SCIENCES

Includes space sciences (general); astronomy; astrophysics; lunar and planetary exploration; solar physics; and space radiation.
For related information see also *Geosciences.*

88 SPACE SCIENCES (GENERAL) N.A.

89 ASTRONOMY N.A.
Includes radio, gamma-ray, and infrared astronomy; and astrometry.

90 ASTROPHYSICS 3235
Includes cosmology; celestial mechanics; space plasmas; and interstellar and interplanetary gases and dust.
For related information see also *75 Plasma Physics.*

91 LUNAR AND PLANETARY EXPLORATION 3238
Includes planetology; and manned and unmanned flights.
For spacecraft design or space stations see *18 Spacecraft Design, Testing and Performance.*

92 SOLAR PHYSICS 3239
Includes solar activity, solar flares, solar radiation and sunspots.
For related information see *93 Space Radiation.*

93 SPACE RADIATION 3239
Includes cosmic radiation; and inner and outer earth's radiation belts.
For biological effects of radiation see *52 Aerospace Medicine.* For theory see *73 Nuclear and High-Energy Physics.*

GENERAL

Includes aeronautical, astronautical, and space science related histories, biographies, and pertinent reports too broad for categorization; histories or broad overviews of NASA programs.

99 GENERAL N.A.

Note: N.A. means that no abstracts were assigned to this category for this issue.

SUBJECT INDEX I-1
PERSONAL AUTHOR INDEX I-51
CORPORATE SOURCE INDEX I-59
CONTRACT NUMBER INDEX I-69
REPORT/ACCESSION NUMBER INDEX I-71

TYPICAL CITATION AND ABSTRACT

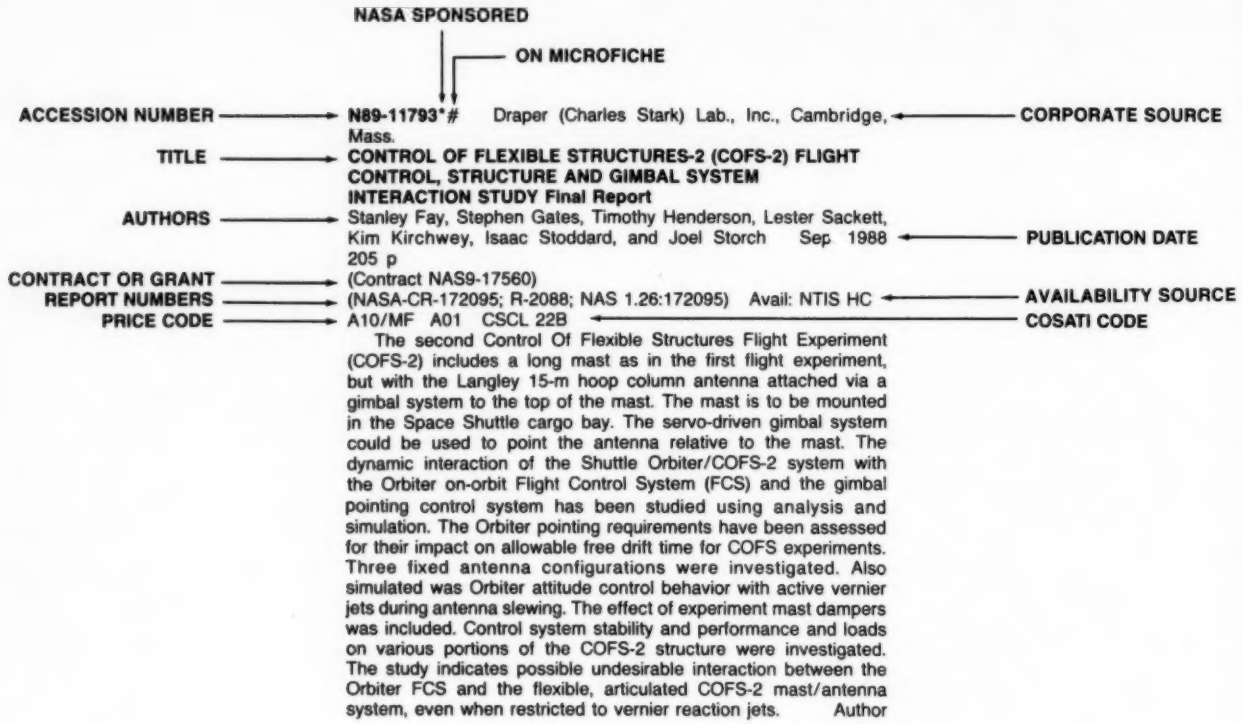
NASA SPONSORED
ON MICROFICHE
ACCESSION NUMBER
N89-11793*# Draper (Charles Stark) Lab., Inc., Cambridge, Mass.
CORPORATE SOURCE
TITLE
CONTROL OF FLEXIBLE STRUCTURES-2 (COFS-2) FLIGHT CONTROL, STRUCTURE AND GIMBAL SYSTEM INTERACTION STUDY Final Report
AUTHORS
Stanley Fay, Stephen Gates, Timothy Henderson, Lester Sackett, Kim Kirchwey, Isaac Stoddard, and Joel Storch Sep. 1988
PUBLICATION DATE
205 p
CONTRACT OR GRANT
(Contract NAS9-17560)
REPORT NUMBERS
(NASA-CR-172095; R-2088; NAS 1.26:172095) Avail: NTIS HC
AVAILABILITY SOURCE
PRICE CODE
A10/MF A01 CSCL 22B
COSATI CODE
The second Control Of Flexible Structures Flight Experiment (COFS-2) includes a long mast as in the first flight experiment, but with the Langley 15-m hoop column antenna attached via a gimbal system to the top of the mast. The mast is to be mounted in the Space Shuttle cargo bay. The servo-driven gimbal system could be used to point the antenna relative to the mast. The dynamic interaction of the Shuttle Orbiter/COFS-2 system with the Orbiter on-orbit Flight Control System (FCS) and the gimbal pointing control system has been studied using analysis and simulation. The Orbiter pointing requirements have been assessed for their impact on allowable free drift time for COFS experiments. Three fixed antenna configurations were investigated. Also simulated was Orbiter attitude control behavior with active vernier jets during antenna slewing. The effect of experiment mast dampers was included. Control system stability and performance and loads on various portions of the COFS-2 structure were investigated. The study indicates possible undesirable interaction between the Orbiter FCS and the flexible, articulated COFS-2 mast/antenna system, even when restricted to vernier reaction jets. Author

VOLUME 27 NUMBER 22 / NOVEMBER 23, 1989

Scientific and Technical Aerospace Reports

A Semimonthly Publication of the National Aeronautics and Space Administration

01 AERONAUTICS (GENERAL)

N89-27632# Army Aviation Engineering Flight Activity, Edwards AFB, CA.
BASELINE PERFORMANCE VERIFICATION OF THE 12TH YEAR PRODUCTION UH-60A BLACK HAWK HELICOPTER Final Report, 15 Aug. - 2 Sep. 1988
John I. Nagata, Joseph L. Piotrowski, Christopher J. Young, William D. Lewis, Paul W. Losier, and Joseph A. Lyle Jan. 1989 74 p
(AD-A208671; USAAEFA-87-32) Avail: NTIS HC A04/MF A01 CSCL 01/3

Testing was conducted to establish a performance baseline of the 12th year production UH-60A helicopter. A total of 19.5 productive hours were flown at two different test sites between 15 August and 2 September 1988. The performance of the 12th year production UH-60A Black Hawk was similar to or slightly degraded from the sixth year production UH-60A. At the primary mission gross weight, the performance met the requirement of the Prime Item Development Specification (PIDS). The out-of-ground effect hover gross weight capability was 17,416 pounds for 95 percent intermediate (30 minute limit) rated power available at 4000 feet pressure altitude and 35 C temperature. The vertical rate of climb of the 12th year aircraft exceeded the PIDS requirement by 21 ft/min. The 12th year production aircraft has an increase in equivalent flat plate area over the sixth year production aircraft. At 4000 ft pressure altitude, 35 C, and maximum continuous power, the cruise airspeed is 139 knots true airspeed, equal to the PIDS requirement. GRA

02 AERODYNAMICS

Includes aerodynamics of bodies, combinations, wings, rotors, and control surfaces; and internal flow in ducts and turbomachinery.

For related information see also *34 Fluid Mechanics and Heat Transfer.*

N89-27633# Vigyan Research Associates, Inc., Hampton, VA.
LOW DENSITY FLOW EFFECTS FOR HYPERVELOCITY VEHICLES Final Report, Aug. 1986 - Jul. 1987
Roop N. Gupta Mar. 1989 41 p
(Contract F33615-86-C-3009)
(AD-A206218; WRDC-TR-89-3034) Avail: NTIS HC A03/MF A01 CSCL 20/4

This work presents results for the surface pressure, drag, heat transfer and skin-friction coefficients for hyperboloids and sphere-cone shaped slender and wide-angle bodies under varying degrees of low-density flow conditions. Recently obtained surface-slip and the corrected shock-slip conditions are employed to account for the low-density effects. The flow cases analyzed include highly cooled and very long slender bodies in high Mach number flows. The present method (limited to the analysis of a perfect gas here) is found to predict various flow field quantities quite accurately when compared with the experimental data. GRA

N89-27634*# National Aeronautics and Space Administration. Langley Research Center, Hampton, VA.
STATIC INTERNAL PERFORMANCE OF A NONAXISYMMETRIC VANED THRUST REVERSER WITH FLOW SPLAY CAPABILITY
Linda S. Bangert and Laurence D. Leavitt Washington Sep. 1989 89 p
(NASA-TP-2933; L-16552; NAS 1.60:2933) Avail: NTIS HC A05/MF A01 CSCL 01A

An investigation was conducted in the Static Test Facility of the Langley 16-Foot Transonic Tunnel on a dual-port, nonaxisymmetric, block-and-turn type thrust reverser model with vane cascades in the reverser ports which turned the flow in the splay direction and aided in turning the flow in the reverse direction. Splaying reverser flow is a method of delaying to lower landing ground roll speeds the reingestion of hot exhaust flow into the inlets. Exhaust flow splay can also help prevent the impingement of hot exhaust gases on the empennage surfaces when the reverser is integrated into an actual airframe. The vane cascades consisted of two sets of perpendicular vanes with a variable number of turning and splay vanes. A skewed vane box was also tested which had only one set of vanes angled to provide both turning and splay. Vane cascades were designed to provide different amounts of flow splay in the top and bottom ports. Inner doors, trim tabs, and an orifice plate all provided means of varying the port area for reverser flow modulation. The outer door position was varied as a means of influencing the flow reverse angle. Nozzle pressure ratio was varied from 1.75 to approximately 6.00. Author

N89-27635# Pacific-Sierra Research Corp., Los Angeles, CA.
AEROSTAT COLD WEATHER STUDY Technical Report, 6 Mar. - 31 Dec. 1988
Dennis L. Kane 13 Mar. 1989 59 p
(Contract MDA903-88-C-0020)
(AD-A207299; PSR-1925) Avail: NTIS HC A04/MF A01 CSCL 04/2

The artic environment and its potential impact on Aerostat design and operations are discussed. Predictive meteorological resources available are summarized. Results of previous Aerostat operations in cold climates are reviewed and potential solutions discussed for the problems encountered. GRA

N89-27636# Air Force Armament Lab., Eglin AFB, FL.
HYPERSONIC PREDICTION COMPARISONS WITH EXPERIMENTAL DATA FOR A CONE-CYLINDER AT MACH 6.86 Final Report, Oct. 1988 - Jan. 1989
Montgomery C. Hughson and Charles J. Cottrell Mar. 1989 10 p Previously announced in IAA as A89-25419
(AD-A207583; AFATL-TP-89-04) Avail: NTIS HC A02/MF A01 CSCL 20/4

Comparisons of computed flowfield predictions to experimental data for a cone-cylinder configurations at Mach 6.86 and angles of attack of 0, 6.7, 14, and 20 degrees are presented. The two inviscid computer codes used were EAGLE and ZEUS, which represent a time-iterative and a space-marching approach, respectively. Specific comparisons were made between the predicted and the experimental pressure distributions along the body at various circumferential locations, as well as aerodynamic

characteristics of normal force coefficient and the location of the center of pressure. The inviscid calculations compare well with experimental data where viscous effects are minimal. GRA

N89-27637# National Aeronautical Lab., Bangalore (India). Computational and Theoretical Fluid Dynamics Div.
COMPUTATION OF TRANSONIC POTENTIAL FLOW PAST RAE-WING-A AND BODY-B2 COMBINATION
Sunil Kumar Chakrabartty Jun. 1989 122 p
(PD-CF-8921) Avail: NTIS HC A06/MF A01

A simple approach has been developed to use the two dimensional grid generation method by solving elliptic partial differential equations to generate the three dimensional grid for wing-fuselage configurations. This simple method can be applied to generate grids for an arbitrary fuselage fitted with any swept wing with dihedral. A three dimensional transonic analysis code TWING, with an approximate factorization (AF2) scheme has been suitably used as a flow solver. As an example, RAE-WING-A with body-B2 configuration has been considered. The results obtained have been compared with available numerical and experimental results. It has been observed in the present computations that AF2 scheme is not sensitive to grid stretching. Author

N89-27638# General Dynamics Corp., Fort Worth, TX.
SMALL SCALE MODEL TESTS IN SMALL WIND AND WATER TUNNELS AT HIGH INCIDENCE AND PITCH RATES. VOLUME 3: WATER TUNNEL (HFF) DATA BASE Final Report, Sep. 1985 - Sep. 1988
Atlee M. Cunningham, Jr., Todd Bushlow, John R. Mercer, Tim A. Wilson, and Steve N. Schwoerke Apr. 1989 179 p
(Contract N00014-85-C-0419)
(AD-A208690) Avail: NTIS HC A09/MF A01 CSCL 01/1

The force testing of small scale models in either a small wind tunnel or a water tunnel was investigated as an inexpensive and quick means to obtain meaningful dynamic force and moment data representative of rapidly maneuvering full scale aircraft. Force tests of flatplate semispan models were conducted in the General Dynamics Aerodynamic Development Facility (ADF) which is a small 14x14 sq in. low speed wind tunnel. Oscillatory model motions up to 48 deg (peak to peak) amplitude were tested at frequencies of 1 to 3 Hz. Force tests of flat and three-dimensional full span models were conducted in the General Dynamics Hydroflow Facility (HFF) which is a horizontal flow water tunnel with a 24x24 sq in. test section. GRA

N89-27639# Georgia Inst. of Tech., Atlanta. School of Aerospace Engineering.
NUMERICAL SIMULATION OF CONTROL OF SUPERSONIC SHEAR LAYERS Semiannual Progress Report, 1 Dec. 1988 - 31 May 1989
L. N. Sankar and Tang Wei 31 May 1989 33 p
(Contract N00014-89-J-1319)
(AD-A209703) Avail: NTIS HC A03/MF A01 CSCL 20/4

The objective of the present research is to investigate the stability and growth characteristics of 2-D and 3-D supersonic free shear layers through direct numerical solution of the 3-D compressible viscous flow equations. An explicit time marching method, patterned after the well known MacCormack scheme is used to integrate the 2-D and 3-D Navier-Stokes equations in time, on a stretched Cartesian grid. The flow being studied consists of shear layers formed at the juncture of two parallel streams at different Mach numbers, densities and temperatures. Assuming an initial velocity, density and temperature distribution at an upstream location, the mean steady flow characteristics of the shear layer are first computed. This is done by marching in time, until an asymptotically steady state solution for the mean flow is obtained. Next, acoustic disturbances composed of streamwise, normal or spanwise sinusoidal velocity perturbations at known frequencies are imposed on the shear layer. The limit cycle behavior of the shear layer is then computed by carrying out the calculations for several cycles of the imposed disturbance. The computed flow field properties are post-processed using standard graphics, techniques to obtain vorticity, pressure and density plots, velocity and Mach numbers of eddies, the Fourier spectrum of the velocity, and pressure field at a number of locations within the shear layer. GRA

N89-27640# McDonnell-Douglas Research Labs., Saint Louis, MO. Dept. of Flight Sciences.
TERMINAL SHOCK RESPONSE IN RAMJET INLETS TO ABRUPT DOWNSTREAM PERTURBATIONS Final Report, 29 Sep. 1983 - 30 Jun. 1987
Miklos Sajben, Thomas J. Bogar, and Joseph C. Kroutil Sep. 1988 47 p
(Contract N60530-83-C-0186)
(AD-A209788; AD-E900851; MDC-Q1285; NWC-TP-6846) Avail: NTIS HC A03/MF A01 CSCL 21/5

The response of a nominally two-dimensional transonic diffuser flow to abrupt downstream perturbations was examined experimentally. GRA

N89-27641# University of Southern California, Los Angeles. Dept. of Aerospace Engineering.
STUDIES OF UNSTEADY VORTEX FLAP AERODYNAMICS Final Report, 1 Aug. 1985 - 31 Jan. 1989
T. Maxworthy and H. K. Cheng 20 Jun. 1989 5 p
(Grant AF-AFOSR-0318-85; AF Proj. 2307)
(AD-A209837; AFOSR-89-0933TR) Avail: NTIS HC A02/MF A01 CSCL 01/1

A joint theoretical and experimental program on the unsteady aerodynamics associated with active vortex flaps employed on delta wings was conducted. Flow visualizations were performed along with quantitative flow field measurements via particle tracking techniques for a range of dynamic conditions. Additionally, a theoretical point vortex approach was employed to study the vortex dynamics and resultant unsteady loads. GRA

03 AIR TRANSPORTATION AND SAFETY

Includes passenger and cargo air transport operations; and aircraft accidents.

For related information see also *16 Space Transportation* and *85 Urban Technology and Transportation.*

N89-27642# Sandia National Labs., Albuquerque, NM.
AN ANALYSIS OF SEVERE AIR TRANSPORT ACCIDENTS
J. D. McClure and R. E. Luna 1989 9 p Presented at the International Symposium on Packaging and Transporting of Radioactive Materials, Washington, DC, 11 Jun. 1989
(Contract DE-AC04-76DP-00789)
(DE89-012642; SAND-89-0922C; CONF-890631-23) Avail: NTIS HC A02/MF A01

The objective of this paper is to analyze the severity of aircraft accidents that may involve the air transport of radioactive materials (RAM). One of the basic aims of this paper is to provide a numerical description of the severity of aircraft transport accidents so that the accident severity can be compared with the accident performance standards that are specified in the International Atomic Energy Authority (IAEA) Safety Series 6, the international packaging standards for the safe movement of RAM. The existing packaging regulations in most countries embrace the packaging standards developed by the IAEA. Historically, the packaging standards for Type B packages have been independent of the transport mode. That is, if the shipment occurs in a certified packaging, then the shipment can take place by any transport mode. In 1975, a legislative action in the U.S. Congress led to the development of a package designed specifically for the air transport of plutonium. Changes were subsequently made to the U.S. packaging regulations to incorporate the plutonium air transport performance standards. These standards were used to certify the air transport package for plutonium which is commonly referred to as PAT-1 (U.S. NRC). The PAT-1 was certified by the U.S. Nuclear Regulatory Commission in September 1978. DOE

N89-27643# Lockheed Aeronautical Systems Co., Burbank, CA.
INVESTIGATION OF TRANSPORT AIRPLANE FUSELAGE FUEL TANK INSTALLATIONS UNDER CRASH CONDITIONS Final Report
Gill Wittlin Jul. 1989 92 p
(Contract DTFA03-86-C-00005)
(DOT/FAA/CT-88/24; LR-31443) Avail: NTIS HC A05/MF A01

Three contemporary fuel tank installation configurations investigated in this study include: (1) a conformable tank containing a bladder and supported within a dedicated structure; (2) a double wall cylindrical strap in an auxiliary tank; and (3) bladder cells fitted in the lower fuselage. Existing crash design criteria are reviewed, as well as current proposals which could affect fuel tank installations. Program KRASH was used to help evaluate the performance of a fuselage mounted tank when subjected to dynamic loads. A total of 21 cases were analyzed, including 12 vertical impacts and 9 longitudinal pulse conditions and/or configurations. The analytical models included 120-inch sections, 300-inch segments and full airplane representations. Results in the form of floor and fuel tank accelerations, floor and fuel tank attachment loads and fuselage crush were obtained. Two test conditions are proposed to represent conditions that best meet the crash design criteria developed in a previous FAA sponsored parametric study, as well as to recognize realistic structures and tests that can be run. Author

N89-27644# Federal Aviation Administration, Washington, DC. Forecast Branch.
TERMINAL AREA FORECASTS: FY 1989 - 2005
Thomas Henry Apr. 1989 527 p
(AD-A209805; FAA-APO-89-5) Avail: NTIS HC A23/MF A01 CSCL 01/5

Forecasts are present for aviation activity of 850 airports in the United States for fiscal years 1989 to 2005. These include 398 airports with FAA air traffic control towers and radar approach control service and 17 FAA contract towers. For each, airport, detailed forecasts are made for the four major users of the air traffic system: air carriers, air taxi/commuters, aviation, and military. Summary tables contain national, FAA regional, and State aviation data and other airport specific highlights. The forecasts have been prepared to meet the budget and planning needs of the constituent units of the FAA headquarters and regional offices and to provide airport-specific information that can be used by State and local aviation authorities, the aviation industry, as a whole, and the general public. GRA

04 AIRCRAFT COMMUNICATIONS AND NAVIGATION

Includes digital and voice communication with aircraft; air navigation systems (satellite and ground based); and air traffic control.

For related information see also *17 Space Communications, Spacecraft Communications, Command and Tracking* and *Communications and Radar.*

N89-27645# Mitre Corp., McLean, VA. Civil Systems Div.
AUTOMATED PLANNING FUNCTION FOR AERA 3: MANEUVER OPTION MANAGER Final Report
William P. Niedringhaus Apr. 1989 45 p
(Contract DTFA01-89-C-00001)
(DOT/FAA/DS-89/21; MTR-88W00048) Avail: NTIS HC A03/MF A01

The Maneuver Option Manager (MOM), a methodology to simplify complex air traffic control (ATC) problems is described. A complex problem is identified here as a set of interrelated potential conflicts between pairs of aircraft. It may involve arbitrarily many aircraft. MOM determines which of six simple maneuver options is available (free of such potential conflicts) for each aircraft. These options involve limited displacements left/right ahead/behind above/below nominal. MOM simplifies a complex problem by protecting (for future use) an available maneuver option for one or more of the involved aircraft. Routinely, a single such maneuver option causes complex problems to be broken into independent, smaller, and simpler problems. Author

N89-27646# Mitre Corp., McLean, VA. Civil Systems Div.
A MATHEMATICAL FORMULATION FOR PLANNING AUTOMATED AIRCRAFT SEPARATIONS FOR AERA 3 Final Report
William P. Niedringhaus Apr. 1989 106 p
(Contract DTFA01-89-C-00001)
(DOT/FAA/DS-89/20; MTR-88W00049) Avail: NTIS HC A06/MF A01

An algorithm, called Gentle-Strict (GS), is given for automated resolution of crossing conflicts between two aircraft, using parallel lateral offset maneuvers. Though other algorithms have been proposed for this purpose, GS uniquely facilitates quantitative analysis of the conflict resolution process itself, as well as quantitative analysis of the links between pairwise conflict resolution and longer lookahead air traffic control (ATC) strategies. The main result of this document is a closed form mathematical formula which relates parameterizations of: (1) the encounter geometry; (2) the pathkeeping uncertainties; (3) the minimum separation achieved by GS; and (4) the gentleness of parallel lateral offset resolution maneuvers (as parameterized by magnitude of offset and by induced delay upon the aircraft). Author

N89-28178*# National Aeronautics and Space Administration. Goddard Space Flight Center, Greenbelt, MD.
NAVIGATIONAL AND ENVIRONMENTAL MEASUREMENT SYSTEM (NEMS) Abstract Only
T. D. Clem *In its* Laboratory for Oceans 1988 p 223-225
(For primary document see N89-28118 22-48)
Avail: NTIS HC A12/MF A01 CSCL 17G

N89-28179*# National Aeronautics and Space Administration. Goddard Space Flight Center, Greenbelt, MD.
AIRBORNE LIDAR GLOBAL POSITIONING INVESTIGATIONS Abstract Only
W. B. Krabill *In its* Laboratory for Oceans 1988 p 227-229
(For primary document see N89-28118 22-48)
Avail: NTIS HC A12/MF A01 CSCL 17G

05 AIRCRAFT DESIGN, TESTING AND PERFORMANCE

Includes aircraft simulation technology.

For related information see also *18 Spacecraft Design, Testing and Performance* and *39 Structural Mechanics.* For land transportation vehicles see *85 Urban Technology and Transportation.*

N89-27647*# Boeing Commercial Airplane Co., Seattle, WA. New Airplane Development.
HIGH-SPEED CIVIL TRANSPORT STUDY. SUMMARY Final Report
Washington Sep. 1989 41 p
(Contract NAS1-18377)
(NASA-CR-4234; NAS 1.26:4234) Avail: NTIS HC A03/MF A01

A system of study of the potential for a high speed commercial transport aircraft addressed technology, economic, and environmental constraints. Market projections indicated a need for fleets of transport with supersonic or greater cruise speeds by the years 2000 to 2005. The associated design requirements called for a vehicle to carry 250 to 300 passengers over a range of 5000 to 6000 nautical miles. The study was initially unconstrained in terms of vehicle characteristics, such as cruise speed, propulsion systems, fuels, or structural materials. Analyses led to a focus on the most promising vehicle concepts. These were concepts that used a kerosene type fuel and cruised at Mach numbers between 2.0 to 3.2. Further systems study identified the impact of

environmental constraints (for community noise, sonic boom, and engine emissions) on economic attractiveness and technological needs. Results showed that current technology cannot produce a viable high speed civil transport. Significant advances are needed to take off gross weight and allow for both economic attractiveness and environment acceptability. Specific technological requirements were identified to meet these needs. Author

N89-27648*# Boeing Commercial Airplane Co., Seattle, WA. New Airplane Development.
HIGH-SPEED CIVIL TRANSPORT STUDY Final Report
Washington Sep. 1989 126 p
(Contract NAS1-18377)
(NASA-CR-4233; NAS 1.26:4233) Avail: NTIS HC A07/MF A01 CSCL 01C

A system study of the potential for a high-speed commercial transport has addressed technological, economic, and environmental constraints. Market projections indicate a need for fleets of transports with supersonic or greater cruise speeds by the year 2000 to 2005. The associated design requirements called for a vehicle to carry 250 to 300 passengers over a range of 5,000 to 6,000 nautical miles. The study was initially unconstrained in terms of vehicle characteristic, such as cruise speed, propulsion systems, fuels, or structural materials. Analyses led to a focus on the most promising vehicle concepts. These were concepts that used a kerosene-type fuel and cruised at Mach numbers between 2.0 to 3.2. Further systems study identified the impact of environmental constraints (for community noise, sonic boom, and engine emissions) on economic attractiveness and technological needs. Results showed that current technology cannot produce a viable high-speed civil transport; significant advances are required to reduce takeoff gross weight and allow for both economic attractiveness and environmental acceptability. Specific technological requirements were identified to meet these needs. Author

N89-27649# Pennsylvania State Univ., University Park. Dept. of Aerospace Engineering.
ANALYSIS OF A SYSTEM TO PREVENT HELICOPTER ROTOR BLADE-AIRFRAME STRIKES Final Report, 1 Nov. 1986 - 31 Dec. 1988
B. W. McCormick and R. G. Melton 1 May 1989 111 p
(Contract DAAL03-87-K-0002)
(AD-A209804; ARO-23726.1-EG) Avail: NTIS HC A06/MF A01 CSCL 01/3

Rotor blade-airframe strikes are rare but they do occur. Three areas of the airframe are particularly vulnerable: the tail boom, canopy and, in the case of the underslung, teetering rotor, the rotor shaft. This latter case is known as mast bumping. This report studies a system to prevent a helicopter rotor blade from striking any part of the airframe. Essentially, the system continuously predicts ahead the rotor blade flapping in response to an input such as pilot control or an atmospheric disturbance. If a blade strike is predicted to occur then an appropriate feedback control is applied to alter the future flapping. The prediction is then begun again with the altered control. In the actual system, an enunciator might warn the pilot at the time that an attempt is made to control input which could be hazardous. Two somewhat independent approaches to the design of the controller are taken. One of the programs is entirely numerical in its approach. The other uses modern control theory and considers the preliminary aspects of implementing the controller in digital hardware. Both methods indicate the feasibility of preventing excessive flapping, although the question of implementation in a dedicated microprocessor is not fully resolved. GRA

06 AIRCRAFT INSTRUMENTATION

Includes cockpit and cabin display devices; and flight instruments.

For related information see also *19 Spacecraft Instrumentation* and *35 Instrumentation and Photography.*

N89-27650# Advisory Group for Aerospace Research and Development, Neuilly-Sur-Seine (France). Avionics Panel.
SYSTEMS ENGINEERING
May 1989 132 p In ENGLISH and FRENCH Lecture series held in Kettering, OH, 15-16 May 1989, in Delft, Netherlands, 22-23 May 1989, and in Rome, Italy, 25-26 May 1989
(AGARD-LS-164; ISBN-92-835-0513-1) Copyright Avail: NTIS HC A07/MF A01

Recent AGARD activities have indicated a strong need for more effective avionics system engineering. There is a growing need for reducing development time, effecting savings in costs of ownership, and in extending the life-time of avionics systems. This must be accomplished along with meeting needs of the user faced with a growing threat. With the growing complexity of avionics systems (as well as other systems), it is important to develop and maintain expertise in system planning, architecture, and management. The important systems engineering aspects of requirements, system integration, prototyping, and design are addressed. In addition, the impact of technology on system architecture are discussed. Methodologies are described and actual case histories will serve as practical examples of modern systems engineering. For individual titles, see N89-27651 through N89-27658.

N89-27651# Rome Air Development Center, Griffiss AFB, NY.
AVIONICS SYSTEM ENGINEERING: AN INTRODUCTION
Fred I. Diamond *In* AGARD, Systems Engineering May 1989 6 p (For primary document see N89-27650 22-06)
Copyright Avail: NTIS HC A07/MF A01

System engineering is the process used in the evolution of systems from identification of a need through construction and/or production and deployment in an operational environment. It is a process that involves the application of appropriate scientific and technical knowledge to transform an operational need into a system configuration with defined parameters, through an iterative process of analysis, design, test, and evaluation; to integrate all performance requirements, including reliability, maintainability, and supportability into the total engineering effort; and to integrate related components to insure interoperability and optimum system performance. It is a process that also considers economic factors such as development and life cycle costs. The life cycle process involves several key steps, many iterative, but in an orderly and controlled manner. These steps include requirements, architecture specification, design, development/construction, test and evaluation, and operational use. With the growing complexity of avionics systems, effective systems engineering is critical. Therefore, greater emphasis is placed on architectures, subsystem design, and interfaces and system integration. Only through a total systems engineering approach from the very initial phases of the system life cycle can a well-engineered system be achieved. The payoff will be reduced cost of ownership and greater mission effectiveness. Author

N89-27652# Westinghouse Electric Corp., Baltimore, MD.
AVIONIC SYSTEM REQUIREMENTS
Harvey M. Paskin *In* AGARD, Systems Engineering May 1989 6 p (For primary document see N89-27650 22-06)
Copyright Avail: NTIS HC A07/MF A01

Avionics system requirements are addressed at the conceptual level in light of changing threats, acquisition strategies, technology, and business environments. The objective is to provide a perspective of total integrated avionics system performance which illuminates broad requirement issues rather than specific subsystem specifications. The fundamental tenet is that although parametric and functional avionic system requirements can be related intuitively to mission related activities, a more global view is necessary to ensure that system requirements aptly address the gamut of factors

which relentlessly bear on the ultimate system design, development, production, and support. The premise is that avionics requirements are driven by four factors: information and data sources, control opportunities and information needs; concepts and algorithmic techniques; and realization technologies. These four factors are set in a generic systems structure which shows their interrelationships and provides the framework for conceptualizing avionic system solutions to meet particular mission needs. The structure focuses on the role of avionics in providing situation assessment, response selection, response implementation, and communications. With this structures in place, avionic system requirements are then examined within the context of architecture, techniques, technology, producibility, and supportability. Author

N89-27653# British Aircraft Corp., Preston (England).
A STRUCTURED APPROACH TO WEAPON SYSTEM DESIGN
J. D. Rowley *In* AGARD, Systems Engineering May 1989 7 p (For primary document see N89-27650 22-06)
Copyright Avail: NTIS HC A07/MF A01

A structured approach is described for the design of a weapon system which British Aerospace (BAe) was able to develop and prove during the design of the avionics system for the Experimental Aircraft Program (EAP) demonstrator aircraft. Brief descriptions are given of the EAP avionics system, the main system design tools used, the activities carried out during the systems design process, and the management and control procedures adopted. In addition a series of observations highlighting some of the findings of the project and providing pointers to the design of future weapon systems are given. Author

N89-27654# Aeronautical Systems Div., Wright-Patterson AFB, OH. Directorate of Design Analysis.
INTEGRATED AVIONICS: CONCEPTUAL DESIGN
Michael J. Breza *In* AGARD, Systems Engineering May 1989 3 p (For primary document see N89-27650 22-06)
Copyright Avail: NTIS HC A07/MF A01

Avionics of modern military aircraft is essential for maximizing performance realization of the total aeronautical system. In the early conceptual phase, aeronautical systems designers give scant attention to the interaction of avionics components. The aircraft design team generally provides weight, volume, and power considerations for the desired avionics functions and assumes that an avionics suite can eventually be assembled. Even less attention is given to the potential synergistic effect avionics can have with the aircraft design process. In contrast, the designers expend a large effort on finding the best balanced combination of airframe and propulsion components which satisfy the design objectives. An attempt is made to show why avionics must be a co-equal member of the aeronautical system along with airframe, propulsion, and armament. In becoming a co-equal partner, avionics must be an element of the system design analysis, commencing with the early conceptual design phase of a new aeronautical system. Author

N89-27655# Air Force Avionics Lab., Wright-Patterson AFB, OH.
THE EVOLUTION OF DIGITAL AVIONICS ARCHITECTURES/SYSTEMS
John C. Ostgaard and D. Reed Morgan *In* AGARD, Systems Engineering May 1989 22 p (For primary document see N89-27650 22-06)
Copyright Avail: NTIS HC A07/MF A01

The evolutionary design/development of modern-day digital information systems is examined. Included are the initial attempts at using digital technology in the early 1970s, the system integration thrusts of the 1980s, and the continued system technology revolution of the 1990s. Author

N89-27656# GEC Avionics Ltd., Rochester (England).
AVIONIC SYSTEM DESIGN METHODOLOGY
M. J. Tooze *In* AGARD, Systems Engineering May 1989 9 p (For primary document see N89-27650 22-06)
Copyright Avail: NTIS HC A07/MF A01

An approach is described for an avionic system design and its application to modular avionic architecture. The approach is to test various candidate architectures using a common functional requirement. The method commences with a requirement analysis carried out in a top-down fashion to arrive at a full functional description. A parallel phase determines the technological base and defines a number of candidate architectures and corresponding component sets (module sets in the case of modular architecture). Thus technological performance and in-place equipment limitations are included at an early stage independent of the requirement. Hence top-down means bottom-up, by taking various architecture candidates and corresponding modular sets and applying the functional description of the requirement, so each architecture may be investigated for its capability to cope with the trial or application system. Assessment of reliability and performance objectives is discussed. Also included is reference to the areas of operating systems and BITE which may form part of the system but are not necessarily directly represented at the boundaries of the system. The philosophy of the approach is evaluated and does not extend to application of the various CASE design tools which exist (or may be specified) in order to carry out such a project in practice. Author

N89-27657# Aeritalia S.p.A., Caselle Torinese (Italy). Gruppo Sistemi e Teleguidati.
RAPID PROTOTYPING OF COMPLEX AVIONICS SYSTEMS
L. Berardi *In* AGARD, Systems Engineering May 1989 18 p (For primary document see N89-27650 22-06)
Copyright Avail: NTIS HC A07/MF A01

The use of a rapid prototyping approach in the initial stages of complex avionics system design can complement some traditional computer design methods. In fact most of the computer aids in engineering and design are aimed to a better, coherent and, as far as possible, complete description of the project, but not too much is done on the verification of the proposed concept implementation. The advantage of having in the early design a software prototype of the system to highlight undesirable characteristics or possible improvements when the system has a high degree of complexity is discussed. Then a design tool called Expert Consultant for Avionics System Transformation Exploitation (ECATE) is described. ECATE is an expert system that prototypes the information handling architecture of an avionics system. The use of knowledge engineering and, in general, artificial intelligence approach for the rapid prototyping has proven very effective, because of the high flexibility, complex domain mastering capability, and heuristic methods typical of these techniques. Finally a description of a complete, integrated environment for the rapid development of prototypes of avionics systems, by using artificial intelligence and computer tools, is given. Author

N89-27658# Avions Marcel Dassault-Breguet Aviation, Saint-Cloud (France).
MODELING FUNCTIONAL SPECIFICATIONS FOR ONBOARD SOFTWARE [MAQUETTAGE DES SPECIFICATIONS FONCTIONNELLES DU LOGICIEL EMBARQUE]
Patrick Schirle *In* AGARD, Systems Engineering May 1989 19 p In FRENCH (For primary document see N89-27650 22-06)
Copyright Avail: NTIS HC A07/MF A01

Software development for military avionics requires extensive documentation of functional and contractual specifications. The modeling of specifications permits: (1) improvement of the formal quality of specifications; (2) functional validation throughout the entire software life cycle; (3) generation of acceptance criteria; and (4) establishment of a functional reference for system integration. The role of specifications modeling in the software development process is discussed and experiences with the Rafale A and Mirage 2000 NC avionics systems are described. Transl. by M.G.

N89-27659# Army Aviation Engineering Flight Activity, Edwards AFB, CA.
VERIFICATION OF THE PRODUCTION SAFE FLIGHT INSTRUMENT CORPORATION OV/RV-1D STALL WARNING SYSTEM Final Report, 17 - 25 Aug. 1988
Joseph C. Miess, Charles Q. Crowell, and Patrick Sullivan Nov. 1988 44 p
(AD-A207392) Avail: NTIS HC A03/MF A01 CSCL 01/4

A Safe Flight Instrument Corporation (SFIC) stall warning system and prototype normal acceleration (g) limit aural warning device were evaluated on an OV-1D(C). Fifteen productive test flight hours were completed. Interchangeability of the SFIC stall warning system between aircraft was demonstrated by the good correlation of data between Grumman's test on aircraft and U.S. Army Aviation Engineering Flight Activity's (AEFA's) test on aircraft. Grumman's data shows adequate warning margin for LSSS on. There were, inadequate stall margins with LSSS not installed for dual-engine unaccelerated stalls, drop tanks only, and no-stores configurations. Single engine warning margins were inadequate, especially with the right engine operating near maximum power. Accelerated stall warning margine were satisfactory for all wing stores configurations. If the SFIC system is installed on operational aircraft without LSSS, the SFIC system should be adjusted to provide approximately 3 knots more warning margin for low power stalls. GRA

N89-27660# Naval Postgraduate School, Monterey, CA.
EVALUATION OF HEAD-UP DISPLAY FORMATS FOR THE F/A-18 HORNET M.S. Thesis
Leah M. Roust Mar. 1989 105 p
(AD-A208651) Avail: NTIS HC A06/MF A01 CSCL 25/3

This study evaluates symbols and formats for the F/A-18 Hornet head-up display (HUD) and Attitude Directional Indicator (ADI) for use by pilots in recovering from unusual aircraft attitudes. Two surveys were conducted to collect pilot opinions on various symbols and formats, based on past experimental research and current recommendations. For the HUD symbols according to the amount of information these symbols provide for the pilot while he is in an unusual attitude. In some cases, the pilots also were asked to choose their preferred symbols. The second survey was based on the results of the first and was administered to 56 F/A-18 pilots. These pilots selected their preferred HUD or ADI display formats, choosing one from two to five possibilities in each case. The specific symbols and formats that were evaluated are described in detail. Survey results are provided, and recommendations are made for display implementation and for further research and testing of symbols and formats. GRA

07 AIRCRAFT PROPULSION AND POWER

Includes prime propulsion systems and systems components, e.g., gas turbine engines and compressors; and onboard auxilliary power plants for aircraft.

For related information see also *20 Spacecraft Propulsion and Power, 28 Propellants and Fuels,* and *44 Energy Production and Conversion.*

N89-27661# Advisory Group for Aerospace Research and Development, Neuilly-Sur-Seine (France). Propulsion and Energetics Panel.
BLADING DESIGN FOR AXIAL TURBOMACHINES
May 1989 212 p Lecture series held in Toronto, Ontario, 1-2 Jun. 1989, in Cologne, Fed. Republic of Germany, 15-16 Jun. 1989, and in Ecully, France, 19-20 Jun. 1989
(AGARD-LS-167; ISBN-92-835-0512-3) Copyright Avail: NTIS HC A10/MF A01

The efficiency and performance of the turbomachinery components of future aero engines can considerably be improved by applying recent advances in understanding the flow behavior of axial compressor and turbine bladings. Thus, the optimal profile pressure distribution as input for new blading design methods has an important effect on losses and flow deflection. The boundary-layer behavior has to be carefully taken into account with respect to laminar/turbulent transition, shock/boundary-layer interaction and separation effects. In addition to these aerodynamical questiona, unsteady effects and the limitations from structural and vibrational conditions also have to be taken into account. Two main topics are discussed: design methods and their principles and limitations, and application to axial compressors and turbines. For individual titles, see N89-27662 through N89-27669.

N89-27662# Hochschule der Bundeswehr, Munich (Germany, F.R.). Inst. fuer Strahlantriebe.
REVIEW ON TURBOMACHINERY BLADING DESIGN PROBLEMS
L. Fottner *In* AGARD, Blading Design for Axial Turbomachines May 1989 13 p (For primary document see N89-27661 22-07)
Copyright Avail: NTIS HC A10/MF A01

Based on the design objectives for the bladings of highly-loaded, high Mach number turbocomponents the main problem areas to be taken into account during the design process are derived. These refer to the flow field conditions with respect to the effect of the Mach number on the profile contour shape, the aerodynamic loading, especially compressor bladings, and the boundary-layer behavior. In addition, blading design has to account for the secondary flow effects and unsteady flow conditions. Author

N89-27663# Deutsche Forschungs- und Versuchsanstalt fuer Luft- und Raumfahrt, Cologne (Germany, F.R.). Inst. fuer Antriebstechnik.
DESIGN CRITERIA FOR OPTIMAL BLADING DESIGN
Hans Starken *In* AGARD, Blading Design for Axial Turbomachines May 1989 17 p (For primary document see N89-27661 22-07)
Copyright Avail: NTIS HC A10/MF A01

Since about 1975 numerical methods are available to compute cascade blade shapes from prescribed surface velocity distributions in compressible flow range. Two-dimensional or quasi three-dimensional inverse or design methods enabled thereby the improvement of compressor and turbine cascades via an optimized blade pressure distribution. The theoretical and experimental development of such pressure distributions is described for the subsonic, supercritical, transonic, and supersonic velocity range of the compressor cascades. The equivalent problems in turbine cascades are indicated. Author

N89-27664# Office National d'Etudes et de Recherches Aeronautiques, Paris (France).
OVERVIEW ON BLADING DESIGN METHODS
G. Meauze *In* AGARD, Blading Design for Axial Turbomachines May 1989 20 p (For primary document see N89-27661 22-07)
Copyright Avail: NTIS HC A10/MF A01

Rather than presenting an exhaustive catalog on the design method calculations, the possible ways to use the calculation methods are discussed, as well as the problems of their practical applications. The complexity of the flow behavior is recalled through a turbomachine and the simplifications which must be adopter, i.e., a mean axisymmetric steady through flow hypothesis. The particular case of an isolated blade row with the possible use of a full 3-D design approach is presented. The well-known quasi 3-D approach combining the mean through flow and the blade-to-blade calculations is discussed where some details are given on direct and inverse methods for both through flow and cascade flow. Author

N89-27665# Iowa State Univ. of Science and Technology, Ames. Dept. of Mechanical Engineering.
PERFORMANCE PREDICTION FOR AXIAL-FLOW COMPRESSOR AND TURBINE BLADING
George K. Serovy *In* AGARD, Blading Design for Axial

Turbomachines May 1989 19 p (For primary document see N89-27661 22-07)
Copyright Avail: NTIS HC A10/MF A01

The performance of compressor and turbine blading must be predicted in all levels of a conventional design system, beginning in the preliminary design phase before blade row geometry is defined. Because of this requirement, many levels of complexity exist in both input and output of prediction methods, and alternative methods exist within each phase of design. A brief review of performance prediction problems and current solutions is presented. Because details of equations and methods cannot and should not be included, reference to original documents in readily available sources are classified according to their place in configuration design and analysis. It is concluded that both quasi-three-dimensional and three-dimensional computation methods have a potential for future development in terms of configuration optimization. Additionally, it is concluded that experimental data correlation is not dead, and that improvement potential exists in every area of the performance estimation problem. Author

N89-27666# Rolls-Royce Ltd., Derby (England).
BLADING DESIGN FOR MULTI-STAGE HP COMPRESSORS
P. Stow *In* AGARD, Blading Design for Axial Turbomachines May 1989 29 p (For primary document see N89-27661 22-07)
Copyright Avail: NTIS HC A10/MF A01

Computer aided turbomachinery blade design is discussed with the emphasis on the mathematical models that are needed in order to account for the important physical phenomena. The various aspects of a typical balde design system are presented covering through-flow and blade-to-blade analysis. The through-flow discussion coveres linked through-flow-blade-to-blade analysis, blade loss models, end-wall boundary layers, secondary flow analysis, and spanwise mixing models. Blade section design using mixed design and analysis methods is covered together with loss prediction using coupled inviscid boundary layer approaches. Limitations of the coupled approach are discussed together with the emerging role of Reynolds averaged Navier-Stokes methods aimed at removing these limitations. The need for fully three-dimensional methods is covered together with their incorporation into the design system. Finally areas for future development and application are discussed. Author

N89-27667# Air Force Wright Aeronautical Labs., Wright-Patterson AFB, OH.
TRANSONIC AND SUPERSONIC COMPRESSOR BLADING DESIGN
A. J. Wennerstrom *In* AGARD, Blading Design for Axial Turbomachines May 1989 22 p (For primary document see N89-27661 22-07)
Copyright Avail: NTIS HC A10/MF A01

A design is presented for axial compressor stages for which the achievement of high performance is both critical from the standpoint of a thermodynamic cycle and also difficult because of high aerodynamic loading, Mach number, or both. The type of method of interest is often termed a through-blade design procedure. The general methodology employed is covered including the computational framework. The kinds of information derived from empiricism is discussed, followed by those areas where design guidance is lacking and logical assumptions are used. The foregoing can theoretically result in an infinite range of solutions. An optimization critieria is presented through striving to obtain the one best solution. Three examples are shown covering the Mach number range of about 0.7 to 1.6 to illustrate the success of the approach. Several other factors which must be taken into account in a design are mentioned. Also, several glaring weaknesses in the present design methods are identified. The lecture concludes with some comments on current design trends and computational goals. Author

N89-27668# Centre de Villaroche, Moissy (France).
BLADING DESIGN FOR COOLED HIGH-PRESSURE TURBINES
P. F. Bry *In* AGARD, Blading Design for Axial Turbomachines May 1989 42 p (For primary document see N89-27661 22-07)
Copyright Avail: NTIS HC A10/MF A01

The past fifty years have seen the tremendous development of jet engine propulsion. Testing has become very complex and has paralleled the increasing complexity observed in the domain of computational methods. The best compromise must be found for the inner and outer shapes of the nozzles and blades. This can only be achieved if internal and external designs are performed by an integrated team of specialists. Tools are described that are available for helping design engineers to reach this objective. Examples of what can be achieved are presented. Both theoretical and experimental aspects are addressed since they are an integral part of the design process. Author

N89-27669# Motoren- und Turbinen-Union Muenchen G.m.b.H. (Germany, F.R.).
AERODYNAMIC DESIGN OF LOW PRESSURE TURBINES
J. Hourmouziadis *In* AGARD, Blading Design for Axial Turbomachines May 1989 40 p (For primary document see N89-27661 22-07)
Copyright Avail: NTIS HC A10/MF A01

The aerodynamic requirements for low pressure (LP) turbines covering a wide range of Mach and Reynolds numbers are derived from the applications for turbofan, shaft, and propfan engines. Designing turbines for high performance levels is based on extensive experience and modern prediction techniques. Methodology, experimental background, measurement techniques, and design systems are reviewed. The merits and limitations of present computation procedures are discussed. The close interaction between research and industrial development is discussed and the differences are pointed out. Two-dimensional pressure distributions can be predicted by a variety of very efficient inviscid methods. Boundary layer prediction is handicapped by complexity including separation and transition. The characteristic of the Prandtl boundary layer is developed and the physical model leading to the concept of Controlled Boundary Layer (CBL) design is presented. The effects of unsteadiness and turbulence in turbomachinery as well as the extension to transonic flow are considered. The understanding of the inviscid 3-D aerodynamics and their introduction in the design systems is presented. Secondary flows and their direct and indirect effects on losses are discussed. The problems to be addressed in the intermediate and long term research and development work are listed and their significance commented upon. Author

N89-27670*# National Aeronautics and Space Administration. Lewis Research Center, Cleveland, OH.
MACH 5 INLET CFD AND EXPERIMENTAL RESULTS
Lois J. Weir, D. R. Reddy, and George D. Rupp (Sverdrup Technology, Inc., Cleveland, OH.) Jul. 1989 16 p Presented at the 25th Joint Propulsion Conference, Monterey, CA, 10-12 Jul. 1989; sponsored in part by AIAA, ASME, SAE, and ASEE
(NASA-TM-102317; E-5011; NAS 1.15:102317; AIAA-89-2355)
Avail: NTIS HC A03/MF A01 CSCL 21E

An experimental research program was conducted in the NASA Lewis Research Center 10 x 10 ft supersonic wind tunnel. The 2-D inlet model was designed to study the Mach 3.0 to 5.0 speed range for an over-under turbojet plus ramjet propulsion system. The model was extensively instrumented to provide both analytical code validation data as well as inlet performance information. Support studies for the program include flow field predictions with both 3-D parabolized Navier-Stokes (PNS) and 3-D full Navier-Stokes (FNS) analytical codes. Analytical predictions and experimental results are compared. Author

08 AIRCRAFT STABILITY AND CONTROL

Includes aircraft handling qualities; piloting; flight controls; and autopilots.

For related information see also *05 Aircraft Design, Testing and Performance.*

N89-27671*# National Aeronautics and Space Administration. Langley Research Center, Hampton, VA.
SUMMARY OF LONGITUDINAL STABILITY AND CONTROL PARAMETERS AS DETERMINED FROM SPACE SHUTTLE CHALLENGER FLIGHT TEST DATA
William T. Suit Jul. 1989 30 p
(NASA-TM-101605; NAS 1.15:101605) Avail: NTIS HC A03/MF A01 CSCL 01C

Estimates of longitudinal stability and control parameters for the space shuttle were determined by applying a maximum likelihood parameter estimation technique to Challenger flight test data. The parameters for pitching moment coefficient, C(m sub alpha), (at different angles of attack), pitching moment coefficient, C(m sub delta e), (at different elevator deflections) and the normal force coefficient, C(z sub alpha), (at different angles of attack) describe 90 percent of the response to longitudinal inputs during Space Shuttle Challenger flights with C(m sub delta e) being the dominant parameter. The values of C(z sub alpha) were found to be input dependent for these tests. However, when C(z sub alpha) was set at preflight predictions, the values determined for C(m sub delta e) changed less than 10 percent from the values obtained when C(z sub alpha) was estimated as well. The preflight predictions for C(z sub alpha) and C(m sub alpha) are acceptable values, while the values of C(z sub delta e) should be about 30 percent less negative than the preflight predictions near Mach 1, and 10 percent less negative, otherwise. Author

N89-27672*# Sverdrup Technology, Inc., Cleveland, OH.
STABILITY ROBUSTNESS IMPROVEMENT OF DIRECT EIGENSPACE ASSIGNMENT BASED FEEDBACK SYSTEMS USING SINGULAR VALUE SENSITIVITIES Final Report
Sanjay Garg Aug. 1989 32 p Presented at the American Control Conference, Pittsburgh, PA, 21-23 Jun.1 989; sponsored in part by American Automatic Control Council
(Contract NAS3-25266)
(NASA-CR-182302; E-4853; NAS 1.26:182302) Avail: NTIS HC A03/MF A01 CSCL 01C

A methodology to improve the stability robustness of feedback control systems designed using direct eigenspace assignment techniques is presented. The method consists of considering the sensitivity of the minimum singular value of the return difference transfer matrix at the plant input to small changes in the desired closed-loop eigenvalues and the specified elements of the desired closed-loop eigenvectors. Closed-form expressions for the gradient of the minimum return difference singular value with respect to desired closed-loop eigenvalue and eigenvector parameters are derived. Closed-form expressions for the gradients of the control feedback gains with respect to the specified eigenspace parameters are obtained as an intermediate step. The use of the gradient information to improve the guaranteed gain and phase margins in eigenspace assignment based designs is demonstrated by application to an advanced fighter aircraft. Author

09 RESEARCH AND SUPPORT FACILITIES (AIR)

Includes airports, hangars and runways; aircraft repair and overhaul facilities; wind tunnels; shock tubes; and aircraft engine test stands.

For related information see also *14 Ground Support Systems and Facilities (Space).*

N89-27673# Central State Univ., Wilberforce, OH. Dept. of Manufacturing Engineering.
THEORETICAL MODEL FOR STABILIZATION OF CLAY-SILT AIRPORT PAVEMENT SUBGRADE SYSTEMS. PHASE 1: LABORATORY INVESTIGATION. PHASE 2: RUTTING TESTS Final Report
William A. Grissom, Abayomi J. Ajayi-Majebi, L. Shelbert Smith, Carl L. White, Mahmoud A. Abd-Allah, and Eugene E. Jones (Tractell, Inc., Dayton, OH.) May 1989 327 p
(Contract DTFA01-84-C-00023)
(DOT/FAA/PM-87/20-Phase-1/2) Avail: NTIS HC A15/MF A01

Theoretical models for low-volume airport pavement stabilization of clay-silt systems are documented. A non-traditional method of soil stabilization is presented for improving the subgrade strength of poorly graded clay-silt. The research (Phase 1) focuses on: (1) identification of a chemical additive capable of increasing the load bearing strength of clay-silt soil; (2) additive application to a clay-silt soil system leading to increased bearing strength; and (3) development of mathematical models for soil strength prediction. Phase 2 focuses on field validation of the test results through studies of pavement rutting. Among several effective non-traditional organic additives tested in this research, the two-part epoxy system, bisphenol A/epichlorohydrin resin plus a polyamide hardener gave the best result as measured by the dry California Bearing Ratio (CBR) test. The choice of the dry CBR test performed to ASTM specification was motivated by a need to capture optimum moisture content as a variable in addition to percent additive, clay-silt ratio, temperature and dry density, using a full factorial experimental design. The statistical regression models developed support the hypothesis that only additive percentage, moisture content and temperature are significant variables influencing the strength of the clay-silt soil system tested. The nomograph developed for CBR prediction enables quick estimates of dry CBR. The marginal increase in CBR values due to a percent increase in epoxy resin application is 11.1 and the marginal degradation of CBR due to a percent increase in moisture level is 5.6. In phase 2, the rutting validation study confirmed the effectiveness of the chemical stabilizing agent identified for strengthening a clay-silt soil at the 4 percent level of additive application. Based on the results of the rutting test conducted on a tire force machine (TFM), the stabilized pavement will sustain an aircraft load of 10,000 lbs applied through 1000 wheel load passes while meeting the 1/2 inch rutting criteria. Author

N89-27674*# Naples Univ. (Italy).
AN EVALUATION OF THREE EXPERIMENTAL PROCESSES FOR TWO-DIMENSIONAL TRANSONIC TESTS
Gennaro Zuppardi Aug. 1989 71 p
(Contract NCC1-47)
(NASA-CR-181871; NAS 1.26:181871) Avail: NTIS HC A04/MF A01 CSCL 14B

The aerodynamic measurements in conventional wind tunnels usually suffer from the interference effects of the sting supporting the model and the test section walls. These effects are particularly severe in the transonic regime. Sting interference effects can be overcome through the Magnetic Suspension technique. Wall effects can be alleviated by: testing airfoils in conventional, ventilated tunnels at relatively small model to tunnel size ratios; treatment of the tunnel wall boundary layers; or by utilization of the Adaptive Wall Test Section (AWTS) concept. The operating capabilities and results from two of the foremost two-dimensional, transonic, AWTS facilities in existence are assessed. These facilities are the NASA 0.3-Meter Transonic Cryogenic Tunnel and the ONERA T-2 facility

located in Toulouse, France. In addition, the results derived from the well known conventional facility, the NAE 5 ft x 5 ft Canadian wind tunnel will be assessed. CAST10/D0A2 Airfoil results will be used in all of the evaluations. Author

N89-27675# Naval Postgraduate School, Monterey, CA.
PARAMETRIC STUDY OF THE AEROTHERMODYNAMICS OF A JET ENGINE TEST FACILITY M.S. Thesis
Todd G. Ratner Mar. 1989 128 p
(AD-A208512) Avail: NTIS HC A07/MF A01 CSCL 01/1

A 3-D numerical analysis of the Jet Engine Hush House located at Naval Air Station Jacksonville, Florida was developed using the PHOENICS computer code. The PHOENICS code was used to determine the steady state aerothermal characteristics in the Hush House produced by a Navy F-4 (Phantom 2) J-79-GE-8 gas turbine engine with afterburner. The PHOENICS generated pressure, velocity, and temperature fields of the test cell facility based on the k-epsilon turbulence model are compared with results generated by a model incorporating a temperature dependent kinematic turbulent viscosity. In addition, for the k-epsilon turbulence model, the effect of augmenter tube length on system behavior was investigated. Lessons learned and recommendations in obtaining a converged solution are included to aid in further applications of the PHOENICS code. GRA

N89-27676# General Dynamics Corp., Fort Worth, TX.
SMALL SCALE MODEL TESTS IN SMALL WIND AND WATER TUNNELS AT HIGH INCIDENCE AND PITCH RATES. VOLUME 2: SMALL WIND TUNNEL (ADF) DATA BASE Final Report, Sep. 1985 - Sep. 1988
Atlee M. Cunningham, Jr., Todd Bushlow, John R. Mercer, Tim A. Wilson, and Steve N. Schwoerke Apr. 1989 149 p
(Contract N00014-85-C-0419)
(AD-A208539) Avail: NTIS HC A07/MF A01 CSCL 01/1

Force testing of small-scale models in either a small wind tunnel or a water tunnel was investigated as an inexpensive and quick means to obtain meaningful dynamic force and moment data representative of rapidly maneuvering full-scale aircraft. Force tests of flat-plate semi-span models were conducted in the General Dynamics Aerodynamic Development Facility (ADF) which is a small 14-in. x 14-in. low speed wind tunnel. Oscillatory model motions up to 48 deg (peak to peak) amplitude were tested at frequencies of 1 to 3 Hz. Force tests of flat and three-dimensional full span models were conducted in G.D.'s Hydroflow Facility (HFF) which is a horizontal flow water tunnel with a 24-in. x 24-in. test section. Pitch/pulse model motions were tested for conditions similar to those tested in the ADF. The test velocities were 100 fps in the ADF and 0.8 fps in the HFF which yielded nominal Reynolds numbers of 0.6 million and 0.06 million respectively (based on root chord). This volume presents the data base generated from tests in the ADF. The normal force, pitching moment and rolling moment data are in plotted and tabulated form for the straked wing, 55 deg and 70 deg delta wings and 70 deg/30 deg cranked wing semi-span models. Steady results along with unsteady results for two frequencies are included for the overall incidence range of 0 deg to 80 deg. Geometric data for the models are also given. GRA

N89-27677# Melbourne Univ., Parkville (Australia).
COMPACTED-SNOW RUNWAYS: GUIDELINES FOR THEIR DESIGN AND CONSTRUCTION IN ANTARCTICA
David S. Russell-Head and William F. Budd Apr. 1989 69 p
(AD-A208910; CRREL-SR-89-10) Avail: NTIS HC A04/MF A01 CSCL 01/5

Only small areas near the margins of the ice cap in Antarctica are ice-free, and only a few of these exposed sites are suitable for the construction of conventional runways. Wheeled aircraft have operated successfully on hard sea ice and exposed glacial ice, and skis have been fitted to a wide range of aircraft for use on snow. There has been a resurgence of interest in making snow runways suitable for use by conventional wheeled aircraft. Laboratory and field work has confirmed that low-density surface snow can be compacted in several ways to yield strong, uniform, load-bearing pavement that can support heavy wheeled aircraft. The Soviets have constructed several full-scale runways in Antarctica. This report provides some of the technical background for the design and construction of compacted-snow runways in Antarctica. The technology is not particularly difficult, and it's likely that the next few decades will see substantial changes to Antarctic air transportation as more snow runways are constructed throughout the continent. GRA

N89-27678# Auburn Univ., AL. Dept. of Civil Engineering.
A COMPARISON OF RUTTING BEHAVIOR OF ASPHALT CONCRETE UNDER THE F-4C/G AND F-15C/D AIRCRAFT Final Report, Jul. - Dec. 1987
James G. Murfee Jun. 1988 145 p
(AF Proj. 2104)
(AD-A208911; AFESC/ESL-TR-88-48) Avail: NTIS HC A07/MF A01 CSCL 13/2

The effect of the F-4 and the F-15 aircraft on rutting performance of standard airfield bituminous mixtures during hot weather conditions were compared. The comparisons and conclusions herein were drawn from trafficking new 4 inch asphalt concrete overlying 12 inches of Portland cement concrete. The asphalt concrete was produced from Ac-30 asphalt cement and 100 percent crushed limestone of 3/4 inch maximum size. Pavement surface temperatures ranged from 80 to 122 F during traffic. Both test strips were trafficked simultaneously, back and forth, in a channelized manner 6,000 times by loadcarts that simulated the heaviest designs of F-4 and F-15 aircraft. In one strip, the F-4 loadcart test wheel was loaded to 27.1 kips with cold tire inflation pressures of 265 psi. In the other strip, the F-15 loadcart test wheel was loaded to 30.5 kips with cold tire inflation pressure of 355 psi. It was learned that it takes 5,000 passes of the F-4 to produce a 0.4 inch rut depth in this particular mix, but only 1,000 passes of the F-15. This rut depth of 0.4 inch was far from failure of the layer and was the maximum reached in the F-4 test strip. The dominant mode of rutting was densification with plastic flow of the mixture estimated to have caused about 12 percent of the rutting. GRA

N89-27679# Dayton Univ., OH. Research Inst.
EFFECT OF THREE-DIMENSIONAL OBJECT TYPE AND DENSITY IN SIMULATED LOW-LEVEL FLIGHT Interim Report, Aug. 1986 - Dec. 1988
James A. Kleiss and David C. Hubbard May 1989 24 p
(Contracts F33615-84-C-0066; F33615-87-C-0012)
(AD-A209756; AFHRL-TR-88-66) Avail: NTIS HC A03/MF A01 CSCL 01/2

Altitude control in simulated low-level flight improves significantly when three-dimensional objects are added to simulator visual scenes. However, the limited processing capacity of computer image generators (CIGs) may be used either to increase the density of objects at the expense of individual object detail and realism, or to increase the detail of objects at the expense of object density. The present investigation sought to determine whether object density or object detail is the more important factor in simulated low-level flight. Three types of three-dimensional object were employed: (1) a control condition consisting of inverted tetrahedrons (the simplest possible three-dimensional shape); (2) highly detailed and realistic pine tree; and (3) a mixture of oak trees, pine trees, and bushes. The four levels of object density employed ranged from 3 objects per square mile to 175 objects per square mile. The task required a perceptual judgement to discriminate a change in altitude and a control action to reestablish the initial target altitude. Results indicated that object density had a greater effect on performance. Limited CIG processing capacity may, therefore, be more effectively used by increasing object density rather than individual object detail. GRA

N89-28161*# National Aeronautics and Space Administration. Goddard Space Flight Center, Greenbelt, MD.
WIND-WAVE-CURRENT TANK RESEARCH FACILITY USAGE AND STATUS Abstract Only
L. F. Bliven and S. R. Long *In its* Laboratory for Oceans

1988 p 159-160 (For primary document see N89-28118 22-48)
Avail: NTIS HC A12/MF A01 CSCL 14B

N89-28173*# National Aeronautics and Space Administration. Goddard Space Flight Center, Greenbelt, MD.
THE LABORATORY FOR OCEANS COMPUTING FACILITY Abstract Only
R. Kao *In its* Laboratory for Oceans 1988 p 205-208 (For primary document see N89-28118 22-48)
Avail: NTIS HC A12/MF A01 CSCL 14B

N89-28192*# National Aeronautics and Space Administration. Goddard Space Flight Center, Greenbelt, MD.
ENVIRONMENTAL CALIBRATION CHAMBER OPERATIONS Abstract Only
D. L. Lester *In its* Laboratory for Oceans 1988 p 275-276 (For primary document see N89-28118 22-48)
Avail: NTIS HC A12/MF A01 CSCL 14B

12 ASTRONAUTICS (GENERAL)

For extraterrestrial exploration see *91 Lunar and Planetary Exploration.*

No abstracts in this category.

13 ASTRODYNAMICS

Includes powered and free-flight trajectories; and orbital and launching dynamics.

N89-27680# Instituto de Pesquisas Espaciais, Sao Jose dos Campos (Brazil).
OPTIMIZATION OF MANEUVERS OF A SPIN-STABILIZED SATELLITE, USING MAGNETIC COILS M.S. Thesis [OTIMIZACAO DE MANOBRAS DE SATELITES ESTABILIZADOS POR SPIN, UTILIZANDO BOBINAS MAGNETICAS]
Victor Orlando GamarraRosado Dec. 1988 86 p In PORTUGUESE; ENGLISH summary
(INPE-4778-TDL/350) Avail: NTIS HC A05/MF A01

Open-loop controls are developed which minimize the attitude maneuver time of a spin-stabilized satellite through the optimization of both polarity and time intervals of actuation of a magnetic coil type actuator. The maneuver control torque is generated by the interaction between the magnetic moment of this coil and the geomagnetic field. The proposed maneuver optimization consists of two phases, both with suboptimal approaches: (1) the optimization of the coil's operating intervals, covering every orbital period separately; and (2) the maneuver global optimization, using the intervals obtained in the previous phase as the starting parameters. The theoretical foundations for the formulation of the problem, the modelling of the satellite attitude dynamics, the optimization treatment to obtain the control, and numerical tests to evaluate the behavior of the procedure are presented. Simulations have verified the feasibility of formulating and obtaining the proposed optimal control. Author

N89-27681# Massachusetts Inst. of Tech., Cambridge.
GPS (GLOBAL POSITIONING SYSTEM) ORBIT DETERMINATION: BOOTSTRAPPING TO RESOLVE CARRIER PHASE AMBIGUITY Technical Report, 29 Apr. 1986 - 10 Feb. 1989
R. E. Abbot, C. C. Counselman, III, S. A. Gourevitch, and J. W. Ladd 11 Feb. 1989 12 p
(Contract F19628-86-K-0009)
(AD-A209974; AFGL-TR-89-0039; SR-3) Avail: NTIS HC A03/MF A01 CSCL 22/3

For Global Positioning System (GPS) satellite orbit determination, the most accurate observable available is carrier phase, differenced between observing stations and between satellites to cancel both transmitter and receiver related errors. For maximum accuracy, the integer cycle ambiguities of such observations must be resolved. To perform this ambiguity resolution, a bootstrapping strategy is effective. This strategy requires the tracking stations to have a wide ranging progression of spacings. Then, by conventional integrated Doppler processing of the observations from the most widely spaced stations, the orbits can be determined well enough to permit resolution can reduce the uncertainty of the orbit determination enough to enable ambiguity resolution for more widely spaced stations, which will reduce the orbital uncertainty further, and enable ambiguity resolution for still more widely spaced stations, and so on. This strategy is tested with two different tracking networks. This limited ambiguity resolution reduced both the formal and the actual errors of GPS orbit determinations by a factor of two. In the second twelve stations were arranged in a spiral with geometrically increasing spacings from 10 to 330 km. By bootstrapping, all ambiguities for baselines up to about 100 km long were resolved. The distance was limited by strong ionospheric variability. Still, orbit-determination uncertainty (3 sigma) was reduced to about 1:1,000,000. GRA

N89-27872*# Jet Propulsion Lab., California Inst. of Tech., Pasadena.
ESTIMATION AND FILTERING TECHNIQUES FOR HIGH-ACCURACY GPS APPLICATIONS
S. M. Lichten *In its* The Telecommunications and Data Acquisition Report 15 May 1989 p 1-20 (For primary document see N89-27871 22-32)
Avail: NTIS HC A17/MF A01 CSCL 22A

14 GROUND SUPPORT SYSTEMS AND FACILITIES (SPACE)

Includes launch complexes, research and production facilities; ground support equipment, e.g., mobile transporters; and simulators.

For related information see also *09 Research and Support Facilities (Air).*

N89-27682# Ballistic Research Labs., Aberdeen Proving Ground, MD.
SMALL SCALE TESTING OF A MASS-STABILIZED ELECTROMAGNETIC PROJECTILE
James M. Garner and Alexander E. Zielinski Mar. 1989 31 p
(AD-A206916; BRL-MR-3740) Avail: NTIS HC A03/MF A01 CSCL 19/1

Few electromagnetic (EM) gun projectiles that incorporate aerodynamic aspects have been fired from an EM gun. A practical EM gun projectile, to be used in atmospheric conditions, should consider how efficiently the projectile package is accelerated as well as the flight characteristics. This report details the firing of a full-bore projectile from an electromagnetic gun. Background projectile design criteria, test procedures, and results are discussed. GRA

15 LAUNCH VEHICLES AND SPACE VEHICLES

Includes boosters; operating problems of launch/space vehicle systems; and reusable vehicles.

For related information see also *20 Spacecraft Propulsion and Power.*

N89-27683# Instituto de Pesquisas Espaciais, Sao Jose dos Campos (Brazil). Dept. of Guidance and Control.
LAUNCH WINDOW FOR THE BRAZILIAN DATA COLLECTING SATELLITE
Valdemir Carrara Dec. 1988 8 p Presented at the 39th Congress of the International Astronautical Federation (IAF), Bangalore, India, 8-15 Oct. 1988
(INPE-4773-PRE/1442; IAF-88-328) Avail: NTIS HC A02/MF A01

The launch window studies establish a relatively significant phase in mission analysis of a given space program. The final result of such an analysis is the time interval of the day during some particular days of the year in which the spacecraft launch could be achieved. The main task is to identify and to formulate mathematically, the several constraints concerning the launch that restrain or modify the launch window. An overview is presented of the launch window studies made for the Data Collecting Satellite (DCS) of the Brazilian Space Program (MECB). Author

N89-27684# Army Stategic Defense Command, Huntsville, AL.
HIGH ENDOATMOSPHERIC DEFENSE INTERCEPTOR (HEDI) TECHNOLOGY TESTING PROGRAM ENVIRONMENTAL ASSESSMENT
Dru Barrineau 31 May 1989 231 p
(AD-A210006) Avail: NTIS HC A11/MF A01 CSCL 15/3

The High Endoatmospheric Defense Interceptor (HEDI) is one of the many technologies being considered in the strategic defense initiative (SDI) technology research program and has the potential to support the requirements for the strategic defense system. The purpose of this environmental assessment (EA) is to analyze the environmental consequences of testing activities for the HEDI technology test program in compliance with the National Environmental Policy Act. The HEDI is a technology that would employ ground-based missiles to intercept and destroy hostile submarine-launched ballistic missiles and intercontinental ballistic missiles during that portion of flight that puts the target in the high endoatmosphere (the terminal portion of an attacking missile trajectory). The HEDI vehicle would consist of a two-stage launch vehicle (booster) and kill vehicle with a conventional warhead. The basic thrust of the efforts already accomplished has been to assess the operational utility of HEDI in the context of a complete strategic defense system. GRA

N89-27685# McDonnell-Douglas Astronautics Co., Saint Louis, MO.
MISSILE DATCOM. VOLUME 2: USER'S MANUAL Final Report, Sep. 1981 - Dec. 1985
Steven R. Vukelich, Stan L. Stoy, and Marvin E. Moore Dec. 1988 140 p
(Contract F33615-81-C-3617)
(AD-A210128; AFWAL-TR-86-3091-Vol-2) Avail: NTIS HC A07/MF A01 CSCL 16/4

The computer code is capable of addressing a wide variety of conventional missile designs. For the purposes of this document, a conventional missile is one which is comprised of the following: an axisymmetric or elliptically-shaped body, one to four fin sets located along the body between the nose and base. Each fin set can be comprised of one to eight identical panels attached around the body at a common longitudinal position, and an airbreathing propulsion system. To minimize the quantity of input data required, commonly used values for many inputs are assumed as defaults. However, all program defaults can be over-ridden by the user in order to more accurately model the configuration of interest. GRA

16 SPACE TRANSPORTATION

Includes passenger and cargo space transportation, e.g., shuttle operations; and space rescue techniques.

For related information see also *03 Air Transportation and Safety* and *18 Spacecraft Design, Testing and Performance.* For space suits see *54 Man/System Technology and Life Support.*

N89-27686# Battelle Columbus Labs., OH.
ENVIRONMENTAL EFFECTS OF SPACE SHUTTLE EXHAUST ON MATERIALS Final Report, Apr. 1986 - Aug. 1987
W. H. Abbott Jan. 1989 42 p
(Contract F08635-85-C-0122; AF Proj. 1900)
(AD-A208813; AFESC/ESL-TR-87-71) Avail: NTIS HC A03/MF A01 CSCL 22/5

Studies were conducted at Vandenberg Air Force Base to monitor the indoor environments associated with ground-based electronics at Shuttle Launch Complex 6 (SLC-6). Phase 1, which is summarized in this report, was designed to determine baseline data prior to first launch of the space shuttle from this facility. During the course of the program, additional but similar studies were made at Vandenberg SLC-4 and Sunnyvale Air Force Station. Results at SLC-6 showed very low indoor pollutant levels, particularly with respect to reactive chlorides. Severity levels, as defined by corrosion monitoring, were exceptionally low at all locations, indicating that baseline conditions were very satisfactory for modern electronics. However, humidity and humidity cycling problems associated with HVAC operations were demonstrated at several locations. This raised the possibility for high corrosion rates on electronic components where reactive chloride infiltration occurred. Significantly higher chloride levels were detected at SLC-4 for both prelaunch and post launch environments. This site was considered marginal with respect to both analyzed and potential corrosion phenomena on electronics. GRA

17 SPACE COMM., SPACECRAFT COMM., COMMAND & TRACKING

Includes telemetry; space communications networks; astronavigation and guidance; and radio blackout.

For related information see also *04 Aircraft Communications and Navigation* and *32 Communications and Radar.*

N89-27900*# Jet Propulsion Lab., California Inst. of Tech., Pasadena.
ACCURACY OF TELEMETRY SIGNAL POWER LOSS IN A FILTER AS AN ESTIMATE FOR TELEMETRY DEGRADATION
M. A. Koerner *In its* The Telecommunications and Data Acquisition Report 15 May 1989 p 285-291 (For primary document see N89-27871 22-32)
Avail: NTIS HC A17/MF A01 CSCL 09F

18 SPACECRAFT DESIGN, TESTING AND PERFORMANCE

Includes satellites; space platforms; space stations; spacecraft systems and components such as thermal and environmental controls; and attitude controls.

For life support systems see *54 Man/System Technology and Life Support.* For related information see also *05 Aircraft Design, Testing and Performance, 39 Structural Mechanics,* and *16 Space Transportation.*

N89-27687*# National Aeronautics and Space Administration. Langley Research Center, Hampton, VA.
NASA IN-HOUSE COMMERCIALLY DEVELOPED SPACE FACILITY (CDSF) STUDY REPORT. VOLUME 1: CONCEPT CONFIGURATION DEFINITION
L. J. DeRyder, H. D. Chiger, D. D. DeRyder, K. N. Detweiler, R. L. DuPree, V. P. Gillespie, J. B. Hall, M. L. Heck, D. C. Herrick, and

S. J. Katzberg et al 28 Apr. 1989 738 p
(NASA-TM-101586-Vol-1; NAS 1.15:101586-Vol-1) Avail: NTIS HC A99/MF E03 CSCL 22B

The results of a NASA in-house team effort to develop a concept definition for a Commercially Developed Space Facility (CDSF) are presented. Science mission utilization definition scenarios are documented, the conceptual configuration definition system performance parameters qualified, benchmark operational scenarios developed, space shuttle interface descriptions provided, and development schedule activity was assessed with respect to the establishment of a proposed launch date. Author

N89-27688# Aerospatiale, Cannes La Bocca (France).
[RADIATORS AND HEAT EXCHANGERS FOR SPACE APPLICATIONS]
1988 16 p
(Rept-882-440-115; ETN-89-94508) Avail: NTIS HC A03/MF A01

Radiator conceptual studies and heat exchangers for hybrid radiators are studied for space applications including Hermes, space stations, and orbiting platforms. Preliminary designs are analyzed and the choices made are described. For individual titles, see N89-27689 through N89-27690.

N89-27689# Aerospatiale, Cannes La Bocca (France).
RADIATOR CONCEPTUAL STUDIES FOR THE HERMES SPACEPLANE
M. Amidieu, J. L. Foret, and G. Sibilo *In its* Radiators and Heat Exchangers for Space Applications 1988 7 p (For primary document see N89-27688 22-18)
Avail: NTIS HC A03/MF A01

Major Hermes critical design areas are discussed including the need for a large radiative surface within a comparatively confined volume, a highly variable outer thermal environment, and severe operational conditions such as heavy structural loads in launch phase and high temperature environment at reentry. It is shown that the problems to be solved will widely differ, depending on whether the deployable, retractable, or the jettisonable concepts are selected. ESA

N89-27690# Aerospatiale, Cannes La Bocca (France).
DEVELOPMENT OF HEAT EXCHANGERS FOR HYBRID RADIATORS
M. Amidieu and T. Lafon (Centre National d'Etudes Spatiales, Toulouse, France) *In its* Radiators and Heat Exchangers for Space Applications 1988 8 p (For primary document see N89-27688 22-18)
Avail: NTIS HC A03/MF A01

Preliminary design concepts of heat exchangers for space station or orbiting platform hybrid radiators are discussed. The selection includes one dry contact exchanger in which the fluid circuit and the heat pipes contact each other through their outer shell and one wet contact exchanger, where one of the fluids comes into contact with the other element. After a comparative analysis taking in account performance, manufacturing and operational use, the dry contact exchanger is selected for future development. ESA

N89-27691# Boston Coll., Chestnut Hill, MA. Space Data Analysis Lab.
DATABASE DEVELOPMENT FOR THE DMSP (DEFENSE METEOROLOGICAL SATELLITE PROGRAM) SSIES EXPERIMENT Scientific Report No. 1, 1 Jan. 1987 - 31 Dec. 1988
Dennis E. Delorey, Paul N. Pruneau, and Carolyn M. Parsons 28 Feb. 1989 41 p
(Contract F19628-87-K-0008; AF Proj. 7601)
(AD-A208712; BC-SDAL-89-1; GL-TR-89-006; SR-1) Avail: NTIS HC A03/MF A01 CSCL 04/1

Processed data bases for the Special Sensor for Ions, Electrons and Scintillators (SSIES) experiments flown on-board the F8 and F9 DMSP vehicles have been created over the lifetime of the two satellites. An historical overview of the DMSP project is presented. The data processing system developed for the SSIES experiments, the payloads on-board the spacecraft and the computer software associated with the data processing are described. The formats of the data bases associated with each phase of the processing are described. GRA

N89-27692# Massachusetts Inst. of Tech., Cambridge.
FEASIBILITY OF MILLIMETER-ACCURACY GEODETIC POSITIONING AND VEHICLE TRACKING WITH REPEATER SATELLITES M.S. Thesis
Laureano A. Cangahuala 27 Jan. 1989 77 p
(Contract F19628-86-K-0009)
(AD-A209958; AFGL-TR-89-0031; SR-2) Avail: NTIS HC A05/MF A01 CSCL 08/5

The feasibility of the GeoBeacon system is studied. In this system, low power radio transmitters are placed on vehicles or at other points whose positions are to be monitored. Tropospheric and ionospheric refraction are also monitored. The number of transmitters is practically unlimited. Signals from all transmitters in view are repeated by satellites to a central site where detection, measurement, and data processing take place. To enable precise geodetic positioning, signals would be emitted at multiple frequencies, including relatively low (e.g., 100 MHz) and relatively high (several GHz) frequencies. The lower frequency signals would aid in the acquisition and tracking of the higher frequency signals in order to reduce transmitter power requirements. Power requirements are calculated as functions of frequency from 100 MHz to 50 GHz, considering both natural phenomena and interference from accidental and intentional radio transmissions. An algorithm is developed for the selection of frequencies by which aided tracking of the highest frequency signal can be maintained. This algorithm is based on a stochastic description of the kinematic and ionospheric contributions to the received signal frequencies and phases. Discrete Kalman filter equations are derived for estimating the covariances of phase and frequency estimates. GRA

N89-28231# Aerospatiale, Cannes La Bocca (France).
THE TWO APPROACHES FOR THE THERMAL CONTROL OF THE COLUMBUS RESOURCE MODULE AND POLAR PLATFORM
B. Poulain and S. Aucel *In* ESA, Third European Symposium on Space Thermal Control and Life Support Systems Dec. 1988 p 127-134 Previously announced as N89-23511 (For primary document see N89-28214 22-54)
Copyright Avail: NTIS HC A99/MF A01; ESA Publications Div., ESTEC, Noordwijk, Netherlands, 80 Dutch guilders or 45 US dollars

N89-28232# Erno Raumfahrttechnik G.m.b.H. Bremen (Germany, F.R.).
REDUNDANCY CONCEPT FOR THE COLUMBUS MAN-TENDED FREE-FLYER THERMAL CONTROL SYSTEM
B. Behrens, C. Bunkenborg, W.-D. Ebeling, and U. Laux *In* ESA, Third European Symposium on Space Thermal Control and Life Support Systems Dec. 1988 p 135-140 (For primary document see N89-28214 22-54)
Copyright Avail: NTIS HC A99/MF A01; ESA Publications Div., ESTEC, Noordwijk, Netherlands, 80 Dutch guilders or 45 US dollars

N89-28233# Aeritalia S.p.A., Turin (Italy).
THERMAL CONTROL OF COLUMBUS PRESSURIZED MODULES
S. Dolce, M. Trichilo, and F. Berardi *In* ESA, Third European Symposium on Space Thermal Control and Life Support Systems Dec. 1988 p 141-147 (For primary document see N89-28214 22-54)
Copyright Avail: NTIS HC A99/MF A01; ESA Publications Div., ESTEC, Noordwijk, Netherlands, 80 Dutch guilders or 45 US dollars

N89-28234# Aeritalia S.p.A., Turin (Italy).
DESIGN CONCEPTS FOR HERMES THERMAL CONTROL
C. Ferro, G. Gianfiglio, and L. Costamagna *In* ESA, Third European Symposium on Space Thermal Control and Life Support Systems Dec. 1988 p 149-156 (For primary document see N89-28214 22-54)
Copyright Avail: NTIS HC A99/MF A01; ESA Publications Div., ESTEC, Noordwijk, Netherlands, 80 Dutch guilders or 45 US dollars

N89-28235# Aerospatiale, Cannes La Bocca (France).
RADIATOR CONCEPTUAL STUDIES FOR THE HERMES SPACEPLANE
M. Amidieu, J. L. Foret, and G. Sibilo *In* ESA, Third European Symposium on Space Thermal Control and Life Support Systems Dec. 1988 p 157-164 (For primary document see N89-28214 22-54)
Copyright Avail: NTIS HC A99/MF A01; ESA Publications Div., ESTEC, Noordwijk, Netherlands, 80 Dutch guilders or 45 US dollars

N89-28236# Contraves Corp., Zurich (Switzerland). Space Dept.
THE SPACE-RIGIDISED THERMAL SHIELD FOR THE ESA FAR-INFRARED SPACE TELESCOPE (FIRST)
M. C. Bernasconi and S. Koese *In* ESA, Third European Symposium on Space Thermal Control and Life Support Systems Dec. 1988 p 165-173 (For primary document see N89-28214 22-54)
(Contract ESTEC-6324/85/NL/PB(SC))
Copyright Avail: NTIS HC A99/MF A01; ESA Publications Div., ESTEC, Noordwijk, Netherlands, 80 Dutch guilders or 45 US dollars

N89-28251# Dornier System G.m.b.H., Friedrichshafen (Germany, F.R.).
THERMAL ANALYSIS OF ROSAT IN LOW-EARTH ECLIPSE ORBIT EMPLOYING STEADY-STATE CALCULATIONS
K. Honnen *In* ESA, Third European Symposium on Space Thermal Control and Life Support Systems Dec. 1988 p 267-271 (For primary document see N89-28214 22-54)
Copyright Avail: NTIS HC A99/MF A01; ESA Publications Div., ESTEC, Noordwijk, Netherlands, 80 Dutch guilders or 45 US dollars

N89-28252# MATRA Espace, Toulouse (France).
THERMAL EFFECTS OF PLUME IMPINGEMENT
P. Cheoux-Damas and C. Koeck *In* ESA, Third European Symposium on Space Thermal Control and Life Support Systems Dec. 1988 p 273-279 (For primary document see N89-28214 22-54)
Copyright Avail: NTIS HC A99/MF A01; ESA Publications Div., ESTEC, Noordwijk, Netherlands, 80 Dutch guilders or 45 US dollars

N89-28253# Danish Research Center for Applied Electronics, Hoersholm.
EFFICIENT IMPLEMENTATION OF A DESCRIPTION LANGUAGE FOR THERMAL SIMULATORS
P. Stangerup *In* ESA, Third European Symposium on Space Thermal Control and Life Support Systems Dec. 1988 p 281-287 (For primary document see N89-28214 22-54)
Copyright Avail: NTIS HC A99/MF A01; ESA Publications Div., ESTEC, Noordwijk, Netherlands, 80 Dutch guilders or 45 US dollars

N89-28254# Aeritalia S.p.A., Turin (Italy).
AN ALGORITHM FOR CALCULATING THERMODYNAMIC PROPERTIES OF SIMPLE FLUIDS SUITABLE FOR SPACE THERMAL CONTROL
C. Actis and N. Nervegna (Politecnico di Torino, Italy) *In* ESA, Third European Symposium Space Thermal Control and Life Support Systems Dec. 1988 p 289-295 (For primary document see N89-28214 22-54)
Copyright Avail: NTIS HC A99/MF A01; ESA Publications Div., ESTEC, Noordwijk, Netherlands, 80 Dutch guilders or 45 US dollars

N89-28255# General Electric Co., Princeton, NJ. Astro-Space Div.
DESIGN TRENDS IN COMMUNICATIONS SATELLITE THERMAL SUBSYSTEMS
D. R. Chalmers, P. H. Burkle, and G. W. Case *In* ESA, Third European Symposium on Space Thermal Control and Life Support Systems Dec. 1988 p 299-310 (For primary document see N89-28214 22-54)
Copyright Avail: NTIS HC A99/MF A01; ESA Publications Div., ESTEC, Noordwijk, Netherlands, 80 Dutch guilders or 45 US dollars

N89-28256# Aeritalia S.p.A., Turin (Italy).
THE THERMAL CONTROL OF EUTELSAT-2
E. Sacchi and M. Koedinger (Aerospatiale, Cannes La Bocca, France) *In* ESA, Third European Symposium on Space Thermal Control and Life Support Systems Dec. 1988 p 311-318 (For primary document see N89-28214 22-54)
Copyright Avail: NTIS HC A99/MF A01; ESA Publications Div., ESTEC, Noordwijk, Netherlands, 80 Dutch guilders or 45 US dollars

N89-28257# Aerospatiale, Cannes La Bocca (France).
TELE-X ANTENNA MODULE THERMAL CONTROL
A. Lanteri and B. Henning (Telefonaktiebolaget L. M. Ericsson, Moelndal, Sweden) *In* ESA, Third European Symposium on Space Thermal Control and Life Support Systems Dec. 1988 p 319-326 (For primary document see N89-28214 22-54)
Copyright Avail: NTIS HC A99/MF A01; ESA Publications Div., ESTEC, Noordwijk, Netherlands, 80 Dutch guilders or 45 US dollars

N89-28258# Fokker B.V., Amsterdam (Netherlands). Space and Systems Div.
A THERMAL CONTROL DESIGN FOR THE QUASAT SPACECRAFT
H. Petersen *In* ESA, Third European Symposium on Space Thermal Control and Life Support Systems Dec. 1988 p 327-332 (For primary document see N89-28214 22-54)
Copyright Avail: NTIS HC A99/MF A01; ESA Publications Div., ESTEC, Noordwijk, Netherlands, 80 Dutch guilders or 45 US dollars

N89-28259# Aerospatiale, Cannes La Bocca (France).
THE VEGETATION PAYLOAD OF THE SPOT-4 SPACECRAFT THERMAL DESIGN AND ANALYSIS
S. Zaninotti *In* ESA, Third European Symposium on Space Thermal Control and Life Support Systems Dec. 1988 p 333-337 (For primary document see N89-28214 22-54)
Copyright Avail: NTIS HC A99/MF A01; ESA Publications Div., ESTEC, Noordwijk, Netherlands, 80 Dutch guilders or 45 US dollars

N89-28260# Fokker B.V., Amsterdam (Netherlands). Space and Systems Div.
PREPARING ULYSSES FOR LAUNCH
H. Petersen *In* ESA, Third European Symposium on Space Thermal Control and Life Support Systems Dec. 1988 p 339-344 (For primary document see N89-28214 22-54)
Copyright Avail: NTIS HC A99/MF A01; ESA Publications Div., ESTEC, Noordwijk, Netherlands, 80 Dutch guilders or 45 US dollars

N89-28261# Dornier System G.m.b.H., Friedrichshafen (Germany, F.R.).
THERMAL ASPECTS OF THE ERS-1 SAR ANTENNA DEPLOYMENT
G. Jander, F. Zilly, and R. Bisanz *In* ESA, Third European Symposium on Space Thermal Control and Life Support Systems Dec. 1988 p 345-350 (For primary document see N89-28214

22-54)
Copyright Avail: NTIS HC A99/MF A01; ESA Publications Div., ESTEC, Noordwijk, Netherlands, 80 Dutch guilders or 45 US dollars

N89-28266# European Space Agency. European Space Research and Technology Center, ESTEC, Noordwijk (Netherlands).
CRYOGENIC ACTIVITIES AT ESTEC
C. Jewell *In its* Third European Symposium on Space Thermal Control and Life Support Systems Dec. 1988 p 381-386 (For primary document see N89-28214 22-54)
Copyright Avail: NTIS HC A99/MF A01; ESA Publications Div., ESTEC, Noordwijk, Netherlands, 80 Dutch guilders or 45 US dollars

N89-28272# Centre National d'Etudes Spatiales, Toulouse (France).
TWO YEARS OF IN-ORBIT LIFE OF SPOT-1 HELIOSYNCHRONOUS PLATFORM
I. Alet *In* ESA, Third European Symposium on Space Thermal Control and Life Support Systems Dec. 1988 p 423-427 (For primary document see N89-28214 22-54)
Copyright Avail: NTIS HC A99/MF A01; ESA Publications Div., ESTEC, Noordwijk, Netherlands, 80 Dutch guilders or 45 US dollars

N89-28273# European Space Agency. European Space Research and Technology Center, ESTEC, Noordwijk (Netherlands).
GIOTTO: THE THERMAL RESPONSES TO ITS ENCOUNTER WITH COMET HALLEY
R. J. Wilson *In its* Third European Symposium on Space Thermal Control and Life Support Systems Dec. 1988 p 429-435 (For primary document see N89-28214 22-54)
Copyright Avail: NTIS HC A99/MF A01; ESA Publications Div., ESTEC, Noordwijk, Netherlands, 80 Dutch guilders or 45 US dollars

N89-28274# Fokker B.V., Amsterdam (Netherlands). Space and Systems Div.
THERMAL ASPECTS OF AN EXTENDED MISSION FOR GIOTTO
A. Hartoog *In* ESA, Third European Symposium on Space Thermal Control and Life Support Systems Dec. 1988 p 437-441 (For primary document see N89-28214 22-54)
Copyright Avail: NTIS HC A99/MF A01; ESA Publications Div., ESTEC, Noordwijk, Netherlands, 80 Dutch guilders or 45 US dollars

N89-28275# Dornier System G.m.b.H., Friedrichshafen (Germany, F.R.).
LESSONS LEARNED FROM ROSAT THERMAL BALANCE TEST: A COMBINED SOLAR SIMULATION/INFRARED TEST
A. Braig, T. Schaefer, and P. Pawlowski (Deutsche Forschungs- und Versuchsanstalt fuer Luft- und Raumfahrt, Cologne, Germany, F.R.) *In* ESA, Third European Symposium on Space Thermal Control and Life Support Systems Dec. 1988 p 443-448 (For primary document see N89-28214 22-54)
Copyright Avail: NTIS HC A99/MF A01; ESA Publications Div., ESTEC, Noordwijk, Netherlands, 80 Dutch guilders or 45 US dollars

N89-28276# Societe des Accumulateurs Fixes et de Traction, Romainville (France).
THERMAL CONTROL OF Ni-H2 BATTERY
C. Bulle and A. Dupuy (Aerospatiale, Cannes La Bocca, France) *In* ESA, Third European Symposium on Space Thermal Control and Life Support Systems Dec. 1988 p 449-455 (For primary document see N89-28214 22-54)
Copyright Avail: NTIS HC A99/MF A01; ESA Publications Div., ESTEC, Noordwijk, Netherlands, 80 Dutch guilders or 45 US dollars

N89-28278# European Space Agency. European Space Research and Technology Center, ESTEC, Noordwijk (Netherlands).
THERMAL SOFTWARE DEVELOPMENTS AT ESTEC
C. Stroom *In its* Third European Symposium on Space Thermal Control and Life Support Systems Dec. 1988 p 463-467 (For primary document see N89-28214 22-54)
Copyright Avail: NTIS HC A99/MF A01; ESA Publications Div., ESTEC, Noordwijk, Netherlands, 80 Dutch guilders or 45 US dollars

N89-28279# European Space Agency. European Space Research and Technology Center, ESTEC, Noordwijk (Netherlands).
SOHO THERMAL MODELLING AND ANALYSIS: THE FIRST APPLICATION OF ESATAN TO A COMPLETE SPACECRAFT
R. J. Wilson *In its* Third European Symposium on Space Thermal Control and Life Support Systems Dec. 1988 p 469-474 (For primary document see N89-28214 22-54)
Copyright Avail: NTIS HC A99/MF A01; ESA Publications Div., ESTEC, Noordwijk, Netherlands, 80 Dutch guilders or 45 US dollars

N89-28280# Aerospatiale, Cannes La Bocca (France).
ASSEMBLING THE ISO THERMAL MODEL WITH ESATAN
A. Rocaboy *In* ESA, Third European Symposium on Space Thermal Control and Life Support Systems Dec. 1988 p 475-482 (For primary document see N89-28214 22-54)
Copyright Avail: NTIS HC A99/MF A01; ESA Publications Div., ESTEC, Noordwijk, Netherlands, 80 Dutch guilders or 45 US dollars

N89-28281# GEC Power Engineering Ltd., Whetstone (England).
ESATAN FHTS: A PIPED FLUID NETWORK CAPABILITY
J. R. Turner, T. J. Swift, T. M. Andrews, and A. Lebru (European Space Agency. European Space Research and Technology Center, ESTEC, Noordwijk, Netherlands) *In* ESA, Third European Symposium on Space Thermal Control and Life Support Systems Dec. 1988 p 483-487 (For primary document see N89-28214 22-54)
Copyright Avail: NTIS HC A99/MF A01; ESA Publications Div., ESTEC, Noordwijk, Netherlands, 80 Dutch guilders or 45 US dollars

N89-28282# Aerospatiale, Cannes La Bocca (France). Space and Strategic Systems Div.
THE FLUIDNET DEVELOPMENT AND APPLICATION TO PRELIMINARY SIZING OF FLUID-LOOP SYSTEMS
S. Andre, J. N. Chelotti, J. F. Gory, and T. Lafon (Centre National d'Etudes Spatiales, Toulouse, France) *In* ESA, Third European Symposium on Space Thermal Control and Life Support Systems Dec. 1988 p 489-495 Previously announced as N89-23845 (For primary document see N89-28214 22-54)
Copyright Avail: NTIS HC A99/MF A01; ESA Publications Div., ESTEC, Noordwijk, Netherlands, 80 Dutch guilders or 45 US dollars

N89-28283# Dornier System G.m.b.H., Friedrichshafen (Germany, F.R.).
EVOLUTION OF THERMAL ANALYSIS METHODS TOWARDS INTEGRATED SYSTEM PERFORMANCE SIMULATION
M. Rothmeyer and W. Schwarzott *In* ESA, Third European Symposium on Space Thermal Control and Life Support Systems Dec. 1988 p 497-505 (For primary document see N89-28214 22-54)
Copyright Avail: NTIS HC A99/MF A01; ESA Publications Div., ESTEC, Noordwijk, Netherlands, 80 Dutch guilders or 45 US dollars

N89-28287# Politecnico di Torino (Italy). Dept. di Energetica.
INTERMEDIATE HEAT EXCHANGER FOR A NUCLEAR-POWERED SPACE POWER SYSTEM
G. DelTin, M. Malandrone, N. Nervegna, N. Valle, P. G. Avanzini,

and A. Torresi (Ansaldo S.p.A., Genoa, Italy) *In* ESA, Third European Symposium on Space Thermal Control and Life Support Systems Dec. 1988 p 529-535 (For primary document see N89-28214 22-54)
Copyright Avail: NTIS HC A99/MF A01; ESA Publications Div., ESTEC, Noordwijk, Netherlands, 80 Dutch guilders or 45 US dollars

N89-28288# Fokker B.V., Amsterdam (Netherlands). Space and Systems Div.
A 1-kW CONDENSER FOR A TWO-PHASE HEAT REJECTION SYSTEM
H. vonLonkhuyzen and N. H. Pennings *In* ESA, Third European Symposium on Space Thermal Control and Life Support Systems Dec. 1988 p 537-541 Sponsored by Dornier System GmbH, Friedrichshafen, Fed. Republic of Germany (For primary document see N89-28214 22-54)
Copyright Avail: NTIS HC A99/MF A01; ESA Publications Div., ESTEC, Noordwijk, Netherlands, 80 Dutch guilders or 45 US dollars

N89-28289# Tokyo Univ. (Japan).
A VERY LOW REFLECTANCE DIFFUSE SURFACE FOR THERMAL DESIGN OF SPACECRAFT
A. Ohnishi, K. Kaneko, and T. Hayashi *In* ESA, Third European Symposium on Space Thermal Control and Life Support Systems Dec. 1988 p 543-545 (For primary document see N89-28214 22-54)
Copyright Avail: NTIS HC A99/MF A01; ESA Publications Div., ESTEC, Noordwijk, Netherlands, 80 Dutch guilders or 45 US dollars

N89-28290# Ansaldo S.p.A., Genoa (Italy).
A MAGNETICALLY-DRIVEN DROPLET RADIATOR CONCEPT
P. G. Avanzini, S. Valentini, and G. Tuninetti *In* ESA, Third European Symposium on Space Thermal Control and Life Support Systems Dec. 1988 p 547-552 (For primary document see N89-28214 22-54)
Copyright Avail: NTIS HC A99/MF A01; ESA Publications Div., ESTEC, Noordwijk, Netherlands, 80 Dutch guilders or 45 US dollars

N89-28291# Messerschmitt-Boelkow-Blohm G.m.b.H., Munich (Germany, F.R.). Space Communications and Propulsions Systems Div.
THERMAL ANALYSIS OF ADVANCED HEAT PROTECTION SYSTEMS
K. Keller and H. Grallert *In* ESA, Third European Symposium on Space Thermal Control and Life Support Systems Dec. 1988 p 555-560 (For primary document see N89-28214 22-54)
Copyright Avail: NTIS HC A99/MF A01; ESA Publications Div., ESTEC, Noordwijk, Netherlands, 80 Dutch guilders or 45 US dollars

N89-28292# Messerschmitt-Boelkow-Blohm G.m.b.H., Bremen (Germany, F.R.).
THERMAL PROTECTION CONCEPTS OF RECOVERABLE CAPSULES
H. Loeser *In* ESA, Third European Symposium on Space Thermal Control and Life Support Systems Dec. 1988 p 561-566 (For primary document see N89-28214 22-54)
Copyright Avail: NTIS HC A99/MF A01; ESA Publications Div., ESTEC, Noordwijk, Netherlands, 80 Dutch guilders or 45 US dollars

N89-28293# Aeritalia S.p.A., Turin (Italy).
CYROGENIC FLUID SINK DEVICE FOR THERMAL CONTROL OF A SPACEPLANE DURING ASCENT AND RE-ENTRY PHASES
D. Nikanpour and M. Petruzziello *In* ESA, Third European Symposium on Space Thermal Control and Life Support Systems Dec. 1988 p 567-572 (For primary document see N89-28214 22-54)
Copyright Avail: NTIS HC A99/MF A01; ESA Publications Div., ESTEC, Noordwijk, Netherlands, 80 Dutch guilders or 45 US dollars

N89-28294# Societe Anonyme Belge de Constructions Aeronautiques, Brussels.
QUALIFICATION PROGRAM ON STAINLESS STEEL A95 HEATPIPE FOR SPACE APPLICATION
R. S. Bhatti and S. VanOost *In* ESA, Third European Symposium on Space Thermal Control and Life Support Systems Dec. 1988 p 575-582 (For primary document see N89-28214 22-54)
Copyright Avail: NTIS HC A99/MF A01; ESA Publications Div., ESTEC, Noordwijk, Netherlands, 80 Dutch guilders or 45 US dollars

N89-28295# Erno Raumfahrttechnik G.m.b.H. Bremen (Germany, F.R.).
THEORETICAL AND EXPERIMENTAL INVESTIGATIONS ON HEAT EXCHANGERS FOR COLUMBUS HYBRID RADIATORS
W.-D. Ebeling and R. Meyer *In* ESA, Third European Symposium on Space Thermal Control and Life Support Systems Dec. 1988 p 583-590 (For primary document see N89-28214 22-54)
Copyright Avail: NTIS HC A99/MF A01; ESA Publications Div., ESTEC, Noordwijk, Netherlands, 80 Dutch guilders or 45 US dollars

N89-28296# Messerschmitt-Boelkow-Blohm G.m.b.H., Bremen (Germany, F.R.).
DEVELOPMENT OF THE HERMES FLEXIBLE EXTERNAL INSULATION
J. Antonenko, W.-D. Ebeling, H.-G Reimerdes, and J. Reininger *In* ESA, Third European Symposium on Space Thermal Control and Life Support Systems Dec. 1988 p 591-597 (For primary document see N89-28214 22-54)
Copyright Avail: NTIS HC A99/MF A01; ESA Publications Div., ESTEC, Noordwijk, Netherlands, 80 Dutch guilders or 45 US dollars

N89-28297# Erno Raumfahrttechnik G.m.b.H. Bremen (Germany, F.R.).
IN-ORBIT DEGRADATION OF THERMO-OPTICAL PROPERTIES ON MARECS GEO-SATELLITE
H.-G. Konzok, A. Soeffker, D. Stuempel, and K. Derbyshire (European Space Agency. European Space Research and Technology Center, ESTEC, Noordwijk, Netherlands) *In* ESA, Third European Symposium on Space Thermal Control and Life Support Systems Dec. 1988 p 599-604 (For primary document see N89-28214 22-54)
(Contract ESTEC-5456/83/NL/DG)
Copyright Avail: NTIS HC A99/MF A01; ESA Publications Div., ESTEC, Noordwijk, Netherlands, 80 Dutch guilders or 45 US dollars

19 SPACECRAFT INSTRUMENTATION

For related information see also *06 Aircraft Instrumentation* and *35 Instrumentation and Photography.*

No abstracts in this category.

20 SPACECRAFT PROPULSION AND POWER

Includes main propulsion systems and components, e.g., rocket engines; and spacecraft auxilliary power sources.

For related information see also *07 Aircraft Propulsion and Power, 28 Propellants and Fuels, 44 Energy Production and Conversion,* and *15 Launch Vehicles and Space Vehicles.*

N89-27693*# Lockheed Missiles and Space Co., Huntsville, AL. Engineering Center.
SPACE SHUTTLE MAIN ENGINE STRUCTURAL ANALYSIS AND DATA REDUCTION/EVALUATION. VOLUME 1: AFT SKIRT ANALYSIS Final Report
David M. Berry and Mark Stansberry Apr. 1989 85 p Original contains color illustrations
(Contract NAS8-37282)
(NASA-CR-183663; NAS 1.26:183663;
LMSC-HEC-TR-F268584-Vol-1) Avail: NTIS HC A05/MF A01 CSCL 21H

Using the ANSYS finite element program, a global model of the aft skirt and a detailed nonlinear model of the failure region was made. The analysis confirmed the area of failure in both STA-2B and STA-3 tests as the forging heat affected zone (HAZ) at the aft ring centerline. The highest hoop strain in the HAZ occurs in this area. However, the analysis does not predict failure as defined by ultimate elongation of the material equal to 3.5 percent total strain. The analysis correlates well with the strain gage data from both the Wyle influence test of the original design aft sjirt and the STA-3 test of the redesigned aft skirt. it is suggested that the sensitivity of the failure area material strength and stress/strain state to material properties and therefore to small manufacturing or processing variables is the most likely cause of failure below the expected material ultimate properties. Author

N89-27694*# Lockheed Missiles and Space Co., Huntsville, AL. Engineering Center.
SPACE SHUTTLE MAIN ENGINE STRUCTURAL ANALYSIS AND DATA REDUCTION/EVALUATION. VOLUME 3A: HIGH PRESSURE OXIDIZER TURBO-PUMP PREBURNER PUMP HOUSING STRESS ANALYSIS REPORT Final Report
Robert V. Shannon, Jr. Apr. 1989 54 p Original contains color illustrations
(Contract NAS8-37282)
(NASA-CR-183665; NAS 1.26:183665;
LMSC-HEC-TR-F268584-Vol-3A) Avail: NTIS HC A04/MF A01 CSCL 21H

The model generation and structural analysis performed for the High Pressure Oxidizer Turbopump (HPOTP) preburner pump volute housing located on the main pump end of the HPOTP in the space shuttle main engine are summarized. An ANSYS finite element model of the volute housing was built and executed. A static structural analysis was performed on the Engineering Analysis and Data System (EADS) Cray-XMP supercomputer Author

N89-27695*# Lockheed Missiles and Space Co., Huntsville, AL. Engineering Center.
SPACE SHUTTLE MAIN ENGINE STRUCTURAL ANALYSIS AND DATA REDUCTION/EVALUATION. VOLUME 3B: HIGH PRESSURE FUEL TURBO-PUMP PREBURNER PUMP BEARING ASSEMBLY ANALYSIS Final Report
Gloria B. Power and Rebeca S. Violett Apr. 1989 41 p
(Contract NAS8-37282)
(NASA-CR-183666; NAS 1.26:183666;
LMSC-HEC-TR-F268584-Vol-3B) Avail: NTIS HC A03/MF A01 CSCL 21H

The analysis performed on the High Pressure Oxidizer Turbopump (HPOTP) preburner pump bearing assembly located on the Space Shuttle Main Engine (SSME) is summarized. An ANSYS finite element model for the inlet assembly was built and executed. Thermal and static analyses were performed. Author

N89-27696*# Lockheed Missiles and Space Co., Huntsville, AL. Engineering Center.
SPACE SHUTTLE MAIN ENGINE STRUCTURAL ANALYSIS AND DATA REDUCTION/EVALUATION. VOLUME 4: HIGH PRESSURE FUEL TURBO-PUMP INLET HOUSING ANALYSIS Final Report
Kirby V. Pool Apr. 1989 100 p Original contains color illustrations
(Contract NAS8-37282)
(NASA-CR-183667; NAS 1.26:183667;
LMSC-HEC-TR-F268584-Vol-4) Avail: NTIS HC A05/MF A01 CSCL 21H

The analysis performed on the Space Shuttle Main Engine (SSME) High Pressure Fuel Turbopump (HPFTP) inlet housings is summarized. Three DIAL finite element models were build to aid in assessing the structural life of the welds and fillets at the vanes. Complete results are given. Author

N89-27697*# Lockheed Missiles and Space Co., Huntsville, AL. Engineering Center.
SPACE SHUTTLE MAIN ENGINE STRUCTURAL ANALYSIS AND DATA REDUCTION/EVALUATION. VOLUME 5: MAIN INJECTOR LOX INLET ANALYSIS Final Report
Rebeca S. Violett Apr. 1989 32 p Original contains color illustrations
(Contract NAS8-37282)
(NASA-CR-183668; NAS 1.26:183668;
LMSC-HEC-TR-F268584-Vol-5) Avail: NTIS HC A03/MF A01 CSCL 21H

The analysis performed on the Main Injector LOX Inlet Assembly located on the Space Shuttle Main Engine is summarized. An ANSYS finite element model of the inlet assemably was built and executed. Static stress analysis was also performed. Author

N89-27698*# Morton Thiokol, Brigham City, UT. Aerospace Group.
FLIGHT SET 360L001 (STS-26) INSULATION COMPONENT. VOLUME 3: FINAL RELEASE Final Report
K. Albrechtsen and J. Passman Apr. 1989 216 p
(Contract NAS8-30490)
(NASA-CR-183674; NAS 1.26:183674; TWR-17272-Vol-3-Rev-A;
ECS-SS-0956) Avail: NTIS HC A10/MF A01 CSCL 21H

The postfire condition of the external and internal insulation for STS-26 is documented and the thermal safety factors of the RSRM-1A and RSRM-1B internal insulation are evaluated. The Insulation Component Program Team assessment of the observation is discussed. Author

N89-27699# Naval Postgraduate School, Monterey, CA.
DEFINITION STUDY AND MODEL FOR A TETHERED SOUNDING ROCKET M.S. Thesis
Sang I. Yoon Dec. 1988 109 p
(AD-A207367) Avail: NTIS HC A06/MF A01 CSCL 22/2

The HOCAT experiment is a sounding rocket payload to measure the coupling of large currents (up to 1 A) from a satellite into the ambient plasma, and the return path through the plasma. The devices used to establish electrical contact with the plasma are hollow cathode plasma sources, using Xenon propellent. Two satellite sections are connected by a 100-m cable, which are used to bias the two satellites with respect to each other. The current through the connecting cable are monitored along with the particle fluxes to the satellites. A fiber optic technique is used to measure the return current flowing through the ambient plasma. Electric fields, densities, and plasma waves are monitored with floating probes. GRA

N89-27700*# Sverdrup Technology, Inc., Cleveland, OH.
ANTIPROTON POWERED PROPULSION WITH MAGNETICALLY CONFINED PLASMA ENGINES Final Report
Michael R. LaPointe Aug. 1989 26 p Presented at the 25th Joint Propulsion Conference, Monterey, CA, 10-12 Jul. 1989; cosponsored by the AIAA, ASME, SAE, and ASEE

(Contract NAS3-25266)
(NASA-CR-185131; E-5025; NAS 1.26:185131; AIAA-89-2334)
Avail: NTIS HC A03/MF A01 CSCL 21H

Matter-antimatter annihilation releases more energy per unit mass than any other method of energy production, making it an attractive energy source for spacecraft propulsion. In the magnetically confined plasma engine, antiproton beams are injected axially into a pulsed magnetic mirror system, where they annihilate with an initially neutral hydrogen gas. The resulting charged annihilation products transfer energy to the hydrogen propellant, which is then exhausted through one end of the pulsed mirror system to provide thrust. The calculated energy transfer efficiencies for a low number density (10(14)/cu cm) hydrogen propellant are insufficient to warrant operating the engine in this mode. Efficiencies are improved using moderate propellant number densities (10(16)/cu cm), but the energy transferred to the plasma in a realistic magnetic mirror system is generally limited to less than 2 percent of the initial proton-antiproton annihilation energy. The energy transfer efficiencies are highest for high number density (10(18)/cu cm) propellants, but plasma temperatures are reduced by excessive radiation losses. Low to moderate thrust over a wide range of specific impulse can be generated with moderate propellant number densities, while higher thrust but lower specific impulse may be generated using high propellant number densities. Significant mass will be required to shield the superconducting magnet coils from the high energy gamma radiation emitted by neutral pion decay. The mass of such a radiation shield may dominate the total engine mass, and could severely diminish the performance of antiproton powered engines which utilize magnetic confinement. The problem is compounded in the antiproton powered plasma engine, where lower energy plasma bremsstrahlung radiation may cause shield surface ablation and degradation. Author

N89-27701*# National Aeronautics and Space Administration. Lewis Research Center, Cleveland, OH.

PERFORMANCE OF A 100 kW CLASS APPLIED FIELD MPD THRUSTER

Maris A. Mantenieks, James S. Sovey, Roger M. Myers, Thomas W. Haag, Paul Raitano, and James E. Parkes (Sverdrup Technology, Inc., Cleveland, OH.) Jul. 1989 18 p Presented at the 25th Joint Propulsion Conference, Monterey, CA, 10-12 Jul. 1989; sponsored in part by AIAA, ASME, SAE, and ASEE
(NASA-TM-102312; E-5006; NAS 1.15:102312; AIAA-89-2710)
Avail: NTIS HC A03/MF A01 CSCL 21H

Performance of a 100 kW, applied field magnetoplasmadynamic (MPD) thruster was evaluated and sensitivities of discharge characteristics to arc current, mass flow rate, and applied magnetic field were investigated. Thermal efficiencies as high as 60 percent, thrust efficiencies up to 21 percent, and specific impulses of up to 1150 s were attained with argon propellant. Thrust levels up to 2.5 N were directly measured with an inverted pendulum thrust stand at discharge input powers up to 57 kW. It was observed that thrust increased monotonically with the product of arc current and magnet current. Author

N89-27702*# National Aeronautics and Space Administration. Lewis Research Center, Cleveland, OH.

DEVELOPMENT AND REFINEMENT OF TEST BED SIMULATIONS

Narayan V. Dravid, Dean R. Miller, Alex G. Patterson, and Frank J. Gombos (Rockwell International Corp., Canoga Park, CA.) Aug. 1989 8 p Presented at the 24th Intersociety Energy Conversion Engineering Conference, Washington, DC, 6-11 Aug. 1989; sponsored in part by IEEE, AIAA, ANS, ASME, SAE, ACS, and AIChE
(NASA-TM-102335; E-5043; NAS 1.15:102335) Avail: NTIS HC A02/MF A01 CSCL 14B

Lewis Research Center of NASA, with support from Rocketdyne, was engaged in non-real time computer simulation effort for the Space Station Freedom Electric Power System (EPS) EASY5, a simulation package, is used as the primary tool for this activity. Early in the design of the EPS, two test beds were set up at Lewis. The Integrated Test Bed (ITB), that combines and upgrades these test beds, is in the planning stage. The test beds are designed to functionally represent many of the components of the EPS and their interconnections. The simulation effort is primarily directed towards these test beds. Model verification is performed using test bed data. Author

N89-27703*# National Aeronautics and Space Administration. Lewis Research Center, Cleveland, OH.

STRUCTURAL AND THERMAL RESPONSE OF 30 cm DIAMETER ION THRUSTER OPTICS

G. S. MacRae, R. J. Zavesky, and S. T. Gooder Jul. 1989 29 p Presented at the 25th Joint Propulsion Conference, Monterey, CA, 10-12 Jul. 1989; sponsored in part by AIAA, ASME, SAE, and ASEE
(NASA-TM-102124; E-4904; NAS 1.15:102124; AIAA-89-2719)
Avail: NTIS HC A03/MF A01 CSCL 21C

Tabular and graphical data are presented which are intended for use in calibrating and validating structural and thermal models of ion thruster optics. A 30 cm diameter, two electrode, mercury ion thruster was operated using two different electrode assembly designs. With no beam extraction, the transient and steady state temperature profiles and center electrode gaps were measured for three discharge powers. The data showed that the electrode mount design had little effect on the temperatures, but significantly impacted the motion of the electrode center. Equilibrium electrode gaps increased with one design and decreased with the other. Equilibrium displacements in excess of 0.5 mm and gap changes of 0.08 mm were measured at 450 W discharge power. Variations in equilibrium gaps were also found among assemblies of the same design. The presented data illustrate the necessity for high fidelity ion optics models and development of experimental techniques to allow their validation. Author

N89-27704*# National Aeronautics and Space Administration. Lewis Research Center, Cleveland, OH.

TOWARD AN ELECTRICAL POWER UTILITY FOR SPACE EXPLORATION

Robert W. Bercaw 1989 6 p Prepared for presentation at the European Space Power Conference, Madrid, Spain, 2-6 Oct. 1989; sponsored in part by ESA
(NASA-TM-102347; E-5055; NAS 1.15:102347) Avail: NTIS HC A02/MF A01 CSCL 10B

Plans for space exploration depend on today's technology programs addressing the novel requirements of space-based enterprise. The requirements for electrical power will be formidable: megawatts in magnitude, reliability for multi-year missions and the flexibility to adapt to needs unanticipated at design time. The reasons for considering the power management and distribution in the various systems from a total mission perspective, rather than simply extrapolating current spacecraft design practice, are discussed. A utility approach to electric power being developed at the Lewis Research Center is described. It integrates requirements from a broad selection of current development programs with studies in which both space and terrestrial technologies are conceptually applied to exploration mission scenarios. Author

N89-27705*# National Aeronautics and Space Administration. Lewis Research Center, Cleveland, OH.

NASA ADVANCED SPACE PHOTOVOLTAIC TECHNOLOGY-STATUS, POTENTIAL AND FUTURE MISSION APPLICATIONS

Dennis J. Flood, Michael Piszczor, Jr., Paul M. Stella, and Gary L. Bennett (National Aeronautics and Space Administration, Washington, DC.) 1989 8 p Prepared for presentation at the European Space Power Conference, Madrid, Spain, 2-6 Oct. 1989; sponsored in part by ESA
(NASA-TM-102093; E-4856; NAS 1.15:102093) Avail: NTIS HC A02/MF A01 CSCL 10B

The NASA program in space photovoltaic research and development encompasses a wide range of emerging options for future space power systems, and includes both cell and array technology development. The long range goals are to develop

technology capable of achieving 300 W/kg for planar arrays, and 300 W/sq m for concentrator arrays. InP and GaAs planar and concentrator cell technologies are under investigation for their potential high efficiency and good radiation resistance. The Advanced Photovoltaic Solar Array (APSA) program is a near term effort aimed at demonstrating 130 W/kg beginning of life specific power using thin (62 micrometer) silicon cells. It is intended to be technology transparent to future high efficiency cells and provides the baseline for development of the 300 W/kg array. Author

N89-27706*# National Aeronautics and Space Administration. Lewis Research Center, Cleveland, OH.
INVESTIGATION OF A LIQUID-FED WATER RESISTOJET PLUME
D. H. Manzella (Sverdrup Technology, Inc., Cleveland, OH.) and L. M. Carney Jul. 1989 10 p Presented at the 25th Joint Propulsion Conference, Monterey, CA, 10-12 Jul. 1989; sponsored in part by AIAA, ASME, SAE, and ASEE
(NASA-TM-102310; E-5005; NAS 1.15:102310; AIAA-89-2840)
Avail: NTIS HC A02/MF A01 CSCL 21H

Measurements of mass flux and flow angle were taken throughout the forward flow region of the exhaust of a liquid-fed water resistojet using a quartz crystal microbalance (QCM). The resistojet operated at a mass flow rate of 0.1 g/s with a power input of 330 Watts. Measured values were compared to theoretical predictions obtained by employing a source flow approximation. Excellent agreement between predicted and measured mass flux values was attained; however, this agreement was highly dependent on knowledge of nozzle flow conditions. Measurements of the temperature at which the exhaust condensed on the QCM were obtained as a function of incident mass flux. Author

N89-27707# Deutsche Gesellschaft fuer Luft- und Raumfahrt, Bonn (Germany, F.R.).
DGLR/AIAA/JSASS 20TH INTERNATIONAL ELECTRIC PROPULSION CONFERENCE: PROCEEDINGS
1988 741 p Conference held in Garmisch-Partenkirchen, Fed. Republic of Germany, 3-6 Oct. 1988 Sponsored by the BMFT, Bonn, Fed. Republic of Germany Original contains color illustrations
(DGLR-Paper-88-02; ISBN-3-92-2010-40-7; ETN-89-95006) Avail: NTIS HC A99/MF E03

Topics discussed at this conference inlcude: magnetoplasmadynamic thrusters; power sources and interactions; field emission electric propulsion; auxiliary propulsion; power conditioning and control; ion thrusters; missions; electrode processes; plasma and plume phenomena; microwave devices; arc jet engines; thruster-spacecraft interactions; and nonpropulsive applications. For individual titles, see N89-27708 through N89-27792.

N89-27708# European Space Agency. European Space Research and Technology Center, ESTEC, Noordwijk (Netherlands). Technical Directorate.
THE ESA POLICY AND PROGRAM FOR THE DEVELOPMENT OF ELECTRIC PROPULSION
W. Berry, C. Bartoli, and A. Trippi *In* DGLR, DGLR/AIAA/JSASS 20th International Electric Propulsion Conference: Proceedings 1988 p 5-16 (For primary document see N89-27707 22-20)
Avail: NTIS HC A99/MF E03

The benefits offered by electric propulsion are analyzed for the four applications of interest to ESA: north-south stationkeeping of geostationary satellites; orbit maneuvering and maintenance of large low-orbiting spacecraft (like the Columbus Man-Tended Free Flyer); primary propulsion for interplanetary missions; and fine pointing, attitude and orbit control of scientific satellites. Developments in electric propulsion include: testing of a multipropellant resistojet for a manned space station; testing of a 15 kW arcjet for orbit maneuvers and maintenance of low orbiting spacecraft; final preparation of the RITA ion engine experiment on the EURECA carrier; preliminary studies of a pre-operational ion propulsion system to be flown on the Agency's SAT-2 satellite in 1993; preparation of a European primary ion propulsion system for interplanetary missions; and further development of the Field Emission Electric Propulsion system for fine attitude and orbit control of scientific spacecraft. ESA

N89-27709# Tokyo Univ., Sagamihara (Japan). Inst. of Space and Astronautical Science.
ELECTRIC PROPULSION PROJECTS AND RESEARCH IN JAPAN
Kyoichi Kuriki and Yoshihiro Nakamura (National Aerospace Lab., Tokyo, Japan) *In* DGLR, DGLR/AIAA/JSASS 20th International Electric Propulsion Conference: Proceedings 1988 p 26-36 (For primary document see N89-27707 22-20)
Avail: NTIS HC A99/MF E03

Electric propulsion activities in Japan from both project and research oriented view points are reviewed. The flight opportunities are Space Flyer Unit Mission 1 for an MPD thruster system and Engineering Test Satellite 6 for an ion engine system. The systems in these missions look forward to near future applications. As for far future applications such as lunar ferry, Mars lander, and deep space explorer, various types of electric propulsion could be candidates. It is essential in designing electric propulsion systems for these missions to take into account the feasible types of power and propellant resources. In other words, the electric propulsion system should be compatible with the future space infrastructures. From this view point the various types of electric propulsion, which may look diversified, are encouraged to be studied as potential options in Japanese research activities. ESA

N89-27710# Academy of Sciences (USSR), Moscow.
RECENT PROGRESS IN THE USSR ELECTRIC PROPULSION
V. V. Zhurin, A. S. Koroteev, A. A. Porotnikov, and B. B. Rodrevich *In* DGLR, DGLR/AIAA/JSASS 20th International Electric Propulsion Conference: Proceedings 1988 p 37-47 (For primary document see N89-27707 22-20)
Avail: NTIS HC A99/MF E03

Stationary plasma thrusters (SPT) and more recent developments are reviewed. Together with SPT in the combined plasma jet unit of space satellites and similar space apparatuses, there is significant interest in electrothermal or thermocatalytic thrusters. Promising results are achieved with magnetoplasmadynamic (MPD) thrusters, which have flow velocities an order of magnitude higher than in plasmatrons and particles concentrations an order higher than in other stationary accelerators. They are used widely in geophysical investigations, on satellites, for ballistic experiments, and are indispensable in the technology of implantation of deposited material in a lining. In these areas the pulsed plasma thrusters which are actually MPD thrusters, can be considered as equal partners. The MPD thrusters could be used for the international flight project to the Mars. ESA

N89-27711# Air Force Astronautics Lab., Edwards AFB, CA.
INTERESTS IN ELECTRIC PROPULSION
Wayne M. Schmidt and John C. Andrews *In* DGLR, DGLR/AIAA/JSASS 20th International Electric Propulsion Conference: Proceedings 1988 p 48-50 (For primary document see N89-27707 22-20)
Avail: NTIS HC A99/MF E03

It is argued that a wide range of orbit transfer and maintenance missions can be greatly improved in terms of deliverable payloads and on-orbit life times through the use of electric propulsion technologies. The trend toward more massive payloads and increasing on-board power availability make electric propulsion competitive with chemical systems. For this reason, the Air Force Astronautics Laboratory (AFAL) is developing 30 kilowatt class arcjets and conducting research on magnetoplasmadynamic (MPD) thrusters. The AFAL's first electric propulsion priority is a space test of a 30 kilowatt class low impedance ammonia arcjet. The AFAL is also developing a high-impedance arcjet which shows potential for both higher efficiencies and longer life times. ESA

N89-27712# International Telecommunications Satellite Organization, Washington, DC.
ELECTRIC PROPULSION: IMPLEMENTATION ISSUES

Rolland Schreib *In* DGLR, DGLR/AIAA/JSASS 20th International Electric Propulsion Conference: Proceedings 1988 p 51-57 (For primary document see N89-27707 22-20)
Avail: NTIS HC A99/MF E03

An overview is given of the process and issues associated with implementing the various electric propulsion (EP) technologies on spacecraft for a range of missions from those currently operational to those high-energy exploratory missions coming into view. It is suggested that a clear, concise, and convincing package of information on EP mission utility, system benefits, spacecraft compatibility, and subsystem readiness must be made available to mission planners and decision makers if the process of selecting EP for advanced missions is to be expedited. Because of the size and power requirements of EP systems for these missions, coordinated leadership and substantial developmental support will be needed in the immediate future. ESA

N89-27713# European Space Agency. European Space Research and Technology Center, ESTEC, Noordwijk (Netherlands). Communications Dept.
THE ROLE OF ELECTRIC PROPULSION IN EXTENDING THE ECONOMIC LIFE-CYCLE OF COMMERCIAL EUROPEAN TELECOMMUNICATION SATELLITES
H. G. Lechte and L. C. vanHoltz *In* DGLR, DGLR/AIAA/JSASS 20th International Electric Propulsion Conference: Proceedings 1988 p 58-61 (For primary document see N89-27707 22-20)
Avail: NTIS HC A99/MF E03

Electric propulsion can play a dominant role in alleviating mass/volume problems in the area of classical unified propulsion, and reducing disturbances to new, sensitive, high pointing accuracy payloads such as laser terminals. It may also contribute to the reduction of spacecraft charging, and hence to elimination of solar array problems and electrostatic discharge phenomena on spacecraft. In Europe, the vehicle to pursue new technologies (payload and platform) is ESA's Payload and Spacecraft Development and Experimentation Program, in which SAT-2 is the dedicated satellite for in-orbit qualification, planned for flight mid-1993. Although communication payload development is the major objective of this program, ion propulsion is envisaged to perform a prominent role in achieving the long term goal of an efficient European communication infrastructure. ESA

N89-27714# Pisa Univ. (Italy). Dipartimento di Ingegneria Aerospaziale.
ELECTRIC PROPULSION FOR LOW EARTH ORBIT APPLICATIONS
M. Andrenucci and A. Trippi (European Space Agency. European Space Research and Technology Center, ESTEC, Noordwijk, Netherlands) *In* DGLR, DGLR/AIAA/JSASS 20th International Electric Propulsion Conference: Proceedings 1988 p 62-68 (For primary document see N89-27707 22-20)
Avail: NTIS HC A99/MF E03

Opportunities for the application of electric propulsion systems arising from the anticipated expansion of low-Earth-orbit activities are reviewed. Inherent characteristics and performance capability of electric propulsion systems are assessed. It is shown that the various thruster concepts should not be regarded as alternative options to be traded off, but rather as a set of answers to future propulsion needs, complementary in nature and graduated in time. Potential applications related to near-Earth activities include orbit maintenance and drag cancellation (representing the most important application in low Earth orbit); and orbit raising to polar orbit and back. A specific example is discussed concerning a man-tended-free-flyer type microgravity laboratory. This example encompasses several propulsion aspects which are common to a variety of near-Earth missions and can provide insight into the applications of different electric propulsion systems in low Earth orbit. ESA

N89-27715# European Space Agency. European Space Research and Technology Center, ESTEC, Noordwijk (Netherlands).
THE ROSETTA/CNSR MISSION: A POSSIBLE APPLICATION OF ELECTRIC PROPULSION TO INTERPLANETARY MISSIONS
A. Atzei *In* DGLR, DGLR/AIAA/JSASS 20th International Electric Propulsion Conference: Proceedings 1988 p 69-74 (For primary document see N89-27707 22-20)
Avail: NTIS HC A99/MF E03

It is shown that for the ROSETTA comet nucleus sample return mission, the most flexible mission design is the so-called hybrid, which utilizes electric propulsion for the Earth to comet cruise and chemical propulsion for the Earth return phase. This type of mission, which would also be compatible with an Ariane-5 launch, features an electric propulsion stage based on 6 RIT-35 thrusters, 32 kW of power and provides a velocity increment of 8.5 km/s. This electric stage is jettisoned at comet encounter after perihelion. The proposed baseline mission is based on a Titan-Centaur G launcher and a stack of three spacecraft, functioning respectively as cruiser, lander, and aerocapsule; the total launch mass is 4000 kg, including 2300 kg of biliquid propellant stored in the cruise spacecraft. The Earth-comet cruise features a 2 yr Earth-gravity-assist trajectory and necessitates a supplementary velocity increment of 1800 m/s by the spacecraft chemical propulsion system. The resulting trajectory will encounter the comet Churymov-Gerasimenko at aphelion, at 5.5 AU, 4.5 yr after launch. The spacecraft will land on a preselected site, where sampling will be carried out by drilling/scooping mechanisms. The cruiser and the aerocapsule will then be injected into an Earth return trajectory (Delta-V = 900 m/s), leaving the lander spacecraft behind on the comet. The aerocapsule will be recovered on Earth following an autonomous parachute-assisted reentry 3.5 yr after comet departure and 8 yr years after launch, in the year 2009. ESA

N89-27716# Snia Viscosa, Colleferro (Italy).
PLASMA PROPULSION ACTIVITES AT SNIA BPD
G. Baiocchi, G. Cruciani, and E. Tosti *In* DGLR, DGLR/AIAA/JSASS 20th International Electric Propulsion Conference: Proceedings 1988 p 75-85 (For primary document see N89-27707 22-20)
Avail: NTIS HC A99/MF E03

Past and ongoing activities on plasma propulsion are reviewed. They are mainly oriented towards the magnetoplasmadynamic (MPD) propulsion and arc jet propulsion development. Future activities in these fields are also mentioned. ESA

N89-27717*# Jet Propulsion Lab., California Inst. of Tech., Pasadena.
SPACECRAFT AND MISSION DESIGN FOR THE SP-100 FLIGHT EXPERIMENT
William D. Deininger and Robert J. Vondra (Schafer, W. J. Associates, Inc., Arlington, VA) *In* DGLR, DGLR/AIAA/JSASS 20th International Electric Propulsion Conference: Proceedings 1988 p 86-98 Sponsored in part by the Strategic Defense Initiative Organization, Washington, DC (For primary document see N89-27707 22-20)
Avail: NTIS HC A99/MF E03 CSCL 10B

The design and performance of a spacecraft employing arcjet nuclear electric propulsion, suitable for use in the SP-100 Space Reactor Power System (SRPS) Flight Experiment, are outlined. The vehicle design is based on a 93 kW(e) ammonia arcjet system operating at an experimentally measured specific impulse of 1031 s and an efficiency of 42.3 percent. The arcjet/gimbal assemblies, power conditioning subsystem, propellant feed system, propulsion system thermal control, spacecraft diagnostic instrumentation, and the telemetry requirements are described. A 100 kW(e) SRPS is assumed. The spacecraft mass is baselined at 5675 kg excluding the propellant and propellant feed system. Four mission scenarios are described which are capable of demonstrating the full capability of the SRPS. The missions considered include spacecraft

deployment to possible surveillance platform orbits, a spacecraft storage mission, and an orbit raising round trip corresponding to possible orbit transfer vehicle (OTV) missions. ESA

N89-27718# Tokyo Univ., Sagamihara (Japan). Inst. of Space and Astronautical Science.
DEVELOPMENT OF AN MPD PROPULSION SYSTEM
Yukio Shimizu, K. Toki, and Kyoichi Kuriki *In* DGLR, DGLR/AIAA/JSASS 20th International Electric Propulsion Conference: Proceedings 1988 p 99-104 (For primary document see N89-27707 22-20)
Avail: NTIS HC A99/MF E03

A 1 kW magnetoplasmadynamic (MPD) thruster system recorded 3 million firings which correspond to 25 days continuous operation demonstrating 34 mN/kW at an Isp of 600 sec. The critical components for system endurance, an MPD thruster head of segmented electrodes with improved thrust performance and a 574 J fail-proof capacitor bank were placed in a vacuum chamber to be operated in 1.4 Hz repetitively pulsed quasi-steady mode. The propellant was hydrazine simulative decomposed gas. Software for automatic control of firings and system diagnosis were also verified without human manipulation for hold and restart. The system was qualified as a breadboard model for EPEX (Electric Propulsion Experiment) onboard SFU (Space Flyer Unit) of which launch is scheduled in the early 1990s. The EPEX system is encouraged to reduce mass and power consumption matched with the SFU accomodation. ESA

N89-27719# Tokyo Univ., Sagamihara (Japan). Inst. of Space and Astronautical Science.
INTERACTION OF HIGH VOLTAGE SOLAR ARRAY WITH IONOSPHERIC PLASMA
H. Kuninaka, S. Satori, Y. Nozaki, and Kyoichi Kuriki *In* DGLR, DGLR/AIAA/JSASS 20th International Electric Propulsion Conference: Proceedings 1988 p 105-114 (For primary document see N89-27707 22-20)
Avail: NTIS HC A99/MF E03

Interference phenomena on a high voltage solar array (HVSA) by the ionospheric plasma were studied. The influence of ion drag on spacecraft motion, and surface degradation by sputtering are pointed out. ESA

N89-27720# Massachusetts Inst. of Tech., Cambridge.
THE INTERACTION BETWEEN A POSITIVELY BIASED CONDUCTOR ON A HIGH VOLTAGE SOLAR ARRAY AND A PLASMA **c75**
Daniel E. Hastings *In* DGLR, DGLR/AIAA/JSASS 20th International Electric Propulsion Conference: Proceedings 1988 p 115-120 (For primary document see N89-27707 22-20)
Avail: NTIS HC A99/MF E03

The physics of a positively biased conductor surrounded by dielectrics in contact with plasma is investigated. It is shown that due to the presence of secondary emission from the surrounding dielectrics the voltage of the surfaces near the conductor can be bistable. One of the bistable solutions always has very low secondary emission while the other has high secondary emission. The secondary current emitted from the neighboring dielectrics is collected by the conductor. When the voltage on the dielectric undergoes a transition from one bistable solution to another this is seen as a concomitant increase in the current collected to the conductor. A theoretical treatment for a conductor surrounded by dielectrics such as silicon dioxide is presented. The theory is applied to explain the snapover effect. The snapover effect is observed on high voltage solar arrays which involve the use of highly biased surfaces in contact with the space environment. When such surfaces are positively biased the current undergoes an anomalous increase at a critical voltage. ESA

N89-27721# Sovonics Solar Systems, Troy, MI.
DEPLOYABLE AEROSPACE PHOTOVOLTAIC ARRAY BASED ON AMORPHOUS SILICON ALLOYS
J. J. Hanak, Lee Walter, David Dobias, and Harvey Flaisher *In* DGLR, DGLR/AIAA/JSASS 20th International Electric Propulsion Conference: Proceedings 1988 p 121-124 (For primary document see N89-27707 22-20)
Avail: NTIS HC A99/MF E03

An ultralight, stowable, and deployable photovoltaic (PV) array is described for aerospace applications such as in lightweight space vehicles and high altitude balloons. The array consists of thin-film, tandem-junction, amorphous silicon alloy solar cells deposited onto a thin metallic foil. The array design utilizes 20 giant-sized cells, 1566 sq cm in area, connected in series to provide power of 207 W at AMO illumination. The weight of the array is only 800 g, which results in a power density of 258 W/kg, one order of magnitude greater than existing space arrays. Each of the cells is fully protected with bypass diodes to prevent damage upon partial shading or cell mismatch. A lightweight mechanism for stowing, deployment and support of the PV array was designed and a prototype constructed. The overall power density for the array and this mechanism is 145 W/kg. ESA

N89-27722# Fabrica Italiana Apparecchiature Radioelettriche S.p.A., Milan.
FEEP POWER CONDITIONING UNIT: DESIGN AND DEVELOPMENT STATUS
A. Bonati, C. Bocchiola, and D. Valentian (Societe Europeenne de Propulsion, Vernon, France) *In* DGLR, DGLR/AIAA/JSASS 20th International Electric Propulsion Conference: Proceedings 1988 p 125-134 (For primary document see N89-27707 22-20)
Avail: NTIS HC A99/MF E03

The design of a power conditioning unit for a field emission electric propulsion (FEEP) system is presented, with special emphasis on north-south stationkeeping application. The propulsion system consists of four thruster pairs (two active at a time and two in cold redundancy) each fed by a thruster dedicated power supply module. A central power and control module provides the bus power distribution, performs the operation control of the overall FEEP system, and exchanges orders and information with the attitude and orbit control system and the ground control directly via the on board data handling bus. The development status, the results achieved, and further steps needed toward the flight model are presented. ESA

N89-27723# Technische Univ., Vienna (Austria).
FIELD EMISSION ELECTRIC PROPULSION: EMISSION OF SLIT-TYPE LIQUID METAL ION SOURCES
J. Mitterauer *In* DGLR, DGLR/AIAA/JSASS 20th International Electric Propulsion Conference: Proceedings 1988 p 135-144 (For primary document see N89-27707 22-20)
(Contract ESTEC-6545/85)
Avail: NTIS HC A99/MF E03

A slit type field ion thruster is discussed. A slit emitter with a closed propellant supply system was fired in any optional direction, requiring in principle no gravitational forces. Quantitative and qualitative data relating the constituents of the residual gas atmosphere to the wetting behavior of the liquid metal propellant, and the emission performance were obtained. Restarting of the emitter after long periods of standby was demonstrated successfully. Major deviations of the current-voltage emission characteristic due to gas adsorption and the related contamination of the slit area of the ion thruster are found as well as a recovery effect probably due to thermal stress during high current ion emission. ESA

N89-27724# Societe Europeenne de Propulsion, Vernon (France).
FIELD EMISSION ELECTRIC PROPULSION (FEEP) ATTITUDE CONTROL CAPABILITIES
D. Valentian, J. P. Bugeat, C. Bartoli, and H. VonRohden (European Space Agency. European Space Research and Technology Center, ESTEC, Noordwijk, Netherlands) *In* DGLR, DGLR/AIAA/JSASS 20th International Electric Propulsion Conference: Proceedings 1988 p 145-152 (For primary document see N89-27707 22-20)
Avail: NTIS HC A99/MF E03

The field emission thruster was tested in pulsed mode. The pulses are reproducible. Either the emitter voltage or the accelerating electrode voltage can be controlled to provide the pulses, and the minimum impulse bit can be as small as 10 E - 8 N.s. Model missions, where FEEP offers significant advantages, are proposed. They deal with fine attitude control and/or drag compensation. The mission analysis leads to the definition of simple and lightweight propulsion systems for each case. A flight experiment to verify these capabilities is proposed. ESA

N89-27725# Stuttgart Univ. (Germany, F.R.). Inst. fuer Raumfahrtsysteme.

CYLINDRICAL STEADY-STATE MPD THRUSTER

H. L. Kurtz, M. Auweter-Kurtz, B. Glocker, H. Habiger, W. D. Merke, and H. O. Schrade *In* DGLR, DGLR/AIAA/JSASS 20th International Electric Propulsion Conference: Proceedings 1988 p 153-162 (For primary document see N89-27707 22-20)
(Contract N00014-87-G-0119)
Avail: NTIS HC A99/MF E03

A water-cooled, continuously running cylindrical magneto-plasmadynamic (MPD) accelerator was built. The cathode is displaceable, hence the discharge can be ignited in a retracted position. When the cathode tip begins to glow, the cathode is protruded to the foreseen position. The anode is divided into three parts to give insight into the current density and heat load distribution, which are compared with the theoretically calculated values. Since the anode rings can be connected separately, this thruster, with displaceable cathode can test a wide range of geometric variations. Two propellant ports are present at the back plate, one in a slit around the cathode, and the other in a slit at the anode radius. The influence of the variation of the propellant fractions at the inlet ports and of the geometry on the voltage/current characteristics and the onset point were evaluated. The temperature on the cathode tip was measured to gain knowledge about the cathode operation. In order to investigate the influence of the operation mode and especially the influence of a cold cathode on these characteristics, a noncooled thruster, similar in geometry and electrode material was built and tested in a quasi-steady discharge mode. The magnetic field distribution was measured to derive the current contour lines. ESA

N89-27726# Mitsubishi Electric Corp., Kanagawa (Japan).

IMPROVED THRUST GENERATION MECHANISM FOR ELECTROTHERMAL/ELECTROMAGNETIC ARCJET

Eiji Nishida, Yukio Shimizu, and Kyoichi Kuriki (Tokyo Univ., Sagamihara, Japan) *In* DGLR, DGLR/AIAA/JSASS 20th International Electric Propulsion Conference: Proceedings 1988 p 163-168 (For primary document see N89-27707 22-20)
Avail: NTIS HC A99/MF E03

The thrust performance of an arcjet was improved with an emphasis on electrothermal/electromagnetic hybrid acceleration. the anode of the arcjet was segmented azimuthally and restricted to the upstream region of outer nozzle. Thrust efficiency was increased from 15 percent to 27 percent around 1000 s of specific impulse. ESA

N89-27727# Stuttgart Univ. (Germany, F.R.). Inst. fuer Raumfahrsysteme.

NOZZLE TYPE MPD THRUSTER EXPERIMENTAL INVESTIGATIONS

W. D. Merke, M. Auweter-Kurtz, H. Habiger, H. L. Kurtz, and H. O. Schrade *In* DGLR, DGLR/AIAA/JSASS 20th International Electric Propulsion Conference: Proceedings 1988 p 169-179 (For primary document see N89-27707 22-20)
Avail: NTIS HC A99/MF E03

Magnetoplasmadynamic (MPD) thrusters were operated in a steady state mode with currents ranging from 200 to 8000 A and mass flow rates of different gases varying between 0.3 and 2.0 g/s. Results with hydrogen as propellant are compared to those with argon and nitrogen with higher molecular weights. The influence of throat geometry variation, i.e., on the one hand a shorter throat length and on the other hand a smaller throat diameter, is investigated. In addition to the other characteristic data, the pressure in the arc chamber is measured. The onset oscillations of the plasma, detected with an electrical probe, are analyzed by a fast Fourier transformation to get the frequency spectrum. A quasi-steady MPD thruster is investigated in order to determine the influence of the mode of operation on the performance. This thruster has the same geometry, electrode materials, and gas injection system as the continuous one. The onset point, defined by the appearance of strong voltage oscillations, lies at lower current values at constant mass flow rates than the steady state onset point. The current contour lines are measured and compared with a theoretical model. ESA

N89-27728# Messerschmitt-Boelkow-Blohm G.m.b.H., Ottobrunn (Germany, F.R.).

STATUS OF THE RITA EXPERIMENT ON EURECA

H. Bassner, H.-P. Berg, C. Bartoli, and A. Trippi (European Space Agency. European Space Research and Technology Center, ESTEC, Noordwijk, Netherlands) *In* DGLR, DGLR/AIAA/JSASS 20th International Electric Propulsion Conference: Proceedings 1988 p 180-185 (For primary document see N89-27707 22-20)
Avail: NTIS HC A99/MF E03

The Radiofrequency Ion Thruster Assembly RITA is built as a flight experiment on EURECA 1. This test flight shall verify the operational use of this electric propulsion system in space by demonstration of operation, lifetime, and reliability. The RITA experiment was adapted to meet the specific constraints imposed by the EURECA spacecraft and by the Space Shuttle as the launcher. Xenon gas will be used as the propellant and the experiment will be operated automatically by means of a dedicated on-board microcomputer system. ESA

N89-27729# Royal Aerospace Establishment, Farnborough (England). Space Dept.

THE PROPOSED DEMONSTRATION OF THE UK-10 ION PROPULSION SYSTEM ON ESA'S SAT-2 SPACECRAFT

D. G. Fearn *In* DGLR, DGLR/AIAA/JSASS 20th International Electric Propulsion Conference: Proceedings 1988 p 186-195 (For primary document see N89-27707 22-20)
Avail: NTIS HC A99/MF E03

The possible demonstration flight of a UK-10 ion propulsion system on ESA's SAT-2 spacecraft, which is due to be launched in mid-1993 to demonstrate advanced communications technologies is discussed. This propulsion system, which provides an exhaust velocity, or specific impulse more than an order of magnitude higher than that attainable with chemical thrusters, can be used for north-south stationkeeping, thereby augmenting the capabilities of the conventional orbit control facilities of the satellite. For a total dry mass of less than 40 kg, the on-station lifetime of the spacecraft can be doubled to 10 years by this means. ESA

N89-27730# Marconi Space Systems Ltd., Portsmouth (England).

DESIGN AND DEVELOPMENT OF THE UK-10 ION PROPULSION SUBSYSTEM

P. Smith *In* DGLR, DGLR/AIAA/JSASS 20th International Electric Propulsion Conference: Proceedings 1988 p 196-202 (For primary document see N89-27707 22-20)
Avail: NTIS HC A99/MF E03

The UK Ion Propulsion Subsystem is based on the UK-10 electrostatic ion thruster which uses xenon propellant to produce thrust in the range 3 to 50 mN. A subsystem for use on a geostationary communications satellite for north-south station-keeping was designed. The design, development, and performance of the subsystem aspects with particular emphasis on spacecraft interfaces, including ground support equipment, are described. ESA

N89-27731# Giessen Univ. (Germany, F.R.). First Inst. of Physics.

AUXILIARY PROPULSION RF ENGINE RIT 15: PROTOTYPE DESIGN AND PERFORMANCE

K. H. Groh, A. Dillmann, H. W. Loeb, and F. Weber *In* DGLR,

DGLR/AIAA/JSASS 20th International Electric Propulsion Conference: Proceedings 1988 p 203-207 (For primary document see N89-27707 22-20)
Avail: NTIS HC A99/MF E03

Advanced north-south stationkeeping (NSSK) requirements are moving towards the 50 mN thrust level and prohibit metal vapors as a propellant. To address these requirements, a prototype of the RIT 15, operated with xenon, was built. The RIT 15 prototype aims at the 20 to 40 mN thrust range at adequate efficiencies. ESA

N89-27732# MATRA Espace, Toulouse (France).
DESIGN AND INTEGRATION OF AN ELECTRIC PROPULSION SYSTEM ON THE EUROSTAR SPACECRAFT
T. Duhamel, P. H. Ricaud, and P. Greff *In* DGLR, DGLR/AIAA/JSASS 20th International Electric Propulsion Conference: Proceedings 1988 p 217-223 (For primary document see N89-27707 22-20)
Avail: NTIS HC A99/MF E03

The implementation of ion propulsion on the 3-axis stabilized geostationary spacecraft EUROSTAR is described. The primary purpose of ion propulsion is to perform north-south stationkeeping. Several thruster configurations are examined and an orbit analysis is performed. The impacts on the spacecraft of the ion propulsion system are reviewed. ESA

N89-27733# Stuttgart Univ. (Germany, F.R.). Inst. fuer Raumfahrtsysteme.
NUMERICAL CODES FOR CYLINDRICAL MPD THRUSTERS
P. C. Sleziona, M. Auweter-Kurtz, and H. O. Schrade *In* DGLR, DGLR/AIAA/JSASS 20th International Electric Propulsion Conference: Proceedings 1988 p 224-234 (For primary document see N89-27707 22-20)
(Contract AF-AFOSR-0337-86; N00014-87-G-0119)
Avail: NTIS HC A99/MF E03

Two fully two-dimensional computer codes were developed to analyze cylindrical, self-field, magnetoplasmadynamic thrusters. Both codes use a magnetogasdynamic description of the gas and the interaction between the magnetic field and the fluid dynamics of the plasma. The fluid dynamic calculation is different in the models. The aim is to test the models for high current to mass flow ratios, up to the critical I to the 2nd power/m, the onset point. The first code was developed in a time dependent formulation and the system of equations is discretized into finite differences. The gasdynamic equations are solved by a modified MacCormack code and the magnetic equations for the steady state phase by a Gauss-Seidel code. A transformation is performed for the magnetogasdynamic equations from an orthogonal, equidistant, computational grid to a geometrically more complex, physical grid. Thus it is possible to obtain a solution for arbitrarily complex engine geometries. High current to mass flow ratios cause difficulties in the calculation of gasdynamic equations. Therefore, a second, finite volume code is applied to calculate the gasdynamic equations, using the program package PHOENICS. The numerical solution from the magnetic equations is handled in the same manner as described above. A comparison for both methods is made for a simplified cylindrical thruster geometry. The results for a mass flow rate of 6 g/s of argon and for currents up to 10 kA are presented. ESA

N89-27734# Massachusetts Inst. of Tech., Cambridge. Space Systems Lab.
FLUID MECHANICS IN A MAGNETOPLASMADYNAMIC THRUSTER
D. J. Hiermerdinger and M. Martinez-Sanchez *In* DGLR, DGLR/AIAA/JSASS 20th International Electric Propulsion Conference: Proceedings 1988 p 235-244 (For primary document see N89-27707 22-20)
(Grant AF-AFOSR-0019-86)
Avail: NTIS HC A99/MF E03

Theoretical and experimental results are presented that: (1) demonstrate the effects of electrode geometry on the operation of the magnetoplasmadynamic (MPD) arc jet; and (2) describe the onset phenomenon not as a single phenomenon but as two distinct phenomena, the first being related to an anode starvation mechanism and the second arising from full single ionization in the plasma bulk. Theory and data both show that the electrode current concentrations can be locally changed by varying the channel's interelectrode separation. The experiment (conducted on a large radius annular geometry) and subsequent theory also show a clear separation between an anode depletion description of onset (caused by the radial component of the thrust vector), indicated by the growth of a large anode voltage drop, and the onset indicated by unsteady large amplitude voltage oscillations which are attributed to a global instability of the electrothermal type occurring near full ionization. ESA

N89-27735# Stuttgart Univ. (Germany, F.R.). Inst. fuer Raumfahrtsysteme.
AN IMPROVED CODE FOR NOZZLE TYPE STEADY STATE MPD THRUSTERS
M. Auweter-Kurtz, S. F. Glaser, H. L. Kurtz, H. O. Schrade, and P. C. Sleziona *In* DGLR, DGLR/AIAA/JSASS 20th International Electric Propulsion Conference: Proceedings 1988 p 245-252 (For primary document see N89-27707 22-20)
(Contract AF-AFOSR-0337-86; N00014-87-G-0119)
Avail: NTIS HC A99/MF E03

In order to predict the overall performance of continuously running, self-field MPD thrusters, a semi-two-dimensional model calculation and computer program was developed. The extended Ohm's law is used to calculate the current contour lines, and a one-dimensional, two-component expansion flow model is employed to obtain velocity, temperature and pressure distributions for calculating the gas properties, which are again used in Ohm's law. In a first step, the expansion flow within the nozzle was assumed to be isothermal for the ions and adiabatic in the case of electrons. Outside the nozzle the expansion flow was considered hyperbolic and adiabatic for both components. This first model was improved. Within the nozzle of the thruster the radial heat transportation and the coupling of electrons and heavy particles are taken into account. The results of the code are compared with measurements in a vacuum tank which always has a residual gas pressure. This ambient gas, which also is at a high temperature (T(e) approx.= 10,000 K) is included in the model with an estimated free stream boundary. The differential equation is solved by means of a finite difference method for the geometry of the nozzle type plasma thruster DT2-IRS investigated experimentally in a steady state as well as in a pulsed mode. The results of these calculations are compared with the experiments. ESA

N89-27736*# Princeton Univ., NJ. Electric Propulsion Lab.
CURRENT DRIVEN INSTABILITIES OF AN ELECTROMAGNETICALLY ACCELERATED PLASMA
E. Y. Choueiri, A. J. Kelly, and R. G. Jahn *In* DGLR, DGLR/AIAA/JSASS 20th International Electric Propulsion Conference: Proceedings 1988 p 253-265 Sponsored in part by Hercules Aerospace; Rocket Research, Inc. and DOE/Princeton Plasma Physics Lab., NJ (For primary document see N89-27707 22-20)
(Contract NAS9-54997)
Avail: NTIS HC A99/MF E03 CSCL 10B

A plasma instability that strongly influences the efficiency and lifetime of electromagnetic plasma accelerators was quantitatively measured. Experimental measurements of dispersion relations (wave phase velocities), spatial growth rates, and stability boundaries are reported. The measured critical wave parameters are in excellent agreement with theoretical instability boundary predictions. The instability is current driven and affects a wide spectrum of longitudinal (electrostatic) oscillations. Current driven instabilities, which are intrinsic to the high-current-carrying magnetized plasma of the magnetoplasmadynmic (MPD) accelerator, were investigated with a kinetic theoretical model based on first principles. Analytical limits of the appropriate dispersion relation yield unstable ion acoustic waves for T(i)/T(e) much less than 1 and electron acoustic waves for T(i)/T(e) much greater than 1. The resulting set of nonlinear equations for the

case of T(i)/T(e) = 1, of most interest to the MPD thruster Plasma Wave Experiment, was numerically solved to yield a multiparameter set of stability boundaries. Under certain conditions, marginally stable waves traveling almost perpendicular to the magnetic field would travel at a velocity equal to that of the electron current. Such waves were termed current waves. Unstable current waves near the upper stability boundary were observed experimentally and are in accordance with theoretical predictions. This provides unambiguous proof of the existence of such instabilites in electromagnetic plasma accelerators. ESA

N89-27737# Stuttgart Univ. (Germany, F.R.). Inst. fuer Raumfahrtsysteme.
INVESTIGATION OF INSTABILITIES IN MPD THRUSTER FLOWS USING A LINEAR DISPERSION RELATION
D. Rempfer, M. Auweter-Kurtz, H. J. Kaeppler, and M. Maurer (Maschinenfabrik Augsburg-Nuernberg A.G., Munich, Germany F.R.) *In* DGLR, DGLR/AIAA/JSASS 20th International Electric Propulsion Conference: Proceedings 1988 p 266-272 (For primary document see N89-27707 22-20)
Avail: NTIS HC A99/MF E03

In order to start a systematic investigation of instabilities occurring in magnetoplasmadynamic (MPD) thruster flows, a linear, as well as a nonlinear, three-fluid system of equations with one chemical reaction (ionization) for a simple thruster model was used to derive the dispersion relation for micro as well as macroinstabilities. The method of solution applied, the quasi-analytical method (QAM), was developed especially for studying nonlinear and turbulent behavior of MPD flows and employs an algebraic computer code. As a first step, the linear dispersion relation was solved for an argon jet, emphasizing the macroinstabilites generated by flow conditions. The acoustic wave instability could be identified. The growth rates and characteristic frequencies of the instability were derived and their behavior investigated. ESA

N89-27738# Royal Aerospace Establishment, Farnborough (England).
DEVELOPMENT OF A FLIGHT STANDARD POWER CONDITIONING AND CONTROL SYSTEM FOR THE T5 ION THRUSTER
Manoj Mohan, David Diani, and David Rees (Wales Polytechnic, Pontypridd.) *In* DGLR, DGLR/AIAA/JSASS 20th International Electric Propulsion Conference: Proceedings 1988 p 283-291 (For primary document see N89-27707 22-20)
Avail: NTIS HC A99/MF E03

The development status of the Power Conditioning and Control System (PCCS) being developed for a test flight of the T5 ion thruster is reviewed. The power and control requirements of the thruster, and how these are provided in the prototype PCCS, built to breadboard standard are described. Problems presented by the thruster are highlighted and details of the techniques used to resolve them are given. The development of the flight packaging of the PCCS is outlined. The approach adopted to ensure reliable operation of the PCCS in the face of the extremities of the space environment (thermal stresses in particular) is shown. ESA

N89-27739# Mitsubishi Electric Corp., Kanagawa (Japan).
VERIFICATION OF PERFORMANCE AND ENDURANCE OF CAPACITOR BANK FOR THE ELECTRIC PROPULSION EXPERIMENT (EPEX)
Y. Kunii, M. Sumida, T. Moriai, H. Sasaki, T. Okamura, H. Harada, K. Ijichi, Yukio Shimizu, and K. Toki (Tokyo Univ., Sagamihara, Japan) *In* DGLR, DGLR/AIAA/JSASS 20th International Electric Propulsion Conference: Proceedings 1988 p 292-299 (For primary document see N89-27707 22-20)
Avail: NTIS HC A99/MF E03

Design requirements and the results of the ground test for the development of the capacitor bank in the power conversion subsystem of EPEX are summarized. The power conversion efficiency in the pulse forming network (PFN), which is a main component of the capacitor bank, is 85 percent. The number of the repetitive discharges amounted to 3 million in a net operation period of 25 days. The basic requirements for the EPEX is confirmed to be feasible by the ground test. ESA

N89-27740# Mitsubishi Electric Corp., Kanagawa (Japan).
VERIFICATION OF CONTROL SEQUENCE AND ALGORITHM FOR THE ELECTRIC PROPULSION EXPERIMENT (EPEX)
M. Sumida, Y. Kunii, T. Moriai, T. Okamura, T. Yoshida, K. Ijichi, Yukio Shimizu, and K. Toki (Tokyo Univ., Sagamihara, Japan) *In* DGLR, DGLR/AIAA/JSASS 20th International Electric Propulsion Conference: Proceedings 1988 p 300-305 (For primary document see N89-27707 22-20)
Avail: NTIS HC A99/MF E03

The control and monitor system based on a microcomputer was composed according to the conceptual design for EPEX system and successfully operated the repetitive discharges of 3 million shots in a net operation period of 25 days, although the hardware of the control and monitor system was composed of equipment for general ground use. The successfull operation verified basic control logics for a magnetoplasmadynamic (MPD) propulsion system. Based on the test results, the conceptual design or requirements for the control and monitor subsystem for EPEX was refined. The monitor signals were evaluated and selected for the flight system. ESA

N89-27741# Hughes Space and Communications Group, El Segundo, CA. Systems Labs.
CONTROLLING A STATIONARY ORBIT USING ELECTRIC PROPULSION
Bernard M. Anzel *In* DGLR, DGLR/AIAA/JSASS 20th International Electric Propulsion Conference: Proceedings 1988 p 306-314 (For primary document see N89-27707 22-20)
Avail: NTIS HC A99/MF E03

Orbit control using two ion engines mounted on the antinadir face of a satellite is considered. Each engine is fired once per orbit sidereal period, and automatically provides acceleration components to correct the inclination, eccentricity, and drift parameters of a stationary orbit. Both engines are canted away from the antinadir face. One engine is primarily thrusting north, and the other south. To control orbit inclination, the south thrusting engine is fired over an arc centered about a right ascension of 90 deg; the north thrusting engine is fired over an arc centered about a right ascension of 270 deg. For equal burn arcs the radial acceleration components are equal so that no net change in eccentricity results. The use of unequal burn arcs, however, results in partial eccentricity control. If the ion engines may be swiveled about the north-south axis, tangential components of acceleration result upon thrusting. These are used to control satellite drift along with eccentricity control. The magnitude depends on the satellite station longitude, precession of the orbit plane caused by solar-lunar gravity, and the cant angle of the engines. Control of satellite drift and orbit inclination is very tight, while control of orbit eccentricity is limited by the requirement that the engine firings are fixed in space. ESA

N89-27742# Osaka Univ. (Japan). Faculty of Engineering Science.
CONTINUOUS OPERATION OF A QUASI-STEADY MPD PROPULSION SYSTEM WITH AN EXTERNAL MAGNETIC FIELD
T. Yoshikawa, Y. Kagaya, H. Tahara, and T. Wasa *In* DGLR, DGLR/AIAA/JSASS 20th International Electric Propulsion Conference: Proceedings 1988 p 315-322 (For primary document see N89-27707 22-20)
Avail: NTIS HC A99/MF E03

An MPD (magnetoplasmadynamic) propulsion system with an external magnetic field was developed for missions near the Earth and tested to solve technological problems for flight model design. The MPD arcjet equipped with a ring coil at the outside of the anode, is of quasi-steady type and was operated at average input power of 1 kW. Cathode erosion is markedly reduced by applying the axial magnetic field. The heat flux to the electrode is 20 percent of the input power, and the temperatures of all components are

kept below 1000 C. From the thermal data of 1 kW power level a 5 kW-class MPD head was designed for future space missions. ESA

N89-27743# Tokyo Univ. (Japan).
OPTIMIZATION OF CURRENT DISTRIBUTION IN AN APPLIED-FIELD MPD THRUSTER
A. Sasoh, A. E. Solem, and Yoshihiro Arakawa *In* DGLR, DGLR/AIAA/JSASS 20th International Electric Propulsion Conference: Proceedings 1988 p 323-332 (For primary document see N89-27707 22-20)
Avail: NTIS HC A99/MF E03

Steady-state applied-field magnetoplasmadynamic (MPD) thrusters were constructed. Thruster performance tests were conducted by varying propellant type, strength and pattern of applied magnetic field, discharge current and mass flow rate. Thrust efficiencies of more than 20 percent are obtained for hydrogen, helium and argon. The performance of nitrogen was low. Thruster performance is found to be closely related to the discharge current distribution. When it is distributed downstream, electromagnetic thrust is produced by interaction with the applied field. Current distribution is found to be determined mainly by propellant type and operating mode. Using a segmented-anode MPD thruster, positive control of current distribution is attained suggesting the feasibility of thruster performance enhancement. ESA

N89-27744# Osaka Univ. (Japan). Faculty of Engineering Science.
HYBRID MPD THRUSTER WITH AXIAL AND CUSP MAGNETIC FIELDS
H. Tahara, Y. Kagaya, and T. Yoshikawa *In* DGLR, DGLR/AIAA/JSASS 20th International Electric Propulsion Conference: Proceedings 1988 p 333-341 (For primary document see N89-27707 22-20)
Avail: NTIS HC A99/MF E03

High-current quasi-steady magnetoplasmadynamic (MPD) thrusters with axial applied magnetic fields were investigated to improve the thrust performance, and to elucidate the mechanisms of propellant heating and acceleration. The discharge voltage and thrust characteristics are ascribed to coexistence of the self-induced and applied fields. Application of pulsed magnetic fields in series with the discharge circuit causes lower discharge voltages and greater thrusts than those for no applied field in such a special condition that the axial field intensity is equal to the azimuthal self-field one only in the main region for current conduction, and it is very small outside the region. Application of the preferred pulsed field brings about effective heating in the upstream region with high pressure and increases the electrothermal component of thrust. A steady MPD thruster with an axial applied magnetic field was designed and tested in the electrothermal, electromagnetic hybrid acceleration mode. ESA

N89-27745# National Aerospace Lab., Tokyo (Japan).
XENON ION THRUSTER TEST FACILITY: DESIGN AND OPERATION
Shoji Kitamura, Katsuhiro Miyazaki, Y. Hayakawa, and Yoshihiro Nakamura *In* DGLR, DGLR/AIAA/JSASS 20th International Electric Propulsion Conference: Proceedings 1988 p 342-348 (For primary document see N89-27707 22-20)
Avail: NTIS HC A99/MF E03

Development of a vacuum facility to test xenon ion thrusters is described. North-south stationkeeping of a 2 ton geostationary satellite for 10 yrs requires its ion propulsion system to operate for over 6000 hrs in total. Long duration tests in ground facilities producing a high and clean vacuum are essential. The facility has a vacuum chamber of 3 m in diameter and 5 m in length. It contains a cryopanel to condense xenon gas, and shrouds and thermal superinsulations to reduce thermal radiation input to the cryopanel to condense xenon gas, and shrouds and thermal superinsulations to reduce thermal radiation input to the cryopanel. The cryopanel and the main shrouds are cooled by circulating helium gas from Stirling cycle cryogenerators. The beam target and the subchamber shroud are cooled by a flon cryogenerator. The facility can be operated without liquid nitrogen. Demonstration tests were conducted using a thruster with 25 mN nominal thrust. Results show that this facility is satisfactory in the thermal design and the attained vacuum. The cryopanel was cooled below 50 K to attain a vacuum of 0.00004 to 0.00005 Pa by 40 hr after starting the cooling. With the ion beam exhaustion, out-gas from the target degraded the vacuum. However, recovery was gradually made to attain a vacuum of 0.0004 to 0.0005 Pa in 20 min. Residual gases were analyzed to give data on the quality of the vacuum. ESA

N89-27746# National Aerospace Lab., Tokyo (Japan).
DISCHARGE PERFORMANCE OF A 12 cm CUSP XENON ION THRUSTER
Yoshihiro Nakamura, Manabu Matsumoto (Tokai Univ., Kanagawa, Japan), Shoji Kitamura, and Katsuhiro Miyazaki *In* DGLR, DGLR/AIAA/JSASS 20th International Electric Propulsion Conference: Proceedings 1988 p 349-357 (For primary document see N89-27707 22-20)
Avail: NTIS HC A99/MF E03

On a 12 cm cusp xenon ion thruster, the effects of configuration parameters in the discharge chamber on the performance were examined by changing them one by one and operating the thruster. The parameters are extracted beam diameter at a screen grid, area at the cathode potential, and the cusped magnetic field to confine a discharge plasma. The diameter of holes on a screen grid should be so large within a discharge chamber that as many ions as possible ions coming to the grid could be extracted. Three ring magnets on the side wall and two rings on the base plate present the best discharge performance. Too many magnet rings distort the magnetic field and bring about performance deterioration. A cathode potential area at the upstream side does not must change the performance. The best performance obtained is an ion production cost of about 230 W/A at propellant utilization efficiency of 90 percent. ESA

N89-27747# United Kingdom Atomic Energy Authority, Culham (England).
HIGH THRUST OPERATION OF THE UK-10 RARE GAS ION THRUSTER (T4A)
A. R. Martin and P. M. Latham *In* DGLR, DGLR/AIAA/JSASS 20th International Electric Propulsion Conference: Proceedings 1988 p 358-363 Sponsored by RAE, Farnborough, United Kingdom (For primary document see N89-27707 22-20)
Avail: NTIS HC A99/MF E03

Changes to the ion thruster used in the UK-10 rare gas electric propulsion system, originally specified for a thrust level of 10 mN, are discussed. With the trend towards larger spacecraft and longer spacecraft lifetime such a relatively low thrust is no longer appropriate to the stationkeeping requirements. Consequently, the thrust limits of an engineering model thruster, designated T4A, were investigated. No modifications were made to the thruster during these high thrust tests. The maximum thrust level achieved is over 70 mN. Detailed characterization of the thermal stability and performance were carried out at 25 mN (the present thrust level specification) and at 40 mN (of interest to a range of more advanced missions). The thruster operation at these elevated thrust levels is described. ESA

N89-27748*# Colorado State Univ., Fort Collins. Dept. of Mechanical Engineering.
RING CUSP/HOLLOW CATHODE DISCHARGE CHAMBER PERFORMANCE STUDIES
J. A. Vaughn and Paul J. Wilbur *In* DGLR, DGLR/AIAA/JSASS 20th International Electric Propulsion Conference: Proceedings 1988 p 364-373 (For primary document see N89-27707 22-20)
(Grant NGR-06-002-112)
Avail: NTIS HC A99/MF E03 CSCL 10B

An experimental study was performed to determine the effects of hollow cathode position, anode position, and ring cusp magnetic field configuration and strength on discharge chamber performance. The results are presented in terms of comparative plasma ion

energy cost, extracted ion fraction, and beam profile data. Such comparisons are used to demonstrate whether changes in performance are caused by changes in the loss rate of primary electrons to the anode or the loss rate of ions to discharge chamber walls or cathode and anode surfaces. Results show: (1) the rate of primary electron loss to the anode decreases as the anode is moved downstream of the ring cusp toward the screen grid; (2) the loss rate of ions to hollow cathode surfaces are excessive if the cathode is located upstream of a point of peak magnetic flux density at the discharge chamber centerline; and (3) the fraction of the ions produced that are lost to discharge chamber walls and ring magnet surfaces is reduced by positioning of the magnet rings so the plasma density is uniform over the grid surface, and adjusting their strength to a level where it is sufficient to prevent excessive ion losses by Bohm diffusion. ESA

N89-27749# Air Force Office of Scientific Research, Bolling AFB, Washington, DC. Directorate of Aerospace Sciences.
SURVEY OF ELECTRIC PROPULSION THRUSTER APPLICABILITY TO NEAR EARTH SPACE MISSIONS
Mitat Birkan and Michael M. Micci (Pennsylvania State Univ., University Park.) *In* DGLR, DGLR/AIAA/JSASS 20th International Electric Propulsion Conference: Proceedings 1988 p 374-382 (For primary document see N89-27707 22-20)
Avail: NTIS HC A99/MF E03

The state-of-the-art performance of nine electric propulsion devices in terms of specific impulse and thruster and power processor efficiency and specific mass are discussed. Initial vehicle mass and strip time for four cases, Delta V of 1 and 6 km/s and payload mass of 3000 and 30,000 kg, were calculated and compared to a state-of-the-art storable chemical propulsion system. Situations where electric propulsion systems give a lower initial vehicle mass than a chemical propulsion system are shown. The advantages of the beamed energy thrusters, the microwave and laser thrusters, which do not carry their power source with them are also shown. The desirability of having a low power supply specific mass for those electric propulsion systems which must carry their power supply with them is demonstrated. ESA

N89-27750# Messerschmitt-Boelkow-Blohm G.m.b.H., Munich (Germany, F.R.). Space Communications and Propulsion Systems Div.
ELECTRICAL TRANSFER VEHICLE ANALYSIS FOR FUTURE SPACE OPERATIONS (MESCATS)
W. Kleinau, D. E. Koelle, and W. Mueller *In* DGLR, DGLR/AIAA/JSASS 20th International Electric Propulsion Conference: Proceedings 1988 p 383-390 (For primary document see N89-27707 22-20)
Avail: NTIS HC A99/MF E03

A modular orbital transfer vehicle for scientific and cargo transportation missions called MESCATS was investigated, in particular for advanced transportations between operational bases as well in a geostationary orbit such as a linar orbit. A cluster of electrical ion-thrusters (RIT 35) was considered as the main propulsion system. The MESCATS is, due to its high specific impulse (up to 38,000 Nsec/kg), an interesting candidate providing not only high delta velocity increments (relevant in particular for scientific missions), but is especially economic for cargo missions (Earth/Moon). It appears feasible to develop an E-OTV like MESCATS which could meet a wide range of operational requirements (such as payload mass, orbital transfer time, velocity increment) with key elements assumed to be available in Europe in the medium term. ESA

N89-27751# Royal Aerospace Establishment, Farnborough (England).
A CASE STUDY OF A MISSION TO THE KORDYLEWSKI CLOUDS USING ION PROPULSION
K. A. Ryden, P. G. Herrington, and N. C. Wallace *In* DGLR, DGLR/AIAA/JSASS 20th International Electric Propulsion Conference: Proceedings 1988 p 391-397 (For primary document see N89-27707 22-20)
Avail: NTIS HC A99/MF E03

A mission to send a spacecraft to one of the stable Earth-Moon Lagrange points is described. The scientific objective of the spacecraft would be to investigate the dust and other material which is expected to have collected at these places, i.e., the Kordylewski clouds. Ground-based and satellite observations of the Kordylewski clouds are reviewed. The main features of the spacecraft are described and analysis of the orbit-raising and rendezvous procedure is discussed. ESA

N89-27752# Royal Aerospace Establishment, Farnborough (England). Space Dept.
A SMALL ION-PROPELLED SPACECRAFT FOR NEAR EARTH EXPERIMENTS
K. A. Ryden and N. C. Wallace *In* DGLR, DGLR/AIAA/JSASS 20th International Electric Propulsion Conference: Proceedings 1988 p 398-404 (For primary document see N89-27707 22-20)
Avail: NTIS HC A99/MF E03

The suitability of ion propulsion for small spacecraft is studied, with particular emphasis on low altitudes where air drag can be a serious problem. It is shown that the use of the UK-10 ion propulsion system can enhance the value of a small spacecraft as a technology demonstration vehicle, permitting the test of a range of devices under realistic conditions. Results of orbit analysis using a numerical program are given for two spacecraft configurations. ESA

N89-27753# Purdue Univ., West Lafayette, IN. School of Mechanical Engineering.
CATHODE PROCESSES IN A MPD ARCJET
K. D. Goodfellow and S. N. B. Murthy *In* DGLR, DGLR/AIAA/JSASS 20th International Electric Propulsion Conference: Proceedings 1988 p 405-415 (For primary document see N89-27707 22-20)
(Grants AF-AFOSR-0335-85; AF-AFOSR-0278-86)
Avail: NTIS HC A99/MF E03

Efforts to develop a methodology for quantitatively examining the plasma-cathode interactive processes in a MPD arcjet within a distance of the order of a recombination length from the surface and to identify limiting operating conditions based on such processes are reviewed. A simple model was developed based on three characteristic lengths in the nonequilibrium, two-temperature plasma and thermionic emission from the cathode under the local electrical field. It is found that the largest changes occur in the sheath region and critical conditions can arise both in the sheath and the outer collisonal non-recombining regions. ESA

N89-27754*# Jet Propulsion Lab., California Inst. of Tech., Pasadena.
THERMAL DESIGN IMPROVEMENTS FOR 30kWe ARCJET ENGINE
William D. Deininger, A. Chopra, D. Q. King, and Thomas J. Pivirotto *In* DGLR, DGLR/AIAA/JSASS 20th International Electric Propulsion Conference: Proceedings 1988 p 416-423
Sponsored in part by Strategic Defense Initiative Organization, Washington, DC (For primary document see N89-27707 22-20)
Avail: NTIS HC A99/MF E03 CSCL 21H

Two thermal design improvements for 30 kWe arcjet engines are described. A ZrB2 high temperature coating was used to increase the surface emissivity of the nozzle radiating surface, enabling lower temperature operation, which should lead to longer nozzle life. The ZrB2-coated engine operated 120 C cooler than the uncoated baseline engine indicating a 30 percent increase in the surface emissivity. An engine design which has fewer active seals than previous designs and operates at lower overall component temperatures is described. The nozzle on the engine operated at 1950 C at 30 kWe while the baseline engine nozzle reached 2000 C at 23 kWe. The back of the engine was more than a factor of two cooler when compared to the baseline engine. ESA

N89-27755*# Jet Propulsion Lab., California Inst. of Tech., Pasadena.
ELECTRODE EROSION IN STEADY-STATE ELECTRIC PROPULSION ENGINES
Thomas J. Pivirotto and William D. Deininger *In* DGLR, DGLR/AIAA/JSASS 20th International Electric Propulsion Conference: Proceedings 1988 p 424-429 Sponsored in part by Strategic Defense Initiative Organization, Washington, DC (For primary document see N89-27707 22-20)
Avail: NTIS HC A99/MF E03 CSCL 21H

The anode and cathode of a 30 kW class arcjet engine were sectioned and analyzed. This arcjet was operated for a total time of 573 hr at power levels between 25 and 30 kW with ammonia at flow rates of 0.25 and 0.27 gm/s. The accumulated run time was sufficient to clearly establish erosion patterns and their causes. The type of electron emission from various parts of the cathode surface was made clear by scanning electron microscope analysis. A scanning electron microscope was used to study recrystallization on the hot anode surface. These electrodes were made of 2 percent thoriated tungsten and the surface thorium content and gradient perpendicular to the surfaces was determined by quantitative microprobe analysis. The results of this material analysis on the electrodes and recommendations for improving electrode operational life time are presented. ESA

N89-27756# Princeton Univ., NJ. Electric Propulsion Lab.
CHARACTERIZATION OF COLD CATHODE EROSION PROCESSES
J. E. Polk, A. J. Kelly, and R. G. Jahn *In* DGLR, DGLR/AIAA/JSASS 20th International Electric Propulsion Conference: Proceedings 1988 p 430-437 (For primary document see N89-27707 22-20)
Avail: NTIS HC A99/MF E03

Measurements of MPD thruster cathode erosion for six different current levels at one mass flow rate using a mass loss detection system called surface layer activation indicate that the cathode erosion rate follows an exponential dependence on the total arc current for currents below a critical point identified as the transition to full ionization. At this point the erosion rate increases by an order of magnitude from that at lower currents, then deviates from the exponential behavior in a drop to an intermediate level. The increase in erosion at the full ionization current is interpreted as a manifestation of an additional mass loss mechanism excited at that point. A related experiment designed to provide preliminary data on the characteristic length scale association with cratering damage in cold cathode erosion by photomicrography of an arced cathode surface yields a mean crater diameter of 1 micron. The diameter of the observed craters is uniform over the cathode surface, indicating that the crater formation processes are relatively insensitive to changes in the discharge occurring along the cathode axis. A simple thermal model of crater formation yields a linear relationship between the diameter and the site current. This relationship coupled with measurements of crater densities suggests that individual emission sites on the cathode surface carry only a few amps and survive for 100 nsec. ESA

N89-27757# Rome Univ. (Italy). Dipartimento di Meccanica e Aeronautica.
ANODE-NOZZLE EXPERIMENTAL ANALYSIS IN A COAXIAL NON-STEADY SOLID PROPELLANT MPD THRUSTER
Giorgi Paccani *In* DGLR, DGLR/AIAA/JSASS 20th International Electric Propulsion Conference: Proceedings 1988 p 438-445 (For primary document see N89-27707 22-20)
Avail: NTIS HC A99/MF E03

The functioning of a coaxial solid propellant MPD thruster with cylindrical and conical anodes was investigated in working conditions characterized by two different discharge waveforms, each one with several different initial discharge energy levels. The effect of the different geometries and working conditions on the electric parameters, on the ablation process, and the theoretical performance was examined. The importance of the ablation process is pointed out in relation to its effect on thruster functioning; a correlation between the ablation process behavior and the current density distribution along the anode is observed. Among the investigated geometries a range of anode lengths in which length variations do not represent a highly-affecting parameter is determined; sharp differences in behavior are observed between cylindrical and flared anodes and between the two operating conditions characterized by the two different waveforms. Nevertheless such differences tend, as a rule, to weaken as the initial discharge energy level increases. ESA

N89-27758# Marconi Space Systems Ltd., Portsmouth (England).
THE PROPELLANT SUPPLY AND MONITORING EQUIPMENT (PSME) FOR THE UK-10 ION PROPULSION SUBSYSTEM
S. D. Watson *In* DGLR, DGLR/AIAA/JSASS 20th International Electric Propulsion Conference: Proceedings 1988 p 446-452 (For primary document see N89-27707 22-20)
Avail: NTIS HC A99/MF E03

The Propellant Supply and Monitoring Equipment (PSME) was designed to interface with the UK-10 electron bombardment ion thruster. Its function is to provide the accurately controlled small xenon mass flow rates to the thruster discharge chamber, cathode and neutralizer. It is shown how the PSME concept was evolved to meet the challenging flow rate requirements consistent with its status as an operational demonstrator model. The various options that were considered for the PSME are described, from basic operating concepts to detailed component selection. The reasoning behind the operating parameter selection is presented. The evolution of the demonstrator from a simple concept-proving model to a piece of equipment being used for thruster testing is described. The operating parameters of the model which were evaluated under test are presented. The flight PSME power requirement, mass, and performance data are given. ESA

N89-27759# Philips Components, Mitcham (England). Central Materials Lab.
A REVIEW OF THE CATHODE CONSTRUCTION FOR THE RAE 10/25mN THRUSTER
S. A. Gair and P. T. Harris *In* DGLR, DGLR/AIAA/JSASS 20th International Electric Propulsion Conference: Proceedings 1988 p 453-459 Sponsored by the United Kingdom Ministry of Defence Procurement Executive (For primary document see N89-27707 22-20)
Avail: NTIS HC A99/MF E03

The constructional details of the cathode and exploratory work which led to the choice of materials and methods for the ion thruster are reviewed. The joining methods are described and examples given to illustrate the criteria for judgement of the adequacy of these methods. The operation for long times at high temperatures requires protection of surfaces from interaction with each other. Work performed to understand these interactions is mentioned. The electrical isolation of the cathode is achieved by the use of ceramic components which have to be ruggedly incorporated into the structure. The thermal insulation is provided by wrapped molybdenum foil which minimizes the power requirements for starting and stabilizes the operation. ESA

N89-27760# Tokyo Univ. (Japan). Dept. of Aeronautics.
DISCHARGE PLASMA CALCULATIONS IN CUSPED ION THRUSTERS USING THE FINITE ELEMENT METHOD
Yoshihiro Arakawa and Paul J. Wilbur (Colorado State Univ., Fort Collins.) *In* DGLR, DGLR/AIAA/JSASS 20th International Electric Propulsion Conference: Proceedings 1988 p 460-466 (For primary document see N89-27707 22-20)
Avail: NTIS HC A99/MF E03

Using the finite element method, a model describing plasma flows in cusped ion thrusters is developed. This model enables one to calculate ion flow fractions to the discharge chamber surfaces for any cusped field configuration. Numerical examples are presented to demonstrate that this model can be used to obtain plasma density distributions in the discharge chamber and to calculate the extracted ion fraction. From the results, it is concluded that this method is a useful tool for optimizing the magnetic field configurations of discharge chambers. ESA

N89-27761*# Colorado State Univ., Fort Collins. Dept. of Mechanical Engineering.

AN APPROACH TO THE PARAMETRIC DESIGN OF ION THRUSTERS

Paul J. Wilbur, John R. Beattie, and Jay Hyman, Jr. (Hughes Research Labs., Malibu, CA.) *In* DGLR, DGLR/AIAA/JSASS 20th International Electric Propulsion Conference: Proceedings 1988 p 467-475 (For primary document see N89-27707 22-20)

(Grant NGR-06-002-112)

Avail: NTIS HC A99/MF E03 CSCL 10B

A methodology that can be used to determine which of several physical constraints can limit ion thruster power and thrust, under various design and operating conditions, is presented. The methodology is exercised to demonstrate typical limitations imposed by grid system span-to-gap ratio, intragrid electric field, discharge chamber power per unit beam area, screen grid lifetime, and accelerator grid lifetime constraints. Limitations on power and thrust for a thruster defined by typical discharge chamber and grid system parameters when it is operated at maximum thrust-to-power are discussed. It is pointed out that other operational objectives such as optimization of payload fraction or mission duration can be substituted for the thrust-to-power objective and that the methodology can be used as a tool for mission analysis. ESA

N89-27762# Pennsylvania State Univ., University Park. Dept. of Aerospace Engineering.

MAGNETIC INDUCTION THRUSTER WITH LITHIUM PROPELLANT

Stewart A. Burston and Michael M. Micci *In* DGLR, DGLR/AIAA/JSASS 20th International Electric Propulsion Conference: Proceedings 1988 p 476-482 (For primary document see N89-27707 22-20)

Avail: NTIS HC A99/MF E03

A performance comparison is made between a lithium and an aluminum reaction mass expelled from a magnetic induction thruster. The lithium reaction mass was expected to produce higher exit velocities due to its lower density. In addition, examination of the reaction mass material properties, geometry dependence, mass dependence, and dynamic properties are conducted. In the magnetic induction thruster an induced current is produced in a ring-shaped reaction mass. The induced current is opposite to the drive coil current, thus creating opposing magnetic fields that provide the accelerating force to expel the reaction mass. A computer code was used to simulate the magnetic induction thruster by numerically integrating the governing ordinary differential equations by a 4th other Runge-Kutta method. The use of lithium as the reaction mass produced an increase in the exit velocity. The desired material properties of the reaction mass are the lowest possible density and resistivity and highest possible specific heat. The geometry of the reaction mass should be a large radius on the order of the drive coil with a very small cross-sectional area relative to the radius. Large masses of the reaction mass are preferred, since this gives a larger net thrust, but at smaller specific impulses. ESA

N89-27763# Toshiba Corp., Kawasaki (Japan).

EXPERIMENTAL STUDY OF DOUBLE STAGE DISCHARGE HALL ION THRUSTER

Y. Yamagiwa and Kyoichi Kuriki (Tokyo Univ., Sagamihara, Japan) *In* DGLR, DGLR/AIAA/JSASS 20th International Electric Propulsion Conference: Proceedings 1988 p 483-489 (For primary document see N89-27707 22-20)

Avail: NTIS HC A99/MF E03

The double stage Hall ion thruster was studied to find the way of improving the performance and to make clear its accelerations and ion production mechanisms. It was experimentally confirmed that the low efficiency in the case of single stage discharge Hall ion thruster is due to the low energy transfer ratio and the poor stability of the discharge in a strong magnetic field. These faults were overcome by installing the plasma source in the upstream end of the acceleration region. The performance obtained with this improvement is 10 mN thrust, 70 percent propellant utilization efficiency, 600 eV/ion ion production cost, and 14% total efficiency at 1800 sec specific impulse. Comparison between experimental results and theoretical analysis confirms that the low acceleration efficiency in the Hall ion thruster is mainly caused by the anomalous electron back flow due to Bohm diffusion and the wall loss of ions. ESA

N89-27764# United Kingdom Atomic Energy Authority, Culham (England). Culham Lab.

ULTIMATE PERFORMANCE LIMITS AND MISSION CAPABILITIES OF ADVANCED ION THRUSTERS

A. R. Martin, A. Bond, and R. A. Bond *In* DGLR, DGLR/AIAA/JSASS 20th International Electric Propulsion Conference: Proceedings 1988 p 490-498 (For primary document see N89-27707 22-20)

Avail: NTIS HC A99/MF E03

The ultimate performance limits and mission capabilities of a nuclear powered, advanced ion thruster propulsion system were examined. This involves consideration of the ultimate ion thruster capability and performance level, together with power supply output level and specific mass values to be expected for such systems. In deriving the system characteristics, realistic extrapolations of current technology are assumed. ESA

N89-27765# City Univ. of New York, NY. Dept. of Natural Sciences.

INTERSTELLAR FLIGHT: ASPECTS OF BEAMED ELECTRIC PROPULSION

G. L. Matloff and E. F. Mallove (Massachusetts Inst. of Tech., Cambridge.) *In* DGLR, DGLR/AIAA/JSASS 20th International Electric Propulsion Conference: Proceedings 1988 p 499-501 (For primary document see N89-27707 22-20)

Avail: NTIS HC A99/MF E03

Beamed-electric propulsion for near-term interstellar flight is discussed. A radiation pressure-supported laser beam receiver system mounted on the starship is considered. Constructed of perforated solar sail material, this device could be applied on both laser rockets and laser ramjets. The potential performance of laser rockets and ramjets is reviewed in light of performance projections for electric rockets. A representative one-way centuries-long interstellar exploration/colonization mission is defined in terms of mass allotments. For this mission, a comparison of beamed electric ramjet and rocket performance is presented. It is shown that rockets and ramjets have comparable performance for expeditions directed to the nearest stars (Proxima/Alpha Centauri and Barnard's Star). For more distant destinations, the laser ramjet (operating with a solar sail first stage) is superior. Both the ramjet and rocket are assumed to decelerate using identical electric/magnetic drag screens. ESA

N89-27766# Tokyo Univ., Sagamihara (Japan). Inst. of Space and Astronautical Science.

QUANTITATIVE IMAGING OF MPD FLOW FIELDS

T. Nakayama, K. Toki, and Kyoichi Kuriki *In* DGLR, DGLR/AIAA/JSASS 20th International Electric Propulsion Conference: Proceedings 1988 p 507-512 (For primary document see N89-27707 22-20)

Avail: NTIS HC A99/MF E03

Quantitative imaging of magnetoplasmodynamic (MPD) flowfields was made by disturbance-free measurements such as magnetic sensitive film for current, CCD images with interference filters for electron temperature, and far infrared Mach-Zehnder Interferometry for plasma density. Distinct cathode jet accompanying a current concentrated at cathode-tip was observed in molecular propellant, hydrogen, and such wall-detaching plasma confinement inside the self-induced magnetic field is found to be very effective for thruster performance improvements. Ion-neutral momentum coupling in atomic propellant, argon, seems to explain many mysterious behaviors of thruster performances such as dependence on mass flow rate, and N-shaped transition in thrust efficiency versus specific impulse characteristics. These real gas

effects together with interelectrode geometry determine the thruster performance and its flow characteristics. ESA

N89-27767# Ohio State Univ., Marion.
ANALYTICAL AND NUMERICAL SOLUTIONS FOR CYLINDRICAL BLAST WAVES IN A PLASMA OF VARYING DENSITY
Bishun D. Pandey *In* DGLR, DGLR/AIAA/JSASS 20th International Electric Propulsion Conference: Proceedings 1988 p 527-529 (For primary document see N89-27707 22-20)
Avail: NTIS HC A99/MF E03

A nonlinear problem concerning the propagation of a blast wave, satisfying the moving boundary conditions at the shock front of a violent explosion in plasma of varying density, is solved. Such a problem arises in connection with the applications of the schok waves in astrophysics, blast-wave propagation in the ionosphere, problems resulting from laser-ray focusing, explosive detonation, or electrical discharge in high-temperature plasma under laboratory conditions, as well as for explosive magnetohydrodynamic generators. The plasma is assumed to be an ideal gas with infinite electrical conductivity and the source of explosion is a supersonic expansion of the corona which drives an outward flow of the solar gas. It is found that solutions admit another discontinuity, cause a violation of continuum theory in the physical plane, and consequently a cavity is formed. The cavity formation and the effects of the varying density distribution and the magnetic pressure are shown through integral curves. ESA

N89-27768# Toshiba Corp., Kawasaki (Japan).
A 30 cm DIAMETER XENON ION THRUSTER: DESIGN AND INITIAL TEST RESULTS
Y. Yamagiwa, Y. Takeshita, H. Kawauchi, H. Yoshida, D. Miyazaki, T. Higuchi, Katsuhiro Miyazaki, Shoji Kitamura, Y. Hayakawa, and Yoshihiro Nakamura (National Aerospace Lab., Tokyo, Japan) *In* DGLR, DGLR/AIAA/JSASS 20th International Electric Propulsion Conference: Proceedings 1988 p 530-534 (For primary document see N89-27707 22-20)
Avail: NTIS HC A99/MF E03

The design and initial test results of a 30 cm diameter xenon cusp type ion thruster are described. The designed thrust and specific impulse of the laboratory model are 150 mN and 3500 sec, respectively, at the exhaust beam energy of 1.0 keV. With the laboratory model, propellant utilization efficiency of 86 percent, and ion production cost of 176 eV/ion are obtained at the extracted beam energy of 1.0 keV. The critical problems with the discharge and the acceleration of the large ion thruster are clarified. ESA

N89-27769# United Kingdom Atomic Energy Authority, Culham (England).
PROPELLANT SELECTION CRITERIA FOR DEEP SPACE ELECTRICALLY PROPELLED MISSIONS
A. R. Martin and P. M. Latham *In* DGLR, DGLR/AIAA/JSASS 20th International Electric Propulsion Conference: Proceedings 1988 p 535-544 Sponsored by RAE, Farnborough, United Kingdom (For primary document see N89-27707 22-20)
Avail: NTIS HC A99/MF E03

The selection of the optimum propellant for electric propulsion systems providing primary propulsion on deep space science missions is discussed. Candidate propellants are mercury and xenon. Spacecraft and systems designers favor xenon because of its inert nature. On the other hand, cosmochemists express reservations over the use of this element for missions involving the return of pristine primordial material (in the context of a comet nucleus sample return, for example). The interaction of propellant efflux with a spacecraft is investigated computationally, modeling the flux of propellant which reaches surfaces on the spacecraft. The physical and chemical effects on materials are also considered. The potential for contamination of a cometary sample is investigated, showing that the efflux from a xenon propelled system does not present any problems. ESA

N89-27770# Giessen Univ. (Germany, F.R.). First Inst. of Physics.
INERT GAS PERFORMANCE OF THE RIT 35 MAIN PROPULSION UNIT
K. H. Groh, H. W. Loeb, W. Schmidt, B. Schuentz, and E. Zarnitz *In* DGLR, DGLR/AIAA/JSASS 20th International Electric Propulsion Conference: Proceedings 1988 p 545-551 Sponsored by MBB GmbH, Munich, Fed. Republic of Germany and ESA/ESTEC, Noordwijk, Netherlands (For primary document see N89-27707 22-20)
Avail: NTIS HC A99/MF E03

After performance mapping with mercury as the propellant, a second phase was started aiming at the inert gas performance of the RIT 35 with xenon as the propellant. After refurbishment and improvement of the test facility, the RIT 35 motor was modified for xenon introducing a new discharge vessel and a flow controller for the gas supply of the motor. Performance mapping was carried out with a flat extraction grid system already used with mercury. Because of the well-known drawbacks of this system, the fabrication of a dished extraction grid system in parallel was started. ESA

N89-27771# Pennsylvania State Univ., University Park. Dept. of Aerospace Engineering.
CHARACTERISTICS OF FREE-FLOATING NITROGEN AND HELIUM PLASMAS GENERATED IN A MICROWAVE RESONANT CAVITY
Philip Balaam, William Maul, and Michael M. Micci *In* DGLR, DGLR/AIAA/JSASS 20th International Electric Propulsion Conference: Proceedings 1988 p 552-558 (For primary document see N89-27707 22-20)
(Grant AF-AFOSR-0048-84)
Avail: NTIS HC A99/MF E03

Results in a program to establish the behavior and physical characteristics of free-floating nitrogen and helium discharges are presented. The discharges are generated in a microwave resonant cavity operating in the TM012 mode at a frequency of 2.45 GHz, within a 10.2 cm diameter quartz sphere, which allows the discharge to be both free floating and accessible to direct visual observation. Input powers up to 3000 W and gas pressures up to 500 kPa (absolute) are obtainable within the experimental apparatus. It is possible to sustain nitrogen plasmas at pressures up to 40 kPa (absolute) with an input power of 450 W, and helium plasmas at pressures up to 330 kPa (absolute) with an input power of 400 W. With no gas flow, and an input power of 400 W, nitrogen plasmas exhibit a maximum coupling efficiency of 40 percent, and helium plasmas 51 percent. When gas flow is introduced, the corresponding maximum coupling efficiency of the helium plasma reaches 63 percent. ESA

N89-27772# Pennsylvania State Univ., University Park. Dept. of Aerospace Engineering.
NUMERICAL AND EXPERIMENTAL INVESTIGATIONS OF A PROPAGATING MICROWAVE-HEATED PLASMA
Juergen Mueller and Michael M. Micci *In* DGLR, DGLR/AIAA/JSASS 20th International Electric Propulsion Conference: Proceedings 1988 p 559-568 (For primary document see N89-27707 22-20)
(Grant AF-AFOSR-0048-84)
Avail: NTIS HC A99/MF E03

A numerical scheme was used to solve the one-dimensional energy equation for the case of a microwave-heated planar propagating plasma. Results for the propagation velocity, temperature profiles, and the absorbed power were obtained for helium and hydrogen at incident power levels ranging from 100 to 7000 W at a frequency of 2.45 GHz for a waveguide of 7.214 x 3.404 cm cross sectional area. A radiation term was included in the energy equation in order to estimate heat radiation losses from the plasma. The results for the propagation velocities were compared to experimentally obtained data in helium for a waveguide of the same dimensions and the same microwave frequency as mentioned above. ESA

N89-27773*# Michigan State Univ., East Lansing. Dept. of Electrical Engineering.

EXPERIMENTS AND ANALYSIS OF A COMPACT ELECTROTHERMAL THRUSTER

Jes Asmussen and Stan Whitehair (IBM Federal Systems Div., Yorktown Heights, NY.) *In* DGLR, DGLR/AIAA/JSASS 20th International Electric Propulsion Conference: Proceedings 1988 p 569-574 (For primary document see N89-27707 22-20)
(Grant NAG3-305)
Avail: NTIS HC A99/MF E03 CSCL 21H

The description and experimental performance of a compact microwave electrothermal thruster (MET) are presented. This thruster uses a coaxial applicator to couple microwave power into a high pressure discharge. Unlike earlier experiments, it uses no fused quartz in the discharge chamber or the nozzle. This allows high temperatures in the discharge chamber without quartz erosion and melting, thereby improving thruster performance and lifetime. The thruster design is compact, enhancing its potential as a space engine. Experimental tests using nitrogen and helium propellants with input powers levels of 200 W to 1.5 kW are presented. Experimental results, which produce energy efficiencies of 20 to 60 percent and specific impulse of 250 to 450 sec, compare favorably to previous experimental MET performance. ESA

N89-27774# Osaka Univ. (Japan). Faculty of Engineering Science.

ELECTROTHERMAL THRUSTERS UTILIZING ELECTRODELESS DISCHARGES

H. Tahara, Y. Tanaka, K. Onoe, and T. Yoshikawa *In* DGLR, DGLR/AIAA/JSASS 20th International Electric Propulsion Conference: Proceedings 1988 p 575-582 (For primary document see N89-27707 22-20)
Avail: NTIS HC A99/MF E03

Electrothermal thrusters utilizing electrodeless discharges, i.e., inductively coupled high-frequency discharge and microwave cavity resonance one, were designed and tested to investigate the fundamental operational characteristics. An inductively coupled plasma thruster was operated with 2 to 4 kW of 3 MHz high frequency input power, and a microwave cavity resonance plasma thruster with 50 to 650 W of 2.45 GHz microwave input power. Regardless of providing larger-diameter throats, the thrust performances of these thrusters compare favorably with those of conventional electrothermal thrusters such as resistojets and arcjets. The inductively coupled plasma thruster achieves a thrust efficiency of 23.3 percent for argon propellant at a maximum specific impulse of 198 sec, and the microwave cavity resonance plasma thruster 38 percent for mixture propellant of N_2+2H_2 at 265 sec. Electrodeless discharge ion sources are reviewed for efficient electrostatic propulsion development. ESA

N89-27775# Stuttgart Univ. (Germany, F.R.). Inst. fuer Raumfahrtsysteme.

PERFORMANCE CALCULATION OF AN H2 ARCJET BY MEANS OF A DUAL CHANNEL MODEL

H. O. Schrade and P. C. Sleziona *In* DGLR, DGLR/AIAA/JSASS 20th International Electric Propulsion Conference: Proceedings 1988 p 583-590 (For primary document see N89-27707 22-20)
(Contract ESTEC-6784/86/NL/PH(SC))
Avail: NTIS HC A99/MF E03

A model calculation to predict the performance of an arcjet and to provide crude design criteria and scaling laws for a constrictor type hydrogen arc thruster is discussed. In this dual channel model calculation, one divides the nozzle flow into a hot plasma core and a surrounding cold gas layer, both with different expansion velocities, but with the same local pressure across any nozzle cross section. The conditions within the nozzle throat are derived by means of a semiempirical approach as a function of the throat geometry, the arc current, and the mass flow rate. ESA

N89-27776# Kyoto Univ. (Japan). Dept. of Aeronautical Engineering.

NUMERICAL STUDIES OF THE FLOW FIELD IN A dc ARCJET THRUSTER

Michio Nishida, Keiji Kaita, and Ken-ichi Tanaka (Mitsubishi Electric Co., Amagasaki, Japan) *In* DGLR, DGLR/AIAA/JSASS 20th International Electric Propulsion Conference: Proceedings 1988 p 591-597 Original contains color illustrations (For primary document see N89-27707 22-20)
Avail: NTIS HC A99/MF E03

Numerical simulation of a 1 kW class dc arcjet thruster was performed, using the same nozzle geometry as used in laboratory experiments. The governing equations for propellant gas flows consist of the axisymmetric Euler type equations coupled with electromagnetic equations. The propellant flow equations were solved by a time dependent technique using the TVD-MacCormack scheme, and the implicit Forward Time Centered Space (FTCS) method was applied to solve the electromagnetic field. Argon was used as propellant. It was considered that the flow was followed by nonequilibrium ionization-recombination. An inlet flow is considered as subsonic. From the numerical data, the details of thruster flow field heated by Joule heating are revealed. The effect of constrictor geometry on the thruster performance was examined for different constrictor lengths. ESA

N89-27777# Mitsubishi Electric Co., Amagasaki (Japan). Central Research Lab.

COMPUTATIONAL INVESTIGATION ON THE CHARACTERISTICS OF A LOW POWER dc ARCJET THRUSTER

Ken-ichi Tanaka, Kazuo Tsuchiya, Keiji Kaita, and Michio Nishida (Kyoto Univ., Japan) *In* DGLR, DGLR/AIAA/JSASS 20th International Electric Propulsion Conference: Proceedings 1988 p 598-605 Original contains color illustrations (For primary document see N89-27707 22-20)
Avail: NTIS HC A99/MF E03

An investigation on the performance of a low power dc arcjet thruster was conduction using the numerical simulation code in which the inlet flow was treated as subsonic and the nonequilibrium ionization-recombination was considered. The nozzle geometry effect on the performance characteristics was also investigated using a simplified calculation model which was developed from the calculation code described above. The results obtained from the numerical simulation and the experiment for two different nozzle geometries, i.e., conical and bell-shaped nozzles, are qualitatively in good agreement. It is revealed by both the numerical simulation and the experiment that the performance of the bell-shaped nozzle was superior to the conical nozzle. ESA

N89-27778# Stuttgart Univ. (Germany, F.R.). Inst. fuer Raumfahrtsysteme.

A 15 kW EXPERIMENTAL ARCJET

H. L. Kurtz, M. Auweter-Kurtz, B. Glocker, W. D. Merke, and H. O. Schrade *In* DGLR, DGLR/AIAA/JSASS 20th International Electric Propulsion Conference: Proceedings 1988 p 606-611 Sponsored in part by ESA/ESTEC, Noordwijk, Netherlands (For primary document see N89-27707 22-20)
(Contract SNIA-BPD-DSR/DHG/74777/LS)
Avail: NTIS HC A99/MF E03

A laboratory model of a 15 to 20 kW arcjet was developed to obtain insight into the mechanisms of discharge and heat loads. This arcjet is a constrictor type device which consists of a coaxial electrode system with a stack of coaxial segments which are individually water cooled and insulated by each other. These segments are made of copper and each of them can serve alone or together with adjacent segments as anodes. The propellant enters a ring-shaped manifold; from there it flows into the plenum section through four bore holes which are directed tangentially and at 30 deg axially in order to induce an arc stabilizing swirl flow in the plenum chamber. The arcjet is mounted on a constructed thrust balance in a stainless steel tank (1.2 m diameter, 4 m long), which is connected to the vacuum system having a pumping speed of 200,000 cum/hr at 0.1 mbar. Experimental results with

argon as propellant are presented. A 1 kW, regeneratively cooled constrictor arcjet with ammonia as a propellant is presented. A high power (100 kW) hydrogen arcjet thruster built from a concept without a constrictor is described. A hollow cathode discharge in a cylindrical anode is stabilized by a small amount of argon and by an applied magnetic field. The plasma is accelerated through an adjacent nozzle. ESA

N89-27779# Osaka Univ. (Japan). Faculty of Engineering Science.

OPERATING CHARACTERISTICS OF 1 kW HYDRAZINE ARCJET THRUSTER

T. Yoshikawa, K. Onoe, H. Yoshida, S. Kotani, H. Suzuki, and K. Uematsu (Ishikawajima-Harima Heavy Industries Co. Ltd., Tokyo, Japan) *In* DGLR, DGLR/AIAA/JSASS 20th International Electric Propulsion Conference: Proceedings 1988 p 612-619 (For primary document see N89-27707 22-20)

Avail: NTIS HC A99/MF E03

A low power arcjet thruster was tested with hydrogen-nitrogen mixture simulating the decomposition products of hydrazine over a range of arc power from 0.4 to 1.5 kW, in order to develop an arcjet capable of operating stably at 0.5 kW power level. The 50 kHz pulse width modulated (PWM) power source, which has potentials of high response and stable operation against current fluctuation, was designed and tested. Energy loss was studied experimentally, and the arc efficiency is estimated to be 85 percent stable and erosion-free operation is attainable by using the developed soft starting method in combination with the PWM power source. To reduce the frozen flow loss and to enhance the thrust performance, it is remarkably effective to use the smaller constrictor diameter of 0.6 mm and an optimum divergent angle is 40 deg). The thrust efficiency of 32 percent and specific impulse of 520 sec are achieved at 0.6 kW power level, using N2+2H2 as propellant. ESA

N89-27780# Mitsubishi Electric Co., Amagasaki (Japan). Central Research Lab.

EXPERIMENTAL INVESTIGATION ON THE CHARACTERISTICS OF A LOW POWER dc ARCJET THRUSTER

Ken-ichi Tanaka, Kazuo Tsuchiya, Keiji Kaita, and Michio Nishida (Kyoto Univ., Japan) *In* DGLR, DGLR/AIAA/JSASS 20th International Electric Propulsion Conference: Proceedings 1988 p 620-626 (For primary document see N89-27707 22-20)

Avail: NTIS HC A99/MF E03

A low power radiation-cooled dc arcjet thruster was developed and tested. Argon was used as propellant and the performance characteristics of the thruster for mass flow rate and discharge current were investigated by thrust measurement. The typical performance is thrust of 0.35 N and specific impulse of 325 s for the mass flow rate of 0.11 g/s and arc current of 120 A. The exhaust plume from the thruster was diagnosed by measurements of electronic excitation temperature. ESA

N89-27781# United Kingdom Atomic Energy Authority, Culham (England).

OPTICAL EMISSION SPECTRUM OF THE UK-10 ION THRUSTER OPERATING ON XENON

P. M. Latham, A. R. Martin, and M. T. Cresdee *In* DGLR, DGLR/AIAA/JSASS 20th International Electric Propulsion Conference: Proceedings 1988 p 627-633 Sponsored by RAE, Farnborough, United Kingdom (For primary document see N89-27707 22-20)

Avail: NTIS HC A99/MF E03

The optical emission spectrum of the UK-10 thruster operating with a xenon propellant was measured. Measurements of relative intensity were made as a function of wavelength in the range 350 to 850 nm. Two fields of view were investigated, one looking towards the beam a little downstream of the extraction grids, the other looking directly at the grids into the discharge chamber. The data obtained were compared with similar published optical measurements on mercury thrusters, and the implications for integration with spacecraft and specific scientific instruments were reconsidered. No problems are anticipated from this point of view. ESA

N89-27782# Royal Aerospace Establishment, Farnborough (England). Space Dept.

DIAGNOSTIC TOOLS FOR AN ION THRUSTER IN SPACE

G. L. Wrenn, K. A. Ryden, D. G. Fearn, A. R. Martin, P. M. Latham, D. R. Rodgers, D. M. Walton, and A. D. Johnstone (Mullard Space Science Lab., Dorking, England) *In* DGLR, DGLR/AIAA/JSASS 20th International Electric Propulsion Conference: Proceedings 1988 p 634-638 (For primary document see N89-27707 22-20)

Avail: NTIS HC A99/MF E03

The prospects for a wider utilization of ion propulsion are outlined as a prerequisite for assessing their possible impact upon spacecraft systems. A manifest is made of all effects which could be detrimental to spacecraft or payload performance and each is examined in terms of the probable risk and available safeguards. In-flight monitoring of the effects will be essential to demonstrate the viability of any particular ion thruster unit, and various diagnostic instruments are discussed. Computer simulation provides a valuable tool for estimating plasma interaction effects, and initial results from NASCAP are presented. Problem areas are identified and solutions proposed. In some cases, special measuring techniques being developed are described. ESA

N89-27783# Stuttgart Univ. (Germany, F.R.). Inst. fuer Raumfahrtsysteme.

STEADY STATE MPD DEVICES FOR REENTRY SIMULATION

M. Auweter-Kurtz, J. Epple, H. Habiger, H. L. Kurtz, O. Loesener, E. Messerschmid, and D. Mulzer *In* DGLR, DGLR/AIAA/JSASS 20th International Electric Propulsion Conference: Proceedings 1988 p 639-646 (For primary document see N89-27707 22-20)

(Contracts CNES-87/CNES/3315; AMD-BA-ROC-1/87(BEH-2001))

Avail: NTIS HC A99/MF E03

A plasma wind tunnel was built for the testing of reusable thermal protection systems for space transportation vehicles. It consists of a 6 m long, 2 m diameter cooled steel tank, which is connected to a vacuum system and a high power rectifier. The test gases are argon and nitrogen/oxygen mixtures with flow rates of typically 10 g/s. The plasma is created by two different arc heaters. One of these plasma sources is based on a magnetoplasmadynamic thruster. It is a concentric device with a hot cathode and a cold water cooled anode. Due to the glowing cathode, only the nitrogen can be injected in the rear of the accelerator; the oxygen is added in the supersonic part of the nozzle. Contrary to thruster applications, the mass flow is high and the corresponding power level low. The characteristic data of this device, such as voltage/current characteristic, specific enthalpy, thermal efficiency, stagnation pressure, velocity and Mach number are presented, together with the limitations of the plasma generator. A second type of plasma source derived from a high power arc jet was built and first experiments with argon were performed. ESA

N89-27784# Academia Sinica, Beijing (China). Space Science and Technology Center.

A 6 cm DIAMETER ION SOURCE FOR ASSISTANT DEPOSITION

Yuan-Zhu Kuang and Yu-Cai Feng *In* DGLR, DGLR/AIAA/JSASS 20th International Electric Propulsion Conference: Proceedings 1988 p 647-652 (For primary document see N89-27707 22-20)

Avail: NTIS HC A99/MF E03

A 6 cm diameter cusp field ion source was designed for assistant deposition. The results of performance tests are presented. It is shown that by matching the parameters, a good performance can be obtained with this source. In the range of low energy, the beam energy could be as low as 50 eV with 20 mA extracting current and 0.91 beam profile flatness parameter. It is very suitable

for assistant deposition. In the range of extracted voltage from 1000 to 1300 V a focusing-like beam with beam current density as high as 4.2 mA/cm sq can be created and it can be used for sputterring deposition. ESA

N89-27785# Giessen Univ. (Germany, F.R.). First Inst. of Physics.

DEVELOPMENT OF HIGH-CURRENT RF PLASMA SOURCES FOR NEUTRAL PARTICLE INJECTIONS

J. Freisinger, H. Hellmann, M. Kaufmann, H. W. Loeb, A. Scharmann, and W. Kraus (Max-Planck-Inst. fuer Plasmaphysik, Garching, Germany, F.R.) *In* DGLR, DGLR/AIAA/JSASS 20th International Electric Propulsion Conference: Proceedings 1988 p 653-664 Sponsored by Deutsche Forschungsgemeinschaft, Bonn, Fed. Republic of Germany and Max-Planck-Inst. fuer Plasmaphysik, Garching, Fed. Republic of Germany (For primary document see N89-27707 22-20)

Avail: NTIS HC A99/MF E03

For the neutral beam injection heating system of the ASDEX Upgrade tokamak (AUG), the use of an RF-plasma source is envisaged. A circular RF-plasma source RIG 20 was put onto a standard ASDEX extration system and operated. A prototype of a PINI-compatible RF-source RIG-HEX was designed, built, and tested. The RF-discharge power of RIG 20 is 20 kW. For 8 sec up 18 A hydrogen ions were extracted at 40 kV. The beam quality is similar to the standard one, when a periplasmatron or Kaufman-type ion source is used. The atomic species fraction is much higher (80 percent). For the actual injection heating of AUG, a neutral power of 6MW is needed. This power will be delivered by one injector box, equipped with four ion sources; each of them has to produce 85 A at 55 kV. The design of these RF-plasma sources is based on the JET PINI-structure. The RIG-HEX was operated up to a maximum rf-discharge power of 140 kW at 1 MHz. The duty cycle is 10 sec pulse/5 min pause. Inside the discharge volume the local distribution of the plasma current density was measured. Compared to dc-ion sources, twice as high ion beam densities (800 mA/cm sq) are observed. ESA

N89-27786# Giessen Univ. (Germany, F.R.). First Inst. of Physics.

NONPROPULSIVE APPLICATION OF THE RF-ION THRUSTER FOR MATERIAL PROCESSING WITH REACTIVE GASES

J. Freisinger, K. H. Groh, J. Krempel-Hesse, J. M. Krumeich, H. W. Loeb, A. Scharmann, and H. W. Velten *In* DGLR, DGLR/AIAA/JSASS 20th International Electric Propulsion Conference: Proceedings 1988 p 665-673 (For primary document see N89-27707 22-20)

Avail: NTIS HC A99/MF E03

Based on experience with RF-ion thrusters of the RIT-type, an RF-ion beam generator, the RIM 10, for material processing was built and successfully tested. The RIM 10 uses the electrodeless, inductively coupled RF-discharge and a redesigned three-grid ion extraction system. Performance mapping shows ion beam currents up to 300 mA at 1 W/mA specific power consumption and 0.03 sccm gas flow rate per 1 mA. The beam energy can be varied between 25 and 3.5 keV. The beam divergence angle is adjustable between 5 and 40 deg. The RIM 10 was operated with 15 different gases, e.g., Ar, O2, N2, CO2, MgF2, CBrF3, C4H8, SF6, CF2Cl2. Owing to the absence of any filament, RIM 10 is well suited for such reactive gases as oxygen or fluorinated and chlorinated hydrocarbons. At present, RIM 10 is used in forming thin films for optical and mechanical layers, in producing thin high dielectric layers for condensors, and in ion beam assisted vapor deposition. ESA

N89-27787# Southampton Univ. (England).

THE USE OF ELECTRIC PROPULSION TECHNIQUES FOR LEO ATOMIC OXYGEN SIMULATION

M. A. Kinnersley and J. P. W. Stark *In* DGLR, DGLR/AIAA/JSASS 20th International Electric Propulsion Conference: Proceedings 1988 p 674-680 (For primary document see N89-27707 22-20)

(Grant MOD-GR/E/07166)

Avail: NTIS HC A99/MF E03

Space environment simulation using electric propulsion technology is proposed. Orbiting space vehicles operating at altitudes below 1000 km are subject to impact by atmospheric species. Within the altitude range 100 to 900 km the dominant species is atomic oxygen. The velocity of the vehicle through this atmosphere results in an impact velocity of 8 km/s; the flux (altitude sensitive) is typically 10 to the 15th power atoms/sqcm/sec within the shuttle orbit. Electric propulsion techniques, yielding velocities of the same order are thus appropriate for sources attempting to simulate the LEO environment. An arc jet atomic oxygen source and its performance are discussed, particularly improving atomic oxygen flux and velocity. ESA

N89-27788# Academy of Space Technology, Lanzhou (China). Inst. of Physics.

PERFORMANCE RESEARCH OF XENON ION ROCKET ENGINE

N. H. Wang, G. F. Wu, Z. Y. Guo, J. Z. Han, J. M. Qin, N. Wang, W. G. Wang, and Y. D. Chen *In* DGLR, DGLR/AIAA/JSASS 20th International Electric Propulsion Conference: Proceedings 1988 p 681-686 (For primary document see N89-27707 22-20)

Avail: NTIS HC A99/MF E03

Specifications for an ion rocket engine using xenon as propellant, and experiments of the engine are reviewed. Thrust is over 5 mN; anode diameter 9 cm (8 to 12 cm), specific impulse 3000 sec; input power is less than 250 W; power to thrust ratio less than 50 W/mN; propellant utilization over 80 percent; discharge loss 350 eV/ion; starting time less than 20 min; cathode operation lifetime (first phase) over 500 hrs; cathode starting cycle (first phase) 1000 times; total weigh 21 kg. ESA

N89-27789# Texas A&M Univ., College Station. Advanced Nuclear Fuels Lab.

KREM: A MODEL FOR EVALUATING ORBITAL TRANSFER VEHICLES UTILIZING NUCLEAR ELECTRIC PROPULSION SYSTEMS

W. F. Lyon *In* DGLR, DGLR/AIAA/JSASS 20th International Electric Propulsion Conference: Proceedings 1988 p 687-692 (For primary document see N89-27707 22-20)

Avail: NTIS HC A99/MF E03

The KREM computer model was designed to evaluate performance of conceptual spacecraft designs utilizing nuclear electric propulsion systems for orbital transfer missions. The code features an interactive input environment so that the user may easily specify the parameters available for characterization of a given mission study. Empirical models for an argon magneto-plasmadynamic (MPD) and a hydrogen arcjet thruster system are included in KREM. There are also two types of nuclear power sources represented. In addition to the thruster and power systems, the user may specify the target orbit and inclination, one-way or roundtrip transfers, the payload mass, power level, and analysis mode. The variety of analysis options available allows KREM to solve for the minimum transfer time, the optimized transfer, or analyze a variety of missions at once. In order to evaluate and demonstrate the operation of KREM, analyses of vehicle performance for a reference low Earth orbit to geosynchronous orbit mission were conducted for both the MPD and arcjet thruster systems. The MPD thruster requires less total mass to complete the reference mission throughout the entire range of operation as compared to the arcjet thruster system. However, the arcjet thruster achieves lower transfer times up to levels of 1300 sec specific impulse. ESA

N89-27790# Maxwell Labs., Inc., San Diego, CA.

CAPACITORS FOR PULSED ELECTRIC PROPULSION

Rolf Dethlefsen and Joel Ennis *In* DGLR, DGLR/AIAA/JSASS 20th International Electric Propulsion Conference: Proceedings 1988 p 693-701 (For primary document see N89-27707 22-20)

Avail: NTIS HC A99/MF E03

Capacitive energy storage for electric propulsion systems is reviewed. Of the major categories of dielectrics, polymer films offer the best characteristics for repetitively pulsed, high average power operation at high specific energy and specific power levels, except at relatively low voltages. Improvements in dielectric film and capacitor manufacturing technology led to order-of-magnitude increases in energy density and a widening range of operating voltage and other parameters since the early 1960s. The current trend in applications is toward low dielectric loss capacitors operated at reduced stress levels and high repetition rates for long life and high average power. ESA

N89-27791*# National Aeronautics and Space Administration. Lyndon B. Johnson Space Center, Houston, TX.
A TANDEM MIRROR HYBRID PLUME PLASMA PROPULSION FACILITY
F. R. Chang-Diaz, T. F. Yang, W. A. Krueger, S. Peng, J. Urbahn, X. Yao, and D. Griffin (Massachusetts Inst. of Tech., Cambridge.) *In* DGLR, DGLR/AIAA/JSASS 20th International Electric Propulsion Conference: Proceedings 1988 p 702-707 Sponsored in part by AFOSR, Washington, DC (For primary document see N89-27707 22-20)
Avail: NTIS HC A99/MF E03 CSCL 10B

A concept in electrodeless plasma propulsion, which is also capable of delivering a variable Isp, is presented. The concept involves a three-stage system of plasma injection, heating, and subsequent ejection through a magnetic nozzle. The nozzle produces the hybrid plume by the coaxial injection of hypersonic neutral gas. The gas layer, thus formed, protects the material walls from the hot plasma and, through increased collisions, helps detach it from the diverging magnetic field. The physics of this concept is evaluated numerically through full spatial and temporal simulations; these explore the operating characteristics of such a device over a wide region of parameter space. An experimental facility to study the plasma dynamics in the hybrid plume was built. The device consists of a tandem mirror operating in an asymmetric mode. A later upgrade of this system will incorporate a cold plasma injector at one end of the machine. Initial experiments involve the full characterization of the operating envelope, as well as extensive measurements of plasma properties at the exhaust. The results of the numerical simulations are described. ESA

N89-27792# European Space Agency. European Space Research and Technology Center, ESTEC, Noordwijk (Netherlands).
FIELD EMISSION ELECTRIC PROPULSION (FEEP): EXPERIMENTAL INVESTIGATIONS ON CONTINUOUS AND PULSED MODES OF OPERATION
C. Petagna, H. vonRohden, C. Bartoli, and D. Valentian (Societe Europeenne de Propulsion, Vernon, France) *In* DGLR, DGLR/AIAA/JSASS 20th International Electric Propulsion Conference: Proceedings 1988 p 708-721 (For primary document see N89-27707 22-20)
Avail: NTIS HC A99/MF E03

The development status of the FEEP system is presented together with an outline of its capabilities for spacecraft orbit control and/or drag compensation. The results of tests with a single slit solid emitter operated in both the continuous and the pulsed mode are reported. The analysis of the results indicates that FEEP thrusters can be successfully operated in pulsed mode and confirms the validity of this operation mode for demanding attitude control missions like fine pointing and fine stationkeeping between clustered spacecraft. ESA

N89-27793# Naval Postgraduate School, Monterey, CA.
PARTICLE SIZING IN SOLID ROCKET MOTORS M.S. Thesis
Douglas Lyle Hovland Mar. 1989 110 p
(Contract F04611-88-X-0021)
(AD-A208740) Avail: NTIS HC A06/MF A01 CSCL 21/8

Particle size distribution measurements were made with a Malvern 2600c forward laser light diffraction system across the exhaust nozzle entrance and exhaust plume of a small two-dimensional rocket motor. The solid propellants tested were GAP propellants containing 2.0 and 4.69 percent aluminum. Surface agglomeration of the aluminum, indicated by the in-motor results, was found to decrease as the motor chamber pressures were increased. At low pressures, increasing the aluminum loading with fixed total solids decreased the mean particle size at the nozzle entrance. Exhaust plume particle size was practically independent of nozzle inlet particle diameters, supporting the critical Weber number particle breakup theory. Initial validation of the Malvern 2600c measurements was accomplished by favorable comparison to exhaust plume particle distribution results obtained using a particle collection probe. GRA

23 CHEMISTRY AND MATERIALS (GENERAL)

No abstracts in this category.

24 COMPOSITE MATERIALS

Includes physical, chemical, and mechanical properties of laminates and other composite materials.
For ceramic materials see *27 Nonmetallic Materials.*

N89-27794# Japan Atomic Energy Research Inst., Tokyo.
IRRADIATION EFFECTS ON RESISTANCE OF THERMAL IMPACT OF COMPOSITE USED IN SPACE
Tsuneo Sasuga, Sigenori Egusa, Akira Udagawa, Tadao Seguchi, Naoyuki Tamura, Takayuki Kamiyama, Noriaki Sugahara, Takeshi Nakao, Yujiro Yoshioa, and Tosio Sakakibara Nov. 1988 34 p In JAPANESE; ENGLISH summary
(DE89-778069; JAERI-M-88-238) Avail: NTIS (US Sales Only) HC A03/MF A01

Electron irradiation effects on mechanical properties at low(-100 C), high(100 C) and room temperatures, and on the cyclic thermal impact from high(100 C) to low(-90 C) were studied for IM-6/R376 composite in which modified TGDDM-DDS matrix was reinforced by a high strength inter mediate modules carbon fiber(IM-6) and T-300/3601 composite which was composed of non-modified TGDDM-DDS matrix and a high strength carbon fiber(T-300), and then adaptability of these materials to environments of space was evaluated. LISS was decreased by irradiation over 10 MGy in IM-6/R6376 composite and 20 MGy in T-300/3601 composite, but the tensile and compression strength at low, high and room temperatures were scarcely affected by irradiation up to 10 MGy. When unirradiated T-300/3601 composite was subjected by thermal impact, many microcracks were produced and the compression strength decrease to 90 percent of the initial value but the production on microcrack and decreasing in the compression strength by thermal impact tended to become less in the irradiated specimen. On the other hand, in the unirradiated IM-6/R6376 composite production of microcrack was not observed by thermal impact and decrease in strength was less but microcracks were produced and the strength decrease by thermal impact after irradiation. In the case of irradiation after thermal impact, radiation effects were not observed. It was concluded from these results that both the composites have enough resistance against environmental radiation in space, and IM-6/R6376 composite is excellent more than T-300/3601 composite in consideration of resistane for thermal impact. DOE

N89-27795*# National Aeronautics and Space Administration. Lewis Research Center, Cleveland, OH.
COMPUTATIONAL SIMULATION OF HIGH TEMPERATURE METAL MATRIX COMPOSITES CYCLIC BEHAVIOR
C. C. Chamis, P. L. N. Murthy, and D. A. Hopkins 8 Nov. 1988 15 p Presented at the ASTM Symposium on Thermal and

Mechanical Behavior of Ceramic and Metal Matrix Composites, Atlanta, GA, 7-8 Nov. 1988
(NASA-TM-102115; E-4888; NAS 1.15:102115) Avail: NTIS HC A03/MF A01 CSCL 11D

A procedure was developed and is described which can be used to computationally simulate the cyclic behavior of high temperature metal matrix composites (HTMMC) and its degradation effects on the structural response. This procedure consists of HTMMC mechanics coupled with a multifactor interaction constituent material relationship and with an incremental iterative nonlinear analysis. The procedure is implemented in a computer code that can be used to computationally simulate the thermomechanical behavior of HTMMC starting from the fabrication process and proceeding through thermomechanical cycling, accounting for the interface/interphase region. Results show that combined thermal/mechanical cycling, the interphase, and in situ matrix properties have significant effects on the structural integrity of HTMMC. Author

N89-27796*# National Aeronautics and Space Administration. Lewis Research Center, Cleveland, OH.
TUNGSTEN FIBER REINFORCED COPPER MATRIX COMPOSITES: A REVIEW
David L. McDanels Sep. 1989 24 p
(NASA-TP-2924; E-4318; NAS 1.60:2924) Avail: NTIS HC A03/MF A01 CSCL 11D

Tungsten fiber reinforced copper matrix (W/Cu) composites have served as an ideal model system with which to analyze the properties of metal matrix composites. A series of research programs were conducted to investigate the stress-strain behavior of W/Cu composites; the effect of fiber content on the strength, modulus, and conductivity of W/Cu composites; and the effect of alloying elements on the behavior of tungsten wire and of W/Cu composites. Later programs investigated the stress-rupture, creep, and impact behavior of these composites at elevated temperatures. Analysis of the results of these programs as allows prediction of the effects of fiber properties, matrix properties, and fiber content on the properties of W/Cu composites. These analyses form the basis for the rule-of-mixtures prediction of composite properties which was universally adopted as the criteria for measuring composite efficiency. In addition, the analyses allows extrapolation of potential properties of other metal matrix composites and are used to select candidate fibers and matrices for development of tungsten fiber reinforced superalloy composite materials for high temperature aircraft and rocket engine turbine applications. The W/Cu composite efforts are summarized, some of the results obtained are described, and an update is provided on more recent work using W/Cu composites as high strength, high thermal conductivity composite materials for high heat flux, elevated temperature applications. Author

N89-27797# Manchester Univ. (England). Materials Science Centre.
HIGH PERFORMANCE COMPOSITES BASED ON POLYURETHANES REINFORCED WITH POLYDIACETYLENES Final Report, Dec. 1986 - Dec. 1987
John L. Stanford and Robert J. Young 4 Apr. 1989 62 p
(Contract DAJA45-86-C-0058; DA Proj. 1L1-61103-BH-57)
(AD-A208436; R/D-4858A-MS-01) Avail: NTIS HC A04/MF A01 CSCL 11/4

This final report covers all the work carried out during the period from December 1986 to December 1987. The scientific program was concerned with the development of high performance composites based on various linear and crosslinked polyurethane matrices reinforced with high strength and high stiffness polydiacetylenes, incorporated either as single crystal fibers or as dispersed hard segment domains. The report is therefore presented in two parts and entitled; Formation and Properties of Fiber Reinforced Composites: polyurethane Resins containing Polydiacetylene Single Crystal Fibers; Formation and Properties of Molecular Composites: Polyurethane-Diacetylene Segmented Copolymers. GRA

N89-27798# Princeton Univ., NJ. Dept. of Chemical Engineering.
ANOMALOUS STRESSES VERSUS EXTENT OF CURE IN AN EPOXY COMPOSITE SPECIMEN Technical Report, 7 Jan. 1987 - 15 Jun. 1989
M. A. Taylor and John K. Gillham Jun. 1989 45 p
(Contract N00014-84-K-0021)
(AD-A208523; TR-20) Avail: NTIS HC A03/MF A01 CSCL 11/4

Recent studies on the properties of high T sub g epoxy systems (i.e., di functional aromatic epoxy resins cured with tetrafunctional aromatic diamines) have shown that, with increasing conversion, the room temperature density increases prior to gelation but decreases after gelation. The lower room temperature modulus and higher equilibrium moisture absorption at higher conversions have been attributed to the lower density. The anomalous behavior has been explained using the concept of free volume and the nonlinear increase of T sub g with conversion. GRA

N89-27799# Texas A&M Univ., College Station. Dept. of Aerospace Engineering and Mechanics and Materials Center.
ULTRASONIC NONDESTRUCTIVE EVALUATION OF DAMAGE IN CONTINUOUS FIBER COMPOSITES Final Report, 1984 - 1988
Vikram K. Kinra and Vinay Dayal 1989 92 p Repr. from Sadhana (India), v. 2, Dec. 1987 p 419-432
(Grant AF-AFOSR-0066-84; AF Proj. 2308)
(AD-A208840; AFOSR-87-2033TR) Avail: NTIS HC A05/MF A01 CSCL 11/4

A new technique for measuring the wavespeed and attenuation in the thickness direction, in extremely thin laminates, and the excitation and detection of Lamb waves in the lengthwise direction was developed. Thus both in-plane and out-of-plane and out-of-plane measurements can be made. Damage in the form of transverse cracking in cross-ply graphite/epoxy laminates was studied by the use of these two techniques. For through-the-thickness measurements the stiffness was found to be insensitive to transverse cracking. The attenuation, however, was found to be quite sensitive and, therefore, was shown to be a reliable damage metric. For the complementary case of Lamb wave propagation in the lengthwise direction, both the stiffness and the attenuation were observed to be sensitive damage parameters. GRA

N89-27800# Israel Inst. of Metals, Haifa.
COATING AND IMPREGNATION OF CARBON-CARBON COMPOSITES WITH CERAMICS BY ELECTROPHORETIC DEPOSITION Final Scientific Report, 1 Mar. 1988 - 28 Feb. 1989
L. Gal-Or and S. Liubovich Apr. 1989 84 p
(Grant AF-AFOSR-0097-88; AF Proj. 2306)
(AD-A208873; AFOSR-89-0685TR) Avail: NTIS HC A05/MF A01 CSCL 11/4

Electrophoretic deposition of ceramic coatings on porous graphite and on a 2-D C-C composite was studied using colloidal and fused SiO2, SiC and SiN. It was shown that all these ceramic materials acquire an electric charge and hence deposit under the electric field. In addition to the formation of a surface deposit, the induction of particles into the pores of porous graphite was demonstrated. The effects of deposition voltage, solvent properties and particle concentration on penetration were studied by examination of cross-sections in the SEM and by quantitative analysis of induced SiO2. Ceramic deposits of CeO2, ZrO2 and Al2O3 were formed on graphite and 2-D C-C by an electrochemical reduction of aqueous solutions containing inorganic salts of the appropriate metals. GRA

N89-27801# University Coll. of North Wales, Bangor. School of Electronic Engineering Science.
PIEZOELECTRIC POLYMER/CERAMIC COMPOSITE Final Report, Jun. 1986 - Aug. 1988
D. K. Das-Gupta 2 May 1989 76 p

(Contract DAJA45-86-C-0034; DA Proj. 1L1-61103-BH-57)
(AD-A208905; R/D-5496-MS-01) Avail: NTIS HC A05/MF A01 CSCL 11/4

Composite films of lead zirconate titanate (PZT)/poly vinylidene fluoride (PVDF), PZT/Copolymer of vinylidene fluoride - trifluorethylene (VDF-TrFE) and Barium titanate (BaTiO3)/PVDF were prepared in our laboratories and their electrical, dielectric and pyroelectric properties were investigated. PZT phase appears to provide a significant contribution to the electrical conductivity of these composites whereas the dielectric dispersion is influenced by the polymer and copolymer phase. The composite film of PZT/VDF-TrFE appears to be an attractive electro-active material with a pyroelectric coefficient an order of magnitude greater than that of PVDF whereas its figure of merit is significantly higher than that of PZT. GRA

N89-27802# Stanford Univ., CA. Div. of Applied Mechanics.
MECHANICAL RESPONSE OF STRUCTURAL ELEMENTS TO DYNAMIC LOADS Final Report, 1 Sep. 1977 - 31 Dec. 1978
George Herrmann Jan. 1979 4 p
(Grant AF-AFOSR-3403-77; AF Proj. 2307)
(AD-A209827; AFOSR-89-0956TR) Avail: NTIS HC A02/MF A01 CSCL 11/4

The general objectives of the activities under this grant consisted of acquiring more detailed and complete knowledge of dynamic response of laminated composites. Specifically, wave propagation in a periodically layered elastic body in plane strain was studied and a considerable number of numerical results were worked out. Both real and complex branches of the dispersion spectrum were considered. The spectrum was shown to be multivalued and quite intricate in detail. Some analytical properties of the Floquet surface were also established. An analytical study of a plane wave in plane strain is exceedingly involved due to the coupling between longitudinal and shear waves. GRA

25 INORGANIC AND PHYSICAL CHEMISTRY

Includes chemical analysis, e.g., chromatography; combustion theory; electrochemistry; and photochemistry.

For related information see also *77 Thermodynamics and Statistical Physics.*.

N89-27803# Cornell Univ., Ithaca, NY. Dept. of Chemistry.
ADSORPTION AND REACTIONS OF CYCLIC SULFIDES ON Mo(110)
Maria Jose Calhorda, Roald Hoffmann, and Cynthia M. Friend (Harvard Univ., Cambridge, MA.) Apr. 1989 56 p
(Contract N00014-82-K-0576)
(AD-A207324; TR-42) Avail: NTIS HC A04/MF A01 CSCL 07/4

Molecular orbital calculations of the chemisorption and reactivity of ethylene sulfide and trimethylene sulfide on molybdenum-110 are presented, and compared to similar binding in model discrete Mo complexes. The calculations suggest preferred bonding of the cyclic sulfides on 2- or 3-fold sites of the surface, by the expected S-lone pair donor mechanism. The concerted elimination of ethylene or cyclopropane is much easier on the surface than it is in model organometallic molecules. The activation barrier for ethylene sulfide decomposition calculated is substantially smaller than for trimethylene sulfide. Various nonconcerted mechanisms and the role of coadsorbed sulfur and hydrogen were also probed. GRA

N89-27804# Rochester Univ., NY. Dept. of Chemistry.
TRANSITION METAL ACTIVATION AND FUNCTIONALIZATION OF CARBON-HYDROGEN BONDS Progress Report, 1 Dec. 1988 - 30 Nov. 1989
William D. Jones Jun. 1989 26 p
(Contract DE-FG02-86ER-13569)
(DE89-012949; DOE/ER-13569/3) Avail: NTIS HC A03/MF A01

The continued investigation of the fundamental thermodynamic and kinetic factors that influence carbon-hydrogen bond activation at homogeneous transition metal centers is examined. The project is also directed toward the conversion of hydrocarbons into functionalized products of potential use to chemical industry. The goals during the grant period will be: (1) to identify new transition metal complexes capable of activating arene and alkane C-H bonds, (2) to quantitatively evaluate the kinetic and thermodynamic stability of these complexes, and (3) to examine routes for functionalization of the activated hydrocarbons. These studies will also contribute toward the formulation of a unified theory of C-H bond activation that applies to other transition metal complexes. The specific complexes involved in these studies are derivatives of the formulation (C5Me5)Rh(PR3)(R)H, Fe(PMe3)2(CNR)3, Ru(PR3)4-(R)H, and Rh(CNR)3H. Functionalization will focus upon isocyanide and acetylene insertion reactions. New compounds that activate hydrocarbon C-H bonds include HRe(PR3)5, HRe(PR3)2(CNR)3, CpRe(PR3)H4, CpRe(PR3)2H2, (eta ^{6}-C6H6)Re(PPh3)2H, and MnH3(dmpe)2. In the third year, significant advances were made in the observation of eta sup 2-arene complexes of (C5Me5)Rh(PMe3). The complex (C5Me5)Rh(PMe3)(eta sup 2-phenanthrene) was structurally characterized. Several other eta sup 2-complexes were also prepared. DOE

N89-27805# Texas Technological Univ., Lubbock. Dept. of Chemistry and Biochemistry.
NOVEL APPROACHES TO IONIC CHROMATOGRAPHY Progress Report, 1 Dec. 1987 - 30 Jun. 1989
Purnendu K. Dasgupta Jul. 1989 19 p
(Contract DE-FG05-84ER-13281)
(DE89-013942; DOE/ER-13281/5) Avail: NTIS HC A03/MF A01

Work continued on ion chromatography. The following research areas are discussed: (1) fluorogenic ligands, chelating surfactants and metal determinations. The use of sulfoxines in fluorescence detection is addressed. Chromatographic detection of Al, Ga, and In was undertaken; (2) membrane suppressers; (3) a novel suppresser reaction and detection of weak acids via indicators reactions; and (4) DC conductivity detection and stopped flow chromoamperometry. DOE

N89-27806# Pacific Northwest Labs., Richland, WA.
ELECTROSPRAY IONIZATION-MASS SPECTROMETRY AND TANDEM MASS SPECTROMETRY
J. A. Loo, C. J. Barinaga, C. G. Edmonds, H. R. Udseth, and R. D. Smith May 1989 3 p Presented at the American Society for Mass Spectroscopy Annual Symposium, Miami Beach, FL, 22-26 May 1989
(Contract DE-AC06-76RL-01830)
(DE89-014465; PNL-SA-16621; CONF-8905166-1) Avail: NTIS HC A02/MF A01

The ability to produce multiply charged molecular ions for biomolecules allows mass spectrometers to analyze compounds with molecular weights much in excess of the instrument's mass limit, but within the mass-to-charge range of most conventional mass spectrometers. In fact, proteins with molecular weights in excess of 130,000 daltons were successfully analyzed by EIS-MS with a quadrupole mass spectrometer of limited m/z range (1700) in the laboratory. The ESI mass spectra of large proteins was compared with and without reduction of its disulfide bridges. By cleavage of cysteine-cysteine bonds and thereby affecting the tertiary structure of the protein, a dramatic increase in the number of positive charges is observed. Highly charged ions desorbed from the droplets are sampled through a nozzle-skimmer orifice to be detected by the quadrupole mass spectrometer. Increasing collision energies also yields significant fragmentation of large peptide and proteins. DOE

N89-27807# SRI International Corp., Menlo Park, CA.
MULTIPHOTON DETECTION TECHNIQUES FOR F AND F2 Annual Technical Report, Apr. 1988 - Mar. 1989
G. W. Faris, M. J. Dyer, and D. L. Huestis 28 Apr. 1989 17 p

(Contract F49620-88-K-0003; AF Proj. 2308)
(AD-A208576; SRI-MP-89-106; AFOSR-89-0712TR) Avail: NTIS HC A02/MF A01 CSCL 07/4

During the last year experiments were performed that will lead to the development of quantitative remote diagnostics for atomic and molecular fluorine, using ultraviolet multiphoton excitation followed by the detection of fluorescence or ionization. The first demonstaton is described for resonant multiphoton excitation of molecular fluorine and the construction of a new apparatus for high-sensitivity detection of atomic fluorine using two-photon absorption of 170-nm radiation from a narrow-band tunable ArF laser, Raman shifted in liquid-nitrogen-cooled HD. GRA

N89-27808# Wisconsin Univ., Madison. Dept. of Chemistry.
SELECTIVE DETECTOR FOR GAS CHROMATOGRAPHY BASED ON ADDUCT-MODULATED SEMICONDUCTOR PHOTOLUMINESCENCE
George C. Lisensky, Gerald J. Meyer, and Arthur B. Ellis 12 May 1989 19 p Submitted for publication Sponsored by 3M Co.
(Contract N00014-85-K-0631)
(AD-A208616; UWIS/DC/TR-89/1) Avail: NTIS HC A02/MF A01 CSCL 14/2

The photoluminescence (PL) of semiconducting n-CdS, Te-doped CdS, and CdSe can be used as the basis for a nondestructive, selective detector for gas chromatography. When placed in a series with the Thermal Conductivity Detector (TCD) of a gas chromatograph, the semiconductor responds in parallel with the TCD to species that can engage in adduct formation: PL intensity is enhanced by Lewis bases-like amines and quenched by Lewis acids such as carboxylic acids, relative to the intensity observed in the He carrier gas. Gases that interact more weakly with the semiconductor surface like hydrocarbons are not detected by the PL-based detector. For a n-CdS:Te detector, linear response regimes and detection limits were determined as being approx. 0.1 to 3.0 micro-g and 0.1 micro-g for n-butylamine and approx. 0.2 to 1.5 mg and 0.2 mg for acetic acid. GRA

N89-27809# Membrane Technology and Research, Inc., Menlo Park, CA.
SEPARATION OF OXYGEN FROM SEAWATER BY MEMBRANE PERMEATION Final Technical Report, 31 Aug. - 28 Feb. 1989
C. M. Bell, P. Chow, and R. W. Baker Mar. 1989 28 p
(Contract DAAA01-88-C-0414)
(AD-A208863) Avail: NTIS HC A03/MF A01 CSCL 07/1

A reliable and compact system able to extract dissolved oxygen from seawater is required for a number of naval applications. This proposal describes the application of a membrane process called pervaporation to the problem of oxygen separation. Seawater containing dissolved air is brought in contact with a suitable membrane, and the dissolved air preferentially permeates the membrane. In this Phase 1 program, two thin-film composite membranes were evaluated, and the feasibility of the approach was demonstrated using a small bench-scale system fitted with a 6-sq m spiral-would membrane module. Approximately 40 percent of the dissolved oxygen in seawater could be removed in a single pass through the membrane module. The oxygen concentration of the permeate gas was 33 percent. A technical analysis was conducted for the application of this technology for: (1) life support on submarines, and (2) oxygen supply for submerged fuel cells. The analysis showed the fuel cell application to be the most promising. In this application, the power consumption of the oxygen extraction process is 25 percent of the energy produced by the fuel cell. GRA

N89-27810# California Univ., Los Angeles. Dept. of Materials Science and Engineering.
OPTICAL SPECTROSCOPY OF COPPER (1) DOPED Na(+) BETA-ALUMINA Technical Report No. 18, Aug. 1988 - Jul. 1989
J. D. Barrie, Bruce Dunn, Gary Hollingsworth, and Jeffrey I. Zink 15 Jun. 1989 28 p Submitted for publication
(Contract N00014-83-K-0498)
(AD-A209819) Avail: NTIS HC A03/MF A01 CSCL 07/4

The luminescence spectra of copper(+) doped sodium(+) Beta alumina single crystals reveal emission bands due to both Cu(+) monomers and Cu(+) - Cu(+) dimers. At low temperature two monomer emissions (410 nm and 440 nm) and two dimer emissions (515 nm and 540 nm) are observed. These bands are assigned to ions in specific sites within the Beta alumina conduction plane. The relative intensities of the emission bands are dependent on the sequence of irradiation and cooling. Changes in the relative intensities are caused by the photo-aggregation of the mobile Cu(+) ions to form dimers. These changes are an example of optical memory. The growth of the dimer emission band under ultraviolet excitation is a diffusion controlled process. The quenching of the monomer emission with increasing temperature correlates well with ionic hopping processes. The dynamics of ion motion which produce the green dimer emission band are quantified by a model based upon the thin film solution of Fick's second law. GRA

N89-27811# Wyoming Univ., Laramie. Dept. of Chemistry.
THE QUARTZ CRYSTAL MICROBALANCE AS AN IN SITU TOOL IN ELECTROCHEMISTRY Technical Report No. 5, Sep. 1988 - Jun. 1989
Daniel A. Buttry 29 Jun. 1989 35 p Submitted for publication
(Contract N00014-89-K-0674)
(AD-A209852) Avail: NTIS HC A03/MF A01 CSCL 07/4

By the very nature of the phenomena studied, electrochemistry deals extensively with interfacial processes. Both in application and in fundamental studies, knowledge of the types and amounts of various species which exist at the electrode/electrolyte interface is essential to a molecular level understanding of the relationship between structure and function in electrochemical phenomena. Consequently, many different types of experimental techniques were applied towards this end. Improvements in the sensitivity of such techniques have pushed the detection limits for interfacial species to monolayer and even submonolayer levels. This Chapter describes the use of the quartz crystal microbalance (QCM) to measure minute mass changes at electrode surfaces, in-situ, during electrochemical processes. It will be seen that, in favorable cases, these mass changes reveal changes in the populations of interfacial species which are associated in some way with the electrochemical processes. This Chapter will focus on the considerations regarding application of the QCM to studies of mass changes at electrode surfaces during redox events and will present some representative examples illustrating what can be achieved with the method. Underpotential deposits, polymer modified electrodes are discussed. GRA

N89-27812# Wyoming Univ., Laramie. Dept. of Chemistry.
APPLICATIONS OF THE QUARTZ CRYSTAL MICROBALANCE TO ELECTROCHEMISTRY Technical Report No. 6, Sep. 1988 - Jun. 1989
Daniel A. Buttry 29 Jun. 1989 92 p Submitted for publication
(Contract N00014-89-K-0674)
(AD-A209853) Avail: NTIS HC A05/MF A01 CSCL 07/4

The quartz crystal microbalance (QCM) is a piezoelectric device capable of extremely sensitive mass measurements. It oscillates in a mechanically resonant shear mode by application of an alternating, high frequency electric field using electrodes which are usually deposited on both sides of the disk. These devices were used for many years to measure the masses of thin films in various types of deposition processes. To the extent that the density of the deposit is known, the thickness may be calculated, so these devices are used in a number of commercial film thickness monitors. Konash, Bastiaans and Nomura demonstrated the use of the QCM in the liquid environment for the determination of mass changes at the crystal surface. These reports made clear the potential utility of the QCM for accurate, in situ determinations of extremely small mass changes of the crystal electrodes or films deposited on them. GRA

N89-27813# Pennsylvania Univ., Philadelphia. Dept. of Materials Science and Engineering.
PROTONIC SOLID ELECTROLYTES: THERMAL STABILITY AND CONDUCTIVITY OF AMMONIUM/HYDRONIUM BETA'-ALUMINA Technical Report No. 9, 1987 - 1989
J. D. DeNuzzio and G. C. Farrington 1989 13 p Submitted for publication
(Contract N00014-81-K-0526)
(AD-A209911) Avail: NTIS HC A03/MF A01 CSCL 07/4

Ammonium/hydronium Beta-alumina, (NH4/H3O)(1.67)-AlMG(0.67)(10.33)O17, is an unusually stable and conductive solid electrolyte for protonic ions. Its conductivity at 200 C, for example, reaches about .01 (ohms/cm). The composition, stability, and ionic conductivity of ammonium/hydronium Beta'-alumina are described by means of chemical analysis, TGA, DSC, and complex impedance analysis. The results demonstrate that ammonium/hydronium Beta'-alumina has a preferential composition of (NH4)1.0(H3O)0.67Mn(0.67)Al-(10.33)O17, which corresponds to a rather elegant, albeit only hypothetical at this time, ordered arrangement of ammonium ions, hydronium ions, and vacancies in the structure . Ammonium/hydronium Beta'-alumina decomposes below 350 C in discrete and reversible reactions that yield water and ammonia. The conductivity of single crystals of (NH4)1.0(H3O)0.67Mg(0.67)Al(10.33)O17 obeys an Arrhenius relationship below 200 C with an activation energy of 0.26 eV (sigma = .001/ohms/cm at 2 C). GRA

N89-27814# Cincinnati Univ., OH. Dept. of Chemistry.
COMPARISON OF VACUUM-ANNEALED AND ELECTROCHEMICALLY CYCLED ELECTRODES IN ADSORPTION AND ELECTROCATALYSIS: AROMATIC COMPOUNDS AT PLATINUM (111) AND POLYCRYSTALLINE PLATINUM
John Y. Gui, Bruce E. Kahn, Laarni Laguren-Davidson, Chiu-Hsun Lin, and Frank Lu 1989 11 p
(Grant AF-AFOSR-0200-86; AF Proj. 2303)
(AD-A210011; AFOSR-89-0925TR) Avail: NTIS HC A03/MF A01 CSCL 07/4

These studies compare adsorbed layer vibrational spectra and packing densities of various aromatic compounds at annealed platinum (111) and polycrystalline Pt surfaces (Pt(poly)) with the behavior of surfaces pretreated by electrochemical cycling (the oxidation-reduction procedure commonly employed to pretreat electrodes prior to use). Surface structural changes produced by cycling exert a profound effect upon each of the properties studied. Absorbates studied represent various types of surface attachment: hydroquinone (HQ), which displays pi-bonding to Pt surfaces (horizontal orientation) when adsorbed from sufficiently dilute aqueous solutions; 2,2',5,5'-tetrahydroxy biphenyl (THBP), which adopts a mixture of horizontal and vertical orientations; 3-thiophene carboxylic acid (3TCA), (3-pyridyl) hydroquinone (3PHQ), and nicotinic acid (NA), which exhibit primarily sigma-bonding (tilted vertical orientation); and benzyl mercaptan (BM) and 2,5-dihydroxy 4-methylbenzyl mercaptan (DMBM), for which attachment occurs through a sulfur atom to form a benzyl pendant. Packing densities (moles adsorbed per unit area) were measured for each compound at each surface by Auger spectroscopy. Surface vibrational spectra were obtained by electron energy loss spectroscopy (EELS) and were assigned by comparison with the IR spectra of the pure compounds. Substrate surfaces were characterized by LEED. Cycling the Pt(111) surface affects the adsorbate packing density by up to 50 percent, while smaller effects are observed for Pt(poly). GRA

N89-27815# Utah Univ., Salt Lake City. Dept. of Chemistry.
QUANTITATIVE ESTIMATION OF COMPONENT AMPLITUDE IN MULTIEXPONENTIAL DATA: APPLICATION TO TIME-RESOLVED FLUORESCENCE SPECTROSCOPY Technical Report, No. 15, Jul. 1988 - Jul. 1989
A. L. Wong and J. M. Harris 1 Jul. 1989 33 p Submitted for publication
(Contract N00014-89-J-1412)
(AD-A210142) Avail: NTIS HC A03/MF A01 CSCL 07/4

Quantitative information of individual component contribution from multiexponential data is obtained by a reiterative, linear least squares algorithm. Uncertainty in the parameter estimates, arising from uncertainty in the data and overlap in the response, are predicted from first principles. The analysis method includes weighting to account for the Poisson error distribution arising from shot-noise limited signals, which increases the accuracy of the amplitude estimates. While the algorithm is applicable to a variety of kinetic methods, it is applied in the present work to the analysis of time resolved fluorescence decay curves. A fluorescence decay curve, written as a row vector, D, is decomposed into two factors: A, a column vector containing the amplitude contribution of each component, and C, a matrix which contains temporal behavioral of each component in its rows. The analysis uses linear least squares to obtain estimates of A, which increases the efficiency by reducing the number of parameters which are searched. The theory of error in linear least squares allows the uncertainty of the component amplitudes to be determined from the C matrix, derived from best estimates of the temporal behavioral of the sample. GRA

26 METALLIC MATERIALS

Includes physical, chemical, and mechanical properties of metals, e.g., corrosion; and metallurgy.

N89-27816# Denver Univ., CO.
AN ACOUSTIC EMISSION INVESTIGATION OF THE TENSILE FAILURE OF CATHODICALLY CHARGED 304 STAINLESS STEEL
Steve H. Carpenter, Xu Wei, and Daniel R. Smith, Jr. 1988 7 p Presented at the 9th International Symposium on Acoustic Emission, Kobe, Japan, 1 Nov. 1988
(Contract DE-FG02-85ER-45182)
(DE89-008752; CONF-8811186-1) Avail: NTIS HC A02/MF A01

It has been shown that by using different heat treatments and cathodic charging, a variety of crack modes could be obtained in 304 stainless steel. Using double cantilever beam specimens, the accoustic emission (AE) generated during crack propagation was measured and characterized. It was found that the type of crack propagation could be identified from the characteristics of the AE waveforms. The purpose of the investigation was to see if similar results could be obtained during the tensile fracture of 304 stainless steel. Results are presented which clearly demonstrate that the type of crack mode in tensile fracture can be determined from careful analysis of the AE waveforms. DOE

N89-27817# Dartmouth Coll., Hanover, NH. School of Engineering.
THE STRUCTURE AND PROPERTIES OF GRAIN BOUNDARIES IN B2 ORDERED ALLOYS Progress Report
I. Baker 21 Apr. 1989 14 p
(Contract DE-FG02-87ER-45311)
(DE89-013266; DOE/ER-45311/2) Avail: NTIS HC A03/MF A01

A number of fine grained alloys of FeAl and NiAl with different aluminum contents were produced by multiple hot extrusion. Thus far, researchers have characterized the extruded microstructures of the alloys; initiated mechanical testing which confirms that with increasing deviation from stoichiometry the yield strength of FeAl decreases while that for NiAl increases and which shows the grain boundary strengthening in NiAl decreases with increasing deviation from stoichiometry; performed grain growth studies of NiAl and FeAl. For FeAl alloys it was found that grain growth is more rapid in the iron-rich composition. An atom probe field ion microscope (APFIM) study was continued of the grain boundary chemistry of NiAl. Boundary chemistry in near-stoichiometric NiAl and FeAl was studied using scanning Auger electron spectroscopy. In-situ

straining experiments in the transmission electron microscope to examine dislocation/grain boundary interactions. DOE

N89-27818*# Ribbon Technology Corp., Gahanna, OH.
RAPIDLY SOLIDIFIED TITANIUM ALLOYS BY MELT OVERFLOW
Thomas A. Gaspar, Thomas J. Bruce, Jr., Lloyd E. Hackman, Susan E. Brasmer, Jonathan A. Dantzig, and William A. Baeslack, III (Ohio State Univ., Columbus.) Washington Sep. 1989 96 p
(Contract NAS1-18288)
(NASA-CR-4253; NAS 1.26:4253) Avail: NTIS HC A05/MF A01 CSCL 11F

A pilot plant scale furnace was designed and constructed for casting titanium alloy strips. The furnace combines plasma arc skull melting techniques with melt overflow rapid solidification technology. A mathematical model of the melting and casting process was developed. The furnace cast strip of a suitable length and width for use with honeycomb structures. Titanium alloys Ti-6Al-4V and Ti-14Al-21 Nb were successfully cast into strips. The strips were evaluated by optical metallography, microhardness measurements, chemical analysis, and cold rolling. Author

N89-27819# National Inst. of Standards and Technology, Gaithersburg, MD. Metallurgy Div.
INSTITUTE FOR MATERIALS SCIENCE AND ENGINEERING: METALLURGY DIVISION, TECHNICAL ACTIVITIES 1988 Annual Report
Dec. 1988 121 p
(PB89-201321; NISTIR-88/3843) Avail: NTIS HC A06/MF A01 CSCL 11F

The FY 1988 activities of the Metallurgy Division of the National Institute of Standards and Technology (NIST) are summarized. Research on the structure-processing-properties relations of metals and alloys and on the methods of their measurement is presented. The generation and evaluation of critical materials data are also reported, along with studies of metallurgical processing, corrosion, mechanical properties, electrodeposition, process sensors, high temperature reactions and magnetic materials. Work done on four cooperative programs with American professional societies and industry is also included: (1) the National Association of Corrosion Engineers (NACE) - NIST Corrosion Data Program; (2) the Aluminum Association - NIST Temperature Sensor Program; (3) the American Iron and Steel Institute (AISI) - NIST Steel Sensor Program; and (4) the ASM INTERNATIONAL (ASM) - NIST Alloy Phase Diagram Program. GRA

N89-27820# Nebraska Univ., Lincoln.
FUNDAMENTAL MAGNETIC STUDIES OF IRON-RARE-EARTH-METALLOID ALLOYS Technical Performance Report
David J. Sellmyer and George C. Hadjipanayis (Kansas State Univ., Manhattan.) 6 Dec. 1988 11 p
(Contracts DE-FG02-86ER-45262; DE-FG02-86ER-45263)
(DE89-013803; DOE/ER-45262/T1) Avail: NTIS HC A03/MF A01

This research is focused on the synthesis of new iron-rare-earth magnetic phases which may have significant technological properties. An important aim is to investigate new methods for producing these materials such as melt spinning and sputtering plus specific heat treatments. Studies are made of the relationship between microstructure and properties such as coercivity, spontaneous magnetization, and anisotropy (magnitude and direction) in bulk and thin film samples. Our goal is to understand these relatively complex materials on the basis of fundamental electronic structure. The theory is of itinerant magnetism and localized 4f electronic states, and the microstructural effects which control the extrinsic properties. To achieve this a broad range of experiments and calculations are performed. DOE

N89-27821# Argonne National Lab., IL.
ION-ASSISTED DEPOSITION OF SILVER FILMS ON CERAMICS FOR FRICTION AND WEAR CONTROL
A. Erdemir, G. R. Fenske, R. A. Erck, and C. C. Cheng 1989 36 p Presented at the 44th Annual STLE Meeting, Atlanta, GA, 1 May 1989
(Contract W-31-109-eng-38)
(DE89-014635; CONF-8905168-1) Avail: NTIS HC A03/MF A01

Development and implementation of novel surface modification methods for controlling friction and wear of ceramic surfaces are of crucial importance to the success of ceramic tribosystems. Frictional heat, tribochemical interactions, and microfracture during sliding contact give rise to severe wear damage and frictional instabilities in tribosystems consisting of ceramic materials. A new approach is introduced to surface modification involving ion assisted deposition (IAD) of silver films on alumina and sapphire ceramics to achieve improved adhesion, friction, and wear behavior. The results of pin-on-disc experiments showed that silver films produced by IAD were very adherent and the wear rates of ceramic substrates coated with IAD silver were negligible. The friction coefficients of ceramic substrates were also substantially reduced by these silver films. Without ion assistance, silver films severely delaminated from the wear tracks of ceramic substrates and the wear rates and friction coefficients were relatively high. DOE

N89-27822# Bhabha Atomic Research Centre, Bombay (India). Radiometallurgy Div.
LASER PROCESSING OF METALS AND ALLOYS
G. L. Goswami, Dilip Kumar, and P. R. Roy 1988 87 p
(DE89-613235; BARC-1431) Avail: NTIS (US Sales Only) HC A05/MF A01

Due to its high degree of coherence, a laser can produce powder density in the range of 10(3) to 10(11) W/sq mm. This high power density of the laser beam enables it to be utilized for many industrial applications, e.g., welding, cutting, drilling, surface treatment, etc. Laser processing of materials has many advantages, e.g., good quality product at high processing speed, least heat affected zone, minimum distortion, etc. In addition, the same laser system can be utilized for different applications, a very cost effective factor for any industry. Therefore laser has been adopted for processing of different materials for a wide range of applications and is now replacing conventional materials processing techniques on commercial merits with several economic and metallurgical advantages. Applications of laser to process materials of different thicknesses varying from 0.1 mm to 100 mm have demonstrated its capability as an important manufacturing tool for engineering industries. While lasers have most widely been utilized in welding, cutting and drilling they have also found applications in surface treatment of metals and alloys, e.g., transformation hardening and annealing. More recently, there is a significant amount of research being undertaken in laser glazing, laser surface alloying and laser cladding for obtaining improved surface properties. The status of laser processing of metals and alloys is reviewed emphasizing its metallurgical aspects and deals with the different laser processes like welding, cutting, drilling and surface treatment highlighting the types and choice of laser and its interaction with metals and alloys and the applications of these processes. DOE

N89-27823# Nottingham Univ. (England). Dept. of Chemistry.
CORROSION OF ALUMINIUM ALLOYS BY IRFNA (INHIBITED RED FUMING NITRIC ACID) Final Report
M. F. Dove, N. Logan, J. P. Mauger, and J. F. Richings Feb. 1989 55 p
(Contract DAJA45-87-C-0050)
(AD-A208326; R/D-5878-CH-01) Avail: NTIS HC A04/MF A01 CSCL 11/6

It has been demonstrated electrochemically (by corrosion potential-time, polarization resistance and Tafel behavior) that the presence of a high concentration of Cu(2+) ions (580 wpm) in IRFNA (Inhibited Red Ruming Nitric Acid) does not lead to an increase in the corrosion rate of aluminum alloy in this liquid oxidizer, or to any significant change in the corrosion potential of the system. The effect of the addition of water, to give an appreciably over-propellant specification level (6.75 wt. percent H2O), on the corrosion rate of aluminum alloy in IRFNA containing

initially 2.79 wt. percent H2O has been investigated by corrosion potential-time polarization resistance and a.c. impedance measurements. The results indicate an order of magnitude increase in corrosion rate and an apparent increase in film thickness, following the addition of water. The effects of variations in IRFNA composition on the corrosion rate of aluminum alloy in IRFNA using four pairs of electrochemical cells, each pair containing IRFNA obtained from a different source, have also been studied. The electrochemical results indicate that the alloy corrodes at a similar rate in IRFNA obtained from three different sources. Auger electron spectroscopy has been used to monitor the effects of certain surface pre-treatments and exposure to IRFNA of samples of aluminum alloy. GRA

N89-27824# Harvard Univ., Cambridge, MA. Dept. of Chemistry.
FORMATION OF MONOLAYERS BY THE COADSORPTION OF THIOLS ON GOLD: VARIATION IN THE LENGTH OF THE ALKYL CHAIN Interim Technical Report
Colin D. Bain (Cambridge Univ., England) and George M. Whitesides May 1989 81 p Submitted for publication
(Contract N00014-85-K-0898; NR Proj. 356-856)
(AD-A208386; TR-18) Avail: NTIS HC A05/MF A01 CSCL 07/4

Mixtures of two long-chain alkanethiols, HS(CH2)nX and HS(CH2)mY (X, Y = CH3, OH; n greater than m), in which the alkyl chains have different lengths, adsorb from solution onto gold and form monolayers comprising a densely packed inner region adjacent to the gold surface and a disordered outer region in contact with the solution. When X = Y = CH3 (n = m), this disordered phase makes the mixed monolayer more oleophilic than the ordered, pure (i.e., single-component) monolayers. When X = Y = OH, the pure monolayers are wet by water, but the mixed monolayers are less hydrophilic because nonpolar polymethylene chains are exposed at the surface. When X = Ch3, Y = OH (n = 21, m = 11), a very sharp transition occurs from a monolayer composed largely of the longer, methyl-terminated component to the shorter, hydroxyl-terminated component as the mole fraction of HS(CH2)11OH in the adsorption solution is increased. From solutions containing two thiols, adsorption of the thiol with the longer chain is preferred. This preference is greater when the monolayers are adsorbed from ethanol than from isooctane. The mixed monolayers do not act as ideal two-dimensional solutions. The adsorption isotherms suggest a positive excess free energy of mixing of the two components in the monolayer. The compositions of the monolayers appear to be determined largely by thermodynamics, although in some cases there is also a kinetic contribution to the composition. GRA

N89-27825# United Kingdom Atomic Energy Authority, Risley (England).
ADVANCED TRIBOLOGICAL COATINGS FOR HIGH SPECIFIC STRENGTH ALLOYS Progress Report No. 4, 29 Sep. 1988 - 29 Mar. 198 9
29 Mar. 1989 3 p
(Contract DAJA45-89-C-0044)
(AD-A208504; R/D-5876-MS-01-4) Avail: NTIS HC A02/MF A01 CSCL 11/3

It was intended to select the most promising surface treatments and arrange coating of rolling contact, fatigue and pin/disc tribometer specimens to evaluate their friction, wear and fatigue properties. GRA

N89-27826# Illinois Univ., Urbana. Dept. of Materials Science and Engineering.
HIGH TEMP TOUGHENING AND CREEP STUDIES Final Report, 1 Jun. 1985 - 28 Feb. 1989
Waltraud M. Kriven 11 May 1989 128 p
(Grant AF-AFOSR-0242-85; AF Proj. 2306)
(AD-A208714; AFOSR-89-0688TR) Avail: NTIS HC A07/MF A01 CSCL 07/2

Early in 1985, the lanthanide sesquioxides (Ln2O3) were identified as potential high temperature transformation tougheners alternative to zirconia (ZrO2). Their 8 to 10 percent volume increase accompanying the monoclinic (B) to cubic (C) transformation suggested that they should be more powerful than ZrO2. In addition, the Ms temperature was raised up to 2200 C indicating that, based on thermodynamics alone, transformation toughening up to this temperature should be possible. Hence a proposal was written with the aim of transformation toughening silicon carbide (SiC) with dispersions of monoclinic dysprosia particles giving a microstructure analogous to Zirconia-Toughened-Alumina (ZTA). GRA

N89-27827# Saarland Univ., Saarbrucken (Germany, F.R.). Inst. for Metal Physics and Metallurgy.
MARTENSITIC PHASE TRANSITIONS IN NANOCRYSTALLINE MATERIALS Final Technical Report, 2 Dec. 1986 - 2 Dec. 1988
Herbert Gleiter 15 May 1989 16 p
(Contract DAJA45-87-C-0008)
(AD-A208804; R/D-5647-MS-01) Avail: NTIS HC A03/MF A01 CSCL 11/6

The martensitic transformation in Fe-Ni alloys (Ni content between 31 wt percent and 36 wt percent) was studied by means of X-ray diffraction and transmission electron microscopy in nanocrystalline specimens (polycrystals with a crystal size of 4 nm) as well as in a loose powder of 4 nm sized, isolated Fe-Ni crystals with the same chemical compositions as the nanocrystalline materials. The isolated crystals were embedded in pure paraffin. The result obtained indicates that a martensitic transformation does not occur in the nanocrystalline material because the formation of a martensitic nuclei is inhibited due to the small size of the crystals. The inhibition of a martensitic phase transition may be of technological interest for the generation of improved superconducting, ferromagnetic and ferroelectric materials. GRA

N89-27828# San Antonio Air Logistics Center, Kelly AFB., TX.
ANALYSIS AND ELIMINATION OF HIGH TEMPERATURE NOTCH INDUCED MICROCRACK INITIATION IN INCONEL 718 NICKEL-BASED ALLOY
1989 56 p
(AD-A209695) Avail: NTIS HC A04/MF A01 CSCL 20/11

A mechanism for eliminating high temperature notch induced microcrack initiation within Inconel 718 was formulated by correlating the dislocation theory of precipitation hardening with plane stress experimental results obtained at elevated temperatures. Elimination of notch sensitivity was found to be possible by means of innovative treatment that increased the average distance between precipitates in this alloy from 50 to 167 atomic spaces without a prohibitive reduction of yield strength. This distance modification is critical as it must be sufficient to enable dislocation line segments to pass between susceptible to notch induced microcrack initiation. It is revealed that it is the spacing and not the size of the precipitates that determine the yield point of Inconel 718. GRA

N89-27829# Lockheed Missiles and Space Co., Palo Alto, CA.
EFFECT OF ALLOYING, RAPID SOLIDIFICATION, AND SURFACE KINETICS ON THE HIGH TEMPERATURE ENVIRONMENTAL RESISTANCE OF NIOBIUM Technical Report, Nov. 1985 - Jan. 1989
R. A. Perkins, K. T. Chiang, G. H. Meier, and R. A. Miller (Pittsburgh Univ., PA.) 23 Jun. 1989 145 p
(Contract F49620-86-C-0018)
(AD-A209934; LMSC/F352227; AFOSR-89-0909TR) Avail: NTIS HC A07/MF A01 CSCL 11/6

Factors affecting the formation of protective alumina scales on niobium-base alloys by selective oxidation have been investigated. Alumina cannot be formed in air at latm. on binary Nb-Al alloys at any N(Al). Theoretical knowledge of selective oxidation has been applied to Nb-Al alloys to alter behavior. The effects of Al-content, temperature, atmosphere, third element additions, and microstructure on the transition from internal to external oxidation of aluminum has been evaluated and conditions under which protective alumina scales can form on Nb-Al alloys

have been defined. Third element additions are required to form protective alumina. The most effective additions are those which can reduce the solubility and diffusivity of oxygen, enhance diffusion of Al, and limit transient oxidation. Additions of Ti, Cr, V and Si were identified as most promising for providing oxidation resistance in Nb-Al alloys. The feasibility of forming compact, adherent alumina scales on Nb alloys at a minimum N(Al)=0.32 in air at 1100 to 1600 C has been demonstrated. Alumina scale could not be formed Relow 1100 C. Preoxidation above 1100 C can be used to preform alumina scales that wil protect at lower temperatures but is effective only if the alloy is not cooled to room temperature prior to exposure at lower temperatures. Rapid solidification processing does not appear to offer any significant benefit. GRA

N89-27830# Illinois Univ., Urbana. Laser Aided Materials Processing Lab.
LASER CLADDING OF Ni, Nb, Mg ALLOYS FOR IMPROVED ENVIRONMENTAL RESISTANCE AT HIGH TEMPERATURES Final Report, Nov. 1985 - Oct. 1988
J. Mazumder, S. Sircar, A. Kar, C. Ribaudo, and R. Lober Jan. 1989 64 p
(Grant AF-AFOSR-0333-85)
(AD-A210134; AFOSR-89-0778TR) Avail: NTIS HC A04/MF A01 CSCL 11/6

This report summarizes experimental and theoretical studies carried out during the period of November 1985 to October 1988 on laser surface modification of Nickel, Niobium, and Magnesium alloys for improved environmental resistance at high temperature. Major emphasis has been on Ni-Cr-Al-Hf system. Microstructural evolution and oxidation properties of Ni and Nb alloys were examined. For Mg alloys microstructural characterization and potentiodynamic corrosion testing were carried out. A one-dimensional diffusion model for finite domain to examine the extended solid solubility in laser cladding was also developed. GRA

27 NONMETALLIC MATERIALS

Includes physical, chemical, and mechanical properties of plastics, elastomers, lubricants, polymers, textiles, adhesives, and ceramic materials.

For composite materials see *24 Composite Materials*.

N89-27831# National Inst. of Standards and Technology, Gaithersburg, MD. Ceramics Div.
VAPOR PHASE DEPOSITION STUDIES OF PHOSPHATE ESTERS ON METAL AND CERAMIC SURFACES Final Report
Douglas E. Deckman, Stephen M. Hsu, and E. Erwin Klaus (Pennsylvania State Univ., University Park.) Sep. 1988 37 p
(PB89-148985; NIST/SP-754; LC-88-600578) Avail: NTIS HC A03/MF A01; also available SOD HC $8.50 as 003-003-02912-2 CSCL 11B

The study focuses on a novel means of lubrication for ceramics and metals at high temperatures called vapor phase lubrication. The deposition rate and mechanisms of tributyl phosphate ester and tricresyl phosphate ester hzve been explored. A Thermalgravimetric Analyzer (TGA) was modified to measure the rate of surface film formation of vapor phase deposition of lubricants on metal surfaces at elevated temperatures. Results from TGA studies showed that the vapor deposition process was a complex function of substrate, time, and temperature. Tricresyl phosphate ester (TCP) and tributyl ester (TBP) were observed to produce similar amounts of film on stainless steel substrates. The observed order of metal activity was copper greater than stainless steel greater than nickel greater than platinum. Film formation on nickel was found to be much more rapid at 600 C than 700 C. Also, the concentration of oxygen present during deposition strongly influenced the amount of film formed. Scanning electron microscopy was conducted on TBP films formed on Si3N4, Al2O3, and alpha-SiC. The films produced contained globule and filamentous structures. The films on each ceramic were unique, demonstrating that vapor deposition is surface sensitive on ceramic substrates. High temperature friction testing was conducted on a TCP coated Al2O3 substrate. The coating reduced the friction level for alumina, thus demonstrating the potential of vapor lubrication for high temperature lubrication of ceramics. Author

N89-27832# Honeywell, Inc., Bloomington, MN. Sensors and Signal Processing Lab.
ELECTRONIC PROPERTIES OF ORDERED LADDER POLYMERS Final Report, 23 Mar. 1986 - 23 Mar. 1988
Samson A. Jenekhe Jan. 1989 91 p
(Contract F33615-85-C-5091)
(AD-A207288; AFWAL-TR-88-4244) Avail: NTIS HC A05/MF A01 CSCL 07/4

Experimental studies of the electronic and electrical properties of high temperature ordered ladder polymers, exemplified by benzimidazobenzophenanthroline type ladder polymer (BBL) and ladder polyhydroquinoxalines (PHQXL), are reported. In addition, results are presented of studies on the structural, electrochemical, and mechanical properties of undoped insulting and doped chain and ladder polymers as well as a novel processing approach for the rigid chain an ladder polymers. The two types of ladder polymers investigated, BBL and PHQXL were found to be insulators in the undoped state. However, upon chemical, electrochemical, or ion implantation doping the room temperature electrical conductivity of films of these ladder polymers was enhanced up to 2 to 220 ohm cm depending on the method of doping. Thus, high temperature potential electronic and aerospace applications. GRA

N89-27833# Army Lab. Command, Watertown, MA. Material Technology Lab.
SOLVENT ASSISTED DELAMINATION CRACK GROWTH BEHAVIOR OF AMORPHOUS THERMOPLASTIC MATERIALS Final Report
Alex J. Hsieh and Janice J. Vanselow Feb. 1989 20 p Presented at CRDEC Conference on Chemical Defense Research, Aberdeen Proving Ground, MD, 15-18 Nov. 1988
(AD-A207365; MTL-TR-89-17) Avail: NTIS HC A03/MF A01 CSCL 11/4

Crack growth studies are being carried out with oxylene in an amorphous thermoplastic, polyetherimide (PEI), via a static deadweight loading apparatus. The three systems evaluated were the neat resin, composite, and adhesively bonded composite. The neat resin specimens show striation-like crack growth band markings on the fracture surfaces. The spacing between the growth bands increases with increasing crack length in each specimen. In the case of the adhesively bonded composite, a characteristic mosaic pattern of intersecting cracks normal to the plane of the adhesive was seen on the fracture surfaces. There cracks, as well as matrix cracks perpendicular to the fibers seen on the fractured composite specimens, appear to result from residual stress driven solvent cracking. Although the rates of crack propagation in the composite systems are much slower than those in the neat resin at most GI values, the mode of solvent-induced degradation is shown to be matrix dominated. GRA

N89-27834# Sandia National Labs., Albuquerque, NM.
CERAMIC JOINING IN THE UNITED STATES
Ronald E. Loehman 1988 11 p Presented at the Conference on Interfaces and Ceramic Joining, Petten, Netherlands, 20 Apr. 1988
(Contract DE-AC04-76DP-00789)
(DE89-009323; SAND-88-1112C; CONF-8804256-1) Avail: NTIS HC A03/MF A01

Most U.S. government-funded ceramic joining research and development is sponsored by the US Department of Energy (DOE). Historically, this work has not been funded as a stand-alone effort, but rather as a component of the ceramic engine program sponsored by DOE. That program had its genesis with the Advanced Gas Turbine (AGT) Project, which was conducted by two teams, each consisting of a turbine manufacturer and an automobile company. The successors to the AGT Project are the Automotive Technology Development Program and the Fossil

Energy Heat Engines Program, both of which are sponsered by DOE. Most of the DOE ceramic research and development related to heat engines is accomplished as part of the Ceramic Technology for Advanced Heat Engines Project managed by Oak Ridge National Laboratory (ORNL). The ORNL Cermamic Technology Project supports the component development portion of the DOE heat engine program. A small amount of joining R and D is funded by the DOE Office of Energy Utilization Research, Energy Conversion and Utilization Technologies (ECUT) division. Short descriptions and fundings for these various projects is given. K.C.D.

N89-27835# Michigan Univ., Ann Arbor. Coll. of Engineering.
NONLINEAR VISCOELASTIC CHARACTERISTICS OF POLYMERIC MATERIALS Final Report, 1 Sep. 1986 - 28 Feb. 1989
S. K. Clark Jun. 1989 8 p
(Contract DE-FG02-86ER-13599)
(DE89-012680; DOE/ER-13599/T1) Avail: NTIS HC A02/MF A01

Results are presented from an experimental program in which the interaction of load, time, and temperature were examined on the deformation characteristics of polymeric cords, with particular emphasis on nylon cord used in tire construction. Thermal contraction effects generally tend to be negative on such materials, but can be overridden by applied loads. These factors are described experimentally and efforts are made to explain the basis for them and to provide an analytical framework for their description. DOE

N89-27836*# National Aeronautics and Space Administration. Lewis Research Center, Cleveland, OH.
ION BEAM AND PLASMA METHODS OF PRODUCING DIAMONDLIKE CARBON FILMS
Diane M. Swec, Michael J. Mirtich, and Bruce A. Banks Aug. 1988 17 p Presented at the 32nd Annual International Technical Symposium on Optical and Optoelectronic Applied Science and Engineering, San Diego, CA, 14-19 Aug. 1988; sponsored in part by Society of Photo-Optical Instrumentation Engineers
(NASA-TM-102301; E-4980; NAS 1.15:102301) Avail: NTIS HC A03/MF A01 CSCL 11G

A variety of plasma and ion beam techniques was employed to generate diamondlike carbon films. These methods included the use of RF sputtering, dc glow discharge, vacuum arc, plasma gun, ion beam sputtering, and both single and dual ion beam deposition. Since films were generated using a wide variety of techniques, the physico-chemical properties of these films varied considerably. In general, these films had characteristics that were desirable in a number of applications. For example, the films generated using both single and dual ion beam systems were evaluated for applications including power electronics as insulated gates and protective coatings on transmitting windows. These films were impervious to reagents which dissolve graphitic and polymeric carbon structures. Nuclear reaction and combustion analysis indicated hydrogen to carbon ratios to be 1.00, which allowed the films to have good transmittance not only in the infrared, but also in the visible. Other evaluated properties of these films include band gap, resistivity, adherence, density, microhardness, and intrinsic stress. The results of these studies and those of the other techniques for depositing diamondlike carbon films are presented. Author

N89-27837# Oak Ridge National Lab., TN.
THE TEXTURE VARIATION IN EXTRUDED GRAPHITE
C. R. Kennedy, D. O. Hobson, and E. M. Woodruff (Westinghouse Hanford Co., Richland, WA.) 1989 2 p Presented at the 19th Biennial Conference on Carbon, University Park, PA, 25 Jun. 1989 Sponsored in part by Martin Marietta Energy Systems, Inc.
(Contracts DE-AC05-84OR-21400; DE-AC06-76RL-01857)
(DE89-014086; CONF-890627-2) Avail: NTIS HC A02/MF A01

The effect of the extrusion process in creating a significant variation in the preferred orientation has been demonstrated. The variation in physical properties, primarily dependent on crystallite orientation (CTE, electrical resistivity, and elastic constants), is shown to be in good agreement with calculated values. TSX graphite is also shown to have a preferred orientation in flaw structure as determined by sonic attenuation measurements. The expected variability in strength, using a fracture mechanics approach, is described. The effect of this variability also has been shown to have a strong effect on the dimensional change in grade TSX under nuclear irradiation. DOE

N89-27838# Massachusetts Inst. of Tech., Cambridge. Dept. of Mechanical Engineering.
EQUIPMENT MODELS FOR PROCESS OPTIMIZATION AND CONTROL USING SMART RESPONSE SURFACES
E. Sachs, G. Prueger, and R. Guerrieri (Bologna Univ., Italy) Mar. 1989 31 p Sponsored in cooperation with the Microelectronics and Computer Technology Corp.
(Contract N00014-85-K-0213)
(AD-A208321; VLSI-Memo-89-513) Copyright Avail: NTIS HC A03/MF A01 CSCL 20/4

An equipment model has been developed for the low pressure chemical vapor deposition of polycrystalline silicon in a horizontal tube furnace. The model predicts the wafer-to-wafer deposition rate down the length of the tube. Inputs to the model include: silane flow rates from three injectors, injector locations, locations of and temperatures of three thermocouples, operating pressure, the number of wafers, wafer diameter, the location of the wafer load, and other physical dimensions of the furnace such as tube length, and inner diameter. The model is intended to aid the process engineer in the operation of equipment, and the equipment designer in the design of new equipment. The one dimensional finite difference model encompasses the convective and diffusive fluxes of silane and hydrogen in the annular space between the wafer load and tube walls. The reaction of silane is modeled, including the generation and transport of hydrogen. Kinetic and injection parameters in the model were calibrated using a series of nine statistically designed experiments. The model accurately predicts the axial deposition profile over the full range of experimentation and demonstrates good extrapolation beyond the range of experimental calibrations. The model was used to predict a set of process parameters that would result in the least variation of deposition rate down the tube. The predicted parameters agree well with experimentally determined optimum conditions. GRA

N89-27839# Massachusetts Inst. of Tech., Cambridge. Microsystems Research Center.
COMPARISON OF EQUIPMENT MODELING METHODS AS APPLIED TO THE LPCVD OF IN-SITU P-DOPED POLYSILICON M.S. Thesis
Parmeet Singh Chaddha Mar. 1989 70 p
(Contracts MDA972-88-K-0008; N00014-85-K-0213)
(AD-A208373; VLSI-Memo-89-517) Copyright Avail: NTIS HC A04/MF A01 CSCL 20/12

The orthogonal array design of experiments for process and equipment optimization is combined with a semi-empirical modelling approach based on dimensional analysis. This methodology is applied to In-Situ Phosphorus Doped Polysilicon Process via LPCVD. Taguchi's method of pure empiricism works well for the optimization of four different responses-thickness uniformity across the wafer, uniformity in a batch, growth rate, and the film resistivity for the process under consideration. The average thickness uniformity growth rate of 998 A/min. and a resistivity of 1.25 mohm-cm are achieved. However, the dependence of Taguchi's method on the assumption that the process is free of parameter interactions distorts the prediction of nominal-is-the-best-signal-to-noise ratio for the film thickness uniformity across the wafer. As a solution to such problems of purely experimental approach a thirteen terms semi-empirical model based on dimensional analysis is evolved for the film thickness uniformity in the process under consideration by using stepwise regression. GRA

N89-27840# Harvard Univ., Cambridge, MA. Dept. of Chemistry.
MODELLING ORGANIC SURFACES WITH SELF-ASSEMBLED MONOLAYERS Interim Technical Report
Colin D. Bain (Cambridge Univ., England) and George M. Whitesides May 1989 37 p Submitted for publication
Sponsored by NSF
(Contract N00014-85-K-0898; NR Proj. 356-856)
(AD-A208385; TR-20) Avail: NTIS HC A03/MF A01 CSCL 07/3

The interfacial properties of organic materials are of critical importance in many applications, especially the control of wettability, adhesion, tribology, and corrosion. The relationships between the microscopic structure of an organic surface and its macroscopic physical properties are, however, only poorly understood. This short review presents a model system that has the ease of preparation and the structural definition required to provide a firm understanding of interfacial phenomena. Long-chain thiols, HS(CH2)nX, adsorb from solution onto gold and form densely packed, oriented monolayers. By varying the terminal functional group, X, of the thiol, organic surfaces can be created having a wide range of structures and properties. GRA

N89-27841# Massachusetts Inst. of Tech., Cambridge. Dept. of Chemistry.
BIRTH, DEATH AND TRANSFIGURATION: THE SYNTHESIS OF PRECERAMIC POLYMERS, THEIR PYROLYSIS AND THEIR CONVERSION TO CERAMICS
Dietmar Seyferth 31 May 1989 43 p Submitted for publication
(Contract N00014-85-K-0645; NR Proj. 631-618)
(AD-A208437; TR-28) Avail: NTIS HC A03/MF A01 CSCL 07/6

An introduction to preceramic polymer chemistry; Applications of preceramic polymers; chemical considerations important in their design and synthesis is presented. Examples from known silicon containing preceramic polymers are studied. Inorganic and organometallic polymers are those macromolecular systems in which the polymer backbone contains elements other than the carbon, oxygen and nitrogen usually found in organic polymers. GRA

N89-27842# Rensselaer Polytechnic Inst., Troy, NY. Dept. of Chemistry.
RESIST SENSITIVITY ENHANCEMENT BY RADIATION-INDUCED MODIFICATION
James A. Moore, Jin-O Choi, Sang-Youl Kim, and John C. Corelli Jun. 1989 32 p Submitted for publication
(Contract N00014-85-K-0632; NR Proj. 625-856)
(AD-A208438; TR-9) Avail: NTIS HC A03/MF A01 CSCL 07/6

Exposure of poly methy methacrylate (PMMA) to electrons, protons, X-rays and ultraviolet radiation creates free radicals which combine with acrylic acid in a chain reaction to form graft and/or block copolymers with solubilities different from PMMA. Appropriate solvents develop negative images generated at doses on the order of 1,000 times less than those needed to form positive images in PMMA. At doses exceeding optimum values growth of the image occurs vertically and laterally. High fidelity replication can be accomplished by controlling dose and by using more aggressive solvents. Enhanced dry etch resistance can be conferred on the acrylic acid-modified PMMA by permitting it to imbibe calcium ion. GRA

N89-27843# Rensselaer Polytechnic Inst., Troy, NY. Dept. of Chemistry.
POLY(ENAMINONITRILES): NOVEL MATERIALS FOR USE IN ELECTRONICS
James A. Moore, Douglas R. Robello, and Parag G. Mehta Jun. 1989 13 p Submitted for publication
(Contract N00014-85-K-0632; NR Proj. 625-826)
(AD-A208439; TR-15) Avail: NTIS HC A03/MF A01 CSCL 07/6

Three new bis(1-chloro-2,2-dicyanovinyl) benzene monomer s have been synthesized. Polymerization of these monomers with two different diamines led to moderate to high molecular weight poly-enaminonitriles possessing excellent thermal stability. These polymers cure without emission of volatile byproducts. Initial thermal, mechanical and dielectric data of these polymers is presented. The dielectric constant of a representative polymer was found to be approximately 8 before heat treatment and 5 afterward. GRA

N89-27844# Rensselaer Polytechnic Inst., Troy, NY. Dept. of Chemistry.
ELECTRON BEAM-POSITIVE POLYIMIDES
James A. Moore and Andrew N. Dasheff Jun. 1989 13 p Submitted for publication
(Contract N00014-85-K-0632; NR Proj. 625-826)
(AD-A208440; TR-14) Avail: NTIS HC A03/MF A01 CSCL 07/6

Polyimides from cyclobutane dianhydrides were prepared and are shown to be sensitive to electron beams as well as to deep UV irradiation. Synthesis, thermal properties and sensitivity data are presented. GRA

N89-27845# University of Southern Mississippi, Hattiesburg. Dept. of Polymer Science.
PHOTODEGRADATION OF POLYIMIDE 1. A SPECTRAL, VISCOMETRIC, CHROMATOGRAPHIC AND WEIGHT LOSS INVESTIGATION OF POLYIMIDES BASED ON A PERFLUORINATED DIANHYDRIDE Technical Report No. 1, 1 Jun. 1988 - 31 May 1989
C. E. Hoyle and E. T. Anzures 31 May 1989 33 p Submitted for publication
(Contract N00014-89-J-1028)
(AD-A208507) Avail: NTIS HC A03/MF A01 CSCL 07/3

The photodegradation of aromatic dianhydride based polyimide films with perfluorinated chromophores in the dianhydride moiety is characterized by significant weight loss and chain cleavage. A conventional polyimide film based on pyromellitic dianhydride yields little decomposition under similar conditions of photolysis. Emission changes on photolysis of polyimide solutions demonstrate an efficient rearrangement to a yield a highly fluorescent species which can be used as an effective tool for following the degradation process. GRA

N89-27846# University of Southern Mississippi, Hattiesburg. Dept. of Polymer Science.
CHARACTERIZATION OF NYLON 6 BY 15N SOLID STATE NMR Technical Report No. 25, 1 Jun. 1988 - 31 May 198 9
Douglas G. Powell and Lon J. Mathias 31 May 1989 32 p Submitted for publication
(Contract N00014-89-J-1225)
(AD-A208508) Avail: NTIS HC A03/MF A01 CSCL 07/3

The solid state N-15 NMR characterization of nylon 6 is reported. Nylon 6 (20 percent N-15 enriched) was prepared by anionic polymerization of isotopically enriched caprolactam. The samples were prepared by three different treatments: quenched from the melt, slowly cooled and annealed, and artificially plasticized with excess caprolactam. CP/MAS spectra of the N-15 enriched samples showed a single sharp peak (alpha crystal form) at 84.2 ppm (relative to glycine) and a broader resonance at 87.2 ppm. Relaxation experiments were conducted to determine T sub n, T sub 1h, and T sub 1p for each sample at 300K. The crystalline resonance was found to have T sub 1n's of 125 to 416s, consistent with crystalling nylon 6. The downfield peak has two measurable T sub 1n's: a short component with T sub 1 of 1 to 3s and a second component with a longer T sub 1 of 19 to 29s. GRA

N89-27847# Ceramic Process Systems Corp., Milford, MA.
COMPOSITE CERAMIC SUPERCONDUCTING WIRES FOR ELECTRIC MOTOR APPLICATIONS Quarterly Report No. 3, 31 Jan. - 31 Mar. 1989
John W. Halloran 28 Apr. 1989 146 p

(Contract N00014-88-C-0512)
(AD-A208598; CPS-89-007) Avail: NTIS HC A07/MF A01 CSCL 11/2

This report describes progress on developing Y-123 wire for a high temperature superconductor (HTSC) motor. The wire is produced by spinning and heat treating fiber to produce metallized superconducting filaments. Development continued on spinning Y-123 green fiber. The diameter of continuous Y-123 green fiber was reduced to 75 microns. A belt furnace is being reconfigured for continuous sintering of fibers and a prototype cladding module for multi-filament ribbon wire is being fabricated. There has been an improvement in 77 K (self-field) critical current density of Y-123 filaments, up to 2400A/sq cm for the best filament, with 1500 A/sq cm for a typical filament. Similar results are seen for silver clad filaments. Preliminary data suggests an important effect of specimen length on transport critical current of thin filaments of weak-linked specimens. The characteristics of dc homopolar, dc heteropolar, reluctance, and induction HTSC motors were determined theoretically. A dc homopolar and an induction motor with superconducting stator windings were selected as final candidates for the proof-of-principle motor. A model for ac losses in HTSC wire, including eddy current and hysteresis losses was also developed. GRA

N89-27848# Stanford Univ., CA. Dept. of Chemical Engineering.
CHARACTERIZATION OF STRUCTURE IN THIN POLYMER RESIST FILMS Technical Report, 1 Jun. 1988 - 31 May 1989
L. L. Kosbar, S. W. Kuan, C. W. Frank, and R. F. Pease 30 May 1989 9 p
(Contract N00014-87-K-0426)
(AD-A208677; SU-TR-18) Avail: NTIS HC A02/MF A01 CSCL 09/1

The structure and homogeneity of thin, multi-component resists prepared by spin casting and Langmuir-Blodgett film formation technologies were investigated. Fluorescence spectroscopy was used to evaluate various casting solvents for spin casting of multi-component films. Films of novolac containing pyrene as a small molecule probe were cast from various ethers and ether alcohols. The small molecules aggregated less when the dipole moment of the solvent closely matched that of the polymer. Langmuir-Blodgett techniques were used to create very thin (40 nm) films of novolac/diazoquinone. Images down to 1 micron were developed in these films and transferred into 50 nm of chrome. These very thin resist films could have various applications in advanced resist technologies, including mask making and deep UV lithography. GRA

N89-27849# Stanford Univ., CA. Dept. of Chemical Engineering.
POLYMER CHAIN CONFIGURATIONS IN CONSTRAINED GEOMETRIES: ULTRATHIN FILMS FOR MICROLITHOGRAPHY Technical Report No.19, 1 Jun. 1988 - 31 May 1989
S. W. Kuan, P. S. Martin, C. W. Frank, and R. F. Pease 30 May 1989 12 p Submitted for publication
(Contract N00014-87-K-0426)
(AD-A208692) Avail: NTIS HC A03/MF A01 CSCL 07/6

Ultrathin (0.9 to 15.3 nm) poly(methyl methacrylate) (PMMA) films prepared by the Langmuir-Blodgett (LB) technique have been explored as high resolution electron beam resists. One eighth micron lines-and-spaces patterns have been achieved by using a Perkin Elmer MEBES I pattern generation system as the exposure tool. The etch resistance of films with thicknesses greater than 4.5 nm is sufficient to allow patterning of chromium film suitable for photomask fabrication. Monolayer PMMA films containing 5 mol percent pyrenedodecanoic acid (PDA) as a probe were prepared by transfer to the substrate at different surface pressures and characterized by fluorescence spectroscopy. The ratio of excimer to monomer emission intensity has a maximum value at 10 dyn/cm, which may be related to a structural rearrangement in the film. Intrinsic bilayer PMMA films prepared at 1 and 19 dyn/cm were also examined by transmission electron microscopy. The wrinkle-like surface topography observed in the 19 dyn/cm sample and not in the 1 dyn/cm sample suggests that the structure in the LB PMMA film depends upon the transfer pressure. GRA

N89-27850# Case Western Reserve Univ., Cleveland, OH. Dept. of Macromolecular Science.
TRANSFORMATION OF A MONOTROPIC MESOPHASE INTO AN ENANTIOTROPIC MESOPHASE BY COPOLYMERIZATION OF THE PARENT POLYMERS' MONOMER PAIR CONTAINING CONSTITUTIONAL ISOMERIC MESOGENIC SIDE GROUPS
Virgil Percec and Dimitris Tomazos 20 Jan. 1989 15 p Submitted for publication
(Contract N00014-89-J-1828)
(AD-A208782; TR-23) Avail: NTIS HC A03/MF A01 CSCL 07/6

The synthesis and the mesomorphic behavior of poly(methylsiloxane)s containing 4-methoxy-4' hydroxy trans-alpha-methylstilbene (4-n-PS) and 4-hydroxy-4' methoxy trans-alpha-methylstilbene (4'-n-PS) connected to the backbone by flexible spacers containing three, six and eleven (n = 3, 6, 11) methylene units, and of some copolymers based on these two constitutional isomeric mesogenic side groups (4,4' (A/B)-n-coPS) is described. The copolymers derived from structural units whose homopolymers displayed enantiotropic mesophases (4,4'(A/B)-3-coPS and 4,4' (A/B)-11-coPS) exhibited a depression of both mesomorphic and crystalline phase transition temperatures. However, the 4,4' (50/50)-6-coPS copolymers, derived from structural units whose homopolymers (4-6-PS and 4'-6-PS) displayed nematic monotropic mesophases, exhibited an enantiotropic nematic mesophase. GRA

N89-27851# Case Western Reserve Univ., Cleveland, OH. Dept. of Macromolecular Science.
THE INFLUENCE OF THE POLYMER BACKBONE FLEXIBILITY ON THE PHASE TRANSITIONS OF SIDE CHAIN LIQUID CRYSTAL POLYMERS CONTAINING 6-(4-(4-METHOXY-BETA-METYLSTYRYL)PHENOXY)HEXYL SIDE GROUPS
Virgil Percec, Dimitris Tomazos, and Reginald A. Willingham (Army Materials Technology Lab., Watertown, MA.) 2 May 1989 11 p Submitted for publication
(Contract N00014-89-J-1828)
(AD-A208821; TR-26) Avail: NTIS HC A03/MF A01 CSCL 07/6

The influence of the polymer backbone flexibility on the phase transition temperatures of side chain liquid crystalline polymethacrylate, polyacrylate, polymethylsiloxane, and polyphosphazene containing 6-(4-(4-methoxy-beta-methylstyryl) phenoxy)hexyl side groups is discussed. Flexible backbones enhance the decoupling of the motions of the side chain and main chain and, therefore, increase the rate of side-chain crystallization. Subsequently, the kinetically controlled crystallization process may transform the thermodynamically controlled mesomorphic phases from enantiotropic into monotropic. However, the highest degree of order in the mesophase is exhibited by the polymers based on the most rigid polymer backbone. GRA

N89-27852# Massachusetts Inst. of Tech., Cambridge. Dpt. of Mechanical Engineering.
SIMULATION OF DEFORMATION AND TEXTURE EVOLUTION IN SEMI-CRYSTALLINE POLYMERS Report No. 17, 1988 - 1989
Ali S. Argon, Said Ahzi, and David M. Parks 29 May 1989 4 p
(Contract N00014-86-K-0768)
(AD-A208854) Avail: NTIS HC A02/MF A01 CSCL 11/9

We developed a spectrum of mechanical based models which can be applied to the study of deformation and texture evolution of semi-crystalline polymers. We applied these models to predict behavior and texture evolution at large deformations. Results obtained from a composite model to polyethylene are presented and compared to the experimental data. The agreement with experiments is satisfactory. GRA

N89-27853# Naval Weapons Center, China Lake, CA. Research Dept.
ENERGETIC POLYOXETANE THERMOPLASTIC ELASTOMERS: SYNTHESIS AND CHARACTERIZATION Progress Report, Oct. 1986 - Sep. 1987
Geoffrey A. Lindsay, Mostafa A. Talukder, Robin A. Nissan, Roxanne L. Quintana, Michael A. Hasting, Rena Y. Yee, Melvin P. Nadler, Alice I. Atwood, Russell Reed, and Gerald E. Manner (Aerojet Solid Propulsion Co., Sacramento, CA.) Dec. 1988 76 p
(AD-A209612; AD-E900879; NWC-TP-6945) Avail: NTIS HC A05/MF A01 CSCL 21/9

This report summarizes our work at the Naval Weapons Center developing improved polymeric binders for energetic materials during Fiscal Year 1987. GRA

N89-27854# Rensselaer Polytechnic Inst., Troy, NY. Dept. of Chemistry.
A SOLUBLE PHOTOSENSITIVE POLYIMIDE
James A. Moore and Andrew N. Dasheff Jun. 1989 10 p Submitted for publication
(Contract N00014-85-K-0632)
(AD-A209634) Avail: NTIS HC A02/MF A01 CSCL 20/6

We have been studying an intrinsically photosensitive polyimide derived from cyclobutane dianhydride and oxydianiline which exhibits both good thermal stability (50 percent weight loss at 460 C) and high deep ultraviolet sensitivity (45 mJ/sq cm. However, the insolubility of cured polyimide films complicates the detailed mechanistic investigation of the photochemical process. We have therefore prepared a soluble homolog of this system which is derived from the photodimer of methyl maleic anhydride (dimethyl cyclobutane dianhydride). This material may also be imaged with deep ultraviolet radiation and exhibits good thermal stability. A discussion of the photochemical behavior of this soluble system will be presented. GRA

N89-27855# California Univ., Los Angeles. Dept. of Materials Science and Engineering.
ENERGY TRANSFER EFFECTS IN BETA-ALUMINA Technical Report No. 21, Aug. 1988 - Jul. 1989
L. A. Momoda, J. D. Barrie, Bruce Dunn, and O. M. Stafsudd 15 Jun. 1989 10 p Submitted for publication
(Contract N00014-83-K-0498)
(AD-A209818) Avail: NTIS HC A02/MF A01 CSCL 07/4

Energy transfer between cerium (+3) and neodynium (+3) exchanged into beta alumina is observed. Synthesis of the crystals was achieved by ion exchange. Both radiative and nonradiative transfer mechanisms are evident. The nonradiative transfer is attributed to electrostatic dipole-quadrupole interactions where the highest measured transfer efficiency was 40 percent. GRA

N89-27856# California Univ., Los Angeles. Dept. of Materials Science and Engineering.
THE USE OF MULTIPLE ION EXCHANGE TO PRODUCE ENERGY TRANSFER IN BETA-ALUMINAS Technical Report No. 19, Aug. 1988 - Jul. 1989
L. A. Momoda, J. D. Barrie, and Bruce Dunn 15 Jun. 1989 10 p Submitted for publication
(Contract N00014-83-K-0498)
(AD-A209821) Avail: NTIS HC A02/MF A01 CSCL 07/4

The preparation of single crystals of Beta alumina containing two trivalent lanthanide species is described. The use of eutectic melts enables the two rare earth species to be introduced during a single ion exchange process. Energy transfer in crystals containing Ce+3/Nd +3 and Ce+3/Tb +3 is shown. High transfer efficiencies were measured for crystals with low sensitizer-to-activator ion concentration ratios. Up-conversion processes were observed in crystals doped with YB+3 and Er+3 ions. GRA

N89-27857# Minnesota Univ., Minneapolis. Dept. of Chemical Engineering and Materials Science.
A STATISTICAL DERIVATION OF THE AVERAGE DEGREE OF POLYMERIZATION IN A STIRRED TANK REACTOR Interim Report
Neil Dotson May 1989 21 p
(Contract N00014-88-K-0366)
(AD-A209873; TR-2) Avail: NTIS HC A03/MF A01 CSCL 07/6

The statistical approach in its many forms is a powerful tool in describing the structural evolution of nonlinear polymers, but is limited in its application to batch processes. This restriction is removed by considering the paradigm of Af homopolymerization in a homogeneous stirred tank reactor. The number-and weight -average degrees of polymerization are derived from the recursive arguments which properly account for the non-random combination of monomers caused by the residence time distribution. The results are in agreement with those derived from the kinetic equations. This route is not necessarily a simpler or more powerful approach than solution of the kinetic equations, but it does provide new insights into this particular problem, as well as demonstrating the versatility of the statistical approach. GRA

N89-27858# Massachusetts Inst. of Tech., Cambridge. Dept. of Civil Engineering.
FIBER REINFORCED STRUCTURAL CERAMICS FOR CONSTRUCTION Final Technical Report, 1 Jan. - 31 Dec. 1988
Victor C. Li and Christopher K. Leung Feb. 1989 36 p
(Contract DAAL03-87-K-0005)
(AD-A209976; ARO-24620.16-EG-UIR) Avail: NTIS HC A03/MF A01 CSCL 11/2

Major findings are summarized for the second year of a five-year research project with the ultimate goal of developing a light-weight, durable, strong and impact-resistant ceramic composite for use in advanced constructed facilities. During the first year of this project, short-fiber reinforced ceramic composites were identified to be the class of ceramic materials with the highest potential for development into a construction material. A model composite system was also chosen. In this project year, work has concentrated on the processing and preliminary testing of model composites as well as on the theoretical prediction of pre-peak behavior of short-fiber composites. Also, a study on the potential of ceramics construction as well as obstacles to its use were carried out to provide a foundation for future work. GRA

N89-27859# Naval Air Development Center, Warminster, PA. Aircraft and Crew Systems Technology Directorate.
AN ADHESIVE FOR FIELD REPAIR OF COMPOSITES Final Report
R. C. Cochran, T. M. Donnellan, J. G. Williams, J. J. Katialaus, and Norman Nemeroff Jun. 1988 29 p
(AD-A209992; NADC-88072-60) Avail: NTIS HC A03/MF A01 CSCL 11/1

The strength, durability, storage, processability and field adaptability of the NADC adhesive were thoroughly demonstrated, and its stress-strain behavior was well characterized. Representative repairs were successfully fabricated using the adducted adhesive system. Under structural evaluation the adhesive provided comfortable margins of safety for field process variability. Field evaluation has demonstrated the safe application of bonded patches under field conditions using existing common ground support equipment and maintenance personnel. The adhesive was qualified to military specification MIL-A-85705 Adhesive, Aircraft for Structural Repair and was approved for use on the AV-8B aircraft as a structural repair adhesive. GRA

N89-27860# Minnesota Univ., Minneapolis. Dept. of Chemical Engineering and Materials Science.
CALCULATION OF NETWORK PARAMETERS OF CROSSLINKED MARKOVIAN POLYMER CHAINS Interim Report
Douglas R. Miller May 1989 12 p Submitted for

publication. Prepared in cooperation with George Washington Univ., Washington, DC
(Contract N00014-88-K-0366)
(AD-A210073; TR-1) Avail: NTIS HC A03/MF A01 CSCL 07/6

Linear copolymer chains form in a chain-addition reaction which includes initiation, homopropagation, crosspropagation, and termination by transfer, disproportionation, and combination. Chain growth obeys the Markov property. Multiple types of monomer units are involved; some types have reactive site, others do not. These chains are then crosslinked by a small monomer crosslinker which may be polydispersed. The resulting network consists of soluble, pendant, and elastically effective fractions. Using classical Markov chain analysis techniques, various statistical properties of the polymer chains are computed. The gel point, weight fractions and other network properties can then be computed. The effects of unequal rates of homopropagation and crosspropagation can be observed. GRA

N89-27861# City Coll. of the City Univ. of New York, NY. Dept. of Chemistry.
NOVEL METHODS FOR REINFORCING ELASTOMERS Final Report, 10 Feb. 1986 - 9 Feb. 1989
J. E. Mark 5 Apr. 1989 5 p
(Contract DAAL03-86-K-0032)
(AD-A210150; ARO-23255.22-MS) Avail: NTIS HC A02/MF A01 CSCL 11/10

The primary goal of this project was the development of new techniques for toughening elastomeric materials. The first approach taken was the in-situ precipitation of reinforcing filler particles into the elastomers. Preliminary studies focused on the elastomer poly(dimethylsiloxane) (PDMS) because of the large number of related studies already carried out on this material. Promising techniques were then extended to other elastomers, such as the polyisobutylene. The second approach was the alignment of ferrite-type filler particles to improve reinforcement, at least in chosen directions. This was done during the curing process and utilized a magnetic field of variable strength. GRA

N89-27862# Iowa State Univ. of Science and Technology, Ames. Dept. of Materials Science and Engineering.
PREPARATION AND CHARACTERIZATION OF COLLOIDAL ZnS PARTICLES
Ahmet Celikkaya and Mufit Akinc 15 Jun. 1989 8 p Submitted for publication
(Contract N00014-87-K-0738)
(AD-A210171; TR-4) Avail: NTIS HC A02/MF A01 CSCL 11/4

The preparation of particles of uniform size, shape, and composition has been of interest to colloid chemists and has received serious attention in the ceramic processing community recently. The interest in making monodispersed sols is not based solely on esthetic appeal of such systems but has evolved from high tech applications which place stringent requirements on the properties of ceramic components and so on starting powders. Uniform particle size and shape are also essential for the evaluation of validity of various sintering models as well as optical, magnetic, and electrokinetic properties of colloidal systems developed assuming uniform particle size and shape. GRA

28 PROPELLANTS AND FUELS

Includes rocket propellants, igniters, and oxidizers; their storage and handling procedures; and aircraft fuels.

For related information see also *07 Aircraft Propulsion and Power, 20 Spacecraft Propulsion and Power,* and *44 Energy Production and Conversion.*

N89-27863# Los Alamos National Lab., NM.
SHOCK INITIATION MODELING OF MULTICOMPONENT EXPLOSIVES
Yehuda Partom May 1989 37 p
(Contract W-7405-eng-36)
(DE89-012259; LA-10773-Add) Avail: NTIS HC A03/MF A01

In the main body of this report, we had developed a characteristics code for shock initiation based on the surface-burn, hot-spot growth mechanism. In this Addendum, we extend the code to include multicomponent materials. We demonstrate the capability of the code by four examples: (1) a two-component system of explosive and inert; (2) a two-component system of two different explosives; (3) prediction of the pop plot of 1.89 g/sq cm PBX 9502 and comparison with experiment; and (4) a three-component system of different grain sizes. We then introduce the concept of critical hot-spot size for ignition and demonstrate its use to model the crossover effect in reaction rate for fine-grained explosives. DOE

N89-27864*# Morton Thiokol, Brigham City, UT. Ordnance Development Section.
SRM PROPELLANT, FRICTION/ESD TESTING
L. A. Campbell 12 May 1989 39 p
(Contract NAS8-30490)
(NASA-CR-183706; NAS 1.26:183706; ECS-SS-3059; Rept-19176) Avail: NTIS HC A03/MF A01 CSCL 21I

Following the Pershing 2 incident in 1985 and the Peacekeeper ignition during core removal in 1987, it was found that propellant can be much more sensitive to Electrostatic Discharges (ESD) than ever before realized. As a result of the Peacekeeper motor near miss incident, a friction machine was designed and fabricated, and used to determine friction hazards during core removal. Friction testing with and electrical charge being applied across the friction plates resulted in propellant ignitions at low friction pressures and extremely low ESD levels. The objective of this test series was to determine the sensitivity of solid rocket propellant to combined friction pressure and electrostatic stimuli and to compare the sensitivity of the SRM propellant to Peacekeeper propellant. The tests are fully discussed, summarized and conclusions drawn.
Author

N89-27865# Texas A&M Univ., College Station. Mechanics and Materials Center.
DYNAMIC FRACTURE AND DEFORMATION OF SOLID PROPELLANT Final Report, Apr. 1986 - Mar. 1989
R. A. Schapery and J. R. Walton 30 May 1989 13 p
(Contract N00014-86-K-0298)
(AD-A208691; MM-5488-89-12) Avail: NTIS HC A03/MF A01 CSCL 19/1

This report summarizes primarily theoretical research on dynamic crack growth in linear viscoelastic media and quasi static deformation behavior of particle filled rubber with propagating or stationary microcracks. Results from both studies are applicable to solid propellant. GRA

N89-27866# Argonne National Lab., IL. Materials and Components Technology Div.
FURTHER INVESTIGATION OF FLOW MODELING DURING SOLID PROPELLANT PROCESSING Final Technical Report, Sep. 1987 - Sep. 1988
Y. S. Cha, H. M. Domanus, W. T. Sha, and S. L. Soo (Illinois Univ., Urbana.) May 1989 35 p
(Contract W-31-109-eng-38; DA Proj. 1L1-61101-A-91-A)
(AD-A209787; AD-E951367; AMSMI/CR-RD-PR-89-1) Avail: NTIS HC A03/MF A01 CSCL 21/9

A two-fluid model is employed to investigate the velocity and volume fraction distributions during the solid propellant casting process. Two important dimensionless parameters, the dimensionless interfacial momentum transfer coefficient D, and the viscosity ratio of the two fluids Z, are identified and varied parametrically in the numerical calculations. The results show that when D is small, separation between the particles and binder occurred and the smaller the D, the larger the degree of separation. When D is large, separation did not occur since the two fluids move like a single fluid when interfacial momentum transfer is dominating. Near the transition point between separation and no

separation (D approx. = 1), an M-shaped profile was observed for the particle volume fraction distribution in an annular duct. The degree of separation is very small and the reason for the existence of such an M-shaped profile is not clearly understood. It is pointed out that a viscosity model recently proposed by Probstein and Sengun may be relevant to the solid propellant system. It is suggested that the next logical step is to incorporate the non-Newtonian behavior of the binder (and the fine particles) into the two-fluid model. GRA

29 MATERIALS PROCESSING

Includes space-based development of products and processes for commercial applications.

For biological materials see *55 Space Biology*.

No abstracts in this category.

31 ENGINEERING (GENERAL)

Includes vacuum technology; control engineering; display engineering; cryogenics; and fire prevention.

N89-27867# Naval Research Lab., Washington, DC.
TESTS OF HALON 1301 TEST GAS SIMULANTS Interim Report, Jan. 1987 - May 1988
H. W. Carhart, J. T. Leonard, P. J. DiNenno, M. D. Starchville, E. W. Forssell, and J. T. Wong (Hughes Associates, Inc., Wheaton, MD.) 28 Feb. 1989 80 p
(AD-A207346; NRL-MR-6424) Avail: NTIS HC A05/MF A01 CSCL 13/12

All new and retrofit installations of Halon 1301 (CBrF3) total flooding fire protection systems in shipboard machinery spaces require full acceptance discharge test. It is desirable to use a suitable simulant test gas in these tests in view of current and future regulation of Halon 1301. Sulfur hexafluoride, SF6, and chlorodifluromethane R-22, were identified as candidate simulants on the basis of their similarity in physical properties to Halon 1301. These two candidates were then evaluated on the basis of leakage from an enclosure. SF6 was determined to be an excellent simulant for Halon 1301 when considering leakage from an enclosure. Further testing of SF6 and R-22 is planned for other important aspects of Halon 1301 systems, i.e., flow hydraulics, initial mixing. GRA

N89-27868*# National Aeronautics and Space Administration. Lewis Research Center, Cleveland, OH.
INDIUM PHOSPHIDE SOLAR CELL RESEARCH IN THE US: COMPARISON WITH NONPHOTOVOLTAIC SOURCES
I. Weinberg, C. K. Swartz, and R. E. Hart, Jr. 1989 13 p Prepared for presentation at the European Space Power Conference, Madrid, Spain, 2-6 Oct. 1989; sponsored in part by ESA
(NASA-TM-102103; E-4869; NAS 1.15:102103) Avail: NTIS HC A03/MF A01 CSCL 10A

Highlights of the InP solar cell research program are presented. Homojunction cells with AMO efficiences approaching 19 percent were demonstrated while 17 percent was achieved for indium tin oxide (ITO)/InP cells. The superior radiation resistance of these latter two cell configurations over both Si and GaAs were demonstrated. InP cells on board the LIPS III satellite show no degradation after more than a year in orbit. Computer modeling calculations were directed toward radiation damage predictions and the specification of concentrator cell parameters. Computed array specific powers, for a specific orbit, are used to compare the performance of an InP solar cell array to solar dynamic and nuclear systems. Author

N89-28267# British Aerospace Public Ltd. Co., Bristol (England). Space and Communications Div.
LONG-LIFE STIRLING CYCLE COOLERS FOR APPLICATIONS IN THE 60 TO 110 K RANGE
C. A. Lewis *In* ESA, Third European Symposium on Space Thermal Control and Life Support Systems Dec. 1988 p 387-391 (For primary document see N89-28214 22-54)
Copyright Avail: NTIS HC A99/MF A01; ESA Publications Div., ESTEC, Noordwijk, Netherlands, 80 Dutch guilders or 45 US dollars

N89-28268# Rutherford High Energy Lab., Chilton (England).
A 4-K MECHANICAL REFRIGERATOR FOR SPACE APPLICATIONS
T. W. Bradshaw and A. H. Orlowska *In* ESA, Third European Symposium on Space Thermal Control and Life Support Systems Dec. 1988 p 393-397 (For primary document see N89-28214 22-54)
Copyright Avail: NTIS HC A99/MF A01; ESA Publications Div., ESTEC, Noordwijk, Netherlands, 80 Dutch guilders or 45 US dollars

N89-28269# Aerospatiale, Cannes La Bocca (France).
THERMAL AND CRYOGENIC ASPECTS OF THE ISO OPTICAL SUBSYSTEM
B. Collaudin and L. DeSa *In* ESA, Third European Symposium on Space Thermal Control and Life Support Systems Dec. 1988 p 399-405 Previously announced as N89-24160 (For primary document see N89-28214 22-54)
Copyright Avail: NTIS HC A99/MF A01; ESA Publications Div., ESTEC, Noordwijk, Netherlands, 80 Dutch guilders or 45 US dollars

N89-28270# Nippon Electric Co. Ltd., Yokohama (Japan). Space Development Div.
THERMAL DESIGN OF A SUPERFLUID HELIUM DEWAR FOR INFRARED TELESCOPE ON-BOARD SPACE FLYER UNIT
G. Fujii, T. Hasui, K. Hama, T. Okamoto, T. Machida, M. Murakami, T. Matsumoto, H. Okuda, and M. Kyoya (Sumitomo Heavy Industries Ltd., Tokyo, Japan) *In* ESA, Third European Symposium on Space Thermal Control and Life Support Systems Dec. 1988 p 407-412 (For primary document see N89-28214 22-54)
Copyright Avail: NTIS HC A99/MF A01; ESA Publications Div., ESTEC, Noordwijk, Netherlands, 80 Dutch guilders or 45 US dollars

N89-28271# Construcciones Aeronauticas S.A., Madrid (Spain). Space Div.
THERMAL CONTROL OF THE GRASP DETECTOR SECTION
P. B. Roig *In* ESA, Third European Symposium on Space Thermal Control and Life Support Systems Dec. 1988 p 413-420 (For primary document see N89-28214 22-54)
Copyright Avail: NTIS HC A99/MF A01; ESA Publications Div., ESTEC, Noordwijk, Netherlands, 80 Dutch guilders or 45 US dollars

N89-28277# Aerospatiale, Cannes La Bocca (France). Cryogenic Lab.
SHAKING IN CRYOGENIC CONDITIONS
S. Taride *In* ESA, Third European Symposium on Space Thermal Control and Life Support Systems Dec. 1988 p 457-460 Previously announced as N89-23939 (For primary document see N89-28214 22-54)
Copyright Avail: NTIS HC A99/MF A01; ESA Publications Div., ESTEC, Noordwijk, Netherlands, 80 Dutch guilders or 45 US dollars

32 COMMUNICATIONS AND RADAR

Includes radar; land and global communications; communications theory; and optical communications.

For related information see also *04 Aircraft Communications and Navigation* and *17 Space Communications, Spacecraft Communications, Command and Tracking.* For search and rescue see *03 Air Transportation and Safety,* and *16 Space Transportation.*

N89-27869# Battelle Columbus Labs., Research Triangle Park, NC.

SOLUTION OF TWO-DIMENSIONAL, TWO-REGION ELECTROMAGNETIC GROUND RESPONSE Final Report, Mar. - Aug. 1987

Ira Kohlberg Mar. 1989 42 p Prepared in cooperation with Kohlberg Associates Inc., Alexandria, VA

(Contract DAAL03-86-D-0001; DA Proj. 1L1-62120-AH-25)

(AD-A206265; BATT-TCN-87-116; HDL-CR-89-001-1) Avail: NTIS HC A03/MF A01 CSCL 20/15

A solution for the two-dimensional, two-region electromagnetic ground response has been developed which relates the surface components of the electric field to the surface components of the magnetic field. This has been accomplished by deriving a universal functional form for a dimensionless Green's function. The Green's function provides increasingly more accurate approximations to the response for each successive reflection from the second layer. This result would appear to provide simplification and reduced computer running time in the numerical modelling of the high-altitude burst electromagnetic pulse (HABEMP) when the ground response is coupled to finite-difference methods for solving the atmospheric part of the problem. GRA

N89-27870*# Ohio State Univ., Columbus. ElectroScience Lab.

TARGET SIGNATURE MODELING AND BISTATIC SCATTERING MEASUREMENT STUDIES Semiannual Report, Sep. 1988 - Feb. 1989

W. D. Burnside, T. H. Lee, R. Rojas, R. J. Marhefka, and D. Bensman Feb. 1989 56 p

(Grant NAG2-542)

(NASA-CR-185434; NAS 1.26:185434; ESL-721432-1; ESL-721446-1; ESL-721447-1; ESL-721711-1) Avail: NTIS HC A04/MF A01 CSCL 17I

Four areas of study are summarized: bistatic scattering measurements studies for a compact range; target signature modeling for test and evaluation hardware in the loop situation; aircraft code modification study; and SATCOM antenna studies on aircraft. Author

N89-27871*# Jet Propulsion Lab., California Inst. of Tech., Pasadena.

THE TELECOMMUNICATIONS AND DATA ACQUISITION REPORT Progress Report, Jan. - Mar. 1989

E. C. Posner, ed. 15 May 1989 394 p

(NASA-CR-185431; JPL-TDA-PR-42-97; NAS 1.26:185431) Avail: NTIS HC A17/MF A01 CSCL 17B

Archival reports on developments in programs managed by the Jet Propulsion Laboratory's Office of Telecommunications and Data Acquisition are provided. Space communications, radio navigation, radio science, and ground based radio and radio astronomy are discussed. Deep Space Network projects are also discussed. For individual titles, see N89-27872 through N89-27906.

N89-27872*# Jet Propulsion Lab., California Inst. of Tech., Pasadena.

ESTIMATION AND FILTERING TECHNIQUES FOR HIGH-ACCURACY GPS APPLICATIONS **c13**

S. M. Lichten *In its* The Telecommunications and Data Acquisition Report 15 May 1989 p 1-20 (For primary document see N89-27871 22-32)

Avail: NTIS HC A17/MF A01 CSCL 22A

Techniques for determination of very precise orbits for satellites of the Global Positioning System (GPS) are currently being studied and demonstrated. These techniques can be used to make cm-accurate measurements of station locations relative to the geocenter, monitor earth orientation over timescales of hours, and provide tropospheric and clock delay calibrations during observations made with deep space radio antennas at sites where the GPS receivers have been collocated. For high-earth orbiters, meter-level knowledge of position will be available from GPS, while at low altitudes, sub-decimeter accuracy will be possible. Estimation of satellite orbits and other parameters such as ground station positions is carried out with a multi-satellite batch sequential pseudo-epoch state process noise filter. Both square-root information filtering (SRIF) and UD-factorized covariance filtering formulations are implemented in the software. Author

N89-27873*# Jet Propulsion Lab., California Inst. of Tech., Pasadena.

HIGH-PRECISION RADIOMETRIC TRACKING FOR PLANETARY APPROACH AND ENCOUNTER IN THE INNER SOLAR SYSTEM

C. S. Christensen, S. W. Thurman, J. M. Davidson, M. H. Finger, and W. M. Folkner *In its* The Telecommunications and Data Acquisition Report 15 May 1989 p 21-46 (For primary document see N89-27871 22-32)

Avail: NTIS HC A17/MF A01 CSCL 20N

The benefits of improved radiometric tracking data have been studied for planetary approach within the inner Solar System using the Mars Rover Sample Return trajectory as a model. It was found that the benefit of improved data to approach and encounter navigation was highly dependent on the a priori uncertainties assumed for several non-estimated parameters, including those for frame-tie, Earth orientation, troposphere delay, and station locations. With these errors at their current levels, navigational performance was found to be insensitive to enhancements in data accuracy. However, when expected improvements in these errors are modeled, performance with current-accuracy data significantly improves, with substantial further improvements possible with enhancements in data accuracy. Author

N89-27874*# Jet Propulsion Lab., California Inst. of Tech., Pasadena.

THE EFFECT OF SPATIAL AND TEMPORAL WET-TROPOSPHERE FLUCTUATIONS ON CONNECTED ELEMENT INTERFEROMETRY **c46**

C. D. Edwards *In its* The Telecommunications and Data Acquisition Report 15 May 1989 p 47-57 (For primary document see N89-27871 22-32)

Avail: NTIS HC A17/MF A01 CSCL 04A

Numerical integrations of the structure function of tropospheric inhomogeneities have been performed to assess the impact of water vapor fluctuations on connected element interferometry (CEI). The expectation value of the RMS troposphere error for a differential spacecraft-quasar observation is derived by integrating the spatial refractivity structure function along raypaths to both the spacecraft and quasar from two spatially separated sites. Correlations between the tropospheric conditions at the two sites, which can become significant for short baseline observations, are fully accounted for in this calculation. Temporal effects are treated by assuming a frozen-flow model in which a fixed spatial distribution blows over both sites. Two nominal observation scenarios are considered, along with variations to study the dependence of the resultant differential troposphere errors on baseline length, observation time, source separation angle, and elevation. Consecutive differential observations are found to be almost completely uncorrelated, implying that averaging many repeated differential observations can quickly reduce the troposphere error. Author

N89-27875*# Jet Propulsion Lab., California Inst. of Tech., Pasadena.

NEW ION TRAP FOR ATOMIC FREQUENCY STANDARD APPLICATIONS **c72**

J. D. Prestage, G. J. Dick, and L. Maleki *In its* The

Telecommunications and Data Acquisition Report 15 May 1989 p 58-63 (For primary document see N89-27871 22-32)
Avail: NTIS HC A17/MF A01 CSCL 20H

A novel linear ion trap that permits storage of a large number of ions with reduced susceptibility to the second-order Doppler effect caused by the radio frequency (RF) confining fields has been designed and built. This new trap should store about 20 times the number of ions a conventional RF trap stores with no corresponding increase in second-order Doppler shift from the confining field. In addition, the sensitivity of this shift to trapping parameters, i.e., RF voltage, RF frequency, and trap size, is greatly reduced. Author

N89-27876*# Jet Propulsion Lab., California Inst. of Tech., Pasadena.
OPERATIONAL PARAMETERS FOR THE SUPERCONDUCTING CAVITY MASER **c36**
R. T. Wang, G. J. Dick, and D. M. Strayer *In its* The Telecommunications and Data Acquisition Report 15 May 1989 p 64-71 (For primary document see N89-27871 22-32)
Avail: NTIS HC A17/MF A01 CSCL 20E

Tests of the superconducting cavity maser (SCM) ultra-stable frequency source have been made for the first time using a hydrogen maser for a frequency reference. In addition to characterizing the frequency stability, the sensitivity of the output frequency to several crucial parameters was determined for various operating conditions. Based on this determination, the refrigeration and thermal control systems of the SCM were modified. Subsequent tests showed substantially improved performance, especially at the longest averaging times. Author

N89-27877*# Jet Propulsion Lab., California Inst. of Tech., Pasadena.
OPERATING AND ENVIRONMENTAL CHARACTERISTICS OF SIGMA TAU HYDROGEN MASERS USED IN THE VERY LONG BASELINE ARRAY (VLBA) **c36**
T. K. Tucker *In its* The Telecommunications and Data Acquisition Report 15 May 1989 p 72-80 (For primary document see N89-27871 22-32)
Avail: NTIS HC A17/MF A01 CSCL 20E

Presented here are the results obtained from performance evaluation of a pair of Sigma Tau Standards Corporation Model VLBA-112 active hydrogen maser frequency standards. These masers were manufactured for the National Radio Astronomy Observatory (NRAO) for use on the Very Long Baseline Array (VLBA) project and were furnished to the Jet Propulsion Laboratory (JPL) for the purpose of these tests. Tests on the two masers were performed in the JPL Frequency Standards Laboratory (FSL) and included the characterization of output frequency stability versus environmental factors such as temperature, humidity, magnetic field, and barometric pressure. The performance tests also included the determination of phase noise and Allan variance using both FSL and Sigma Tau masers as references. All tests were conducted under controlled laboratory conditions, with only the desired environmental and operational parameters varied to determine sensitivity to external environment. Author

N89-27878*# Jet Propulsion Lab., California Inst. of Tech., Pasadena.
STATE-OF-THE-ART FIBER OPTICS FOR SHORT DISTANCE FREQUENCY REFERENCE DISTRIBUTION **c74**
G. F. Lutes and L. E. Primas *In its* The Telecommunications and Data Acquisition Report 15 May 1989 p 81-87 (For primary document see N89-27871 22-32)
Avail: NTIS HC A17/MF A01 CSCL 20F

A number of recently developed fiber-optic components that hold the promise of unprecedented stability for passively stabilized frequency distribution links are characterized. These components include a fiber-optic transmitter, an optical isolator, and a new type of fiber-optic cable. A novel laser transmitter exhibits extremely low sensitivity to intensity and polarization changes of reflected light due to cable flexure. This virtually eliminates one of the shortcomings in previous laser transmitters. A high-isolation, low-loss optical isolator has been developed which also virtually eliminates laser sensitivity to changes in intensity and polarization of reflected light. A newly developed fiber has been tested. This fiber has a thermal coefficient of delay of less than 0.5 parts per million per deg C, nearly 20 times lower than the best coaxial hardline cable and 10 times lower than any previous fiber-optic cable. These components are highly suitable for distribution systems with short extent, such as within a Deep Space Communications Complex. Here, these new components are described and the test results presented. Author

N89-27879*# Jet Propulsion Lab., California Inst. of Tech., Pasadena.
STABILIZED FIBER-OPTIC FREQUENCY DISTRIBUTION SYSTEM **c74**
L. E. Primas, G. F. Lutes, and R. L. Sydnor *In its* The Telecommunications and Data Acquisition Report 15 May 1989 p 88-97 (For primary document see N89-27871 22-32)
Avail: NTIS HC A17/MF A01 CSCL 20F

A technique for stabilizing reference frequencies transmitted over fiber-optic cable in a frequency distribution system is discussed. The distribution system utilizes fiber-optic cable as the transmission medium to distribute precise reference signals from a frequency standard to remote users. The stability goal of the distribution system is to transmit a 100-MHz signal over a 22-km fiber-optic cable and maintain a stability of 1 part in 10(17) for 1000-second averaging times. Active stabilization of the link is required to reduce phase variations produced by environmental effects, and is achieved by transmitting the reference signal from the frequency standard to the remote unit and then reflecting back to the reference unit over the same optical fiber. By comparing the phase of the transmitted and reflected signals at the reference unit, phase variations of the remote signal can be measured. An error voltage derived from the phase difference between the two signals is used to add correction phase. Author

N89-27880*# Jet Propulsion Lab., California Inst. of Tech., Pasadena.
A NEW METHOD FOR ANALYSIS OF LIMIT CYCLE BEHAVIOR OF THE NASA/JPL 70-METER ANTENNA AXIS SERVOS **c33**
R. E. Hill *In its* The Telecommunications and Data Acquisition Report 15 May 1989 p 98-111 (For primary document see N89-27871 22-32)
Avail: NTIS HC A17/MF A01 CSCL 09A

A piecewise linear method of analyzing the effects of discontinuous nonlinearities on control system performance is described. The limit cycle oscillatory behavior of the system resulting from the nonlinearities is described in terms of a sequence of linear system transient responses. The equations are derived which relate the initial and the terminal conditions of successive transients and the boundary conditions imposed by the non-linearities. The method leads to a convenient computation algorithm for prediction of limit cycle characteristics resulting from discontinuous nonlinearities such as friction, deadzones, and hysteresis. Author

N89-27881*# Jet Propulsion Lab., California Inst. of Tech., Pasadena.
APPLICATION OF OPTIMAL CONTROL THEORY TO THE DESIGN OF THE NASA/JPL 70-METER ANTENNA SERVOS **c33**
L. S. Alvarez and J. Nickerson *In its* The Telecommunications and Data Acquisition Report 15 May 1989 p 112-126 (For primary document see N89-27871 22-32)
Avail: NTIS HC A17/MF A01 CSCL 09A

The application of Linear Quadratic Gaussian (LQG) techniques to the design of the 70-m axis servos is described. Linear quadratic optimal control and Kalman filter theory are reviewed, and model development and verification are discussed. Families of optimal controller and Kalman filter gain vectors were generated by varying weight parameters. Performance specifications were used to select final gain vectors. Author

N89-27882*# Jet Propulsion Lab., California Inst. of Tech., Pasadena.
PRECISION POINTING COMPENSATION FOR DSN ANTENNAS WITH OPTICAL DISTANCE MEASURING SENSORS **c33**
R. E. Scheid *In its* The Telecommunications and Data Acquisition Report 15 May 1989 p 127-140 (For primary document see N89-27871 22-32)
Avail: NTIS HC A17/MF A01 CSCL 09A

The pointing control loops of Deep Space Network (DSN) antennas do not account for unmodeled deflections of the primary and secondary reflectors. As a result, structural distortions due to unpredictable environmental loads can result in uncompensated boresight shifts which degrade pointing accuracy. The design proposed here can provide real-time bias commands to the pointing control system to compensate for environmental effects on pointing performance. The bias commands can be computed in real time from optically measured deflections at a number of points on the primary and secondary reflectors. Computer simulations with a reduced-order finite-element model of a DSN antenna validate the concept and lead to a proposed design by which a ten-to-one reduction in pointing uncertainty can be achieved under nominal uncertainty conditions. Author

N89-27883*# Jet Propulsion Lab., California Inst. of Tech., Pasadena.
THE EFFECTS OF ATMOSPHERIC TURBULENCE ON PRECISION OPTICAL MEASUREMENTS USED FOR ANTENNA-POINTING COMPENSATION **c74**
N. Nerheim *In its* The Telecommunications and Data Acquisition Report 15 May 1989 p 141-148 (For primary document see N89-27871 22-32)
Avail: NTIS HC A17/MF A01 CSCL 20F

Blind pointing of the Deep Space Network (DSN) 70-meter antennas can be improved if distortions of the antenna structure caused by unpredictable environmental loads can be measured in real-time, and the resulting boresight shifts evaluated and incorporated into the pointing control loops. The measurement configuration of a proposed pointing compensation system includes an optical range sensor that measures distances to selected points on the antenna surface. The effect of atmospheric turbulence on the accuracy of optical distance measurements and a method to make in-situ determinations of turbulence-induced measurement errors are discussed. Author

N89-27884*# Jet Propulsion Lab., California Inst. of Tech., Pasadena.
A MULTIFLARE HORN WITH 1-MEGAWATT POWER HANDLING CAPABILITY
D. J. Hoppe *In its* The Telecommunications and Data Acquisition Report 15 May 1989 p 149-155 (For primary document see N89-27871 22-32)
Avail: NTIS HC A17/MF A01 CSCL 17I

The design and testing of the prototype horn for the proposed 1-megawatt radar are described. The unique features of this square horn include a multiflare design in which flare angle changes rather than corrugations are used to generate the required higher-order modes. A five-port combining section is used at the input. The design of this section and the multiflare section are described. Measured radiation patterns are in good agreement with theoretical patterns. Author

N89-27885*# Jet Propulsion Lab., California Inst. of Tech., Pasadena.
THERMAL MEASUREMENTS OF MICROWAVE TRANSMITTER FEEDHORN WINDOW
R. M. Perez and D. J. Hoppe *In its* The Telecommunications and Data Acquisition Report 15 May 1989 p 156-161 (For primary document see N89-27871 22-32)
Avail: NTIS HC A17/MF A01 CSCL 20N

Thermal measurements of microwave transmitter feedhorn windows were performed using an imaging infrared radiometer. The measurement technique is described and results are presented for windows made of 0.001-in. Kapton (trademark of Dupont Chemical Co.) and 0.1-in. HTP-6 (Space Shuttle tile material). Measured and calculated temperatures agree well. Author

N89-27886*# Jet Propulsion Lab., California Inst. of Tech., Pasadena.
A NEW ANALYSIS OF BEAM-WAVEGUIDE ANTENNAS CONSIDERING THE PRESENCE OF THE ENCLOSURE
A. G. Cha *In its* The Telecommunications and Data Acquisition Report 15 May 1989 p 162-168 (For primary document see N89-27871 22-32)
Avail: NTIS HC A17/MF A01 CSCL 20N

Beam-waveguide (BWG) antennas provide multiple frequency band operations and other operational benefits for large ground-station antennas. Present design practices use diffraction analyses that ignore the presence of the BWG enclosure and may be inaccurate at lower frequency bands for ground-station antennas operating over multiple frequency bands. Introduced here is a new analysis approach that considers the presence of the BWG enclosure. Results based on the new analysis have revealed new understandings of the performance degradation mechanisms in a BWG antenna and have provided direction for potential design improvements. Author

N89-27887*# Jet Propulsion Lab., California Inst. of Tech., Pasadena.
MULTIPURPOSE EXCITER WITH LOW PHASE NOISE **c33**
B. Conroy and D. Le *In its* The Telecommunications and Data Acquisition Report 15 May 1989 p 169-174 (For primary document see N89-27871 22-32)
Avail: NTIS HC A17/MF A01 CSCL 09A

Results of an effort to develop a lower-cost exciter with high stability, low phase noise, and controllable phase and frequency for use in Deep Space Network and Goldstone Solar System Radar applications are discussed. Included is a discussion of the basic concept, test results, plans, and concerns. Author

N89-27888*# Jet Propulsion Lab., California Inst. of Tech., Pasadena.
SOFTWARE PACKAGE FOR PERFORMING EXPERIMENTS ABOUT THE CONVOLUTIONALLY ENCODED VOYAGER 1 LINK **c61**
U. Cheng *In its* The Telecommunications and Data Acquisition Report 15 May 1989 p 175-179 (For primary document see N89-27871 22-32)
Avail: NTIS HC A17/MF A01 CSCL 09B

A software package enabling engineers to conduct experiments to determine the actual performance of long constraint-length convolutional codes over the Voyager 1 communication link directly from the Jet Propulsion Laboratory (JPL) has been developed. Using this software, engineers are able to enter test data from the Laboratory in Pasadena, California. The software encodes the data and then sends the encoded data to a personal computer (PC) at the Goldstone Deep Space Complex (GDSC) over telephone lines. The encoded data are sent to the transmitter by the PC at GDSC. The received data, after being echoed back by Voyager 1, are first sent to the PC at GDSC, and then are sent back to the PC at the Laboratory over telephone lines for decoding and further analysis. All of these operations are fully integrated and are completely automatic. Engineers can control the entire software system from the Laboratory. The software encoder and the hardware decoder interface were developed for other applications, and have been modified appropriately for integration into the system so that their existence is transparent to the users. This software provides: (1) data entry facilities, (2) communication protocol for telephone links, (3) data displaying facilities, (4) integration with the software encoder and the hardware decoder, and (5) control functions. Author

N89-27889*# Jet Propulsion Lab., California Inst. of Tech., Pasadena.
THE USE OF INTERLEAVING FOR REDUCING RADIO LOSS IN TRELLIS-CODED MODULATION SYSTEMS

D. Divsalar and M. K. Simon *In its* The Telecommunications and Data Acquisition Report 15 May 1989 p 180-193 (For primary document see N89-27871 22-32)
Avail: NTIS HC A17/MF A01 CSCL 20N

It is demonstrated how the use of interleaving/deinterleaving in trellis-coded modulation (TCM) systems can reduce the signal-to-noise ratio loss due to imperfect carrier demodulation references. Both the discrete carrier (phase-locked loop) and suppressed carrier (Costas loop) cases are considered and the differences between the two are clearly demonstrated by numerical results. These results are of great importance for future communication links to the Deep Space Network (DSN), especially from high Earth orbiters, which may be bandwidth limited. Author

N89-27890*# Jet Propulsion Lab., California Inst. of Tech., Pasadena.
PERFORMANCE OF CONCATENATED CODES USING 8-BIT AND 10-BIT REED-SOLOMON CODES c61
F. Pollara and K.-M. Cheung *In its* The Telecommunications and Data Acquisition Report 15 May 1989 p 194-201 (For primary document see N89-27871 22-32)
Avail: NTIS HC A17/MF A01 CSCL 09B

The performance improvement of concatenated coding systems using 10-bit instead of 8-bit Reed-Solomon codes is measured by simulation. Three inner convolutional codes are considered: (7,1/2), (15,1/4), and (15,1/6). It is shown that approximately 0.2 dB can be gained at a bit error rate of 10(-6). The loss due to nonideal interleaving is also evaluated. Performance comparisons at very low bit error rates may be relevant for systems using data compression. Author

N89-27891*# Jet Propulsion Lab., California Inst. of Tech., Pasadena.
DECODING OF 1/2-RATE (24,12) GOLAY CODES c61
T.-K. Truong, I. S. Reed, and X. Yin *In its* The Telecommunications and Data Acquisition Report 15 May 1989 p 202-207 (For primary document see N89-27871 22-32)
Avail: NTIS HC A17/MF A01 CSCL 09B

A decoding method for a (23,12) Golay code is extended to the important 1/2-rate (24,12) Golay code so that three errors can be corrected and four errors can be detected. It is shown that the method can be extended to any decoding method which can correct three errors in the (23,12) Golay code. Author

N89-27892*# Jet Propulsion Lab., California Inst. of Tech., Pasadena.
THE WEIGHT DISTRIBUTION AND RANDOMNESS OF LINEAR CODES c61
K.-M. Cheung *In its* The Telecommunications and Data Acquisition Report 15 May 1989 p 208-215 (For primary document see N89-27871 22-32)
Avail: NTIS HC A17/MF A01 CSCL 09B

Finding the weight distributions of block codes is a problem of theoretical and practical interest. Yet the weight distributions of most block codes are still unknown except for a few classes of block codes. Here, by using the inclusion and exclusion principle, an explicit formula is derived which enumerates the complete weight distribution of an (n,k,d) linear code using a partially known weight distribution. This expression is analogous to the Pless power-moment identities - a system of equations relating the weight distribution of a linear code to the weight distribution of its dual code. Also, an approximate formula for the weight distribution of most linear (n,k,d) codes is derived. It is shown that for a given linear (n,k,d) code over GF(q), the ratio of the number of codewords of weight u to the number of words of weight u approaches the constant Q = q(-)(n-k) as u becomes large. A relationship between the randomness of a linear block code and the minimum distance of its dual code is given, and it is shown that most linear block codes with rigid algebraic and combinatorial structure also display certain random properties which make them similar to random codes with no structure at all. Author

N89-27893*# Jet Propulsion Lab., California Inst. of Tech., Pasadena.
EFFECTIVE AMPLIFIER NOISE FOR AN OPTICAL RECEIVER BASED ON LINEAR MODE AVALANCHE PHOTODIODES c74
C.-C. Chen *In its* The Telecommunications and Data Acquisition Report 15 May 1989 p 216-220 (For primary document see N89-27871 22-32)
Avail: NTIS HC A17/MF A01 CSCL 20F

The rms noise charge induced by the amplifier for an optical receiver based on the linear-mode avalanche photodiode (APD) was analyzed. It is shown that for an amplifier with a 1-pF capacitor and a noise temperature of 100 K, the rms noise charge due to the amplifier is about 300. Since the noise charge must be small compared to the signal gain, APD gains on the order of 1000 will be required to operate the receiver in the linear mode. Author

N89-27894*# Jet Propulsion Lab., California Inst. of Tech., Pasadena.
A VISIBILITY CHARACTERIZATION PROGRAM FOR OPTICAL COMMUNICATIONS THROUGH THE ATMOSPHERE c74
K. Cowles *In its* The Telecommunications and Data Acquisition Report 15 May 1989 p 221-225 (For primary document see N89-27871 22-32)
Avail: NTIS HC A17/MF A01 CSCL 20F

A program is described for characterizing the atmosphere as it affects optical communications from a spacecraft. Cloud cover patterns and optical transmission will be determined by setting up three automated observatories in the Southwestern United States. Methods of site selection and operation of hardware and software components are presented, as well as plans for term deployment. Author

N89-27895*# Jet Propulsion Lab., California Inst. of Tech., Pasadena.
OPTIONS FOR DAYTIME MONITORING OF ATMOSPHERIC VISIBILITY IN OPTICAL COMMUNICATIONS c46
D. Erickson and K. Cowles *In its* The Telecommunications and Data Acquisition Report 15 May 1989 p 226-234 (For primary document see N89-27871 22-32)
Avail: NTIS HC A17/MF A01 CSCL 04A

Techniques for daytime detection of atmospheric transmission and cloud cover to determine the capabilities of future deep-space optical communications links are considered. A modification of the planned nighttime photometry program will provide the best data while minimizing the need for further equipment. Greater degrees of modification will provide increased detection capabilities. Future testing of the equipment will better define the improvement offered by each level of modification. Daytime photometry is favored at certain wavelengths because of higher transmission and lower background noise, thus giving an increased signal-to-noise ratio. A literature search has provided a list of stars brighter than second magnitude at these wavelengths. Author

N89-27896*# Jet Propulsion Lab., California Inst. of Tech., Pasadena.
SITE SELECTION CRITERIA FOR THE OPTICAL ATMOSPHERIC VISIBILITY MONITORING TELESCOPES c47
K. Cowles *In its* The Telecommunications and Data Acquisition Report 15 May 1989 p 235-239 (For primary document see N89-27871 22-32)
Avail: NTIS HC A17/MF A01 CSCL 04B

A description of each of the criteria used to decide where to locate the Atmospheric Visibility Monitoring (AVM) telescope systems is given, along with a weighting factor for each of them. These criteria include low probability of clouds, fog, smog, haze, low scattering, low turbulence, availability of security and maintenance, and suitability of a site for a potential optical reception station. They will be used to determine which three of several sites under consideration will be used for monitoring visibility through the atmosphere as it applies to an optical ground-based receiving network as may be used in NASA space missions in decades to come. Author

N89-27897*# Jet Propulsion Lab., California Inst. of Tech., Pasadena.
A NOVEL APPROACH TO A PPM-MODULATED FREQUENCY-DOUBLED ELECTRO-OPTIC CAVITY-DUMPED Nd:YAG LASER **c36**
D. L. Robinson *In its* The Telecommunications and Data Acquisition Report 15 May 1989 p 240-247 (For primary document see N89-27871 22-32)
Avail: NTIS HC A17/MF A01 CSCL 20E

A technique which can provide frequency doubling, with high efficiency, while cavity dumping a laser for pulse position M-ary modulation while being used for an optical communication link is discussed. This approach uses a secondary cavity that provides feedback of the undoubled fundamental light, which is normally lost, into the primary cavity to be recirculated and frequency doubled. Specific operations of the electrooptic modulator and frequency-doubling crystal are described along with the overall modulation scheme and experimental setup. Author

N89-27898*# Jet Propulsion Lab., California Inst. of Tech., Pasadena.
MICROWAVE TIME DELAYS FOR THE X/S-BAND FEED SYSTEM AT X-BAND **c33**
J. Chen *In its* The Telecommunications and Data Acquisition Report 15 May 1989 p 248-251 (For primary document see N89-27871 22-32)
Avail: NTIS HC A17/MF A01 CSCL 09A

The X-band time delays for the X/S feed system of the 34-meter high efficiency antenna are required to refine current X-band downlink (8450 plus or minus 50 MHz) calibrations and prepare for the Magellan uplink (7190 plus or minus 45 MHz). The time delays of elements in the X-band feed system are obtained mostly via computer calculation and partly via measurement. The methods used and results obtained are presented. There is good agreement with theory. Author

N89-27899*# Jet Propulsion Lab., California Inst. of Tech., Pasadena.
DSN RADIO SCIENCE SYSTEM DESIGN AND TESTING FOR VOYAGER-NEPTUNE ENCOUNTER
N. C. Ham, T. A. Rebold, and J. F. Weese *In its* The Telecommunications and Data Acquisition Report 15 May 1989 p 252-284 (For primary document see N89-27871 22-32)
Avail: NTIS HC A17/MF A01 CSCL 20N

The Deep Space Network (DSN) Radio Science System presently implemented within the Deep Space Network was designed to meet stringent requirements imposed by the demands of the Voyager-Neptune encounter and future missions. One of the initial parameters related to frequency stability is discussed. The requirement, specification, design, and methodology for measuring this parameter are described. A description of special instrumentation that was developed for the test measurements and initial test data resulting from the system tests performed at Canberra, Australia and Usuda, Japan are given. Author

N89-27900*# Jet Propulsion Lab., California Inst. of Tech., Pasadena.
ACCURACY OF TELEMETRY SIGNAL POWER LOSS IN A FILTER AS AN ESTIMATE FOR TELEMETRY DEGRADATION **c17**
M. A. Koerner *In its* The Telecommunications and Data Acquisition Report 15 May 1989 p 285-291 (For primary document see N89-27871 22-32)
Avail: NTIS HC A17/MF A01 CSCL 09F

When telemetry data is transmitted through a communication link, some degradation in telemetry performance occurs as a result of the imperfect frequency response of the channel. The term telemetry degradation as used here is the increase in received signal power required to offset this filtering. The usual approach to assessing this degradation is to assume that it is equal to the signal power loss in the filtering, which is easily calculated. However, this approach neglects the effects of the nonlinear phase response of the filter, the effect of any reduction of the receiving system noise due to the filter, and intersymbol interference. Here, an exact calculation of the telemetry degradation, which includes all of the above effects, is compared with the signal power loss calculation for RF filtering of NRZ data on a carrier. The signal power loss calculation is found to be a reasonable approximation when the filter follows the point at which the receiving system noise is introduced, especially if the signal power loss is less than 0.5 dB. The signal power loss approximation is less valid when the receiving system noise is not filtered. Author

N89-27901*# Jet Propulsion Lab., California Inst. of Tech., Pasadena.
THE DSS-14 C-BAND EXCITER **c33**
D. R. Rowan *In its* The Telecommunications and Data Acquisition Report 15 May 1989 p 292-299 (For primary document see N89-27871 22-32)
Avail: NTIS HC A17/MF A01 CSCL 09A

The development and implementation of a C-band exciter for use with the Block IV Receiver-Exciter Subsystem at Deep Space Station 14 (DSS-14) has been completed. The exciter supplements the standard capabilities of the Block IV system by providing a drive signal for the C-band transmitter while generating coherent translation frequencies for C-band (5-GHz) to S-band (2.2- to 2.3-GHz) Doppler extraction, C-band to L-band (1.6-GHz) zero delay measurements, and a level calibrated L-band test signal. Exciter functions are described, and a general explanation and description of the C-band uplink controller is presented. Author

N89-27902*# Jet Propulsion Lab., California Inst. of Tech., Pasadena.
ORTHOGONAL SETS OF DATA WINDOWS CONSTRUCTED FROM TRIGONOMETRIC POLYNOMIALS **c64**
C. A. Greenhall *In its* The Telecommunications and Data Acquisition Report 15 May 1989 p 300-305 (For primary document see N89-27871 22-32)
Avail: NTIS HC A17/MF A01 CSCL 12A

Suboptimal, easily computable substitutes for the discrete prolate-spheroidal windows used by Thomson for spectral estimation are given. Trigonometric coefficients and energy leakages of the window polynomials are tabulated. Author

N89-27903*# Jet Propulsion Lab., California Inst. of Tech., Pasadena.
DSN 70-METER ANTENNA MICROWAVE OPTICS DESIGN AND PERFORMANCE IMPROVEMENTS. PART 1: DESIGN OPTIMIZATION **c74**
D. A. Bathker and S. D. Slobin *In its* The Telecommunications and Data Acquisition Report 15 May 1989 p 306-313 (For primary document see N89-27871 22-32)
Avail: NTIS HC A17/MF A01 CSCL 20F

The design optimizations associated with the microwave and structural upgrade of the DSN 64-m antennas are discussed. Expected area efficiency/gain performances at S- and X-band are given for both the original 64-m systems and the upgraded 70-m systems, and error estimates are developed. The DSN 70-m Upgrade Project specifications, based on predesign estimates, were 1.4-dB gain at S-band and 1.9-dB at X-band, with no degradation to critical receiving system noise temperatures. The measurements show an S-band gain increase of 1.9 dB and an average increase of 2.1 dB at X-band. The Project also delivered small receiving system noise decreases at both frequency bands. The three DSN 70-m antennas, in the initial state of mechanical adjustment as of the end of calendar year 1988, are performing with very high peak microwave area efficiencies at very nearly the engineering design expectations of 76 percent at S-band and 71 percent at X-band. Author

N89-27904*# Jet Propulsion Lab., California Inst. of Tech., Pasadena.
DSN 70-METER ANTENNA X- AND S-BAND CALIBRATION. PART 1: GAIN MEASUREMENTS
P. H. Richter and S. D. Slobin *In its* The Telecommunications

and Data Acquisition Report 15 May 1989 p 314-351 (For primary document see N89-27871 22-32)
Avail: NTIS HC A17/MF A01 CSCL 20N

Aperture efficiency measurements made during 1988 on the three 70-m stations (DSS-14, DSS-43, and DSS-63) at X-band (8420 MHz) and S-band (2295 MHz) have been analyzed and reduced to yield best estimates of antenna gain versus elevation. The analysis has been carried out by fitting the gain data to a theoretical expression based on the Ruze formula. Newly derived flux density and source-size correction factors for the natural radio calibration sources used in the measurements have been used in the reduction of the data. Peak gains measured at the three stations were 74.18 (plus or minus 0.10) dBi at X-band, and 63.34 (plus or minus 0.03) dBi at S-band, with corresponding peak aperture efficiencies of 0.687 (plus or minus 0.015) and 0.762 (plus or minus 0.006), respectively. The values quoted assume no atmosphere is present, and the estimated absolute accuracy of the gain measurements is approximately plus or minus 0.2 dB at X-band and plus or minus 0.1 dB at S-band (1-sigma values). Author

N89-27905*# Jet Propulsion Lab., California Inst. of Tech., Pasadena.
DSN 70-METER ANTENNA X- AND S-BAND CALIBRATION. PART 2: SYSTEM NOISE TEMPERATURE MEASUREMENTS AND TELECOMMUNICATIONS LINK EVALUATION
S. D. Slobin and P. H. Richter *In its* The Telecommunications and Data Acquisition Report 15 May 1989 p 352-366 (For primary document see N89-27871 22-32)
Avail: NTIS HC A17/MF A01 CSCL 20N

The X- and S-band system operating noise temperatures of the Deep Space Network (DSN) 70-m antennas are presented. Models of atmosphere and ground noise temperature contributions, as they affect the antenna calibrations, are given for future use in telecommunications link modeling. The measured 70-m antenna network gain/system noise temperature (G/T) performance is presented. Compared with the earlier 64-m antenna network, G/T improvements of from 1.8 dB to 2.5 dB, depending on elevation angle, were achieved. G/T comparisons are made with the DSN/Flight Project Design Handbook and the Voyager telecommunications design control table. Actual Voyager telecommunications link performance is compared with predictions made by TPAP (the Voyager telecommunications prediction and analysis program) and with measured performance of the individual 70-m antennas. A modification in the use of antenna gain, system noise temperature, and atmospheric attenuation in existing telecommunications design control tables is suggested. Author

N89-27906*# Jet Propulsion Lab., California Inst. of Tech., Pasadena.
REANALYSIS, COMPATIBILITY AND CORRELATION IN ANALYSIS OF MODIFIED ANTENNA STRUCTURES
R. Levy *In its* The Telecommunications and Data Acquisition Report 15 May 1989 p 367-381 (For primary document see N89-27871 22-32)
Avail: NTIS HC A17/MF A01 CSCL 20N

A simple computational procedure is synthesized to process changes in the microwave-antenna pathlength-error measure when there are changes in the antenna structure model. The procedure employs structural modification reanalysis methods combined with new extensions of correlation analysis to provide the revised rms pathlength error. Mainframe finite-element-method processing of the structure model is required only for the initial unmodified structure, and elementary postprocessor computations develop and deal with the effects of the changes. Several illustrative computational examples are included. The procedure adapts readily to processing spectra of changes for parameter studies or sensitivity analyses. Author

N89-27907*# Jet Propulsion Lab., California Inst. of Tech., Pasadena.
PROCEEDINGS OF THE MOBILE SATELLITE SYSTEM ARCHITECTURES AND MULTIPLE ACCESS TECHNIQUES WORKSHOP
Khaled Dessouky Mar. 1989 116 p Workshop held in Pasadena, CA, 7-8 Mar. 1989
(Contract NAS7-918)
(NASA-CR-184564; JPL-Publ-89-13; NAS 1.26:184564) Avail: NTIS HC A06/MF A01 CSCL 17B

The Mobile Satellite System Architectures and Multiple Access Techniques Workshop served as a forum for the debate of system and network architecture issues. Particular emphasis was on those issues relating to the choice of multiple access technique(s) for the Mobile Satellite Service (MSS). These proceedings contain articles that expand upon the 12 presentations given in the workshop. Contrasting views on Frequency Division Multiple Access (FDMA), Code Division Multiple Access (CDMA), and Time Division Multiple Access (TDMA)-based architectures are presented, and system issues relating to signaling, spacecraft design, and network management constraints are addressed. An overview article that summarizes the issues raised in the numerous discussion periods of the workshop is also included. For individual titles, see N89-27908 through N89-27918.

N89-27908*# Transit Communications, Inc., Pasadena, CA.
THE AMSC MOBILE SATELLITE SYSTEM: DESIGN SUMMARY AND COMPARATIVE ANALYSIS
Gary K. Noreen *In* Jet Propulsion Lab., California Inst. of Tech., Proceedings of the Mobile Satellite System Architectures and Multiple Access Techniques Workshop Mar. 1989 p 15-22 (For primary document see N89-27907 22-32)
Avail: NTIS HC A06/MF A01 CSCL 17B

Mobile satellite communications will be provided in the United States by the American Mobile Satellite Consortium (AMSC). Telesat Mobile, Inc. (TMI) and AMSC are jointly developing MSAT, the first regional Mobile Satellite Service (MSS) system. MSAT will provide diverse mobile communications services - including voice, data and position location - to mobiles on land, water, and in the air throughout North America. Described here are the institutional relationships between AMSC, TMI and other organizations participating in MSAT, including the Canadian Department of Communications and NASA. The regulatory status of MSAT in the United States and international allocations to MSS are reviewed. The baseline design is described. Author

N89-27909*# International Maritime Satellite Organization, London (England).
CHOICE OF FDMA/SCPC ACCESS TECHNIQUE FOR AERONAUTICAL SATELLITE VOICE SYSTEM
G. K. Smith *In* Jet Propulsion Lab., California Inst. of Tech., Proceedings of the Mobile Satellite System Architectures and Multiple Access Techniques Workshop Mar. 1989 p 23-28 (For primary document see N89-27907 22-32)
Avail: NTIS HC A06/MF A01 CSCL 17B

A worldwide aeronautical mobile satellite system is about to become operational. The system architecture and access methods have been debated extensively, resulting in the selection of Time Division Multiplexing/Time Division Multiple Access (TDM/TDMA) access for packet data, and Single Channel Per Carrier (SCPC) for voice. These have become standards for airline use, and also satisfy the known requirements of ICAO for safety related communications. Voice communications are expected to absorb a high proportion of satellite bandwidth and power in the future. Here, it is explained why INMARSAT selected Frequency Division Multiple Access/SCPC satellite access for this application. Author

N89-27910*# Jet Propulsion Lab., California Inst. of Tech., Pasadena.
PERFORMANCE OF DA/FDMA ARCHITECTURE PROPOSED FOR MSS
Charles Wang, Tsun-Yee Yan, and Khaled Dessouky *In its*

Proceedings of the Mobile Satellite System Architectures and Multiple Access Techniques Workshop Mar. 1989 p 29-36 (For primary document see N89-27907 22-32)
Avail: NTIS HC A06/MF A01 CSCL 17B

The system architecture proposed for the Mobile Satellite Service (MSS) by the National Aeronautics and Space Administration (NASA)/JPL is presented. The demand assigned Frequency Division Multiple Access (FDMA) scheme is described, and results for the associated network access protocol developed by JPL are presented. Both the total number of users that the system can support and the system spectral efficiency are given for a variety of traffic conditions, including those postulated for the Mobile Satellite System Architectures and Multiple Access Techniques Workshop. The results are given for both first- and second-generation one- and two-satellite systems. Author

N89-27911*# Geostar Messaging Corp., Washington, DC. System Implementation.
GEOSTAR'S SYSTEM ARCHITECTURES
Ronald J. Lepkowski *In* Jet Propulsion Lab., California Inst. of Tech., Proceedings of the Mobile Satellite System Architectures and Multiple Access Techniques Workshop Mar. 1989 p 37-41 (For primary document see N89-27907 22-32)
Avail: NTIS HC A06/MF A01 CSCL 17B

Geostar is currently constructing a radiodetermination satellite system to provide position fixes and vehicle surveillance services, and has proposed a digital land mobile satellite service to provide data, facsimile and digitized voice services to low cost mobile users. The different system architectures for these two systems, are reviewed. Author

N89-27912*# Qualcomm, Inc., San Diego, CA.
WHY IS CDMA THE SOLUTION FOR MOBILE SATELLITE COMMUNICATION
Klein S. Gilhousen, Irwin M. Jacobs, Roberto Padovani, and Lindsay A. Weaver *In* Jet Propulsion Lab., California Inst. of Tech., Proceedings of the Mobile Satellite System Architectures and Multiple Access Techniques Workshop Mar. 1989 p 57-70 Presented at the Mobile Satellite Conference, Pasadena, CA, May 1988 Sponsored in part by Hughes Aircraft Company (For primary document see N89-27907 22-32)
Avail: NTIS HC A06/MF A01 CSCL 17B

It is demonstrated that spread spectrum Code Division Multiple Access (CDMA) systems provide an economically superior solution to satellite mobile communications by increasing the system maximum capacity with respect to single channel per carrier Frequency Division Multiple Access (FDMA) systems. Following the comparative analysis of CDMA and FDMA systems, the design of a model that was developed to test the feasibility of the approach and the performance of a spread spectrum system in a mobile environment. Results of extensive computer simulations as well as laboratory and field tests results are presented. Author

N89-27913*# Hughes Communications, Inc., Los Angeles, CA.
SYSTEM LEVEL COMPARISON OF FDMA VS. CDMA (UNDER CONFERENCE GUIDELINE CONSTRAINT)
Ken Renshaw *In* Jet Propulsion Lab., California Inst. of Tech., Proceedings of the Mobile Satellite System Architectures and Multiple Access Techniques Workshop Mar. 1989 p 71-76 (For primary document see N89-27907 22-32)
Avail: NTIS HC A06/MF A01 CSCL 17B

The margin that is required to mitigate the near-far problem in a Code Division Multiple Access (CDMA) mobile satellite system is determined by the radio-propagation model selected, the distribution of the users in clear and shadowed environments, and implementation techniques. The use of revenue potential as a means of evaluating the relative merits of CDMA and Frequency Division Multiple Access (FDMA) systems is a convenient way to rationalize the performance of systems using high-gain and low-gain antennas. The revenue potential of CDMA is much greater than the revenue potential for FDMA for a particular satellite design considered. Author

N89-27914*# Spread Spectrum Systems, Inc., Olney, MD.
ALTERNATIVE MULTIPLE-ACCESS TECHNIQUES FOR MOBILE SATELLITE SYSTEMS
Patrick O. Smith and Evaggelos Geraniotis *In* Jet Propulsion Lab., California Inst. of Tech., Proceedings of the Mobile Satellite System Architectures and Multiple Access Techniques Workshop Mar. 1989 p 77-82 (For primary document see N89-27907 22-32)
Avail: NTIS HC A06/MF A01 CSCL 17B

The use of Code Division Multiple Access (CDMA) to satisfy the diverse requirements of a generic (land, maritime, aeronautical) mobile satellite system (MSS) network design is discussed. Comparisons between CDMA and Frequency Division Multiple Access (FDMA) show that a CDMA network design can support significantly more voice channel allocations than FDMA when relatively simple CDMA correlation receivers are employed, provided that there is sufficient space segment equivalent isotropically radiated power (EIRP). The use of more advanced CDMA receivers can improve the spectral and power efficiency. Although the use of CDMA may not gain immediate and widespread support in the international MSS community, provision for the use of CDMA for a domestic system in the U.S., and possibly for a regional system throughout North America, is likely. Author

N89-27915*# Telesat Mobile, Inc., Ottawa (Ontario).
PRACTICAL CONSTRAINTS ON NETWORK ARCHITECTURE AND SIGNALLING IN THE MSAT SYSTEM
N. George Davies *In* Jet Propulsion Lab., California Inst. of Tech., Proceedings of the Mobile Satellite System Architectures and Multiple Access Techniques Workshop Mar. 1989 p 85-90 (For primary document see N89-27907 22-32)
Avail: NTIS HC A06/MF A01 CSCL 17B

Telesat Mobile Inc. plans to provide mobile satellite communications services in Canada in 1993/4, in close cooperation with the American Mobile Satellite Consortium Inc., which will be providing services in the U.S.A. L-band frequencies will be used in multiple beams for communication with mobile terminals. Ku-band frequencies will be used for the feeder-links to fixed stations. The system will support voice and data communications. The baseline Canadian system will support approximately 450 assignable voice channels, some fraction of which will be the equivalent in data channels. The method of multiple access will be Frequency Division Multiple Access/Single Channel Per Carrier. The availability of frequencies, the availability of technology and the time scale for implementation all constrain the network architecture for the system. Further, it is important to have an open specification to encourage multiple equipment vendors. The interplay of these constraints is discussed. Author

N89-27916*# Spar Aerospace Ltd., Ste-Anne-de-Bellevue (Quebec). Communications Group.
MSAT SIGNALLING AND NETWORK MANAGEMENT ARCHITECTURES
Peter Garland and J. Malcolm Keelty *In* Jet Propulsion Lab., California Inst. of Tech., Proceedings of the Mobile Satellite System Architectures and Multiple Access Techniques Workshop Mar. 1989 p 91-101 (For primary document see N89-27907 22-32)
Avail: NTIS HC A06/MF A01 CSCL 17B

Spar Aerospace has been active in the design and definition of Mobile Satellite Systems since the mid 1970's. In work sponsored by the Canadian Department of Communications, various payload configurations have evolved. In addressing the payload configuration, the requirements of the mobile user, the service provider and the satellite operator have always been the most important consideration. The current Spar 11 beam satellite design is reviewed, and its capabilities to provide flexibility and potential for network growth within the WARC87 allocations are explored. To enable the full capabilities of the payload to be realized, a large amount of ground based Switching and Network Management infrastructure will be required, when space segment becomes available. Early indications were that a single custom designed Demand Assignment Multiple Access (DAMA) switch should be implemented to provide efficient use of the space segment. As

MSAT has evolved into a multiple service concept, supporting many service providers, this architecture should be reviewed. Some possible signalling and Network Management solutions are explored. Author

N89-27917*# Aussat Proprietary Ltd., Sydney (Australia).
A ROBUST SIGNALLING SYSTEM FOR LAND MOBILE SATELLITE SERVICES
Dale Irish, Gary Shmith, Nick Hart, and Marie Wines *In* Jet Propulsion Lab., California Inst. of Tech., Proceedings of the Mobile Satellite System Architectures and Multiple Access Techniques Workshop Mar. 1989 p 103-108 (For primary document see N89-27907 22-32)
Avail: NTIS HC A06/MF A01 CSCL 17B

Presented here is a signalling system optimized to ensure expedient call set-up for satellite telephony services in a land mobile environment. In a land mobile environment, the satellite to mobile link is subject to impairments from multipath and shadowing phenomena, which result in signal amplitude and phase variations. Multipath, caused by signal scattering and reflections, results in sufficient link margin to compensate for these variations. Direct signal attenuation caused by shadowing due to buildings and vegetation may result in attenuation values in excess of 10 dB and commonly up to 20 dB. It is not practical to provide a link with sufficient margin to enable communication when the signal is blocked. When a moving vehicle passes these obstacles, the link will experience rapid changes in signal strength due to shadowing. Using statistical models of attenuation as a function of distance travelled, a communication strategy has been defined for the land mobile environment. Author

N89-27918*# Stanford Telecommunications, Inc., Santa Clara, CA.
AERONAUTICAL MOBILE TDMA/MCTDMA SYSTEM
Thomas Magill and Wayne Pierzga (Arinc Research Corp., Santa Ana, CA.) *In* Jet Propulsion Lab., California Inst. of Tech., Proceedings of the Mobile Satellite System Architectures and Multiple Access Techniques Workshop Mar. 1989 p 109-114 (For primary document see N89-27907 22-32)
Avail: NTIS HC A06/MF A01 CSCL 17B

A multiple carrier Time Division Multiple Access (TDMA) system capable of supporting voice, stream data, and packet data traffic between aircraft and ground terminals is presented. Demand assignment permits efficient resource sharing for voice and stream data. The bandwidth efficiency of uncoded A Quadrature Phase Shift Keying (AQPSK) is 1 bps/Hz. High time efficiency (approximately equals 83 percent) is achieved through the use of symbol synchronous TDMA. Demodulation is achieved without loop hang-up while requiring only a 16 symbol preamble each burst. A concatenated coding system provides reliable transmission under multipath conditions. Author

N89-27919# Naval Postgraduate School, Monterey, CA.
AN EXPERIMENTAL AND COMPUTER MODELING STUDY OF STEPPED RADIUS MONOPOLE ANTENNAS M.S. Thesis
Jae Yong Yim Dec. 1988 63 p
(AD-A207356) Avail: NTIS HC A04/MF A01 CSCL 12/5

The input impedance numerically calculated by MIN INEC, NEC, and NECGS are compared with experimental results on stepped radius monopole antennas for swept frequencies. This determines the limitation of computer codes and gives guidelines for Yagi and Log Periodic (LP) antenna designs which use Tapered Linear Antenna Elements (TLAE's) NEC and MININEC, thin wire modeling codes, use different Electric Field Integral Equation (EFIE) formulations of the method of moments for the solution of currents. A cylindrical wire cage model is used via NECGS. Four groups of computer models are developed, varying the number of segments from 1 to 70 for 27 to 31 MHz. Reflection coefficients of seven experimental models are measured at the antenna feed point, and the input impedances are calculated by an auxiliary computer program. The input impedance is then analyzed by comparing the computer simulation results with measured results. Surprisingly, the input impedance of MININEC is closest to experimental results for monopoles which were constructed with ratios of radius-to-wavelength up to 0.0026. GRA

N89-27920# Naval Postgraduate School, Monterey, CA.
ANALYSIS OF MARITIME MOBILE SATELLITE COMMUNICATION SYSTEMS M.S. Thesis
Augusto J. Zapata Dec. 1988 83 p
(AD-A207358) Avail: NTIS HC A05/MF A01 CSCL 25/2

The communication channel between a satellite and a ship earth station (SES) is described by a model which includes multipath fading, Doppler shift and noise. Multipath fading is caused by reflections from the sea surface. These reflections can affect the system performance, especially at low elevation angles or when SES is using low gain antennas. Doppler shift is a very important effect when using low altitude satellites, because of the high velocities involved. A software simulator is described and a simulator is presented for multipath fading in the maritime communications environment. Analysis of throughput of an unslotted Aloha maritime mobile satellite communication channel is also presented. GRA

N89-27921# Massachusetts Inst. of Tech., Cambridge. Dept. of Civil Engineering.
PROPAGATION CHARACTERISTICS OF ELECTROMAGNETIC WAVES IN CONCRETE Technical Report, Jan. - Dec. 1988
Udaya B. Halabe, Kenneth Maser, and Eduardo Kausel Mar. 1989 106 p
(Contract DAAL03-87-K-0005)
(AD-A207387; ARO-24620.3-EG-UIR) Avail: NTIS HC A06/MF A01 CSCL 20/14

This research develops models which can predict the velocity and attenuation of electromagnetic waves in concrete as a function of frequency, temperature, moisture content, chloride content and concrete mix constituents. These models were proposed to predict the electromagnetic properties of concrete by aggregating the electromagnetic properties of its constituents. Water and the dissolved salt are the constituents having the most prominent effect on the dielectric behavior of concrete. A comparative study of three existing three-phase mixture models was carried out. Numerical results were generated using the most representative Discrete model. These results have shown that the real part of complex concrete permittivity (and therefore the velocity of electromagnetic waves) is independent of salinity or frequency in the 0.6 to 3.0 GHz frequency range. On the other hand, these results show that the attenuation coefficient and dielectric conductivity vary almost linearly with frequency in this same frequency range. The real part of concrete permittivity and the attenuation coefficient also show a linear dependence with respect to the degree of saturation of water in the concrete mixture. This suggests that future research should focus on approximating the complex models presented in this research by simple equations. GRA

N89-27922# North Carolina Univ., Chapel Hill. Dept. of Statistics.
CAPACITY OF DISCRETE TIME GAUSSIAN CHANNEL WITH AND WITHOUT FEEDBACK, 2
Shunsuke Ihara and Kenjiro Yanagi May 1988 26 p
(Contract N00014-84-C-0212)
(AD-A207388; LISS-26-2) Avail: NTIS HC A03/MF A01 CSCL 12/4

The problem considered in this paper is whether the capacity of a discrete time Gaussian channel is increased by feedback or not. It is well known that the capacity of a white Gaussian channel under the average power constraint is not changed by feedback. Some conditions are given under which the capacity of a discrete time Gaussian channel is increased by feedback. It is also shown that there exists a non-white Gaussian channel whose capacity is not increased by feedback. GRA

N89-27923*# National Aeronautics and Space Administration. Lewis Research Center, Cleveland, OH.
PARAMETRIC STUDY OF ELECTROMAGNETIC WAVES PROPAGATING IN ABSORBING CURVED S DUCTS
Kenneth J. Baumeister Jul. 1989 25 p
(NASA-TM-102024; E-4761; NAS 1.15:102024) Avail: NTIS HC A03/MF A01 CSCL 20N

A finite-element Galerkin formulation has been developed to study attenuation of transverse magnetic (TM) waves propagating in two-dimensional S-curved ducts with absorbing walls. In the frequency range where the duct diameter and electromagnetic wave length are nearly equal, the effect of duct length, curvature (duct offset), and absorber wall thickness was examined. For a given offset in the curved duct, the length of the S-duct was found to significantly affect both the absorptive and reflective characteristics of the duct. For a straight and a curved duct with perfect electric conductor terminations, power attenuation contours were examined to determine electromagnetic wall properties associated with maximum input signal absorption. Offset of the S-duct was found to significantly affect the value of the wall permittivity associated with the optimal attenuation of the incident electromagnetic wave. Author

N89-27924# Sandia National Labs., Albuquerque, NM.
SCATTERING FROM FRACTALS
Alan J. Hurd 1989 7 p Presented at the NSF Workshop on Future Directions in Electromagnetics Research, Boston, MA, 25 Jul. 1989
(Contract DE-AC04-76DP-00789)
(DE89-013451; SAND-89-1346C; CONF-890791-1) Avail: NTIS HC A02/MF A01

The realization that structures in Nature often can be described by Mandelbrot's fractals has led to a revolution in many areas of physics. The interaction of waves with fractal systems has, understandably, become intensely studied since scattering is the method of choice to probe delicate fractal structures such as chainlike particle aggregates. Not all of these waves are electromagnetic. Neutron scattering, for example, is an important complementary tool to structural studies by X-ray and light scattering. Since the phenomenology of small-angle neutron scattering (SANS), as it is applied to fractal systems, is identical to that of small-angle X-ray scattering (SAXS), it falls within the scope of this paper. DOE

N89-27925# Sandia National Labs., Albuquerque, NM.
THE EFFECTS OF SNOW ON LANDMARKS IN K(SUB u) BAND SAR IMAGES
M. Murray Apr. 1989 127 p
(Contract DE-AC04-76DP-00789)
(DE89-014578; SAND-88-3153) Avail: NTIS HC A07/MF A01

The effects of snow on candidate landmarks for the TFS radar are documented. It includes a discussion of a simple snow model, relevant backscatter data from previous ground based collections, predictions of the effects of snow coverage based on this data, a discussion of the snow data collection with the TFS radar, and an analysis of the results of that collection. All SAR images are for a K sub u band radar, with HH polarization, and a 30 deg depression angle. The images have 3 m resolution and a 1 km swath. SAR images were collected of both rural and urban landmarks. DOE

N89-27926# International Centre for Theoretical Physics, Trieste (Italy).
ALGEBRAIC ANALYSIS OF THE ELECTROMAGNETIC WAVE INTERACTION WITH THE TWO-LEVEL SYSTEM WITH TWO-FOLD DEGENERATED STATES
K. A. Rustamov Nov. 1988 5 p Submitted for publication
(DE89-611932; IC-88/358) Avail: NTIS (US Sales Only) HC A02/MF A01

Algebraic properties of the analytical model, describing electro-magnetic weak interaction with the two-level system with two-fold degenerate state are considered. The expressions for the coherent states and Green's function of the system are obtained. DOE

N89-27927*# National Aeronautics and Space Administration. Lewis Research Center, Cleveland, OH.
DIGITAL CODEC FOR REAL-TIME PROCESSING OF BROADCAST QUALITY VIDEO SIGNALS AT 1.8 BITS/PIXEL
Mary Jo Shalkhauser and Wayne A. Whyte, Jr. 1989 10 p Prepared for presentation at the Global Telecommunications Conference, Dallas, TX, 27-30 Nov. 1989; sponsored in part by IEEE
(NASA-TM-102325; E-5026; NAS 1.15:102325) Avail: NTIS HC A02/MF A01 CSCL 17B

Advances in very large-scale integration and recent work in the field of bandwidth efficient digital modulation techniques have combined to make digital video processing technically feasible and potentially cost competitive for broadcast quality television transmission. A hardware implementation was developed for a DPCM-based digital television bandwidth compression algorithm which processes standard NTSC composite color television signals and produces broadcast quality video in real time at an average of 1.8 bits/pixel. The data compression algorithm and the hardware implementation of the CODEC are described, and performance results are provided. Author

N89-27928 ANT Nachrichtentechnik, Backnang (Germany, F.R.).
COMMUNICATION ENGINEERING REPORTS. FUNDAMENTAL DEVELOPMENTS. THEORETICAL WORK [NACHRICHTENTECHNISCHE BERICHTE. GRUNDLAGENENTWICKLUNG. THEORETISCHE ARBEITEN]
Hans Gschwendtner, ed. and Waldemar Hauk, ed. Nov. 1988 128 p In GERMAN Original contains color illustrations
(ETN-89-94623) Copyright Avail: Fachinformationszentrum Karlsruhe, 7514 Eggenstein-Leopoldshafen 2, Fed. Republic of Germany, 35 DM

A method for systems development was developed with a view to the increase of productivity and quality. A technical data base was realized for computer-assisted quality assurance. Coded frequency shift keying is presented. A theory of value-discrete adaptive compensation filters was developed. Receiver synchronization for the ISDN basic connection and for spread spectrum transmission was studied. A concept for carrier recovery for higher-stage quadrature-amplitude-modulated signals was developed. The dimensioning of baseband equalizers for digital radio relay links was studied. Digital demultiplexers and demodulators for mobile satellite communication were designed. A speech code was developed. Field theory simulation of nonreciprocal microwave components was performed. A method for the calculation of losses in waveguide networks was developed. For individual titles, see N89-27929 through N89-27942.

N89-27929 ANT Nachrichtentechnik, Backnang (Germany, F.R.).
MODEL AND METHOD FOR SYSTEMS DEVELOPMENT [MODELL UND METHODE FUER DIE SYSTEMENTWICKLUNG]
Erich Behl and Michael Rittel *In its* Communication Engineering Reports. Fundamental Developments. Theoretical Work Nov. 1988 p 4-9 In GERMAN (For primary document see N89-27928 22-32)
Copyright Avail: Fachinformationszentrum Karlsruhe, 7514 Eggenstein-Leopoldshafen 2, Fed. Republic of Germany, 35 DM

A method for systems development was developed with a view to the increase of productivity and quality. The basic approaches are a standard consideration of software and hardware and the rapid prototyping procedure. The methodological procedure is strongly characterized by the reuse of available concepts as well as of hardware and software components. The method is supported by a systems development environment which contains adjusted aids and automates a serres of activities. ESA

N89-27930 ANT Nachrichtentechnik, Backnang (Germany, F.R.).
REQUIREMENTS FOR A TECHNICAL DATA BASE [ANFORDERUNGEN AN EINE TECHNISCHE DATENBANK]
c82
Burkhardt Lowe *In its* Communication Engineering Reports. Fundamental Developments. Theoretical Work Nov. 1988 p 10-23 In GERMAN (For primary document see N89-27928

22-32)
Copyright Avail: Fachinformationszentrum Karlsruhe, 7514 Eggenstein-Leopoldshafen 2, Fed. Republic of Germany, 35 DM

A technical data base was realized for computer assisted quality assurance of glass fiber cable production as well as for the further development of optical cable techniques. The emphasis was on the storage of physical and optical data. The different tasks of the data base are presented. The conceptual design as well as the logical and physical design of the data base are described. The data dictionary and the field of applications are depicted. Practical experience with the glass fiber data base is very positive. ESA

N89-27931 ANT Nachrichtentechnik, Backnang (Germany, F.R.).
MINIMUM SHIFT KEYING. A MODULATION SYSTEM WITH CODING [MINIMUM SHIFT KEYING. EIN MODULATIONSSYSTEM MIT CODIERUNG]
Rudolf Wrzesinsky *In its* Communication Engineering Reports. Fundamental Developments. Theoretical Work Nov. 1988 p 24-29 In GERMAN (For primary document see N89-27928 22-32)
Copyright Avail: Fachinformationszentrum Karlsruhe, 7514 Eggenstein-Leopoldshafen 2, Fed. Republic of Germany, 35 DM

The digital modulation method Minimum Shift Keying (MSK) is presented as coded Frequency Shift Keying (FSK) with a view to the transmission of digital signals via nonlinear channels. The elimination of the coding up to a trivial difference coding is possible using a basic change in the signal space. The equivalence is demonstrated between the representation of MSK as continuous phase modulation and as offset quadrature amplitude modulation. The maximum likelihood receiver can directly be specified. The Massey receiver results from a simple transformation. ESA

N89-27932 ANT Nachrichtentechnik, Backnang (Germany, F.R.).
ANALYSIS AND DIMENSIONING OF A VALUE-DISCRETE ADAPTIVE COMPENSATION FILTER [ANALYSE UND DIMENSIONIERUNG WERTDISKRETER ADAPTIVER KOMPENSATIONSFILTER] **c33**
Bernd Friedrichs *In its* Communication Engineering Reports. Fundamental Developments. Theoretical Work Nov. 1988 p 30-39 In GERMAN (For primary document see N89-27928 22-32)
Copyright Avail: Fachinformationszentrum Karlsruhe, 7514 Eggenstein-Leopoldshafen 2, Fed. Republic of Germany, 35 DM

A closed theory of value-discrete adaptive compensation filters was developed. The exact theoretical analysis of adaptive compensation filters is outlined. Simple formulas were used to calculate the residual errors and the convergence speed as a function of the quantization operations and the amplitude distributions of the signals, resulting in a secure dimensioning. The theory is demonstrated by an adaptive echo cancellation for full-duplex data transmission. ESA

N89-27933 ANT Nachrichtentechnik, Backnang (Germany, F.R.).
SYNCHRONIZATION OF THE RECEIVER FOR THE ISDN BASIC CONNECTION [ZUR SYNCHRONISATION DES EMPFAENGERS FUER DEN ISDN-BASISANSCHLUSS]
Volker Hespelt and Fritz Widmann *In its* Communication Engineering Reports. Fundamental Developments. Theoretical Work Nov. 1988 p 40-49 In GERMAN Sponsored by the Bundesministerium fuer Forschung und Technologie, Bonn, Fed. Republic of Germany (For primary document see N89-27928 22-32)
Copyright Avail: Fachinformationszentrum Karlsruhe, 7514 Eggenstein-Leopoldshafen 2, Fed. Republic of Germany, 35 DM

The UIC component, required for user connection to ISDN, is presented. The UIC component realizes the full duplex transmission with a 144 kbit/s bit rate on the two-wire user connection circuit. The substantial requirements for signal processing, switching technique, and technology imposed by the necessary direction separation are discussed. The complexity of the UIC component, as well as the efficiency of the digital signal processing are presented. The concept of the receiver synchronization with its five control circuits is explained. ESA

N89-27934 ANT Nachrichtentechnik, Backnang (Germany, F.R.).
RECEIVER SYNCHRONIZATION FOR SPREAD SPECTRUM TRANSMISSION [EMPFAENGER-SYNCHRONISATION BEI SPREAD-SPECTRUM-UEBERTRAGUNG]
Peter Harz, Manfred Ottka, and Udo Seier *In its* Communication Engineering Reports. Fundamental Developments. Theoretical Work Nov. 1988 p 50-58 In GERMAN (For primary document see N89-27928 22-32)
Copyright Avail: Fachinformationszentrum Karlsruhe, 7514 Eggenstein-Leopoldshafen 2, Fed. Republic of Germany, 35 DM

The synchronization method coherent addition for spread spectrum systems is presented. Basic considerations concerning the properties and applicability of the spread spectrum technique are given. The principle of spread spectrum transmission is explained by the so-called direct-sequence method. The properties of the coherent addition synchronization method are presented, together with advantages compared to other methods. An experimental system, programmable in essential parameters, is described. It allows the study of problems which could not be solved using an analytical description or digital simulation due to the outstanding complexity of the system. ESA

N89-27935 ANT Nachrichtentechnik, Backnang (Germany, F.R.).
CARRIER DERIVATION IN HIGHER-STAGE QAM-SIGNALS [ZUR TRAEGERABLEITUNG BEI HOHERSTUFIGEN QAM-SIGNALEN]
Michael H. W. Hoffmann *In its* Communication Engineering Reports. Fundamental Developments. Theoretical Work Nov. 1988 p 59-66 In GERMAN (For primary document see N89-27928 22-32)
Copyright Avail: Fachinformationszentrum Karlsruhe, 7514 Eggenstein-Leopoldshafen 2, Fed. Republic of Germany, 35 DM

A concept for the carrier recovery of a QAM-signal is presented, for application to higher-stage QAM-signals. Starting from the requirements for a good phase detector, the status of the methods for carrier regeneration of a QAM-signal is outlined. The concept is based on decisions concerning amplitude and phase of the complex envelope of the input signal. It leads to phase detector characteristics which combine good acquisition behavior with good properties after synchronization. A realization, suited for applications with high data rates, is presented. ESA

N89-27936 ANT Nachrichtentechnik, Backnang (Germany, F.R.).
BASEBAND EQUALIZER FOR DIGITAL RADIO RELAY LINKS [BASISBANDENTZERRER FUER DIGITALE RICHTFUNKVERBINDUNGEN]
Peter Herbig *In its* Communication Engineering Reports. Fundamental Developments. Theoretical Work Nov. 1988 p 67-74 In GERMAN (For primary document see N89-27928 22-32)
Copyright Avail: Fachinformationszentrum Karlsruhe, 7514 Eggenstein-Leopoldshafen 2, Fed. Republic of Germany, 35 DM

The dimensioning of linear and nonlinear baseband equalizers for digital radio relay links was studied. Equalizers without quantized feedback need pure delay time lines as partial circuits. All-pass circuits are less suited due to eigendistortions. In transversal equalizers overscanning is the first choice to improve the equalizing quality. Quantized feedback is required to equalize deeper fading drops. The most important point in quantized equalizers is the system delay time which determines the equalizing quality, especially for non-minimum-phase distortions. It is shown that there exist system delay times for which minimum-phase and non-minimum-phase channel types are equally well equalized. In some equalizer configurations unwanted high coefficient values can occur; they can however be reduced by optimization. ESA

N89-27937 ANT Nachrichtentechnik, Backnang (Germany, F.R.).
DIGITAL DEMULTIPLIER FOR MOBILE SATELLITE COMMUNICATION [DIGITALER DEMULTIPLEXER FUER DEN MOBILEN SATELLITENFUNK]

Heinz Goeckler and Helmut Eyssele *In its* Communication Engineering Reports. Fundamental Developments. Theoretical Work Nov. 1988 p 75-82 In GERMAN Original contains color illustrations (For primary document see N89-27928 22-32)
(Contract ESTEC-6497/85)
Copyright Avail: Fachinformationszentrum Karlsruhe, 7514 Eggenstein-Leopoldshafen 2, Fed. Republic of Germany, 35 DM

A digital demultiplexer for single channel per carrier signal in frequency multiplexing was designed, as part of a multicarrier demodulator for mobile satellite communication systems. This demultiplexer is a variant of the hierarchically constructed multistage method (tree structure). Specific characteristics of this highly modular system are: scanning of bandpass signals, over scanning by a factor two in all stages, processing of analytical signals, and exclusive use of linearly phased FIR filters. ESA

N89-27938 ANT Nachrichtentechnik, Backnang (Germany, F.R.).
DIGITAL DEMODULATOR FOR MOBILE SATELLITE COMMUNICATION [DIGITALER DEMODULATOR FUER DEN MOBILEN SATELLITENFUNK]
Thomas Alberty and Volker Hespelt *In its* Communication Engineering Reports. Fundamental Developments. Theoretical Work Nov. 1988 p 83-92 In GERMAN Original contains color illustrations (For primary document see N89-27928 22-32)
(Contract ESTEC-6497/85)
Copyright Avail: Fachinformationszentrum Karlsruhe, 7514 Eggenstein-Leopoldshafen 2, Fed. Republic of Germany, 35 DM

A digital demodulator was designed to fulfil very stringent synchronization requirements in satellite-supported mobile communication systems. The fully digital systems concept is outlined. The control circuits for scanning cycle, carrier frequency, and carrier phase are discussed. Examples demonstrate the efficiency of the synchronization. Instructions for the realization of a demonstration model are given. ESA

N89-27939 ANT Nachrichtentechnik, Backnang (Germany, F.R.).
RELP: SPEECH CODING USING ANALYSIS BY SYNTHESIS [RELP-SPRACHCODIERUNG MITTELS ANALYSE DURCH SYNTHESE]
Joerg-Martin Mueller and Helmut Scheuermann *In its* Communication Engineering Reports. Fundamental Developments. Theoretical Work Nov. 1988 p 93-105 In GERMAN (For primary document see N89-27928 22-32)
Copyright Avail: Fachinformationszentrum Karlsruhe, 7514 Eggenstein-Leopoldshafen 2, Fed. Republic of Germany, 35 DM

The RELP speech code, based on analysis by synthesis is presented. Optimal and suboptimal algorithms are given for multipulse excitation with scalar quantization as well as for stochastic excitation via vector quantization. Tables, indicating the computation effort for several methods, simplify the choice of a signal processor for real-time realizations. ESA

N89-27940 ANT Nachrichtentechnik, Backnang (Germany, F.R.).
FIELD THEORY SIMULATION OF NONRECIPROCAL MICROWAVE COMPONENTS [FELDTHEORETISCHE SIMULATION NICHTREZIPROKER MIKROWELLENKOMPONENTEN] **c33**
Wolfgang Hauth *In its* Communication Engineering Reports. Fundamental Developments. Theoretical Work Nov. 1988 p 106-113 In GERMAN Original contains color illustrations (For primary document see N89-27928 22-32)
Copyright Avail: Fachinformationszentrum Karlsruhe, 7514 Eggenstein-Leopoldshafen 2, Fed. Republic of Germany, 35 DM

Field theory simulation is treated with a view to the design and optimization of microwave components. The theoretical fundamentals of the method are outlined. Based on a generally formulated theoretical method, simulation programs were made for a series of nonreciprocal components, and successfully applied. The broad domain of applications covers circulators in microstrip technique, electronically controllable phase shifters, and high power circulators for nuclear research. ESA

N89-27941 ANT Nachrichtentechnik, Backnang (Germany, F.R.).
THE CALCULATION OF LOSSES IN WAVEGUIDE NETWORKS [ZUR BERECHNUNG VON VERLUSTEN IN HOHLLEITER-NETZWERKEN] **c33**
Reinhard Keller *In its* Communication Engineering Reports. Fundamental Developments. Theoretical Works Nov. 1988 p 114-120 In GERMAN Original contains color illustrations (For primary document see N89-27928 22-32)
Copyright Avail: Fachinformationszentrum Karlsruhe, 7514 Eggenstein-Leopoldshafen 2, Fed. Republic of Germany, 35 DM

An approximation method for the calculation of losses in waveguide networks was developed for computer-aided dimensioning of such networks. For a number of waveguide network elements, numerical calculation procedures were deduced using field theory approximation methods, especially taking into account the effect of the standing wave distribution on the waveguide losses. The validity of the theory was demonstrated by practical application examples. ESA

N89-27942 ANT Nachrichtentechnik, Backnang (Germany, F.R.).
CALCULATION OF PLANAR STRUCTURES FOR OPTICAL WAVELENGTH MULTIPLEXERS [BERECHNUNG PLANARER STRUKTUREN FUER OPTISCHE WELLENLAENGENMULTIPLEXER] **c74**
Thomas Schwander *In its* Communication Engineering Reports. Fundamental Developments. Theoretical Work Nov. 1988 p 121-127 In GERMAN (For primary document see N89-27928 22-32)
Copyright Avail: Fachinformationszentrum Karlsruhe, 7514 Eggenstein-Leopoldshafen 2, Fed. Republic of Germany, 35 DM

The dimensioning of extremely broadband, planar wavelength multiplexers in LiNbO3 was studied for the separation of the wavelength ranges 1.3 and 1.55 microns. The wave propagation in LiNbO3 wavelength multiplexers was simulated using the beam propagation method. From this dimensioning, guidelines were deduced for the production of broadband structures for the separation of the wavelength ranges 1.3 and 1.5 microns. These are partially in contrast with presently known design criteria for strongly wavelength-selective multiplexers. ESA

N89-27943# Messerschmitt-Boelkow-Blohm G.m.b.H., Munich (Germany, F.R.). Space Communications and Propulsions Systems Div.
STUDY ON THE APPLICABILITY OF ASYNCHRONOUS TIME DIVISION (ATD) TECHNIQUES TO SATELLITE COMMUNICATIONS SYSTEMS Final Report
H. Kuhlen, G. Hertel, M. Moerzinga, A. Zambra, M. Merri, A. Vernucci, F. DelliPriscoli, and A. Roveri (Rome Univ., Italy) Paris, France ESA Jul. 1988 267 p
(Contract ESA-7300/87/F/RD(SC))
(ESA-CR(P)-2742; ETN-89-94464) Avail: NTIS HC A12/MF A01

Applicability of asynchronous transfer mode (ATM) in satellite communication systems of the fixed satellite service (FSS) was studied using two models: one model typical for a network, and another typical for a user oriented scenario. Equipment complexity and typical hardware required in an ATM oriented system for the space and ground segment were considered. The applicability of ATM in an environment of the future Data Relay Satellite (DRS) system, considered as a special case of the user oriented scenario, was also studied. It is concluded that ATM is very attractive for broadband communication systems such as the glass fiber oriented systems of the future broadband network. The user scenario appears to be a good candidate for an immediate application but probably at higher bitrates, while the situation of the network scenario is completely open on all system aspects. Here the satellite community, ESA and industry, should follow very closely the process of standardization and implementation of ATM to be prepared for the right satellite at the right moment. The hardware technology already under development for terrestrial applications will create no significant problems for the introduction of appropriate satellite payloads. ESA

N89-27944# Maryland Univ., College Park. Dept. of Electrical Engineering.
STUDIES OF THE PROPAGATION OF SHORT BURST, HIGH POWER MICROWAVE RADIATION THROUGH NEUTRAL AND IONIZED MEDIA Final Report, 1 Dec. 1985 - 30 Nov. 1988
William W. Destler and Charles D. Striffler Mar. 1989 84 p
(Grant AF-AFOSR-0046-86; AF Proj. 2301)
(AD-A208664; AFOSR-89-0710TR) Avail: NTIS HC A05/MF A01 CSCL 20/14

Experiments were completed on the propagation of very high power (500 kw/cmsq), short burst (3 to 30 ms) microwaves through a neutral media. Results indicate that breakdown field strengths are about a factor of two higher when the test cell is shielded from X-rays generated by the microwave source. Standard theoretical models were shown to give very accurate predictions of actual observations for all cases except when the RF frequency was near the plasma frequency. GRA

N89-27945# Martin Marietta Aerospace, Washington, DC. Information and Communications System.
A COMPARATIVE STUDY OF SHF (SUPER HIGH FREQUENCY) AND EHF (EXTREMELY HIGH FREQUENCY) SATELLITE COMMUNICATIONS, VOLUME 1 Final Report, Aug. - Sep. 1987
William E. Leavitt, Phillip M. Hooten, Charles Green, E. M. Anderson, and Everett Ayers Sep. 1989 231 p Prepared in cooperation with ARINC Research Corp., Washington, DC
Prepared for Naval Research Lab., Washington, DC
(Contract N00014-87-M-0258)
(AD-A208850; ATC-HDQ/S/87-274) Avail: NTIS HC A11/MF A01 CSCL 25/2

This study evaluates the use of an Extremely High Frequency (EHF) alternative for the Super High Frequency (SHF) baseline for the Ultra High Frequency (UHF) Follow-On Satellite Tracking, Telemetry, and Control (TT&C) subsystem. It also compares and characterizes EHF, SHF, and UHF links, and identifies possible recommended future enhancements for the UHF Follow-On Satellite. Susceptibility to uplink jamming is considered the most critical criteria in this comparison. Adding EHF communications to the UHF Follow-On Satellite would affect the number of UHF communications channels that could be accommodated. Satellite spot beams would be necessary to operate at EHF with currently sized terminals. This report recommends retaining the SHF baseline for TT&C. GRA

N89-27946# Massachusetts Inst. of Tech., Lexington. Lincoln Lab.
ADAPTIVE PREPROCESSING OF NONSTATIONARY SIGNALS
M. D. Eggers and T. S. Khoun 9 May 1989 82 p
(Contract F19628-85-C-0002)
(AD-A209646; ESD-TR-88-329) Avail: NTIS HC A05/MF A01 CSCL 12/9

As the number and bandwidth of sensors increase, an acute demand for preprocessing sensor data obtained for machine-based decision making arises. Especially in a data fusion context, the data from numerous sensors must first be preprocessed to prevent saturation of the decision making mechanism-albeit man or machine. Presented is a general preprocessing approach which provides a compact representation (feature vector) of sensor data. The approach, supported by a signal decomposition theorem, adaptively models in recursive fashion, the detrended sensor data as an autoregressive (AR) process of sufficiently high order. Provisions are included to accommodate nonstationary data by incorporating an information-theoretic transition detector to identify the segments of near-stationary data segments which are scale invariant, translation invariant, normalized, and represent sufficient statistics. Furthermore, the merit of the preprocessor is quantitatively determined in a continuous manner from the resulting innovations (modeling error process). Specific application results utilizing nonstationary radar data demonstrate the ability to simultaneously reduce data and maintain information content, without requiring a priori statistics and/or expert rules. GRA

N89-27947# Naval Postgraduate School, Monterey, CA.
THEORY OF MULTI-FREQUENCY MODULATION (MFM) DIGITAL COMMUNICATIONS Interim Report, Oct. 1988 - Mar. 1989
Paul H. Moose 5 May 1989 44 p
(AD-A209737; NPS62-89-019) Avail: NTIS HC A03/MF A01 CSCL 25/5

Multi-frequency modulation (MFM) is a new digital signal processing (DSP) oriented communications signal developed at NPS specifically for computer-to-computer communications links and information exchange networks. MFM utilizes the hardware and software of the host computers to generate and to demodulate coherent communications discrete time signals. In this report, the theory behind MFM generation and reception is presented. Auto-correlation functions and power spectral densities of MFM signals are derived and examples presented for lowpass and bandpass white MFM sequences. The bit error rates are computed for three types of MFM: MFBPSK, MFQPSK and MF16-QAM. These modulation formats provide one, two and four bits per Hz of channel bandwidth respectively. Optimization arguments show that best system performance is obtained by using the maximum possible number of tones with the limit on the number of tones being set either by the packet length or the coherence time of the channel, whichever is shorter. GRA

N89-27948# Naval Weapons Center, China Lake, CA. Dept. of Attack Weapons.
NOISE AND FALSE ALARM RATE CHARACTERISTICS FOR ENVELOPE DETECTOR SYSTEMS PRECEDED BY RF AMPLIFICATION Final Report, Aug. 1986 - May 1988
Brad Wiitala Nov. 1988 49 p
(Contract AIRTASK-A540-5402)
(AD-A209789; AD-E900865; NWC-TP-6953) Avail: NTIS HC A03/MF A01 CSCL 17/9

The noise and false alarm rate (FAR) characteristics at the video output of square-law envelope-detector systems preceded by RF amplification are explored. GRA

N89-27949# City Coll. of the City Univ. of New York, NY. Communications Systems Lab.
COMMUNICATIONS USING CHANNELS FORMED BY METEOR BURSTS Final Technical Report, 1 Jul. 1985 - 30 Nov. 1988
Donald L. Schilling and Eliphaz Hibshoosh 30 Nov. 1988 146 p
(Grant AF-AFOSR-0234-85; AF Proj. 2305)
(AD-A209856; AFOSR-89-0821TR) Avail: NTIS HC A07/MF A01 CSCL 25/5

The use of the meteor burst channel in communication systems is studied by investigating the following important aspects: (1) the development and enhancement of an accurate and reliable channel model based on recently available empirical data. Analysis of this model results in analytical expressions for communication parameters such as channel duration and throughput to be used as design and analysis tools, (2) the optimization of throughput for fixed transmission rate under the constraint of a given maximum bit error rate. This will demonstrate the room for improvement in existing systems using constant transmission rate, (3) the feasibility of efficiently communicating over the MBC using variable bit rate and employing a feedback protocol to monitor the channel. This approach will dramatically improve the throughput in comparison with constant transmission rate systems, and (4) analysis of Automatic-Repeat-Request (ARQ) Transmission over MBC by studying performance measures such as duty cycle, throughput and waiting time as a function of packet length, coding, data rate, and modulation technique. GRA

N89-27950# Southwest Research Inst., San Antonio, TX.
A STUDY OF SPACECRAFT ELECTROMAGNETIC CONTAMINATION OF ARTIFICIAL ELECTRON BEAMS Final Report, 1 Aug. 1987 - 31 Sep. 1988
C. S. Lin 31 Dec. 1988 54 p
(Contract F19628-85-K-0004)

(AD-A209954; GL-TR-89-0121) Avail: NTIS HC A04/MF A01 CSCL 20/3

The numerical code developed for solving the dispersion equation of the electromagnetic dispersion equation for a finite radius electron beam in a neutralizing background is documented. Derivation of the dispersion equation from the fluid equation and Maxwell's equations is described. To study electromagnetic radiation induced by electron beam injection from the Space Shuttle, the numerical code is applied to solve for the instability growth rates for the beam and whistler modes. The numerical solutions indicate that a finite radius electron beam injected into the ionosphere with the beam energy around 1 keV and current about 100 mA can drive the beam and whistler modes unstable. The results can explain the whistler waves radiated from the keV electron beam injected from Spacelab 2. GRA

N89-27951# Mission Research Corp., Nashua, NH.
MATH AND PHYSICS STUDIES-MULTI-PROJECT SUPPORT ENTROPY-BASED IMAGE RESTORATION: MODIFICATIONS AND ADDDITIONAL RESULTS Technical Report, 29 Sep. 1987 - 29 Sep. 1988
John P. Kennealy and Rose M. Korte 31 Oct. 1988 11 p
(Contract F19628-87-C-0230)
(AD-A209972; MRC-NSH-R-88-0008; AFGL-TR-88-0330; SR-1)
Avail: NTIS HC A03/MF A01 CSCL 17/5

The contract effort was toward the development of a data management program for the SDIO Infrared Background Signature Survey, a shuttle-based experiment to be launched in mid 1990, and the super resolution of special data observations of IRAS satellite sensor images of galaxies. The attached report addresses the latter. A new approach to the application of maximum entropy principles in image restoration is being developed. It is an iterative process which combines a Wiener filter restoration and modification to the Weiner image that are Entropy based. The result is an image with well restored frequency content and very little of the spuriousness commonly introduced by inverse filters. The algorithm is fast, stable to convergence, and will accommodate any specifiable distorting function. GRA

N89-27952# Stanford Univ., CA. Information Systems Lab.
STUDIES IN STATISTICAL SIGNAL PROCESSING Final Technical Report, 1 Jul. 1983 - 30 Jun. 1988
Thomas Kailath 30 Jun. 1988 21 p
(Grant AF-AFOSR-0228-83; AF Proj. 2304)
(AD-A210054; AFOSR-89-0916TR) Avail: NTIS HC A03/MF A01 CSCL 12/3

The primary objective of our research is to develop efficient and numerically stable algorithms for nonstationary signal processing problems by understanding and exploiting special structures, both deterministic and stochastic, in the problems. We also strive to establish and broaden links with related disciplines, such as cascade filter synthesis, scattering theory, numerical linear algebra, and mathematical operator theory for the purpose of cross fertilization of ideas and techniques. These explorations have led to new results both in estimation theory and in these other fields, e.g., to new algorithms for triangular and QR factorization of structured matrices, new techniques for root location and stability testing, new recursions for orthogonal polynomials on the unit circle and the real line as well as on other curves, and new approaches to overcome singularities and ill-conditioning in the recursions. GRA

N89-27953# Illinois Univ., Urbana. Coordinated Science Lab.
ELECTROMAGNETIC SCATTERING FROM A STRUCTURED SLAB COMPRISED OF PERIODICALLY PLACED RESISTIVE CARDS
Roy E. Jorgenson and Raj Mittra May 1989 274 p
(Contract N00014-84-C-0149)
(AD-A210145; UILU-ENG-89-2218) Avail: NTIS HC A12/MF A01 CSCL 20/14

The structured slab, which is constructed by arranging cells composed of thin, lossy, dielectric cards on a one- or two-dimensional lattice, is an important material in the aerospace industry because of its high strength-to-weight ratio. Recently, the structured slab has also been used to reduce the radar cross section of various aircraft. It is important, therefore, to characterize how an electromagnetic wave scatters from this slab. The structured slabs discussed herein are constructed by repeating lossy strips periodically in one dimension or lossy plates in two dimensions. An electric field integral equation is formulated which has as its unknown the electric current flowing in a single unit cell of the structure. The periodicity of the structure is accounted for by using an efficiently calculated periodic Green's function. The loss is modeled by resistive boundary condition. The integral equation is solved by the method of moments using subdomain basis functions. The generalized scattering matrix is calculated and the propagating reflection coefficients are plotted as a function of frequency for various structures. The oblique scattering from one-dimensional arrays of strips is examined for various configurations of unit cells and various resistances. A depolarizing effect of the structure is found to be a function of incident angle and symmetry in the unit cell. The reflection from two-dimensional arrays of plates connected to form slabs of zigzag plates and honeycomb is also examined. GRA

N89-28119*# National Aeronautics and Space Administration. Goddard Space Flight Center, Greenbelt, MD.
OCEAN TOPOGRAPHY EXPERIMENT (TOPEX) RADAR ALTIMETER Abstract Only
L. C. Rossi, D. W. Hancock, and G. S. Hayne *In its* Laboratory for Oceans 1988 p 19-21 (For primary document see N89-28118 22-48)
Avail: NTIS HC A12/MF A01 CSCL 17I

N89-28120*# National Aeronautics and Space Administration. Goddard Space Flight Center, Greenbelt, MD.
MARS OBSERVER RADAR ALTIMETER RADIOMETER (MORAR) Abstract Only
L. C. Rossi, D. W. Hancock, and G. S. Hayne *In its* Laboratory for Oceans 1988 p 23-24 (For primary document see N89-28118 22-48)
Avail: NTIS HC A12/MF A01 CSCL 17I

N89-28159*# National Aeronautics and Space Administration. Goddard Space Flight Center, Greenbelt, MD.
SURFACE CONTOUR RADAR (SCR) CONTRIBUTIONS TO FASINEX Abstract Only
E. J. Walsh *In its* Laboratory for Oceans 1988 p 153-155 (For primary document see N89-28118 22-48)
Avail: NTIS HC A12/MF A01 CSCL 17I

N89-28176*# National Aeronautics and Space Administration. Goddard Space Flight Center, Greenbelt, MD.
THIRD INTERNATIONAL SATELLITE DIRECT BROADCAST SERVICES USER'S CONFERENCE Abstract Only
J. Kamowski and C. Vermillion *In its* Laboratory for Oceans 1988 p 217-218 Conference held in Linthicum, MD, 20-24 Jun. 1988 (For primary document see N89-28118 22-48)
Avail: NTIS HC A12/MF A01 CSCL 17B

33 ELECTRONICS AND ELECTRICAL ENGINEERING

Includes test equipment and maintainability; components, e.g., tunnel diodes and transistors; microminiaturization; and integrated circuitry.

For related information see also *60 Computer Operations and Hardware* and *76 Solid-State Physics.*

N89-27954# Allied-Signal Aerospace Co., Torrance, CA. Airesearch Div.
ADVANCED MOTOR AND MOTOR CONTROL DEVELOPMENT Final Report, Dec. 1982 - Dec. 1987
Kenneth L. Wuertz and Edward D. Beauchamp Aug. 1988 106 p

(Contract F33615-82-C-2233)
(AD-A207332; Rept-88-61112; AFWAL-TR-88-2047) Avail: NTIS HC A06/MF A01 CSCL 09/1

The capability of operating a high speed permanent magnet brushless dc motor with electronic controller over a wide load and speed range was demonstrated. A centrifugal pump was used as the loading mechanism and hydraulic fluid was pumped in simulation of an aircraft engine fuel pump requirement. A motor speed of 45,000 rpm was reached and a maximum output of 68.5 hp was demonstrated. The response of the system to step commands for speed change was established. Reduction of size and weight of electronic control was established as a primary future goal. The program system concept with minor rotating machine improvements is viable for high speed drive applications up to 100-hp level. GRA

N89-27955# Sandia National Labs., Albuquerque, NM.
A ONE MICROSECOND, THIRTY-FIVE KILOJOULE, ONE HERTZ PULSE GENERATOR
R. S. Clark, L. R. Rinehart, M. T. Buttram, and D. L. Green 1989 14 p Presented at the 7th IEEE Pulsed Power Conference, Monterey, CA, 12 Jun. 1989
(Contract DE-AC04-76DP-00789)
(DE89-013074; SAND-88-3475C; CONF-890665-7) Avail: NTIS HC A03/MF A01

A repetitive high-voltage pulser has been developed at Sandia National Laboratories that will drive a vacuum diode for electron beam production. It is a 1-ms, 200-kV, 1-ohm, 35-kJ unit that is designed to operate in the 1 to 10 Hz range (the 1-Hz operation is studied). The design concept utilizes a pulse forming network (PFN) to form the output waveshape. The pulser is developed in a modular concept that will allow series/parallel operation of the PFNs to meet changing energy and/or voltage needs. Achieving sufficiently low inductance is generally the chief design challenge in producing a low-impedance PFN. Because it allows the greatest amount of inductance in the circuit, the Guillemin type C PFN is used in each module. Several capacitive stages are charged to + or - 100 kV (maximum) and then discharged (by spark-gap switches) through turned inductances to obtain a relatively square waveform. A PFN consisting of two stages (the main energy storage stage and a pulse shaping stage) was evaluated. Each stage generates a different harmonic of the desired waveshape. When the outputs of both stages are added together at the load, the resultant waveform has the desired shape and amplitude. The design and operation of the high voltage module and a pulser which was developed using two of the modules in series were studied. Design philosophy, module fabrication, and operational results are presented. Each component of the pulser is discussed. DOE

N89-27956# SRI International Corp., Menlo Park, CA.
DEVELOPMENT OF ANODES FOR ALUMINUM/AIR BATTERIES: SOLUTION PHASE INHIBITION OF CORROSION Final Report
Digby D. Macdonald, Catherine English, and Mirna Urquidi-Macdonald Mar. 1989 43 p Prepared in cooperation with California Univ. Lawrence Berkeley Lab.
(Contract DE-AC03-76SF-00098)
(DE89-012839; LBL-26999) Avail: NTIS HC A03/MF A01

Solution-phase inhibition is a promising strategy for controlling the corrosion of the aluminum fuel in alkaline aluminum/air batteries. Development of effective inhibitors would permit the use of scrap aluminum as fuel and thereby significantly improve the economics of the battery, because the cost of the fuel would have been partly or wholly defrayed by its previous use. In this study, we explored the discharge characteristics of aluminum in inhibited and uninhibited 4 M KOH at 50 C and compared the performance of the fuel with that for two leading alloy fuels that had been evaluated in our previous work, Alloy BDW (Al1Mg(o,1)In(0.2)Mn) and Alloy 21 (Al(0.2)Ga(0.1)IN(0.1)Tl). The inhibitors employed in this study, SnO3(-2), In(OH)3, Ga(OH)4(-1), MnO4(-2), and binary combinations thereof, are either alloying elements of Alloys BDW and 21 or were investigated previously. It was found that potassium manganate and Na2SnO3 + In(OH)3 are effective inhibitor systems. Particularly at high discharge rates, but at low discharge rates only manganate offers a significant advantage in coulombic efficiency over the uninhibited solution. Alloy BDW exhibits a very low open circuit (standby) corrosion rate, but its coulombic efficiency under discharge, as determined by delineating the particle anodic and cathodic reactions, was found to be no better than that of aluminum in the same uninhibited solution. Alloy 21 was found to exhibit a comparable performance to Alloy BDW under open circuit conditions and a much higher coulombic efficiency at low discharge rates, but the performance of this alloy under high discharge rate conditions was not determined. Alloy 21 has the significant disadvantage that it contains thallium. DOE

N89-27957# Sandia National Labs., Albuquerque, NM. Microwave Physics Div.
LINE/CIRCUIT ANALYSIS PROGRAM: CROSS-COUPLING ON PC (PRINTED CIRCUIT) BOARD TRACES INCLUDING DISCONTINUITIES AND CIRCUIT ELEMENTS
L. D. Bacon and R. P. Toth Jun. 1989 45 p
(Contract DE-AC04-76DP-00789)
(DE89-013884; SAND-89-0037) Avail: NTIS HC A03/MF A01

A program has been written that allows us to predict the trace-to-trace cross-coupling on printed circuit boards for many geometries of practical interest. It combines multiconductor transmission line analysis with circuit analysis in the time domain. Multiple sections of uniform lines, of varying number and characteristics, can be interconnected by passive circuit elements. These circuit elements may represent physical components or the effects of discontinuities in the lines. These predictions were compared with measurements for simple geometries, with good agreement in both waveshape and amplitude. The major discrepancies were in the amplitudes of fast rising spikes and are probably due to the fact that the predictions did not account for the increasing attenuation at high frequencies. DOE

N89-27958# Los Alamos National Lab., NM.
A BATTERY-POWERED FLUX COMPRESSION GENERATOR SYSTEM
J. E. Vorthman, C. M. Fowler, R. F. Hoeberling, and M. V. Fazio 1989 6 p Presented at the 5th International Conference on Megagauss Magnetic Field Generation and Related Topics, Novosibirsk, USSR, 3-7 Jul. 1989
(Contract W-7405-eng-36)
(DE89-014230; LA-UR-89-2097; CONF-890710-5) Avail: NTIS HC A02/MF A01

Flux compression generators (FCGs) are primarily used as energy amplifiers. While a FCG can be made small, typically the seed energy that the FCG amplifies comes from a capacitator bank much larger and heavier than the FCG. If seed energy was supplied by a compact device, FCGs could be used as portable power supplies. One application of interest is to combine a compact seed source with a FCG and transformer. The result would be a self-contained power supply capable of producing a microsecond long, megavolt pulse. The described objective was to make a seed source capable of energizing a standard Los Alamos plate FCG. The power supply was to be relatively small, light weight, and able to deliver at least 100-kJ to a 280-nH inductive load, e.g., plate FCG. DOE

N89-27959# Los Alamos National Lab., NM.
HIGH VOLTAGE POWER CONDITION SYSTEMS POWERED BY FLUX COMPRESSION GENERATORS
R. E. Reinovsky, I. R. Lindemuth, and J. E. Vorthman 1989 5 p Presented at the 7th IEEE Pulsed Power Conference, Monterey, CA, 11-14 Jun. 1989
(Contract W-7405-eng-36)
(DE89-014259; LA-UR-89-1941; CONF-890665-29) Avail: NTIS HC A02/MF A01

Compact, high-gain magnetic flux compressors (FCGs) are convenient sources of substantial energy for plasma-physics and electron-beam-physics experiments, but the need for high-voltage,

fast-rising pulses is difficult to meet directly with conventional generators. While a variety of novel concepts employing simultaneous, axially-detonated explosive systems are under development, power-conditioning systems based on fuse opening switches and high-voltage transformers constitute another approach that complements the fundamental size, weight, and configuration of the small helical flux compressor. In this paper, we consider first a basic inductive store/opening switch circuit and the implications associated with, specifically, a fuse opening switch and an FCG energy source. We develop a general solution to a transformer/opening switch circuit---which also includes (as a special case) the direct inductive store/opening switch circuit (without transformer) and we report results of one elementary experiment demonstrating the feasibility of the approach. DOE

N89-27960# Los Alamos National Lab., NM.
HIGH-PERFORMANCE, HIGH-CURRENT FUSES FOR FLUX COMPRESSION GENERATOR DRIVEN INDUCTIVE STORE POWER CONDITIONING APPLICATIONS
R. E. Reinovsky, I. R. Lindemuth, J. H. Goforth, R. S. Caird, and C. M. Fowler 1989 21 p Presented at the 5th International Conference on Megagauss Magnetic Field Generation and Related Topics, Novosibirsk, USSR, 3-7 Jul. 1989
(Contract W-7405-eng-36)
(DE89-014274; LA-UR-89-2194; CONF-890710-7) Avail: NTIS HC A03/MF A01

Large-scale helical flux compression generators deliver energies in the range of 10 to 50 MJ in economical, flexible packages for powering a variety of plasma and electron beam experiments. While conventional, end-detonating, helical generators are simple and reliable, they have the disadvantage of delivering their energy over long timescales, up to 400 to 500 microseconds, and at relatively low output voltages. Many experiments require faster risetimes than can be delivered by a helical FCG directly, and inductive systems utilizing high current interrupting switches can be employed to match generator performance to load requirements. For this experiment, a 15-MJ class helical flux compression generator was selected as the primary energy source. This flux compressor is a modification of a design proposed by Pavlovski in 1979 and used routinely in Los Alamos programs. The generator consists of a multiple conductor, multiple pitch, helical stator and a hollow copper armature containing a 60-kg charge of PBX 9501 high explosive (HE) which is initiated by a small plane wave lens at the end opposite the output. DOE

N89-27961# Los Alamos National Lab., NM.
A SIMULTANEOUS HELICAL GENERATOR
D. G. Rickel, B. L. Freeman, C. M. Fowler, J. E. Vorthman, and S. P. Marsh 1989 8 p Presented at the 5th International Conference on Megagauss Magnetic Field Generation and Related Topics, Novosibirsk, USSR, 3-7 Jul. 1989
(Contract W-7405-eng-36)
(DE89-014284; LA-UR-89-2163; CONF-890710-4) Avail: NTIS HC A02/MF A01

A need is emerging for a class of short-pulse, high-voltage, magnetic flux compression generators (FCGs). It is desirable that these generators be compact, inexpensive and have modest prime power requirements. Toward this end several concepts have been worked on in our Laboratory, one of which is the conical helical generator described. DOE

N89-27962# Naval Research Lab., Washington, DC. Plasma Radiation Branch.
ZPIMP: A ZERO-D Z-PINCH IMPLOSION CODE Interim Report
John L. Giuliani and John Rogerson 25 Apr. 1989 54 p Sponsored by DNA and ONR
(AD-A208381; NRL-MR-6448) Avail: NTIS HC A04/MF A01 CSCL 20/9

The discharge of electrical energy through a cylindrical gas puff is a well tested means of creating an intense burst of high energy radiation. Typical output from an imploding neon Z-pinch is a few kJ of X-rays when the peak current is about 1 MA on the GAMBLE 2 pulsed-power device at the Naval Research Laboratory. The experimental program to produce a bright and consistent Plasma Radiation Source (PRS) on GAMBLE 2 and on other facilities has evolved over the past several years. A new single zone, radiation-hydrodynamics code (ZPIMP) for modeling current driven gas puff implosions is developed. The hydrodynamics is based upon the finite difference equations for a standard multizone simulation. An analytic solution for the diffusion of the magnetic field in a moving medium is used to calculate the resistive heating and Maxwell stresses. A non-LTE ionization dynamics is self-consistently coupled to radiation transport for the single plasma zone. A circuit equation is solved for the input current to the plasma load. The problem of complete energy conservation in a numerical finite difference code is addressed in detail. The ZPIMP code is applied to the implosion of an aluminum vapor on GAMBLE 2. A brief comparison of the results for annular shells and filled cylinders is presented. GRA

N89-27963# Naval Ocean Systems Center, San Diego, CA.
DARPA (DEFENSE ADVANCED RESEARCH PROJECTS AGENCY) REVIEW ON EHF DEVICES
Apr. 1989 487 p Review held in San Diego, CA, 24-25 Jan. 1989
(AD-A208564; NOSC/TD-1532) Avail: NTIS HC A21/MF A01 CSCL 09/1

Topics addressed include: Overview of Millimeter Wave Components and Systems for Army Military Applications; Ballistic Transport in the Vertical and Lateral Domains; Permeable Base Transistor and Regrowth FET Development; Transport Considerations for EHF Devices; GaA1As/GaAs Heterojunction Bipolar Transistors for mm-Wave Applications; Heterojunction Power FET Technology; Molecular Beam Epitaxy and Resonant Tunneling Devices; Array Applications; MM-Wave Phased-Array Antenna Concepts; Materials Choice for Ballistic and Drift Transport Devices; AlInAs-GaInAs HEMTs for high speed applications; Measurement of Response of High Speed Tunneling Devices; EHF HBT Development; and On Wafer Characterization of High Speed Circuits. GRA

N89-27964# Colorado Univ., Boulder. Dept. of Electrical and Computer Engineering.
QUADRATIC ESTIMATORS OF THE POWER SPECTRUM
C. T. Mullis and Louis L. Scharf Apr. 1989 82 p
(Contracts N00014-89-J-1070; DAAL03-88-K-0058; NSF MIP-87-17714)
(AD-A208601; CU/ONR/2) Avail: NTIS HC A05/MF A01 CSCL 12/3

Among nonparametric estimators of the power spectrum, quadratic estimators are the only ones that are dimensionally correct. This report motivates interest in quadratic estimators by setting up idealized experiments for spectrum analysis and deriving maximum likelihood estimates for narrowband power. These idealized experiments show that quadratic functions of the experimental data are sufficient statistics for estimating power. The maximum likelihood estimates show that low-rank projection operators play a fundamental role in the theory of spectrum analysis. The projection operator plays the same role as a bandpass filter in a conventional swept frequency spectrum analyzer. The mean-squared error of a maximum likelihood estimator of power is inversely proportional to the rank of the estimator. With our maximum likelihood result in hand, we turn to a systematic study of quadratic estimators of the power spectrum. GRA

N89-27965# State Univ. of New York, Buffalo. Dept. of Chemistry.
EXPERIMENTAL DETERMINATION OF THE COEFFICIENT IN THE STEADY STATE CURRENT EQUATION FOR SPHERICAL SEGMENT MICROELECTRODES
Zbigniew Stojek (Warsaw Univ., Poland) and Janet Osteryoung 31 May 1989 20 p Submitted for publication
(Contract N00014-84-K-0052)
(AD-A208662; TR-22) Avail: NTIS HC A03/MF A01 CSCL 07/2

The coefficient in the steady state current equation for spherical

segment microelectrodes has been evaluated experimentally for various values of the height of the spherical segment. For this purpose chronoamperometric reduction of Hg2+2 ion at a silver microdisc electrode in perchloric acid solution has been employed. The diffusion coefficient of Hg2+2 in 0.25 M HC104 at 30 C was determined as .0000112 sq cm/s. GRA

N89-27966# California Inst. of Tech., Pasadena. Dept. of Electrical Engineering.
ACOUSTOOPTIC PROCESSING OF TWO DIMENSIONAL SIGNALS USING TEMPORAL AND SPATIAL INTEGRATION Final Report, 1 May 1988 - 28 Feb. 1989
Demetri Psaltis, John Hong, Scott Hudson, Jeff Yu, Fai Mok, Mark Neifeld, Nabeel Riza, and Dave Brady 12 May 1989 126 p
(Grant AF-AFOSR-0332-85; AF Proj. 2305)
(AD-A208686; AFOSR-89-0730TR) Avail: NTIS HC A07/MF A01 CSCL 09/1

Acoustooptic signal processing architectures and methods are developed for a variety of 2-D problems. A formulation of the universe synthetic aperture radar problem as an energy minimization procedure is reported. Acoustooptic systems for multiple target detection and 2-D spectrum analysis are experimentally demonstrated. The application of acoustooptics to the adaptive beam forming for broadband antenna arrays is described. GRA

N89-27967# Illinois Univ. at Urbana-Champaign, Savoy. Coordinated Science Lab.
AVERAGE INTERCONNECTION LENGTH AND INTERCONNECTION DISTRIBUTION FOR RECTANGULAR ARRAYS
Carol Gura and Jacob A. Abraham May 1989 21 p
(Contract N00014-84-C-0149)
(AD-A209848; UILU-ENG-89-2212-CSG-101; CSG-101) Avail: NTIS HC A02/MF A01 CSCL 09/1

It is shown that it is necessary to utilize different partitioning coefficients in interconnection length analyses which are based on Rent's rule, depending on whether one- or two-dimensional placement strategies are used. Beta is the partitioning coefficient in the power-law relationship Alpha Beta which provides a measure of the number of interconnection that cross a boundary which encioses Beta blocks. The partitioning coefficients are Beta = p/2 and Beta = p for two- and one-dimensional arrays, respectively, where p is the experimental coefficient, of the Rent relationship. Based on these separate partitioning coefficients, an average interconnection length prediction is presented for rectangular arrays that out performs existing predictions. Examples are given to support this theory. GRA

N89-27968# Princeton Univ., NJ. Dept. of Electrical Engineering and Computer Science.
SYSTEM THEORETIC MODELS FOR HIGH DENSITY VLSI STRUCTURES Final Technical Report
Bradley W. Dickinson and William E. Hopkins, Jr. 1989 42 p
(Contract N00014-83-K-0577)
(AD-A209901) Avail: NTIS HC A03/MF A01 CSCL 09/1

This research project involved the development of mathematical models for analysis, synthesis, and simulation of large systems of interacting devices. The work was motivated by problems that may become important in high density VLSI chips with characteristic feature sizes less than 1 micron: it is anticipated that interactions of neighboring devices will play an important role in the determination of circuit properties. It is hoped that the combination of high device densities and such local interactions can somehow be exploited to increase circuit speed and to reduce power consumption. To address these issues from the point of view of system theory, research was pursued in the areas of nonlinear and stochastic systems and into neural network models. Statistical models were developed to characterize various features of the dynamic behavior of interacting systems. Random process models for studying the resulting asynchronous modes of operation were investigated. The local interactions themselves may be modeled as stochastic effects. The resulting behavior was investigated through the use of various scaling limits, and by a combination of other analytical and simulation techniques. Techniques arising in a variety of disciplines where models of interaction were formulated and explored were considered and adapted for use. GRA

N89-27969# Space Computer Corp., Santa Monica, CA.
HYBRID WAFER-SCALE PROCESSOR Final Report, 15 Jul. 1988 - 14 Jan. 1989
William J. Jacobi 14 Mar. 1989 35 p
(Contract DAAL03-88-C-0007)
(AD-A209944; SCC-R-104-F; ARO-26019.1-EL-SBI) Avail: NTIS HC A03/MF A01 CSCL 09/1

The basic goal of this project is to develop and demonstrate techniques for the reduction of power consumption of space-based processors for infrared surveillance systems. The primary technique is to minimize the capacitive loading encountered in off-chip communications for highly concurrent processing architectures. Both processing architecture and chip packaging are simultaneously considered to maximize MOPS (million operations per second) per watt by increasing throughput while reducing system capacitance, signal delay, noise, voltage swing, and power consumption (the costs of system communications). With conventional packaging technology, highly concurrent processing architectures result in hardware implementations that are extremely large, very heavy, and that consume excessive power. Monolithic wafer-scale integration is theoretically ideal but requires an extensive amount of redundant circuitry and provisions for circuit reconstructurability because of manufacturing yield problems. In the hybrid wafer-scale integration (HWSI) approach, individual pre-tested chips are bonded to a fine-line interconnect structure fabricated on the surface of a wafer-scale substrate. With this technique, high yields can be achieved without redundancy. GRA

N89-27970# Texas Univ., Austin. Electronics Research Center.
ELECTRONICS RESEARCH AT THE UNIVERSITY OF TEXAS AT AUSTIN Final Report, 1 Apr. 1986 - 31 Mar. 1989
Edward J. Powers 31 May 1989 28 p
(Contract F49620-86-C-0045)
(AD-A209989; TR-39; AFOSR-89-0800TR) Avail: NTIS HC A03/MF A01 CSCL 09/1

This final report covers the period from April 1, 1986 through March 31, 1989. The progress reported concerns research conducted by ten faculty members and approximately thirty graduate students from the Department of Electrical and Computer Engineering and the Department of Physics. The University of Texas DoD JSEP program is a broad-based program with four research units in Solid State Electronics, two in Electromagnetics, two in Quantum Electronics, and two in Information Electronics. Solid State Electronics includes work on implantation and annealing of InP and related compounds; molecular beam epitaxy with high-speed device applications; epitaxial growth, structure and electronic properties of silicides on silicon surfaces; and femtosecond processes in condensed matter. In Quantum Electronics, nonlinear optical interactions and nonlinear Raman scattering from molecular ions have been investigated. Work in Electromagnetics includes millimeter-wave monolithic array components and nonlinear wave phenomena, while electronic signal processing and nonlinear estimation and detection were studied in Information Electronics. GRA

N89-27971# George Mason Univ., Fairfax, VA. Center for Computational Statistics.
HYPERDIMENSIONAL DATA ANALYSIS AND STRUCTURAL INFERENCE Final Technical Report, 1 Apr. 1987 - 31 Mar. 1989
Edward J. Weaman 18 May 1989 7 p
(Grant AF-AFOSR-0179-87; AF Proj. 2304)
(AD-A210056; AFOSR-89-0914TR) Avail: NTIS HC A02/MF A01 CSCL 12/3

This research project was based on belief that modern technology has substantially changed the flavor of problems being presented to the statistician. Electronic instrumentation implies an

ability to acquire a large amount of high dimensional data very rapidly. While such capabilities have existed for some time, the emergence of cheap random access memory in the 1980's has given us the ability to store and access that data in an active computer memory. This represents a challenge for statisticians which is substantially different in kind. The majority of existing methodology is focused on the univariate, iid random variable model. Even in the circumstance that a multivariate model is allowed, it is usually assumed to be multivariate normal. While arbitrary sample size is frequently assumed, the truth of the matter is that these techniques implicitly assume small to moderate sample sizes. For example, a regression problem with 5 design variables and 1000 observations would represent no problem for traditional techniques. By contrast, a regression problem with 40,000 design variables and 8 million observations would. The reason is clear. In the former case the emphasis is on statistical efficiency which is the operational goal for most current statistical technology. By contrast, in the latter case, emphasis must be clearly on computational efficiency. The emphasis on parsimony in many contemporary books and papers is a further reflection of the mind-set that implicitly focuses on small to moderate sample sizes, since few parameters do not make sense in context of very large sample sizes. GRA

N89-27972# Northrop Research and Technology Center, Palos Verdes Peninsula, CA.
INVESTIGATION OF RADIATION EFFECTS ON SEMICONDUCTOR DEVICES AND INTEGRATED CIRCUITS
Technical Report, 17 Apr. 1984 - 17 Jun. 1988
Zef Shanfield, Joseph R. Srour, Melvin Moriwaki, Kerry S. Kitazaki, and Robert A. Hartmann 16 Sep. 1988 160 p
(Contract DNA001-84-C-0196)
(AD-A210165; NRTC-88-22-R; DNA-TR-88-221) Avail: NTIS HC A08/MF A01 CSCL 09/1

Results of a study of radiation effects on electronic materials, devices, and integrated circuits are presented in this report. Emphasis was placed on determining the underlying mechanisms responsible for observed radiation effects with a view toward gaining understanding of value in the development of radiation-hardened devices. Measurements and analyses were made of the effects of single energetic neutrons and protons on silicon integrated circuits. In addition, a detailed description is given of the effects of radiation-induced displacement damage on device depletion regions. Single event upset studies included charge collection and transient current measurements on Si and GaAs devices following a single alpha-particle strike. The angular dependence of charge funneling was also investigated. The mechanisms of ionizing radiation effects on Si MOS devices were explored in detail using the thermally stimulated current technique and other measurement approaches. Data obtained by several techniques show that use of the radiation-induced shift of the capacitance-voltage curve at midgap is not generally valid for determining oxide trapped charge. GRA

N89-27880*# Jet Propulsion Lab., California Inst. of Tech., Pasadena.
A NEW METHOD FOR ANALYSIS OF LIMIT CYCLE BEHAVIOR OF THE NASA/JPL 70-METER ANTENNA AXIS SERVOS
R. E. Hill *In its* The Telecommunications and Data Acquisition Report 15 May 1989 p 98-111 (For primary document see N89-27871 22-32)
Avail: NTIS HC A17/MF A01 CSCL 09A

N89-27881*# Jet Propulsion Lab., California Inst. of Tech., Pasadena.
APPLICATION OF OPTIMAL CONTROL THEORY TO THE DESIGN OF THE NASA/JPL 70-METER ANTENNA SERVOS
L. S. Alvarez and J. Nickerson *In its* The Telecommunications and Data Acquisition Report 15 May 1989 p 112-126 (For primary document see N89-27871 22-32)
Avail: NTIS HC A17/MF A01 CSCL 09A

N89-27882*# Jet Propulsion Lab., California Inst. of Tech., Pasadena.
PRECISION POINTING COMPENSATION FOR DSN ANTENNAS WITH OPTICAL DISTANCE MEASURING SENSORS
R. E. Scheid *In its* The Telecommunications and Data Acquisition Report 15 May 1989 p 127-140 (For primary document see N89-27871 22-32)
Avail: NTIS HC A17/MF A01 CSCL 09A

N89-27887*# Jet Propulsion Lab., California Inst. of Tech., Pasadena.
MULTIPURPOSE EXCITER WITH LOW PHASE NOISE
B. Conroy and D. Le *In its* The Telecommunications and Data Acquisition Report 15 May 1989 p 169-174 (For primary document see N89-27871 22-32)
Avail: NTIS HC A17/MF A01 CSCL 09A

N89-27898*# Jet Propulsion Lab., California Inst. of Tech., Pasadena.
MICROWAVE TIME DELAYS FOR THE X/S-BAND FEED SYSTEM AT X-BAND
J. Chen *In its* The Telecommunications and Data Acquisition Report 15 May 1989 p 248-251 (For primary document see N89-27871 22-32)
Avail: NTIS HC A17/MF A01 CSCL 09A

N89-27901*# Jet Propulsion Lab., California Inst. of Tech., Pasadena.
THE DSS-14 C-BAND EXCITER
D. R. Rowan *In its* The Telecommunications and Data Acquisition Report 15 May 1989 p 292-299 (For primary document see N89-27871 22-32)
Avail: NTIS HC A17/MF A01 CSCL 09A

N89-27932 ANT Nachrichtentechnik, Backnang (Germany, F.R.).
ANALYSIS AND DIMENSIONING OF A VALUE-DISCRETE ADAPTIVE COMPENSATION FILTER [ANALYSE UND DIMENSIONIERUNG WERTDISKRETER ADAPTIVER KOMPENSATIONSFILTER]
Bernd Friedrichs *In its* Communication Engineering Reports. Fundamental Developments. Theoretical Work Nov. 1988 p 30-39 In GERMAN (For primary document see N89-27928 22-32)
Copyright Avail: Fachinformationszentrum Karlsruhe, 7514 Eggenstein-Leopoldshafen 2, Fed. Republic of Germany, 35 DM

N89-27940 ANT Nachrichtentechnik, Backnang (Germany, F.R.).
FIELD THEORY SIMULATION OF NONRECIPROCAL MICROWAVE COMPONENTS [FELDTHEORETISCHE SIMULATION NICHTREZIPROKER MIKROWELLENKOMPONENTEN]
Wolfgang Hauth *In its* Communication Engineering Reports. Fundamental Developments. Theoretical Work Nov. 1988 p 106-113 In GERMAN Original contains color illustrations (For primary document see N89-27928 22-32)
Copyright Avail: Fachinformationszentrum Karlsruhe, 7514 Eggenstein-Leopoldshafen 2, Fed. Republic of Germany, 35 DM

N89-27941 ANT Nachrichtentechnik, Backnang (Germany, F.R.).
THE CALCULATION OF LOSSES IN WAVEGUIDE NETWORKS [ZUR BERECHNUNG VON VERLUSTEN IN HOHLLEITER-NETZWERKEN]
Reinhard Keller *In its* Communication Engineering Reports. Fundamental Developments. Theoretical Works Nov. 1988 p 114-120 In GERMAN Original contains color illustrations (For primary document see N89-27928 22-32)
Copyright Avail: Fachinformationszentrum Karlsruhe, 7514 Eggenstein-Leopoldshafen 2, Fed. Republic of Germany, 35 DM

34 FLUID MECHANICS AND HEAT TRANSFER

Includes boundary layers; hydrodynamics; fluidics; mass transfer; and ablation cooling.

For related information see also *02 Aerodynamics* and *77 Thermodynamics and Statistical Physics.*

N89-27973# Naval Postgraduate School, Monterey, CA.
BUBBLE DETECTION USING A DUAL FREQUENCY SOUND FIELD M.S. Thesis
Ernest R. Lineberger, III Dec. 1988 130 p
(AD-A207286) Avail: NTIS HC A07/MF A01 CSCL 20/1

The design, testing and analysis of a dual frequency system to detect and determine the resonance frequency (and hence the size) of bubbles ranging from 100 to 7 micro radius is reported. The resonance frequencies were compared to estimates based on the rise time of the bubbles. In general these comparisons agreed to within 5 percent. Although the system is not ideal for field measurements, it identifies important requirements concerning the size of the sample volume, the frequency and amplitude ranges of the sound fields and signal processing techniques to make an effective system. Bubbles are distinguished from non-gaseous particles by the nature of their nonlinear response to the dual sound field. The system is versatile and can be modified to suit many research purposes. GRA

N89-27974# Naval Postgraduate School, Monterey, CA.
EFFECTS OF AN EMBEDDED VORTEX ON A SINGLE FILM-COOLING JET IN A TURBULENT BOUNDARY LAYER M.S. Thesis
Warren W. Williams Jun. 1988 223 p
(AD-A207374) Avail: NTIS HC A10/MF A01 CSCL 20/13

Effects of embedded longitudinal vortices on heat transfer in a turbulent boundary layer film cooled from a single injections hole are discussed. Film coolant was injected at blowing ratios 0.50 to 1.50 at a freestream velocity of 10 m/s. A single longitudinal vortex was induced upstream of the film cooling holes. Heat transfer measurement were made downstream of injection. Flow visualization tests were conducted after the injectant was contaminated with smoke. Surveys of mean velocity and mean temperature were also made in different spanwise normal planes. For all blowing ratios examined, the embedded vortices cause significant alterations to wall heat transfer and to film cooling distributions. GRA

N89-27975# Los Alamos National Lab., NM.
KIVA-2: A COMPUTER PROGRAM FOR CHEMICALLY REACTIVE FLOWS WITH SPRAYS
A. A. Amsden, P. J. ORourke, and T. D. Butler May 1989 164 p
(Contract W-7405-eng-36)
(DE89-012805; LA-11560-MS) Avail: NTIS HC A08/MF A01

This report documents the KIVA-2 computer program for the numerical calculation of transient, two- and three-dimensional, chemically reactive fluid flows with sprays. KIVA-2 extends and enhances the earlier KIVA code, improving its computational accuracy and efficiency and its ease-of-use. The KIVA-2 equations and numerical solution procedures are very general and can be applied to laminar or turbulent flows, subsonic or supersonic flows, and single-phase or dispersed two-phase flows. Arbitrary numbers of species and chemical reactions are allowed. A stochastic particle method is used to calculate evaporating liquid sprays, including the effects of droplet collisions and aerodynamic breakups. Although the initial and boundary conditions and mesh generation have been written for internal combustion engine calculations, the logic for these specifications can be easily modified for a variety of other applications. Following an overview of the principal features of the KIVA-2 program, we describe in detail the equations solved, the numerical solution procedure, and the structure of the computer program. Sixteen appendices provide additional details concerning the numerical solution procedure. DOE

N89-27976# Colorado School of Mines, Golden.
AN EXPERIMENTAL STUDY TO DETERMINE THE RELATIVE INFLUENCE OF FLUID-FLUID INTERACTIONS AND MEDIA HETEROGENEITIES ON THE GROWTH OF IMMISCIBLE VISCOUS FINGERS Ph.D. Thesis
Daniel M. Stoelzel 1988 153 p
(Contract DE-FG22-87BC-14152)
(DE89-013122; DOE/BC-14152/2) Avail: NTIS HC A08/MF A01

The relative influence of transport media heterogeneities or fluid-fluid interactions on the formation of immiscible viscous fingers was evaluated. Comparisons of experimental flows in a Hele-Shaw cell show that the spatial variations (heterogeneities) in the glass surface play a more significant role in finger growth than do random fluid-fluid instabilities. Visual records of over two hundred experimental runs were analyzed using digital video image processing and fractal dimension measurements. Digital overlays of the images show that finger patterns sweep essentially the same areas and have the same fractal dimension for different experimental conditions. This shows that heterogeneity in the flow regime is more significant in governing fluid displacements than the mobility controlled instabilities. DOE

N89-27977*# National Aeronautics and Space Administration. Langley Research Center, Hampton, VA.
A CRITICAL COMPARISON OF TURBULENCE MODELS FOR HOMOGENEOUS SHEAR FLOWS IN A ROTATING FRAME Final Report
Charles G. Speziale, Thomas B. Gatski, and Nessan MacGiollaMhuiris (Case Western Reserve Univ., Cleveland, OH.) Jun. 1989 24 p Presented at the 7th Symposium on Turbulent Shear Flows
(Contract NAS1-18605)
(NASA-CR-181864; NAS 1.26:181864; ICASE-89-43) Avail: NTIS HC A03/MF A01 CSCL 20D

A variety of turbulence models, including five second-order closure models and four two equation models, are tested for the problem of homogeneous turbulent shear flow in a rotating frame. The model predictions for the time evolution of the turbulent kinetic energy and dissipation rate, as well as those for the equilibrium states, are compared with the results of physical and numerical experiments. Most of the two-equation models predict the same results for all rotation rates (omega/S) in which there is an exponential time growth of the turbulent kinetic energy and dissipation rate. The second-order closures are qualitatively superior since, consistent with physical and numerical experiments, they only predict this type of unstable flow for intermediate rotation rates in the range -0.1 less than or equal to omega/S less than or equal to 1.6. For rotation rates outside this range, there is an exchange of stabilities with a solution whose kinetic energy and dissipation rate decay with time. Although the second-order closures are superior to the two-equation models, there are still problems with the quantitative accuracy of their predictions. Author

N89-27978*# Analytical Services and Materials, Inc., Hampton, VA.
SPATIAL THREE-DIMENSIONAL SECONDARY INSTABILITY COMPRESSIBLE BOUNDARY-LAYER FLOWS
Nabil M. El-Hady Washington Sep. 1989 37 p
(Contract NAS1-18599)
(NASA-CR-4251; NAS 1.26:4251) Avail: NTIS HC A03/MF A01 CSCL 20D

Three-dimensional linear secondary instability theory is extended for compressible and high Mach number boundary layer flows. The small but finite amplitude compressible Tollmien-Schlichting wave effect on the growth of 3-D perturbations is investigated. The focus is on principal parametric resonance responsible for the strong growth of subharmonic in low disturbance environment. The effect of increasing Mach number on the onset, growth, the shape of eigenfunctions of the subharmonic is assessed, and the resulting vortical structure is examined. Author

N89-27979*# Prairie View Agricultural and Mechanical Coll., TX. Dept. of Mechanical Engineering.

FLOW BOILING WITH ENHANCEMENT DEVICES FOR COLD PLATE COOLANT CHANNEL DESIGN Final Report

Ronald D. Boyd, Jerry C. Turknett, and Alvin Smith 28 Aug. 1989 14 p

(Grant NAG9-310)

(NASA-CR-185840; NAS 1.26:185840) Avail: NTIS HC A03/MF A01 CSCL 20D

The effects of enhancement devices on flow boiling heat transfer in circular coolant channels, which are heated over a fraction of their perimeters, are studied. The variations were examined in both the mean and local (axial, and circumferential) heat transfer coefficients for a circular coolant channel with either smooth walls or with both a twisted tape and spiral finned walls. Improvements were initiated in the present data reduction analysis. These efforts should lead to the development of heat transfer correlations which include effects of single side heat flux and enhancement device configuration. It is hoped that a stage will be set for the study of heat transfer and pressure drop in single sided heated systems under zero gravity conditions. Author

N89-27980*# National Aeronautics and Space Administration. Lewis Research Center, Cleveland, OH.

EXPERIENCE WITH ADVANCED INSTRUMENTATION IN A HOT SECTION CASCADE

Frederick C. Yeh and Herbert J. Gladden 1989 14 p Prepared for presentation at the Winter Annual Meeting of the American Society of Mechanical Engineers, San Francisco, CA, 10-15 Dec. 1989

(NASA-TM-102294; E-4962; NAS 1.15:102294) Avail: NTIS HC A03/MF A01 CSCL 20D

The Lewis Research Center gas turbine Hot Section Test Facility was developed to provide a real engine environment with known boundary conditions for the aerothermal performance evaluation and verification of computer design codes. This verification process requires experimental measurements in a hostile environment. The research instruments used in this facility are presented, and their characteristics and how they perform in this environment are discussed. The research instrumentation consisted of conventional pressure and temperature sensors, as well as thin-film thermocouples and heat flux gages. The hot gas temperature was measured by an aspirated temperature probe and by a dual-element, fast-response temperature probe. The data acquisition mode was both steady state and time dependent. These experiments were conducted over a wide range of gas Reynolds numbers, exit gas Mach numbers, and heat flux levels. This facility was capable of testing at temperatures up to 1600 K, and at pressures up to 18 atm. These corresponded to an airfoil exit Reynolds number range of 0.5 x 10(6) to 2.5 x 10(6) based on the airfoil chord of 5.55 cm. The results characterize the performance capability and the durability of the instrumentation. The challenge of making measurements in hostile environments is also discussed. The instruments exhibited more than adequate durability to achieve the measurement profile. About 70 percent of the thin-film thermocouples and the dual-element temperature probe survived several hundred thermal cycles and more than 35 hr at gas temperatures up to 1600 K. Within the experimental uncertainty, the steady-state and transient heat flux measurements were comparable and consistent over the range of Reynolds numbers tested. Author

N89-27981# Argonne National Lab., IL. Reactor Analysis and Safety Div.

A CENTRAL DIFFERENCE TYPE APPROXIMATION OF CONVECTION IN FLUID FLOW

Constantine P. Tzanos 1989 6 p Presented at the Annual Meeting of the American Nuclear Society, Atlanta, GA, 4 Jun. 1989

(Contract W-31-109-eng-38)

(DE89-013282; CONF-890604-12) Avail: NTIS HC A02/MF A01

In fluid flow and heat transfer problems, to eliminate instability and oscillations resulting from the numerical approximation of the convection term, it is common practice to use first order upwind differencing. For example, first order upwind differencing is used in codes like COMMIX and PHOENICS. However, in problems characterized by high Peclet numbers, this approach is highly inaccurate unless an excessive number of nodes is used. To eliminate this difficulty, a method of grid adaptation using central differencing in one-dimensional problems was presented. In the effort to extend this approach to 2-D and 3-D problems a new method was developed for multidimensional problems that is superior to first order upwind differencing even for a few non-adaptive grid points. This method is presented in this work. DOE

N89-27982# Argonne National Lab., IL. Reactor Analysis and Safety Div.

INTERFACIAL AREA MEASUREMENT METHODS

M. J. Tan 1989 19 p Presented at the 3rd American Society of Civil Engineers/ASME Conference, San Diego, CA, 9 Jul. 1989

(Contract W-31-109-eng-38)

(DE89-013426; CONF-890794-1) Avail: NTIS HC A03/MF A01

Knowledge of local specific interfacial area is required for analysis and prediction of transient and steady characteristics of two-phase flow systems using the two-fluid models. Based on a survey of published work on the subject of specific interfacial area, it is recognized that there is virtually no data base for local specific interfacial area. This report describes the ongoing development of experimental techniques for measurement of local specific interfacial area in gas-liquid and liquid-liquid two-phase systems. Mathematical relations between local specific interfacial area and measurable quantities are derived based on kinematics and geometry. Two methods for determining local specific interfacial area are identified; both entail detection of passage of interfaces through fixed locations in the flow field. A multiple-sensor electrical-resistivity-probe technique is being developed for determination of local specific interfacial area in vertical gas-liquid bubbly flows. The technique consists of simultaneous measurements at two or four locations in the two-phase flow field of the local electrical resistivity of the two-phase mixture. Methods for data analysis are described. Limitations of the technique are briefly discussed. DOE

N89-27983# Du Pont de Nemours (E. I.) and Co., Aiken, SC. Savannah River Lab.

SUBCOOLED BOILING OF DOWNWARD FLOW IN A VERTICAL ANNULUS

B. S. Johnston 1989 21 p Presented at the ASME/AIChE National Heat Transfer Conference, Philadelphia, PA, 6-9 Aug. 1989 Submitted for publication

(Contract DE-AC09-76SR-00001)

(DE89-005320; DP-MS-88-217; CONF-890819-1) Avail: NTIS HC A03/MF A01

Measurements of steady state pressure drop were made for the downward flow of water in a vertical annulus at low pressure. The inner wall was uniformly heated to allow subcooled boiling. The minimum in the test section demand curve was compared to the onset of significant void (OSV) at the exit of the annulus. As expected, OSV was found to serve as a conservative predictor for avoiding flow excursions. However, at low flow rates the demand curve minima were significantly different from those obtained for upward flow. Similarly, conditions for OSV in downward flow were not predicted by the correlation of Saha and Zuber. More data are needed to establish a general correlation for OSV in downward flow. DOE

N89-27984# Argonne National Lab., IL. Materials and Components Technology Div.

ANALYSIS OF PRESSURE DROP AND HEAT TRANSFER DATA FROM THE REVERSING FLOW TEST FACILITY

Paul D. Roach and Kenneth J. Bell May 1989 33 p

(Contract W-31-109-eng-38)

(DE89-013907; ANL/MCT-88/2) Avail: NTIS HC A03/MF A01

The Reversing Flow Test Facility is part of the heat engine R

and D capabilities at Argonne National Laboratory. The facility permits the study of heat transfer and pressure drop under conditions of rapidly reversing flow. The results are summarized that were obtained from more than 100 data sets that cover a wide range of temperatures, pressures, and frequencies. Pressure drop data are presented as normalized pressure drop vs. the Reynolds number calculated from the amplitude of the oscillatory flow. Heat transfer data for the regenerators are presented as regenerator effectiveness vs. Reynolds number. Three significant conclusions are derived from the analysis of the data: (1) no frequency dependence is observed in either the pressure drop or the heat transfer data; (2) the measured pressure drops for the heater and coolers are distinctly higher than those calculated from steady-flow correlations; and (3) the heat transfer coefficient in the heater is about 80 percent of that predicted by steady flow correlations. The correlations presented provide the basis for improving existing models. DOE

N89-27985# Von Karman Inst. for Fluid Dynamics, Rhode-Saint-Genese (Belgium).
AN INTRODUCTION TO COMPUTATIONAL FLUID DYNAMICS
1989 483 p Lecture series held in Rhode-Saint-Genese, Belgium, 16-20 Jan. 1989
(VKI-LS-1989-02; ISSN-0377-8312; ETN-89-94967) Avail: NTIS HC A21/MF A01

Boundary layer equations and methods of solution, finite volume techniques, finite element techniques, and implicit time dependent methods for inviscid and viscous compressible flows, with a discussion of the concept of numerical dissipation, are presented. For individual titles, see N89-27986 through N89-27990.

N89-27986# Maryland Univ., College Park. Dept. of Aerospace Engineering.
INTRODUCTION
J. D. Anderson, Jr. *In* VKI, An Introduction to Computational Fluid Dynamics 1989 269 p (For primary document see N89-27985 22-34)
Avail: NTIS HC A21/MF A01

Governing equations of fluid dynamics; mathematical properties of fluid dynamic equations; discretization of partial differential equations; transformations and grids; incompressible inviscid flows: source and vortex panel methods; and explicit finite difference methods applied to inviscid and viscous flows are introduced. ESA

N89-27987# Von Karman Inst. for Fluid Dynamics, Rhode-Saint-Genese (Belgium).
BOUNDARY LAYER EQUATIONS AND METHODS OF SOLUTION
R. Grundmann *In its* An Introduction to Computational Fluid Dynamics 1989 31 p (For primary document see N89-27985 22-34)
Avail: NTIS HC A21/MF A01

Prandtl's boundary layer equations; the hierarchy of boundary layer equations; transformation of the boundary layer equations; numerical solution methods; and sample calculations are discussed. ESA

N89-27988# Ghent Univ. (Belgium). Dept. of Machinery.
INTRODUCTION TO FINITE ELEMENT TECHNIQUES IN COMPUTATIONAL FLUID DYNAMICS
E. Dick *In* VKI, An Introduction to Computational Fluid Dynamics 1989 27 p (For primary document see N89-27985 22-34)
Avail: NTIS HC A21/MF A01

Strong and weak formulations of a boundary value problem; piecewise defined shape functions; implementation of the finite element method; and finite element method applications to fluid dynamics are explained. ESA

N89-27989# Ghent Univ. (Belgium). Dept. of Machinery.
INTRODUCTION TO FINITE VOLUME TECHNIQUES IN COMPUTATIONAL FLUID DYNAMICS
E. Dick *In* VKI, An Introduction to Computational Fluid Dynamics 1989 26 p (For primary document see N89-27985 22-34)
Avail: NTIS HC A21/MF A01

Finite-element like finite volume techniques; finite difference like finite volume techniques; and methods which use modes not at cell centers or at cell vertices are outlined. ESA

N89-27990# Sherbrooke Univ. (Quebec). Dept. of Mechanical Engineering.
IMPLICIT TIME DEPENDENT METHODS FOR INVISCID AND VISCOUS COMPRESSIBLE FLOWS, WITH A DISCUSSION OF THE CONCEPT OF NUMERICAL DISSIPATION
G. Degrez *In* VKI, An Introduction to Computational Fluid Dynamics 1989 135 p (For primary document see N89-27985 22-34)
Avail: NTIS HC A21/MF A01

Solution techniques for simple flows and their failures for Euler/Navier-Stokes equations; implicit methods for time-dependent problems; numerical dissipation; and conservative upwind discretization for hyperbolic systems are discussed. ESA

N89-27991# Lehigh Univ., Bethlehem, PA.
THREE-DIMENSIONAL VORTEX INTERACTIONS IN TURBULENT BOUNDARY LAYERS Final Report, 7 Jan. 1985 - 30 Nov. 1988
C. R. Smith and J. D. A. Walker 15 Apr. 1989 73 p
(Contract F49620-85-C-0108; AF Proj. 2307)
(AD-A208624; AFOSR-89-0689TR) Avail: NTIS HC A04/MF A01 CSCL 20/4

The results and accomplishments of a combined analytical-experimental research program, aimed at understanding and modeling the three-dimensional vortex interactions that take place in turbulent boundary layers, are described. The central theme of the program is that hairpin vortices are the basic building block of boundary-layer turbulence and that many of the observed dynamic features of turbulent shear flows can be explained in terms of how hairpin vortices interact with the background shear, with each other and the viscous flow near solid walls. A basic intent of the program is to cross-compare detailed experimental flow visualization-imaging studies of well-defined three-dimensional hairpin vortices with computational studies of the behavior, evolution and induced effects of comparable vortices. Based on these investigations, a model of the dynamics of turbulent flows near a wall is proposed. GRA

N89-27992# Aerospace Corp., El Segundo, CA. Engineering Group.
A METHOD FOR CALCULATING ASYMMETRIC FLOW THROUGH NOZZLES Final Report, Jan. - Aug. 1988
Rudolf X. Meyer Jan. 1989 24 p
(Contract F04701-88-C-0089)
(AD-A209689; TR-0088(4392-11)-1; SD-TR-89-20) Avail: NTIS HC A03/MF A01 CSCL 20/4

The asymmetric steady state, inviscous, adiabatic flow of a perfect gas through a subsonic/supersonic nozzle is considered. The nozzle itself is either of rectangular cross section or is axisymmetric. A first-order small asymmetry induced by an entrance flow which is oblique to the nozzle axis and has a transverse pressure gradient is allowed. The cross section of the nozzle is assumed to vary only slowly as a function of the axial distance; the case considered here is therefore an extension of the well known theory of the quasi-1-D flow of a perfect gas treated in standard textbooks. An integral method is used to obtain approximate results. The method is simple, yet in a test case (supersonic flow at an angle of attack through a rectangular channel) where the exact first-order result is known, a comparison shows surprisingly good agreement. Numerical results are tabulated for axisymmetric nozzles with polynomial Mach number dependence. GRA

N89-27993# Clarkson Univ., Potsdam, NY. Dept. of Mathematics and Computer Science.
NONLINEAR WAVES

Mark J. Ablowitz and Athanassios S. Fokas 15 Jun. 1989 9 p
(Contract N00014-88-K-0447)
(AD-A209822) Avail: NTIS HC A02/MF A01 CSCL 20/4

The investigators have been working in the general area of nonlinear wave propagation for over twenty years. The main focus herein is the understanding of the nonlinear phenomena involved with the wave propagation arising in physical problems. The work has application to numerous areas of physics, engineering and mathematics. Applications include fluid dynamics, waves in stratified fluids, surface gravity waves and wave excitation phenomena related to moving pressure distributions; numerical approximation and computation; nonlinear optics; and plasma physics. Moreover the study of solutions to some of the underlying nonlinear evolution equations has led naturally to the investigation and new results in the separate but closely related field of inverse scattering. Developments to both one and multidimensional inverse problems were made. GRA

35 INSTRUMENTATION AND PHOTOGRAPHY

Includes remote sensors; measuring instruments and gages; detectors; cameras and photographic supplies; and holography.

For aerial photography see *43 Earth Resources and Remote Sensing*. For related information see also *06 Aircraft Instrumentation*, and *19 Spacecraft Instrumentation*.

N89-27994*# Microtronics Associates, Pittsburgh, PA.
HIGH DYNAMIC RANGE INFRARED RADIOMETRY AND IMAGING Final Report
Darryl D. Coon, R. P. G. Karunasiri, and K. M. S. V. Bandara 20 Aug. 1988 33 p Original contains color illustrations
(Contracts NAS5-30282; DASG60-86-C-0075)
(NASA-CR-183439; NAS 1.26:183439) Avail: NTIS HC A03/MF A01 CSCL 14B

The use is described of cryogenically cooled, extrinsic silicon infrared detectors in an unconventional mode of operation which offers an unusually large dynamic range. The system performs intensity-to-frequency conversion at the focal plane via simple circuits with very low power consumption. The incident IR intensity controls the repetition rate of short duration output pulses over a pulse rate dynamic range of about 10(6). Theory indicates the possibility of monotonic and approx. linear response over the full dynamic range. A comparison between the theoretical and the experimental results shows that the model provides a reasonably good description of experimental data. Some measurements of survivability with a very intense IR source were made on these devices and found to be very encouraging. Evidence continues to indicate that some variations in interpulse time intervals are deterministic rather than probabilistic. Author

N89-27995*# National Aeronautics and Space Administration. Langley Research Center, Hampton, VA.
PHOTOGRAMMETRIC TECHNIQUE FOR IN-FLIGHT RANGING OF TRAILING VORTICES USING ENTRAINED BALLOONS
Walter L. Snow, Alpheus W. Burner, and William K. Goad 1989 1 p
(NASA-TM-4129; L-16551; NAS 1.15:4129) Avail: NTIS HC A03/MF A01 CSCL 14E

A method for experimentally determining the radial distance of a probe aircraft from a trailing vortex is described. The method relies on photogrammetric triangulation of targets entrained in the vortex core. The theory and preliminary testing were described using laboratory mock-ups. Solid state video cameras were to provide data at 300 Hz rates. Practical methods for seeding the vortex are under separate investigation and are not addressed. Author

N89-27996# Maryland Univ., College Park. Dept. of Mechanical Engineering.
THE USE OF STEREO OPTICAL FLOW FIELDS IN THE DETERMINATION OF THREE-DIMENSIONAL MOTION AND STEREO CORRESPONDENCE Progress Report, May 1988 - Apr. 1989
J. H. Duncan May 1989 30 p
(Contract DE-FG05-87ER-13782)
(DE89-012518; DOE/ER-13782/3) Avail: NTIS HC A03/MF A01

A method has been developed that can determine the motion of a stereo-camera platform and the relative three-dimensional position of image features using data from stereo image sequences as input. In the first step of the method, the motion is found from a set of linear equations whose coefficients are averages of functions of the measured positions and velocities of image features. In the second step of the method, the same equations are used with the computed translational velocities to determine the correspondence of features in the left and right images. Separate theories were developed which use the full optical flow as input or the normal flow at contours as input. The theory using the full optical flow as derived for six-component, three-dimensional motions, while the theory for the normal flow was derived for translational motion only. The theories require only that the data in the left and right images come from regions corresponding to objects with the same relative velocity. Thus, in the case of a camera platform moving through a stationary environment these regions include the entire images. The theories have been tested with synthetic image sequences and appear to be promising. A stereo camera system for use in the laboratory has just been constructed and will be used to test the methods with real images from laboratory scenes. In the following, the theory for motion recovery with the full optical flow data is presented first. This is followed by the theory for the recovery of the translational motion from the normal flow data. A discussion of the determination of stereo correspondence follows. Then the results of experiments with synthetic images are presented and the conclusions are given. DOE

N89-27997# Notre Dame Univ., IN. Dept. of Physics.
SCINTILLATING FIBER DETECTOR DEVELOPMENT FOR THE SSC Annual Progress Report
Randal C. Ruchti 29 May 1989 14 p
(Contract DE-AC02-87ER-40372)
(DE89-013118; DOE/ER-40372/02) Avail: NTIS HC A03/MF A01

During the past year, considerable effort was applied to the development of scintillating fiber detectors in several areas: new scintillation liquids and studies of their fluorescence properties; new fluorescent dyes based on non-intramolecular proton transfer; new dyes based on intramolecular proton transfer; incorporation of these new dyes in plastic (polystyrene) and liquid scintillation solutions; development of small cross section glass capillaries for the containment of liquid scintillators; studies of waveguide characteristics; and studies of image intensifier phosphor screen characteristics. Other areas are: initial steps to form a collaboration to study and develop appropriate new properties of the Solid State Photomultiplier. Construction of a new laboratory at Notre Dame to enhance the capabilities for further measurements and studies; and organization of and execution of a Workshop on Scintillating Fiber Detector Development for the SSC, held at Fermilab, November 14 to 16, 1988. DOE

N89-27998*# National Aeronautics and Space Administration. Lewis Research Center, Cleveland, OH.
COMPENSATION FOR EFFECTS OF AMBIENT TEMPERATURE ON RARE-EARTH DOPED FIBER OPTIC THERMOMETER
G. Adamovsky, J. L. Sotomayor, M. J. Krasowski, and J. G. Eustace (John Carroll Univ., Cleveland, OH.) 1989 14 p Presented at the Fiber Optic and Laser Sensors 7, Boston, MA, 5-8 Sep. 1989; sponsored by the Society of Photo-Optical Instrumentation Engineers

(Grant NAG3-984)
(NASA-TM-102282; E-4946; NAS 1.15:102282) Avail: NTIS HC A03/MF A01 CSCL 14B

Variations in ambient temperature have a negative effect on the performance of any fiber optic sensing system. A change in ambient temperature may alter the design parameters of fiber optic cables, connectors, sources, detectors, and other fiber optic components and eventually the performance of the entire system. The thermal stability of components is especially important in a system which employs intensity modulated sensors. Several referencing schemes have been developed to account for the variable losses that occur within the system. However, none of these conventional compensating techniques can be used to stabilize the thermal drift of the light source in a system based on the spectral properties of the sensor material. The compensation for changes in ambient temperature becomes especially important in fiber optic thermometers doped with rare earths. Different approaches to solving this problem are searched and analyzed. Author

N89-27999*# National Aeronautics and Space Administration. Lewis Research Center, Cleveland, OH.
SPECKLE INTERFEROMETRY USING FIBER OPTIC PHASE STEPPING
Carolyn R. Mercer and Glenn Beheim Aug. 1989 9 p Presented at the Symposium on Optical and Optoelectronic Applied Science and Engineering, San Diego, CA, 6-11 Aug. 1989; sponsored in part by Society of Photo-Optical Instrumentation Engineers
(NASA-TM-102331; E-5040; NAS 1.15:102331) Avail: NTIS HC A02/MF A01 CSCL 14B

A system employing closed-loop phase-stepping is used to measure the out-of-plane deformation of a diffusely reflecting object. Optical fibers are used to provide reference and object beam illumination for a standard two-beam speckle interferometer, providing set-up flexibility and ease of alignment. Piezoelectric fiber-stretchers and a phase-measurement/servo system are used to provide highly accurate phase steps. Intensity data is captured with a charge-injection-device camera, and is converted into a phase map using a desktop computer. The closed-loop phase-stepping system provides 90 deg phase steps which are accurate to 0.02 deg, greatly improving this system relative to open-loop interferometers. The system is demonstrated on a speckle interferometer, measuring the rigid-body translation of a diffusely reflecting object with an accuracy + or - 10 deg, or roughly + or - 15 nanometers. This accuracy is achieved without the use of a pneumatically mounted optics table. Author

N89-28000# Lawrence Livermore National Lab., CA. Environmental Sciences Div.
HIGH-TEMPERATURE OPTICAL-FIBER PH SENSOR Final Report
S. M. Angel and J. F. Poco Jun. 1989 31 p Prepared for Electric Power Research Inst.
(Contract W-7405-eng-48)
(DE89-014103; UCRL-21083; EPRI-RP-2614-5) Avail: NTIS HC A03/MF A01

The results of research on high-temperature optical-fiber pH sensors will be presented. It is shown that these sensors (optrodes) can be made to work in very-high-temperature (300 C) water for long periods and that it is possible to measure pH using fluorescent inorganic ions doped into solid matrices. A high-temperature pH optrode can be made using these techniques; however, more research is needed into the chemistry of the carrier matrices and fluorescent dopants. New types of materials should be studied, including solid polymer ionic conductors and high-temperature epoxies. Particular emphasis should be placed on developing an Eh optrode because it also will be very useful and probably more easily developed. Transition-metal ions and complexes, as well as certain stable organic dyes, (materials that are very stable at high temperature) should also be investigated as dopants. DOE

N89-28001# Army Missile Command, Redstone Arsenal, AL. Research Directorate.
COMPUTER GENERATED MATCHED FILTERS WITH SPATIAL FREQUENCY TAILORING Final Technical Report, Jun. - Oct. 1988
Don A. Gregory, Kevin Worchester, Larry Z. Kennedy, and J. Graeme Duthie (Alabama Univ., Huntsville.) Apr. 1989 43 p
(AD-A209786; AD-E951363; AMSMI/TR-RD-RE-89-2) Avail: NTIS HC A03/MF A01 CSCL 09/1

Computer generated Fourier transform matched filters have been constructed using e-beam lithography. These filters were then evaluated by placing them in a VanderLugt optical correlator and addressing them with the original scene used to make the filters. Results show that the spatial frequency content of a filter may be tailored so as to obtain good signal-to-noise correlations while maintaining high diffraction efficiency. GRA

N89-28125*# National Aeronautics and Space Administration. Goddard Space Flight Center, Greenbelt, MD.
MONOCULAR ELECTRO-OPTICAL STEREO SCANNER Abstract Only
C. Vermillion, H. Maurer, V. Salomonson, C. Cote, J. Catena, H. Rampariyan, and J. Smith *In its* Laboratory for Oceans 1988 p 35-36 (For primary document see N89-28118 22-48)
Avail: NTIS HC A12/MF A01 CSCL 14B

N89-28128*# National Aeronautics and Space Administration. Goddard Space Flight Center, Greenbelt, MD.
ADVANCED ALTIMETRY Abstract Only
C. L. Parsons, S. A. Bailey, D. E. Hines, D. W. Shirk, C. W. Wright, and A. R. Selser *In its* Laboratory for Oceans 1988 p 45-47 (For primary document see N89-28118 22-48)
Avail: NTIS HC A12/MF A01 CSCL 14B

N89-28129*# National Aeronautics and Space Administration. Goddard Space Flight Center, Greenbelt, MD.
EARTH OBSERVING SYSTEM (EOS) ADVANCED ALTIMETRY Abstract Only
C. L. Parsons and E. J. Walsh *In its* Laboratory for Oceans 1988 p 49-51 (For primary document see N89-28118 22-48)
Avail: NTIS HC A12/MF A01 CSCL 14B

N89-28132*# National Aeronautics and Space Administration. Goddard Space Flight Center, Greenbelt, MD.
OCEANOGRAPHIC WIDE FIELD SENSOR Abstract Only
R. G. Kirk *In its* Laboratory for Oceans 1988 p 59-60 (For primary document see N89-28118 22-48)
Avail: NTIS HC A12/MF A01 CSCL 14B

N89-28142*# National Aeronautics and Space Administration. Goddard Space Flight Center, Greenbelt, MD.
NASA CHARGE COUPLED DEVICE (CCD) SPECTROMETER SYSTEM (NCSS) Abstract Only
C. W. Wright, S. A. Bailey, and C. R. Piazza *In its* Laboratory for Oceans 1988 p 91-94 (For primary document see N89-28118 22-48)
Avail: NTIS HC A12/MF A01 CSCL 14B

N89-28145*# National Aeronautics and Space Administration. Goddard Space Flight Center, Greenbelt, MD.
COASTAL ZONE COLOR SCANNER Abstract Only
B. Johnson *In its* Laboratory for Oceans 1988 p 101-103 (For primary document see N89-28118 22-48)
Avail: NTIS HC A12/MF A01 CSCL 14B

N89-28146*# National Aeronautics and Space Administration. Goddard Space Flight Center, Greenbelt, MD.
THE MULTICHANNEL OCEAN COLOR SENSOR (MOCS) Abstract Only
J. D. Oberholtzer and C. R. Vaughn *In its* Laboratory for Oceans 1988 p 105-106 (For primary document see N89-28118 22-48)
Avail: NTIS HC A12/MF A01 CSCL 14B

N89-28181*# National Aeronautics and Space Administration. Goddard Space Flight Center, Greenbelt, MD.
SYNTHETIC APERTURE MICROWAVE RADIOMETER Abstract Only
D. M. LeVine *In its* Laboratory for Oceans 1988 p 237-238 (For primary document see N89-28118 22-48)
Avail: NTIS HC A12/MF A01 CSCL 14B

N89-28183*# National Aeronautics and Space Administration. Goddard Space Flight Center, Greenbelt, MD.
ADVANCED SOLIDSTATE ARRAY SPECTRORADIOMETER Abstract Only
F. G. Huegel and J. Irons *In its* Laboratory for Oceans 1988 p 243-245 (For primary document see N89-28118 22-48)
Avail: NTIS HC A12/MF A01 CSCL 14B

N89-28189*# National Aeronautics and Space Administration. Goddard Space Flight Center, Greenbelt, MD.
NASA AIRCRAFT-SATELLITE INSTRUMENT CALIBRATION PROJECT Abstract Only
B. W. Guenther *In its* Laboratory for Oceans 1988 p 267-268 (For primary document see N89-28118 22-48)
Avail: NTIS HC A12/MF A01 CSCL 14B

N89-28190*# National Aeronautics and Space Administration. Goddard Space Flight Center, Greenbelt, MD.
FLIGHT CALIBRATION SOURCE DEVELOPMENT Abstract Only
S. Glicker *In its* Laboratory for Oceans 1988 p 269 (For primary document see N89-28118 22-48)
Avail: NTIS HC A12/MF A01 CSCL 14B

N89-28193*# National Aeronautics and Space Administration. Goddard Space Flight Center, Greenbelt, MD.
CALIBRATION SOURCE MAINTENANCE, CHARACTERIZATION AND DEVELOPMENT Abstract Only
J. T. McLean *In its* Laboratory for Oceans 1988 p 277 (For primary document see N89-28118 22-48)
Avail: NTIS HC A12/MF A01 CSCL 14B

N89-28194*# National Aeronautics and Space Administration. Goddard Space Flight Center, Greenbelt, MD.
INTEGRATING SPHERE AND HEMISPHERE CALIBRATION UPDATE Abstract Only
J. T. McLean *In its* Laboratory for Oceans 1988 p 279-281 (For primary document see N89-28118 22-48)
Avail: NTIS HC A12/MF A01 CSCL 14B

36 LASERS AND MASERS

Includes parametric amplifiers.
For related information see also *76 Solid-State Physics*.

N89-28002# SRI International Corp., Menlo Park, CA.
GMBU (GROUND MOBILE BREADBOARD UPGRADE) LIDAR AND BUBBLER CORRELATION STUDY AT DUGWAY PROVING GROUND Technical Report, Aug. - Dec. 1988
Peter L. Holland 17 Mar. 1989 30 p
(Contract DAAK11-82-C-0158)
(AD-A207297; DPG-FR-89-901) Avail: NTIS HC A03/MF A01 CSCL 17/5

Infrared differential adsorption lidar (IR DIAL) was used for real time vapor concentration measurements. As part of the 1988 Thermal Image Test Program, a correlation study was made between conventional sequentially aspirated bubblers and the DIAL system. Six lidar bubbler correlation trials were performed using diethyl malonate (DEM) as a simulant. The DEM was disseminated from a 100 m line source with the lidar aimed along a single line of sight directly over 21 bubbler stations spaced at approximately 30 m intervals. High correlations between lidar and bubbler DEM vapor concentration measurements were observed. For the 1 min integration period generally used the lidar sensitivity limit is estimated to be less than 1mg/cu m for DEM. GRA

N89-28003# Naval Research Lab., Washington, DC.
EFFICIENT SECOND HARMONIC CONVERSION OF BROADBAND HIGH-PEAK-POWER ND:GLASS LASER RADIATION USING LARGE-APERTURE KDP CRYSTALS IN QUADRATURE
M. Pronko, R. Lehmberg, S. Obenschain, C. Pawley, C. Manka, and R. Eckardt (Stanford Univ., CA.) 23 Jun. 1989 41 p
(Contract DE-AI03-79DP-40092)
(DE89-012961; NRL-MR-6453) Avail: NTIS HC A03/MF A01

We have investigated the second harmonic conversion efficiency of broadband Nd:glass laser light (delta nu/c is less than 30/cm FWHM). Using two KDP crystals in a quadrature arrangement we obtained energy conversion efficiencies approximately 55 percent with an initial bandwidth for the fundamental of delta nu/c is approximately 17/cm FWHM. For these conditions, we observed a modest increase (approximately 70 percent) in the harmonic bandwidth (FWHM) relative to the fundamental. The usual theory of three-wave mixing in dispersive birefringent nonlinear crystals is extended to describe the broadband harmonic conversion process; the generalized theory includes the statistical properties of the light and phase mismatch effects on the spectral components in the complex field amplitudes. Good agreement is shown between the code calculations and the measurements. DOE

N89-28004*# Planning Research Corp., Hampton, VA. Aerospace Technologies Div.
APPROACHES TOWARD A BLUE SEMICONDUCTOR LASER Report, Sep. 1987 - Sep. 1988
I. Ladany Washington Sep. 1989 90 p
(Contract NAS1-18000)
(NASA-CR-4252; NAS 1.26:4252) Avail: NTIS HC A05/MF A01 CSCL 20E

Possible approaches for obtaining semiconductor diode laser action in the blue region of the spectrum are surveyed. A discussion of diode lasers is included along with a review of the current status of visible emitters, presently limited to 670 nm. Methods are discussed for shifting laser emission toward shorter wavelengths, including the use of II-IV materials, the increase in the bandgap of III-V materials by addition of nitrogen, and changing the bandstructure from indirect to direct by incorporating interstitial atoms or by constructing superlattices. Non-pn-junction injection methods are surveyed, including avalanche breakdown, Langmuir-Blodgett diodes, heterostructures, carrier accumulation, and Berglund diodes. Prospects of inventing new multinary semiconducting materials are discussed, and a number of novel materials described in the literature are tabulated. New approaches available through the development of quantum wells and superlattices are described, including resonant tunneling and the synthesis of arbitrary bandgap materials through multiple quantum wells. Author

N89-28005# California Univ., Berkeley. Lawrence Berkeley Lab. Accelerator and Fusion Research Div.
HIGH-POWER, HIGH-EFFICIENCY FELS
Andrew M. Sessler Apr. 1989 17 p Presented at the CERN Accelerator School, Chester, United Kingdom, 6 Apr. 1989
(Contract DE-AC03-76SF-00098)
(DE89-013002; LBL-27035; CONF-8904228-2) Avail: NTIS HC A03/MF A01

High power, high efficiency free electron lasers (FELs) require tapering, as the particles loose energy, so as to maintain resonance between the electromagnetic wave and the particles. They also require focusing of the particles (usually done with curved pole faces) and focusing of the electromagnetic wave (i.e., optical guiding). In addition, one must avoid transverse beam instabilities (primarily resistive wall) and longitudinal instabilities (i.e., sidebands). DOE

N89-28006# Lawrence Livermore National Lab., CA.
MULTI-SEGMENT Nd:GLASS DISK AMPLIFIERS
J. E. Murray, A. C. Erlandson, F. A. Frick, K. S. Jancaitis, C. E. Hurley, and H. T. Powell Jun. 1989 21 p Presented at the

CLEO 1989: Conference on Lasers and Electro Optics, Baltimore, MD, 24 Apr. 1989
(Contract W-7405-eng-48)
(DE89-014043; UCRL-101266; CONF-890423-11) Avail: NTIS HC A03/MF A01

Initial designs of a multi-megajoule laser system call for compact, segmented aperture disk amplifiers which are substantially different from conventional amplifiers. We have experimentally investigated several of the new issues introduced by these amplifiers. DOE

N89-28007# Los Alamos National Lab., NM.
KrF LASERS FOR INERTIAL CONFINEMENT FUSION
David B. Harris, David C. Cartwright, Joseph F. Figueira, Thomas E. McDonald, and Michael E. Sorem 1989 13 p Presented at the 5th International Conference on Emerging Nuclear Energy Systems: ICENES '89, Karlsruhe, Federal Republic of Germany, 3-6 Jul. 1989
(Contract W-7405-eng-36)
(DE89-014272; LA-UR-89-2205; CONF-890711-1) Avail: NTIS HC A03/MF A01

The KrF laser was proposed for inertial confinement fusion (ICF) since its discovery in 1975. Since that time, the laser has seen significant development and was increased in energy many orders of magnitude to the several kilojoule energy level. The suitability of the KrF laser as a driver for ICF energy applications was continually reviewed. The latest assessments indicate that the KrF laser still appears to be the leading laser candidate. A worldwide effort exists to advance the KrF laser for ICF applications. DOE

N89-28008# Tokyo Univ., Tanashi (Japan). Inst. for Nuclear Study.
LASERTRON: A PULSED RF-SOURCE USING LASER TRIGGERED PHOTOCATHODE
Masakazu Yoshioka Dec. 1988 30 p
(DE89-778130; INS-726) Avail: NTIS (US Sales Only) HC A03/MF A01

A new pulsed RF-source, Lasertron, are being developed as a possible RF power source for future electron-positron linear colliders. In a series of systematic study, a prototype lasertron has been fabricated and tested. A peak power of 80 kW is attained at 2.856 GHz RF-frequency in 1-ms time duration. The experimental results of the lasertron are described including the developments of the photocathode and the laser system. Test results are compared with the analysis of beam dynamics in the lasertron. DOE

N89-28009# Lawrence Livermore National Lab., CA.
PULSED LASER PROPULSION FOR LOW COST, HIGH VOLUME LAUNCH TO ORBIT
Jordin Kare 2 Jun. 1989 11 p Presented at the International Astronautics Federation Conference on Space Power, Cleveland, OH, 5 Jun. 1989
(Contract W-7405-eng-48)
(DE89-014049; UCRL-101139; CONF-8906169-1) Avail: NTIS HC A03/MF A01

Pulsed laser propulsion offers the prospect of delivering high thrust at high specific impulse (500 to 1000 seconds) from a very simple thruster, using the energy of a remote ground-based laser to heat an inert propellant. Current analyses indicate that payloads of approximately 1 kg per megawatt of average laser power can be launched at a rate of one payload every 15 minutes and a marginal cost of $20 to $200 per kg. A 20 MW entry-level launch system could be built using current technology at a cost of $500 million or less; it would be capable of placing 600 tons per year into LEO. The SDIO Laser Propulsion Program has been developing the technology for such a launch system since 1987. The program has conducted theoretical and experimental research on a particular class of laser-driven thruster, the planar double-pulse LSD-wave thruster, which could be used for a near-term launcher. The double-pulse thruster offers several advantages, including extreme simplicity, design flexibility, and the ability to guide a vehicle remotely by precise control of the laser beam. Small-scale experiments have demonstrated the operation of this thruster at a specific impulse of 600 seconds and 10 percent efficiency; larger experiments now under way are expected to increase this to at least 20 percent efficiency. DOE

N89-28010# Ortel Corp., Alhambra, CA.
BAND STRUCTURE ENGINEERING FOR ULTRA-LOW THRESHOLD LASER DIODES Final Progress Report
I. Ury and Kam Y. Lau 1988 45 p
(Contract N00014-88-C-0611)
(AD-A208629) Avail: NTIS HC A03/MF A01 CSCL 09/3

While semiconductor lasers of a high level of sophistication and reliability have been developed for present day fiberoptic telecommunications, demands for ultralow lasing threshold and ultrahigh modulation speed stem mainly from applications involving relatively short distance interconnections within a computer. The need for optics in computers arises from the increasing parallelism in modern computer architectures, which places heavy demands on input/output functions at gigahertz clock rates. Further consideration of using semiconductor lasers in computer optical interconnects shows that conventional semiconductor lasers are unacceptable for such purposes, the main problem being that they must be biased at or above lasing threshold for proper modulation behavior. This mode of operation requires a monitor photodiode and an active feedback circuit to stabilize the operating point. In a supercomputer where there are as many as a few hundred thousand interconnections, such feedback circuits will occupy a large amount of real estate and the bias current required will consume an unacceptable amount of power. GRA

N89-28011# Defense Intelligence Agency, Washington, DC. Directorate for Scientific and Technical Intelligence.
BIBLIOGRAPHY OF SOVIET LASER DEVELOPMENTS: JANUARY - FEBRUARY 1988
21 Feb. 1989 138 p
(AD-A209802; DIA-DST-2700Z-007-89; Rept-93) Avail: NTIS HC A07/MF A01 CSCL 09/3

This is the Soviet Laser Bibliography for January and February 1988, and is No. 93 in a continuing series on Soviet Laser developments. The coverage includes basic research on solid state, liquid, gas, and chemical lasers; components; nonlinear optics; spectroscopy of laser materials; ultrashort pulse generation; theoretical aspects of advanced lasers; and general laser theory. Laser applications are listed under biological effects; communications systems; beam propagation; adaptive optics; computer technology; holography; laser induced chemical reactions; measurement of laser parameters; laser measurement applications; laser excited optical effects; laser spectroscopy; beam target interaction; and plasma generation and diagnostics. GRA

N89-28012# Ortel Corp., Alhambra, CA.
PIGTAILED SINGLE-MODE DIODE LASERS Final Report, 20 Sep. 1988 - 30 Apr. 1989
Norman Kwong 30 Apr. 1989 33 p
(Contract N00014-88-C-2033)
(AD-A209913) Avail: NTIS HC A03/MF A01 CSCL 09/3

In choosing a scheme for single mode fiber coupling, the final evaluation should of course be based on an experimental comparison between the alternative. However, such an evaluation will generally not reveal the essential limitations of any scheme. While the possible sources of less than ideal performance are well known, their relative significance is not so obvious. It is clear that in order to make significant improvements in the state of fiber coupling technology, the relevant limitations must be clarified in order to guide further efforts in fruitful directions. As such, an analysis was conducted for several aspects of the fiber coupling problem which is presented. Preliminary to the consideration of any particular system, the importance of the zeroth and first order properties of the coupling system are briefly discussed. To go beyond this, the higher order aberrations of the optical coupling system must be included in the analysis. To do this, an algorithm to calculate the mode coupling performance of any optical system

was developed using the ray tracing features of an optical design program. This algorithm is described along with the results of an analysis of coupling with graded index lenses which were found to work well experimentally. GRA

N89-28013# University of Southern California, Los Angeles. Center for Laser Studies.
NEW, EFFICIENT OPTICALLY PUMPED SOLID STATE LASERS Final Report, 15 Aug. 1984 - 14 Nov. 1988
Michael Bass and Milton Birnbaum 21 Feb. 1989 51 p
(Grant AF-AFOSR-0378-84; AF Proj. 2301)
(AD-A209998; AFOSR-89-0919TR) Avail: NTIS HC A04/MF A01 CSCL 09/3

This effort explored the effects on laser operation of ion-ion interactions in crystalline solids. The work on the doubly-doubly Nd,Er:YAG and Nd,Ho:YAG lasers has demonstrated not only simultaneous lasing of both ionic species but also drastic lifetime productions in the lower laser states of both Er and Ho. This work has enabled the prediction of crystals in which 4 level operations at 2.9 microns can be achieved and initial verification was obtained with Er,Nd:YALO. GRA

N89-27876*# Jet Propulsion Lab., California Inst. of Tech., Pasadena.
OPERATIONAL PARAMETERS FOR THE SUPERCONDUCTING CAVITY MASER
R. T. Wang, G. J. Dick, and D. M. Strayer *In its* The Telecommunications and Data Acquisition Report 15 May 1989 p 64-71 (For primary document see N89-27871 22-32)
Avail: NTIS HC A17/MF A01 CSCL 20E

N89-27877*# Jet Propulsion Lab., California Inst. of Tech., Pasadena.
OPERATING AND ENVIRONMENTAL CHARACTERISTICS OF SIGMA TAU HYDROGEN MASERS USED IN THE VERY LONG BASELINE ARRAY (VLBA)
T. K. Tucker *In its* The Telecommunications and Data Acquisition Report 15 May 1989 p 72-80 (For primary document see N89-27871 22-32)
Avail: NTIS HC A17/MF A01 CSCL 20E

N89-27897*# Jet Propulsion Lab., California Inst. of Tech., Pasadena.
A NOVEL APPROACH TO A PPM-MODULATED FREQUENCY-DOUBLED ELECTRO-OPTIC CAVITY-DUMPED Nd:YAG LASER
D. L. Robinson *In its* The Telecommunications and Data Acquisition Report 15 May 1989 p 240-247 (For primary document see N89-27871 22-32)
Avail: NTIS HC A17/MF A01 CSCL 20E

N89-28134*# National Aeronautics and Space Administration. Goddard Space Flight Center, Greenbelt, MD.
LUNAR OBSERVER LASER ALTIMETER Abstract Only
J. L. Bufton *In its* Laboratory for Oceans 1988 p 63-65 (For primary document see N89-28118 22-48)
Avail: NTIS HC A12/MF A01 CSCL 20E

N89-28135*# National Aeronautics and Space Administration. Goddard Space Flight Center, Greenbelt, MD.
YAG AEROSOL LIDAR Abstract Only
R. Sullivan *In its* Laboratory for Oceans 1988 p 67-68 (For primary document see N89-28118 22-48)
Avail: NTIS HC A12/MF A01 CSCL 20E

N89-28141*# National Aeronautics and Space Administration. Goddard Space Flight Center, Greenbelt, MD.
OCEANOGRAPHIC APPLICATIONS OF LASER TECHNOLOGY Abstract Only
F. E. Hoge *In its* Laboratory for Oceans 1988 p 85-94 (For primary document see N89-28118 22-48)
Avail: NTIS HC A12/MF A01 CSCL 20E

N89-28143*# National Aeronautics and Space Administration. Goddard Space Flight Center, Greenbelt, MD.
AIRBORNE OCEANOGRAPHIC LIDAR (AOL) FLIGHT MISSION PARTICIPATION Abstract Only
F. E. Hoge *In its* Laboratory for Oceans 1988 p 95-97 (For primary document see N89-28118 22-48)
Avail: NTIS HC A12/MF A01 CSCL 20E

N89-28185*# National Aeronautics and Space Administration. Goddard Space Flight Center, Greenbelt, MD.
DIODE-PUMPED LASER RESEARCH
L. Ramos-Izquierdo, J. L. Bufton, and K. Chan *In its* Laboratory for Oceans 1988 p 249-252 (For primary document see N89-28118 22-48)
Avail: NTIS HC A12/MF A01 CSCL 20E

N89-28186*# National Aeronautics and Space Administration. Goddard Space Flight Center, Greenbelt, MD.
LARGE APERTURE SCANNING AIRBORNE LIDAR Abstract Only
J. Smith, R. Bindschadler, R. Boers, J. L. Bufton, D. Clem, J. Garvin, and S. H. Melfi *In its* Laboratory for Oceans 1988 p 253-256 (For primary document see N89-28118 22-48)
Avail: NTIS HC A12/MF A01 CSCL 20E

N89-28187*# National Aeronautics and Space Administration. Goddard Space Flight Center, Greenbelt, MD.
A MULTIPROCESSOR AIRBORNE LIDAR DATA SYSTEM Abstract Only
C. W. Wright, S. A. Bailey, G. E. Heath, and C. R. Piazza *In its* Laboratory for Oceans 1988 p 257-259 (For primary document see N89-28118 22-48)
Avail: NTIS HC A12/MF A01 CSCL 20E

37 MECHANICAL ENGINEERING

Includes auxiliary systems (nonpower); machine elements and processes; and mechanical equipment.

N89-28014# Naval Civil Engineering Lab., Port Hueneme, CA.
DEVELOPMENT OF A LIGHTWEIGHT, HIGH STRENGTH, COLLAPSIBLE HOSE Final Technical Report, Oct. 1984 - Jun. 1988
Laurence Nixon Feb. 1989 148 p
(AD-A207292; NCEL-TN-1793) Avail: NTIS HC A07/MF A01 CSCL 13/11

An exploratory development effort to produce a 6-inch diameter, lightweight, high strength, collapsible, layflat hose using aramid yarn as the hose reinforcing material is reported. The design goals were to produce a hose with a 100,000-pound tensile strength and 1,800-psi burst pressure. The project had three phases: (1) a feasibility study, (2) manufacturing trials with a 4-inch hose, and (3) the design and fabrication of 6-inch hose on the production line. The work failed to produce the desired hose primarily because of strength losses incurred in the aramid during the manufacturing process. However, the project did produce a relatively high performance polyester reinforced hose (47,000-pound tensile strength) that may have applications for fuel transfer. GRA

N89-28015*# National Aeronautics and Space Administration. Lewis Research Center, Cleveland, OH.
TOPOLOGY OF MODIFIED HELICAL GEARS
F. L. Litvin, J. Zhang, R. F. Handschuh (Army Aviation Systems Command, Cleveland, OH.), and J. J. Coy 1989 21 p Presented at the 5th International Power Transmission and Gearing Conference, Chicago, IL, 24-27 Apr. 1989; sponsored by the ASME
(DA Proj. 1L1-62209-A-47-A)
(NASA-TM-102134; E-4054; NAS 1.15:102134; AVSCOM-TR-89-C-004) Avail: NTIS HC A03/MF A01 CSCL 13I

The topology of several types of modified surfaces of helical gears is proposed. The modified surfaces allow absorption of a

linear or almost linear function of transmission errors. These errors are caused by gear misalignment and an improvement of the contact of gear tooth surfaces. Principles and corresponding programs for computer aided simulation of meshing and contact of gears have been developed. The results of this investigation are illustrated with numerical examples. Author

N89-28016*# Catholic Univ. of America, Washington, DC. Dept. of Electrical Engineering.
JOINT-SPACE ADAPTIVE CONTROL OF A 6 DOF END-EFFECTOR WITH CLOSED-KINEMATIC CHAIN MECHANISM
Charles C. Nguyen and Zhen-Lei Zhou Aug. 1989 16 p
(Grant NAG5-780)
(NASA-CR-185861; NAS 1.26:185861) Avail: NTIS HC A03/MF A01 CSCL 13I

The development is presented for a joint-space adaptive scheme that controls the joint position of a six-degree-of-freedom (DOF) robot end-effector performing fine and precise motion within a very limited workspace. The end-effector was built to study autonomous assembly of NASA hardware in space. The design of the adaptive controller is based on the concept of model reference adaptive control (MRAC) and Lyapunov direct method. In the development, it is assumed that the end-effector performs slowly varying motion. Computer simulation is performed to investigate the performance of the developed control scheme on position control of the end-effector. Simulation results manifest that the adaptive control scheme provides excellent tracking of several test paths. Author

N89-28017*# Catholic Univ. of America, Washington, DC. Dept. of Electrical Engineering.
DESIGN OF AN ADAPTIVE CONTROLLER FOR A TELEROBOT MANIPULATOR Semiannual Technical Report
Charles C. Nguyen and Zhen-Lei Zhou Aug. 1989 14 p
(Grant NAG5-1124)
(NASA-CR-185863; NAS 1.26:185863) Avail: NTIS HC A03/MF A01 CSCL 13I

The design of a joint-space adaptive control scheme is presented for controlling the slave arm motion of a dual-arm telerobot system developed at Goddard Space Flight Center (GSFC) to study telerobotic operations in space. Each slave arm of the dual-arm system is a kinematically redundant manipulator with 7 degrees of freedom (DOF). Using the concept of model reference adaptive control (MRAC) and Lyapunov direct method, an adatation algorithm is derived which adjusts the PD controller gains of the control scheme. The development of the adaptive control scheme assumes that the slave arm motion is non-compliant and slowly-varying. The implementation of the derived control scheme does not need the computation of the manipulator dynamics, which makes the control scheme sufficiently fast for real-time applications. Computer simulation study performed for the 7-DOF slave arm shows that the developed control scheme can efficiently adapt to sudden change in payloads while tracking various test trajectories such as ramp or sinusoids with negligible position errors. Author

N89-28018# Massachusetts Inst. of Tech., Cambridge. Artificial Intelligence Lab.
DESIGN CONSIDERATIONS FOR AN EARTH BASED FLEXIBLE ROBOTIC SYSTEM
Andrew D. Christian and Warren P. Seering Apr. 1989 18 p
(Contract N00014-86-K-0685)
(AD-A209635; AI-M-1115) Avail: NTIS HC A03/MF A01 CSCL 12/9

Insights are provided into the problems of designing a robot with joint and link flexibility. The relationship between the deflection of the robot under gravity is correlated with the fundamental frequency of vibration. Different types of link geometry are considered and the flexibility potential of different materials are evaluated. Some general conclusions and guidelines for constructing a flexible robot are given. GRA

N89-28019# Stanford Univ., CA. Dept. of Computer Science.
ROBOT MOTION PLANNING: A DISTRIBUTED REPRESENTATION APPROACH
Jerome Barraquand and Jean-Claude Latombe May 1989 57 p
(Contracts DAAA21-89-C-0002; N00014-88-K-0620)
(AD-A209890; SU-STAN-CS-89-1257) Avail: NTIS HC A04/MF A01 CSCL 12/9

In this paper, we propose a new approach for planning the motion of robotic systems among obstacles, which is based on a distributed representation of the world model. Within this approach, we designed and implemented a general purpose path planner with five new capabilities: (1) It is able to generate very complex motions for robots with many degrees of freedom. In particular, we succeeded in generating complex paths for a 10 DOF non-serial manipulator arm made with both revolute and prismatic joints. (2) It is drastically faster (between 1 and 2 orders of magnitude) than existing systems on a sequential computer. We generated complex paths for a 3 DOF bar in a 2D workspace in about 1 second on a MIPS-based workstations, as opposed to minutes or even tens of minutes for other algorithms. The planner outputs a path for the robot in configuration space, while the goal is specified in operational space. Hence, the inverse kinematic problem is completely avoided. Furthermore, any kind of redundancy of the robot arms can be handled without modification. GRA

N89-28020# Massachusetts Inst. of Tech., Cambridge. Lab. for Manufacturing and Productivity.
FUNDAMENTAL MECHANISMS OF TRIBOLOGY AND THEIR IMPLICATIONS Final Technical Report, 1 May 1982 - 31 Jan. 1986
Nam P. Suh, Nannaji Saka, and Kyriakos Komvopoulos 30 May 1989 75 p
(Contract N00014-82-K-0520)
(AD-A209941) Avail: NTIS HC A04/MF A01 CSCL 11/8

The objective of the proposed research was to create hard layers on metallic surfaces in boundary-lubricated sliding and to investigate their tribological behavior. In addition, the goal was to investigate the basic mechanism of friction of lubricated metallic surfaces. We have investigated the following aspects: (1) experimental investigation of the tribological behavior of metallic and coated surfaces in boundary lubrication, and (2) finite element analysis of friction and wear of the coated surfaces, and the delamination process at the interface. GRA

N89-28021# Cornell Univ., Ithaca, NY. Dept. of Computer Science.
GENERIC SINGULARITIES OF ROBOT MANIPULATORS
Dinesh K. Pai and M. C. Leu 1988 7 p Prepared in cooperation with New Jersey Inst. of Technology
(Contracts N00014-88-K-0591; N00014-86-K-0281; NSF MSM-84-51074; NSF DMS-86-17355)
(AD-A210116) Avail: NTIS HC A02/MF A01 CSCL 12/9

The singularities of the differential kinematic map, i.e., of the manipulator Jacobian, are considered. We first examine the notion of a generic kinematic map, whose singularities form smooth manifolds of prescribed dimension in the joint space of the manipulator. For 3-joint robots, an equivalent condition for genericity using determinants is derived. The condition lends itself to symbolic computation and is sufficient for the study of decoupled manipulators, i.e., manipulators which can be separated into a 3-joint translating part and a 3-joint orienting part. The results are illustrated by analyzing the singularities of two classes of 3-joint positioning robots. GRA

38 QUALITY ASSURANCE AND RELIABILITY

Includes product sampling procedures and techniques; and quality control.

N89-28022# University of Southern California, Los Angeles. Dept. of Electrical Engineering.
BASIC RESEARCH IN RELIABILITY FOR REAL SYSTEMS Final Technical Report, 15 Jul. 1986 - 14 Jul. 1988
Victor O. Li 5 Aug. 1988 6 p
(Grant AF-AFOSR-0269-84; AF Proj. 2304)
(AD-A209649; AFOSR-89-0783TR) Avail: NTIS HC A02/MF A01 CSCL 12/7

The goal of this research is to develop practical models and efficient algorithms to analyze the reliability, availability and maintainability of complex systems in which component failures are statistically dependent and each component is subject to degradations before complete failure. The Event-Based Reliability Model (EBRM) was developed to model and analyze the reliability of a network in which component failures are statistically dependent. In EBRM, the events that could cause component failures were modeled explicitly. This approach required much fewer parameters than the traditional model employing conditional probabilities. The EBRM was also proved to be a completely general model which could be applied to various types of failure dependencies. For reliability evaluations, many existing algorithms for computing network reliability could be used with minor modifications and no significant increase in computational complexity. An improved algorithm for the approximate evaluation of network performance was also developed. For multi-state systems, ordered enumeration was used to approximate and bound system reliabilities and other performance measures, and an efficient algorithm was developed for this purpose. The author has been studying network management algorithms which are resilient to network failures. GRA

N89-28023# Illinois Univ., Chicago. Dept. of Mathematics Statistics and Computer Science.
DESIGN OF EXPERIMENTS AND RELIABILITY MODELS Final Report, 1 Aug. 1985 - 31 Oct. 1988
A. S. Hedayat and E. El-Neweihi 1 May 1989 51 p
(Grant AF-AFOSR-0320-85; AF Proj. 2304)
(AD-A209880; AFOSR-89-0772TR) Avail: NTIS HC A04/MF A01 CSCL 14/2

The research in design of experiments included the following areas: (1) efficient designs for experiments involving several factors; (2) efficient designs for repeated measurements models; (3) trade off in designs; (4) flexible orthogonal arrays; (5) efficient designs for comparing test treatments with controls; and (6) designs for collecting data through sampling. The research in reliability was mainly directed to the following areas: multistate reliability models; optimal assembly of coherent systems (both in the binary and multistate cases); redundancy importance and allocation of spares in coherent systems; closure properties of classes of life distributions; and optimal inspection policies. GRA

N89-28024# Northwestern Univ., Evanston, IL. Dept. of Mechanical Engineering.
MONTE CARLO RELIABILITY ANALYSIS Final Report, 1 Jul. 1984 - 31 Dec. 1988
Elmir E. Lewis 24 Apr. 1989 8 p
(Grant AF-AFOSR-0340-84; AF Proj. 2304)
(AD-A210052; AFOSR-89-0915TR) Avail: NTIS HC A02/MF A01 CSCL 12/3

The research resulted in major improvements in Markov models to be used in Monte Carlo modeling of reliability problems. These include a number of component dependency models and modeling of unrevealed failures. A new sampling technique, the method of self-transitions, is developed for treating time dependent failure rates, and non Markovian generalizations are made to model replacement of ageing parts and as-good-as-new repair. GRA

39 STRUCTURAL MECHANICS

Includes structural element design and weight analysis; fatigue; and thermal stress.

For applications see *05 Aircraft Design, Testing and Performance* and *18 Spacecraft Design, Testing and Performance*.

N89-28025# Vibration Inst., Clarendon Hills, IL.
THE SHOCK AND VIBRATION DIGEST, VOLUME 21, NO. 4 Monthly Report
Vicki M. Pate, ed. Apr. 1989 76 p
Avail: NTIS HC A05/MF A01

Damping in Structural Joints; Recent Advances on the Dynamic Behavior of Stiffened Plates; and abstracts from current literature are presented. For individual titles, see N89-28026 through N89-28027.

N89-28026# Imperial Coll. of Science and Technology, London (England). Dept. of Mechanical Engineering.
DAMPING IN STRUCTURAL JOINTS
C. F. Beards *In* Vibration Inst., The Shock and Vibration Digest, Volume 21, No. 4 Apr. 1989 p 3-5 (For primary document see N89-28025 22-39)
Avail: NTIS HC A05/MF A01

Friction damping in joints is the major source of inherent damping in most fabricated structures. Although analysis techniques are becoming more refined, it can still be difficult to accurately predict the effect of controlled joint damping on the vibration response of a structure. The range and scope of applications in which it is desirable to provide increased joint damping continues to expand. Author

N89-28027# Indian Inst. of Tech., Kharagpur. Dept. of Naval Architecture.
RECENT ADVANCES ON THE DYNAMIC BEHAVIOR OF STIFFENED PLATES
M. Mukhopadhyay and A. Mukherjee (Indian Inst. of Tech., Bombay.) *In* Vibration Inst., The Shock and Vibration Digest, Volume 21, No. 4 Apr. 1989 p 6-9 (For primary document see N89-28025 22-39)
Avail: NTIS HC A05/MF A01

A continuation of a survey published in 1986 reviews the literature after mid-1985 on the dynamic behavior of stiffened plates. It caters to all aspects of dynamic behavior -- free vibration, forced vibration, random vibration and experimental investigations. Author

N89-28028# Naval Research Lab., Washington, DC. Condensed Matter and Radiation Sciences Div.
THE INADEQUACIES OF DAMAGE ENERGY AS A MEASURE OF DISPLACEMENT DAMAGE Interim Report
George P. Mueller 10 Apr. 1989 29 p
(AD-A207376; NRL-MR-6443) Avail: NTIS HC A03/MF A01 CSCL 07/4

The Lindhard, Nielson, Scharff and Thompson equations for the partitioning of an ion's energy into electronic and damage portions are widely used to estimate the number of displacements produced in a solid by an impinging ion. The LNST approach was extended by including a displacement energy at all stages of the calculation, which allows the formation an integral equation that yields the number of displacements Nv(E) directly, rather than estimating it from the damage energy D(E). The results are compared with both the LNST approach and with the collision simulation code MARLOWE. The approach is found to approximate the MARLOWE results reasonably well, but the the damage energy is a poor estimator of displacement damage, because Nv(E) and D(E) have different dependencies on the interatomic potential and on the low energy portion of the inelastic loss function. GRA

N89-28029*# National Aeronautics and Space Administration. Lewis Research Center, Cleveland, OH.
A DATA ACQUISITION AND CONTROL PROGRAM FOR AXIAL-TORSIONAL FATIGUE TESTING

Sreeramesh Kalluri and Peter J. Bonacuse (Army Aviation Systems Command, Cleveland, OH.) May 1989 23 p Presented at the Symposium on the Applications of Automation Technology to Fatigue and Fracture Testing, Kansas City, MO, 22-23 May 1989; sponsored in part by the American Society for Testing and Materials Prepared in cooperation with Army Aviation Systems Command, Cleveland, OH
(NASA-TM-102041; E-4790; NAS 1.15:102041; AVSCOM-TR-89-C-002) Avail: NTIS HC A03/MF A01 CSCL 20K

A computer program was developed for data acquisition and control of axial-torsional fatigue experiments. The multitasked, interrupt-driven program was written in Pascal and Assembly. This program is capable of dual-channel control and six-channel data acquisition. It can be utilized to perform inphase and out-of-phase axial-torsional isothermal fatigue or deformation experiments. The program was successfully used to conduct inphase axial-torsional fatigue experiments on 304 stainless steel at room temperature and on Hastelloy X at 800 C. The details of the software and some of the results generated to date are presented. Author

N89-28030*# National Aeronautics and Space Administration. Lewis Research Center, Cleveland, OH.
PROBABILISTIC STRUCTURAL ANALYSIS METHODS OF HOT ENGINE STRUCTURES
C. C. Chamis and D. A. Hopkins Jun. 1989 17 p Presented at the 34th International Gas Turbine and Aeroengine Congress and Exposition, Toronto, Ontario, 4-8 Jun. 1989; sponsored in part by ASME
(NASA-TM-102091; E-4855; NAS 1.15:102091) Avail: NTIS HC A03/MF A01 CSCL 20K

Development of probabilistic structural analysis methods for hot engine structures at Lewis Research Center is presented. Three elements of the research program are: (1) composite load spectra methodology; (2) probabilistic structural analysis methodology; and (3) probabilistic structural analysis application. Recent progress includes: (1) quantification of the effects of uncertainties for several variables on high pressure fuel turbopump (HPFT) turbine blade temperature, pressure, and torque of the space shuttle main engine (SSME); (2) the evaluation of the cumulative distribution function for various structural response variables based on assumed uncertainties in primitive structural variables; and (3) evaluation of the failure probability. Collectively, the results demonstrate that the structural durability of hot engine structural components can be effectively evaluated in a formal probabilistic/reliability framework. Author

N89-28031# Oak Ridge National Lab., TN.
THE SIGMAJIG: AN IMPROVED HOT-CRACKING TEST
Gene M. Goodwin 1989 4 p Presented at the International Congress on Technology and Technology Exchange, New York, NY, 28 Jun. 1989 Sponsored in part by Martin Marietta Energy Systems, Inc.
(Contract DE-AC05-84OR-21400)
(DE89-013029; CONF-8906135-1) Avail: NTIS HC A02/MF A01

This report covers the newly developed Sigmajig test system. This system when combined with a gas tungsten arc provides a method to test weldability for the evaluation of hot cracking sensitivity. Initial use has been with thin sheet (0.2 to 1.5 mm) although there is no inherent thickness limitation. DOE

N89-28032# Sandia National Labs., Albuquerque, NM.
THERMAL STRAINS IN A BIMATERIAL JOINT: EXPERIMENTAL AND NUMERICAL ANALYSIS
J. D. Wood, M. Y. Tsai, D. Post, J. Morton, V. J. Parks (Catholic Univ. of America, Washington, DC.), and F. P. Gerstle, Jr. 1989 9 p Presented at the SEM Spring Meeting, Cambridge, MA, 28 May 1989
(Contracts DE-AC04-76DP-00789; SNL-75-8962; N00014-86-K-0799)
(DE89-013935; SAND-89-0815C; CONF-8905107-4) Avail: NTIS HC A02/MF A01

A comprehensive stress analysis was performed for a bimaterial plate subjected to a uniform change of temperature. The steel and brass portions of the specimen were bonded along a common edge. Whole-field measurements were made by high-sensitivity moire interferometry. A companion finite element numerical analysis of a similar body was conducted to help interpret the experimental results. The experiments documented a strong free-edge effect along the entire perimeter of the joint, an effect akin to a line singularity along the perimeter. High stresses in the edge-effected zone were determined from measurements, and enormous stress gradients were deduced by analysis. The largest stresses were found at the corner, where two edge-effected zones intersected. DOE

N89-28033# International Centre for Theoretical Physics, Trieste (Italy).
SOLITON BEHAVIOUR OF CRACK PROPAGATION IN BRITTLE MATERIALS
Tong Hu Oct. 1988 7 p Submitted for publication
(DE89-612190; IC-88/350) Avail: NTIS (US Sales Only) HC A02/MF A01

An equation is given to describe the process of crack propagation with high speed in brittle materials. According to this equation, it was found that a soliton behavior occurs when the crack propagates with high speeds. This result will provide a new method to calculate many problems of crack propagation with high speed in brittle materials. DOE

N89-28034*# National Aeronautics and Space Administration. Ames Research Center, Moffett Field, CA.
EVALUATION OF A STRAIN-GAGE LOAD CALIBRATION ON A LOW-ASPECT-RATIO WING STRUCTURE AT ELEVATED TEMPERATURE
Lawrence F. Reardon Jun. 1989 39 p
(NASA-TP-2921; H-1331; NAS 1.60:2921) Avail: NTIS HC A03/MF A01 CSCL 20K

The environmental aspect of elevated temperature and its relationship to the science of strain gage calibrations of aircraft structures are addressed. A section of a wing designed for a high-speed aircraft structure was used to study this problem. This structure was instrumented with strain gages calibrated at both elevated and room temperatures. Load equations derived from a high-temperature load calibration were compared with equations derived from an identical load calibration at room temperature. The implications of the high temperature load calibration were studied from the viewpoint of applicability and necessity. Load equations derived from the room temperature load calibration resulted in generally lower equation standard errors than equations derived from the elevated temperature load calibration. A distributed load was applied to the structure at elevated temperature and strain gage outputs were measured. This applied load was then calculated using equations derived from both the room temperature and elevated temperature calibration data. It was found that no significant differences between the two equation systems existed in terms of computing this applied distributed load, as long as the thermal shifts resulting from thermal stresses could be identified. This identification requires a heating of the structure. Therefore, it is concluded that for this structure, a high temperature load calibration is not required. However, a heating of the structure is required to determine thermal shifts. Author

N89-28035*# National Aeronautics and Space Administration. Langley Research Center, Hampton, VA.
RESEARCH AND TECHNOLOGY PLANS FOR FY 1989 AND ACCOMPLISHMENTS FOR FY 1988
Kay S. Bales Apr. 1989 95 p
(NASA-TM-101592; NAS 1.15:101592) Avail: NTIS HC A05/MF A01 CSCL 20K

The Objectives, FY 1989 Plans, Approach, and FY 1989 Milestones for the Structural Mechanics Division's research programs are presented. Fiscal year 1988 Accomplishments are presented where applicable. This information is useful in program

coordination with other governmental organizations in areas of mutual interest. Author

N89-28036*# National Aeronautics and Space Administration. Lewis Research Center, Cleveland, OH.
REFINEMENTS IN A VISCOPLASTIC MODEL
A. D. Freed and K. P. Walker (Engineering Science Software, Inc., Smithfield, RI.) 1989 18 p Prepared for presentation at the Winter Annual Meeting of the American Society of Mechanical Engineers, San Francisco, CA, 10-15 Dec. 1989
(NASA-TM-102338; E-4988; NAS 1.15:102338) Avail: NTIS HC A03/MF A01 CSCL 20K

A thermodynamically admissible theory of viscoplasticity with two internal variables (a back stress and a drag strength) is presented. Six material functions characterize a specific viscoplastic model. In the pursuit of compromise between accuracy and simplicity, a model is developed that is a hybrid of two existing viscoplastic models. A limited number of applications of the model to Al, Cu, and Ni are presented. A novel implicit integration method is also discussed. Applications are made to obtain solutions using this viscoplastic model. Author

N89-28037# Institut National Polytechnique, Grenoble (France). Lab. de Genie Physique et Mecanique des Materiaux.
MECHANICAL AND PHYSICAL STUDY OF THE BEHAVIOR UNDER SEQUENTIAL LOADS OF COPPER AND STEEL PLATES Ph.D. Thesis [ETUDE MECANIQUE ET PHYSIQUE DU COMPORTEMENT EN SOLLICITATIONS SEQUENTIELLES DE TOLES D'ACIER ET DE CUIVRE]
En Lai Shen (Shanghai Polytechnic Univ., China) 1988 311 p In FRENCH
(ETN-89-94805) Avail: NTIS HC A14/MF A01

The behavior of mild steel and pure copper thin plates under sequential loading is studied. A macroscopic model is developed and a Hill criterion is identified to define a mode and a predeformation rate in agreement with the experimental results. The copper anisotropic macroscopic model does not describe correctly the behavior found in experiments. Further development of the presented models is discussed. ESA

N89-28038# Sandia National Labs., Albuquerque, NM.
DISCRETE ENFORCEMENT OF UNCERTAIN OSCILLATOR GAUSSIAN RESPONSE
Linda J. Branstetter and Garrett D. Jeong (Purdue Univ., West Lafayette, IN.) 1989 8 p Presented at the 5th International Conference on Structural Safety and Reliability, San Francisco, CA, 8 Aug. 1989
(Contract DE-AC04-76DP-00789)
(DE89-005595; SAND-88-1304C; CONF-890835-1) Avail: NTIS HC A02/MF A01

A limited number of step-by-step procedures were developed to recursively evaluate the response moments of uncertain systems. In several of these procedures, the recursive evaluation depends on discrete enforcement of a Gaussian approximation to the displacement and velocity response random processes. The error associated with such an approximation is isolated for a simple system using an analytic method which is not itself approximate in the manner of perturbation or Monte Carlo approaches. DOE

N89-28039# Sandia National Labs., Albuquerque, NM.
MODEL BASED DAMPING OF COUPLED HORIZONTAL AND VERTICAL OSCILLATIONS IN A FLEXIBLE ROD
B. J. Petterson and R. D. Robinett 1989 24 p Presented at the Guidance, Navigation, and Control Conference, Boston, MA, 14 Aug. 1989
(Contract DE-AC04-76DP-00789)
(DE89-007034; SAND-88-2876C; CONF-890818-3) Avail: NTIS HC A03/MF A01

The theory associated with vibrations of angularly accelerated cantilevered beams which display significant gravitational sag (coupling the out-of-plane dynamics of the flexible beam) is reviewed and a control approach is formulated for moving such beams to damp residual first horizontal and vertical modes of oscillation. An experimental implementation of the control strategy using an open-loop, single axis torque that is shaped for simultaneous damping of the horizontal and vertical vibrations is described. The experimental control strategy demonstrates more than 99 percent reduction in the coupled residual vibrations. DOE

N89-28040# New Jersey Inst. of Tech., Newark. Office of Sponsored Projects.
PLASTIC DEFORMATION OF GRANULAR MATERIALS Final Report, 1 Apr. 1988 - 31 Mar. 1989
E. Bruce Pitman (Minnesota Univ., Minneapolis.) 31 Mar. 1989 11 p
(Grant AF-AFOSR-0182-88; AF Proj. 2304)
(AD-A208589; AFOSR-89-0723TR) Avail: NTIS HC A02/MF A01 CSCL 07/4

The deformation of granular materials occurs in a variety of applications: soil dynamics; avalanch flows; and grain flow in bins. The goal in this project is to develop a more complete understanding of the mechanics of granular flow. The project consists of two distinct but related phases. One phase is a study of the mathematical structure of constitutive relations used to model the granular medium. The research here is primarily concerned with the stability and well posedness of the evolution equations governing flow. Most of the efforts have concentrated on the Critical State Theory of Soil Mechanics, a mathematically attractive theory which has some success in modeling soil deformations. In particular, the Critical State Theory is reasonably successful at modeling the deformation of so called Cam clay , a type of clay tested by the Cambridge soil mechanics group in the late 1950's. GRA

N89-28041# Carnegie-Mellon Univ., Pittsburgh, PA.
NON-LINEAR DYNAMICS AND CHAOTIC MOTIONS IN FEEDBACK CONTROLLED ELASTIC SYSTEM Final Report, 1 Dec. 1983 - 30 Sep. 1988
1988 9 p
(Grant AF-AFOSR-0051-84; AF Proj. 2304)
(AD-A208628; AFOSR-89-0725TR) Avail: NTIS HC A02/MF A01 CSCL 20/11

Work was continued on the global dynamics and bifurcations of O(2) symmetric ODEs. Such systems are obtained as finite dimensional projections or reductions of spatially translation- and reflection-invariant PDE S, for example. In 1987/88, partially supported by this grant, a complete analysis was provided for the heteroclinic cycles and modulated travelling waves in two mode (k:2K) interacting systems. In particular, it was pointed out that heteroclinic cycles are structurally stable features in such systems. GRA

N89-28042# Georgetown Univ., Washington, DC. Dept. of Mathematics.
STUDIES IN STABILIZATION AND CONTROL OF BEAMS AND PLATES Final Report, 1 Jun. 1986 - 31 Aug. 1988
John E. Lagnese 31 Aug. 1988 3 p
(Grant AF-AFOSR-0162-86; AF Proj. 2304)
(AD-A208635; AFOSR-89-0726TR) Avail: NTIS HC A02/MF A01 CSCL 13/13

The principal achievement of the research undertaken under this grant was the development of comprehensive theories of exact controllability and stabilization of thin plate dynamics by means of forces and moments applied on the edge of the plate, based on continuum models of plates. Two major research monographs, which lay the foundations of the theories, were written. The motivation for this study, and its ultimate goal, is the design and analysis of practical strategies for active control and vibration suppression in flexible structures. A second, related, area of research was the design of feedback controls acting on the edge of the plate which uniformly stabilize plate motion, i.e, which cause all of the modes to decay at some uniform rate. Once again, such control strategies were sought for a wide variety of plate models, including nonlinear models. In fact, our results for nonlinear

models (in which the nonlinearities may be both in the dynamics and in the feedback control) are probably the first of their kind. GRA

N89-28043# Rhode Island Univ., Kingston. Solid Mechanics Lab.
PROBABILISTIC DESCRIPTION OF FATIGUE CRACK GROWTH UNDER CONSTANT-AND VARIABLE-AMPLITUDE LOADING Final Report, 16 Sep. 1985 - 15 Nov. 1988
H. Ghonem and M. Zeng Mar. 1989 188 p
(Grant AF-AFOSR-0362-85; AF Proj. 2302)
(AD-A208717; URI-MSL-891; AFOSR-89-0716TR) Avail: NTIS HC A09/MF A01 CSCL 11/6

This report is concerned with the description of the development and application of a stochastic crack growth model. It is built as a discontinuous Markov process and is inhomogeneous with respect to the number of cycles required for the crack to reach a specified crack length. The model is then used to describe the evolution of the crack length in terms of growth curves, each of whose points possess equal probability of advancing from one position to another forward position. The validity of the model is established by applying it to constant as well as to variable amplitude loading. In those applications the theoretical constant probability crack growth curves generated by the model compared to those experimentally obtained using Al 7075-T6 and Al 2024-T3 material for constant-amplitude loading while Ti-6Al-4V was used in single overload application. Results of these comparisons indicate the ability of the proposed model when fitted with parameters whose values can be obtained from a limited numbers of experimental tests, to predict the crack growth statistics under different loading conditions. GRA

N89-28044# Materials Research Labs., Ascot Vale (Australia).
STRESS INTENSITY CALIBRATION OF A RING SPECIMEN USING A FINITE ELEMENT TECHNIQUE
G. Clark and T. V. Rose Jan. 1989 29 p
(AD-A208878; MRL-TN-549; DODA-AR-005-679) Avail: NTIS HC A03/MF A01 CSCL 12/5

A finite element technique has been used to determine the stress intensity at the tip of a bore crack in a cylindrical fracture specimen. This technical note describes the detailed input for the computer programs which perform the stress analyses. Much of the preparatory work involves generating a suitable mesh of elements which represents the elastic properties of the specimen. The constraints which are imposed on the mesh geometry are described. GRA

N89-28045# Naval Research Lab., Washington, DC. Physical Acoustics Branch.
ANALYSIS OF A LIMITING-AMPLITUDE PROBLEM IN ACOUSTO-ELASTIC INTERACTIONS, 1 Interim Report
Allan G. Dallas 15 May 1989 63 p
(AD-A209741; NRL-9172-1) Avail: NTIS HC A04/MF A01 CSCL 20/11

Time-harmonic scattering and radiation by an elastic body into an inviscid fluid is studied as a problem of limiting amplitude. By supposing that all is known about the exterior Neumann-radiation problem and a certain interior traction eigenvalue problem, the interface problem is reduced to an interior one with a nonlocal boundary condition, which is shown to be well-posed in weak sense, modulo the satisfaction of a solvability condition. The convergence of a solution-approximating Galerkin procedure is established. It is shown that the acoustic field can be computed without examining the mentioned eigenvalue problem. GRA

N89-28046# Johns Hopkins Univ., Baltimore, MD. Dept. of Mechanical Engineering.
DYNAMIC FRACTURE TOUGHNESS TESTING Final Report, 1 Sep. 1985 - 28 Feb. 1989
W. N. Sharpe, Jr. and A. S. Douglas 15 May 1989 6 p
(Contract DAAG29-85-K-0218)
(AD-A209948; ARO-22684.3-EG) Avail: NTIS HC A02/MF A01 CSCL 11/6

An optical technique for measuring the Crack-Tip Opening Displacement (CTOD) of pre-cracked three-point bend specimens subjected to impact loading was developed. Procedures for computing a dynamic Load-CTOD plot were also developed; this enables one to determine the dynamic fracture toughness. Finite element analyses were used to verify and extend the procedures. GRA

42 GEOSCIENCES (GENERAL)

No abstracts in this category.

43 EARTH RESOURCES AND REMOTE SENSING

Includes remote sensing of earth resources by aircraft and spacecraft; photogrammetry; and aerial photography.

For instrumentation see *35 Instrumentation and Photography.*

N89-28047*# State Univ. of New York, Binghamton. Dept. of Geological Sciences.
LITHOLOGIC MAPPING OF MAFIC INTRUSIONS IN EAST GREENLAND USING LANDSAT THEMATIC MAPPER DATA Final Report
H. Richard Naslund, R. W. Birnie, and J. T. Parr (Analytic Sciences Corp., Reading, MA.) 24 Apr. 1989 63 p Original contains color illustrations
(Contract NAS5-28738)
(NASA-CR-183440; NAS 1.26:183440) Avail: NTIS HC A01/MF A01 CSCL 08B

The East Greenland Tertiary Igneous Province contains a variety of intrusive and extrusive rock types. The Skaergaard complex is the most well known of the intrusive centers. Landsat thematic mapping (TM) was used in conjunction with field spectrometer data to map these mafic intrusions. These intrusions are of interest as possible precious metal ore deposits. They are spectrally distinct from the surrounding Precambrian gneisses. However, subpixel contamination by snow, oxide surface coatings, lichen cover and severe topography limit the discrimination of lithologic units within the gabbro. Imagery of the Skaergaard and surrounding vicinity, and image processing and enhancement techniques are presented. Student theses and other publications resulting from this work are also listed. K.C.D.

N89-28048# Instituto de Pesquisas Espaciais, Sao Jose dos Campos (Brazil). Dept. de Processamento de Imagens-DPI.
THE USE OF DIGITAL ELEVATION MODEL FOR CORRECTING THE EFFECTS OF PROJECTIONS IN REFORRESTATIONS OF EUCALYPTUS IN MOUNTAINOUS REGIONS [USO DE MODELO DIGITAL DE ELEVACAO PARA CORRIGIR O EFEITO DO RELEVO EM REFLORESTAMENTO DE EUCALYPTUS EM REGIOES MONTANHOSAS]
Luiz Alberto VieiraDias, Flavio Jorge Ponzoni, and Eni AlvimdeOliveira Dec. 1988 8 p In PORTUGUESE; ENGLISH summary Presented at the 5th Brazilian Symposium on Remote Sensing, Natal, RN, 11-15 Oct. 1988
(INPE-4763-PRE/1432) Avail: NTIS HC A02/MF A01

The radiance arriving to a remote sensing satellite depends on the target illumination and reflection, and on the angles between: the terrain normal and the illuminating source, and the satellite sensor. For reforestations in mountainous regions the illumination angles are a prime factor. It is assumed that the forest reflection is Lambertian. The inclinations were obtained from a Digital Elevation Model of the area. The LANDSAT TM channels used were 3, 4 and 5, and the region was classified taking and not

taking into account the terrain relief effect. A maximum likelihood classification has shown better results in the corrected image.
Author

N89-28049# Instituto de Pesquisas Espaciais, Sao Jose dos Campos (Brazil).
AUTOMATIC CHANGE IN CONTOUR DIAGRAMS ON THE OCCASION OF SCALE REDUCTION USING A MATERIAL MORPHOLOGY [MUDANCA AUTOMATICA NO TRACADO DE CONTORNOS POR OCASIAO DE REDUCAO DE ESCALA UTILIZANDO A MORFOLOGIA MATEMATICA]
Fernando Augusto Mit li, Luiz Alberto VieiraDias, Julio Cesar LimadAlge, and Junior Barrera Dec. 1988 8 p In PORTUGUESE; ENGLISH summary Presented at the 5th Brazilian Symposium on Remote Sensing, Natal, RN, 11-15 Oct. 1988
(INPE-4769-PRE/1438) Avail: NTIS HC A02/MF A01

As the map is a reduced representation of the topographic surface, the scale of the map determines the amount of information which can be shown. The consequence of scale reduction is generalization: the smaller the scale the greater the degree of generalization. An automatic solution is proposed based on the Mathematical Morphology operations of erosion and dilation. Using the SITIM, INPE's image processing system, an example of automatic scale reduction from 1:50,000 to 1:250,000 of a portion of Ilha Grande (RJ) is presented and compared to the existing topographic map.
Author

N89-28050# Instituto de Pesquisas Espaciais, Sao Jose dos Campos (Brazil).
THE USE OF EDGE DETECTORS BASED ON MATHEMATICAL MORPHOLOGY IN REMOTE SENSING IMAGERY
Erivaldo A. daSilva and Nelson D. A. Mascarenhas Dec. 1988 11 p In PORTUGUESE; ENGLISH summary Presented at the 5th Brazilian Symposium on Remote Sensing, Brazil, 11-15 Oct. 1988
(INPE-4777-PRE/1446) Avail: NTIS HC A03/MF A01

The edge detection problem has great importance in digital image processing. A large number of such detectors have been proposed in the literature. Recently, the theory of mathematical morphology was used as the basis for the proposal of new edge detectors. This work tests the use of one of these detectors on LANDSAT TM satellite images and compares its performance with a detector based on a digital approximation of the gradient.
Author

N89-28051# Instituto de Pesquisas Espaciais, Sao Jose dos Campos (Brazil).
REPORT OF THE PROJECT ESTIMA, PHASE 2: LANDSAT-TM DATA AND AGROMETEOROLOGY IN CROP YIELD ESTIMATION OF WHEAT AT THE FARM LEVEL [RELATORIO DA FASE II DO PROJETO ESTIMA - DADOS LANDSAT-TM E AGROMETEOROLOGICOS NA ESTIMATIVA DA PRODUTIVIDADE DA CULTURA DO TRIGO AO NIVEL DE PROPRIEDADES RURAIS]
Bernardo Friedrich T Rudorff and Getulio Teixeira Batista May 1989 45 p In PORTUGUESE; ENGLISH summary Sponsored by Banco de Brazil
(INPE-4782-RPE/582-Phase-2) Avail: NTIS HC A03/MF A01

Wheat plays an important role in the Brazilian commodity production. Therefore, objective and reliable methods for yield estimation are needed, especially at the farm level where several management actions have to be taken. LANDSAT TM and agrometeorological data were integrated in order to obtain a model for wheat yield estimation at the farm level for a test site in the southwest of Sao Paulo State. LANDSAT data for the crop years of 1986 (three acquisitions) and 1987 (two acquisitions), agronomic and meteorological data were related to yield estimates at the field level (250 fields, approximately). Results have shown that vegetation index derived from LANDSAT TM explained 64 and 46 percent of wheat yield variability for the two crop year analyzed. The joint use of both vegetation index and agrometeorological data in a single model improved the results to 71 and 53 percent, respectively, for the crop year of 86 and 87. The proposed model is to be validated for future crop seasons. Nevertheless it provided objective and accurate results for wheat estimation on the two crop seasons analyzed.
Author

N89-28052# Montana State Univ., Bozeman. Dept. of C/AE.
EVALUATION OF NEW THERMOMECHANICAL CONSTITUTIVE THEORY FOR SNOW Final Report
R. L. Brown Feb. 1989 48 p
Avail: NTIS HC A03/MF A01

The thermomechanical properties of snow have been described in terms of microstructural processes. The constitutive theory was formulated in a form consistent with the second law of thermodynamics. The deformation was described in terms of such microstructural processes as pressure sintering, shearing deformations within the necks connecting the ice grains, and intergranular glide. The matrix material (ice) was modeled as an elastic-viscoplastic material such that transient response as well as steady state response to loading can be described. The formulation also has the ability to describe the development of material anisotropy which evolves as a result of sustained deformation. In conjunction with this, an experimental technique was developed to enable one to measure the change in the microstructure of the material due to deformation. This had to be done in order to determine if the constitutive theory was correctly describing the microstructural deformation processes. This technique involved the use of an image analysis system to quantitatively determine the important microstructural processes (grain size, pore size, neck length, bond radius, bonds/grain). Computer software had to be developed in order to automate the process as much as possible. Finally the changes in microstructure due to thermal effects were studied.
Author

N89-28053# Massachusetts Inst. of Tech., Cambridge. Marine Industry Collegium.
SATELLITE IMAGE ANALYSIS FOR MARINE APPLICATIONS Opportunity Brief
John Moore, Jr., ed. 9 Mar. 1989 24 p Presented at the MIT/Marine Industry Colleguim, Cambridge, MA, 9 Mar. 1989
(Grant NOAA-NA86AA-D-SG089)
(PB89-187330; MITSG-89-3; OPPORTUNITY BRIEF-53) Avail: NTIS HC A03/MF A01 CSCL 08C

The presentations included in the workshop are: Acquisition of environmental satellite data; NOAA satellite data availability; intelligent browsing of image data; data assimilation studies with models of ocean circulation; industry data needs through the 1990s and beyond; and remarks on future satellite and data systems.
GRA

N89-28054# Los Alamos National Lab., NM.
MAGNETOPAUSE STRUCTURE AND DYNAMICS: ISSUES FOR GEM
R. C. Elphic 1989 18 p Presented at the 1st Geospace Environment Modeling (GEM) Workshop, San Diego, CA, 19-21 Feb. 1989
(Contract NAG5-536; NAGw-1663; W-7405-eng-36)
(DE89-012620; LA-UR-89-1595; CONF-8902115-1) Avail: NTIS HC A03/MF A01

Recent multi-spacecraft observations of the magnetopause have allowed us to establish its structure and dynamical behavior. The magnetopause current sheet is thicker than expected, often ten magnetosheath ion gyroradii or more. One very important result has been the confirmation of magnetic reconnection in both its quasi-steady and transient forms. A boundary layer of magnetosheath-like plasma is often, but not always, observed earthward of the magnetopause current layer. There is considerable small-scale magnetic structure within the current layer, suggesting the presence of filamentary currents much smaller than an ion gyroradius. Such micro-structure may be important in particle diffusion and, hence, reconnection. There are many outstanding questions, among them: How does the low latitude boundary layer form. Why is the magnetopause current layer so thick. What is the detailed structure and topology of FTEs. How are quasi-steady

and transient reconnection related. The GEM program may help us address these issues. DOE

N89-28055# European Space Agency, Paris (France).
EUROPEAN COORDINATED EFFORT FOR MONITORING THE EARTH'S ENVIRONMENT. A PILOT PROJECT CAMPAIGN ON LANDSAT THEMATIC MAPPER APPLICATIONS (1985-1987)
T. Duc Guyenne, ed. and Gianna Calabresi, ed. May 1989 350 p In ENGLISH and FRENCH Workshop held in Frascati, Italy, Dec. 1987 Original contains color illustrations
(ESA-SP-1102; ISBN-9-29-092000-9; ETN-89-95009) Copyright Avail: NTIS HC A15/MF A01; ESA Publications Div., ESTEC, Noordwijk, Netherlands, 80 Dutch guilders or 40 US dollars

In 1985 Earthnet decided to promote the use of the Thematic Mapper in Europe. A considerable volume of data received was made available to the user community to stimulate a wide range of projects. The results presented at the workshop refer to subjects which include snow cover, hydrology, coastal waters, geology, land use, forestry and cartography. For individual titles, see N89-28056 through N89-28091.

N89-28056# Innsbruck Univ. (Austria). Inst. fuer Meteorologie und Geophysik.
IMPROVED SNOW AND GLACIER MONITORING BY THE LANDSAT THEMATIC MAPPER
H. Rott and G. Markl *In* ESA, European Coordinated Effort for Monitoring the Earth's Environment. A Pilot Project Campaign on LANDSAT Thematic Mapper Applications (1985-1987) May 1989 p 3-12 Sponsored by the Austrian Fonds zur Foerderung der Wissenschaftlichen Forschung and the Oesterreichische Akademie der Wissenschaften, Vienna, Austria Original contains color illustrations (For primary document see N89-28055 22-43)
Copyright Avail: NTIS HC A15/MF A01; ESA Publications Div., ESTEC, Noordwijk, Netherlands, 80 Dutch guilders or 40 US dollars

The significance of the improved spectral and spatial capabilities of the LANDSAT Thematic Mapper (TM) are investigated. Digital methods are applied for snow mapping in two drainage basins of the Austrian Alps using spectral ratios of the TM bands 3 and 5 for the compensation of topographic effects. An algorithm is developed for estimating the snow extent in partly cloud covered scenes, based on the altitude distribution of the different surface classes in the cloud free areas. LANDSAT TM is found an excellent tool for snow mapping in Alpine drainage basins and for investigations of snow and ice areas on Alpine glaciers. ESA

N89-28057# Gesellschaft fuer Angewandte Fernerkundung, Munich (Germany, F.R.).
MULTITEMPORAL SNOW CLASSIFICATION WITH TM DATA
Ute Gangkofner *In* ESA, European Coordinated Effort for Monitoring the Earth's Environment. A Pilot Project Campaign on LANDSAT Thematic Mapper Applications (1985-1987) May 1989 p 13-21 Original contains color illustrations (For primary document see N89-28055 22-43)
Copyright Avail: NTIS HC A15/MF A01; ESA Publications Div., ESTEC, Noordwijk, Netherlands, 80 Dutch guilders or 40 US dollars

The areal extent of snow cover in an region of Austrian Alps is determined on TM images from April to July 1984, by means of supervised maximum likelihood classification. Interpretation is severely restricted by saturation: TM1 totally saturates over snow; TM2 and TM3 largely, and even TM4 saturates to some extent. Besides snow mapping, the major vegetation types in the July image are classified. TM band 5 proves to be of major importance not only for snow cloud discrimination, but also for differentiation within the snow covered area and the vegetation types. ESA

N89-28058# University Coll., Dublin (Ireland). Dept. of Computer Science.
UTILITY OF THEMATIC MAPPER DATA FOR NATIONAL SURVEY OF IRISH LAKES
B. C. Reardon and M. L. McGarrigle (An Foras Forbartha, Castlebar, Ireland) *In* ESA, European Coordinated Effort for Monitoring the Earth's Environment. A Pilot Project Campaign on LANDSAT Thematic Mapper Applications (1985-1987) May 1989 p 25-31 (For primary document see N89-28055 22-43)
Copyright Avail: NTIS HC A15/MF A01; ESA Publications Div., ESTEC, Noordwijk, Netherlands, 80 Dutch guilders or 40 US dollars

The utility of TM data with its increased number of narrower spectral bands and better spatial resolution is investigated to see whether this data is more suitable for water quality monitoring purposes. The software system used to extract lake statistics from TM data is described. Cluster analysis and Monte Carlo simulation techniques were used. In general, clusters correspond to various lake trophic states, indicating that TM data is capable of separating such characteristics. Some anomalies were noted and are discussed. Different regression curves should be used for different lake types, with clustering used to determine these groups. ESA

N89-28059# Muenster Univ. (Germany, F.R.). Dept. of Geography.
APPLICATION OF LANDSAT DATA TO HYDROLOGICAL MAPPING
Ludger Paus and Ulrich Streit *In* ESA, European Coordinated Effort for Monitoring the Earth's Environment. A Pilot Project Campaign on LANDSAT Thematic Mapper Applications (1985-1987) May 1989 p 33-39 Original contains color illustrations (For primary document see N89-28055 22-43)
Copyright Avail: NTIS HC A15/MF A01; ESA Publications Div., ESTEC, Noordwijk, Netherlands, 80 Dutch guilders or 40 US dollars

A hydrological model for estimating flood hydrographs in all subcatchments of a larger river basin is developed based on a spatial disaggregation approach. LANDSAT 5 TM data are used for a spatially detailed land use classification as an essential input of the module, which transforms rainfall to direct runoff. A rough distinction between forest types, land types, impervious and water areas is sufficient for runoff estimation. The results are presented as chorological runoff maps for several components and different levels of spatial resolution in the upper Lenne basin. ESA

N89-28060# Instituut voor Culturrtechniek en Waterhuishouding, Wageningen (Netherlands).
APPLICATION OF REMOTE SENSING TO IRRIGATION WATER MANAGEMENT IN TWO ITALIAN IRRIGATION DISTRICTS
S. Azzali and M. Menenti *In* ESA, European Coordinated Effort for Monitoring the Earth's Environment. A Pilot Project Campaign on LANDSAT Thematic Mapper Applications (1985-1987) May 1989 p 41-48 Original contains color illustrations (For primary document see N89-28055 22-43)
Copyright Avail: NTIS HC A15/MF A01; ESA Publications Div., ESTEC, Noordwijk, Netherlands, 80 Dutch guilders or 40 US dollars

The feasibility of a remote sensing method to determine quantity, type, and water shortage (water stress) of crops by means of LANDSAT TM images is demonstrated in two irrigation districts in the Po valley. It is shown that an accurate crop calendar applying for each area is required for the multitemporal analysis to be successful. Reflectance measurements in bands 3, 4, 5, and 7 are more reliable than estimates of surface temperature with band 6 measurements in detecting shortage of water availability in crops. ESA

N89-28061# Centro de Estudios y Experimentacion de Obras Publicas, Madrid (Spain).
REMOTE SENSING OF LIMNOLOGICAL PARAMETERS IN RESERVOIRS
J. L. OrtizCasas and R. PenaMartinez *In* ESA, European Coordinated Effort for Monitoring the Earth's Environment. A Pilot Project Campaign on LANDSAT Thematic Mapper Applications (1985-1987) May 1989 p 49-56 Original contains color illustrations (For primary document see N89-28055 22-43)
Copyright Avail: NTIS HC A15/MF A01; ESA Publications

Div., ESTEC, Noordwijk, Netherlands, 80 Dutch guilders or 40 US dollars

Evaluation and mapping of surface limnological variables in reservoirs is made on a single date basis by making use of LANDSAT 5 TM imagery. The variables used are water temperature, chlorophyll concentration and Secchi depth transparency. In total eight images/dates are included in the study involving up to eleven reservoirs. Reliable maps of chlorophyll and Secchi depth transparency are developed in most instances. ESA

N89-28062# Geneva Univ. (Switzerland). Dept. of Geology.
COLOR ANALYSIS OF INLAND WATERS USING LANDSAT TM DATA
J.-M. Jaquet and B. Zand (United Nations Environment Programme, Geneva, Switzerland) *In* ESA, European Coordinated Effort for Monitoring the Earth's Environment. A Pilot Project Campaign on LANDSAT Thematic Mapper Applications (1985-1987) May 1989 p 57-67 Original contains color illustrations (For primary document see N89-28055 22-43)
Copyright Avail: NTIS HC A15/MF A01; ESA Publications Div., ESTEC, Noordwijk, Netherlands, 80 Dutch guilders or 40 US dollars

Chromaticity transforms based on bands 1, 2, and 3 are computed for over 50 inland water bodies located in western Switzerland and southeastern France. Their trophic state varies between oligotrophic and eutrophic. In chomaticity space, the range from green blue, moderately saturated (clear water) to green, less saturated (high chlorophyll). A third pole is located towards isoradiance point (high mineral turbidity). Targets with bottom signal influence plot in between. It is shown that color transforms yield more information on water bodies typology and features than principal component analysis based on band radiances. ESA

N89-28063# University Coll., Dublin (Ireland). Dept. of Biochemistry.
USE OF SATELLITE IMAGERY FOR THE INVESTIGATION OF POLLUTION-RELATED CHARACTERISTICS OF DUBLIN BAY, IRELAND
Bartholomew Masterson and Dymphna Conry-McDermott *In* ESA, European Coordinated Effort for Monitoring the Earth's Environment. A Pilot Project Campaign on LANDSAT Thematic Mapper Applications (1985-1987) May 1989 p 71-75 Original contains color illustrations (For primary document see N89-28055 22-43)
Copyright Avail: NTIS HC A15/MF A01; ESA Publications Div., ESTEC, Noordwijk, Netherlands, 80 Dutch guilders or 40 US dollars

The use of satellite imagery in the context of a proposed water quality management plan is considered. A synoptic appreciation of the heterogeneity of the Dublin Bay water body is obtained. The results, based on the reflectance patterns, generally reinforce the limited published hydrological data and the known behavior of point discharges, but suggets that the complexity of the dispersion processes is greater than that hitherto observed. ESA

N89-28064# Norwegian Hydrodynamic Labs., Trondheim.
LANDSAT-5 TM STUDY OF SUSPENDED SEDIMENTS IN A FJORD SYSTEM IN WESTERN NORWAY
J. Nilsen, I. Selseth, and V. Nilsen (Forut, Tromsoe, Norway) *In* ESA, European Coordinated Effort for Monitoring the Earth's Environment. A Pilot Project Campaign on LANDSAT Thematic Mapper Applications (1985-1987) May 1989 p 77-87 Original contains color illustrations (For primary document see N89-28055 22-43)
Copyright Avail: NTIS HC A15/MF A01; ESA Publications Div., ESTEC, Noordwijk, Netherlands, 80 Dutch guilders or 40 US dollars

The spreading of suspended sediments discharged from rivers into fjords are studied using visible and infrared TM data. Different methods are used to study the distribution of the surface turbidity and temperature. The color coding of brightness levels from channels 1, 2, and 3 seem to give the best resolution. Supervised classification techniques are useful in determining the presence of classes defined in a nearby control area. Visible channels are found more useful for studying the spreading of the suspended sediments. ESA

N89-28065# Trinity Coll., Dublin (Ireland).
THE USE OF THEMATIC MAPPER IMAGERY FOR PEATLAND MAPPING AND MINERAL EXPLORATION IN IRELAND
G. W. Horgan and M. F. Critchley *In* ESA, European Coordinated Effort for Monitoring the Earth's Environment. A Pilot Project Campaign on LANDSAT Thematic Mapper Applications (1985-1987) May 1989 p 91-97 Original contains color illustrations (For primary document see N89-28055 22-43)
Copyright Avail: NTIS HC A15/MF A01; ESA Publications Div., ESTEC, Noordwijk, Netherlands, 80 Dutch guilders or 40 US dollars

A two stage approach is used in the mapping of peatlands. Techniques base upon mathematical morphology are used to separate peatlands from other types of land cover. Maximum likelihood methods are then used to classify different types of peatlands. Using these methods it was possible to distinguish between areas of undisturbed, machine cut, hand cut, and burnt peat. Edge enhanced and directionally filtered band 4 imagery is used in mineral exploration to map geological structures. Statistical pattern analysis is found a useful method for this case. TM imagery is however hindered by agricultural features. ESA

N89-28066# Freie Univ., Berlin (Germany, F.R.). Inst. of Applied Geology.
LANDSAT TM STUDY OF SABKHA SURFACES IN THE QATTARA DEPRESSION, NORTHWESTERN EGYPT
Frank K. List, Doris Linne, and Bernd Meissner *In* ESA, European Coordinated Effort for Monitoring the Earth's Environment. A Pilot Project Campaign on LANDSAT Thematic Mapper Applications (1985-1987) May 1989 p 99-110 Sponsored by the Deutsche Forschungsgeimschaft, Bonn, Fed. Republic of Germany Original contains color illustrations (For primary document see N89-28055 22-43)
Copyright Avail: NTIS HC A15/MF A01; ESA Publications Div., ESTEC, Noordwijk, Netherlands, 80 Dutch guilders or 40 US dollars

A digital LANDSAT TM scene of January 1986 was studied in detail for a better discrimination of the different types of sabkha surfaces. Several combinations of spectral bands were examined in order to find out what type of color composite imagery would be best suited to visual interpretation. The digital classification by a maximum likelihood classifier, though rendering more detailed discrimination of the sabkha surfaces than visual interpretation alone, represents only an intermediary stage in the information extraction process. ESA

N89-28067# Karlsruhe Univ. (Germany, F.R.). Dept. of Photogrammetry and Remote Sensing.
IMAGE PROCESSING STRATEGIES FOR MINERAL EXPLORATION IN ARID AREAS BY USE OF TM DATA
H. Kaufmann *In* ESA, European Coordinated Effort for Monitoring the Earth's Environment. A Pilot Project Campaign on LANDSAT Thematic Mapper Applications (1985-1987) May 1989 p 111-125 Original contains color illustrations (For primary document see N89-28055 22-43)
Copyright Avail: NTIS HC A15/MF A01; ESA Publications Div., ESTEC, Noordwijk, Netherlands, 80 Dutch guilders or 40 US dollars

Investigations were carried out in the Wadi Araba to trace the relationship between diagnostic signals received from LANDSAT TM data and several mineralized ground districts. Rationing, principal component analysis, and IHS decorrelation processing are used to enhance diagnostic features associated with hydrothermally altered areas. The ratio and PC approaches often fail to clearly discriminate between the diagnostic features. The main reasons are attributed to similarities in relative intensities of vegetation and minerals and to disadvantages that arise through the techniques themselves. ESA

N89-28068# Technische Univ., Munich (Germany, F.R.). Arbeitsgruppe Fernerkundung.
APPLICABILITY OF LANDSAT TM DATA FOR GEOSCIENTIFIC PURPOSES IN ICELAND
F. Jaskolla and K. Arnason *In* ESA, European Coordinated Effort for Monitoring the Earth's Environment. A Pilot Project Campaign on LANDSAT Thematic Mapper Applications (1985-1987) May 1989 p 127-139 Original contains color illustrations (For primary document see N89-28055 22-43)
Copyright Avail: NTIS HC A15/MF A01; ESA Publications Div., ESTEC, Noordwijk, Netherlands, 80 Dutch guilders or 40 US dollars

Daytime images of Iceland were studied in order to examine whether the data might be attractive for future geothermal investigations. The comparison with older HCMM images (spatial resolution 600 m) shows an enormous qualitative increase in the information content of TM images. The thermal emission from geothermal fields may be recognized. The capability of the satellite to register subtle changes in thermal anomalies of the ocean is of particular interest as these changes are coupled with climatic variations, which often have great impacts on fishery and farming. ESA

N89-28069# Karlsruhe Univ. (Germany, F.R.). Lehrstuhl fuer Angewandte Geologie.
KARST DRAINAGE IN THE PELOPONNESUS AREA: A CASE STUDY FOR APPLICATION OF TM DATA IN HYDROGEOLOGY
B. Reichert, H. Hoetzl, and H. Kaufmann *In* ESA, European Coordinated Effort for Monitoring the Earth's Environment. A Pilot Project Campaign on LANDSAT Thematic Mapper Applications (1985-1987) May 1989 p 141-148 Original contains color illustrations (For primary document see N89-28055 22-43)
Copyright Avail: NTIS HC A15/MF A01; ESA Publications Div., ESTEC, Noordwijk, Netherlands, 80 Dutch guilders or 40 US dollars

The drainage system between the catchment areas and the various springs on the coast were investigated and possible ways of collection of fresh water before its submarine discharge were studied. The use of special band combinations of the reflective data made a separation of the main hydrogeological units possible. A fracture pattern is detected which permits new conclusions on possible underground paths of the water. ESA

N89-28070# Bundesanstalt fuer Geowissenschaften und Rohstoffe, Hannover (Germany, F.R.).
DETECTION OF SHORT-TERM CHANGES IN TIDAL FLAT GEOMORPHOLOGY
J. Ehlers and F. Boeker *In* ESA, European Coordinated Effort for Monitoring the Earth's Environment. A Pilot Project Campaign on LANDSAT Thematic Mapper Applications (1985-1987) May 1989 p 149-159 Original contains color illustrations (For primary document see N89-28055 22-43)
Copyright Avail: NTIS HC A15/MF A01; ESA Publications Div., ESTEC, Noordwijk, Netherlands, 80 Dutch guilders or 40 US dollars

Results from LANDSAT 5 TM imagery were studied. Attention is focused on large scale features formed by wind induced drift currents on the tidal flats, tidal current flow patterns, and the application of satellite imagery for tracing morphological changes in the Wangerooge and Mellum areas. The results demonstrate that satellite image evaluation is applicable to track major morphological changes in the Wadden Sea. ESA

N89-28071# Karlsruhe Univ. (Germany, F.R.). Inst. of Geology.
METHODICAL AND STRUCTURAL MSS AND TM INVESTIGATIONS IN THE SWABIAN ALB, SW GERMANY
R. Stellrecht, A. Hoydem, H. Kaufmann, and W. Weisbrich *In* ESA, European Coordinated Effort for Monitoring the Earth's Environment. A Pilot Project Campaign on LANDSAT Thematic Mapper Applications (1985-1987) May 1989 p 161-168 Original contains color illustrations (For primary document see N89-28055 22-43)
Copyright Avail: NTIS HC A15/MF A01; ESA Publications Div., ESTEC, Noordwijk, Netherlands, 80 Dutch guilders or 40 US dollars

Synchronous records of data are compared with each other and with geological field data. The structural features known from field investigations are also presented in both satellite data direction roses. TM image give better details than MSS. Geodynamic statements in the investigated area are scarcely possible. ESA

N89-28072# Geological Survey of Norway, Trondheim.
LANDSAT TM DATA USED IN THE MAPPING OF LARGE-SCALE GEOLOGICAL STRUCTURES IN COASTAL AREAS IN TRONDELAG, CENTRAL NORWAY
Bjorn Rindstad and Arne Gronlie *In* ESA, European Coordinated Effort for Monitoring the Earth's Environment. A Pilot Project Campaign on LANDSAT Thematic Mapper Applications (1985-1987) May 1989 p 169-181 Sponsored by the Technical Research Council of Norway Original contains color illustrations (For primary document see N89-28055 22-43)
Copyright Avail: NTIS HC A15/MF A01; ESA Publications Div., ESTEC, Noordwijk, Netherlands, 80 Dutch guilders or 40 US dollars

Both standard B/W photographs and digital data were employed to map linear structures in coastal areas. Linear processing consisted of linear stretching of individual TM channels and generation of color composites. TM imagery is proven useful for detailed interpretation of geological structures. An image processing system suitable for TM data should at least be able to display 1024 x 1024 pixels in a color monitor. ESA

N89-28073# Universite Catholique de Louvain (Belgium). Lab. de Teledetection.
EVALUATION OF THE LANDSAT TM SATELLITE IN URBAN MEDIA: APPLICATION TO THE CASE OF BRUSSELS, BELGIUM [EVALUATION DES POTENTIALITES DU SATELLITE LANDSAT TM EN MILIEU URBAIN - APPLICATION AU CAS DE BRUXELLES (BELGIQUE)]
M. L. DeKeersmaecker *In* ESA, European Coordinated Effort for Monitoring the Earth's Environment. A Pilot Project Campaign on LANDSAT Thematic Mapper Applications (1985-1987) May 1989 p 185-189 In FRENCH; ENGLISH summary Original contains color illustrations (For primary document see N89-28055 22-43)
Copyright Avail: NTIS HC A14/MF A01; ESA Publications Div., ESTEC, Noordwijk, Netherlands, 80 Dutch guilders or 40 US dollars

The results from different analysis methods are presented. The study's goals include land use classification in an urban area, study of homogeneous wards in an urban system and modeling the spatial distribution of the components of the urban system. An algorithm based on a mobile window is described. The Clark relation is used to establish a relationship between population density and distance to the center of the city. The results confirm the applicability of remote sensing methods. ESA

N89-28074# Freiburg Univ. (Germany, F.R.). Dept. of Hydrology.
AGRICULTURAL LAND-USE CLASSIFICATION IN THE UPPER RHINE VALLEY USING MULTITEMPORAL TM DATA
Wolfram Mauser *In* ESA, European Coordinated Effort for Monitoring the Earth's Environment. A Pilot Project Campaign on LANDSAT Thematic Mapper Applications (1985-1987) May 1989 p 191-198 Original contains color illustrations (For primary document see N89-28055 22-43)
Copyright Avail: NTIS HC A15/MF A01; ESA Publications Div., ESTEC, Noordwijk, Netherlands, 80 Dutch guilders or 40 US dollars

Maximum likelihood classifications of different combinations of spectral bands and dates were compared in their accuracy in separating the different plant species. The training areas were chosen to cover different varieties of forest, corn, wheat, barley, sugarbeet, potatoes, grassland, built-up areas and water. It is concluded that the resolution of TM data is sufficient to recognize

the major fields in the study area. The use of multitemporal data improves the classification accuracy, especially when moving from spring to summer. ESA

N89-28075# Tromsoe Univ. (Norway). Inst. of Biology and Geology.
MAPPING WINTER GRAZING AREAS FOR REINDEER ON SVALBARD USING LANDSAT THEMATIC MAPPER DATA
Sigmund Spjelkavik and Arve Elvebakk *In* ESA, European Coordinated Effort for Monitoring the Earth's Environment. A Pilot Project Campaign on LANDSAT Thematic Mapper Applications (1985-1987) May 1989 p 199-206 Sponsored by ESA and the Norwegian Polar Research Inst. (For primary document see N89-28055 22-43)
Copyright Avail: NTIS HC A15/MF A01; ESA Publications Div., ESTEC, Noordwijk, Netherlands, 80 Dutch guilders or 40 US dollars

A vegetation map was made on panchromatic aerial photos in a limited area and later compared with enhanced and classified TM images. Moss communities are recognized on the mountain plateaus. Faeces counting is used as an indication of reindeer grazing. The spatial and spectral resolution of the TM system seems to be sufficient for rangeland mapping in this artic region. ESA

N89-28076# Instituto de Edafologia y Fisiologia Vegetal, Madrid (Spain).
REMOTE SENSING OF THE MADRID AREA ECOSYSTEMS
Jose Luis LabranderoSanz *In* ESA, European Coordinated Effort for Monitoring the Earth's Environment. A Pilot Project Campaign on LANDSAT Thematic Mapper Applications (1985-1987) May 1989 p 207-211 Original contains color illustrations (For primary document see N89-28055 22-43)
Copyright Avail: NTIS HC A15/MF A01; ESA Publications Div., ESTEC, Noordwijk, Netherlands, 80 Dutch guilders or 40 US dollars

The characterization and definition of the land elements was carried out in June 1984 and March 1985 using information provided by the TM sensors of LANDSAT 5 satellite. Pilot areas of 256 x 256 pixels were analyzed with the aid of the Pericolor 1000 system as a means of interpreting information from the sensor and concluding its importance in the study of the different land elements which define ecosystems. The combination of bands 1, 2 and 3 enhance the cartographic units of the soils, and is of great assistance in the control of soil degradation. ESA

N89-28077# Instituto Nacional de Investigaciones Agronomicas, Madrid (Spain). Seccion de Proceso de Datos.
COMPARISON OF THE CLASSIFICATION RESULTS OBTAINED WITH TM AND MSS DATA IN LAND USES IDENTIFICATION OF THE COMMUNIDAD AUTONOMA DE CANTABRIA
Federico GonzalezAlonso and Jose Maria UrenaFrances (Universidad de Santander, Spain) *In* ESA, European Coordinated Effort for Monitoring the Earth's Environment. A Pilot Project Campaign on LANDSAT Thematic Mapper Applications (1985-1987) May 1989 p 213-219 Sponsored by the Spanish National Point of Contact Original contains color illustrations (For primary document see N89-28055 22-43)
Copyright Avail: NTIS HC A15/MF A01; ESA Publications Div., ESTEC, Noordwijk, Netherlands, 80 Dutch guilders or 40 US dollars

Several radiometric corrections are made with the aim of making the indices obtained from the TM and MSS data more easily comparable. Training areas for the different types of canopy are delimited, and the study zone is classified using the intervals obtained for the normalized vegetation index in each class. The results are compared in a pilot zone and show that the radiometric correction of the digital values is a useful technique to attenuate the different calibration of the sensors. ESA

N89-28078# Bodenkultur Univ., Vienna (Austria). Inst. fuer Vermessungswesen und Fernerkundung.
FOREST DAMAGE MAPPING IN AUSTRIA WITH THE AID OF LANDSAT TM IMAGE DATA
W. Schneider *In* ESA, European Coordinated Effort for Monitoring the Earth's Environment. A Pilot Project Campaign on LANDSAT Thematic Mapper Applications (1985-1987) May 1989 p 223-231 Sponsored in part by Austrian Fonds zur Foerderung der Wissenschaftlichen Forschung Original contains color illustrations (For primary document see N89-28055 22-43)
(Contract BMWF-37.007/1-25/85)
Copyright Avail: NTIS HC A15/MF A01; ESA Publications Div., ESTEC, Noordwijk, Netherlands, 80 Dutch guilders or 40 US dollars

Temporal/spectral signatures of forest stands of different species composition, age class, crown closure, and crown condition are analyzed. It is confirmed that channels 5 and 7 (mid-infrared) are valuable and the most important for separating forest categories. There is a correlation between crown condition and crown closure in the area studied. It could not be decided whether it is the crown condition proper or the crown closure which is sensed by TM. ESA

N89-28079# Institute for Image Processing Computer Mapping, Graz (Austria).
DISCRIMINATION OF GEOBOTANICAL ANOMALIES IN CONIFEROUS FORESTS FROM LANDSAT TM DATA
C. Banninger *In* ESA, European Coordinated Effort for Monitoring the Earth's Environment. A Pilot Project Campaign on LANDSAT Thematic Mapper Applications (1985-1987) May 1989 p 233-240 Sponsored by the Bundesministerium fuer Wissenschaft und Forschung, Vienna, Austria and the Styrian Scientific Research Office Original contains color illustrations (For primary document see N89-28055 22-43)
Copyright Avail: NTIS HC A15/MF A01; ESA Publications Div., ESTEC, Noordwijk, Netherlands, 80 Dutch guilders or 40 US dollars

A statistical analysis of multitemporal TM data from a test site in Austria analyzes the relationship between soil metal content, canopy leaf density and canopy reflectance and defines the TM bands and transformations best suited for distinguishing geobotanical anomalies in forest stands, particularly those related to changes in canopy structure. The results indicate the incipient or subtle levels of heavy metal stress are most likely manifested by morphological rather then physiological changes in a canopy. ESA

N89-28080# Gewerkschaften Brigitta und Elwerath Betriebsfuehrungsgesellschaft m.b.H., Hanover (Germany, F.R.). Lab. of Remote Sensing and Forest Management.
CLASSIFICATION OF SMALL-SCALE FORESTS IN FLANDERS USING LANDSAT TM DIGITAL DATA: PRELIMINARY RESULTS
Robert R. DeWulf and Roland E. Goossens *In* ESA, European Coordinated Effort for Monitoring the Earth's Environment. A Pilot Project Campaign on LANDSAT Thematic Mapper Applications (1985-1987) May 1989 p 241-249 Original contains color illustrations (For primary document see N89-28055 22-43)
Copyright Avail: NTIS HC A15/MF A01; ESA Publications Div., ESTEC, Noordwijk, Netherlands, 80 Dutch guilders or 40 US dollars

The feasibility of TM for forest classification in Flanders is investigated. A supervised classification scheme is adopted, with emphasis on the assessment of classification accuracy on different levels of detail. Channel ratios and linear combinations are tested against single TM channels. It is concluded that the type of classification algorithm does not significantly influence classification results. Forest-non forest distinction is possible with an accuracy ranging between 79 and 92 percent. Coniferous species can be recognized with an accuracy ranging between 60 and 82 percent. ESA

N89-28081# Deutsche Forschungs- und Versuchsanstalt fuer Luft- und Raumfahrt, Oberpfaffenhofen (West Germany).
FOREST CLASSIFICATION WITH TM DATA IN THE AREA OF FREIBURG, FEDERAL REPUBLIC OF GERMANY
M. Schardt *In* ESA, European Coordinated Effort for Monitoring the Earth's Environment. A Pilot Project Campaign on LANDSAT Thematic Mapper Applications (1985-1987) May 1989 p 251-259 Original contains color illustrations (For primary document see N89-28055 22-43)
Copyright Avail: NTIS HC A15/MF A01; ESA Publications Div., ESTEC, Noordwijk, Netherlands, 80 Dutch guilders or 40 US dollars

Data is digitally classified to delineate its information content according to forest inventories. Data from two different seasons are used. The separation of deciduous and coniferous forests, forested and agricultural areas, and age classes of trees were tested. To avoid misclassifications caused by the influence of topography, the additional information of a digital terrain model was integrated. It is found that pure poplar stands can be clearly separated from mixed deciduous forest stands in band TM5, the middle infrared band. The three species classified could be separated with an accuracy of over 90 percent. ESA

N89-28082# Freiburg Univ. (Germany, F.R.). Abteilung Luftbildmessung und Fernerkundung.
USE OF LANDSAT TM DATA FOR FOREST DAMAGE INVENTORY
A. Kadro *In* ESA, European Coordinated Effort for Monitoring the Earth's Environment. A Pilot Project Campaign on LANDSAT Thematic Mapper Applications (1985-1987) May 1989 p 261-270 Original contains color illustrations (For primary document see N89-28055 22-43)
Copyright Avail: NTIS HC A15/MF A01; ESA Publications Div., ESTEC, Noordwijk, Netherlands, 80 Dutch guilders or 40 US dollars

Several investigations on spectral signatures of different TM bands were performed. The analysis resulted in clear separability of different degrees of damages. Band 5 and 7 are not yet sufficiently evaluated. Computer aided classifications in form of ratioing (B5/B4) show positive results in separating damaged and healthy sites. Correlation of TM simulation data and direct observation and IR photo is acceptable. ESA

N89-28083# Tromsoe Univ. (Norway). Inst. of Biology and Geology.
USE OF REMOTE SENSING IN MAPPING OF VEGETATION IN THE DIVIDALEN AREA CENTRAL TROMS, NORTHERN NORWAY
Hans Tommervik *In* ESA, European Coordinated Effort for Monitoring the Earth's Environment. A Pilot Project Campaign on LANDSAT Thematic Mapper Applications (1985-1987) May 1989 p 271-278 Original contains color illustrations (For primary document see N89-28055 22-43)
Copyright Avail: NTIS HC A15/MF A01; ESA Publications Div., ESTEC, Noordwijk, Netherlands, 80 Dutch guilders or 40 US dollars

The identification of different vegetation cover types using TM data is evaluated. Digital image processing (supervised classification) done on the imagery showed that it is possible to classify the most phenological developed vegetation cover types with an overall accuracy of 90 percent and more, in spite of the early spring season. Visual interpretation on both the spring scene and the autumn scene combined with digital classification done on serveral band combinations is a good tool to improve the interpretation of each imagery. ESA

N89-28084# Alcala de Henares Univ., Madrid (Spain). Dept. of Geography.
MULTITEMPORAL ANALYSIS OF TM IMAGES: APPLICATION TO FOREST FIRE MAPPING AND INVENTORY IN A MEDITERRANEAN ENVIRONMENT
Emilio Chuvieco *In* ESA, European Coordinated Effort for Monitoring the Earth's Environment. A Pilot Project Campaign on LANDSAT Thematic Mapper Applications (1985-1987) May 1989 p 279-285 Original contains color illustrations (For primary document see N89-28055 22-43)
Copyright Avail: NTIS HC A15/MF A01; ESA Publications Div., ESTEC, Noordwijk, Netherlands, 80 Dutch guilders or 40 US dollars

The test area was disturbed by a big conflagration in 1985. Images before and after the fire were selected for multitemporal comparison. Cluster analysis was employed to group supervised and unsupervised training statistics, while discriminant analysis tested the strength of the grouping process. The results presented include the evaluation of the area burned by land cover types. ESA

N89-28085# Ecole Polytechnique Federale de Lausanne (Switzerland). Inst. of Rural Engineering.
LARGE-SCALE FOREST MANAGEMENT USING LANDSAT THEMATIC MAPPER DATA
R. Caloz and T. Blaser *In* ESA, European Coordinated Effort for Monitoring the Earth's Environment. A Pilot Project Campaign on LANDSAT Thematic Mapper Applications (1985-1987) May 1989 p 287-291 Original contains color illustrations (For primary document see N89-28055 22-43)
Copyright Avail: NTIS HC A15/MF A01; ESA Publications Div., ESTEC, Noordwijk, Netherlands, 80 Dutch guilders or 40 US dollars

The information that can be drawn from TM data is evaluated by studying two typical small forests of the Swiss Plateau. Existing inventories are described and the sequences used for image processing are analyzed. It is shown that it is possible at a municipal scale to give the physical limits actualization of the forestal area at a scale of 1:25000 and the inventory and spatial distribution of the species. ESA

N89-28086# Freie Univ., Berlin (Germany, F.R.). Inst. fuer Meteorologie.
MULTITEMPORAL ANALYSIS OF FOREST AREAS IN SURROUNDINGS OF INNSBRUCK, AUSTRIA
Franz H. Berger *In* ESA, European Coordinated Effort for Monitoring the Earth's Environment. A Pilot Project Campaign on LANDSAT Thematic Mapper Applications (1985-1987) May 1989 p 293-298 Sponsored by the Austrian Solar and Space Agency, Vienna, and the Bundesministerium fuer Wissenschaft und Forschung, Vienna, Austria Original contains color illustrations (For primary document see N89-28055 22-43)
Copyright Avail: NTIS HC A15/MF A01; ESA Publications Div., ESTEC, Noordwijk, Netherlands, 80 Dutch guilders or 40 US dollars

The seasonal variations in 1984 to 1985 of directional vegation reflectance was analyzed for various forested areas (mainly coniferous forests). A simple radiative model was applied to correct for atmospheric effects. This resulted in spectral surface reflectances of each TM band. The correlation and the multiple correlation between the different TM channels were computed. Channel 4 is the least correlated to all the other channels, and its combination with one of them results in a maximum of information. ESA

N89-28087# Office de la Recherche Scientifique et Technique, Bondy (France). Atelier de Teledetection.
COMPARISON OF MSS AND TM LANDSAT DATA FOR CARTOGRAPHY OF SURFACE STRUCTURES IN ARID REGIONS (SOUTHERN TUNISIA) [COMPARAISON DES DONNEES LANDSAT MSS ET TM POUR LA CARTOGRAPHIE DES FORMATIONS SUPERFICIELLES EN ZONE ARIDE (TUNISIE MERIDIONALE)]
R. Escadafal and J. Pouget *In* ESA, European Coordinated Effort for Monitoring the Earth's Environment. A Pilot Project Campaign on LANDSAT Thematic Mapper Applications (1985-1987) May 1989 p 301-307 In FRENCH; ENGLISH summary Original contains color illustrations (For primary document see N89-28055 22-43)

Copyright Avail: NTIS HC A15/MF A01; ESA Publications Div., ESTEC, Noordwijk, Netherlands, 80 Dutch guilders or 40 US dollars

The image acquired the 5th August 1984 was analyzed by color coding associating channels 2, 3, and 4 and associating the visible channels 1 and 3 to channel 7 (medium infrared). Channel 7 is shown to be strongly correlated to the mineralogical content of the soil surface in the studied area. This enables to easily distinguish gypsum from carbonate and quartz dominated soils. ESA

N89-28088# RSDE S.R.L., Milan (Italy).
PROCESSING AND INTERPRETATION OF THEMATIC MAPPER IMAGES IN THE PROVINCE OF PIACENZA (ITALY)
Alessandro Annoni, Enrico Zini, and Rita Arcozzi (Region of Emilia-Romagna, Bologne, Italy) *In* ESA, European Coordinated Effort for Monitoring the Earth's Environment. A Pilot Project Campaign on LANDSAT Thematic Mapper Applications (1985-1987) May 1989 p 309-314 Original contains color illustrations (For primary document see N89-28055 22-43)
Copyright Avail: NTIS HC A15/MF A01; ESA Publications Div., ESTEC, Noordwijk, Netherlands, 80 Dutch guilders or 40 US dollars

TM data was used to obtain soil maps of the Po plain following the methodology used by the Cartographical Office of the region. The image processing methods available are discussed. The different levels of water retention were studied from images taken after a long dry spell and after several rainy days. The spring image is considered to be the most interesting, the best image processing being color coding of bands 4, 5, and 3 simply enhanced by contrast stretching. ESA

N89-28089# Technische Univ., Berlin (Germany, F.R.). Fachgebiet Photogrammetrie und Kartographie.
PRODUCTION OF SATELLITE IMAGE MAPS FROM TM DATA
Joerg Albertz and Alfred Mehlbreuer *In* ESA, European Coordinated Effort for Monitoring the Earth's Environment. A Pilot Project Campaign on LANDSAT Thematic Mapper Applications (1985-1987) May 1989 p 315-321 Sponsored by the Deutsche Forschungsgemeinschaft, Bonn, Fed. Republic of Germany Original contains color illustrations (For primary document see N89-28055 22-43)
Copyright Avail: NTIS HC A15/MF A01; ESA Publications Div., ESTEC, Noordwijk, Netherlands, 80 Dutch guilders or 40 US dollars

A software system for digital image processing is presented. The system is characterized by the fact that the satellite scanner data are handled in digital form until the final printing plates are generated. Mosaicing of several images is achieved by special techniques utilizing the multiple information in the overlapping sections of adjacent scenes. ESA

N89-28090# Centro Nazionale Univ. per il Calcolo Elettronico, Pisa (Italy).
INTEGRATING TM AND CARTOGRAPHIC DATA
P. Mogorovich *In* ESA, European Coordinated Effort for Monitoring the Earth's Environment. A Pilot Project Campaign on LANDSAT Thematic Mapper Applications (1985-1987) May 1989 p 323-331 Original contains color illustrations (For primary document see N89-28055 22-43)
Copyright AvaiL: NTIS HC A15/MF A01; ESA Publications Div., ESTEC, Noordwijk, Netherlands, 80 Dutch guilders or 40 US dollars

The types of problems arising from integration are investigated. The objective is to superimpose TM and cartographic data so that similar features can be documented and updated at different times for visual comparisons. It is shown that the set of necessary operations is rather complex. Consequently it does not appear advisable to propose the introduction of this system into public administration. ESA

N89-28091# Politecnico di Milano (Italy). Istituto di Topografia, Fotogrammetria e Geofisica.
TESTS OF TOPOGRAPHIC MAPPING WITH THEMATIC MAPPER IMAGES
G. Togliatti, G. Lechi, and A. Moriondo *In* ESA, European Coordinated Effort for Monitoring the Earth's Environment. A Pilot Project Campaign on LANDSAT Thematic Mapper Applications (1985-1987) May 1989 p 333-338 Previously announced in IAA as A89-20712 (For primary document see N89-28055 22-43)
Copyright Avail: NTIS HC A15/MF A01; ESA Publications Div., ESTEC, Noordwijk, Netherlands, 80 Dutch guilders or 40 US dollars

TM images were studied to identify the most suitable bands to use in order to prepare the positive transparencies on which to perform measures, the types of image enhancement most suitable for topographic mapping purposes, and which pixel size would be most acceptable to the operators eyes. The geometric accuracy seems to meet the expectations. The topographic mapping on 1:50000 scale is nearly impossible with the present European specification. ESA

N89-28092# Institut fuer Angewandte Geodaesie, Frankfurt am Main (Germany, F.R.).
REPORTS ON CARTOGRAPHY AND GEODESY. SPECIAL ISSUE: HISTORY OF PHOTOGRAMMETRY, NUMBER 1 [NACHRICHTEN AUS DEM KARTEN- UND VERMESSUNGSWESEN. SONDERHEFT: GESCHICHTE DER PHOTOGRAMMETRIE, BAND 1]
1988 188 p In GERMAN Original contains color illustrations 3-D glasses as supplement
(ISSN-0344-5879; ETN-89-94678) Avail: NTIS HC A09/MF A01

The historical evolution of photogrammetry from the early period till the invention of the aircraft is surveyed. The main developments in the fields of analog methods and instruments in photogrammetry are presented. For individual titles, see N89-28093 through N89-28094.

N89-28093# Institut fuer Angewandte Geodaesie, Frankfurt am Main (Germany, F.R.).
THE EARLY PERIOD OF PHOTOGRAMMETRY TILL THE INVENTION OF THE AIRCRAFT [DIE FRUEHZEIT DER PHOTOGRAMMETRIE BIS ZUR ERFINDUNG DES FLUGZEUGES]
Teodor J. Blachut *In its* Reports on Cartography and Geodesy. Special Issue: History of Photogrammetry, Number 1 1988 p 17-63 In GERMAN (For primary document see N89-28092 22-43)
Avail: NTIS HC A09/MF A01

The historical evolution of photogrammetry is surveyed. The preceding events, the beginning of photogrammetry, the further development in cartographic applications of photography, and the spreading of photogrammetric procedures are depicted. Remarks concerning the development of terrestrial chambers and phototheodolites are given. The early developments in evaluating instruments (measuring and mapping instruments) are described. The development of balloons and the first balloon flights; balloon photography and its application to cartography; and the use of kites for aerial photography are presented. ESA

N89-28094# Institut fuer Angewandte Geodaesie, Frankfurt am Main (Germany, F.R.).
ANALOG METHODS AND INSTRUMENTS [ANALOGE VERFAHREN UND INSTRUMENTE]
Rudolf Burkhardt *In its* Reports on Cartography and Geodesy. Special Issue: History of Photogrammetry, Number 1 1988 p 65-172 In GERMAN Original contains color illustrations (For primary document see N89-28092 22-43)
Avail: NTIS HC A09/MF A01

The main developments in the fields of analog methods and instruments in photogrammetry are treated. Methods and instruments for the rectification of single pictures are presented:

nonphotographic and photographic rectification, the development of rectification instruments, and the accuracy and costs of rectification are discussed. The photographic layout for rough areas, and the orthophoto are described. Analog methods and instruments for stereomapping (multipicture photogrammetry) are presented. Analog plane image triangulation procedures are outlined. The analog spatial aerotriangulation is presented. ESA

N89-28095# Ohio State Univ., Columbus. Dept. of Geodetic Science and Surveying.
DETERMINATION OF LOCAL EMPIRICAL COVARIANCE FUNCTIONS FROM RESIDUAL TERRAIN REDUCED ALTIMETER DATA
Per Knudsen Nov. 1988 65 p
(Contract F19628-86-K-0016)
(AD-A208678; OSU/DGSS-395; AFGL-TR-89-0016; SR-5) Avail: NTIS HC A04/MF A01 CSCL 08/5

Local empirical covariance functions have been estimated from cross-over adjusted high-pass filtered SEASAT/GEOS-3 altimeter data in three local 2 x 2 deg areas in the North Atlantic ocean. The high-pass filtering was needed in order to remove remaining long wavelength parts of the gravity field due to errors in the spherical harmonic expansion that was used, and effects from sea surface topography and correlated parts of radial orbit errors. After a subtraction of noise variances geoid height variances associated with harmonic degrees above 180 of 0.213 sq m, 0.112 sq m, and 1.217 sq m were obtained in the three local areas respectively. Then residual terrain effects were computed from Airy-Heiskanen isostatic earth models using Fourier techniques and SYNBAPS bathymetry. The depths of compensation were increased in order to simulate regional Vening Meinesz models. Comparisons of altimetric and bathymetric geoid heights showed that the magnitudes of the unmodelled parts of the gravity fields practically were unaffected by changes in the depths of compensation from 50 km to 70 km. Estimations of local empirical covariance functions from the terrain reduced altimetry showed that the geoid height variances were reduced by about 3 dB, and 9 dB to values of 0.096 sq m, 0.108 sq m and 0.147 sq m respectively. GRA

N89-28096# New Mexico State Univ., Las Cruces. Dept. of Mathematical Sciences.
DIFFERENTIAL GEODESY OF THE EOTVOS TORSION BALANCE Final Report, 24 Jun. 1986 - 23 Jun. 1988
J. D. Zund 26 Apr. 1989 15 p
(Contract F19628-86-K-0028.)
(AD-A208711; GL-TR-89-0087) Avail: NTIS HC A03/MF A01 CSCL 08/5

The differential geodesy of the Eotvos torsion balance is examined by using the fourth and fifth fundamental tensors of the geopotential surfaces of a rotating Earth. It is shown that both these tensors involve curvature differences which are measureable by the Eotvos torsion balance. This suggests that the inability to determine the individual curvatures is not only a physical limitation, but also a geometric one. The fundamental tensors are expressed using the Hotine 2-leg formalism and their components are explicitly exhibited for the case of a spheroid. GRA

N89-28097# Vexcell Corp., Boulder, CO.
A SMART, MAPPING, CHARTING AND GEODESY CONTROL GENERATOR, PHASE 2 Final Report, Oct. 1987 - Jun. 1988
Franz Leberl, Woody Kober, M. Karspect, and J. Curlander Dec. 1988 155 p
(Contract DACA72-87-C-0011)
(AD-A208806; ETL-0523) Avail: NTIS HC A08/MF A01 CSCL 08/2

The real-time automated registration of multi-sensor imagery begins with the generation of control information. A specific application may require the registration of newly acquired data to an existing spatial database (absolute registration), or to other images of a series (relative registration). This study examines the feasibility and upper-level design of a system capable of providing the control information required for a range of image registration tasks and image types. In general, the control generator we suggest will be guided by a spatial database maintaining information about the feature content of the area of interest. A rule-based query generator will extract candidate ground control optimized for the particular image type and geometry at hand. GRA

N89-28098# Creative Optics, Inc., Bedford, MA.
NOVEL METHODOLOGY FOR APPLICATION OF ADAPTIVE SYSTEMS TECHNIQUES TO DMSP (DEFENSE METEOROLOGICAL SATELLITE PROGRAM) REMOTE TEMPERATURE SENSING Final Report, Jul. - Nov. 1988
Robert G. Hohlfeld, James C. Kilian, Thomas W. Drueding, and John F. Ebersole 29 Nov. 1988 44 p
(Contract F19628-88-C-0151)
(AD-A209975; COI-SR-26; AFGL-TR-88-0323) Avail: NTIS HC A03/MF A01 CSCL 04/1

Two new theoretical algorithms for the bias-free determination of atmospheric temperatures from upwelling radiance data were implemented in this research--the Differential Inversion (DI) algorithm and Optical Measure Theory (OMT). DI and OMT are complementary bias-free approaches to the construction of atmospheric temperature profiles. Previous work on DI was extended to permit the computation of partial atmospheric temperature profiles (at three altitudes) from Tiros Operational Vertical Sounder (TOVS) data. These partial temperature profiles demonstrated the utility of DI for the important operational problem of determination of the tropopause altitude. In OMT, atmospheric temperature profiles are the fundamental theoretical entities. Application of OMT to TOVS data in this research has resulted in the first bias-free computation of a complete atmospheric temperature profile from upwelling radiance data. This profile exhibits a meteorological character which is a natural consequence of the physical principles of radiative energy transfer on which OMT is based. Algorithmic studies in the development of DI and OMT have further elucidated the classic problems associated with the inversion of radiance data to obtain atmospheric temperature profiles. In addition to the TOVS data, data sets from the Defense Meteorological Satellite Program (DMSP) and the high-resolution Interferometer Sounder (HIS) were investigated for their suitability for inversion to atmospheric temperature profiles by DI and OMT. GRA

N89-28130*# National Aeronautics and Space Administration. Goddard Space Flight Center, Greenbelt, MD.
WIDE BAND DATA COLLECTION SYSTEM Abstract Only
J. M. Turkiewicz *In its* Laboratory for Oceans 1988 p 53-56 (For primary document see N89-28118 22-48)
Avail: NTIS HC A12/MF A01 CSCL 08B

N89-28131*# National Aeronautics and Space Administration. Goddard Space Flight Center, Greenbelt, MD.
CALIBRATION SUPPORT FOR THE EARTH OBSERVING SYSTEM PROJECT Abstract Only
B. W. Guenther *In its* Laboratory for Oceans 1988 p 57 (For primary document see N89-28118 22-48)
Avail: NTIS HC A12/MF A01 CSCL 08B

N89-28180*# National Aeronautics and Space Administration. Goddard Space Flight Center, Greenbelt, MD.
MICROWAVE REMOTE SENSING OF SOIL MOISTURE Abstract Only
J. C. Shiue and J. R. Wang *In its* Laboratory for Oceans 1988 p 231-235 (For primary document see N89-28118 22-48)
Avail: NTIS HC A12/MF A01 CSCL 08B

N89-28182*# National Aeronautics and Space Administration. Goddard Space Flight Center, Greenbelt, MD.
RADAR SCATTERING AND SOIL MOISTURE Abstract Only
D. M. LeVine and P. O. Neill *In its* Laboratory for Oceans 1988 p 239-241 (For primary document see N89-28118 22-48)
Avail: NTIS HC A12/MF A01 CSCL 17I

N89-28184*# National Aeronautics and Space Administration. Goddard Space Flight Center, Greenbelt, MD.
AGRICULTURE MULTIBAND EXPERIMENT RADIOMETER Abstract Only
W. H. Jones, J. Schutt, and B. Holben *In its* Laboratory for Oceans 1988 p 247-248 (For primary document see N89-28118 22-48)
Avail: NTIS HC A12/MF A01 CSCL 02C

44 ENERGY PRODUCTION AND CONVERSION

Includes specific energy conversion systems, e.g., fuel cells; global sources of energy; geophysical conversion; and windpower.

For related information see also *07 Aircraft Propulsion and Power, 20 Spacecraft Propulsion and Power,* and *28 Propellants and Fuels.*

N89-28099# Midwest Research Inst., Golden, CO. Solar Energy Research Inst.
PHOTOVOLTAIC PROGRAM BRANCH ANNUAL REPORT, FY 1988
Mar. 1989 303 p
(Contract DE-AC02-83CH-10093)
(DE89-000898; SERI/PR-211-3483) Avail: NTIS HC A14/MF A01

This report summarizes the progress of the Photovoltaic (PV) Program Branch of the Solar Energy Research Institute (SERI) from October 1, 1987 through September 30, 1988. The branch is responsible for the management of the subcontracted portion of SERI's PV Advanced Research and Development Project. In fiscal year 1988, this included more than 55 subcontracts with a total annualized funding of approximately $13.5 million. Approximately two-thirds of the subcontracts were with universities at a total funding of nearly $4.7 million. The six technical sections of the report cover the main areas of the subcontracted program: the Amorphous Silicon Research Project, Polycrystalline Thin Films, Crystalline Silicon Materials Research, High-Efficiency Concepts, the New Ideas Program, and the University Participation Program. Technical summaries of each of the subcontracted programs provide a discussion of approaches, major accomplishments in FY 1988, and future research directions. DOE

N89-28100# Midwest Research Inst., Golden, CO.
PROGRESS IN PARABOLIC DISH TECHNOLOGY
William B. Stine Jun. 1989 53 p
(Contract DE-AC02-83CH-10093)
(DE89-009427; SERI/SP-220-3237) Avail: NTIS HC A04/MF A01

This report describes the current status of parabolic dish technology. Its purpose is to communicate the principal outcomes of DOE's parabolic dish technology R and D efforts carried out at the Solar Energy Research Institute; Sandia National Laboratory, Albuquerque; the Jet Propulsion Laboratory; and other DOE national laboratories. It is written for those in industry, academia, and government who have a special interest in solar thermal systems that use parabolic dishes as collectors. The evolution of parabolic technology is described, and examples of projects in operation and under construction are included. Solar thermal dish technology can supply either electric or thermal energy to various applications over a broad range of system sizes and temperatures. These solar energy systems will be available by the time this country needs additional electric generation capacity -- in the mid to late 1990s -- at costs competitive with other energy sources. DOE

N89-28101# Applied Microwave Plasma Concepts, Carlsbad, CA.
EFFICIENT ENERGY STORAGE AND CONVERSION USING ADIABATIC COMPRESSION OF RELATIVISTIC-ELECTRON PLASMAS Final Report, 15 May 1986 - 31 Dec. 1988
Gareth E. Guest, Raphael A. Dandl, and Robert L. Miller 17 Jan. 1989 34 p
(Contract F49620-86-C-0055)
(AD-A208657; AMPC-028-036; AFOSR-89-0711TR) Avail: NTIS HC A03/MF A01 CSCL 10/4

The Plasma Electron Microwave Source (PEMS) concept in a relativistic-electron plasma confined in a magnetic-mirror device. The stored energy is transformed into microwave through amplification of whistler waves that can be launched externally for amplifier operation or generated spontaneously for oscillator operation. The anisotropy of the hot-electron temperature governs the maximum plasma energy density that can be stored, the amplification rates, and the saturated power level of the unstable whistler waves. The results of theoretical studies are summarized of the critical aspects of hot electron plasmas generated by ECH techniques, such as the Upper Off-Resonant Heating pioneered by Dandl in the ELMO series of experiments; and, the spatial amplification rates of unstable whistler waves in these plasmas. It is shown that a substantial fraction of the energy stored in a hot electron plasma can be transformed into repetitive pulses of microwave power by employing the PEMS approach, with typical values of gain, about 40db and bandwidth. GRA

N89-28102# Pennsylvania State Univ., University Park. Dept. of Mechanical Engineering.
COUPLING BETWEEN RADIATION AND GAS DYNAMICS Final Report, 1 Feb. 1988 - 1 Feb. 1989
Charles L. Merkle and Michael M. Micci 24 May 1989 39 p
(Grant AF-AFOSR-0048-84; AF Proj. 2308)
(AD-A209657; AFOSR-89-0784TR) Avail: NTIS HC A03/MF A01 CSCL 09/3

Heat addition in flowing gases by electromagnetic wave absorption is being considered for propulsive purposes. The research includes both microwave and solar radiation. In the microwave studies, an experimental investigation of helium and nitrogen discharges has shown that free-floating plasmas can be established in either medium for a range of input powers and gas flow rates, although helium gives the broader range of stable limits. The discharges are being set up in a 10.2 cm quartz sphere. For pressure ranges from 0.5 to 5.0 atm and input powers to 3 kW, maximum coupling efficiencies are measured to be between 40 and 65 percent with higher efficiencies for cases with larger flow rates. Spectroscopic techniques are being introduced to provide detailed local measurements of conditions inside the discharge. In companion analytical efforts, computational techniques are being used to model the experimental flowfields to provide improved understanding of the absorption process and to enable us to extend the experimental findings to broader conditions. In the solar radiation studies, the feasibility of direct absorption of solar energy in flowing conditions is studied. Similar computational studies are also being used to study the absorption of solar radiation in hydrogen with alkali seedants. Results show peak gas temperatures of about 3500 to 4000 K can be reached with reasonable solar concentration ratios. GRA

45 ENVIRONMENT POLLUTION

Includes atmospheric, noise, thermal, and water pollution.

N89-28103# Lenox Inst. for Research, Inc., MA.
ANALYTICAL PROCEDURES FOR ENVIRONMENTAL QUALITY CONTROL, VOLUME 2
Lawrence K. Wang, ed. and Mu Hao Sung Wang, ed. (New York State Dept. of Environmental Conservation, Albany.) 15 Jan. 1989 274 p Prepared in cooperation with Massachusetts Dept. of Environmental Quality Engineering, Boston; Hach Co., Loveland, CO.; Environmental Associates Ltd., Limestone, NY; EPA, Washington, DC
(PB89-158612; LIR/01-89/332-Vol-2) Avail: NTIS HC A12/MF A01 CSCL 13B

Topics covered in this report include: (1) the determination of the maximum total trihalomethane potential; (2) nationwide approval

of an alternative test procedure for the analysis of trihalomethanes; (3) volatile organic compounds in water by purge and trap capillary column gas chromatography with photoionization and electrolytic conductivity detectors in series; (4) analysis of organohalide pesticides and aroclors in drinking water by microextraction and gas chromatography; (4) testing for lead in school drinking water; (5) simplified methods for food and feed testing; (6) determination of chlorinated herbicides in drinking water; (7) measurement of N-methyl carbamoyloximes and N-methyl carbamates in drinking water; (8) determination of nitroaromatic compounds, isophorone, haloethers, phthalates, TCDD, pesticides, PCBs, volatile organics, and polynuclear aromatic hydrocarbons in industrial and municipal wastewater; and (9) sampling for Giardia and/or Crytosporidium.

GRA

N89-28104# Lenox Inst. for Research, Inc., MA.
ANALYTICAL PROCEDURES FOR ENVIRONMENTAL QUALITY CONTROL, VOLUME 3
Lawrence K. Wang, ed. and Mu Hao Sung Wang, ed. (New York State Dept. of Environmental Conservation, Albany.) 15 Jan. 1989 215 p Prepared in cooperation with EPA, Washington, DC; New York State Dept. of Health, Albany; Connecticut Dept. of Environmental Protection and Dept. of Health Services, Hartford; National Sanitation Foundation, Ann Arbor, MI; American Water Works Associ
(PB89-158620; LIR/01-89/333-Vol-3) Avail: NTIS HC A08/MF A01 CSCL 13B

The report covers ten important topics: (1) a procedure for determination of total trihalomethane formation potential; (2) trihalomethane formation potential; (3) summary of code revision of the maximum contaminant levels (MCL) of organic contaminants in public drinking waters; (4) sampling, exposure, and analysis of samples; (5) statewide screening of municipal sewage discharges initial assessments: chemical and toxicological characterizations; (6) determination of nitrosamines in industrial and municipal wastewaters; (7) determination of benzidines in industrial and municipal wastewaters; (8) determination of polychlorinated biphenyls (PCB) in potable water, fish and sediments; (9) specialty environmental GC columns, EPA methods and dioxin columns; and (10) volatile organic chemicals (VOC) detection limit requirements of large water utilities. GRA

N89-28105# Lawrence Livermore National Lab., CA. Atmospheric and Geophysical Sciences Div.
BACKGROUNDER CONTRIBUTION NO. 18: CLIMATE SCENARIOS FOR THE FIRST UC/DOE WORKSHOP
Joseph B. Knox May 1989 38 p
(Contract W-7405-eng-48)
(DE89-014302; UCID-21634) Avail: NTIS HC A03/MF A01

The purpose of this contribution is to provide a more detailed discussion of our workshop climate scenarios for the periods: (1) 2000 to 2010, and (2) 2030 to 2070 summarized in the introduction. The description considers the rationale or method of preparation of each element in the climate scenarios, the associated references and source documents, and an estimate of the uncertainty associated with the elements of the scenarios. In addition, a description is included of the climate scenario presently being used in the State of California's Study of Global Warming, and supportive material in regard to the climate scenario used in the Australian assessment of global warming and its effects on that nation. The summary table of the two workshop climate scenarios is reproduced here in this chapter for ease of reference, with the scenario elements labelled alphabetically for discussion purposes. DOE

N89-28164*# National Aeronautics and Space Administration. Goddard Space Flight Center, Greenbelt, MD.
CORRELATIVE MEASUREMENTS PROGRAM Abstract Only
C. L. Parsons *In its* Laboratory for Oceans 1988 p 169-173
(For primary document see N89-28118 22-48)
Avail: NTIS HC A12/MF A01 CSCL 13B

N89-28165*# National Aeronautics and Space Administration. Goddard Space Flight Center, Greenbelt, MD.
OZONE MEASUREMENTS USING BALLOON-BORNE OZONESONDES Abstract Only
A. L. Torres *In its* Laboratory for Oceans 1988 p 175-178
(For primary document see N89-28118 22-48)
Avail: NTIS HC A12/MF A01 CSCL 13B

N89-28166*# National Aeronautics and Space Administration. Goddard Space Flight Center, Greenbelt, MD.
MOBILE LIDAR SYSTEM FOR MEASUREMENT OF WATER VAPOR MIXING RATIO AND OZONE NUMBER DENSITY Abstract Only
D. Whiteman *In its* Laboratory for Oceans 1988 p 179-183
(For primary document see N89-28118 22-48)
Avail: NTIS HC A12/MF A01 CSCL 13B

N89-28171*# National Aeronautics and Space Administration. Goddard Space Flight Center, Greenbelt, MD.
TROPOSPHERIC NITRIC OXIDE MEASUREMENTS Abstract Only
A. L. Torres *In its* Laboratory for Oceans 1988 p 197-198
(For primary document see N89-28118 22-48)
Avail: NTIS HC A12/MF A01 CSCL 13B

46 GEOPHYSICS

Includes aeronomy; upper and lower atmosphere studies; ionospheric and magnetospheric physics; and geomagnetism.

For space radiation see *93 Space Radiation.*

N89-28106# Iowa Univ., Iowa City. Dept. of Physics and Astronomy.
PARTICLE SIMULATIONS IN MAGNETOSPHERIC PLASMAS Final Report, 1 Nov. 1987 - 31 Oct. 1988
Ken-Ichi Nishikawa 14 Mar. 1989 13 p
(Contract N00014-88-K-2007)
(AD-A206252) Avail: NTIS HC A03/MF A01 CSCL 04/1

Plasma physics processes occurring in magnetospheric plasmas were studied by means of numerical simulations. This study has included the excitation of instabilities due to electron currents and/or ion beams due to the presence of nonuniform electric fields. The investigations also included the heating and transport of plasma in the presence of particle interactions with excited waves in a collisionless plasma. Extensive numerical simulations were performed along with the development of analytic theories. These simulations allowed assessment of the affect of inherent nonlinear processes on plasma dynamics and to compare the simulation results with the observed data. GRA

N89-28107# Brookhaven National Lab., Upton, NY. Dept. of Applied Science.
SYNCHROTRON X-RAY FLUORESCENCE ANALYSES OF STRATOSPHERIC COSMIC DUST: NEW RESULTS FOR CHONDRITIC AND NICKEL-DEPLETED PARTICLES
G. J. Flynn and S. R. Sutton (Chicago Univ., IL.) Jun. 1989 20 p Presented at the Lunar Planetary Science Conference, Houston, TX, 12 Mar. 1989
(Contract NAG9-106; NAG9-257; DE-AC02-76CH-00016; NSF EAR-83-13683)
(DE89-014032; BNL-42627; CONF-8903111-4) Avail: NTIS HC A03/MF A01

Trace element abundance determinations were performed using synchrotron X-ray fluorescence on nine particles collected from the stratosphere and classified as cosmic. Improvements to the Synchrotron Light Source allowed the detection of all elements between Cr and Mo, with the exceptions of Co and As, in our largest particle. The minor and trace element abundance patterns of three Ni-depleted particles were remarkably similar to those of extraterrestrial igneous rocks. Fe/Ni and Fe/Mn ratios suggest that one of these may be of lunar origin. All nine particles exhibited

an enrichment in Br, ranging form 1.3 to 38 times the Cl concentration. Br concentrations were uncorrelated with particle size, as would be expected for a surface correlated component acquires from the stratosphere. DOE

N89-28108# Lawrence Livermore National Lab., CA. Atmospheric and Geophysical Sciences Div.
EVALUATING CFC (CHLOROFLUOROCARBON) ALTERNATIVES FROM THE ATMOSPHERIC VIEWPOINT, REVISION 1
Peter S. Connell and Donald J. Wuebbles May 1989 13 p Presented at the 82nd Air and Waste Management Association Annual Meeting and Exhibition, Anaheim, CA, 25 Jun. 1989
(Contract W-7405-eng-48)
(DE89-014268; UCRL-99927-Rev-1; CONF-890692-13-Rev-1)
Avail: NTIS HC A03/MF A01

Current understanding of atmospheric processes in the troposphere and stratosphere, in particular stratospheric ozone-controlling photochemistry, allows evaluation of the effects on the stratosphere of chlorine-containing compounds envisioned as CFC (chlorofluorocarbon) replacements prior to their production and release. Such evaluations can help to direct decisions on selecting CFC alternatives and define acceptable levels of production or emission. A two-dimensional (latitude and altitude) computational representation of the troposphere and stratosphere is employed which incorporates physical processes, e.g., species transport and radiative transfer, and homogeneous photochemical processes. Laboratory measurements of OH and $O(^1D)$ reactivity and spectral parameters of the alternative HCFC (hydrochlorofluorocarbon) compounds were used as input. The model-derived ozone depletion potential (ODP) is a defined quantity relating the effect on ozone of emission of a species to the model-calculated effect of a standard compound, here CFC-11 (CFCl3). Globally and annually averaged ozone depletion potentials vary from less than .02 to greater than 1.0 for various CFCs and HCFCs, primarily as a result of differences in calculated atmospheric lifetimes. Differences in stratospheric photochemistry among CFCs and HCFCs play a smaller but significant role. Zonally averaged ODPs for some compounds can range over a factor of three with latitude, however, as a result of differences in stratospheric lifetime and the altitude profile of Cl release in CFC or HCFC loss processes. While globally defined ODPs are useful in designing methods to reduce the overall stratospheric Cl burden and its impact on ozone, latitudinally and seasonally varying ODPs must be additionally considered as knowledge of specific areas of the impacts of decreasing ozone column abundance increases. DOE

N89-28109# Air Force Geophysics Lab., Hanscom AFB, MA.
USER'S GUIDE FOR THE AIR FORCE SURFACE-LAYER WINDFLOW MODEL (AFWIND) Environmental Research Papers, Jun. 1987 - Jun. 1988
Bruce A. Kunkel 8 Jul. 1988 19 p
(AD-A208710; AFGL-TR-88-0157; AFGL-ERP-1008) Avail: NTIS HC A03/MF A01 CSCL 04/1

AFWIND is a 2-D (xy plane) surface layer wind flow model for complex terrain. The model runs on most IBM compatible microcomputers with enhanced graphics capability. The model accepts single or multiple observations of surface winds. The model then performs a variational analysis of the wind field, adjusting the winds through a relaxation technique until the wind field conforms to effects of topography, stability, ambient flow conditions, and mass continuity. Atmospheric stability is determined from either date/time, wind speed, and cloud cover, or from vertical temperature profile measurements. The model is designed to produce high resolution wind analyses, typically running on domains on th order of 10 x 10 km, with horizontal grid spacing of 100 to 200 m. The structure of the computer code is described code and the input data requirements. An example run is given. GRA

N89-28110# Naval Ocean Systems Center, San Diego, CA.
AEROSOL MODEL SELECTION USING SURFACE MEASUREMENTS OF IR HORIZON RADIANCES AND SATELLITE DETECTED VISIBLE RADIANCES
Hubert G. Hughes and Douglas R. Jensen Jun. 1989 5 p
(AD-A209638) Avail: NTIS HC A02/MF A01 CSCL 04/1

In the absence of size distribution measurements, we must presently rely on the models in the LOWTRAN 6 code to calculate the effects of aerosols on atmospheric transmittances and background radiances using measured meteorological parameters as inputs. These aerosol models were developed to be as representative as possible to different atmospheric conditions. This model is the sum of three lognormal size distributions. In this publication a remote sensing technique is presented whereby an appropriate aerosol size distribution model can be selected which is applicable to transmittance and radiance calculations in both the visible and IR wave-length bands. GRA

N89-28111# Naval Research Lab., Washington, DC. Geophysical and Plasma Dynamics Branch.
SCALING LAWS FOR THE SPECTRUM OF INTERCHANGE INSTABILITIES IN THE HIGH LATITUDE IONOSPHERE Interim Report
M. J. Keskinen 15 Jun. 1989 27 p
(Contract MIPR-88-526)
(AD-A209993; NRL-MR-6481) Avail: NTIS HC A03/MF A01 CSCL 04/1

Constraints on and scaling laws associated with the power spectrum of interchange instabilities in the inertial regime in the high latitude ionosphere are derived using conservation laws implied by the fundamental nonlinear plasma fluid equations. Applications to large scale convecting high latitude ionospheric plasma density structures, patches, and enhancements are made. GRA

N89-28112# OptiMetrics, Inc., Burlington, MA.
A NEW BACKGROUND STRATOSPHERIC AEROSOL MODEL FOR USE IN ATMOSPHERIC RADIATION MODELS
John R. Hummel, Eric P. Shettle, and David R. Longtin 30 Jul. 1988 70 p
(Contract F19628-85-C-0178)
(AD-A210110; OMI-298; AFGL-TR-88-0166; SR-8) Avail: NTIS HC A04/MF A01 CSCL 04/1

The current background stratospheric aerosol model is based on laboratory measurements of indices of refraction for a solution of H2SO4 taken at 300 K and a size distribution based on a modified gamma distribution. Stratospheric temperatures are considerably colder than this. Also, recent satellite measurements indicate that a log normal size distribution is more representative of stratospheric aerosols. Therefore, a new background stratospheric aerosol model is presented based on temperature dependent indices of refraction and a log normal size distribution that is consistent with the literature. A set of indices of refraction have been calculated using Lorentz-Lorenz corrections and interpolated values of the available laboratory measurements of the index of refraction of a mixture of 75 percent H2SO4 in water. Indices of refraction at 215 K have been taken as representative of an averaged, midlatitude stratosphere. The log normal size distribution is based on recommendations from an experts meeting on aerosols and climatic effects held by the World Climate Programme. The proposed extinction coefficients are essentially unchanged for wavelengths up to about 5 microns. Above 5 microns, the proposed values are smaller than that in LOWTRAN 6. The differences are due almost entirely to changes in the absorption coefficient as a result of the smaller imaginary components of the index of refraction. Also, the results are insensitive to changes in size distribution. GRA

N89-27874*# Jet Propulsion Lab., California Inst. of Tech., Pasadena.
THE EFFECT OF SPATIAL AND TEMPORAL WET-TROPOSPHERE FLUCTUATIONS ON CONNECTED ELEMENT INTERFEROMETRY
C. D. Edwards *In its* The Telecommunications and Data

Acquisition Report 15 May 1989 p 47-57 (For primary document see N89-27871 22-32)
Avail: NTIS HC A17/MF A01 CSCL 04A

N89-27895*# Jet Propulsion Lab., California Inst. of Tech., Pasadena.
OPTIONS FOR DAYTIME MONITORING OF ATMOSPHERIC VISIBILITY IN OPTICAL COMMUNICATIONS
D. Erickson and K. Cowles *In its* The Telecommunications and Data Acquisition Report 15 May 1989 p 226-234 (For primary document see N89-27871 22-32)
Avail: NTIS HC A17/MF A01 CSCL 04A

N89-28133*# National Aeronautics and Space Administration. Goddard Space Flight Center, Greenbelt, MD.
THE EARTH RADIATION BUDGET EXPERIMENT Abstract Only
A. T. Mecherikunnel *In its* Laboratory for Oceans 1988 p 61-62 (For primary document see N89-28118 22-48)
Avail: NTIS HC A12/MF A01 CSCL 04A

N89-28167*# National Aeronautics and Space Administration. Goddard Space Flight Center, Greenbelt, MD.
ROCKET TEMPERATURE SOUNDINGS Abstract Only
F. J. Schmidlin *In its* Laboratory for Oceans 1988 p 185-187 (For primary document see N89-28118 22-48)
Avail: NTIS HC A12/MF A01 CSCL 04A

N89-28168*# National Aeronautics and Space Administration. Goddard Space Flight Center, Greenbelt, MD.
ELECTRODYNAMICS, WIND AND TEMPERATURE Abstract Only
F. J. Schmidlin *In its* Laboratory for Oceans 1988 p 189 (For primary document see N89-28118 22-48)
Avail: NTIS HC A12/MF A01 CSCL 04A

N89-28169*# National Aeronautics and Space Administration. Goddard Space Flight Center, Greenbelt, MD.
RADIOSONDE INTERCOMPARISON Abstract Only
F. J. Schmidlin *In its* Laboratory for Oceans 1988 p 191-193 (For primary document see N89-28118 22-48)
Avail: NTIS HC A12/MF A01 CSCL 04A

N89-28170*# National Aeronautics and Space Administration. Goddard Space Flight Center, Greenbelt, MD.
SATELLITE/RADIOSONDE COMPARISON Abstract Only
F. J. Schmidlin *In its* Laboratory for Oceans 1988 p 195 (For primary document see N89-28118 22-48)
Avail: NTIS HC A12/MF A01 CSCL 04A

N89-28172*# National Aeronautics and Space Administration. Goddard Space Flight Center, Greenbelt, MD.
CLOUD ABSORPTION RADIOMETER Abstract Only
M. G. Strange *In its* Laboratory for Oceans 1988 p 199-202 (For primary document see N89-28118 22-48)
Avail: NTIS HC A12/MF A01 CSCL 04A

47 METEOROLOGY AND CLIMATOLOGY

Includes weather forecasting and modification.

N89-28113*# Ohio State Univ., Columbus. Dept. of Physics.
ZONAL WINDS BETWEEN 25 AND 120 km RETRIEVED FROM SOLAR OCCULTATION SPECTRA Ph.D. Thesis Final Report
Garrett Warren vanCleef and John H. Shaw Jul. 1989 305 p Previously announced in IAA as A88-23175
(Grant NAGw-1129)
(NASA-CR-180086; NAS 1.26:180086) Avail: NTIS HC A14/MF A01 CSCL 04B

Atmospheric winds at heights between 25 and 120 km have been retrieved with precisions of 5/ms from the Doppler shifts of atmospheric absorption lines measured from a satellite-borne instrument. Lines of the upsilon 3 CO2 and upsilon 2 H2O rotation-vibration bands caused by gases in the instrument allowed the instrumental frequency scale to be absolutely calibrated so that accurate relative speeds could be obtained. By comparing the positions of both sets of instrumental lines the calibration of the frequency scale was determined to be stable to a precision of less than 2 x 10(-5) cm during the course of each occultation. It was found that the instrumental resolution of 0.015 cm after apodization, the signal to noise ratio of about 100 and stable calibration allowed relative speeds to be determined to a precision of 5 ms or better by using small numbers of absorption lines between 1600 and 3200 cm. Absolute absorption line positions were simultaneously recovered to precisions of 5 x 10(-5) cm or better. The wind speed profiles determined from four sunset occultations and one sunrise occultation show remarkable similarities in the magnitudes and directions of the zonal wind velocities as functions of height. These wind profiles appear to be manifestations of atmospheric tides. Author

N89-28114# Instituto de Pesquisas Espaciais, Sao Jose dos Campos (Brazil).
METEOROLOGY IN THE PRESS [A METEOROLOGIA NA IMPRENSA]
Beatriz Correa Pires Dornelles Dec. 1988 10 p In PORTUGESE Presented at the 5th Brazilian Conference on Meteorology, Rio de Janeiro, Brazil, 7-11 Nov. 1988
(INPE-4762-PRE/1432) Avail: NTIS HC A02/MF A01

Analysis of press coverage in the area of meteorology in the period 1983 to 1988 involves eight means of communication. The topic is subdivided into eight themes, not considering daily weather forecasts and non-scientific materials. Statistics, results, and conclusions are presented. Author

N89-28115*# Electro Magnetic Applications, Inc., Lakewood, CO.
INTERPRETATION OF F106B AND CV580 IN-FLIGHT LIGHTNING DATA AND FORM FACTOR DETERMINATION
T. Rudolph, J. Horembala, F. J. Eriksen, H. S. Weigel, J. R. Elliott, S. L. Parker, and R. A. Perala Washington Sep. 1989 156 p
(Contract NAS1-17748)
(NASA-CR-4250; NAS 1.26:4250; EMA-89-R-33) Avail: NTIS HC A08/MF A01 CSCL 04B

Two topics of in-flight aircraft/lightning interaction are addressed. The first is the analysis of measured data from the NASA F106B Thunderstorm Research Aircraft and the CV580 research program run by the FAA and Wright-Patterson Air Force Base. The CV580 data was investigated in a mostly qualitative sense, while the F106B data was subjected to both statistical and quantitative analysis using linear triggered lightning finite difference models. The second main topic is the analysis of field mill data and the calibration of the field mill systems. The calibration of the F106B field mill system was investigated using an improved finite difference model of the aircraft having a spatial resolution of one-quarter meter. The calibration was applied to measured field mill data acquired during the 1985 thunderstorm season. The experimental determination of form factors useful for field mill calibration was also investigated both experimentally and analytically. The experimental effort involved the use of conducting scale models and an electrolytic tank. An analytic technique was developed to aid in the understanding of the experimental results. Author

N89-28116# Research and Data Systems, Inc., Greenbelt, MD.
EVALUATION OF THE AFGL (AIR FORCE GEOPHYSICS LABORATORY) CLOUD SIMULATION MODELS USING SATELLITE DATA Final Report, 1 Apr. 1985 - 15 Oct. 1988
Joseph V. Fiore, Jr., Lanning M. Penn, and Gary Rasmussen (Analytic Sciences Corp., Reading, MA.) Dec. 1988 160 p
(Contract F19628-85-C-0007; AF Proj. 6670)
(AD-A208713; AFGL-TR-88-0328) Avail: NTIS HC A08/MF A01 CSCL 04/2

This report presents the results of the validation of three empirical models of the distribution of the total sky cover over lines and areas: the Burger Area Algorithm (BAA), Burger Line

Algorithm (BLA) and the Gringorten Interval Algorithm (GIA). The generation of a sky cover database from satellite imagery, the determination of appropriate sample size and the determination of goodness-of-fit error bounds are discussed. The models are run, and their output compared to empirical cloud cover distributions. Goodness-of-fit statistics are used to evaluate the results of the models. Conclusions and recommendations concerning the utility of the models are presented. GRA

N89-28117# Stanford Univ., CA. Dept. of Computer Science.
ADAPTIVE GRID METHODS FOR NUMERICAL WEATHER PREDICTION Final Report, 1 Mar. 1984 - 31 Dec. 1988
Joseph Oliger and Robert L. Street Jun. 1989 5 p
(Contract N00014-84-K-0267)
(AD-A209950) Avail: NTIS HC A02/MF A01 CSCL 04/2

The major objective of this project was to develop automatic adaptive grid methods for numerical weather prediction based upon computed error estimates. GRA

N89-27896*# Jet Propulsion Lab., California Inst. of Tech., Pasadena.
SITE SELECTION CRITERIA FOR THE OPTICAL ATMOSPHERIC VISIBILITY MONITORING TELESCOPES
K. Cowles *In its* The Telecommunications and Data Acquisition Report 15 May 1989 p 235-239 (For primary document see N89-27871 22-32)
Avail: NTIS HC A17/MF A01 CSCL 04B

N89-28121*# National Aeronautics and Space Administration. Goddard Space Flight Center, Greenbelt, MD.
BANGLADESH AGRO-CLIMATIC ENVIRONMENTAL MONITORING PROJECT Abstract Only
C. Vermillion, H. Maurer, M. Williams, J. Kamowski, T. Moore, W. Maksimovich, H. Obler, and E. Gilbert *In its* Laboratory for Oceans 1988 p 25-26 (For primary document see N89-28118 22-48)
Avail: NTIS HC A12/MF A01 CSCL 04B

N89-28122*# National Aeronautics and Space Administration. Goddard Space Flight Center, Greenbelt, MD.
NASA FOLLOW-ON TO THE BANGLADESH AGRO-CLIMATIC ENVIRONMENTAL MONITORING PROJECT Abstract Only
C. Vermillion, H. Maurer, M. Williams, M. DesJardins, E. Mollo-Christensen, C. D. Mason, A. Kerber, J. Gervin, and J. Elrod *In its* Laboratory for Oceans 1988 p 27 (For primary document see N89-28118 22-48)
Avail: NTIS HC A12/MF A01 CSCL 04B

N89-28123*# National Aeronautics and Space Administration. Goddard Space Flight Center, Greenbelt, MD.
FIJI SOUTH PACIFIC SEVERE STORM DETECTION AND WARNING SYSTEM PROJECT (SPSSD/WS) Abstract Only
C. Vermillion, H. Maurer, M. Williams, J. Kamowski, T. Moore, W. Maksimovich, and A. Hasler *In its* Laboratory for Oceans 1988 p 29-30 (For primary document see N89-28118 22-48)
Avail: NTIS HC A12/MF A01 CSCL 04B

N89-28124*# National Aeronautics and Space Administration. Goddard Space Flight Center, Greenbelt, MD.
NASA FOLLOW-ON ON THE FIJI SOUTH PACIFIC SEVERE STORM WARNING SYSTEM PROJECT (SPSSD/WS) Abstract Only
C. Vermillion, H. Maurer, M. Williams, J. Kamowski, T. Moore, W. Maksimovich, and A. Hasler *In its* Laboratory for Oceans 1988 p 31-33 (For primary document see N89-28118 22-48)
Avail: NTIS HC A12/MF A01 CSCL 04B

N89-28126*# National Aeronautics and Space Administration. Goddard Space Flight Center, Greenbelt, MD.
TROPICAL RAINFALL MEASUREMENT MISSION Abstract Only
T. T. Wilheit *In its* Laboratory for Oceans 1988 p 37-40 (For primary document see N89-28118 22-48)
Avail: NTIS HC A12/MF A01 CSCL 04B

N89-28127*# National Aeronautics and Space Administration. Goddard Space Flight Center, Greenbelt, MD.
SPACEBORNE METEOROLOGICAL RADAR STUDIES Abstract Only
R. Meneghini *In its* Laboratory for Oceans 1988 p 41-43 (For primary document see N89-28118 22-48)
Avail: NTIS HC A12/MF A01 CSCL 04B

N89-28151*# National Aeronautics and Space Administration. Goddard Space Flight Center, Greenbelt, MD.
SEA ICE/CLIMATE STUDIES Abstract Only
C. L. Parkinson *In its* Laboratory for Oceans 1988 p 123-125 (For primary document see N89-28118 22-48)
Avail: NTIS HC A12/MF A01 CSCL 04B

N89-28156*# National Aeronautics and Space Administration. Goddard Space Flight Center, Greenbelt, MD.
CLIMATOLOGICAL ASPECTS OF NIMBUS-7 SMMR DATA Abstract Only
P. Gloersen *In its* Laboratory for Oceans 1988 p 143-145 (For primary document see N89-28118 22-48)
Avail: NTIS HC A12/MF A01 CSCL 04B

N89-28160*# National Aeronautics and Space Administration. Goddard Space Flight Center, Greenbelt, MD.
RAINFALL ON MICROWAVE RETURN FROM THE SEA SURFACE Abstract Only
L. F. Bliven and J.-P. Giovanangeli *In its* Laboratory for Oceans 1988 p 157-158 (For primary document see N89-28118 22-48)
Avail: NTIS HC A12/MF A01 CSCL 04B

N89-28163*# National Aeronautics and Space Administration. Goddard Space Flight Center, Greenbelt, MD.
WATER VAPOR PROFILING USING MICROWAVE RADIOMETRY Abstract Only
J. R. Wang and T. T. Wilheit *In its* Laboratory for Oceans 1988 p 165-167 (For primary document see N89-28118 22-48)
Avail: NTIS HC A12/MF A01 CSCL 04B

N89-28188*# National Aeronautics and Space Administration. Goddard Space Flight Center, Greenbelt, MD.
METEOROLOGICAL SENSOR CALIBRATION FACILITY Abstract Only
F. J. Schmidlin *In its* Laboratory for Oceans 1988 p 263-265 (For primary document see N89-28118 22-48)
Avail: NTIS HC A12/MF A01 CSCL 04B

48 OCEANOGRAPHY

Includes biological, dynamic, and physical oceanography; and marine resources.

For related information see also *43 Earth Resources and Remote Sensing.*

N89-28118*# National Aeronautics and Space Administration. Goddard Space Flight Center, Greenbelt, MD.
LABORATORY FOR OCEANS Activities Report, Feb. - Apr. 1988 Abstracts Only
1988 272 p
(NASA-TM-101257; NAS 1.15:101257) Avail: NTIS HC A12/MF A01 CSCL 20L

A review is made of the activities of the Laboratory for Oceans. The staff and the research activities are nearly evenly divided between engineering and scientific endeavors. The Laboratory contributes engineering design skills to aircraft and ground based experiments in terrestrial and atmospheric sciences in cooperation with scientists from labs in Earth sciences. For individual titles, see N89-28119 through N89-28194.

N89-28119*# National Aeronautics and Space Administration. Goddard Space Flight Center, Greenbelt, MD.
OCEAN TOPOGRAPHY EXPERIMENT (TOPEX) RADAR ALTIMETER Abstract Only **c32**
L. C. Rossi, D. W. Hancock, and G. S. Hayne *In its* Laboratory for Oceans 1988 p 19-21 (For primary document see N89-28118 22-48)
Avail: NTIS HC A12/MF A01 CSCL 17I

A spaceflight qualified Radar Altimeter capable of achieving the TOPEX Mission measurement precision requirement of 2-centimeters, is provided and its performance (Engineering Assessment) will be evaluated after launch and continuously during its 3-year mission operational period. Information will be provided to JPL about the calibration of the TOPEX Radar Altimeter. The specifications for the required data processing algorithms which will be necessary to convert the Radar Altimeter mission telemetry data into the geophysical data will also be provided. The stringent 2 cm precision requirement for ocean topography determination from space necessitated examining existing Radar Altimeter designs for their applicability towards TOPEX. As a result, a system configuration evolved using some flight proven designs in conjunction with needed improvements which include: (1) a second frequency or channel to remove the range delay or apparent height bias caused by the electron content of the ionosphere; (2) higher transmit pulse repetition frequencies for correlation benefits at higher sea states to maintain precision; and (3) a faster microprocessor to accommodate two channels of altimetry data. Additionally, examination of past altimeter programs associated data processing algorithms was accomplished to establish the TOPEX-class Radar Altimeter data processing algorithms, and the necessary direction was outlined to begin to generate these for the TOPEX Mission. Author

N89-28120*# National Aeronautics and Space Administration. Goddard Space Flight Center, Greenbelt, MD.
MARS OBSERVER RADAR ALTIMETER RADIOMETER (MORAR) Abstract Only **c32**
L. C. Rossi, D. W. Hancock, and G. S. Hayne *In its* Laboratory for Oceans 1988 p 23-24 (For primary document see N89-28118 22-48)
Avail: NTIS HC A12/MF A01 CSCL 17I

The Mars Observer Project will permit the advancement of the state of the topographic and hypsometric knowledge of Mars to a level of 10 m or better over the surface of the planet Mars, the measurement of microwave surface brightness temperature of Mars with an accuracy of 15 to 20 K over 24 hours, and the measurement, globally, of surface returned power related to radar cross section with an accuracy of 1 dB and a repeatability of .5 dB. The MORAR Hardware Development, Ground Data Processing, and the Mission Operations will allow the accomplishment of these scientific objectives to define globally the topography of Mars at sufficient vertical resolution and spatial scale to address both large-scale geophysical and small-scale geologic problems, and to obtain global surface electrical and scattering properties of the upper several centimeters of the Martian surface for assessment of the composition, physical state, and volatile distribution of the surface. Author

N89-28121*# National Aeronautics and Space Administration. Goddard Space Flight Center, Greenbelt, MD.
BANGLADESH AGRO-CLIMATIC ENVIRONMENTAL MONITORING PROJECT Abstract Only **c47**
C. Vermillion, H. Maurer, M. Williams, J. Kamowski, T. Moore, W. Maksimovich, H. Obler, and E. Gilbert *In its* Laboratory for Oceans 1988 p 25-26 (For primary document see N89-28118 22-48)
Avail: NTIS HC A12/MF A01 CSCL 04B

The Agro-Climatic Environmental Monitoring Project (ACEMP) is based on a Participating Agency Service Agreement (PASA) between the Agency for International Development (AID) and the National Oceanic and Atmospheric Administration (NOAA). In FY80, the Asia Bureau and Office of Federal Disaster Assistance (OFDA), worked closely to develop a funding mechanism which would meet Bangladesh's needs both for flood and cyclone warning capability and for application of remote sensing data to development problems. In FY90, OFDA provided for a High Resolution Picture Transmission (HRPT) receiving capability to improve their forecasting accuracy for cyclones, flooding and storm surges. That equipment is primarily intended as a disaster prediction and preparedness measure. The ACEM Project was designed to focus on the development applications of remote sensing technology. Through this Project, AID provided to the Bangladesh Government (BDG) the equipment, technical assistance, and training necessary to collect and employ remote sensing data made available by satellites as well as hydrological data obtained from data collection platforms placed in major rivers. The data collected will enable the BDG to improve the management of its natural resources. Author

N89-28122*# National Aeronautics and Space Administration. Goddard Space Flight Center, Greenbelt, MD.
NASA FOLLOW-ON TO THE BANGLADESH AGRO-CLIMATIC ENVIRONMENTAL MONITORING PROJECT Abstract Only **c47**
C. Vermillion, H. Maurer, M. Williams, M. DesJardins, E. Mollo-Christensen, C. D. Mason, A. Kerber, J. Gervin, and J. Elrod *In its* Laboratory for Oceans 1988 p 27 (For primary document see N89-28118 22-48)
Avail: NTIS HC A12/MF A01 CSCL 04B

The NASA responsibility and activities for the follow-on to the original Agro-Climatic Environmental Monitoring Project (ACEMP) which was completed during 1987 is described. Five training sessions which comprise the NASA ACEMP follow-on are: Agrometeorology, Meteorology of Severe Storms Using GEMPAK, Satellite Oceanography, Hydrology, and Meteorology with TOVS. The objective of the follow-on is to train Bangladesh Government staff in the use of satellite data for remote sensing applications. This activity also encourages the scientific connection between NASA/Goddard Space Flight Center and The Bangladesh Space and Remote Sensing Organization (SPARRSO). Author

N89-28123*# National Aeronautics and Space Administration. Goddard Space Flight Center, Greenbelt, MD.
FIJI SOUTH PACIFIC SEVERE STORM DETECTION AND WARNING SYSTEM PROJECT (SPSSD/WS) Abstract Only **c47**
C. Vermillion, H. Maurer, M. Williams, J. Kamowski, T. Moore, W. Maksimovich, and A. Hasler *In its* Laboratory for Oceans 1988 p 29-30 (For primary document see N89-28118 22-48)
Avail: NTIS HC A12/MF A01 CSCL 04B

In August 1986, a South Pacific Severe Storm Detection and Warning System (SPSSD/WS) was installed by NASA at the Fiji Meteorological Service (FMS) in Nadi, Fiji. The system consists of a 6.1 meter parabolic dish antenna, a satellite ground station, and computer and image processing facilities. The system allows tracking of all South Pacific tropical cyclones with real-time, high resolution reception of visible and infrared cloud images from both the Japanese Geostationary Meteorological Satellite (GMS) and the U.S. Geostationary Operational Environmental Satellite (GOES-WEST). Training was also provided in system usage and operations. In December 1986, the U.S. AID Office of U.S. Foreign Disaster Assistance (OFDA) commissioned an evaluation of the SPSSD/WS. The system was recognized as one of the most advanced of its kind in the Pacific Basin. It has functioned successfully since installation with only minor interruptions, and it has become the prime tool in supporting the FMS' role as the regional tropical cyclone warning center for the Southwest Pacific. However, it was noted that there are needed enhancements to the system. Author

N89-28124*# National Aeronautics and Space Administration. Goddard Space Flight Center, Greenbelt, MD.
NASA FOLLOW-ON ON THE FIJI SOUTH PACIFIC SEVERE STORM WARNING SYSTEM PROJECT (SPSSD/WS) Abstract Only **c47**
C. Vermillion, H. Maurer, M. Williams, J. Kamowski, T. Moore, W.

Maksimovich, and A. Hasler *In its* Laboratory for Oceans 1988 p 31-33 (For primary document see N89-28118 22-48)
Avail: NTIS HC A12/MF A01 CSCL 04B

The follow-on agreement will implement needed systems enhancements of the satellite ground station installed under the previous SPSSD/WS project. These enhancements include the purchase and installation of an Uninterruptible Power Supply (UPS) and lightning protection unit, hardware modifications to provide system redundancy and increased data storage capacity, software modifications for the new Japanese GMS digital data, upgrades of the image processing software, and both hardware maintenance and tropical cyclone analysis training, and a non-renewable grant to provide emergency field repairs and replacement/spare parts. In March 1988, the UPS and lightning protection unit was installed at the Fiji Meteorological Service by NASA personnel. A tape recorder and demodulator was shipped to Fiji to record the new digital GMS data. Data tapes are not yet available from the Japanese Meteorological Service of the new digital format. This data is required to test the GMS digital software being developed for the Fiji SPSSD/WS facility. Author

N89-28125*# National Aeronautics and Space Administration. Goddard Space Flight Center, Greenbelt, MD.
MONOCULAR ELECTRO-OPTICAL STEREO SCANNER Abstract Only **c35**
C. Vermillion, H. Maurer, V. Salomonson, C. Cote, J. Catena, H. Rampariyan, and J. Smith *In its* Laboratory for Oceans 1988 p 35-36 (For primary document see N89-28118 22-48)
Avail: NTIS HC A12/MF A01 CSCL 14B

MEOSS is a single optics and single spectral band camera. Three CCD's working in pushbroom mode are mounted perpendicular to the flight direction on a common focal plate. Their oblique views of + and - 23 degrees forward and backward, as well as nadir oriented, lead to threefold stereoscopic images. This principle allows a nearly simultaneous generation of all three images of a stereo triplet. The time gap between the forward and aft looking images guarantees constant illumination conditions. The ground resolution of MEOSS will be 52 by 80 m ground pixel size, height resolution of 55 m and swath width of 255 km. The drifting ground coverage pattern of MEOSS is unique compared to polar orbiting satellites and will allow images of an area to be taken at different times of the day. A scene will consist of 3144 scan lines, with each having 3236 pixels. The data will be received by the Deep Space Network of JPL Goldstone and mailed to Goddard. Author

N89-28126*# National Aeronautics and Space Administration. Goddard Space Flight Center, Greenbelt, MD.
TROPICAL RAINFALL MEASUREMENT MISSION Abstract Only **c47**
T. T. Wilheit *In its* Laboratory for Oceans 1988 p 37-40 (For primary document see N89-28118 22-48)
Avail: NTIS HC A12/MF A01 CSCL 04B

It has long been noted that anomalies in the sea surface temperature (SST) in the tropics are strongly correlated with climate in the temperate latitudes on a seasonal time scale. The ability to measure the global SST and the atmospheric pressure/temperature patterns has made great progress. However, rainfall measurement, the putative connection between the two, is poorly accomplished. The Tropical Rainfall Measurement Mission (TRMM) was conceived to fill this gap. The TRMM spacecraft would fly in a low inclination, (about 35 deg), orbit which would concentrate the sampling in the very important tropical latitudes. The precession of such an orbit would enable observations at all times of the day over the span of a month which would permit corrections for the diurnal cycle of precipitation which is quite marked in parts of the tropics. The payload of the TRMM spacecraft is carefully designed to provide accurate measurements of rain. It consists of microwave radiometers, a microwave radar and visible/infrared radiometer. The two types of microwave instruments provide direct measurements of the hydrometeors, each having strengths which compensate for weaknesses of the other. The VIS/IR instrument provides a connection to the long time series of VIS/IR measurements from polar and Geosynchronous spacecraft which are currently the best available source of global rainfall estimates. The TRMM is currently in a phase A (feasibility) study. Author

N89-28127*# National Aeronautics and Space Administration. Goddard Space Flight Center, Greenbelt, MD.
SPACEBORNE METEOROLOGICAL RADAR STUDIES Abstract Only **c47**
R. Meneghini *In its* Laboratory for Oceans 1988 p 41-43 (For primary document see N89-28118 22-48)
Avail: NTIS HC A12/MF A01 CSCL 04B

Various radar designs and methods are studied for the estimation of rainfall parameters from space. An immediate goal is to support the development of the spaceborne radar that has been proposed for the Tropical Rain Measuring Mission (TRMM). The effort is divided into two activities: a cooperative airborne rain measuring experiment with the Radio Research Laboratory of Japan (RRL), and the modelling of spaceborne weather radars. An airborne rain measuring experiment was conducted at Wallops Flight Facility in 1985 to 1986 using the dual-wavelength radar/radiometer developed by RRL. The data are presently being used to test a number of methods that are relevant to spaceborne weather radars. An example is shown of path-averaged rain rates as estimated from three methods: the standard reflectivity rain rate method (Z-R), a dual-wavelength method, and a surface reference method. The results from the experiment shows for the first time the feasibility of using attenuation methods from space. The purposes of the modelling are twofold: to understand in a quantitative manner the relationships between a particular radar design and its capability for estimating precipitation parameters and to help devise and test new methods. The models are being used to study the impact of various TRMM radar designs on the accuracy of rain rate estimation as well as to test the performance of range-profiling algorithms, the mirror-image method, and some recently devised graphical methods for the estimation of the drop size distribution. Author

N89-28128*# National Aeronautics and Space Administration. Goddard Space Flight Center, Greenbelt, MD.
ADVANCED ALTIMETRY Abstract Only **c35**
C. L. Parsons, S. A. Bailey, D. E. Hines, D. W. Shirk, C. W. Wright, and A. R. Selser *In its* Laboratory for Oceans 1988 p 45-47 (For primary document see N89-28118 22-48)
Avail: NTIS HC A12/MF A01 CSCL 14B

The radar altimeter being developed for the Ocean Topography Experiment (TOPEX) will have an inherent instrument precision of 2 to 3 cm. While some minor refinements may be possible in the future, major geophysical advances could be made if altimetric measurements over a wide swath of the Earth's surface were possible. The NASA Headquarters Oceanic Processes Branch is supporting a 3-year investigation of the technological issues inherent in the precision measurement of topography from spaceborne platforms at angles off-nadir. To explore the off-nadir measurement of topography, a flexible, airborne radar instrument system is being developed. Its hardware design is now complete, and it is made up of several subsystems. The antenna selected is a dielectric lens of .894 m diameter. The RF subsystem uses phase-locked oscillators, FET solid-state amplifiers, and times four frequency multipliers to develop a transmit signal at a frequency of 36.0 GHz and a local oscillator signal at a frequency of 35.4 GHz. Lecroy 6880 digitizers under computer control digitize the five receiver outputs. The digital subsystem consists of six single-board Heurikon processors. At this time, the instrument construction continues with final system integration planned for November 1988. Author

N89-28129*# National Aeronautics and Space Administration. Goddard Space Flight Center, Greenbelt, MD.
EARTH OBSERVING SYSTEM (EOS) ADVANCED ALTIMETRY Abstract Only **c35**
C. L. Parsons and E. J. Walsh *In its* Laboratory for Oceans 1988 p 49-51 (For primary document see N89-28118 22-48)
Avail: NTIS HC A12/MF A01 CSCL 14B

In the post-TOPEX era, satellite radar altimeters will be developed with the capability of measuring the earth's surface topography over a wide swath of coverage, rather than just at the satellite's nadir. The identification of potential spacecraft flight missions in the future was studied. The best opportunity was found to be the Earth Observing System (EOS). It is felt that an instrument system that has a broad appeal to the earth sciences community stands a much better chance of being selected as an EOS instrument. Consequently, the Topography and Rain Radar Imager (TARRI) will be proposed as a system that has the capability to profile the Earth's topography regardless of the surface type. The horizontal and height resolutions of interest are obviously significantly different over land, ice, and water; but, the use of radar to provide an all-weather observation capability is applicable to the whole earth. The scientific guidance for the design and development of this instrument and the eventual scientific utilization of the data produced by the TARRI will be provided by seven science teams. The teams are formed around scientific disciplines and are titled: Geology/Geophysics, Hydrology/Rain, Oceanography, Ice/Snow, Geodesy/Orbit/Attitude, Cartography, and Surface Properties/Techniques. Author

N89-28130*# National Aeronautics and Space Administration. Goddard Space Flight Center, Greenbelt, MD.
WIDE BAND DATA COLLECTION SYSTEM Abstract Only c43
J. M. Turkiewicz *In its* Laboratory for Oceans 1988 p 53-56 (For primary document see N89-28118 22-48)
Avail: NTIS HC A12/MF A01 CSCL 08B

The Incorporated Research Institutes for Seismology (IRIS) approached NASA Headquarters in 1986 about the need to collect data daily from seismic stations around the world as part of the Earth Observing System (EOS) mission. A typical IRIS Seismic Station generates 16 Megabytes of data per day when there is seismic activity. The Preliminary Design Parameters of the Wide Band Data Collection System are summarized. Author

N89-28131*# National Aeronautics and Space Administration. Goddard Space Flight Center, Greenbelt, MD.
CALIBRATION SUPPORT FOR THE EARTH OBSERVING SYSTEM PROJECT Abstract Only c43
B. W. Guenther *In its* Laboratory for Oceans 1988 p 57 (For primary document see N89-28118 22-48)
Avail: NTIS HC A12/MF A01 CSCL 08B

The Earth Observing System Project (EOS) program guidelines establishes significantly more stringent requirements on calibrations of instruments. This requirement is driven by the need for long-term continuity of acquired data sets and the use of measurements in interdisciplinary investigations. Personnel from the Standards and Calibration Office have been supporting the Program and Project in interpreting these goals into specific requirements. Contributions to EOS have included participation in the Panel of Experts which produced a list of consensus items necessary for accomplishing an accurate calibration and suggested EOS Project Calibration Policy, and drafting the announcement of opportunity and bidders information package positions on instrument calibration and data product validation. Technical staffing was provided to the NASA delegates to the Committee on Earth Orbiting Satellites (club of space-faring nations) for the standing working group on Calibration and Data Validation. Author

N89-28132*# National Aeronautics and Space Administration. Goddard Space Flight Center, Greenbelt, MD.
OCEANOGRAPHIC WIDE FIELD SENSOR Abstract Only c35
R. G. Kirk *In its* Laboratory for Oceans 1988 p 59-60 (For primary document see N89-28118 22-48)
Avail: NTIS HC A12/MF A01 CSCL 14B

The Oceanographic Wide Field Sensor (SeaWiFS) science project will provide measurements of ocean color from space to which will support research into: (1) the character of ocean physical and biological processes; (2) to assess the global oceanic biomass; and (3) to better understand the role of oceanic processes in modulating the Earth's biogeochemical cycles, including the CO2 cycle as it is affected by fossil fuel combustion. The present work extends previous work to study the feasibility of an ocean color mission using the proposed compact Wide-Field Sensor (SeaWiFS) and the EOSAT Corporation's LANDSAT-6 satellite. A Phase A study was conducted which defines a NASA Facility Data System and accompanying Science Program for the EOSAT Company's commercial ocean color instrument called SeaWiFS to be launched on board LANDSAT-6 in 1991. Author

N89-28133*# National Aeronautics and Space Administration. Goddard Space Flight Center, Greenbelt, MD.
THE EARTH RADIATION BUDGET EXPERIMENT Abstract Only c46
A. T. Mecherikunnel *In its* Laboratory for Oceans 1988 p 61-62 (For primary document see N89-28118 22-48)
Avail: NTIS HC A12/MF A01 CSCL 04A

The Earth Radiation Budget Experiment (ERBE) data studied at present are as follows: (1) Solar Data from ERBS, NOAA-9, and NOAA-10. The solar total irradiance data obtained by the ERBE solar monitors serve as a calibration check on the earth viewing radiometers, as well as provide the experimental value of the solar constant needed in the net radiation computations. (2) The collocated satellite altitude irradiances from ERBS and Nimbus-7 Earth Radiation Budget Measurements are investigated. The sun-synchronous, near-local-noon Nimbus-7 satellite has coincident orbital intersections with the non-sun-synchronous ERBS spacecraft. The objective here is to compare the WFOV and MFOV (wide and medium field-of-view) observations of the ERBS/ERBE, and the Nimbus-7 ERB data sets at the points of their orbital intersections. (3) Globally and zonally averaged ERBE/ERBS data are examined. Investigations of the globally and zonally averaged ERB obtained from the ERBS SCANNER, MFOV and WFOV and the Nimbus-7 WFOV is being carried out to assess the sensor performance. Author

N89-28134*# National Aeronautics and Space Administration. Goddard Space Flight Center, Greenbelt, MD.
LUNAR OBSERVER LASER ALTIMETER Abstract Only c36
J. L. Bufton *In its* Laboratory for Oceans 1988 p 63-65 (For primary document see N89-28118 22-48)
Avail: NTIS HC A12/MF A01 CSCL 20E

Understanding the global topography of the Moon is especially important for answering questions concerning lunar origin and evolution. Many outstanding problems in lunar science can be addressed with high resolution topographic data. The severe power, mass, size, and data-rate limitations imposed by the Lunar Geoscience Observer (LGO) and other Observer-class missions are major challenges for all instruments capable of measuring topography. A radar altimeter that meets these strict requirements could obtain a global prespective of lunar topography with a few kilometers spatial resolution and 10 m vertical resolution from a lunar orbit of 100 km. A prototype model is being constructed of the Lunar Observer Laser Altimeter (LOLA) capable of continuously measuring the range to the lunar surface with sub-meter vertical resolution within a 30 to 300 m diameter surface footprint. This same instrument is also designed to provide a direct measure of the surface height distribution in the footprint by waveform analysis of the backscattered laser pulse. Both these measurements are to be made in a continuous, nadir profile across the lunar surface from a 100 km orbit. The wavelength of the altimeter is 1064 nm. A short-pulse (2 nsec), diode-pumped Nd:YAG laser combined with a 25 cm diameter telescope, silicon avalanche photodiode detector, ranging electronics, and instrument computer was designed to make these measurements and meet all the requirements of the LGO mission. Author

N89-28135*# National Aeronautics and Space Administration. Goddard Space Flight Center, Greenbelt, MD.
YAG AEROSOL LIDAR Abstract Only c36
R. Sullivan *In its* Laboratory for Oceans 1988 p 67-68 (For primary document see N89-28118 22-48)
Avail: NTIS HC A12/MF A01 CSCL 20E

The Global Atmospheric Backscatter Experiment (GLOBE) Mission, using the NASA DC-8 aircraft platform, is designed to

provide the magnitude and statistical distribution of atmospheric backscatter cross section at lidar operating wavelengths. This is a fundamental parameter required for the Doppler lidar proposed to be used on a spacecraft platform for global wind field measurements. The prime measurements will be made by a CO2 lidar instrument in the 9 to 10 micron range. These measurements will be complemented with the Goddard YAG Aerosol Lidar (YAL) data in two wavelengths, 0.532 and 1.06 micron, in the visible and near-infrared. The YAL, is being designed to utilize as much existing hardware, as feasible, to minimize cost and reduce implementation time. The laser, energy monitor, telescope and detector package will be mounted on an optical breadboard. The optical breadboard is mounted through isolation mounts between two low boy racks. The detector package will utilize a photomultiplier tube for the 0.532 micron channel and a silicon avalanche photo detector (APD) for the 1.06 micron channel.
Author

N89-28136*# National Aeronautics and Space Administration. Goddard Space Flight Center, Greenbelt, MD.
APPLICATIONS OF THE COASTAL ZONE COLOR SCANNER IN OCEANOGRAPHY Abstract Only
C. R. McClain *In its* Laboratory for Oceans 1988 p 71-72 (For primary document see N89-28118 22-48)
Avail: NTIS HC A12/MF A01 CSCL 08C

Research activity has continued to be focused on the applications of the Coastal Zone Color Scanner (CZCS) imagery in oceanography. A number of regional studies were completed including investigations of temporal and spatial variability of phytoplankton populations in the South Atlantic Bight, Northwest Spain, Weddell Sea, Bering Sea, Caribbean Sea and in tropical Atlantic Ocean. In addition to the regional studies, much work was dedicated to developing ancillary global scale meteorological and hydrographic data sets to complement the global CZCS processing products. To accomplish this, SEAPAK's image analysis capability was complemented with an interface to GEMPAK (Severe Storm Branch's meteorological analysis software package) for the analysis and graphical display of gridded data fields. Plans are being made to develop a similar interface to SEAPAK for hydrographic data using EPIC (a hydrographic data analysis package developed by NOAA/PMEL). Author

N89-28137*# National Aeronautics and Space Administration. Goddard Space Flight Center, Greenbelt, MD.
OCEAN COLOR OBSERVATIONS OF PHYTOPLANKTON DISTRIBUTIONS AND PRIMARY PRODUCTIVITY Abstract Only
W. Esaias *In its* Laboratory for Oceans 1988 p 73-75 (For primary document see N89-28118 22-48)
Avail: NTIS HC A12/MF A01 CSCL 08C

The primary goal of this activity is to develop the means to assess the mean and variability of phytoplankton biomass and primary productivity on global scales. There are three major approaches whose goals are to provide global scale observations. These are processing and analysis of the complete CZCS data set in a consistent manner; preparing science mission and project implementation plans for the SeaWiFS sensor to be launched on LANDSAT 6 in 1991; and providing guidance to EOS flight projects for ocean color observations using the MODIS sensor planned for the Polar Platform in the mid 1990's. This processing presents the first consistent view of phytoplankton pigments on global scales, and analysis of this temporally undersampled data set is proving very instructive in specifying mission requirements for SeaWiFS and future algorithm development. Author

N89-28138*# National Aeronautics and Space Administration. Goddard Space Flight Center, Greenbelt, MD.
COASTAL ZONE COLOR SCANNER STUDIES Abstract Only
J. Elrod *In its* Laboratory for Oceans 1988 p 77 (For primary document see N89-28118 22-48)
Avail: NTIS HC A12/MF A01 CSCL 08C

Activities over the past year have included cooperative work with a summer faculty fellow using the Coastal Zone Color Scanner (CZCS) imagery to study the effects of gradients in trophic resources on coral reefs in the Caribbean. Other research included characterization of ocean radiances specific to an acid-waste plume. Other activities include involvement in the quality control of imagery produced in the processing of the global CZCS data set, the collection of various other data global sets, and the subsequent data comparison and analysis. Author

N89-28139*# National Aeronautics and Space Administration. Goddard Space Flight Center, Greenbelt, MD.
REMOTE SENSING OF OCEAN COLOR IN THE ARCTIC Abstract Only
N. G. Maynard *In its* Laboratory for Oceans 1988 p 79-80 (For primary document see N89-28118 22-48)
Avail: NTIS HC A12/MF A01 CSCL 08C

The main objectives of the research are: to increase the understanding of biological production (and carbon fluxes) along the ice edge, in frontal regions, and in open water areas of the Arctic and the physical factors controlling that production through the use of satellite and aircraft remote sensing techniques; and to develop relationships between measured radiances from the Multichannel Aircraft Radiometer System (MARS) and the bio-optical properties of the water in the Arctic and adjacent seas. Several recent Coastal Zone Color Scanner (CZCS) studies in the Arctic have shown that, despite constraints imposed by cloud cover, satellite ocean color is a useful means of studying mesoscale physical and biological oceanographic phenomena at high latitudes. The imagery has provided detailed information on ice edge and frontal processes such as spring breakup and retreat of the ice edge, influence of ice on ice effects of stratification on phytoplankton production, river sediment transport, effects of spring runoff, water mass boundaries, circulation patterns, and eddy formation in Icelandic waters and in the Greenland, Barents, Norwegian, and Bering Seas. Author

N89-28140*# National Aeronautics and Space Administration. Goddard Space Flight Center, Greenbelt, MD.
AIRBORNE IN-SITU SPECTRAL CHARACTERIZATION AND CONCENTRATION ESTIMATES OF FLUORESCENT ORGANICS AS A FUNCTION OF DEPTH Abstract Only
R. A. Tittle *In its* Laboratory for Oceans 1988 p 81-83 (For primary document see N89-28118 22-48)
Avail: NTIS HC A12/MF A01 CSCL 08C

The primary purpose of many in-situ airborne light scattering experiments in natural waters is to spectrally characterize the subsurface fluorescent organics and estimate their relative concentrations. This is often done by shining a laser beam into the water and monitoring its subsurface return signal. To do this with the proper interpretation, depth must be taken into account. If one disregards depth dependence when taking such estimates, both their spectral characteristics and their concentrations estimates can be rather ambiguous. A simple airborne lidar configuration is used to detect the subsurface return signal from a particular depth and wavelength. Underwater scatterometer were employed to show that in-situ subsurface organics are very sensitive to depth, but they also require the use of slow moving boats to cover large sample areas. Also, their very entry into the water disturbs the sample it is measuring. The method described is superior and simplest to any employed thus far. Author

N89-28141*# National Aeronautics and Space Administration. Goddard Space Flight Center, Greenbelt, MD.
OCEANOGRAPHIC APPLICATIONS OF LASER TECHNOLOGY Abstract Only **c36**
F. E. Hoge *In its* Laboratory for Oceans 1988 p 85-94 (For primary document see N89-28118 22-48)
Avail: NTIS HC A12/MF A01 CSCL 20E

Oceanographic activities with the Airborne Oceanographic Lidar (AOL) for the past several years have primarily been focussed on using active (laser induced pigment fluorescence) and concurrent passive ocean color spectra to improve existing ocean color algorithms for estimating primary production in the world's oceans. The most significant results were the development of a technique

for selecting optimal passive wavelengths for recovering phytoplankton photopigment concentration and the application of this technique, termed active-passive correlation spectroscopy (APCS), to various forms of passive ocean color algorithms. Included in this activity is use of airborne laser and passive ocean color for development of advanced satellite ocean color sensors. Promising on-wavelength subsurface scattering layer measurements were recently obtained. A partial summary of these results are shown.
Author

N89-28142*# National Aeronautics and Space Administration. Goddard Space Flight Center, Greenbelt, MD.
NASA CHARGE COUPLED DEVICE (CCD) SPECTROMETER SYSTEM (NCSS) Abstract Only **c35**
C. W. Wright, S. A. Bailey, and C. R. Piazza *In its* Laboratory for Oceans 1988 p 91-94 (For primary document see N89-28118 22-48)
Avail: NTIS HC A12/MF A01 CSCL 14B

A small lightweight NCSS was designed, constructed, and is now being bench tested at Wallops. The unit provides 256, 2.7 nm wide channels in the visible spectrum from approximately 400 to 1100 nm. The present input slit provides a spectral impulse response of about 10 nm. Up to five NCSS sensors may be bused to one data system interface. The NCSS contains a high speed, 16 bit analog to digital converter (ADC) with an integral wide-band sample-and-hold amplifier. The NCSS was developed primarily for use with the Airbone Oceanographic Lidar (AOL). A prototype NCSS is presently interfaced to the AOL. The AOL will use two new NCSS units onboard the Goddard P-3A aircraft. They will provide the AOL with high resolution sky and ocean spectra. The up-looking NCSS will provide the AOL data system (AOLDS) with down-welling solar radiance, and the down-looking NCSS will provide ocean color spectra. The solar radiance will be used to correct various ocean color algorithms now being researched.
Author

N89-28143*# National Aeronautics and Space Administration. Goddard Space Flight Center, Greenbelt, MD.
AIRBORNE OCEANOGRAPHIC LIDAR (AOL) FLIGHT MISSION PARTICIPATION Abstract Only **c36**
F. E. Hoge *In its* Laboratory for Oceans 1988 p 95-97 (For primary document see N89-28118 22-48)
Avail: NTIS HC A12/MF A01 CSCL 20E

From February 1986 to the present, the AOL participated in six interagency flight missions. (1) Shelf Edge Exchange Processes (SEEP II) (Department of Energy). The SEEP experiments are designed to assess the assimilative capacity of the Continental Shelf to absorb the energy by-products introduced into the near-shore ocean environment from coastal communities and marine activities such as energy production plants and offshore oil operations. (2) BIOWATT II (Office of Naval Research). The major objective of this study was to provide a better understanding of the relationships between ocean physics, biology, bioluminescence, and optics in oligotrophic portions of the Atlantic Ocean. (3) Fall Experiment (FLEX) (Department of Energy). The FLEX studies were designed to determine the fate of low salinity water in the coastal boundary zone that is advected south towards the Florida coast during autumn. (4) Greenland Sea and Icelandic Marine Biological Experiments (NASA). The investigations were designed to evaluate the distribution of surface layer chlorophyll in the Greeland Sea and in the coastal waters in the vicinity of Iceland. (5) Submerged Oceanic Scattering Layer Experiment (Naval Ocean Systems Center). This flight experiment demonstrated for the first time the feasibility of detecting and metrically measuring the depth to submerged layers of particulate matter in the shelf break region and in the inner coastal zone. (6) Microbial Exchanges and Coupling in Coastal Atlantic Systems (National Science Foundation). This investigation was designed to study the transportation and fate of particulates in coastal waters and in particular the Chesapeake Bay/coastal Atlantic Ocean. Shortly after the conduct of the flight experiments, airborne laser-induced chlorophyll a and phycoerythrin fluorescence data, as well as sea surface temperature and airborne expendable bathythermograph water column temperature profiles are supplied to cooperating institutions.
Author

N89-28144*# National Aeronautics and Space Administration. Goddard Space Flight Center, Greenbelt, MD.
OCEAN DATA ACQUISITION SYSTEM Abstract Only
B. Johnson, J. Cavanaugh, J. Smith, and W. Esaias *In its* Laboratory for Oceans 1988 p 99-100 (For primary document see N89-28118 22-48)
Avail: NTIS HC A12/MF A01 CSCL 08C

The Ocean Data Acquisition System (ODAS) is a low cost instrument with potential commercial application. It is easily mounted on a small aircraft and flown over the coastal zone ocean to remotely measure sea surface temperature and three channels of ocean color information. From this data, chlorophyll levels can be derived for use by ocean scientists, fisheries, and environmental offices. Data can be transmitted to shipboard for real-time use with sea truth measurements, ocean productivity estimates and fishing fleet direction. The aircraft portion of the system has two primary instruments: an IR radiometer to measure sea surface temperature and a three channel visible spectro-radiometer for 460, 490, and 520 nm wavelength measurements from which chlorophyll concentration can be derived. The aircraft package contains a LORAN-C unit for aircraft location information, clock, on-board data processor and formatter, digital data storage, packet radio terminal controller, and radio transceiver for data transmission to a ship. The shipboard package contains a transceiver, packet terminal controller, data processing and storage capability, and printer. Both raw data and chlorophyll concentrations are available for real-time analysis.
Author

N89-28145*# National Aeronautics and Space Administration. Goddard Space Flight Center, Greenbelt, MD.
COASTAL ZONE COLOR SCANNER Abstract Only **c35**
B. Johnson *In its* Laboratory for Oceans 1988 p 101-103 (For primary document see N89-28118 22-48)
Avail: NTIS HC A12/MF A01 CSCL 14B

The Coastal Zone Color Scanner (CZCS) spacecraft ocean color instrument is capable of measuring and mapping global ocean surface chlorophyll concentration. It is a scanning radiometer with multiband capability. With new electronics and some mechanical, and optical re-work, it probably can be made flight worthy. Some additional components of a second flight model are also available. An engineering study and further tests are necessary to determine exactly what effort is required to properly prepare the instrument for spaceflight and the nature of interfaces to prospective spacecraft. The CZCS provides operational instrument capability for monitoring of ocean productivity and currents. It could be a simple, low cost alternative to developing new instruments for ocean color imaging. Researchers have determined that with global ocean color data they can: specify quantitatively the role of oceans in the global carbon cycle and other major biogeochemical cycles; determine the magnitude and variability of annual primary production by marine phytoplankton on a global scale; understand the fate of fluvial nutrients and their possible affect on carbon budgets; elucidate the coupling mechanism between upwelling and large scale patterns in ocean basins; answer questions concerning the large scale distribution and timing of spring blooms in the global ocean; acquire a better understanding of the processes associated with mixing along the edge of eddies, coastal currents, western boundary currents, etc., and acquire global data on marine optical properties.
Author

N89-28146*# National Aeronautics and Space Administration. Goddard Space Flight Center, Greenbelt, MD.
THE MULTICHANNEL OCEAN COLOR SENSOR (MOCS) Abstract Only **c35**
J. D. Oberholtzer and C. R. Vaughn *In its* Laboratory for Oceans 1988 p 105-106 (For primary document see N89-28118 22-48)
Avail: NTIS HC A12/MF A01 CSCL 14B

The MOCS is an imaging spectroradiometer with a sensitivity

that matches the light upwelling from open bodies of water. Twenty contiguous spectral channels in the visible are recorded in a line scanning mode from an aircraft. The system also supports a thermal infrared radiometer and will accept input from a position location system. The sensor in the MOCS system is an image dissector tube. A spectral curvature algorithm was developed. No atmospheric correction to the data is needed for low flying aircraft gathering chlorophyll data using this algorithm. Although the MOCS is now about 15 years old, because its response has been so stable, its data recording system was upgraded to the system used by the Aircraft Oceanographic Lidar where possible. The MOCS has been a reliable instrument for recording ocean color from low flying aircraft. As NASA enters the next period of ocean color investigations from space, such a device can play an important role in calibration of the space instrument, as well as provide support for programs developing the next generation of spaceborne devices. Author

N89-28147*# National Aeronautics and Space Administration. Goddard Space Flight Center, Greenbelt, MD.
ARCTIC SEA ICE STUDIES WITH PASSIVE MICROWAVE SATELLITE OBSERVATIONS Abstract Only
D. J. Cavalieri *In its* Laboratory for Oceans 1988 p 109-111 (For primary document see N89-28118 22-48)
Avail: NTIS HC A12/MF A01 CSCL 08C

The objectives of this research are: (1) to improve sea ice concentration determinations from passive microwave space observations; (2) to study the role of Arctic polynyas in the production of sea ice and the associated salinization of Arctic shelf water; and (3) to study large scale sea ice variability in the polar oceans. The strategy is to analyze existing data sets and data acquired from both the DMSP SSM/I and recently completed aircraft underflights. Special attention will be given the high resolution 85.5 GHz SSM/I channels for application to thin ice algorithms and processes studies. Analysis of aircraft and satellite data sets is expected to provide a basis for determining the potential of the SSM/I high frequency channels for improving sea ice algorithms and for investigating oceanic processes. Improved sea ice algorithms will aid the study of Arctic coastal polynyas which in turn will provide a better understanding of the role of these polynyas in maintaining the Arctic watermass structure. Analysis of satellite and archived meteorological data sets will provide improved estimates of annual, seasonal and shorter-term sea ice variability. Author

N89-28148*# National Aeronautics and Space Administration. Goddard Space Flight Center, Greenbelt, MD.
MICROWAVE REMOTE SENSING OF SEA ICE Abstract Only
J. C. Comiso *In its* Laboratory for Oceans 1988 p 113-115 (For primary document see N89-28118 22-48)
Avail: NTIS HC A12/MF A01 CSCL 08C

The long term objectives are: (1) to understand the physics of the multispectral microwave radiative characteristics of sea ice as it goes through different phases; (2) to improve characterization of sea ice cover using satellite microwave sensors; and (3) to study ice/ocean physical and biological processes associated with polynya formations and variability of the marginal sea ice region. Two field experiments were conducted to pursue these objectives. One involved measurements of radiative and physical characteristics of sea ice from a ship during a 3-month long cruise through the Weddell Sea ice pack during the Austral winter of 1986. The other involved similar measurements from two aircrafts and a submarine over the Central Arctic and Greenland Sea region. Preliminary results have already led to an enhanced understanding of the microwave signatures of pancake ice, nilas, first year ice, multiyear ice and effects of snow cover. Coastal and deep ocean polynyas and their role in bottom water formation and ocean circulation were studied using a time series of ice images from SMMR. An unsupervised cluster analysis of Arctic sea ice using SMMR and THIR emissivity and brightness temperature data was implemented. The analysis indicates the existence of several unique and persistent clusters in the Central Arctic region during winter and that the sum of the area of these clusters excluding those of first year ice is about 20 percent less than minimum ice cover area inferred from a previous summer data. This result is consistent with saline surface for some multiyear ice floes as observed during MIZEZ and suggests that a significant fraction of multiyear ice floes in the Arctic have first year ice signatures. Author

N89-28149*# National Aeronautics and Space Administration. Goddard Space Flight Center, Greenbelt, MD.
ANALYSIS OF SEA ICE DYNAMICS Abstract Only
J. Zwally *In its* Laboratory for Oceans 1988 p 117-120 (For primary document see N89-28118 22-48)
Avail: NTIS HC A12/MF A01 CSCL 08C

The ongoing work has established the basis for using multiyear sea ice concentrations from SMMR passive microwave for studies of largescale advection and convergence/divergence of the Arctic sea ice pack. Comparisons were made with numerical model simulations and buoy data showing qualitative agreement on daily to interannual time scales. Analysis of the 7-year SMMR data set shows significant interannual variations in the total area of multiyear ice. The scientific objective is to investigate the dynamics, mass balance, and interannual variability of the Arctic sea ice pack. The research emphasizes the direct application of sea ice parameters derived from passive microwave data (SMMR and SSMI) and collaborative studies using a sea ice dynamics model. The possible causes of observed interannual variations in the multiyear ice area are being examined. The relative effects of variations in the large scale advection and convergence/divergence within the ice pack on a regional and seasonal basis are investigated. The effects of anomolous atmospheric forcings are being examined, including the long-lived effects of synoptic events and monthly variations in the mean geostrophic winds. Estimates to be made will include the amount of new ice production within the ice pack during winter and the amount of ice exported from the pack. Author

N89-28150*# National Aeronautics and Space Administration. Goddard Space Flight Center, Greenbelt, MD.
ICE SHEET RADAR ALTIMETRY Abstract Only
J. Zwally *In its* Laboratory for Oceans 1988 p 121-122 (For primary document see N89-28118 22-48)
Avail: NTIS HC A12/MF A01 CSCL 08C

The surface topography of the Greenland and Antarctic ice sheets between 72 degrees north and south was mapped using radar altimetry data from the U.S. Navy GEOSAT. The glaciological objectives of this activity were to study the dynamics of the ice flow, changes in the position of floating ice-shelf fronts, and ultimately to measure temporal changes in ice surface elevation indicative of ice sheet mass balance. Author

N89-28151*# National Aeronautics and Space Administration. Goddard Space Flight Center, Greenbelt, MD.
SEA ICE/CLIMATE STUDIES Abstract Only **c47**
C. L. Parkinson *In its* Laboratory for Oceans 1988 p 123-125 (For primary document see N89-28118 22-48)
Avail: NTIS HC A12/MF A01 CSCL 04B

The objectives were to determine and analyze the annual cycle of sea ice extents in the Arctic Ocean and peripheral seas and bays over the period 1973 to 1986, looking in particular for any long term trends; to examine the relationship between local sea ice covers and the surrounding atmosphere and ocean; and to examine sea ice as a potential early indicator of climate change. The work involves creating regional and hemispheric time series of sea ice variables from satellite passive microwave data and analyzing these through various intercomparisons amongst themselves and with oceanographic and atmospheric fields. Author

N89-28152*# National Aeronautics and Space Administration. Goddard Space Flight Center, Greenbelt, MD.
ICE SHEET STUDIES USING SYNTHETIC APERTURE RADAR Abstract Only
R. Bindschadler *In its* Laboratory for Oceans 1988 p 127

(For primary document see N89-28118 22-48)
Avail: NTIS HC A12/MF A01 CSCL 08C

The objective was to demonstrate the utility of synthetic aperture radar in ice sheet studies. The major advantage of SAR imagery over visible imagery is the all-weather capability of radar and the ability to specify look angle. Available digital SAR imagery over ice sheets was collected and examined both qualitatively and quantitatively using corroborative data, such as LANDSAT imagery, to confirm feature identification and interpretations. A simple scattering model will be developed to assess the relative importance of surface topography, composition, and subsurface layering to the intensity of radar backscatter. Recommendations of system parameters will be made for optimal SAR operation over ice sheets. Author

N89-28153*# National Aeronautics and Space Administration. Goddard Space Flight Center, Greenbelt, MD.
WAVE/CURRENT INTERACTION MODEL Abstract Only
A. K. Liu *In its* Laboratory for Oceans 1988 p 131-133
(For primary document see N89-28118 22-48)
Avail: NTIS HC A12/MF A01 CSCL 08C

The wave-current interaction for the application to remote sensing data via numerical simulations and data comparison is modelled. Using the field data of surface current shear, wind condition and ambient wave spectrum, the numerical simulations of directional wave spectrum evolution were used to interpret and to compare with the aircraft data from Radar Ocean Wave Spectrometer (ROWS) and Surface Contour Radar (SCR) across the front during Frontal Air Sea Interaction Experiment (FASINEX). The wave-ice interaction was inspired by the observation of large amplitude waves hundreds of kms inside the ice pack in the Weddell Sea, resulting in breakup of the ice pack. The developed analysis of processes includes the refraction of waves at the pack edge, the effects of pack compression on wave propagation, wave train stability and buckling stability in the ice pack. Sources of pack compression and interaction between wave momentum and pack compression are investigated. Viscous camping of propagating waves in the marginal ice zone are also studied. The analysis suggests an explanation for the change in wave dispersion observed from the ship and the sequence of processes that cause ice pack breakup, pressure ridge formation and the formation of open bands of water. Author

N89-28154*# National Aeronautics and Space Administration. Goddard Space Flight Center, Greenbelt, MD.
OCEAN DRIFTER PROJECT Abstract Only
C. D. Mason *In its* Laboratory for Oceans 1988 p 135-138
(For primary document see N89-28118 22-48)
Avail: NTIS HC A12/MF A01 CSCL 08C

Four drifting buoys were fabricated from mostly local hardware plus animal locating transmitters. The first two working models were dropped from a Wallops aircraft, to test the mechanical integrity and to test the ability of the whole system to withstand the drop and provide usable data. There are two temperature sensors on board, one to measure sea surface temperature and the other to measure air temperature. An onboard computer controls the transmissions, sending three water temperature readings for each air temperature reading in order to differentiate one from the other after data reduction. Guidelines for the development and test of optical drifting buoys include: air deployable and expendable, reasonable cost for multiple deployment, 1 year lifetime, use of existing technology and a minimal validation parameter set. Author

N89-28155*# National Aeronautics and Space Administration. Goddard Space Flight Center, Greenbelt, MD.
ANALYSES OF THE WIND-DRIVEN RESPONSE OF TROPICAL OCEANS Abstract Only
A. J. Busalacchi *In its* Laboratory for Oceans 1988 p 141-142 (For primary document see N89-28118 22-48)
Avail: NTIS HC A12/MF A01 CSCL 08C

Numerical and analytical models are used to study the upper-ocean response to surface wind stress estimates from the tropical Atlantic and Pacific Oceans. These models are used to identify regions of important variability in the wind field, analyze the oceanic response, and demonstrate the applicability of remotely sensed vector wind stress and altimetry data. Both model and XBT depictions of the mean seasonal cycle, 1979 to 1981, were analyzed along the major ship tracks in the western, central, and eastern tropical Pacific. Model solutions were also used to address array design questions in observing system simulation experiments. Subsequent analyses of the 1982 to 1983 solutions will be performed with respect to differences from the mean seasonal cycle 1979 to 1981, as well as, differences in the three wind products. Author

N89-28156*# National Aeronautics and Space Administration. Goddard Space Flight Center, Greenbelt, MD.
CLIMATOLOGICAL ASPECTS OF NIMBUS-7 SMMR DATA Abstract Only **c47**
P. Gloersen *In its* Laboratory for Oceans 1988 p 143-145
(For primary document see N89-28118 22-48)
Avail: NTIS HC A12/MF A01 CSCL 04B

An algorithm was developed for calculating simultaneously SSTs, SWs, and TAUs on a global basis using only the 6.6 and 18 GHz channels of the SMMR. Samples of the retrievals were calculated in each of eight of the SMMR years and found to produce independent results, consistent with weather charts and climatic records, even in the presence of high winds. Another new algorithm for calculating high-latitude scalar winds from Nimbus-7 Scanning Multichannel Microwave Radiometer (SMMR) data was devised and tuned with surface observations from a number of documented Arctic Polar Low events. The algorithm utilizes the horizontally and vertically polarized radiances from the 0.8 and 1.7 cm wavelength channels of the ten-channel SMMR to retrieve near surface oceanic scalar winds and cloud water in the column, and takes advantage of the relatively small fluctuations in atmospheric water vapor at high latitudes. An advantage of this algorithm for high latitude winds from SMMR over the global algorithm is an inherently better spatial resolution as a result of the shorter wavelengths used. Author

N89-28157*# National Aeronautics and Space Administration. Goddard Space Flight Center, Greenbelt, MD.
MICROSCALE OCEAN DYNAMICS Abstract Only
N. Huang *In its* Laboratory for Oceans 1988 p 147-148
(For primary document see N89-28118 22-48)
Avail: NTIS HC A12/MF A01 CSCL 08C

The detailed dynamics of the micro-scale ocean surface phenomena are studied along with the relationships among the surface signatures with the underlying dynamical processes. The approach to advance the understanding in this area is as follows: (1) Conduct rigorous theoretical studies of the ocean surface wave dynamics and statistical properties; (2) Conduct process-oriented laboratory experiments to verify the theoretical results, and to provide guidance for further studies; and (3) Prepare testable hypotheses for field verifications and comparisons during the ONR/NASA sponsored Surface Wave Dynamics Experiment (SWADE). An analytic model was established for wave breaking probability to study the influence of wave breaking on the spectrum shape in both deep and finite-depth waters. The spectrum was processed along with the structures of the water surface under the influence of wind and existing waves. Author

N89-28158*# National Aeronautics and Space Administration. Goddard Space Flight Center, Greenbelt, MD.
MICROWAVE RADAR OCEANOGRAPHIC INVESTIGATIONS Abstract Only
F. C. Jackson *In its* Laboratory for Oceans 1988 p 149-152
(For primary document see N89-28118 22-48)
Avail: NTIS HC A12/MF A01 CSCL 08C

The Radar Ocean Wave Spectrometer (ROWS) technique was developed and demonstrated for measuring ocean wave directional spectra from air and space platforms. The measurement technique was well demonstrated with data collected in a number of flight experiments involving wave spectral comparisons with wave buoys

and the Surface Contour Radar (SCR). Recent missions include the SIR-B underflight experiment (1984), FASINEX (1986), and LEWEX (1987). ROWS related activity is presently concentrating on using the aircraft instrument for wave-processes investigations and obtaining the necessary support (consensus) for a satellite instrument development program. Prospective platforms include EOS and the Canadian RADARSAT. Author

N89-28159*# National Aeronautics and Space Administration. Goddard Space Flight Center, Greenbelt, MD.
SURFACE CONTOUR RADAR (SCR) CONTRIBUTIONS TO FASINEX Abstract Only **c32**
E. J. Walsh *In its* Laboratory for Oceans 1988 p 153-155 (For primary document see N89-28118 22-48)
Avail: NTIS HC A12/MF A01 CSCL 17I

The SCR was asked to participate in the Frontal Air-Sea Interaction Experiment (FASINEX) to provide directional wave spectra. The NASA P-3 carrying the SCR, the Radar Ocean Wave Spectrometer, and the Airborne Oceanographic Lidar was one of five aircrafts and two ocean research ships participating in this coordinated study of the air sea interaction in the vicinity of a sea surface temperature front near 28 deg N, 70 deg W. Analysis of data from the February 1986 experiment is still ongoing, but results already submitted for publication strengthen the hypothesis that off-nadir radar backscatter is closely correlated to wind stress. The SCR provided valuable information on the directional wave spectrum and its spatial variation. Author

N89-28160*# National Aeronautics and Space Administration. Goddard Space Flight Center, Greenbelt, MD.
RAINFALL ON MICROWAVE RETURN FROM THE SEA SURFACE Abstract Only **c47**
L. F. Bliven and J.-P. Giovanangeli *In its* Laboratory for Oceans 1988 p 157-158 (For primary document see N89-28118 22-48)
Avail: NTIS HC A12/MF A01 CSCL 04B

The long range goal remains unchanged; to conduct experiments and develop/test theoretical models to permit useful algorithms to be constructed for microwave systems that observe oceanic processes. This topic is relevant to altimeters, scatterometers, and rain rate measurements. The current focus is attention to scatterometer wind velocity measurement. One component of the laboratory efforts is an experiment conducted, in the wind wave tank at the GSFC/WFF, to quantify the effect of rain-generated surface wave brightening of radar cross section. Laboratory conditions can be characterized as light wind, functional rain rates, a single drop size, and a 36 GHz radar system at 30 degrees inclination. Author

N89-28161*# National Aeronautics and Space Administration. Goddard Space Flight Center, Greenbelt, MD.
WIND-WAVE-CURRENT TANK RESEARCH FACILITY USAGE AND STATUS Abstract Only **c09**
L. F. Bliven and S. R. Long *In its* Laboratory for Oceans 1988 p 159-160 (For primary document see N89-28118 22-48)
Avail: NTIS HC A12/MF A01 CSCL 14B

This summary is to provide information as to: (1) research activities, and (2) facilities status of the wind-wave-current tank research facility located at the GSFC/WFF. Research Activities include: (1) Wave-Turbulence Interaction; (2) Velocity Structure Below Waves; (3) Short-Wave Modification by Long-Waves; (4) Wind-Wave Generation Time Scale; (5) Wave-Current Interaction; (6) Rain Effects on Microwave Scattering from the Sea-Surface; and (7) Gas Exchange Rates versus Scatterometer Power.
Author

N89-28162*# National Aeronautics and Space Administration. Goddard Space Flight Center, Greenbelt, MD.
THE SURFACE WAVE DYNAMICS EXPERIMENT (SWADE) Abstract Only
S. R. Long, J. D. Oberholtzer, C. W. Wright, and H. G. Shirk *In its* Laboratory for Oceans 1988 p 161-162 (For primary document see N89-28118 22-48)
Avail: NTIS HC A12/MF A01 CSCL 08C

SWADE was developed to study the dynamics of the wave field development in the open ocean with the following specific objectives: (1) to understand the development of the wave directional spectrum under various conditions; (2) to determine the effect of waves on the air/sea transfers of momentum, heat, and mass; (3) to determine breaking distributions as a function of sea state, wind, and boundary stability; and (4) to provide data and analyses for ERS-1 validation. The experiment is designed for the winter of 1990 to 1991. Four buoys will be deployed for 6 months starting October 1990 and ending March 1991. During that time period, three intensive periods of 2 weeks duration each will be selected for frequent aircraft flights for wave data collection to satisfy scientific studies, as well as ERS-1 validation needs.
Author

N89-28163*# National Aeronautics and Space Administration. Goddard Space Flight Center, Greenbelt, MD.
WATER VAPOR PROFILING USING MICROWAVE RADIOMETRY Abstract Only **c47**
J. R. Wang and T. T. Wilheit *In its* Laboratory for Oceans 1988 p 165-167 (For primary document see N89-28118 22-48)
Avail: NTIS HC A12/MF A01 CSCL 04B

Water vapor is one of the most important constituents in the Earth's atmosphere. Its spatial and temporal variations affect a wide spectrum of meteorological phenomena ranging from the formation of clouds to the development of severe storms. The passive microwave technique offers an excellent means for water vapor measurements. It can provide both day and night coverage under most cloud conditions. Two water vapor absorption features, at 22 and 183 GHz, were explored in the past years. The line strengths of these features differ by nearly two orders of magnitude. As a consequence, the techniques and the final products of water vapor measurements are also quite different. The research effort in the past few years was to improve and extend the retrieval algorithm to the measurements of water vapor profiles under cloudy conditions. In addition, the retrieval of total precipitable water using 183 GHz measurements, but in a manner analogous to the use of 22 GHz measurements, to increase measurement sensitivity for atmospheres of very low moisture content was also explored.
Author

N89-28164*# National Aeronautics and Space Administration. Goddard Space Flight Center, Greenbelt, MD.
CORRELATIVE MEASUREMENTS PROGRAM Abstract Only **c45**
C. L. Parsons *In its* Laboratory for Oceans 1988 p 169-173 (For primary document see N89-28118 22-48)
Avail: NTIS HC A12/MF A01 CSCL 13B

The GSFC Correlative Measurements Program at the Wallops Flight Facility was represented on the Satellite/Satellite Intercomparisons Working Group. The Correlative Measurements Program uses the Rocket Ozonesonde (ROCOZ-A) and the Electrochemical Concentration Cell (ECC) balloon borne ozonesonde to measure the vertical profile of ozone amount in the atmosphere. The balloon work is described in a separate report. The ROCOZ-A instrument was used for many years to provide in situ truth data for various satellite ozone measuring systems, such as SBUV on Nimbus-7, SAGE-II, SBUV-II on the NOAA series of polar orbiting satellites, SME, LIMS, etc. The particular data sets of interest to the Ozone Trends Panel Working Group were collected at Natal, Brazil. The major results produced for and used by the Ozone Trends Panel are shown. The ROCOZ-A average ozone density profile is plotted versus altitude on the left. ECC ozonesondes were used for the portion of the profile below 20 km, the lower limit for ROCOZ-A. The difference between SAGE-II and ROCOZ-A average density profiles is shown.
Author

N89-28165*# National Aeronautics and Space Administration. Goddard Space Flight Center, Greenbelt, MD.
OZONE MEASUREMENTS USING BALLOON-BORNE OZONESONDES Abstract Only **c45**
A. L. Torres *In its* Laboratory for Oceans 1988 p 175-178 (For primary document see N89-28118 22-48)
Avail: NTIS HC A12/MF A01 CSCL 13B

Vertical profiles of atmospheric ozone have been measured for a number of years by WFF personnel using small balloon borne ozonesondes. These sondes are interfaced with meteorological radiosondes so that both ozone data and meterological data (pressure, temperature, humidity, wind speed and direction) are obtained from ground level up to 30 to 35 km. Efforts at Wallops have been focused in three areas. The first involves biweekly launches from two sites (Wallops and Natal, Brazil), timed to coincide with overpasses of satellite borne ozone sensors such as the Solar Backscattered Ultraviolet. The resulting data are reported to the World Ozone Data Center and are used for satellite correlative support, as well as, for studies of both tropospheric and stratospheric ozone. The second activity consists of field campaigns in remote locations in support of special projects. The third is a continuing activity to quantitatively evaluate and improve the sonde's performance under stratospheric conditions. Author

N89-28166*# National Aeronautics and Space Administration. Goddard Space Flight Center, Greenbelt, MD.
MOBILE LIDAR SYSTEM FOR MEASUREMENT OF WATER VAPOR MIXING RATIO AND OZONE NUMBER DENSITY Abstract Only **c45**
D. Whiteman *In its* Laboratory for Oceans 1988 p 179-183 (For primary document see N89-28118 22-48)
Avail: NTIS HC A12/MF A01 CSCL 13B

The Water Vapor Lidar was modified and extended to make differential absorption measurements of ozone. Water vapor measurements make use of a weak molecular scattering process known as Raman scattering. It is characterized by a shift in wavelength of the scattered beam of light relative to the incident one. Some of the energy of the incident photon is converted to vibrational or rotational energy within the molecule leaving the scattered photon shifted to a slightly longer wavelength. When performing water vapor measurements, profiles are acquired of water vapor mixing ratio from near the ground to beyond 7 km every 2 minutes. By forming a color composite image of the individual profiles, the spatial and temporal evolution of water vapor is visible with vertical resolution of 75 to 150m and temporal resolution of 2 minutes. The ozone lidar is intended for use as a cross calibration facility for other stationary ozone lidar systems. The ozone measurement employs the technique known as differential absorption. The backscattered laser radiation from two different wavelengths is measured. Successful measurements of 308 nm returns were made from 80 km with an averaging period of 6 hours. Using these data and a standard atmosphere density curve, an ozone number density profile was made which agrees very well with the standard ozone curve between 20 and 40 km. Author

N89-28167*# National Aeronautics and Space Administration. Goddard Space Flight Center, Greenbelt, MD.
ROCKET TEMPERATURE SOUNDINGS Abstract Only **c46**
F. J. Schmidlin *In its* Laboratory for Oceans 1988 p 185-187 (For primary document see N89-28118 22-48)
Avail: NTIS HC A12/MF A01 CSCL 04A

In situ rocket-borne measurements of temperature and wind contribute to a better determination and understanding of stratospheric behavior and, hence, to a better understanding of processes that control the dynamical and chemical behavior of this region. Concern over ozone depletion and the difficulty generally involved in determining actual ozone trends has generated significant interest in temperature behavior, especially trends. Recent analysis of rocketsonde acquired temperature data between 1969 and 1986 contains evidence that the stratosphere may indeed be cooling. It is the intention of the RTOP to continue to provide rocketsonde measurements to: maintain the long term data stratospheric-mesospheric data base already established for Wallops; provide ground truth for remote measurements; and continue studies of atmospheric structure and morphology of disturbances and anomalous events as resources permit. Author

N89-28168*# National Aeronautics and Space Administration. Goddard Space Flight Center, Greenbelt, MD.
ELECTRODYNAMICS, WIND AND TEMPERATURE Abstract Only **c46**
F. J. Schmidlin *In its* Laboratory for Oceans 1988 p 189 (For primary document see N89-28118 22-48)
Avail: NTIS HC A12/MF A01 CSCL 04A

This RTOP provides for correlative meteorological wind and temperature measurements with atmospheric electrodynamic measurements. Meteorological rocketsondes were launched as part of a number of electrodynamic investigations in Alaska, Norway, Peru, Sweden, and at the Wallops Flight Facility, Wallops Island, Virginia. Measurements obtained as part of the MAC/Epsilon campaign during October 1987 from Andoya, Norway, were in conjunction with electric field, ion mobility, conductivity, and energy deposition studies. The measurements obtained between 30 and 90 km are to evaluate and correlate changes in the atmospheric electrical structure caused by the neutral wind and temperature, or changes in the neutral atmosphere resulting from electrical anomalies. Author

N89-28169*# National Aeronautics and Space Administration. Goddard Space Flight Center, Greenbelt, MD.
RADIOSONDE INTERCOMPARISON Abstract Only **c46**
F. J. Schmidlin *In its* Laboratory for Oceans 1988 p 191-193 (For primary document see N89-28118 22-48)
Avail: NTIS HC A12/MF A01 CSCL 04A

The largest amount of material ever collected from a radiosonde comparison was examined. Radiosondes from Australia, Finland, India, and the United States were involved. Data were received from 100 soundings, each of which was a simultaneous in situ test of four different instrument types. The simultaneous temperature comparison of participating operational radiosondes in daylight was about 1 C at the 100 hPa level and about 4 C at the 10 hPa level, while the corresponding comparison for geopotential was about 40 meters at 100 hPa and 100 meters at 10 hPa. Estimates of the reproducibility of standard level temperatures are given. The reproducibility obtained from the in situ comparisons is, in general, slightly better than corresponding results from monitoring measurements in a real-time mode at analysis centers. Conclusions from the intercomparison are many; the following call for particular attention: (1) fully automated radiosonde systems were able to reproduce geopotential measurements better than non-automated systems, mainly due to a decrease in observer mistakes; (2) observed temperature differences between radiosonde measurements were as large during the night as during the day; and (3) significant inconsistencies still exist between the night time and day time measurements, as well as significant bias errors in the pressure measurements of some radiosonde types. Author

N89-28170*# National Aeronautics and Space Administration. Goddard Space Flight Center, Greenbelt, MD.
SATELLITE/RADIOSONDE COMPARISON Abstract Only **c46**
F. J. Schmidlin *In its* Laboratory for Oceans 1988 p 195 (For primary document see N89-28118 22-48)
Avail: NTIS HC A12/MF A01 CSCL 04A

Collocated measurements of radiosonde and TIROS Operational Vertical Sounder (TOVS) data are compared to determine whether significant latitudinal, seasonal, or instrumental biases exist. Long-wave structure determined by each system is being examined for correlation. Because U.S. radiosonde data are archived uncorrected, an effort to correct the measurements is being considered. These corrections will be applied to 7 years of measurements. New comparisons will then be made using corrected radiosonde and TOVS data. A regression method is used to retrieve temperatures, and radiosonde zonal means are

used to update the regression coefficients. Preliminary results of auto-correlation analysis indicate that detection of long-wave structure in each set of data is slightly different with some levels and locations experiencing different wave periods or amplitudes. Scatter diagrams and linear regression for each layer show bias in the mean temperatures. Winter-time measurements show poorer correlations due to noisy measurements. Author

N89-28171*# National Aeronautics and Space Administration. Goddard Space Flight Center, Greenbelt, MD.
TROPOSPHERIC NITRIC OXIDE MEASUREMENTS Abstract Only **c45**
A. L. Torres *In its* Laboratory for Oceans 1988 p 197-198 (For primary document see N89-28118 22-48)
Avail: NTIS HC A12/MF A01 CSCL 13B

Nitric oxide (NO) plays a key role in tropospheric photo-chemistry. The photochemical oxidation of hydrocarbons, for example, can serve as either a source or a sink for ozone, depending on the local abundance of NO. Nitric oxide also helps govern atmospheric concentrations of the hydroxyl (OH) radical. The OH radical is the single most important player in photochemical transformations because it controls the atmospheric lifetimes of so many chemical species. Although NO serves as a very effective catalyst in many important chemical processes, its concentration is low enough to normally be expressed in units of parts per trillion by volume (pptv). Consequently, commercially available detectors for NO (with detection limits of about one part per billion) have proven to be unsuitable for use anywhere except in urban areas and near other local pollution sources. Under the sponsorship of NASA's Global Tropospheric Experiment (GTE), Wallops has developed an extremely sensitive detector with a detection limit of a few pptv. The system was specifically designed for aircraft use, with the objective of applying it in global aircraft studies of tropospheric chemistry. Studies with the detector are examined. Author

N89-28172*# National Aeronautics and Space Administration. Goddard Space Flight Center, Greenbelt, MD.
CLOUD ABSORPTION RADIOMETER Abstract Only **c46**
M. G. Strange *In its* Laboratory for Oceans 1988 p 199-202 (For primary document see N89-28118 22-48)
Avail: NTIS HC A12/MF A01 CSCL 04A

The Cloud Absorption Radiometer (CAR) was developed to measure spectrally how light is scattered by clouds and to determine the single scattering albedo, important to meteorology and climate studies, with unprecedented accuracy. This measurement is based on ratios of downwelling to upwelling radiation within clouds, and so is not strongly dependent upon absolute radiometric calibration of the instrument. The CAR has a 5-inch aperture and 1 degree IFOV, and spatially scans in a plane orthogonal to the flight vector from the zenith to nadir at 1.7 revolutions per second. Incoming light is measured in 13 spectral bands, using silicon, germanium, and indium-antimonide detectors. Data from each channel is digitally recorded in flight with 10-bit (0.1 percent) resolution. The instrument incorporates several novel features. These features are briefly detailed. Author

N89-28173*# National Aeronautics and Space Administration. Goddard Space Flight Center, Greenbelt, MD.
THE LABORATORY FOR OCEANS COMPUTING FACILITY Abstract Only **c09**
R. Kao *In its* Laboratory for Oceans 1988 p 205-208 (For primary document see N89-28118 22-48)
Avail: NTIS HC A12/MF A01 CSCL 14B

The first VAX computer in the Laboratory for Oceans Computing Facility (LOCF) was installed and the facility was largely expanded. The growth is not only in hardware and software, but also in the number of users and in supporting research and development projects. The LOCF serves as a general purpose computing facility for: ocean color research projects, sea ice research projects, processing of the Nimbus-7 Coastal Zone Color Scanner data set, real time ingest and analysis of TIROS-N satellite data, study of the Synthetic Aperture Radar data, study of LANDSAT data, and many others. The physical space and the electrical power layout of the computing room were modified to accommodate all the equipment. The LOCF has several image processing stations which include two International Imaging Systems (IIS) model 75 processors and one Adage processor. The facility has the capability of ingesting the TIROS-N HRPT satellite data on a real time basis. More than 30 software packages were installed on the systems. System software packages, network software, FORTRAN and C compilers, database management software, image processing software, graphics, mathematics and statistics packages, TAE, Catalog Manager, GEMPAK, LAS and many other software developed on the LOCF computers such as SEAPAK have greatly advanced the capability of the LOCF. Author

N89-28174*# National Aeronautics and Space Administration. Goddard Space Flight Center, Greenbelt, MD.
CODE 672 OBSERVATIONAL SCIENCE BRANCH COMPUTER NETWORKS Abstract Only **c62**
D. W. Hancock and H. G. Shirk *In its* Laboratory for Oceans 1988 p 209-212 (For primary document see N89-28118 22-48)
Avail: NTIS HC A12/MF A01 CSCL 09B

In general, networking increases productivity due to the speed of transmission, easy access to remote computers, ability to share files, and increased availability of peripherals. Two different networks within the Observational Science Branch are described in detail. Author

N89-28175*# National Aeronautics and Space Administration. Goddard Space Flight Center, Greenbelt, MD.
PERSONAL COMPUTERS ON ETHERNET Abstract Only **c60**
R. Kao *In its* Laboratory for Oceans 1988 p 213-215 (For primary document see N89-28118 22-48)
Avail: NTIS HC A12/MF A01 CSCL 09B

Many researchers in the Division have projects which require transferring large files between their personal computers (PC) and VAX computers in the Laboratory for Oceans Computing Facility (LOCF). Since Ethernet local area network provides high speed communication channels which make file transfers (among other capabilities) practical, a network plan was assembled to connect IBM and IBM compatible PC's to Ethernet for participating personnel. The design employs ThinWire Ethernet technology. A simplified configuration diagram is shown. A DEC multiport repeater (DEMPR) is used for connection of ThinWire Ethernet segments. One port of DEMPR is connected to a H4000 transceiver and the transceiver is clamped onto the Goddard Ethernet backbonecoaxial cable so that the PC's can be optionally on the SPAN network. All these common elements were successfully installed and tested. Author

N89-28176*# National Aeronautics and Space Administration. Goddard Space Flight Center, Greenbelt, MD.
THIRD INTERNATIONAL SATELLITE DIRECT BROADCAST SERVICES USER'S CONFERENCE Abstract Only **c32**
J. Kamowski and C. Vermillion *In its* Laboratory for Oceans 1988 p 217-218 Conference held in Linthicum, MD, 20-24 Jun. 1988 (For primary document see N89-28118 22-48)
Avail: NTIS HC A12/MF A01 CSCL 17B

A workshop titled, The Third International Satellite Direct Broadcast Services User's Conference, jointly sponsored by NASA and NOAA/NESDIS was scheduled to be held June 20 to 24, 1988, at the International Hotel located at the Baltimore-Washington Airport. Details concerning the organizing of the conference are given. Author

N89-28177*# National Aeronautics and Space Administration. Goddard Space Flight Center, Greenbelt, MD.
LOW COST REAL TIME INTERACTIVE ANALYSIS SYSTEM Abstract Only **c60**
F. Stetina *In its* Laboratory for Oceans 1988 p 219-220 (For primary document see N89-28118 22-48)
Avail: NTIS HC A12/MF A01 CSCL 09B

Efforts continue to develop a low cost real time interactive

analysis system for the reception of satellite data. A multi-purpose ingest hardware software frame formatter was demonstrated for GOES and TIROS data and work is proceeding on extending the capability to receive GMS data. A similar system was proposed as an archival and analysis system for use with INSAT data and studies are underway to modify the system to receive the planned SeaWiFS (ocean color) data. This system was proposed as the core of a number of international programs in support of U.S. AID activities. Systems delivered or nearing final testing are listed. Author

N89-28178*# National Aeronautics and Space Administration. Goddard Space Flight Center, Greenbelt, MD.
NAVIGATIONAL AND ENVIRONMENTAL MEASUREMENT SYSTEM (NEMS) Abstract Only **c04**
T. D. Clem *In its* Laboratory for Oceans 1988 p 223-225 (For primary document see N89-28118 22-48)
Avail: NTIS HC A12/MF A01 CSCL 17G

The NEMS concept and design were initiated from the need to measure and record positional and environmental information during aircraft flights of developmental science research instrumentation. The unit was designed as a stand-alone system which could serve the needs of instruments whose developmental nature did not justify the cost and complexity of including these measurements within the instrument data system. Initially, the system was comprised of a Loran-C receiver and a portable IBM compatible computer recording position and time. Later, the system was interfaced with the Wallops aircraft inertial navigation system (INS), and various other sensors were supplied and shared by the Goddard science users. Real-time position mapping on video monitors was added for investigator's use and information. In 1987, the use of a Global Positioning System (GPS) receiver was included in some missions. A total configuration of the system and the various sensors which can be incorporated are shown. Author

N89-28179*# National Aeronautics and Space Administration. Goddard Space Flight Center, Greenbelt, MD.
AIRBORNE LIDAR GLOBAL POSITIONING INVESTIGATIONS Abstract Only **c04**
W. B. Krabill *In its* Laboratory for Oceans 1988 p 227-229 (For primary document see N89-28118 22-48)
Avail: NTIS HC A12/MF A01 CSCL 17G

The Global Positioning System (GPS) network of satellites shows high promise of revolutionizing methods for conducting surveying, navigation, and positioning. This is especially true in the case of airborne or satellite positioning. A single GPS receiver (suitably adapted for aircraft deployment) can yield positioning accuracies (world-wide) in the order of 30 to 50 m vertically, as well as horizontally. This accuracy is dramatically improved when a second GPS receiver is positioned at a known horizontal and vertical reference. Absolute horizontal and vertical positioning of 1 to 2 m are easily achieved over areas of separation of tens of km. If four common satellites remain in lock in both receivers, then differential phase pseudo-ranges on the GPS L-band carrier can be utilized to achieve accuracies of + or - 10 cm and perhaps as good as + or - 2 cm. The initial proof of concept investigation for airborne positioning using the phase difference between the airborne and stationary GPS receivers was conducted and is examined. Author

N89-28180*# National Aeronautics and Space Administration. Goddard Space Flight Center, Greenbelt, MD.
MICROWAVE REMOTE SENSING OF SOIL MOISTURE Abstract Only **c43**
J. C. Shiue and J. R. Wang *In its* Laboratory for Oceans 1988 p 231-235 (For primary document see N89-28118 22-48)
Avail: NTIS HC A12/MF A01 CSCL 08B

Knowledge of soil moisture is important to many disciplines, such as agriculture, hydrology, and meteorology. Soil moisture distribution of vast regions can be measured efficiently only with remote sensing techniques from airborne or satellite platforms. At low microwave frequencies, water has a much larger dielectric constant than dry soil. This difference manifests itself in surface emissivity (or reflectivity) change between dry and wet soils, and can be measured by a microwave radiometer or radar. The Microwave Sensors and Data Communications Branch is developing microwave remote sensing techniques using both radar and radiometry, but primarily with microwave radiometry. The efforts in these areas range from developing algorithms for data interpretation to conducting feasibility studies for space systems, with a primary goal of developing a microwave radiometer for soil moisture measurement from satellites, such as EOS or the Space Station. These efforts are listed. Author

N89-28181*# National Aeronautics and Space Administration. Goddard Space Flight Center, Greenbelt, MD.
SYNTHETIC APERTURE MICROWAVE RADIOMETER Abstract Only **c35**
D. M. LeVine *In its* Laboratory for Oceans 1988 p 237-238 (For primary document see N89-28118 22-48)
Avail: NTIS HC A12/MF A01 CSCL 14B

Realizing the full potential of microwave remote sensing from space requires putting relatively large antennas in orbit. Research is being conducted to develop synthetic aperture antennas to reduce the physical collecting area required of sensors in space, and to possibly open the door to new applications of microwave remote sensing. The technique under investigation involves using a correlation interferometer with multiple baselines. The Microwave Sensors and Data Collection Branch has been engaged in research to develop this technique for applications to remote sensing of soil moisture from space. Soil moisture is important for agricultural applications and for understanding the global hydrologic cycle. An aircraft prototype of an instrument suitable for making such measurements was developed. This is an L-band radiometer called ESTAR which is hoped will become part of the Earth Observing System (EOS). ESTAR is a hybrid instrument which uses both real aperture antennas (long sticks to obtain resolution in the along-track dimension) and aperture synthesis (correlation between sticks to obtain resolution in the cross track dimension). The hybrid was chosen as a compromise to increase the sensitivity (T) of the instrument. Author

N89-28182*# National Aeronautics and Space Administration. Goddard Space Flight Center, Greenbelt, MD.
RADAR SCATTERING AND SOIL MOISTURE Abstract Only **c43**
D. M. LeVine and P. O. Neill *In its* Laboratory for Oceans 1988 p 239-241 (For primary document see N89-28118 22-48)
Avail: NTIS HC A12/MF A01 CSCL 17I

Research is being conducted on microwave scattering from vegetation. The objective is to develop techniques for measuring parameters of the vegetation canopy (such as biomass) needed for understanding global biogeochemical cycles and to develop techniques for correcting microwave measurements of soil moisture for the effects of the vegetation canopy. Measurements of vegetation and soil moisture are important for understanding the environment on a global scale. For example, moisture in the soil is an important, highly variable, element in the global hydrologic cycle. The hydrologic cycle, in turn, is strongly coupled to weather and climate through moisture (and energy) fluxes at the surface. The amount and distribution of vegetation is an important element in biogeochemical cycles; and knowledge of both the vegetation canopy and soil moisture is of practical importance in agricultural management. These theories are examined. Author

N89-28183*# National Aeronautics and Space Administration. Goddard Space Flight Center, Greenbelt, MD.
ADVANCED SOLIDSTATE ARRAY SPECTRORADIOMETER Abstract Only **c35**
F. G. Huegel and J. Irons *In its* Laboratory for Oceans 1988 p 243-245 (For primary document see N89-28118 22-48)
Avail: NTIS HC A12/MF A01 CSCL 14B

During the Summer of 1987, the Advanced Solidstate Array Spectroradiometer (ASAS) was installed and flown on the NASA

Ames C-130 in support of the First International Field Experiment (FIFE) missions. The study site was over the grassland areas of the Konza Prairie in Kansas. The data collected with ASAS during these flights has been used to produce the first nearly simultaneous multiangular/multispectral images of selected terrestrial study sites. This data will be valuable in the study of surface bidirectional reflectance and albedo. The data will also be useful for the development of data analysis algorithms for future spaceborne instruments such as the Goddard MODIS-T and JPL's HIRIS. The flight data acquired is further analyzed. Author

N89-28184*# National Aeronautics and Space Administration. Goddard Space Flight Center, Greenbelt, MD.
AGRICULTURE MULTIBAND EXPERIMENT RADIOMETER Abstract Only **c43**
W. H. Jones, J. Schutt, and B. Holben *In its* Laboratory for Oceans 1988 p 247-248 (For primary document see N89-28118 22-48)
Avail: NTIS HC A12/MF A01 CSCL 02C

Agriculture Multiband Experiment Radiometer (Amber) was designed and built in 1979 to 1980 and deployed in 1981. Amber was designed to simultaneously measure sunlight reflected from vegetation in 15 optical bands. In 1982, program interest shifted from ground truth to satellite image reduction and Amber was retired. Early in 1987, the project scientists concluded that Amber, because of its 15 simple and independent optical systems, would be ideally suited to study polarized light. Changes were made to add polarimeter capability to the instrument. The changes are listed and briefly discussed. Author

N89-28185*# National Aeronautics and Space Administration. Goddard Space Flight Center, Greenbelt, MD.
DIODE-PUMPED LASER RESEARCH **c36**
L. Ramos-Izquierdo, J. L. Bufton, and K. Chan *In its* Laboratory for Oceans 1988 p 249-252 (For primary document see N89-28118 22-48)
Avail: NTIS HC A12/MF A01 CSCL 20E

The Laboratory for Oceans is currently working on the development of compact laser diode array (LD) pumped Nd:YAG lasers for use in space-based altimetry and ranging. Laser diode-array pumping technology promises to increase the electrical to optical efficiency of solid state lasers by an order of magnitude with a lifetime increase of nearly three orders of magnitude relative to today's conventional flashlamp-pumped laser systems. The small size, efficiency, and ruggedness make LD-pumped solid state lasers ideal for space based applications. In an in-house RTOP effort, a novel multiple-pass LD-pumped Nd:YAG laser amplifier was designed and tested to increase the 100 microjoule output pulse energy of the Lightwave laser oscillator. Preliminary results have yielded a round trip amplifier gain of about 15 percent using 7 microjoule LD-pump energy. As a parallel activity, funding was recently obtained to investigate the possible use of custom made fiber optic arrays to obtain an efficient optical coupling mechanism between the emitting laser diode-arrays and the target solid state laser material. Fiber optic coupling arrays would allow for the easy manipulation of the spatial emitting pattern of the diode pump sources to match either an end or side pumping laser configuration. Author

N89-28186*# National Aeronautics and Space Administration. Goddard Space Flight Center, Greenbelt, MD.
LARGE APERTURE SCANNING AIRBORNE LIDAR Abstract Only **c36**
J. Smith, R. Bindschadler, R. Boers, J. L. Bufton, D. Clem, J. Garvin, and S. H. Melfi *In its* Laboratory for Oceans 1988 p 253-256 (For primary document see N89-28118 22-48)
Avail: NTIS HC A12/MF A01 CSCL 20E

A large aperture scanning airborne lidar facility is being developed to provide important new capabilities for airborne lidar sensor systems. The proposed scanning mechanism allows for a large aperture telescope (25 in. diameter) in front of an elliptical flat (25 x 36 in.) turning mirror positioned at a 45 degree angle with respect to the telescope optical axis. The lidar scanning capability will provide opportunities for acquiring new data sets for atmospheric, earth resources, and oceans communities. This completed facility will also make available the opportunity to acquire simulated EOS lidar data on a near global basis. The design and construction of this unique scanning mechanism presents exciting technological challenges of maintaining the turning mirror optical flatness during scanning while exposed to extreme temperatures, ambient pressures, aircraft vibrations, etc. Author

N89-28187*# National Aeronautics and Space Administration. Goddard Space Flight Center, Greenbelt, MD.
A MULTIPROCESSOR AIRBORNE LIDAR DATA SYSTEM Abstract Only **c36**
C. W. Wright, S. A. Bailey, G. E. Heath, and C. R. Piazza *In its* Laboratory for Oceans 1988 p 257-259 (For primary document see N89-28118 22-48)
Avail: NTIS HC A12/MF A01 CSCL 20E

A new multiprocessor data acquisition system was developed for the existing Airborne Oceanographic Lidar (AOL). This implementation simultaneously utilizes five single board 68010 microcomputers, the UNIX system V operating system, and the real time executive VRTX. The original data acquisition system was implemented on a Hewlett Packard HP 21-MX 16 bit minicomputer using a multi-tasking real time operating system and a mixture of assembly and FORTRAN languages. The present collection of data sources produce data at widely varied rates and require varied amounts of burdensome real time processing and formatting. It was decided to replace the aging HP 21-MX minicomputer with a multiprocessor system. A new and flexible recording format was devised and implemented to accommodate the constantly changing sensor configuration. A central feature of this data system is the minimization of non-remote sensing bus traffic. Therefore, it is highly desirable that each micro be capable of functioning as much as possible on-card or via private peripherals. The bus is used primarily for the transfer of remote sensing data to or from the buffer queue. Author

N89-28188*# National Aeronautics and Space Administration. Goddard Space Flight Center, Greenbelt, MD.
METEOROLOGICAL SENSOR CALIBRATION FACILITY Abstract Only **c47**
F. J. Schmidlin *In its* Laboratory for Oceans 1988 p 263-265 (For primary document see N89-28118 22-48)
Avail: NTIS HC A12/MF A01 CSCL 04B

The meteorological sensor calibration facility is designed to test and assess radiosonde measurement quality through actual flights in the atmosphere. United States radiosonde temperature measurements are deficient in that they require correction for errors introduced by long- and short-wave radiation. The effect of not applying corrections results in a large bias between day time and night time measurements. This day/night bias has serious implications for users of radiosonde data, of which NASA is one. The derivation of corrections for the U.S. radiosonde is quite important. Determination of corrections depends on solving the heat transfer equation of the thermistor using laboratory measurements of the emissivity and absorptivity of the thermistor coating. The U.S. radiosonde observations from the World Meteorological Organization International Radiosonde Intercomparison were used as the data base to test whether the day/night height bias can be removed. Twenty-five noon time and 26 night time observations were used. Corrected temperatures were used to calculate new geopotentials. Day/night bias in the geopotentials decreased significantly when corrections were introduced. Some testing of thermal lag attendant with the standard carbon hygristor took place. Two radiosondes with small bead thermistors imbedded in the hygristor were flown. Detailed analysis was not accomplished; however, cursory examination of the data showed that the hygristor is at a higher temperature than the external thermistor indicates. Author

N89-28189*# National Aeronautics and Space Administration. Goddard Space Flight Center, Greenbelt, MD.
NASA AIRCRAFT-SATELLITE INSTRUMENT CALIBRATION PROJECT Abstract Only **c35**
B. W. Guenther *In its* Laboratory for Oceans 1988 p 267-268 (For primary document see N89-28118 22-48)
Avail: NTIS HC A12/MF A01 CSCL 14B

Ground based prelaunch calibration of satellite instruments usually is not adequate to provide an accurate characterization of the in-orbit performance of a satellite instrument. This is because the ground calibrations may not simulate the in-orbit environment observations of the satellite sensor, or because the sensor characteristics have changed during launch and in-orbit operations. One technique to obtain a meaningful in-orbit calibration of satellite sensors is to acquire simultaneous observations of an Earth scene with the satellite and a well calibrated aircraft or shuttle sensor which has similar characteristics to the satellite sensor. This is a direct in-orbit calibration technique and is usually called vicarious calibration. The experiment with the control instrument must occur above the sensible atmosphere as measured by the satellite sensor to provide a useful improvement to the calibration of the satellite sensor. Some observations on the experiments are made. Author

N89-28190*# National Aeronautics and Space Administration. Goddard Space Flight Center, Greenbelt, MD.
FLIGHT CALIBRATION SOURCE DEVELOPMENT Abstract Only **c35**
S. Glicker *In its* Laboratory for Oceans 1988 p 269 (For primary document see N89-28118 22-48)
Avail: NTIS HC A12/MF A01 CSCL 14B

An important element in monitoring the sensitivity of flight instrumentation throughout a flight is a reliable reference. Tungsten filament quartz halogen and deuterium UV sources were tested for this purpose. All three types were obtained from available commercial supplies and were tested against various mission requirements, particularly long term stability characteristics. Stability tests were made before and after thermal vacuum and vibration tests. Author

N89-28191*# National Aeronautics and Space Administration. Goddard Space Flight Center, Greenbelt, MD.
RADIANCE STANDARDS Abstract Only **c74**
D. L. Lester *In its* Laboratory for Oceans 1988 p 271-274 (For primary document see N89-28118 22-48)
Avail: NTIS HC A12/MF A01 CSCL 20F

Two radiometric calibration sources that are utilized by various groups are maintained and operated. One source is a 6-ft diameter sphere and the other a 4-ft diameter hemisphere. Both are internally coated with multiple layers of barium sulfate and house an array of 12 tungsten filament-quartz iodine lamps that provide a uniform diffuse target of radiance traceable to NBS. The lamps are baffled and arranged so that they are not part of the scene during calibrations. Both systems have a 10-inch viewing aperture. The hemisphere is somewhat more versatile in that the aperture can be changed and the system is movable so calibrations can be done at other sites. Together, these systems have supported numerous GSFC projects and missions during this review period. They are listed. Author

N89-28192*# National Aeronautics and Space Administration. Goddard Space Flight Center, Greenbelt, MD.
ENVIRONMENTAL CALIBRATION CHAMBER OPERATIONS Abstract Only **c09**
D. L. Lester *In its* Laboratory for Oceans 1988 p 275-276 (For primary document see N89-28118 22-48)
Avail: NTIS HC A12/MF A01 CSCL 14B

Thermal vacuum capabilities are provided for the development, calibration, and functional operation checks of flight sensors, sources, and laboratory and field instruments. Two systems are available. The first is a 46 cm diameter diffusion pumped vacuum chambler of the bell jar variety. It has an internal thermal shroud, LN2 old trap, two viewing ports, and various electrical and fluid feedthroughs. The other, also an oil diffusion pumped system, consists of a 1.8 m diameter by 2.5 m long stainless steel vacuum tank, associated pumping and control equipment, a liquid nitrogen storage and transfer system and internal IR/visible calibration sources. This is a two story system with the chamber located on one floor and the pumping/cryogenic systems located on the floor below. Author

N89-28193*# National Aeronautics and Space Administration. Goddard Space Flight Center, Greenbelt, MD.
CALIBRATION SOURCE MAINTENANCE, CHARACTERIZATION AND DEVELOPMENT Abstract Only **c35**
J. T. McLean *In its* Laboratory for Oceans 1988 p 277 (For primary document see N89-28118 22-48)
Avail: NTIS HC A12/MF A01 CSCL 14B

The Standards and Calibration Office maintains visible and near infrared calibration sources for the use of various GSFC organizations instrument calibration needs and related field activities. These are large aperture spherical and hemispherical integrating sources designed to provide a spatially uniform absolute spectral radiance with a well-defined angular uniformity characteristic. In essence, the calibration and characterization efforts involve monitoring and documenting the stability and the absolute radiance of these calibration sources. These sources are recalibrated on a regular basis to both document any changes that might occur in the output of the sources and to provide the most up-to-date calibration data for the source users. Efforts included comparing the calibration numbers with those of a commercial calibration laboratory that was engaged to do independent calibrations. However, the most recent calibrations done by the independent laboratory and those done by GSFC personnel show a rather large discrepancy (10 to 15 percent). Efforts are underway to resolve these differences. Author

N89-28194*# National Aeronautics and Space Administration. Goddard Space Flight Center, Greenbelt, MD.
INTEGRATING SPHERE AND HEMISPHERE CALIBRATION UPDATE Abstract Only **c35**
J. T. McLean *In its* Laboratory for Oceans 1988 p 279-281 (For primary document see N89-28118 22-48)
Avail: NTIS HC A12/MF A01 CSCL 14B

This background information relates to the conclusions reached about the GSFC/Optronic calibrations for the 6-foot sphere. Both the hemispherical and the spherical integrating sources were remeasured in February 1988 by two experimenters and the results show a decrease in the output of the sphere. But the discrepancy between GSFC data and Optronic Data remains. The decrease in the output can be accounted for by a correction in the current value of power supplies Number 2 and Number 3. The supplies were running about 1.75 percent high. Minor differences were noted in the short wavelength end of the hemisphere. Efforts to resolve the discrepancy between GSFC and Optronic Labs as well as improve the ability to make more accurate and precise measurements are underway. Author

N89-28195# Colorado Univ., Boulder. Center for Astrodynamics Research.
OCEAN MODELLING AND THE USE OF ALTIMETRY DATA Final Report, 1 Jul. 1986 - 30 Sep. 1988
George Born and Patrick Weidman 1 Feb. 1989 2 p
(Contract N00014-86-K-0728)
(AD-A206841) Avail: NTIS HC A02/MF A01 CSCL 08/3

The objective of the subject contract was to develop methodology for effectively using satellite altimetry for oceanographic applications. Another task was to examine techniques for measuring and monitoring rotating fluid phenomena. In addition, a task was added later by NORDA to develop ice motion techniques from sequential AVHRR imagery. The ice motion work involved the use of filtered cross correlation between relatively cloud free sequential AVHRR images to examine temporal changes in the patterns of sea ice motion. Most of this work was the interpolation of GEOSAT ERM altimetry time series for the purpose

of wave detection. Considerable work was done in the tropical Pacific on Kelvin wave detection techniques. This work has been presented at several conferences (see list of presentations), but has not yet been fully documented in the open literature. This work is still in progress and its results should be published during the next year. GRA

N89-28196# Lamont-Doherty Geological Observatory, Palisades, NY.
CLOUD/CRYOSPHERE INTERACTIONS Final Report, Nov. 1985 - Oct. 1988
George Kukla and David A. Robinson (Rutgers - The State Univ., New Brunswick, NJ.) 19 Apr. 1989 46 p
(Contract DE-AC02-81EV-10665; AF-AFOSR-0053-86; NSF ATM-83-18676; NSF ATM-85-05558; NSF ATM-87-19865; NSF ATM-87-12020; AF Proj. 2310)
(AD-A208377; AFOSR-89-0590TR) Avail: NTIS HC A03/MF A01 CSCL 08/12

Major objectives included investigating cryospheric dynamics, particularly relationships and feedbacks between clouds and the cryosphere when snow cover is forming or dissipating, and assessing algorithms and climatologies used in Air Force (A.F.) operational snow and cloud cover products. Study results have led to increased understanding of: (1) seasonal and interannual variations in snow and cloud cover; (2) dynamics of the onset of melt season in arctic regions; (3) performance of A.F. nephanalyses in marginal cryosphere regions; and (4) performance of the A.F. SNODEP model. Some of the results include: (1) Cloud cover in the Arctic Basin has a late May-early June maximum in extent and thickness, followed by a period of less extensive and thinner cover extending into early August. Cloud conditions are associated with the distribution of surface pressure and the flow of air into the Basin at the surface and aloft; (2) Over arctic lands and sea ice, the timing and duration of the snow melt season, which strongly influence surface mobility of personnel and machinery, vary geographically within a year and across the region from year to year; and (3) Increased spring cloudiness and onset of the melt season over sea ice coincide, suggesting that both are related to northward transport of moist air into the Basin by synoptic disturbances, rather than one solely driving the other. Results over arctic lands are less conclusive. Varying conditions of snow pack, surface albedo, seasonal and latitudinal distribution of solar insolation reaching the top of the atmosphere are among other factors influencing melt. GRA

N89-28197# Naval Research Lab., Washington, DC. Acoustic Systems Branch.
MODELING OF OCEAN SURFACE SPECTRUM AND SURFACE SCATTERING. APPLICATIONS TO REVERBERATION PREDICTION IN THE AAUS PROGRAM Memorandum Report, Oct. 1983 - Sep. 1984
T. D. Ngoc, E. R. Franchi, and B. B. Adams 23 Jun. 1989 84 p
(AD-A210127; NRL-MR-6205) Avail: NTIS HC A05/MF A01 CSCL 20/1

Current scattering theories for sound interaction with the ocean surface and empirical descriptions of the ocean surface wave spectrum are examined for incorporation into the NRL Reverberation Model (RASP). The intent is to provide surface scattering strength estimates using such theories to augment the empirical data bases in surface scattering strength already included in RASP. Since the input surface wave spectrum plays a critical role in determining the scattering strength, a comprehensive assessment of available empirical models of surface wave spectra was performed and the most updated version of the Pierson model was selected for use in combination with the azimuthal distribution model proposed by Mitsuyasu et al. This study focussed on those scattering theories that perform best in the low frequency (less than 500 Hz), low-grazing angle (less than 20 deg) regime. As a result, scattering models such as the small perturbation method and the composite roughness approach were selected for incorporation into RASP in addition to two empirical models, Martin and Chapman-Harris. Illustrations of the surface wave two-dimensional spectrum are presented, and sample computations of the scattering strength using the selected models are given for different combinations of the principal parameters, which include frequency, wind speed, wind direction, and scattering geometry. GRA

51 LIFE SCIENCES (GENERAL)

N89-28198# California Univ., Santa Barbara. Marine Science Inst.
MOLECULAR BIOLOGY OF THE PHOTOREGULATION OF PHOTOSYNTHETIC LIGHT-HARVESTING COMPLEXES IN MARINE DINOFLAGELLATES Annual Report, 15 Jun. 1988 - 15 Jun. 1989
Barbara B. Prezelin and Edward L. Triplett 2 Jun. 1989 14 p
(Contract N00014-88-K-0060)
(AD-A209650) Avail: NTIS HC A03/MF A01 CSCL 06/3

The goal is to continue to use biotechnological techniques to study the genetic bases of light- and nutrient-regulation of photosynthetic light-harvesting complexes in marine dinoflagellates and their consequences for the bio-optical features of these algae. The studies are significant to determining the molecular bases of environmental regulation of gene expression and photosynthetic performance in marine phytoplankton. Results also contribute to understanding the linkages between light environments and cell optical properties, key elements in physiologically-based bio-optical models being developed to predict ocean primary production. GRA

52 AEROSPACE MEDICINE

Includes physiological factors; biological effects of radiation; and effects of weightlessness on man and animals.

N89-28199# Los Alamos National Lab., NM.
THE HUMAN TELOMERE
Robert K. Moyzis 1989 15 p Presented at the 6th Conversation in the Discipline Biomolecular Stereodynamics, Albany, NY, 6 Jun. 1989
(Contract W-7405-eng-36)
(DE89-014252; LA-UR-89-1989; CONF-8906159-2) Avail: NTIS HC A03/MF A01

An ultimate goal of human genetics is the generation of a complete physical and functional map of the human genome. Twenty-five percent of human DNA, however, consists of repetitive DNA sequences. These repetitive DNA sequences are thought to arise by many mechanisms, from direct sequence amplification by the unequal recombination of homologous DNA regions to the reverse flow of genetic information. A general outline of the chromosomal organization of these repetitive sequences will be discussed. Our working hypothesis is that certain classes of human repetitive DNA sequences encode the information necessary for defining long-range genomic structure. Evidence will be presented that the first goal of this research, the identification and cloning of the human telomere, has been achieved. A human repetitive DNA library was constructed from randomly sheared, reassociated, and oligo(G-C)-tailed DNA, a method that minimizes the potential loss of sequences devoid of a given restriction enzyme site. Sequences too large to clone efficiently in cosmid or lambda vectors, such as centromeric repeats, or telomeric sequences with an end incompatible for cloning, should be present in this library. In order to isolate highly conserved repetitive DNA sequences, this library was screened with radiolabeled hamster Cot50 repetitive DNA. Two clones, containing tandem arrays of the sequence (TTAGGG), were isolated by this method. DOE

N89-28200# Aerospace Medical Research Labs., Wright-Patterson AFB, OH.
THE EFFECT OF VARIOUS STRAINING MANEUVERS ON CARDIAC VOLUMES AT 1G AND DURING +Gz ACCELERATION Final Report, Jan. 1984 - Aug. 1985
Tom Jennings, Lloyd Tripp, Lora Howell, John Seaworth, and David Ratino Jan. 1989 20 p
(AD-A208846; AAMRL-TR-89-011) Avail: NTIS HC A03/MF A01 CSCL 06/5

The purpose of this study was to evaluate the effect of Valsalva (Val), isometric contraction (Iso) and the L-1 maneuvers (L-1) on cardiac volumes at 1G and during 4G. Two-dimensional echocardiography was used to measure volumes. 1G Phase: Eight seated male subjects performed the three maneuvers. The end-diastolic volume (EDV) decreased during Val and L-1 (p less than 0.05). EDV decreased initially but then returned to baseline with Iso. 4G Phase: Seven male subjects experienced three 30 second 4G epochs while performing the three maneuvers. During 4G, 3 of 7 performing Val, 2 of 7 performing Iso, and none performing L-1, experienced peripheral light loss. EDV decreased and stabilized below baseline during the 4Gz epoch (p less than 0.05). Heart rate and cardiac output increased for all maneuvers. Differences between the effects of Val, Iso, and L-1 on G-tolerance do not appear to be related to a differential ability to maintain cardiac volumes. L-1 must provide more G protection due to the isometric contraction component of the maneuver and provide more G protection due to the isometric contraction component of the maneuver and its ability to increase blood pressure. GRA

N89-28201# Army Research Inst. of Environmental Medicine, Natick, MA. Health and Performance Div.
EFFECTS OF HIGH TERRESTRIAL ALTITUDE ON MILITARY PERFORMANCE
Louis E. Banderet and Richard L. Burse 18 Apr. 1989 45 p
(AD-A209614; USARIEM-M-33-89) Avail: NTIS HC A03/MF A01 CSCL 06/4

At high altitude, several adverse physical characteristics make coping, functioning, and survival very difficult: hypoxia, cold, wind, dryness, solar radiation, and ultraviolet radiation. The proportion of oxygen in the air is constant at 20.93 percent, even at altitudes up to 100,000 m. The decreased atmospheric pressure at high altitudes results in a proportional reduction of the partial pressure of oxygen (Po2). This lessens the amount of oxygen carried on the blood. The barometric pressures of two regions at the same elevation may differ, since atmospheric pressure also depends on latitude, thickness of the earth's crust, and weather. The relationship between altitude and atmospheric pressure is described in table which include adjustment factors for specific location conditions. GRA

N89-28202# Army Research Inst. of Environmental Medicine, Natick, MA.
ACETYLCHOLINESTERASE INHIBITOR, PYRIDOSTIGMINE BROMIDE, REDUCES SKIN BLOOD FLOW IN HUMANS
Lou A. Stephenson and Margaret A. Kolka May 1989 26 p
(AD-A209615; USARIEM-M-49-89) Avail: NTIS HC A03/MF A01 CSCL 06/15

Five subjects exercised on a cycle ergometer for 30 min at 55 percent peak VO2 on two occasions in a slightly warm environment. Pyridostigmine bromide (PYR), an acetylcholinesterase (AChE) inhibitor, was ingested (30 mg) approximately 150 min before one experiment, and no drug was administered during the other experiment (control). Red cell AChE inhibition averaged 40 (+ or - 7) percent during PYR treatment. Esophageal temperature (Tes), a derived mean skin temperature, forearm blood flow (venous occlusion plethysmography), cutaneous perfusion, and metabolic rate were measured. Cutaneous perfusion decreased after PYR treatment compared to control. Forearm blood flow, which included inactive muscle, skin, fat and bone tissue, was not different between treatments, which implies that blood flow to one of those tissues may have increased while skin blood flow decreased during PYR treatment. The increased threshold for initiation of cutaneous vasodilation with AChE inhibition by PYR suggests that the drug activates central modulation of thermoregulation. One of several possible mechanisms activated may be through increased ACh accumulation at preganglionic sites. This could potentiate adrenergic transmission to cutaneous blood vessels, and enhance vasoconstrictor tone. GRA

N89-28203# Rutgers - The State Univ., New Brunswick, NJ. Dept. of Psychology.
EYE MOVEMENTS AND VISUAL INFORMATION PROCESSING Interim Report, 1 Apr. 1988 - 31 Mar. 1989
Eileen Kowler 27 Apr. 1989 3 p
(Grant AF-AFOSR-0171-88; AF Proj. 2313)
(AD-A209817; AFOSR-89-0808TR) Avail: NTIS HC A02/MF A01 CSCL 05/8

Eye movements place a limit on the processing of visual information because they determine the location and the velocity of the retinal image. Thus, to understand how we see it is necessary to understand how eye moments are controlled. Work this year in my laboratory has concentrated on the roles of expectations and selective attention in the programming of smooth and saccadic eye movements. We have: (1) demonstrated distinct roles for past experience and expectations in the control of smooth eye movement and found that expectation will predominate in the presence of cues about the direction of future motion; (2) found that brisk initial pursuit requires that expectation that target motion will continue; and (3) showed that saccadic eye movements are not attracted to visual backgrounds (as had been claimed) unless subjects pay attention to the background. These studies show that central representations of visual scenes, containing information about the position, motion and future motion of selected objects, are the natural effective stimulus for human eye movement. GRA

N89-28204# Colorado State Univ., Fort Collins.
THE PHOTOTOXICITY OF BLUE LIGHT ON THE FUNCTIONAL PROPERTIES OF THE RETINAL PIGMENT EPITHELIUM Annual Report, 1 May 1988 - 30 Apr. 1989
E. L. Paulter May 1989 17 p
(Grant AF-AFOSR-0189-87; AF Proj. 2312)
(AD-A209834; AFOSR-89-0930TR) Avail: NTIS HC A02/MF A01 CSCL 06/10

The phototoxic effect of blue light on isolated pigment epithelium was investigated. The emphasis was on functional changes rather than a description of pathology. The pigment epithelium is analogous to the blood-brain barrier; therefore, the principal functions investigated were the integrity of the barrier system and the transport system and the transport systems known to operate in the pigment epithelium. The effects of blue light on leucine transport across the isolated bovine retinal pigment epithelium (RPE) were continued to determine if Vitamin E and melatonin provided any protective action. Similar studies on the transport of glutamate in the retina to choroid direction were also completed. GRA

N89-28205# New York Univ., New York. Dept. of Psychology.
HIGHER ORDER MECHANISMS OF COLOR VISION Progress Report No. 1, 15 Sep. 1986 - 14 Mar. 1989
John Krauskopf 12 May 1989 16 p
(Grant AF-AFOSR-0334-86; AF Proj. 2313)
(AD-A209838; AFOSR-89-0931TR) Avail: NTIS HC A02/MF A01 CSCL 06/4

The main accomplishments during this reporting period were: (1) a comprehensive study of the effects of chromatic content, blur and contrast of targets on vernier acuity and on stereo acuity; (2) the use of a new method of measuring chromatic discrimination under conditions of constant adaptation; (3) continuation of the study of the chromatic properties of single cells in the monkey cortex; and (4) experiments on the significance color in the perception of motion. GRA

N89-28206# Johns Hopkins Univ., Baltimore, MD.
PRE-ATTENTIVE AND ATTENTIVE VISUAL INFORMATION PROCESSING Annual Report, 2 Apr. 1988 - 3 Mar. 1989

H. E. Egeth 1 Jun. 1989 17 p
(Grant AF-AFOSR-0180-87; AF Proj. 2313)
(AD-A209884; AFOSR-89-0815TR) Avail: NTIS HC A03/MF A01 CSCL 06/4

Research on several interrelated topics is described. These projects are focused on the analysis of feature and conjunction detection, models of selective attention, and curve tracing. One project examines the effects of a heterogeneous background on feature search. Another assesses spatial factors (such a target-distractor separation) in the detection of targets defined in terms of simple features. A third project has the goal of developing methods for determining the extent to which processing is serial or parallel. A fourth represents initial efforts to determine whether conjoined features are represented in retinotopic or spatiotopic maps. A fifth explores top-down and bottom-up factors in visual search. A sixth makes use of an inhibitory priming method to test early-and late-selection models of selective attention. Finally, a project is reported in which the operation of visual curve tracing is studied. GRA

N89-28207# New York Univ., New York.
ATTENTION, IMAGERY AND MEMORY: A NEUROMAGNETIC INVESTIGATION Annual Report, 1 Mar. 1988 - 28 Feb. 1989
Lloyd Kaufman 12 May 1989 7 p
(Contract F49620-88-K-0004)
(AD-A209917; AFOSR-89-0960TR) Avail: NTIS HC A02/MF A01 CSCL 05/8

This report describes a number of experiments related to the effects of mental imagery and other high-level cognitive tasks on the spontaneous activity of the brain. The basic procedure involves narrowly bandpassing the magnetoencephalogram (MEG), computing the average response to a stimulus or event within that bandpass, and computing the variance around the average. The variance at any point in time subsequent to the stimulus is a measure of mean square field (power). Power in the alpha band (8 to 12 Hz) was found to show a prominent change in level subsequent to presentation of form. Simply watching the form results in a dip in alpha power, but when subjects attempt to determine if the form had been seen previously, the duration of the reduction in alpha power increases significantly, and is correlated with reaction time (RT). In an experiment subjects tried to form an image of an object represented by a visually presented word, or to find a rhyming word. The latter task did not produce a change in activity of visual cortex, while the same words produced a profound change in activity cortex during imaging. Acoustically presented words were also found to produce changes in MEG activity. GRA

N89-28208# New York Univ., New York. Dept. of Physics and Psychology.
MODULATION OF SPONTANEOUS BRAIN ACTIVITY DURING MENTAL IMAGERY Report, 1 Mar. 1988 - 28 Feb. 1989
Lloyd Kaufman, Barry Swartz, Carlo Salustri, and Samuel J. Williamson 12 May 1989 14 p
(Contract F49620-88-K-0004)
(AD-A209918; AFOSR-89-0961TR) Avail: NTIS HC A03/MF A01 CSCL 06/4

Magnetic measurements of average power of human alpha activity over the occipital and parietal areas of the scalp reveal spatially selective suppression when abstract figures are briefly presented visually. The duration of suppression increases along with reaction time during a search of visual memory. This implies that the visual system is involved in mental imagery. GRA

N89-28209# Massachusetts Inst. of Tech., Lexington. Lincoln Lab.
OPTICAL SPATIAL TRACKING USING COHERENT DETECTION IN THE PUPIL PLANE
Eric A. Swanson, Gary M. Carter, D. J. Bernays, and David M. Hodsdon 19 May 1989 41 p
(Contract F19628-85-C-0002)
(AD-A209970; TR-823) Avail: NTIS HC A03/MF A01 CSCL 17/5

Design considerations for a heterodyne spatial tracking system utilizing pupil-plane processing techniques and its advantages over traditional focal-plane processing are described. Noise performance bounds, optimal and suboptimal local oscillator distributions, pull-in performance, and applications other than spatial tracking are discussed. Experimental verification of a one-axis closed-loop tracking system is presented. GRA

N89-28210# New York Univ., New York. Dept. of Physics and Psychology.
VISUALIZING AND RHYMING CAUSE DIFFERENCES IN ALPHA SUPPRESSION Report, 1 Mar. 1988 - 28 Feb. 1989
Lloyd Kaufman, M. Glanzer, Y. Cycowicz, and S. J. Williamson 12 May 1989 5 p
(Contracts F49620-88-K-0004; F49620-86-C-0141; AF Proj. 2313)
(AD-A210005; AFOSR-89-0962TR) Avail: NTIS HC A02/MF A01 CSCL 06/4

Alpha rhythms of the EEG are strongest at the occipital regions of the head, and the visual cortex is apparently a major contributor. It has been suggested that visual cortex is involved in forming and processing mental images. The purpose of this experiment is to determine if a task that involves visualizing objects represented by words produces changes in alpha rhythms of the MEG that differ from changes associated with finding rhymes of the same or related verbal stimuli. By hypothesis, the visual areas of the cortex play a less prominent role in the latter task than they do in the visualizing task. This inference is consistent with the finding that visual imagery is accompanied by attenuation of the alpha rhythm over the occipital scalp, in the proximity of visual cortex cognitive factors, such as memorization and classification of words, affects the pattern of alpha blockage across the occipital and parietal area, but this does not establish that visual cortex per se is involved. Subjects responded by forming mental images of the objects represented by the words. The event related potentials associated with presentation of the words were larger in amplitude than they were when the subjects silently pronounced words that rhymed with the stimuli instead of forming mental images. This effect was more evident at occipital electrodes than it was at other locations. There may well be differential suppression of alpha activity depending on the degree to which visual resources are engaged in various mental tasks, such as imaging. GRA

53 BEHAVIORAL SCIENCES

Includes psychological factors; individual and group behavior; crew training and evaluation; and psychiatric research.

No abstracts in this category.

54 MAN/SYSTEM TECHNOLOGY AND LIFE SUPPORT

Includes human engineering; biotechnology; and space suits and protective clothing.

For related information see also *16 Space Transportation.*

N89-28211*# Good Samaritan Hospital and Medical Center, Portland, OR. Dept. of Neuro-otology.
AGE-RELATED CHANGES IN HUMAN VESTIBULO-OCULAR REFLEXES: SINUSOIDAL ROTATION AND CALORIC TESTS
R. J. Peterka, F. O. Black, and M. B. Schoenhoff 1989 15 p
(Grant NAG9-117)
(NASA-CR-185857; NAS 1.26:185857) Avail: NTIS HC A03/MF A01 CSCL 05H

The dynamic response properties of horizontal vestibulo-ocular reflex (VOR) were characterized in 216 human subjects ranging in

age from 7 to 81 years. The object of this cross-sectional study was to determine the effects of aging on VOR dynamics, and to identify the distributions of parameters which describe VOR responses to caloric and to sinusoidal rotational stimuli in a putatively normal population. Caloric test parameters showed no consistent trend with age. Rotation test parameters showed declining response amplitude and slightly less compensatory response phase with increasing age. The magnitudes of these changes were not large relative to the variability within the population. The age-related trends in VOR were not consistent with the anatomic changes in the periphery reported by others which showed an increasing rate of peripheral hair cell and nerve fiber loss in subjects over 55 years. The poor correlation between physiological and anatomical data suggest that adaptive mechanisms in the central nervous system are important in maintaining the VOR. Author

N89-28212*# Good Samaritan Hospital and Medical Center, Portland, OR. Dept. of Neuro-otology.
AGE-RELATED CHANGES IN HUMAN POSTURE CONTROL: SENSORY ORGANIZATION TESTS
R. J. Peterka and F. O. Black 1989 17 p
(Grant NAG9-117)
(NASA-CR-185858; NAS 1.26:185858) Avail: NTIS HC A03/MF A01 CSCL 05H

Postural control was measured in 214 human subjects ranging in age from 7 to 81 years. Sensory organization tests measured the magnitude of anterior-posterior body sway during six 21 s trials in which visual and somatosensory orientation cues were altered (by rotating the visual surround and support surface in proportion to the subject's sway) or vision eliminated (eyes closed) in various combinations. No age-related increase in postural sway was found for subjects standing on a fixed support surface with eyes open or closed. However, age-related increases in sway were found for conditions involving altered visual or somatosensory cues. Subjects older than about 55 years showed the largest sway increases. Subjects younger than about 15 years were also sensitive to alteration of sensory cues. On average, the older subjects were more affected by altered visual cues whereas younger subjects had more difficulty with altered somatosensory cues. Author

N89-28213*# Good Samaritan Hospital and Medical Center, Portland, OR. Dept. of Neuro-otology.
AGE-RELATED CHANGES IN HUMAN VESTIBULO-OCULAR AND OPTOKINETIC REFLEXES: PSEUDORANDOM ROTATION TESTS
R. J. Peterka, F. O. Black, and M. B. Schoenhoff 1989 16 p
(Grant NAG9-117)
(NASA-CR-185856; NAS 1.26:185856) Avail: NTIS HC A03/MF A01 CSCL 05H

The dynamic response properties of horizontal vestibulo-ocular reflex (VOR) and optokinetic reflex (OKR) were characterized in 216 human subjects ranging in age from 7 to 81 years. The object of this cross-sectional study was to determine the effects of aging on VOR and OKR reflex dynamics, and to identify the distributions of parameters which describe VOR and OKR responses to pseudorandom stimuli in a putatively normal population. In general, VOR and OKR response parameters changed in a manner consistent with declining function with increasing age. For the VOR this was reflected in declining response amplitudes, although the magnitude of the decline was small relative to the variability of the data. For the OKR the lag time of the response, probably associated with the time required for visual information processing, increased linearly with age at a rate of about 1 ms per year. Author

N89-28214# European Space Agency, Paris (France).
THIRD EUROPEAN SYMPOSIUM ON SPACE THERMAL CONTROL AND LIFE SUPPORT SYSTEMS
T. Duc Guyenne, ed. and J. Hunt, ed. Dec. 1988 629 p Symposium held in Noordwijk, Netherlands, 3-6 Oct. 1988
(ESA-SP-288; ISSN-0379-6566; ETN-89-95012) Copyright Avail: NTIS HC A99/MF A01; ESA Publications Div., ESTEC, Noordwijk, Netherlands, 80 Dutch guilders or 45 US dollars

Environmental control and life support systems; heat transport systems; orbital systems thermal control; atmosphere management; EVA; analysis methods; satellite thermal control; liquid management and habitability; cryogenics; in-orbit performance and testing; thermal control technology; and reentry and thermal protection systems were discussed. For individual titles, see N89-28215 through N89-28297.

N89-28215*# National Aeronautics and Space Administration. Marshall Space Flight Center, Huntsville, AL.
STATUS OF THE US SPACE STATION ECLSS AND INTERNAL TCS
R. Humphries, L. Turner, J. Reuter, and D. Patterson *In* ESA, Third European Symposium on Space Thermal Control and Life Support Systems Dec. 1988 p 5-13 (For primary document see N89-28214 22-54)
Copyright Avail: NTIS HC A99/MF A01; ESA Publications Div., ESTEC, Noordwijk, Netherlands, 80 Dutch guilders or 45 US dollars

The space station environmental control and life support system (ECLSS) and internal thermal control system (ITCS) are outlined. The ECLSS is composed of six subsystem groups: the temperature humidity control, the atmosphere control and supply, the air revitalization, water reclamation and management, fecal waste management, and the fire detection and suppression subsystems. The ITCS consists of all WP01 elements of passive and active thermal measures. The ECLSS and ITCS provide services for the permanently orbiting pressurized modules as well as the pressurized and unpressurized logistics carriers. All internal cooling of the permanent orbital elements are provided via internal active fluid loops within the elements utilizing water as the transport media. Cabin and equipment cooling are provided by forced air flow and coldplate heat sinks. An active cooling loop is provided in the laboratory module to accommodate experiments and other payloads. Coatings and insulation are used in conjunction with the active components to passively limit heat losses/gains. The most challenging ECLSS new technology issues relate to oxygen and water recovery. Closure of the oxygen loop requires the use of regenerative CO2 removal and concentration techniques, CO2 reduction to convert the CO2 to water with a waste by-product, and the electrolysis of water to produce breathing oxygen for water recovery. ESA

N89-28216# Entwicklungsring Nord, Bremen (Germany, F.R.).
SYSTEM ASPECTS OF COLUMBUS THERMAL CONTROL AND LIFE SUPPORT
U. Laux, B. Behrens, and R. Lawson *In* ESA, Third European Symposium on Space Thermal Control and Life Support Systems Dec. 1988 p 15-23 (For primary document see N89-28214 22-54)
Copyright Avail: NTIS HC A99/MF A01; ESA Publications Div., ESTEC, Noordwijk, Netherlands, 80 Dutch guilders or 45 US dollars

Thermal Control and Life Support Systems of the Columbus flight configurations, the Attached Pressurized Module (APM), the Man Tended Free Flyer (MTFF) and the Polar Platform (PPF) are described. The overall APM and MTFF Environmental Control and Life Support System (ECLSS) is strongly affected by the interfaces to the International Space Station (ISS) and Hermes. It is proposed to centralize particular ECLSS functions of both the APM and MTFF for reasons of cost, mass, power, and complexity reduction and to operate the MTFF-ECLSS in a power saving mode during the free flying phase. Rejection of the APM generated heat is performed totally by the ISS, whereas the MTFF Thermal Control is fully autonomous in the free flying and Hermes servicing phase. The preferred MTFF orientation, which is driven by the very stringent microgravity requirement, is in conflict with the heat rejection capabilities of the TCS. ESA

N89-28217# Aerospatiale Usines de Toulouse (France).
THE HERMES SPACEPLANE PROGRAM: STATUS REPORT ON THE THERMAL CONTROL, ENVIRONMENT CONTROL AND LIFE SUPPORT ACTIVITIES
H. Lacaze, P. Bisiaux, and C. Rodiere *In* ESA, Third European Symposium on Space Thermal Control and Life Support Systems Dec. 1988 p 25-36 (For primary document see N89-28214 22-54)
Copyright Avail: NTIS HC A99/MF A01; ESA Publications Div., ESTEC, Noordwijk, Netherlands, 80 Dutch guilders or 45 US dollars

The status of the Hermes, the thermal protection subsystem, thermal control subsystem, and environmental control and life support subsystem is outlined. Each one contributes to the thermal control of some part of the vehicle and is therefore influenced by the two others. Due to severe constraints coming from the launcher performances, the Hermes mass budget is critical and renders necessary elaborate design studies and use of advanced techniques for most component parts. ESA

N89-28218# Dornier System G.m.b.H., Friedrichshafen (Germany, F.R.).
EUROPEAN LIFE SUPPORT SYSTEMS FOR SPACE APPLICATIONS
H. Preiss *In* ESA, Third European Symposium on Space Thermal Control and Life Support Systems Dec. 1988 p 39-44 (For primary document see N89-28214 22-54)
Copyright Avail: NTIS HC A99/MF A01; ESA Publications Div., ESTEC, Noordwijk, Netherlands, 80 Dutch guilders or 45 US dollars

The environmental control and life support systems (ECLSS) for Columbus and Hermes are described, and the ECLSS requirements for European missions to Mars, the Moon, and an LEO station are outlined. It is argued that to meet these demands, international cooperation is necessary. ESA

N89-28219# Dornier System G.m.b.H., Friedrichshafen (Germany, F.R.).
ENVIRONMENTAL CONTROL AND LIFE SUPPORT SYSTEMS FOR PRESSURIZED MODULES: FROM SPACELAB TO COLUMBUS
K.-O. Hienerwadel and G. Kring *In* ESA, Third European Symposium on Space Thermal Control and Life Support Systems Dec. 1988 p 45-50 (For primary document see N89-28214 22-54)
Copyright Avail: NTIS HC A99/MF A01; ESA Publications Div., ESTEC, Noordwijk, Netherlands, 80 Dutch guilders or 45 US dollars

The Columbus environmental control and life support system (ECLSS) is compared with the Spacelab ECLSS. The individual Columbus ECLSS equipment characteristics are identified, stating whether they are identical, modified, and advanced or completely new compared to the Spacelab capabilities. Although the basic ECLSS functions of Columbus are similar to those of Spacelab there are considerable differences in design and performance between the two systems. These differences are mainly caused by two factors. The first one is the mission duration characterized by the in orbit life time of the module and the uninterrupted attendance of one crew before change of shift. The second one is the required full automatic operation capability caused by the 180 days free flying and unmanned period of the Man-Tended Free Flyer. ESA

N89-28220# Dornier System G.m.b.H., Friedrichshafen (Germany, F.R.).
THE DEFINITION STATUS OF THE ENVIRONMENTAL CONTROL AND LIFE SUPPORT SUBSYSTEMS FOR HERMES
R. Schaefer *In* ESA, Third European Symposium on Space Thermal Control and Life Support Systems Dec. 1988 p 51-55 (For primary document see N89-28214 22-54)
Copyright Avail: NTIS HC A99/MF A01; ESA Publications Div., ESTEC, Noordwijk, Netherlands, 80 Dutch guilders or 45 US dollars

The status of the Hermes environmental control and life support system (ECLSS) and the main differences compared with the Spacelab ECLSS are outlined. Requirements development from Phase A (6 men, 2 volumes) to Phase B (3 men, 3 volumes) and the relevant configurations are described. The atmosphere pressure control section; air conditioning section; liquid management section; food galley management section; hygiene and solid waste management section; and monitoring, control, and power management section are described. ESA

N89-28221# Nelson Space Services Ltd., London (England).
PHYSICO-CHEMICAL ATMOSPHERE REVITALISATION: THE QUALITATIVE AND QUANTITATIVE SELECTION OF REGENERATIVE DESIGNS
R. C. Hunttenbach, A. R. Kaiser, J. D. Radford, and R. A. Binot (European Space Agency. European Space Research and Technology Center, ESTEC, Noordwijk, Netherlands) *In* ESA, Third European Symposium on Space Thermal Control and Life Support Systems Dec. 1988 p 57-64 (For primary document see N89-28214 22-54)
Copyright Avail: NTIS HC A99/MF A01; ESA Publications Div., ESTEC, Noordwijk, Netherlands, 80 Dutch guilders or 45 US dollars

The systems engineering needs of regenerative physico-chemical atmosphere revitalization is discussed from the qualitative point of view, and a procedure that can be used to quantify the prospective merits of competing designs at an early stage in their development cycle is described. This procedure involves the preparation of energy and multicomponent material balances, the derivation of weight penalties for various power generation/supply and heat rejection technologies, the calculation of equivalent weights versus duration of mission and the use of spreadsheets to analyze the sensitivity of results when input data such as the weight of flight qualified equipment is subject to uncertainty. The methodology can be applied to other systems including water management and future biological options on manned space missions. ESA

N89-28222# Centre d'Etude de l'Energie Nucleaire, Mol (Belgium).
MELISSA: A MICRO-ORGANISMS-BASED MODEL FOR CELSS DEVELOPMENT
M. Mergeay, W. Verstraete, G. Dubertret, M. Lefort-Tran, C. Chipaux, and R. A. Binot (European Space Agency. European Space Research and Technology Center, ESTEC, Noordwijk, Netherlands) *In* ESA, Third European Symposium on Space Thermal Control and Life Support Systems Dec. 1988 p 65-68 (For primary document see N89-28214 22-54)
Copyright Avail: NTIS HC A99/MF A01; ESA Publications Div., ESTEC, Noordwijk, Netherlands, 80 Dutch guilders or 45 US dollars

The MELISSA was conceived as a microorganism based ecosystem, being a simplified, model of a future biological life support system for manned missions. The driving element is the reprocessing of edible biomass from waste, CO2, and minerals with the direct use of sunlight as a source of energy for biological photosynthesis. A four compartments ecosystem is selected allowing the closure of the material loop around a central food and O2 reprocessing compartment by the growth of the filamentous cyanobacterium SPIRULINA. Nitrates, CO2, and minerals required by SPIRULINA are produced by the other microbial compartments, namely an anaerobic digestion system and a nitrifying compartment. The anaerobic digestion system includes a thermophilic solubilization and fermentation compartment (CLOSTRIDIA) followed by a second light dependent compartment, colonized by RHODOBACTER, removing tne soluble organics (mainly fatty acids) and leaving the minerals requested by SPIRULINA, and producing a biomass of high food value. Nitrification of ammonium from the anaerobic step to nitrate for SPIRULINA, is performed by NITROBACTERIA, with a very low biomass production, in the fourth compartment. For a consumer added to the loop, MELISSA ensures food and oxygen recycling through complete carbon, nitrogen, sulfur

and minerals cycles, driven in axenic conditions by genetically well-known, nonpathogenic strains. ESA

N89-28223# MATRA Espace, Paris-Velizy (France).
POSSIBLE USE OF A GAS MONITORING SYSTEM IN SPACE RESPIROMETRY STUDIES
C. Lasseur, C. Chipaux, M. Andre, F. X. Cote, and J. Massimino (Commissariat a l'Energie Atomique, Saint-Paul-les-Durance, France) *In* ESA, Third European Symposium on Space Thermal Control and Life Support Systems Dec. 1988 p 69-72 (For primary document see N89-28214 22-54)
Copyright Avail: NTIS HC A99/MF A01; ESA Publications Div., ESTEC, Noordwijk, Netherlands, 80 Dutch guilders or 45 US dollars

The C23A system (automatic culture chambers in artificial atmosphere) was used in respiratory studies on a small animal, Triturus Walt I.I. The multiplexed analyzers allow use of the same analyzer for several different applications, e.g., respirometry, or atmosphere. This method permits to decrease weight and reduce the number of gas calibrations. Similarly the design of the computing system anticipates the full separation between automation in space and control-command on ground. ESA

N89-28224# Dornier System G.m.b.H., Friedrichshafen (Germany, F.R.).
TWO-PHASE HEAT TRANSPORT SYSTEMS: CRITICAL COMPONENTS
H. Kreeb and R. Siepmann *In* ESA, Third European Symposium on Space Thermal Control and Life Support System Dec. 1988 p 75-82 (For primary document see N89-28214 22-54)
Copyright Avail: NTIS HC A99/MF A01; ESA Publications Div., ESTEC, Noordwijk, Netherlands, 80 Dutch guilders or 45 US dollars

Within the preparatory support technology program for COLUMBUS a mechanically pumped two-phase heat transport system is developed. A preparatory study recommended system based on a parallel arrangement of evaporator cold plates and heat exchangers, condenser units, and a conventional mechanical pump. Important characteristics of this system include the controlled flooding of the condensers with liquid to achieve temperature control and the ability to use the evaporators also as condensers to permit heat load sharing between payload elements. In order to meet Columbus-requirements the system is specified to work at a maximum heat load of 10 to 20 kW at a nominal temperature of 20 C. The working medium is freon R 114. The design of the overall system, the breadboard development of the critical components, and the planned test-bed verification are outlined. ESA

N89-28225# Societe Anonyme Belge de Constructions Aeronautiques, Brussels.
FEASIBILITY DEMONSTRATION MODEL OF A CAPILLARY PUMPING LOOP
R. S. Bhatti, S. VanOost, and C. J. Savage (European Space Agency. European Space Research and Technology Center, ESTEC, Noordwijk, Netherlands) *In* ESA, Third European Symposium on Space Thermal Control and Life Support Systems Dec. 1988 p 83-88 (For primary document see N89-28214 22-54)
Copyright Avail: NTIS HC A99/MF A01; ESA Publications Div., ESTEC, Noordwijk, Netherlands, 80 Dutch guilders or 45 US dollars

The general objectives, the design concept, and the potential performances of the two-phase capillary pumping loop (CPL) as a heat transportation system are reviewed. Results obtained on the first breadboard CPL model are reported with comparison of predicted against tested performances. ESA

N89-28226# Entwicklungsring Nord, Bremen (Germany, F.R.).
DESIGN AND TEST OF A TWO-PHASE COLDPLATE
R. Mueller *In* ESA, Third European Symposium on Space Thermal Control and Life Support Systems Dec. 1988 p 89-95 (For primary document see N89-28214 22-54)
Copyright Avail: NTIS HC A99/MF A01; ESA Publications Div., ESTEC, Noordwijk, Netherlands, 80 Dutch guilders or 45 US dollars

The design and the results of a performance test for a two phase cold plate are presented. The cold plate consists of 7 parallel aluminum evaporator tubes and a 50 x 50 cm mounting plate. The evaporator tubes are equipped with capillary circumferential grooves and an internal structure to separate liquid and vapor. The cold plate is suitable for application in mechanically, as well as capillary pumped loops. In the test the heat transport limit of the evaporator tubes, i.e., the dryout of their circumferential grooves, was evaluated. The test was conducted in the mechanically pumped mode using ammonia as a working fluid. It demonstrates the feasibility of the selected design of the cold plate evaporator tubes. Heat flux limits ranging from 2.4 and 10.7 W/sq cm and heat transfer coefficients between 0.14 and 1.35 W/sq cm-K are were measured for the different evaporator tubes. ESA

N89-28227# Minelectrotechprom, Moscow (USSR).
NON-CONDENSIBLE GAS EFFECTS ON THE LOW-TEMPERATURE HEAT PIPE CHARACTERISTICS
M. D. Parfentiev *In* ESA, Third European Symposium on Space Thermal Control and Life Support Systems Dec. 1988 p 97-101 (For primary document see N89-28214 22-54)
Copyright Avail: NTIS HC A99/MF A01; ESA Publications Div., ESTEC, Noordwijk, Netherlands, 80 Dutch guilders or 45 US dollars

Results of studies on noncondensable gas (NCG) distribution in condensation zones of low temperature heat pipes (LTHP) and estimates of its effect on distribution of both localized heat flows and localized heat-exchange coefficients as well as LTHP was temperature profile in condensation zone are described. Based on visual studies on vapor-gas mixture distribution in LTHP condensation zone, a NCG distribution model is proposed which considers distribution irregularities both in axial and radial directions. Using the accepted NCG distribution model as the base, the heat balance equation for a condenser wall component which considers variable thermal resistance of a NCG layer was obtained. ESA

N89-28228# Tokyo Univ., Sagamihara (Japan).
MICRO-FLUID DYNAMICAL ANALYSIS OF EVAPORATING FLOWS IN HEAT PIPES
K. Oshima and N. Izutsu *In* ESA, Third European Symposium on Space Thermal Control and Life Support Systems Dec. 1988 p 103-108 (For primary document see N89-28214 22-54)
Copyright Avail: NTIS HC A99/MF A01; ESA Publications Div., ESTEC, Noordwijk, Netherlands, 80 Dutch guilders or 45 US dollars

Heat pipe systems utilizing phase changing heat transfer concepts are introduced, including micro heat pipes, a separate type heat pipe heat exchanger, and heat pipe turbines. Inside these heat pipes, contrary to the conventional thermosyphon, evaporation and condensation processes are heavily influenced by the surface tension effect. This effect is also dominant in heat pipes operating under microgravity in space. Similarity parameters concerning these phenomena are discussed. Laboratory experiments as well as numerical simulations of the flows relating to evaporative heat transfer were carried out. It is found that heat transfer by the evaporation process is decreased in such conditions. ESA

N89-28229# Minelectrotechprom, Moscow (USSR).
EXPRESS-METHOD INVESTIGATION AND ITS APPLICATION FOR HEAT PIPE QUALITY CONTROL
A. D. Lobanov and A. A. Parentieva *In* ESA, Third European Symposium on Space Thermal Control and Life Support Systems Dec. 1988 p 109-112 (For primary document see N89-28214 22-54)
Copyright Avail: NTIS HC A99/MF A01; ESA Publications Div., ESTEC, Noordwijk, Netherlands, 80 Dutch guilders or 45 US dollars

Results of studies and application of a heat pipe quality control

method applicable in the pipe series production (and introduced) into the heat pipe production process and on installing the heat pipes on cooled and controlled temperature instruments and equipment, with no pipes disconnected from these instruments, are described. A heat short time action (heat flux density ranges from unities to tens of W/sq m and time interval, from unities to tens of seconds) is applied upon an envelope of a working fluid filled and sealed heat pipe locally, that is on its small section (an area of 1 sq m) and the pipe envelope temperature increase at the heat short time action input section is registered during its effect time or a shorter period. It is possible to determine a heat pipe parameter controlled by making comparison with an increase in temperature premeasured at a reference device subjected to a similar effect. The method is used to check working fluid availability in a heat pipe, to test noncondensible gas absence (or presence of its given amount) therein. The method markedly accelerates heat pipe rejection and improve quality control reliability (one heat pipe requires only 30 sec for its testing). ESA

N89-28230# National Aerospace Lab., Emmeloord (Netherlands). Space Div.

DEVELOPMENT OF A SENSOR FOR HIGH-QUALITY TWO-PHASE FLOW

A. A. M. Delil and J. F. Heemskerk *In* ESA, Third European Symposium on Space Thermal Control and Life Support Systems Dec. 1988 p 113-123 Sponsored in part by the Netherlands Agency for Aerospace Programs (For primary document see N89-28214 22-54)

Copyright Avail: NTIS HC A99/MF A01; ESA Publications Div., ESTEC, Noordwijk, Netherlands, 80 Dutch guilders or 45 US dollars

Based on a tradeoff of quality monitoring concepts, a dedicated quality sensor for two phase mixtures was developed, based on the axial capacitance principle. Its theoretically demonstrated feasibility as quality and wetting sensor was experimentally confirmed by experiments using liquid layer simulating plastic sheets and annular air/liquid flow. Experiments in a two-phase freon test loop show the sensor to be an accurate, fast responding, sensitive instrument. It was accepted for further development as a component of the two-phase heat transport system developed by the European Space Agency. Performance figures, obtained by calibrations in a freon 114 loop, are given. Recommendations for future work and applications are indicated. ESA

N89-28231# Aerospatiale, Cannes La Bocca (France).

THE TWO APPROACHES FOR THE THERMAL CONTROL OF THE COLUMBUS RESOURCE MODULE AND POLAR PLATFORM **c18**

B. Poulain and S. Aucel *In* ESA, Third European Symposium on Space Thermal Control and Life Support Systems Dec. 1988 p 127-134 Previously announced as N89-23511 (For primary document see N89-28214 22-54)

Copyright Avail: NTIS HC A99/MF A01; ESA Publications Div., ESTEC, Noordwijk, Netherlands, 80 Dutch guilders or 45 US dollars

The impact of the requirements of the Columbus program such as long life time and servicing on system architecture and subsequently on thermal control systems (TCS) design is discussed. Based on these requirements two completely different approaches were selected for polar platform (PPF) and resources module (RM) architectures. The system architecture/TCS approach used for the PPF (individual TCS of ORU) led to an optimized TCS in terms of mass and performance (i.e., launch cost) having nevertheless certain penalties: on power budget (improvements are possible); and on servicing mass (acceptable). The RM system architecture/TCS approach (centralized TCS) is optimized with respect to servicing operations and power budget but has penalties on TCS mass and performance. These penalties are compensated by global savings at MTFF level. One of the prime drivers leading to the difference between the two approaches is the use of Hermes as servicing vehicle for RM and not for PPF (additional constraint on RM). Although the TCS performances are quite different, the selected designs of both spacecraft are the best compromises which could be achieved at system level. ESA

N89-28232# Erno Raumfahrttechnik G.m.b.H. Bremen (Germany, F.R.).

REDUNDANCY CONCEPT FOR THE COLUMBUS MAN-TENDED FREE-FLYER THERMAL CONTROL SYSTEM **c18**

B. Behrens, C. Bunkenborg, W.-D. Ebeling, and U. Laux *In* ESA, Third European Symposium on Space Thermal Control and Life Support Systems Dec. 1988 p 135-140 (For primary document see N89-28214 22-54)

Copyright Avail: NTIS HC A99/MF A01; ESA Publications Div., ESTEC, Noordwijk, Netherlands, 80 Dutch guilders or 45 US dollars

The Columbus Man-Tended Free Flyer (MTFF) thermal control system (TCS) is described. The redundancy philosophy for TCS is discussed and the resulting thermal control concept presented. Effects of the failure tolerance requirements on the overall MTFF thermal control architecture as well as the arrangement of subsystem units within the MTFF for thermal control reasons is considered. Reliability analyses are outlined. For operating the MTFF at a required reliability level of 0.93 for nominal payload support for 180 days, the items aboard are classified in three criticality categories. Therefore various required failure tolerances have to be provided by an appropriate redundancy concept for each of these criticality categories. ESA

N89-28233# Aeritalia S.p.A., Turin (Italy).

THERMAL CONTROL OF COLUMBUS PRESSURIZED MODULES **c18**

S. Dolce, M. Trichilo, and F. Berardi *In* ESA, Third European Symposium on Space Thermal Control and Life Support Systems Dec. 1988 p 141-147 (For primary document see N89-28214 22-54)

Copyright Avail: NTIS HC A99/MF A01; ESA Publications Div., ESTEC, Noordwijk, Netherlands, 80 Dutch guilders or 45 US dollars

The thermal control architecture of Columbus Pressurized Modules (PM); tradeoffs and design activities performed up to the present phase CO; and the baseline design solutions at loop and at component level are discussed. Active thermal control architecture consists of: module internal water loops collecting heat from directly interfacing P/L's and S/S's, avionic and cabin air loops; space station external freon loop (PM2 only) providing removal and transportation of water loop heat loads to the heat rejection system; based thermal bus providing removal and rejection of docked element water loops heat loads; and loop control and monitoring functions provided by modulating pumps and valves, temperature, pressure, and flow sensors interfacing with an intelligent control unit. Passive thermal control architecture consists of: MLI to insulate the modules and limit heat leaks, gains; coatings to provide the required thermo-optical properties; and internal insulation to avoid condensation. ESA

N89-28234# Aeritalia S.p.A., Turin (Italy).

DESIGN CONCEPTS FOR HERMES THERMAL CONTROL **c18**

C. Ferro, G. Gianfiglio, and L. Costamagna *In* ESA, Third European Symposium on Space Thermal Control and Life Support Systems Dec. 1988 p 149-156 (For primary document see N89-28214 22-54)

Copyright Avail: NTIS HC A99/MF A01; ESA Publications Div., ESTEC, Noordwijk, Netherlands, 80 Dutch guilders or 45 US dollars

The Hermes spaceplane configuration and the possible mission profile are discussed with regard to the major thermal requirements. The design approach and the optimization criteria are described, highlighting procedures for the overall mass minimization. The design concept is illustrated for the ATCS (Active Thermal Control Section) and the PTCS (Passive Thermal Control Section). The ATCS performances mainly rely on the adoption of fluid loops (dual option), collecting and transporting heat loads from the thermal sources to the sink devices. The possible architectures of

the loops are identified addressing the significant functions and the level of performance for the various components. The PTCS consists of foam/fibrous and/or multilayer insulation blankets, thermal control coatings and tapes, applied throughout the fuselage and on internal items and parts, in order to avoid excessive temperature excursions and heat leaks or gains from or to other spaceplane subsystems such as ATCS, Environmental Control and Life Support Subsystem, Power Units. Further temperature control is achieved by means of a dedicated heater system. Subsystem areas which will be the subject of investigation and development are addressed. ESA

N89-28235# Aerospatiale, Cannes La Bocca (France).
RADIATOR CONCEPTUAL STUDIES FOR THE HERMES SPACEPLANE **c18**
M. Amidieu, J. L. Foret, and G. Sibilo *In* ESA, Third European Symposium on Space Thermal Control and Life Support Systems Dec. 1988 p 157-164 (For primary document see N89-28214 22-54)
Copyright Avail: NTIS HC A99/MF A01; ESA Publications Div., ESTEC, Noordwijk, Netherlands, 80 Dutch guilders or 45 US dollars

The Hermes radiator design is discussed. The radiator assembly consists of a number of radiative panels, with internal fluid circulation, connected to freon loops. Resulting from the performance requirement, the major critical areas are: the need for a large radiative surface within a comparatively confined volume; a highly variable outer thermal environment, inducing wide fluctuations heat on the rejection capacity, thus conflicting with the strict requirement on the fluid output temperature; and severe operational conditions, i.e., heavy structural loads in launch phase and high temperature environment at reentry. ESA

N89-28236# Contraves Corp., Zurich (Switzerland). Space Dept.
THE SPACE-RIGIDISED THERMAL SHIELD FOR THE ESA FAR-INFRARED SPACE TELESCOPE (FIRST) **c18**
M. C. Bernasconi and S. Koese *In* ESA, Third European Symposium on Space Thermal Control and Life Support Systems Dec. 1988 p 165-173 (For primary document see N89-28214 22-54)
(Contract ESTEC-6324/85/NL/PB(SC))
Copyright Avail: NTIS HC A99/MF A01; ESA Publications Div., ESTEC, Noordwijk, Netherlands, 80 Dutch guilders or 45 US dollars

Results of the feasibility investigation of an inflatable space rigidized thermal shield for the FIRST-mission are presented. Possible ISRS-shield configurations were surveyed. The configuration study confirms the use of a truncated cylinder shield concept. Stowage patterns and deployment sequences are discussed, leading to an overview of the rigidization aspects. For a proper cure, the rigidizable structure must be heated to a predefined temperature by proper orientation with respect to the Sun. The cure analysis shows that the structure can be cured within 9 hrs, using an external gaseous catalyst. Evaluation of the thermal efficiency shows that the thermal requirements can be satisfied with a 6-layer MLI blanket. The structural analysis shows that the shield meets the 2-Hz stiffness requirement. ESA

N89-28237# Dornier System G.m.b.H., Friedrichshafen (Germany, F.R.).
REGENERATIVE CO2-CONTROL
H. Preiss and H. Funke *In* ESA, Third European Symposium on Space Thermal Control and Life Support Systems Dec. 1988 p 177-183 Sponsored by the Bundesministerium fuer Forschung und Technologie, Bonn, Fed. Republic of Germany (For primary document see N89-28214 22-54)
Copyright Avail: NTIS HC A99/MF A01; ESA Publications Div., ESTEC, Noordwijk, Netherlands, 80 Dutch guilders or 45 US dollars

Technological work for a regenerative CO2-control system, applicable for longterm space missions, especially the Columbus program, is described. Regenerative CO2-control is required for this program, because the previous use of expendable chemical agents as applied for Spacelab leads to unacceptable mass and volume penalties. In regenerative CO2-control, the adsorber material can accumulate and release CO2 in a periodic way. However the regeneration process needs energy, which is not necessary for the expendables. Major design parameters, which allow the sizing and interface definition of a regenerative CO2-control for an actual space application were derived. This is demonstrated by the successful operation of an advanced breadboard, where predicted and measured performance are in good agreement. Two adsorber materials were tested, showing adequate performance. The research material has better stability than the commercial product and is the favored material. ESA

N89-28238# Draegerwerk A.G., Luebeck (Germany, F.R.).
ELECTROCHEMICAL REMOVAL AND CONCENTRATION OF CO2
S. Haupt *In* ESA, Third European Symposium on Space Thermal Control and Life Support Systems Dec. 1988 p 185-186 (For primary document see N89-28214 22-54)
Copyright Avail: NTIS HC A99/MF A01; ESA Publications Div., ESTEC, Noordwijk, Netherlands, 80 Dutch guilders or 45 US dollars

It is argued that because electrochemical reactions can be performed with high power efficiencies, and because of the direct transfer of the removed CO2 into hydrogen, the electrochemical method has advantages in comparison to other methods, when requirements such as power consumption, efficiency, mass and volume are concerned. An electrochemical assembly similar to a fuel cell can meet the requirements for CO2 removal in space application. For the construction of an effective system for CO2 removal and concentration, all electrode processes and transport mechanisms have to be studied in detail. Using ion selective membranes, the transport processes can be controlled effectively. ESA

N89-28239# Draegerwerk A.G., Luebeck (Germany, F.R.).
THE CATALYTIC OXIDERZER: DESCRIPTION AND FIRST RESULTS OF A BREADBOARD MODEL FOR A COMPONENT OF THE COLUMBUS ECLSS
K. Ammann *In* ESA, Third European Symposium on Space Thermal Control and Life Support Systems Dec. 1988 p 187-192 (For primary document see N89-28214 22-54)
Copyright Avail: NTIS HC A99/MF A01; ESA Publications Div., ESTEC, Noordwijk, Netherlands, 80 Dutch guilders or 45 US dollars

A technological breadboard of a catalytic oxidizer system was designed to remove the low boiling point hydrocarbons, hydrogen, and carbon monoxide from a space station atmosphere. With respect to the necessary flow rate, CO turned out to be the design driver, while CH4 (which needs a flow rate significantly lower than CO) is the design driver for the temperature required. For energy saving, a two catalyst system which consists of a high flow/low temperature catalyst for CO oxidation and a low flow/high temperature catalyst for the oxidation of methane, hydrogen and the other candidate contaminants was chosen. Results of performance tests including experiments with selected catalyst poisons are discussed. ESA

N89-28240# Nord-Micro Elektronic Feinmechanik G.m.b.H., Frankfort (Germany, F.R.).
CONDENSING HEAT EXCHANGERS FOR EUROPEAN SPACECRAFT ECLSS
P. Kuhn and F. Petter *In* ESA, Third European Symposium on Space Thermal Control and Life Support Systems Dec. 1988 p 193-197 Sponsored by the Bundesministerium fuer Forschung und Technologie, Bonn, Fed. Republic of Germany and Aerospatiale, France (For primary document see N89-28214 22-54)
Copyright Avail: NTIS HC A99/MF A01; ESA Publications Div., ESTEC, Noordwijk, Netherlands, 80 Dutch guilders or 45 US dollars

Based on an earlier concept, a condensing heat exchanger

type with lower complexity and reduced weight and volume compared with previous configurations was developed. Probe units with extremely low leakage were obtained both by careful selection of materials and processes and close control of manufacturing parameters. Hydrophilic coatings on the basis of borosilicate glass and polysilicate ceramic, providing wettable surfaces to the air passes and slurpers of condensing heat exchangers were developed. ESA

N89-28241# Dornier System G.m.b.H., Friedrichshafen (Germany, F.R.).
THE ATMOSPHERE PRESSURE CONTROL SECTION OF THE HERMES ECLSS
G. Hauser *In* ESA, Third European Symposium on Space Thermal Control and Life Support Systems Dec. 1988 p 199-204 (For primary document see N89-28214 22-54)
Copyright Avail: NTIS HC A99/MF A01; ESA Publications Div., ESTEC, Noordwijk, Netherlands, 80 Dutch guilders or 45 US dollars

The Atmosphere Pressure and Control Section (APCS) is part of the Hermes Environmental Control and Life Support Subsystem (ECLSS), which has to provide a safe and habitable environment for the crew. The APCS maintains the cabin total pressure and oxygen partial pressure in the specified limits, and supplies gas to several users, e.g., EVA suits, oxygen masks, docked MTFF. It has the capability to restore the atmosphere after depressurization of the airlock at the end of EVA as well as after evacuation of the total habitable volume after fire/contamination. Calculated performance data are presented. The location of all APCS-assemblies within the different Hermes volumes and conceptual details such as redundancy and safety provisions are shown. ESA

N89-28242# Deutsche Forschungs- und Versuchsanstalt fuer Luft- und Raumfahrt, Cologne (Germany, F.R.). Space Station Program Office.
COME TO FLIGHT RULES: RATIONALE ON ENVIRONMENTAL CONTROL AND LIFE SUPPORT SYSTEMS
H. Bauer *In* ESA, Third European Symposium on Space Thermal Control and Life Support Systems Dec. 1988 p 205-208 (For primary document see N89-28214 22-54)
Copyright Avail: NTIS HC A99/MF A01; ESA Publications Div., ESTEC, Noordwijk, Netherlands, 80 Dutch guilders or 45 US dollars

Critical aspects of the Hermes-MTFF system flight rule definition are discussed. The most constraining life support system is the cabin pressure integrity, the O2 and CO2 concentration. It starts with an emergency landing requirement abort once around, or if it is worse with a transatlantic landing or even with a return to landing site. Loss of two H2O loops within the air revitalization system requires also an abort once around. For all other failures a work-around solution according operational flight rules can be found. Failure in the flash evaporator system may not cause an emergency landing, but evaluating existing systems and relevant flight rules can keep the crew busy in solving the problems and to continue the flight with constraints. ESA

N89-28243# Dornier System G.m.b.H., Friedrichshafen (Germany, F.R.).
THE EUROPEAN SPACE SUIT SYSTEM
N. Herber *In* ESA, Third European Symposium on Space Thermal Control and Life Support Systems Dec. 1988 p 211-219 (For primary document see N89-28214 22-54)
Copyright Avail: NTIS HC A99/MF A01; ESA Publications Div., ESTEC, Noordwijk, Netherlands, 80 Dutch guilders or 45 US dollars

The European Space Suit System (ESSS) status is foreseen for servicing of various elements of space infrastructure within typical operational scenarios based on Hermes. As a result of different EVA studies the ESSS concept was defined and structured in three modules: the EVA Suit Enclosure Module, the EVA Life Support Module, and the EVA Information and Communication Module. The fourth equipment which has to be seen as a part of the Space Suit System as well, is the EVA Support and Verification Equipment responsible for suit accommodation, recharging, check out and the like. ESA

N89-28244# European Space Agency. European Space Research and Technology Center, ESTEC, Noordwijk (Netherlands).
LIFE SUPPORT FOR EVA: THE EUROPEAN SYSTEM BASELINE
J. Witt, B. Svensson, and R. Vaeth (Dornier System G.m.b.H., Friedrichshafen, Germany, F.R.) *In its* Third European Symposium on Space Thermal Control and Life Support Systems Dec. 1988 p 221-226 (For primary document see N89-28214 22-54)
Copyright Avail: NTIS HC A99/MF A01; ESA Publications Div., ESTEC, Noordwijk, Netherlands, 80 Dutch guilders or 45 US dollars

Based on earlier system studies the EVA Life Support Module (ELSM) was studied. A review of metabolic design factors set the performance limits of the ELSM. Various design solutions for the physical realization of the ELSM functions were studied and traded-off against each other. The design baseline for the ELSM established is presented. The further development of life support for EVA in Europe is timed for a first manned flight of Hermes in 1999. ESA

N89-28245# Avions Marcel Dassault-Breguet Aviation, Saint-Cloud (France).
THERMAL MODELLING OF THE EVA-SUITED ASTRONAUT
L. Simionesco and D. Hornet *In* ESA, Third European Symposium on Space Thermal Control and Life Support Systems Dec. 1988 p 227-232 (For primary document see N89-28214 22-54)
Copyright Avail: NTIS HC A99/MF A01; ESA Publications Div., ESTEC, Noordwijk, Netherlands, 80 Dutch guilders or 45 US dollars

A computer thermal model which integrates the man-in-the-loop was developed in order to analyze the interactions between the human self-regulating thermal mechanisms and the behavior of the ELSS, water and gas heat transport loops. Because the human thermodynamic behavior is dependent on its own thermal status (metabolic activity and core temperature) and on its environment (gas constituants partial pressures and relevant temperatures) those variables had to be introduced into the conventional heat and mass transfer scheme. ESA

N89-28246# European Space Agency. European Space Research and Technology Center, ESTEC, Noordwijk (Netherlands).
EVA AND HUMAN PHYSIOLOGY
B. Svensson, L. Vogt, and N. Herber (Dornier System G.m.b.H., Friedrichshafen, Germany, F.R.) *In its* Third European Symposium on Space Thermal Control and Life Support Systems Dec. 1988 p 233-238 (For primary document see N89-28214 22-54)
Copyright Avail: NTIS HC A99/MF A01; ESA Publications Div., ESTEC, Noordwijk, Netherlands, 80 Dutch guilders or 45 US dollars

The crew requirements for the European EVA space suit are divided into human safety, human physiology, and crew performance and productivity requirements. The human physiology requirements addresses areas like anthropometry, biomechanics, psychosensory performance and protection, atmosphere composition and pressure, metabolism, weightlessness effects and radiation. It is planned to perform validation of critical parameters by tests, e.g., the establishment of risk factors for decompression sickness. Considerations and test results of physiological parameters will be given to the ESA medical board, which will give recommendations on acceptable risk factors, maximum and minimum exposure levels, and comfort levels for the EVA crew members. ESA

N89-28247# Dornier System G.m.b.H., Friedrichshafen (Germany, F.R.).
ADVANCED MODULAR SOFTWARE DEVELOPMENT IN THERMAL ENGINEERING

R. Bisanz and F. Zilly *In* ESA, Third European Symposium on Space Thermal Control and Life Support Systems Dec. 1988 p 241-248 (For primary document see N89-28214 22-54)
Copyright Avail: NTIS HC A99/MF A01; ESA Publications Div., ESTEC, Noordwijk, Netherlands, 80 Dutch guilders or 45 US dollars

A Concept for Simulation and Analysis of Space Systems (COSIMA) was developed utilizing advanced modular software engineering techniques and the software management system RSYST. Realizations in various disciplines and project applications demonstrated the advantages of this concept. The main components of COSIMA and its application to thermal radiation software development, and a materials data base are described. Help facilities are outlined. ESA

N89-28248# Fokker B.V., Amsterdam (Netherlands). Space and Systems Div.
LUMPING, A POWERFUL DESIGN TOOL FOR THERMAL CONTROL
W. Kruidhof *In* ESA, Third European Symposium on Space Thermal Control and Life Support Systems Dec. 1988 p 249-253 (For primary document see N89-28214 22-54)
Copyright Avail: NTIS HC A99/MF A01; ESA Publications Div., ESTEC, Noordwijk, Netherlands, 80 Dutch guilders or 45 US dollars

Temperatures calculated for electronics boxes of the HIPPARCOS spacecraft with a so-called lumped thermal mathematical model (LTMM) and a comprehensive thermal mathematical model (CTMM) are compared. The temperatures predicted with the LTMM and the temperatures actually measured for the electronic boxes during the HIPPARCOS PFM test are also compared. It is demonstrated that the box temperatures as predicted with the LTMM can be correlated within a bandwidth of + or - 6 C with the CTMM (all boxes considered) and within a bandwidth of + or - 7 C with the PFM test results (only units of which temperature was monitored in PFM test considered). ESA

N89-28249# MATRA Espace, Toulouse (France).
IMPROVED RAY TRACING TECHNIQUE FOR RADIATIVE HEAT TRANSFER MODELLING
C. Koeck *In* ESA, Third European Symposium on Space Thermal Control and Life Support Systems Dec. 1988 p 255-260 (For primary document see N89-28214 22-54)
Copyright Avail: NTIS HC A99/MF A01; ESA Publications Div., ESTEC, Noordwijk, Netherlands, 80 Dutch guilders or 45 US dollars

The implementation of an optimized ray-tracing technique in a thermal radiation software based on Monte-Carlo gave an efficient tool to compute radiative exchange factors and external heat fluxes. The software presents the advantages of the Monte-Carlo method: better physical modeling, simplicity of use, without its usual drawback: computer run time. As an indication, computation of view-factors within an enclosure of hundred surfaces can be 100 times faster than when using the double summation method of VWHEAT. Features such as surface specularity or transparency are accounted for in the simulation. ESA

N89-28250# European Space Agency. European Space Research and Technology Center, ESTEC, Noordwijk (Netherlands).
APPLICATION OF EXPERT SYSTEMS TO THE THERMAL CONFIGURATION OF GIOTTO
G. Limouzin and R. J. Wilson *In its* Third European Symposium on Space Thermal Control and Life Support Systems Dec. 1988 p 261-266 (For primary document see N89-28214 22-54)
Copyright Avail: NTIS HC A99/MF A01; ESA Publications Div., ESTEC, Noordwijk, Netherlands, 80 Dutch guilders or 45 US dollars

An experimental expert system was developed to monitor and control the thermal subsystem of a spacecraft. Its aim was to demonstrate the feasibility of such a system to assist non-experts in managing the spacecraft's thermal behavior. Giotto was taken as the test case as its thermal control was performed by ground command during its flight towards comet Halley. A knowledge based expert system was constructed and its conception was made easy to use for non-computer specialists. Based on a rules production system, this mock-up was written in PROLOG and was implemented on a VAX/750 minicomputer. ESA

N89-28251# Dornier System G.m.b.H., Friedrichshafen (Germany, F.R.).
THERMAL ANALYSIS OF ROSAT IN LOW-EARTH ECLIPSE ORBIT EMPLOYING STEADY-STATE CALCULATIONS **c18**
K. Honnen *In* ESA, Third European Symposium on Space Thermal Control and Life Support Systems Dec. 1988 p 267-271 (For primary document see N89-28214 22-54)
Copyright Avail: NTIS HC A99/MF A01; ESA Publications Div., ESTEC, Noordwijk, Netherlands, 80 Dutch guilders or 45 US dollars

Although ROSAT is thermally characterized by strongly varying orbital heat loads, for the lay-out of the thermal control system, steady-state calculations with average values for the heat loads were employed to avoid excessive computing time. Due to the nonlinearity of thermal radiation, the calculated steady-state temperatures differ from the actual mean transient temperatures. A method to take the effect of these nonlinear thermal couplings into account in steady-state analysis was developed and applied. Resulting steady-state temperatures are identical to calculated average transient temperatures. ESA

N89-28252# MATRA Espace, Toulouse (France).
THERMAL EFFECTS OF PLUME IMPINGEMENT **c18**
P. Cheoux-Damas and C. Koeck *In* ESA, Third European Symposium on Space Thermal Control and Life Support Systems Dec. 1988 p 273-279 (For primary document see N89-28214 22-54)
Copyright Avail: NTIS HC A99/MF A01; ESA Publications Div., ESTEC, Noordwijk, Netherlands, 80 Dutch guilders or 45 US dollars

A computer code for plume impingement modeling in space was used to analyze thermal effects on several satellites (thermal control analysis and thermal protection dimensioning). This code allows the simulation of convective and radiative heat fluxes due to the plume. The contents of the plume computation code from the combustion chamber to the outside plume expansion, and plume impingement modeling are described. The validation tests and simulation examples illustrate the results of the plume impingement code in real cases. ESA

N89-28253# Danish Research Center for Applied Electronics, Hoersholm.
EFFICIENT IMPLEMENTATION OF A DESCRIPTION LANGUAGE FOR THERMAL SIMULATORS **c18**
P. Stangerup *In* ESA, Third European Symposium on Space Thermal Control and Life Support Systems Dec. 1988 p 281-287 (For primary document see N89-28214 22-54)
Copyright Avail: NTIS HC A99/MF A01; ESA Publications Div., ESTEC, Noordwijk, Netherlands, 80 Dutch guilders or 45 US dollars

It is shown which requirements should be made to the description language of a thermal simulator and how this language is implemented. It is demonstrated that the only thermal components required are: conductors, capacitors, source of heat flow rate, and source of applied temperature. This is true if all component values in the description language can be expressed as arbitrary functions of system variables. The ideas which ensure a high degree of generality are implemented in the ESACAP program, available on IBM compatible PC's. ESA

N89-28254# Aeritalia S.p.A., Turin (Italy).
AN ALGORITHM FOR CALCULATING THERMODYNAMIC PROPERTIES OF SIMPLE FLUIDS SUITABLE FOR SPACE THERMAL CONTROL **c18**
C. Actis and N. Nervegna (Politecnico di Torino, Italy) *In* ESA, Third European Symposium Space Thermal Control and Life Support Systems Dec. 1988 p 289-295 (For primary document

see N89-28214 22-54)
Copyright Avail: NTIS HC A99/MF A01; ESA Publications Div., ESTEC, Noordwijk, Netherlands, 80 Dutch guilders or 45 US dollars

A method for calculating equilibrium thermodynamic properties of a simple fluid is proposed. Following the rigorous theory of statistical mechanics an equation of state that describes both the liquid and vapor state of a two parameter fluid is developed. The formulation is not purely analytic being based on an algorithm implemented in a FORTRAN package. At the modeling stage the real fluid behavior is portrayed via a quasi Lennard-Jones molecular interaction potential. The perturbation theory of Barker and Henderson is used while a variational minimization criterion leads to the selection of the hard-sphere particles diameter thus identifying the reference system. By so doing, the isotropic pair interaction is dictated by a hard sphere potential perturbed by an attractive term. Of significance is the fact that potential parameters are made dependent on both specific volume and temperature. The method was tested for argon due to its nonpolar characteristics and simple molecular structure. Argon is of interest in both cryogenics and dynamic energy conversion systems for space use, especially in connection with mixtures where molecular mass values can be adjusted to compromise rotating machinery vs heat transfer efficiencies. Results from this formulation are compared with other correlations as well as with experimental data a specific state points. ESA

N89-28255# General Electric Co., Princeton, NJ. Astro-Space Div.
DESIGN TRENDS IN COMMUNICATIONS SATELLITE THERMAL SUBSYSTEMS **c18**
D. R. Chalmers, P. H. Burkle, and G. W. Case *In* ESA, Third European Symposium on Space Thermal Control and Life Support Systems Dec. 1988 p 299-310 (For primary document see N89-28214 22-54)
Copyright Avail: NTIS HC A99/MF A01; ESA Publications Div., ESTEC, Noordwijk, Netherlands, 80 Dutch guilders or 45 US dollars

Design trends in spacecraft radiators; heat pipes; thermal materials; heater control; and insulation are reviewed. Thermal analysis; satellite design/mission issues; and spacecraft thermal testing are discussed. ESA

N89-28256# Aeritalia S.p.A., Turin (Italy).
THE THERMAL CONTROL OF EUTELSAT-2 **c18**
E. Sacchi and M. Koedinger (Aerospatiale, Cannes La Bocca, France) *In* ESA, Third European Symposium on Space Thermal Control and Life Support Systems Dec. 1988 p 311-318 (For primary document see N89-28214 22-54)
Copyright Avail: NTIS HC A99/MF A01; ESA Publications Div., ESTEC, Noordwijk, Netherlands, 80 Dutch guilders or 45 US dollars

The EUTELSAT system constraints assigned to the thermal control subsystem are described for the transfer and geosynchronous phases. The thermal control is based on passive concepts complemented with heat pipes and heaters. The multilayer insulation blankets are classical. The thermal analysis is conducted using a 400 node global mathematical model, and local models for external units. The verification and test plan set-up for the thermal control subsystem within the overall development plan of the program, and the status of the manufacturing, integration and test activities are presented. ESA

N89-28257# Aerospatiale, Cannes La Bocca (France).
TELE-X ANTENNA MODULE THERMAL CONTROL **c18**
A. Lanteri and B. Henning (Telefonaktiebolaget L. M. Ericsson, Moelndal, Sweden) *In* ESA, Third European Symposium on Space Thermal Control and Life Support Systems Dec. 1988 p 319-326 (For primary document see N89-28214 22-54)
Copyright Avail: NTIS HC A99/MF A01; ESA Publications Div., ESTEC, Noordwijk, Netherlands, 80 Dutch guilders or 45 US dollars

Thermal control for the 3-axis stabilized Telecom satellite TELE-X, including antenna module (AM) and variable conductance heat pipes (VCHPs), which regulate the transmitter feed is described. At both AM and VCHP levels, the design support simulations are described. Tests whereby thermal design was qualified, as well as the flight predictions yielding expected in-orbit thermal behavior of the AM are summarized. ESA

N89-28258# Fokker B.V., Amsterdam (Netherlands). Space and Systems Div.
A THERMAL CONTROL DESIGN FOR THE QUASAT SPACECRAFT **c18**
H. Petersen *In* ESA, Third European Symposium on Space Thermal Control and Life Support Systems Dec. 1988 p 327-332 (For primary document see N89-28214 22-54)
Copyright Avail: NTIS HC A99/MF A01; ESA Publications Div., ESTEC, Noordwijk, Netherlands, 80 Dutch guilders or 45 US dollars

Quasat's requirements to its thermal subsystem are discussed. The payload preamplifiers have to be cooled in the 100 K region by Stirling cycle coolers. The preamps must be close to the feed, so the coolers operate in the heart of the satellite and their heat has to be carried away by heat pipes. Heat pipes are necessary anyway to transport all equipment dissipation from the platform to and over the radiator, because this radiator is relatively small and remote. The spacecraft environment is dominated by the large antenna, of which the temperature can change between -230 C and +130 C dependent on the solar aspect angle and the eclipse length, which can be 2 hr. The envisaged solution employs Variable Conductance Heat Pipes to control emission by the radiator. ESA

N89-28259# Aerospatiale, Cannes La Bocca (France).
THE VEGETATION PAYLOAD OF THE SPOT-4 SPACECRAFT THERMAL DESIGN AND ANALYSIS **c18**
S. Zaninotti *In* ESA, Third European Symposium on Space Thermal Control and Life Support Systems Dec. 1988 p 333-337 (For primary document see N89-28214 22-54)
Copyright Avail: NTIS HC A99/MF A01; ESA Publications Div., ESTEC, Noordwijk, Netherlands, 80 Dutch guilders or 45 US dollars

The VEGETATION instrument, a payload of the SPOT 4, is presented. It is composed of a number of optical cameras and detectors requiring a high image quality and stability. The approach selected for the thermal control of this instrument is outlined. The mathematical models and the performances of the VEGETATION thermal control are discussed. The proposed development plan is shown. ESA

N89-28260# Fokker B.V., Amsterdam (Netherlands). Space and Systems Div.
PREPARING ULYSSES FOR LAUNCH **c18**
H. Petersen *In* ESA, Third European Symposium on Space Thermal Control and Life Support Systems Dec. 1988 p 339-344 (For primary document see N89-28214 22-54)
Copyright Avail: NTIS HC A99/MF A01; ESA Publications Div., ESTEC, Noordwijk, Netherlands, 80 Dutch guilders or 45 US dollars

The analysis program being carried out for Ulysses during launch is discussed. This analysis is important because the launch phase may be lengthy and Ulysses internal temperatures run high during ascent, partly because of the operating status of the spacecraft, partly because of high temperatures in the cargo bay. The launch scenario is discussed, and agreements with NASA to decrease the heat loads on the spacecraft are mentioned. Consequences from the decreasing electrical output of the RTG are discussed. A plume heating problem is indicated. Measurements on a blanket from the spacecraft indicate that no degradation due to aging and an ice phenomenon during vacuum testing occur. ESA

N89-28261# Dornier System G.m.b.H., Friedrichshafen (Germany, F.R.).
THERMAL ASPECTS OF THE ERS-1 SAR ANTENNA DEPLOYMENT **c18**

G. Jander, F. Zilly, and R. Bisanz *In* ESA, Third European Symposium on Space Thermal Control and Life Support Systems Dec. 1988 p 345-350 (For primary document see N89-28214 22-54)
Copyright Avail: NTIS HC A99/MF A01; ESA Publications Div., ESTEC, Noordwijk, Netherlands, 80 Dutch guilders or 45 US dollars

Transferring the deployable elements of the ERS-1 SAR antenna from stowed into deployed configuration is considered as the most critical activity within the LEOP (Launch and Early Orbit Phase) operational sequence. The deployment of the different elements of the ERS-1 has to be studied carefully and the operational sequencing of events has to be embedded into an overall LEOP scenario considering various constraints. Besides the nominal operational conditions the deployment was studied for various scenarios, including failure cases (contingency scenarios). Relevant scenarios including partly deployed antenna panels and their analytical treatment, e.g., standard thermal mathematical models, raytracing techniques for sun trapping, and engineering assessment are described. ESA

N89-28262*# National Aeronautics and Space Administration. Lyndon B. Johnson Space Center, Houston, TX.
TEST RESULTS ON RE-USE OF RECLAIMED SHOWER WATER: SUMMARY
C. E. Verostko, R. Garcia, R. Sauer, A. T. Linton, T. Elms, and R. P. Reysa (Boeing Aerospace Co., Houston, TX.) *In* ESA, Third European Symposium on Space Thermal Control and Life Support Systems Dec. 1988 p 353-360 (For primary document see N89-28214 22-54)
Copyright Avail: NTIS HC A99/MF A01; ESA Publications Div., ESTEC, Noordwijk, Netherlands, 80 Dutch guilders or 45 US dollars CSCL 05H

A microgravity whole body shower (WBS) and waste water recovery systems (WWRS) were evaluated in three separate closed loop tests. Following a protocol similar to that anticipated for the U.S. Space Station, test subjects showered in a prototype whole body shower. The WWRS processes evaluated during the test series were phase change and reverse osmosis (RO). A preprototype Thermoelectric Integrated Hollow Fiber Membrane Evaporation Subsystem phase change process was used for the initial test with chemical pretreatment of the shower water waste input. The second and third tests concentrated on RO technologies. The second test evaluated a dynamic RO membrane consisting of zirconium oxide polyacrylic acid (ZOPA) membranes deposited on the interior diameter of 316L porous stainless steel tubes while the final test employed a thin semipermeable RO membrane deposited on the interior surface of polysulfone hollow fibers. All reclaimed water was post-treated for purity using ion exchange and granular activated carbon beds immediately followed by microbial control treatment using both heat and iodine. The test hardware, controls exercised for whole body showering, types of soaps evaluated, shower subject response to reclaimed water showering, and shower water collection and chemical pretreatment (if required) for microbial control are described. The WWRS recovered water performance and the effectiveness of the reclaimed water post-treatment techniques used for maintaining water purity and microorganism control are compared. Results on chemical and microbial impurity content of the water samples obtained from various locations in the shower water reuse system are summarized. ESA

N89-28263# Dornier System G.m.b.H., Friedrichshafen (Germany, F.R.).
THE LIQUID MANAGEMENT SECTION OF THE HERMES ECLSS
R. Strittmatter *In* ESA, Third European Symposium on Space Thermal Control and Life Support Systems Dec. 1988 p 361-366 (For primary document see N89-28214 22-54)
Copyright Avail: NTIS HC A99/MF A01; ESA Publications Div., ESTEC, Noordwijk, Netherlands, 80 Dutch guilders or 45 US dollars

The equipment required and the processes used to provide the crew of Hermes with potable water and to collect waste liquids within the habitable area and the airlock are described. The treated water flowing steadily at 1.5 kg/hr in average from the fuel cells will be stored in double redundant tanks of 50 liters each while quality controlled and processed for multiple uses (drink/food preparation, washing, cooling purposes). Two tanks for the collection and temporary storage of waste liquids, provisions for overboard dumping of excess liquids and for transfer to and from docked modules (MTFF, Space Station) are foreseen. ESA

N89-28264# Osterreichische Raumfahrt- und Systemtechnik G.m.b.H., Vienna (Austria).
HERMES: DRINK/FOOD-WATER SUPPLY ASSEMBLY
H. W. Malnig *In* ESA, Third European Symposium on Space Thermal Control and Life Support Systems Dec. 1988 p 367-371 (For primary document see N89-28214 22-54)
Copyright Avail: NTIS HC A99/MF A01; ESA Publications Div., ESTEC, Noordwijk, Netherlands, 80 Dutch guilders or 45 US dollars

A recommendation for a Hermes food/drink Water Supply Assembly (WSA) is presented. The main components of the WSA are the chiller which provides cold potable water and the heater for hot water for food preparation. Tradeoffs in combination with the pressurization system result in the following concepts. Chiller: a cylindric batch tank with a concentric cooling coil and swirler yielding an equivalent to free convection, the quantity of in- and out-flowing water is balanced. Heater: two joined externally heated hemispheric shells with an equatorial bladder, which is reciprocating under incoming water inherent pressure, balancing in- and out-flowing water volume. ESA

N89-28265# Osterreichische Raumfahrt- und Systemtechnik G.m.b.H., Vienna (Austria).
NUTRITION FOR SHORT-DURATION SPACE MISSIONS
C. Dammermann *In* ESA, Third of the 3rd European Symposium on Space Thermal Control and Life Support Systems Dec. 1988 p 373-377 (For primary document see N89-28214 22-54)
Copyright Avail: NTIS HC A99/MF A01; ESA Publications Div., ESTEC, Noordwijk, Netherlands, 80 Dutch guilders or 45 US dollars

The role food/galley management (FGM) and nutrition plays within the context of the Hermes ECLSS is discussed. Human physiological and phychological needs as well as Hermes spacecraft mission requirements are presented. The analysis of possible concepts and the definition of the optimum solution were performed under the following constraints: the size of the spaceplane makes it mass and power critical which places a significant constraint on power consumption and mass of the FGMS. Tests for the practical analysis of temperature and palatability aspects of the proposed food were conducted. ESA

N89-28266# European Space Agency. European Space Research and Technology Center, ESTEC, Noordwijk (Netherlands). **c18**
CRYOGENIC ACTIVITIES AT ESTEC
C. Jewell *In its* Third European Symposium on Space Thermal Control and Life Support Systems Dec. 1988 p 381-386 (For primary document see N89-28214 22-54)
Copyright Avail: NTIS HC A99/MF A01; ESA Publications Div., ESTEC, Noordwijk, Netherlands, 80 Dutch guilders or 45 US dollars

The main cryogenic activity in ESTEC revolves around the preparation of ISO for launch in 1993. However many other projects such as Meteosat, FIRST, GRASP, QUASAT, and X-ray detection with STJ junctions all need cooling to 80 K or less. At these temperatures the use of reasonably sized radiators is limited by cooling power and pointing constraints while the use of cryogen cooling is often limited by the lifetime. Hence ESTEC is involved in the study and development of mechanical coolers for work in the temperature ranges of 80, 20, and 4 K. ESA

N89-28267# British Aerospace Public Ltd. Co., Bristol (England). Space and Communications Div.

LONG-LIFE STIRLING CYCLE COOLERS FOR APPLICATIONS IN THE 60 TO 110 K RANGE **c31**

C. A. Lewis *In* ESA, Third European Symposium on Space Thermal Control and Life Support Systems Dec. 1988 p 387-391 (For primary document see N89-28214 22-54)

Copyright Avail: NTIS HC A99/MF A01; ESA Publications Div., ESTEC, Noordwijk, Netherlands, 80 Dutch guilders or 45 US dollars

A mechanical, long life refrigerator which can replace stored cryogens and low temperature radiators in the 60 to 110 K range is presented. Design guidelines are given for the accommodation of these coolers on 3-axis and spin stabilized spacecraft. The growth of a cooler system from a single unit may require additional hardware such as thermal switches, momentum compensators, and cold plumbing. A modular philosophy towards this cryogenic hardware is proposed, enabling the user to design a system which exactly meets the mission requirements with respect to performance, reliability and flexibility. ESA

N89-28268# Rutherford High Energy Lab., Chilton (England).

A 4-K MECHANICAL REFRIGERATOR FOR SPACE APPLICATIONS **c31**

T. W. Bradshaw and A. H. Orlowska *In* ESA, Third European Symposium on Space Thermal Control and Life Support Systems Dec. 1988 p 393-397 (For primary document see N89-28214 22-54)

Copyright Avail: NTIS HC A99/MF A01; ESA Publications Div., ESTEC, Noordwijk, Netherlands, 80 Dutch guilders or 45 US dollars

A long life 4 K mechanical refrigerator for space applications was developed. The refrigerator consists of a Stirling cycle precooler operating at 20 K and a Joule-Thomson system using helium to achieve temperatures in the region of 4 K with a cooling power of a few milliwatts. The precooler is a two stage Stirling cycle cooler and is based on earlier work on long life single stage coolers. The Joule-Thomson stage uses compressors that are similar to those used in the precooler. ESA

N89-28269# Aerospatiale, Cannes La Bocca (France).

THERMAL AND CRYOGENIC ASPECTS OF THE ISO OPTICAL SUBSYSTEM **c31**

B. Collaudin and L. DeSa *In* ESA, Third European Symposium on Space Thermal Control and Life Support Systems Dec. 1988 p 399-405 Previously announced as N89-24160 (For primary document see N89-28214 22-54)

Copyright Avail: NTIS HC A99/MF A01; ESA Publications Div., ESTEC, Noordwijk, Netherlands, 80 Dutch guilders or 45 US dollars

The ISO Optical Subsystem is composed of a cold telescope, a main baffle, and a sunshade. Low temperatures are needed to reduce infrared noise produced by thermal self emission. The telescope and the baffle are cooled down to 3 K and 8 K by heat exchange with helium gas evaporated from a superfluid helium tank. The sunshade is cooled by radiation towards space, using a radiator. The analyses were performed using VWHEAT/ESATAN thermal models. A bulk model was used for design. Detailed models of the telescope, of the main baffle, and of the sun shade were established for local analysis and design. The design fulfills the requirements. ESA

N89-28270# Nippon Electric Co. Ltd., Yokohama (Japan). Space Development Div.

THERMAL DESIGN OF A SUPERFLUID HELIUM DEWAR FOR INFRARED TELESCOPE ON-BOARD SPACE FLYER UNIT **c31**

G. Fujii, T. Hasui, K. Hama, T. Okamoto, T. Machida, M. Murakami, T. Matsumoto, H. Okuda, and M. Kyoya (Sumitomo Heavy Industries Ltd., Tokyo, Japan) *In* ESA, Third European Symposium on Space Thermal Control and Life Support Systems Dec. 1988 p 407-412 (For primary document see N89-28214 22-54)

Copyright Avail: NTIS HC A99/MF A01; ESA Publications Div., ESTEC, Noordwijk, Netherlands, 80 Dutch guilders or 45 US dollars

The Infrared Telescope in Space (IRTS) onboard Space Flyer Unit is cooled down to 1.8 K by stored superfluid helium, allowing spectroscopic observation even in far infrared regions. The cooled mission life time is longer than several weeks. Minimization of heat leak to the lowest temperature level is one of the primary design goals for the maximum life time. The superfluid helium management at the launching site and also in the zero-g situation should also be well planned. ESA

N89-28271# Construcciones Aeronauticas S.A., Madrid (Spain). Space Div.

THERMAL CONTROL OF THE GRASP DETECTOR SECTION **c31**

P. B. Roig *In* ESA, Third European Symposium on Space Thermal Control and Life Support Systems Dec. 1988 p 413-420 (For primary document see N89-28214 22-54)

Copyright Avail: NTIS HC A99/MF A01; ESA Publications Div., ESTEC, Noordwijk, Netherlands, 80 Dutch guilders or 45 US dollars

The necessity of keeping GRASP telescope (Gamma Ray Astronomy with Spectroscopy and Positioning) detectors at working temperatures within an adequate range (85 + or - 15 K for the germanium and 283 + or - 20 K for CsI) is discussed. Thermal control based in cryogenic liquid tanks is not considered the most suitable solution because of mass and lifetime considerations. Instead of this conventional solution, a concept using a combination of passive and active cooling systems was chosen. It combines the features of a corrugated radiator panel, thermal shields, MLI blankets, and an extra cooling system based on the Stirling cycle engine. ESA

N89-28272# Centre National d'Etudes Spatiales, Toulouse (France).

TWO YEARS OF IN-ORBIT LIFE OF SPOT-1 HELIOSYNCHRONOUS PLATFORM **c18**

I. Alet *In* ESA, Third European Symposium on Space Thermal Control and Life Support Systems Dec. 1988 p 423-427 (For primary document see N89-28214 22-54)

Copyright Avail: NTIS HC A99/MF A01; ESA Publications Div., ESTEC, Noordwijk, Netherlands, 80 Dutch guilders or 45 US dollars

The flight data of the SPOT-1 satellite were analyzed to serve the future programs on the same type of orbit. The thermal control system of the platform proves to be correctly designed and works very well. The temperatures are in good agreement with predictions. The rise of the internal temperatures is significant for the first year (2 to 3 C), but very smooth (1 C) for the second year. The good behavior of the system allows optimism as to a long life of SPOT-1. ESA

N89-28273# European Space Agency. European Space Research and Technology Center, ESTEC, Noordwijk (Netherlands).

GIOTTO: THE THERMAL RESPONSES TO ITS ENCOUNTER WITH COMET HALLEY **c18**

R. J. Wilson *In its* Third European Symposium on Space Thermal Control and Life Support Systems Dec. 1988 p 429-435 (For primary document see N89-28214 22-54)

Copyright Avail: NTIS HC A99/MF A01; ESA Publications Div., ESTEC, Noordwijk, Netherlands, 80 Dutch guilders or 45 US dollars

Giotto passed within 596 km of the comet Halley nucleus and suffered dust damage to protruding experiments and the lower parts of the spacecraft. The dust impacts caused immediate temperature increases followed by revised thermal characteristics as a result of the damage. The exposed areas changed by up to 24 C, while 12 C increases were seen at internal locations. Damage hypotheses and how these would combine to produce the changed thermal behavior seen after the encounter are discussed. Giotto was put into hibernation 20 days after the encounter. It is hoped

to reactivate it early in 1990 and later to retarget it for another cometary encounter in 1992. ESA

N89-28274# Fokker B.V., Amsterdam (Netherlands). Space and Systems Div.
THERMAL ASPECTS OF AN EXTENDED MISSION FOR GIOTTO **c18**
A. Hartoog *In* ESA, Third European Symposium on Space Thermal Control and Life Support Systems Dec. 1988 p 437-441 (For primary document see N89-28214 22-54)
Copyright Avail: NTIS HC A99/MF A01; ESA Publications Div., ESTEC, Noordwijk, Netherlands, 80 Dutch guilders or 45 US dollars

Damage to Giotto as a result of the Halley encounter is explained in terms of the deteriorative effects of the cometary dust. The hibernation period following encounter is analyzed, revealing the unfortunate thermal situation where the spacecraft is illuminated on the topside with an intensity of 2600 W/sq m every time it passes through perihelion. The present proposal for a general health check of Giotto calls for a reactivation of the spacecraft in January 1990. A feasible mission scenario, accounting for thermal and power considerations is developed, which would end just before an Earth flyby July 1990. This flyby will change Giotto's orbit to an average distance to the Sun above 1 AU. A thermal configuration was chosen to provide the best possible thermal conditions during a second hibernation period (June 1990 to June 1992). A thermal strategy is developed for encounter with Grigg-Skjellerup on 10 July 1992. ESA

N89-28275# Dornier System G.m.b.H., Friedrichshafen (Germany, F.R.).
LESSONS LEARNED FROM ROSAT THERMAL BALANCE TEST: A COMBINED SOLAR SIMULATION/INFRARED TEST **c18**
A. Braig, T. Schaefer, and P. Pawlowski (Deutsche Forschungs- und Versuchsanstalt fuer Luft- und Raumfahrt, Cologne, Germany, F.R.) *In* ESA, Third European Symposium on Space Thermal Control and Life Support Systems Dec. 1988 p 443-448 (For primary document see N89-28214 22-54)
Copyright Avail: NTIS HC A99/MF A01; ESA Publications Div., ESTEC, Noordwijk, Netherlands, 80 Dutch guilders or 45 US dollars

The structural/thermal model of the German X-ray observatory ROSAT was successfully thermal balance tested in a solar simulation chamber. Due to a complicated orbital thermal environment and dimensional constraints, the test conditions could not fully be adopted to the orbit conditions. The experiments, combining solar simulation and infrared test methods are described. Recommendations for improving the test quality are given. ESA

N89-28276# Societe des Accumulateurs Fixes et de Traction, Romainville (France).
THERMAL CONTROL OF NI-H2 BATTERY **c18**
C. Bulle and A. Dupuy (Aerospatiale, Cannes La Bocca, France) *In* ESA, Third European Symposium on Space Thermal Control and Life Support Systems Dec. 1988 p 449-455 (For primary document see N89-28214 22-54)
Copyright Avail: NTIS HC A99/MF A01; ESA Publications Div., ESTEC, Noordwijk, Netherlands, 80 Dutch guilders or 45 US dollars

The thermal design of a 50 Ah battery including sleeve and radiative plate is described. The thermal mathematical model built to predict temperatures of one cell during flight operation and which is adapted to predict temperatures during thermal cycling vacuum test is presented. The program, temperature measurements, and main results of this thermal test are provided. The thermal design adequacy of the battery is verified by the thermal vacuum test performed on the two cell specimen. The mathematical model is also qualified and allows cell temperature during battery operation to be predicted. ESA

N89-28277# Aerospatiale, Cannes La Bocca (France). Cryogenic Lab.
SHAKING IN CRYOGENIC CONDITIONS **c31**
S. Taride *In* ESA, Third European Symposium on Space Thermal Control and Life Support Systems Dec. 1988 p 457-460 Previously announced as N89-23939 (For primary document see N89-28214 22-54)
Copyright Avail: NTIS HC A99/MF A01; ESA Publications Div., ESTEC, Noordwijk, Netherlands, 80 Dutch guilders or 45 US dollars

Test equipment was developed to perform vibration tests on the whole ISOCAM instrument, which weights 9 kg, along the three axes, in sine and random, according to the level specified by the ISO project (up to 23 g). It is possible to measure the acceleration levels at the specimen interface as well as inside the specimen, at 4 K. The equipment can cool the instrument down to 4 K and to maintain in thus for hours, in order to analyze the low level sine curves before running qualification levels. It also has to keep the specimen under class 100 cleanness environment during preparation and under very clean vacuum during cooling down, shaking, and warming up. ESA

N89-28278# European Space Agency. European Space Research and Technology Center, ESTEC, Noordwijk (Netherlands).
THERMAL SOFTWARE DEVELOPMENTS AT ESTEC **c18**
C. Stroom *In its* Third European Symposium on Space Thermal Control and Life Support Systems Dec. 1988 p 463-467 (For primary document see N89-28214 22-54)
Copyright Avail: NTIS HC A99/MF A01; ESA Publications Div., ESTEC, Noordwijk, Netherlands, 80 Dutch guilders or 45 US dollars

The major software activities of the Thermal Control and Life Support Division of ESTEC are reviewed. Ongoing activities are listed and the outline for future activities is given. The role of ESTEC in the support and maintenance of the distributed software is emphasized. ESA

N89-28279# European Space Agency. European Space Research and Technology Center, ESTEC, Noordwijk (Netherlands).
SOHO THERMAL MODELLING AND ANALYSIS: THE FIRST APPLICATION OF ESATAN TO A COMPLETE SPACECRAFT **c18**
R. J. Wilson *In its* Third European Symposium on Space Thermal Control and Life Support Systems Dec. 1988 p 469-474 (For primary document see N89-28214 22-54)
Copyright Avail: NTIS HC A99/MF A01; ESA Publications Div., ESTEC, Noordwijk, Netherlands, 80 Dutch guilders or 45 US dollars

Application to a whole spacecraft of ESA's finite difference thermal analyzer ESATAN is discussed. The ESATAN model of SOHO took advantage of the many facilities offered, such as sub-models and super-nodes. The SOHO model structure and the way in which the model was operated are described along with the use of models that existed in a stand-alone form. Advice to potential users on the construction of models is given. ESA

N89-28280# Aerospatiale, Cannes La Bocca (France).
ASSEMBLING THE ISO THERMAL MODEL WITH ESATAN **c18**
A. Rocaboy *In* ESA, Third European Symposium on Space Thermal Control and Life Support Systems Dec. 1988 p 475-482 (For primary document see N89-28214 22-54)
Copyright Avail: NTIS HC A99/MF A01; ESA Publications Div., ESTEC, Noordwijk, Netherlands, 80 Dutch guilders or 45 US dollars

The ISO satellite, the associated mission requirements, the thermal concept, and thermal analysis conducted at system level for the demonstration of the helium cryostat operational lifetime are described. In a first step the thermal analysis is performed using separate models for each module of the spacecraft. These sub-models are condensed and assembled using the modular

structure of ESATAN and subroutines and through numerical interface specification. The global model (550 nodes) is used for the update of thermal interfaces between submodels and the verification of thermal performances of the design in terms of temperature distribution and lifetime, at system level. Guidelines to be applied in assembling submodels are presented. Positive features of ESATAN for the ISO application are emphasized and recommendations for improvement are suggested. ESA

N89-28281# GEC Power Engineering Ltd., Whetstone (England).
ESATAN FHTS: A PIPED FLUID NETWORK CAPABILITY c18
J. R. Turner, T. J. Swift, T. M. Andrews, and A. Lebru (European Space Agency. European Space Research and Technology Center, ESTEC, Noordwijk, Netherlands) *In* ESA, Third European Symposium on Space Thermal Control and Life Support Systems Dec. 1988 p 483-487 (For primary document see N89-28214 22-54)
Copyright Avail: NTIS HC A99/MF A01; ESA Publications Div., ESTEC, Noordwijk, Netherlands, 80 Dutch guilders or 45 US dollars

The ESATAN thermal analysis package was extended to incorporate predictions of fluid pressure and mass flow rate in one-dimensional, piped fluid networks. This is in addition to the original capability of thermal analysis. The ESATAN Fluid Heat Transport System (FHTS) is capable of steady state or transient analyses, with single or two-phase fluid flow. Users are able to construct piped fluid systems from basic node and conductance data, and also incorporate predefined elements which are used to simulate hardware such as pumps and heat exchangers. Previous thermal model input decks are compatible with the new system. Analysis may be all-fluid, all-thermal, or both fluid and thermal simultaneously. ESA

N89-28282# Aerospatiale, Cannes La Bocca (France). Space and Strategic Systems Div.
THE FLUIDNET DEVELOPMENT AND APPLICATION TO PRELIMINARY SIZING OF FLUID-LOOP SYSTEMS c18
S. Andre, J. N. Chelotti, J. F. Gory, and T. Lafon (Centre National d'Etudes Spatiales, Toulouse, France) *In* ESA, Third European Symposium on Space Thermal Control and Life Support Systems Dec. 1988 p 489-495 Previously announced as N89-23845 (For primary document see N89-28214 22-54)
Copyright Avail: NTIS HC A99/MF A01; ESA Publications Div., ESTEC, Noordwijk, Netherlands, 80 Dutch guilders or 45 US dollars

Fluidnet is a computer program for preliminary sizing of fluid loop networks used in space thermal control systems. Fluidnet is an interactive application, whose main features are: easy implementation, rapidity, portability, flexible architecture. It is complementary with design tools like FLUINT and FHTS (fluid loop analysis extensions from SINDA and ESATAN). The current version is applied to thermal and hydraulic analysis of single phase fluid loops in steady state. ESA

N89-28283# Dornier System G.m.b.H., Friedrichshafen (Germany, F.R.).
EVOLUTION OF THERMAL ANALYSIS METHODS TOWARDS INTEGRATED SYSTEM PERFORMANCE SIMULATION c18
M. Rothmeyer and W. Schwarzott *In* ESA, Third European Symposium on Space Thermal Control and Life Support Systems Dec. 1988 p 497-505 (For primary document see N89-28214 22-54)
Copyright Avail: NTIS HC A99/MF A01; ESA Publications Div., ESTEC, Noordwijk, Netherlands, 80 Dutch guilders or 45 US dollars

A loose integration of thermal analysis tools into a common software system is described. The requirements for thermal modeling within future space projects and the software tools which are being developed are listed. Using the thermal simulation of the habitable volumes of Hermes as an example, the benefits of integrated thermal models are discussed. ESA

N89-28284# Dornier System G.m.b.H., Friedrichshafen (Germany, F.R.).
ECLS SIMULATION PROGRAM
G. Kirschner *In* ESA, Third European Symposium on Space Thermal Control and Life Support Systems Dec. 1988 p 507-511 (For primary document see N89-28214 22-54)
Copyright Avail: NTIS HC A99/MF A01; ESA Publications Div., ESTEC, Noordwijk, Netherlands, 80 Dutch guilders or 45 US dollars

Showing the importance and advantages of an integrated simulation, models for EVA, Hermes and Columbus ECLS systems have to be developed. Using modular program technique the same subroutines for equal functions can be used for the different simulation models. The tasks of the single modules are described and it is shown how existing commercial programs are used for in- and out-put, documentation, and data representation. An example from already programmed modules and an outlook for further program development is given. ESA

N89-28285# Aerospatiale, Cannes La Bocca (France).
DEVELOPMENT OF HEAT EXCHANGERS FOR HYBRID RADIATORS
M. Amidieu and T. Lafon (Centre National d'Etudes Spatiales, Toulouse, France) *In* ESA, Third European Symposium on Space Thermal Control and Life Support Systems Dec. 1988 p 515-522 (For primary document see N89-28214 22-54)
Copyright Avail: NTIS HC A99/MF A01; ESA Publications Div., ESTEC, Noordwijk, Netherlands, 80 Dutch guilders or 45 US dollars

A preliminary study yielded two basic concepts for a heat exchanger, namely: one dry contact exchanger in which the fluid circuit and the heat pipes contact each other through their outer shell; one wet contact exchanger, where one of the fluids comes into contact with the other element. From a comparative analysis of the two concepts, taking into account criteria of performance, manufacturing and operational use, the dry contact exchanger was selected for development. ESA

N89-28286# Martin Marietta Aerospace, Denver, CO. Astronautics Group.
DEVELOPMENT OF A NOVEL HIGH-PERFORMANCE CONTACT HEAT EXCHANGER
W. H. Miller and T. Buna *In* ESA, Third European Symposium on Space Thermal Control and Life Support Systems Dec. 1988 p 523-528 (For primary document see N89-28214 22-54)
Copyright Avail: NTIS HC A99/MF A01; ESA Publications Div., ESTEC, Noordwijk, Netherlands, 80 Dutch guilders or 45 US dollars

The development of a contact heat exchanger for space station type applications with the objective of providing on-orbit replaceability of damaged or degraded radiators is described. The device is to provide disconnect type thermal coupling between heat pipe radiators and the internal heat transport fluid loops of the thermal management system. The key issue to be resolved was to ensure precise mating between the contact surfaces, determined to be a necessary condition for ensuring the required high conductance. This was achieved by the use of precision manufacturing techniques and the use of a conical contact geometry. Analyses, test approach, and results are presented indicating a highly competitive thermal performance. ESA

N89-28287# Politecnico di Torino (Italy). Dept. di Energetica.
INTERMEDIATE HEAT EXCHANGER FOR A NUCLEAR-POWERED SPACE POWER SYSTEM c18
G. DelTin, M. Malandrone, N. Nervegna, N. Valle, P. G. Avanzini, and A. Torresi (Ansaldo S.p.A., Genoa, Italy) *In* ESA, Third European Symposium on Space Thermal Control and Life Support Systems Dec. 1988 p 529-535 (For primary document see N89-28214 22-54)
Copyright Avail: NTIS HC A99/MF A01; ESA Publications Div., ESTEC, Noordwijk, Netherlands, 80 Dutch guilders or 45 US dollars

The analysis and design of an Intermediate Heat Exchanger

(IHX) operated under constraints of power, temperature, pressure, redundancy and size, and suitable for integration in a 200 kWe space nuclear generator system is presented. Exchanged thermal power is in the range of 1050 kW being liquid lithium the IHX shell side coolant fluid. Tube side fluid is an He-Xe mixture, rated at the molecular mass of Ar (39.9) to compromise turbomachinery performances and heat exchange processes. Specifications on normal operating temperatures are: in the selected counterflow arrangement lithium enters the shell side at 1197 C, while the gas mixture enters the IHX at 735 C. Since the two existing lithium loops are low pressure operated and being low velocity, for which a typical transition flow regime must be accounted. Secondary loops, four at normal operating conditions, are wholly independent and arranged in parallel with an operating pressure of 10 bar and a compression ratio of 2.2. Thus, the flow is fully turbulent. The selected containment material for the lithium side is the (MoRe) alloy, while a (TaW) alloy was designated for the gas side. Straight tubes partitioned in four bundles individually feed respective turbomachines, this solution providing some degree of redundancy in case of failure of one rotating unit. ESA

N89-28288# Fokker B.V., Amsterdam (Netherlands). Space and Systems Div.

A 1-kW CONDENSER FOR A TWO-PHASE HEAT REJECTION SYSTEM **c18**

H. vonLonkhuyzen and N. H. Pennings *In* ESA, Third European Symposium on Space Thermal Control and Life Support Systems Dec. 1988 p 537-541 Sponsored by Dornier System GmbH, Friedrichshafen, Fed. Republic of Germany (For primary document see N89-28214 22-54)

Copyright Avail: NTIS HC A99/MF A01; ESA Publications Div., ESTEC, Noordwijk, Netherlands, 80 Dutch guilders or 45 US dollars

A breadboard model of a 1 kW spacecraft condenser unit was designed, manufactured, and tested. The condenser forms part of a 15 kW mechanically pumped two-phase flow (TPF) heat rejection system. A thermal-hydraulic analysis of such a heat rejection system shows that a parallel layout of radiator panels and condenser branches is preferred. The 1 kW condenser consists of two parallel branches. Each branch is made of an aluminum extrusion profile with 15 parallel channels and a porous plug. The condenser can be integrated in a two-sided radiating panel of 1.8 x 1.8 m sq. The test results of the condenser breadboard model show that the thermal-hydraulic behavior is a factor 1.5 to 2 better than the performance predicted by the Lockhart-Martinelli theory. For a 1 kW heatload the pressure drop over the condenser is 0.02 bar and the temperature drop from the TPF mixture to the outer surface of the condenser is 1.5 C. ESA

N89-28289# Tokyo Univ. (Japan).

A VERY LOW REFLECTANCE DIFFUSE SURFACE FOR THERMAL DESIGN OF SPACECRAFT **c18**

A. Ohnishi, K. Kaneko, and T. Hayashi *In* ESA, Third European Symposium on Space Thermal Control and Life Support Systems Dec. 1988 p 543-545 (For primary document see N89-28214 22-54)

Copyright Avail: NTIS HC A99/MF A01; ESA Publications Div., ESTEC, Noordwijk, Netherlands, 80 Dutch guilders or 45 US dollars

A very low reflectance diffuse surface for thermal control coating of spacecraft is proposed. This method is based on electrostatic flocking of carbon fiber to a surface previously coated with adhesive to fix the fiber vertically to the surface. The surface region surrounded by carbon fiber behaves microscopically as a lossy terminal for electromagnetic waves in visible and IR regions, and diffuse black surface with high stability would be attained. ESA

N89-28290# Ansaldo S.p.A., Genoa (Italy).

A MAGNETICALLY-DRIVEN DROPLET RADIATOR CONCEPT **c18**

P. G. Avanzini, S. Valentini, and G. Tuninetti *In* ESA, Third European Symposium on Space Thermal Control and Life Support Systems Dec. 1988 p 547-552 (For primary document see N89-28214 22-54)

Copyright Avail: NTIS HC A99/MF A01; ESA Publications Div., ESTEC, Noordwijk, Netherlands, 80 Dutch guilders or 45 US dollars

The liquid droplet radiator (LDR) is described. It features a solenoid magnet constraining a radiating surface of droplets in a toroidal configuration. An annular droplet generator surrounds the magnet. Two streams of ferromagnetic droplets are generated in opposite directions, driven by the magnetic field along curvilinear trajectories, collected inside the magnet, and recirculated to the generator after cooling in a heat exchanger interfacing heat rejection and thermal control loops. Advantages are expected in system compactness and reduction of coolant losses. A model is developed to predict the motion of a ferromagnetic droplet in a magnetic field, in order to investigate the feasibility of the concept. ESA

N89-28291# Messerschmitt-Boelkow-Blohm G.m.b.H., Munich (Germany, F.R.). Space Communications and Propulsions Systems Div.

THERMAL ANALYSIS OF ADVANCED HEAT PROTECTION SYSTEMS **c18**

K. Keller and H. Grallert *In* ESA, Third European Symposium on Space Thermal Control and Life Support Systems Dec. 1988 p 555-560 (For primary document see N89-28214 22-54)

Copyright Avail: NTIS HC A99/MF A01; ESA Publications Div., ESTEC, Noordwijk, Netherlands, 80 Dutch guilders or 45 US dollars

Heat transfer in fibrous insulations with reflective foils is discussed. The dependence of radiative transfer on foil reflectivity, foil number, and basic fiber characteristics is studied. With respect to heat conduction by air, it is found that besides the commonly known dependence on fiber diameter, porosity, and ambient pressure, additionally the fiber orientation has to be considered. Results concerning radiation-conduction coupling and convection are presented. ESA

N89-28292# Messerschmitt-Boelkow-Blohm G.m.b.H., Bremen (Germany, F.R.).

THERMAL PROTECTION CONCEPTS OF RECOVERABLE CAPSULES **c18**

H. Loeser *In* ESA, Third European Symposium on Space Thermal Control and Life Support Systems Dec. 1988 p 561-566 (For primary document see N89-28214 22-54)

Copyright Avail: NTIS HC A99/MF A01; ESA Publications Div., ESTEC, Noordwijk, Netherlands, 80 Dutch guilders or 45 US dollars

Recoverable capsule thermal protection system concepts are discussed, e.g., reradiative systems, heat sinks, and ablative systems. The relative merits of the three systems are quantified by numerical results obtained for a capsule to be flown with a sounding rocket and returning with sub-circular entry velocity. ESA

N89-28293# Aeritalia S.p.A., Turin (Italy).

CYROGENIC FLUID SINK DEVICE FOR THERMAL CONTROL OF A SPACEPLANE DURING ASCENT AND RE-ENTRY PHASES **c18**

D. Nikanpour and M. Petruzziello *In* ESA, Third European Symposium on Space Thermal Control and Life Support Systems Dec. 1988 p 567-572 (For primary document see N89-28214 22-54)

Copyright Avail: NTIS HC A99/MF A01; ESA Publications Div., ESTEC, Noordwijk, Netherlands, 80 Dutch guilders or 45 US dollars

The use of a cryogenic fluid store in supplying a low temperature fluid as the heat sink device is discussed. Candidate fluids such as liquid helium and hydrogen were investigated and shown to provide high heat transport capability per unit mass by sensibly heating the gas, exploiting the low initial temperatures and high specific heat capacities of the fluid. Design features of the heat sink device are discussed and critical areas requiring technology development for its safe implementation are highlighted. ESA

N89-28294# Societe Anonyme Belge de Constructions Aeronautiques, Brussels.
QUALIFICATION PROGRAM ON STAINLESS STEEL A95 HEATPIPE FOR SPACE APPLICATION **c18**
R. S. Bhatti and S. VanOost *In* ESA, Third European Symposium on Space Thermal Control and Life Support Systems Dec. 1988 p 575-582 (For primary document see N89-28214 22-54)
Copyright Avail: NTIS HC A99/MF A01; ESA Publications Div., ESTEC, Noordwijk, Netherlands, 80 Dutch guilders or 45 US dollars

High performance wicked stainless steel/ammonia heat pipes (VCHP and CCHP) were subjected to qualification as enumerated in ESA-PSS-49. Different lengths and various bend configurations were considered to cover all possible cases. Qualification tests are listed. Tests results are analyzed. The heat pipes in A95 steel meet specifications. ESA

N89-28295# Erno Raumfahrttechnik G.m.b.H. Bremen (Germany, F.R.).
THEORETICAL AND EXPERIMENTAL INVESTIGATIONS ON HEAT EXCHANGERS FOR COLUMBUS HYBRID RADIATORS **c18**
W.-D. Ebeling and R. Meyer *In* ESA, Third European Symposium on Space Thermal Control and Life Support Systems Dec. 1988 p 583-590 (For primary document see N89-28214 22-54)
Copyright Avail: NTIS HC A99/MF A01; ESA Publications Div., ESTEC, Noordwijk, Netherlands, 80 Dutch guilders or 45 US dollars

Parallel to the development of the Columbus system, ESA initiated a Preparatory Support Technology Programme (PSTP). In the frame of PSTP1, of a hybrid radiator Technical Demonstration Model (TDM) was developed. The thermo-hydraulic acceptance tests of the heat exchanger TDM show that the requirements concerning minimum heat transfer rate and maximum allowable pressure drop are met at the design point. The component tests on fin packages of different geometry show that the theoretical determination of thermohydraulic properties of offset strip fin packages using empirical correlations concerning the heat transfer rate is limited. Flow instabilities may cause a steep decrease in the convection coefficient within a limited Reynolds-number regime. Therefore, thermohydraulic component tests on selected fin geometries are required for the selection of a best suited fin configuration. This procedure which is applied for the development of the heat exchanger TDM is justified by the results of the component tests. ESA

N89-28296# Messerschmitt-Boelkow-Blohm G.m.b.H., Bremen (Germany, F.R.).
DEVELOPMENT OF THE HERMES FLEXIBLE EXTERNAL INSULATION **c18**
J. Antonenko, W.-D. Ebeling, H.-G Reimerdes, and J. Reininger *In* ESA, Third European Symposium on Space Thermal Control and Life Support Systems Dec. 1988 p 591-597 (For primary document see N89-28214 22-54)
Copyright Avail: NTIS HC A99/MF A01; ESA Publications Div., ESTEC, Noordwijk, Netherlands, 80 Dutch guilders or 45 US dollars

The Hermes flexible external insulation (FEI) is part of the thermal protection subsystem (PTS). It is applied in those areas where the external temperatures remain below 500 C under nominal reentry conditions. The extension of the maximum temperature limit up to 800 C is under consideration. The insulation blanket shall protect the structure from temperature rising beyond 200 C. It shall maintain full integrity under all mechanical and aerodynamical loads for 15 yr or 30 missions. The selected FEI configuration consists of a fibrous insulation core between fiber fabrics which are sewed together. Design features are discussed and results from thermal and mechanical investigations performed during the predevelopment phase are presented. ESA

N89-28297# Erno Raumfahrttechnik G.m.b.H. Bremen (Germany, F.R.).
IN-ORBIT DEGRADATION OF THERMO-OPTICAL PROPERTIES ON MARECS GEO-SATELLITE **c18**
H.-G. Konzok, A. Soeffker, D. Stuempel, and K. Derbyshire (European Space Agency. European Space Research and Technology Center, ESTEC, Noordwijk, Netherlands) *In* ESA, Third European Symposium on Space Thermal Control and Life Support Systems Dec. 1988 p 599-604 (For primary document see N89-28214 22-54)
(Contract ESTEC-5456/83/NL/DG)
Copyright Avail: NTIS HC A99/MF A01; ESA Publications Div., ESTEC, Noordwijk, Netherlands, 80 Dutch guilders or 45 US dollars

Observations from the initial 6 yr of flight for MCS-A and 3 yr; for MCS-B2 are discussed. There is a noticeable general temperature increase within the satellites. The temperature rise at equinox is larger than expected. The additional rise seen at solstices when the radiators are Sun illuminated is within the expected range. The calculated degradation rates compare well to those generated by DERTS. ESA

N89-28298# Army Research Inst. of Environmental Medicine, Natick, MA.
ANALYSIS OF ARTICULATED MANIKIN BASED CONVECTIVE HEAT TRANSFER DURING WALKING
Stephen KW. Chang and Richard R. Gonzalez Mar. 1989 43 p
(DA Proj. 3E1-62787-A-878)
(AD-A208299; USARIEM-T-11-89) Avail: NTIS HC A03/MF A01 CSCL 06/4

Using the articulated manikin at U.S. Army Research Institute of Environmental Medicine (USARIEM) as a model, the effect of the walking motion on the local convective heat transfer at various body sites was studied. The forced convective heat transfer coefficient (hc) was determined by the naphthalene sublimation technique. The results showed that the arm movement during walking, unexpectedly, diminished the local convective transfer coefficient. Increasing gait actually resulted in a decrease in hc, as measured on the arms and legs. On the non-moving body trunk, no significant difference in hc was observed with changing gait. When the manikin was held stationary and the chamber wind speed increased, a corresponding increase in hc was observed. Thus, during walking, motion of the swinging limbs, the pendulum effect, tends to decrease the forced convective heat transfer as observed locally on the limbs. GRA

N89-28299# Georgia Inst. of Tech., Atlanta.
IDENTIFICATION OF VARIABLES DETERMINING INTRAHEMISPHERIC INTERFERENCE BETWEEN PROCESSING DEMANDS Final Report, 1981-1985
Joanne Green Apr. 1989 166 p
(Contract MDA903-81-C-0443)
(AD-A208435; ARI-RN-89-17) Avail: NTIS HC A08/MF A01 CSCL 05/8

This research note describes basic research aimed at understanding principles of brain hemisphere functioning which can be used to improve human performance. The research is most relevant for understanding performance based on visual information perceived by peripheral vision, and examines how intrahemispheric interference affects performance degradation when two task-related activities depend on the same hemisphere of the brain. It was found that even in apparently simple tasks, small changes increasing or decreasing the difficulty of cognitive decision making are very powerful in determining how interactions within hemispheres will affect performance. When intrahemispheric interference occurred, changes in response requirements simplifying the decisional processes necessary to organize the response served to reduce interference. Effects of intrahemispheric interference may reduce performance based on stimuli in a particular location, or reduce it by one hand relative to the other. There are individual differences in the magnitude of intrahemispheric interference and its effects degrading performance as well. GRA

N89-28300# Universal Energy Systems, Inc., Dayton, OH. Biomedical Applications Research Div.
ANTHROPOMETRIC MEASUREMENTS OF AVIATORS WITHIN THE AVIATION EPIDEMIOLOGY DATA REGISTER Final Report
Robert H. Schrimsher and Thomas J. Burke Mar. 1989 46 p
(DA Proj. 3E1-62787-A-878)
(AD-A208609; USAARL-89-5) Avail: NTIS HC A03/MF A01 CSCL 06/4

Beginning in 1983, the U.S. Army Aviation Epidemiology Data Register (AEDR) was developed. The AEDR is a permanent, computer-accessible repository of medical information on the Army aviation population. This automated database system provides data for developing and evaluating aviation medical selection and retention standards, for conducting epidemiologic studies on health risk factors, and the natural history of disease in the aviation environment, for evaluating health hazards in the aviation environment, and for providing human factors input to engineers developing aircraft, weapons, and life support equipment. Twenty anthropometric measurements on 22,000 male flight school applicants, 29,000 male aviators, 800 female flight school applicants, and 600 female aviators are recorded in the Aviation Epidemiology Data Register (AEDR). Summary statistics for the anthropometric measurements of these four populations, including mean, standard deviation, and the 1, 5, 50, 95, and 99 percentile values, are reported. These values are reported in a tabular format with the corresponding values from five other Department of Defense anthropometric studies. GRA

N89-28301# Northwestern Univ., Evanston, IL. Neuroscience Lab.
PERCEPTION OF MOTION IN STATISTICALLY-DEFINED DISPLAYS Final Scientific Report, 1 Oct. 1985 - 30 Sep. 1988
Robert Sekuler 15 Apr. 1989 278 p
(Grant AF-AFOSR-0370-85; AF Proj. 2313)
(AD-A208695; AFOSR-89-0769TR) Avail: NTIS HC A13/MF A01 CSCL 06/5

This project used statistically-complex displays to probe higher-orders of human motion perception. The project's overall aim was to establish the characteristics of human visual mechanisms that extract information from these and other displays. A fundamental contribution was the systematic refinement and extension of a model in which motion information is extracted and processed, via non-linear interactions, by directionally-selective visual mechanisms. Prior work has shown that a percept of global coherent motion can be produced from the combination of many different, localized motion vectors. Using random-dot cinematograms, we established that hysteresis is strongly associated with such percepts. It was previously found that practice seemed to produce direction-selective improvement in observers' ability to discriminate between highly similar directions of motion. Investigators clarified the basis for this improvement by recording an observers eye movements while they target motion. Investigators also created random-dot cinematograms in which each dot's successive movements were independently drawn from a Gaussian distribution of directions of some characteristic bandwidth. GRA

N89-28302# Rice Univ., Houston, TX. Dept. of Psychology.
HUMAN COGNITION AND INFORMATION DISPLAY IN C3I SYSTEM TASKS Research Note Oct. 1985 - Nov. 1986
William C. Howell, David M. Lane, and Kritina L. Holden Dec. 1988 42 p
(Contract MDA903-85-C-0347)
(AD-A210012; Rept-86-1; ARI-RN-88-106) Avail: NTIS HC A03/MF A01 CSCL 25/5

It is widely recognized that the growing demands of modern warfare strain and in some cases exceed human cognitive capabilities. Although modern command, control, communication, and intelligence (C3I) systems incorporate a number of advanced design concepts to reduce the burden on operators, it is essential that they retain certain key controlling functions. Therefore, efforts toward improving our understanding of how various design concepts affect human (and overall system) performance must continue. In particular, it is not always clear how general design principles relate to the specific kinds of critical tasks performed by operators in C3I systems. The purpose of this report is to present a highly selective review of the literature on C3I tasks, display principles, and human information processing functions with an eye toward identifying promising variables or concepts for evaluation in a simulated system context. GRA

N89-28303# Naval Air Development Center, Warminster, PA. Air Vehicle and Crew Systems Technology Dept.
EVALUATION OF THERMAL STRESS INDUCED BY HELICOPTER AIRCREW CHEMICAL, BIOLOGICAL, RADIOLOGICAL (CBR) PROTECTIVE ENSEMBLE Final Report, 3 Nov. 1987 - 17 Dec. 1988
Jonathan W. Kaufman, Katherine Y. Dejneka, Stephen Morrissey, and Alvah Bittner, Jr. 15 Jun. 1988 31 p Prepared in cooperation with Analytics, Inc., Willow Grove, PA
(AD-A210123; NADC-89009-60) Avail: NTIS HC A03/MF A01 CSCL 15/6

The A/P22P-9(V) Chemical, Biological, Radiological (CBR) Protective Assembly for helicopter aircrews has been evaluated for the additional thermal stress it imparts to users in a hot environment. The standard aircrew life support system for helicopters, based on the CWU-27/P flight coverall, was employed as the experimental control. Two environmental conditions were studied: (1) a simulated hot aircraft interior (hot), with chamber temperatures maintained at dry bulb temperatures = 32.8C and a wet bulb temperature = 25.0C; and (2) a control environment (cool), with chamber temperatures maintained at 20.9C. Three males, aged 24 to 35 years, were exposed twice to each garment/environment condition combination, for a total of eight exposures each, except for one subject who was studied in cool conditions only once in each of the configurations, for a total of six runs. Heat durations were designed for 480 minutes. Comparison by ensemble show significant differences observed for exposure durations, while rectal temperatures were significantly different (p less than 0.05) between ensembles only in hot conditions. Ambient conditions significantly impacted on nearly all measured parameters. The results indicate that the CBR ensemble represents a limiting factor in performance in a hot environment. GRA

55 SPACE BIOLOGY

Includes exobiology; planetary biology; and extraterrestrial life.

N89-28304*# National Aeronautics and Space Administration. Ames Research Center, Moffett Field, CA.
LIFE SCIENCE RESEARCH OBJECTIVES AND REPRESENTATIVE EXPERIMENTS FOR THE SPACE STATION
Catherine C. Johnson, ed., Roger D. Arno, ed., and Richard Mains, ed. (Mains Associates, Moffett Field, CA.) Apr. 1989 299 p
(NASA-TM-89445; A-87160; NAS 1.15:89445) Avail: NTIS HC A13/MF A01 CSCL 06C

A workshop was convened to develop hypothetical experiments to be used as a baseline for space station designer and equipment specifiers to ensure responsiveness to the users, the life science community. Sixty-five intra- and extramurai scientists were asked to describe scientific rationales, science objectives, and give brief representative experiment descriptions compatible with expected space station accommodations, capabilities, and performance envelopes. Experiment descriptions include hypothesis, subject types, approach, equipment requirements, and space station support requirements. The 171 experiments are divided into 14 disciplines. Author

59 MATHEMATICAL AND COMPUTER SCIENCES (GENERAL)

No abstracts in this category.

60 COMPUTER OPERATIONS AND HARDWARE

Includes hardware for computer graphics, firmware, and data processing.

For components see *33 Electronics and Electrical Engineering.*

N89-28305# Instituto de Pesquisas Espaciais, Sao Jose dos Campos (Brazil).
PERFORMANCE AUGMENTATION OF SITIM-150 THROUGH A HIGH PERFORMANCE NUMERICAL PROCESSOR [AUMENTO DA PERFORMANCE DO SITIM-150 ATRAVES DE UM PROCESSADOR NUMERICO DE ALTO DESEMPENHO]
Jose Claudio Mura Dec. 1988 8 p In PORTUGUESE; ENGLISH summary Presented at the 5th Brazilian Symposium on Remote Sensing, Natal, RN, 11-15 Oct. 1988
(INPE-4770-PRE/1439) Avail: NTIS HC A02/MF A01

The Image Processing System, SITIM-150, and the Numerical Processor, PN25, based on DSP TMS320C25 is described. The results are presented of the processing times, obtained for some image processing algorithms with PN25 and without it. Author

N89-28306# National Aeronautical Lab., Bangalore (India). Systems Engineering Div.
VED EDITOR FOR MC5600 COMPUTER SYSTEM
N. S. Badriprasad, N. N. Murthy, and V. Kothandaraman May 1989 15 p
(Proj. SE-0-135)
(PD-SE-8907) Avail: NTIS HC A03/MF A01

The ved is a test editor of the Masscomp MC5600. A guide to the ved user is presented. A major advantage of this editor is that it involves the use of few keys to invoke commands, making it easy to use. Using this editor involves the constant use of the control key. Author

N89-28307# National Aeronautical Lab., Bangalore (India). Systems Engineering Div.
VI EDITOR FOR MC56000 COMPUTER SYSTEM
Preetish Nijhawan, N. N. Murthy, and V. Kothandaraman May 1989 22 p
(Proj. SE-0-135)
(PD-SE-8906) Avail: NTIS HC A03/MF A01

Vi is a powerful editor on MASSCOMP 5600 system. It has numerous facilities: easy editing, lots of options, indenting, to edit the files without exiting vi, easy moving of between files and so on. Author

N89-28308# Oak Ridge National Lab., TN. Engineering Technology Div.
APPROACHING DISTRIBUTED DATABASE APPLICATIONS USING A PROGRAMMABLE TERMINAL EMULATOR
J. A. Clinard, J. J. Robinson, J. T. Phillips, Jr., and G. L. Johnson Jun. 1989 68 p Sponsored in part by Pacific Missile Testing Center
(Contract DE-AC05-84OT-21400)
(DE89-014831; K/DSRD-80) Avail: NTIS HC A04/MF A01

Two separate approaches were used to develop a prototype for entering data into a remote host computer in an automated manner. In the first approach, revisions were implemented in the IBM PC's terminal emulator VTEK 4.2. These revisions allowed prewritten script files to be processed to the host based operating system and applications software as if the script file information had been entered on the keyboard. The script processing capability was implemented taking advantage of existing user defined key capability and the DEC VT100 asynchronous terminal emulation of VTEK communications software. At present the script command and data files must be manually created at the PC using an editor or word processor. The script processing capability works with any host based operating system or application software that interacts with a DEC VT100 terminal. An example is provided where VTEK script processing is used to automatically interact with a VAX-based Database Management System (DBMS), INGRES, appending PC resident data records to an INGRES table, creating a default report, aborting to VMS, and disposing of the report, all without touching a key. An appendix is provided which discusses the second approach of developing a prototype VT100 emulator specifically designed for data entry to a remote host computer system. This software loads data automatically into a Vax Datatrieve data base. It provides an alternative method of prototype development. The challenges for future development are identified and discussed. The use of the programmable terminal emulator for data control in the case of distributed database applications is also discussed. DOE

N89-28175*# National Aeronautics and Space Administration. Goddard Space Flight Center, Greenbelt, MD.
PERSONAL COMPUTERS ON ETHERNET Abstract Only
R. Kao *In its* Laboratory for Oceans 1988 p 213-215 (For primary document see N89-28118 22-48)
Avail: NTIS HC A12/MF A01 CSCL 09B

N89-28177*# National Aeronautics and Space Administration. Goddard Space Flight Center, Greenbelt, MD.
LOW COST REAL TIME INTERACTIVE ANALYSIS SYSTEM Abstract Only
F. Stetina *In its* Laboratory for Oceans 1988 p 219-220 (For primary document see N89-28118 22-48)
Avail: NTIS HC A12/MF A01 CSCL 09B

61 COMPUTER PROGRAMMING AND SOFTWARE

Includes computer programs, routines, alogorithms, and specific applications, e.g., CAD/CAM.

N89-28309*# Research Inst. for Advanced Computer Science, Moffett Field, CA.
A SURVEY OF VISUAL PREPROCESSING AND SHAPE REPRESENTATION TECHNIQUES
Bruno A. Olshausen Nov. 1988 64 p
(Contract NCC2-408)
(NASA-CR-185418; NAS 1.26:185418; RIACS-TR-88.35) Avail: NTIS HC A04/MF A01 CSCL 09B

Many recent theories and methods proposed for visual preprocessing and shape representation are summarized. The survey brings together research from the fields of biology, psychology, computer science, electrical engineering, and most recently, neural networks. It was motivated by the need to preprocess images for a sparse distributed memory (SDM), but the techniques presented may also prove useful for applying other associative memories to visual pattern recognition. The material of this survey is divided into three sections: an overview of biological visual processing; methods of preprocessing (extracting parts of shape, texture, motion, and depth); and shape representation and recognition (form invariance, primitives and structural descriptions, and theories of attention). Author

N89-28310# Naval Postgraduate School, Monterey, CA.
OPTIMAL THREE-DIMENSIONAL PATH PLANNING USING VISIBILITY CONSTRAINTS M.S. Thesis
David H. Lewis Dec. 1988 228 p
(AD-A207357) Avail: NTIS HC A11/MF A01 CSCL 12/9

An algorithm is presented for finding optimal 3-D paths above polyhedral models of terrain. Airspace is modeled as irregularly shaped regions of homogeneous probability-of-detection, with respect to one or more fixed observers. Paths are planned by first finding an optimal set of contiguous visibility regions, then an optimal piecewise linear flight path through this envelope, using Snells Law to find locally-optimal maneuver points. The performance of the region finding algorithm favorably compares with an alternate approach using regular cubic regions. GRA

N89-28311# Instituto de Pesquisas Espaciais, Sao Jose dos Campos (Brazil).
PRELIMINARY STATISTICAL IDENTIFICATION OF RADAR IMAGERY: AUTOREGRESSIVE-MOVING AVERAGE (ARMA) MODELS [IDENTIFICACAO ESTATISTICA PRELIMINAR DE IMAGENS DE RADAR: MODELOS AUTORREGRESSIVOS E MEDIA MOVEL (ARMA)]
Luciano VieiraDutra Dec. 1988 11 p In PORTUGUESE; ENGLISH summary Presented at the 5th Brazilian Symposium on Remote Sensing, Natal, RN, 11-15 Oct. 1988
(INPE-4771-PRE/1440) Avail: NTIS HC A03/MF A01

The preliminary results of statistical modelling studies for image processing is reported. The identification phase is the basic problem of the modelling task (that is, the order determination of the type of model being considered). An image is represented by a bidimensional stochastic process, and a model, with two independent variables brings additional difficulties to the identification. To overcome this difficulty, one looks for identification using a linearized version of the image, lexicographically organizing the image by lines or by columns. For radar images other questions arise because of the type of noise present in the image, which some authors claim to be multiplicative. The ARMA (autoregressive-moving average) model is used on the original and log transformed data (which transforms the multiplicative noise in additive, if present). The image that was used is a full 512 x 512 resolution SAR-580 image. Results showed that radar is composed by a 2D nonseparable stochastic field which is class independent. This fact indicates that natural textures is hidden by radar characteristics. Also the model in homomorphic space showed in general, lower correlations indicating a higher random character of noise coherent with the hypothesis of lower signal-noise dependence in this space. Author

N89-28312# Instituto de Pesquisas Espaciais, Sao Jose dos Campos (Brazil).
MODE FILTERS AND THEIR APPLICATIONS [FILTROS MODAIS E SUAS APLICACOES]
Virginia RagonideMoraesCorreia and Luciano VieiraDutra Dec. 1988 12 p In PORTUGUESE; ENGLISH summary Presented at the 5th Brazilian Symposium on Remote Sensing, Natal, RN, 11-15 Oct. 1988
(INPE-4748-PRE/1421) Avail: NTIS HC A03/MF A01

The development of a mode filter is reported. The output of this filter is the mode of a smooth histogram computed in a neighborhood of the input image pixel. This smooth histogram is obtained in the same way as in density estimation by the kernel approach. The value at which the histogram is maximum is called the mode and the original point is replaced by the mode provided that the frequency of the mode is higher than a given threshold. The threshold and the kernel are user defined. Two types of applications were tested. First the mode filter was applied to reduce speckle noise in a SAR580 radar image using several neighborhoods dimensions and types of kernels. The procedure worked better compared to simple mean filter because frontiers are not blurred and the granular aspect reduced. Second application tested was reduction of the noisy aspect of the per point classification results using a single point kernel. The procedure was tested using a classified area nearby Sao Jose dos Campos, and a good improvement of the classification aspect was achieved. Author

N89-28313# National Aeronautical Lab., Bangalore (India). Computational and Theoretical Fluid Dynamics Div.
EXTENDED KALMAN FILTER (EKF) ALGORITHM
P. Ramamoorthy Jun. 1989 13 p
(PD-CF-8922) Avail: NTIS HC A03/MF A01

An extended Kalman filter (EKF) algorithm is implemented on UNIVAC 1100/70. As an example, the longitudinal states, characterizing the short period dynamics of an aircraft are obtained from noisy measured data. This algorithm, with minor modifications and the incorporation of a stiff differential equation solution algorithm, could be implemented for extraction of stability and control derivatives from noisy flight test data. Author

N89-28314*# National Aeronautics and Space Administration. Langley Research Center, Hampton, VA.
THE POTENTIAL APPLICATION OF THE BLACKBOARD MODEL OF PROBLEM SOLVING TO MULTIDISCIPLINARY DESIGN
James L. Rogers Jul. 1989 12 p Prepared for presentation at the 7th AIAA Computers in Aerospace Conference, Monterey, CA, 3-5 Oct. 1989
(NASA-TM-101633; NAS 1.15:101633; AIAA-89-3071) Avail: NTIS HC A03/MF A01 CSCL 09B

The potential application of the blackboard model of problem solving to multidisciplinary design is discussed. Multidisciplinary design problems are complex, poorly structured, and lack a predetermined decision path from the initial starting point to the final solution. The final solution is achieved using data from different engineering disciplines. Ideally, for the final solution to be the optimum solution, there must be a significant amount of communication among the different disciplines plus intradisciplinary and interdisciplinary optimization. In reality, this is not what happens in today's sequential approach to multidisciplinary design. Therefore it is highly unlikely that the final solution is the true optimum solution from an interdisciplinary optimization standpoint. A multilevel decomposition approach is suggested as a technique to overcome the problems associated with the sequential approach, but no tool currently exists with which to fully implement this technique. A system based on the blackboard model of problem solving appears to be an ideal tool for implementing this technique because it offers an incremental problem solving approach that requires no a priori determined reasoning path. Thus it has the potential of finding a more optimum solution for the multidisciplinary design problems found in today's aerospace industries. Author

N89-28315# Los Alamos National Lab., NM.
PARAGRAPH-RTS: A PARALLEL REDUCTION-BASED RUN-TIME SYSTEM
Bonnie Yantis, David Rich, and Randy Michelsen 1989 10 p Presented at the International Conference on Parallel Processing, St. Charles, IL, 8-12 Aug. 1989
(Contract W-7405-eng-36)
(DE89-005457; LA-UR-88-4110; CONF-890834-1) Avail: NTIS HC A02/MF A01

The use is investigated of the functional programming paradigm on multiprocessor computers. A parallel graph reduction was developed run time system called ParaGraph-RTS (Parallel Graph Reduction) that provides both significant amounts of exploitable parallelism and the robustness to support development of large scientific codes. This system allows the empirical investigation of the functional programming paradigm within computationally intensive application domains. An implementation is described of ParaGraph-RTS on a shared memory multiprocessor. The implementation strategy reflects inbsights gained through performance characterizations of the reduction process. Preliminary performance results and analyses are presented. DOE

N89-28316# Massachusetts Inst. of Tech., Cambridge. Dept. of Electrical Engineering and Computer Science.
APPROACHES TO MULTI-LEVEL SEQUENTIAL LOGIC SYNTHESIS
Srinivas Devadas Mar. 1989 9 p

(Contract N00014-87-K-0825)
(AD-A208322; VLSI-Memo-89-509) Copyright Avail: NTIS HC A02/MF A01 CSCL 09/1

This paper presents approaches to multi-level sequential logic synthesis (algorithms and techniques for the area and performance optimization of interconnected finite state machine descriptions). Interacting finite state machines are common in industrial chip designs. While optimization techniques for single finite state machines are relatively well developed, the problem of optimization across latch boundaries has received much less attention. Techniques to optimize pipelined combinational logic so as to improve area/throughput have been proposed. However, logic cannot be straightforwardly migrated across latch boundaries when the basic blocks are sequential rather than combinational circuits. We present new techniques for the exploitation of sequential don't cares in arbitrary, interconnected sequential machine structures. Exploiting these don't care sequences can result in significant improvements in area and performance. We address the problem of migrating logic across state machine boundaries so as to make particular machines less complex at the possible expense of making others more complex. This can be useful from both an area and performance point of view. We present new optimization algorithms that incrementally modify state machine structures across latch boundaries. We discuss the use of more global state machine decomposition and factorization algorithms for area optimization. Finally, we present experimental results using these algorithms on sequential circuits. GRA

N89-28317# Massachusetts Inst. of Tech., Cambridge. Microsystems Research Center.
A FAST MULTIPOLE ALGORITHM FOR CAPACITANCE EXTRACTION OF COMPLEX 3-D GEOMETRIES
K. Nabors and J. K. White Feb. 1989 12 p Presented at the Custom Integrated Circuits Conference, San Diego, CA, 15-18 May 1989 Sponsored in cooperation with IBM Corp., and Analog Devices
(Contract N00014-87-K-0825)
(AD-A208374; VLSI-Memo-89-508) Copyright Avail: NTIS HC A03/MF A01 CSCL 20/3

A fast algorithm for computing the capacitance of a complicated 3-D geometry of ideal conductors in a uniform dielectric is described. The method is an acceleration of the standard integral equation approach for multiconductor capacitance extraction. These integral equation methods are slow because they lead to dense matrix problems which are typically solved with some form of Gaussian elimination. This implies the computation grows like mn, where m is the number of tiles needed to accurately discretize the conductor surface charges. A preconditioned conjugate gradient iterative algorithm is presented with a multipole approximation to compute the iterates. This reduces the complexity so that accurate multiconductor capacitance calculations grow as nm where m is the number of conductors. GRA

N89-28318# Naval Postgraduate School, Monterey, CA.
FIXED INTERVAL SMOOTHING ALGORITHM FOR AN EXTENDED KALMAN FILTER FOR OVER-THE-HORIZON SHIP TRACKING M.S. Thesis
William J. Galinis Mar. 1989 97 p
(AD-A208555) Avail: NTIS HC A05/MF A01 CSCL 17/11

The performance of an extended Kalman filter used to track a maneuvering surface target using HFDF lines-of-bearing is substantially improved by implementing a fixed interval smoothing algorithm and a maneuver detection method that uses a noise variance estimator process. This tracking routine is designed and implemented in a computer program. The Hall noise model is used to accurately evaluate the performance of the tracking algorithm in a noisy environment. Several tracking scenarios are simulated and analyzed. The application of the Kalman tracker to a tropical storm tracking is investigated. Actual storm tracks obtained from the Joint Typhoon Warning Center in Guam, Mariana Islands are used for this research. GRA

N89-28319# California Univ., Irvine. Dept. of Electrical Engineering.
STATISTICAL ANALYSIS OF THE LMS AND MODIFIED STOCHASTIC GRADIENT ALGORITHMS Annual Report, 15 May 1988 - 14 May 1989
Neil J. Bershad 14 May 1989 23 p
(Grant AF-AFOSR-0093-86; AF Proj. 2304)
(AD-A208618; AFOSR-89-0701TR) Avail: NTIS HC A02/MF A01 CSCL 09/1

During the period April 15 1989, the Air Force Office of Scientific Research supported research work on the stochastic behavior of the LMS and related adaptive algorithms yielded results in two major areas: Digital Implementation of Stochastic Gradient Type adaptive Algorithms; and LMS and RLS Performance Comparison for Tracking a Chirped Sinusoid in Noise. GRA

N89-28320# Stanford Univ., CA. Systems Optimization Lab.
AN EFFICIENT EXACT ALGORITHM FOR THE LEAST SQUARES IMAGE REGISTRATION PROBLEM
Karel Zikan (Hughes Research Labs., Malibu, CA.) May 1989 17 p
(Contracts N00014-89-J-1659; DE-FG03-87ER-25028; NSF DMS-88-00589)
(AD-A208725; SU-SOL-89-5) Avail: NTIS HC A02/MF A01 CSCL 12/9

Image registration involves estimating how one set of n-dimensional points is rotated, scaled, and translated into a second set of n-dimensional points. In practice, n is usually 2 or 3. We give an exact algorithm to solve the least-squares formulation of the two-dimensional registration problem. The algorithm, which is based on parametric linear programming, can be viewed as a refinement of the O(k cubed) approximation method proposed by Zikan and Silberberg. GRA

N89-28321# Air Force Flight Dynamics Lab., Wright-Patterson AFB, OH.
AEROSPACE STRUCTURES DESIGN ON COMPUTERS Final Report, Dec. 1988 - Mar. 1989
Vipperla B. Venkayya Mar. 1989 216 p
(AD-A208811; WRDC-TR-89-3045) Avail: NTIS HC A10/MF A01 CSCL 12/5

This report, prepared for training, is intended to bring out the elements of structural design optimization on modern computers. The first section gives a cursory description of the requirements and essential disciplines involved in aircraft structural design. The second section is an optimization paper that provides the basis for optimization using large finite element assemblies. The third section provides a summary of design sensitivity analysis which is an essential element of optimization. The two appendices are the descriptions of two training programs for analysis and optimization. Each of these sections has their own references. This is an informal report intended for training and is a collection material entirely from the open literature. GRA

N89-28322# Naval Postgraduate School, Monterey, CA. Dept. of Electrical and Computer Engineering.
PARAMETER PLANE DESIGN METHOD M.S. Thesis
Dong Ryong Shin Mar. 1989 103 p
(AD-A209845) Avail: NTIS HC A06/MF A01 CSCL 12/5

When analyzing or designing a control system, it is important to study the effects on overall system performance of varying one or more parameters (mass, inertia, gain, resistance, etc). It is equally important to determine whether a desired dynamic behavior can be achieved with any set of values for the parameters...if not, redesign is indicated. The analysis and synthesis of linear feedback control systems, or the compensation of same, can be realized by parameter plane methods. The parameter plane method, which works well for two variable parameters and which may be extended to three or more parameters, is purely algebraic, and the resulting plots are valuable aids to analysis. Furthermore, the performance index cost curves in terms of integral-square error and other cost functions can be superimposed on the parameter plane graphically. The object is to develop a user friendly interactive computer

program to plot families of performance index cost curves. A secondary objectives is to demonstrate the use of the these curves in the design of the system. The design procedure starts with the performance index cost curves superimposed on parameter plane cures. The result of the analysis is a choice of values for the parameters such that the system performance is the best available compromise between transient performance and cost. GRA

N89-28323# California Univ., San Diego. Inst. for Cognitive Science.
THE BACK PROPAGATION TECHNIQUE FOR MODELING CORTICAL COMPUTATION Final Technical Report, 1 Feb. 1988 - 1 Jan. 1989
David Zipser 31 Jan. 1989 20 p
(Grant AF-AFOSR-0062-86; AF Proj. 2312)
(AD-A209855; AFOSR-89-0911TR) Avail: NTIS HC A02/MF A01 CSCL 12/9

Over the past several years powerful learning procedures were developed that can program simulated neural networks to compute a wide variety of functions. This has made it possible to use learning procedures to train model networks to do computations that occur in the brain. While there was so a priori reason to suppose that the individual neuro-like units in these model networks would resemble the brain in any way, the empirical observations is that they do. Good results were achieved applying this paradigm to modeling monkey parietal area 7a. Various aspects of the primary visual area were also successfully modeled using this approach. The results raise the interesting possibility that learning procedures and particularly the back propagation algorithm used in these studies, can serve as a general technique to account for how the brain implements computations. While these observations do not imply that back propagation is actually used in the brain, they do raise the possibility that some analogous learning procedure is used there. GRA

N89-28324# Massachusetts Inst. of Tech., Cambridge. Artificial Intelligence Lab.
QUANTITATIVE INFERENCE IN A MECHANICAL DESIGN COMPILER
Allen C. Ward and Warren P. Seering Jan. 1989 18 p
(Contract N00014-86-K-0685)
(AD-A209900; AI-M-1062) Avail: NTIS HC A03/MF A01 CSCL 13/7

This paper presents the ideas underlying a computer program that takes as input a schematic of a mechanical or hydraulic power transmission system, plus specifications and a utility function, and returns catalog numbers from predefined catalogs for the optimal selection of components implementing the design. Unlike programs for designing single components or systems, this program provides the designer with a high level language in which to compose new designs. It then performs some of the detailed design process for him. The process of compilation, or transformation from a high to a low level description, is based on a formalization of quantitative inferences about hierarchically organized sets of artifacts and operating conditions. This allows compilation without the exhaustive enumeration of alternatives. The paper introduces the formalism, illustrating its use with examples. It then outlines some differences from previous work, and summarizes early tests and conclusions. GRA

N89-28325# New York Univ. Medical Center. Dept. of Psychiatry.
AUTOMATIC CONSTRUCTION OF POLYHEDRAL SURFACES FROM VOXEL REPRESENTATIONS
Eric L. Schwartz and Alan Shaw Jun. 1989 26 p Prepared in cooperation with New York Univ., NY
(Grant AF-AFOSR-0341-85; AF Proj. 2313)
(AD-A210009; TR-381; RR-158; AFOSR-89-0978TR) Avail: NTIS HC A03/MF A01 CSCL 12/9

Various applications require triangulations, or polyhedral representations, of surfaces which are represented as serial sections. Heuristic methods are in common use to triangulate such data. These methods work well on segments of a generalized cylinder, i.e., runs of sections containing single loops, but they often fail when attempting to process highly convoluted surfaces. This is because the topology of the sections changes when a critical point of the surface is encountered. The equivalent of the full adjacency graph of the surface (provided by a voxel model) is used to classify the changes in topology of the sections of the surface, and thereby guide the triangulation process. For a voxel surface which is a discrete sampling of a smooth manifold in general position, we are able to exhaustively classify the small set of possible topological changes in the sections of the surface. We then deal with these cases exhaustively. To the best of our knowledge, this is the first description of an algorithm which can in theory and practice triangulate surfaces as complex as that of a brain, from serial sections, without human interaction. GRA

N89-28326# Cornell Univ., Ithaca, NY. Dept. of Computer Science.
ALGORITHMIC CONTROL OF WALKING
A. J. Stewart and James F. Cremer 1989 6 p
(Contracts N00014-86-K-0281; N00014-88-K-0591; NSF DMC-86-17355)
(AD-A210117) Avail: NTIS HC A02/MF A01 CSCL 12/9

We suggest that there are two components required in most control schemes: an algorithmic component which takes a high-level goal and generates joint trajectories, and a dynamics component which takes a high-level goal and generates joint trajectories, and a dynamics component which takes these joint trajectories and generates the required joint torques. The joint torques are then sent to the mechanism, which (hopefully) achieves the high-level goal. We present an approach that simplifies the programming of the algorithmic component for high degree of freedom objects. Instead of supplying a complete set of joint trajectories as a function of time, the algorithm controls other, more intuitive, degrees of freedom. These degrees of freedom are automatically converted to the more conventional joint trajectories. This approach is applied to generate joint trajectories for a walking biped. GRA

N89-28327# Illinois Univ., Urbana. Coordinated Science Lab.
LOAD BALANCING IN MULTIPROCESSOR SYSTEMS
Michael C. Loui and Milind A. Sohoni Jun. 1989 12 p
(Contract N00014-85-K-0570)
(AD-A210144; UILU-ENG-89-2219; ACT-107) Avail: NTIS HC A03/MF A01 CSCL 12/6

We present an algorithm for dynamic load balancing in a multiprocessor system that minimizes the number of accesses to the shared memory. The algorithm assumes no information, probabilistic or otherwise, regarding task arrivals or processing requirements. For k processors to process n tasks, the algorithm incurs O(k log k log n) potential memory collisions in the worst case. The algorithm itself is a simple variation of the strategy of visiting the longest queue. The key idea is to delay reporting task arrivals and completions, where the delay is a function of dynamic loading conditions. GRA

N89-27888*# Jet Propulsion Lab., California Inst. of Tech., Pasadena.
SOFTWARE PACKAGE FOR PERFORMING EXPERIMENTS ABOUT THE CONVOLUTIONALLY ENCODED VOYAGER 1 LINK
U. Cheng *In its* The Telecommunications and Data Acquisition Report 15 May 1989 p 175-179 (For primary document see N89-27871 22-32)
Avail: NTIS HC A17/MF A01 CSCL 09B

N89-27890*# Jet Propulsion Lab., California Inst. of Tech., Pasadena.
PERFORMANCE OF CONCATENATED CODES USING 8-BIT AND 10-BIT REED-SOLOMON CODES
F. Pollara and K.-M. Cheung *In its* The Telecommunications and Data Acquisition Report 15 May 1989 p 194-201 (For primary document see N89-27871 22-32)
Avail: NTIS HC A17/MF A01 CSCL 09B

N89-27891*# Jet Propulsion Lab., California Inst. of Tech., Pasadena.
DECODING OF 1/2-RATE (24,12) GOLAY CODES
T.-K. Truong, I. S. Reed, and X. Yin *In its* The Telecommunications and Data Acquisition Report 15 May 1989 p 202-207 (For primary document see N89-27871 22-32)
Avail: NTIS HC A17/MF A01 CSCL 09B

N89-27892*# Jet Propulsion Lab., California Inst. of Tech., Pasadena.
THE WEIGHT DISTRIBUTION AND RANDOMNESS OF LINEAR CODES
K.-M. Cheung *In its* The Telecommunications and Data Acquisition Report 15 May 1989 p 208-215 (For primary document see N89-27871 22-32)
Avail: NTIS HC A17/MF A01 CSCL 09B

62 COMPUTER SYSTEMS

Includes computer networks and special application computer systems.

N89-28328*# Worcester Polytechnic Inst., MA.
EVIDENCE FLOW GRAPH METHODS FOR VALIDATION AND VERIFICATION OF EXPERT SYSTEMS
Lee A. Becker, Peter G. Green, and Jayant Bhatnagar Jul. 1989 46 p
(Grant NAG1-809)
(NASA-CR-181810; NAS 1.26:181810) Avail: NTIS HC A03/MF A01 CSCL 09B

The results of an investigation into the use of evidence flow graph techniques for performing validation and verification of expert systems are given. A translator to convert horn-clause rule bases into evidence flow graphs, a simulation program, and methods of analysis were developed. These tools were then applied to a simple rule base which contained errors. It was found that the method was capable of identifying a variety of problems, for example that the order of presentation of input data or small changes in critical parameters could affect the output from a set of rules. Author

N89-28329# Clemson Univ., SC. Dept. of Industrial Engineering.
COMM-Q: A SIMULATION MODEL TO DETERMINE SATURATION POINTS IN NODAL TYPE NETWORKS M.S. Thesis Final Report
Richard A. Paradiso, Jr. May 1989 15 p Sponsored by Army Signal Center, Fort Gordon, GA
(AD-A207294) Avail: NTIS HC A03/MF A01 CSCL 25/2

The phenomenon of saturation can be a severe problem in nodal type networks where many customers compete for limited resources. The identification of how and at what point saturation affects a network must be accomplished by network managers so that appropriate control measures can be applied to their network to avoid saturation. The objective of this thesis is to develop a computer simulation model to determine the point at which saturation begins to affect a specific nodal type network and to assess the performance of that network under various loading conditions. The model developed in this research is titled the COMM-Q model. The COMM-Q model represents the MSRT-RAU portions of the U.S. Army's Mobile Subscriber equipment tactical communications system. The outputs of the COMM-Q model are the generic network performance measures: Link Utilization, Radio Utilization, Saturation Level and Grade of Service. The research reveals that network saturation will be a problem for the MSE network resulting in a low Grade of Service. The saturation level is highly dependent on call arrival rate and a very narrow transition range exists where the network shifts from a high saturation level and an acceptable grade of service. The call holding time is a predominant factor in saturation level in that it determines at what point this transition range will occur. GRA

N89-28330# Naval Postgraduate School, Monterey, CA.
CONVERSION OF MASS STORAGE HIERARCHY IN AN IBM COMPUTER NETWORK M.S. Thesis
Linda S. Mauck Mar. 1989 47 p
(AD-A208520) Avail: NTIS HC A03/MF A01 CSCL 05/1

With the shift from batch applications to online systems supporting the strategic role of information, corporate or institutional goals tie directly to the information management functions. This has been true at the Naval Postgraduate School (NPS). Like many other Government installations, the NPS Computer Center has to meet its objectives with less than state-of-the-art hardware. In the early 1980's, the Center employed IBM's 3850 Mass Storage Subsystem (MSS) for online storage of student and faculty data sets. It was installed in December 1980 and performed well for over six years. Faced with IBM's announcement (in February 1985) of the limited future connectivity and compatibility and the increasing maintenance costs, the decision was made to replace the MSS with hardware/software alternative that would use a more modern and reliable architecture. The solution, and data set migration process is defined, and the early experience with a multi-level, software-managed, storage system are described. GRA

N89-28331# Naval Postgraduate School, Monterey, CA.
A COMPUTATIONAL COMPARISON OF THE PRIMAL SIMPLEX AND RELAXATION ALGORITHMS FOR SOLVING MINIMUM COST FLOW NETWORKS M.S. Thesis
Michael B. Sagaser Mar. 1989 80 p
(AD-A208534) Avail: NTIS HC A05/MF A01 CSCL 12/4

The relative computational efficiencies are examined for two advanced network minimum cost flow problem solution methodologies: the primal simplex specialization to networks developed by Bradley, Brown and Graves (1977)--GNET and XNET, and a Lagrangian relaxation method developed by Bertsekas and Tseng (1988)--RELAX-2 and RELAX-2. Additionally, the relaxation method description is clarified and potential implementation improvements are investigated. Research by Bertsekas and Tseng has shown the relaxation codes to be on the order of four to five times faster than the primal simplex codes. This thesis fails to duplicate those results. While the relaxation codes do perform faster in many circumstances when solving purely random problems, the primal simplex codes are still closely competitive. In particular, the primal simplex codes appear more efficient at solving capacitated transshipment problems in networks with an echelon structure, and in networks with many more sinks than sources. Primal simplex codes also require about half the computer storage of the relaxation codes. The research has produced compelling evidence that the relaxation algorithms can be further refined. All indications appear to reinforce the desirability of prioritizing by absolute deficit the node selection process used in both relaxation codes. Further research is recommended. GRA

N89-28332# Massachusetts Univ., Amherst. Dept. of Electrical and Computer Engineering.
RESOURCE CONTENTION MANAGEMENT IN PARALLEL SYSTEMS Final Report, Jun. - Dec. 1987
Christos G. Cassandras, James F. Kurose, and Don Towsley Apr. 1989 151 p
(Contract F30602-81-C-0169)
(AD-A208809; RADC-TR-89-48) Avail: NTIS HC A08/MF A01 CSCL 12/7

This research effort explored two issues: (1) The comparative study of simple load balancing algorithms for distributed real-time systems which showed that simple policies perform just as well as complex policies in a majority of the cases; (2) The second task was to development of on-line optimization procedures for load balancing algorithms and of task scheduling policies with real-time constraints. GRA

N89-28174*# National Aeronautics and Space Administration. Goddard Space Flight Center, Greenbelt, MD.
CODE 672 OBSERVATIONAL SCIENCE BRANCH COMPUTER NETWORKS Abstract Only

D. W. Hancock and H. G. Shirk *In its* Laboratory for Oceans 1988 p 209-212 (For primary document see N89-28118 22-48)
Avail: NTIS HC A12/MF A01 CSCL 09B

63 CYBERNETICS

Includes feedback and control theory, artificial intelligence, robotics and expert systems.

For related information see also *54 Man/System Technology and Life Support.*

N89-28333# Instituto de Pesquisas Espaciais, Sao Jose dos Campos (Brazil).
IMPLEMENTATION OF A DIGITAL TORQUE CONTROLLER OF A REACTION WHEEL WITH AN INCREMENTAL COMPUTER [IMPLEMENTACAO DE UM CONTROLADOR DIGITAL DE TORQUE DE UMA RODA DE REACAO COM UM COMPUTADOR INCREMENTAL]
Joao Benedito Diehl, Gilberto daCunha Trivelato, and Juan Sune Perez Jan. 1989 8 p In PORTUGUESE; ENGLISH summary Presented at the 7th SBA (Brazilian Conference on Automation), Sao Jose dos Campos, Brazil, 15-19 Aug. 1988
(INPE-4784-PRE/1447) Avail: NTIS HC A02/MF A01

A real-time application of a digital incremental computer in the realization of a digital torque controller of a reaction wheel is discussed. The objectives are: (1) to evaluate the application of incremental computation techniques; (2) to apply this technique in real time controller; (3) to verify the performance of the implemented digital controller. Initially, description is given of: the computer architecture, the implemented structure of control and the parameters which were utilized in the system. Afterwards, experimental results obtained with tests made in laboratory with the resulting control system are presented. These results indicate that the computer and the adopted algorithm comply with the specifications of the control system project which was built and tested. Author

N89-28334# Northeast Artificial Intelligence Consortium, Syracuse, NY.
NORTHEAST ARTIFICIAL INTELLIGENCE CONSORTIUM ANNUAL REPORT 1987. VOLUME 6: ARTIFICIAL INTELLIGENCE APPLICATIONS TO SPEECH RECOGNITION Interim Report, Dec. 1986 - Dec. 1987
Harvey E. Rhody, James Hillenbrand, and John A. Biles Mar. 1989 39 p
(Contract F30602-85-C-0008; AF Proj. 5581)
(AD-A208380; RADC-TR-88-324-Vol-6) Avail: NTIS HC A03/MF A01 CSCL 12/9

The Northeast Artificial Intelligence Consortium (NAIC) conducted pertinent research in artificial intelligence and performed activities ancillary to this research. Progress is described that was made in the third year of the existence of the NAIC on the technical research tasks undertaken at the member universities. The topics covered in general are: versatile expert system for equipment maintenance, distributed AI for communications system control, automatic photo interpretation, time-oriented problem solving, speech understanding systems, knowledge base maintenance, hardware architectures for very large systems, knowledge-based reasoning and planning, and a knowledge acquisition, assistance, and explanation system. The specific topic for this volume is the design and implementation of a knowledge-based system to read speech spectro grams. The primary goal the RIT NAIC project is the development of techniques that can be applied to most difficult type of speech understanding system: the speaker independent, continuous speech, large vocabulary system. GRA

N89-28335# Maryland Univ., Baltimore.
CONTROL AND SYSTEM THEORY, OPTIMIZATION, INVERSE AND ILL-POSED PROBLEMS Final Report, 15 Sep. 1987 - 14 Sep. 1988
Thomas I. Seidman 14 Sep. 1988 10 p
(Grant AF-AFOSR-0350-87; AF Proj. 2304)
(AD-A208570; AFOSR-89-0618TR) Avail: NTIS HC A02/MF A01 CSCL 12/4

Research activities are summarized in applied mathematics, including control of distributed systems, optimization, and inverse problems. Results published in 23 journal articles are summarized. Results include a new method for computing solutions to ill-posed problems via optimal filtering and new results for the analysis and control of switching systems. GRA

N89-28336# Syracuse Univ., NY.
NORTHEAST ARTIFICIAL INTELLIGENCE CONSORTIUM ANNUAL REPORT FOR 1987. VOLUME 4: RESEARCH IN AUTOMATED PHOTOINTERPRETATION Interim Report, Dec. 1986 - Dec. 1987
James Modestino Mar. 1989 92 p
(Contract F30602-85-C-0008; AF Proj. 2304)
(AD-A208610; RADC-TR-88-324-Vol-4) Avail: NTIS HC A05/MF A01 CSCL 12/9

The Northeast Artificial Intelligence Consortium (NAIC) purpose is to conduct pertinent research in artificial intelligence and to perform activities ancillary to this research. Progress is described that was made in the third year of the existence of the NAIC on the technical research tasks undertaken at the member universities. The topics covered in general are: versatile expert system for equipment maintenance, distributed AI for communications system control, automatic photointerpretation, time-oriented problem solving, speech understanding systems, knowledge base maintenance, hardware architectures for very large system, knowledge-based reasoning and planning, and a knowledge acquisition, assistance, and explanation system. The specific topics for this volume are the use of expert systems for automated photointerpretation and other AI techniques to image segmentation and region identification. GRA

N89-28337# Carnegie-Mellon Univ., Pittsburgh, PA. Dept. of Mathematics.
SINGULAR AND BANG-BANG STOCHASTIC CONTROL Final Report, 30 Sep. 1985 - 30 Sep. 1988
Steven E. Shreve 1988 5 p
(Grant AF-AFOSR-0360-85; AF Proj. 2304)
(AD-A208627; AFOSR-89-0724TR) Avail: NTIS HC A02/MF A01 CSCL 12/3

The proposal which formed the basis for this grant consisted of three parts: research on singular stochastic control, research on bang-band stochastic control, and the creation of a graduate text which would make these two topics widely accessible. Significant progress was made in the two research areas, although a number of important questions remain. The proposed graduate text was completed and a copy was provided to the Air Force Office of Scientific Research in December 1987. Each of these three topics is discussed in turn. GRA

N89-28338# Illinois Univ., Urbana. Dept. of Computer Science.
LEARNING FROM PHYSICAL ANALOGIES: A STUDY IN ANALOGY AND THE EXPLANATION PROCESS Ph.D. Thesis
Brian Carl Falkenhainer 27 Dec. 1988 273 p
(Contracts N00014-85-K-0559; N00014-89-J-1272)
(AD-A208689; UIUCDCS-R-88-1479; UILU-ENG-88-1785) Avail: NTIS HC A12/MF A01 CSCL 12/9

To make programs that understand and interact with the world as well as people do, the kind of flexibility people exhibit when conjecturing plausible explanations of the diverse physical phenomena they encounter must be duplicated. This process often involves drawing upon physical analogies; viewing the situation and its behavior as similar to familiar phenomena, conjecturing that they share analogous underlying causes, and using the plausible interpretation as a foothold to further understanding, analysis, and hypothesis refinement. Analogical reasoning and learning applied to the task of constructing qualitative explanations of observed physical phenomena is investigated. Primary emphasis is placed on two central questions. First, how are analogies elaborated to sanction new inferences about a novel situation.

This problem is addressed by contextual structure mapping, a knowledge intensive adaptation of Gentner's structure mapping theory. It presents analogy elaboration as a map and analyze cycle, in which two situations are placed in correspondence, followed by problem solving and inference production focused on correspondence inadequacies. These ideas are illustrated via PHINEAS, a program which uses similarity to posit qualitative explanations for time-varying descriptions of physical behaviors. It builds upon existing work in qualitative physics to provide a rich environment in which to describe and reason with theories of the physical world. GRA

N89-28339# Naval Weapons Center, China Lake, CA.
STATE-SPACE THEORY OF STRUCTURED UNCERTAINTY WITH EXAMPLES Final Report, Jan. - Nov. 1988
G. A. Hewer, Charles Kenney, and Richard Klabunde Mar. 1989 39 p
(AD-A209968; AD-E900902; NWC-TP-6971) Avail: NTIS HC A03/MF A01 CSCL 12/9

A state space mode is documented for additive errors that is algebraically and dynamically equivalent to Doyle's structured singular values. GRA

N89-28340# Stanford Univ., CA. Dept. of Computer Science.
A THEORY OF JUSTIFIED REFORMULATIONS Ph.D. Thesis
Devika Subramanian Mar. 1989 148 p
(Contract N00014-81-K-0004)
(AD-A210153; SU-STAN-CS-89-1260) Avail: NTIS HC A07/MF A01 CSCL 12/9

Present day systems, intelligent or otherwise, are limited by the conceptualizations of the world given to them by their designers. Issues in the construction of adaptive systems that can e incrementally reformulate their conceptulizations to achieve computational efficiency or descriptional adequacy are explored. A detailed account of a special case of the reformulation problem is presented: we reconceptualize a knowledge base in terms of new abstract objects and relations in order to make the computation of a given class of queries more efficient. Automatic reformulation will not be possible unless a reformulator can justify a shift in conceptualization. A new class of meta-theoretical justification is presented for a reformulation, called irrelevance explanations. A logical irrelevance explanation proves that certain distinctions made in the formulation are not necessary for the computation of a given class of problems. A computational irrelevance explanation proves that some distinctions are not useful with respect to a given problem solver for a given class of problems. Inefficient formulations make irrelevant distinctions and the irrelevance principle logically minimizes a formulation by removing all facts and distinctions in it that are not needed for the specified goals. The automation of the irrelevance principle is demonstrated with the generation of abstractions from first principles. The implementation of an irrelevance reformulator is described with experimental results that confirm the theory. GRA

64 NUMERICAL ANALYSIS

Includes iteration, difference equations, and numerical approximation.

N89-28341*# Institute for Computer Applications in Science and Engineering, Hampton, VA.
BUNCH-KAUFMAN FACTORIZATION FOR REAL SYMMETRIC INDEFINITE BANDED MATRICES Final Report
Mark T. Jones (Duke Univ., Durham, NC.) and Merrell L. Patrick May 1989 15 p Submitted for publication
(Contracts NAS1-18107; NAS1-18605; NAG1-466; AF-AFOSR-0117-88)
(NASA-CR-181860; NAS 1.26:181860; ICASE-89-37) Avail: NTIS HC A03/MF A01 CSCL 12A

The Bunch-Kaufman algorithm for factoring symmetric indefinite matrices was rejected for banded matrices because it destroys the banded structure of the matrix. Herein, it is shown that for a subclass of real symmetric matrices which arise in solving the generalized eigenvalue problem using Lanczos's method, the Bunch-Kaufman algorithm does not result in major destruction of the bandwidth. Space time complexities of the algorithm are given and used to show that the Bunch-Kaufman algorithm is a significant improvement over LU factorization. Author

N89-28342*# Institute for Computer Applications in Science and Engineering, Hampton, VA.
AN INTEGRATING MATRIX FORMULATION FOR BUCKLING OF ROTATING BEAMS INCLUDING THE EFFECTS OF CONCENTRATED MASSES Final Report
William D. Lakin and Raymond G. Kvaternik (National Aeronautics and Space Administration. Langley Research Center, Hampton, VA.) May 1989 25 p Submitted for publication
(Contracts NAS1-18107; NAS1-18605)
(NASA-CR-181862; ICASE-89-39; NAS 1.26:181862) Avail: NTIS HC A03/MF A01 CSCL 12A

The integrating matrix technique of computational mechanics is extended to include the effects of concentrated masses. The stability of a flexible rotating beam with discrete masses is analyzed to determine the critical rotational speeds for buckling in the inplane and out-of-plane directions. In this problem, the beam is subjected to compressive centrifugal forces arising from steady rotation about an axis which does not pass through the clamped end of the beam. To determine the eigenvalues from which stability is assessed, the differential equations of motion are solved numerically by combining the extended integrating matrix method with an eigenanalysis. Stability boundaries for a discrete mass representation of a uniform beam are shown to asymptotically approach the stability boundaries for the corresponding continuous mass beam as the number of concentrated masses is increased. An error in the literature is also noted for the discrete mass problem concerning the behavior of the critical rotational speed for inplane buckling as the radius of rotation of the clamped end of the beam is reduced. Author

N89-28343# International Centre for Theoretical Physics, Trieste (Italy).
SOME BASIC THEOREMS ON THE CROSS-SUMS OF CERTAIN CLASS OF NUMBERS (M-1) WHEN THE OPERATIONS ARE DONE WITH DIFFERENT BASES M OF THE ARITHMETIC
P. C. Ozoemena and C. A. Onwumechili (University Coll., Cardiff, Wales) Nov. 1988 22 p Submitted for publication
(DE89-611892; IC-88/374) Avail: NTIS (US Sales Only) HC A03/MF A01

Some new theorems were propounded for the numbers (M-1), as they relate to other numerals, through the basic arithmetical operations, at different bases M. For some reason, the proof is given of the theorems for the case M=10 using mathematical induction, and by Peano's fifth axiom make the generalizations. Comments are made in respect of the numbers (M-1), (in this case 9). Apart from the theorems facilitating mathematical operations, evidences have also been given, from different sources of the interesting properties of this class of numbers, represented in this case by the numeral 9. The theorems neither violate the divisibility rule for 9 nor are they a consequence of it. From symmetry, a suggestion is made in respect of the possible origin of the numeration in base 10, and the case of a ten dimensional Universe reconsidered. DOE

N89-28344# International Centre for Theoretical Physics, Trieste (Italy).
ORBITS WHICH ALWAYS HAVE AFFINE INVARIANT NEIGHBOURHOODS
Krzysztof Trautman Dec. 1988 9 p
(DE89-611895; IC-88/393) Avail: NTIS (US Sales Only) HC A02/MF A01

Actions of a connected reductive algebraic group, G, on normal algebraic varieties over an algebraically closed field of characteristic, O, are considered. The group was characterized

theoretically, the subgroups H of G such that whenever H is the stabilizer of a point of a G-variety, there exists an affine invariant neighborhood of the point. DOE

N89-28345# International Centre for Theoretical Physics, Trieste (Italy).
TWO EXAMPLES OF ESCAPING HARMONIC MAPS
A. PereiradoValle and A. Verjovsky Dec. 1988 13 p Submitted for publication
(DE89-611896; IC-88/408) Avail: NTIS (US Sales Only) HC A03/MF A01

The existence of special harmonic maps on complete non-compact Riemannian manifolds is studied. The notion is generalized of escaping geodesic and some results on the existence of escaping harmonic maps are proven. DOE

N89-28346# Brown Univ., Providence, RI. Center for Control Sciences.
A UNIFORMLY DIFFERENTIABLE APPROXIMATION SCHEME FOR DELAY SYSTEMS USING SPLINES
K. Ito and F. Kappel (Graz Univ., Austria) Apr. 1989 51 p
(Contract NAG1-517; F49620-86-C-0111; NSF UINT-85-21208; AF-AFOSR-0398-84; FWF-S3206; FWF-P6005; AF Proj. 2304)
(AD-A208567; LCDS/CCS-89-8; AFOSR-89-0698TR) Avail: NTIS HC A04/MF A01 CSCL 12/1

A new spline-based scheme is developed for linear retarded functional differential equations within the framework for semigroups on a certain Hilbert space formula. The approximating semigroups inherit in uniform way the characterization for differentiable semigroups from the solution semigroup of the delay system (e.g., among other things the logarithmic sectorial property for the spectrum). Convergence of the scheme in state spaces was proved. The uniform differentiability of the approximating semigroups enables the establishment of error estimates including quadratic convergence for certain classes of initial data. The scheme was also applied for computing the feedback solutions to linear quadratic optimal control problems. GRA

N89-28347# Rutgers - The State Univ., New Brunswick, NJ. Center for the Mathematical Sciences.
A RUTCOR PROJECT ON DISCRETE APPLIED MATHEMATICS Final Technical Report, 1 Aug. 1985 - 30 Sep. 1988
Peter L. Hammer and Fred S. Roberts 30 Jan. 1989 47 p
(Grant AF-AFOSR-0271-85; AF Proj. 2304)
(AD-A208572; AFOSR-89-0619TR) Avail: NTIS HC A03/MF A01 CSCL 12/1

This project was concerned with theoretical, algorithmic, and applied research in six areas of discrete applied mathematics. Work on graph theory and its applications was concerned with graph coloring and stability, special classes of graphs, and graphs and discrete optimization. Work on discrete optimization has also dealt with location problems, preprocessing and decomposition, approximation, and applications of combinatorial optimization to nonlinear problems. Research on posets and other combinatorial structures and their applications was concerned with linear extensions and ideals, graphs and posets, posets and discrete optimization, and other useful combinatorial structures. The effort in the area of computational complexity and efficient algorithms has concentrated on foundations on computational complexity and heuristics. Work on applications of discrete mathematics to decision making has involved group decision making, measurement and decision making, and multiple conclusion logic. Work on large scale scheduling problems has concentrated on the STORM 1 and STORM 2 models for routing aircraft, the aircrew scheduling problem, and the single base aircrews staging problem. Among the many applications considered are frequency assignment, task scheduling and air crew scheduling, location of warehouses and communication centers, maintenance problems, communications over noisy channels, and expert systems. GRA

N89-28348# Columbia Univ., New York, NY. Dept. of Mathematics.
DIFFERENTIAL EQUATIONS, RELATED PROBLEMS OF PADE APPROXIMATIONS AND COMPUTER APPLICATIONS Final Technical Report, 1 Jan. 1987 - 31 Dec. 1988
D. V. Chudnovsky and G. V. Chudnovsky 1988 62 p
(Grant AF-AFOSR-0117-87; AF Proj. 2304)
(AD-A208590; AFOSR-89-0729TR) Avail: NTIS HC A04/MF A01 CSCL 12/2

During the past period of the Grant, this work focused on the study of analytic, arithmetic and algorithmic properties of differential equations applied to solutions of problems in theoretical mathematics, mathematical and theoretical physics, numerical methods and computer science. GRA

N89-28349# Florida Univ., Gainesville. Dept. of Computer and Information Sciences.
IMAGE ALGEBRA FORTRAN PREPROCESSOR: USER'S MANUAL Final Report, Jan. - Dec. 1987
Joseph N. Wilson, D. Clay Wilson, and G. X. Ritter Mar. 1989 82 p Sponsored by DARPA
(Contract F08635-84-C-0295; AF Proj. 2068)
(AD-A208612; AD-E801892; AFATL-TR-88-156) Avail: NTIS HC A05/MF A01 CSCL 12/9

An algorithm developer is provided with a user's manual for the Image Algebra, FORTRAN 77, Preprocessor. The manual contains a thorough description of the capabilities and limitations of the preprocessor's code. Its emphasis is on providing a variety of step-by-step descriptions, with illustrations, that clearly demonstrate how to use the preprocessor syntax to express image processing transformations and information extraction techniques. GRA

N89-28350# Iowa State Univ. of Science and Technology, Ames. Dept. of Mathematics.
ANALYSIS AND NUMERICAL ANALYSIS OF SOME PROPERLY AND IMPROPERLY POSED PROBLEMS IN APPLIED MATHEMATICS Final Report, 15 Oct. 1987 - 14 Oct. 1988
Howard A. Levine 14 Oct. 1988 18 p
(Grant AF-AFOSR-0031-88; AF Proj. 2304)
(AD-A208633; AFOSR-89-0702TR) Avail: NTIS HC A02/MF A01 CSCL 12/1

Several different types of problems involving par tial differential equations which arise naturally in applications are studied. Some applications are: Qualitative behavior of solutions of nonlinear evolution equations; and Parameter identification problems. GRA

N89-28351# Brown Univ., Providence, RI. Center for Dynamical Systems.
A NUMERICAL STUDY OF AN AUGMENTED LAGRANGIAN METHOD FOR THE ESTIMATION OF PARAMETERS IN ELLIPTIC SYSTEMS
K. Ito, M. Kroller, and K. Kunisch Jan. 1989 37 p
(Contract F49620-86-C-0111)
(AD-A208658; AFOSR-89-0697TR) Avail: NTIS HC A03/MF A01 CSCL 12/3

A method based on an augmented Lagrangian formulation is developed which allows one to estimate coefficients in an elliptic differential equation from measurements of the state. This is a hybrid method combining the output-least-squares and the equation-error technique. Seminorm regularization is employed, and convergence and stability properties are discussed. Several aspects of an efficient implementation are described. Finally the effectiveness of the method is demonstrated by means of one and two dimensional examples. GRA

N89-28352# Stanford Univ., CA. Systems Optimization Lab.
THE PRINCIPAL PIVOTING METHOD REVISITED
Richard W. Cottle Apr. 1989 21 p
(Contracts N00014-89-J-1659; DE-FG03-87ER-25028; NSF DMS-88-00589)

(AD-A208796; SU-SOL-89-3) Avail: NTIS HC A03/MF A01 CSCL 12/4

The Principal Pivoting Method (PPM) for the Linear Complementarity Problem (LCP) is shown to be applicable to the class of LCPs involving the newly identified class of sufficient matrices. The classes of row sufficient and column sufficient matrices were recently introduced in a paper by Cottle, Pang, and Venkateswaran. It was shown there that such matrices provide answers to natural theoretical questions concerning the linear complementarity problem (LCP). Further, on the algorithmic side, it was noted that Lemke's Method (Scheme 1) for the LCP can process any problem in which the matrix is row sufficient. In fact, by a theorem of Aganagic' and Cottle', the latter is true for any Qo-matrix having non-negative principal minors, and row sufficient matrices are of this sort. These observations prompt one to ask whether the Principal Pivoting Method (PPM) is also applicable to this class of LCPs. This question is especially relevant inasmuch as the kinds of matrices that the principal pivoting method can handle have heretofore been limited to P-matrices and Positive Semi-Definite (PSD) matrices, both of which types are row sufficient as well as column sufficient. Thus, a demonstration that the PPM can process LCPs with row sufficient matrices amounts to a unification of the existing theory of the PPM and an extension of its scope. GRA

N89-28353# Stanford Univ., CA. Dept. of Statistics.
SUBSET COMPLEMENT ADDITION UPPER BOUNDS: AN IMPROVED INCLUSION/EXCLUSION METHOD
Donald R. Hoover 20 Apr. 1989 15 p
(Contract N00014-86-K-0156; NR Proj. 042-267)
(AD-A208797; SU-TR-416) Avail: NTIS HC A03/MF A01 CSCL 12/3

The Subset Complement Addition Upper Bound (SCAUB) procedure are presented which produces upper bounds for probabilities of unions of n events given that probabilities of unions and/or intersections of subsets including up to k events are known. The SCAUB method is an extension of Hunter's (1976) improved Bonferroni bounds. The SCAUB inequality is much simpler to calculate than are other distribution free upper bounds proposed in the past. It is also a distribution free analog of Glaz and Johnson's (1984) product type bounds. We prove that for any fixed n events, the SCAUB inequality monotonically decreases with k. SCAUB upper bounds are applied to the multivariate normal (or t) simultaneous interference interval problem. GRA

N89-28354# Notre Dame Univ., IN. Dept. of Aerospace and Mechanical Engineering.
TIME SERIES MODELING FOR STRUCTURAL RESPONSE PREDICTION Final Report, 1 Mar. 1985 - 1 Aug. 1988
Stephen M. Batill and Joseph J. Hollkamp 14 Nov. 1988 167 p
(Contract F33615-85-C-3205)
(AD-A208808; AFWAL-TR-88-3114) Avail: NTIS HC A08/MF A01 CSCL 12/3

A numerical and experimental study of time domain methods for modeling and parameter identification of structural systems is presented. Models are developed which can be used to predict the transient response of multiple-degree-of-freedom systems subjected to arbitrary input. The linear, discrete time transfer function is expressed in a a form called the Autoregressive Moving Average (ARMA) model. The ARMA model is a minimum parameter model that may be parameterized with a minimum number of measured quantities. The ARMA model is contrasted to traditional models such as differential equation models and modal methods. The ARMA model indentification algorithms are also compared to time domain modal methods. Though it has proven useful for a number of low-order systems, the identification of the ARMA model is often hampered by the sensitivity of parameter estimates to measurement noise bias. GRA

N89-28355# Stanford Univ., CA. Dept. of Computer Science.
COMPUTATIONAL METHODS AND SYSTEMS FOR PROBLEMS IN SCIENCE AND ENGINEERING Final Report, 1 Jun. 1987 - 31 May 1988
Joseph Oliger Jun. 1989 5 p
(Contract N00014-87-K-0384)
(AD-A209951) Avail: NTIS HC A02/MF A01 CSCL 20/4

The major objective related to adaptive grid methods for engineering problems in fluid dynamics and the development of parallel algorithms for the same class of problems. GRA

N89-28356# Massachusetts Inst. of Tech., Lexington.
BINARY SEQUENCES OF ARBITRARY LENGTH WITH NEAR-IDEAL CORRELATION
Patrick R. Hirschler-Marchand 13 Jun. 1989 33 p
(Contract F19628-85-C-0002)
(AD-A209956; TR-851; ESD-TR-89-107) Avail: NTIS HC A03/MF A01 CSCL 12/1

Binary sequences having two-valued correlation are very much sought after. Their applications are found in many areas such as error correcting codes, synchronization, spread spectrum communication, time resolution measurements, ranging, picture transmission, acoustics, radar, and antenna design. Many sequences are known to have two-valued periodic correlation. Perhaps, the most famous of these are maximum length sequences. Maximum length sequences have two-valued periodic correlations and power spectra. They satisfy linear recursions which are a consequence of Galois field theory and are very easily implemented with linear shift registers. Barker sequences have correlations less than or equal to 1, except at the origin. Twin-prime (p,p + 2) sequences have correlation of p(p+2) at the origin and -1 elsewhere. Hall sequences and quadratic-residue or Legendre sequences also have the same two-valued periodic correlations and power spectra. The above sequences have remarkable correlation properties but only come in certain lengths. Specifically, developed are: a dense class of binary sequences, called Mac sequences having arbitrary length and ideal correlation properties over a limited range around the peak; and a general algorithm to construct Mac sequences of any length. GRA

N89-28357# Wisconsin Univ., Madison.
SOME PROBLEMS IN NONLINEAR ANALYSIS Final Report, 1 Jun. 1987 - 31 Jan. 1989
Michael G. Crandall 1989 4 p
(Grant AF-AFOSR-0202-87; AF Proj. 2304)
(AD-A209991; AFOSR-89-0918TR) Avail: NTIS HC A02/MF A01 CSCL 12/2

A program for obtaining the basic results of Kato's theory of quasilinear evolution equations was obtained by the simpler methods of nonlinear semigroup theory (implicit differencing in time). Certain classes of parabolic and Hamilton-Jacobi equations show the existence and uniqueness of solutions if initial boundary value problems with singular (e.g., identically infinite) initial data and the continuous dependence of these singular solutions as the diffusion coefficient tends to zero. This work shows how certain PDE questions motivated by the theory of large deviations can be treated in greater generality and provides a certain abstract framework for this as well as concrete estimates. GRA

N89-28358# Naval Surface Warfare Center, Dahlgren, VA.
SIGNIFICANT DIGIT COMPUTATION OF THE INCOMPLETE BETA FUNCTION RATIOS Final Report
Armido R. DiDonato and Alfred H. Morris, Jr. Nov. 1988 81 p
(AD-A210118; NSWC/TR-88-365) Avail: NTIS HC A05/MF A01 CSCL 12/3

An algorithm is given for evaluating the incomplete beta function ratio I sub x (a,b) and its complement 1-I sub x (a,b). Two new procedures are used with classical results. A listing of a transportable FORTRAN subroutine using this algorithm is given. The subroutine is accurate to 14 significant digits when the precision is not restricted by inherent error. GRA

N89-28359# Vanderbilt Univ., Nashville, TN. Dept. of Mathematics.
CLAW-FREE MAXIMAL PLANAR GRAPHS
Michael D. Plummer 1989 22 p
(Contract N00014-85-K-0488)
(AD-A210179) Avail: NTIS HC A02/MF A01 CSCL 12/2

A graph G is claw-free if it contains no induced subgraph isomorphic to the complete bipartite graph K. Such graphs have been widely studied with respect to such other graph properties as matching, perfection, vertex-packing, Hamiltonian cycles and related questions on traversability, and reconstruction. A planar graph is said to be maximal planar (or a triangulation) if, given any imbedding of G in the plane, every face boundary is a triangle. The abbreviations MAXP and CFMAXP are used for the properties maximal planar and claw-free maximal planar respectively. (Recall that every maximal planar graph with at least three points is either the complete graph K3 or else is 3-connected and thus it follows that such a graph has a unique imbedding in the plane). GRA

N89-27902*# Jet Propulsion Lab., California Inst. of Tech., Pasadena.
ORTHOGONAL SETS OF DATA WINDOWS CONSTRUCTED FROM TRIGONOMETRIC POLYNOMIALS
C. A. Greenhall *In its* The Telecommunications and Data Acquisition Report 15 May 1989 p 300-305 (For primary document see N89-27871 22-32)
Avail: NTIS HC A17/MF A01 CSCL 12A

65 STATISTICS AND PROBABILITY

Includes data sampling and smoothing; Monte Carlo method; and stochastic processes.

N89-28360# Illinois Univ., Urbana. Psychometric Group.
A NEW ITEM RESPONSE THEORY MODELING APPROACH WITH APPLICATIONS TO UNIDIMENSIONALITY ASSESSMENT AND ABILITY ESTIMATION
William F. Stout Mar. 1989 58 p
(Contract N00014-87-K-0277; RR04024)
(AD-A207301; Rept-89-1-ONR) Avail: NTIS HC A04/MF A01 CSCL 12/3

Using an infinite item test framework, it is argued that the usual assumption of local independence be replaced by a weaker assumption, essential independence. A fortiori, the usual assumption of unidimensionality is replaced by a weaker and arguably more appropriate statistically testable assumption of essential unidimensionality. Essential unidimensionality implies the existence of a unique unidimensional latent ability. Essential unidimensionality is equivalent to the consistent estimation of this latent ability in an ordinal scaling sense using any balanced linear formula scoring scheme. A variation of this estimation approach allows consistent estimation of ability on the given latent ability scale. GRA

N89-28361# Naval Ship Research and Development Center, Bethesda, MD. Ship Materials Engineering Dept.
ESTIMATION OF LOWER BOUND PROPERTIES FROM MATERIAL TEST DATA Research and Development Report, Sep. 1987 - Jan. 1989
M. T. Kirk Jan. 1989 28 p
(AD-A207378; DTRC/SME-88-63) Avail: NTIS HC A03/MF A01 CSCL 20/11

Monte Carlo simulations were performed to determine how the accuracy of lower bound values estimated from experimental data is influenced by sampled size required confidence level, and assumed statistical mode. Population distributions having different degrees of skewness, selected to bracket those expected in actual experimental data, were studied. For nearly every case considered, lower bound estimates calculated using Log-Normal statistics were more accurate than estimates calculated using either Normal or Weibull statistics. It was demonstrated that testing more than three samples per condition can greatly reduce the error associated with the lower bound estimate. However, after the thirteenth sample no additional sample will reduce the lower bound estimation error by more than 2.5 percent for all statistical distribution/ confidence level combinations considered. When applied to material properties for which the population distribution has been established by previous testing, it was demonstrated that a Monte Carlo simulation can be used to assess the maximum expected lower bound estimation error as a function of sample size and confidence level. GRA

N89-28362# Princeton Univ., NJ. Dept. of Civil Engineering and Operations Research.
MARKOV PROCESSES APPLIED TO CONTROL, RELIABILITY AND REPLACEMENT Final Report, Oct. 1987 - Sep. 1988
Erhan Cinlar Apr. 1989 5 p
(Grant AF-AFOSR-0050-87; AF Proj. 2304)
(AD-A208634; AFOSR-89-0700TR) Avail: NTIS HC A02/MF A01 CSCL 12/3

This reports on the work done on stochastic comparisons of semimartingale Markov processes, opportunistic replacement policies, stochastic flows, and the book project on probability theory and stochastic processes. GRA

N89-28363# Massachusetts Inst. of Tech., Cambridge. Artificial Intelligence Lab.
THE COMBINATORICS OF HEURISTIC SEARCH TERMINATION FOR OBJECT RECOGNITION IN CLUTTERED ENVIRONMENTS
W. Eric L. Grimson May 1989 32 p
(Contracts N00014-86-K-0685; N00014-85-K-0124; DACA76-85-C-0010)
(AD-A209690; AI-M-1111) Avail: NTIS HC A03/MF A01 CSCL 12/9

Many current recognition systems use constrained search to locate objects in cluttered environments. Earlier analysis of one class of methods has shown that the expected amount of search is quadratic in the number of model and date features, if all the data is known to come from a single object, but is exponential when spurious data is included. To overcome this, many methods terminate search once an interpretation that is good enough is found. This paper formally examines the combinations of this approach, showing that choosing correct termination procedures can dramatically reduce the search. In particular, conditions are provided for the object model and the scene clutter such that the expected search is polynomial. The analytic results are shown to be in agreement with empirical data for cluttered object recognition. GRA

N89-28364# North Carolina Univ., Chapel Hill. Dept. of Statistics.
RESEARCH IN STOCHASTIC PROCESSES Final Report, 1 Sep. 1987 - 31 Aug. 1988
Stamatis Cambanis, Raymond J. Carroll, Gopinath Kallianpur, and M. R. Leadbetter 31 Aug. 1988 73 p
(Contract F49620-85-C-0144)
(AD-A209935; AFOSR-89-0913TR) Avail: NTIS HC A04/MF A01 CSCL 12/3

Research was conducted in the areas of stochastic processes and statistical inference. Main areas of research include: (1) non-Gaussian signal processing; (2) nonlinear filtering and prediction; (3) extremal theory for moderately behaved stationary sequences; and (4) weighted least squares methods with weights estimated by replication. GRA

66 SYSTEMS ANALYSIS

Includes mathematical modeling; network analysis; and operations research.

N89-28365# Army War Coll., Carlisle Barracks, PA.
SPACE ASSET MODELING FOR WARGAME INTEGRATION

Roger A. Cunning 2 Mar. 1989 45 p
(AD-A207350) Avail: NTIS HC A03/MF A01 CSCL 15/6

As more nations develop or participate in space activity, the impacts or effects of space assets and their degradation must be analyzed prior to a devastating event. Existing wargames which model space assets as an integral component of the game are reviewed. Differences between wargames, simulations and exercises are acknowledged; recommendations for each type of gaming activity are provided. In reviewing the various wargaming activities, stated policies of the United States and the Soviet Union are examined; space asset wargaming is approached from the viewpoint of supporting national policy. Since wargaming develops leadership skills and provides a degree of education to leaders, emphasis is placed on the ability of wargames to convey a sense of national priority. The possibility of creating a wargame suitable for all communities versus the addition of a module of a space package into any existing wargame was examined. Finally, a description of necessary components and human interface to a space module in a wargame are examined and a recommendation for effective operation is provided. GRA

N89-28366# Los Alamos National Lab., NM.
GOALS FOR LIMITED STRATEGIC DEFENSES
Gregory H. Canavan May 1989 44 p
(Contract W-7405-eng-36)
(DE89-012260; LA-11419-MS) Avail: NTIS HC A03/MF A01

The nature of near and mid-term accidental, third-country, and limited threats, discusses the technologies available to defend against them is reviewed and examines the development programs required. DOE

N89-28367# Los Alamos National Lab., NM.
CONSTELLATION SIZING FOR MODEST DIRECTED ENERGY PLATFORMS
Gregory H. Canavan Jun. 1989 11 p
(Contract W-7405-eng-36)
(DE89-012826; LA-11573-MS) Avail: NTIS HC A03/MF A01

Discussions of boost-phase, directed energy scaling have concentrated on large lasers and mirrors requiring development. Modest lasers that could be deployed sooner if their performance and effectiveness were found to be adequate are explored. DOE

N89-28368# Strategic Defense Initiative Organization, Washington, DC.
THE 1989 REPORT TO THE CONGRESS ON THE STRATEGIC DEFENSE INITIATIVE
13 Mar. 1989 358 p
(PB89-196661) Avail: NTIS HC A16/MF A01 CSCL 12B

A summary of the Strategic Defense Initiative (SDI) legacy is presented. The best current program for the resolution of remaining technical issues, the validation of technologies, and the demonstration of the ability to integrate them is assessed in detail. The program of research, development and testing would, if adequately funded, support a fully informed decision by the President and Congress in the future on whether to deploy a strategic defense of the United States. Such defenses could enhance deterrence and increase stability. GRA

67 THEORETICAL MATHEMATICS

Includes topology and number theory.

No abstracts in this category.

70 PHYSICS (GENERAL)

For precision time and time interval (PTTI) see *35 Instrumentation and Photography;* for geophysics, astrophysics or solar physics see *46 Geophysics, 90 Astrophysics,* or *92 Solar Physics.*

N89-28369# Air Force Academy, CO.
SYMMETRY IN THE BASIC SCIENCES Final Report, Aug. 1988 - Apr. 1989
Joseph E. Toole, David W. Jensen, Mark E. Rogers, Paul J. Chernek, and Thomas E. Erstfeld Apr. 1989 75 p
(AD-A207371; USAFA-TR-89-3) Avail: NTIS HC A04/MF A01 CSCL 12/2

The basic mathematical theory behind plane symmetry groups is presented. This theory is then applied in classifying the symmetry of bounded figures, frieze patterns and wallpaper patterns. Recently developed algorithms are included to help analyze complex designs. Symmetry operations relevant to 3-D crystallography are discussed. In particular, the seven crystal systems that classify the 32 crystallographic point groups are described. These are then used to construct the Bravais lattices. The role is investigated of symmetry in biological forms. Specifically, work on growth and form of molluscan shells is reviewed with an attempt to explain the consequences of that growth and form to the natural history of the Chambered Nautilus and its ancestors. The central role symmetry has increasingly played in physics is looked at by examining the Principle of Least Action and the invariance of the Lagrangian under a transformation. Noether's Theorem guarantees that a conservation law is associated with each of these symmetries. Examples include the conservation of energy, linear momentum, and angular momentum, as well as the purely quantum mechanical symmetry of invariance under an exchange operation. A brief look at gauge theories is the final example of how symmetry has become a guiding principle in the formulation of new theories. GRA

71 ACOUSTICS

Includes sound generation, transmission and attenuation. For noise pollution see *45 Environmental Pollution.*

N89-28370# Naval Research Lab., Washington, DC. Acoustic Systems Branch.
SOUND PROPAGATION IN BUBBLY LIQUIDS: A REVIEW Memorandum Report, Jun. - Aug. 1988
S. Temkin (Rutgers Univ., New Brunswick, NJ.) 5 Apr. 1989 46 p
(AD-A207377; NRL-MR-6403) Avail: NTIS HC A03/MF A01 CSCL 20/1

This report considers the propagation of plane sound waves in a liquid containing a homogeneous distribution of small, nondiffusing gas bubbles. We have concentrated on the basic theories of Wood and Kennard for phase speed in equilibrium conditions, and at finite frequencies, respectively. A derivation of phase speed from first principles indicates the Wood's equation is an accurate approximation for dilute mixtures of gas bubbles in a liquid. The conditions under which Wood's equation does not apply are discussed based on the analytic expressions obtained from the fundamental derivation. Kennard's equation is based on assumptions which have not been critically examined, particularly in regard to the compressibility model on which is based, and on the frequency dependence of the relevant damping coefficients. GRA

N89-28371# Texas Univ., Austin. Applied Research Lab.
REFLECTION AND REFRACTION OF FINITE AMPLITUDE ACOUSTIC WAVES AT A FLUID-FLUID INTERFACE Ph.D. Thesis Technical Report
Frederick D. Cotaras (Defence Research Establishment Atlantic, Dartmouth, Nova Scotia) 3 Jan. 1989 134 p
(Contracts N00014-89-J-1109; N00014-84-K-0574)

(AD-A209800; ARL-TR-89-1) Avail: NTIS HC A07/MF A01 CSCL 20/1

A theoretical investigation is presented of the nonlinear effects in reflection and refraction of plane finite-amplitude acoustic waves at an initially plane interface between two lossless fluids. In the first part, the terms in the equations of motion for a homogeneous, thermoviscous fluid with a single relaxation mechanism are rank ordered to determine the most important nonlinear and dissipation terms. The equations are then combined to form a general wave equation that includes the most important effects of nonlinearity and dissipation. In the second part, the terms in the boundary conditions between two lossless fluids are rank ordered to include the most important nonlinear effects. Subject to these boundary conditions, a solution of the lossless form of the aforementioned wave equation is obtained by way of second order perturbation expansion. The lossless form of the wave equation and the lossless boundary conditions are expanded, and the O (epsilon) and O (epsilon-sq) systems are solved in terms of a modified velocity potential. The analysis is performed for oblique incidence, and the boundary condition at the source is arbitrary. Effects examined include the finite displacement of the interface and the variation of the direction of the normal to the interface, both of which are caused by the motion of the interface as it responds to the incident sound. GRA

72 ATOMIC AND MOLECULAR PHYSICS

Includes atomic structure, electron properties, and molecular spectra.

N89-28372# Boston Univ., MA.
FLUORESCENCE PROBES OF SPECTROSCOPIC AND DYNAMICAL ASPECTS OF MOLECULAR PHOTOIONIZATION Final Report, 1 Jul. 1984 - 30 Jun. 1988
Erwin D. Poliakoff Nov. 1988 5 p
(Grant AF-AFOSR-0261-84; AF Proj. 2301)
(AD-A207185; AFOSR-89-0473TR) Avail: NTIS HC A02/MF A01 CSCL 07/2

Studies were made of vibrationally resolved aspects of shape resonant excitation in the photoionization of N(2)0. This experiment was performed by generating dispersed fluorescence spectra from electronically excited photoions. These results are the first vibrationally resolved results on a polyatomic shape resonance. In vibrationally resolved measurements, different internuclear configurations are probed by sampling alternative vibrational levels of the ion. As a result, the continuum electron behavior can be mapped out most clearly, and the qualitative aspects of the electron ejection can be understood clearly. A central motivation for studying polyatomic shape resonances is that alternative vibrational modes may be explored, revealing facets that are nonexistent for diatomic systems, which are the only systems that have been characterized previously. GRA

N89-28373# Max-Planck-Institut fuer Stroemungsforschung, Goettingen (Germany, F.R.).
VIBRATIONAL PREDISSOCIATION OF SHOCK-SELECTED C2H4 AND NH3 CLUSTERS Thesis [SCHWINGUNGSPRAEDISSOZIATION VON STOSSSELEKTIERTEN C2H4- UND NH3-CLUSTERN]
Thomas Pertsch Feb. 1988 175 p In ENGLISH and GERMAN
(MPIS-6/1988; ISSN-0436-1199; ETN-89-94383) Avail: NTIS HC A08/MF A01; Max-Planck-Inst. fuer Stroemungsforschung, Boettinger Strasse 6, 3400 Goettingen, Fed. Republic of Germany, 36 DM

The infrared vibrational predissociation of C2H4 and NH3-clusters was investigated. Infrared photodissociation spectroscopy of selected, internally cold, weakly bound ethylene clusters was performed. Infrared photodissociation experiments were carried out on (C2H4)n-clusters, selectively prepared by molecular beam scattering. A computer controlled time of flight analyzer, incorporated in a CAMAC system, was developed for the analysis of supersonic molecular beams. For individual titles, see N89-28374 through N89-28377.

N89-28374# Max-Planck-Institut fuer Stroemungsforschung, Goettingen (Germany, F.R.).
VIBRATIONAL PREDISSOCIATION OF SHOCK-SELECTED C2H4 AND NH3 CLUSTERS, INTRODUCTION [SCHWINGUNGSPRAEDISSOZIATION VON STOSSSELEKTIERTEN C2H4- UND NH3-CLUSTERN]
Thomas Pertsch *In its* Vibrational Predissociation of Shock-Selected C2H4 and NH3 Clusters Feb. 1988 p 1-142 In GERMAN (For primary document see N89-28373 22-72)
Avail: NTIS HC A08/MF A01; Max-Planck-Inst. fuer Stroemungsforschung, Boettinger Strasse 6, 3400 Goettingen, Fed. Republic of Germany, 36 DM

The IR vibrational predissociation of clusters of the weak binding type was investigated. A cluster beam was crossed with the beam of a CO2 laser tunable at discrete frequencies. For suitable frequencies, a monomer unit in the cluster is vibrationally excited leading to dissociation. Subsequently, the cluster beam is dispersed by an atomic He-beam. The combination of IR photodissociation and scattering analysis provides a selective spectroscopic method. The frequency dependence of the IR-photodissociation spectra of all investigated C2H4 clusters is the same. The dependence of the dissociation on the laser energy was determined. Infrared photodissociation spectra of NH3-clusters were measured; the frequency dependence depends on the cluster size; the dissocation distributions of trimers, tetramers and pentamers show a blue shift compared with the dimer dissociation bands. ESA

N89-28375# Max-Planck-Institut fuer Stroemungsforschung, Goettingen (Germany, F.R.).
INFRARED PHOTODISSOCIATION AND CLUSTER-SPECIFIC DETECTION OF INTERNALLY COLD (C2H4) VAN DER WAALS COMPLEXES
Friedrich Huisken and Thomas Pertsch *In its* Vibrational Predissociation of Shock-Selected C2H4 and NH3 Clusters Feb. 1988 p 143-150 Repr. from J. Chem. Phys. (American Inst. of Physics), v. 86, no. 1, 1 Jan. 1987 p 106-113 (For primary document see N89-28373 22-72)
Avail: NTIS HC A08/MF A01; Max-Planck-Inst. fuer Stroemungsforschung, Boettinger Strasse 6, 3400 Goettingen, Fed. Republic of Germany, 36 DM

Infrared photodissociation spectroscopy of selected, internally cold, weakly bound van der Waals ethylene clusters was performed. A steady molecular beam of C2H4 clusters is crossed by the IR radiation of a pulser CO2 laser. Subsequent scattering by a secondary He-beam disperses the cluster beam and allows unequivocal detection of selected cluster species which is not disturbed by fragmentation processes in an ionizer. The dependence of IR photon absorption on cluster size was investigated in the region of the nu-7 vibration of C2H4; predissociation spectra were recorded for (C2H4)n complexes with n=2,3,4, and 5. The absorption profiles are structureless and all have, regardless of cluster size, the same width and the peak at the same position. From the dependence of the dissociation yield on the laser fluence, transition probabilites were determined for n=2,3, and 4. ESA

N89-28376# Max-Planck-Institut fuer Stroemungsforschung, Goettingen (Germany, F.R.).
INFRARED PHOTODISSOCIATION OF VAN DER WAALS COMPLEXES SELECTIVELY PREPARED BY MOLECULAR BEAM SCATTERING
U. Buck, Friedrich Huisken, Ch. Lauenstein, Thomas Pertsch, and R. Sroka *In its* Vibrational Predissociation of Shock-Selected C2H4 and NH3 Clusters Feb. 1988 p 151-161 Repr. from Structure and Dynamics of Weakly Bound Molecular Complexes (D. Reidel Publishing Co.), 1987 p 477-487 (For primary document see N89-28373 22-72)
Avail: NTIS HC A08/MF A01; Max-Planck-Inst. fuer

Stroemungsforschung, Boettinger Strasse 6, 3400 Goettingen, Fed. Republic of Germany, 36 DM

Infrared photodissociation experiments were carried out on (C2H4)n-clusters, which were prepared according to their size by scattering them from a helium beam. The ethylene clusters were dissociated upon absorption of a CO2-laser photon by exciting the nu-7 mode of the monomer. Since an appreciable amount of energy is transferred to the cluster during the collision, the laser photons interact with internally cold or hot clusters depending on whether the interaction is before or after the collision center. The frequency and fluence dependences of the photodissociation cross sections were measured for cold and hot clusters from n=2 to n=6. The spectra of the cold clusters show the same shape and line width for all cluster sizes investigated, while those of the hot clusters are characterized by large variations in shape and line width. The very structured dimer spectrum is explained by the excitation of hot bands. ESA

N89-28377# Max-Planck-Institut fuer Stroemungsforschung, Goettingen (Germany, F.R.).

CAMAC TIME-OF-FLIGHT ANALYZER FOR MOLECULAR BEAM DIAGNOSTICS

Friedrich Huisken and Thomas Pertsch *In its* Vibrational Predissociation of Shock-Selected C2H4 and NH3 Clusters Feb. 1988 p 163-166 Repr. from Rev. Sci. Instrum. (American Inst. of Physics), v. 58, no. 6, Jun. 1987 p 1038-1041 (For primary document see N89-28373 22-72)

Avail: NTIS HC A08/MF A01; Max-Planck-Inst. fuer Stroemungsforschung, Boettinger Strasse 6, 3400 Goettingen, Fed. Republic of Germany, 36 DM

A computer-controlled time of flight (TOF) analyzer, incorporated in a CAMAC system, was developed for the analysis of supersonic molecular beams. The measured arrival times are stored in a histogramming memory module and transferred to a minicomputer for further processing. The system features four independent multichannel analyzers which can be selected. Each unit has 4096 24-bit channels. Dwell times are programmable between 1 and 255 microsec and the maximum counting rate is 1 MHz. The system is intended for ordinary single pulse or pseudorandom TOF analysis, and can also be used in photodissociation experiments employing pulsed lasers. The calibration of the TOF analyzer is described and examples of measurements are presented. ESA

N89-28378# Max-Planck-Institut fuer Stroemungsforschung, Goettingen (Germany, F.R.).

CHARGE TRANSFER AND INELASTIC SCATTERING IN PROTON-MOLECULE COLLISIONS Thesis [LADUNGAUSTAUSCH UND INELASTISCHE STREUUNG IN PROTON-MOLEKUEL-STOESSEN]

Gereon Niedner Jun. 1988 320 p In ENGLISH and GERMAN

(MPIS-13/1988; ISSN-0436-1199; ETN-89-94569) Avail: NTIS HC A14/MF A01; Max Planck-Inst. fuer Stroemungsforschung, Boettinger Strasse 6, 3400 Goettingen, Fed. Republic of Germany, 56 DM

Differential charge transfer cross sections in proton-molecule collisions were investigated by direct detection of the produced H-atoms. Potential energy curves for the ArH(+) and NeH(+) systems were deduced from the interplay of theory and experiments. The dynamics of H(+) +Kr and H(+) +Xe elastic and charge transfer collisions at low collision energies was investigated. Vibrationally resolved charge transfer in H(+)+H2 was observed. A 3-D quantum mechanical close coupling study of state-to-state charge transfer cross sections of the system H(+) +H2 was made. A 3-D quantum mechanical close coupling study of vibrational inelastic and charge transfer processes of the system H(+) +H2 was carried out. Charge transfer and structured vibrational distributions in the system H(+) +CH4 were studied for low energy collisions. For individual titles, see N89-28379 through N89-28385.

N89-28379# Max-Planck-Institut fuer Stroemungsforschung, Goettingen (Germany, F.R.).

CHARGE TRANSFER AND INELASTIC SCATTERING IN PROTON-MOLECULE COLLISIONS, INTRODUCTION [LADUNGSAUSTAUSCH UND INELASTISCHE STREUUNG IN PROTON-MOLEKUEL-STOESSEN]

Gereon Niedner *In its* Charge Transfer and Inelastic Scattering in Proton-Molecule Collisions Jun. 1988 p 1-165 In GERMAN (For primary document see N89-28378 22-72)

Avail: NTIS HC A14/MF A01; Max Planck-Inst. fuer Stroemungsforschung, Boettinger Strasse 6, 3400 Goettingen, Fed. Republic of Germany, 56 DM

Differential charge transfer cross sections in proton-molecule collisions were investigated by direct detection of the produced H-atoms. The experimental system, the measurement procedure, the calculation concept, and the H-atom detector are described. The theoretical models are overviewed. In the experiments, a broad spectrum of several species was tested as target molecules (ion-atoms, ion-diatoms, and ion-polyatoms). Where possible, theoretical calculations or symmetry considerations were made in addition to the experimental observations. ESA

N89-28380# Max-Planck-Institut fuer Stroemungsforschung, Goettingen (Germany, F.R.).

POTENTIAL ENERGY CURVES FOR THE (ArH(+)) AND (NeH(+)) SYSTEMS FROM THE INTERPLAY OF THEORY AND EXPERIMENTS

F. A. Gianturco, Gereon Niedner, Martin Noll, E. Semprini, F. Stefani (Consiglio Nazionale delle Ricerche, Rome, Italy), and J. Peter Toennies *In its* Charge Transfer and Inelastic Scattering in Proton-Molecule Collisions Jun. 1988 p 166-173 Repr. from Z. Phys. D. - Atoms, Molecules and Clusters (Springer-Verlag), v. 7, 1987 p 281-288 Sponsored in part by the Alexander von Humboldt Stiftung (For primary document see N89-28378 22-72)

Avail: NTIS HC A14/MF A01; Max Planck-Inst. fuer Stroemungsforschung, Boettinger Strasse 6, 3400 Goettingen, Fed. Republic of Germany, 56 DM

The ground state potential energy curves for protons interacting with Ar and Ne atoms were investigated by the analysis of highly accurate measurements of the elastic differential cross sections at a collision energy of 14.8 eV. Accompanying theoretical results were used as starting points to generate analytical potentials to fit all available experimental cross sections for both systems. The final results provide the full shape of the potential curves and give the test existing fit to the measured cross sections for elastic scattering at several energies between 2 and 30 eV. ESA

N89-28381# Max-Planck-Institut fuer Stroemungsforschung, Goettingen (Germany, F.R.).

DYNAMICS OF H(+) + Kr AND H(+) + Xe ELASTIC AND CHARGE-TRANSFER COLLISIONS: STATE-SELECTED DIFFERENTIAL CROSS SECTIONS AT LOW COLLISION ENERGIES

Michael Baer, Rudolf Dueren, Bretislav Friedrich (Ceskoslovenska Akademie Ved, Prague.), Gereon Niedner, Martin Noll, and J. Peter Toennies *In its* Charge Transfer and Inelastic Scattering in Proton-Molecule Collisions Jun. 1988 p 174-183 Repr. from Physical Review A (American Physical Society), v. 36, no. 3, 1 Aug. 1987 p 1063-1072 Sponsored in part by the Alexander von Humboldt Stiftung (For primary document see N89-28378 22-72)

Avail: NTIS HC A14/MF A01; Max Planck-Inst. fuer Stroemungsforschung, Boettinger Strasse 6, 3400 Goettingen, Fed. Republic of Germany, 56 DM

Elastic and charge transfer scattering of protons by Kr and Xe targets was investigated in a crossed beam experiment at collision energies of 30.6 and 51.7 eV. The charge transfer collisions led to the formation of Kr(+) (2P3/2, 2P1/2) + H(n=1) and Xe(+) (2P3/2, 2P1/2) + H(n=1, n=2) products, respectively. Interference patterns in the state-selected relative differential cross sections were clearly resolved and ascribed to primary and secondary rainbows and/or Stueckelberg-type oscillations. The

H(+) +Xe collisions were also investigated theoretically by the exact close-coupling method. Good agreement between theory and experiment is found. A method for the determination of the absolute H-atom detection efficiency is suggested. ESA

N89-28382# Max-Planck-Institut fuer Stroemungsforschung, Goettingen (Germany, F.R.).
OBSERVATION OF VIBRATIONALLY RESOLVED CHARGE TRANSFER IN H(+) + H2 AT A COLLISION ENERGY Ecm = 20 eV
Gereon Niedner, Martin Noll, J. Peter Toennies, and Ch. Schlier (Freiburg Univ., Germany, F.R.) *In its* Charge Transfer and Inelastic Scattering in Proton-Molecule Collisions Jun. 1988 p 184-193 Repr. from J. Chem. Phys. (American Inst. of Physics), v. 87, no. 5, 1 Sep. 1987 p 2685-2694 (For primary document see N89-28378 22-72)
Avail: NTIS HC A14/MF A01; Max Planck-Inst. fuer Stroemungsforschung, Boettinger Strasse 6, 3400 Goettingen, Fed. Republic of Germany, 56 DM

The doubly differential cross sections for both the scattered protons and H-atoms were measured at E sub cm = 20 eV and scattering angles between 0 and 18 deg for the reactions H(+) +H2 yields H(+) +H2 (delta E = 0.01v) and H(+) +H2 yields H(+) +H2(+) (delta E = 1.83 eV). The energy resolution is sufficient to resolve final vibrational states in both reactions. Clear experimental evidence is found of a two-step charge transfer mechanism: vibrational excitation on the lower H(+) +H2 surface is followed by charge transfer in the outgoing collision for only those H2-molecules which are excited vibrationally high enough (nu-f greater than or=4) overcome the endoergic barrier (delta E = 1.83 eV). The final vibration distributions of H2(+) are very similar to those of H2 for nu-f greater than or=4. The comparison with classical trajectory surface hopping calculations points to disagreement which can probably be attributed to the potential surface used. ESA

N89-28383# Max-Planck-Institut fuer Stroemungsforschung, Goettingen (Germany, F.R.).
A COMPARISON BETWEEN THEORETICAL AND EXPERIMENTAL STATE-TO-STATE CHARGE TRANSFER CROSS SECTIONS FOR H(+) + H2 AT 20 eV: EVIDENCE FOR QUANTUM EFFECTS
Michael Baer (Soreq Research Establishment, Israel Atomic Energy Commission, Yavneh.), Gereon Niedner, and J. Peter Toennies *In its* Charge Transfer and Inelastic Scattering in Proton-Molecule Collisions Jun. 1988 p 194-195 (For primary document see N89-28378 22-72)
Avail: NTIS HC A14/MF A01; Max Planck-Inst. fuer Stroemungsforschung, Boettinger Strasse 6, 3400 Goettingen, Fed. Republic of Germany, 56 DM

A 3-D quantum mechanical close coupling study for the system H(+) +H2 is communicated. The quantum calculations, caried out in the finite order swiden approximation, show a better fit to previous experiments than the classical trajectory surface hopping (TSH) calculations, and provide direct evidence for the usefulness of a quantum treatment in predicting charge transfer (CT) processes. The total differential cross sections (summed over all final vibrational states) for the CT processes were calculated, in good agreement with experimental results. It is shown that a quantum mechanical treatment of both the inelastic and the charge transfer nonadiabatic processes is feasible and provides a superior description of the experiments compared to the TSH treatment. This demonstrates the importance of quantum effects in ion-molecule charge transfer. ESA

N89-28384# Max-Planck-Institut fuer Stroemungsforschung, Goettingen (Germany, F.R.).
A THREE-DIMENSIONAL QUANTUM MECHANICAL STUDY OF VIBRATIONAL INELASTIC AND CHARGE TRANSFER PROCESSES IN H(+) + H2 AT A COLLISION ENERGY Ecm = 20 eV
Michael Baer (Soreq Research Establishment, Israel Atomic Energy Commission, Yavneh.), Gereon Niedner, and J. Peter Toennies *In its* Charge Transfer and Inelastic Scattering in Proton-Molecule Collisions Jun. 1988 p 196-244 (For primary document see N89-28378 22-72)
Avail: NTIS HC A14/MF A01; Max Planck-Inst. fuer Stroemungsforschung, Boettinger Strasse 6, 3400 Goettingen, Fed. Republic of Germany, 56 DM

A 3-D quantum mechanical close coupling study of the system H(+) + H2 was carried out within the infinite order sudden approximation. Vibrational inelastic an charge transfer processes were treated. Steric factors, opacity functions, angular distributions, and integral cross sections were calculated. The measurable quantities were compared with experimental results, with in general very good agreement. Comparisons with trajectory surface hopping results demonstrate shortcomings of this semi-classical approach. ESA

N89-28385# Max-Planck-Institut fuer Stroemungsforschung, Goettingen (Germany, F.R.).
CHARGE TRANSFER AND STRUCTURED VIBRATIONAL DISTRIBUTIONS IN H(+) + CH4 LOW-ENERGY COLLISIONS
Y. N. Chiu, Bretislav Friedrich (Ceskoslovenska Akademie Ved, Prague.), W. Maring, Gereon Niedner, Martin Noll, and J. Peter Toennies *In its* Charge Transfer and Inelastic Scattering in Proton-Molecule Collisions Jun. 1988 p 262-314 Submitted for publication Sponsored in part by Alexander von Humboldt Stiftung (For primary document see N89-28378 22-72)
Avail: NTIS HC A14/MF A01; Max Planck-Inst. fuer Stroemungsforschung, Boettinger Strasse 6, 3400 Goettingen, Fed. Republic of Germany, 56 DM

In elastic and charge transfer collisions of protons with methane molecules were investigated in a perpendicular-plane crossed beam experiment via the detection of the scattered protons and H-atoms, respectively. Time of flight analysis provided information on internal structured energy distributions of the CH4 and CH4(+) products. For scattering angles greater than 4 deg, the energy transfer increases steeply up to the dissociation limit while the vibrational structure is no longer resolved. In the case of charge transfer, the observed narrow internal energy distribution is centered at the recombination energy of the proton, indicating a quasi-resonant charge transfer. The mass spectrometric analysis results of the fragmentation of CH4(+) are in good agreement with the known values. A mechanism, based on vibronic symmetry correlation theory, is proposed to explain the experimental results. The effects of Jahn-Teller distortions of the CH4(+) charge transfer product are discussed. ESA

N89-28386# University Coll. of Wales, Aberystwyth. Dept. of Physics.
VIBRATIONALLY EXCITED IONS: QUENCHING, REACTION AND LIFETIMES Final Report, Mar. 1988 - Jan. 1989
Norman Twiddy 20 Jan. 1989 51 p Sponsored by Science and Engineering Research Council Prepared in cooperation with Paris-Sud Univ., Orsay, France
(Grant AF-AFOSR-0122-88; AF Proj. 2301)
(AD-A208503; EOARD-TR-89-07) Avail: NTIS HC A04/MF A01 CSCL 07/4

The topics addressed include: Vibrational quenching studies of HCl(+) (v=1) and DCl(+) (v=1); Ion chemistry of HBr(+); Measurement of vibrational lifetimes; Proton affinity measurements. GRA

N89-28387# California Univ., Santa Barbara. Dept. of Physics.
QUANTUM CORRECTIONS FOR INELASTIC ATOM-SURFACE SCATTERING Technical Report No. 23, 1 Jan. - 31 Dec. 1989
J. H. Jensen and W. Kohn 21 Jun. 1989 22 p Submitted for publication
(Contract N00014-84-K-0548; NR Proj. 372-160)
(AD-A209850) Avail: NTIS HC A02/MF A01 CSCL 20/10

Simple and exact expressions are derived for the leading quantum corrections to the angular and energy distributions of an atom scattered inelastically from a solid crystalline surface. The quantum corrections are given in terms of classical trajectories and equilibrium correlation functions for the solid surface. The

results are useful when the incident atom has an energy of about 1 electron volt and the surface has a temperature less than or comparable to the Debye temperature. GRA

N89-28388# Utah Univ., Salt Lake City. Dept. of Chemistry.
MODIFIED ROTATIONALLY ADIABATIC MODEL FOR ROTATIONAL AUTOIONIZATION OF DIPOLE-BOUND MOLECULAR ANIONS Technical Report No. 2, Jan. - Jun. 1989
Jack Simons (Joint Inst. for Lab. Astrophysics, Boulder, CO.) 28 Jun. 1989 24 p Submitted for publication
(Contract N00014-89-J-1497; NSF CHE-88-14765)
(AD-A209851) Avail: NTIS HC A02/MF A01 CSCL 07/2

Modifications are introduced to a rotationally adiabatic model developed and successfully applied by Clary to describe rotational autoionization of dipole-bound molecular anions. These modifications address branching ratios for forming neutrals in various final rotational states. Also produced are rate-enhancement corrections to the original model in the neighborhoods of channel openings. Example calculations are presented and the essential ingredients of the corrections are tabulated in a manner that permits straight-forward application to any linear or pseudo-linear anion. GRA

N89-28389# State Univ. of New York, Buffalo. Dept. of Chemistry.
EXTRAORDINARY BEHAVIOR OF ATOMS NEAR A PHASE CONJUGATOR
Henk F. Arnoldus and Thomas F. George Jun. 1989 10 p
(Contract N00014-86-K-0043)
(AD-A209946; UBUFFALO/DC/TR-103) Avail: NTIS HC A02/MF A01 CSCL 20/5

An atom near a phase conjugator (PC) is theoretically seen to behave quite differently than an atom in empty space or an atom near an ordinary (linear) surface. With two laser beams which pump the nonlinear crystal (PC), it is found that an atom in its ground state can fluoresce if it is sufficiently close to a PC. The possible mechanism involves the atomic transition dipole polarizing the PC, which then spontaneously emits a photon focused on the atom. With stimulated absorption and subsequent spontaneous emission, the net effect is that the atom remains in its ground state. GRA

N89-28390# State Univ. of New York, Buffalo. Dept. of Chemistry.
ELECTROMAGNETIC REACTION TO MOLECULAR RELAXATION AND ITS EFFECT ON ABSORPTION NEAR A ROUGH SURFACE
Purna C. Das, Ashok Puri, and Thomas F. George Jun. 1989 20 p Submitted for publication
(Contract N00014-86-K-0043)
(AD-A210069; UBUFFALO/DR/TR-102) Avail: NTIS HC A03/MF A01 CSCL 07/4

The effect of electromagnetic reaction to relaxation of a molecule adsorbed on a rough surface is considered. The reaction fields are included due to the system dipole relaxing by both photon radiation and decay to delocalized surface plasmon damping is shown to be important for both small and large sized roughness features. GRA

N89-27875*# Jet Propulsion Lab., California Inst. of Tech., Pasadena.
NEW ION TRAP FOR ATOMIC FREQUENCY STANDARD APPLICATIONS
J. D. Prestage, G. J. Dick, and L. Maleki *In its* The Telecommunications and Data Acquisition Report 15 May 1989 p 58-63 (For primary document see N89-27871 22-32)
Avail: NTIS HC A17/MF A01 CSCL 20H

73 NUCLEAR AND HIGH-ENERGY PHYSICS

Includes elementary and nuclear particles; and reactor theory.
For space radiation see *93 Space Radiation.*

No abstracts in this category.

74 OPTICS

Includes light phenomena; and optical devices.
For lasers see *36 Lasers and Masers.*

N89-28391# Rockwell International Corp., Thousand Oaks, CA. Science Center.
STUDIES OF PHASE-CONJUGATE OPTICAL DEVICE CONCEPTS Final Report, 1 Apr. 1985 - 30 Jun. 1988
I. C. McMichael and P. A. Yeh Mar. 1989 180 p
(Contract N00014-85-C-0219)
(AD-A206219; SC5424.FR) Avail: NTIS HC A09/MF A01 CSCL 20/6

Phase-conjugate gyroscopy is a new area promising significant advances in state-of-the-art inertial navigation. This contract demonstrated the first phase-conjugate fiber-optic gyros (PCFOG's) and their ability to use low cost multimode fiber components. The development of the PCFOG is now at the stage where its sources of noise and drift can be isolated, and its competitiveness with conventional fiber optic gyros can be tested. To come to this stage in development, several scientific and technical issues had to be resolved. For example, to correct for the modal scrambling of multimode fibers, the theory and practice of polarization preserving conjugators that worked at milliwatt power levels had to be developed and tested. Another issue was the mutual coherence requirement for two beams interacting with a self-pumped conjugator that at first restricted the PCFOG from using the most desireable form of biasing (fast phase modulation). This issue was resolved only recently when a new class of phase conjugators (mutually pumped conjugators) was developed that have the ability to operate with mutually incoherent beams. Almost as quickly as the first mutually pumped conjugators were discovered, this contract demonstrated the first PCFOG to use one. In addition to, and in the process of developing the PCFOG, this contract investigated several new photorefractive phenomena. GRA

N89-28392# Colorado Univ., Boulder. Optoelectronic Computing Systems Center.
FIBER-OPTIC DELAY LINE STORAGE IN DIGITAL OPTICAL COMPUTERS BASED ON DIRECTIONAL COUPLERS Interim Report
David B. Sarrazin Jan. 1989 49 p Prepared in cooperation with Colorado State Univ., Fort Collins
(Grant NSF CDR-86-22236)
(PB89-185318; OCS-TR-89-04) Avail: NTIS HC A03/MF A01 CSCL 20F

The use of optical fiber for delay-line memory in LiNbO3-switch-based digital optical computers is investigated. Errors caused by the thermal sensitivity of optical fiber could lead to memory failure in a synchronous design if not properly controlled. Intermittent regeneration errors occur at the electro-optic boundary, in part due to optical attenuation. Fiber dispersion, switch crosstalk, polarization effects, and compositional variation in the switch are expected to have negligible effects on the proposed implementation. Suggestions for overcoming these limitations are presented, along with considerations for future developments. GRA

N89-28393# Oak Ridge National Lab., TN.
NONCONTACTING LASER DIFFRACTION STRAIN EXTENSOMETER FOR MATERIAL PROPERTIES CHARACTERIZATION AT HIGH TEMPERATURES
K. C. Liu and H. Pih 1989 6 p Presented at the International Congress on Technology and Technology Exchange, New York, NY, 28 Jun. 1989
(Contract DE-AC05-84OR-21400)
(DE89-013551; CONF-8906147-1) Avail: NTIS HC A02/MF A01

A noncontacting optical system, utilizing the interference fringes produced by the diffraction of laser light passing through a narrow slit, has been developed for measuring static and dynamic strain deformations at elevated temperatures above 1300 C. Basic optical theory, details of instrumentation, system operation, and sample applications are presented. Examples utilizing SiN and Ti alloy composite are given. DOE

N89-28394# Environmental Research Inst. of Michigan, Ann Arbor.
SENSITIVITY ANALYSIS OF REFLECTION ERRORS IN INFRARED IMAGE SIMULATION
B. E. Morey and D. J. Witte Sep. 1988 44 p
(Contract MDA908-87-C-3056)
(AD-A208600; ERIM-205200-12-T) Avail: NTIS HC A03/MF A01 CSCL 17/5

The question of how much error is present in a simulated infrared signature if reflections are neglected was studied using a sensitivity analysis approach. The purpose was to determine whether it is necessary to model reflections in the current FSTC method of simulating IR signatures. To gain insight the following steps were performed. A sensitivity analysis approach was chosen for the study. An equation isolating the major components of an IR signature was derived. The equation was used to determine error present in a simulation when emissivity was estimated to be always 0.95. This was accomplished by using a simulation of a complicated tank applied with actual, measured emissivity that had specular characteristics. A weighted average error figure was derived and applied to the results of histogramming emissivities for the simulated tank. It was determined that in some cases, error could be as high as 35 percent on an absolute scale. However, most of the errors calculated in section 3.0 were found to be less than 10 percent, which corresponds to about 6 K apparent temperature error for ambient targets. GRA

N89-28395# University of Southern California, Los Angeles.
INTEGRATED OPTO-ELECTRONIC COMPUTING Final Report, 1 Jul. 1988 - 31 Jan. 1989
W. H. Steier and A. A. Sawchuk 15 Apr. 1989 3 p
(Grant AF-AFOSR-0211-88; AF Proj. 2305)
(AD-A209936; Rept-53-4502-0337; AFOSR-89-0910TR) Avail: NTIS HC A02/MF A01 CSCL 20/6

Research assistants supported by this grant have worked in a variety of optical computing projects. These projects are summarized briefly in this report. GRA

N89-28396# Creative Optics, Inc., Bedford, MA.
APPLICATION OF OPTICAL MEASURE THEORY TO ATMOSPHERIC TEMPERATURE SOUNDING FROM TOVS (TIROS OPERATIONAL VERTICAL SOUNDER) RADIANCES Final Report, Dec. 1988 - May 1989
Robert G. Hohlfeld, Thomas W. Drueding, and John F. Ebersole 2 May 1989 35 p
(Contract F19628-88-C-0151)
(AD-A209955; COI-SR-31; GL-TR-89-0120) Avail: NTIS HC A03/MF A01 CSCL 20/6

Robust algorithms were demonstrated for generating fits in Optical Measure Theory (OMT) to radiance data from the TIROS Operational Vertical Sounder (TOVS). These algorithms generated physically meaningful fits on 100 percent of a test set of 45 TOVS radiance scans, and were successful both on short wavelength (667/cm) and on long wavelength (2250/cm) TOVS data. The resulting OMT temperature profiles exhibit meteorological characteristics and appear to be suitable for determination of atmospheric structure parameters characterizing the large-scale vertical temperature of the atmosphere, and also suitable for generation of input data for numerical weather prediction codes. GRA

N89-28397# Environmental Research Inst. of Michigan, Ann Arbor. Optical Science Lab.
GENERALIZED BEAMFORMING WITH MULTIPLE COMPUTER ORIGINATED HOLOGRAMS Final Report, Oct. 1985 - Oct. 1988
J. N. Cederquist, A. M. Tai, M. T. Eismann, M. A. Stuff, and J. R. Fienup Dec. 1988 102 p
(Contract DAAL03-86-K-0006)
(AD-A210175; ERIM-192400-13-F) Avail: NTIS HC A06/MF A01 CSCL 14/1

Generalized beamforming with optical systems using multiple computer-originated holographic optical elements (HOEs) was studied theoretically, through computer simulations, and through fabrication and experiments. A two HOE system was built for polar formatting of spotlight synthetic aperture radar data and was used with a spatial light modulator and a third phase-correcting HOE for real-time image formation. A two HOE system was designed using a novel iterative algorithm and successfully used for energy-efficient conversion of a Gaussian beam to a uniform far-field beam. A necessary condition was derived that a one-to-one coordinate transformation must satisfy to enable it to be performed with only two optical coordinate tranformations, each using the stationary phase approximation. Because of the importance of computer-generated holograms to this work, a brief study was made of computer-generated hologram fabrication facilities. GRA

N89-27878*# Jet Propulsion Lab., California Inst. of Tech., Pasadena.
STATE-OF-THE-ART FIBER OPTICS FOR SHORT DISTANCE FREQUENCY REFERENCE DISTRIBUTION
G. F. Lutes and L. E. Primas *In its* The Telecommunications and Data Acquisition Report 15 May 1989 p 81-87 (For primary document see N89-27871 22-32)
Avail: NTIS HC A17/MF A01 CSCL 20F

N89-27879*# Jet Propulsion Lab., California Inst. of Tech., Pasadena.
STABILIZED FIBER-OPTIC FREQUENCY DISTRIBUTION SYSTEM
L. E. Primas, G. F. Lutes, and R. L. Sydnor *In its* The Telecommunications and Data Acquisition Report 15 May 1989 p 88-97 (For primary document see N89-27871 22-32)
Avail: NTIS HC A17/MF A01 CSCL 20F

N89-27883*# Jet Propulsion Lab., California Inst. of Tech., Pasadena.
THE EFFECTS OF ATMOSPHERIC TURBULENCE ON PRECISION OPTICAL MEASUREMENTS USED FOR ANTENNA-POINTING COMPENSATION
N. Nerheim *In its* The Telecommunications and Data Acquisition Report 15 May 1989 p 141-148 (For primary document see N89-27871 22-32)
Avail: NTIS HC A17/MF A01 CSCL 20F

N89-27893*# Jet Propulsion Lab., California Inst. of Tech., Pasadena.
EFFECTIVE AMPLIFIER NOISE FOR AN OPTICAL RECEIVER BASED ON LINEAR MODE AVALANCHE PHOTODIODES
C.-C. Chen *In its* The Telecommunications and Data Acquisition Report 15 May 1989 p 216-220 (For primary document see N89-27871 22-32)
Avail: NTIS HC A17/MF A01 CSCL 20F

N89-27894*# Jet Propulsion Lab., California Inst. of Tech., Pasadena.
A VISIBILITY CHARACTERIZATION PROGRAM FOR OPTICAL COMMUNICATIONS THROUGH THE ATMOSPHERE

K. Cowles *In its* The Telecommunications and Data Acquisition Report 15 May 1989 p 221-225 (For primary document see N89-27871 22-32)
Avail: NTIS HC A17/MF A01 CSCL 20F

N89-27903*# Jet Propulsion Lab., California Inst. of Tech., Pasadena.
DSN 70-METER ANTENNA MICROWAVE OPTICS DESIGN AND PERFORMANCE IMPROVEMENTS. PART 1: DESIGN OPTIMIZATION
D. A. Bathker and S. D. Slobin *In its* The Telecommunications and Data Acquisition Report 15 May 1989 p 306-313 (For primary document see N89-27871 22-32)
Avail: NTIS HC A17/MF A01 CSCL 20F

N89-27942 ANT Nachrichtentechnik, Backnang (Germany, F.R.).
CALCULATION OF PLANAR STRUCTURES FOR OPTICAL WAVELENGTH MULTIPLEXERS [BERECHNUNG PLANARER STRUKTUREN FUER OPTISCHE WELLENLAENGENMULTIPLEXER]
Thomas Schwander *In its* Communication Engineering Reports. Fundamental Developments. Theoretical Work Nov. 1988 p 121-127 In GERMAN (For primary document see N89-27928 22-32)
Copyright Avail: Fachinformationszentrum Karlsruhe, 7514 Eggenstein-Leopoldshafen 2, Fed. Republic of Germany, 35 DM

N89-28191*# National Aeronautics and Space Administration. Goddard Space Flight Center, Greenbelt, MD.
RADIANCE STANDARDS Abstract Only
D. L. Lester *In its* Laboratory for Oceans 1988 p 271-274 (For primary document see N89-28118 22-48)
Avail: NTIS HC A12/MF A01 CSCL 20F

75 PLASMA PHYSICS

Includes magnetohydrodynamics and plasma fusion.
For ionospheric plasmas see *46 Geophysics*. For space plasmas see *90 Astrophysics*.

N89-28398# Department of Energy, Washington, DC. Office of the Deputy Assistant Secretary for Oil, Gas, Shale and Special Technologies.
MHD (MAGNETOHYDRODYNAMICS) PROGRAM PLAN, FY 1989
May 1989 43 p
(DE89-012232; DOE/FE-0129) Avail: NTIS HC A03/MF A01
The essential elements of the current program, which is a continuation of the program outlined in the FY 1988 MHD Program Plan, are to: develop technical and environmental data for the integrated MHD topping cycle system through long-term (1000 hours) proof of concept (POC) testing; develop technical and environmental data for the integrated MHD bottoming cycle subsystem through long-term (4000 hours) POC testing; design and construct a seed regeneration system capable of independent operation, using spent seed materials from the MHD process; prepare a conceptual design for an MHD retrofit plant; and continue system studies and supporting research necessary for system testing. Results of the topping cycle POC tests at the Component Development and Integration Facility (CDIF), coupled with the bottoming cycle POC test results obtained at the Coal Fired Flow Facility (CFFF), and the seed regeneration POC effort will provide the critical engineering data base for the private sector's final decision on proceeding with the design, construction, and operation of an MHD retrofit. The development schedule, decision points, and resource requirements are discussed. As part of the MHD program, international activities of several nations are monitored and evaluated through contact with the international MHD scientific and technical community. DOE

N89-28399# Nagoya Univ. (Japan). Inst. of Plasma Physics.
ROLE OF EDGE MAGNETIC SHEAR ON THE LIMITER H-MODE TRANSITION OF THE JIPP T-IIU TOKAMAK
K. Toi, K. Kawahata, S. Morita, T. Watari, R. Kumazawa, K. Ida, A. Ando, Y. Oka, M. Sakamoto, and Y. Hamada et al Apr. 1989 17 p Prepared in cooperation with Chubu Univ., Kasugai, Japan
(IPPJ-906; ISSN-0469-4732) Avail: NTIS HC A03/MF A01
In a circular cross section plasma bounded by a limiter, the H-mode transition is triggered by rapid ramp-down in a plasma current during additional heating, even in the case that the edge electron temperature decays gradually prior to the transition. This result suggests that the enhancement of a magnetic shear near the plasma edge by the ramp-down plays a crucial role on the transition, and that the transition in a limiter-bounded plasma is essentially governed by the current density profile near the edge. Author

N89-28400# Nagoya Univ. (Japan). Inst. of Plasma Physics.
EXTENSION OF STELLARATOR APPROXIMATION IN MAGNETOHYDRODYNAMIC EQUILIBRIUM AND STABILITY OF TOROIDAL HELICAL SYSTEMS
Jiro Todoroki Apr. 1989 31 p
(IPPJ-905) Avail: NTIS HC A03/MF A01
Formulation is made to solve a 3-D MHD equilibrium problem on the basis of the coordinate transformation. The 3-D problem is divided into three steps: (1) the hyperbolic equations to determine the coordinate transformation; (2) averaged equation in 2-D; and (3) the 3-D elliptic equation to deal with magnetic potential. The usual stellarator approximation or averaging method is regarded as the first step of the iteration procedure to get the solution of the full 3-D problems. In formulating linear stability problem, the stellarator ordering is required; the resonance effect should be omitted in the averaging formulation. Some comparison is made to check the validity of the above formulation. Author

N89-28401# Nagoya Univ. (Japan). Inst. of Plasma Physics.
EXPERIMENTAL STUDY ON THE DEPOSITION PROFILE OF THE ICRF POWER AND ELECTRON THERMAL DIFFUSIVITY
Y. Ogawa, R. Ando, E. Kako, K. Kawahata, Y. Kawasumi, S. Morita, T. Watari, R. Akiyama, Y. Hamada, and S. Hirokura Apr. 1989 27 p
(IPPJ-908; ISSN-0469-4732) Avail: NTIS HC A03/MF A01
In Ion Cyclotron Range of Frequencies (ICRF) heating experiments the deposition profile in electrons was derived experimentally, and comparison with theory was performed. It was found that the deposition profile is relatively broad (Prf,e(r) = Prf,e(0)(1-(r/a)2)k with k = 1.8), and this is interpreted in terms of characteristics of the mode-converted Ion Bernstein Wave. The distribution of the RF power to each species (electrons, hydrogen and deuterium ions) is in good agreement with theoretical predictions. With the deposition profile experimentally obtained, the electron thermal diffusivity Xe has been calculated, resulting in Xe approximately 0.65 m(2)/s at antineutron e = 9x10(19) m(-3). Author

N89-28402# Georgia Inst. of Tech., Atlanta. Fusion Research Center.
REVIEW OF EFFECTS OF NBI (NEUTRAL BEAM INJECTION) AND ROTATION ON PLASMA TRANSPORT IN TOKAMAKS
Weston M. Stacey, Jr. Jun. 1989 20 p
(Contract DE-AS05-78ET-52025)
(DE89-014109; GTFR-91) Avail: NTIS HC A03/MF A01
The experimental and theoretical indications of effects of unbalanced neutral beam injection and plasma rotation on plasma transport in tokamaks are reviewed. DOE

N89-28403# Los Alamos National Lab., NM.
THE STABILITY OF THE HIGH-DENSITY Z-PINCH
A. H. Glasser and R. A. Nebel 1989 16 p Presented at the 2nd International Conference on High-Density Pinches (ICHOP-2), Laguna Beach, CA, 26-28 Apr. 1989
(Contract W-7405-eng-36)
(DE89-014276; LA-UR-89-2188; CONF-8904107-7) Avail: NTIS HC A03
Fiber-initiated High Density Z-Pinches at Los Alamos, NRL, and Karlsruhe have shown anomalously good stability. Kink modes

are never seen, and sausage modes are at least delayed until late in the discharge. The success of these devices in reaching fusion conditions may depend on maintaining and understanding this anomalous stability. Two numerical methods were developed to study the stability in the regime where fluid theory is valid. While the methods are applicable to all modes, they are described only for the m = 0 sausage mode. The appearance of sausage modes late in the discharge and the total absence of kink modes suggest that an understanding of sausage modes is more urgent, and it is also simpler. DOE

N89-28404# Applied Microwave Plasma Concepts, Carlsbad, CA.
A TWO-STREAM PLASMA ELECTRON MICROWAVE SOURCE FOR HIGH-POWER MILLIMETER WAVE GENERATION, PHASE 1 Final Report, 1 Aug. 1988 - 31 Jan. 1989
Gareth E. Guest and Raphael A. Dandl 29 Mar. 1989 64 p
(Contract F49620-88-C-0101)
(AD-A209942; AMPC-033-038; AFOSR-89-0840TR) Avail: NTIS HC A04/MF A01 CSCL 20/9

A novel high power millimeter/microwave source is proposed in which one or more pairs of interpenetrating streams of electrons, flowing through a background plasma in a static magnetic field are used to generate a hot-electron plasma that is confined in a mirror-like magnetic field. Energy stored in the anisotropic, hot-electron plasma is then used to amplify pulses of unstable plasma waves to large amplitude by selective deactivation of mechanisms that stabilize the hot-electron plasma during the energy accumulation phase when the density of hot electrons is rapidly increased through the beam-plasma interaction. The Phase 1 program has yielded a design for an experimental arrangement capable of verifying the key aspects of this novel source concept, as well as a theoretical framework for interpreting the empirical Phase 2 results produced by the experimental device and extrapolating those results to evaluate the suitability of the proposed source to meet the requirements of various high power microwave and millimeter wave defense and industrial applications. The experiments will be carried out in a timely and cost-effective way by employing the AMPHED (a CW magetic mirror) experimental facility at Applied Microwave Plasma Concepts (AMPC). GRA

N89-27720# Massachusetts Inst. of Tech., Cambridge.
THE INTERACTION BETWEEN A POSITIVELY BIASED CONDUCTOR ON A HIGH VOLTAGE SOLAR ARRAY AND A PLASMA
Daniel E. Hastings *In* DGLR, DGLR/AIAA/JSASS 20th International Electric Propulsion Conference: Proceedings 1988 p 115-120 (For primary document see N89-27707 22-20)
Avail: NTIS HC A99/MF E03

76 SOLID-STATE PHYSICS

Includes superconductivity.

For related information, see also *33 Electronics and Electrical Engineering* and *36 Lasers and Masers.*

N89-28405# National Inst. of Standards and Technology, Boulder, CO. Electromagnetic Technology Div.
HIGH-TEMPERATURE SUPERCONDUCTIVITY: ABSTRACTS OF NIST (NATIONAL INSTITUTE OF STANDARDS AND TECHNOLOGY) PUBLICATIONS, 1987-1988 Final Report
Mary E. DeWeese, ed., Robert A. Kamper, ed., and Ronald M. Powell, ed. Nov. 1988 37 p
(PB89-148340; NIST/SP-759; LC-88-600602) Avail: NTIS HC A03/MF A01; also available SOD HC $2.00 as SN003-003-02902-5 CSCL 20L

Abstracts were collected from 61 papers published between March 1987 and May 1988 covering various aspects of superconductivity research. The work of nine divisions of the National Institute of Standards and Technology (formerly the National Bureau of Standards), in both Boulder, Colorado, and Gaithersburg, Maryland, is represented. GRA

N89-28406# Central Inst. of Physics, Bucharest (Romania).
SUPERCONDUCTIVITY IN THE Ba(0.69)Y(0.46)CuO(3.15-DELTA) COMPOUND
I. Ursu, E. Labusca, I. Mihai, A. Novacu, H. Petrascu, and M. Petrascu Oct. 1987 5 p
(DE88-706000; ICEFIZ-CS-12-1987) Avail: NTIS (US Sales Only) HC A02/MF A01

High critical temperature T sub c equals 119 K and onset temperature T equals 135 K was observed in Ba(0.69)Y(0.46)CuO-(3.15 - delta) compound. This compound corresponds to the calculated admixture of 80 percent of the superconducting Ba2YCuO(9 - delta) phase, with 20 percent of the semiconductor Y2BaCuO5 phas. A decrease in time was observed for T sub c , but also for the temperature width delta T. The zero resistence point and the onset temperature are not significantly modified after a period of 3 months. DOE

N89-28407# Massachusetts Inst. of Tech., Cambridge. Dept. of Materials Science and Engineering.
EVIDENCE AGAINST THE EXISTENCE OF STRONG DIFFUSE X-RAY SCATTERING FROM GOLD TWIST BOUNDARIES AT ROOM TEMPERATURE
I. Majid, P. D. Bristowe, and R. W. Balluffi May 1989 7 p
(Contract DE-FG02-87ER-45310)
(DE89-012726; DOE/ER-45310/18) Avail: NTIS HC A02/MF A01

Research on diffuse scattering from twist boundaries in gold is reported. In order to obtain an unambiguous measure of the diffuse scattering from the boundary, we developed a technique in which the total diffuse scattering is measured from the same specimen containing the boundary, and then not containing the boundary, and then determining any difference. This is accomplished by first measuring the diffuse scattering from the bilayer specimen containing the boundary. The specimen is then removed from its polymer film support and annealed gently at 175 C in order to convert the metastable layered bicrystal into a more stable structure consisting of columnar grains separated by short transverse boundaries. In this process, the original flat twist boundary is eliminated. The specimen is then remounted on a polymer film support in as reproducible a manner as possible, and the diffuse scattering is again measured. DOE

N89-28408# Cornell Univ., Ithaca, NY. Dept. of Materials Science and Engineering.
EXPERIMENTAL STUDIES OF THE STRUCTURE OF GRAIN BOUNDARIES Progress Report
S. L. Sass Feb. 1989 16 p
(Contract DE-FG02-85ER-45211)
(DE89-012954; DOE/ER-45211/13) Avail: NTIS HC A03/MF A01

The long reach goals are to obtain information on the atomic structure and properties of grain boundaries in bcc metals and ceramics, to understand how solute segregation influences grain boundary structure and causes boundaries to become embrittled in Fe-base alloys, to understand the role of boron and non-stoichiometry in making brittle boundaries in Ni3Al ductile, and to understand how solute segregation influences the boundary structure in ceramic materials. The topics covered are: the influence of solute segregation on the structure of grain boundaries in Fe-base alloys; and the influence of boron segregation on the structure of grain boundaries in Ni3Al. DOE

N89-28409# California Univ., Berkeley. Lawrence Berkeley Lab. Materials and Chemical Sciences Div.
BIBLIOGRAPHY OF HIGH-T SUB c SUPERCONDUCTING FILMS
J. Talvacchio Jan. 1989 62 p Prepared in cooperation with Westinghouse Electric Corp., Pittsburgh, PA
(Contract DE-AC03-76SF-00098)
(DE89-013395; LBL-26578) Avail: NTIS HC A04/MF A01

An effort is made to make bibliographic information on high T sub c superconductor films available to those who cannot access the on-line database at the Westinghouse R and D Center. The

database contains a growing list of references (approx. 5000) each of which is identified by a set of two letter keywords. The database is used the same way as as INSPEC's, but its fixed set of standard keywords enables the user to obtain a complete list of references on keyworded topics. Since a single keyword (or search term) such as sputtering creates a bibliography that is too long for practical use, the database is used most effectively by combining a series of keywords using Boolean algebra to identify a handful of relevant references. The structure of this document is intended to present the subset of papers concerning high T sub c films (725 papers) in a compact format as a substitute for on-line searches. Rather than listing separate bibliographies for each of the 185 keywords, a single list of all the references is contained in Section 6, and indices based on the keywords are contained in Sections 3 to 5. This is a true bibliography and does not contain any informative text. DOE

N89-28410# Argonne National Lab., IL. Materials Science Div.
GRAIN BOUNDARIES IN SILICON FROM ZERO TEMPERATURE THROUGH MELTING
S. R. Phillpot and D. Wolf Dec. 1988 16 p Presented at the Symposium on Interface Structure and Reactions, San Francisco, CA, 23 Oct. 1988 Submitted for publication
(Contracts W-31-109-eng-38; N00014-88-F-0019)
(DE89-013186; CONF-8810377-1) Avail: NTIS HC A03/MF A01

Recent atomistic simulations of silicon grain boundaries are reviewed and compared with similar studies in metals. Three aspects are discussed in detail: (1) the zero-temperature structure-energy correlation, (2) the elastic anomalies near a grain boundary at zero temperature, and (3) the high-temperature stability of a twist boundary and its role in thermodynamic melting. In each case striking similarities with studies on metals are found. DOE

N89-28411# Brookhaven National Lab., Upton, NY. Chemistry Dept.
SUPEREXCHANGE COUPLING MECHANISMS FOR ELECTRON TRANSFER PROCESSES
M. D. Newton 1989 14 p Presented at the 22nd Jerusalem Symposium on Quantum Chemistry, Jerusalem, Israel, 15 May 1989
(Contract DE-AC02-76CH-00016)
(DE89-013568; BNL-42831; CONF-8905146-1) Avail: NTIS HC A03/MF A01

Electron transfer matrix elements for electron exchange between various pairs of transition metal complexes in close contact have been calculated and analyzed for a variety of approach geometries for the two reactants. The coupling between the nominal metal ion donor/acceptor sites is achieved by superexchange of the hole type arising from ligand-to-metal charge transfer (LMCT), the dominant ligand-field interaction for the electron-donor ligands considered (H sub 2 O, NH sub 3, the cyclopentadienide anion). The pronounced variations of H sub if with geometry are not correlated with the separation distance of the metal ions (between which the direct overlap is negligible) and span the range from non-adiabatic to strongly adiabatic electronic coupling. The values for metallocene/metallocinium redox pairs bracket recently reported experimental values. Analysis of the results using the method of corresponding orbitals demonstrates the validity of an effective 1-electron model for the electron transfer process to within about 10 percent for the class of systems considered. A higher-order superexchange mechanism was encountered for the Co(NH sub 3) sub 6 (2+/3+) exchange process, in which the LMCT-driven hole-transport mechanism couples excited local states of the metal ions, which in turn are connected to the corresponding ground states by spin-orbit mixing. This mechanism yields on electronic transmission factor within two orders of magnitude of unity. DOE

N89-28412# Sandia National Labs., Albuquerque, NM.
PHONON-DRAG THERMOELECTRIC POWER IN HIGH MAGNETIC FIELDS IN HETEROJUNCTIONS
S. K. Lyo 1989 10 p Presented at the 4th International Conference on Modulated Semiconductor Structures, Ann Arbor, MI, 17 Jul. 1989
(Contract DE-AC04-76DP-00789)
(DE89-013921; SAND-89-0542C; CONF-890746-1) Avail: NTIS HC A02/MF A01

A theory is presented for the low-temperature (T) phonon-drag thermopower S sub xx in a semiconductor heterojunction in a strong magnetic field. Gigantic quantum oscillations (much larger than electron-diffusion contributions) are obtained. When the Landau-level width is larger than k sub B/T, the one-phonon intra-Landau-level absorption and emission processes are dominant. In the opposite limit, the two-phonon Raman processes give major contributions. The temperature and field dependences of S sub xx agree reasonably with recent data in GaAs Al sub x Ga sub 1-x/As heterojunctions. Effects of localized states on S sub xx are discussed. DOE

N89-28413# Stanford Univ., CA.
APPLICATION OF QUATERNARY PHASE DIAGRAMS TO COMPOUND SEMICONDUCTOR PROCESSING Progress Report, 1 Apr. - 31 Dec. 1988
Alan Schwartzman 1989 20 p
(Contract DE-FG03-84ER-45085)
(DE89-014537; DOE/ER-45085/T1) Avail: NTIS HC A03/MF A01

Work is summarized for phase equilibria in II-VI quaternary systems over the last year. In general, the phase diagram depicts the geometric relationship among thermodynamic variables for phases in equilibrium with each other under an established set of conditions. Each type of thermodynamic system has a particular set of intensive variables which, when plotted against each other, best elucidate the equilibrium conditions. Isobaric, isothermal phase diagrams are used to predict solid state reactions in ternary and quaternary systems. This research has illustrated that a rigorous and methodical technique using the computer to construct quaternary phase diagrams can be successfully applied to a wide range of II-VI semiconductor systems, even for systems with solid solubility. DOE

N89-28414# Sandia National Labs., Albuquerque, NM.
DIAMAGNETIC SHIELDING AND FLUX CREEP IN A Tl-Ba-Ca-Cu-O THIN FILM
E. L. Venturini, J. F. Kwak, D. S. Ginley, R. J. Baughman, and B. Morosin 1989 3 p Presented at the International Conference on Materials and Mechanisms of Superconductivity. High-Temperature Superconductors, Stanford, CA, 23 Jul. 1989
(Contract DE-AC04-76DP-00789)
(DE89-014550; SAND-89-0506C; CONF-890718-6) Avail: NTIS HC A02/MF A01

Static magnetization data for a superconducting thin film based on the Tl-Ba-Ca-Cu-O system are presented and discussed. The film, deposited by electron-beam evaporation onto a single crystal SrTiO3 substrate, consists of large grains of two superconducting structural phases with their crystallographic c axes normal to the substrate. It exhibits substantial transport critical current density, large diamagnetic shielding, and activated flux creep, consistent with strong intergranular links but weak flux pinning. DOE

N89-28415# Argonne National Lab., IL.
THE TOPOLOGICAL STRUCTURE OF GRAIN BOUNDARIES
N. Rivier Jun. 1989 12 p Presented at the Les Houches International Workshop on Number Theory and Physics, Les Houches, France, 7 Mar. 1989
(Contract W-31-109-eng-38)
(DE89-014676; CONF-8903140-1) Avail: NTIS HC A03/MF A01

Grain boundaries are shown to be quasiperiodic tillings made of inflatable sequences of structural units. A general grain boundary is a quasiperiodic grid of dislocations with the same inflation multiplier (a quadratic irrational) in every direction. DOE

N89-28416# International Centre for Theoretical Physics, Trieste (Italy).
DIFFERENTIAL GEOMETRIC ASPECTS OF THE THEORY OF FERROELECTRICITY
V. T. Khosiainov Nov. 1988 12 p Submitted for publication
(DE89-612191; IC-88/365) Avail: NTIS (US Sales Only) HC A03/MF A01

In connection with the problem of the ferroelectricity a differential formalism is developed as a tool to describe the fine electronic properties in solids. This includes the gauge invariant definition of the differentiation in k-space (position operator), the notion of holonomy group and characteristic gauge field in k-space of electron states. A variational principle and possible solutions of resulting field equations are discussed. A criterion for the appearance of the ferroelectricity is proposed. DOE

N89-28417# Brasilia Univ. (Brazil). Dept. de Fisica.
THEORY OF PHOTON-DRAG EFFECT IN BULK MAGNETIC SEMICONDUCTORS
C. Rodrigues-Costa and O. A. C. Nunes Sep. 1988 37 p Submitted for publication
(DE89-612214; UnB-FIS-10/88) Avail: NTIS (US Sales Only) HC A03/MF A01

The theory of the photo-drag effect in magnetic semiconducting crystals is considered using the s-d (or s-f) exchange model of interaction between the electron and the magnon. An equation is derived for the electric field generated by this effect. Numerical examples are given for CdCr2SE4 crystals. DOE

N89-28418# Joint Inst. for Nuclear Research, Dubna (USSR). Lab. of Nuclear Problems.
GLASSY BEHAVIOUR OF YBa2Cu3O7
S. Sahling 1988 8 p Submitted for publication
(DE89-613399; JINR-E-8-88-638) Avail: NTIS (US Sales Only) HC A02/MF A01

Long time power released in YBa2Cu3O7 after rapid cooling from the equilibrium temperature T sub 1 (2.35 K less than or equal to T sub 1 less than or equal to 15.11 K) to T sub 0 = 1.5 K and the heat capacity (1.2 K less than or equal to T less than or equal to 100 K) were measured. The observed power release is similar to those of amorphous solids. The resulting density of states of two level systems is close to the values obtained from heat capacity and acoustic measurements from heat capacity and acoustic measurements. DOE

N89-28419# Wisconsin Univ., Madison. Dept. of Chemistry.
SEMICONDUCTOR-OLEFIN ADDUCTS. PHOTOLUMINESCENT PROPERTIES OF CADMIUM SULFIDE AND CADMIUM SELENIDE IN THE PRESENCE OF BUTENES Technical Report, 31 Oct. 1988
Gerald J. Meyer, Larry K. Leung, Jim C. Yu, George C. Lisensky, and Arthur B. Ellis 12 May 1989 19 p Submitted for publication
(Contract N00014-85-K-0631)
(AD-A208348; UWIS/DC/TR-89/3) Avail: NTIS HC A03/MF A01 CSCL 07/2

Direct evidence for adduct formation between butenes and etched, single-crystal n-CdS and n-CdSe(CdS(e)) surfaces has been obtained from photoluminescence (PL) measurements. Exposure of CdS(e) to butenes causes enhancement of the solids' band edge PL relative to a N2 ambient. For 30 percent mixtures of the olefins in N2, the magnitude of the enhancement follows the order, 1,3-butadiene is greater than cis-2-butene trans-2-butene is greater than isobutylene 1-butene, and correlates with the olefin basicities, based on photoionization potentials. Enhancements in PL intensity can be fit to a dead-layer model, allowing the determination of the reduction in depletion width in the semiconductor resulting from olefin exposure; depletion width reductions reach a few hundred Angstroms for adducts of 1,3-butadiene with CdS(e). The PL changes were used in conjunction with the Langmuir adsorption isotherm model to yield equilibrium constants for adduct formation of 1,3-butadiene with CdS(e) of 9 plus or minus 4/atm at 293 K. Surface interactions that may contribute to the observed PL changes are discussed. GRA

N89-28420# Rensselaer Polytechnic Inst., Troy, NY. Dept. of Chemistry.
DECOMPOSITION KINETICS AND FILM FORMATION OF AN ORGANOMETALLIC PRECURSOR TO SiC ON Si(100) Technical Report No. 6
Leonard Interrante, Wei Lee, Klaus Lenz, Krishna Rajan, and John B. Hudson 15 May 1989 23 p Submitted for publication
(Contract N00014-85-K-0632; NSF CHE-84-06078)
(AD-A208384; TR-6) Avail: NTIS HC A02/MF A01 CSCL 07/2

The absorption and decomposition kinetics of the SiC precursor (CH3Si(H)mu(CH2)2Si(CH3) CH2SiH2CH3) have been studied on the Si(100) surface using a combination of molecular beam mass spectrometry and Auger electron spectroscopy. The intact precursor adsorbs with a heat of adsorption of about 10 kcal/mol. The decomposition rate becomes measurable at about 800 K, and increases with increasing temperatures. The resulting films are stoichiometric, polycrystalline SiC, with partial epitaxial orientation relative to the substrate. GRA

N89-28421# Hypress, Inc., Elmsford, NY.
MM WAVECOMPONENTS - SIS (SUPERCONDUCTOR-INSULATOR-SUPERCONDUCTOR) MIXERS Final Report, Nov. 1986 - Dec. 1988
Stephen R. Whiteley 26 Apr. 1989 50 p
(Contract F49620-87-C-0014; AF Proj. 3005)
(AD-A208632; AFOSR-89-0620TR) Avail: NTIS HC A03/MF A01 CSCL 09/1

Superconductor-Insulator-Superconductor (SIS) tunnel junction mixers are known to provide ultra-high sensitivity receiver applications above 30 GHz. In this two year (Phase 2) program, HYPRES, in collaboration with the National Radio Astronomy Observatory, developed novel fully integrated SIS mixer circuits, and demonstrated a unique high efficiency cooling system. The integrated SIS mixer chip contains, aside from the actual mixer elements, passive tuning components, an IF filter, a coplanar transmission line, and a waveguide coupler, necessary components heretofore realized off-chip. Fabrication of the integrated mixer required development of a nine level process and optimization of the process dependent electrical parameters of the SIS devices. The device performs efficiently in the range of 75-115 GHz. A novel dewar-based cooler, which makes use of the extremely low thermal conductivity of the fused silica chip substrate to achieve an incremental thermal load of 25 mW, was fabricated and demonstrated. Such a cryostat allows relatively long term unattended operation of SIS, or other, cryogenic devices. GRA

N89-28422# Naval Weapons Center, China Lake, CA. Chemistry Div.
CRYSTAL CHEMISTRY, SYNTHESIS, AND CHARACTERIZATION OF INFRARED OPTICAL MATERIALS
D. O. Kipp, C. K. Lowe-Ma, and T. A. Vanderah 1988 10 p Presented at the Materials Research Society Meeting, San Diego, CA, 24-28 Apr. 1989 Sponsored by ONR
(AD-A208723) Avail: NTIS HC A02/MF A01 CSCL 07/4

Non-oxide inorganic compounds such as sulfides, phosphides, and mixed-anion sulfide-phosphides are of interest as possible infrared window materials. Our research on the solid state chemistry and structure-property relationships of these materials includes the directed synthesis of new compounds as well as the study of compounds that have been reported in the literature but which have been incompletely characterized for this application. The present work includes investigations of three ternary sulfide systems: ZnGa2S4, AIn2S4(A = Ca, Sr, Ba), and CaY2S4. Samples were prepared in polycrystalline form and/or as crystals. New compounds were obtained in our studies of the CaIn2S4, SrIn2S4, and CaY2S4 systems. Compounds were characterized by X-ray diffraction, elemental analysis, Fourier Transform Infrared Radiometry, and thermogravimetric analysis. GRA

N89-28423# Brown Univ., Providence, RI. Dept. of Chemistry.
GROWTH AND CHARACTERIZATION OF ZINC SULFIDE FILMS BY CONVERSION OF ZINC OXIDE FILMS WITH H2S
Y-M. Gao, P. Wu, J. Baglio (GTE Labs., Inc., Waltham, MA.), Kirby Dwight, and A. Wold 30 May 1989 9 p Sponsored in part by Eastman Kodak Co., Rochester, NY
(Contract N00014-85-K-0177; NSF DMR-88-03184)
(AD-A208727; TR-11) Avail: NTIS HC A02/MF A01 CSCL 20/12

Zinc sulfide is an IR window material and a transparent semiconductor with a large direct band gap. It also possesses piezoelectric, photoconductive and electroluminescent properties. Thin films of zinc sulfide can be utilized for infrared antireflection coatings, Light-Emitting Diodes (LEDs), electroluminescent (EL) displays, multilayer dielectric filters, optical phase modulation and light guiding in integrated optics. In recent years, there has been a large amount of effort directed at the growth of high quality films of ZnS. Various fabrication techniques have been employed, such as ion beam sputtering, Atomic Layer Epitaxy (ALE), Molecular Beam Epitaxy (MBE), metal organic chemical vapor deposition and spray pyrolysis. Zinc sulfide films were prepared by conversion of zinc oxide films in the presence of hydrogen sulfide. The films which contained both the hexagonal and cubic forms of zinc sulfide were shown to be uniform and gave a measured band gap of 3.65 eV. The electrical resistances of the films prepared were greater than 10 to the 7th ohms. GRA

N89-28424# Brown Univ., Providence, RI. Dept. of Chemistry.
PREPARATION AND CHARACTERIZATION OF SEVERAL CONDUCTION TRANSITION METAL OXIDES
Aaron Wold and Kirby Dwight 24 May 1989 13 p
(Contract N00014-86-K-0234)
(AD-A208895; TR-21) Avail: NTIS HC A03/MF A01 CSCL 20/12

The structure-property relationships of several conducting transition metal oxides, as well as their preparative methods, are presented. The importance of preparing homogenous phases with precisely known stoichiometry is emphasized. A comparison is also made of the various techniques used to prepare both polycrystalline and single crystal samples. For transition metal oxides, the metallic properties are discussed either in terms of metal-metal distances which are short enough to result in metallic behavior, or in terms of the formation of a conduction band resulting from covalent metal-oxygen interactions. Metallic behavior is observed when the conduction bands are populated with either electrons or holes. The concentration of these carriers can be affected by either cation or anion or anion substitutions. The discussion in this presentation will be limited to the elements Re, Ti, V, Cr, Mo and Cu. GRA

N89-28425# Massachusetts Inst. of Tech., Cambridge. Dept. of Mechanical Engineering.
POLYCRYSTALLINE PLASTIC DEFORMATION AND TEXTURE EVOLUTION FOR CRYSTALS LACKING FIVE INDEPENDENT SLIP SYSTEMS Interim Technical Report No. 20, 1988 - 1989
David M. Parks and Said Ahzi 29 May 1989 45 p
(Contract N00014-86-K-0768)
(AD-A208902) Avail: NTIS HC A03/MF A01 CSCL 20/2

The kinematic constraints are elucidated, and the corresponding kinematic indeterminacy of part of the deviatoric stress tensor, in a rigid-viscoplastic single crystal lacking five independent slip systems. The indeterminate stress component is a Lagrange multiplier enforcing the kinematic constraint, and it must be determined from equilibrium considerations. A simple polycrystalline model is constructed which precisely satisfies local kinematic constraints as well as global compatibility. Volume-average global stresses are obtained by approximating the local constraint stress as the correspcnding projection of the (to-be-determined) global stress. Applications of the model to hexagonal crystals without pyramidal slip, and to large deformation and texturing of orthorhombic polycrystalline materials (olivine; HDPE) are made. GRA

N89-28426# Massachusetts Inst. of Tech., Lexington. Lincoln Lab.
SOLID STATE RESEARCH Quarterly Technical Report, 1 May - 31 Jul. 1988
Alan L. McWhorter 7 Mar. 1989 100 p
(Contract F19628-85-C-0002)
(AD-A209645; Rept-1988; Rept-3; ESD-TR-88-209) Avail: NTIS HC A05/MF A01 CSCL 20/12

The Solid State division of Lexington Lincoln Lab reports on its progress for this quarter. The areas of study are: Time Dye Laser Using Integrated Optics; GaP Microlenses by Mass Transport; A New OMVPE Reactor for Growth of InP and Related Alloys; Microchannel Heat Sinks for Two-Dimensional High Power-Density Diode Laser Arrays; Novel Scalloped-Mirror Diffraction-Coupled Laser Arrays; Three-Mirror Ti:Al2O3 Ring Laser Cavity; Femtosecond TiAl2O3 Injection-Seeded Laser; End-Pumped Nd:LaF3 and Nd:LaMgA11O19 Lasers; Single Frequency Mixing of Frequency Modulated Laser Radiation; Vertical Rotating Disk OMVPE Reactor; New Electron Beam Lithography System; Dry Etching Induced Damage on Vertical Sidewalls of GaAs Channels; Homoepitaxial Semiconducting Diamond; 420 X 420 CCD Frame Transfer Imager; Technique for Monolithically Integrating GaAs/AlGaAs Lasers of Different Wavelengths; Superconducting Thin Films of BiSrCaCuO; and Nb Thin Film Capacitors for Superconductive Circuits. GRA

N89-28427# Pittsburgh Univ., PA. Surface Science Center.
THE ORIENTATION OF CHEMICAL BONDS AT SURFACES: A KEY TO UNDERSTANDING THE STRUCTURE AND BONDING OF SURFACE SPECIES Final Report, 15 Apr. 1986 - 14 Apr. 1989
John T. Yates, Jr. 22 Jun. 1989 18 p
(Grant AF-AFOSR-0107-86; AF Proj. 2303)
(AD-A209833; AFOSR-89-0928TR) Avail: NTIS HC A02/MF A01 CSCL 20/2

The development and use of the digital ESDIAD method for studying the molecular structure and the dynamics of adsorbates on metal single crystal surfaces is examined. A number of new findings were made involving the following phenomena: (1) First direct observation of the hindered rotation of a chemisorbed molecule; (2) Observation of hydrogen bonding forces between adsorbates causing hinderance of molecular rotation; (3) Structural determination of bonding site for coordinatively unsaturated radical species, PF2 and PF on Ni(111); (4) Discovery of alkali metal sensitization of H+ ESD yield on metals; and (E) Discovery of copious metastable CO yield in ESD from CO on Pt(111). GRA

N89-28428# Princeton Univ., NJ. Dept. of Electrical Engineering and Computer Science.
TRANSPORT AND SUBMILLIMETER WAVE SPECTROSCOPY OF GaAs/Al SUB xGa SUB 1-xAs HETEROSTRUCTURES Final Report, Jul. 1985 - Sep. 1988
D. C. Tsui 16 Jun. 1989 43 p
(Grant AF-AFOSR-0204-85; AF Proj. 2305)
(AD-A209836; AFOSR-89-0934TR) Avail: NTIS HC A03/MF A01 CSCL 20/12

The research emphasized the physics of the electronic processes in GaAs/Al(x)Ga(1-x)As and In(x)Ga(1-x)As/InP heterojunction thin film structures and focuses in two directions: one in superlattice materials and the other in submillimeter wave spectroscopy. After a brief description of the accomplishments in both directions, together with a list of the publications of work supported by the contract, a detailed account is made of the systematic investigation of transport through In(x)Ga(1-x)As/InP superlattices grown by Chemical Beam Epitaxy. GRA

N89-28429# Stanford Univ., CA. Solid-State Electronics Lab.
DEVELOPMENT OF SUPERLATTICES FOR ULTRA HIGH-SPEED ELECTRONIC AND OPTOELECTRONIC DEVICES Final Technical Report, 1 Apr. 1986 - 31 Mar. 1989
James S. Harris 31 Mar. 1989 99 p
(Contract N00014-86-K-0530)
(AD-A209874) Avail: NTIS HC A05/MF A01 CSCL 20/12

The remarkable advances in computation and communications technologies in the last half century have been made possible by the invention and development of a vast array of solid state electronic and optical devices. By striving to achieve higher speeds of operation, and greater levels of integration, ever more powerful computing and communications tools have been created. The transistor, the laser and a host of other devices have been invented and reinvented many times in a multitude of materials systems. As materials growth and fabrication technologies continue to improve, it becomes possible to use new physical phenomena in solid state devices, in addition to optimizing the performance of existing devices. Optical interconnects are attracting attention as a means to overcome the interconnection bottleneck in high speed electronic systems. The best type of light source for such schemes is sometimes a continuous-wave laser used in conjunction with a light modulator, which acts as an external switch. Modulators that operate in perpendicular geometry, with light directed normal to the plane of the device, allow simple fabrication of two-dimensional arrays: these are of interest for multiple parallel optical interconnections and for optical information processing. GRA

N89-28430# Manchester Coll. of Science and Technology (England). Dept. of Chemistry.
ZINC TELLURIDE GROWTH ON InP Annual Report
J. O. Williams and Nicholas Maung 14 Jan. 1989 51 p
(Grant AF-AFOSR-0109-88; AF Proj. 2301)
(AD-A209924; EOARD-TR-89-09) Avail: NTIS HC A04/MF A01 CSCL 20/12

Initial studies have concentrated on the preparation of epitaxial Zinc Selenide on Indium Phosphide (100) substrates and an optimum bakeout procedure for the substrates determined. Subsequently, the doping of ZnSe with small amounts of Tellurium (up to ca 5 at percent) was achieved and the structural, compositional and optical properties of the epitaxial layers investigated. It was demonstrated by photoluminescence measurement that in small concentrations Te acts as an isolated isoelectronic trap in ZnSe and at higher concentrations clusters of Te atoms form. This results in broadened photoluminescence emission peaks. It proved impossible with our atmospheric pressure MOCVD reactor and using a conventional source of Te to prepare epitaxial layers of the ternary ZnSe(1-y)Te(y) with Te concentration in excess of ca 5 at percent. GRA

N89-28431# Massachusetts Inst. of Tech., Lexington. Lincoln Lab.
SOLID STATE RESEARCH Quarterly Technical Report, 1 Aug. - 31 Oct. 1988
Alan L. McWhorter 15 Nov. 1988 84 p
(Contract F19628-85-C-0002)
(AD-A209969; Rept-88-4; ESD-TR-88-250) Avail: NTIS HC A05/MF A01 CSCL 20/3

The solid state research of the Lexington Lincoln Lab is review for this time period. Areas of study are: Microwave Bandpass Modulators in Lithium Niobate; Surface Energy and Temperature Effect on Etched Structures in Compound Semiconductors Model of the Mass Transport Phenomenon; Kinetics of Mass Transport of Etched Structures in InP Due to Surface Energy Minimization; A Simple Model of Amplified Spontaneous Emission Spectral Narrowing High Power, Diffraction Limited, Narrowband External Cavity Diode Laser; Si-on-Insulator Films Prepared by Zone Melting Recrystallization with Enhanced Radiative Heating; Selective Plasma Etching of Si from GaAs-on-Si Wafers; Selective Area Laser Photodeposition of Transparent Conductive SnO2 Films; Electrical Characteristics of Ultrashallow Junction Diodes Fabricated by Laser Doping; Patterned Excimer Laser Etching of GaAs Within a Molecular Beam Epitaxy Machine; PBT Amplification at 94 GHz; A 64 X 64-Pixel Back Illuminated CCD Imager with Low Noise and High Frame Rates; High Speed Resonant Tunneling Diodes Made from the Pseudomorphic In(0.53)Ga(0.47) As/AlAs System; Superconductive Nb Thin Film Capacitors with Ta2O5 Dielectric; Deposition of YBa2Cu3Ox Films by Sequential RF Diode Sputtering; and Microwave Surface Resistance of BiSrCaCuO Films. GRA

77 THERMODYNAMICS AND STATISTICAL PHYSICS

Includes quantum mechanics; theoretical physics; and Bose and Fermi statistics.

For related information see also *25 Inorganic and Physical Chemistry* and *34 Fluid Mechanics and Heat Transfer.*

N89-28432# Sandia National Labs., Albuquerque, NM.
REAL GAS EQUATIONS OF STATE FOR CHEMKIN
P. Barry Butler Mar. 1989 40 p
(Contract DE-AC04-76DP-00789)
(DE89-012794; SAND-88-3118) Avail: NTIS HC A03/MF A01

CHEMKIN is a chemical kinetics FORTRAN program developed to treat the gas-phase kinetics and associated thermodynamics for a set of user-defined chemical reactions. A key assumption made in CHEMKIN is that the gas behaves as a perfect gas, a restriction that results in noninterference of the individual species in a gas mixture (i.e., partial molal properties equal specific properties of pure component). Recently, the code was modified to account for real gas behavior according to the general limit method. The appropriate departure integrals for two real gas equations of state were calculated and included in a modified version of the code. The equations of state considered in this work were: a constant-covolume Noble-Abel function, and the Becker-Kistiakowsky-Wilson formulation. DOE

N89-28433# Colorado State Univ., Fort Collins. Dept. of Chemical Engineering.
STUDY OF IMPROVED METHODS FOR PREDICTING CHEMICAL EQUILIBRIA Progress Report, 1 Jul. 1986 - 30 Jun. 1989
Terry G. Lenz and John D. Vaughan 1989 62 p
(Contract DE-FG02-86ER-13582)
(DE89-014535; DOE/ER-13582/T2) Avail: NTIS HC A04/MF A01

The research involves developing general computational methods for predicting the thermodynamic properties of condensed state chemically reactive systems. The overall effort has encompassed both computer studies, and parallel laboratory experimental work to support the evolving computational models. To date, the soundness of molecular mechanics/force-field techniques were demonstrated for accurate prediction of the thermodynamic properties of chemically reactive systems. Extensive work was done with three molecular mechanics models, Boyd's MOLBD3, Allinger's MMP2 and the Warshel/Lifson/Karplus QCFF/PI program. Not one of these programs at present has general full thermodynamic output capability. Modification of the QCFF/PI is well on its way to full thermodynamic capability. Supporting laboratory studies have involved careful bomb calorimetry for H(sub f)° information, X-ray structure determination for accurate molecular geometry data, and kinetics/equilibrium determinations for various prototypical Diels-Alder reactions. Vapor pressure studies for candidate Diels-Alder compounds are also underway. The bomb calorimetric and greater initial effort on vapor pressure studies have replaced the original solvent effect and hindered rotation NMR studies planned, on the basis of most critical data needs for correct computational model development. DOE

N89-28434# Los Alamos National Lab., NM.
ISSUES AND FUTURE DIRECTIONS IN SUBSECOND THERMOPHYSICS
J. W. Shaner 1989 6 p Presented at the 10th Symposium on Thermophysical Properties, Gaithersburg, MD, 20-23 Jun. 1989
(Contract W-7405-eng-36)
(DE89-014228; LA-UR-89-2105; CONF-8906164-1) Avail: NTIS HC A02/MF A01

The primary motivations for trying to measure thermophysical properties of materials on subsecond timescales are to extend measurements to higher temperatures than can be conveniently maintained continuously, or to make measurements on systems out of thermodynamic equilibrium. Since these measurements are

difficult, one must keep in mind the needs for the data. These include the ability to use materials cleverly in new high-pressure/high-temperature applications, as well as the development of calibrated models for the response of materials to rapid energy deposition, by laser pulses, for example. Several key areas have been identified in which effort is needed for substantial progress in subsecond measurements, and which have unusual promise for useful new scientific results. These areas include the problems of high-temperature standards, equilibration during rapid heating, measurements at higher temperatures combined with higher pressures, measurements on specific interesting materials, and measurement of microstructural properties at high temperature and their relation to macroscopic response. Each of these areas will be touched upon here. DOE

N89-28435# Los Alamos National Lab., NM.
THERMOPHYSICAL PROPERTIES OF LIQUID NIOBIUM
R. S. Hixson and M. A. Winkler 1989 9 p Presented at the AIRAPT and EHPRG International High Pressure Science and Technology Conference, Paderborn, Federal Republic of Germany, 17 Jul. 1989
(Contract W-7405-eng-36)
(DE89-014288; LA-UR-89-2150; CONF-890798-1-Vugraphs)
Avail: NTIS HC A02/MF A01

Thermophysical properties of most liquid metals are difficult to measure because of the very high temperatures and pressures required, but they are important for several reasons. These include understanding the fundamental physics of liquid metals and experimental modeling and design of exploding wires, foils and fuses. The melting points of all but a few metals are at high temperatures, with many exceeding 2000 K. The critical points of most metals exceed temperatures and pressures that may be easily achieved in static high-pressure systems. Because of the limitations on temperatures that may be reached in static high-pressure experiments, various dynamic techniques have been developed to study liquid metals. We use a resistive pule heating method in which a cylindrical wire-shaped sample is made to expand along a isobaric path. During an experiment the sample is heated, made to melt, and enthalpy, temperature, and specific volume are measured. After the liquid end state is reached, a single sound speed measurement per experiment is made. From these fundamental properties, other properties such as thermal expansion coefficient bulk modulii, and compressibilities may be calculated. Here we report measurements that we have recently made on liquid niobium. DOE

80 SOCIAL SCIENCES (GENERAL)

Includes educational matters.

No abstracts in this category.

81 ADMINISTRATION AND MANAGEMENT

Includes management planning and research.

N89-28436# Universal Energy Systems, Inc., Dayton, OH.
UNITED STATES AIR FORCE RESEARCH INITIATION PROGRAM FOR 1987, VOLUME 1 Interim Report
Rodney C. Darrah Apr. 1989 782 p
(Contract F49620-85-C-0013)
(AD-A209726; AFOSR-89-0329TR-Vol-1) Avail: NTIS HC A99/MF E03 CSCL 05/1

The U.S. Air Force Research Initiation Program has caused study in many areas. This is volume 1 of 4 volumes. Some areas studied are: Effects of Bending Flexibility on the Aerodynamic Characteristics of Slender Cylinders Determined from Free Flight Ballistic Data; Image Complexity Measures and Edge Detection; Advanced Gun Gas Diversion; A Physical and Numerical Study of Pressure Attenuation in Solids; Pyroelectric Sensing for Potential Multi-Mode Use; Gaseous Fuel Injection and Mixing in a Supersonic Combustor; Systems Effectiveness for Targets with Repair or Replacement; A Pattern Recognition Application in Elastic-Plastic Boundary Element, Hybrid Stress Analysis; Vectorized Perturbed Functional Iterative Scheme (VPFIS): A Large Scale Nonlinear System Solver; Liquid Film Cooling in Rocket Engines; Estimation of Autocorrelation and Power Spectral Density for Randomly Sampled Systems; Fracture in Solid Propellant: Damage Effects upon Crack Propagation; Novel Conversion of Organometallics to Energetic Nitro Compounds; Correlations of Spontaneous Ignition Temperatures with Molecular Structures of Flammable with Molecular Structures of Flammable Compounds; The Estimation of Stature from Fragments of the Femur: A Revision of the Steele Method; Effects of Water Solubility and Functional Group Content on the Interactions of Organic Solutes with Soil Organic Matter; A Study of Semihardened Concrete Arch Structure Response Under Protective Layers; and Stress Wave Propagation in Layered Media. GRA

N89-28437# Universal Energy Systems, Inc., Dayton, OH.
UNITED STATES AIR FORCE RESEARCH INITIATION PROGRAM FOR 1987, VOLUME 3 Interim Report
Rodney C. Darrah Apr. 1989 526 p
(Contract F49620-85-C-0013)
(AD-A209728; AFOSR-89-0831TR-Vol-3) Avail: NTIS HC A23/MF A01 CSCL 05/1

The U.S. Air Force Research Initiation Program has caused study in many areas. This is volume 3 of 4. Some areas of study are: A Numerical Study of the Flow Field and Heat Transfer in a Rectangular Passage with a Turbulator; Analysis of an Algorithm for Multiple Frequency Resolution; Signal Processing in EW Environment; Implementation of Blackboard Systems in Ada; Surface States and Electron Transport Properties in Semi-Insulating Gallium Arsenide; Investigate Feasibility of Implementing Associative Memories Using Luminescent Rebroadcasting Devices; Automated Translation of Digital Logic Equation into Optimized VHDL Code; Analytical Model and Computer Program of F-16 Nose Gear and F-16 ALGS; Development of a Technique for Prediction of Internal Heat Transfer in Actively Cooled Structures; Radiation Hypersonic Aerodynamics; A Chemical Kinetics Model for Mach 5 to 14 Hypersonic Flow; Development of a Microcomputer Lateral Resupply Simulation System; Development of Expert System Control of a Carbon Fiber Production Process; Influence of Microstructural Variations on the Thermomechanical Processing in Dynamic Material Modeling of Titanium Aluminides; Studies on the Compatibility of Potential Matrix and Reinforcement Materials in Ceramic Composites for High Temperature, Aerospace Applications; Synthesis of Compounds Capable of Intramolecular Cyclization - Aromatization Reactions; Leaky Rayleigh and Lamb Waves on Composites; and Performance Improvement in Knowledge-Based Process Control Systems. GRA

N89-28438# Universal Energy Systems, Inc., Dayton, OH.
UNITED STATES AIR FORCE RESEARCH INITIATION PROGRAM FOR 1987, VOLUME 4 Interim Report
Rodney C. Darrah Apr. 1989 783 p
(Contract F49620-85-C-0013)
(AD-A209729; AFOSR-89-0832TR-Vol-4) Avail: NTIS HC A99/MF E03 CSCL 05/1

The U.S. Air Force Research Initiation Program has caused study into many areas. This is volume 4 of 4. Some areas of study are: Development of Implantable Devices for Sustained Delivery of Volatile Hydrocarbons in Rats; In Situ Detection of Osteoprogenitor Cells in an Actively Growing Bone System; Trauma Activated Periosteum Derived Osteogenic Cells: Response to Selected Growth Factors; Assessing the Attributes of Expert Judgement: Measuring Bias in Subjective Uncertainty Estimates; Mathematical Modeling; Learning Behavior of Adaptive Filters for Evoked Brain Potentials; The Rhetoric of Hypertext: An Examination of Document Database Concepts and The Integrated Maintenance

Information System; Structural Representations of Multi-Dimensional Criterion Construct Space; Comparison of Supervisor's and Incumbent's Estimates of SDy; The Role of Fourier Descriptions for Shape in Visual Form Perception; Comprehensibility of Technical Test; Mechanisms of Contrast and Lightness Constancy; Phytotoxicity of Soil Residues of JP-4 Aviation Fuel; The Contracting Out of In-House Analytical Services at the USAF Occupational and Environmental Health Laboratory-Brooks AFB, San Antonio, Texas; Effects of Metal Mutagens on the Synthesis and Accumulation of Macromolecules; Development of a Rapid and Sensitive Assay Procedure for the Detection of the Protozoan Parasite Giardia Lamblia in Drinking Water; Limitations to Heavy Work of Personnel Wearing at 21 C: U.S. Military Chemical Defense Ensemble. GRA

N89-28439# Department of Defense, Washington, DC.
CRITICAL TECHNOLOGIES PLAN FOR THE COMMITTEES ON ARMED SERVICES, UNITED STATES CONGRESS, REVISION
5 May 1989 137 p Superseded report dated 15 Mar. 1989, AD-A206130
(AD-A210170) Avail: NTIS HC A07/MF A01 CSCL 15/3

Public Law 100-456, the National Defense Authorization Act for Fiscal Year 1989, authorizes a report to Congress annually of a Critical Technologies Plan. This is the first such submission. It is the result of a series of meetings involving representatives of the military departments and defense agencies with responsibilities for science and technology programs, and representatives from the Department of Energy, Assistant Secretary for Defense Programs. The scope of the report is defined and outlined, the DoD planning process for science and technology, selection criteria for critical technologies are presented. Technologies related to nuclear weapons and their effects, because of their special nature, are not included in this plan. Critical technologies are technologies with great promise of ensuring the long-term superiority of the United States weapon system. The following critical technologies were selected: Microelectronic Circuits and Their Fabrication, Preparation of GaAs and Other Compound Semi-Conductors, Software Producibility, Parallel Computer Architectures, Machine Intelligence/Robotics, Simulation and Modeling, Integrated Optics, Fiber Optics, Sensitive Radars, Passive Sensors, Automatic Target Recognition, Phased Arrays, Data Fusion, Signature Control, Computational Fluid Dynamics, Air Breathing Propulsion, High Power Microwaves, Pulsed Power, Hypervelocity Projectiles, High Temperature/High Strength/Light Weight Composite Materials, and Superconductors. GRA

82 DOCUMENTATION AND INFORMATION SCIENCE

Includes information management; information storage and retrieval technology; technical writing; graphic arts; and micrography.

For computer documentation see *61 Computer Programming and Software.*

N89-28440*# George Washington Univ., Washington, DC.
[DATA BASE DEVELOPMENT AND RESEARCH AND EDITORIAL SUPPORT] Final Report, 17 Apr. 1978 - 30 Jun. 1988
30 Jun. 1988 100 p
(Contract NASw-3165)
(NASA-CR-183249; NAS 1.26:183249) Avail: NTIS HC A05/MF A01 CSCL 05B

The Life Sciences Bibliographic Data Base was created in 1981 and subsequently expanded. A systematic, professional system was developed to collect, organize, and disseminate information about scientific publications resulting from research. The data base consists of bibliographic information and hard copies of all research papers published by Life Sciences-supported investigators. Technical improvements were instituted in the database. To minimize costs, take advantage of advances in personal computer technology, and achieve maximum flexibility and control, the data base was transferred from the JSC computer to personal computers at George Washington University (GWU). GWU also performed a range of related activities such as conducting in-depth searches on a variety of subjects, retrieving scientific literature, preparing presentations, summarizing research progress, answering correspondence requiring reference support, and providing writing and editorial support. Author

N89-28441# National Inst. of Standards and Technology, Gaithersburg, MD. Information Resources and Services Div.
DATA BASES AVAILABLE AT THE NATIONAL INSTITUTE OF STANDARDS AND TECHNOLOGY RESEARCH INFORMATION CENTER Final Report
Diane Cunningham Nov. 1988 117 p
(PB89-160014; NIST/SP-753; LC-88-600602) Avail: NTIS HC A06/MF A01 CSCL 05B

Data bases available online at the National Institute of Standards and Technology (NIST) Research Information Center are listed by acronym and by full title. In addition, descriptions of the data bases, periods of coverage, producers, corresponding hard copy titles and principal sources and vendors are listed. A general subject index and a cross reference index are also supplied. Author

N89-28442# Naval Postgraduate School, Monterey, CA.
AN IMPLEMENTATION OF A DATA DEFINITION FACILITY FOR THE GRAPHICS LANGUAGE FOR DATABASE M.S. Thesis
Michael L. Williamson Dec. 1988 89 p
(AD-A207380) Avail: NTIS HC A05/MF A01 CSCL 12/5

This research is an implementation of the data definition facility for the Graphics Language for Database (GLAD). GLAD is a graphics-oriented database management system which is primarily concerned with ease of learning and efficiency of use. The system uses an object-relationship approach to data base design. Entities of the database are represented graphically as objects. With this method, users can visualize the schema of the database and can quickly comprehend how the entities relate. Every effort was made to design GLAD so that a new user can quickly learn to create and manipulate a database without the need of a dedicated database administrator. GRA

N89-28443# Lawrence Livermore National Lab., CA.
ENGINEERING DRAWING TRANSFER TEST WITH DOUGLAS AIRCRAFT COMPANY: MIL-D-28000 CLASS II (IGES)
2 May 1989 56 p Prepared for Air Force Logistics Command
(Contract W-7405-eng-48)
(DE89-012810; UCID-21677) Avail: NTIS HC A04/MF A01

The DOD Computer-aided Acquisition and Logistic Support (CALS) Test Network (CTN) is conducting tests of the military standard for the Automated Interchange of Technical Information, MIL-STD-1840A (1840A) (OSDA88) and its companion suite of military specifications. The CTN is a DOD sponsored confederation of voluntary participants from industry and Government, managed jointly by a technical staff at Air Force Logistics Command (AFLC) and Lawrence Livermore National Laboratory (LLNL). The objective of the CTN tests is to demonstrate and evaluate the interchange and functional use of digital technical information between industry and government using the CALS Standards. This test was CTN Planned Test (CPT) (CTN89) with Douglas Aircraft Company (DAC). It was conducted at a DAC facility in Long Beach, California, February 7 to 9, 1989. The objective of the CPT was to test the engineering drawing subset of Initial Graphics Exchange Specifications (IGES) (NBS88) entities defined in the Military Specifications for the Digital Representation for Communication of Product Data: IGES Application Subsets, MIL-D-28000 Amendment 1 (28000) (OSDD88). Since DAC is preparing to accept data from a subcontractor in conjunction with its DOD C17 contract, the primary goal of this test was to demonstrate, test, and evaluate DAC's ability to interchange and use digital data in 1840A/28000 form. A secondary goal was to evaluate the CTN's 28000 Class 2 Reference Material utilized for the first time in this test and scheduled for use in subsequent tests of 28000. DOE

N89-28444*# Dartmouth Coll., Hanover, NH. Dept. of Mathematics and Computer Science.
THEFT OF INFORMATION IN THE TAKE-GRANT PROTECTION MODEL
Matt Bishop 1989 27 p
(Grant NAG2-480)
(NASA-CR-185835; NAS 1.26:185835; PCS-TR88-137) Avail: NTIS HC A03/MF A01 CSCL 05B

Using the information transfer extensions to the Take-Grant Protection Model, the concept of theft of information is defined and necessary and sufficient conditions for such theft to occur are presented, as well as bounds on the number of actors involved in such theft. Finally, the application of these results to reference monitors are explored. Author

N89-28445*# Dartmouth Coll., Hanover, NH. Dept. of Mathematics and Computer Science.
THE SHARING OF RIGHTS AND INFORMATION IN A CAPABILITY-BASED PROTECTION SYSTEM
Matt Bishop 1989 36 p Sponsored in part by a Burke Award from Dartmouth Coll.
(Grant NAG2-480)
(NASA-CR-185388; NAS 1.26:185388; PCS-TR88-136) Avail: NTIS HC A03/MF A01 CSCL 05B

The question of sharing of rights and information in the Take-Grant Protection Model is examined by concentrating on the similarities between the two; in order to do this, new theorems are stated and proven for each that specifically show the similarities. The proof for one of the original theorems is also provided. These statements of necessary and sufficient conditions are contrasted to illustrate the proposition that transferring rights and transferring information are fundamentally the same, as one would expect in a capability-based system. Directions are then discussed for future research in light of these results. Author

N89-28446*# Dartmouth Coll., Hanover, NH. Dept. of Mathematics and Computer Science.
A MODEL OF SECURITY MONITORING
Matt Bishop 1989 23 p
(Grant NAG2-480)
(NASA-CR-185845; NAS 1.26:185845) Avail: NTIS HC A03/MF A01 CSCL 05B

A model of security monitoring is presented that distinguishes between two types of logging and auditing. Implications for the design and use of security monitoring mechanisms are drawn from this model. The usefulness of the model is then demonstrated by analyzing several different monitoring mechanisms. Author

N89-28447# Lawrence Livermore National Lab., CA.
PROBLEMS AND SOLUTIONS IN ONLINE DOCUMENTATION SYSTEMS
Jean Shuler Jun. 1989 6 p Presented at the Cray User's Group Conference, Los Angeles, CA, 24 Apr. 1989
(Contract W-7405-eng-48)
(DE89-014092; UCRL-101237; CONF-8904210-7) Avail: NTIS HC A02/MF A01

Pogo says we are surrounded by insurmountable opportunities. DOCUMENT, the online document system at NMFECC, has been continually enhanced and modified in the past 12 years to meet customer needs by analyzing the insurmountable opportunities (commonly called problems) that have arisen. We have analyzed where these documentation retrieval problems exist and solved these problems. The greatest challenge was to provide the customer with a stable system using the existing database of documents while adding new features and programs to retrieve information. Listed are four of the problems we have encountered, solutions are given and some indicators of success are shown. DOE

N89-27930 ANT Nachrichtentechnik, Backnang (Germany, F.R.).
REQUIREMENTS FOR A TECHNICAL DATA BASE [ANFORDERUNGEN AN EINE TECHNISCHE DATENBANK]
Burkhardt Lowe *In its* Communication Engineering Reports. Fundamental Developments. Theoretical Work Nov. 1988 p 10-23 In GERMAN (For primary document see N89-27928 22-32)
Copyright Avail: Fachinformationszentrum Karlsruhe, 7514 Eggenstein-Leopoldshafen 2, Fed. Republic of Germany, 35 DM

83 ECONOMICS AND COST ANALYSIS

Includes cost effectiveness studies.

N89-28448*# Management Information Services, Inc., Washington, DC.
THE PRIVATE SECTOR ECONOMIC AND EMPLOYMENT BENEFITS TO THE NATION AND TO EACH STATE OF PROPOSED FY 1990 NASA PROCUREMENT EXPENDITURES
Apr. 1989 77 p Prepared for NASA Alumni League, Washington, DC
(NASA-CR-185894; NAS 1.26:185894) Avail: NTIS HC A05/MF A01 CSCL 05C

The private sector economic and employment benefits (disaggregated among 80 industries and 475 occupations) of the proposed FY 1990 NASA procurement expenditures to the nation and to each state are estimated. Nationwide, it is found that FY 1990 NASA procurement expenditures of $11.3 billion will have an economic multiplier of 2.1 and will create, directly and indirectly, 237,000 jobs, $23.2 billion in total industry sales, $2.4 billion in corporate profits, and $7.4 billion in Federal, state, and local government tax revenues. These benefits are widely dispersed throughout the United States and are significant in many states not normally considered to be major beneficiaries of NASA spending. The indirect economic benefits are identified for each state resulting from the second-, third-, and fourth rounds of industry purchases generated by NASA procurement expenditures. Each state is ranked on the basis of several criteria, including the total benefits, indirect benefits, and per capita benefits received from NASA spending. The estimates developed are important for maintaining a viable U.S. Space Program through the remainder of this century. B.G.

84 LAW, POLITICAL SCIENCE AND SPACE POLICY

Includes NASA appropriation hearings; aviation law; space law and policy; international law; international cooperation; and patent policy.

N89-28449# Army War Coll., Carlisle Barracks, PA.
CRISIS DECISION-MAKING: THE IMPACT OF COMMERCIAL SATELLITES ON THE MEDIA, MILITARY AND NATIONAL LEADERS
Raymond J. Dolan 7 Mar. 1989 45 p
(AD-A207334) Avail: NTIS HC A03/MF A01 CSCL 22/2

Technological advances will have a significant impact on future crises. Decision making will become more difficult and complex as the amount of information available to decision makers and the public increases substantially. Photos from commercial satellites have just begun to have an effect on governments and their policies. The rapid increase in technology will provide capabilities to the news media that will profoundly affect the relationship among the media, military and national leaders. The old ways of doing business have changed. The launching of a media satellite is certain to raise many issues that must be addressed and solved. The media's use of their own satellite will generate conflicts between first amendment rights and U.S. national security and foreign policy interests. A mediasat will also affect military strategy and tactics. These issues are addressed in a hypothetical scenario in a generate awareness of potential problems and postulate some solutions. GRA

N89-28450# Committee on Science, Space and Technology (U.S. House).
THE 1990 NATIONAL AERONAUTICS AND SPACE ADMINISTRATION AUTHORIZATION
1989 69 p Hearing before the Subcommittee on Transportation, Aviation and Materials of the Committee on Science, Space and Technology, 100th Congress, 1st Session, no. 17, 26 Apr. 1989, volume 1
(GPO-99-550) Avail: Subcommittee on Transportation, Aviation and Materials, House of Representatives, Washington, D.C. 20515 SOD HC $2.25

Hearings before a subcommittee on transportation, aviation, and materials of the U.S. House of Representatives are presented for the fiscal year 1990 NASA aeronautics research and technology program are presented. All written testimony and submittals for the record are included. Justifications for research and development of high-speed air transportation are provided. B.G.

N89-28451# Committee on Science and Technology (U.S. House).
NATIONAL AERONAUTICS AND SPACE ADMINISTRATION MULTIYEAR AUTHORIZATION ACT OF 1989
Washington GPO 1989 51 p A bill, H.R. 1759, referred to the Committee on Science, Space and Technology, 101st Congress, 1st Session, 10 Apr. 1989
(H-Rept-101-226) Avail: Document Room, House of Representatives, Washington, D.C. 20515 HC free

Hearings before a subcommittee of U.S. House of Representatives are presented to authorize appropriations for the National Aeronautics and Space Administration for the fiscal year 1990. All written testimony and submittals for the record are also included. The budget estimates provide a detailed outline of the budgetary information and justifications for research and development, space flight, control and data communications, construction of facilities, and research and program management. B.G.

85 URBAN TECHNOLOGY AND TRANSPORTATION

Includes applications of space technology to urban problems; technology transfer; technology assessment; and surface and mass transportation.

For related information see also *03 Air Transportation and Safety, 16 Space Transportation,* and *44 Energy Production and Conversion.*

N89-28452# Army War Coll., Carlisle Barracks, PA.
INTERNATIONAL TECHNOLOGY TRANSFER: THE ROPE TO HANG THE WEST
Neil W. Grotegut 28 Mar. 1989 39 p
(AD-A207347) Avail: NTIS HC A03/MF A01 CSCL 05/1

The United States relies on the superior technology of its defense systems as a competitive edge against overwhelming Soviet numerical advantages. There is strong evidence to suggest that the U.S.S.R. is rapidly reducing the U.S. technology lead through the transfer and assimilation of technology gained from the West. The relevant issues of West to East technology transfer is examined in order to provide awareness and appreciation of its importance to the security of the U.S. GRA

N89-28453# Lawrence Livermore National Lab., CA.
ENGINEERING RESEARCH AND DEVELOPMENT: THRUST AREA REPORT FY 88
E. Lafranchi Jun. 1988 313 p
(Contract W-7405-eng-48)
(DE89-014320; UCRL-53868-88) Avail: NTIS HC A14/MF A01

This annual report describes the accomplishments of the Engineering Research Program for fiscal year 1988. Sixty-seven research and development projects are covered. For each project, goal(s), technical description, and an overview of future work are provided. DOE

88 SPACE SCIENCES (GENERAL)

No abstracts in this category.

89 ASTRONOMY

Includes radio, gamma-ray, and infrared astronomy, and astrometry.

No abstracts in this category.

90 ASTROPHYSICS

Includes cosmology; celestial mechanics; space plasmas; and interstellar and interplanetary gases and dust.

For related information see also *75 Plasma Physics.*

N89-28454*# Jet Propulsion Lab., California Inst. of Tech., Pasadena.
INTERPLANETARY PARTICLE ENVIRONMENT. PROCEEDINGS OF A CONFERENCE
Joan Feynman, ed. and Stephen Gabriel, ed. 15 Apr. 1988 165 p Conference held in Pasadena, CA, 16-17 Mar. 1987
(Contract NAS7-918)
(NASA-CR-185461; JPL-Publ-88-28; NAS 1.26:185461) Avail: NTIS HC A08/MF A01 CSCL 03B

A workshop entitled the Interplanetary Charged Particle Environment was held at the Jet Propulsion Laboratory (JPL) on March 16 and 17, 1987. The purpose of the Workshop was to define the environment that will be seen by spacecraft operating in the 1990s. It focused on those particles that are involved in single event upset, latch-up, total dose and displacement damage in spacecraft microelectronic parts. Several problems specific to Magellan were also discussed because of the sensitivity of some electronic parts to single-event phenomena. Scientists and engineers representing over a dozen institutions took part in the meeting. The workshop consisted of two major activities, reviews of the current state of knowledge and the formation of working groups and the drafting of their reports. For individual titles, see N89-28455 through N89-28470.

N89-28455*# Jet Propulsion Lab., California Inst. of Tech., Pasadena.
TOWARD A DESCRIPTIVE MODEL OF SOLAR PARTICLES IN THE HELIOSPHERE
M. A. Shea, D. F. Smart, James H. Adams, Jr., D. Chenette, Joan Feynman, Douglas C. Hamilton, G. R. Heckman, A. Konradi, Martin A. Lee, and D. S. Nachtwey (National Aeronautics and Space Administration. Lyndon B. Johnson Space Center, Houston, TX.) et al *In its* Interplanetary Particle Environment. Proceedings of a Conference 15 Apr. 1988 p 3-13 (For primary document see N89-28454 22-90)
Avail: NTIS HC A08/MF A01 CSCL 03B

During a workshop on the interplanetary charged particle environment held in 1987, a descriptive model of solar particles in the heliosphere was assembled. This model includes the fluence, composition, energy spectra, and spatial and temporal variations of solar particles both within and beyong 1 AU. The ability to predict solar particle fluences was also discussed. Suggestions for specific studies designed to improve the basic model were also made. Author

N89-28456*# Jet Propulsion Lab., California Inst. of Tech., Pasadena.
TOWARD A DESCRIPTIVE MODEL OF GALACTIC COSMIC RAYS IN THE HELIOSPHERE **c93**
R. A. Mewaldt, A. C. Cummings, James H. Adams, Jr., Paul Evenson, W. Fillius, J. R. Jokipii, R. B. McKibben (Chicago Univ., IL.), and Paul A. Robinson, Jr. *In its* Interplanetary Particle Environment. Proceedings of a Conference 15 Apr. 1988 p 14-32 (For primary document see N89-28454 22-90)
Avail: NTIS HC A08/MF A01 CSCL 03B

Researchers review the elements that enter into phenomenological models of the composition, energy spectra, and the spatial and temporal variations of galactic cosmic rays, including the so-called anomalous cosmic ray component. Starting from an existing model, designed to describe the behavior of cosmic rays in the near-Earth environment, researchers suggest possible updates and improvements to this model, and then propose a quantitative approach for extending such a model into other regions of the heliosphere. Author

N89-28457*# Jet Propulsion Lab., California Inst. of Tech., Pasadena.
THE EFFECTS OF HIGH ENERGY PARTICLES ON PLANETARY MISSIONS
Paul A. Robinson, Jr. *In its* Interplanetary Particle Environment. Proceedings of a Conference 15 Apr. 1988 p 35-47 (For primary document see N89-28454 22-90)
Avail: NTIS HC A08/MF A01 CSCL 03B

Researchers review the background and motivation for the detailed study of the variability and uncertainty of the particle environment from a space systems planning perspective. The engineering concern raised by each environment is emphasized rather than the underlying physics of the magnetosphere or the sun. Missions now being planned span the short term range of one to three years to periods over ten years. Thus the engineering interest is beginning to stretch over periods of several solar cycles. Coincidentally, detailed measurements of the environment are now becoming available over that period of time. Both short term and long term environmental predictions are needed for proper mission planning. Short term predictions, perhaps based on solar indices, real time observations, or short term systematics, are very useful in near term planning -- launches, EVAs (extravehicular activities), coordinated observations, and experiments which require the magnetosphere to be in a certain state. Long term predictions of both average and extreme conditions are essential to mission design. Engineering considerations are many times driven by the worst case environment. Knowledge of the average conditions and their variability allows trade-off studies to be made, implementation of designs which degrade gracefully under multi-stress environments. Author

N89-28458*# Naval Research Lab., Washington, DC. Center for Space Research.
CURRENT MODELS OF THE INTENSELY IONIZING PARTICLE ENVIRONMENT IN SPACE **c93**
James H. Adams, Jr. *In* Jet Propulsion Lab., California Inst. of Tech., Interplanetary Particle Environment. Proceedings of a Conference 15 Apr. 1988 p 49-56 (For primary document see N89-28454 22-90)
Avail: NTIS HC A08/MF A01 CSCL 03B

The Cosmic Ray Effects on MicroElectronics (CREME) model that is currently in use to estimate single event effect rates in spacecraft is described. The CREME model provides a description of the radiation environment in interplanetary space near the orbit of the earth that contains no major deficiencies. The accuracy of the galactic cosmic ray model is limited by the uncertainties in solar modulation. The model for solar energetic particles could be improved by making use of all the data that has been collected on solar energetic particle events. There remain major uncertainties about the environment within the earth's magnetosphere, because of the uncertainties over the charge states of the heavy ions in the anomalous component and solar flares, and because of trapped heavy ions. The present CREME model is valid only at 1 AU, but it could be extended to other parts of the heliosphere. There is considerable data on the radiation environment from 0.2 to 35 AU in the ecliptic plane. This data could be used to extend the CREME model. Author

N89-28459*# Jet Propulsion Lab., California Inst. of Tech., Pasadena.
A NEW PROTON FLUENCE MODEL FOR E GREATER THAN 10 MeV **c93**
Joan Feynman, T. P. Armstrong, L. Dao-Gibner, and S. Silverman (Boston Coll., Chestnut Hill, MA.) *In its* Interplanetary Particle Environment. Proceedings of a Conference 15 Apr. 1988 p 58-71 (For primary document see N89-28454 22-90)
(Grant NSF ATM-83-05537)
Avail: NTIS HC A08/MF A01 CSCL 03B

Researchers describe a new engineering model for the fluence of protons with energies greater than 10 MeV. The data set used is a combination of observations made primarily from the Earth's surface between 1956 and 1963 and observations made from spacecraft in the vicinity of Earth between 1963 and 1985. With this data set we find that the distinction between ordinary proton events and anomalously large proton events made in earlier work disappears. The greater than 10 MeV fluences at 1 AU calculated with the new model are about twice those expected on the basis of models now in use. In contrast to earlier models, results do not depend critically on the fluence from any one event. Author

N89-28460*# Air Force Geophysics Lab., Hanscom AFB, MA.
INTENSITY/TIME PROFILES OF SOLAR PARTICLE EVENTS AT ONE ASTRONOMICAL UNIT **c92**
M. A. Shea *In* Jet Propulsion Lab., California Inst. of Tech., Interplanetary Particle Environment. Proceedings of a Conference 15 Apr. 1988 p 75-84 (For primary document see N89-28454 22-90)
Avail: NTIS HC A08/MF A01 CSCL 03B

A description of the intensity-time profiles of solar proton events observed at the orbit of the earth is presented. The discussion, which includes descriptive figures, presents a general overview of the subject without the detailed mathematical description of the physical processes which usually accompany most reviews. Author

N89-28461*# Maryland Univ., College Park. Dept. of Physics and Astronomy.
THE RADIAL DEPENDENCE OF THE SOLAR ENERGETIC PARTICLE FLUX **c92**
Douglas C. Hamilton *In* Jet Propulsion Lab., California Inst. of Tech., Interplanetary Particle Environment. Proceedings of a Conference 15 Apr. 1988 p 86-90 (For primary document see N89-28454 22-90)
Avail: NTIS HC A08/MF A01 CSCL 03B

Researchers discuss the radial dependence of the peak flux and the fluence of solar flare produced energetic particles under the assumption that they propagate diffusively in the heliosphere. Author

N89-28462*# National Oceanic and Atmospheric Administration, Boulder, CO.
SOLAR PROTON EVENT FORECASTS **c92**
G. R. Heckman *In* Jet Propulsion Lab., California Inst. of Tech., Interplanetary Particle Environment. Proceedings of a Conference 15 Apr. 1988 p 91-100 (For primary document see N89-28454 22-90)
Avail: NTIS HC A08/MF A01 CSCL 03B

The United States operates a space weather service to provide information on space hazards including solar proton events to Federal government agencies and other users who operate systems that are affected by disturbances in the upper atmosphere and interplanetary environment. The observation and prediction of solar proton events has been continuous through solar cycle 21 (1976 to 1986), establishing a base of experience that can be used in providing similar support to space operations in the 1990's. The observations, indices, alerts, and forecasts used in the service

are described. Also provided is a short summary of the experience obtained from making proton event predictions in solar cycle 21 including the years 1976 to 1986. Author

N89-28463*# Air Force Geophysics Lab., Hanscom AFB, MA.
PREDICTING THE ARRIVAL TIMES OF SOLAR PARTICLES **c92**
D. F. Smart *In* Jet Propulsion Lab., California Inst. of Tech., Interplanetary Particle Environment. Proceedings of a Conference 15 Apr. 1988 p 101-110 (For primary document see N89-28454 22-90)
Avail: NTIS HC A08/MF A01 CSCL 03B

A procedure has been developed to generate a computerized time-intensity profile of the solar proton intensity expected at the earth after the occurrence of a significant solar flare on the sun. This procedure is a combination of many pieces of independent research and theoretical results. Many of the concepts used were first reported by Smart and Shea (1979) and are summarized by Smart and Shea (1985). Extracts from the general procedure that relate to predicting the expected onset time and time of maximum at the earth after the occurrence of a solar flare are presented. Author

N89-28464*# New Hampshire Univ., Durham. Inst. for the Study of Earth, Oceans and Space.
PARTICLES ACCELERATED BY SHOCKS IN THE HELIOSPHERE **c92**
Martin A. Lee *In* Jet Propulsion Lab., California Inst. of Tech., Interplanetary Particle Environment. Proceedings of a Conference 15 Apr. 1988 p 111-116 (For primary document see N89-28454 22-90)
(Grants NAG5-728; NAGw-76; NSF ATM-85-13363)
Avail: NTIS HC A08/MF A01 CSCL 03B

The populations of energetic ions accelerated by shocks in the heliosphere are reviewed briefly. Characteristic spectra and representative fluxes are given. Author

N89-28465*# Jet Propulsion Lab., California Inst. of Tech., Pasadena.
HIGH-ENERGY PARTICLES VERY NEAR THE SUN Abstract Only **c92**
B. E. Goldstein *In its* Interplanetary Particle Environment. Proceedings of a Conference 15 Apr. 1988 p 117 (For primary document see N89-28454 22-90)
Avail: NTIS HC A08/MF A01 CSCL 03B

NASA's long range plans include a Solar Probe (Star Probe) mission in which a spacecraft is placed in an eccentric orbit with perihelion at four solar radii. As part of the study effort for this mission, a Solar Probe Environment Workshop was sponsored by JPL. The report of this committee was issued in September 1978 as JPL Publication 78-64. A brief abstract of this document is given. There are considerable uncertainties in the models of solar energetic particle release and transport. The committee addressed this problem by using different modelling techniques when possible to provide a cross-check on the estimates. These models were used to extrapolate observation at 1 AU to the vicinity of the Sun. Additionally, the occurrence of a flare of a given magnitude must be estimated on a statistical basis. Therefore, it is possible to state a likelihood that the fluxes and fluences will be less than a certain magnitude, but in the event of an extremely large solar flare (occurrence of perhaps once a decade, e.g., August 4, 1972) it is likely that the hazard would be insurmountable. A brief first look indicates that the near-solar particle environment is not a worse hazard than Jupiter. Author

N89-28466*# California Inst. of Tech., Pasadena.
ELEMENTAL COMPOSITION AND ENERGY SPECTRA OF GALACTIC COSMIC RAYS **c93**
R. A. Mewaldt *In* Jet Propulsion Lab., California Inst. of Tech., Interplanetary Particle Environment. Proceedings of a Conference 15 Apr. 1988 p 121-132 (For primary document see N89-28454 22-90)
(Grants NGR-05-002-160; NAG5-722)
Avail: NTIS HC A08/MF A01 CSCL 03B

A brief review is presented of the major features of the elemental composition and energy spectra of galactic cosmic rays. The requirements for phenomenological models of cosmic ray composition and energy spectra are discussed, and possible improvements to an existing model are suggested. Author

N89-28467*# California Inst. of Tech., Pasadena.
THE ANOMALOUS COSMIC-RAY COMPONENT **c93**
A. C. Cummings and E. C. Stone *In* Jet Propulsion Lab., California Inst. of Tech., Interplanetary Particle Environment. Proceedings of a Conference 15 Apr. 1988 p 133-134 (For primary document see N89-28454 22-90)
(Contract NAS7-918; NGR-05-002-160)
Avail: NTIS HC A08/MF A01 CSCL 03B

This brief report is intended to update the anomalous component section of the summary report of the galactic cosmic-ray working group (Mewaldt et al., 1987), which was drafted at the March 1987 Workshop on the Interplanetary Charged Particle Environment at the Jet Propulsion Laboratory. The description of the spectrum of the anomalous cosmic-ray component is contained in section 3.3 of that report. That description is based on data analyzed through day 310 of 1986, and in it we proposed that the energy spectrum of the various species of the anomalous component could be derived by scaling from two generic spectra. Two generic spectra were required because the energy spectrum of the anomalous component changed shape near the time of the solar magnetic field reversal in 1980. These two generic spectra are shown in Figure 2 of the summary report. Author

N89-28468*# Chicago Univ., IL.
GRADIENTS OF GALACTIC COSMIC RAYS AND ANOMALOUS COMPONENTS **c93**
R. B. McKibben *In* Jet Propulsion Lab., California Inst. of Tech., Interplanetary Particle Environment. Proceedings of a Conference 15 Apr. 1988 p 135-148 (For primary document see N89-28454 22-90)
Avail: NTIS HC A08/MF A01 CSCL 03B

Measurements of radial and latitudinal gradients of galactic cosmic rays and anomalous components now cover radii from 0.3 to 40 AU from the sun and latitudes up to 30 deg above the ecliptic plane for particle energies from approx. 10 MeV/n up to relativistic energies. The most accurate measurements cover the period 1972 through 1987, which includes more than one full 11 year cycle of solar activity. Radial gradients for glactic cosmic rays of all energies and species are small (similar to less than 10 percent AU), and variable in time, reaching a minimum of near 0 percent AU out to 30 AU for some species at solar maximum. Gradients for anomalous components are larger, of order 15 percent AU, may show similar time variability, and are relatively independent of particle species and energy. For the period 1985 through 1986 the intensity decreased away from the ecliptic for all species and energies. For galactic cosmic rays, the measured gradients are approx. 0.5 percent/degree near 20 AU, while for anomalous components the gradients are larger, ranging from 3 to 6 percent/degree. Comparison with a similar measurement for anomalous helium in 1975 through 1976 suggests that the latitude gradients for anomalous components have changed sign between 1975 and 1985. For galactic cosmic rays, the available evidence suggests no change in sign of the latitudinal gradient for relativistic particles. Author

N89-28469*# Delaware Univ., Newark.
TIME VARIATION OF GALACTIC COSMIC RAYS **c93**
Paul Evenson *In* Jet Propulsion Lab., California Inst. of Tech., Interplanetary Particle Environment. Proceedings of a Conference 15 Apr. 1988 p 149-161 (For primary document see N89-28454 22-90)
(Grants NAG5-374; NSF ATM-86-03192)
Avail: NTIS HC A08/MF A01 CSCL 03B

Time variations in the flux of galactic cosmic rays are the result of changing conditions in the solar wind. Maximum cosmic

ray fluxes, which occur when solar activity is at a minimum, are well defined. Reductions from this maximum level are typically systematic and predictable but on occasion are rapid and unexpected. Models relating the flux level at lower energy to that at neutron monitor energy are typically accurate to 20 percent of the total excursion at that energy. Other models, relating flux to observables such as sunspot number, flare frequency, and current sheet tilt are phenomenological but nevertheless can be quite accurate. Author

N89-28470*# Arizona Univ., Tucson.
GALACTIC COSMIC RAYS IN THREE DIMENSIONS Abstract Only c93
J. R. Jokipii *In* Jet Propulsion Lab., California Inst. of Tech., Interplanetary Particle Environment. Proceedings of a Conference 15 Apr. 1988 p 162-163 (For primary document see N89-28454 22-90)
Avail: NTIS HC A08/MF A01 CSCL 03B

A general conclusion is that the cosmic rays increase with increasing distance from the Sun at approximately 2 percent a.u. There is a strong correlation of the cosmic ray intensity with distance with the tilt of the heliospheric current sheet. Moreover, researchers find that the variation of the cosmic rays with time changes in alternate sun spot cycles. Finally, it seems that during alternate sun spot minima (1965 and 1985) the cosmic rays access to the inner solar system was along the equatorial current sheet, wheras in 1975 the cosmic rays came in over the poles. The recently discovered anomalous component of cosmic rays is very much related to this whole problem, and probably corresponds to particles being accelerated at the termination of the solar wind at some 50 to 100 astonomical units from the sun. In summary, many predictions of the models remain controversial in detail. Nonetheless, it appears now that we can expect more cosmic rays over the poles in the next sunspot cycle, and the intensity will continue to increase with heliocentric radius out to the interstellar medium. Author

N89-28471*# Bell Telephone Labs., Inc., New York, NY.
SILICON CHEMISTRY IN INTERSTELLAR CLOUDS
William D. Langer and A. E. Glassgold 26 May 1989 32 p
Prepared in cooperation with New York Univ., NY
(Grant NAGw-630)
(NASA-CR-185862; NAS 1.26:185862) Avail: NTIS HC A03/MF A01 CSCL 03B

Interstellar SiO was discovered shortly after CO but it has been detected mainly in high density and high temperature regions associated with outflow sources. A new model of interstellar silicon chemistry that explains the lack of SiO detections in cold clouds is presented which contains an exponential temperature dependence for the SiO abundance. A key aspect of the model is the sensitivity of SiO production by neutral silicon reactions to density and temperature, which arises from the dependence of the rate coefficients on the population of the excited fine structure levels of the silicon atom. This effect was originally pointed out in the context of neutral reactions of carbon and oxygen by Graff, who noted that the leading term in neutral atom-molecule interactions involves the quadrupole moment of the atom. Similar to the case of carbon, the requirement that Si has a quadrupole moment requires population of the J = 1 level, which lies 111K above the J = 0 ground state and has a critical density n(cr) equal to or greater than 10(6)/cu cm. The SiO abundance then has a temperature dependence proportional to exp(-111/T) and a quadratic density dependence for n less than n(cr). As part of the explanation of the lack of SiO detections at low temperatures and densities, this model also emphasizes the small efficiencies of the production routes and the correspondingly long times needed to reach equilibrium. Measurements of the abundance of SiO, in conjunction with theory, can provide information on the physical properties of interstellar clouds such as the abundances of oxygen bearing molecules and the depletion of interstellar silicon. Author

N89-28472# Instituto de Fisica Teorica, Sao Paulo (Brazil).
INFORMATION ASPECTS OF TYPE 9 COSMOLOGICAL MODELS
Gerson Francisco 1987 30 p
(DE89-612518; IFT-P-03/87) Avail: NTIS (US Sales Only) HC A03/MF A01

A study of amounts of information necessary to localize the trajectory of a dynamical system known as the Mixmaster universe is presented. The main result is that less information is necessary near the cosmological singularity of the system than far away. This conclusion is obtained by evolving probability distributions towards the singularity and comparing the associated information functions. Qualitative methods of dynamical systems theory present a phenomenon that might be related to this loss of information. DOE

N89-28473# Hiroshima Univ., Takehara (Japan). Research Inst. for Theoretical Physics.
STOCHASTIC APPROACH TO CHAOTIC INFLATION AND THE DISTRIBUTION OF UNIVERSES
Yasusada Nambu and Masao Sasaki Nov. 1988 15 p
(DE89-778051; RRK-88-35) Avail: NTIS (US Sales Only) HC A03/MF A01

Using the Fokker-Planck equation derived from stochastic approach to inflation, the dynamics and global structure of the chaotic inflationary universe are investigated. Full account was taken of the difference in the physical volume of each horizon size region in the Fokker-Planck equation. It was found that the modified Fokker-Planck equation admits a normalizable stationary solution, contrary to the original equation. The approximate form of the solution was evaluatedand it describes both the distribution of quantum universes out of which the universes was born and that of large classical (grow-up) universes like ours. In particular, for lambda phi sup 4 theory, the distribution of classical universes has a power law spectrum. Thus there appears no characteristic scale and the distribution of classical universes has a fractal structure. DOE

91 LUNAR AND PLANETARY EXPLORATION

Includes planetology; and manned and unmanned flights. For spacecraft design or space stations see *18 Spacecraft Design, Testing and Performance.*

N89-28474*# National Aeronautics and Space Administration, Washington, DC.
TIME-VARIABLE PHENOMENA IN THE JOVIAN SYSTEM
Michael J. S. Belton, ed., Robert A. West, ed. (Jet Propulsion Lab., California Inst. of Tech., Pasadena.), Jurgen Rahe, ed., and Margarita Pereyda 1989 406 p Workshop held in Flagstaff, AZ, 25-27 Aug. 1987 Original contains color illustrations
(NASA-SP-494; NAS 1.21:494; LC-88-25450) Avail: NTIS HC A18/MF A01 CSCL 03B

The current state of knowledge of dynamic processes in the Jovian system is assessed and summaries are provided of both theoretical and observational foundations upon which future research might be based. There are three sections: satellite phenomena and rings; magnetospheric phenomena, Io's torus, and aurorae; and atmospheric phenomena. Each chapter discusses time dependent theoretical framework for understanding and interpreting what is observed; others describe the evidence and nature of observed changes or their absence. A few chapters provide historical perspective and attempt to present a comprehensive synthesis of the current state of knowledge. Author

N89-28475*# Hampton Inst., VA. Dept. of Computer Science.
PARALLEL ARCHITECTURES FOR PLANETARY EXPLORATION REQUIREMENTS (PAPER) Interim Report
Ruknet Cezzar and Ranjan K. Sen 25 Jun. 1989 57 p

(Grant NAG1-949)
(NASA-CR-185370; NAS 1.26:185370) Avail: NTIS HC A04/MF A01 CSCL 03B

The Parallel Architectures for Planetary Exploration Requirements (PAPER) project is essentially research oriented towards technology insertion issues for NASA's unmanned planetary probes. It was initiated to complement and augment the long-term efforts for space exploration with particular reference to NASA/LaRC's (NASA Langley Research Center) research needs for planetary exploration missions of the mid and late 1990s. The requirements for space missions as given in the somewhat dated Advanced Information Processing Systems (AIPS) requirements document are contrasted with the new requirements from JPL/Caltech involving sensor data capture and scene analysis. It is shown that more stringent requirements have arisen as a result of technological advancements. Two possible architectures, the AIPS Proof of Concept (POC) configuration and the MAX Fault-tolerant dataflow multiprocessor, were evaluated. The main observation was that the AIPS design is biased towards fault tolerance and may not be an ideal architecture for planetary and deep space probes due to high cost and complexity. The MAX concepts appears to be a promising candidate, except that more detailed information is required. The feasibility for adding neural computation capability to this architecture needs to be studied. Key impact issues for architectural design of computing systems meant for planetary missions were also identified. K.C.D.

92 SOLAR PHYSICS

Includes solar activity, solar flares, solar radiation and sunspots.

For related information see *93 Space Radiation*.

N89-28476*# Smithsonian Astrophysical Observatory, Cambridge, MA.
CORONAGRAPH OBSERVATIONS AND ANALYSES OF THE ULTRAVIOLET SOLAR CORONA Semiannual Status Report, 1 Apr. 1987 - 31 Mar. 1989
John L. Kohl Mar. 1989 20 p
(Grant NAG5-613)
(NASA-CR-185830; NAS 1.26:185830; SASR-10; SASR-11; SASR-12; SASR-13) Avail: NTIS HC A03/MF A01 CSCL 03B

The major activities on the Spartan Ultraviolet Coronal Spectrometer project include both scientific and experimental/technical efforts. In the scientific area, a detailed analysis of the previously reported Doppler dimming of HI Ly-alpha from the July 1982 rocket flight has determined an outflow velocity at 2 solar radii from sun center to be between 153 and 251 km/s at 67 percent confidence. The technical activities include, several improvements made to the instrument that will result in enhanced scientific performance or in regaining a capability that had deteriorated during the delay time in the launch date. These include testing and characterizing the detector for OVI radiation, characterizing a serrated occulter at UV and visible wavelengths, fabricating and testing telescope mirrors with improved edges, testing and evaluating a new array detector system, modifying the slit mask mechanism and installing a mask in the instrument to block the Ly-alpha resonance line when the electron scattered component is being observed. Author

N89-28460*# Air Force Geophysics Lab., Hanscom AFB, MA.
INTENSITY/TIME PROFILES OF SOLAR PARTICLE EVENTS AT ONE ASTRONOMICAL UNIT
M. A. Shea *In* Jet Propulsion Lab., California Inst. of Tech., Interplanetary Particle Environment. Proceedings of a Conference 15 Apr. 1988 p 75-84 (For primary document see N89-28454 22-90)
Avail: NTIS HC A08/MF A01 CSCL 03B

N89-28461*# Maryland Univ., College Park. Dept. of Physics and Astronomy.
THE RADIAL DEPENDENCE OF THE SOLAR ENERGETIC PARTICLE FLUX
Douglas C. Hamilton *In* Jet Propulsion Lab., California Inst. of Tech., Interplanetary Particle Environment. Proceedings of a Conference 15 Apr. 1988 p 86-90 (For primary document see N89-28454 22-90)
Avail: NTIS HC A08/MF A01 CSCL 03B

N89-28462*# National Oceanic and Atmospheric Administration, Boulder, CO.
SOLAR PROTON EVENT FORECASTS
G. R. Heckman *In* Jet Propulsion Lab., California Inst. of Tech., Interplanetary Particle Environment. Proceedings of a Conference 15 Apr. 1988 p 91-100 (For primary document see N89-28454 22-90)
Avail: NTIS HC A08/MF A01 CSCL 03B

N89-28463*# Air Force Geophysics Lab., Hanscom AFB, MA.
PREDICTING THE ARRIVAL TIMES OF SOLAR PARTICLES
D. F. Smart *In* Jet Propulsion Lab., California Inst. of Tech., Interplanetary Particle Environment. Proceedings of a Conference 15 Apr. 1988 p 101-110 (For primary document see N89-28454 22-90)
Avail: NTIS HC A08/MF A01 CSCL 03B

N89-28464*# New Hampshire Univ., Durham. Inst. for the Study of Earth, Oceans and Space.
PARTICLES ACCELERATED BY SHOCKS IN THE HELIOSPHERE
Martin A. Lee *In* Jet Propulsion Lab., California Inst. of Tech., Interplanetary Particle Environment. Proceedings of a Conference 15 Apr. 1988 p 111-116 (For primary document see N89-28454 22-90)
(Grants NAG5-728; NAGw-76; NSF ATM-85-13363)
Avail: NTIS HC A08/MF A01 CSCL 03B

N89-28465*# Jet Propulsion Lab., California Inst. of Tech., Pasadena.
HIGH-ENERGY PARTICLES VERY NEAR THE SUN Abstract Only
B. E. Goldstein *In its* Interplanetary Particle Environment. Proceedings of a Conference 15 Apr. 1988 p 117 (For primary document see N89-28454 22-90)
Avail: NTIS HC A08/MF A01 CSCL 03B

93 SPACE RADIATION

Includes cosmic radiation; and inner and outer earth's radiation belts.

For biological effects of radiation see *52 Aerospace Medicine*. For theory see *73 Nuclear and High-Energy Physics*.

N89-28477# Lawrence Livermore National Lab., CA. Dept. of Physics.
GAMMA RAY BURSTS: CONFRONTATION BETWEEN THEORY AND OBSERVATIONAL DATA
Edison P. Liang 15 May 1989 21 p Presented at the Gamma Ray Observatory Science Workshop, Greenbelt, MD, 10-12 Apr. 1989
(Contract W-7405-eng-48)
(DE89-012936; UCRL-101121; CONF-8904216-3) Avail: NTIS HC A03/MF A01

The current observational data and theoretical models of cosmic gamma ray bursts are reviewed. The evidences for and physics issues of a teragauss field neutron star interpretation are summarized. Constraints on the baseline emission scenario are highlighted. A brief comparison is given of some popular astrophysical models. Some priorities for future observations and data analyses are suggested. DOE

N89-28478# Oak Ridge National Lab., TN. Biology Div.
RISK ASSESSMENT AND LATE EFFECTS OF RADIATION IN LOW-EARTH ORBITS
R. J. M. Fry 1989 15 p Presented at the Symposium on Radiation Hazards in Space and Biological Consequences, Washington, DC, 11 May 1989 Sponsored in part by Martin Marietta Energy Systems, Inc.
(Contract DE-AC05-84OR-21400)
(DE89-013043; CONF-8905157-1) Avail: NTIS HC A03/MF A01

The radiation dose rates in low-earth orbits are dependent on the altitude and orbital inclination. The doses to which the crews of space vehicles are exposed is governed by the duration of the mission and the shielding, and in low-earth orbit missions protons are the dominant particles encountered. The risk of concern with the low dose rates and the relatively low total doses of radiation that will be incurred on the space station is excess cancer. The National Council on Radiation Protection and Measurements has recently recommended career dose-equivalent limits that take into account sex and age. The new recommendations for career limits range from 1.0 Sv to 4 Sv, depending on sex and on the age at the time of their first space mission, compared to a single career limit of 4.0 Sv previously used by NASA. Risk estimates for radiated-induced cancer are evolving and changes in the current guidance may be required in the next few years. DOE

N89-28479# Lockheed Missiles and Space Co., Palo Alto, CA. Space Sciences Lab..
A SPACE RADIATION TEST MODEL STUDY Final Report, 20 May 1985 - 17 Feb. 1989
R. W. Nightingale, Y. T. Chiu, G. T. Davidson, W. E. Francis, and M. A. Rinaldi 17 Feb. 1989 92 p
(Contract F19628-85-C-0073)
(AD-A208760; LMSC/F297919; AFGL-TR-89-0036) Avail: NTIS HC A05/MF A01 CSCL 04/1

The tools for dynamic modeling of the energetic populations in the outer radiation belts are being developed to better understand the extreme variations of particle flux in response to magnetospheric and solar activity. The study utilizes the SCATHA SC3 high-energy electron data for energies from 200 keV to 2 MeV, with fine pitch-angle measurements over the L-shell range of 5.3 to 7 for quiet and moderate geomagnetic periods in April 1979 and June 1980. A solution of the simultaneous bimodal (radial and pitch-angle) diffusion equation for the radiation belts was developed with special regard for the requirements of satellite radiation belt data analysis. The solution was used to test the bimodal theory of outer-electron-belt diffusion by confronting it with satellite data. The data representation requires and provides diffusion parameters that are in agreement with all previous experimental and theoretical determinations of such diffusion coefficients. Such a representation satisfies the basic requirements towards the dynamic modeling of the outer electron radiation belt for L is less than 7 at quiet and moderate geomagnetic conditions. The presentation was also shown to be unique when projected off of the satellite trajectory in (L,t)-space. For L about 7 the representation has difficulties with butterfly distributions that may signify energetic electron encounters with the magnetopause.
GRA

N89-28480# Naval Research Lab., Washington, DC. Gamma and Cosmic Ray Astrophysics Branch.
DETECTION OF ARTIFICIAL SOURCES OF NUCLEAR RADIATION IN SPACE, REVISION Memorandum Report, Feb. 1980 - May 1981
G. H. Share, J. D. Kurfess, K. W. Marlow, J. A. Eisele, E. L. Chupp, and I. B. Strong (Los Alamos National Lab., NM.) 31 May 1989 36 p Revised
(AD-A209720; NRL-MR-6466; NRL-MR-4596-Rev) Avail: NTIS HC A03/MF A01 CSCL 18/4

The gamma-ray experiment on board NASA's Solar Maximum Mission Satellite (SMM) has detected nuclear radiation emitted from the reactor on COSMOS 1176. Direct observations of gamma-rays and possibly neutrons from this reactor were made at distances as close as about 350 km. Nuclear line features were observed in the gamma-ray spectrum. Explanations for some of these features are presented. The absolute power of the reactor is difficult to estimate at present; however, there is evidence that both the intensity and spectral shape of the emitted radiation changed significantly during the operational period of COSMOS. The reactor was also detected at distances of greater than or = 6,300 km in an indirect manner. Positrons and electrons escaping from the COSMOS spacecraft following production by the intense gamma-radiation are stored temporarily in the Earth's magnetic field and unambiguous signal due to their characteristic annihilation into gamma-rays at 511 keV. Details of these observations and their implications are discussed. GRA

N89-28481# Naval Research Lab., Washington, DC. Gamma and Cosmic Ray Astrophysics Branch.
MONITORING SOURCES OF NUCLEAR RADIATION IN SPACE. PART 1: EARLY 1984 OBSERVATIONS, REVISION
G. H. Share, J. D. Kurfess, and D. C. Messina (Sachs/Freeman Associates, Inc., Landover, MD.) 31 May 1989 14 p Revised
(AD-A209721; NRL-MR-6467-Pt-1; NRL-MR-5617-Pt-1-Rev)
Avail: NTIS HC A03/MF A01 CSCL 18/4

Nuclear radiation from the reactor powered satellite COSMOS 1579 was monitored by the gamma ray spectrometer (GRS) on NASA's Solar Maximum Mission satellite (SMM). Gamma rays from the RORSAT (Radar Ocean Reconnaissance Satellites) were detected about every 4 days as it passed within about 500 km of SMM. In addition, events attributed to positrons emitted from the outer shell of COSMOS 1579 were detected on the average of once every about 1.5 days. These positrons were detected at large distances (less than or = 5000 km) from COSMOS after being stored in the earth's magnetic field for seconds or minutes. The rate of the positron detections is about a factor of two higher than observed for most of the earlier RORSAT's detected by SMM. At present, this increase is unexplained. The qualitative features of the measured gamma-ray spectrum from COSMOS 1579 are similar to those of preceding satellites; however, the spectral features are clearer. A model is presented for the origin of these features which suggests the presence of significant amounts of beryllium, sodium, potassium, molybdenum and lithium and/or hydrogen lying with tens of gm/sq cm of material. There is also spectral evidence for the presence of either iron or aluminum. Based on this model, a conservative lower limit was obtained to the thermal power of the reactor on COSMOS 1579. This lower limit is 30 kW. GRA

N89-28482# Naval Research Lab., Washington, DC. Gamma and Cosmic Ray Astrophysics Branch.
MONITORING SOURCES OF NUCLEAR RADIATION IN SPACE 1980-1984 OBSERVATIONS, REVISION Memorandum Report, Apr. 1980 - Jan. 1985
G. H. Share, J. D. Kurfess, and D. C. Messina (Sachs/Freeman Associates, Inc., Landover, MD.) 31 May 1989 31 p Revised
(AD-A209722; NRL-MR-6468; NRL-MR-5862-Rev) Avail: NTIS HC A03/MF A01 CSCL 18/4

Details are provided of SMM's observations of the seven RORSATS (Radar Ocean Reconnaissance Satellites) launched from 1980 through 1984. Estimates are obtained of the relative power of the reactors from integral gamma ray intensities measured at distances less than 400 km. The average intensities from the seven satellites, after correcting for distance of separation, are consistent with each other to within 30 percent. In contrast, the rate of distant detections of positrons increased with time over the four year period. The rate of detections was about 0.2/day in 1980 and 0.7/day in 1984. This increasing rate is due to the decreasing atmospheric density above a few hundred km in the transition from maximum to minimum solar activity. The positron storage time in the geomagnetic field is expected to increase with decreasing density. A composite gamma ray spectrum created from a summation of close-approach sightings of the seven RORSATS are presented. It is not possible to obtain a unique interpretation of this spectrum. One relatively simple model of the gamma ray spectrum emitted from the RORSATS which fits the

data reasonably well includes the following components: a fission continuum from U-235 and neutron capture lines from molybdenum embedded within tens of g/sq cm of material; two unresolved lines near 500 keV attributed to a line at 511 keV from positron-annihilation and to a line near 477 keV from boron. GRA

N89-28483# Naval Research Lab., Washington, DC. Gamma and Cosmic Ray Astrophysics Branch.
MONITORING SOURCES OF NUCLEAR RADIATION IN SPACE 1985-1987 OBSERVATIONS, REVISION
G. H. Share, J. D. Kurfess, and D. C. Messina (Sachs/Freeman Associates, Inc., Landover, MD.) 31 May 1989 23 p Revised (AD-A209723; NRL-MR-6469; NRL-MR-6297-Rev) Avail: NTIS HC A03/MF A01 CSCL 18/4

The gamma-ray spectrometer (GRS) on NASA's Solar Maximum Mission satellite (SMM) has been monitoring Soviet nuclear reactors in space since 1980 when it detected radiation from COSMOS 1176. Direct observations of gamma radiation were made within about 500 km when the RORSATS (Radar Ocean Reconnaissance Satellites) were not occulted by a significant amount of material in SMM. Indirect observations were also made up to distances in excess of a few thousand kilometers. These observations were made when positrons and electrons produced in the outer layers of the reactor powered spacecraft reached SMM after being stored in the Earth's magnetic field. Details are provided of SMM's observations of the four RORSATS launched in 1985 and 1986, and are compared with measurements made of the seven RORSATS detected from 1980 to 1984. The average intensities from all the eleven reactor-powered satellites are consistent with each other, after correcting for distance of separation. The observed increase in the rate of distant detections of positrons from 1980 to 1984 is due to the decreasing atmospheric density above a few hundred km in the transition from maximum to minimum solar activity. The rate did not change significantly between 1984 and 1986. GRA

N89-28484# Utah Univ., Salt Lake City. Dept. of Physics.
STUDIES OF THE COSMIC RAY PENUMBRA Final Report, 9 Sep. 1980 - 30 Sep. 1985
David J. Cooke 11 Aug. 1988 110 p
(Contract F19628-81-K-0020)
(AD-A210109; AFGL-TR-88-0203) Avail: NTIS HC A06/MF A01 CSCL 03/2

The penumbra is the term used to refer to the interval of space which lies, for any given particle rigidity, between the solid angle zone within which all such particles have free access, and the region within which particle access is completely forbidden. The term is also used to refer, in a specific direction, to the rigidity interval between the lowest rigidity for which any particle may enter in the given direction, and the rigidity below which particle access is completely forbidden in the same direction. Typically the penumbra consists of a mixture of allowed and forbidden trajectories. This question of access of charged primary cosmic rays to points within the magnetic field of a plant is of great interest in numbers of areas of physics. It is very difficult, however, to map the allowed and forbidden regions of access, because of the time-consuming nature of the calculations involved. The present research has involved a systematic study of the nature of the characteristic zones of access in order to produce techniques by which information about the cosmic ray penumbra may efficiently be derived. The work has then focused on the mapping and study of the phenomenology of the penumbra. GRA

N89-28456*# Jet Propulsion Lab., California Inst. of Tech., Pasadena.
TOWARD A DESCRIPTIVE MODEL OF GALACTIC COSMIC RAYS IN THE HELIOSPHERE
R. A. Mewaldt, A. C. Cummings, James H. Adams, Jr., Paul Evenson, W. Fillius, J. R. Jokipii, R. B. McKibben (Chicago Univ., IL.), and Paul A. Robinson, Jr. *In its* Interplanetary Particle Environment. Proceedings of a Conference 15 Apr. 1988 p 14-32 (For primary document see N89-28454 22-90)
Avail: NTIS HC A08/MF A01 CSCL 03B

N89-28458*# Naval Research Lab., Washington, DC. Center for Space Research.
CURRENT MODELS OF THE INTENSELY IONIZING PARTICLE ENVIRONMENT IN SPACE
James H. Adams, Jr. *In* Jet Propulsion Lab., California Inst. of Tech., Interplanetary Particle Environment. Proceedings of a Conference 15 Apr. 1988 p 49-56 (For primary document see N89-28454 22-90)
Avail: NTIS HC A08/MF A01 CSCL 03B

N89-28459*# Jet Propulsion Lab., California Inst. of Tech., Pasadena.
A NEW PROTON FLUENCE MODEL FOR E GREATER THAN 10 MeV
Joan Feynman, T. P. Armstrong, L. Dao-Gibner, and S. Silverman (Boston Coll., Chestnut Hill, MA.) *In its* Interplanetary Particle Environment. Proceedings of a Conference 15 Apr. 1988 p 58-71 (For primary document see N89-28454 22-90)
(Grant NSF ATM-83-05537)
Avail: NTIS HC A08/MF A01 CSCL 03B

N89-28466*# California Inst. of Tech., Pasadena.
ELEMENTAL COMPOSITION AND ENERGY SPECTRA OF GALACTIC COSMIC RAYS
R. A. Mewaldt *In* Jet Propulsion Lab., California Inst. of Tech., Interplanetary Particle Environment. Proceedings of a Conference 15 Apr. 1988 p 121-132 (For primary document see N89-28454 22-90)
(Grants NGR-05-002-160; NAG5-722)
Avail: NTIS HC A08/MF A01 CSCL 03B

N89-28467*# California Inst. of Tech., Pasadena.
THE ANOMALOUS COSMIC-RAY COMPONENT
A. C. Cummings and E. C. Stone *In* Jet Propulsion Lab., California Inst. of Tech., Interplanetary Particle Environment. Proceedings of a Conference 15 Apr. 1988 p 133-134 (For primary document see N89-28454 22-90)
(Contract NAS7-918; NGR-05-002-160)
Avail: NTIS HC A08/MF A01 CSCL 03B

N89-28468*# Chicago Univ., IL.
GRADIENTS OF GALACTIC COSMIC RAYS AND ANOMALOUS COMPONENTS
R. B. McKibben *In* Jet Propulsion Lab., California Inst. of Tech., Interplanetary Particle Environment. Proceedings of a Conference 15 Apr. 1988 p 135-148 (For primary document see N89-28454 22-90)
Avail: NTIS HC A08/MF A01 CSCL 03B

N89-28469*# Delaware Univ., Newark.
TIME VARIATION OF GALACTIC COSMIC RAYS
Paul Evenson *In* Jet Propulsion Lab., California Inst. of Tech., Interplanetary Particle Environment. Proceedings of a Conference 15 Apr. 1988 p 149-161 (For primary document see N89-28454 22-90)
(Grants NAG5-374; NSF ATM-86-03192)
Avail: NTIS HC A08/MF A01 CSCL 03B

N89-28470*# Arizona Univ., Tucson.
GALACTIC COSMIC RAYS IN THREE DIMENSIONS Abstract Only
J. R. Jokipii *In* Jet Propulsion Lab., California Inst. of Tech., Interplanetary Particle Environment. Proceedings of a Conference 15 Apr. 1988 p 162-163 (For primary document see N89-28454 22-90)
Avail: NTIS HC A08/MF A01 CSCL 03B

99 GENERAL

No abstracts in this category.

Typical Subject Index Listing

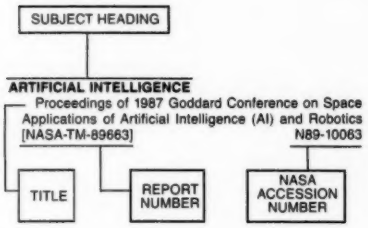

The subject heading is a key to the subject content of the document. Titles, report numbers, and accession numbers of pertinent documents are provided under each subject heading. When the title is insufficiently descriptive of the document content, a title extension has been added, separated from the title by three hyphens. The report number helps to indicate the type of document cited (e.g., NASA report, NASA translation, NASA contractor report). The NASA accession number is the number by which the document abstracts are arranged in this journal and by which the document is sold or requested. The titles, with title extensions if present, are arranged under each subject heading in ascending accession number order. The subject headings have been selected from the latest revision of the *NASA Thesaurus* (NASA SP-7064).

A

ABILITIES
A new item response theory modeling approach with applications to unidimensionality assessment and ability estimation
[AD-A207301] N89-28360

ABSORBERS (MATERIALS)
Parametric study of electromagnetic waves propagating in absorbing curved S ducts
[NASA-TM-102024] N89-27923

ABSTRACTS
The Shock and Vibration Digest, volume 21, no. 4 N89-28025
High-temperature superconductivity: Abstracts of NIST (National Institute of Standards and Technology) publications, 1987-1988
[PB89-148340] N89-28405

ACCELERATION (PHYSICS)
Particles accelerated by shocks in the heliosphere N89-28464

ACCELERATION TOLERANCE
The effect of various straining maneuvers on cardiac volumes at 1G and during +Gz acceleration
[AD-A208846] N89-28200

ACCESS CONTROL
The sharing of rights and information in a capability-based protection system
[NASA-CR-185388] N89-28445

ACCIDENT PREVENTION
Analysis of a system to prevent helicopter rotor blade-airframe strikes
[AD-A209804] N89-27649

ACCURACY
High-precision radiometric tracking for planetary approach and encounter in the inner solar system N89-27873

ACETYLENE
High performance composites based on polyurethanes reinforced with polydiacetylenes
[AD-A208436] N89-27797

ACOUSTIC ATTENUATION
Reflection and refraction of finite amplitude acoustic waves at a fluid-fluid interface
[AD-A209800] N89-28371

ACOUSTIC EMISSION
An acoustic emission investigation of the tensile failure of cathodically charged 304 stainless steel
[DE89-008752] N89-27816

ACOUSTIC MEASUREMENT
The texture variation in extruded graphite
[DE89-014086] N89-27837
Glassy behaviour of YBa2Cu3O7
[DE89-613399] N89-28418

ACOUSTIC PROPERTIES
Modeling of ocean surface spectrum and surface scattering. Applications to reverberation prediction in the AAUS program
[AD-A210127] N89-28197

ACOUSTIC SCATTERING
Analysis of a limiting-amplitude problem in acousto-elastic interactions, 1
[AD-A209741] N89-28045
Modeling of ocean surface spectrum and surface scattering. Applications to reverberation prediction in the AAUS program
[AD-A210127] N89-28197

ACOUSTIC VELOCITY
Sound propagation in bubbly liquids: A review
[AD-A207377] N89-28370

ACOUSTICS
Numerical simulation of control of supersonic shear layers
[AD-A209703] N89-27639

ACOUSTO-OPTICS
Acoustooptic processing of two dimensional signals using temporal and spatial integration
[AD-A208686] N89-27966

ACRYLIC RESINS
The influence of the polymer backbone flexibility on the phase transitions of side chain liquid crystal polymers containing
yl side groups
[AD-A208821] N89-27851

ACTIVATION ENERGY
Transition metal activation and functionalization of carbon-hydrogen bonds
[DE89-012949] N89-27804

ACTUATORS
A new method for analysis of limit cycle behavior of the NASA/JPL 70-meter antenna axis servos N89-27880

ADAPTATION
Adaptive preprocessing of nonstationary signals
[AD-A209646] N89-27946

ADAPTIVE CONTROL
Joint-space adaptive control of a 6 DOF end-effector with closed-kinematic chain mechanism
[NASA-CR-185861] N89-28016
Design of an adaptive controller for a telerobot manipulator
[NASA-CR-185863] N89-28017
Adaptive grid methods for numerical weather prediction
[AD-A209950] N89-28117

ADAPTIVE FILTERS
Analysis and dimensioning of a value-discrete adaptive compensation filter N89-27932

ADDITIVES
Theoretical model for stabilization of clay-silt airport pavement subgrade systems. Phase 1: Laboratory investigation. Phase 2: Rutting tests
[DOT/FAA/PM-87/20-PHASE-1/2] N89-27673

ADHESION
Ceramic joining in the United States
[DE89-009323] N89-27834

ADHESIVES
An adhesive for field repair of composites
[AD-A209992] N89-27859

ADIABATIC CONDITIONS
Efficient energy storage and conversion using adiabatic compression of relativistic-electron plasmas
[AD-A208657] N89-28101
Modified rotationally adiabatic model for rotational autoionization of dipole-bound molecular anions
[AD-A209651] N89-28388

ADSORPTION
Comparison of vacuum-annealed and electrochemically cycled electrodes in adsorption and electrocatalysis: Aromatic compounds at platinum (111) and polycrystalline platinum
[AD-A210011] N89-27814
Formation of monolayers by the coadsorption of thiols on gold: Variation in the length of the alkyl chain
[AD-A208386] N89-27824
Decomposition kinetics and film formation of an organometallic precursor to SiC on Si(100)
[AD-A208384] N89-28420

AERODYNAMIC CHARACTERISTICS
Numerical simulation of control of supersonic shear layers
[AD-A209703] N89-27639
Studies of unsteady vortex flap aerodynamics
[AD-A209837] N89-27641
United States Air Force Research Initiation Program for 1987, volume 1
[AD-A209726] N89-28436

AERODYNAMIC COEFFICIENTS
Hypersonic prediction comparisons with experimental data for a cone-cylinder at mach 6.86
[AD-A207583] N89-27636
Summary of longitudinal stability and control parameters as determined from Space Shuttle Challenger flight test data
[NASA-TM-101605] N89-27671

AERODYNAMIC CONFIGURATIONS
Aerodynamic design of low pressure turbines N89-27669

AERODYNAMIC DRAG
Low density flow effects for hypervelocity vehicles
[AD-A206218] N89-27633
A small ion-propelled spacecraft for near earth experiments N89-27752

AERODYNAMIC FORCES
Hypersonic prediction comparisons with experimental data for a cone-cylinder at mach 6.86
[AD-A207583] N89-27636
Small scale model tests in small wind and water tunnels at high incidence and pitch rates. Volume 2: Small wind tunnel (ADF) data base
[AD-A208539] N89-27676

AERODYNAMIC STABILITY
Studies of unsteady vortex flap aerodynamics
[AD-A209837] N89-27641

AERODYNAMIC STALLING
Verification of the production safe flight instrument corporation OV/RV-1D stall warning system
[AD-A207392] N89-27659

AERODYNAMICS
United States Air Force Research Initiation Program for 1987, volume 3
[AD-A209728] N89-28437

AERONAUTICAL ENGINEERING
Aerospace structures design on computers
[AD-A208811] N89-28321

AEROSOLS
Aerosol model selection using surface measurements of IR horizon radiances and satellite detected visible radiances
[AD-A209638] N89-28110
A new background stratospheric aerosol model for use in atmospheric radiation models
[AD-A210110] N89-28112
YAG aerosol lidar N89-28135

AEROSPACE MEDICINE
Anthropometric measurements of aviators within the Aviation Epidemiology Data Register
[AD-A208609] N89-28300

AEROSPACE PLANES
Cyrogenic fluid sink device for thermal control of a spaceplane during ascent and re-entry phases N89-28293
AEROSPACE SYSTEMS
European life support systems for space applications N89-28218
Space asset modeling for wargame integration [AD-A207350] N89-28365
United States Air Force Research Initiation Program for 1987, volume 3 [AD-A209728] N89-28437
AEROSPACE VEHICLES
Aerospace structures design on computers [AD-A208811] N89-28321
AEROTHERMODYNAMICS
Low density flow effects for hypervelocity vehicles [AD-A206218] N89-27633
Parametric study of the aerothermodynamics of a jet engine test facility [AD-A206512] N89-27675
Research and technology plans for FY 1989 and accomplishments for FY 1988 — Structural Mechanics Division [NASA-TM-101592] N89-28035
AGE FACTOR
Age-related changes in human vestibulo-ocular reflexes: Sinusoidal rotation and caloric tests [NASA-CR-185857] N89-28211
Age-related changes in human posture control: Sensory organization tests [NASA-CR-185858] N89-28212
Age-related changes in human vestibulo-ocular and optokinetic reflexes: Pseudorandom rotation tests [NASA-CR-185856] N89-28213
AGRICULTURE
Report of the Project Estima, phase 2: LANDSAT-TM data and agrometeorology in crop yield estimation of wheat at the farm level [INPE-4782-RPE/582-PHASE-2] N89-28051
AGROCLIMATOLOGY
Bangladesh Agro-Climatic Environmental Monitoring Project N89-28121
NASA follow-on to the Bangladesh Agro-Climatic Environmental Monitoring Project N89-28122
AGROMETEOROLOGY
Report of the Project Estima, phase 2: LANDSAT-TM data and agrometeorology in crop yield estimation of wheat at the farm level [INPE-4782-RPE/582-PHASE-2] N89-28051
AIR BREATHING ENGINES
Missile Datcom. Volume 2: User's manual [AD-A210128] N89-27685
AIR CONDITIONING
Physico-chemical atmosphere revitalisation: The qualitative and quantitative selection of regenerative designs N89-28221
AIR PURIFICATION
Electrochemical removal and concentration of CO2 N89-28238
AIR SEA ICE INTERACTIONS
Sea ice/climate studies N89-28151
Wave/current interaction model N89-28153
Climatological aspects of Nimbus-7 SMMR data N89-28156
AIR TRAFFIC CONTROL
Terminal area forecasts: FY 1989 - 2005 [AD-A209805] N89-27644
Automated planning function for AERA 3: Maneuver option manager [DOT/FAA/DS-89/21] N89-27645
AIR TRANSPORTATION
Compacted-snow runways: Guidelines for their design and construction in Antarctica [AD-A208910] N89-27677
AIR WATER INTERACTIONS
Analyses of the wind-driven response of tropical oceans N89-28155
Surface Contour Radar (SCR) contributions to FASINEX N89-28159
The Surface Wave Dynamics Experiment (SWADE) N89-28162
AIRBORNE EQUIPMENT
Airborne Oceanographic Lidar (AOL) flight mission participation N89-28143
Navigational and Environmental Measurement System (NEMS) N89-28178
Airborne lidar global positioning investigations N89-28179
Large aperture scanning airborne lidar N89-28186
A multiprocessor airborne lidar data system N89-28187
AIRBORNE LASERS
NASA Charge Coupled Device (CCD) Spectrometer System (NCSS) N89-28142
AIRBORNE/SPACEBORNE COMPUTERS
Modeling functional specifications for onboard software N89-27658
Effect of three-dimensional object type and density in simulated low-level flight [AD-A209756] N89-27679
AIRCRAFT ACCIDENTS
An analysis of severe air transport accidents [DE89-012642] N89-27642
AIRCRAFT COMMUNICATION
Aeronautical mobile TDMA/MCTDMA system N89-27918
AIRCRAFT CONFIGURATIONS
Computation of transonic potential flow past RAE-Wing-A and Body-B2 combination [PD-CF-8921] N89-27637
Evaluation of a strain-gage load calibration on a low-aspect-ratio wing structure at elevated temperature [NASA-TP-2921] N89-28034
AIRCRAFT CONSTRUCTION MATERIALS
Research and technology plans for FY 1989 and accomplishments for FY 1988 — Structural Mechanics Division [NASA-TM-101592] N89-28035
AIRCRAFT DESIGN
Aerostat cold weather study [AD-A207299] N89-27635
High-speed civil transport study. Summary [NASA-CR-4234] N89-27647
AIRCRAFT ENGINES
Blading Design for Axial Turbomachines [AGARD-LS-167] N89-27661
AIRCRAFT FUEL SYSTEMS
Investigation of transport airplane fuselage fuel tank installations under crash conditions [DOT/FAA/CT-88/24] N89-27643
AIRCRAFT FUELS
United States Air Force Research Initiation Program for 1987, volume 4 [AD-A209729] N89-28438
AIRCRAFT GUIDANCE
Automated planning function for AERA 3: Maneuver option manager [DOT/FAA/DS-89/21] N89-27645
AIRCRAFT HAZARDS
Investigation of transport airplane fuselage fuel tank installations under crash conditions [DOT/FAA/CT-88/24] N89-27643
Analysis of a system to prevent helicopter rotor blade-airframe strikes [AD-A209804] N89-27649
AIRCRAFT INDUSTRY
Terminal area forecasts: FY 1989 - 2005 [AD-A209805] N89-27644
AIRCRAFT INSTRUMENTS
NASA Aircraft-Satellite Instrument Calibration Project N89-28189
AIRCRAFT LANDING
A comparison of rutting behavior of asphalt concrete under the F-4C/G and F-15C/D aircraft [AD-A208911] N89-27678
AIRCRAFT MANEUVERS
Automated planning function for AERA 3: Maneuver option manager [DOT/FAA/DS-89/21] N89-27645
A mathematical formulation for planning automated aircraft separations for AERA 3 [DOT/FAA/DS-89/20] N89-27646
Small scale model tests in small wind and water tunnels at high incidence and pitch rates. Volume 2: Small wind tunnel (ADF) data base [AD-A208539] N89-27676
AIRCRAFT PRODUCTION
Baseline performance verification of the 12th year production UH-60A Black Hawk helicopter [AD-A208671] N89-27632
AIRCRAFT SAFETY
An analysis of severe air transport accidents [DE89-012642] N89-27642
Investigation of transport airplane fuselage fuel tank installations under crash conditions [DOT/FAA/CT-88/24] N89-27643
AIRCRAFT STRUCTURES
Evaluation of a strain-gage load calibration on a low-aspect-ratio wing structure at elevated temperature [NASA-TP-2921] N89-28034
Aerospace structures design on computers [AD-A208811] N89-28321
AIRCRAFT WAKES
Photogrammetric technique for in-flight ranging of trailing vortices using entrained balloons [NASA-TM-4129] N89-27995
AIRFRAMES
Analysis of a system to prevent helicopter rotor blade-airframe strikes [AD-A209804] N89-27649
AIRLINE OPERATIONS
Terminal area forecasts: FY 1989 - 2005 [AD-A209805] N89-27644
AIRPORT PLANNING
Terminal area forecasts: FY 1989 - 2005 [AD-A209805] N89-27644
AIRSHIPS
Aerostat cold weather study [AD-A207299] N89-27635
AIRSPEED
Baseline performance verification of the 12th year production UH-60A Black Hawk helicopter [AD-A208671] N89-27632
ALBEDO
Advanced Solidstate Array Spectroradiometer N89-28183
ALGEBRA
Algebraic analysis of the electromagnetic wave interaction with the two-level system with two-fold degenerated states [DE89-011932] N89-27926
Parameter plane design method [AD-A209845] N89-28322
Orbits which always have affine invariant neighbourhoods [DE89-011895] N89-28344
Image Algebra FORTRAN preprocessor: User's manual [AD-A208612] N89-28349
ALGORITHMS
A mathematical formulation for planning automated aircraft separations for AERA 3 [DOT/FAA/DS-89/20] N89-27646
Verification of control sequence and algorithm for the electric propulsion experiment (EPEX) N89-27740
Quantitative estimation of component amplitude in multiexponential data: Application to time-resolved fluorescence spectroscopy [AD-A210142] N89-27815
Decoding of 1/2-rate (24,12) Golay codes N89-27891
Math and physics studies-multi-project support entropy-based image restoration: Modifications and addditional results [AD-A209972] N89-27951
Studies in statistical signal processing [AD-A210054] N89-27952
Pigtailed single-mode diode lasers [AD-A209913] N89-28012
Basic research in reliability for real systems [AD-A209649] N89-28022
Novel methodology for application of adaptive systems techniques to DMSP (Defense Meteorological Satellite Program) remote temperature sensing [AD-A209975] N89-28098
Ocean topography experiment (TOPEX) radar altimeter N89-28119
Oceanographic applications of laser technology N89-28141
Climatological aspects of Nimbus-7 SMMR data N89-28156
Rainfall on microwave return from the sea surface N89-28160
An algorithm for calculating thermodynamic properties of simple fluids suitable for space thermal control N89-28254
Performance augmentation of SITIM-150 through a high performance numerical processor [INPE-4770-PRE/1439] N89-28305
Optimal three-dimensional path planning using visibility constraints [AD-A207357] N89-28310
Extended Kalman Filter (EKF) algorithm [PD-CF-8922] N89-28313
A fast multipole algorithm for capacitance extraction of complex 3-D geometries [AD-A208374] N89-28317
Fixed interval smoothing algorithm for an extended Kalman filter for over-the-horizon ship tracking [AD-A208555] N89-28318
Statistical analysis of the LMS and modified stochastic gradient algorithms [AD-A208618] N89-28319
An efficient exact algorithm for the least squares image registration problem [AD-A208725] N89-28320
Automatic construction of polyhedral surfaces from voxel representations [AD-A210009] N89-28325
Algorithmic control of walking [AD-A210117] N89-28326
Load balancing in multiprocessor systems [AD-A210144] N89-28327

A computational comparison of the primal simplex and relaxation algorithms for solving minimum cost flow networks
[AD-A208534] N89-28331
Resource contention management in parallel systems
[AD-A208809] N89-28332
A RUTCOR project on discrete applied mathematics
[AD-A208572] N89-28347
Computational methods and systems for problems in science and engineering
[AD-A209951] N89-28355
Binary sequences of arbitrary length with near-ideal correlation
[AD-A209956] N89-28356
Significant digit computation of the incomplete beta function ratios
[AD-A210118] N89-28358
Symmetry in the basic sciences
[AD-A207371] N89-28369

ALIGNMENT
Topology of modified helical gears
[NASA-TM-102134] N89-28015

ALLOYING
Effect of alloying, rapid solidification, and surface kinetics on the high temperature environmental resistance of niobium
[AD-A209934] N89-27829

ALLOYS
Institute for Materials Science and Engineering: Metallurgy Division, technical activities 1988
[PB89-201321] N89-27819

ALPINE METEOROLOGY
Improved snow and glacier monitoring by the LANDSAT Thematic Mapper N89-28056
Multitemporal snow classification with TM data N89-28057

ALTIMETERS
Determination of local empirical covariance functions from residual terrain reduced altimeter data
[AD-A208678] N89-28095

ALTITUDE CONTROL
Effect of three-dimensional object type and density in simulated low-level flight
[AD-A209756] N89-27679

ALUMINIDES
Advanced tribological coatings for high specific strength alloys
[AD-A208504] N89-27825

ALUMINUM
Development of anodes for aluminum/air batteries: Solution phase inhibition of corrosion
[DE89-012839] N89-27956

ALUMINUM ALLOYS
The structure and properties of grain boundaries in B2 ordered alloys
[DE89-013266] N89-27817
Corrosion of aluminium alloys by IRFNA (Inhibited Red Fuming Nitric Acid)
[AD-A208326] N89-27823
Probabilistic description of fatigue crack growth under constant-and variable-amplitude loading
[AD-A208717] N89-28043

ALUMINUM GALLIUM ARSENIDES
Transport and submillimeter wave spectroscopy of GaAs/Al sub xGa sub 1-xAs heterostructures
[AD-A209836] N89-28428

ALUMINUM OXIDES
Optical spectroscopy of copper (1) doped Na(+) beta-alumina
[AD-A209819] N89-27810
Protonic solid electrolytes: Thermal stability and conductivity of ammonium/hydronium beta'-alumina
[AD-A209911] N89-27813
Effect of alloying, rapid solidification, and surface kinetics on the high temperature environmental resistance of niobium
[AD-A209934] N89-27829
Energy transfer effects in beta-alumina
[AD-A209818] N89-27855
The use of multiple ion exchange to produce energy transfer in beta-aluminas
[AD-A209821] N89-27856

AMBIENT TEMPERATURE
Compensation for effects of ambient temperature on rare-earth doped fiber optic thermometer
[NASA-TM-102282] N89-27998

AMMONIA
Vibrational predissociation of shock-selected C2H4 and NH3 clusters, introduction N89-28374

AMMONIUM COMPOUNDS
Protonic solid electrolytes: Thermal stability and conductivity of ammonium/hydronium beta'-alumina
[AD-A209911] N89-27813

AMORPHOUS MATERIALS
Solvent assisted delamination crack growth behavior of amorphous thermoplastic materials
[AD-A207365] N89-27833

AMORPHOUS SILICON
Photovoltaic Program Branch annual report, FY 1988
[DE89-000898] N89-28099

AMPLIFICATION
DSN 70-meter antenna X- and S-band calibration. Part 1: Gain measurements N89-27904
DSN 70-meter antenna X- and S-band calibration. Part 2: System noise temperature measurements and telecommunications link evaluation N89-27905
Noise and false alarm rate characteristics for envelope detector systems preceded by RF amplification
[AD-A209789] N89-27948

AMPLIFIERS
A multiflare horn with 1-megawatt power handling capability N89-27884
Noise and false alarm rate characteristics for envelope detector systems preceded by RF amplification
[AD-A209789] N89-27948

AMPLITUDE MODULATION
Minimum shift keying. A modulation system with coding N89-27931
Carrier derivation in higher-stage QAM-signals N89-27935

ANALOG DATA
Analog methods and instruments N89-28094

ANALOGIES
Learning from physical analogies: A study in analogy and the explanation process
[AD-A208689] N89-28338

ANALYTICAL CHEMISTRY
Analytical procedures for environmental quality control, volume 3
[PB89-158620] N89-28104

ANHYDRIDES
Photodegradation of polyimide 1. A spectral, viscometric, chromatographic and weight loss investigation of polyimides based on a perfluorinated dianhydride
[AD-A208507] N89-27845

ANIONS
Modified rotationally adiabatic model for rotational autoionization of dipole-bound molecular anions
[AD-A209851] N89-28388

ANISOTROPIC PLATES
Mechanical and physical study of the behavior under sequential loads of copper and steel plates
[ETN-89-94805] N89-28037

ANNIHILATION REACTIONS
Antiproton powered propulsion with magnetically confined plasma engines
[NASA-CR-185131] N89-27700

ANNUAL VARIATIONS
Multitemporal analysis of forest areas in surroundings of Innsbruck, Austria N89-28086
Analysis of sea ice dynamics N89-28149
Sea ice/climate studies N89-28151

ANNULAR FLOW
Further investigation of flow modeling during solid propellant processing
[AD-A209787] N89-27866

ANODES
Anode-nozzle experimental analysis in a coaxial non-steady solid propellant MPD thruster N89-27757
Development of anodes for aluminum/air batteries: Solution phase inhibition of corrosion
[DE89-012839] N89-27956

ANTARCTIC REGIONS
Compacted-snow runways: Guidelines for their design and construction in Antarctica
[AD-A208910] N89-27677
Correlative Measurements Program N89-28164

ANTENNA ARRAYS
DARPA (Defense Advanced Research Projects Agency) Review on EHF Devices
[AD-A208564] N89-27963

ANTENNA COMPONENTS
A multiflare horn with 1-megawatt power handling capability N89-27884

ANTENNA DESIGN
Target signature modeling and bistatic scattering measurement studies
[NASA-CR-185434] N89-27870
The Telecommunications and Data Acquisition Report
[NASA-CR-185431] N89-27871
A multiflare horn with 1-megawatt power handling capability N89-27884
A new analysis of beam-waveguide antennas considering the presence of the enclosure N89-27886
DSN 70-meter antenna microwave optics design and performance improvements. Part 1: Design optimization N89-27903
Reanalysis, compatibility and correlation in analysis of modified antenna structures N89-27906
An experimental and computer modeling study of stepped radius monopole antennas
[AD-A207356] N89-27919

ANTENNA FEEDS
Microwave time delays for the X/S-band feed system at X-band N89-27898
TELE-X antenna module thermal control N89-28257

ANTENNA RADIATION PATTERNS
A multiflare horn with 1-megawatt power handling capability N89-27884
A new analysis of beam-waveguide antennas considering the presence of the enclosure N89-27886

ANTENNAS
A new method for analysis of limit cycle behavior of the NASA/JPL 70-meter antenna axis servos N89-27880
Application of optimal control theory to the design of the NASA/JPL 70-meter antenna servos N89-27881
Precision pointing compensation for DSN antennas with optical distance measuring sensors N89-27882
The effects of atmospheric turbulence on precision optical measurements used for antenna-pointing compensation N89-27883
Microwave time delays for the X/S-band feed system at X-band N89-27898
DSN 70-meter antenna microwave optics design and performance improvements. Part 1: Design optimization N89-27903
DSN 70-meter antenna X- and S-band calibration. Part 1: Gain measurements N89-27904
DSN 70-meter antenna X- and S-band calibration. Part 2: System noise temperature measurements and telecommunications link evaluation N89-27905

ANTHROPOMETRY
Anthropometric measurements of aviators within the Aviation Epidemiology Data Register
[AD-A208609] N89-28300

ANTICHOLINERGICS
Acetylcholinesterase inhibitor, pyridostigmine bromide, reduces skin blood flow in humans
[AD-A209615] N89-28202

ANTIMISSILE DEFENSE
High Endoatmospheric Defense Interceptor (HEDI) technology testing program environmental assessment
[AD-A210006] N89-27684
The 1989 report to the Congress on the Strategic Defense Initiative
[PB89-196661] N89-28368

ANTIMISSILE MISSILES
High Endoatmospheric Defense Interceptor (HEDI) technology testing program environmental assessment
[AD-A210006] N89-27684

ANTIPROTONS
Antiproton powered propulsion with magnetically confined plasma engines
[NASA-CR-185131] N89-27700

ANTIREFLECTION COATINGS
Growth and characterization of zinc sulfide films by conversion of zinc oxide films with H2S
[AD-A208727] N89-28423

APERTURES
Large aperture scanning airborne lidar N89-28186

APPLICATIONS PROGRAMS (COMPUTERS)
Modeling functional specifications for onboard software N89-27658
KIVA-2: A computer program for chemically reactive flows with sprays
[DE89-012805] N89-27975
A data acquisition and control program for axial-torsional fatigue testing
[NASA-TM-102041] N89-28029
Real gas equations of state for CHEMKIN
[DE89-012794] N89-28432

APPROACH
High-precision radiometric tracking for planetary approach and encounter in the inner solar system N89-27873

APPROACH CONTROL
Automated planning function for AERA 3: Maneuver option manager
[DOT/FAA/DS-89/21] N89-27645

APPROPRIATIONS
National Aeronautics and Space Administration Multiyear Authorization Act of 1989
[H-REPT-101-226] N89-28451

APPROXIMATION
A central difference type approximation of convection in fluid flow
[DE89-013282] N89-27981
A uniformly differentiable approximation scheme for delay systems using splines
[AD-A208567] N89-28346

ARC DISCHARGES
Performance of a 100 kW class applied field MPD thruster
[NASA-TM-102312] N89-27701

A 15 kW experimental arcjet N89-27778

ARC JET ENGINES

Interests in electric propulsion N89-27711
Improved thrust generation mechanism for electrothermal/electromagnetic arcjet N89-27726
Fluid mechanics in a magnetoplasmadynamic thruster N89-27734
Continuous operation of a quasi-steady MPD propulsion system with an external magnetic field N89-27742
Cathode processes in a MPD arcjet N89-27753
Thermal design improvements for 30kWe arcjet engine N89-27754
Electrode erosion in steady-state electric propulsion engines N89-27755
Experiments and analysis of a compact electrothermal thruster N89-27773
Performance calculation of an H2 arcjet by means of a dual channel model N89-27775
Numerical studies of the flow field in a dc arcjet thruster N89-27776
Computational investigation on the characteristics of a low power dc arcjet thruster N89-27777
A 15 kW experimental arcjet N89-27778
Operating characteristics of 1 kW hydrazine arcjet thruster N89-27779
Experimental investigation on the characteristics of a low power dc arcjet thruster N89-27780

ARC WELDING

The Sigmajig: An improved hot-cracking test [DE89-013029] N89-28031

ARCHITECTURE (COMPUTERS)

Avionic system design methodology N89-27656
Rapid prototyping of complex avionics systems N89-27657
Line/Circuit Analysis Program: Cross-coupling on PC (Printed Circuit) board traces including discontinuities and circuit elements [DE89-013884] N89-27957
Hybrid wafer-scale processor [AD-A209944] N89-27969
Band structure engineering for ultra-low threshold laser diodes [AD-A208629] N89-28010
Approaching distributed database applications using a programmable terminal emulator [DE89-014831] N89-28308
Conversion of mass storage hierarchy in an IBM computer network [AD-A208520] N89-28330
Northeast Artificial Intelligence Consortium annual report 1987. Volume 6: Artificial intelligence applications to speech recognition [AD-A208380] N89-28334
Northeast Artificial Intelligence Consortium annual report for 1987. Volume 4: Research in automated photointerpretation [AD-A208610] N89-28336
Critical technologies plan for the Committees on Armed Services, United States Congress, revision [AD-A210170] N89-28439
Problems and solutions in online documentation systems [DE89-014092] N89-28447
Parallel Architectures for Planetary Exploration Requirements (PAPER) [NASA-CR-185370] N89-28475

ARCTIC OCEAN

Cloud/cryosphere interactions [AD-A208377] N89-28196

ARCTIC REGIONS

Aerostat cold weather study [AD-A207299] N89-27635
Remote sensing of ocean color in the Arctic N89-28139
Arctic Sea ice studies with passive microwave satellite observations N89-28147
Cloud/cryosphere interactions [AD-A208377] N89-28196

ARGON

Potential energy curves for the (ArH(+)) and (NeH(+)) systems from the interplay of theory and experiments N89-28380

ARGON PLASMA

Performance of a 100 kW class applied field MPD thruster [NASA-TM-102312] N89-27701

ARID LANDS

Comparison of MSS and TM LANDSAT data for cartography of surface structures in arid regions (southern Tunisia) N89-28087

AROMATIC COMPOUNDS

Analytical procedures for environmental quality control, volume 2 [PB89-158612] N89-28103
Analytical procedures for environmental quality control, volume 3 [PB89-158620] N89-28104

ARTIFICIAL INTELLIGENCE

Optimal three-dimensional path planning using visibility constraints [AD-A207357] N89-28310
The potential application of the blackboard model of problem solving to multidisciplinary design [NASA-TM-101633] N89-28314
The back propagation technique for modeling cortical computation [AD-A209855] N89-28323
Northeast Artificial Intelligence Consortium annual report 1987. Volume 6: Artificial intelligence applications to speech recognition [AD-A208380] N89-28334
Northeast Artificial Intelligence Consortium annual report for 1987. Volume 4: Research in automated photointerpretation [AD-A208610] N89-28336
Learning from physical analogies: A study in analogy and the explanation process [AD-A208689] N89-28338
A theory of justified reformulations [AD-A210153] N89-28340
Critical technologies plan for the Committees on Armed Services, United States Congress, revision [AD-A210170] N89-28439

ASPHALT

A comparison of rutting behavior of asphalt concrete under the F-4C/G and F-15C/D aircraft [AD-A208911] N89-27678

ASTRONAUT PERFORMANCE

EVA and human physiology N89-28245

ASTRONOMICAL MODELS

Information aspects of type 9 cosmological models [DE89-612518] N89-28472

ASTRONOMY

Options for daytime monitoring of atmospheric visibility in optical communications N89-27895

ASYMMETRY

A method for calculating asymmetric flow through nozzles [AD-A209689] N89-27992

ATLANTIC OCEAN

Determination of local empirical covariance functions from residual terrain reduced altimeter data [AD-A208678] N89-28095

ATMOSPHERIC ATTENUATION

A visibility characterization program for optical communications through the atmosphere N89-27894
Options for daytime monitoring of atmospheric visibility in optical communications N89-27895
Site selection criteria for the optical atmospheric visibility monitoring telescopes N89-27896
DSN 70-meter antenna X- and S-band calibration. Part 2: System noise temperature measurements and telecommunications link evaluation N89-27905

ATMOSPHERIC CHEMISTRY

Evaluating CFC (Chlorofluorocarbon) alternatives from the atmospheric viewpoint, revision 1 [DE89-014268] N89-28108
Scaling laws for the spectrum of interchange instabilities in the high latitude ionosphere [AD-A209993] N89-28111

ATMOSPHERIC CIRCULATION

Zonal winds between 25 and 120 km retrieved from solar occultation spectra [NASA-CR-180086] N89-28113

ATMOSPHERIC COMPOSITION

Evaluating CFC (Chlorofluorocarbon) alternatives from the atmospheric viewpoint, revision 1 [DE89-014268] N89-28108
Correlative Measurements Program N89-28164
Ozone measurements using balloon-borne ozonesondes N89-28165
Tropospheric nitric oxide measurements N89-28171

ATMOSPHERIC DENSITY

Mobile lidar system for measurement of water vapor mixing ratio and ozone number density N89-28166

ATMOSPHERIC GENERAL CIRCULATION MODELS

Backgrounder contribution No. 18: Climate scenarios for the first UC/DOE workshop [DE89-014302] N89-28105

ATMOSPHERIC MODELS

User's guide for the Air Force surface-layer windflow model (AFWIND) [AD-A208710] N89-28109
Aerosol model selection using surface measurements of IR horizon radiances and satellite detected visible radiances [AD-A209638] N89-28110
A new background stratospheric aerosol model for use in atmospheric radiation models [AD-A210110] N89-28112
Evaluation of the AFGL (Air Force Geophysics Laboratory) cloud simulation models using satellite data [AD-A208713] N89-28116

ATMOSPHERIC MOISTURE

Water vapor profiling using microwave radiometry N89-28163

ATMOSPHERIC PRESSURE

Effects of high terrestrial altitude on military performance [AD-A209614] N89-28201
The atmosphere pressure control section of the Hermes ECLSS N89-28241

ATMOSPHERIC REFRACTION

A new background stratospheric aerosol model for use in atmospheric radiation models [AD-A210110] N89-28112

ATMOSPHERIC SCATTERING

Aerosol model selection using surface measurements of IR horizon radiances and satellite detected visible radiances [AD-A209638] N89-28110

ATMOSPHERIC SOUNDING

Application of optical measure theory to atmospheric temperature sounding from TOVS (TIROS Operational Vertical Sounder) radiances [AD-A209955] N89-28396

ATMOSPHERIC TEMPERATURE

Ocean Drifter Project N89-28154
Satellite/radiosonde comparison N89-28170
Application of optical measure theory to atmospheric temperature sounding from TOVS (TIROS Operational Vertical Sounder) radiances [AD-A209955] N89-28396

ATMOSPHERIC TURBULENCE

The effects of atmospheric turbulence on precision optical measurements used for antenna-pointing compensation N89-27883

ATOMIC BEAMS

Potential energy curves for the (ArH(+)) and (NeH(+)) systems from the interplay of theory and experiments N89-28380
Quantum corrections for inelastic atom-surface scattering [AD-A209850] N89-28387

ATOMIC COLLISIONS

Dynamics of H(+) + Kr and H(+) + Xe elastic and charge-transfer collisions: State-selected differential cross sections at low collision energies N89-28381

ATOMIC ENERGY LEVELS

New ion trap for atomic frequency standard applications N89-27875

ATOMIC SPECTRA

Extraordinary behavior of atoms near a phase conjugator [AD-A209946] N89-28389

ATOMIC STRUCTURE

Experimental studies of the structure of grain boundaries [DE89-012954] N89-28408
Differential geometric aspects of the theory of ferroelectricity [DE89-612191] N89-28416

ATTENTION

Attention, imagery and memory: A neuromagnetic investigation [AD-A209917] N89-28207

ATTENUATION

A robust signalling system for land mobile satellite services N89-27917

ATTENUATION COEFFICIENTS

Propagation characteristics of electromagnetic waves in concrete [AD-A207387] N89-27921

ATTITUDE (INCLINATION)

Evaluation of head-up display formats for the F/A-18 hornet [AD-A208651] N89-27660

ATTITUDE CONTROL

A comparative study of SHF (Super High Frequency) and EHF (Extremely High Frequency) satellite communications, volume 1 [AD-A208850] N89-27945

ATTITUDE INDICATORS

Evaluation of head-up display formats for the F/A-18 hornet [AD-A208651] N89-27660

AUSTRIA

Forest damage mapping in Austria with the aid of LANDSAT TM image data N89-28078

AUTOCORRELATION

Theory of multi-frequency modulation (MFM) digital communications [AD-A209737] N89-27947

AUTOIONIZATION
Modified rotationally adiabatic model for rotational autoionization of dipole-bound molecular anions
[AD-A209851] N89-28388
AUTOMATED EN ROUTE ATC
Automated planning function for AERA 3: Maneuver option manager
[DOT/FAA/DS-89/21] N89-27645
A mathematical formulation for planning automated aircraft separations for AERA 3
[DOT/FAA/DS-89/20] N89-27646
AUTOMATIC CONTROL
Implementation of a digital torque controller of a reaction wheel with an incremental computer
[INPE-4784-PRE/1447] N89-28333
Northeast Artificial Intelligence Consortium annual report for 1987. Volume 4: Research in automated photointerpretation
[AD-A208610] N89-28336
AUTOREGRESSIVE PROCESSES
Preliminary statistical identification of radar imagery: Autoregressive-moving average (ARMA) models
[INPE-4771-PRE/1440] N89-28311
AUXILIARY PROPULSION
Design and development of the UK-10 ion propulsion subsystem N89-27730
Auxiliary propulsion RF engine RIT 15: Prototype design and performance N89-27731
AVALANCHE DIODES
Effective amplifier noise for an optical receiver based on linear mode avalanche photodiodes N89-27893
AVIONICS
Systems Engineering
[AGARD-LS-164] N89-27650
Avionics system engineering: An introduction N89-27651
Avionic system requirements N89-27652
A structured approach to weapon system design N89-27653
Integrated avionics: Conceptual design N89-27654
The evolution of digital avionics architectures/systems N89-27655
Avionic system design methodology N89-27656
Rapid prototyping of complex avionics systems N89-27657
Modeling functional specifications for onboard software N89-27658
AXIAL FLOW
Blading Design for Axial Turbomachines
[AGARD-LS-167] N89-27661
Performance prediction for axial-flow compressor and turbine blading N89-27665
AXIAL STRAIN
A data acquisition and control program for axial-torsional fatigue testing
[NASA-TM-102041] N89-28029

B

BACKGROUND RADIATION
Aerosol model selection using surface measurements of IR horizon radiances and satellite detected visible radiances
[AD-A209638] N89-28110
BACKSCATTERING
Modeling of ocean surface spectrum and surface scattering. Applications to reverberation prediction in the AAUS program
[AD-A210127] N89-28197
BALANCE
Age-related changes in human posture control: Sensory organization tests
[NASA-CR-185858] N89-28212
BALANCING
Load balancing in multiprocessor systems
[AD-A210144] N89-28327
BALLISTICS
DARPA (Defense Advanced Research Projects Agency) Review on EHF Devices
[AD-A208564] N89-27963
BALLOONS
Photogrammetric technique for in-flight ranging of trailing vortices using entrained balloons
[NASA-TM-4129] N89-27995
BANDPASS FILTERS
Quadratic estimators of the power spectrum
[AD-A208601] N89-27964
BANDWIDTH
Adaptive preprocessing of nonstationary signals
[AD-A209646] N89-27946
BARIUM OXIDES
Superconductivity in the Ba(0.69)Y(0.46)CuO(3.15-delta) compound
[DE88-706000] N89-28406
BATCH PROCESSING
A statistical derivation of the average degree of polymerization in a stirred tank reactor
[AD-A209873] N89-27857
BATHING
Test results on re-use of reclaimed shower water: Summary — space stations N89-28262
BAYS (TOPOGRAPHIC FEATURES)
Use of satellite imagery for the investigation of pollution-related characteristics of Dublin Bay, Ireland N89-28063
BEAM INJECTION
Development of high-current RF plasma sources for neutral particle injections N89-27785
Review of effects of NBI (Neutral Beam Injection) and rotation on plasma transport in tokamaks
[DE89-014109] N89-28402
BEAMS (RADIATION)
Generalized beamforming with multiple computer originated holograms
[AD-A210175] N89-28397
BEAMS (SUPPORTS)
Recent advances on the dynamic behavior of stiffened plates N89-28027
Studies in stabilization and control of beams and plates
[AD-A208635] N89-28042
An integrating matrix formulation for buckling of rotating beams including the effects of concentrated masses
[NASA-CR-181862] N89-28342
BEARINGS
Space Shuttle Main Engine structural analysis and data reduction/evaluation. Volume 3B: High pressure fuel turbo-pump preburner pump bearing assembly analysis
[NASA-CR-183666] N89-27695
BELGIUM
Evaluation of the LANDSAT TM satellite in urban media: Application to the case of Brussels, Belgium N89-28073
BIBLIOGRAPHIES
Bibliography of Soviet laser developments: January - February 1988
[AD-A209802] N89-28011
Bibliography of high-T sub c superconducting films
[DE89-013395] N89-28409
Data bases available at the National Institute of Standards and Technology Research Information Center
[PB89-160014] N89-28441
BICRYSTALS
Evidence against the existence of strong diffuse X-ray scattering from gold twist boundaries at room temperature
[DE89-012726] N89-28407
Grain boundaries in silicon from zero temperature through melting
[DE89-013186] N89-28410
BIDIRECTIONAL REFLECTANCE
Advanced Solidstate Array Spectroradiometer N89-28183
BIMETALS
Thermal strains in a bimaterial joint: Experimental and numerical analysis
[DE89-013935] N89-28032
BINARY DATA
Binary sequences of arbitrary length with near-ideal correlation
[AD-A209956] N89-28356
BIOCHEMISTRY
Identification of variables determining intrahemispheric interference between processing demands
[AD-A208435] N89-28299
BIOELECTRICITY
Modulation of spontaneous brain activity during mental imagery
[AD-A209918] N89-28208
Identification of variables determining intrahemispheric interference between processing demands
[AD-A208435] N89-28299
BIOMASS
Ocean color observations of phytoplankton distributions and primary productivity N89-28137
MELISSA: A micro-organisms-based model for CELSS development N89-28222
BIOMEDICAL DATA
Anthropometric measurements of aviators within the Aviation Epidemiology Data Register
[AD-A208609] N89-28300
BIT SYNCHRONIZATION
Synchronization of the receiver for the ISDN basic connection N89-27933
BITUMENS
A comparison of rutting behavior of asphalt concrete under the F-4C/G and F-15C/D aircraft
[AD-A208911] N89-27678
BLOOD CIRCULATION
Acetylcholinesterase inhibitor, pyridostigmine bromide, reduces skin blood flow in humans
[AD-A209615] N89-28202
BLOOD FLOW
Acetylcholinesterase inhibitor, pyridostigmine bromide, reduces skin blood flow in humans
[AD-A209615] N89-28202
BLOOD PRESSURE
The effect of various straining maneuvers on cardiac volumes at 1G and during +Gz acceleration
[AD-A208846] N89-28200
BODY SWAY TEST
Age-related changes in human posture control: Sensory organization tests
[NASA-CR-185858] N89-28212
BODY TEMPERATURE
Thermal modelling of the EVA-suited astronaut N89-28245
BOILING
Flow boiling with enhancement devices for cold plate coolant channel design
[NASA-CR-185840] N89-27979
Subcooled boiling of downward flow in a vertical annulus
[DE89-005320] N89-27983
BORESIGHT ERROR
Precision pointing compensation for DSN antennas with optical distance measuring sensors N89-27882
The effects of atmospheric turbulence on precision optical measurements used for antenna-pointing compensation N89-27883
BOUNDARY LAYER EQUATIONS
Boundary layer equations and methods of solution N89-27987
BOUNDARY LAYER FLOW
Spatial three-dimensional secondary instability compressible boundary-layer flows
[NASA-CR-4251] N89-27978
Boundary layer equations and methods of solution N89-27987
BOUNDARY LAYER STABILITY
Spatial three-dimensional secondary instability compressible boundary-layer flows
[NASA-CR-4251] N89-27978
BOUNDARY LAYERS
Magnetopause structure and dynamics: Issues for GEM
[DE89-012620] N89-28054
BOUNDARY LUBRICATION
Fundamental mechanisms of tribology and their implications
[AD-A209941] N89-28020
BOUNDARY VALUE PROBLEMS
Control and system theory, optimization, inverse and ill-posed problems
[AD-A208570] N89-28335
Some problems in nonlinear analysis
[AD-A209991] N89-28357
Estimation of lower bound properties from material test data
[AD-A207378] N89-28361
BRAIN
Attention, imagery and memory: A neuromagnetic investigation
[AD-A209917] N89-28207
Modulation of spontaneous brain activity during mental imagery
[AD-A209918] N89-28208
BRASSES
Thermal strains in a bimaterial joint: Experimental and numerical analysis
[DE89-013935] N89-28032
BRAZIL
Report of the Project Estima, phase 2: LANDSAT-TM data and agrometeorology in crop yield estimation of wheat at the farm level
[INPE-4782-RPE/582-PHASE-2] N89-28051
BRAZILIAN SPACE PROGRAM
Launch window for the Brazilian Data Collecting Satellite
[INPE-4773-PRE/1442] N89-27683
BREADBOARD MODELS
GMBU (Ground Mobile Breadboard Upgrade) lidar and bubbler correlation study at Dugway Proving Ground
[AD-A207297] N89-28002
BRITTLE MATERIALS
Soliton behaviour of crack propagation in brittle materials
[DE89-612190] N89-28033
BROADBAND
Wide band data collection system N89-28130
BROADCASTING
Digital CODEC for real-time processing of broadcast quality video signals at 1.8 bits/pixel
[NASA-TM-102325] N89-27927

BROMIDES
Acetylcholinesterase inhibitor, pyridostigmine bromide, reduces skin blood flow in humans
[AD-A209615] N89-28202
BUBBLES
Bubble detection using a dual frequency sound field
[AD-A207286] N89-27973
Sound propagation in bubbly liquids: A review
[AD-A207377] N89-28370
BUCKLING
An integrating matrix formulation for buckling of rotating beams including the effects of concentrated masses
[NASA-CR-181862] N89-28342
BUOYS
Ocean Drifter Project N89-28154
BURSTS
Solution of two-dimensional, two-region electromagnetic ground response
[AD-A206265] N89-27869
BUTENES
Semiconductor-olefin adducts. Photoluminescent properties of cadmium sulfide and cadmium selenide in the presence of butenes
[AD-A208348] N89-28419

C

C BAND
The DSS-14 C-band exciter N89-27901
CADMIUM SELENIDES
Semiconductor-olefin adducts. Photoluminescent properties of cadmium sulfide and cadmium selenide in the presence of butenes
[AD-A208348] N89-28419
CADMIUM SULFIDES
Selective detector for gas chromatography based on adduct-modulated semiconductor photoluminescence
[AD-A208616] N89-27808
Semiconductor-olefin adducts. Photoluminescent properties of cadmium sulfide and cadmium selenide in the presence of butenes
[AD-A208348] N89-28419
CALIBRATING
DSN 70-meter antenna X- and S-band calibration. Part 1: Gain measurements N89-27904
DSN 70-meter antenna X- and S-band calibration. Part 2: System noise temperature measurements and telecommunications link evaluation N89-27905
Evaluation of a strain-gage load calibration on a low-aspect-ratio wing structure at elevated temperature
[NASA-TP-2921] N89-28034
Stress intensity calibration of a ring specimen using a finite element technique
[AD-A208878] N89-28044
Comparison of the classification results obtained with TM and MSS data in land uses identification of the Communidad Autonoma de Cantabria N89-28077
Calibration support for the Earth Observing System Project N89-28131
NASA Aircraft-Satellite Instrument Calibration Project N89-28189
Flight calibration source development N89-28190
Radiance standards N89-28191
Environmental calibration chamber operations N89-28192
Calibration source maintenance, characterization and development N89-28193
Integrating sphere and hemisphere calibration update N89-28194
CAMERAS
The use of stereo optical flow fields in the determination of three-dimensional motion and stereo correspondence
[DE89-012518] N89-27996
CANOPIES (VEGETATION)
Comparison of the classification results obtained with TM and MSS data in land uses identification of the Communidad Autonoma de Cantabria N89-28077
Use of remote sensing in mapping of vegetation in the Dividalen area central Troms, northern Norway N89-28083
Radar scattering and soil moisture N89-28182
CANTILEVER BEAMS
Model based damping of coupled horizontal and vertical oscillations in a flexible rod
[DE89-007034] N89-28039
CAPACITANCE
A fast multipole algorithm for capacitance extraction of complex 3-D geometries
[AD-A208374] N89-28317
CAPACITORS
Verification of performance and endurance of capacitor bank for the electric propulsion experiment (EPEX) N89-27739
Capacitors for pulsed electric propulsion N89-27790
CAPILLARY FLOW
Feasibility demonstration model of a capillary pumping loop N89-28225
CARBON
Transition metal activation and functionalization of carbon-hydrogen bonds
[DE89-012949] N89-27804
Ion beam and plasma methods of producing diamondlike carbon films
[NASA-TM-102301] N89-27836
CARBON DIOXIDE CONCENTRATION
Regenerative CO2-control --- Columbus N89-28237
Electrochemical removal and concentration of CO2 N89-28238
CARBON DIOXIDE LASERS
Pulsed laser propulsion for low cost, high volume launch to orbit
[DE89-014049] N89-28009
CARBON FIBER REINFORCED PLASTICS
Irradiation effects on resistance of thermal impact of composite used in space
[DE89-778069] N89-27794
CARBON FIBERS
A very low reflectance diffuse surface for thermal design of spacecraft N89-28289
CARBON-CARBON COMPOSITES
Coating and impregnation of carbon-carbon composites with ceramics by electrophoretic deposition
[AD-A208873] N89-27800
CARBONACEOUS MATERIALS
Issues and future directions in subsecond thermophysics
[DE89-014228] N89-28434
CARRIER FREQUENCIES
The use of interleaving for reducing radio loss in trellis-coded modulation systems N89-27889
CARRIER WAVES
Carrier derivation in higher-stage QAM-signals N89-27935
CASSEGRAIN OPTICS
DSN 70-meter antenna microwave optics design and performance improvements. Part 1: Design optimization N89-27903
CASTING
Further investigation of flow modeling during solid propellant processing
[AD-A209787] N89-27866
CATALYSIS
Comparison of vacuum-annealed and electrochemically cycled electrodes in adsorption and electrocatalysis: Aromatic compounds at platinum (111) and polycrystalline platinum
[AD-A210011] N89-27814
CATALYSTS
The catalytic oxiderzer: Description and first results of a breadboard model for a component of the Columbus ECLSS N89-28239
CAVITY RESONATORS
Characteristics of free-floating nitrogen and helium plasmas generated in a microwave resonant cavity N89-27771
CENTRAL PROCESSING UNITS
Hybrid wafer-scale processor
[AD-A209944] N89-27969
CERAMIC BONDING
Ceramic joining in the United States
[DE89-009323] N89-27834
CERAMIC COATINGS
Coating and impregnation of carbon-carbon composites with ceramics by electrophoretic deposition
[AD-A208873] N89-27800
CERAMIC FIBERS
Composite ceramic superconducting wires for electric motor applications
[AD-A208598] N89-27847
CERAMICS
Ion-assisted deposition of silver films on ceramics for friction and wear control
[DE89-014635] N89-27821
Vapor phase deposition studies of phosphate esters on metal and ceramic surfaces
[PB89-148985] N89-27831
Birth, death and transfiguration: The synthesis of preceramic polymers, their pyrolysis and their conversion to ceramics
[AD-A208437] N89-27841
Fiber reinforced structural ceramics for construction
[AD-A209976] N89-27858
Preparation and characterization of colloidal ZnS particles
[AD-A210171] N89-27862
High-temperature superconductivity: Abstracts of NIST (National Institute of Standards and Technology) publications, 1987-1988
[PB89-148340] N89-28405
Experimental studies of the structure of grain boundaries
[DE89-012954] N89-28408
CEREBRAL CORTEX
Higher order mechanisms of color vision
[AD-A209838] N89-28205
Visualizing and rhyming cause differences in alpha suppression
[AD-A210005] N89-28210
The back propagation technique for modeling cortical computation
[AD-A209855] N89-28323
CEREBRUM
Identification of variables determining intrahemispheric interference between processing demands
[AD-A208435] N89-28299
CERIUM
Energy transfer effects in beta-alumina
[AD-A209818] N89-27855
CHALLENGER (ORBITER)
Summary of longitudinal stability and control parameters as determined from Space Shuttle Challenger flight test data
[NASA-TM-101605] N89-27671
CHANNEL CAPACITY
COMM-Q: A simulation model to determine saturation points in nodal type networks
[AD-A207294] N89-28329
CHANNEL FLOW
Flow boiling with enhancement devices for cold plate coolant channel design
[NASA-CR-185840] N89-27979
CHANNEL NOISE
Capacity of discrete time Gaussian channel with and without feedback, 2
[AD-A207388] N89-27922
CHANNELS (DATA TRANSMISSION)
Communications using channels formed by meteor bursts
[AD-A209656] N89-27949
CHAOS
Non-linear dynamics and chaotic motions in feedback controlled elastic system
[AD-A208628] N89-28041
CHARACTERIZATION
Characterization of structure in thin polymer resist films
[AD-A208677] N89-27848
CHARGE COUPLED DEVICES
NASA Charge Coupled Device (CCD) Spectrometer System (NCSS) N89-28142
CHARGE EXCHANGE
Charge transfer and inelastic scattering in proton-molecule collisions
[MPIS-13/1988] N89-28378
Charge transfer and inelastic scattering in proton-molecule collisions, introduction N89-28379
Dynamics of H(+) + Kr and H(+) + Xe elastic and charge-transfer collisions: State-selected differential cross sections at low collision energies N89-28381
Observation of vibrationally resolved charge transfer in H(+) + H2 at a collision energy Ecm = 20 eV N89-28382
A comparison between theoretical and experimental state-to-state charge transfer cross sections for H(+) + H2 at 20 eV: Evidence for quantum effects N89-28383
A three-dimensional quantum mechanical study of vibrational inelastic and charge transfer processes in H(+) + H2 at a collision energy Ecm = 20 eV N89-28384
Charge transfer and structured vibrational distributions in H(+) + CH4 low-energy collisions N89-28385
Superexchange coupling mechanisms for electron transfer processes
[DE89-013568] N89-28411
CHARTS
A smart, mapping, charting and geodesy control generator, phase 2
[AD-A208806] N89-28097
CHEMICAL ANALYSIS
Protonic solid electrolytes: Thermal stability and conductivity of ammonium/hydronium beta'-alumina
[AD-A209911] N89-27813
Analytical procedures for environmental quality control, volume 3
[PB89-158620] N89-28104
Crystal chemistry, synthesis, and characterization of infrared optical materials
[AD-A208723] N89-28422
CHEMICAL BONDS
Transition metal activation and functionalization of carbon-hydrogen bonds
[DE89-012949] N89-27804
Electronic properties of ordered ladder polymers
[AD-A207288] N89-27832

Calculation of network parameters of crosslinked Markovian polymer chains
[AD-A210073] N89-27860
The orientation of chemical bonds at surfaces: A key to understanding the structure and bonding of surface species
[AD-A209833] N89-28427

CHEMICAL COMPOSITION
Separation of oxygen from seawater by membrane permeation
[AD-A208863] N89-27809
Synchrotron X-ray fluorescence analyses of stratospheric cosmic dust: New results for chondritic and nickel-depleted particles
[DE89-014032] N89-28107
Elemental composition and energy spectra of galactic cosmic rays N89-28466

CHEMICAL DEFENSE
United States Air Force Research Initiation Program for 1987, volume 4
[AD-A209729] N89-28438

CHEMICAL EQUILIBRIUM
Study of improved methods for predicting chemical equilibria
[DE89-014535] N89-28433

CHEMICAL LASERS
Bibliography of Soviet laser developments: January - February 1988
[AD-A209802] N89-28011

CHEMICAL REACTIONS
KIVA-2: A computer program for chemically reactive flows with sprays
[DE89-012805] N89-27975
Real gas equations of state for CHEMKIN
[DE89-012794] N89-28432
Study of improved methods for predicting chemical equilibria
[DE89-014535] N89-28433

CHEMICAL REACTORS
A statistical derivation of the average degree of polymerization in a stirred tank reactor
[AD-A209873] N89-27857

CHEMICAL WARFARE
Evaluation of thermal stress induced by helicopter aircrew Chemical, Biological, Radiological (CBR) protective ensemble
[AD-A210123] N89-28303

CHEMISORPTION
Adsorption and reactions of cyclic sulfides on Mo(110)
[AD-A207324] N89-27803
The orientation of chemical bonds at surfaces: A key to understanding the structure and bonding of surface species
[AD-A209833] N89-28427

CHIPS (ELECTRONICS)
Average interconnection length and interconnection distribution for rectangular arrays
[AD-A209848] N89-27967
Hybrid wafer-scale processor
[AD-A209944] N89-27969
MM wavecomponents - SIS (Superconductor-Insulator-Superconductor) mixers
[AD-A208632] N89-28421

CHLORIDES
Environmental effects of space shuttle exhaust on materials
[AD-A208813] N89-27686

CHLORINE FLUORIDES
Tests of Halon 1301 test gas simulants
[AD-A207346] N89-27867

CHLOROCARBONS
Evaluating CFC (Chlorofluorocarbon) alternatives from the atmospheric viewpoint, revision 1
[DE89-014268] N89-28108

CHLOROPHYLLS
Coastal Zone Color Scanner N89-28145

CHOLINESTERASE
Acetylcholinesterase inhibitor, pyridostigmine bromide, reduces skin blood flow in humans
[AD-A209615] N89-28202

CHROMATOGRAPHY
Novel approaches to ionic chromatography
[DE89-013942] N89-27805

CHROMOSOMES
The human telomere
[DE89-014252] N89-28199

CIRCUITS
Development of superlattices for ultra high-speed electronic and optoelectronic devices
[AD-A209874] N89-28429

CIRCULATORS (PHASE SHIFT CIRCUITS)
Field theory simulation of nonreciprocal microwave components N89-27940

CITIES
Evaluation of the LANDSAT TM satellite in urban media: Application to the case of Brussels, Belgium N89-28073

CIVIL AVIATION
High-speed civil transport study. Summary
[NASA-CR-4234] N89-27647
High-speed civil transport study
[NASA-CR-4233] N89-27648

CLADDING
Laser processing of metals and alloys
[DE89-613235] N89-27822
Laser cladding of Ni, Nb, Mg alloys for improved environmental resistance at high temperatures
[AD-A210134] N89-27830

CLASSIFICATIONS
Classification of small-scale forests in Flanders using LANDSAT TM digital data: Preliminary results N89-28080
The human telomere
[DE89-014252] N89-28199
Northeast Artificial Intelligence Consortium annual report 1987. Volume 6: Artificial intelligence applications to speech recognition
[AD-A208380] N89-28334

CLAYS
Theoretical model for stabilization of clay-silt airport pavement subgrade systems. Phase 1: Laboratory investigation. Phase 2: Rutting tests
[DOT/FAA/PM-87/20-PHASE-1/2] N89-27673

CLIMATE CHANGE
Sea ice/climate studies N89-28151

CLIMATOLOGY
Climatological aspects of Nimbus-7 SMMR data N89-28156
Cloud/cryosphere interactions
[AD-A208377] N89-28196

CLOSED ECOLOGICAL SYSTEMS
Status of the US Space Station ECLSS and internal TCS N89-28215
Physico-chemical atmosphere revitalisation: The qualitative and quantitative selection of regenerative designs N89-28221
MELISSA: A micro-organisms-based model for CELSS development N89-28222
The catalytic oxiderzer: Description and first results of a breadboard model for a component of the Columbus ECLSS N89-28239
Nutrition for short-duration space missions N89-28265

CLOTHING
Evaluation of thermal stress induced by helicopter aircrew Chemical, Biological, Radiological (CBR) protective ensemble
[AD-A210123] N89-28303

CLOUD COVER
A visibility characterization program for optical communications through the atmosphere N89-27894
Options for daytime monitoring of atmospheric visibility in optical communications N89-27895
Evaluation of the AFGL (Air Force Geophysics Laboratory) cloud simulation models using satellite data
[AD-A208713] N89-28116
Cloud/cryosphere interactions
[AD-A208377] N89-28196

CLOUD PHYSICS
Cloud absorption radiometer N89-28172
Cloud/cryosphere interactions
[AD-A208377] N89-28196

CLOUDS (METEOROLOGY)
Cloud/cryosphere interactions
[AD-A208377] N89-28196

CLUSTERS
Vibrational predissociation of shock-selected C2H4 and NH3 clusters
[MPIS-6/1988] N89-28373
Vibrational predissociation of shock-selected C2H4 and NH3 clusters, introduction N89-28374
Infrared photodissociation and cluster-specific detection of internally cold (C2H4) van der Waals complexes N89-28375
Infrared photodissociation of van der Waals complexes selectively prepared by molecular beam scattering N89-28376

COAL UTILIZATION
MHD (Magnetohydrodynamics) Program Plan, FY 1989
[DE89-012232] N89-28398

COASTAL WATER
LANDSAT TM data used in the mapping of large-scale geological structures in coastal areas in Trondelag, central Norway N89-28072

COASTAL ZONE COLOR SCANNER
Applications of the Coastal Zone Color Scanner in oceanography N89-28136
Coastal Zone Color Scanner studies N89-28138
Remote sensing of ocean color in the Arctic N89-28139
Coastal Zone Color Scanner N89-28145

COATINGS
Advanced tribological coatings for high specific strength alloys
[AD-A208504] N89-27825

COAXIAL PLASMA ACCELERATORS
Anode-nozzle experimental analysis in a coaxial non-steady solid propellant MPD thruster N89-27757

CODE DIVISION MULTIPLE ACCESS
Proceedings of the Mobile Satellite System Architectures and Multiple Access Techniques Workshop
[NASA-CR-184564] N89-27907
Why is CDMA the solution for mobile satellite communication N89-27912
System level comparison of FDMA vs. CDMA (under conference guideline constraint) N89-27913
Alternative multiple-access techniques for mobile satellite systems N89-27914

CODING
Software package for performing experiments about the convolutionally encoded Voyager 1 link N89-27888
The use of interleaving for reducing radio loss in trellis-coded modulation systems N89-27889
Performance of concatenated codes using 8-bit and 10-bit Reed-Solomon codes N89-27890
Decoding of 1/2-rate (24,12) Golay codes N89-27891
The weight distribution and randomness of linear codes N89-27892

COGNITION
Identification of variables determining intrahemispheric interference between processing demands
[AD-A208435] N89-28299
Human cognition and information display in C3I system tasks
[AD-A210012] N89-28302

COLD CATHODES
Cylindrical steady-state MPD thruster N89-27725
Characterization of cold cathode erosion processes N89-27756

COLD SURFACES
Effect of alloying, rapid solidification, and surface kinetics on the high temperature environmental resistance of niobium
[AD-A209934] N89-27829
Design and test of a two-phase coldplate N89-28226

COLD WEATHER
Aerostat cold weather study
[AD-A207299] N89-27635

COLLISION AVOIDANCE
A mathematical formulation for planning automated aircraft separations for AERA 3
[DOT/FAA/DS-89/20] N89-27648

COLLOIDS
Preparation and characterization of colloidal ZnS particles
[AD-A210171] N89-27862

COLOR
The phototoxicity of blue light on the functional properties of the retinal pigment epithelium
[AD-A209834] N89-28204

COLOR CODING
Color analysis of inland waters using LANDSAT TM data N89-28062
LANDSAT TM study of sabkha surfaces in the Qattara Depression, northwestern Egypt N89-28066

COLOR VISION
Higher order mechanisms of color vision
[AD-A209838] N89-28205

COLUMBUS SPACE STATION
System aspects of Columbus thermal control and life support N89-28216
Environmental control and life support systems for pressurized modules: From Spacelab to Columbus N89-28219
Two-phase heat transport systems: Critical components --- Columbus N89-28224
The two approaches for the thermal control of the Columbus resource module and polar platform N89-28231
Redundancy concept for the Columbus man-tended free-flyer thermal control system N89-28232
Thermal control of Columbus pressurized modules N89-28233
Regenerative CO2-control --- Columbus N89-28237
The catalytic oxiderzer: Description and first results of a breadboard model for a component of the Columbus ECLSS N89-28239
Theoretical and experimental investigations on heat exchangers for Columbus hybrid radiators N89-28295

COMBINATORIAL ANALYSIS
A RUTCOR project on discrete applied mathematics
[AD-A208572] N89-28347

The combinatorics of heuristic search termination for object recognition in cluttered environments
[AD-A209690] N89-28363
COMBUSTIBLE FLOW
KIVA-2: A computer program for chemically reactive flows with sprays
[DE89-012805] N89-27975
COMBUSTION CHAMBERS
United States Air Force Research Initiation Program for 1987, volume 1
[AD-A209726] N89-28436
COMBUSTION PHYSICS
Real gas equations of state for CHEMKIN
[DE89-012794] N89-28432
COMET NUCLEI
The ROSETTA/CNSR mission: A possible application of electric propulsion to interplanetary missions N89-27715
COMMAND AND CONTROL
Human cognition and information display in C3I system tasks
[AD-A210012] N89-28302
COMMERCE
The private sector economic and employment benefits to the nation and to each state of proposed FY 1990 NASA procurement expenditures
[NASA-CR-185894] N89-28448
COMMERCIAL SPACECRAFT
Crisis decision-making: The impact of commercial satellites on the media, military and national leaders
[AD-A207334] N89-28449
COMMUNICATION CABLES
State-of-the-art fiber optics for short distance frequency reference distribution N89-27878
Stabilized fiber-optic frequency distribution system N89-27879
COMMUNICATION NETWORKS
Site selection criteria for the optical atmospheric visibility monitoring telescopes N89-27896
Study on the applicability of Asynchronous Time Division (ATD) techniques to satellite communications systems
[ESA-CR(P)-2742] N89-27943
Theory of multi-frequency modulation (MFM) digital communications
[AD-A209737] N89-27947
COMMUNICATION SATELLITES
The role of electric propulsion in extending the economic life-cycle of commercial European telecommunication satellites N89-27713
The AMSC mobile satellite system: Design summary and comparative analysis N89-27908
Choice of FDMA/SCPC access technique for aeronautical satellite voice system N89-27909
Performance of DA/FDMA architecture proposed for MSS N89-27910
Geostar's system architectures N89-27911
Why is CDMA the solution for mobile satellite communication N89-27912
System level comparison of FDMA vs. CDMA (under conference guideline constraint) N89-27913
Alternative multiple-access techniques for mobile satellite systems N89-27914
Practical constraints on network architecture and signalling in the MSAT system N89-27915
MSAT signalling and network management architectures N89-27916
Aeronautical mobile TDMA/MCTDMA system N89-27918
A comparative study of SHF (Super High Frequency) and EHF (Extremely High Frequency) satellite communications, volume 1
[AD-A208850] N89-27945
Design trends in communications satellite thermal subsystems N89-28255
The thermal control of EUTELSAT-2 N89-28256
COMMUNICATION THEORY
Theory of multi-frequency modulation (MFM) digital communications
[AD-A209737] N89-27947
A RUTCOR project on discrete applied mathematics
[AD-A208572] N89-28347
COMPENSATORS
Analysis and dimensioning of a value-discrete adaptive compensation filter N89-27932
COMPILERS
Quantitative inference in a mechanical design compiler
[AD-A209900] N89-28324
COMPLEX COMPOUNDS
Transition metal activation and functionalization of carbon-hydrogen bonds
[DE89-012949] N89-27804
COMPLEX SYSTEMS
Basic research in reliability for real systems
[AD-A209649] N89-28022
COMPOSITE MATERIALS
High performance composites based on polyurethanes reinforced with polydiacetylenes
[AD-A208436] N89-27797
Piezoelectric polymer/ceramic composite
[AD-A208905] N89-27801
High temp toughening and creep studies
[AD-A208714] N89-27826
Composite ceramic superconducting wires for electric motor applications
[AD-A208598] N89-27847
An adhesive for field repair of composites
[AD-A209992] N89-27859
Research and technology plans for FY 1989 and accomplishments for FY 1988 --- Structural Mechanics Division
[NASA-TM-101592] N89-28035
United States Air Force Research Initiation Program for 1987, volume 3
[AD-A209728] N89-28437
COMPOSITE STRUCTURES
Simulation of deformation and texture evolution in semi-crystalline polymers
[AD-A208854] N89-27852
COMPRESSIBLE BOUNDARY LAYER
Spatial three-dimensional secondary instability compressible boundary-layer flows
[NASA-CR-4251] N89-27978
COMPRESSIBLE FLOW
Implicit time dependent methods for inviscid and viscous compressible flows, with a discussion of the concept of numerical dissipation N89-27990
COMPRESSOR BLADES
Design criteria for optimal blading design N89-27663
Blading design for multi-stage HP compressors N89-27666
Transonic and supersonic compressor blading design N89-27667
COMPRESSORS
Blading Design for Axial Turbomachines
[AGARD-LS-167] N89-27661
Overview on blading design methods N89-27664
Performance prediction for axial-flow compressor and turbine blading N89-27665
COMPUTATION
Reanalysis, compatibility and correlation in analysis of modified antenna structures N89-27906
A computational comparison of the primal simplex and relaxation algorithms for solving minimum cost flow networks
[AD-A208534] N89-28331
A RUTCOR project on discrete applied mathematics
[AD-A208572] N89-28347
Significant digit computation of the incomplete beta function ratios
[AD-A210118] N89-28358
COMPUTATIONAL FLUID DYNAMICS
Computation of transonic potential flow past RAE-Wing-A and Body-B2 combination
[PD-CF-8921] N89-27637
Performance prediction for axial-flow compressor and turbine blading N89-27665
Blading design for multi-stage HP compressors N89-27666
Blading design for cooled high-pressure turbines N89-27668
Mach 5 inlet CFD and experimental results
[NASA-TM-102317] N89-27670
Numerical codes for cylindrical MPD thrusters N89-27733
KIVA-2: A computer program for chemically reactive flows with sprays
[DE89-012805] N89-27975
A critical comparison of turbulence models for homogeneous shear flows in a rotating frame
[NASA-CR-181864] N89-27977
An Introduction to Computational Fluid Dynamics
[VKI-LS-1989-02] N89-27985
Introduction --- computational fluid dynamics N89-27986
Boundary layer equations and methods of solution N89-27987
Introduction to finite element techniques in computational fluid dynamics N89-27988
Introduction to finite volume techniques in computational fluid dynamics N89-27989
Implicit time dependent methods for inviscid and viscous compressible flows, with a discussion of the concept of numerical dissipation N89-27990
Computational methods and systems for problems in science and engineering
[AD-A209951] N89-28355
COMPUTATIONAL GRIDS
Computation of transonic potential flow past RAE-Wing-A and Body-B2 combination
[PD-CF-8921] N89-27637
Adaptive grid methods for numerical weather prediction
[AD-A209950] N89-28117
COMPUTER AIDED DESIGN
Blading design for multi-stage HP compressors N89-27666
Advanced modular software development in thermal engineering --- spacecraft design N89-28247
Improved ray tracing technique for radiative heat transfer modelling N89-28249
Assembling the ISO thermal model with ESATAN N89-28280
The Fluidnet development and application to preliminary sizing of fluid-loop systems N89-28282
Aerospace structures design on computers
[AD-A208811] N89-28321
Quantitative inference in a mechanical design compiler
[AD-A209900] N89-28324
Automatic construction of polyhedral surfaces from voxel representations
[AD-A210009] N89-28325
COMPUTER AIDED MANUFACTURING
Requirements for a technical data base N89-27930
COMPUTER GRAPHICS
Effect of three-dimensional object type and density in simulated low-level flight
[AD-A209756] N89-27679
The combinatorics of heuristic search termination for object recognition in cluttered environments
[AD-A209690] N89-28363
An implementation of a data definition facility for the graphics language for database
[AD-A207380] N89-28442
COMPUTER INFORMATION SECURITY
Theft of information in the take-grant protection model
[NASA-CR-185835] N89-28444
The sharing of rights and information in a capability-based protection system
[NASA-CR-185388] N89-28445
A model of security monitoring
[NASA-CR-185845] N89-28446
COMPUTER NETWORKS
Software package for performing experiments about the convolutionally encoded Voyager 1 link N89-27888
Theory of multi-frequency modulation (MFM) digital communications
[AD-A209737] N89-27947
The Laboratory for Oceans Computing Facility N89-28173
Code 672 observational science branch computer networks N89-28174
Low cost real time interactive analysis system N89-28177
Conversion of mass storage hierarchy in an IBM computer network
[AD-A208520] N89-28330
A computational comparison of the primal simplex and relaxation algorithms for solving minimum cost flow networks
[AD-A208534] N89-28331
Engineering drawing transfer test with Douglas Aircraft Company: MIL-D-28000 Class II (IGES)
[DE89-012810] N89-28443
COMPUTER PROGRAMMING
Modeling functional specifications for onboard software N89-27658
Production of satellite image maps from TM data N89-28089
Integrating TM and cartographic data N89-28090
Approaching distributed database applications using a programmable terminal emulator
[DE89-014831] N89-28308
A theory of justified reformulations
[AD-A210153] N89-28340
COMPUTER PROGRAMS
Computation of transonic potential flow past RAE-Wing-A and Body-B2 combination
[PD-CF-8921] N89-27637
Rapid prototyping of complex avionics systems N89-27657
Space Shuttle Main Engine structural analysis and data reduction/evaluation. Volume 1: Aft Skirt analysis
[NASA-CR-183663] N89-27693
Space Shuttle Main Engine structural analysis and data reduction/evaluation. Volume 3B: High pressure fuel turbo-pump preburner pump bearing assembly analysis
[NASA-CR-183666] N89-27695
An improved code for nozzle type steady state MPD thrusters N89-27735
Software package for performing experiments about the convolutionally encoded Voyager 1 link N89-27888
An experimental and computer modeling study of stepped radius monopole antennas
[AD-A207356] N89-27919

Evaluation of new thermomechanical constitutive theory for snow N89-28052
The Laboratory for Oceans Computing Facility N89-28173
ECLS simulation program N89-28284
ParaGraph-RTS: A parallel reduction-based run-time system
[DE89-005457] N89-28315
Fixed interval smoothing algorithm for an extended Kalman filter for over-the-horizon ship tracking
[AD-A208555] N89-28318
Parameter plane design method
[AD-A209845] N89-28322
Northeast Artificial Intelligence Consortium annual report for 1987. Volume 4: Research in automated photointerpretation
[AD-A208610] N89-28336
Learning from physical analogies: A study in analogy and the explanation process
[AD-A208689] N89-28338
Computational methods and systems for problems in science and engineering
[AD-A209951] N89-28355
Study of improved methods for predicting chemical equilibria
[DE89-014535] N89-28433

COMPUTER STORAGE DEVICES
Load balancing in multiprocessor systems
[AD-A210144] N89-28327
Conversion of mass storage hierarchy in an IBM computer network
[AD-A208520] N89-28330

COMPUTER SYSTEMS DESIGN
Modeling functional specifications for onboard software N89-27658
Code 672 observational science branch computer networks N89-28174
The potential application of the blackboard model of problem solving to multidisciplinary design
[NASA-TM-101633] N89-28314
A theory of justified reformulations
[AD-A210153] N89-28340
A model of security monitoring
[NASA-CR-185845] N89-28446

COMPUTER SYSTEMS PERFORMANCE
Hyperdimensional data analysis and structural inference
[AD-A210056] N89-27971
Code 672 observational science branch computer networks N89-28174
A theory of justified reformulations
[AD-A210153] N89-28340

COMPUTER SYSTEMS PROGRAMS
Model and method for systems development N89-27929
The Fluidnet development and application to preliminary sizing of fluid-loop systems N89-28282

COMPUTER TECHNIQUES
Hyperdimensional data analysis and structural inference
[AD-A210056] N89-27971
The potential application of the blackboard model of problem solving to multidisciplinary design
[NASA-TM-101633] N89-28314
Evidence flow graph methods for validation and verification of expert systems
[NASA-CR-181810] N89-28328
Northeast Artificial Intelligence Consortium annual report 1987. Volume 6: Artificial intelligence applications to speech recognition
[AD-A208380] N89-28334
Differential equations, related problems of Pade approximations and computer applications
[AD-A208590] N89-28348
Generalized beamforming with multiple computer originated holograms
[AD-A210175] N89-28397

COMPUTERIZED SIMULATION
Design criteria for optimal blading design N89-27663
Parametric study of the aerothermodynamics of a jet engine test facility
[AD-A208512] N89-27675
Development and refinement of test bed simulations
[NASA-TM-102335] N89-27702
Numerical codes for cylindrical MPD thrusters N89-27733
Analytical and numerical solutions for cylindrical blast waves in a plasma of varying density N89-27767
Numerical studies of the flow field in a dc arcjet thruster N89-27776
Computational investigation on the characteristics of a low power dc arcjet thruster N89-27777
KREM: A model for evaluating orbital transfer vehicles utilizing nuclear electric propulsion systems N89-27789
Computational simulation of high temperature metal matrix composites cyclic behavior
[NASA-TM-102115] N89-27795
Indium phosphide solar cell research in the US: Comparison with nonphotovoltaic sources
[NASA-TM-102103] N89-27868
An experimental and computer modeling study of stepped radius monopole antennas
[AD-A207356] N89-27919
Joint-space adaptive control of a 6 DOF end-effector with closed-kinematic chain mechanism
[NASA-CR-185861] N89-28016
Particle simulations in magnetospheric plasmas
[AD-A206252] N89-28106
Evaluation of the AFGL (Air Force Geophysics Laboratory) cloud simulation models using satellite data
[AD-A208713] N89-28116
Thermal software developments at ESTEC N89-28278
SOHO thermal modelling and analysis: The first application of ESATAN to a complete spacecraft N89-28279
Evolution of thermal analysis methods towards integrated system performance simulation N89-28283
The back propagation technique for modeling cortical computation
[AD-A209855] N89-28323
Evidence flow graph methods for validation and verification of expert systems
[NASA-CR-181810] N89-28328
COMM-Q: A simulation model to determine saturation points in nodal type networks
[AD-A207294] N89-28329
Generalized beamforming with multiple computer originated holograms
[AD-A210175] N89-28397

COMPUTERS
Band structure engineering for ultra-low threshold laser diodes
[AD-A208629] N89-28010

CONCENTRATION (COMPOSITION)
Airborne in-situ spectral characterization and concentration estimates of fluorescent organics as a function of depth N89-28140

CONCRETES
A comparison of rutting behavior of asphalt concrete under the F-4C/G and F-15C/D aircraft
[AD-A208911] N89-27678
Propagation characteristics of electromagnetic waves in concrete
[AD-A207387] N89-27921

CONCURRENT PROCESSING
Hybrid wafer-scale processor
[AD-A209944] N89-27969

CONDENSERS (LIQUEFIERS)
A 1-kW condenser for a two-phase heat rejection system N89-28288

CONDENSING
Condensing heat exchangers for European spacecraft ECLSS N89-28240

CONDUCTION BANDS
Preparation and characterization of several conduction transition metal oxides
[AD-A208895] N89-28424

CONDUCTORS
The interaction between a positively biased conductor on a high voltage solar array and a plasma N89-27720

CONFERENCES
DGLR/AIAA/JSASS 20th International Electric Propulsion Conference: Proceedings
[DGLR-PAPER-88-02] N89-27707
Proceedings of the Mobile Satellite System Architectures and Multiple Access Techniques Workshop
[NASA-CR-184564] N89-27907
An Introduction to Computational Fluid Dynamics
[VKI-LS-1989-02] N89-27985
European Coordinated Effort for Monitoring the Earth's Environment. A Pilot Project Campaign on LANDSAT Thematic Mapper Applications (1985-1987)
[ESA-SP-1102] N89-28055
Third International Satellite Direct Broadcast Services User's Conference N89-28176
Third European Symposium on Space Thermal Control and Life Support Systems
[ESA-SP-288] N89-28214
Life science research objectives and representative experiments for the space station
[NASA-TM-89445] N89-28304
Interplanetary Particle Environment. Proceedings of a Conference
[NASA-CR-185461] N89-28454

CONFIDENCE
Discrete enforcement of uncertain oscillator Gaussian response
[DE89-005595] N89-28038

CONFIDENCE LIMITS
Estimation of lower bound properties from material test data
[AD-A207378] N89-28361

CONGRESSIONAL REPORTS
The 1989 report to the Congress on the Strategic Defense Initiative
[PB89-196661] N89-28368
The 1990 National Aeronautics and Space Administration authorization
[GPO-99-550] N89-28450
National Aeronautics and Space Administration Multiyear Authorization Act of 1989
[H-REPT-101-226] N89-28451

CONICAL BODIES
Hypersonic prediction comparisons with experimental data for a cone-cylinder at mach 6.86
[AD-A207583] N89-27636

CONICAL FLOW
Hypersonic prediction comparisons with experimental data for a cone-cylinder at mach 6.86
[AD-A207583] N89-27636

CONIFERS
Discrimination of geobotanical anomalies in coniferous forests from LANDSAT TM data N89-28079

CONJUGATE GRADIENT METHOD
A fast multipole algorithm for capacitance extraction of complex 3-D geometries
[AD-A208374] N89-28317

CONSTELLATIONS
Constellation sizing for modest directed energy platforms
[DE89-012826] N89-28367

CONSTRUCTION
Fiber reinforced structural ceramics for construction
[AD-A209976] N89-27858

CONTAMINANTS
Analytical procedures for environmental quality control, volume 3
[PB89-158620] N89-28104

CONTOUR SENSORS
Surface Contour Radar (SCR) contributions to FASINEX N89-28159

CONTOURS
Automatic construction of polyhedral surfaces from voxel representations
[AD-A210009] N89-28325

CONTROL STABILITY
Stability robustness improvement of direct eigenspace assignment based feedback systems using singular value sensitivities
[NASA-CR-182302] N89-27672

CONTROL SYSTEMS DESIGN
Stability robustness improvement of direct eigenspace assignment based feedback systems using singular value sensitivities
[NASA-CR-182302] N89-27672
Development of a flight standard power conditioning and control system for the T5 ion thruster N89-27738
Application of optimal control theory to the design of the NASA/JPL 70-meter antenna servos N89-27881
Joint-space adaptive control of a 6 DOF end-effector with closed-kinematic chain mechanism
[NASA-CR-185861] N89-28016
Design of an adaptive controller for a telerobot manipulator
[NASA-CR-185863] N89-28017
Thermal control of Columbus pressurized modules N89-28233
Design concepts for Hermes thermal control N89-28234
The atmosphere pressure control section of the Hermes ECLSS N89-28241
A thermal control design for the Quasat spacecraft N89-28258
Development of heat exchangers for hybrid radiators N89-28285
Parameter plane design method
[AD-A209845] N89-28322
Implementation of a digital torque controller of a reaction wheel with an incremental computer
[INPE-4784-PRE/1447] N89-28333
Singular and bang-bang stochastic control
[AD-A208627] N89-28337

CONTROL THEORY
The Telecommunications and Data Acquisition Report
[NASA-CR-185431] N89-27871
Application of optimal control theory to the design of the NASA/JPL 70-meter antenna servos N89-27881
Control and system theory, optimization, inverse and ill-posed problems
[AD-A208570] N89-28335

CONTROLLABILITY
Markov processes applied to control, reliability and replacement
[AD-A208634] N89-28362

CONTROLLERS
A new method for analysis of limit cycle behavior of the NASA/JPL 70-meter antenna axis servos N89-27880
Application of optimal control theory to the design of the NASA/JPL 70-meter antenna servos N89-27881
Design of an adaptive controller for a telerobot manipulator [NASA-CR-185863] N89-28017
Implementation of a digital torque controller of a reaction wheel with an incremental computer [INPE-4784-PRE/1447] N89-28333

CONVECTION
A central difference type approximation of convection in fluid flow [DE89-013282] N89-27981

CONVECTIVE HEAT TRANSFER
Thermal effects of plume impingement N89-28252
Theoretical and experimental investigations on heat exchangers for Columbus hybrid radiators N89-28295
Analysis of articulated manikin based convective heat transfer during walking [AD-A208299] N89-28298

COOLANTS
Flow boiling with enhancement devices for cold plate coolant channel design [NASA-CR-185840] N89-27979

COOLERS
A thermal control design for the Quasat spacecraft N89-28258

COOLING
Blading design for cooled high-pressure turbines N89-27668
Glassy behaviour of YBa2Cu3O7 [DE89-613399] N89-28418

COOLING SYSTEMS
Radiators and heat exchangers for space applications [REPT-882-440-115] N89-27688
Radiator conceptual studies for the Hermes spaceplane N89-27689
Development of heat exchangers for hybrid radiators N89-27690

COORDINATE TRANSFORMATIONS
Extension of stellarator approximation in magnetohydrodynamic equilibrium and stability of toroidal helical systems [IPPJ-905] N89-28400

COPOLYMERIZATION
Transformation of a monotropic mesophase into an enantiotropic mesophase by copolymerization of the parent polymers' monomer pair containing constitutional isomeric mesogenic side groups [AD-A208782] N89-27850
Calculation of network parameters of crosslinked Markovian polymer chains [AD-A210073] N89-27860

COPOLYMERS
Resist sensitivity enhancement by radiation-induced modification [AD-A208438] N89-27842
Transformation of a monotropic mesophase into an enantiotropic mesophase by copolymerization of the parent polymers' monomer pair containing constitutional isomeric mesogenic side groups [AD-A208782] N89-27850

COPPER
Tungsten fiber reinforced copper matrix composites: A review [NASA-TP-2924] N89-27796
Optical spectroscopy of copper (1) doped Na(+) beta-alumina [AD-A209819] N89-27810

COPPER OXIDES
Superconductivity in the Ba(0.69)Y(0.46)CuO(3.15-delta) compound [DE88-706000] N89-28406

CORRELATION
The effect of spatial and temporal wet-troposphere fluctuations on connected element interferometry N89-27874
Reanalysis, compatibility and correlation in analysis of modified antenna structures N89-27906
GMBU (Ground Mobile Breadboard Upgrade) lidar and bubbler correlation study at Dugway Proving Ground [AD-A207297] N89-28002
Correlative Measurements Program N89-28164

CORROSION
Institute for Materials Science and Engineering: Metallurgy Division, technical activities 1988 [PB89-201321] N89-27819

CORROSION RESISTANCE
Corrosion of aluminium alloys by IRFNA (Inhibited Red Fuming Nitric Acid) [AD-A208328] N89-27823
Development of anodes for aluminum/air batteries: Solution phase inhibition of corrosion [DE89-012639] N89-27956

COSMIC DUST
Synchrotron X-ray fluorescence analyses of stratospheric cosmic dust: New results for chondritic and nickel-depleted particles [DE89-014032] N89-28107

COSMIC RAYS
The anomalous cosmic-ray component N89-28467
Studies of the cosmic ray penumbra [AD-A210109] N89-28484

COSMIC X RAYS
Gamma ray bursts: Confrontation between theory and observational data [DE89-012936] N89-28477

COSMOLOGY
Information aspects of type 9 cosmological models [DE89-612518] N89-28472
Stochastic approach to chaotic inflation and the distribution of universes [DE89-778051] N89-28473

COST ANALYSIS
Parameter plane design method [AD-A209845] N89-28322
The 1989 report to the Congress on the Strategic Defense Initiative [PB89-196661] N89-28368

COST EFFECTIVENESS
A computational comparison of the primal simplex and relaxation algorithms for solving minimum cost flow networks [AD-A208534] N89-28331

COUPLINGS
Development of a novel high-performance contact heat exchanger N89-28286

COVARIANCE
High-precision radiometric tracking for planetary approach and encounter in the inner solar system N89-27873
Determination of local empirical covariance functions from residual terrain reduced altimeter data [AD-A208678] N89-28095

CRACK GEOMETRY
Stress intensity calibration of a ring specimen using a finite element technique [AD-A208878] N89-28044

CRACK INITIATION
Analysis and elimination of high temperature notch induced microcrack initiation in Inconel 718 nickel-based alloy [AD-A209695] N89-27828

CRACK OPENING DISPLACEMENT
Dynamic fracture toughness testing [AD-A209948] N89-28046

CRACK PROPAGATION
An acoustic emission investigation of the tensile failure of cathodically charged 304 stainless steel [DE89-008752] N89-27816
Solvent assisted delamination crack growth behavior of amorphous thermoplastic materials [AD-A207385] N89-27833
Dynamic fracture and deformation of solid propellant [AD-A208691] N89-27865
Soliton behaviour of crack propagation in brittle materials [DE89-612190] N89-28033
Probabilistic description of fatigue crack growth under constant-and variable-amplitude loading [AD-A208717] N89-28043
Stress intensity calibration of a ring specimen using a finite element technique [AD-A208878] N89-28044
United States Air Force Research Initiation Program for 1987, volume 1 [AD-A209726] N89-28436

CRACK TIPS
Dynamic fracture toughness testing [AD-A209948] N89-28046

CRACKS
The Sigmajig: An improved hot-cracking test [DE89-013029] N89-28031
Probabilistic description of fatigue crack growth under constant-and variable-amplitude loading [AD-A208717] N89-28043

CRASHES
An analysis of severe air transport accidents [DE89-012642] N89-27642
Investigation of transport airplane fuselage fuel tank installations under crash conditions [DOT/FAA/CT-88/24] N89-27643

CRATERING
Characterization of cold cathode erosion processes N89-27756

CREEP PROPERTIES
High temp toughening and creep studies [AD-A208714] N89-27826
Diamagnetic shielding and flux creep in a Tl-Ba-Ca-Cu-O thin film [DE89-014550] N89-28414

CRITERIA
Site selection criteria for the optical atmospheric visibility monitoring telescopes N89-27896

CROP GROWTH
Report of the Project Estima, phase 2: LANDSAT-TM data and agrometeorology in crop yield estimation of wheat at the farm level [INPE-4782-RPE/582-PHASE-2] N89-28051
Application of remote sensing to irrigation water management in two Italian irrigation districts N89-28060

CROP INVENTORIES
Forest classification with TM data in the area of Freiburg, Federal Republic of Germany N89-28081
Large-scale forest management using LANDSAT Thematic Mapper data N89-28085

CROSS POLARIZATION
Characterization of nylon 6 by 15N solid state NMR [AD-A208508] N89-27846

CROSSLINKING
High performance composites based on polyurethanes reinforced with polydiacetylenes [AD-A208436] N89-27797
Calculation of network parameters of crosslinked Markovian polymer chains [AD-A210073] N89-27860

CRYOGENIC COOLING
Cryogenic activities at ESTEC N89-28266
Long-life Stirling cycle coolers for applications in the 60 to 110 K range N89-28267
A 4-K mechanical refrigerator for space applications N89-28268
Thermal and cryogenic aspects of the ISO optical subsystem N89-28269
Thermal design of a superfluid helium dewar for infrared telescope on-board space flyer unit N89-28270
Cyrogenic fluid sink device for thermal control of a spaceplane during ascent and re-entry phases N89-28293

CRYOGENIC EQUIPMENT
Cryogenic activities at ESTEC N89-28266
A 4-K mechanical refrigerator for space applications N89-28268
Thermal and cryogenic aspects of the ISO optical subsystem N89-28269
Thermal design of a superfluid helium dewar for infrared telescope on-board space flyer unit N89-28270
Shaking in cryogenic conditions N89-28277

CRYOGENICS
Operational parameters for the superconducting cavity maser N89-27876
MM wavecomponents - SIS (Superconductor-Insulator-Superconductor) mixers [AD-A208632] N89-28421

CRYSTAL DEFECTS
The texture variation in extruded graphite [DE89-014086] N89-27837

CRYSTAL DISLOCATIONS
The topological structure of grain boundaries [DE89-014676] N89-28415

CRYSTAL GROWTH
Equipment models for process optimization and control using smart response surfaces [AD-A208321] N89-27838

CRYSTAL LATTICES
The topological structure of grain boundaries [DE89-014676] N89-28415
Zinc telluride growth on InP [AD-A209924] N89-28430

CRYSTAL STRUCTURE
High-temperature superconductivity: Abstracts of NIST (National Institute of Standards and Technology) publications, 1987-1988 [PB89-148340] N89-28405
Grain boundaries in silicon from zero temperature through melting [DE89-013186] N89-28410
Polycrystalline plastic deformation and texture evolution for crystals lacking five independent slip systems [AD-A208902] N89-28425

CRYSTAL SURFACES
Applications of the quartz crystal microbalance to electrochemistry [AD-A209853] N89-27812

CRYSTALLIZATION
The influence of the polymer backbone flexibility on the phase transitions of side chain liquid crystal polymers containing yl side groups [AD-A208821] N89-27851

Simulation of deformation and texture evolution in semi-crystalline polymers
[AD-A208854] N89-27852

CRYSTALS
Differential geometric aspects of the theory of ferroelectricity
[DE89-612191] N89-28416
Crystal chemistry, synthesis, and characterization of infrared optical materials
[AD-A208723] N89-28422

CURING
Anomalous stresses versus extent of cure in an epoxy composite specimen
[AD-A208523] N89-27798
Novel methods for reinforcing elastomers
[AD-A210150] N89-27861

CURRENT DISTRIBUTION
Optimization of current distribution in an applied-field MPD thruster N89-27743

CYCLES
A new method for analysis of limit cycle behavior of the NASA/JPL 70-meter antenna axis servos N89-27880

CYCLIC LOADS
Nonlinear viscoelastic characteristics of polymeric materials
[DE89-012680] N89-27835
Probabilistic description of fatigue crack growth under constant-and variable-amplitude loading
[AD-A208717] N89-28043

D

DAMAGE ASSESSMENT
Ultrasonic nondestructive evaluation of damage in continuous fiber composites
[AD-A208840] N89-27799
The inadequacies of damage energy as a measure of displacement damage
[AD-A207376] N89-28028
Use of LANDSAT TM data for forest damage inventory N89-28082
Giotto: The thermal responses to its encounter with comet Halley N89-28273
Thermal aspects of an extended mission for Giotto N89-28274

DAMPING
The Shock and Vibration Digest, volume 21, no. 4 N89-28025
Damping in structural joints N89-28026

DATA ACQUISITION
The Telecommunications and Data Acquisition Report
[NASA-CR-185431] N89-27871
A visibility characterization program for optical communications through the atmosphere N89-27894
Design of experiments and reliability models
[AD-A209880] N89-28023
A data acquisition and control program for axial-torsional fatigue testing
[NASA-TM-102041] N89-28029
Wide band data collection system N89-28130

DATA BASE MANAGEMENT SYSTEMS
Approaching distributed database applications using a programmable terminal emulator
[DE89-014831] N89-28308
Conversion of mass storage hierarchy in an IBM computer network
[AD-A208520] N89-28330
Data base development and research and editorial support
[NASA-CR-183249] N89-28440
An implementation of a data definition facility for the graphics language for database
[AD-A207380] N89-28442
Problems and solutions in online documentation systems
[DE89-014092] N89-28447

DATA BASES
Small scale model tests in small wind and water tunnels at high incidence and pitch rates. Volume 3: Water tunnel (HFF) data base
[AD-A208690] N89-27638
Database development for the DMSP (Defense Meteorological Satellite Program) SSIES experiment
[AD-A208712] N89-27691
Requirements for a technical data base N89-27930
Evaluation of the AFGL (Air Force Geophysics Laboratory) cloud simulation models using satellite data
[AD-A208713] N89-28116
Anthropometric measurements of aviators within the Aviation Epidemiology Data Register
[AD-A208609] N89-28300
Data base development and research and editorial support
[NASA-CR-183249] N89-28440
Data bases available at the National Institute of Standards and Technology Research Information Center
[PB89-160014] N89-28441
An implementation of a data definition facility for the graphics language for database
[AD-A207380] N89-28442

DATA COMPRESSION
Digital CODEC for real-time processing of broadcast quality video signals at 1.8 bits/pixel
[NASA-TM-102325] N89-27927

DATA LINKS
Software package for performing experiments about the convolutionally encoded Voyager 1 link N89-27888

DATA MANAGEMENT
Math and physics studies-multi-project support entropy-based image restoration: Modifications and addditional results
[AD-A209972] N89-27951

DATA PROCESSING
Adaptive preprocessing of nonstationary signals
[AD-A209646] N89-27946
Report of the Project Estima, phase 2: LANDSAT-TM data and agrometeorology in crop yield estimation of wheat at the farm level
[INPE-4782-RPE/582-PHASE-2] N89-28051
Extended Kalman Filter (EKF) algorithm
[PD-CF-8922] N89-28313
A computational comparison of the primal simplex and relaxation algorithms for solving minimum cost flow networks
[AD-A208534] N89-28331

DATA PROCESSING TERMINALS
Synchronization of the receiver for the ISDN basic connection N89-27933

DATA REDUCTION
Determination of local empirical covariance functions from residual terrain reduced altimeter data
[AD-A208678] N89-28095

DATA RETRIEVAL
Data base development and research and editorial support
[NASA-CR-183249] N89-28440

DATA SAMPLING
Hyperdimensional data analysis and structural inference
[AD-A210056] N89-27971

DATA TRANSMISSION
Software package for performing experiments about the convolutionally encoded Voyager 1 link N89-27888
Accuracy of telemetry signal power loss in a filter as an estimate for telemetry degradation N89-27900
Analysis and dimensioning of a value-discrete adaptive compensation filter N89-27932
Communications using channels formed by meteor bursts
[AD-A209856] N89-27949

DAYTIME
Options for daytime monitoring of atmospheric visibility in optical communications N89-27895

DECISION MAKING
Identification of variables determining intrahemispheric interference between processing demands
[AD-A208435] N89-28299
Crisis decision-making: The impact of commercial satellites on the media, military and national leaders
[AD-A207334] N89-28449

DECOMPOSITION
A RUTCOR project on discrete applied mathematics
[AD-A208572] N89-28347
Decomposition kinetics and film formation of an organometallic precursor to SiC on Si(100)
[AD-A208384] N89-28420

DEEP SPACE NETWORK
The Telecommunications and Data Acquisition Report
[NASA-CR-185431] N89-27871
Stabilized fiber-optic frequency distribution system N89-27879
Precision pointing compensation for DSN antennas with optical distance measuring sensors N89-27882
The effects of atmospheric turbulence on precision optical measurements used for antenna-pointing compensation N89-27883
A multiflare horn with 1-megawatt power handling capability N89-27884
Multipurpose exciter with low phase noise N89-27887
DSN radio science system design and testing for Voyager-Neptune encounter N89-27899
The DSS-14 C-band exciter N89-27901
DSN 70-meter antenna microwave optics design and performance improvements. Part 1: Design optimization N89-27903
DSN 70-meter antenna X- and S-band calibration. Part 1: Gain measurements N89-27904
DSN 70-meter antenna X- and S-band calibration. Part 2: System noise temperature measurements and telecommunications link evaluation N89-27905

DEFENSE PROGRAM
High Endoatmospheric Defense Interceptor (HEDI) technology testing program environmental assessment
[AD-A210006] N89-27684
Goals for limited strategic defenses
[DE89-012260] N89-28386
The 1989 report to the Congress on the Strategic Defense Initiative
[PB89-196661] N89-28368
Critical technologies plan for the Committees on Armed Services, United States Congress, revision
[AD-A210170] N89-28439

DEFLECTORS
Static internal performance of a nonaxisymmetric vaned thrust reverser with flow splay capability
[NASA-TP-2933] N89-27634

DEFORMATION
Nonlinear viscoelastic characteristics of polymeric materials
[DE89-012680] N89-27835
Dynamic fracture and deformation of solid propellant
[AD-A208691] N89-27865
Speckle interferometry using fiber optic phase stepping
[NASA-TM-102331] N89-27999
Evaluation of new thermomechanical constitutive theory for snow N89-28052

DEGRADATION
Photodegradation of polyimide 1. A spectral, viscometric, chromatographic and weight loss investigation of polyimides based on a perfluorinated dianhydride
[AD-A208507] N89-27845
Probabilistic structural analysis methods of hot engine structures
[NASA-TM-102091] N89-28030

DEGREES OF FREEDOM
Algorithmic control of walking
[AD-A210117] N89-28326

DELAMINATING
Solvent assisted delamination crack growth behavior of amorphous thermoplastic materials
[AD-A207365] N89-27833

DELAY LINES (COMPUTER STORAGE)
Fiber-optic delay line storage in digital optical computers based on directional couplers
[PB89-185318] N89-28392

DELTA WINGS
Studies of unsteady vortex flap aerodynamics
[AD-A209837] N89-27641

DEMAND ASSIGNMENT MULTIPLE ACCESS
Performance of DA/FDMA architecture proposed for MSS N89-27910
MSAT signalling and network management architectures N89-27916

DEMODULATION
Aeronautical mobile TDMA/MCTDMA system N89-27918

DEMODULATORS
Digital demodulator for mobile satellite communication N89-27938

DEMULTIPLEXING
Digital demultiplier for mobile satellite communication N89-27937

DEOXYRIBONUCLEIC ACID
Molecular biology of the photoregulation of photosynthetic light-harvesting complexes in marine dinoflagellates
[AD-A209650] N89-28198

DEPLOYMENT
Thermal aspects of the ERS-1 SAR antenna deployment N89-28261
The 1989 report to the Congress on the Strategic Defense Initiative
[PB89-196661] N89-28368

DEPOSITION
A 6 cm diameter ion source for assistant deposition N89-27784
Laser processing of metals and alloys
[DE89-613235] N89-27822
Ion beam and plasma methods of producing diamondlike carbon films
[NASA-TM-102301] N89-27836
Experimental study on the deposition profile of the ICRF power and electron thermal diffusivity
[IPPJ-908] N89-28401

DESERTS
LANDSAT TM study of sabkha surfaces in the Qattara Depression, northwestern Egypt N89-28066
Image processing strategies for mineral exploration in arid areas by use of TM data N89-28067

DESIGN ANALYSIS
Systems Engineering
[AGARD-LS-164] N89-27650

Avionics system engineering: An introduction N89-27651
Avionic system requirements N89-27652
A structured approach to weapon system design N89-27653
Integrated avionics: Conceptual design N89-27654
The evolution of digital avionics architectures/systems N89-27655
Blading design for cooled high-pressure turbines N89-27668
Radiators and heat exchangers for space applications [REPT-882-440-115] N89-27688
Development of heat exchangers for hybrid radiators N89-27690
The potential application of the blackboard model of problem solving to multidisciplinary design [NASA-TM-101633] N89-28314

DESORPTION
Applications of the quartz crystal microbalance to electrochemistry [AD-A209853] N89-27812

DESTRUCTIVE TESTS
The Sigmajig: An improved hot-cracking test [DE89-013029] N89-28031

DETECTION
Optical spatial tracking using coherent detection in the pupil plane [AD-A209970] N89-28209
Detection of artificial sources of nuclear radiation in space, revision [AD-A209720] N89-28480

DIAMAGNETISM
Diamagnetic shielding and flux creep in a Tl-Ba-Ca-Cu-O thin film [DE89-014550] N89-28414

DIAMINES
Poly(enaminonitriles): Novel materials for use in electronics [AD-A208439] N89-27843

DIAMONDS
Ion beam and plasma methods of producing diamondlike carbon films [NASA-TM-102301] N89-27836

DIELECTRICS
The interaction between a positively biased conductor on a high voltage solar array and a plasma N89-27720
Piezoelectric polymer/ceramic composite [AD-A208905] N89-27801
Electromagnetic scattering from a structured slab comprised of periodically placed resistive cards [AD-A210145] N89-27953
A fast multipole algorithm for capacitance extraction of complex 3-D geometries [AD-A208374] N89-28317
Growth and characterization of zinc sulfide films by conversion of zinc oxide films with H2S [AD-A208727] N89-28423

DIFFERENTIAL EQUATIONS
A uniformly differentiable approximation scheme for delay systems using splines [AD-A209567] N89-28346
Differential equations, related problems of Pade approximations and computer applications [AD-A208590] N89-28348

DIFFRACTION PATTERNS
Noncontacting laser diffraction strain extensometer for material properties characterization at high temperatures [DE89-013551] N89-28393

DIFFUSION
A central difference type approximation of convection in fluid flow [DE89-013282] N89-27981
Experimental study on the deposition profile of the ICRF power and electron thermal diffusivity [IPPJ-908] N89-28401

DIFFUSION COEFFICIENT
Experimental determination of the coefficient in the steady state current equation for spherical segment microelectrodes [AD-A208662] N89-27965

DIGITAL COMPUTERS
Implementation of a digital torque controller of a reaction wheel with an incremental computer [INPE-4784-PRE/1447] N89-28333
Fiber-optic delay line storage in digital optical computers based on directional couplers [PB89-185318] N89-28392

DIGITAL DATA
The evolution of digital avionics architectures/systems N89-27655
The use of digital elevation model for correcting the effects of projections in reforrestations of eucalyptus in mountainous regions [INPE-4763-PRE/1432] N89-28048

DIGITAL FILTERS
Computer generated matched filters with spatial frequency tailoring [AD-A209786] N89-28001

DIGITAL SIMULATION
Field theory simulation of nonreciprocal microwave components N89-27940
A study of spacecraft electromagnetic contamination of artificial electron beams [AD-A209954] N89-27950
Thermal modelling of the EVA-suited astronaut N89-28245
Thermal effects of plume impingement N89-28252

DIGITAL SYSTEMS
Digital demultiplier for mobile satellite communication N89-27937
Digital demodulator for mobile satellite communication N89-27938
Theory of multi-frequency modulation (MFM) digital communications [AD-A209737] N89-27947
Engineering drawing transfer test with Douglas Aircraft Company: MIL-D-28000 Class II (IGES) [DE89-012810] N89-28443

DIGITAL TECHNIQUES
The evolution of digital avionics architectures/systems N89-27655

DIGITS
Significant digit computation of the incomplete beta function ratios [AD-A210118] N89-28358

DIODES
A one microsecond, thirty-five kilojoule, one hertz pulse generator [DE89-013074] N89-27955
Diode-pumped laser research N89-28185

DIPOLE MOMENTS
Characterization of structure in thin polymer resist films [AD-A208677] N89-27848

DIRECT BROADCAST SATELLITES
Third International Satellite Direct Broadcast Services User's Conference N89-28176

DIRECT CURRENT
Numerical studies of the flow field in a dc arcjet thruster N89-27776
Computational investigation on the characteristics of a low power dc arcjet thruster N89-27777
Experimental investigation on the characteristics of a low power dc arcjet thruster N89-27780

DIRECTION FINDING
Fixed interval smoothing algorithm for an extended Kalman filter for over-the-horizon ship tracking [AD-A208555] N89-28318

DIRECTIONAL COUPLERS
Fiber-optic delay line storage in digital optical computers based on directional couplers [PB89-185318] N89-28392

DISCRIMINANT ANALYSIS (STATISTICS)
Perception of motion in statistically-defined displays [AD-A208695] N89-28301

DISPLACEMENT
An experimental study to determine the relative influence of fluid-fluid interactions and media heterogeneities on the growth of immiscible viscous fingers [DE89-013122] N89-27976
The inadequacies of damage energy as a measure of displacement damage [AD-A207376] N89-28028

DISPLAY DEVICES
Perception of motion in statistically-defined displays [AD-A208695] N89-28301
Human cognition and information display in C3I system tasks [AD-A210012] N89-28302

DISSOCIATION
Electrospray ionization-mass spectrometry and tandem mass spectrometry [DE89-014465] N89-27806

DISTANCE MEASURING EQUIPMENT
Precision pointing compensation for DSN antennas with optical distance measuring sensors N89-27882
The effects of atmospheric turbulence on precision optical measurements used for antenna-pointing compensation N89-27883

DISTORTION
Precision pointing compensation for DSN antennas with optical distance measuring sensors N89-27882

DISTRIBUTED PROCESSING
Approaching distributed database applications using a programmable terminal emulator [DE89-014831] N89-28308
Resource contention management in parallel systems [AD-A208809] N89-28332

DMSP SATELLITES
Database development for the DMSP (Defense Meteorological Satellite Program) SSIES experiment [AD-A208712] N89-27691

DOPED CRYSTALS
Optical spectroscopy of copper (1) doped Na(+) beta-alumina [AD-A209819] N89-27810

DOPPLER EFFECT
New ion trap for atomic frequency standard applications N89-27875

DOPPLER NAVIGATION
High-precision radiometric tracking for planetary approach and encounter in the inner solar system N89-27873

DOPPLER RADAR
YAG aerosol lidar N89-28135

DOWNLINKING
Microwave time delays for the X/S-band feed system at X-band N89-27898
Geostar's system architectures N89-27911

DRAG
Theory of photon-drag effect in bulk magnetic semiconductors [DE89-612214] N89-28417

DRAINAGE
Application of LANDSAT data to hydrological mapping N89-28059

DRILLING
Laser processing of metals and alloys [DE89-613235] N89-27822

DROPS (LIQUIDS)
A magnetically-driven droplet radiator concept N89-28290

DUCTS
Parametric study of electromagnetic waves propagating in absorbing curved S ducts [NASA-TM-102024] N89-27923

DUMMIES
Analysis of articulated manikin based convective heat transfer during walking [AD-A208299] N89-28298

DYE LASERS
Solid state research [AD-A209645] N89-28426

DYNAMIC CHARACTERISTICS
The Shock and Vibration Digest, volume 21, no. 4 N89-28025
Recent advances on the dynamic behavior of stiffened plates N89-28027
Non-linear dynamics and chaotic motions in feedback controlled elastic system [AD-A208628] N89-28041
Magnetopause structure and dynamics: Issues for GEM [DE89-012620] N89-28054
Engineering research and development: Thrust area report FY 88 [DE89-014320] N89-28453
Time-Variable Phenomena in the Jovian System [NASA-SP-494] N89-28474
A space radiation test model study [AD-A208760] N89-28479

DYNAMIC CONTROL
Studies in stabilization and control of beams and plates [AD-A208635] N89-28042
Algorithmic control of walking [AD-A210117] N89-28326

DYNAMIC LOADS
Mechanical response of structural elements to dynamic loads [AD-A209827] N89-27802
Dynamic fracture toughness testing [AD-A209948] N89-28046

DYNAMIC MODELS
Three-dimensional vortex interactions in turbulent boundary layers [AD-A208624] N89-27991
A space radiation test model study [AD-A208760] N89-28479

DYNAMIC RESPONSE
Mechanical response of structural elements to dynamic loads [AD-A209827] N89-27802
System theoretic models for high density VLSI structures [AD-A209901] N89-27968
Damping in structural joints N89-28026
Discrete enforcement of uncertain oscillator Gaussian response [DE89-005595] N89-28038
Time series modeling for structural response prediction [AD-A208808] N89-28354

DYNAMIC STABILITY
The stability of the High-Density Z-Pinch
[DE89-014276] N89-28403

E

EARTH ATMOSPHERE
Studies of the propagation of short burst, high power microwave radiation through neutral and ionized media
[AD-A208664] N89-27944
EARTH IONOSPHERE
Interaction of high voltage solar array with ionospheric plasma N89-27719
Scaling laws for the spectrum of interchange instabilities in the high latitude ionosphere
[AD-A209993] N89-28111
A space radiation test model study
[AD-A208760] N89-28479
EARTH MAGNETOSPHERE
A space radiation test model study
[AD-A208760] N89-28479
EARTH OBSERVING SYSTEM (EOS)
Earth Observing System (EOS) advanced altimetry N89-28129
Wide band data collection system N89-28130
Calibration support for the Earth Observing System Project N89-28131
EARTH ORBITAL ENVIRONMENTS
The use of electric propulsion techniques for LEO atomic oxygen simulation N89-27787
EARTH ORBITS
Electric propulsion for low earth orbit applications N89-27714
Estimation and filtering techniques for high-accuracy GPS applications N89-27872
EARTH PLANETARY STRUCTURE
Solution of two-dimensional, two-region electromagnetic ground response
[AD-A206265] N89-27869
EARTH RADIATION BUDGET
The Earth Radiation Budget Experiment N89-28133
EARTH RADIATION BUDGET EXPERIMENT
The Earth Radiation Budget Experiment N89-28133
EARTH ROTATION
Differential geodesy of the Eotvos torsion balance
[AD-A208711] N89-28096
EARTH SURFACE
Solution of two-dimensional, two-region electromagnetic ground response
[AD-A206265] N89-27869
ECHOCARDIOGRAPHY
The effect of various straining maneuvers on cardiac volumes at 1G and during +Gz acceleration
[AD-A208846] N89-28200
ECHOES
Statistical analysis of the LMS and modified stochastic gradient algorithms
[AD-A208618] N89-28319
ECONOMIC ANALYSIS
High-speed civil transport study
[NASA-CR-4233] N89-27648
System level comparison of FDMA vs. CDMA (under conference guideline constraint) N89-27913
ECONOMIC IMPACT
The private sector economic and employment benefits to the nation and to each state of proposed FY 1990 NASA procurement expenditures
[NASA-CR-185894] N89-28448
ECOSYSTEMS
Remote sensing of the Madrid area ecosystems N89-28076
EDGES
The use of edge detectors based on mathematical morphology in remote sensing imagery
[INPE-4777-PRE/1446] N89-28050
EDITING
Ved editor for MC5600 computer system
[PD-SE-8907] N89-28306
Vi editor for MC56000 computer system
[PD-SE-8906] N89-28307
EDITING ROUTINES (COMPUTERS)
Ved editor for MC5600 computer system
[PD-SE-8907] N89-28306
Vi editor for MC56000 computer system
[PD-SE-8906] N89-28307
EGYPT
LANDSAT TM study of sabkha surfaces in the Qattara Depression, northwestern Egypt N89-28066
EIGENVALUES
Stability robustness improvement of direct eigenspace assignment based feedback systems using singular value sensitivities
[NASA-CR-182302] N89-27672
EIGENVECTORS
Stability robustness improvement of direct eigenspace assignment based feedback systems using singular value sensitivities
[NASA-CR-182302] N89-27672
ELASTIC PROPERTIES
Mechanical response of structural elements to dynamic loads
[AD-A209827] N89-27802
Non-linear dynamics and chaotic motions in feedback controlled elastic system
[AD-A208628] N89-28041
Analysis of a limiting-amplitude problem in acousto-elastic interactions, 1
[AD-A209741] N89-28045
Grain boundaries in silicon from zero temperature through melting
[DE89-013186] N89-28410
ELASTIC SCATTERING
Infrared photodissociation of van der Waals complexes selectively prepared by molecular beam scattering N89-28376
Potential energy curves for the (ArH(+)) and (NeH(+)) systems from the interplay of theory and experiments N89-28380
Dynamics of H(+) + Kr and H(+) + Xe elastic and charge-transfer collisions: State-selected differential cross sections at low collision energies N89-28381
ELASTIC WAVES
Terminal shock response in ramjet inlets to abrupt downstream perturbations
[AD-A209788] N89-27640
ELASTOMERS
Novel methods for reinforcing elastomers
[AD-A210150] N89-27861
ELECTRIC BATTERIES
A battery-powered flux compression generator system
[DE89-014230] N89-27958
ELECTRIC CONDUCTORS
A fast multipole algorithm for capacitance extraction of complex 3-D geometries
[AD-A208374] N89-28317
ELECTRIC CONNECTORS
Average interconnection length and interconnection distribution for rectangular arrays
[AD-A209848] N89-27967
Band structure engineering for ultra-low threshold laser diodes
[AD-A208629] N89-28010
Development of superlattices for ultra high-speed electronic and optoelectronic devices
[AD-A209874] N89-28429
ELECTRIC CONTACTS
Advanced motor and motor control development
[AD-A207332] N89-27954
ELECTRIC CURRENT
Experimental determination of the coefficient in the steady state current equation for spherical segment microelectrodes
[AD-A208662] N89-27965
ELECTRIC DISCHARGES
Discharge performance of a 12 cm cusp xenon ion thruster N89-27746
Ring cusp/hollow cathode discharge chamber performance studies — ion propulsion N89-27748
SRM propellant, friction/ESD testing
[NASA-CR-183706] N89-27864
ELECTRIC FIELDS
Definition study and model for a tethered sounding rocket
[AD-A207367] N89-27699
Solution of two-dimensional, two-region electromagnetic ground response
[AD-A206265] N89-27869
Interpretation of F106B and CV580 in-flight lightning data and form factor determination
[NASA-CR-4250] N89-28115
Theory of photon-drag effect in bulk magnetic semiconductors
[DE89-612214] N89-28417
ELECTRIC MOTORS
Composite ceramic superconducting wires for electric motor applications
[AD-A208598] N89-27847
Advanced motor and motor control development
[AD-A207332] N89-27954
ELECTRIC POTENTIAL
New ion trap for atomic frequency standard applications N89-27875
ELECTRIC POWER SUPPLIES
Development and refinement of test bed simulations
[NASA-TM-102335] N89-27702
ELECTRIC PROPULSION
DGLR/AIAA/JSASS 20th International Electric Propulsion Conference: Proceedings
[DGLR-PAPER-88-02] N89-27707
The ESA policy and program for the development of electric propulsion N89-27708
Electric propulsion projects and research in Japan N89-27709
Recent progress in the USSR electric propulsion N89-27710
Interests in electric propulsion N89-27711
Electric propulsion: Implementation issues N89-27712
Electric propulsion for low earth orbit applications N89-27714
FEEP power conditioning unit: Design and development status N89-27722
Survey of electric propulsion thruster applicability to near earth space missions N89-27749
Magnetic induction thruster with lithium propellant N89-27762
Propellant selection criteria for deep space electrically propelled missions N89-27769
Experiments and analysis of a compact electrothermal thruster N89-27773
The use of electric propulsion techniques for LEO atomic oxygen simulation N89-27787
KREM: A model for evaluating orbital transfer vehicles utilizing nuclear electric propulsion systems N89-27789
Capacitors for pulsed electric propulsion N89-27790
ELECTRIC ROCKET ENGINES
Field Emission Electric Propulsion (FEEP) attitude control capabilities N89-27724
ELECTRO-OPTICS
A novel approach to a PPM-modulated frequency-doubled electro-optic cavity-dumped Nd:YAG laser N89-27897
Monocular electro-optical stereo scanner N89-28125
Integrated opto-electronic computing
[AD-A209936] N89-28395
ELECTROCATALYSTS
Comparison of vacuum-annealed and electrochemically cycled electrodes in adsorption and electrocatalysis: Aromatic compounds at platinum (111) and polycrystalline platinum
[AD-A210011] N89-27814
ELECTROCHEMICAL CORROSION
Corrosion of aluminium alloys by IRFNA (Inhibited Red Fuming Nitric Acid)
[AD-A208326] N89-27823
ELECTROCHEMISTRY
The quartz crystal microbalance as an in situ tool in electrochemistry
[AD-A209852] N89-27811
Applications of the quartz crystal microbalance to electrochemistry
[AD-A209853] N89-27812
Electrochemical removal and concentration of CO2 N89-28238
ELECTRODELESS DISCHARGES
Electrothermal thrusters utilizing electrodeless discharges N89-27774
ELECTRODEPOSITION
Coating and impregnation of carbon-carbon composites with ceramics by electrophoretic deposition
[AD-A208873] N89-27800
Institute for Materials Science and Engineering: Metallurgy Division, technical activities 1988
[PB89-201321] N89-27819
ELECTRODES
Electrode erosion in steady-state electric propulsion engines N89-27755
Comparison of vacuum-annealed and electrochemically cycled electrodes in adsorption and electrocatalysis: Aromatic compounds at platinum (111) and polycrystalline platinum
[AD-A210011] N89-27814
Experimental determination of the coefficient in the steady state current equation for spherical segment microelectrodes
[AD-A208662] N89-27965
ELECTRODYNAMICS
Definition study and model for a tethered sounding rocket
[AD-A207367] N89-27699
Electrodynamics, wind and temperature N89-28168
ELECTROENCEPHALOGRAPHY
Attention, imagery and memory: A neuromagnetic investigation
[AD-A209917] N89-28207
Visualizing and rhyming cause differences in alpha suppression
[AD-A210005] N89-28210
ELECTROLYTIC CELLS
Corrosion of aluminium alloys by IRFNA (Inhibited Red Fuming Nitric Acid)
[AD-A208326] N89-27823
ELECTROMAGNETIC ABSORPTION
Multiphoton detection techniques for F and F2
[AD-A208576] N89-27807

Parametric study of electromagnetic waves propagating in absorbing curved S ducts
[NASA-TM-102024] N89-27923
ELECTROMAGNETIC FIELDS
Small scale testing of a mass-stabilized electromagnetic projectile
[AD-A206916] N89-27682
High-power, high-efficiency FELs
[DE89-013002] N89-28005
ELECTROMAGNETIC INTERACTIONS
Algebraic analysis of the electromagnetic wave interaction with the two-level system with two-fold degenerated states
[DE89-611932] N89-27926
ELECTROMAGNETIC MEASUREMENT
Aerosol model selection using surface measurements of IR horizon radiances and satellite detected visible radiances
[AD-A209638] N89-28110
ELECTROMAGNETIC NOISE
Noise and false alarm rate characteristics for envelope detector systems preceded by RF amplification
[AD-A209789] N89-27948
ELECTROMAGNETIC PROPERTIES
Electromagnetic reaction to molecular relaxation and its effect on absorption near a rough surface
[AD-A210069] N89-28390
ELECTROMAGNETIC PROPULSION
Improved thrust generation mechanism for electrothermal/electromagnetic arcjet N89-27726
ELECTROMAGNETIC PULSES
Solution of two-dimensional, two-region electromagnetic ground response
[AD-A206265] N89-27869
Line/Circuit Analysis Program: Cross-coupling on PC (Printed Circuit) board traces including discontinuities and circuit elements
[DE89-013884] N89-27957
ELECTROMAGNETIC RADIATION
Propagation characteristics of electromagnetic waves in concrete
[AD-A207387] N89-27921
Parametric study of electromagnetic waves propagating in absorbing curved S ducts
[NASA-TM-102024] N89-27923
Algebraic analysis of the electromagnetic wave interaction with the two-level system with two-fold degenerated states
[DE89-611932] N89-27926
A study of spacecraft electromagnetic contamination of artificial electron beams
[AD-A209954] N89-27950
Electromagnetic scattering from a structured slab comprised of periodically placed resistive cards
[AD-A210145] N89-27953
Coupling between radiation and gas dynamics
[AD-A209657] N89-28102
ELECTROMAGNETIC SCATTERING
Electromagnetic scattering from a structured slab comprised of periodically placed resistive cards
[AD-A210145] N89-27953
ELECTROMAGNETIC WAVE TRANSMISSION
Parametric study of electromagnetic waves propagating in absorbing curved S ducts
[NASA-TM-102024] N89-27923
Studies of the propagation of short burst, high power microwave radiation through neutral and ionized media
[AD-A208664] N89-27944
ELECTROMAGNETS
A magnetically-driven droplet radiator concept N89-28290
ELECTRON BEAMS
Irradiation effects on resistance of thermal impact of composite used in space
[DE89-778069] N89-27794
Electron beam-positive polyimides
[AD-A208440] N89-27844
A study of spacecraft electromagnetic contamination of artificial electron beams
[AD-A209954] N89-27950
A one microsecond, thirty-five kilojoule, one hertz pulse generator
[DE89-013074] N89-27955
Computer generated matched filters with spatial frequency tailoring
[AD-A209786] N89-28001
ELECTRON CYCLOTRON HEATING
A tandem mirror hybrid plume plasma propulsion facility N89-27791
ELECTRON ENERGY
Experimental study on the deposition profile of the ICRF power and electron thermal diffusivity
[IPPJ-908] N89-28401
A space radiation test model study
[AD-A208760] N89-28479
ELECTRON MICROSCOPY
Martensitic phase transitions in nanocrystalline materials
[AD-A208804] N89-27827
ELECTRON PLASMA
Efficient energy storage and conversion using adiabatic compression of relativistic-electron plasmas
[AD-A208657] N89-28101
A two-stream plasma electron microwave source for high-power millimeter wave generation, phase 1
[AD-A209942] N89-28404
ELECTRON TRANSFER
Experimental study on the deposition profile of the ICRF power and electron thermal diffusivity
[IPPJ-908] N89-28401
Superexchange coupling mechanisms for electron transfer processes
[DE89-013568] N89-28411
ELECTRONIC CONTROL
Advanced motor and motor control development
[AD-A207332] N89-27954
ELECTRONIC EQUIPMENT
Environmental effects of space shuttle exhaust on materials
[AD-A208813] N89-27686
Electronics research at the University of Texas at Austin
[AD-A209989] N89-27970
ELECTRONIC PACKAGING
Hybrid wafer-scale processor
[AD-A209944] N89-27969
ELECTRONS
Database development for the DMSP (Defense Meteorological Satellite Program) SSIES experiment
[AD-A208712] N89-27691
ELECTROPHORESIS
Coating and impregnation of carbon-carbon composites with ceramics by electrophoretic deposition
[AD-A208873] N89-27800
Theory of photon-drag effect in bulk magnetic semiconductors
[DE89-612214] N89-28417
ELECTROPHYSICS
Electronics research at the University of Texas at Austin
[AD-A209989] N89-27970
ELECTROSTATIC CHARGE
SRM propellant, friction/ESD testing
[NASA-CR-183706] N89-27864
ELECTROSTATIC DRAG
Interaction of high voltage solar array with ionospheric plasma N89-27719
ELECTROTHERMAL ENGINES
Electrothermal thrusters utilizing electrodeless discharges N89-27774
ELLIPTIC DIFFERENTIAL EQUATIONS
A numerical study of an augmented Lagrangian method for the estimation of parameters in elliptic systems
[AD-A208658] N89-28351
EMISSION SPECTRA
Optical spectroscopy of copper (1) doped Na(+) beta-alumina
[AD-A209819] N89-27810
Gamma ray bursts: Confrontation between theory and observational data
[DE89-012936] N89-28477
EMPLOYMENT
The private sector economic and employment benefits to the nation and to each state of proposed FY 1990 NASA procurement expenditures
[NASA-CR-185894] N89-28448
ENCLOSURES
A new analysis of beam-waveguide antennas considering the presence of the enclosure N89-27886
END EFFECTORS
Joint-space adaptive control of a 6 DOF end-effector with closed-kinematic chain mechanism
[NASA-CR-185861] N89-28016
ENERGETIC PARTICLES
The effects of high energy particles on planetary missions N89-28457
Current models of the intensely ionizing particle environment in space N89-28458
Intensity/time profiles of solar particle events at one astronomical unit N89-28460
The radial dependence of the solar energetic particle flux N89-28461
Predicting the arrival times of solar particles N89-28463
ENERGY CONVERSION EFFICIENCY
Efficient second harmonic conversion of broadband high-peak-power Nd:glass laser radiation using large-aperture KDP crystals in quadrature
[DE89-012961] N89-28003
Efficient energy storage and conversion using adiabatic compression of relativistic-electron plasmas
[AD-A208657] N89-28101
ENERGY DISSIPATION
The calculation of losses in waveguide networks N89-27941
ENERGY DISTRIBUTION
Charge transfer and inelastic scattering in proton-molecule collisions
[MPIS-13/1988] N89-28378
Charge transfer and structured vibrational distributions in H(+) + CH4 low-energy collisions N89-28385
ENERGY LEVELS
The inadequacies of damage energy as a measure of displacement damage
[AD-A207376] N89-28028
ENERGY POLICY
MHD (Magnetohydrodynamics) Program Plan, FY 1989
[DE89-012232] N89-28398
ENERGY SPECTRA
Elemental composition and energy spectra of galactic cosmic rays N89-28466
The anomalous cosmic-ray component N89-28467
ENERGY STORAGE
Progress in parabolic dish technology
[DE89-009427] N89-28100
Efficient energy storage and conversion using adiabatic compression of relativistic-electron plasmas
[AD-A208657] N89-28101
ENERGY TECHNOLOGY
Photovoltaic Program Branch annual report, FY 1988
[DE89-000898] N89-28099
ENERGY TRANSFER
Energy transfer effects in beta-alumina
[AD-A209818] N89-27855
The use of multiple ion exchange to produce energy transfer in beta-aluminas
[AD-A209821] N89-27856
Novel methodology for application of adaptive systems techniques to DMSP (Defense Meteorological Satellite Program) remote temperature sensing
[AD-A209975] N89-28098
ENGINE DESIGN
Blading Design for Axial Turbomachines
[AGARD-LS-167] N89-27661
Aerodynamic design of low pressure turbines N89-27669
Thermal design improvements for 30kWe arcjet engine N89-27754
ENGINE INLETS
Terminal shock response in ramjet inlets to abrupt downstream perturbations
[AD-A209788] N89-27640
Mach 5 inlet CFD and experimental results
[NASA-TM-102317] N89-27670
ENGINE MONITORING INSTRUMENTS
The Propellant Supply and Monitoring Equipment (PSME) for the UK-10 ion propulsion subsystem N89-27758
Diagnostic tools for an ion thruster in space N89-27782
ENGINE TESTS
Parametric study of the aerothermodynamics of a jet engine test facility
[AD-A208512] N89-27675
ENGINEERING DRAWINGS
Engineering drawing transfer test with Douglas Aircraft Company: MIL-D-28000 Class II (IGES)
[DE89-012810] N89-28443
ENTHALPY
Thermophysical properties of liquid niobium
[DE89-014288] N89-28435
ENVIRONMENT EFFECTS
High-speed civil transport study. Summary
[NASA-CR-4234] N89-27647
High-speed civil transport study
[NASA-CR-4233] N89-27648
High Endoatmospheric Defense Interceptor (HEDI) technology testing program environmental assessment
[AD-A210006] N89-27654
Environmental effects of space shuttle exhaust on materials
[AD-A208813] N89-27686
ENVIRONMENT SIMULATORS
Environmental calibration chamber operations N89-28192
ENVIRONMENTAL CONTROL
Third European Symposium on Space Thermal Control and Life Support Systems
[ESA-SP-288] N89-28214
Status of the US Space Station ECLSS and internal TCS N89-28215
The Hermes spaceplane program: Status report on the thermal control, environment control and life support activities N89-28217

European life support systems for space applications N89-28218
Environmental control and life support systems for pressurized modules: From Spacelab to Columbus N89-28219
The definition status of the environmental control and life support subsystems for Hermes N89-28220
Regenerative CO2-control --- Columbus N89-28237
The catalytic oxiderzer: Description and first results of a breadboard model for a component of the Columbus ECLSS N89-28239
Condensing heat exchangers for European spacecraft ECLSS N89-28240
Come to flight rules: Rationale on environmental control and life support systems --- Hermes N89-28242
ECLS simulation program N89-28284

ENVIRONMENTAL MONITORING
Environmental effects of space shuttle exhaust on materials
[AD-A208813] N89-27686
Analytical procedures for environmental quality control, volume 2
[PB89-158612] N89-28103
Analytical procedures for environmental quality control, volume 3
[PB89-158620] N89-28104
Bangladesh Agro-Climatic Environmental Monitoring Project N89-28121
NASA follow-on to the Bangladesh Agro-Climatic Environmental Monitoring Project N89-28122
Navigational and Environmental Measurement System (NEMS) N89-28178

ENVIRONMENTAL SURVEYS
High Endoatmospheric Defense Interceptor (HEDI) technology testing program environmental assessment
[AD-A210006] N89-27684
Environmental effects of space shuttle exhaust on materials
[AD-A208813] N89-27686

ENVIRONMENTAL TESTS
Operating and environmental characteristics of Sigma Tau hydrogen masers used in the Very Long Baseline Array (VLBA) N89-27877

EPIDEMIOLOGY
Anthropometric measurements of aviators within the Aviation Epidemiology Data Register
[AD-A208609] N89-28300

EPITAXY
Zinc telluride growth on InP
[AD-A209924] N89-28430

EPITHELIUM
The phototoxicity of blue light on the functional properties of the retinal pigment epithelium
[AD-A209834] N89-28204

EPOXY COMPOUNDS
Energetic polyoxetane thermoplastic elastomers: Synthesis and characterization
[AD-A209612] N89-27853

EPOXY RESINS
Anomalous stresses versus extent of cure in an epoxy composite specimen
[AD-A208523] N89-27798

EQUALIZERS (CIRCUITS)
Communication engineering reports. Fundamental developments. Theoretical work
[ETN-89-94623] N89-27928
Baseband equalizer for digital radio relay links N89-27936

EQUATIONS OF MOTION
Soliton behaviour of crack propagation in brittle materials
[DE89-612190] N89-28033
Model based damping of coupled horizontal and vertical oscillations in a flexible rod
[DE89-007034] N89-28039

EQUATIONS OF STATE
Experimental determination of the coefficient in the steady state current equation for spherical segment microelectrodes
[AD-A208662] N89-27965
Real gas equations of state for CHEMKIN
[DE89-012794] N89-28432

EQUIPMENT SPECIFICATIONS
Life science research objectives and representative experiments for the space station
[NASA-TM-89445] N89-28304

EROSION
Electrode erosion in steady-state electric propulsion engines N89-27755
Characterization of cold cathode erosion processes N89-27756

ERROR ANALYSIS
Analysis and dimensioning of a value-discrete adaptive compensation filter N89-27932
A uniformly differentiable approximation scheme for delay systems using splines
[AD-A208567] N89-28346
Sensitivity analysis of reflection errors in infrared image simulation
[AD-A208600] N89-28394

ERROR CORRECTING CODES
Decoding of 1/2-rate (24,12) Golay codes N89-27891
The weight distribution and randomness of linear codes N89-27892

ERROR SIGNALS
Adaptive preprocessing of nonstationary signals
[AD-A209646] N89-27946

ERRORS
The effect of spatial and temporal wet-troposphere fluctuations on connected element interferometry N89-27874

ERS-1 (ESA SATELLITE)
Thermal aspects of the ERS-1 SAR antenna deployment N89-28261

ESA SATELLITES
The role of electric propulsion in extending the economic life-cycle of commercial European telecommunication satellites N89-27713
The proposed demonstration of the UK-10 ion propulsion system on ESA's SAT-2 spacecraft N89-27729
Design and integration of an electric propulsion system on the Eurostar spacecraft N89-27732
The space-rigidised thermal shield for the ESA Far-Infrared Space Telescope (FIRST) N89-28236
A thermal control design for the Quasat spacecraft N89-28258
Thermal control of the GRASP detector section N89-28271
SOHO thermal modelling and analysis: The first application of ESATAN to a complete spacecraft N89-28279

ESTERS
Vapor phase deposition studies of phosphate esters on metal and ceramic surfaces
[PB89-148985] N89-27831

ESTIMATING
Estimation and filtering techniques for high-accuracy GPS applications N89-27872

ETHYLENE
Vibrational predissociation of shock-selected C2H4 and NH3 clusters, introduction N89-28374
Infrared photodissociation and cluster-specific detection of internally cold (C2H4) van der Waals complexes N89-28375
Infrared photodissociation of van der Waals complexes selectively prepared by molecular beam scattering N89-28376

EURECA (ESA)
Electric propulsion for low earth orbit applications N89-27714
Status of the RITA experiment on EURECA N89-27728

EUROPEAN SPACE PROGRAMS
The ESA policy and program for the development of electric propulsion N89-27708
Plasma propulsion activites at SNIA BPD N89-27716
FEEP power conditioning unit: Design and development status N89-27722
Field emission electric propulsion: Emission of slit-type liquid metal ion sources N89-27723
European life support systems for space applications N89-28218
Cryogenic activities at ESTEC N89-28266

EUTROPHICATION
Color analysis of inland waters using LANDSAT TM data N89-28062

EVAPORATION
Micro-fluid dynamical analysis of evaporating flows in heat pipes N89-28228

EVAPORATORS
Design and test of a two-phase coldplate N89-28226

EXCITATION
Vibrationally excited ions: Quenching, reaction and lifetimes
[AD-A208503] N89-28386

EXERCISE PHYSIOLOGY
The effect of various straining maneuvers on cardiac volumes at 1G and during +Gz acceleration
[AD-A208846] N89-28200

EXHAUST EMISSION
Environmental effects of space shuttle exhaust on materials
[AD-A208813] N89-27686

EXOBIOLOGY
Life science research objectives and representative experiments for the space station
[NASA-TM-89445] N89-28304

EXPERIMENT DESIGN
Design of experiments and reliability models
[AD-A209880] N89-28023
Life science research objectives and representative experiments for the space station
[NASA-TM-89445] N89-28304

EXPERT SYSTEMS
Rapid prototyping of complex avionics systems N89-27657
Application of expert systems to the thermal configuration of Giotto N89-28250
Evolution of thermal analysis methods towards integrated system performance simulation N89-28283
The potential application of the blackboard model of problem solving to multidisciplinary design
[NASA-TM-101633] N89-28314
Evidence flow graph methods for validation and verification of expert systems
[NASA-CR-181810] N89-28328

EXPOSURE
Evaluation of thermal stress induced by helicopter aircrew Chemical, Biological, Radiological (CBR) protective ensemble
[AD-A210123] N89-28303

EXTENSOMETERS
Noncontacting laser diffraction strain extensometer for material properties characterization at high temperatures
[DE89-013551] N89-28393

EXTRATERRESTRIAL RADIATION
A space radiation test model study
[AD-A208760] N89-28479
Detection of artificial sources of nuclear radiation in space, revision
[AD-A209720] N89-28480

EXTRAVEHICULAR ACTIVITY
Life support for EVA: The European system baseline N89-28244
Thermal modelling of the EVA-suited astronaut N89-28245
EVA and human physiology N89-28246

EXTREMELY HIGH FREQUENCIES
A comparative study of SHF (Super High Frequency) and EHF (Extremely High Frequency) satellite communications, volume 1
[AD-A208850] N89-27945
DARPA (Defense Advanced Research Projects Agency) Review on EHF Devices
[AD-A208564] N89-27963

EXTRUDING
The structure and properties of grain boundaries in B2 ordered alloys
[DE89-013266] N89-27817
The texture variation in extruded graphite
[DE89-014086] N89-27837

EYE (ANATOMY)
Eye movements and visual information processing
[AD-A209817] N89-28203
Optical spatial tracking using coherent detection in the pupil plane
[AD-A209970] N89-28209

EYE MOVEMENTS
Eye movements and visual information processing
[AD-A209817] N89-28203
Age-related changes in human vestibulo-ocular reflexes: Sinusoidal rotation and caloric tests
[NASA-CR-185857] N89-28211
Age-related changes in human vestibulo-ocular and optokinetic reflexes: Pseudorandom rotation tests
[NASA-CR-185856] N89-28213
Perception of motion in statistically-defined displays
[AD-A208695] N89-28301

F

FACTORIZATION
Computation of transonic potential flow past RAE-Wing-A and Body-B2 combination
[PD-CF-8921] N89-27637
Bunch-Kaufman factorization for real symmetric indefinite banded matrices
[NASA-CR-181860] N89-28341

FAILURE ANALYSIS
Space Shuttle Main Engine structural analysis and data reduction/evaluation. Volume 1: Aft Skirt analysis
[NASA-CR-183663] N89-27693
An acoustic emission investigation of the tensile failure of cathodically charged 304 stainless steel
[DE89-008752] N89-27816
Monte Carlo reliability analysis
[AD-A210052] N89-28024
Probabilistic structural analysis methods of hot engine structures
[NASA-TM-102091] N89-28030

FALSE ALARMS
Noise and false alarm rate characteristics for envelope detector systems preceded by RF amplification
[AD-A209789] N89-27948
FAR INFRARED RADIATION
The space-rigidised thermal shield for the ESA Far-Infrared Space Telescope (FIRST) N89-28236
FATIGUE (MATERIALS)
Probabilistic description of fatigue crack growth under constant-and variable-amplitude loading
[AD-A208717] N89-28043
Dynamic fracture toughness testing
[AD-A209948] N89-28046
FATIGUE LIFE
Probabilistic structural analysis methods of hot engine structures
[NASA-TM-102091] N89-28030
FATIGUE TESTS
A data acquisition and control program for axial-torsional fatigue testing
[NASA-TM-102041] N89-28029
FEASIBILITY ANALYSIS
Separation of oxygen from seawater by membrane permeation
[AD-A208863] N89-27809
FEDERAL BUDGETS
The private sector economic and employment benefits to the nation and to each state of proposed FY 1990 NASA procurement expenditures
[NASA-CR-185894] N89-28448
The 1990 National Aeronautics and Space Administration authorization
[GPO-99-550] N89-28450
National Aeronautics and Space Administration Multiyear Authorization Act of 1989
[H-REPT-101-226] N89-28451
FEEDBACK CIRCUITS
Band structure engineering for ultra-low threshold laser diodes
[AD-A208629] N89-28010
FEEDBACK CONTROL
Analysis of a system to prevent helicopter rotor blade-airframe strikes
[AD-A209804] N89-27649
Stability robustness improvement of direct eigenspace assignment based feedback systems using singular value sensitivities
[NASA-CR-182302] N89-27672
A new method for analysis of limit cycle behavior of the NASA/JPL 70-meter antenna axis servos N89-27880
Application of optimal control theory to the design of the NASA/JPL 70-meter antenna servos N89-27881
Parameter plane design method
[AD-A209845] N89-28322
State-space theory of structured uncertainty with examples
[AD-A209968] N89-28339
FERROELECTRICITY
Differential geometric aspects of the theory of ferroelectricity
[DE89-612191] N89-28416
FERROMAGNETIC MATERIALS
Martensitic phase transitions in nanocrystalline materials
[AD-A208804] N89-27827
FIBER COMPOSITES
Tungsten fiber reinforced copper matrix composites: A review
[NASA-TP-2924] N89-27796
Ultrasonic nondestructive evaluation of damage in continuous fiber composites
[AD-A208840] N89-27799
Fiber reinforced structural ceramics for construction
[AD-A209976] N89-27858
FIBER OPTICS
State-of-the-art fiber optics for short distance frequency reference distribution N89-27878
Stabilized fiber-optic frequency distribution system N89-27879
Compensation for effects of ambient temperature on rare-earth doped fiber optic thermometer
[NASA-TM-102282] N89-27998
Speckle interferometry using fiber optic phase stepping
[NASA-TM-102331] N89-27999
Band structure engineering for ultra-low threshold laser diodes
[AD-A208629] N89-28010
Studies of phase-conjugate optical device concepts
[AD-A206219] N89-28391
Fiber-optic delay line storage in digital optical computers based on directional couplers
[PB89-185318] N89-28392
FIELD EFFECT TRANSISTORS
DARPA (Defense Advanced Research Projects Agency) Review on EHF Devices
[AD-A208564] N89-27963
FIELD EMISSION
FEEP power conditioning unit: Design and development status N89-27722
Field emission electric propulsion: Emission of slit-type liquid metal ion sources N89-27723
Field Emission Electric Propulsion (FEEP) attitude control capabilities N89-27724
Field Emission Electric Propulsion (FEEP): Experimental investigations on continuous and pulsed modes of operation N89-27792
FIELD OF VIEW
Oceanographic wide field sensor N89-28132
FIELD THEORY (ALGEBRA)
Orbits which always have affine invariant neighbourhoods
[DE89-611895] N89-28344
FIELD THEORY (PHYSICS)
Field theory simulation of nonreciprocal microwave components N89-27940
FILLERS
Novel methods for reinforcing elastomers
[AD-A210150] N89-27861
FILM COOLING
Effects of an embedded vortex on a single film-cooling jet in a turbulent boundary layer
[AD-A207374] N89-27974
FILM THICKNESS
Comparison of equipment modeling methods as applied to the LPCVD of in-situ P-doped polysilicon
[AD-A208373] N89-27839
FINITE DIFFERENCE THEORY
SOHO thermal modelling and analysis: The first application of ESATAN to a complete spacecraft N89-28279
Assembling the ISO thermal model with ESATAN N89-28280
ESATAN FHTS: A piped fluid network capability N89-28281
FINITE ELEMENT METHOD
Space Shuttle Main Engine structural analysis and data reduction/evaluation. Volume 1: Aft Skirt analysis
[NASA-CR-183663] N89-27693
Space Shuttle Main Engine structural analysis and data reduction/evaluation. Volume 3A: High pressure oxidizer turbo-pump preburner pump housing stress analysis report
[NASA-CR-183665] N89-27694
Space Shuttle Main Engine structural analysis and data reduction/evaluation. Volume 3B: High pressure fuel turbo-pump preburner pump bearing assembly analysis
[NASA-CR-183666] N89-27695
Space Shuttle Main Engine structural analysis and data reduction/evaluation. Volume 4: High pressure fuel turbo-pump inlet housing analysis
[NASA-CR-183667] N89-27696
Space Shuttle Main Engine structural analysis and data reduction/evaluation. Volume 5: Main Injector LOX Inlet analysis
[NASA-CR-183668] N89-27697
Structural and thermal response of 30 cm diameter ion thruster optics
[NASA-TM-102124] N89-27703
Discharge plasma calculations in cusped ion thrusters using the finite element method N89-27760
Introduction to finite element techniques in computational fluid dynamics N89-27988
Thermal strains in a bimaterial joint: Experimental and numerical analysis
[DE89-013935] N89-28032
Stress intensity calibration of a ring specimen using a finite element technique
[AD-A208878] N89-28044
FINITE VOLUME METHOD
Introduction to finite volume techniques in computational fluid dynamics N89-27989
FIORDS
LANDSAT-5 TM study of suspended sediments in a fjord system in western Norway N89-28064
FIRE EXTINGUISHERS
Tests of Halon 1301 test gas simulants
[AD-A207346] N89-27867
FIRE PREVENTION
Tests of Halon 1301 test gas simulants
[AD-A207346] N89-27867
FLEXIBILITY
The influence of the polymer backbone flexibility on the phase transitions of side chain liquid crystal polymers containing
yl side groups
[AD-A208821] N89-27851
Design considerations for an earth based flexible robotic system
[AD-A209635] N89-28018
Development of the Hermes flexible external insulation N89-28296
FLEXIBLE BODIES
Studies in stabilization and control of beams and plates
[AD-A208635] N89-28042
An integrating matrix formulation for buckling of rotating beams including the effects of concentrated masses
[NASA-CR-181862] N89-28342
FLIGHT CHARACTERISTICS
Small scale testing of a mass-stabilized electromagnetic projectile
[AD-A206916] N89-27682
FLIGHT CONTROL
A structured approach to weapon system design N89-27653
FLIGHT CREWS
Evaluation of thermal stress induced by helicopter aircrew Chemical, Biological, Radiological (CBR) protective ensemble
[AD-A210123] N89-28303
FLIGHT INSTRUMENTS
Verification of the production safe flight instrument corporation OV/RV-1D stall warning system
[AD-A207392] N89-27659
FLIGHT RULES
Come to flight rules: Rationale on environmental control and life support systems --- Hermes N89-28242
FLIGHT SAFETY
Verification of the production safe flight instrument corporation OV/RV-1D stall warning system
[AD-A207392] N89-27659
FLIGHT SIMULATION
Effect of three-dimensional object type and density in simulated low-level flight
[AD-A209756] N89-27679
Steady state MPD devices for reentry simulation N89-27783
FLIGHT SIMULATORS
Effect of three-dimensional object type and density in simulated low-level flight
[AD-A209756] N89-27679
FLIGHT TESTS
Flight calibration source development N89-28190
FLOW DEFLECTION
Static internal performance of a nonaxisymmetric vaned thrust reverser with flow splay capability
[NASA-TP-2933] N89-27634
FLOW DISTRIBUTION
Low density flow effects for hypervelocity vehicles
[AD-A206218] N89-27633
Hypersonic prediction comparisons with experimental data for a cone-cylinder at mach 6.86
[AD-A207583] N89-27636
Numerical simulation of control of supersonic shear layers
[AD-A209703] N89-27639
Studies of unsteady vortex flap aerodynamics
[AD-A209837] N89-27641
Design criteria for optimal blading design N89-27663
Overview on blading design methods N89-27664
Blading design for cooled high-pressure turbines N89-27668
Mach 5 inlet CFD and experimental results
[NASA-TM-102317] N89-27670
Quantitative imaging of MPD flow fields N89-27766
Numerical studies of the flow field in a dc arcjet thruster N89-27776
Spatial three-dimensional secondary instability compressible boundary-layer flows
[NASA-CR-4251] N89-27978
Subcooled boiling of downward flow in a vertical annulus
[DE89-005320] N89-27983
The use of stereo optical flow fields in the determination of three-dimensional motion and stereo correspondence
[DE89-012518] N89-27996
FLOW EQUATIONS
Low density flow effects for hypervelocity vehicles
[AD-A206218] N89-27633
Numerical studies of the flow field in a dc arcjet thruster N89-27776
An Introduction to Computational Fluid Dynamics
[VKI-LS-1989-02] N89-27985
Introduction --- computational fluid dynamics N89-27986
Boundary layer equations and methods of solution N89-27987
Introduction to finite volume techniques in computational fluid dynamics N89-27989

FLOW GEOMETRY
Small scale model tests in small wind and water tunnels at high incidence and pitch rates. Volume 2: Small wind tunnel (ADF) data base
[AD-A208539] N89-27676
FLOW MEASUREMENT
Development of a sensor for high-quality two-phase flow N89-28230
FLOW THEORY
Markov processes applied to control, reliability and replacement
[AD-A208634] N89-28362
Reflection and refraction of finite amplitude acoustic waves at a fluid-fluid interface
[AD-A209800] N89-28371
FLOW VELOCITY
An experimental study to determine the relative influence of fluid-fluid interactions and media heterogeneities on the growth of immiscible viscous fingers
[DE89-013122] N89-27976
FLOW VISUALIZATION
Studies of unsteady vortex flap aerodynamics
[AD-A209837] N89-27641
Quantitative imaging of MPD flow fields N89-27766
FLOWMETERS
Development of a sensor for high-quality two-phase flow N89-28230
FLUENCE
A new proton fluence model for E greater than 10 MeV N89-28459
The radial dependence of the solar energetic particle flux N89-28461
FLUID BOUNDARIES
Analysis of a limiting-amplitude problem in acousto-elastic interactions, 1
[AD-A209741] N89-28045
Reflection and refraction of finite amplitude acoustic waves at a fluid-fluid interface
[AD-A209800] N89-28371
FLUID DYNAMICS
Micro-fluid dynamical analysis of evaporating flows in heat pipes N89-28228
FLUID FLOW
KIVA-2: A computer program for chemically reactive flows with sprays
[DE89-012805] N89-27975
An experimental study to determine the relative influence of fluid-fluid interactions and media heterogeneities on the growth of immiscible viscous fingers
[DE89-013122] N89-27976
A central difference type approximation of convection in fluid flow
[DE89-013282] N89-27981
FLUID MANAGEMENT
The liquid management section of the Hermes ECLSS N89-28263
The Fluidnet development and application to preliminary sizing of fluid-loop systems N89-28282
FLUORESCENCE
Novel approaches to ionic chromatography
[DE89-013942] N89-27805
Quantitative estimation of component amplitude in multiexponential data: Application to time-resolved fluorescence spectroscopy
[AD-A210142] N89-27815
Characterization of structure in thin polymer resist films
[AD-A208677] N89-27848
High-temperature optical-fiber pH sensor
[DE89-014103] N89-28000
Airborne in-situ spectral characterization and concentration estimates of fluorescent organics as a function of depth N89-28140
Extraordinary behavior of atoms near a phase conjugator
[AD-A209946] N89-28389
FLUOROCARBONS
Evaluating CFC (Chlorofluorocarbon) alternatives from the atmospheric viewpoint, revision 1
[DE89-014268] N89-28108
FLUX PINNING
Diamagnetic shielding and flux creep in a Tl-Ba-Ca-Cu-O thin film
[DE89-014550] N89-28414
FOCUSING
High-power, high-efficiency FELs
[DE89-013002] N89-28005
Optical spatial tracking using coherent detection in the pupil plane
[AD-A209970] N89-28209
FOKKER-PLANCK EQUATION
Stochastic approach to chaotic inflation and the distribution of universes
[DE89-778051] N89-28473
FOLDING STRUCTURES
Deployable aerospace photovoltaic array based on amorphous silicon alloys N89-27721
FOOD PRODUCTION (IN SPACE)
MELISSA: A micro-organisms-based model for CELSS development N89-28222
FORCE DISTRIBUTION
Summary of longitudinal stability and control parameters as determined from Space Shuttle Challenger flight test data
[NASA-TM-101605] N89-27671
FORECASTING
Terminal area forecasts: FY 1989 - 2005
[AD-A209805] N89-27644
Backgrounder contribution No. 18: Climate scenarios for the first UC/DOE workshop
[DE89-014302] N89-28105
FOREIGN POLICY
Crisis decision-making: The impact of commercial satellites on the media, military and national leaders
[AD-A207334] N89-28449
FOREST FIRES
Multitemporal analysis of TM images: Application to forest fire mapping and inventory in a Mediterranean environment N89-28084
FOREST MANAGEMENT
Forest damage mapping in Austria with the aid of LANDSAT TM image data N89-28078
Discrimination of geobotanical anomalies in coniferous forests from LANDSAT TM data N89-28079
Classification of small-scale forests in Flanders using LANDSAT TM digital data: Preliminary results N89-28080
Forest classification with TM data in the area of Freiburg, Federal Republic of Germany N89-28081
Use of LANDSAT TM data for forest damage inventory N89-28082
Large-scale forest management using LANDSAT Thematic Mapper data N89-28085
Multitemporal analysis of forest areas in surroundings of Innsbruck, Austria N89-28086
FORM FACTORS
Interpretation of F106B and CV580 in-flight lightning data and form factor determination
[NASA-CR-4250] N89-28115
FORMULATIONS
A uniformly differentiable approximation scheme for delay systems using splines
[AD-A208567] N89-28346
FOUNDATIONS
Studies in stabilization and control of beams and plates
[AD-A208635] N89-28042
FOURIER TRANSFORMATION
Computer generated matched filters with spatial frequency tailoring
[AD-A209786] N89-28001
FRACTALS
Scattering from fractals
[DE89-013451] N89-27924
FRACTURE MECHANICS
Solvent assisted delamination crack growth behavior of amorphous thermoplastic materials
[AD-A207365] N89-27833
The texture variation in extruded graphite
[DE89-014086] N89-27837
Dynamic fracture and deformation of solid propellant
[AD-A208691] N89-27865
Probabilistic structural analysis methods of hot engine structures
[NASA-TM-102091] N89-28030
Dynamic fracture toughness testing
[AD-A209948] N89-28046
FRACTURE STRENGTH
Dynamic fracture toughness testing
[AD-A209948] N89-28046
FRACTURING
Dynamic fracture and deformation of solid propellant
[AD-A208691] N89-27865
FRANCE
Color analysis of inland waters using LANDSAT TM data N89-28062
FREE ELECTRON LASERS
High-power, high-efficiency FELs
[DE89-013002] N89-28005
Bibliography of Soviet laser developments: January - February 1988
[AD-A209802] N89-28011
FREE RADICALS
Resist sensitivity enhancement by radiation-induced modification
[AD-A208438] N89-27842
FREQUENCY CONTROL
Multipurpose exciter with low phase noise N89-27887
FREQUENCY CONVERTERS
High dynamic range infrared radiometry and imaging
[NASA-CR-183439] N89-27994
FREQUENCY DIVISION MULTIPLE ACCESS
Proceedings of the Mobile Satellite System Architectures and Multiple Access Techniques Workshop
[NASA-CR-184564] N89-27907
Choice of FDMA/SCPC access technique for aeronautical satellite voice system N89-27909
Performance of DA/FDMA architecture proposed for MSS N89-27910
Why is CDMA the solution for mobile satellite communication N89-27912
System level comparison of FDMA vs. CDMA (under conference guideline constraint) N89-27913
Alternative multiple-access techniques for mobile satellite systems N89-27914
FREQUENCY RANGES
High dynamic range infrared radiometry and imaging
[NASA-CR-183439] N89-27994
FREQUENCY RESPONSE
Accuracy of telemetry signal power loss in a filter as an estimate for telemetry degradation N89-27900
FREQUENCY SHIFT KEYING
Minimum shift keying. A modulation system with coding N89-27931
FREQUENCY STABILITY
DSN radio science system design and testing for Voyager-Neptune encounter N89-27899
Orthogonal sets of data windows constructed from trigonometric polynomials N89-27902
FREQUENCY STANDARDS
New ion trap for atomic frequency standard applications N89-27875
Operating and environmental characteristics of Sigma Tau hydrogen masers used in the Very Long Baseline Array (VLBA) N89-27877
State-of-the-art fiber optics for short distance frequency reference distribution N89-27878
Stabilized fiber-optic frequency distribution system N89-27879
Orthogonal sets of data windows constructed from trigonometric polynomials N89-27902
FREQUENCY SYNTHESIZERS
Multipurpose exciter with low phase noise N89-27887
The DSS-14 C-band exciter N89-27901
FRICTION
Advanced tribological coatings for high specific strength alloys
[AD-A208504] N89-27825
Vapor phase deposition studies of phosphate esters on metal and ceramic surfaces
[PB89-148985] N89-27831
A new method for analysis of limit cycle behavior of the NASA/JPL 70-meter antenna axis servos N89-27880
Fundamental mechanisms of tribology and their implications
[AD-A209941] N89-28020
The Shock and Vibration Digest, volume 21, no. 4 N89-28025
Damping in structural joints N89-28026
FRICTION REDUCTION
Ion-assisted deposition of silver films on ceramics for friction and wear control
[DE89-014635] N89-27821
FRONTS (METEOROLOGY)
Surface Contour Radar (SCR) contributions to FASINEX N89-28159
FUEL CELLS
Separation of oxygen from seawater by membrane permeation
[AD-A208863] N89-27809
FUEL INJECTION
United States Air Force Research Initiation Program for 1987, volume 1
[AD-A209726] N89-28436
FUEL PUMPS
Advanced motor and motor control development
[AD-A207332] N89-27954
FUEL SPRAYS
KIVA-2: A computer program for chemically reactive flows with sprays
[DE89-012805] N89-27975
FUEL SYSTEMS
Development of a lightweight, high strength, collapsible hose
[AD-A207292] N89-28014
FUEL TANKS
Investigation of transport airplane fuselage fuel tank installations under crash conditions
[DOT/FAA/CT-88/24] N89-27643
FUNCTIONAL DESIGN SPECIFICATIONS
Modeling functional specifications for onboard software N89-27658

FURNACES
Equipment models for process optimization and control using smart response surfaces
[AD-A208321] N89-27838
FUSELAGES
Investigation of transport airplane fuselage fuel tank installations under crash conditions
[DOT/FAA/CT-88/24] N89-27643

G

GALACTIC CLUSTERS
Stochastic approach to chaotic inflation and the distribution of universes
[DE89-778051] N89-28473
GALACTIC COSMIC RAYS
Interplanetary Particle Environment. Proceedings of a Conference
[NASA-CR-185461] N89-28454
Toward a descriptive model of galactic cosmic rays in the heliosphere N89-28456
Current models of the intensely ionizing particle environment in space N89-28458
Elemental composition and energy spectra of galactic cosmic rays N89-28466
Gradients of galactic cosmic rays and anomalous components N89-28468
Time variation of galactic cosmic rays N89-28469
Galactic cosmic rays in three dimensions N89-28470
GALLIUM ARSENIDE LASERS
Solid state research
[AD-A209645] N89-28426
GAMMA RAY ASTRONOMY
Thermal control of the GRASP detector section N89-28271
GAMMA RAY BURSTS
Gamma ray bursts: Confrontation between theory and observational data
[DE89-012936] N89-28477
GAMMA RAY SPECTRA
Gamma ray bursts: Confrontation between theory and observational data
[DE89-012936] N89-28477
Monitoring sources of nuclear radiation in space. Part 1: Early 1984 observations, revision
[AD-A209721] N89-28481
Monitoring sources of nuclear radiation in space 1980-1984 observations, revision
[AD-A209722] N89-28482
Monitoring sources of nuclear radiation in space 1985-1987 observations, revision
[AD-A209723] N89-28483
GAMMA RAY SPECTROMETERS
Thermal control of the GRASP detector section N89-28271
GAMMA RAYS
Detection of artificial sources of nuclear radiation in space, revision
[AD-A209720] N89-28480
GAS CHROMATOGRAPHY
Selective detector for gas chromatography based on adduct-modulated semiconductor photoluminescence
[AD-A208616] N89-27808
GAS DETECTORS
Selective detector for gas chromatography based on adduct-modulated semiconductor photoluminescence
[AD-A208616] N89-27808
Tropospheric nitric oxide measurements N89-28171
GAS DYNAMICS
Numerical codes for cylindrical MPD thrusters N89-27733
Coupling between radiation and gas dynamics
[AD-A209657] N89-28102
GAS FLOW
Equipment models for process optimization and control using smart response surfaces
[AD-A208321] N89-27838
A method for calculating asymmetric flow through nozzles
[AD-A209689] N89-27992
Coupling between radiation and gas dynamics
[AD-A209657] N89-28102
Non-condensible gas effects on the low-temperature heat pipe characteristics N89-28227
GAS LASERS
Bibliography of Soviet laser developments: January - February 1988
[AD-A209602] N89-28011
GAS METERS
Possible use of a gas monitoring system in space respirometry studies N89-28223
GAS MIXTURES
Real gas equations of state for CHEMKIN
[DE89-012794] N89-28432
GAS TEMPERATURE
Experience with advanced instrumentation in a hot section cascade
[NASA-TM-102294] N89-27980
GAS TURBINE ENGINES
Blading Design for Axial Turbomachines
[AGARD-LS-167] N89-27661
GAS TURBINES
Ceramic joining in the United States
[DE89-009323] N89-27834
GASES
Possible use of a gas monitoring system in space respirometry studies N89-28223
Real gas equations of state for CHEMKIN
[DE89-012794] N89-28432
GATES (CIRCUITS)
Average interconnection length and interconnection distribution for rectangular arrays
[AD-A209848] N89-27967
GEAR TEETH
Topology of modified helical gears
[NASA-TM-102134] N89-28015
GEARS
Topology of modified helical gears
[NASA-TM-102134] N89-28015
GELATION
Anomalous stresses versus extent of cure in an epoxy composite specimen
[AD-A208523] N89-27798
GENETIC ENGINEERING
Molecular biology of the photoregulation of photosynthetic light-harvesting complexes in marine dinoflagellates
[AD-A209650] N89-28198
GENETICS
The human telomere
[DE89-014252] N89-28199
GEOBOTANY
Discrimination of geobotanical anomalies in coniferous forests from LANDSAT TM data N89-28079
GEODESIC LINES
Two examples of escaping harmonic maps
[DE89-611896] N89-28345
GEODESY
Feasibility of millimeter-accuracy geodetic positioning and vehicle tracking with repeater satellites
[AD-A209958] N89-27692
Differential geodesy of the Eotvos torsion balance
[AD-A208711] N89-28096
A smart, mapping, charting and geodesy control generator, phase 2
[AD-A208806] N89-28097
GEODETIC SATELLITES
Feasibility of millimeter-accuracy geodetic positioning and vehicle tracking with repeater satellites
[AD-A209958] N89-27692
GEOMAGNETISM
A space radiation test model study
[AD-A208760] N89-28479
Detection of artificial sources of nuclear radiation in space, revision
[AD-A209720] N89-28480
GEOMETRIC RECTIFICATION (IMAGERY)
Analog methods and instruments N89-28094
GEOMETRICAL OPTICS
A new analysis of beam-waveguide antennas considering the presence of the enclosure N89-27886
GEOMORPHOLOGY
Detection of short-term changes in tidal flat geomorphology N89-28070
Methodical and structural MSS and TM investigations in the Swabian Alb, SW Germany N89-28071
GEOPHYSICS
Ocean topography experiment (TOPEX) radar altimeter N89-28119
GEOPOTENTIAL
Differential geodesy of the Eotvos torsion balance
[AD-A208711] N89-28096
GEOPOTENTIAL HEIGHT
Radiosonde intercomparison N89-28169
GEOTHERMAL ANOMALIES
Applicability of LANDSAT TM data for geoscientific purposes in Iceland N89-28068
GEOTHERMAL RESOURCES
Applicability of LANDSAT TM data for geoscientific purposes in Iceland N89-28068
GERMANY
Application of LANDSAT data to hydrological mapping N89-28059
Methodical and structural MSS and TM investigations in the Swabian Alb, SW Germany N89-28071
GIOTTO MISSION
Application of expert systems to the thermal configuration of Giotto N89-28250
Giotto: The thermal responses to its encounter with comet Halley N89-28273
Thermal aspects of an extended mission for Giotto N89-28274
GLACIERS
Ice sheet radar altimetry N89-28150
GLASS
Multi-segment Nd:glass disk amplifiers
[DE89-014043] N89-28006
GLASS FIBERS
Requirements for a technical data base N89-27930
Scintillating fiber detector development for the SSC
[DE89-013118] N89-27997
GLASS LASERS
Efficient second harmonic conversion of broadband high-peak-power Nd:glass laser radiation using large-aperture KDP crystals in quadrature
[DE89-012961] N89-28003
GLASS TRANSITION TEMPERATURE
Anomalous stresses versus extent of cure in an epoxy composite specimen
[AD-A208523] N89-27798
GLOBAL POSITIONING SYSTEM
GPS (Global Positioning System) orbit determination: Bootstrapping to resolve carrier phase ambiguity
[AD-A209974] N89-27681
The Telecommunications and Data Acquisition Report
[NASA-CR-185431] N89-27871
Estimation and filtering techniques for high-accuracy GPS applications N89-27872
High-precision radiometric tracking for planetary approach and encounter in the inner solar system N89-27873
Airborne lidar global positioning investigations N89-28179
GOLD
Formation of monolayers by the coadsorption of thiols on gold: Variation in the length of the alkyl chain
[AD-A208386] N89-27824
Modelling organic surfaces with self-assembled monolayers
[AD-A208385] N89-27840
Evidence against the existence of strong diffuse X-ray scattering from gold twist boundaries at room temperature
[DE89-012726] N89-28407
GOVERNMENT PROCUREMENT
The private sector economic and employment benefits to the nation and to each state of proposed FY 1990 NASA procurement expenditures
[NASA-CR-185894] N89-28448
GRADIENTS
Gradients of galactic cosmic rays and anomalous components N89-28468
GRAIN BOUNDARIES
The structure and properties of grain boundaries in B2 ordered alloys
[DE89-013266] N89-27817
Evidence against the existence of strong diffuse X-ray scattering from gold twist boundaries at room temperature
[DE89-012726] N89-28407
Experimental studies of the structure of grain boundaries
[DE89-012954] N89-28408
Grain boundaries in silicon from zero temperature through melting
[DE89-013186] N89-28410
The topological structure of grain boundaries
[DE89-014676] N89-28415
GRANULAR MATERIALS
Plastic deformation of granular materials
[AD-A208589] N89-28040
GRAPH THEORY
Claw-free maximal planar graphs
[AD-A210179] N89-28359
GRAPHITE
Coating and impregnation of carbon-carbon composites with ceramics by electrophoretic deposition
[AD-A208873] N89-27800
The texture variation in extruded graphite
[DE89-014086] N89-27837
GRAVITATIONAL EFFECTS
Design considerations for an earth based flexible robotic system
[AD-A209635] N89-28018
GRAZING
Mapping winter grazing areas for reindeer on Svalbard using LANDSAT Thematic Mapper data N89-28075
GREECE
Karst drainage in the Peloponnesus area: A case study for application of TM data in hydrogeology N89-28069
GREENLAND
Lithologic mapping of mafic intrusions in East Greenland using Landsat Thematic Mapper data
[NASA-CR-183440] N89-28047

GRID GENERATION (MATHEMATICS)
Computational methods and systems for problems in science and engineering
[AD-A209951] N89-28355
GRIGG-SKJELLERUP COMET
Thermal aspects of an extended mission for Giotto N89-28274
GROUND EFFECT (AERODYNAMICS)
Baseline performance verification of the 12th year production UH-60A Black Hawk helicopter
[AD-A208671] N89-27632
GROUND STATIONS
High-precision radiometric tracking for planetary approach and encounter in the inner solar system N89-27873
A new analysis of beam-waveguide antennas considering the presence of the enclosure N89-27886
DSN radio science system design and testing for Voyager-Neptune encounter N89-27899
The DSS-14 C-band exciter N89-27901
GROUND TESTS
Verification of performance and endurance of capacitor bank for the electric propulsion experiment (EPEX) N89-27739
GROUND WIND
User's guide for the Air Force surface-layer windflow model (AFWIND)
[AD-A208710] N89-28109
GROUP THEORY
Some problems in nonlinear analysis
[AD-A209991] N89-28357
GYROSCOPES
Studies of phase-conjugate optical device concepts
[AD-A206219] N89-28391

H

HALL ACCELERATORS
Experimental study of double stage discharge Hall ion thruster N89-27763
HALL EFFECT
Binary sequences of arbitrary length with near-ideal correlation
[AD-A209956] N89-28356
HALOCARBONS
Analytical procedures for environmental quality control, volume 2
[PB89-158612] N89-28103
Analytical procedures for environmental quality control, volume 3
[PB89-158620] N89-28104
HAMILTONIAN FUNCTIONS
Claw-free maximal planar graphs
[AD-A210179] N89-28359
HARDENING (MATERIALS)
Theoretical model for stabilization of clay-silt airport pavement subgrade systems. Phase 1: Laboratory investigation. Phase 2: Rutting tests
[DOT/FAA/PM-87/20-PHASE-1/2] N89-27673
HARMONIC ANALYSIS
Two examples of escaping harmonic maps
[DE89-611896] N89-28345
HARMONIC RADIATION
Efficient second harmonic conversion of broadband high-peak-power Nd:glass laser radiation using large-aperture KDP crystals in quadrature
[DE89-012961] N89-28003
HARMONICS
Efficient second harmonic conversion of broadband high-peak-power Nd:glass laser radiation using large-aperture KDP crystals in quadrature
[DE89-012961] N89-28003
Analysis of a limiting-amplitude problem in acousto-elastic interactions, 1
[AD-A209741] N89-28045
HEAD-UP DISPLAYS
Evaluation of head-up display formats for the F/A-18 hornet
[AD-A208651] N89-27660
HEART
The effect of various straining maneuvers on cardiac volumes at 1G and during +Gz acceleration
[AD-A208846] N89-28200
HEART RATE
The effect of various straining maneuvers on cardiac volumes at 1G and during +Gz acceleration
[AD-A208846] N89-28200
HEAT AFFECTED ZONE
Space Shuttle Main Engine structural analysis and data reduction/evaluation. Volume 1: Aft Skirt analysis
[NASA-CR-183663] N89-27693
HEAT EXCHANGERS
Condensing heat exchangers for European spacecraft ECLSS N89-28240
Development of heat exchangers for hybrid radiators N89-28285
Development of a novel high-performance contact heat exchanger N89-28286
Intermediate heat exchanger for a nuclear-powered space power system N89-28287
Theoretical and experimental investigations on heat exchangers for Columbus hybrid radiators N89-28295
HEAT FLUX
Experience with advanced instrumentation in a hot section cascade
[NASA-TM-102294] N89-27980
Express-method investigation and its application for heat pipe quality control N89-28229
HEAT PIPES
Non-condensible gas effects on the low-temperature heat pipe characteristics N89-28227
Micro-fluid dynamical analysis of evaporating flows in heat pipes N89-28228
Express-method investigation and its application for heat pipe quality control N89-28229
Development of a novel high-performance contact heat exchanger N89-28286
Qualification program on stainless steel A95 heatpipe for space application N89-28294
HEAT PUMPS
Two-phase heat transport systems: Critical components — Columbus N89-28224
Feasibility demonstration model of a capillary pumping loop N89-28225
HEAT RESISTANT ALLOYS
Thermal design improvements for 30kWe arcjet engine N89-27754
Computational simulation of high temperature metal matrix composites cyclic behavior
[NASA-TM-102115] N89-27795
Analysis and elimination of high temperature notch induced microcrack initiation in Inconel 718 nickel-based alloy
[AD-A209695] N89-27828
HEAT SHIELDING
Steady state MPD devices for reentry simulation N89-27783
The Hermes spaceplane program: Status report on the thermal control, environment control and life support activities N89-28217
The space-rigidised thermal shield for the ESA Far-Infrared Space Telescope (FIRST) N89-28236
Thermal analysis of advanced heat protection systems — hypersonic vehicles N89-28291
HEAT SINKS
Cyrogenic fluid sink device for thermal control of a spaceplane during ascent and re-entry phases N89-28293
HEAT TOLERANCE
Evaluation of thermal stress induced by helicopter aircrew Chemical, Biological, Radiological (CBR) protective ensemble
[AD-A210123] N89-28303
HEAT TRANSFER
Radiators and heat exchangers for space applications
[REPT-882-440-115] N89-27688
Radiator conceptual studies for the Hermes spaceplane N89-27689
Development of heat exchangers for hybrid radiators N89-27690
Effects of an embedded vortex on a single film-cooling jet in a turbulent boundary layer
[AD-A207374] N89-27974
Flow boiling with enhancement devices for cold plate coolant channel design
[NASA-CR-185840] N89-27979
Experience with advanced instrumentation in a hot section cascade
[NASA-TM-102294] N89-27980
A central difference type approximation of convection in fluid flow
[DE89-013282] N89-27981
Interfacial area measurement methods
[DE89-013426] N89-27982
Subcooled boiling of downward flow in a vertical annulus
[DE89-005320] N89-27983
Analysis of pressure drop and heat transfer data from the reversing flow test facility
[DE89-013907] N89-27984
ESATAN FHTS: A piped fluid network capability N89-28281
Experimental study on the deposition profile of the ICRF power and electron thermal diffusivity
[IPPJ-908] N89-28401
United States Air Force Research Initiation Program for 1987, volume 3
[AD-A209728] N89-28437
HEAT TREATMENT
Laser processing of metals and alloys
[DE89-613235] N89-27822
HELICOPTER PERFORMANCE
Baseline performance verification of the 12th year production UH-60A Black Hawk helicopter
[AD-A208671] N89-27632
HELICOPTERS
Evaluation of thermal stress induced by helicopter aircrew Chemical, Biological, Radiological (CBR) protective ensemble
[AD-A210123] N89-28303
HELIOSPHERE
Interplanetary Particle Environment. Proceedings of a Conference
[NASA-CR-185461] N89-28454
Toward a descriptive model of solar particles in the heliosphere N89-28455
Toward a descriptive model of galactic cosmic rays in the heliosphere N89-28456
Current models of the intensely ionizing particle environment in space N89-28458
Intensity/time profiles of solar particle events at one astronomical unit N89-28460
The radial dependence of the solar energetic particle flux N89-28461
Particles accelerated by shocks in the heliosphere N89-28464
HELIUM PLASMA
Characteristics of free-floating nitrogen and helium plasmas generated in a microwave resonant cavity N89-27771
Numerical and experimental investigations of a propagating microwave-heated plasma N89-27772
Coupling between radiation and gas dynamics
[AD-A209657] N89-28102
HEMISPHERICAL SHELLS
Integrating sphere and hemisphere calibration update N89-28194
HERMES MANNED SPACEPLANE
Radiators and heat exchangers for space applications
[REPT-882-440-115] N89-27688
Radiator conceptual studies for the Hermes spaceplane N89-27689
The Hermes spaceplane program: Status report on the thermal control, environment control and life support activities N89-28217
The definition status of the environmental control and life support subsystems for Hermes N89-28220
Design concepts for Hermes thermal control N89-28234
Radiator conceptual studies for the Hermes spaceplane N89-28235
The atmosphere pressure control section of the Hermes ECLSS N89-28241
Come to flight rules: Rationale on environmental control and life support systems — Hermes N89-28242
The European space suit system N89-28243
Life support for EVA: The European system baseline N89-28244
The liquid management section of the Hermes ECLSS N89-28263
Hermes: Drink/food-water supply assembly N89-28264
Nutrition for short-duration space missions N89-28265
Development of the Hermes flexible external insulation N89-28296
HETEROJUNCTIONS
Phonon-drag thermoelectric power in high magnetic fields in heterojunctions
[DE89-013921] N89-28412
Transport and submillimeter wave spectroscopy of GaAs/Al sub xGa sub 1-xAs heterostructures
[AD-A209836] N89-28428
HEURISTIC METHODS
Quadratic estimators of the power spectrum
[AD-A208601] N89-27964
Automatic construction of polyhedral surfaces from voxel representations
[AD-A210009] N89-28325
The combinatorics of heuristic search termination for object recognition in cluttered environments
[AD-A209690] N89-28363
HEXYL COMPOUNDS
The influence of the polymer backbone flexibility on the phase transitions of side chain liquid crystal polymers containing
yl side groups
[AD-A208821] N89-27851
HIERARCHIES
Conversion of mass storage hierarchy in an IBM computer network
[AD-A208520] N89-28330

HIGH ALTITUDE
Effects of high terrestrial altitude on military performance
[AD-A209614] N89-28201
HIGH RESOLUTION
Math and physics studies-multi-project support entropy-based image restoration: Modifications and additional results
[AD-A209972] N89-27951
Novel methodology for application of adaptive systems techniques to DMSP (Defense Meteorological Satellite Program) remote temperature sensing
[AD-A209975] N89-28098
HIGH STRENGTH
Development of a lightweight, high strength, collapsible hose
[AD-A207292] N89-28014
HIGH STRENGTH ALLOYS
Advanced tribological coatings for high specific strength alloys
[AD-A208504] N89-27825
HIGH TEMPERATURE
High temp toughening and creep studies
[AD-A208714] N89-27826
Evaluation of thermal stress induced by helicopter aircrew Chemical, Biological, Radiological (CBR) protective ensemble
[AD-A210123] N89-28303
HIGH TEMPERATURE ENVIRONMENTS
Effect of alloying, rapid solidification, and surface kinetics on the high temperature environmental resistance of niobium
[AD-A209934] N89-27829
Laser cladding of Ni, Nb, Mg alloys for improved environmental resistance at high temperatures
[AD-A210134] N89-27830
Vapor phase deposition studies of phosphate esters on metal and ceramic surfaces
[PB89-148985] N89-27831
Experience with advanced instrumentation in a hot section cascade
[NASA-TM-102294] N89-27980
Evaluation of a strain-gage load calibration on a low-aspect-ratio wing structure at elevated temperature
[NASA-TP-2921] N89-28034
HIGH TEMPERATURE PLASMAS
A two-stream plasma electron microwave source for high-power millimeter wave generation, phase 1
[AD-A209942] N89-28404
HIGH TEMPERATURE SUPERCONDUCTORS
Composite ceramic superconducting wires for electric motor applications
[AD-A208598] N89-27847
High-temperature superconductivity: Abstracts of NIST (National Institute of Standards and Technology) publications, 1987-1988
[PB89-148340] N89-28405
Bibliography of high-T sub c superconducting films
[DE89-013395] N89-28409
Diamagnetic shielding and flux creep in a Tl-Ba-Ca-Cu-O thin film
[DE89-014550] N89-28414
Glassy behaviour of YBa2Cu3O7
[DE89-613399] N89-28418
HIGH THRUST
High thrust operation of the UK-10 rare gas ion thruster (T4A) N89-27747
HIGH VOLTAGES
High voltage power condition systems powered by flux compression generators
[DE89-014259] N89-27959
HISTOGRAMS
Mode filters and their applications
[INPE-4748-PRE/1421] N89-28312
HISTORIES
Reports on cartography and geodesy. Special issue: History of photogrammetry, number 1
[ISSN-0344-5879] N89-28092
The early period of photogrammetry till the invention of the aircraft N89-28093
HOLLOW CATHODES
Ring cusp/hollow cathode discharge chamber performance studies --- ion propulsion N89-27748
A review of the cathode construction for the RAE 10/25mN thruster N89-27759
HOLOGRAPHY
Computer generated matched filters with spatial frequency tailoring
[AD-A209786] N89-28001
Generalized beamforming with multiple computer originated holograms
[AD-A210175] N89-28397
HOMOGENEITY
A statistical derivation of the average degree of polymerization in a stirred tank reactor
[AD-A209873] N89-27857
HOMOGENEOUS TURBULENCE
A critical comparison of turbulence models for homogeneous shear flows in a rotating frame
[NASA-CR-181864] N89-27977
HONEYCOMB STRUCTURES
Electromagnetic scattering from a structured slab comprised of periodically placed resistive cards
[AD-A210145] N89-27953
HORIZON
Aerosol model selection using surface measurements of IR horizon radiances and satellite detected visible radiances
[AD-A209638] N89-28110
HORSESHOE VORTICES
Three-dimensional vortex interactions in turbulent boundary layers
[AD-A208624] N89-27991
HOSES
Development of a lightweight, high strength, collapsible hose
[AD-A207292] N89-28014
HOT SURFACES
Effect of alloying, rapid solidification, and surface kinetics on the high temperature environmental resistance of niobium
[AD-A209934] N89-27829
HOUSINGS
Space Shuttle Main Engine structural analysis and data reduction/evaluation. Volume 3A: High pressure oxidizer turbo-pump preburner pump housing stress analysis report
[NASA-CR-183665] N89-27694
Space Shuttle Main Engine structural analysis and data reduction/evaluation. Volume 4: High pressure fuel turbo-pump inlet housing analysis
[NASA-CR-183667] N89-27696
HUMAN BEINGS
Modulation of spontaneous brain activity during mental imagery
[AD-A209918] N89-28208
Perception of motion in statistically-defined displays
[AD-A208695] N89-28301
HUMAN FACTORS ENGINEERING
Anthropometric measurements of aviators within the Aviation Epidemiology Data Register
[AD-A208609] N89-28300
Human cognition and information display in C3I system tasks
[AD-A210012] N89-28302
HUMAN PERFORMANCE
Effects of high terrestrial altitude on military performance
[AD-A209614] N89-28201
Age-related changes in human vestibulo-ocular and optokinetic reflexes: Pseudorandom rotation tests
[NASA-CR-185856] N89-28213
Human cognition and information display in C3I system tasks
[AD-A210012] N89-28302
HUMAN REACTIONS
Age-related changes in human vestibulo-ocular reflexes: Sinusoidal rotation and caloric tests
[NASA-CR-185857] N89-28211
HUMAN TOLERANCES
Age-related changes in human vestibulo-ocular reflexes: Sinusoidal rotation and caloric tests
[NASA-CR-185857] N89-28211
HUMAN WASTES
MELISSA: A micro-organisms-based model for CELSS development N89-28222
HUMIDITY MEASUREMENT
Meteorological Sensor Calibration Facility N89-28188
HYBRID CIRCUITS
Hybrid wafer-scale processor
[AD-A209944] N89-27969
HYBRID PROPULSION
The ROSETTA/CNSR mission: A possible application of electric propulsion to interplanetary missions N89-27715
HYDRAULIC EQUIPMENT
A new method for analysis of limit cycle behavior of the NASA/JPL 70-meter antenna axis servos N89-27880
HYDRAULIC TEST TUNNELS
Small scale model tests in small wind and water tunnels at high incidence and pitch rates. Volume 3: Water tunnel (HFF) data base
[AD-A208690] N89-27638
Small scale model tests in small wind and water tunnels at high incidence and pitch rates. Volume 2: Small wind tunnel (ADF) data base
[AD-A208539] N89-27676
HYDRAZINE ENGINES
Operating characteristics of 1 kW hydrazine arcjet thruster N89-27779
HYDRODYNAMICS
ZPIMP: A zero-D Z-pinch implosion code
[AD-A208381] N89-27962
HYDROGEN
Transition metal activation and functionalization of carbon-hydrogen bonds
[DE89-012949] N89-27804
Observation of vibrationally resolved charge transfer in H(+) + H2 at a collision energy Ecm = 20 eV N89-28382
A comparison between theoretical and experimental state-to-state charge transfer cross sections for H(+) + H2 at 20 eV: Evidence for quantum effects N89-28383
A three-dimensional quantum mechanical study of vibrational inelastic and charge transfer processes in H(+) + H2 at a collision energy Ecm = 20 eV N89-28384
HYDROGEN FUELS
Antiproton powered propulsion with magnetically confined plasma engines
[NASA-CR-185131] N89-27700
Operating characteristics of 1 kW hydrazine arcjet thruster N89-27779
HYDROGEN MASERS
Operational parameters for the superconducting cavity maser N89-27876
Operating and environmental characteristics of Sigma Tau hydrogen masers used in the Very Long Baseline Array (VLBA) N89-27877
HYDROGEN PLASMA
Antiproton powered propulsion with magnetically confined plasma engines
[NASA-CR-185131] N89-27700
Numerical and experimental investigations of a propagating microwave-heated plasma N89-27772
Performance calculation of an H2 arcjet by means of a dual channel model N89-27775
Coupling between radiation and gas dynamics
[AD-A209657] N89-28102
HYDROGEOLOGY
Karst drainage in the Peloponnesus area: A case study for application of TM data in hydrogeology N89-28069
HYDROGRAPHY
Applications of the Coastal Zone Color Scanner in oceanography N89-28136
HYDROLOGY
European Coordinated Effort for Monitoring the Earth's Environment. A Pilot Project Campaign on LANDSAT Thematic Mapper Applications (1985-1987)
[ESA-SP-1102] N89-28055
Color analysis of inland waters using LANDSAT TM data N89-28062
HYDROLOGY MODELS
Application of LANDSAT data to hydrological mapping N89-28059
HYDROTHERMAL SYSTEMS
Image processing strategies for mineral exploration in arid areas by use of TM data N89-28067
Applicability of LANDSAT TM data for geoscientific purposes in Iceland N89-28068
HYPERCUBE MULTIPROCESSORS
ParaGraph-RTS: A parallel reduction-based run-time system
[DE89-005457] N89-28315
Parallel Architectures for Planetary Exploration Requirements (PAPER)
[NASA-CR-185370] N89-28475
HYPERSONIC FLOW
Hypersonic prediction comparisons with experimental data for a cone-cylinder at mach 6.86
[AD-A207583] N89-27636
HYPERSONIC VEHICLES
Low density flow effects for hypervelocity vehicles
[AD-A206218] N89-27633
Thermal analysis of advanced heat protection systems --- hypersonic vehicles N89-28291
HYPERTHERMIA
Evaluation of thermal stress induced by helicopter aircrew Chemical, Biological, Radiological (CBR) protective ensemble
[AD-A210123] N89-28303
HYPERVELOCITY GUNS
Small scale testing of a mass-stabilized electromagnetic projectile
[AD-A206916] N89-27682
HYPSOGRAPHY
Mars Observer Radar Altimeter Radiometer (MORAR) N89-28120
HYSTERESIS
A new method for analysis of limit cycle behavior of the NASA/JPL 70-meter antenna axis servos N89-27880
A data acquisition and control program for axial-torsional fatigue testing
[NASA-TM-102041] N89-28029

I

IBM COMPUTERS
Conversion of mass storage hierarchy in an IBM computer network
[AD-A208520] N89-28330
ICE FORMATION
Microwave remote sensing of sea ice N89-28148
ICE MAPPING
Ice sheet radar altimetry N89-28150
Ice sheet studies using synthetic aperture radar N89-28152
IMAGE ANALYSIS
High dynamic range infrared radiometry and imaging
[NASA-CR-183439] N89-27994
The use of edge detectors based on mathematical morphology in remote sensing imagery
[INPE-4777-PRE/1446] N89-28050
Evaluation of new thermomechanical constitutive theory for snow N89-28052
Satellite image analysis for marine applications
[PB89-187330] N89-28053
Multitemporal analysis of TM images: Application to forest fire mapping and inventory in a Mediterranean environment N89-28084
Coastal Zone Color Scanner studies N89-28138
Sea ice/climate studies N89-28151
Low cost real time interactive analysis system N89-28177
IMAGE ENHANCEMENT
Tests of topographic mapping with Thematic Mapper images N89-28091
IMAGE PROCESSING
Effect of three-dimensional object type and density in simulated low-level flight
[AD-A209756] N89-27679
Target signature modeling and bistatic scattering measurement studies
[NASA-CR-185434] N89-27870
The use of stereo optical flow fields in the determination of three-dimensional motion and stereo correspondence
[DE89-012518] N89-27996
Computer generated matched filters with spatial frequency tailoring
[AD-A209786] N89-28001
Automatic change in contour diagrams on the occasion of scale reduction using a material morphology
[INPE-4769-PRE/1438] N89-28049
The use of edge detectors based on mathematical morphology in remote sensing imagery
[INPE-4777-PRE/1446] N89-28050
European Coordinated Effort for Monitoring the Earth's Environment. A Pilot Project Campaign on LANDSAT Thematic Mapper Applications (1985-1987)
[ESA-SP-1102] N89-28055
Improved snow and glacier monitoring by the LANDSAT Thematic Mapper N89-28056
Multitemporal snow classification with TM data N89-28057
Utility of Thematic Mapper data for national survey of Irish lakes N89-28058
Application of LANDSAT data to hydrological mapping N89-28059
Application of remote sensing to irrigation water management in two Italian irrigation districts N89-28060
Remote sensing of limnological parameters in reservoirs N89-28061
Color analysis of inland waters using LANDSAT TM data N89-28062
Use of satellite imagery for the investigation of pollution-related characteristics of Dublin Bay, Ireland N89-28063
LANDSAT-5 TM study of suspended sediments in a fjord system in western Norway N89-28064
The use of Thematic Mapper imagery for peatland mapping and mineral exploration in Ireland N89-28065
LANDSAT TM study of sabkha surfaces in the Qattara Depression, northwestern Egypt N89-28066
Image processing strategies for mineral exploration in arid areas by use of TM data N89-28067
Applicability of LANDSAT TM data for geoscientific purposes in Iceland N89-28068
Karst drainage in the Peloponnesus area: A case study for application of TM data in hydrogeology N89-28069
Detection of short-term changes in tidal flat geomorphology N89-28070
Methodical and structural MSS and TM investigations in the Swabian Alb, SW Germany N89-28071
LANDSAT TM data used in the mapping of large-scale geological structures in coastal areas in Trondelag, central Norway N89-28072
Evaluation of the LANDSAT TM satellite in urban media: Application to the case of Brussels, Belgium N89-28073
Agricultural land-use classification in the Upper Rhine Valley using multitemporal TM data N89-28074
Mapping winter grazing areas for reindeer on Svalbard using LANDSAT Thematic Mapper data N89-28075
Remote sensing of the Madrid area ecosystems N89-28076
Forest damage mapping in Austria with the aid of LANDSAT TM image data N89-28078
Discrimination of geobotanical anomalies in coniferous forests from LANDSAT TM data N89-28079
Classification of small-scale forests in Flanders using LANDSAT TM digital data: Preliminary results N89-28080
Forest classification with TM data in the area of Freiburg, Federal Republic of Germany N89-28081
Use of LANDSAT TM data for forest damage inventory N89-28082
Multitemporal analysis of TM images: Application to forest fire mapping and inventory in a Mediterranean environment N89-28084
Large-scale forest management using LANDSAT Thematic Mapper data N89-28085
Multitemporal analysis of forest areas in surroundings of Innsbruck, Austria N89-28086
Comparison of MSS and TM LANDSAT data for cartography of surface structures in arid regions (southern Tunisia) N89-28087
Processing and interpretation of Thematic Mapper images in the Province of Piacenza (Italy) N89-28088
Production of satellite image maps from TM data N89-28089
Integrating TM and cartographic data N89-28090
Tests of topographic mapping with Thematic Mapper images N89-28091
Performance augmentation of SITIM-150 through a high performance numerical processor
[INPE-4770-PRE/1439] N89-28305
Preliminary statistical identification of radar imagery: Autoregressive-moving average (ARMA) models
[INPE-4771-PRE/1440] N89-28311
Northeast Artificial Intelligence Consortium annual report for 1987. Volume 4: Research in automated photointerpretation
[AD-A208610] N89-28336
Image Algebra FORTRAN preprocessor: User's manual
[AD-A208612] N89-28349
Engineering research and development: Thrust area report FY 88
[DE89-014320] N89-28453
IMAGE RECONSTRUCTION
Math and physics studies-multi-project support entropy-based image restoration: Modifications and addditional results
[AD-A209972] N89-27951
IMAGE RESOLUTION
The effects of snow on landmarks in K(sub u) band SAR images
[DE89-014578] N89-27925
IMAGERY
Attention, imagery and memory: A neuromagnetic investigation
[AD-A209917] N89-28207
Modulation of spontaneous brain activity during mental imagery
[AD-A209918] N89-28208
IMAGES
Pre-attentive and attentive visual information processing
[AD-A209884] N89-28206
Attention, imagery and memory: A neuromagnetic investigation
[AD-A209917] N89-28207
Generalized beamforming with multiple computer originated holograms
[AD-A210175] N89-28397
IMAGING SPECTROMETERS
NASA Charge Coupled Device (CCD) Spectrometer System (NCSS) N89-28142
The Multichannel Ocean Color Sensor (MOCS) N89-28146
IMAGING TECHNIQUES
The use of stereo optical flow fields in the determination of three-dimensional motion and stereo correspondence
[DE89-012518] N89-27996
Multitemporal snow classification with TM data N89-28057
A survey of visual preprocessing and shape representation techniques
[NASA-CR-185418] N89-28309
An efficient exact algorithm for the least squares image registration problem
[AD-A208725] N89-28320
Sensitivity analysis of reflection errors in infrared image simulation
[AD-A208600] N89-28394
IMPACT DAMAGE
The inadequacies of damage energy as a measure of displacement damage
[AD-A207376] N89-28028
IMPACT RESISTANCE
United States Air Force Research Initiation Program for 1987, volume 4
[AD-A209729] N89-28438
IMPLOSIONS
ZPIMP: A zero-D Z-pinch implosion code
[AD-A208381] N89-27962
IN-FLIGHT MONITORING
Interpretation of F106B and CV580 in-flight lightning data and form factor determination
[NASA-CR-4250] N89-28115
INCOMPRESSIBLE FLOW
Computational methods and systems for problems in science and engineering
[AD-A209951] N89-28355
INCONEL (TRADEMARK)
Analysis and elimination of high temperature notch induced microcrack initiation in Inconel 718 nickel-based alloy
[AD-A209695] N89-27828
INDIUM PHOSPHIDES
Indium phosphide solar cell research in the US: Comparison with nonphotovoltaic sources
[NASA-TM-102103] N89-27868
Transport and submillimeter wave spectroscopy of GaAs/Al sub xGa sub 1-xAs heterostructures
[AD-A209836] N89-28428
Zinc telluride growth on InP
[AD-A209924] N89-28430
INDUCTANCE
A one microsecond, thirty-five kilojoule, one hertz pulse generator
[DE89-013074] N89-27955
INDUCTION (MATHEMATICS)
Some basic theorems on the cross-sums of certain class of numbers (M-1) when the operations are done with different bases M of the arithmetic
[DE89-611892] N89-28343
INELASTIC COLLISIONS
Charge transfer and inelastic scattering in proton-molecule collisions
[MPIS-13/1988] N89-28378
Charge transfer and inelastic scattering in proton-molecule collisions, introduction N89-28379
Observation of vibrationally resolved charge transfer in H(+) + H2 at a collision energy Ecm = 20 eV N89-28382
A three-dimensional quantum mechanical study of vibrational inelastic and charge transfer processes in H(+) + H2 at a collision energy Ecm = 20 eV N89-28384
INELASTIC SCATTERING
Quantum corrections for inelastic atom-surface scattering
[AD-A209850] N89-28387
INERTIAL CONFINEMENT FUSION
Multi-segment Nd:glass disk amplifiers
[DE89-014043] N89-28006
KrF lasers for inertial confinement fusion
[DE89-014272] N89-28007
INERTIAL NAVIGATION
Studies of phase-conjugate optical device concepts
[AD-A206219] N89-28391
INFERENCE
Quantitative inference in a mechanical design compiler
[AD-A209900] N89-28324
INFORMATION
Estimation and filtering techniques for high-accuracy GPS applications N89-27872
INFORMATION DISSEMINATION
Data bases available at the National Institute of Standards and Technology Research Information Center
[PB89-160014] N89-28441
Theft of information in the take-grant protection model
[NASA-CR-185835] N89-28444
INFORMATION PROCESSING (BIOLOGY)
Pre-attentive and attentive visual information processing
[AD-A209884] N89-28206
Visualizing and rhyming cause differences in alpha suppression
[AD-A210005] N89-28210
Human cognition and information display in C3I system tasks
[AD-A210012] N89-28302
A survey of visual preprocessing and shape representation techniques
[NASA-CR-185418] N89-28309
INFORMATION RETRIEVAL
Problems and solutions in online documentation systems
[DE89-014092] N89-28447

INFORMATION SYSTEMS
The evolution of digital avionics architectures/systems N89-27655
Anthropometric measurements of aviators within the Aviation Epidemiology Data Register
[AD-A208609] N89-28300
Data base development and research and editorial support
[NASA-CR-183249] N89-28440
Engineering drawing transfer test with Douglas Aircraft Company: MIL-D-28000 Class II (IGES)
[DE89-012810] N89-28443
INFORMATION THEORY
Capacity of discrete time Gaussian channel with and without feedback, 2
[AD-A207388] N89-27922
Information aspects of type 9 cosmological models
[DE89-012518] N89-28472
INFORMATION TRANSFER
Engineering drawing transfer test with Douglas Aircraft Company: MIL-D-28000 Class II (IGES)
[DE89-012810] N89-28443
Theft of information in the take-grant protection model
[NASA-CR-185835] N89-28444
INFRARED DETECTORS
Math and physics studies-multi-project support entropy-based image restoration: Modifications and addditional results
[AD-A209972] N89-27951
High dynamic range infrared radiometry and imaging
[NASA-CR-183439] N89-27994
INFRARED IMAGERY
Math and physics studies-multi-project support entropy-based image restoration: Modifications and addditional results
[AD-A209972] N89-27951
High dynamic range infrared radiometry and imaging
[NASA-CR-183439] N89-27994
Sensitivity analysis of reflection errors in infrared image simulation
[AD-A208600] N89-28394
INFRARED INSTRUMENTS
Long-life Stirling cycle coolers for applications in the 60 to 110 K range N89-28267
INFRARED RADIATION
GMBU (Ground Mobile Breadboard Upgrade) lidar and bubbler correlation study at Dugway Proving Ground
[AD-A207297] N89-28002
Aerosol model selection using surface measurements of IR horizon radiances and satellite detected visible radiances
[AD-A209638] N89-28110
Ocean Data Acquisition System N89-28144
INFRARED RADIOMETERS
High dynamic range infrared radiometry and imaging
[NASA-CR-183439] N89-27994
INFRARED SIGNATURES
Math and physics studies-multi-project support entropy-based image restoration: Modifications and addditional results
[AD-A209972] N89-27951
INFRARED SPACE OBSERVATORY (ISO)
Thermal and cryogenic aspects of the ISO optical subsystem N89-28269
Shaking in cryogenic conditions N89-28277
Assembling the ISO thermal model with ESATAN N89-28280
INFRARED SPECTRA
Vibrational predissociation of shock-selected C2H4 and NH3 clusters
[MPIS-6/1988] N89-28373
Vibrational predissociation of shock-selected C2H4 and NH3 clusters, introduction N89-28374
Infrared photodissociation and cluster-specific detection of internally cold (C2H4) van der Waals complexes N89-28375
Infrared photodissociation of van der Waals complexes selectively prepared by molecular beam scattering N89-28376
INFRARED TELESCOPES
The space-rigidised thermal shield for the ESA Far-Infrared Space Telescope (FIRST) N89-28236
Thermal design of a superfluid helium dewar for infrared telescope on-board space flyer unit N89-28270
INFRARED WINDOWS
Crystal chemistry, synthesis, and characterization of infrared optical materials
[AD-A208723] N89-28422
INHIBITORS
Acetylcholinesterase inhibitor, pyridostigmine bromide, reduces skin blood flow in humans
[AD-A209615] N89-28202
INITIATION
Shock initiation modeling of multicomponent explosives
[DE89-012259] N89-27863
INJECTION
Effects of an embedded vortex on a single film-cooling jet in a turbulent boundary layer
[AD-A207374] N89-27974
INJECTORS
Space Shuttle Main Engine structural analysis and data reduction/evaluation. Volume 5: Main Injector LOX Inlet analysis
[NASA-CR-183668] N89-27697
INLET FLOW
Computational investigation on the characteristics of a low power dc arcjet thruster N89-27777
INORGANIC COMPOUNDS
Crystal chemistry, synthesis, and characterization of infrared optical materials
[AD-A208723] N89-28422
INSTALLING
Investigation of transport airplane fuselage fuel tank installations under crash conditions
[DOT/FAA/CT-88/24] N89-27643
INSTRUMENT ERRORS
Radiosonde intercomparison N89-28169
Satellite/radiosonde comparison N89-28170
NASA Aircraft-Satellite Instrument Calibration Project N89-28189
Flight calibration source development N89-28190
Radiance standards N89-28191
Calibration source maintenance, characterization and development N89-28193
INSULATION
Flight set 360L001 (STS-26) insulation component. Volume 3: Final release
[NASA-CR-183674] N89-27698
INTAKE SYSTEMS
Space Shuttle Main Engine structural analysis and data reduction/evaluation. Volume 4: High pressure fuel turbo-pump inlet housing analysis
[NASA-CR-183667] N89-27696
Space Shuttle Main Engine structural analysis and data reduction/evaluation. Volume 5: Main Injector LOX Inlet analysis
[NASA-CR-183668] N89-27697
INTEGRATED CIRCUITS
Electronics research at the University of Texas at Austin
[AD-A209989] N89-27970
Investigation of radiation effects on semiconductor devices and integrated circuits
[AD-A210165] N89-27972
INTEGRATED OPTICS
Growth and characterization of zinc sulfide films by conversion of zinc oxide films with H2S
[AD-A208727] N89-28423
Solid state research
[AD-A209645] N89-28426
INTERFACES
The quartz crystal microbalance as an in situ tool in electrochemistry
[AD-A209852] N89-27811
Modelling organic surfaces with self-assembled monolayers
[AD-A208385] N89-27840
Interfacial area measurement methods
[DE89-013426] N89-27982
Reflection and refraction of finite amplitude acoustic waves at a fluid-fluid interface
[AD-A209800] N89-28371
INTERFEROMETRY
The effect of spatial and temporal wet-troposphere fluctuations on connected element interferometry N89-27874
Synthetic aperture microwave radiometer N89-28181
INTERMETALLICS
Fundamental magnetic studies of iron-rare-earth-metalloid alloys
[DE89-013803] N89-27820
INTERNAL COMBUSTION ENGINES
KIVA-2: A computer program for chemically reactive flows with sprays
[DE89-012805] N89-27975
INTERNATIONAL COOPERATION
The AMSC mobile satellite system: Design summary and comparative analysis N89-27906
INTERPLANETARY FLIGHT
The ROSETTA/CNSR mission: A possible application of electric propulsion to interplanetary missions N89-27715
INTERPLANETARY NAVIGATION
High-precision radiometric tracking for planetary approach and encounter in the inner solar system N89-27873
INTERSTELLAR CHEMISTRY
Silicon chemistry in interstellar clouds
[NASA-CR-185862] N89-28471
INTERSTELLAR GAS
Silicon chemistry in interstellar clouds
[NASA-CR-185862] N89-28471
INTERSTELLAR SPACECRAFT
Interstellar flight: Aspects of beamed electric propulsion N89-27765
INTERSTELLAR TRAVEL
Interstellar flight: Aspects of beamed electric propulsion N89-27765
INTERVALS
Orthogonal sets of data windows constructed from trigonometric polynomials N89-27902
INVARIANT IMBEDDINGS
Orbits which always have affine invariant neighbourhoods
[DE89-611895] N89-28344
INVERSIONS
Novel methodology for application of adaptive systems techniques to DMSP (Defense Meteorological Satellite Program) remote temperature sensing
[AD-A209975] N89-28098
Control and system theory, optimization, inverse and ill-posed problems
[AD-A208570] N89-28335
INVISCID FLOW
Implicit time dependent methods for inviscid and viscous compressible flows, with a discussion of the concept of numerical dissipation N89-27990
ION BEAMS
Nonpropulsive application of the RF-ion thruster for material processing with reactive gases N89-27786
ION CYCLOTRON RADIATION
Experimental study on the deposition profile of the ICRF power and electron thermal diffusivity
[IPPJ-908] N89-28401
ION EMISSION
Optical spectroscopy of copper (1) doped Na(+) beta-alumina
[AD-A209819] N89-27810
ION ENGINES
Structural and thermal response of 30 cm diameter ion thruster optics
[NASA-TM-102124] N89-27703
Field emission electric propulsion: Emission of slit-type liquid metal ion sources N89-27723
A review of the cathode construction for the RAE 10/25mN thruster N89-27759
Experimental study of double stage discharge Hall ion thruster N89-27763
Optical emission spectrum of the UK-10 ion thruster operating on xenon N89-27781
Nonpropulsive application of the RF-ion thruster for material processing with reactive gases N89-27786
Performance research of xenon ion rocket engine N89-27788
ION EXCHANGING
Energy transfer effects in beta-alumina
[AD-A209818] N89-27855
The use of multiple ion exchange to produce energy transfer in beta-aluminas
[AD-A209821] N89-27856
ION IMPACT
The inadequacies of damage energy as a measure of displacement damage
[AD-A207376] N89-28028
ION PROPULSION
The role of electric propulsion in extending the economic life-cycle of commercial European telecommunication satellites N89-27713
Field emission electric propulsion: Emission of slit-type liquid metal ion sources N89-27723
Field Emission Electric Propulsion (FEEP) attitude control capabilities N89-27724
Status of the RITA experiment on EURECA N89-27728
The proposed demonstration of the UK-10 ion propulsion system on ESA's SAT-2 spacecraft N89-27729
Design and development of the UK-10 ion propulsion subsystem N89-27730
Design and integration of an electric propulsion system on the Eurostar spacecraft N89-27732
Development of a flight standard power conditioning and control system for the T5 ion thruster N89-27738
Controlling a stationary orbit using electric propulsion N89-27741
Xenon ion thruster test facility: Design and operation N89-27745
Discharge performance of a 12 cm cusp xenon ion thruster N89-27746
High thrust operation of the UK-10 rare gas ion thruster (T4A) N89-27747
Ring cusp/hollow cathode discharge chamber performance studies --- ion propulsion N89-27748
A case study of a mission to the Kordylewski clouds using ion propulsion N89-27751

A small ion-propelled spacecraft for near earth experiments N89-27752

The Propellant Supply and Monitoring Equipment (PSME) for the UK-10 ion propulsion subsystem N89-27758

A review of the cathode construction for the RAE 10/25mN thruster N89-27759

An approach to the parametric design of ion thrusters N89-27761

Experimental study of double stage discharge Hall ion thruster N89-27763

Ultimate performance limits and mission capabilities of advanced ion thrusters N89-27764

A 30 cm diameter xenon ion thruster: Design and initial test results N89-27768

Diagnostic tools for an ion thruster in space N89-27782

A 6 cm diameter ion source for assistant deposition N89-27784

Field Emission Electric Propulsion (FEEP): Experimental investigations on continuous and pulsed modes of operation N89-27792

ION SOURCES

Ring cusp/hollow cathode discharge chamber performance studies --- ion propulsion N89-27748

A 6 cm diameter ion source for assistant deposition N89-27784

Development of high-current RF plasma sources for neutral particle injections N89-27785

A one microsecond, thirty-five kilojoule, one hertz pulse generator
[DE89-013074] N89-27955

ION TRAPS (INSTRUMENTATION)

New ion trap for atomic frequency standard applications N89-27875

IONIZATION

Electrospray ionization-mass spectrometry and tandem mass spectrometry
[DE89-014465] N89-27806

Current models of the intensely ionizing particle environment in space N89-28458

IONS

Database development for the DMSP (Defense Meteorological Satellite Program) SSIES experiment
[AD-A208712] N89-27691

Protonic solid electrolytes: Thermal stability and conductivity of ammonium/hydronium beta'-alumina
[AD-A209911] N89-27813

New, efficient optically pumped solid state lasers
[AD-A209998] N89-28013

IRELAND

Utility of Thematic Mapper data for national survey of Irish lakes N89-28058

Use of satellite imagery for the investigation of pollution-related characteristics of Dublin Bay, Ireland N89-28063

The use of Thematic Mapper imagery for peatland mapping and mineral exploration in Ireland N89-28065

IRON ALLOYS

Martensitic phase transitions in nanocrystalline materials
[AD-A208804] N89-27827

IRRADIANCE

The Earth Radiation Budget Experiment N89-28133

IRRADIATION

Irradiation effects on resistance of thermal impact of composite used in space
[DE89-778069] N89-27794

Resist sensitivity enhancement by radiation-induced modification
[AD-A208438] N89-27842

Electron beam-positive polyimides
[AD-A208440] N89-27844

IRRIGATION

Application of remote sensing to irrigation water management in two Italian irrigation districts N89-28060

ISOLATORS

State-of-the-art fiber optics for short distance frequency reference distribution N89-27878

ISOTHERMAL LAYERS

Formation of monolayers by the coadsorption of thiols on gold: Variation in the length of the alkyl chain
[AD-A208386] N89-27824

ITALY

Application of remote sensing to irrigation water management in two Italian irrigation districts N89-28060

Processing and interpretation of Thematic Mapper images in the Province of Piacenza (Italy) N89-28088

J

JAMMING

A comparative study of SHF (Super High Frequency) and EHF (Extremely High Frequency) satellite communications, volume 1
[AD-A208850] N89-27945

JAPANESE SPACE PROGRAM

Electric propulsion projects and research in Japan N89-27709

Development of an MPD propulsion system N89-27718

JAPANESE SPACECRAFT

Thermal design of a superfluid helium dewar for infrared telescope on-board space flyer unit N89-28270

JET ENGINES

Parametric study of the aerothermodynamics of a jet engine test facility
[AD-A208512] N89-27675

JET IMPINGEMENT

Thermal effects of plume impingement N89-28252

JOINTS (JUNCTIONS)

Flight set 360L001 (STS-26) insulation component. Volume 3: Final release
[NASA-CR-183674] N89-27698

Ceramic joining in the United States
[DE89-009323] N89-27834

An adhesive for field repair of composites
[AD-A209992] N89-27859

Design considerations for an earth based flexible robotic system
[AD-A209635] N89-28018

Robot motion planning: A distributed representation approach
[AD-A209890] N89-28019

The Shock and Vibration Digest, volume 21, no. 4 N89-28025

Damping in structural joints N89-28026

JOSEPHSON JUNCTIONS

High-temperature superconductivity: Abstracts of NIST (National Institute of Standards and Technology) publications, 1987-1988
[PB89-148340] N89-28405

JUPITER ATMOSPHERE

Time-Variable Phenomena in the Jovian System
[NASA-SP-494] N89-28474

JUPITER RINGS

Time-Variable Phenomena in the Jovian System
[NASA-SP-494] N89-28474

JUPITER SATELLITES

Time-Variable Phenomena in the Jovian System
[NASA-SP-494] N89-28474

K

K-EPSILON TURBULENCE MODEL

Parametric study of the aerothermodynamics of a jet engine test facility
[AD-A208512] N89-27675

KALMAN FILTERS

Application of optimal control theory to the design of the NASA/JPL 70-meter antenna servos N89-27881

Extended Kalman Filter (EKF) algorithm
[PD-CF-8922] N89-28313

Fixed interval smoothing algorithm for an extended Kalman filter for over-the-horizon ship tracking
[AD-A208555] N89-28318

KAPTON (TRADEMARK)

Thermal measurements of microwave transmitter feedhorn window N89-27885

KINEMATICS

Joint-space adaptive control of a 6 DOF end-effector with closed-kinematic chain mechanism
[NASA-CR-185861] N89-28016

Robot motion planning: A distributed representation approach
[AD-A209890] N89-28019

Generic singularities of robot manipulators
[AD-A210116] N89-28021

KINETIC EQUATIONS

A statistical derivation of the average degree of polymerization in a stirred tank reactor
[AD-A209873] N89-27857

KINETICS

Effect of alloying, rapid solidification, and surface kinetics on the high temperature environmental resistance of niobium
[AD-A209934] N89-27829

Decomposition kinetics and film formation of an organometallic precursor to SiC on Si(100)
[AD-A208384] N89-28420

KNOWLEDGE BASES (ARTIFICIAL INTELLIGENCE)

Evidence flow graph methods for validation and verification of expert systems
[NASA-CR-181810] N89-28328

KRYPTON

Dynamics of H(+) + Kr and H(+) + Xe elastic and charge-transfer collisions: State-selected differential cross sections at low collision energies N89-28381

KRYPTON FLUORIDE LASERS

KrF lasers for inertial confinement fusion
[DE89-014272] N89-28007

L

LAGRANGE MULTIPLIERS

A numerical study of an augmented Lagrangian method for the estimation of parameters in elliptic systems
[AD-A208658] N89-28351

LAGRANGIAN EQUILIBRIUM POINTS

A case study of a mission to the Kordylewski clouds using ion propulsion N89-27751

LAKES

Utility of Thematic Mapper data for national survey of Irish lakes N89-28058

LAMB WAVES

Ultrasonic nondestructive evaluation of damage in continuous fiber composites
[AD-A208840] N89-27799

LAMINATES

Ultrasonic nondestructive evaluation of damage in continuous fiber composites
[AD-A208840] N89-27799

Mechanical response of structural elements to dynamic loads
[AD-A209827] N89-27802

Fundamental mechanisms of tribology and their implications
[AD-A209941] N89-28020

LAND USE

Agricultural land-use classification in the Upper Rhine Valley using multitemporal TM data N89-28074

Remote sensing of the Madrid area ecosystems N89-28076

LANDSAT SATELLITES

Report of the Project Estima, phase 2: LANDSAT-TM data and agrometeorology in crop yield estimation of wheat at the farm level
[INPE-4782-RPE/582-PHASE-2] N89-28051

LANDSAT 5

Improved snow and glacier monitoring by the LANDSAT Thematic Mapper N89-28056

LARGE SPACE STRUCTURES

Research and technology plans for FY 1989 and accomplishments for FY 1988 --- Structural Mechanics Division
[NASA-TM-101592] N89-28035

LASER ALTIMETERS

Lunar observer laser altimeter N89-28134

LASER APPLICATIONS

Multiphoton detection techniques for F and F2
[AD-A208576] N89-27807

Laser processing of metals and alloys
[DE89-613235] N89-27822

Laser cladding of Ni, Nb, Mg alloys for improved environmental resistance at high temperatures
[AD-A210134] N89-27830

KrF lasers for inertial confinement fusion
[DE89-014272] N89-28007

Bibliography of Soviet laser developments: January - February 1988
[AD-A209802] N89-28011

Noncontacting laser diffraction strain extensometer for material properties characterization at high temperatures
[DE89-013551] N89-28393

LASER INTERFEROMETRY

Noncontacting laser diffraction strain extensometer for material properties characterization at high temperatures
[DE89-013551] N89-28393

LASER OUTPUTS

Approaches toward a blue semiconductor laser
[NASA-CR-4252] N89-28004

Extraordinary behavior of atoms near a phase conjugator
[AD-A209946] N89-28389

LASER PROPULSION

Interstellar flight: Aspects of beamed electric propulsion N89-27765

Pulsed laser propulsion for low cost, high volume launch to orbit
[DE89-014049] N89-28009

LASER PUMPING

New, efficient optically pumped solid state lasers
[AD-A209998] N89-28013

Diode-pumped laser research N89-28185

Extraordinary behavior of atoms near a phase conjugator
[AD-A209946] N89-28389

LASER SPECTROSCOPY
New, efficient optically pumped solid state lasers
[AD-A209998] N89-28013

LASER WEAPONS
Goals for limited strategic defenses
[DE89-012260] N89-28366
Constellation sizing for modest directed energy platforms
[DE89-012826] N89-28367

LASER WELDING
Laser processing of metals and alloys
[DE89-613235] N89-27822

LASERS
Development of superlattices for ultra high-speed electronic and optoelectronic devices
[AD-A209874] N89-28429

LASING
New, efficient optically pumped solid state lasers
[AD-A209998] N89-28013

LAUNCH WINDOWS
Launch window for the Brazilian Data Collecting Satellite
[INPE-4773-PRE/1442] N89-27683

LEARNING
The back propagation technique for modeling cortical computation
[AD-A209855] N89-28323
Learning from physical analogies: A study in analogy and the explanation process
[AD-A208689] N89-28336

LEAST SQUARES METHOD
Quantitative estimation of component amplitude in multiexponential data: Application to time-resolved fluorescence spectroscopy
[AD-A210142] N89-27815
Statistical analysis of the LMS and modified stochastic gradient algorithms
[AD-A208618] N89-28319
An efficient exact algorithm for the least squares image registration problem
[AD-A208725] N89-28320
A numerical study of an augmented Lagrangian method for the estimation of parameters in elliptic systems
[AD-A208658] N89-28351

LEG (ANATOMY)
Analysis of articulated manikin based convective heat transfer during walking
[AD-A208299] N89-28298

LIAPUNOV FUNCTIONS
State-space theory of structured uncertainty with examples
[AD-A209968] N89-28339

LIFE (DURABILITY)
Experience with advanced instrumentation in a hot section cascade
[NASA-TM-102294] N89-27980

LIFE SCIENCES
Life science research objectives and representative experiments for the space station
[NASA-TM-89445] N89-28304
Data base development and research and editorial support
[NASA-CR-183249] N89-28440

LIFE SUPPORT SYSTEMS
Separation of oxygen from seawater by membrane permeation
[AD-A208863] N89-27809
Third European Symposium on Space Thermal Control and Life Support Systems
[ESA-SP-288] N89-28214
System aspects of Columbus thermal control and life support N89-28216
The Hermes spaceplane program: Status report on the thermal control, environment control and life support activities N89-28217
European life support systems for space applications N89-28218
Environmental control and life support systems for pressurized modules: From Spacelab to Columbus N89-28219
The definition status of the environmental control and life support subsystems for Hermes N89-28220
Condensing heat exchangers for European spacecraft ECLSS N89-28240
Come to flight rules: Rationale on environmental control and life support systems --- Hermes N89-28242
Life support for EVA: The European system baseline N89-28244
ECLS simulation program N89-28284

LIGHT EMITTING DIODES
Compensation for effects of ambient temperature on rare-earth doped fiber optic thermometer
[NASA-TM-102282] N89-27998

LIGHT MODULATION
Computer generated matched filters with spatial frequency tailoring
[AD-A209786] N89-28001
Generalized beamforming with multiple computer originated holograms
[AD-A210175] N89-28397
Development of superlattices for ultra high-speed electronic and optoelectronic devices
[AD-A209874] N89-28429

LIGHT SCATTERING
Scattering from fractals
[DE89-013451] N89-27924
Airborne in-situ spectral characterization and concentration estimates of fluorescent organics as a function of depth N89-28140
Cloud absorption radiometer N89-28172

LIGHT SOURCES
Development of superlattices for ultra high-speed electronic and optoelectronic devices
[AD-A209874] N89-28429

LIGHTNING
Interpretation of F106B and CV580 in-flight lightning data and form factor determination
[NASA-CR-4250] N89-28115

LIMITERS (FUSION REACTORS)
Role of edge magnetic shear on the limiter H-mode transition of the JIPP T-IIU tokamak
[IPPJ-906] N89-28399

LIMNOLOGY
Remote sensing of limnological parameters in reservoirs N89-28061

LINEAR ACCELERATORS
Lasertron: A pulsed RF-source using laser triggered photocathode
[DE89-778130] N89-28006

LINEAR EQUATIONS
A uniformly differentiable approximation scheme for delay systems using splines
[AD-A208567] N89-28346

LINEAR FILTERS
Estimation and filtering techniques for high-accuracy GPS applications N89-27872
Mode filters and their applications
[INPE-4748-PRE/1421] N89-28312

LINEAR PROGRAMMING
An efficient exact algorithm for the least squares image registration problem
[AD-A208725] N89-28320

LINEAR QUADRATIC GAUSSIAN CONTROL
Application of optimal control theory to the design of the NASA/JPL 70-meter antenna servos N89-27881

LINEAR SYSTEMS
Parameter plane design method
[AD-A209845] N89-28322

LIQUID COOLING
An algorithm for calculating thermodynamic properties of simple fluids suitable for space thermal control N89-28254
United States Air Force Research Initiation Program for 1987, volume 1
[AD-A209726] N89-28436

LIQUID CRYSTALS
Transformation of a monotropic mesophase into an enantiotropic mesophase by copolymerization of the parent polymers' monomer pair containing constitutional isomeric mesogenic side groups
[AD-A208782] N89-27850
The influence of the polymer backbone flexibility on the phase transitions of side chain liquid crystal polymers containing
yl side groups
[AD-A208821] N89-27851

LIQUID LASERS
Bibliography of Soviet laser developments: January - February 1988
[AD-A209802] N89-28011

LIQUID METALS
Field emission electric propulsion: Emission of slit-type liquid metal ion sources N89-27723
Thermophysical properties of liquid niobium
[DE89-014288] N89-28435

LIQUID NITROGEN
Operating characteristics of 1 kW hydrazine arcjet thruster N89-27779

LIQUID SURFACES
Applications of the quartz crystal microbalance to electrochemistry
[AD-A209853] N89-27812

LIQUID-GAS MIXTURES
Non-condensible gas effects on the low-temperature heat pipe characteristics N89-28227

LIQUID-LIQUID INTERFACES
An experimental study to determine the relative influence of fluid-fluid interactions and media heterogeneities on the growth of immiscible viscous fingers
[DE89-013122] N89-27976

LIQUIDS
Sound propagation in bubbly liquids: A review
[AD-A207377] N89-28370

LITHIUM
Magnetic induction thruster with lithium propellant N89-27762

LITHIUM NIOBATES
Calculation of planar structures for optical wavelength multiplexers N89-27942
Fiber-optic delay line storage in digital optical computers based on directional couplers
[PB89-185318] N89-28392

LITHIUM OXIDES
Calculation of planar structures for optical wavelength multiplexers N89-27942

LITHOGRAPHY
Characterization of structure in thin polymer resist films
[AD-A208677] N89-27848
Computer generated matched filters with spatial frequency tailoring
[AD-A209786] N89-28001

LITHOLOGY
Lithologic mapping of mafic intrusions in East Greenland using Landsat Thematic Mapper data
[NASA-CR-183440] N89-28047

LOAD TESTS
Theoretical model for stabilization of clay-silt airport pavement subgrade systems. Phase 1: Laboratory investigation. Phase 2: Rutting tests
[DOT/FAA/PM-87/20-PHASE-1/2] N89-27673
A data acquisition and control program for axial-torsional fatigue testing
[NASA-TM-102041] N89-28029
Evaluation of a strain-gage load calibration on a low-aspect-ratio wing structure at elevated temperature
[NASA-TP-2921] N89-28034
Probabilistic description of fatigue crack growth under constant-and variable-amplitude loading
[AD-A208717] N89-28043

LOADS (FORCES)
Research and technology plans for FY 1989 and accomplishments for FY 1988 --- Structural Mechanics Division
[NASA-TM-101592] N89-28035
Mechanical and physical study of the behavior under sequential loads of copper and steel plates
[ETN-89-94805] N89-28037
Probabilistic description of fatigue crack growth under constant-and variable-amplitude loading
[AD-A208717] N89-28043

LOCAL AREA NETWORKS
Personal computers on Ethernet N89-28175

LOG PERIODIC ANTENNAS
An experimental and computer modeling study of stepped radius monopole antennas
[AD-A207356] N89-27919

LOGIC CIRCUITS
Average interconnection length and interconnection distribution for rectangular arrays
[AD-A209848] N89-27967
Approaches to multi-level sequential logic synthesis
[AD-A208322] N89-28316

LONGITUDINAL STABILITY
Summary of longitudinal stability and control parameters as determined from Space Shuttle Challenger flight test data
[NASA-TM-101605] N89-27671

LOSSES
The calculation of losses in waveguide networks N89-27941

LOSSY MEDIA
Electromagnetic scattering from a structured slab comprised of periodically placed resistive cards
[AD-A210145] N89-27953

LOW ALTITUDE
Effect of three-dimensional object type and density in simulated low-level flight
[AD-A209756] N89-27679

LOW ASPECT RATIO WINGS
Evaluation of a strain-gage load calibration on a low-aspect-ratio wing structure at elevated temperature
[NASA-TP-2921] N89-28034

LOW DENSITY FLOW
Low density flow effects for hypervelocity vehicles
[AD-A206218] N89-27633

LOW NOISE
Multipurpose exciter with low phase noise N89-27867

LOW PRESSURE
Aerodynamic design of low pressure turbines N89-27669
LOW SPEED WIND TUNNELS
Small scale model tests in small wind and water tunnels at high incidence and pitch rates. Volume 2: Small wind tunnel (ADF) data base
[AD-A208539] N89-27676
LUBRICANT TESTS
Vapor phase deposition studies of phosphate esters on metal and ceramic surfaces
[PB89-148985] N89-27831
LUBRICANTS
Fundamental mechanisms of tribology and their implications
[AD-A209941] N89-28020
LUBRICATION
Vapor phase deposition studies of phosphate esters on metal and ceramic surfaces
[PB89-148985] N89-27831
LUNAR FLIGHT
A case study of a mission to the Kordylewski clouds using ion propulsion N89-27751
LUNAR GEOLOGY
Lunar observer laser altimeter N89-28134
LUNAR PROBES
Lunar observer laser altimeter N89-28134
LUNAR SURFACE
Lunar observer laser altimeter N89-28134

M

MACH NUMBER
Mach 5 inlet CFD and experimental results
[NASA-TM-102317] N89-27670
MAGNESIUM ALLOYS
Laser cladding of Ni, Nb, Mg alloys for improved environmental resistance at high temperatures
[AD-A210134] N89-27830
MAGNET COILS
Optimization of maneuvers of a spin-stabilized satellite, using magnetic coils
[INPE-4778-TDL/350] N89-27680
MAGNETIC COMPRESSION
A battery-powered flux compression generator system
[DE89-014230] N89-27958
High voltage power condition systems powered by flux compression generators
[DE89-014259] N89-27959
High-performance, high-current fuses for flux compression generator driven inductive store power conditioning applications
[DE89-014274] N89-27960
A simultaneous helical generator
[DE89-014284] N89-27961
MAGNETIC CONTROL
Optimization of maneuvers of a spin-stabilized satellite, using magnetic coils
[INPE-4778-TDL/350] N89-27680
MAGNETIC FIELD CONFIGURATIONS
Hybrid MPD thruster with axial and cusp magnetic fields N89-27744
Discharge plasma calculations in cusped ion thrusters using the finite element method N89-27760
MAGNETIC FIELDS
Hybrid MPD thruster with axial and cusp magnetic fields N89-27744
Solution of two-dimensional, two-region electromagnetic ground response
[AD-A206265] N89-27869
Modulation of spontaneous brain activity during mental imagery
[AD-A209918] N89-28208
The stability of the High-Density Z-Pinch
[DE89-014276] N89-28403
Phonon-drag thermoelectric power in high magnetic fields in heterojunctions
[DE89-013921] N89-28412
MAGNETIC FLUX
High-performance, high-current fuses for flux compression generator driven inductive store power conditioning applications
[DE89-014274] N89-27960
MAGNETIC INDUCTION
Magnetic induction thruster with lithium propellant N89-27762
Solution of two-dimensional, two-region electromagnetic ground response
[AD-A206265] N89-27869
MAGNETIC MATERIALS
Institute for Materials Science and Engineering: Metallurgy Division, technical activities 1988
[PB89-201321] N89-27819
MAGNETIC PROPERTIES
Fundamental magnetic studies of iron-rare-earth-metalloid alloys
[DE89-013803] N89-27820
Magnetopause structure and dynamics: Issues for GEM
[DE89-012620] N89-28054
MAGNETIC SHIELDING
Diamagnetic shielding and flux creep in a Tl-Ba-Ca-Cu-O thin film
[DE89-014550] N89-28414
MAGNETIC SUSPENSION
An evaluation of three experimental processes for two-dimensional transonic tests
[NASA-CR-181871] N89-27674
MAGNETOHYDRODYNAMIC FLOW
Numerical codes for cylindrical MPD thrusters N89-27733
Quantitative imaging of MPD flow fields N89-27766
MAGNETOHYDRODYNAMIC GENERATORS
MHD (Magnetohydrodynamics) Program Plan, FY 1989
[DE89-012232] N89-28398
MAGNETOHYDRODYNAMIC SHEAR HEATING
Role of edge magnetic shear on the limiter H-mode transition of the JIPP T-IIU tokamak
[IPPJ-906] N89-28399
MAGNETOHYDRODYNAMIC STABILITY
Current driven instabilities of an electromagnetically accelerated plasma N89-27736
Investigation of instabilities in MPD thruster flows using a linear dispersion relation N89-27737
Extension of stellarator approximation in magnetohydrodynamic equilibrium and stability of toroidal helical systems
[IPPJ-905] N89-28400
The stability of the High-Density Z-Pinch
[DE89-014276] N89-28403
MAGNETOHYDRODYNAMICS
A simultaneous helical generator
[DE89-014284] N89-27961
MHD (Magnetohydrodynamics) Program Plan, FY 1989
[DE89-012232] N89-28398
MAGNETOPAUSE
Magnetopause structure and dynamics: Issues for GEM
[DE89-012620] N89-28054
MAGNETOPLASMADYNAMICS
Performance of a 100 kW class applied field MPD thruster
[NASA-TM-102312] N89-27701
Development of an MPD propulsion system N89-27718
Cylindrical steady-state MPD thruster N89-27725
Nozzle type MPD thruster experimental investigations N89-27727
Numerical codes for cylindrical MPD thrusters N89-27733
Fluid mechanics in a magnetoplasmadynamic thruster N89-27734
An improved code for nozzle type steady state MPD thrusters N89-27735
Investigation of instabilities in MPD thruster flows using a linear dispersion relation N89-27737
Optimization of current distribution in an applied-field MPD thruster N89-27743
Hybrid MPD thruster with axial and cusp magnetic fields N89-27744
Cathode processes in a MPD arcjet N89-27753
Anode-nozzle experimental analysis in a coaxial non-steady solid propellant MPD thruster N89-27757
Quantitative imaging of MPD flow fields N89-27766
Steady state MPD devices for reentry simulation N89-27783
KREM: A model for evaluating orbital transfer vehicles utilizing nuclear electric propulsion systems N89-27789
A tandem mirror hybrid plume plasma propulsion facility N89-27791
MAGNETOSPHERES
Particle simulations in magnetospheric plasmas
[AD-A206252] N89-28106
MAGNONS
Theory of photon-drag effect in bulk magnetic semiconductors
[DE89-612214] N89-28417
MAINTAINABILITY
Basic research in reliability for real systems
[AD-A209649] N89-28022
MAN MACHINE SYSTEMS
Identification of variables determining intrahemispheric interference between processing demands
[AD-A208435] N89-28299
MAN TENDED FREE FLYERS
Electric propulsion for low earth orbit applications N89-27714
MAN-COMPUTER INTERFACE
An implementation of a data definition facility for the graphics language for database
[AD-A207380] N89-28442
MANAGEMENT ANALYSIS
Basic research in reliability for real systems
[AD-A209649] N89-28022
MANAGEMENT SYSTEMS
Resource contention management in parallel systems
[AD-A208809] N89-28332
MANEUVERS
Fixed interval smoothing algorithm for an extended Kalman filter for over-the-horizon ship tracking
[AD-A208555] N89-28318
MANIPULATORS
Design of an adaptive controller for a telerobot manipulator
[NASA-CR-185863] N89-28017
Generic singularities of robot manipulators
[AD-A210116] N89-28021
MAPPING
Automatic change in contour diagrams on the occasion of scale reduction using a material morphology
[INPE-4769-PRE/1438] N89-28049
European Coordinated Effort for Monitoring the Earth's Environment. A Pilot Project Campaign on LANDSAT Thematic Mapper Applications (1985-1987)
[ESA-SP-1102] N89-28055
LANDSAT TM data used in the mapping of large-scale geological structures in coastal areas in Trondelag, central Norway N89-28072
Evaluation of the LANDSAT TM satellite in urban media: Application to the case of Brussels, Belgium N89-28073
Use of remote sensing in mapping of vegetation in the Dividalen area central Troms, northern Norway N89-28083
Multitemporal analysis of TM images: Application to forest fire mapping and inventory in a Mediterranean environment N89-28084
Large-scale forest management using LANDSAT Thematic Mapper data N89-28085
Multitemporal analysis of forest areas in surroundings of Innsbruck, Austria N89-28086
Processing and interpretation of Thematic Mapper images in the Province of Piacenza (Italy) N89-28088
Production of satellite image maps from TM data N89-28089
Integrating TM and cartographic data N89-28090
A smart, mapping, charting and geodesy control generator, phase 2
[AD-A208806] N89-28097
The human telomere
[DE89-014252] N89-28199
Two examples of escaping harmonic maps
[DE89-611896] N89-28345
MAPS
Generic singularities of robot manipulators
[AD-A210116] N89-28021
MARECS MARITIME SATELLITES
In-orbit degradation of thermo-optical properties on MARECS GEO-satellite N89-28297
MARINE TECHNOLOGY
Satellite image analysis for marine applications
[PB89-187330] N89-28053
MARITIME SATELLITES
Analysis of maritime mobile satellite communication systems
[AD-A207358] N89-27920
MARKET RESEARCH
High-speed civil transport study. Summary
[NASA-CR-4234] N89-27647
MARKETING
High-speed civil transport study
[NASA-CR-4233] N89-27648
MARKOV PROCESSES
Calculation of network parameters of crosslinked Markovian polymer chains
[AD-A210073] N89-27860
Markov processes applied to control, reliability and replacement
[AD-A208634] N89-28362
MARS OBSERVER
Mars Observer Radar Altimeter Radiometer (MORAR) N89-28120
MARS SURFACE
Mars Observer Radar Altimeter Radiometer (MORAR) N89-28120
MARTENSITE
Martensitic phase transitions in nanocrystalline materials
[AD-A208804] N89-27827
MASS
The quartz crystal microbalance as an in situ tool in electrochemistry
[AD-A209852] N89-27811

An integrating matrix formulation for buckling of rotating beams including the effects of concentrated masses [NASA-CR-181862] N89-28342
MASS FLOW
Investigation of a liquid-fed water resistojet plume [NASA-TM-102310] N89-27706
MASS SPECTROMETERS
Electrospray ionization-mass spectrometry and tandem mass spectrometry [DE89-014465] N89-27806
MASS TRANSFER
Interfacial area measurement methods [DE89-013426] N89-27982
Solid state research [AD-A209969] N89-28431
MATCHED FILTERS
Computer generated matched filters with spatial frequency tailoring [AD-A209786] N89-28001
MATHEMATICAL MODELS
Numerical simulation of control of supersonic shear layers [AD-A209703] N89-27639
Blading design for multi-stage HP compressors N89-27666
Space Shuttle Main Engine structural analysis and data reduction/evaluation. Volume 3A: High pressure oxidizer turbo-pump preburner pump housing stress analysis report [NASA-CR-183665] N89-27694
Space Shuttle Main Engine structural analysis and data reduction/evaluation. Volume 3B: High pressure fuel turbo-pump preburner pump bearing assembly analysis [NASA-CR-183666] N89-27695
Structural and thermal response of 30 cm diameter ion thruster optics [NASA-TM-102124] N89-27703
Investigation of a liquid-fed water resistojet plume [NASA-TM-102310] N89-27706
Rapidly solidified titanium alloys by melt overflow [NASA-CR-4253] N89-27818
Fiber reinforced structural ceramics for construction [AD-A209976] N89-27858
Further investigation of flow modeling during solid propellant processing [AD-A209787] N89-27866
Model and method for systems development N89-27929
Studies of the propagation of short burst, high power microwave radiation through neutral and ionized media [AD-A208664] N89-27944
System theoretic models for high density VLSI structures [AD-A209901] N89-27968
Monte Carlo reliability analysis [AD-A210052] N89-28024
Recent advances on the dynamic behavior of stiffened plates N89-28027
Refinements in a viscoplastic model [NASA-TM-102338] N89-28036
Discrete enforcement of uncertain oscillator Gaussian response [DE89-005595] N89-28038
Model based damping of coupled horizontal and vertical oscillations in a flexible rod [DE89-007034] N89-28039
Plastic deformation of granular materials [AD-A208589] N89-28040
Determination of local empirical covariance functions from residual terrain reduced altimeter data [AD-A208678] N89-28095
Backgrounder contribution No. 18: Climate scenarios for the first UC/DOE workshop [DE89-014302] N89-28105
Evaluating CFC (Chlorofluorocarbon) alternatives from the atmospheric viewpoint, revision 1 [DE89-014268] N89-28108
Analyses of the wind-driven response of tropical oceans N89-28155
Modeling of ocean surface spectrum and surface scattering. Applications to reverberation prediction in the AAUS program [AD-A210127] N89-28197
Lumping, a powerful design tool for thermal control N89-28248
Assembling the ISO thermal model with ESATAN N89-28280
Preliminary statistical identification of radar imagery: Autoregressive-moving average (ARMA) models [INPE-4771-PRE/1440] N89-28311
Fixed interval smoothing algorithm for an extended Kalman filter for over-the-horizon ship tracking [AD-A208555] N89-28318
Statistical analysis of the LMS and modified stochastic gradient algorithms [AD-A208618] N89-28319
COMM-Q: A simulation model to determine saturation points in nodal type networks [AD-A207294] N89-28329
United States Air Force Research Initiation Program for 1987, volume 3 [AD-A209728] N89-28437
United States Air Force Research Initiation Program for 1987, volume 4 [AD-A209729] N89-28438
A model of security monitoring [NASA-CR-185845] N89-28446
Toward a descriptive model of solar particles in the heliosphere N89-28455
Toward a descriptive model of galactic cosmic rays in the heliosphere N89-28456
Current models of the intensely ionizing particle environment in space N89-28458
A new proton fluence model for E greater than 10 MeV N89-28459
High-energy particles very near the sun N89-28465
Elemental composition and energy spectra of galactic cosmic rays N89-28466
MATHEMATICAL PROGRAMMING
ParaGraph-RTS: A parallel reduction-based run-time system [DE89-005457] N89-28315
MATRICES (MATHEMATICS)
Bunch-Kaufman factorization for real symmetric indefinite banded matrices [NASA-CR-181860] N89-28341
The principal pivoting method revisited [AD-A208796] N89-28352
MATRIX MATERIALS
High performance composites based on polyurethanes reinforced with polydiacetylenes [AD-A208436] N89-27797
MATRIX THEORY
The principal pivoting method revisited [AD-A208796] N89-28352
MATTER-ANTIMATTER PROPULSION
Antiproton powered propulsion with magnetically confined plasma engines [NASA-CR-185131] N89-27700
MAXIMUM LIKELIHOOD ESTIMATES
Quadratic estimators of the power spectrum [AD-A208601] N89-27964
MAXWELL EQUATION
A study of spacecraft electromagnetic contamination of artificial electron beams [AD-A209954] N89-27950
MEASURE AND INTEGRATION
Novel methodology for application of adaptive systems techniques to DMSP (Defense Meteorological Satellite Program) remote temperature sensing [AD-A209975] N89-28098
MEASURING INSTRUMENTS
Database development for the DMSP (Defense Meteorological Satellite Program) SSIES experiment [AD-A208712] N89-27691
Institute for Materials Science and Engineering: Metallurgy Division, technical activities 1988 [PB89-201321] N89-27819
Calibration support for the Earth Observing System Project N89-28131
MECHANICAL DEVICES
Quantitative inference in a mechanical design compiler [AD-A209900] N89-28324
MECHANICAL ENGINEERING
Quantitative inference in a mechanical design compiler [AD-A209900] N89-28324
MECHANICAL PROPERTIES
Institute for Materials Science and Engineering: Metallurgy Division, technical activities 1988 [PB89-201321] N89-27819
The texture variation in extruded graphite [DE89-014086] N89-27837
An adhesive for field repair of composites [AD-A209992] N89-27859
MEDIA
Studies of the propagation of short burst, high power microwave radiation through neutral and ionized media [AD-A208664] N89-27944
Crisis decision-making: The impact of commercial satellites on the media, military and national leaders [AD-A207334] N89-28449
MEMBRANES
Separation of oxygen from seawater by membrane permeation [AD-A208863] N89-27809
MEMORY
Attention, imagery and memory: A neuromagnetic investigation [AD-A209917] N89-28207
Modulation of spontaneous brain activity during mental imagery [AD-A209918] N89-28208
MEMORY (COMPUTERS)
Fiber-optic delay line storage in digital optical computers based on directional couplers [PB89-185318] N89-28392
MENTAL PERFORMANCE
Attention, imagery and memory: A neuromagnetic investigation [AD-A209917] N89-28207
Visualizing and rhyming cause differences in alpha suppression [AD-A210005] N89-28210
MERCURY (METAL)
Propellant selection criteria for deep space electrically propelled missions N89-27769
Inert gas performance of the RIT 35 main propulsion unit N89-27770
Experimental determination of the coefficient in the steady state current equation for spherical segment microelectrodes [AD-A208662] N89-27965
METAL AIR BATTERIES
Development of anodes for aluminum/air batteries: Solution phase inhibition of corrosion [DE89-012839] N89-27956
METAL BONDING
The orientation of chemical bonds at surfaces: A key to understanding the structure and bonding of surface species [AD-A209833] N89-28427
METAL CRYSTALS
Martensitic phase transitions in nanocrystalline materials [AD-A208804] N89-27827
Experimental studies of the structure of grain boundaries [DE89-012954] N89-28408
METAL CUTTING
Laser processing of metals and alloys [DE89-613235] N89-27822
METAL FILMS
Ion-assisted deposition of silver films on ceramics for friction and wear control [DE89-014635] N89-27821
METAL MATRIX COMPOSITES
Computational simulation of high temperature metal matrix composites cyclic behavior [NASA-TM-102115] N89-27795
Tungsten fiber reinforced copper matrix composites: A review [NASA-TP-2924] N89-27796
Institute for Materials Science and Engineering: Metallurgy Division, technical activities 1988 [PB89-201321] N89-27819
METAL OXIDE SEMICONDUCTORS
Investigation of radiation effects on semiconductor devices and integrated circuits [AD-A210165] N89-27972
METAL OXIDES
Preparation and characterization of several conduction transition metal oxides [AD-A208895] N89-28424
METAL PLATES
Mechanical and physical study of the behavior under sequential loads of copper and steel plates [ETN-89-94805] N89-28037
METAL SURFACES
Vapor phase deposition studies of phosphate esters on metal and ceramic surfaces [PB89-148985] N89-27831
METALLIC GLASSES
Glassy behaviour of YBa2Cu3O7 [DE89-613399] N89-28418
METALLOGRAPHY
Institute for Materials Science and Engineering: Metallurgy Division, technical activities 1988 [PB89-201321] N89-27819
METALS
Institute for Materials Science and Engineering: Metallurgy Division, technical activities 1988 [PB89-201321] N89-27819
Issues and future directions in subsecond thermophysics [DE89-014228] N89-28434
METEOROLOGICAL PARAMETERS
Aerosol model selection using surface measurements of IR horizon radiances and satellite detected visible radiances [AD-A209638] N89-28110
METEOROLOGICAL RADAR
Spaceborne meteorological radar studies N89-28127

METEOROLOGICAL SATELLITES
Novel methodology for application of adaptive systems techniques to DMSP (Defense Meteorological Satellite Program) remote temperature sensing
[AD-A209975] N89-28098
Fiji South Pacific Severe Storm Detection and Warning System Project (SPSSD/WS) N89-28123
NASA follow-on on the Fiji South Pacific Severe Storm Warning System Project (SPSSD/WS) N89-28124
Earth Observing System (EOS) advanced altimetry N89-28129
Application of optical measure theory to atmospheric temperature sounding from TOVS (TIROS Operational Vertical Sounder) radiances
[AD-A209955] N89-28396
METEOROLOGY
Meteorology in the press
[INPE-4762-PRE/1432] N89-28114
Laboratory for Oceans
[NASA-TM-101257] N89-28118
Applications of the Coastal Zone Color Scanner in oceanography N89-28136
METHANE
Charge transfer and structured vibrational distributions in H(+) + CH4 low-energy collisions N89-28385
MICROBALANCES
Applications of the quartz crystal microbalance to electrochemistry
[AD-A209853] N89-27812
MICROCRACKS
Analysis and elimination of high temperature notch induced microcrack initiation in Inconel 718 nickel-based alloy
[AD-A209695] N89-27828
MICROELECTRONICS
Electronics research at the University of Texas at Austin
[AD-A209989] N89-27970
Critical technologies plan for the Committees on Armed Services, United States Congress, revision
[AD-A210170] N89-28439
Interplanetary Particle Environment. Proceedings of a Conference
[NASA-CR-185461] N89-28454
Toward a descriptive model of solar particles in the heliosphere N89-28455
MICROGRAVITY APPLICATIONS
NASA in-house Commercially Developed Space Facility (CDSF) study report. Volume 1: Concept configuration definition
[NASA-TM-101586-VOL-1] N89-27687
MICROSTRUCTURE
The structure and properties of grain boundaries in B2 ordered alloys
[DE89-013266] N89-27817
High temp toughening and creep studies
[AD-A208714] N89-27826
Modelling organic surfaces with self-assembled monolayers
[AD-A208385] N89-27840
Evaluation of new thermomechanical constitutive theory for snow N89-28052
MICROWAVE ANTENNAS
The Telecommunications and Data Acquisition Report
[NASA-CR-185431] N89-27871
A new analysis of beam-waveguide antennas considering the presence of the enclosure N89-27886
Reanalysis, compatibility and correlation in analysis of modified antenna structures N89-27906
MICROWAVE COUPLING
Coupling between radiation and gas dynamics
[AD-A209657] N89-28102
MICROWAVE EQUIPMENT
Communication engineering reports. Fundamental developments. Theoretical work
[ETN-89-94623] N89-27928
Field theory simulation of nonreciprocal microwave components N89-27940
Engineering research and development: Thrust area report FY 88
[DE89-014320] N89-28453
MICROWAVE IMAGERY
Rainfall on microwave return from the sea surface N89-28160
MICROWAVE RADIOMETERS
Spaceborne meteorological radar studies N89-28127
Arctic Sea ice studies with passive microwave satellite observations N89-28147
Water vapor profiling using microwave radiometry N89-28163
Microwave remote sensing of soil moisture N89-28180
Synthetic aperture microwave radiometer N89-28181
MICROWAVE SCATTERING
Radar scattering and soil moisture N89-28182
MICROWAVE SENSORS
Microwave remote sensing of sea ice N89-28148
Analysis of sea ice dynamics N89-28149
Microwave remote sensing of soil moisture N89-28180
MICROWAVE TRANSMISSION
Thermal measurements of microwave transmitter feedhorn window N89-27885
Studies of the propagation of short burst, high power microwave radiation through neutral and ionized media
[AD-A208664] N89-27944
MICROWAVES
Characteristics of free-floating nitrogen and helium plasmas generated in a microwave resonant cavity N89-27771
Microwave time delays for the X/S-band feed system at X-band N89-27898
DSN 70-meter antenna microwave optics design and performance improvements. Part 1: Design optimization N89-27903
A two-stream plasma electron microwave source for high-power millimeter wave generation, phase 1
[AD-A209942] N89-28404
MILITARY AIR FACILITIES
Environmental effects of space shuttle exhaust on materials
[AD-A208813] N89-27686
MILITARY OPERATIONS
High Endoatmospheric Defense Interceptor (HEDI) technology testing program environmental assessment
[AD-A210006] N89-27684
The 1989 report to the Congress on the Strategic Defense Initiative
[PB89-196661] N89-28368
MILITARY TECHNOLOGY
DARPA (Defense Advanced Research Projects Agency) Review on EHF Devices
[AD-A208564] N89-27963
The 1989 report to the Congress on the Strategic Defense Initiative
[PB89-196661] N89-28368
International technology transfer: The rope to hang the west
[AD-A207347] N89-28452
MILLIMETER WAVES
DARPA (Defense Advanced Research Projects Agency) Review on EHF Devices
[AD-A208564] N89-27963
A two-stream plasma electron microwave source for high-power millimeter wave generation, phase 1
[AD-A209942] N89-28404
MINERAL EXPLORATION
The use of Thematic Mapper imagery for peatland mapping and mineral exploration in Ireland N89-28065
Image processing strategies for mineral exploration in arid areas by use of TM data N89-28067
Comparison of MSS and TM LANDSAT data for cartography of surface structures in arid regions (southern Tunisia) N89-28087
MISALIGNMENT
Topology of modified helical gears
[NASA-TM-102134] N89-28015
MISSILE CONFIGURATIONS
Missile Datcom. Volume 2: User's manual
[AD-A210128] N89-27685
MISSILE DEFENSE
Goals for limited strategic defenses
[DE89-012260] N89-28366
MISSILE DESIGN
Missile Datcom. Volume 2: User's manual
[AD-A210128] N89-27685
MISSILES
Missile Datcom. Volume 2: User's manual
[AD-A210128] N89-27685
MISSION PLANNING
Avionic system requirements N89-27652
Toward an electrical power utility for space exploration
[NASA-TM-102347] N89-27704
NASA advanced space photovoltaic technology-status, potential and future mission applications
[NASA-TM-102093] N89-27705
Spacecraft and mission design for the SP-100 flight experiment N89-27717
MIXING CIRCUITS
MM wavecomponents - SIS (Superconductor-Insulator-Superconductor) mixers
[AD-A208632] N89-28421
MIXING HEIGHT
Mobile lidar system for measurement of water vapor mixing ratio and ozone number density N89-28166
MOBILE COMMUNICATION SYSTEMS
Proceedings of the Mobile Satellite System Architectures and Multiple Access Techniques Workshop
[NASA-CR-184564] N89-27907
The AMSC mobile satellite system: Design summary and comparative analysis N89-27908
Choice of FDMA/SCPC access technique for aeronautical satellite voice system N89-27909
Performance of DA/FDMA architecture proposed for MSS N89-27910
Geostar's system architectures N89-27911
Why is CDMA the solution for mobile satellite communication N89-27912
System level comparison of FDMA vs. CDMA (under conference guideline constraint) N89-27913
Alternative multiple-access techniques for mobile satellite systems N89-27914
Practical constraints on network architecture and signalling in the MSAT system N89-27915
MSAT signalling and network management architectures N89-27916
A robust signalling system for land mobile satellite services N89-27917
Aeronautical mobile TDMA/MCTDMA system N89-27918
Analysis of maritime mobile satellite communication systems
[AD-A207358] N89-27920
Digital demultiplier for mobile satellite communication N89-27937
Digital demodulator for mobile satellite communication N89-27938
MODELS
Communications using channels formed by meteor bursts
[AD-A209856] N89-27949
Robot motion planning: A distributed representation approach
[AD-A209890] N89-28019
Modified rotationally adiabatic model for rotational autoionization of dipole-bound molecular anions
[AD-A209851] N89-28388
Sensitivity analysis of reflection errors in infrared image simulation
[AD-A208600] N89-28394
Semiconductor-olefin adducts. Photoluminescent properties of cadmium sulfide and cadmium selenide in the presence of butenes
[AD-A208348] N89-28419
MODULATION
Theory of multi-frequency modulation (MFM) digital communications
[AD-A209737] N89-27947
Communications using channels formed by meteor bursts
[AD-A209856] N89-27949
Modulation of spontaneous brain activity during mental imagery
[AD-A209918] N89-28208
MODULATORS
The DSS-14 C-band exciter N89-27901
MOISTURE CONTENT
The effect of spatial and temporal wet-troposphere fluctuations on connected element interferometry N89-27874
MOLECULAR ABSORPTION
Electromagnetic reaction to molecular relaxation and its effect on absorption near a rough surface
[AD-A210069] N89-28390
MOLECULAR BEAM EPITAXY
Electronics research at the University of Texas at Austin
[AD-A209989] N89-27970
Decomposition kinetics and film formation of an organometallic precursor to SiC on Si(100)
[AD-A208384] N89-28420
Growth and characterization of zinc sulfide films by conversion of zinc oxide films with H2S
[AD-A208727] N89-28423
MOLECULAR BEAMS
Vibrational predissociation of shock-selected C2H4 and NH3 clusters
[MPIS-6/1988] N89-28373
Infrared photodissociation of van der Waals complexes selectively prepared by molecular beam scattering N89-28376
CAMAC time-of-flight analyzer for molecular beam diagnostics N89-28377
MOLECULAR BIOLOGY
Molecular biology of the photoregulation of photosynthetic light-harvesting complexes in marine dinoflagellates
[AD-A209650] N89-28198
MOLECULAR CHAINS
Electronic properties of ordered ladder polymers
[AD-A207288] N89-27832
Polymer chain configurations in constrained geometries: Ultrathin films for microlithography
[AD-A208692] N89-27849
Calculation of network parameters of crosslinked Markovian polymer chains
[AD-A210073] N89-27860

MOLECULAR CLOUDS
Silicon chemistry in interstellar clouds
[NASA-CR-185862] N89-28471
MOLECULAR COLLISIONS
Electrospray ionization-mass spectrometry and tandem mass spectrometry
[DE89-014465] N89-27806
Charge transfer and inelastic scattering in proton-molecule collisions
[MPIS-13/1988] N89-28378
Charge transfer and inelastic scattering in proton-molecule collisions, introduction N89-28379
MOLECULAR EXCITATION
Multiphoton detection techniques for F and F2
[AD-A208576] N89-27807
Fluorescence probes of spectroscopic and dynamical aspects of molecular photoionization
[AD-A207185] N89-28372
MOLECULAR ORBITALS
Adsorption and reactions of cyclic sulfides on Mo(110)
[AD-A207324] N89-27803
MOLECULAR OSCILLATIONS
Vibrationally excited ions: Quenching, reaction and lifetimes
[AD-A208503] N89-28386
MOLECULAR RELAXATION
Characterization of nylon 6 by 15N solid state NMR
[AD-A208508] N89-27846
Electromagnetic reaction to molecular relaxation and its effect on absorption near a rough surface
[AD-A210069] N89-28390
MOLECULAR ROTATION
The orientation of chemical bonds at surfaces: A key to understanding the structure and bonding of surface species
[AD-A209833] N89-28427
MOLECULAR SPECTROSCOPY
Multiphoton detection techniques for F and F2
[AD-A208576] N89-27807
MOLECULAR STRUCTURE
Electrospray ionization-mass spectrometry and tandem mass spectrometry
[DE89-014465] N89-27806
Preparation and characterization of several conduction transition metal oxides
[AD-A208895] N89-28424
The orientation of chemical bonds at surfaces: A key to understanding the structure and bonding of surface species
[AD-A209833] N89-28427
United States Air Force Research Initiation Program for 1987, volume 1
[AD-A209726] N89-28436
MOLYBDENUM ISOTOPES
Adsorption and reactions of cyclic sulfides on Mo(110)
[AD-A207324] N89-27803
MONITORS
Options for daytime monitoring of atmospheric visibility in optical communications N89-27895
Site selection criteria for the optical atmospheric visibility monitoring telescopes N89-27896
Possible use of a gas monitoring system in space respirometry studies N89-28223
MONOCULAR VISION
Monocular electro-optical stereo scanner N89-28125
MONOMERS
Poly(enaminonitriles): Novel materials for use in electronics
[AD-A208439] N89-27843
Polymer chain configurations in constrained geometries: Ultrathin films for microlithography
[AD-A208692] N89-27849
Transformation of a monotropic mesophase into an enantiotropic mesophase by copolymerization of the parent polymers' monomer pair containing constitutional isomeric mesogenic side groups
[AD-A208782] N89-27850
MONOPOLE ANTENNAS
An experimental and computer modeling study of stepped radius monopole antennas
[AD-A207356] N89-27919
MONOTONE FUNCTIONS
A new item response theory modeling approach with applications to unidimensionality assessment and ability estimation
[AD-A207301] N89-28360
MONTE CARLO METHOD
Monte Carlo reliability analysis
[AD-A210052] N89-28024
Improved ray tracing technique for radiative heat transfer modeling N89-28249
State-space theory of structured uncertainty with examples
[AD-A209968] N89-28339
Estimation of lower bound properties from material test data
[AD-A207378] N89-28361
MORPHOLOGY
Automatic change in contour diagrams on the occasion of scale reduction using a material morphology
[INPE-4769-PRE/1438] N89-28049
MULTIPATH TRANSMISSION
Aeronautical mobile TDMA/MCTDMA system N89-27918
Analysis of maritime mobile satellite communication systems
[AD-A207358] N89-27920
MULTIPLEXING
Calculation of planar structures for optical wavelength multiplexers N89-27942
MULTIPOLES
A fast multipole algorithm for capacitance extraction of complex 3-D geometries
[AD-A208374] N89-28317
MULTIPROCESSING (COMPUTERS)
A multiprocessor airborne lidar data system N89-28187
Load balancing in multiprocessor systems
[AD-A210144] N89-28327
Resource contention management in parallel systems
[AD-A208809] N89-28332
Parallel Architectures for Planetary Exploration Requirements (PAPER)
[NASA-CR-185370] N89-28475
MULTISPECTRAL BAND SCANNERS
Improved snow and glacier monitoring by the LANDSAT Thematic Mapper N89-28056
Multitemporal snow classification with TM data N89-28057
Comparison of MSS and TM LANDSAT data for cartography of surface structures in arid regions (southern Tunisia) N89-28087
Coastal Zone Color Scanner N89-28145
The Multichannel Ocean Color Sensor (MOCS) N89-28146
MULTISTATIC RADAR
Target signature modeling and bistatic scattering measurement studies
[NASA-CR-185434] N89-27870
MULTIVARIATE STATISTICAL ANALYSIS
Subset complement addition upper bounds: An improved inclusion/exclusion method
[AD-A208797] N89-28353

N

NASA PROGRAMS
The private sector economic and employment benefits to the nation and to each state of proposed FY 1990 NASA procurement expenditures
[NASA-CR-185894] N89-28448
The 1990 National Aeronautics and Space Administration authorization
[GPO-99-550] N89-28450
National Aeronautics and Space Administration Multiyear Authorization Act of 1989
[H-REPT-101-226] N89-28451
NASA SPACE PROGRAMS
Spacecraft and mission design for the SP-100 flight experiment N89-27717
NASTRAN
Space Shuttle Main Engine structural analysis and data reduction/evaluation. Volume 1: Aft Skirt analysis
[NASA-CR-183663] N89-27693
NATIONAL AEROSPACE PLANE PROGRAM
The 1990 National Aeronautics and Space Administration authorization
[GPO-99-550] N89-28450
National Aeronautics and Space Administration Multiyear Authorization Act of 1989
[H-REPT-101-226] N89-28451
NAVIER-STOKES EQUATION
Mach 5 inlet CFD and experimental results
[NASA-TM-102317] N89-27670
Introduction — computational fluid dynamics N89-27986
NAVIGATION INSTRUMENTS
Navigational and Environmental Measurement System (NEMS) N89-28178
NEODYMIUM
Energy transfer effects in beta-alumina
[AD-A209818] N89-27855
NEODYMIUM LASERS
A novel approach to a PPM-modulated frequency-doubled electro-optic cavity-dumped Nd:YAG laser N89-27897
Efficient second harmonic conversion of broadband high-peak-power Nd:glass laser radiation using large-aperture KDP crystals in quadrature
[DE89-012961] N89-28003
Multi-segment Nd:glass disk amplifiers
[DE89-014043] N89-28006
Diode-pumped laser research N89-28185
NEON
Potential energy curves for the (ArH(+)) and (NeH(+)) systems from the interplay of theory and experiments N89-28380
NEPHANALYSIS
Cloud/cryosphere interactions
[AD-A208377] N89-28196
NETWORK ANALYSIS
Study on the applicability of Asynchronous Time Division (ATD) techniques to satellite communications systems
[ESA-CR(P)-2742] N89-27943
Basic research in reliability for real systems
[AD-A209649] N89-28022
Personal computers on Ethernet N89-28175
NETWORK CONTROL
MSAT signalling and network management architectures N89-27916
Synchronization of the receiver for the ISDN basic connection N89-27933
Personal computers on Ethernet N89-28175
COMM-Q: A simulation model to determine saturation points in nodal type networks
[AD-A207294] N89-28329
NEURAL NETS
System theoretic models for high density VLSI structures
[AD-A209901] N89-27968
A survey of visual preprocessing and shape representation techniques
[NASA-CR-185418] N89-28309
The back propagation technique for modeling cortical computation
[AD-A209855] N89-28323
NEUROLOGY
Identification of variables determining intrahemispheric interference between processing demands
[AD-A208435] N89-28299
NEUROMUSCULAR TRANSMISSION
Identification of variables determining intrahemispheric interference between processing demands
[AD-A208435] N89-28299
NEUROPHYSIOLOGY
Modulation of spontaneous brain activity during mental imagery
[AD-A209918] N89-28208
NEUTRAL ATMOSPHERES
Electrodynamics, wind and temperature N89-28168
NEUTRAL BEAMS
Development of high-current RF plasma sources for neutral particle injections N89-27785
NEUTRAL SHEETS
Electrodynamics, wind and temperature N89-28168
NEWS
Meteorology in the press
[INPE-4762-PRE/1432] N89-28114
NEWS MEDIA
Meteorology in the press
[INPE-4762-PRE/1432] N89-28114
NICKEL
Laser cladding of Ni, Nb, Mg alloys for improved environmental resistance at high temperatures
[AD-A210134] N89-27830
NICKEL ALLOYS
The structure and properties of grain boundaries in B2 ordered alloys
[DE89-013266] N89-27817
Martensitic phase transitions in nanocrystalline materials
[AD-A208804] N89-27827
NICKEL HYDROGEN BATTERIES
Thermal control of Ni-H2 battery — spacecraft battery N89-28276
NIOBIUM
Laser cladding of Ni, Nb, Mg alloys for improved environmental resistance at high temperatures
[AD-A210134] N89-27830
Thermophysical properties of liquid niobium
[DE89-014288] N89-28435
NIOBIUM ALLOYS
Effect of alloying, rapid solidification, and surface kinetics on the high temperature environmental resistance of niobium
[AD-A209934] N89-27829
NITRIC ACID
Corrosion of aluminium alloys by IRFNA (Inhibited Red Fuming Nitric Acid)
[AD-A208326] N89-27823
NITRIC OXIDE
Tropospheric nitric oxide measurements N89-28171

NITRIDING
Advanced tribological coatings for high specific strength alloys
[AD-A208504] N89-27825
NITRILES
Poly(enaminonitriles): Novel materials for use in electronics
[AD-A208439] N89-27843
NITROGEN OXIDES
Fluorescence probes of spectroscopic and dynamical aspects of molecular photoionization
[AD-A207185] N89-28372
NITROGEN PLASMA
Characteristics of free-floating nitrogen and helium plasmas generated in a microwave resonant cavity N89-27771
Coupling between radiation and gas dynamics
[AD-A209657] N89-28102
NITROGEN POLYMERS
Birth, death and transfiguration: The synthesis of preceramic polymers, their pyrolysis and their conversion to ceramics
[AD-A208437] N89-27841
NOISE TEMPERATURE
DSN 70-meter antenna X- and S-band calibration. Part 2: System noise temperature measurements and telecommunications link evaluation N89-27905
NONCONDENSABLE GASES
Non-condensible gas effects on the low-temperature heat pipe characteristics N89-28227
NONDESTRUCTIVE TESTS
Ultrasonic nondestructive evaluation of damage in continuous fiber composites
[AD-A208840] N89-27799
NONLINEAR EQUATIONS
Some problems in nonlinear analysis
[AD-A209991] N89-28357
NONLINEAR EVOLUTION EQUATIONS
Nonlinear waves
[AD-A209822] N89-27993
Analysis and numerical analysis of some properly and improperly posed problems in applied mathematics
[AD-A208633] N89-28350
NONLINEAR FEEDBACK
Non-linear dynamics and chaotic motions in feedback controlled elastic system
[AD-A208628] N89-28041
Studies in stabilization and control of beams and plates
[AD-A208635] N89-28042
NONLINEAR FILTERS
Research in stochastic processes
[AD-A209935] N89-28364
NONLINEAR OPTICS
Nonlinear waves
[AD-A209822] N89-27993
NONLINEAR SYSTEMS
Electronics research at the University of Texas at Austin
[AD-A209989] N89-27970
NONLINEARITY
A new method for analysis of limit cycle behavior of the NASA/JPL 70-meter antenna axis servos N89-27880
Nonlinear waves
[AD-A209822] N89-27993
NONSTABILIZED OSCILLATION
Model based damping of coupled horizontal and vertical oscillations in a flexible rod
[DE89-007034] N89-28039
NORMAL DENSITY FUNCTIONS
Subset complement addition upper bounds: An improved inclusion/exclusion method
[AD-A208797] N89-28353
NORWAY
LANDSAT-5 TM study of suspended sediments in a fjord system in western Norway N89-28064
LANDSAT TM data used in the mapping of large-scale geological structures in coastal areas in Trondelag, central Norway N89-28072
NOTCH SENSITIVITY
Analysis and elimination of high temperature notch induced microcrack initiation in Inconel 718 nickel-based alloy
[AD-A209695] N89-27828
NOZZLE EFFICIENCY
Nozzle type MPD thruster experimental investigations N89-27727
An improved code for nozzle type steady state MPD thrusters N89-27735
Anode-nozzle experimental analysis in a coaxial non-steady solid propellant MPD thruster N89-27757
NOZZLE FLOW
An improved code for nozzle type steady state MPD thrusters N89-27735
Computational investigation on the characteristics of a low power dc arcjet thruster N89-27777
A method for calculating asymmetric flow through nozzles
[AD-A209689] N89-27992
NOZZLE GEOMETRY
Nozzle type MPD thruster experimental investigations N89-27727
A method for calculating asymmetric flow through nozzles
[AD-A209689] N89-27992
NOZZLE THRUST COEFFICIENTS
An improved code for nozzle type steady state MPD thrusters N89-27735
NUCLEAR FUELS
An analysis of severe air transport accidents
[DE89-012642] N89-27642
NUCLEAR MAGNETIC RESONANCE
Characterization of nylon 6 by 15N solid state NMR
[AD-A208508] N89-27846
NUCLEAR RADIATION
Detection of artificial sources of nuclear radiation in space, revision
[AD-A209720] N89-28480
Monitoring sources of nuclear radiation in space. Part 1: Early 1984 observations, revision
[AD-A209721] N89-28481
Monitoring sources of nuclear radiation in space 1980-1984 observations, revision
[AD-A209722] N89-28482
Monitoring sources of nuclear radiation in space 1985-1987 observations, revision
[AD-A209723] N89-28483
NUCLEAR ROCKET ENGINES
Spacecraft and mission design for the SP-100 flight experiment N89-27717
Ultimate performance limits and mission capabilities of advanced ion thrusters N89-27764
KREM: A model for evaluating orbital transfer vehicles utilizing nuclear electric propulsion systems N89-27789
NUCLEAR WEAPONS
Critical technologies plan for the Committees on Armed Services, United States Congress, revision
[AD-A210170] N89-28439
NUMBER THEORY
Particle sizing in solid rocket motors
[AD-A208740] N89-27793
NUMERICAL STABILITY
Implicit time dependent methods for inviscid and viscous compressible flows, with a discussion of the concept of numerical dissipation N89-27990
NUMERICAL WEATHER FORECASTING
Adaptive grid methods for numerical weather prediction
[AD-A209950] N89-28117
NUTRITION
Molecular biology of the photoregulation of photosynthetic light-harvesting complexes in marine dinoflagellates
[AD-A209650] N89-28198
NUTRITIONAL REQUIREMENTS
Nutrition for short-duration space missions N89-28265
NYLON (TRADEMARK)
Nonlinear viscoelastic characteristics of polymeric materials
[DE89-012680] N89-27835
Characterization of nylon 6 by 15N solid state NMR
[AD-A208508] N89-27846

O

OCEAN COLOR SCANNER
Oceanographic wide field sensor N89-28132
Ocean color observations of phytoplankton distributions and primary productivity N89-28137
OCEAN CURRENTS
Microwave remote sensing of sea ice N89-28148
Wave/current interaction model N89-28153
Ocean Drifter Project N89-28154
Wind-Wave-Current Tank Research Facility usage and status N89-28161
OCEAN DATA ACQUISITIONS SYSTEMS
Airborne Oceanographic Lidar (AOL) flight mission participation N89-28143
Ocean Data Acquisition System N89-28144
OCEAN DYNAMICS
Analysis of sea ice dynamics N89-28149
Microscale ocean dynamics N89-28157
The Surface Wave Dynamics Experiment (SWADE) N89-28162
OCEAN MODELS
Satellite image analysis for marine applications
[PB89-187330] N89-28053
Analyses of the wind-driven response of tropical oceans N89-28155
Ocean modelling and the use of altimetry data
[AD-A206841] N89-28195
OCEAN SURFACE
Determination of local empirical covariance functions from residual terrain reduced altimeter data
[AD-A208678] N89-28095
Coastal Zone Color Scanner N89-28145
Surface Contour Radar (SCR) contributions to FASINEX N89-28159
Rainfall on microwave return from the sea surface N89-28160
Modeling of ocean surface spectrum and surface scattering. Applications to reverberation prediction in the AAUS program
[AD-A210127] N89-28197
Fixed interval smoothing algorithm for an extended Kalman filter for over-the-horizon ship tracking
[AD-A208555] N89-28318
OCEANOGRAPHIC PARAMETERS
Oceanographic applications of laser technology N89-28141
OCEANOGRAPHY
Laboratory for Oceans
[NASA-TM-101257] N89-28118
Ocean topography experiment (TOPEX) radar altimeter N89-28119
Oceanographic wide field sensor N89-28132
Applications of the Coastal Zone Color Scanner in oceanography N89-28136
NASA Charge Coupled Device (CCD) Spectrometer System (NCSS) N89-28142
Airborne Oceanographic Lidar (AOL) flight mission participation N89-28143
The Laboratory for Oceans Computing Facility N89-28173
A multiprocessor airborne lidar data system N89-28187
OFF-ON CONTROL
Singular and bang-bang stochastic control
[AD-A208627] N89-28337
ON-LINE SYSTEMS
Conversion of mass storage hierarchy in an IBM computer network
[AD-A208520] N89-28330
Problems and solutions in online documentation systems
[DE89-014092] N89-28447
ONBOARD DATA PROCESSING
Database development for the DMSP (Defense Meteorological Satellite Program) SSIES experiment
[AD-A208712] N89-27691
ONBOARD EQUIPMENT
Interplanetary Particle Environment. Proceedings of a Conference
[NASA-CR-185461] N89-28454
OPERATING SYSTEMS (COMPUTERS)
Theft of information in the take-grant protection model
[NASA-CR-185835] N89-28444
OPTICAL COMMUNICATION
The Telecommunications and Data Acquisition Report
[NASA-CR-185431] N89-27871
A visibility characterization program for optical communications through the atmosphere N89-27894
Options for daytime monitoring of atmospheric visibility in optical communications N89-27895
Site selection criteria for the optical atmospheric visibility monitoring telescopes N89-27896
A novel approach to a PPM-modulated frequency-doubled electro-optic cavity-dumped Nd:YAG laser N89-27897
OPTICAL COMPUTERS
Fiber-optic delay line storage in digital optical computers based on directional couplers
[PB89-185318] N89-28392
OPTICAL COUPLING
Pigtailed single-mode diode lasers
[AD-A209913] N89-28012
OPTICAL DATA PROCESSING
Integrated opto-electronic computing
[AD-A209936] N89-28395
OPTICAL EMISSION SPECTROSCOPY
Optical emission spectrum of the UK-10 ion thruster operating on xenon N89-27781
Optical spectroscopy of copper (1) doped Na(+) beta-alumina
[AD-A209819] N89-27810
OPTICAL EQUIPMENT
Pigtailed single-mode diode lasers
[AD-A209913] N89-28012
Generalized beamforming with multiple computer originated holograms
[AD-A210175] N89-28397
OPTICAL FIBERS
Requirements for a technical data base N89-27930

Compensation for effects of ambient temperature on rare-earth doped fiber optic thermometer [NASA-TM-102282] N89-27998
High-temperature optical-fiber pH sensor [DE89-014103] N89-28000
Fiber-optic delay line storage in digital optical computers based on directional couplers [PB89-185318] N89-28392

OPTICAL MATERIALS
Crystal chemistry, synthesis, and characterization of infrared optical materials [AD-A208723] N89-28422

OPTICAL MEASUREMENT
The effects of atmospheric turbulence on precision optical measurements used for antenna-pointing compensation N89-27883

OPTICAL MEASURING INSTRUMENTS
Compensation for effects of ambient temperature on rare-earth doped fiber optic thermometer [NASA-TM-102282] N89-27998
High-temperature optical-fiber pH sensor [DE89-014103] N89-28000

OPTICAL PATHS
Development of superlattices for ultra high-speed electronic and optoelectronic devices [AD-A209874] N89-28429

OPTICAL PROPERTIES
In-orbit degradation of thermo-optical properties on MARECS GEO-satellite N89-28297
Semiconductor-olefin adducts. Photoluminescent properties of cadmium sulfide and cadmium selenide in the presence of butenes [AD-A208348] N89-28419

OPTICAL PUMPING
Multi-segment Nd:glass disk amplifiers [DE89-014043] N89-28006

OPTICAL RADAR
GMBU (Ground Mobile Breadboard Upgrade) lidar and bubbler correlation study at Dugway Proving Ground [AD-A207297] N89-28002
YAG aerosol lidar N89-28135
Airborne Oceanographic Lidar (AOL) flight mission participation N89-28143
Mobile lidar system for measurement of water vapor mixing ratio and ozone number density N89-28166
Airborne lidar global positioning investigations N89-28179
Large aperture scanning airborne lidar N89-28186
A multiprocessor airborne lidar data system N89-28187

OPTICAL SCANNERS
Monocular electro-optical stereo scanner N89-28125

OPTICAL TRACKING
Optical spatial tracking using coherent detection in the pupil plane [AD-A209970] N89-28209

OPTICAL WAVEGUIDES
Calculation of planar structures for optical wavelength multiplexers N89-27942

OPTIMIZATION
Optimization of maneuvers of a spin-stabilized satellite, using magnetic coils [INPE-4778-TDL/350] N89-27680
Equipment models for process optimization and control using smart response surfaces [AD-A208321] N89-27838
DSN 70-meter antenna microwave optics design and performance improvements. Part 1: Design optimization N89-27903
Communications using channels formed by meteor bursts [AD-A209656] N89-27949
Design of experiments and reliability models [AD-A209880] N89-28023
The potential application of the blackboard model of problem solving to multidisciplinary design [NASA-TM-101633] N89-28314
Approaches to multi-level sequential logic synthesis [AD-A208322] N89-28316
Control and system theory, optimization, inverse and ill-posed problems [AD-A208570] N89-28335
The principal pivoting method revisited [AD-A208796] N89-28352

OPTOELECTRONIC DEVICES
Development of superlattices for ultra high-speed electronic and optoelectronic devices [AD-A209874] N89-28429

ORBIT CALCULATION
GPS (Global Positioning System) orbit determination: Bootstrapping to resolve carrier phase ambiguity [AD-A209974] N89-27681

ORBIT TRANSFER VEHICLES
Electrical transfer vehicle analysis for future space operations (MESCATS) N89-27750
KREM: A model for evaluating orbital transfer vehicles utilizing nuclear electric propulsion systems N89-27789

ORBITAL MANEUVERS
Optimization of maneuvers of a spin-stabilized satellite, using magnetic coils [INPE-4778-TDL/350] N89-27680

ORGANIC MATERIALS
Airborne in-situ spectral characterization and concentration estimates of fluorescent organics as a function of depth N89-28140

ORGANIC SULFUR COMPOUNDS
Novel approaches to ionic chromatography [DE89-013942] N89-27805

ORGANOMETALLIC COMPOUNDS
Decomposition kinetics and film formation of an organometallic precursor to SiC on Si(100) [AD-A208384] N89-28420

ORGANOMETALLIC POLYMERS
Birth, death and transfiguration: The synthesis of preceramic polymers, their pyrolysis and their conversion to ceramics [AD-A208437] N89-27841

ORTHOGONALITY
Orthogonal sets of data windows constructed from trigonometric polynomials N89-27902
Design of experiments and reliability models [AD-A209880] N89-28023

ORTHOPHOTOGRAPHY
Analog methods and instruments N89-28094

OSCILLATING FLOW
Analysis of pressure drop and heat transfer data from the reversing flow test facility [DE89-013907] N89-27984

OSCILLATION DAMPERS
Model based damping of coupled horizontal and vertical oscillations in a flexible rod [DE89-007034] N89-28039

OSCILLATIONS
Applications of the quartz crystal microbalance to electrochemistry [AD-A209853] N89-27812

OVER-THE-HORIZON RADAR
Fixed interval smoothing algorithm for an extended Kalman filter for over-the-horizon ship tracking [AD-A208555] N89-28318

OXIDATION
Effect of alloying, rapid solidification, and surface kinetics on the high temperature environmental resistance of niobium [AD-A209934] N89-27829

OXIDATION RESISTANCE
Effect of alloying, rapid solidification, and surface kinetics on the high temperature environmental resistance of niobium [AD-A209934] N89-27829

OXIDATION-REDUCTION REACTIONS
The quartz crystal microbalance as an in situ tool in electrochemistry [AD-A209852] N89-27811
Applications of the quartz crystal microbalance to electrochemistry [AD-A209853] N89-27812

OXIDE FILMS
Growth and characterization of zinc sulfide films by conversion of zinc oxide films with H2S [AD-A208727] N89-28423

OXIDIZERS
The catalytic oxiderzer: Description and first results of a breadboard model for a component of the Columbus ECLSS N89-28239

OXYGEN
The use of electric propulsion techniques for LEO atomic oxygen simulation N89-27787
Separation of oxygen from seawater by membrane permeation [AD-A208863] N89-27809

OXYGEN CONSUMPTION
Effects of high terrestrial altitude on military performance [AD-A209614] N89-28201

OXYGEN SUPPLY EQUIPMENT
Separation of oxygen from seawater by membrane permeation [AD-A208863] N89-27809

OZONE
Evaluating CFC (Chlorofluorocarbon) alternatives from the atmospheric viewpoint, revision 1 [DE89-014268] N89-28108
Mobile lidar system for measurement of water vapor mixing ratio and ozone number density N89-28166
Tropospheric nitric oxide measurements N89-28171

OZONE DEPLETION
Correlative Measurements Program N89-28164
Rocket temperature soundings N89-28167

OZONOSPHERE
Rocket temperature soundings N89-28167

P

PACKAGING
An analysis of severe air transport accidents [DE89-012642] N89-27642

PACKING DENSITY
Comparison of vacuum-annealed and electrochemically cycled electrodes in adsorption and electrocatalysis: Aromatic compounds at platinum (111) and polycrystalline platinum [AD-A210011] N89-27814

PADE APPROXIMATION
Differential equations, related problems of Pade approximations and computer applications [AD-A208590] N89-28348

PANEL METHOD (FLUID DYNAMICS)
Introduction --- computational fluid dynamics N89-27986

PARABOLIC REFLECTORS
Progress in parabolic dish technology [DE89-009427] N89-28100

PARALLEL PROCESSING (COMPUTERS)
Performance augmentation of SITIM-150 through a high performance numerical processor [INPE-4770-PRE/1439] N89-28305
ParaGraph-RTS: A parallel reduction-based run-time system [DE89-005457] N89-28315
Resource contention management in parallel systems [AD-A208809] N89-28332
Computational methods and systems for problems in science and engineering [AD-A209951] N89-28355
Parallel Architectures for Planetary Exploration Requirements (PAPER) [NASA-CR-185370] N89-28475

PARAMETER IDENTIFICATION
An approach to the parametric design of ion thrusters N89-27761
Analysis and numerical analysis of some properly and improperly posed problems in applied mathematics [AD-A208633] N89-28350
Time series modeling for structural response prediction [AD-A208808] N89-28354

PARAMETERIZATION
A numerical study of an augmented Lagrangian method for the estimation of parameters in elliptic systems [AD-A208658] N89-28351

PARTIAL DIFFERENTIAL EQUATIONS
Analysis and numerical analysis of some properly and improperly posed problems in applied mathematics [AD-A208633] N89-28350
Some problems in nonlinear analysis [AD-A209991] N89-28357

PARTICLE COLLISIONS
Lasertron: A pulsed RF-source using laser triggered photocathode [DE89-778130] N89-28008

PARTICLE INTERACTIONS
New, efficient optically pumped solid state lasers [AD-A209998] N89-28013
Particle simulations in magnetospheric plasmas [AD-A206252] N89-28106
Vibrationally excited ions: Quenching, reaction and lifetimes [AD-A208503] N89-28388

PARTICLE SIZE DISTRIBUTION
Particle sizing in solid rocket motors [AD-A208740] N89-27793
Further investigation of flow modeling during solid propellant processing [AD-A209787] N89-27866
Synchrotron X-ray fluorescence analyses of stratospheric cosmic dust: New results for chondritic and nickel-depleted particles [DE89-014032] N89-28107
Aerosol model selection using surface measurements of IR horizon radiances and satellite detected visible radiances [AD-A209638] N89-28110

PARTITIONS (MATHEMATICS)
Average interconnection length and interconnection distribution for rectangular arrays [AD-A209848] N89-27967

PATTERN RECOGNITION
Computer generated matched filters with spatial frequency tailoring [AD-A209786] N89-28001
Use of satellite imagery for the investigation of pollution-related characteristics of Dublin Bay, Ireland N89-28063
Ice sheet studies using synthetic aperture radar N89-28152

A survey of visual preprocessing and shape representation techniques
[NASA-CR-185418] N89-28309
Mode filters and their applications
[INPE-4748-PRE/1421] N89-28312
The combinatorics of heuristic search termination for object recognition in cluttered environments
[AD-A209690] N89-28363

PATTERN REGISTRATION
A smart, mapping, charting and geodesy control generator, phase 2
[AD-A208806] N89-28097
An efficient exact algorithm for the least squares image registration problem
[AD-A208725] N89-28320

PAVEMENTS
Theoretical model for stabilization of clay-silt airport pavement subgrade systems. Phase 1: Laboratory investigation. Phase 2: Rutting tests
[DOT/FAA/PM-87/20-PHASE-1/2] N89-27673

PAYLOADS
Database development for the DMSP (Defense Meteorological Satellite Program) SSIES experiment
[AD-A208712] N89-27691

PEAT
The use of Thematic Mapper imagery for peatland mapping and mineral exploration in Ireland N89-28065

PENUMBRAS
Studies of the cosmic ray penumbra
[AD-A210109] N89-28484

PERCEPTION
Pre-attentive and attentive visual information processing
[AD-A209884] N89-28206

PERCHLORIC ACID
Experimental determination of the coefficient in the steady state current equation for spherical segment microelectrodes
[AD-A208662] N89-27965

PERFLUORO COMPOUNDS
Photodegradation of polyimide 1. A spectral, viscometric, chromatographic and weight loss investigation of polyimides based on a perfluorinated dianhydride
[AD-A208507] N89-27845

PERFORMANCE PREDICTION
Blading Design for Axial Turbomachines
[AGARD-LS-167] N89-27661
Performance prediction for axial-flow compressor and turbine blading N89-27665
Aerodynamic design of low pressure turbines N89-27669
Performance calculation of an H2 arcjet by means of a dual channel model N89-27775
KREM: A model for evaluating orbital transfer vehicles utilizing nuclear electric propulsion systems N89-27789
Parameter plane design method
[AD-A209845] N89-28322

PERFORMANCE TESTS
Blading design for cooled high-pressure turbines N89-27668
An adhesive for field repair of composites
[AD-A209992] N89-27859
Indium phosphide solar cell research in the US: Comparison with nonphotovoltaic sources
[NASA-TM-102103] N89-27868
Operating and environmental characteristics of Sigma Tau hydrogen masers used in the Very Long Baseline Array (VLBA) N89-27877
Development of anodes for aluminum/air batteries: Solution phase inhibition of corrosion
[DE89-012839] N89-27956
Pigtailed single-mode diode lasers
[AD-A209913] N89-28012
Design of experiments and reliability models
[AD-A209880] N89-28023
Qualification program on stainless steel A95 heatpipe for space application N89-28294

PERMANENT MAGNETS
Advanced motor and motor control development
[AD-A207332] N89-27954

PERMEATING
Separation of oxygen from seawater by membrane permeation
[AD-A208863] N89-27809

PERMITTIVITY
Poly(enaminonitriles): Novel materials for use in electronics
[AD-A208439] N89-27843
Microwave remote sensing of soil moisture N89-28180

PERSONAL COMPUTERS
Personal computers on Ethernet N89-28175

PERSONNEL
Integrated opto-electronic computing
[AD-A209936] N89-28395

PERTURBATION
Terminal shock response in ramjet inlets to abrupt downstream perturbations
[AD-A209788] N89-27640

PERTURBATION THEORY
Modeling of ocean surface spectrum and surface scattering. Applications to reverberation prediction in the AAUS program
[AD-A210127] N89-28197

PH
High-temperature optical-fiber pH sensor
[DE89-014103] N89-28000

PHASE CONJUGATION
Extraordinary behavior of atoms near a phase conjugator
[AD-A209946] N89-28389

PHASE DIAGRAMS
Application of quaternary phase diagrams to compound semiconductor processing
[DE89-014537] N89-28413

PHASE MODULATION
The use of interleaving for reducing radio loss in trellis-coded modulation systems N89-27889
The DSS-14 C-band exciter N89-27901

PHASE SHIFT
Speckle interferometry using fiber optic phase stepping
[NASA-TM-102331] N89-27999

PHASE SHIFT KEYING
Why is CDMA the solution for mobile satellite communication N89-27912
Aeronautical mobile TDMA/MCTDMA system N89-27918
Minimum shift keying. A modulation system with coding N89-27931

PHASE TRANSFORMATIONS
Martensitic phase transitions in nanocrystalline materials
[AD-A208804] N89-27827
The influence of the polymer backbone flexibility on the phase transitions of side chain liquid crystal polymers containing
yl side groups
[AD-A208821] N89-27851

PHASED ARRAYS
DARPA (Defense Advanced Research Projects Agency) Review on EHF Devices
[AD-A208564] N89-27963

PHENANTHRENE
Electronic properties of ordered ladder polymers
[AD-A207288] N89-27832

PHENOLS
The influence of the polymer backbone flexibility on the phase transitions of side chain liquid crystal polymers containing
yl side groups
[AD-A208821] N89-27851

PHOSPHATES
Vapor phase deposition studies of phosphate esters on metal and ceramic surfaces
[PB89-148985] N89-27831

PHOSPHAZENE
The influence of the polymer backbone flexibility on the phase transitions of side chain liquid crystal polymers containing
yl side groups
[AD-A208821] N89-27851

PHOTOCATHODES
Lasertron: A pulsed RF-source using laser triggered photocathode
[DE89-778130] N89-28008

PHOTOCHEMICAL REACTIONS
A soluble photosensitive polyimide
[AD-A209634] N89-27854
Tropospheric nitric oxide measurements N89-28171
The phototoxicity of blue light on the functional properties of the retinal pigment epithelium
[AD-A209834] N89-28204
Silicon chemistry in interstellar clouds
[NASA-CR-185862] N89-28471

PHOTODECOMPOSITION
Photodegradation of polyimide 1. A spectral, viscometric, chromatographic and weight loss investigation of polyimides based on a perfluorinated dianhydride
[AD-A208507] N89-27845

PHOTODIODES
Effective amplifier noise for an optical receiver based on linear mode avalanche photodiodes N89-27893
Band structure engineering for ultra-low threshold laser diodes
[AD-A208629] N89-28010

PHOTODISSOCIATION
Vibrational predissociation of shock-selected C2H4 and NH3 clusters
[MPIS-6/1988] N89-28373
Vibrational predissociation of shock-selected C2H4 and NH3 clusters, introduction N89-28374
Infrared photodissociation and cluster-specific detection of internally cold (C2H4) van der Waals complexes N89-28375
Infrared photodissociation of van der Waals complexes selectively prepared by molecular beam scattering N89-28376
CAMAC time-of-flight analyzer for molecular beam diagnostics N89-28377

PHOTOGRAMMETRY
Photogrammetric technique for in-flight ranging of trailing vortices using entrained balloons
[NASA-TM-4129] N89-27995
Reports on cartography and geodesy. Special issue: History of photogrammetry, number 1
[ISSN-0344-5879] N89-28092
The early period of photogrammetry till the invention of the aircraft N89-28093
Analog methods and instruments N89-28094

PHOTOINTERPRETATION
Classification of small-scale forests in Flanders using LANDSAT TM digital data: Preliminary results N89-28080
Use of LANDSAT TM data for forest damage inventory N89-28082
Use of remote sensing in mapping of vegetation in the Dividalen area central Troms, northern Norway N89-28083
Northeast Artificial Intelligence Consortium annual report 1987. Volume 6: Artificial intelligence applications to speech recognition
[AD-A208380] N89-28334

PHOTOIONIZATION
Fluorescence probes of spectroscopic and dynamical aspects of molecular photoionization
[AD-A207185] N89-28372
Semiconductor-olefin adducts. Photoluminescent properties of cadmium sulfide and cadmium selenide in the presence of butenes
[AD-A208348] N89-28419

PHOTOLITHOGRAPHY
Polymer chain configurations in constrained geometries: Ultrathin films for microlithography
[AD-A208692] N89-27849

PHOTOLUMINESCENCE
Selective detector for gas chromatography based on adduct-modulated semiconductor photoluminescence
[AD-A208616] N89-27808
Semiconductor-olefin adducts. Photoluminescent properties of cadmium sulfide and cadmium selenide in the presence of butenes
[AD-A208348] N89-28419

PHOTOLYSIS
Photodegradation of polyimide 1. A spectral, viscometric, chromatographic and weight loss investigation of polyimides based on a perfluorinated dianhydride
[AD-A208507] N89-27845

PHOTOMAPPING
Comparison of MSS and TM LANDSAT data for cartography of surface structures in arid regions (southern Tunisia) N89-28087
Tests of topographic mapping with Thematic Mapper images N89-28091

PHOTONS
Effective amplifier noise for an optical receiver based on linear mode avalanche photodiodes N89-27893
Theory of photon-drag effect in bulk magnetic semiconductors
[DE89-612214] N89-28417

PHOTOSENSITIVITY
A soluble photosensitive polyimide
[AD-A209634] N89-27854

PHOTOSYNTHESIS
Molecular biology of the photoregulation of photosynthetic light-harvesting complexes in marine dinoflagellates
[AD-A209650] N89-28198

PHOTOVOLTAIC CELLS
NASA advanced space photovoltaic technology-status, potential and future mission applications
[NASA-TM-102093] N89-27705

PHOTOVOLTAIC CONVERSION
Photovoltaic Program Branch annual report, FY 1988
[DE89-000898] N89-28099

PHYSIOLOGICAL EFFECTS
Effects of high terrestrial altitude on military performance
[AD-A209614] N89-28201

PHYSIOLOGICAL FACTORS
EVA and human physiology N89-28246

PHYSIOLOGICAL RESPONSES
Thermal modelling of the EVA-suited astronaut N89-28245

PHYTOPLANKTON
Applications of the Coastal Zone Color Scanner in oceanography N89-28136
Ocean color observations of phytoplankton distributions and primary productivity N89-28137
Remote sensing of ocean color in the Arctic N89-28139
Oceanographic applications of laser technology N89-28141
Molecular biology of the photoregulation of photosynthetic light-harvesting complexes in marine dinoflagellates
[AD-A209650] N89-28198
PIEZOELECTRIC CERAMICS
Piezoelectric polymer/ceramic composite
[AD-A208905] N89-27801
PIEZOELECTRICITY
Piezoelectric polymer/ceramic composite
[AD-A208905] N89-27801
Applications of the quartz crystal microbalance to electrochemistry
[AD-A209853] N89-27812
PIGMENTS
Ocean color observations of phytoplankton distributions and primary productivity N89-28137
The phototoxicity of blue light on the functional properties of the retinal pigment epithelium
[AD-A209834] N89-28204
PILOT PERFORMANCE
Identification of variables determining intrahemispheric interference between processing demands
[AD-A208435] N89-28299
PILOT SELECTION
Anthropometric measurements of aviators within the Aviation Epidemiology Data Register
[AD-A208609] N89-28300
PIPE FLOW
ESATAN FHTS: A piped fluid network capability N89-28281
PITCHING MOMENTS
Summary of longitudinal stability and control parameters as determined from Space Shuttle Challenger flight test data
[NASA-TM-101605] N89-27671
PIXELS
Digital CODEC for real-time processing of broadcast quality video signals at 1.8 bits/pixel
[NASA-TM-102325] N89-27927
PLAINS
Processing and interpretation of Thematic Mapper images in the Province of Placenza (Italy) N89-28088
PLANAR STRUCTURES
Calculation of planar structures for optical wavelength multiplexers N89-27942
Claw-free maximal planar graphs
[AD-A210179] N89-28359
PLANT DISEASES
Use of LANDSAT TM data for forest damage inventory N89-28082
PLASMA ACCELERATORS
Cylindrical steady-state MPD thruster N89-27725
Current driven instabilities of an electromagnetically accelerated plasma N89-27736
PLASMA ARC WELDING
Rapidly solidified titanium alloys by melt overflow
[NASA-CR-4253] N89-27818
PLASMA COMPRESSION
Efficient energy storage and conversion using adiabatic compression of relativistic-electron plasmas
[AD-A208657] N89-28101
PLASMA CONTROL
Antiproton powered propulsion with magnetically confined plasma engines
[NASA-CR-185131] N89-27700
A tandem mirror hybrid plume plasma propulsion facility N89-27791
PLASMA CURRENTS
Definition study and model for a tethered sounding rocket
[AD-A207367] N89-27699
Current driven instabilities of an electromagnetically accelerated plasma N89-27736
Hybrid MPD thruster with axial and cusp magnetic fields N89-27744
Role of edge magnetic shear on the limiter H-mode transition of the JIPP T-IIU tokamak
[IPPJ-906] N89-28399
PLASMA DENSITY
Analytical and numerical solutions for cylindrical blast waves in a plasma of varying density N89-27767
Scaling laws for the spectrum of interchange instabilities in the high latitude ionosphere
[AD-A209993] N89-28111
PLASMA DIAGNOSTICS
Discharge plasma calculations in cusped ion thrusters using the finite element method N89-27760
Characteristics of free-floating nitrogen and helium plasmas generated in a microwave resonant cavity N89-27771
Diagnostic tools for an ion thruster in space N89-27782
PLASMA ENGINES
Antiproton powered propulsion with magnetically confined plasma engines
[NASA-CR-185131] N89-27700
PLASMA EQUILIBRIUM
Extension of stellarator approximation in magnetohydrodynamic equilibrium and stability of toroidal helical systems
[IPPJ-905] N89-28400
PLASMA ETCHING
Solid state research
[AD-A209969] N89-28431
PLASMA GENERATORS
ZPIMP: A zero-D Z-pinch implosion code
[AD-A208381] N89-27962
A two-stream plasma electron microwave source for high-power millimeter wave generation, phase 1
[AD-A209942] N89-28404
PLASMA HEATING
Numerical and experimental investigations of a propagating microwave-heated plasma N89-27772
Role of edge magnetic shear on the limiter H-mode transition of the JIPP T-IIU tokamak
[IPPJ-906] N89-28399
Experimental study on the deposition profile of the ICRF power and electron thermal diffusivity
[IPPJ-908] N89-28401
PLASMA INTERACTIONS
Interaction of high voltage solar array with ionospheric plasma N89-27719
The interaction between a positively biased conductor on a high voltage solar array and a plasma N89-27720
PLASMA JET WIND TUNNELS
Steady state MPD devices for reentry simulation N89-27783
PLASMA JETS
Discharge plasma calculations in cusped ion thrusters using the finite element method N89-27760
PLASMA PROPULSION
Antiproton powered propulsion with magnetically confined plasma engines
[NASA-CR-185131] N89-27700
Performance of a 100 kW class applied field MPD thruster
[NASA-TM-102312] N89-27701
Plasma propulsion activites at SNIA BPD N89-27716
Development of an MPD propulsion system N89-27718
Cylindrical steady-state MPD thruster N89-27725
Nozzle type MPD thruster experimental investigations N89-27727
Numerical codes for cylindrical MPD thrusters N89-27733
Fluid mechanics in a magnetoplasmadynamic thruster N89-27734
Current driven instabilities of an electromagnetically accelerated plasma N89-27736
Investigation of instabilities in MPD thruster flows using a linear dispersion relation N89-27737
Verification of performance and endurance of capacitor bank for the electric propulsion experiment (EPEX) N89-27739
Verification of control sequence and algorithm for the electric propulsion experiment (EPEX) N89-27740
Continuous operation of a quasi-steady MPD propulsion system with an external magnetic field N89-27742
Optimization of current distribution in an applied-field MPD thruster N89-27743
Hybrid MPD thruster with axial and cusp magnetic fields N89-27744
Cathode processes in a MPD arcjet N89-27753
Thermal design improvements for 30kWe arcjet engine N89-27754
Electrode erosion in steady-state electric propulsion engines N89-27755
Characterization of cold cathode erosion processes N89-27756
Anode-nozzle experimental analysis in a coaxial non-steady solid propellant MPD thruster N89-27757
Discharge plasma calculations in cusped ion thrusters using the finite element method N89-27760
Quantitative imaging of MPD flow fields N89-27766
Performance calculation of an H2 arcjet by means of a dual channel model N89-27775
A tandem mirror hybrid plume plasma propulsion facility N89-27791
PLASMA RADIATION
Studies of the propagation of short burst, high power microwave radiation through neutral and ionized media
[AD-A208664] N89-27944
ZPIMP: A zero-D Z-pinch implosion code
[AD-A208381] N89-27962
PLASMA WAVES
Analytical and numerical solutions for cylindrical blast waves in a plasma of varying density N89-27767
Numerical and experimental investigations of a propagating microwave-heated plasma N89-27772
A two-stream plasma electron microwave source for high-power millimeter wave generation, phase 1
[AD-A209942] N89-28404
PLASMAS (PHYSICS)
ZPIMP: A zero-D Z-pinch implosion code
[AD-A208381] N89-27962
Particle simulations in magnetospheric plasmas
[AD-A206252] N89-28106
Experimental study on the deposition profile of the ICRF power and electron thermal diffusivity
[IPPJ-908] N89-28401
Review of effects of NBI (Neutral Beam Injection) and rotation on plasma transport in tokamaks
[DE89-014109] N89-28402
PLASMATRONS
Development of high-current RF plasma sources for neutral particle injections N89-27785
PLASTIC DEFORMATION
Simulation of deformation and texture evolution in semi-crystalline polymers
[AD-A208854] N89-27852
Mechanical and physical study of the behavior under sequential loads of copper and steel plates
[ETN-89-94805] N89-28037
Plastic deformation of granular materials
[AD-A208589] N89-28040
Polycrystalline plastic deformation and texture evolution for crystals lacking five independent slip systems
[AD-A208902] N89-28425
PLATES
The Shock and Vibration Digest, volume 21, no. 4 N89-28025
PLATES (STRUCTURAL MEMBERS)
Recent advances on the dynamic behavior of stiffened plates N89-28027
PLATINUM
Comparison of vacuum-annealed and electrochemically cycled electrodes in adsorption and electrocatalysis: Aromatic compounds at platinum (111) and polycrystalline platinum
[AD-A210011] N89-27814
PLUMES
Investigation of a liquid-fed water resistojet plume
[NASA-TM-102310] N89-27706
Particle sizing in solid rocket motors
[AD-A208740] N89-27793
PLUTONIUM
An analysis of severe air transport accidents
[DE89-012642] N89-27642
POINTING CONTROL SYSTEMS
The Telecommunications and Data Acquisition Report
[NASA-CR-185431] N89-27871
Application of optimal control theory to the design of the NASA/JPL 70-meter antenna servos N89-27881
Precision pointing compensation for DSN antennas with optical distance measuring sensors N89-27882
The effects of atmospheric turbulence on precision optical measurements used for antenna-pointing compensation N89-27883
POLAR REGIONS
Mapping winter grazing areas for reindeer on Svalbard using LANDSAT Thematic Mapper data N89-28075
POLARIMETERS
Agriculture Multiband Experiment Radiometer N89-28184
POLICIES
Design of experiments and reliability models
[AD-A209880] N89-28023
POLLUTION MONITORING
Environmental effects of space shuttle exhaust on materials
[AD-A208813] N89-27686
Analytical procedures for environmental quality control, volume 2
[PB89-158612] N89-28103
Analytical procedures for environmental quality control, volume 3
[PB89-158620] N89-28104
POLYCRYSTALS
Comparison of vacuum-annealed and electrochemically cycled electrodes in adsorption and electrocatalysis: Aromatic compounds at platinum (111) and polycrystalline platinum
[AD-A210011] N89-27814
Martensitic phase transitions in nanocrystalline materials
[AD-A208804] N89-27827

Polycrystalline plastic deformation and texture evolution for crystals lacking five independent slip systems
[AD-A208902] N89-28425

POLYESTERS
Nonlinear viscoelastic characteristics of polymeric materials
[DE89-012680] N89-27835

POLYETHER RESINS
Energetic polyoxetane thermoplastic elastomers: Synthesis and characterization
[AD-A209612] N89-27853

POLYETHYLENES
Piezoelectric polymer/ceramic composite
[AD-A208905] N89-27801
Simulation of deformation and texture evolution in semi-crystalline polymers
[AD-A208854] N89-27852

POLYHEDRONS
Automatic construction of polyhedral surfaces from voxel representations
[AD-A210009] N89-28325

POLYIMIDE RESINS
Photodegradation of polyimide 1. A spectral, viscometric, chromatographic and weight loss investigation of polyimides based on a perfluorinated dianhydride
[AD-A208507] N89-27845
A soluble photosensitive polyimide
[AD-A209634] N89-27854

POLYIMIDES
Electron beam-positive polyimides
[AD-A208440] N89-27844
Photodegradation of polyimide 1. A spectral, viscometric, chromatographic and weight loss investigation of polyimides based on a perfluorinated dianhydride
[AD-A208507] N89-27845

POLYMER CHEMISTRY
Electronic properties of ordered ladder polymers
[AD-A207288] N89-27832
Birth, death and transfiguration: The synthesis of preceramic polymers, their pyrolysis and their conversion to ceramics
[AD-A208437] N89-27841

POLYMER PHYSICS
Characterization of nylon 6 by 15N solid state NMR
[AD-A208508] N89-27846

POLYMERIC FILMS
Capacitors for pulsed electric propulsion N89-27790
Electronic properties of ordered ladder polymers
[AD-A207288] N89-27832
Photodegradation of polyimide 1. A spectral, viscometric, chromatographic and weight loss investigation of polyimides based on a perfluorinated dianhydride
[AD-A208507] N89-27845
Characterization of structure in thin polymer resist films
[AD-A208677] N89-27848
Polymer chain configurations in constrained geometries: Ultrathin films for microlithography
[AD-A208692] N89-27849

POLYMERIZATION
Poly(enaminonitriles): Novel materials for use in electronics
[AD-A208439] N89-27843
Electron beam-positive polyimides
[AD-A208440] N89-27844
Characterization of nylon 6 by 15N solid state NMR
[AD-A208508] N89-27846
A statistical derivation of the average degree of polymerization in a stirred tank reactor
[AD-A209873] N89-27857

POLYMETHYL METHACRYLATE
Resist sensitivity enhancement by radiation-induced modification
[AD-A208438] N89-27842
Polymer chain configurations in constrained geometries: Ultrathin films for microlithography
[AD-A208692] N89-27849

POLYNOMIALS
Orthogonal sets of data windows constructed from trigonometric polynomials N89-27902
Differential equations, related problems of Pade approximations and computer applications
[AD-A208590] N89-28348

POLYQUINOXALINES
Electronic properties of ordered ladder polymers
[AD-A207288] N89-27832

POLYSTATION DOPPLER TRACKING SYSTEM
GPS (Global Positioning System) orbit determination: Bootstrapping to resolve carrier phase ambiguity
[AD-A209974] N89-27681

POLYURETHANE RESINS
High performance composites based on polyurethanes reinforced with polydiacetylenes
[AD-A208436] N89-27797

POPULATION THEORY
Estimation of lower bound properties from material test data
[AD-A207378] N89-28361

POSITION (LOCATION)
Application of optimal control theory to the design of the NASA/JPL 70-meter antenna servos N89-27881
Geostar's system architectures N89-27911

POSITION INDICATORS
Navigational and Environmental Measurement System (NEMS) N89-28178

POSITRONS
Monitoring sources of nuclear radiation in space. Part 1: Early 1984 observations, revision
[AD-A209721] N89-28481
Monitoring sources of nuclear radiation in space 1980-1984 observations, revision
[AD-A209722] N89-28482
Monitoring sources of nuclear radiation in space 1985-1987 observations, revision
[AD-A209723] N89-28483

POSTFLIGHT ANALYSIS
Flight set 360L001 (STS-26) insulation component. Volume 3: Final release
[NASA-CR-183674] N89-27698

POSTURE
Age-related changes in human posture control: Sensory organization tests
[NASA-CR-185858] N89-28212

POTABLE WATER
Hermes: Drink/food-water supply assembly N89-28264

POTENTIAL FLOW
Computation of transonic potential flow past RAE-Wing-A and Body-B2 combination
[PD-CF-8921] N89-27637

POWDER (PARTICLES)
Preparation and characterization of colloidal ZnS particles
[AD-A210171] N89-27862

POWER AMPLIFIERS
Multi-segment Nd:glass disk amplifiers
[DE89-014043] N89-28006

POWER CONDITIONING
FEEP power conditioning unit: Design and development status N89-27722
Development of a flight standard power conditioning and control system for the T5 ion thruster N89-27738
High voltage power condition systems powered by flux compression generators
[DE89-014259] N89-27959
High-performance, high-current fuses for flux compression generator driven inductive store power conditioning applications
[DE89-014274] N89-27960

POWER SPECTRA
Orthogonal sets of data windows constructed from trigonometric polynomials N89-27902
Quadratic estimators of the power spectrum
[AD-A208601] N89-27964
Scaling laws for the spectrum of interchange instabilities in the high latitude ionosphere
[AD-A209993] N89-28111
Binary sequences of arbitrary length with near-ideal correlation
[AD-A209956] N89-28356

PREBURNERS
Space Shuttle Main Engine structural analysis and data reduction/evaluation. Volume 3A: High pressure oxidizer turbo-pump preburner pump housing stress analysis report
[NASA-CR-183665] N89-27694
Space Shuttle Main Engine structural analysis and data reduction/evaluation. Volume 3B: High pressure fuel turbo-pump preburner pump bearing assembly analysis
[NASA-CR-183666] N89-27695

PRECISION
The effects of atmospheric turbulence on precision optical measurements used for antenna-pointing compensation N89-27883

PREDICTION ANALYSIS TECHNIQUES
Studies of the propagation of short burst, high power microwave radiation through neutral and ionized media
[AD-A208664] N89-27944
Time series modeling for structural response prediction
[AD-A208808] N89-28354

PREDICTIONS
Study of improved methods for predicting chemical equilibria
[DE89-014535] N89-28433
Predicting the arrival times of solar particles N89-28463

PREFLIGHT ANALYSIS
Launch window for the Brazilian Data Collecting Satellite
[INPE-4773-PRE/1442] N89-27683

PREPROCESSING
Adaptive preprocessing of nonstationary signals
[AD-A209646] N89-27945
A survey of visual preprocessing and shape representation techniques
[NASA-CR-185418] N89-28309
Image Algebra FORTRAN preprocessor: User's manual
[AD-A208612] N89-28349

PRESSURE DISTRIBUTION
Hypersonic prediction comparisons with experimental data for a cone-cylinder at mach 6.86
[AD-A207583] N89-27636
Nonlinear waves
[AD-A209822] N89-27993

PRESSURE EFFECTS
Issues and future directions in subsecond thermophysics
[DE89-014228] N89-28434

PRESSURE OSCILLATIONS
Terminal shock response in ramjet inlets to abrupt downstream perturbations
[AD-A209788] N89-27640

PRESSURE REDUCTION
Subcooled boiling of downward flow in a vertical annulus
[DE89-005320] N89-27983
Analysis of pressure drop and heat transfer data from the reversing flow test facility
[DE89-013907] N89-27984

PRESSURE REGULATORS
The atmosphere pressure control section of the Hermes ECLSS N89-28241

PRINTED CIRCUITS
Line/Circuit Analysis Program: Cross-coupling on PC (Printed Circuit) board traces including discontinuities and circuit elements
[DE89-013884] N89-27957

PRIVACY
Theft of information in the take-grant protection model
[NASA-CR-185835] N89-28444
A model of security monitoring
[NASA-CR-185845] N89-28446

PROBABILITY DISTRIBUTION FUNCTIONS
Capacity of discrete time Gaussian channel with and without feedback, 2
[AD-A207388] N89-27922
Probabilistic structural analysis methods of hot engine structures
[NASA-TM-102091] N89-28030
Information aspects of type 9 cosmological models
[DE89-012518] N89-28472

PROBABILITY THEORY
Discrete enforcement of uncertain oscillator Gaussian response
[DE89-005595] N89-28038
Subset complement addition upper bounds: An improved inclusion/exclusion method
[AD-A208797] N89-28353
Markov processes applied to control, reliability and replacement
[AD-A208634] N89-28362

PROBLEM SOLVING
Review on turbomachinery blading design problems N89-27662
The potential application of the blackboard model of problem solving to multidisciplinary design
[NASA-TM-101633] N89-28314
Northeast Artificial Intelligence Consortium annual report 1987. Volume 6: Artificial intelligence applications to speech recognition
[AD-A208380] N89-28334
Learning from physical analogies: A study in analogy and the explanation process
[AD-A208689] N89-28338
A theory of justified reformulations
[AD-A210153] N89-28340

PROCESS CONTROL (INDUSTRY)
Vapor phase deposition studies of phosphate esters on metal and ceramic surfaces
[PB89-148985] N89-27831
Comparison of equipment modeling methods as applied to the LPCVD of in-situ P-doped polysilicon
[AD-A208373] N89-27839
Growth and characterization of zinc sulfide films by conversion of zinc oxide films with H2S
[AD-A208727] N89-28423

PRODUCT DEVELOPMENT
Reports on cartography and geodesy. Special issue: History of photogrammetry, number 1
[ISSN-0344-5879] N89-28092

The early period of photogrammetry till the invention of the aircraft N89-28093
Analog methods and instruments N89-28094
CAMAC time-of-flight analyzer for molecular beam diagnostics N89-28377

PRODUCTION ENGINEERING
Requirements for a technical data base N89-27930

PROGRAMMING LANGUAGES
Efficient implementation of a description language for thermal simulators N89-28253
An implementation of a data definition facility for the graphics language for database [AD-A207380] N89-28442

PROJECT MANAGEMENT
The 1989 report to the Congress on the Strategic Defense Initiative [PB89-196661] N89-28368

PROJECT PLANNING
MHD (Magnetohydrodynamics) Program Plan, FY 1989 [DE89-012232] N89-28398

PROJECT SETI
Life science research objectives and representative experiments for the space station [NASA-TM-89445] N89-28304

PROJECTILES
Small scale testing of a mass-stabilized electromagnetic projectile [AD-A206916] N89-27662

PROPAGATION VELOCITY
Propagation characteristics of electromagnetic waves in concrete [AD-A207387] N89-27921
Sound propagation in bubbly liquids: A review [AD-A207377] N89-28370

PROPELLANT SENSITIVITY
SRM propellant, friction/ESD testing [NASA-CR-183706] N89-27864

PROPELLANT TESTS
Inert gas performance of the RIT 35 main propulsion unit N89-27770

PROPELLANT TRANSFER
The Propellant Supply and Monitoring Equipment (PSME) for the UK-10 ion propulsion subsystem N89-27758
Development of a lightweight, high strength, collapsible hose [AD-A207292] N89-28014

PROPELLANTS
Propellant selection criteria for deep space electrically propelled missions N89-27769
Inert gas performance of the RIT 35 main propulsion unit N89-27770
Pulsed laser propulsion for low cost, high volume launch to orbit [DE89-014049] N89-28009

PROPULSION SYSTEM CONFIGURATIONS
Development of an MPD propulsion system N89-27718
Nozzle type MPD thruster experimental investigations N89-27727
Status of the RITA experiment on EURECA N89-27728
The proposed demonstration of the UK-10 ion propulsion system on ESA's SAT-2 spacecraft N89-27729
Controlling a stationary orbit using electric propulsion N89-27741
Continuous operation of a quasi-steady MPD propulsion system with an external magnetic field N89-27742
Optimization of current distribution in an applied-field MPD thruster N89-27743
Electrical transfer vehicle analysis for future space operations (MESCATS) N89-27750
A small ion-propelled spacecraft for near earth experiments N89-27752

PROPULSION SYSTEM PERFORMANCE
Performance of a 100 kW class applied field MPD thruster [NASA-TM-102312] N89-27701
Spacecraft and mission design for the SP-100 flight experiment N89-27717
Design and development of the UK-10 ion propulsion subsystem N89-27730
An improved code for nozzle type steady state MPD thrusters N89-27735
Continuous operation of a quasi-steady MPD propulsion system with an external magnetic field N89-27742
Optimization of current distribution in an applied-field MPD thruster N89-27743
Ultimate performance limits and mission capabilities of advanced ion thrusters N89-27764

PROPULSIVE EFFICIENCY
Antiproton powered propulsion with magnetically confined plasma engines [NASA-CR-185131] N89-27700
Performance of a 100 kW class applied field MPD thruster [NASA-TM-102312] N89-27701
Improved thrust generation mechanism for electrothermal/electromagnetic arcjet N89-27726
Nozzle type MPD thruster experimental investigations N89-27727
Optimization of current distribution in an applied-field MPD thruster N89-27743
Hybrid MPD thruster with axial and cusp magnetic fields N89-27744
Discharge performance of a 12 cm cusp xenon ion thruster N89-27746
Magnetic induction thruster with lithium propellant N89-27762

PROTECTIVE COATINGS
Ion beam and plasma methods of producing diamondlike carbon films [NASA-TM-102301] N89-27836
Fundamental mechanisms of tribology and their implications [AD-A209941] N89-28020
United States Air Force Research Initiation Program for 1987, volume 1 [AD-A209726] N89-28436

PROTOCOL (COMPUTERS)
Software package for performing experiments about the convolutionally encoded Voyager 1 link N89-27888

PROTON BEAMS
Charge transfer and inelastic scattering in proton-molecule collisions, introduction N89-28379
Observation of vibrationally resolved charge transfer in H(+) + H2 at a collision energy Ecm = 20 eV N89-28382
A comparison between theoretical and experimental state-to-state charge transfer cross sections for H(+) + H2 at 20 eV: Evidence for quantum effects N89-28383
A three-dimensional quantum mechanical study of vibrational inelastic and charge transfer processes in H(+) + H2 at a collision energy Ecm = 20 eV N89-28384
Charge transfer and structured vibrational distributions in H(+) + CH4 low-energy collisions N89-28385

PROTON DAMAGE
Investigation of radiation effects on semiconductor devices and integrated circuits [AD-A210165] N89-27972

PROTONS
Protonic solid electrolytes: Thermal stability and conductivity of ammonium/hydronium beta'-alumina [AD-A209911] N89-27813

PROTOTYPES
Systems Engineering [AGARD-LS-164] N89-27650
Rapid prototyping of complex avionics systems N89-27657

PSYCHOLOGICAL TESTS
A new item response theory modeling approach with applications to unidimensionality assessment and ability estimation [AD-A207301] N89-28360

PSYCHOLOGY
Identification of variables determining intrahemispheric interference between processing demands [AD-A208435] N89-28299

PSYCHOMETRICS
A new item response theory modeling approach with applications to unidimensionality assessment and ability estimation [AD-A207301] N89-28360

PSYCHOMOTOR PERFORMANCE
Eye movements and visual information processing [AD-A209817] N89-28203

PSYCHOPHYSIOLOGY
Higher order mechanisms of color vision [AD-A209838] N89-28205

PULMONARY CIRCULATION
The effect of various straining maneuvers on cardiac volumes at 1G and during +Gz acceleration [AD-A208846] N89-28200

PULSE COMMUNICATION
Theory of multi-frequency modulation (MFM) digital communications [AD-A209737] N89-27947

PULSE GENERATORS
A one microsecond, thirty-five kilojoule, one hertz pulse generator [DE89-013074] N89-27955
A battery-powered flux compression generator system [DE89-014230] N89-27958
High voltage power condition systems powered by flux compression generators [DE89-014259] N89-27959
High-performance, high-current fuses for flux compression generator driven inductive store power conditioning applications [DE89-014274] N89-27960
A simultaneous helical generator [DE89-014284] N89-27961
ZPIMP: A zero-D Z-pinch implosion code [AD-A208381] N89-27962

PULSE POSITION MODULATION
A novel approach to a PPM-modulated frequency-doubled electro-optic cavity-dumped Nd:YAG laser N89-27897

PULSED JET ENGINES
Antiproton powered propulsion with magnetically confined plasma engines [NASA-CR-185131] N89-27700

PULSED LASERS
Lasertron: A pulsed RF-source using laser triggered photocathode [DE89-778130] N89-28008
Pulsed laser propulsion for low cost, high volume launch to orbit [DE89-014049] N89-28009

PULSED RADIATION
Studies of the propagation of short burst, high power microwave radiation through neutral and ionized media [AD-A208864] N89-27944

PULSEJET ENGINES
Capacitors for pulsed electric propulsion N89-27790

PUMPS
Space Shuttle Main Engine structural analysis and data reduction/evaluation. Volume 3B: High pressure fuel turbo-pump preburner pump bearing assembly analysis [NASA-CR-183666] N89-27695

PUPILS
Optical spatial tracking using coherent detection in the pupil plane [AD-A209970] N89-28209

PYROELECTRICITY
Piezoelectric polymer/ceramic composite [AD-A208905] N89-27801

PYROLYSIS
Birth, death and transfiguration: The synthesis of preceramic polymers, their pyrolysis and their conversion to ceramics [AD-A208437] N89-27841

Q

Q SWITCHED LASERS
A novel approach to a PPM-modulated frequency-doubled electro-optic cavity-dumped Nd:YAG laser N89-27897

QUADRATIC EQUATIONS
Quadratic estimators of the power spectrum [AD-A208601] N89-27964
A uniformly differentiable approximation scheme for delay systems using splines [AD-A208567] N89-28346

QUADRUPOLES
New ion trap for atomic frequency standard applications N89-27875

QUALITY CONTROL
Analytical procedures for environmental quality control, volume 2 [PB89-158612] N89-28103
Analytical procedures for environmental quality control, volume 3 [PB89-158620] N89-28104
Express-method investigation and its application for heat pipe quality control N89-28229

QUANTUM ELECTRONICS
Electronics research at the University of Texas at Austin [AD-A209989] N89-27970

QUANTUM MECHANICS
Algebraic analysis of the electromagnetic wave interaction with the two-level system with two-fold degenerated states [DE89-611932] N89-27926
Charge transfer and inelastic scattering in proton-molecule collisions [MPIS-13/1988] N89-28378
A comparison between theoretical and experimental state-to-state charge transfer cross sections for H(+) + H2 at 20 eV: Evidence for quantum effects N89-28383
A three-dimensional quantum mechanical study of vibrational inelastic and charge transfer processes in H(+) + H2 at a collision energy Ecm = 20 eV N89-28384

QUANTUM THEORY
Quantum corrections for inelastic atom-surface scattering [AD-A209850] N89-28387

QUANTUM WELLS
Potential energy curves for the (ArH(+)) and (NeH(+)) systems from the interplay of theory and experiments N89-28380

QUARTZ CRYSTALS
The quartz crystal microbalance as an in situ tool in electrochemistry
[AD-A209852] N89-27811
Applications of the quartz crystal microbalance to electrochemistry
[AD-A209853] N89-27812
QUASARS
The effect of spatial and temporal wet-troposphere fluctuations on connected element interferometry N89-27874
QUATERNARY ALLOYS
Application of quaternary phase diagrams to compound semiconductor processing
[DE89-014537] N89-28413
QUENCHING (ATOMIC PHYSICS)
Vibrationally excited ions: Quenching, reaction and lifetimes
[AD-A208503] N89-28386
QUENCHING (COOLING)
Rapidly solidified titanium alloys by melt overflow
[NASA-CR-4253] N89-27818

R

RADAR
Noise and false alarm rate characteristics for envelope detector systems preceded by RF amplification
[AD-A209789] N89-27948
RADAR ANTENNAS
A multiflare horn with 1-megawatt power handling capability N89-27884
Synthetic aperture microwave radiometer N89-28181
RADAR CROSS SECTIONS
Electromagnetic scattering from a structured slab comprised of periodically placed resistive cards
[AD-A210145] N89-27953
RADAR IMAGERY
The effects of snow on landmarks in K(sub u) band SAR images
[DE89-014578] N89-27925
Acoustooptic processing of two dimensional signals using temporal and spatial integration
[AD-A208686] N89-27966
Laboratory for Oceans
[NASA-TM-101257] N89-28118
Ice sheet studies using synthetic aperture radar N89-28152
Wave/current interaction model N89-28153
Microwave radar oceanographic investigations N89-28158
Surface Contour Radar (SCR) contributions to FASINEX N89-28159
Preliminary statistical identification of radar imagery: Autoregressive-moving average (ARMA) models
[INPE-4771-PRE/1440] N89-28311
Mode filters and their applications
[INPE-4748-PRE/1421] N89-28312
RADAR RECEIVERS
Noise and false alarm rate characteristics for envelope detector systems preceded by RF amplification
[AD-A209789] N89-27948
RADAR SCANNING
Large aperture scanning airborne lidar N89-28186
RADAR SCATTERING
Target signature modeling and bistatic scattering measurement studies
[NASA-CR-185434] N89-27870
Radar scattering and soil moisture N89-28182
RADAR TRANSMITTERS
A multiflare horn with 1-megawatt power handling capability N89-27884
RADIANCE
The use of digital elevation model for correcting the effects of projections in reforrestations of eucalyptus in mountainous regions
[INPE-4763-PRE/1432] N89-28048
Aerosol model selection using surface measurements of IR horizon radiances and satellite detected visible radiances
[AD-A209638] N89-28110
Coastal Zone Color Scanner studies N89-28138
Remote sensing of ocean color in the Arctic N89-28139
Radiance standards N89-28191
Calibration source maintenance, characterization and development N89-28193
Integrating sphere and hemisphere calibration update N89-28194
Application of optical measure theory to atmospheric temperature sounding from TOVS (TIROS Operational Vertical Sounder) radiances
[AD-A209955] N89-28396
RADIATION ABSORPTION
Coupling between radiation and gas dynamics
[AD-A209657] N89-28102
Cloud absorption radiometer N89-28172
Extraordinary behavior of atoms near a phase conjugator
[AD-A209946] N89-28389
RADIATION BELTS
A space radiation test model study
[AD-A208760] N89-28479
RADIATION DAMAGE
High-energy particles very near the sun N89-28465
RADIATION DETECTORS
Effective amplifier noise for an optical receiver based on linear mode avalanche photodiodes N89-27893
Coronagraph observations and analyses of the ultraviolet solar corona
[NASA-CR-185830] N89-28476
RADIATION EFFECTS
Irradiation effects on resistance of thermal impact of composite used in space
[DE89-778069] N89-27794
Resist sensitivity enhancement by radiation-induced modification
[AD-A208438] N89-27842
Indium phosphide solar cell research in the US: Comparison with nonphotovoltaic sources
[NASA-TM-102103] N89-27868
The phototoxicity of blue light on the functional properties of the retinal pigment epithelium
[AD-A209834] N89-28204
Toward a descriptive model of galactic cosmic rays in the heliosphere N89-28456
The effects of high energy particles on planetary missions N89-28457
Current models of the intensely ionizing particle environment in space N89-28458
A new proton fluence model for E greater than 10 MeV N89-28459
Risk assessment and late effects of radiation in low-earth orbits
[DE89-013043] N89-28478
RADIATION HARDENING
Investigation of radiation effects on semiconductor devices and integrated circuits
[AD-A210165] N89-27972
RADIATION MEASUREMENT
A new background stratospheric aerosol model for use in atmospheric radiation models
[AD-A210110] N89-28112
Gradients of galactic cosmic rays and anomalous components N89-28468
RADIATION PROTECTION
Risk assessment and late effects of radiation in low-earth orbits
[DE89-013043] N89-28478
RADIATION SOURCES
Monitoring sources of nuclear radiation in space. Part 1: Early 1984 observations, revision
[AD-A209721] N89-28481
Monitoring sources of nuclear radiation in space 1980-1984 observations, revision
[AD-A209722] N89-28482
Monitoring sources of nuclear radiation in space 1985-1987 observations, revision
[AD-A209723] N89-28483
RADIATION TRANSPORT
ZPIMP: A zero-D Z-pinch implosion code
[AD-A208381] N89-27962
RADIATIVE HEAT TRANSFER
Improved ray tracing technique for radiative heat transfer modelling N89-28249
Thermal effects of plume impingement N89-28252
Thermal and cryogenic aspects of the ISO optical subsystem N89-28269
Thermal protection concepts of recoverable capsules N89-28292
RADIO ALTIMETERS
Ocean topography experiment (TOPEX) radar altimeter N89-28119
Mars Observer Radar Altimeter Radiometer (MORAR) N89-28120
Advanced altimetry N89-28128
Earth Observing System (EOS) advanced altimetry N89-28129
Ice sheet radar altimetry N89-28150
RADIO ANTENNAS
Estimation and filtering techniques for high-accuracy GPS applications N89-27872
RADIO BEACONS
Feasibility of millimeter-accuracy geodetic positioning and vehicle tracking with repeater satellites
[AD-A209958] N89-27692
RADIO FILTERS
Accuracy of telemetry signal power loss in a filter as an estimate for telemetry degradation N89-27900
RADIO FREQUENCIES
New ion trap for atomic frequency standard applications N89-27875
Accuracy of telemetry signal power loss in a filter as an estimate for telemetry degradation N89-27900
Noise and false alarm rate characteristics for envelope detector systems preceded by RF amplification
[AD-A209789] N89-27948
Lasertron: A pulsed RF-source using laser triggered photocathode
[DE89-778130] N89-28008
RADIO FREQUENCY HEATING
Numerical and experimental investigations of a propagating microwave-heated plasma N89-27772
Development of high-current RF plasma sources for neutral particle injections N89-27785
RADIO FREQUENCY SHIELDING
Studies of the propagation of short burst, high power microwave radiation through neutral and ionized media
[AD-A208664] N89-27844
RADIO INTERFEROMETERS
Feasibility of millimeter-accuracy geodetic positioning and vehicle tracking with repeater satellites
[AD-A209958] N89-27692
RADIO NAVIGATION
The Telecommunications and Data Acquisition Report
[NASA-CR-185431] N89-27871
Geostar's system architectures N89-27911
RADIO RELAY SYSTEMS
Baseband equalizer for digital radio relay links N89-27936
RADIO TRACKING
Feasibility of millimeter-accuracy geodetic positioning and vehicle tracking with repeater satellites
[AD-A209958] N89-27692
RADIO TRANSMITTERS
Feasibility of millimeter-accuracy geodetic positioning and vehicle tracking with repeater satellites
[AD-A209958] N89-27692
The DSS-14 C-band exciter N89-27901
RADIOACTIVE MATERIALS
An analysis of severe air transport accidents
[DE89-012642] N89-27642
RADIOLOGY
Evaluation of thermal stress induced by helicopter aircrew Chemical, Biological, Radiological (CBR) protective ensemble
[AD-A210123] N89-28303
RADIOMETERS
High-precision radiometric tracking for planetary approach and encounter in the inner solar system N89-27873
Comparison of the classification results obtained with TM and MSS data in land uses identification of the Communidad Autonoma de Cantabria N89-28077
Cloud absorption radiometer N89-28172
Agriculture Multiband Experiment Radiometer N89-28184
RADIOMETRIC CORRECTION
The use of digital elevation model for correcting the effects of projections in reforrestations of eucalyptus in mountainous regions
[INPE-4763-PRE/1432] N89-28048
Comparison of the classification results obtained with TM and MSS data in land uses identification of the Communidad Autonoma de Cantabria N89-28077
Meteorological Sensor Calibration Facility N89-28188
Radiance standards N89-28191
RADIOMETRIC RESOLUTION
Calibration source maintenance, characterization and development N89-28193
RADIOSONDES
Ozone measurements using balloon-borne ozonesondes N89-28165
Radiosonde intercomparison N89-28169
Satellite/radiosonde comparison N89-28170
Meteorological Sensor Calibration Facility N89-28188
RAILGUN ACCELERATORS
Goals for limited strategic defenses
[DE89-012260] N89-28366
RAIN
Tropical Rainfall Measurement Mission N89-28126
Rainfall on microwave return from the sea surface N89-28160
RAIN GAGES
Spaceborne meteorological radar studies N89-28127
RAMJET ENGINES
Terminal shock response in ramjet inlets to abrupt downstream perturbations
[AD-A209788] N89-27640
RANDOM ACCESS MEMORY
Hyperdimensional data analysis and structural inference
[AD-A210056] N89-27971

RANDOM VARIABLES
Markov processes applied to control, reliability and replacement
[AD-A208634] N89-28362
RANGELANDS
Mapping winter grazing areas for reindeer on Svalbard using LANDSAT Thematic Mapper data N89-28075
RAY TRACING
Pigtailed single-mode diode lasers
[AD-A209913] N89-28012
Improved ray tracing technique for radiative heat transfer modelling N89-28249
REACTION KINETICS
Quantitative estimation of component amplitude in multiexponential data: Application to time-resolved fluorescence spectroscopy
[AD-A210142] N89-27815
Effect of alloying, rapid solidification, and surface kinetics on the high temperature environmental resistance of niobium
[AD-A209934] N89-27829
Equipment models for process optimization and control using smart response surfaces
[AD-A206321] N89-27838
Energetic polyoxetane thermoplastic elastomers: Synthesis and characterization
[AD-A209612] N89-27853
Shock initiation modeling of multicomponent explosives
[DE89-012259] N89-27863
Real gas equations of state for CHEMKIN
[DE89-012794] N89-28432
REACTION WHEELS
Implementation of a digital torque controller of a reaction wheel with an incremental computer
[INPE-4784-PRE/1447] N89-28333
REACTIVITY
Adsorption and reactions of cyclic sulfides on Mo(110)
[AD-A207324] N89-27803
REAL GASES
Real gas equations of state for CHEMKIN
[DE89-012794] N89-28432
REAL TIME OPERATION
The effects of atmospheric turbulence on precision optical measurements used for antenna-pointing compensation N89-27883
Digital CODEC for real-time processing of broadcast quality video signals at 1.8 bits/pixel
[NASA-TM-102325] N89-27927
Low cost real time interactive analysis system N89-28177
RECEIVERS
Synchronization of the receiver for the ISDN basic connection N89-27933
Receiver synchronization for spread spectrum transmission N89-27934
RECEPTION DIVERSITY
A robust signalling system for land mobile satellite services N89-27917
RECOVERABLE SPACECRAFT
Thermal protection concepts of recoverable capsules N89-28292
RECTANGULAR WAVEGUIDES
The calculation of losses in waveguide networks N89-27941
RECYCLING
MELISSA: A micro-organisms-based model for CELSS development N89-28222
REDUCTION (CHEMISTRY)
Experimental determination of the coefficient in the steady state current equation for spherical segment microelectrodes
[AD-A208662] N89-27965
REDUNDANCY
Design of experiments and reliability models
[AD-A209880] N89-28023
Redundancy concept for the Columbus man-tended free-flyer thermal control system N89-28232
REENTRY EFFECTS
Steady state MPD devices for reentry simulation N89-27763
REENTRY SHIELDING
Thermal protection concepts of recoverable capsules N89-28292
REFLECTANCE
An experimental and computer modeling study of stepped radius monopole antennas
[AD-A207356] N89-27919
REFLEXES
Age-related changes in human vestibulo-ocular and optokinetic reflexes: Pseudorandom rotation tests
[NASA-CR-185856] N89-28213
REFORESTATION
The use of digital elevation model for correcting the effects of projections in reforrestations of eucalyptus in mountainous regions
[INPE-4763-PRE/1432] N89-28048
REFRACTED WAVES
Reflection and refraction of finite amplitude acoustic waves at a fluid-fluid interface
[AD-A209800] N89-28371
REFRACTION
Reflection and refraction of finite amplitude acoustic waves at a fluid-fluid interface
[AD-A209800] N89-28371
REFRACTORY MATERIALS
Institute for Materials Science and Engineering: Metallurgy Division, technical activities 1988
[PB89-201321] N89-27819
REFRIGERATING
A 4-K mechanical refrigerator for space applications N89-28268
REGENERATION (ENGINEERING)
Physico-chemical atmosphere revitalisation: The qualitative and quantitative selection of regenerative designs N89-28221
REGRESSION ANALYSIS
Quantitative estimation of component amplitude in multiexponential data: Application to time-resolved fluorescence spectroscopy
[AD-A210142] N89-27815
Hyperdimensional data analysis and structural inference
[AD-A210056] N89-27971
REINFORCING MATERIALS
Novel methods for reinforcing elastomers
[AD-A210150] N89-27861
RELATIVISTIC PLASMAS
Efficient energy storage and conversion using adiabatic compression of relativistic-electron plasmas
[AD-A208657] N89-28101
RELAXATION METHOD (MATHEMATICS)
A computational comparison of the primal simplex and relaxation algorithms for solving minimum cost flow networks
[AD-A208534] N89-28331
RELIABILITY
Basic research in reliability for real systems
[AD-A209649] N89-28022
RELIABILITY ANALYSIS
Design of experiments and reliability models
[AD-A209880] N89-28023
Monte Carlo reliability analysis
[AD-A210052] N89-28024
REMOTE SENSING
The use of edge detectors based on mathematical morphology in remote sensing imagery
[INPE-4777-PRE/1446] N89-28050
Report of the Project Estima, phase 2: LANDSAT-TM data and agrometeorology in crop yield estimation of wheat at the farm level
[INPE-4782-RPE/582-PHASE-2] N89-28051
Remote sensing of the Madrid area ecosystems N89-28076
Comparison of the classification results obtained with TM and MSS data in land uses identification of the Communidad Autonoma de Cantabria N89-28077
Use of remote sensing in mapping of vegetation in the Dividalen area central Troms, northern Norway N89-28083
Laboratory for Oceans
[NASA-TM-101257] N89-28118
Bangladesh Agro-Climatic Environmental Monitoring Project N89-28121
NASA follow-on to the Bangladesh Agro-Climatic Environmental Monitoring Project N89-28122
Remote sensing of ocean color in the Arctic N89-28139
Microwave remote sensing of sea ice N89-28148
The Surface Wave Dynamics Experiment (SWADE) N89-28162
REMOTE SENSORS
Determination of local empirical covariance functions from residual terrain reduced altimeter data
[AD-A208678] N89-28095
Aerosol model selection using surface measurements of IR horizon radiances and satellite detected visible radiances
[AD-A209638] N89-28110
The vegetation payload of the SPOT-4 spacecraft thermal design and analysis N89-28259
REQUIREMENTS
Avionic system requirements N89-27652
A structured approach to weapon system design N89-27653
Avionic system design methodology N89-27656
RESEARCH AIRCRAFT
Interpretation of F106B and CV580 in-flight lightning data and form factor determination
[NASA-CR-4250] N89-28115
RESEARCH AND DEVELOPMENT
The 1990 National Aeronautics and Space Administration authorization
[GPO-99-550] N89-28450
National Aeronautics and Space Administration Multiyear Authorization Act of 1989
[H-REPT-101-226] N89-28451
RESEARCH FACILITIES
NASA in-house Commercially Developed Space Facility (CDSF) study report. Volume 1: Concept configuration definition
[NASA-TM-101586-VOL-1] N89-27687
RESEARCH MANAGEMENT
Basic research in reliability for real systems
[AD-A209649] N89-28022
RESERVOIRS
Remote sensing of limnological parameters in reservoirs N89-28061
RESISTOJET ENGINES
Investigation of a liquid-fed water resistojet plume
[NASA-TM-102310] N89-27706
RESONANCE FLUORESCENCE
Multiphoton detection techniques for F and F2
[AD-A208576] N89-27807
Fluorescence probes of spectroscopic and dynamical aspects of molecular photoionization
[AD-A207185] N89-28372
RESONANCE PROBES
Fluorescence probes of spectroscopic and dynamical aspects of molecular photoionization
[AD-A207185] N89-28372
RESONANT FREQUENCIES
Bubble detection using a dual frequency sound field
[AD-A207286] N89-27973
RESONANT VIBRATION
Fluorescence probes of spectroscopic and dynamical aspects of molecular photoionization
[AD-A207185] N89-28372
RESPIROMETERS
Possible use of a gas monitoring system in space respirometry studies N89-28223
RETINA
The phototoxicity of blue light on the functional properties of the retinal pigment epithelium
[AD-A209834] N89-28204
RETINAL IMAGES
Eye movements and visual information processing
[AD-A209817] N89-28203
RETURN TO EARTH SPACE FLIGHT
The ROSETTA/CNSR mission: A possible application of electric propulsion to interplanetary missions N89-27715
REVERSED FLOW
Analysis of pressure drop and heat transfer data from the reversing flow test facility
[DE89-013907] N89-27984
RHYTHM (BIOLOGY)
Visualizing and rhyming cause differences in alpha suppression
[AD-A210005] N89-28210
RIEMANN MANIFOLD
Two examples of escaping harmonic maps
[DE89-611896] N89-28345
RISK
Anthropometric measurements of aviators within the Aviation Epidemiology Data Register
[AD-A208609] N89-28300
Risk assessment and late effects of radiation in low-earth orbits
[DE89-013043] N89-28478
RIT ENGINES
The ROSETTA/CNSR mission: A possible application of electric propulsion to interplanetary missions N89-27715
Status of the RITA experiment on EURECA N89-27728
Auxiliary propulsion RF engine RIT 15: Prototype design and performance N89-27731
Electrical transfer vehicle analysis for future space operations (MESCATS) N89-27750
Inert gas performance of the RIT 35 main propulsion unit N89-27770
ROBOTICS
Joint-space adaptive control of a 6 DOF end-effector with closed-kinematic chain mechanism
[NASA-CR-185861] N89-28016
Design of an adaptive controller for a telerobot manipulator
[NASA-CR-185863] N89-28017
Design considerations for an earth based flexible robotic system
[AD-A209635] N89-28018

Robot motion planning: A distributed representation approach
[AD-A209890] N89-28019
Algorithmic control of walking
[AD-A210117] N89-28326

ROBOTS
Robot motion planning: A distributed representation approach
[AD-A209890] N89-28019
Generic singularities of robot manipulators
[AD-A210116] N89-28021

ROBUSTNESS (MATHEMATICS)
Stability robustness improvement of direct eigenspace assignment based feedback systems using singular value sensitivities
[NASA-CR-182302] N89-27672
State-space theory of structured uncertainty with examples
[AD-A209968] N89-28339

ROCK INTRUSIONS
Lithologic mapping of mafic intrusions in East Greenland using Landsat Thematic Mapper data
[NASA-CR-183440] N89-28047

ROCKET ENGINE CASES
Flight set 360L001 (STS-26) insulation component. Volume 3: Final release
[NASA-CR-183674] N89-27698

ROCKET ENGINE CONTROL
Development of a flight standard power conditioning and control system for the T5 ion thruster N89-27738
Verification of control sequence and algorithm for the electric propulsion experiment (EPEX) N89-27740

ROCKET ENGINE DESIGN
DGLR/AIAA/JSASS 20th International Electric Propulsion Conference: Proceedings
[DGLR-PAPER-88-02] N89-27707
Interests in electric propulsion N89-27711
Plasma propulsion activites at SNIA BPD N89-27716
Development of an MPD propulsion system N89-27718
FEEP power conditioning unit: Design and development status N89-27722
Field Emission Electric Propulsion (FEEP) attitude control capabilities N89-27724
Nozzle type MPD thruster experimental investigations N89-27727
The proposed demonstration of the UK-10 ion propulsion system on ESA's SAT-2 spacecraft N89-27729
Design and development of the UK-10 ion propulsion subsystem N89-27730
Numerical codes for cylindrical MPD thrusters N89-27733
Fluid mechanics in a magnetoplasmadynamic thruster N89-27734
Thermal design improvements for 30kWe arcjet engine N89-27754
An approach to the parametric design of ion thrusters N89-27761
A 30 cm diameter xenon ion thruster: Design and initial test results N89-27768
Electrothermal thrusters utilizing electrodeless discharges N89-27774
Performance calculation of an H2 arcjet by means of a dual channel model N89-27775
A 15 kW experimental arcjet N89-27778
Performance research of xenon ion rocket engine N89-27788

ROCKET ENGINES
Performance of a 100 kW class applied field MPD thruster
[NASA-TM-102312] N89-27701
United States Air Force Research Initiation Program for 1987, volume 1
[AD-A209726] N89-28436

ROCKET EXHAUST
Optical emission spectrum of the UK-10 ion thruster operating on xenon N89-27781
Thermal effects of plume impingement N89-28252

ROCKET NOZZLES
A method for calculating asymmetric flow through nozzles
[AD-A209689] N89-27992

ROCKET SOUNDING
Rocket temperature soundings N89-28167

ROCKET TEST FACILITIES
Xenon ion thruster test facility: Design and operation N89-27745

ROCKET THRUST
Improved thrust generation mechanism for electrothermal/electromagnetic arcjet N89-27726
High thrust operation of the UK-10 rare gas ion thruster (T4A) N89-27747

ROCKS
Lithologic mapping of mafic intrusions in East Greenland using Landsat Thematic Mapper data
[NASA-CR-183440] N89-28047

ROOM TEMPERATURE
Anomalous stresses versus extent of cure in an epoxy composite specimen
[AD-A208523] N89-27798

ROSAT MISSION
Thermal analysis of ROSAT in low-earth eclipse orbit employing steady-state calculations N89-28251
Lessons learned from ROSAT thermal balance test: A combined solar simulation/infrared test N89-28275

ROTARY WINGS
Analysis of a system to prevent helicopter rotor blade-airframe strikes
[AD-A209804] N89-27649

ROTATING BODIES
An integrating matrix formulation for buckling of rotating beams including the effects of concentrated masses
[NASA-CR-181862] N89-28342

ROTATING FLUIDS
Ocean modelling and the use of altimetry data
[AD-A206841] N89-28195

ROTATING PLASMAS
Review of effects of NBI (Neutral Beam Injection) and rotation on plasma transport in tokamaks
[DE89-014109] N89-28402

ROTATION
Age-related changes in human vestibulo-ocular reflexes: Sinusoidal rotation and caloric tests
[NASA-CR-185857] N89-28211
Age-related changes in human posture control: Sensory organization tests
[NASA-CR-185858] N89-28212
Modified rotationally adiabatic model for rotational autoionization of dipole-bound molecular anions
[AD-A209851] N89-28388

RUBBER
Dynamic fracture and deformation of solid propellant
[AD-A208691] N89-27865

RUN TIME (COMPUTERS)
Performance augmentation of SITIM-150 through a high performance numerical processor
[INPE-4770-PRE/1439] N89-28305

RUNWAY CONDITIONS
A comparison of rutting behavior of asphalt concrete under the F-4C/G and F-15C/D aircraft
[AD-A208911] N89-27678

RUNWAYS
Theoretical model for stabilization of clay-silt airport pavement subgrade systems. Phase 1: Laboratory investigation. Phase 2: Rutting tests
[DOT/FAA/PM-87/20-PHASE-1/2] N89-27673
Compacted-snow runways: Guidelines for their design and construction in Antarctica
[AD-A208910] N89-27677

S

SALINITY
Arctic Sea ice studies with passive microwave satellite observations N89-28147

SAMARIUM COMPOUNDS
Fundamental magnetic studies of iron-rare-earth-metalloid alloys
[DE89-013803] N89-27820

SAMPLING
Evaluation of the AFGL (Air Force Geophysics Laboratory) cloud simulation models using satellite data
[AD-A208713] N89-28116

SATELLITE ALTIMETRY
Ocean topography experiment (TOPEX) radar altimeter N89-28119
Mars Observer Radar Altimeter Radiometer (MORAR) N89-28120
Advanced altimetry N89-28128
Earth Observing System (EOS) advanced altimetry N89-28129
Ocean modelling and the use of altimetry data
[AD-A206841] N89-28195

SATELLITE ANTENNAS
A comparative study of SHF (Super High Frequency) and EHF (Extremely High Frequency) satellite communications, volume 1
[AD-A208850] N89-27945
TELE-X antenna module thermal control N89-28257
Thermal aspects of the ERS-1 SAR antenna deployment N89-28261

SATELLITE ATTITUDE CONTROL
Optimization of maneuvers of a spin-stabilized satellite, using magnetic coils
[INPE-4778-TDL/350] N89-27680
Launch window for the Brazilian Data Collecting Satellite
[INPE-4773-PRE/1442] N89-27683
Field Emission Electric Propulsion (FEEP) attitude control capabilities N89-27724

SATELLITE COMMUNICATION
Feasibility of millimeter-accuracy geodetic positioning and vehicle tracking with repeater satellites
[AD-A209958] N89-27692
Target signature modeling and bistatic scattering measurement studies
[NASA-CR-185434] N89-27870
The use of interleaving for reducing radio loss in trellis-coded modulation systems N89-27889
A visibility characterization program for optical communications through the atmosphere N89-27894
Digital demultiplier for mobile satellite communication N89-27937
Digital demodulator for mobile satellite communication N89-27938
A comparative study of SHF (Super High Frequency) and EHF (Extremely High Frequency) satellite communications, volume 1
[AD-A208850] N89-27945

SATELLITE COMMUNICATIONS SHIPS
Analysis of maritime mobile satellite communication systems
[AD-A207358] N89-27920

SATELLITE CONTROL
Controlling a stationary orbit using electric propulsion N89-27741

SATELLITE DESIGN
MSAT signalling and network management architectures N89-27916
Design trends in communications satellite thermal subsystems N89-28255
Two years of in-orbit life of SPOT-1 heliosynchronous platform N89-28272

SATELLITE IMAGERY
Lithologic mapping of mafic intrusions in East Greenland using Landsat Thematic Mapper data
[NASA-CR-183440] N89-28047
Satellite image analysis for marine applications
[PB89-187330] N89-28053
Utility of Thematic Mapper data for national survey of Irish lakes N89-28058
Remote sensing of limnological parameters in reservoirs N89-28061
Use of satellite imagery for the investigation of pollution-related characteristics of Dublin Bay, Ireland N89-28063
Production of satellite image maps from TM data N89-28089
Laboratory for Oceans
[NASA-TM-101257] N89-28118
Coastal Zone Color Scanner studies N89-28138
Ice sheet radar altimetry N89-28150
Climatological aspects of Nimbus-7 SMMR data N89-28156
Low cost real time interactive analysis system N89-28177
Microwave remote sensing of soil moisture N89-28180
The vegetation payload of the SPOT-4 spacecraft thermal design and analysis N89-28259

SATELLITE INSTRUMENTS
Diagnostic tools for an ion thruster in space N89-27782
NASA Aircraft-Satellite Instrument Calibration Project N89-28189

SATELLITE NETWORKS
Study on the applicability of Asynchronous Time Division (ATD) techniques to satellite communications systems
[ESA-CR(P)-2742] N89-27943
Airborne lidar global positioning investigations N89-28179

SATELLITE OBSERVATION
Novel methodology for application of adaptive systems techniques to DMSP (Defense Meteorological Satellite Program) remote temperature sensing
[AD-A209975] N89-28098
Bangladesh Agro-Climatic Environmental Monitoring Project N89-28121
NASA follow-on to the Bangladesh Agro-Climatic Environmental Monitoring Project N89-28122
Fiji South Pacific Severe Storm Detection and Warning System Project (SPSSD/WS) N89-28123
NASA follow-on on the Fiji South Pacific Severe Storm Warning System Project (SPSSD/WS) N89-28124
Monocular electro-optical stereo scanner N89-28125
Tropical Rainfall Measurement Mission N89-28126
Advanced altimetry N89-28128
Calibration support for the Earth Observing System Project N89-28131
Oceanographic wide field sensor N89-28132
Arctic Sea ice studies with passive microwave satellite observations N89-28147

SATELLITE ORBITS
Estimation and filtering techniques for high-accuracy GPS applications N89-27872

SATELLITE ORIENTATION
Thermal aspects of the ERS-1 SAR antenna deployment N89-28261
SATELLITE SOUNDING
Satellite/radiosonde comparison N89-28170
Application of optical measure theory to atmospheric temperature sounding from TOVS (TIROS Operational Vertical Sounder) radiances [AD-A209955] N89-28396
SATELLITE TRACKING
A comparative study of SHF (Super High Frequency) and EHF (Extremely High Frequency) satellite communications, volume 1 [AD-A208850] N89-27945
Fiji South Pacific Severe Storm Detection and Warning System Project (SPSSD/WS) N89-28123
NASA follow-on on the Fiji South Pacific Severe Storm Warning System Project (SPSSD/WS) N89-28124
SATELLITE TRANSMISSION
Wide band data collection system N89-28130
SATELLITE-BORNE INSTRUMENTS
Long-life Stirling cycle coolers for applications in the 60 to 110 K range N89-28267
SATELLITE-BORNE PHOTOGRAPHY
Evaluation of the AFGL (Air Force Geophysics Laboratory) cloud simulation models using satellite data [AD-A208713] N89-28116
SCALE (RATIO)
Large-scale forest management using LANDSAT Thematic Mapper data N89-28085
SCALE EFFECT
Automatic change in contour diagrams on the occasion of scale reduction using a material morphology [INPE-4769-PRE/1438] N89-28049
SCALE MODELS
Small scale model tests in small wind and water tunnels at high incidence and pitch rates. Volume 3: Water tunnel (HFF) data base [AD-A208690] N89-27638
Small scale model tests in small wind and water tunnels at high incidence and pitch rates. Volume 2: Small wind tunnel (ADF) data base [AD-A208539] N89-27676
SCALING LAWS
Scaling laws for the spectrum of interchange instabilities in the high latitude ionosphere [AD-A209993] N89-28111
Constellation sizing for modest directed energy platforms [DE89-012826] N89-28367
SCATTERING
Site selection criteria for the optical atmospheric visibility monitoring telescopes N89-27896
A robust signalling system for land mobile satellite services N89-27917
Modeling of ocean surface spectrum and surface scattering. Applications to reverberation prediction in the AAUS program [AD-A210127] N89-28197
Detection of artificial sources of nuclear radiation in space, revision [AD-A209720] N89-28480
SCATTERING AMPLITUDE
Analysis of a limiting-amplitude problem in acousto-elastic interactions, 1 [AD-A209741] N89-28045
SCATTERING CROSS SECTIONS
A comparison between theoretical and experimental state-to-state charge transfer cross sections for H(+) + H2 at 20 eV: Evidence for quantum effects N89-28383
SCHEDULING
Resource contention management in parallel systems [AD-A208809] N89-28332
SCHMIDT TELESCOPES
A visibility characterization program for optical communications through the atmosphere N89-27894
SCINTILLATION
Database development for the DMSP (Defense Meteorological Satellite Program) SSIES experiment [AD-A208712] N89-27691
SCINTILLATION COUNTERS
Scintillating fiber detector development for the SSC [DE89-013118] N89-27997
SEA ICE
Arctic Sea ice studies with passive microwave satellite observations N89-28147
Microwave remote sensing of sea ice N89-28148
Analysis of sea ice dynamics N89-28149
Sea ice/climate studies N89-28151
Ice sheet studies using synthetic aperture radar N89-28152
Wave/current interaction model N89-28153
Ocean modelling and the use of altimetry data [AD-A206841] N89-28195
SEA SURFACE TEMPERATURE
Tropical Rainfall Measurement Mission N89-28126
Ocean Data Acquisition System N89-28144
Ocean Drifter Project N89-28154
Climatological aspects of Nimbus-7 SMMR data N89-28156
SEA WATER
Separation of oxygen from seawater by membrane permeation [AD-A208863] N89-27809
SEARCHING
The combinatorics of heuristic search termination for object recognition in cluttered environments [AD-A209690] N89-28363
SECONDARY FLOW
Effects of an embedded vortex on a single film-cooling jet in a turbulent boundary layer [AD-A207374] N89-27974
SECURITY
Crisis decision-making: The impact of commercial satellites on the media, military and national leaders [AD-A207334] N89-28449
SEDIMENT TRANSPORT
LANDSAT-5 TM study of suspended sediments in a fjord system in western Norway N89-28064
SEDIMENTS
Theoretical model for stabilization of clay-silt airport pavement subgrade systems. Phase 1: Laboratory investigation. Phase 2: Rutting tests [DOT/FAA/PM-87/20-PHASE-1/2] N89-27673
SEISMOLOGY
Wide band data collection system N89-28130
SELENIDES
Selective detector for gas chromatography based on adduct-modulated semiconductor photoluminescence [AD-A208616] N89-27808
SEMICONDUCTING FILMS
Growth and characterization of zinc sulfide films by conversion of zinc oxide films with H2S [AD-A208727] N89-28423
SEMICONDUCTOR DEVICES
Theory of photon-drag effect in bulk magnetic semiconductors [DE89-612214] N89-28417
SEMICONDUCTOR DIODES
Approaches toward a blue semiconductor laser [NASA-CR-4252] N89-28004
Solid state research [AD-A209969] N89-28431
SEMICONDUCTOR JUNCTIONS
Phonon-drag thermoelectric power in high magnetic fields in heterojunctions [DE89-013921] N89-28412
SEMICONDUCTOR LASERS
Approaches toward a blue semiconductor laser [NASA-CR-4252] N89-28004
Band structure engineering for ultra-low threshold laser diodes [AD-A208629] N89-28010
Pigtailed single-mode diode lasers [AD-A209913] N89-28012
SEMICONDUCTOR PLASMAS
Solid state research [AD-A209969] N89-28431
SEMICONDUCTORS (MATERIALS)
Selective detector for gas chromatography based on adduct-modulated semiconductor photoluminescence [AD-A208616] N89-27808
Photovoltaic Program Branch annual report, FY 1988 [DE89-000898] N89-28099
Application of quaternary phase diagrams to compound semiconductor processing [DE89-014537] N89-28413
Semiconductor-olefin adducts. Photoluminescent properties of cadmium sulfide and cadmium selenide in the presence of butenes [AD-A208348] N89-28419
SENSITIVITY
Sensitivity analysis of reflection errors in infrared image simulation [AD-A208600] N89-28394
SEQUENCING
Approaches to multi-level sequential logic synthesis [AD-A208322] N89-28316
Binary sequences of arbitrary length with near-ideal correlation [AD-A209956] N89-28356
SEQUENTIAL COMPUTERS
Approaches to multi-level sequential logic synthesis [AD-A208322] N89-28316
SERVICE LIFE
Design of experiments and reliability models [AD-A209880] N89-28023
Refinements in a viscoplastic model [NASA-TM-102338] N89-28036
Long-life Stirling cycle coolers for applications in the 60 to 110 K range N89-28267
A 4-K mechanical refrigerator for space applications N89-28268
Two years of in-orbit life of SPOT-1 heliosynchronous platform N89-28272
Thermal software developments at ESTEC N89-28278
Assembling the ISO thermal model with ESATAN N89-28280
SERVOMECHANISMS
A new method for analysis of limit cycle behavior of the NASA/JPL 70-meter antenna axis servos N89-27880
Application of optimal control theory to the design of the NASA/JPL 70-meter antenna servos N89-27881
SHAPES
A survey of visual preprocessing and shape representation techniques [NASA-CR-185418] N89-28309
SHEAR FLOW
A critical comparison of turbulence models for homogeneous shear flows in a rotating frame [NASA-CR-181864] N89-27977
SHEAR LAYERS
Numerical simulation of control of supersonic shear layers [AD-A209703] N89-27639
Mechanical response of structural elements to dynamic loads [AD-A209827] N89-27802
SHEAR PROPERTIES
Three-dimensional vortex interactions in turbulent boundary layers [AD-A208624] N89-27991
SHIFT REGISTERS
Binary sequences of arbitrary length with near-ideal correlation [AD-A209956] N89-28356
SHOCK LAYERS
Low density flow effects for hypervelocity vehicles [AD-A206218] N89-27633
SHOCK WAVE INTERACTION
Terminal shock response in ramjet inlets to abrupt downstream perturbations [AD-A209788] N89-27640
SHOCK WAVE PROPAGATION
Analytical and numerical solutions for cylindrical blast waves in a plasma of varying density N89-27767
Particles accelerated by shocks in the heliosphere N89-28464
SHOCK WAVES
Shock initiation modeling of multicomponent explosives [DE89-012259] N89-27863
The Shock and Vibration Digest, volume 21, no. 4 N89-28025
Particles accelerated by shocks in the heliosphere N89-28464
SIGNAL DETECTORS
Carrier derivation in higher-stage QAM-signals N89-27935
Adaptive preprocessing of nonstationary signals [AD-A209646] N89-27946
SIGNAL DISTORTION
Baseband equalizer for digital radio relay links N89-27936
SIGNAL ENCODING
RELP: Speech coding using analysis by synthesis N89-27939
SIGNAL FADING
Accuracy of telemetry signal power loss in a filter as an estimate for telemetry degradation N89-27900
A robust signalling system for land mobile satellite services N89-27917
Analysis of maritime mobile satellite communication systems [AD-A207358] N89-27920
SIGNAL GENERATORS
Multipurpose exciter with low phase noise N89-27887
SIGNAL PROCESSING
RELP: Speech coding using analysis by synthesis N89-27939
Theory of multi-frequency modulation (MFM) digital communications [AD-A209737] N89-27947
Studies in statistical signal processing [AD-A210054] N89-27952
Acoustooptic processing of two dimensional signals using temporal and spatial integration [AD-A208686] N89-27966
Electronics research at the University of Texas at Austin [AD-A209989] N89-27970
Bubble detection using a dual frequency sound field [AD-A207286] N89-27973

Northeast Artificial Intelligence Consortium annual report 1987. Volume 6: Artificial intelligence applications to speech recognition
[AD-A208380] N89-28334
Research in stochastic processes
[AD-A209935] N89-28364
United States Air Force Research Initiation Program for 1987, volume 3
[AD-A209728] N89-28437

SIGNAL RECEPTION
A robust signalling system for land mobile satellite services N89-27917

SIGNAL REFLECTION
Stabilized fiber-optic frequency distribution system N89-27879
A robust signalling system for land mobile satellite services N89-27917
Analysis of maritime mobile satellite communication systems
[AD-A207358] N89-27920

SIGNAL TO NOISE RATIOS
Performance of concatenated codes using 8-bit and 10-bit Reed-Solomon codes N89-27890

SIGNAL TRANSMISSION
State-of-the-art fiber optics for short distance frequency reference distribution N89-27878
Stabilized fiber-optic frequency distribution system N89-27879
A robust signalling system for land mobile satellite services N89-27917

SIGNATURE ANALYSIS
Target signature modeling and bistatic scattering measurement studies
[NASA-CR-185434] N89-27870
Forest damage mapping in Austria with the aid of LANDSAT TM image data N89-28078

SILICON
Equipment models for process optimization and control using smart response surfaces
[AD-A208321] N89-27838
Effective amplifier noise for an optical receiver based on linear mode avalanche photodiodes N89-27893
Grain boundaries in silicon from zero temperature through melting
[DE89-013186] N89-28410
Silicon chemistry in interstellar clouds
[NASA-CR-185862] N89-28471

SILICON ALLOYS
Deployable aerospace photovoltaic array based on amorphous silicon alloys N89-27721

SILICON CARBIDES
High temp toughening and creep studies
[AD-A208714] N89-27826

SILICON DIOXIDE
Coating and impregnation of carbon-carbon composites with ceramics by electrophoretic deposition
[AD-A208873] N89-27800
High temp toughening and creep studies
[AD-A208714] N89-27826

SILICON FILMS
Decomposition kinetics and film formation of an organometallic precursor to SiC on Si(100)
[AD-A208384] N89-28420

SILICON NITRIDES
Noncontacting laser diffraction strain extensometer for material properties characterization at high temperatures
[DE89-013551] N89-28393

SILICON OXIDES
Silicon chemistry in interstellar clouds
[NASA-CR-185862] N89-28471

SILICON POLYMERS
Comparison of equipment modeling methods as applied to the LPCVD of in-situ P-doped polysilicon
[AD-A208373] N89-27839

SILOXANES
Transformation of a monotropic mesophase into an enantiotropic mesophase by copolymerization of the parent polymers' monomer pair containing constitutional isomeric mesogenic side groups
[AD-A208782] N89-27850
Novel methods for reinforcing elastomers
[AD-A210150] N89-27861

SILVER
Ion-assisted deposition of silver films on ceramics for friction and wear control
[DE89-014635] N89-27821

SIMULATION
Simulation of deformation and texture evolution in semi-crystalline polymers
[AD-A208854] N89-27852
Space asset modeling for wargame integration
[AD-A207350] N89-28365

SINGLE CHANNEL PER CARRIER TRANSMISSION
Choice of FDMA/SCPC access technique for aeronautical satellite voice system N89-27909
Why is CDMA the solution for mobile satellite communication N89-27912
Practical constraints on network architecture and signalling in the MSAT system N89-27915
Digital demultiplier for mobile satellite communication N89-27937

SINGLE CRYSTALS
Protonic solid electrolytes: Thermal stability and conductivity of ammonium/hydronium beta'-alumina
[AD-A209911] N89-27813
The use of multiple ion exchange to produce energy transfer in beta-aluminas
[AD-A209821] N89-27856
The orientation of chemical bonds at surfaces: A key to understanding the structure and bonding of surface species
[AD-A209833] N89-28427

SINGULARITY (MATHEMATICS)
Generic singularities of robot manipulators
[AD-A210116] N89-28021

SINTERED ALUMINUM POWDER
High temp toughening and creep studies
[AD-A208714] N89-27826

SINTERING
Preparation and characterization of colloidal ZnS particles
[AD-A210171] N89-27862

SIS (SEMICONDUCTORS)
MM wavecomponents - SIS (Superconductor-Insulator-Superconductor) mixers
[AD-A208632] N89-28421

SISO (CONTROL SYSTEMS)
Stability robustness improvement of direct eigenspace assignment based feedback systems using singular value sensitivities
[NASA-CR-182302] N89-27672
State-space theory of structured uncertainty with examples
[AD-A209968] N89-28339

SITE SELECTION
Site selection criteria for the optical atmospheric visibility monitoring telescopes N89-27896

SKIN FRICTION
Low density flow effects for hypervelocity vehicles
[AD-A206218] N89-27633

SKIRTS
Space Shuttle Main Engine structural analysis and data reduction/evaluation. Volume 1: Aft Skirt analysis
[NASA-CR-183663] N89-27693

SLENDER BODIES
Low density flow effects for hypervelocity vehicles
[AD-A206218] N89-27633

SLIDING
Fundamental mechanisms of tribology and their implications
[AD-A209941] N89-28020

SNELLS LAW
Optimal three-dimensional path planning using visibility constraints
[AD-A207357] N89-28310

SNOW
Compacted-snow runways: Guidelines for their design and construction in Antarctica
[AD-A208910] N89-27677
Evaluation of new thermomechanical constitutive theory for snow N89-28052
Cloud/cryosphere interactions
[AD-A208377] N89-28196

SNOW COVER
The effects of snow on landmarks in K(sub u) band SAR images
[DE89-014578] N89-27925
European Coordinated Effort for Monitoring the Earth's Environment. A Pilot Project Campaign on LANDSAT Thematic Mapper Applications (1985-1987)
[ESA-SP-1102] N89-28055
Improved snow and glacier monitoring by the LANDSAT Thematic Mapper N89-28056
Multitemporal snow classification with TM data N89-28057
Cloud/cryosphere interactions
[AD-A208377] N89-28196

SODIUM
Optical spectroscopy of copper (1) doped Na(+) beta-alumina
[AD-A209819] N89-27810

SOFTWARE ENGINEERING
Modeling functional specifications for onboard software N89-27658
Software package for performing experiments about the convolutionally encoded Voyager 1 link N89-27888
Thermal software developments at ESTEC N89-28278

SOIL MECHANICS
Plastic deformation of granular materials
[AD-A208589] N89-28040

SOIL MOISTURE
Microwave remote sensing of soil moisture N89-28180
Radar scattering and soil moisture N89-28182

SOILS
Theoretical model for stabilization of clay-silt airport pavement subgrade systems. Phase 1: Laboratory investigation. Phase 2: Rutting tests
[DOT/FAA/PM-87/20-PHASE-1/2] N89-27673

SOLAR ACTIVITY
Gradients of galactic cosmic rays and anomalous components N89-28466
A space radiation test model study
[AD-A208760] N89-28479
Monitoring sources of nuclear radiation in space 1980-1984 observations, revision
[AD-A209722] N89-28482

SOLAR ACTIVITY EFFECTS
Interplanetary Particle Environment. Proceedings of a Conference
[NASA-CR-185461] N89-28454
Intensity/time profiles of solar particle events at one astronomical unit N89-28460
Solar proton event forecasts N89-28462
Predicting the arrival times of solar particles N89-28463
Particles accelerated by shocks in the heliosphere N89-28464
Galactic cosmic rays in three dimensions N89-28470

SOLAR ARRAYS
NASA advanced space photovoltaic technology-status, potential and future mission applications
[NASA-TM-102093] N89-27705
Interaction of high voltage solar array with ionospheric plasma N89-27719
The interaction between a positively biased conductor on a high voltage solar array and a plasma N89-27720
Deployable aerospace photovoltaic array based on amorphous silicon alloys N89-27721

SOLAR CELLS
NASA advanced space photovoltaic technology-status, potential and future mission applications
[NASA-TM-102093] N89-27705
Deployable aerospace photovoltaic array based on amorphous silicon alloys N89-27721
Indium phosphide solar cell research in the US: Comparison with nonphotovoltaic sources
[NASA-TM-102103] N89-27868
Photovoltaic Program Branch annual report, FY 1988
[DE89-000898] N89-28099

SOLAR CORONA
Coronagraph observations and analyses of the ultraviolet solar corona
[NASA-CR-185830] N89-28476

SOLAR CYCLES
Toward a descriptive model of solar particles in the heliosphere N89-28455
Toward a descriptive model of galactic cosmic rays in the heliosphere N89-28456
Time variation of galactic cosmic rays N89-28469

SOLAR ENERGY
Progress in parabolic dish technology
[DE89-009427] N89-28100

SOLAR ENERGY CONVERSION
Progress in parabolic dish technology
[DE89-009427] N89-28100

SOLAR FLARES
Intensity/time profiles of solar particle events at one astronomical unit N89-28460
The radial dependence of the solar energetic particle flux N89-28461
Predicting the arrival times of solar particles N89-28463
Particles accelerated by shocks in the heliosphere N89-28464
High-energy particles very near the sun N89-28465
Time variation of galactic cosmic rays N89-28469

SOLAR MAGNETIC FIELD
The anomalous cosmic-ray component N89-28467

SOLAR OBSERVATORIES
SOHO thermal modelling and analysis: The first application of ESATAN to a complete spacecraft N89-28279

SOLAR PHYSICS
Interplanetary Particle Environment. Proceedings of a Conference
[NASA-CR-185461] N89-28454
Toward a descriptive model of solar particles in the heliosphere N89-28455
Toward a descriptive model of galactic cosmic rays in the heliosphere N89-28456

SOLAR PROBES
High-energy particles very near the sun N89-28465

SOLAR PROTONS
Interplanetary Particle Environment. Proceedings of a Conference
[NASA-CR-185461] N89-28454
Toward a descriptive model of solar particles in the heliosphere N89-28455
A new proton fluence model for E greater than 10 MeV N89-28459
Intensity/time profiles of solar particle events at one astronomical unit N89-28460
Solar proton event forecasts N89-28462
Predicting the arrival times of solar particles N89-28463
High-energy particles very near the sun N89-28465
SOLAR RADIATION
The Earth Radiation Budget Experiment N89-28133
Current models of the intensely ionizing particle environment in space N89-28458
SOLAR SIMULATION
Lessons learned from ROSAT thermal balance test: A combined solar simulation/infrared test N89-28275
SOLAR SPECTRA
Zonal winds between 25 and 120 km retrieved from solar occultation spectra
[NASA-CR-180086] N89-28113
Coronagraph observations and analyses of the ultraviolet solar corona
[NASA-CR-185830] N89-28476
SOLAR WIND
Coupling between radiation and gas dynamics
[AD-A209657] N89-28102
Interplanetary Particle Environment. Proceedings of a Conference
[NASA-CR-185461] N89-28454
Particles accelerated by shocks in the heliosphere N89-28464
Galactic cosmic rays in three dimensions N89-28470
A space radiation test model study
[AD-A208760] N89-28479
SOLAR X-RAYS
Intensity/time profiles of solar particle events at one astronomical unit N89-28460
SOLENOIDS
Line/Circuit Analysis Program: Cross-coupling on PC (Printed Circuit) board traces including discontinuities and circuit elements
[DE89-013884] N89-27957
A magnetically-driven droplet radiator concept N89-28290
SOLID ELECTROLYTES
Protonic solid electrolytes: Thermal stability and conductivity of ammonium/hydronium beta'-alumina
[AD-A209911] N89-27813
The use of multiple ion exchange to produce energy transfer in beta-aluminas
[AD-A209821] N89-27856
SOLID PROPELLANT IGNITION
SRM propellant, friction/ESD testing
[NASA-CR-183706] N89-27864
United States Air Force Research Initiation Program for 1987, volume 1
[AD-A209726] N89-28436
SOLID PROPELLANT ROCKET ENGINES
Anode-nozzle experimental analysis in a coaxial non-steady solid propellant MPD thruster N89-27757
Particle sizing in solid rocket motors
[AD-A208740] N89-27793
SOLID PROPELLANTS
Dynamic fracture and deformation of solid propellant
[AD-A208691] N89-27865
Further investigation of flow modeling during solid propellant processing
[AD-A209787] N89-27866
SOLID ROCKET BINDERS
Energetic polyoxetane thermoplastic elastomers: Synthesis and characterization
[AD-A209612] N89-27853
Further investigation of flow modeling during solid propellant processing
[AD-A209787] N89-27866
SOLID ROCKET PROPELLANTS
SRM propellant, friction/ESD testing
[NASA-CR-183706] N89-27864
SOLID STATE
Solid state research
[AD-A209969] N89-28431
SOLID STATE DEVICES
Solid state research
[AD-A209645] N89-28426
Development of superlattices for ultra high-speed electronic and optoelectronic devices
[AD-A209874] N89-28429
Solid state research
[AD-A209969] N89-28431
SOLID STATE LASERS
Bibliography of Soviet laser developments: January - February 1988
[AD-A209802] N89-28011
Solid state research
[AD-A209645] N89-28426
SOLIDIFICATION
Rapidly solidified titanium alloys by melt overflow
[NASA-CR-4253] N89-27818
Effect of alloying, rapid solidification, and surface kinetics on the high temperature environmental resistance of niobium
[AD-A209934] N89-27829
SOLIDS
Quantum corrections for inelastic atom-surface scattering
[AD-A209850] N89-28387
SOLITARY WAVES
Soliton behaviour of crack propagation in brittle materials
[DE89-012190] N89-28033
SOLVENTS
Solvent assisted delamination crack growth behavior of amorphous thermoplastic materials
[AD-A207365] N89-27833
SOUND FIELDS
Bubble detection using a dual frequency sound field
[AD-A207286] N89-27973
Analysis of a limiting-amplitude problem in acousto-elastic interactions, 1
[AD-A209741] N89-28045
SOUND PROPAGATION
Sound propagation in bubbly liquids: A review
[AD-A207377] N89-28370
SOUND TRANSMISSION
The Shock and Vibration Digest, volume 21, no. 4 N89-28025
Sound propagation in bubbly liquids: A review
[AD-A207377] N89-28370
SOUND WAVES
Reflection and refraction of finite amplitude acoustic waves at a fluid-fluid interface
[AD-A209800] N89-28371
SOUNDING ROCKETS
Definition study and model for a tethered sounding rocket
[AD-A207367] N89-27699
SPACE CAPSULES
Thermal protection concepts of recoverable capsules N89-28292
SPACE COMMERCIALIZATION
NASA in-house Commercially Developed Space Facility (CDSF) study report. Volume 1: Concept configuration definition
[NASA-TM-101586-VOL-1] N89-27687
SPACE DEBRIS
A case study of a mission to the Kordylewski clouds using ion propulsion N89-27751
SPACE ELECTRIC ROCKET TESTS
Verification of performance and endurance of capacitor bank for the electric propulsion experiment (EPEX) N89-27739
Experimental study of double stage discharge Hall ion thruster N89-27763
SPACE ENVIRONMENT SIMULATION
The use of electric propulsion techniques for LEO atomic oxygen simulation N89-27787
SPACE EXPLORATION
Toward an electrical power utility for space exploration
[NASA-TM-102347] N89-27704
DSN radio science system design and testing for Voyager-Neptune encounter N89-27899
The effects of high energy particles on planetary missions N89-28457
SPACE FLIGHT
Risk assessment and late effects of radiation in low-earth orbits
[DE89-013043] N89-28478
SPACE FLIGHT FEEDING
Hermes: Drink/food-water supply assembly N89-28264
Nutrition for short-duration space missions N89-28265
SPACE MISSIONS
Electric propulsion: Implementation issues N89-27712
SPACE PLASMAS
Interaction of high voltage solar array with ionospheric plasma N89-27719
The interaction between a positively biased conductor on a high voltage solar array and a plasma N89-27720
SPACE PLATFORMS
Microwave radar oceanographic investigations N89-28158
Constellation sizing for modest directed energy platforms
[DE89-012826] N89-28367
SPACE POWER REACTORS
Intermediate heat exchanger for a nuclear-powered space power system N89-28287
Monitoring sources of nuclear radiation in space 1980-1984 observations, revision
[AD-A209722] N89-28482
Monitoring sources of nuclear radiation in space 1985-1987 observations, revision
[AD-A209723] N89-28483
SPACE SHUTTLE MAIN ENGINE
Space Shuttle Main Engine structural analysis and data reduction/evaluation. Volume 1: Aft Skirt analysis
[NASA-CR-183663] N89-27693
Space Shuttle Main Engine structural analysis and data reduction/evaluation. Volume 3B: High pressure fuel turbo-pump preburner pump bearing assembly analysis
[NASA-CR-183666] N89-27695
Space Shuttle Main Engine structural analysis and data reduction/evaluation. Volume 5: Main Injector LOX Inlet analysis
[NASA-CR-183668] N89-27697
Probabilistic structural analysis methods of hot engine structures
[NASA-TM-102091] N89-28030
SPACE SHUTTLE MISSION 51-F
Flight set 360L001 (STS-26) insulation component. Volume 3: Final release
[NASA-CR-183674] N89-27698
SPACE SHUTTLES
Environmental effects of space shuttle exhaust on materials
[AD-A208813] N89-27686
Cyrogenic fluid sink device for thermal control of a spaceplane during ascent and re-entry phases N89-28293
SPACE STATION PAYLOADS
Life science research objectives and representative experiments for the space station
[NASA-TM-89445] N89-28304
SPACE STATION POLAR PLATFORMS
The two approaches for the thermal control of the Columbus resource module and polar platform N89-28231
SPACE STATION POWER SUPPLIES
Development and refinement of test bed simulations
[NASA-TM-102335] N89-27702
SPACE STATION PROPULSION
The ESA policy and program for the development of electric propulsion N89-27708
Electric propulsion for low earth orbit applications N89-27714
SPACE STATION STRUCTURES
Research and technology plans for FY 1989 and accomplishments for FY 1988 --- Structural Mechanics Division
[NASA-TM-101592] N89-28035
SPACE STATIONS
State-of-the-art fiber optics for short distance frequency reference distribution N89-27878
Status of the US Space Station ECLSS and internal TCS N89-28215
Test results on re-use of reclaimed shower water: Summary --- space stations N89-28262
Development of a novel high-performance contact heat exchanger N89-28286
National Aeronautics and Space Administration Multiyear Authorization Act of 1989
[H-REPT-101-226] N89-28451
SPACE SUITS
The European space suit system N89-28243
Thermal modelling of the EVA-suited astronaut N89-28245
SPACE TRANSPORTATION SYSTEM
National Aeronautics and Space Administration Multiyear Authorization Act of 1989
[H-REPT-101-226] N89-28451
SPACE WEAPONS
Goals for limited strategic defenses
[DE89-012260] N89-28366
Constellation sizing for modest directed energy platforms
[DE89-012826] N89-28367
SPACEBORNE EXPERIMENTS
Spaceborne meteorological radar studies N89-28127
Possible use of a gas monitoring system in space respirometry studies N89-28223
SPACEBORNE TELESCOPES
The space-rigidised thermal shield for the ESA Far-Infrared Space Telescope (FIRST) N89-28236
Thermal design of a superfluid helium dewar for infrared telescope on-board space flyer unit N89-28270

SPACECRAFT CABIN ATMOSPHERES
Physico-chemical atmosphere revitalisation: The qualitative and quantitative selection of regenerative designs N89-28221
Regenerative CO2-control --- Columbus N89-28237
Electrochemical removal and concentration of CO2 N89-28238
The atmosphere pressure control section of the Hermes ECLSS N89-28241
SPACECRAFT CHARGING
The effects of high energy particles on planetary missions N89-28457
SPACECRAFT COMMUNICATION
The Telecommunications and Data Acquisition Report [NASA-CR-185431] N89-27871
Software package for performing experiments about the convolutionally encoded Voyager 1 link N89-27888
Performance of concatenated codes using 8-bit and 10-bit Reed-Solomon codes N89-27890
Site selection criteria for the optical atmospheric visibility monitoring telescopes N89-27896
A novel approach to a PPM-modulated frequency-doubled electro-optic cavity-dumped Nd:YAG laser N89-27897
DSN radio science system design and testing for Voyager-Neptune encounter N89-27899
Accuracy of telemetry signal power loss in a filter as an estimate for telemetry degradation N89-27900
Orthogonal sets of data windows constructed from trigonometric polynomials N89-27902
DSN 70-meter antenna microwave optics design and performance improvements. Part 1: Design optimization N89-27903
DSN 70-meter antenna X- and S-band calibration. Part 1: Gain measurements N89-27904
DSN 70-meter antenna X- and S-band calibration. Part 2: System noise temperature measurements and telecommunications link evaluation N89-27905
SPACECRAFT COMPONENTS
A 1-kW condenser for a two-phase heat rejection system N89-28288
Qualification program on stainless steel A95 heatpipe for space application N89-28294
SPACECRAFT CONFIGURATIONS
Spacecraft and mission design for the SP-100 flight experiment N89-27717
SPACECRAFT CONTAMINATION
A study of spacecraft electromagnetic contamination of artificial electron beams [AD-A209954] N89-27950
SPACECRAFT CONTROL
Summary of longitudinal stability and control parameters as determined from Space Shuttle Challenger flight test data [NASA-TM-101605] N89-27671
SPACECRAFT DESIGN
NASA in-house Commercially Developed Space Facility (CDSF) study report. Volume 1: Concept configuration definition [NASA-TM-101586-VOL-1] N89-27687
Radiators and heat exchangers for space applications [REPT-882-440-115] N89-27688
Radiator conceptual studies for the Hermes spaceplane N89-27689
Development of heat exchangers for hybrid radiators N89-27690
Spacecraft and mission design for the SP-100 flight experiment N89-27717
Status of the US Space Station ECLSS and internal TCS N89-28215
Environmental control and life support systems for pressurized modules: From Spacelab to Columbus N89-28219
The definition status of the environmental control and life support subsystems for Hermes N89-28220
Design concepts for Hermes thermal control N89-28234
Advanced modular software development in thermal engineering --- spacecraft design N89-28247
Improved ray tracing technique for radiative heat transfer modelling N89-28249
The Fluidnet development and application to preliminary sizing of fluid-loop systems N89-28282
SPACECRAFT ENVIRONMENTS
Status of the US Space Station ECLSS and internal TCS N89-28215
The Hermes spaceplane program: Status report on the thermal control, environment control and life support activities N89-28217
European life support systems for space applications N89-28218
Environmental control and life support systems for pressurized modules: From Spacelab to Columbus N89-28219
The definition status of the environmental control and life support subsystems for Hermes N89-28220
The catalytic oxiderzer: Description and first results of a breadboard model for a component of the Columbus ECLSS N89-28239
Condensing heat exchangers for European spacecraft ECLSS N89-28240
Toward a descriptive model of solar particles in the heliosphere N89-28455
Toward a descriptive model of galactic cosmic rays in the heliosphere N89-28456
The effects of high energy particles on planetary missions N89-28457
Current models of the intensely ionizing particle environment in space N89-28458
A new proton fluence model for E greater than 10 MeV N89-28459
Solar proton event forecasts N89-28462
High-energy particles very near the sun N89-28465
SPACECRAFT EQUIPMENT
A 4-K mechanical refrigerator for space applications N89-28268
Shaking in cryogenic conditions N89-28277
SPACECRAFT LAUNCHING
Launch window for the Brazilian Data Collecting Satellite [INPE-4773-PRE/1442] N89-27683
Preparing Ulysses for launch N89-28260
SPACECRAFT MODELS
Thermal effects of plume impingement N89-28252
Efficient implementation of a description language for thermal simulators N89-28253
SOHO thermal modelling and analysis: The first application of ESATAN to a complete spacecraft N89-28279
ESATAN FHTS: A piped fluid network capability N89-28281
SPACECRAFT MODULES
The two approaches for the thermal control of the Columbus resource module and polar platform N89-28231
Redundancy concept for the Columbus man-tended free-flyer thermal control system N89-28232
Thermal control of Columbus pressurized modules N89-28233
SPACECRAFT ORBITS
Two years of in-orbit life of SPOT-1 heliosynchronous platform N89-28272
SPACECRAFT PERFORMANCE
Two years of in-orbit life of SPOT-1 heliosynchronous platform N89-28272
Giotto: The thermal responses to its encounter with comet Halley N89-28273
Thermal aspects of an extended mission for Giotto N89-28274
Evolution of thermal analysis methods towards integrated system performance simulation N89-28283
In-orbit degradation of thermo-optical properties on MARECS GEO-satellite N89-28297
SPACECRAFT POWER SUPPLIES
Toward an electrical power utility for space exploration [NASA-TM-102347] N89-27704
NASA advanced space photovoltaic technology-status, potential and future mission applications [NASA-TM-102093] N89-27705
Thermal control of Ni-H2 battery --- spacecraft battery N89-28276
SPACECRAFT PROPULSION
DGLR/AIAA/JSASS 20th International Electric Propulsion Conference: Proceedings [DGLR-PAPER-88-02] N89-27707
The ESA policy and program for the development of electric propulsion N89-27708
Electric propulsion projects and research in Japan N89-27709
Recent progress in the USSR electric propulsion N89-27710
Interests in electric propulsion N89-27711
Electric propulsion: Implementation issues N89-27712
Electric propulsion for low earth orbit applications N89-27714
Spacecraft and mission design for the SP-100 flight experiment N89-27717
FEEP power conditioning unit: Design and development status N89-27722
Auxiliary propulsion RF engine RIT 15: Prototype design and performance N89-27731
Survey of electric propulsion thruster applicability to near earth space missions N89-27749
Interstellar flight: Aspects of beamed electric propulsion N89-27765
Propellant selection criteria for deep space electrically propelled missions N89-27769
Experiments and analysis of a compact electrothermal thruster N89-27773
A 15 kW experimental arcjet N89-27778
Field Emission Electric Propulsion (FEEP): Experimental investigations on continuous and pulsed modes of operation N89-27792
SPACECRAFT RADIATORS
Radiators and heat exchangers for space applications [REPT-882-440-115] N89-27688
Radiator conceptual studies for the Hermes spaceplane N89-27689
Development of heat exchangers for hybrid radiators N89-27690
Design and test of a two-phase coldplate N89-28226
Radiator conceptual studies for the Hermes spaceplane N89-28235
Development of heat exchangers for hybrid radiators N89-28285
Development of a novel high-performance contact heat exchanger N89-28286
A 1-kW condenser for a two-phase heat rejection system N89-28288
A magnetically-driven droplet radiator concept N89-28290
Theoretical and experimental investigations on heat exchangers for Columbus hybrid radiators N89-28295
SPACECRAFT REENTRY
Steady state MPD devices for reentry simulation N89-27783
Development of the Hermes flexible external insulation N89-28296
SPACECRAFT STABILITY
Summary of longitudinal stability and control parameters as determined from Space Shuttle Challenger flight test data [NASA-TM-101605] N89-27671
A study of spacecraft electromagnetic contamination of artificial electron beams [AD-A209954] N89-27950
SPACECRAFT TEMPERATURE
Third European Symposium on Space Thermal Control and Life Support Systems [ESA-SP-288] N89-28214
Status of the US Space Station ECLSS and internal TCS N89-28215
System aspects of Columbus thermal control and life support N89-28216
Two-phase heat transport systems: Critical components --- Columbus N89-28224
Feasibility demonstration model of a capillary pumping loop N89-28225
Design and test of a two-phase coldplate N89-28226
Micro-fluid dynamical analysis of evaporating flows in heat pipes N89-28228
Express-method investigation and its application for heat pipe quality control N89-28229
The two approaches for the thermal control of the Columbus resource module and polar platform N89-28231
Redundancy concept for the Columbus man-tended free-flyer thermal control system N89-28232
Thermal control of Columbus pressurized modules N89-28233
Design concepts for Hermes thermal control N89-28234
Radiator conceptual studies for the Hermes spaceplane N89-28235
Advanced modular software development in thermal engineering --- spacecraft design N89-28247
Lumping, a powerful design tool for thermal control N89-28248
Application of expert systems to the thermal configuration of Giotto N89-28250
Thermal analysis of ROSAT in low-earth eclipse orbit employing steady-state calculations N89-28251
Efficient implementation of a description language for thermal simulators N89-28253
An algorithm for calculating thermodynamic properties of simple fluids suitable for space thermal control N89-28254
Design trends in communications satellite thermal subsystems N89-28255
The thermal control of EUTELSAT-2 N89-28256
TELE-X antenna module thermal control N89-28257
A thermal control design for the Quasat spacecraft N89-28258
Cryogenic activities at ESTEC N89-28266
Giotto: The thermal responses to its encounter with comet Halley N89-28273
Thermal aspects of an extended mission for Giotto N89-28274
ESATAN FHTS: A piped fluid network capability N89-28281
The Fluidnet development and application to preliminary sizing of fluid-loop systems N89-28282
Evolution of thermal analysis methods towards integrated system performance simulation N89-28283
Development of heat exchangers for hybrid radiators N89-28285

A 1-kW condenser for a two-phase heat rejection system N89-28288
A very low reflectance diffuse surface for thermal design of spacecraft N89-28289
Thermal analysis of advanced heat protection systems — hypersonic vehicles N89-28291
Cyrogenic fluid sink device for thermal control of a spaceplane during ascent and re-entry phases N89-28293

SPACECRAFT TRAJECTORIES
The ROSETTA/CNSR mission: A possible application of electric propulsion to interplanetary missions N89-27715

SPACELAB
Environmental control and life support systems for pressurized modules: From Spacelab to Columbus N89-28219

SPATIAL DISTRIBUTION
A smart, mapping, charting and geodesy control generator, phase 2
[AD-A208806] N89-28097
Evaluation of the AFGL (Air Force Geophysics Laboratory) cloud simulation models using satellite data
[AD-A208713] N89-28116
Water vapor profiling using microwave radiometry N89-28163
Pre-attentive and attentive visual information processing
[AD-A209884] N89-28206

SPATIAL FILTERING
Computer generated matched filters with spatial frequency tailoring
[AD-A209786] N89-28001

SPECIFIC HEAT
Glassy behaviour of YBa2Cu3O7
[DE89-613399] N89-28418

SPECIFICATIONS
Practical constraints on network architecture and signalling in the MSAT system N89-27915

SPECKLE INTERFEROMETRY
Speckle interferometry using fiber optic phase stepping
[NASA-TM-102331] N89-27999

SPECKLE PATTERNS
Mode filters and their applications
[INPE-4748-PRE/1421] N89-28312

SPECTRAL BANDS
Approaches toward a blue semiconductor laser
[NASA-CR-4252] N89-28004
Agricultural land-use classification in the Upper Rhine Valley using multitemporal TM data N89-28074
Tests of topographic mapping with Thematic Mapper images N89-28091

SPECTRAL CORRELATION
Oceanographic applications of laser technology N89-28141

SPECTRAL EMISSION
Approaches toward a blue semiconductor laser
[NASA-CR-4252] N89-28004

SPECTRAL REFLECTANCE
The use of digital elevation model for correcting the effects of projections in reforrestations of eucalyptus in mountainous regions
[INPE-4763-PRE/1432] N89-28048
Multitemporal analysis of forest areas in surroundings of Innsbruck, Austria N89-28086
Microwave remote sensing of soil moisture N89-28180
Agriculture Multiband Experiment Radiometer N89-28184

SPECTRAL RESOLUTION
Classification of small-scale forests in Flanders using LANDSAT TM digital data: Preliminary results N89-28080
Forest classification with TM data in the area of Freiburg, Federal Republic of Germany N89-28081
Calibration source maintenance, characterization and development N89-28193

SPECTRAL SIGNATURES
Forest damage mapping in Austria with the aid of LANDSAT TM image data N89-28078
Microscale ocean dynamics N89-28157

SPECTRORADIOMETERS
Ocean Data Acquisition System N89-28144
The Multichannel Ocean Color Sensor (MOCS) N89-28146
Advanced Solidstate Array Spectroradiometer N89-28183

SPECTROSCOPY
Quantitative estimation of component amplitude in multiexponential data: Application to time-resolved fluorescence spectroscopy
[AD-A210142] N89-27815
Transport and submillimeter wave spectroscopy of GaAs/Al sub xGa sub 1-xAs heterostructures
[AD-A209836] N89-28428

SPECTRUM ANALYSIS
Quadratic estimators of the power spectrum
[AD-A208601] N89-27964
Acoustooptic processing of two dimensional signals using temporal and spatial integration
[AD-A208686] N89-27966
Monitoring sources of nuclear radiation in space. Part 1: Early 1984 observations, revision
[AD-A209721] N89-28481
Monitoring sources of nuclear radiation in space 1980-1984 observations, revision
[AD-A209722] N89-28482
Monitoring sources of nuclear radiation in space 1985-1987 observations, revision
[AD-A209723] N89-28483

SPECULAR REFLECTION
Sensitivity analysis of reflection errors in infrared image simulation
[AD-A208600] N89-28394

SPEECH RECOGNITION
RELP: Speech coding using analysis by synthesis N89-27939
Northeast Artificial Intelligence Consortium annual report 1987. Volume 6: Artificial intelligence applications to speech recognition
[AD-A208380] N89-28334

SPHERES
Integrating sphere and hemisphere calibration update N89-28194

SPIN DYNAMICS
Characterization of structure in thin polymer resist films
[AD-A208677] N89-27848

SPIN STABILIZATION
Optimization of maneuvers of a spin-stabilized satellite, using magnetic coils
[INPE-4778-TDL/350] N89-27680

SPLINES
A uniformly differentiable approximation scheme for delay systems using splines
[AD-A208567] N89-28346

SPOT (FRENCH SATELLITE)
The vegetation payload of the SPOT-4 spacecraft thermal design and analysis N89-28259
Two years of in-orbit life of SPOT-1 heliosynchronous platform N89-28272

SPREAD SPECTRUM TRANSMISSION
Why is CDMA the solution for mobile satellite communication N89-27912
Receiver synchronization for spread spectrum transmission N89-27934

SPUTTERING
Ion beam and plasma methods of producing diamondlike carbon films
[NASA-TM-102301] N89-27836

STABILITY
Operational parameters for the superconducting cavity maser N89-27876

STABILITY TESTS
Flight calibration source development N89-28190

STABILIZATION
Small scale testing of a mass-stabilized electromagnetic projectile
[AD-A206916] N89-27682
Studies in stabilization and control of beams and plates
[AD-A208635] N89-28042

STABILIZERS (AGENTS)
Theoretical model for stabilization of clay-silt airport pavement subgrade systems. Phase 1: Laboratory investigation. Phase 2: Rutting tests
[DOT/FAA/PM-87/20-PHASE-1/2] N89-27673

STAINLESS STEELS
An acoustic emission investigation of the tensile failure of cathodically charged 304 stainless steel
[DE89-008752] N89-27816
Qualification program on stainless steel A95 heatpipe for space application N89-28294

STANDARDS
Risk assessment and late effects of radiation in low-earth orbits
[DE89-013043] N89-28478

STARS
Options for daytime monitoring of atmospheric visibility in optical communications N89-27895

STATIC TESTS
Static internal performance of a nonaxisymmetric vaned thrust reverser with flow splay capability
[NASA-TP-2933] N89-27634

STATIONARY ORBITS
Controlling a stationary orbit using electric propulsion N89-27741

STATIONKEEPING
FEEP power conditioning unit: Design and development status N89-27722
Auxiliary propulsion RF engine RIT 15: Prototype design and performance N89-27731
Design and integration of an electric propulsion system on the Eurostar spacecraft N89-27732
Controlling a stationary orbit using electric propulsion N89-27741

STATISTICAL ANALYSIS
A statistical derivation of the average degree of polymerization in a stirred tank reactor
[AD-A209873] N89-27857
Studies in statistical signal processing
[AD-A210054] N89-27952
Quadratic estimators of the power spectrum
[AD-A208601] N89-27964
Basic research in reliability for real systems
[AD-A209649] N89-28022
Discrimination of geobotanical anomalies in coniferous forests from LANDSAT TM data N89-28079
Statistical analysis of the LMS and modified stochastic gradient algorithms
[AD-A208618] N89-28319
A new item response theory modeling approach with applications to unidimensionality assessment and ability estimation
[AD-A207301] N89-28360

STATISTICAL DISTRIBUTIONS
The weight distribution and randomness of linear codes N89-27892
Evaluation of the AFGL (Air Force Geophysics Laboratory) cloud simulation models using satellite data
[AD-A208713] N89-28116

STEADY STATE
Nozzle type MPD thruster experimental investigations N89-27727
An improved code for nozzle type steady state MPD thrusters N89-27735
Steady state MPD devices for reentry simulation N89-27783
Thermal analysis of ROSAT in low-earth eclipse orbit employing steady-state calculations N89-28251

STELLAR OCCULTATION
Zonal winds between 25 and 120 km retrieved from solar occultation spectra
[NASA-CR-180086] N89-28113

STELLARATORS
Extension of stellarator approximation in magnetohydrodynamic equilibrium and stability of toroidal helical systems
[IPPJ-905] N89-28400

STEREOPHOTOGRAPHY
Analog methods and instruments N89-28094
Monocular electro-optical stereo scanner N89-28125

STEREOSCOPY
Effect of three-dimensional object type and density in simulated low-level flight
[AD-A209756] N89-27679

STIFFENING
Recent advances on the dynamic behavior of stiffened plates N89-28027

STIMULATED EMISSION
Extraordinary behavior of atoms near a phase conjugator
[AD-A209946] N89-28389

STIRLING CYCLE
Long-life Stirling cycle coolers for applications in the 60 to 110 K range N89-28267

STOCHASTIC PROCESSES
Statistical analysis of the LMS and modified stochastic gradient algorithms
[AD-A208618] N89-28319
Singular and bang-bang stochastic control
[AD-A208627] N89-28337
Markov processes applied to control, reliability and replacement
[AD-A208634] N89-28362
Research in stochastic processes
[AD-A209935] N89-28364
Stochastic approach to chaotic inflation and the distribution of universes
[DE89-778051] N89-28473

STOICHIOMETRY
Preparation and characterization of several conduction transition metal oxides
[AD-A208895] N89-28424

STORMS (METEOROLOGY)
Fiji South Pacific Severe Storm Detection and Warning System Project (SPSSD/WS) N89-28123
NASA follow-on on the Fiji South Pacific Severe Storm Warning System Project (SPSSD/WS) N89-28124

STRAIN GAGES
Evaluation of a strain-gage load calibration on a low-aspect-ratio wing structure at elevated temperature
[NASA-TP-2921] N89-28034

STRAIN MEASUREMENT
Noncontacting laser diffraction strain extensometer for material properties characterization at high temperatures
[DE89-013551] N89-28393
STRAIN RATE
Refinements in a viscoplastic model
[NASA-TM-102338] N89-28036
STRATEGY
Crisis decision-making: The impact of commercial satellites on the media, military and national leaders
[AD-A207334] N89-28449
STRATOSPHERE
Synchrotron X-ray fluorescence analyses of stratospheric cosmic dust: New results for chondritic and nickel-depleted particles
[DE89-014032] N89-28107
A new background stratospheric aerosol model for use in atmospheric radiation models
[AD-A210110] N89-28112
Correlative Measurements Program N89-28164
Ozone measurements using balloon-borne ozonesondes N89-28165
STRATOSPHERE RADIATION
A new background stratospheric aerosol model for use in atmospheric radiation models
[AD-A210110] N89-28112
STRESS (PHYSIOLOGY)
Evaluation of thermal stress induced by helicopter aircrew Chemical, Biological, Radiological (CBR) protective ensemble
[AD-A210123] N89-28303
STRESS ANALYSIS
Space Shuttle Main Engine structural analysis and data reduction/evaluation. Volume 3A: High pressure oxidizer turbo-pump preburner pump housing stress analysis report
[NASA-CR-183665] N89-27694
Thermal strains in a bimaterial joint: Experimental and numerical analysis
[DE89-013935] N89-28032
Stress intensity calibration of a ring specimen using a finite element technique
[AD-A208878] N89-28044
STRESS INTENSITY FACTORS
Stress intensity calibration of a ring specimen using a finite element technique
[AD-A208878] N89-28044
STRESS TENSORS
Polycrystalline plastic deformation and texture evolution for crystals lacking five independent slip systems
[AD-A208902] N89-28425
STRESS-STRAIN RELATIONSHIPS
Tungsten fiber reinforced copper matrix composites: A review
[NASA-TP-2924] N89-27796
Simulation of deformation and texture evolution in semi-crystalline polymers
[AD-A208854] N89-27852
An adhesive for field repair of composites
[AD-A209992] N89-27859
Refinements in a viscoplastic model
[NASA-TM-102338] N89-28036
STRONGLY COUPLED PLASMAS
Definition study and model for a tethered sounding rocket
[AD-A207367] N89-27699
STRUCTURAL ANALYSIS
Avionic system design methodology N89-27656
Space Shuttle Main Engine structural analysis and data reduction/evaluation. Volume 3A: High pressure oxidizer turbo-pump preburner pump housing stress analysis report
[NASA-CR-183665] N89-27694
Space Shuttle Main Engine structural analysis and data reduction/evaluation. Volume 3B: High pressure fuel turbo-pump preburner pump bearing assembly analysis
[NASA-CR-183666] N89-27695
Space Shuttle Main Engine structural analysis and data reduction/evaluation. Volume 4: High pressure fuel turbo-pump inlet housing analysis
[NASA-CR-183667] N89-27696
Space Shuttle Main Engine structural analysis and data reduction/evaluation. Volume 5: Main Injector LOX Inlet analysis
[NASA-CR-183668] N89-27697
Structural and thermal response of 30 cm diameter ion thruster optics
[NASA-TM-102124] N89-27703
Fiber reinforced structural ceramics for construction
[AD-A209976] N89-27858
An adhesive for field repair of composites
[AD-A209992] N89-27859
Reanalysis, compatibility and correlation in analysis of modified antenna structures N89-27906
Probabilistic structural analysis methods of hot engine structures
[NASA-TM-102091] N89-28030
Research and technology plans for FY 1989 and accomplishments for FY 1988 — Structural Mechanics Division
[NASA-TM-101592] N89-28035
Time series modeling for structural response prediction
[AD-A208808] N89-28354
United States Air Force Research Initiation Program for 1987, volume 4
[AD-A209729] N89-28438
STRUCTURAL DESIGN
High-speed civil transport study
[NASA-CR-4233] N89-27648
Review on turbomachinery blading design problems N89-27662
Design criteria for optimal blading design N89-27663
Overview on blading design methods N89-27664
Performance prediction for axial-flow compressor and turbine blading N89-27665
Blading design for multi-stage HP compressors N89-27666
Transonic and supersonic compressor blading design N89-27667
STRUCTURAL ENGINEERING
Precision pointing compensation for DSN antennas with optical distance measuring sensors N89-27882
Research and technology plans for FY 1989 and accomplishments for FY 1988 — Structural Mechanics Division
[NASA-TM-101592] N89-28035
Discrete enforcement of uncertain oscillator Gaussian response
[DE89-005595] N89-28038
Aerospace structures design on computers
[AD-A208611] N89-28321
STRUCTURAL MEMBERS
Damping in structural joints N89-28026
STRUCTURAL STABILITY
An integrating matrix formulation for buckling of rotating beams including the effects of concentrated masses
[NASA-CR-181862] N89-28342
SUBMILLIMETER WAVES
Transport and submillimeter wave spectroscopy of GaAs/Al sub xGa sub 1-xAs heterostructures
[AD-A209836] N89-28428
SUBROUTINES
Significant digit computation of the incomplete beta function ratios
[AD-A210118] N89-28358
SUBSONIC FLOW
A method for calculating asymmetric flow through nozzles
[AD-A209689] N89-27992
SULFIDES
Adsorption and reactions of cyclic sulfides on Mo(110)
[AD-A207324] N89-27803
SULFUR FLUORIDES
Tests of Halon 1301 test gas simulants
[AD-A207346] N89-27867
SULFURIC ACID
A new background stratospheric aerosol model for use in atmospheric radiation models
[AD-A210110] N89-28112
SUN
Interplanetary Particle Environment. Proceedings of a Conference
[NASA-CR-185461] N89-28454
Toward a descriptive model of solar particles in the heliosphere N89-28455
Toward a descriptive model of galactic cosmic rays in the heliosphere N89-28456
Current models of the intensely ionizing particle environment in space N89-28458
A new proton fluence model for E greater than 10 MeV N89-28459
Intensity/time profiles of solar particle events at one astronomical unit N89-28460
The radial dependence of the solar energetic particle flux N89-28461
Solar proton event forecasts N89-28462
Predicting the arrival times of solar particles N89-28463
Particles accelerated by shocks in the heliosphere N89-28464
High-energy particles very near the sun N89-28465
The anomalous cosmic-ray component N89-28467
Time variation of galactic cosmic rays N89-28469
Galactic cosmic rays in three dimensions N89-28470
SUNSPOTS
Interplanetary Particle Environment. Proceedings of a Conference
[NASA-CR-185461] N89-28454
Galactic cosmic rays in three dimensions N89-28470
SUPERCOMPUTERS
Parallel Architectures for Planetary Exploration Requirements (PAPER)
[NASA-CR-185370] N89-28475
SUPERCONDUCTING FILMS
Bibliography of high-T sub c superconducting films
[DE89-013395] N89-28409
SUPERCONDUCTING SUPER COLLIDER
Scintillating fiber detector development for the SSC
[DE89-013118] N89-27997
SUPERCONDUCTIVITY
Operational parameters for the superconducting cavity maser N89-27876
High-temperature superconductivity: Abstracts of NIST (National Institute of Standards and Technology) publications, 1987-1988
[PB89-148340] N89-28405
Superconductivity in the Ba(0.69)Y(0.46)CuO(3.15-delta) compound
[DE88-706000] N89-28406
SUPERCONDUCTORS
Martensitic phase transitions in nanocrystalline materials
[AD-A208804] N89-27827
Superconductivity in the Ba(0.69)Y(0.46)CuO(3.15-delta) compound
[DE88-706000] N89-28406
SUPERHIGH FREQUENCIES
Microwave time delays for the X/S-band feed system at X-band N89-27898
DSN radio science system design and testing for Voyager-Neptune encounter N89-27899
DSN 70-meter antenna microwave optics design and performance improvements. Part 1: Design optimization N89-27903
DSN 70-meter antenna X- and S-band calibration. Part 1: Gain measurements N89-27904
DSN 70-meter antenna X- and S-band calibration. Part 2: System noise temperature measurements and telecommunications link evaluation N89-27905
A comparative study of SHF (Super High Frequency) and EHF (Extremely High Frequency) satellite communications, volume 1
[AD-A208850] N89-27945
SUPERLATTICES
Development of superlattices for ultra high-speed electronic and optoelectronic devices
[AD-A209874] N89-28429
SUPERSONIC FLOW
Numerical simulation of control of supersonic shear layers
[AD-A209703] N89-27639
Transonic and supersonic compressor blading design N89-27667
SUPERSONIC NOZZLES
A method for calculating asymmetric flow through nozzles
[AD-A209689] N89-27992
SUPPORT INTERFERENCE
An evaluation of three experimental processes for two-dimensional transonic tests
[NASA-CR-181871] N89-27674
SUPPRESSORS
Studies in stabilization and control of beams and plates
[AD-A208635] N89-28042
SURFACE COOLING
Effect of alloying, rapid solidification, and surface kinetics on the high temperature environmental resistance of niobium
[AD-A209934] N89-27829
SURFACE GEOMETRY
Automatic construction of polyhedral surfaces from voxel representations
[AD-A210009] N89-28325
SURFACE LAYERS
Formation of monolayers by the coadsorption of thiols on gold: Variation in the length of the alkyl chain
[AD-A208386] N89-27824
Modelling organic surfaces with self-assembled monolayers
[AD-A208385] N89-27840
Fundamental mechanisms of tribology and their implications
[AD-A209941] N89-28020
Semiconductor-olefin adducts. Photoluminescent properties of cadmium sulfide and cadmium selenide in the presence of butenes
[AD-A208348] N89-28419
SURFACE PROPERTIES
Low density flow effects for hypervelocity vehicles
[AD-A208218] N89-27633
A comparison of rutting behavior of asphalt concrete under the F-4C/G and F-15C/D aircraft
[AD-A208911] N89-27678

SURFACE REACTIONS
The quartz crystal microbalance as an in situ tool in electrochemistry
[AD-A209852] N89-27811
Modelling organic surfaces with self-assembled monolayers
[AD-A208385] N89-27840
SURFACE ROUGHNESS
Modeling of ocean surface spectrum and surface scattering. Applications to reverberation prediction in the AAUS program
[AD-A210127] N89-28197
Electromagnetic reaction to molecular relaxation and its effect on absorption near a rough surface
[AD-A210069] N89-28390
SURFACE WAVES
Microscale ocean dynamics N89-28157
The Surface Wave Dynamics Experiment (SWADE) N89-28162
Modeling of ocean surface spectrum and surface scattering. Applications to reverberation prediction in the AAUS program
[AD-A210127] N89-28197
SURVEYS
Evaluation of head-up display formats for the F/A-18 hornet
[AD-A208651] N89-27660
Data base development and research and editorial support
[NASA-CR-183249] N89-28440
SURVIVAL
Effects of high terrestrial altitude on military performance
[AD-A209614] N89-28201
SWITZERLAND
Color analysis of inland waters using LANDSAT TM data N89-28062
SYMMETRY
Bunch-Kaufman factorization for real symmetric indefinite banded matrices
[NASA-CR-181860] N89-28341
Symmetry in the basic sciences
[AD-A207371] N89-28369
SYNCHRONISM
Receiver synchronization for spread spectrum transmission N89-27934
System theoretic models for high density VLSI structures
[AD-A209901] N89-27968
SYNCHROTRONS
Synchrotron X-ray fluorescence analyses of stratospheric cosmic dust: New results for chondritic and nickel-depleted particles
[DE89-014032] N89-28107
SYNTHESIS (CHEMISTRY)
Birth, death and transfiguration: The synthesis of preceramic polymers, their pyrolysis and their conversion to ceramics
[AD-A208437] N89-27841
SYNTHETIC APERTURE RADAR
The effects of snow on landmarks in K(sub u) band SAR images
[DE89-014578] N89-27925
Acoustooptic processing of two dimensional signals using temporal and spatial integration
[AD-A208686] N89-27966
Ice sheet studies using synthetic aperture radar N89-28152
Synthetic aperture microwave radiometer N89-28181
Preliminary statistical identification of radar imagery: Autoregressive-moving average (ARMA) models
[INPE-4771-PRE/1440] N89-28311
SYNTHETIC FOOD
Nutrition for short-duration space missions N89-28265
SYSTEMS ANALYSIS
System theoretic models for high density VLSI structures
[AD-A209901] N89-27968
SYSTEMS ENGINEERING
Systems Engineering
[AGARD-LS-164] N89-27650
Avionics system engineering: An introduction N89-27651
Avionic system requirements N89-27652
A structured approach to weapon system design N89-27653
Integrated avionics: Conceptual design N89-27654
Avionic system design methodology N89-27656
Rapid prototyping of complex avionics systems N89-27657
Modeling functional specifications for onboard software N89-27658
NASA in-house Commercially Developed Space Facility (CDSF) study report. Volume 1: Concept configuration definition
[NASA-TM-101586-VOL-1] N89-27687
A new method for analysis of limit cycle behavior of the NASA/JPL 70-meter antenna axis servos N89-27880
A multiflare horn with 1-megawatt power handling capability N89-27884
DSN radio science system design and testing for Voyager-Neptune encounter N89-27899
Proceedings of the Mobile Satellite System Architectures and Multiple Access Techniques Workshop
[NASA-CR-184564] N89-27907
Performance of DA/FDMA architecture proposed for MSS N89-27910
System level comparison of FDMA vs. CDMA (under conference guideline constraint) N89-27913
Alternative multiple-access techniques for mobile satellite systems N89-27914
MSAT signalling and network management architectures N89-27916
Communication engineering reports. Fundamental developments. Theoretical work
[ETN-89-94623] N89-27928
Model and method for systems development N89-27929
Study on the applicability of Asynchronous Time Division (ATD) techniques to satellite communications systems
[ESA-CR(P)-2742] N89-27943
A battery-powered flux compression generator system
[DE89-014230] N89-27958
Navigational and Environmental Measurement System (NEMS) N89-28178
Radiator conceptual studies for the Hermes spaceplane N89-28235
Intermediate heat exchanger for a nuclear-powered space power system N89-28287
SYSTEMS INTEGRATION
Avionics system engineering: An introduction N89-27651
Integrated avionics: Conceptual design N89-27654
The evolution of digital avionics architectures/systems N89-27655
Investigation of a liquid-fed water resistojet plume
[NASA-TM-102310] N89-27706
Evolution of thermal analysis methods towards integrated system performance simulation N89-28283
SYSTEMS MANAGEMENT
Resource contention management in parallel systems
[AD-A208809] N89-28332
SYSTEMS SIMULATION
Efficient implementation of a description language for thermal simulators N89-28253
ECLS simulation program N89-28284

T

TARGET ACQUISITION
Fixed interval smoothing algorithm for an extended Kalman filter for over-the-horizon ship tracking
[AD-A208555] N89-28318
TARGET RECOGNITION
Target signature modeling and bistatic scattering measurement studies
[NASA-CR-185434] N89-27870
Acoustooptic processing of two dimensional signals using temporal and spatial integration
[AD-A208686] N89-27966
TASKS
Human cognition and information display in C3I system tasks
[AD-A210012] N89-28302
TATB
Shock initiation modeling of multicomponent explosives
[DE89-012259] N89-27863
TECHNOLOGICAL FORECASTING
Critical technologies plan for the Committees on Armed Services, United States Congress, revision
[AD-A210170] N89-28439
International technology transfer: The rope to hang the west
[AD-A207347] N89-28452
TECHNOLOGY ASSESSMENT
NASA advanced space photovoltaic technology-status, potential and future mission applications
[NASA-TM-102093] N89-27705
Survey of electric propulsion thruster applicability to near earth space missions N89-27749
KrF lasers for inertial confinement fusion
[DE89-014272] N89-28007
TECHNOLOGY TRANSFER
International technology transfer: The rope to hang the west
[AD-A207347] N89-28452
TECHNOLOGY UTILIZATION
Avionic system design methodology N89-27656
The use of electric propulsion techniques for LEO atomic oxygen simulation N89-27787
TELECOMMUNICATION
Communication engineering reports. Fundamental developments. Theoretical work
[ETN-89-94623] N89-27928
A comparative study of SHF (Super High Frequency) and EHF (Extremely High Frequency) satellite communications, volume 1
[AD-A208850] N89-27945
Communications using channels formed by meteor bursts
[AD-A209856] N89-27949
Northeast Artificial Intelligence Consortium annual report for 1987. Volume 4: Research in automated photointerpretation
[AD-A208610] N89-28336
Development of superlattices for ultra high-speed electronic and optoelectronic devices
[AD-A209874] N89-28429
TELEMETRY
Database development for the DMSP (Defense Meteorological Satellite Program) SSIES experiment
[AD-A208712] N89-27691
Accuracy of telemetry signal power loss in a filter as an estimate for telemetry degradation N89-27900
A comparative study of SHF (Super High Frequency) and EHF (Extremely High Frequency) satellite communications, volume 1
[AD-A208850] N89-27945
Evaluation of the AFGL (Air Force Geophysics Laboratory) cloud simulation models using satellite data
[AD-A208713] N89-28116
A space radiation test model study
[AD-A208760] N89-28479
TELEOPERATORS
Design of an adaptive controller for a telerobot manipulator
[NASA-CR-185863] N89-28017
TELEPHONY
A robust signalling system for land mobile satellite services N89-27917
TELESCOPES
Site selection criteria for the optical atmospheric visibility monitoring telescopes N89-27896
TEMPERATURE COMPENSATION
Compensation for effects of ambient temperature on rare-earth doped fiber optic thermometer
[NASA-TM-102282] N89-27998
TEMPERATURE CONTROL
Operational parameters for the superconducting cavity maser N89-27876
Third European Symposium on Space Thermal Control and Life Support Systems
[ESA-SP-288] N89-28214
Status of the US Space Station ECLSS and internal TCS N89-28215
System aspects of Columbus thermal control and life support N89-28216
The Hermes spaceplane program: Status report on the thermal control, environment control and life support activities N89-28217
Two-phase heat transport systems: Critical components — Columbus N89-28224
Feasibility demonstration model of a capillary pumping loop N89-28225
Design and test of a two-phase coldplate N89-28226
Micro-fluid dynamical analysis of evaporating flows in heat pipes N89-28228
Express-method investigation and its application for heat pipe quality control N89-28229
The two approaches for the thermal control of the Columbus resource module and polar platform N89-28231
Redundancy concept for the Columbus man-tended free-flyer thermal control system N89-28232
Thermal control of Columbus pressurized modules N89-28233
Design concepts for Hermes thermal control N89-28234
Radiator conceptual studies for the Hermes spaceplane N89-28235
Advanced modular software development in thermal engineering — spacecraft design N89-28247
Lumping, a powerful design tool for thermal control N89-28248
Application of expert systems to the thermal configuration of Giotto N89-28250
Thermal analysis of ROSAT in low-earth eclipse orbit employing steady-state calculations N89-28251

An algorithm for calculating thermodynamic properties of simple fluids suitable for space thermal control N89-28254
Design trends in communications satellite thermal subsystems N89-28255
The thermal control of EUTELSAT-2 N89-28256
TELE-X antenna module thermal control N89-28257
A thermal control design for the Quasat spacecraft N89-28258
The vegetation payload of the SPOT-4 spacecraft thermal design and analysis N89-28259
Preparing Ulysses for launch N89-28260
Cryogenic activities at ESTEC N89-28266
Thermal control of the GRASP detector section N89-28271
Thermal aspects of an extended mission for Giotto N89-28274
Lessons learned from ROSAT thermal balance test: A combined solar simulation/infrared test N89-28275
Thermal control of Ni-H2 battery --- spacecraft battery N89-28276
Thermal software developments at ESTEC N89-28278
The Fluidnet development and application to preliminary sizing of fluid-loop systems N89-28282
A 1-kW condenser for a two-phase heat rejection system N89-28288
A very low reflectance diffuse surface for thermal design of spacecraft N89-28289
Thermal analysis of advanced heat protection systems --- hypersonic vehicles N89-28291
Cyrogenic fluid sink device for thermal control of a spaceplane during ascent and re-entry phases N89-28293
In-orbit degradation of thermo-optical properties on MARECS GEO-satellite N89-28297

TEMPERATURE EFFECTS
Effect of alloying, rapid solidification, and surface kinetics on the high temperature environmental resistance of niobium [AD-A209934] N89-27829
Thermal aspects of the ERS-1 SAR antenna deployment N89-28261
Issues and future directions in subsecond thermophysics [DE89-014228] N89-28434

TEMPERATURE MEASUREMENT
Thermal measurements of microwave transmitter feedhorn window N89-27885
Experience with advanced instrumentation in a hot section cascade [NASA-TM-102294] N89-27980
High-temperature optical-fiber pH sensor [DE89-014103] N89-28000
Rocket temperature soundings N89-28167
Electrodynamics, wind and temperature N89-28168
Radiosonde intercomparison N89-28169
Meteorological Sensor Calibration Facility N89-28188
Issues and future directions in subsecond thermophysics [DE89-014228] N89-28434

TEMPERATURE MEASURING INSTRUMENTS
Thermal measurements of microwave transmitter feedhorn window N89-27885

TEMPERATURE PROBES
Experience with advanced instrumentation in a hot section cascade [NASA-TM-102294] N89-27980

TEMPERATURE PROFILES
Non-condensible gas effects on the low-temperature heat pipe characteristics N89-28227
Application of optical measure theory to atmospheric temperature sounding from TOVS (TIROS Operational Vertical Sounder) radiances [AD-A209955] N89-28396

TEMPORAL DISTRIBUTION
Ocean color observations of phytoplankton distributions and primary productivity N89-28137
Water vapor profiling using microwave radiometry N89-28163

TEMPORAL RESOLUTION
Agricultural land-use classification in the Upper Rhine Valley using multitemporal TM data N89-28074

TENSILE PROPERTIES
An acoustic emission investigation of the tensile failure of cathodically charged 304 stainless steel [DE89-008752] N89-27816

TERMINAL FACILITIES
Terminal area forecasts: FY 1989 - 2005 [AD-A209805] N89-27644

TERRAIN
Determination of local empirical covariance functions from residual terrain reduced altimeter data [AD-A208678] N89-28095
User's guide for the Air Force surface-layer windflow model (AFWIND) [AD-A208710] N89-28109

TERRAIN ANALYSIS
Advanced Solidstate Array Spectroradiometer N89-28183

TEST CHAMBERS
Environmental calibration chamber operations N89-28192

TEST FACILITIES
Parametric study of the aerothermodynamics of a jet engine test facility [AD-A208512] N89-27675

TETHERING
Definition study and model for a tethered sounding rocket [AD-A207367] N89-27699

TEXTURES
The texture variation in extruded graphite [DE89-014086] N89-27837
Simulation of deformation and texture evolution in semi-crystalline polymers [AD-A208854] N89-27852
Polycrystalline plastic deformation and texture evolution for crystals lacking five independent slip systems [AD-A208902] N89-28425

THEMATIC MAPPERS (LANDSAT)
European Coordinated Effort for Monitoring the Earth's Environment. A Pilot Project Campaign on LANDSAT Thematic Mapper Applications (1985-1987) [ESA-SP-1102] N89-28055
Improved snow and glacier monitoring by the LANDSAT Thematic Mapper N89-28056
Multitemporal snow classification with TM data N89-28057
Utility of Thematic Mapper data for national survey of Irish lakes N89-28058
Application of LANDSAT data to hydrological mapping N89-28059
Application of remote sensing to irrigation water management in two Italian irrigation districts N89-28060
Remote sensing of limnological parameters in reservoirs N89-28061
Color analysis of inland waters using LANDSAT TM data N89-28062
Use of satellite imagery for the investigation of pollution-related characteristics of Dublin Bay, Ireland N89-28063
LANDSAT-5 TM study of suspended sediments in a fjord system in western Norway N89-28064
The use of Thematic Mapper imagery for peatland mapping and mineral exploration in Ireland N89-28065
LANDSAT TM study of sabkha surfaces in the Qattara Depression, northwestern Egypt N89-28066
Image processing strategies for mineral exploration in arid areas by use of TM data N89-28067
Applicability of LANDSAT TM data for geoscientific purposes in Iceland N89-28068
Karst drainage in the Peloponnesus area: A case study for application of TM data in hydrogeology N89-28069
Detection of short-term changes in tidal flat geomorphology N89-28070
Methodical and structural MSS and TM investigations in the Swabian Alb, SW Germany N89-28071
LANDSAT TM data used in the mapping of large-scale geological structures in coastal areas in Trondelag, central Norway N89-28072
Evaluation of the LANDSAT TM satellite in urban media: Application to the case of Brussels, Belgium N89-28073
Agricultural land-use classification in the Upper Rhine Valley using multitemporal TM data N89-28074
Mapping winter grazing areas for reindeer on Svalbard using LANDSAT Thematic Mapper data N89-28075
Remote sensing of the Madrid area ecosystems N89-28076
Comparison of the classification results obtained with TM and MSS data in land uses identification of the Communidad Autonoma de Cantabria N89-28077
Forest damage mapping in Austria with the aid of LANDSAT TM image data N89-28078
Discrimination of geobotanical anomalies in coniferous forests from LANDSAT TM data N89-28079
Classification of small-scale forests in Flanders using LANDSAT TM digital data: Preliminary results N89-28080
Forest classification with TM data in the area of Freiburg, Federal Republic of Germany N89-28081
Use of LANDSAT TM data for forest damage inventory N89-28082
Use of remote sensing in mapping of vegetation in the Dividalen area central Troms, northern Norway N89-28083
Multitemporal analysis of TM images: Application to forest fire mapping and inventory in a Mediterranean environment N89-28084
Large-scale forest management using LANDSAT Thematic Mapper data N89-28085
Multitemporal analysis of forest areas in surroundings of Innsbruck, Austria N89-28086
Comparison of MSS and TM LANDSAT data for cartography of surface structures in arid regions (southern Tunisia) N89-28087
Processing and interpretation of Thematic Mapper images in the Province of Piacenza (Italy) N89-28088
Production of satellite image maps from TM data N89-28089
Integrating TM and cartographic data N89-28090
Tests of topographic mapping with Thematic Mapper images N89-28091

THEMATIC MAPPING
Lithologic mapping of mafic intrusions in East Greenland using Landsat Thematic Mapper data [NASA-CR-183440] N89-28047
The use of edge detectors based on mathematical morphology in remote sensing imagery [INPE-4777-PRE/1446] N89-28050
Report of the Project Estima, phase 2: LANDSAT-TM data and agrometeorology in crop yield estimation of wheat at the farm level [INPE-4782-RPE/582-PHASE-2] N89-28051
The use of Thematic Mapper imagery for peatland mapping and mineral exploration in Ireland N89-28065

THEOREM PROVING
The sharing of rights and information in a capability-based protection system [NASA-CR-185388] N89-28445

THEOREMS
Some basic theorems on the cross-sums of certain class of numbers (M-1) when the operations are done with different bases M of the arithmetic [DE89-611892] N89-28343
Symmetry in the basic sciences [AD-A207371] N89-28369

THERMAL ABSORPTION
Coupling between radiation and gas dynamics [AD-A209657] N89-28102
Decomposition kinetics and film formation of an organometallic precursor to SiC on Si(100) [AD-A208384] N89-28420

THERMAL ANALYSIS
Flight set 360L001 (STS-26) insulation component. Volume 3: Final release [NASA-CR-183674] N89-27698
Structural and thermal response of 30 cm diameter ion thruster optics [NASA-TM-102124] N89-27703
Research and technology plans for FY 1989 and accomplishments for FY 1988 --- Structural Mechanics Division [NASA-TM-101592] N89-28035
Lumping, a powerful design tool for thermal control N89-28248
Thermal analysis of ROSAT in low-earth eclipse orbit employing steady-state calculations N89-28251
Efficient implementation of a description language for thermal simulators N89-28253
Design trends in communications satellite thermal subsystems N89-28255
TELE-X antenna module thermal control N89-28257
The vegetation payload of the SPOT-4 spacecraft thermal design and analysis N89-28259
Preparing Ulysses for launch N89-28260
Thermal aspects of the ERS-1 SAR antenna deployment N89-28261
Thermal software developments at ESTEC N89-28278
SOHO thermal modelling and analysis: The first application of ESATAN to a complete spacecraft N89-28279
Assembling the ISO thermal model with ESATAN N89-28280
ESATAN FHTS: A piped fluid network capability N89-28281
Evolution of thermal analysis methods towards integrated system performance simulation N89-28283
Thermal analysis of advanced heat protection systems --- hypersonic vehicles N89-28291

THERMAL CONDUCTIVITY
MM wavecomponents - SIS (Superconductor-Insulator-Superconductor) mixers [AD-A208632] N89-28421

THERMAL CONTROL COATINGS
A very low reflectance diffuse surface for thermal design of spacecraft N89-28289

THERMAL CYCLING TESTS
Computational simulation of high temperature metal matrix composites cyclic behavior [NASA-TM-102115] N89-27795

THERMAL DEGRADATION
Computational simulation of high temperature metal matrix composites cyclic behavior
[NASA-TM-102115] N89-27795
THERMAL ENERGY
Progress in parabolic dish technology
[DE89-009427] N89-28100
Intermediate heat exchanger for a nuclear-powered space power system N89-28287
THERMAL ENVIRONMENTS
Analysis of articulated manikin based convective heat transfer during walking
[AD-A208299] N89-28298
Evaluation of thermal stress induced by helicopter aircrew Chemical, Biological, Radiological (CBR) protective ensemble
[AD-A210123] N89-28303
THERMAL INSULATION
A review of the cathode construction for the RAE 10/25mN thruster N89-27759
Development of the Hermes flexible external insulation N89-28296
THERMAL PROTECTION
The space-rigidised thermal shield for the ESA Far-Infrared Space Telescope (FIRST) N89-28236
THERMAL RESISTANCE
Effect of alloying, rapid solidification, and surface kinetics on the high temperature environmental resistance of niobium
[AD-A209934] N89-27829
THERMAL SHOCK
Irradiation effects on resistance of thermal impact of composite used in space
[DE89-778069] N89-27794
THERMAL SIMULATION
Lessons learned from ROSAT thermal balance test: A combined solar simulation/infrared test N89-28275
THERMAL STABILITY
Protonic solid electrolytes: Thermal stability and conductivity of ammonium/hydronium beta'-alumina
[AD-A209911] N89-27813
THERMAL STRESSES
Thermal strains in a bimaterial joint: Experimental and numerical analysis
[DE89-013935] N89-28032
Studies in stabilization and control of beams and plates
[AD-A208635] N89-28042
Evaluation of thermal stress induced by helicopter aircrew Chemical, Biological, Radiological (CBR) protective ensemble
[AD-A210123] N89-28303
THERMAL VACUUM TESTS
Environmental calibration chamber operations N89-28192
Thermal control of Ni-H2 battery — spacecraft battery N89-28276
THERMIONIC CATHODES
Cathode processes in a MPD arcjet N89-27753
THERMISTORS
Meteorological Sensor Calibration Facility N89-28188
THERMOCOUPLES
Experience with advanced instrumentation in a hot section cascade
[NASA-TM-102294] N89-27980
THERMODYNAMIC PROPERTIES
Institute for Materials Science and Engineering: Metallurgy Division, technical activities 1988
[PB89-201321] N89-27819
Electron beam-positive polyimides
[AD-A208440] N89-27844
Refinements in a viscoplastic model
[NASA-TM-102338] N89-28036
An algorithm for calculating thermodynamic properties of simple fluids suitable for space thermal control N89-28254
In-orbit degradation of thermo-optical properties on MARECS GEO-satellite N89-28297
Application of quaternary phase diagrams to compound semiconductor processing
[DE89-014537] N89-28413
THERMODYNAMICS
Formation of monolayers by the coadsorption of thiols on gold: Variation in the length of the alkyl chain
[AD-A208386] N89-27824
Evaluation of new thermomechanical constitutive theory for snow N89-28052
Grain boundaries in silicon from zero temperature through melting
[DE89-013186] N89-28410
Real gas equations of state for CHEMKIN
[DE89-012794] N89-28432
Study of improved methods for predicting chemical equilibria
[DE89-014535] N89-28433
Issues and future directions in subsecond thermophysics
[DE89-014228] N89-28434
THERMOELECTRIC POWER GENERATION
Monitoring sources of nuclear radiation in space. Part 1: Early 1984 observations, revision
[AD-A209721] N89-28481
THERMOELECTRICITY
Phonon-drag thermoelectric power in high magnetic fields in heterojunctions
[DE89-013921] N89-28412
THERMOMETERS
Compensation for effects of ambient temperature on rare-earth doped fiber optic thermometer
[NASA-TM-102282] N89-27998
THERMOPHYSICAL PROPERTIES
Thermophysical properties of liquid niobium
[DE89-014288] N89-28435
THERMOPLASTIC RESINS
Solvent assisted delamination crack growth behavior of amorphous thermoplastic materials
[AD-A207365] N89-27833
THERMOPLASTICITY
Energetic polyoxetane thermoplastic elastomers: Synthesis and characterization
[AD-A209612] N89-27853
THERMOREGULATION
Acetylcholinesterase inhibitor, pyridostigmine bromide, reduces skin blood flow in humans
[AD-A209615] N89-28202
THIN FILMS
Nonpropulsive application of the RF-ion thruster for material processing with reactive gases N89-27786
Separation of oxygen from seawater by membrane permeation
[AD-A208863] N89-27809
Applications of the quartz crystal microbalance to electrochemistry
[AD-A209853] N89-27812
Ion beam and plasma methods of producing diamondlike carbon films
[NASA-TM-102301] N89-27836
Characterization of structure in thin polymer resist films
[AD-A208677] N89-27848
Polymer chain configurations in constrained geometries: Ultrathin films for microlithography
[AD-A208692] N89-27849
Photovoltaic Program Branch annual report, FY 1988
[DE89-000898] N89-28099
Evidence against the existence of strong diffuse X-ray scattering from gold twist boundaries at room temperature
[DE89-012726] N89-28407
Diamagnetic shielding and flux creep in a Tl-Ba-Ca-Cu-O thin film
[DE89-014550] N89-28414
Growth and characterization of zinc sulfide films by conversion of zinc oxide films with H2S
[AD-A208727] N89-28423
Transport and submillimeter wave spectroscopy of GaAs/Al sub xGa sub 1-xAs heterostructures
[AD-A209836] N89-28428
Zinc telluride growth on InP
[AD-A209924] N89-28430
THIOLS
Formation of monolayers by the coadsorption of thiols on gold: Variation in the length of the alkyl chain
[AD-A208386] N89-27824
Modelling organic surfaces with self-assembled monolayers
[AD-A208385] N89-27840
THREAT EVALUATION
Goals for limited strategic defenses
[DE89-012260] N89-28366
THREE AXIS STABILIZATION
Design and integration of an electric propulsion system on the Eurostar spacecraft N89-27732
THREE DIMENSIONAL BOUNDARY LAYER
Three-dimensional vortex interactions in turbulent boundary layers
[AD-A208624] N89-27991
THREE DIMENSIONAL FLOW
Spatial three-dimensional secondary instability compressible boundary-layer flows
[NASA-CR-4251] N89-27978
Three-dimensional vortex interactions in turbulent boundary layers
[AD-A208624] N89-27991
THREE DIMENSIONAL MODELS
Overview on blading design methods N89-27664
Space Shuttle Main Engine structural analysis and data reduction/evaluation. Volume 5: Main Injector LOX Inlet analysis
[NASA-CR-183668] N89-27697
THREE DIMENSIONAL MOTION
The use of stereo optical flow fields in the determination of three-dimensional motion and stereo correspondence
[DE89-012518] N89-27996
THRESHOLDS (PERCEPTION)
Higher order mechanisms of color vision
[AD-A209838] N89-28205
THRUST
Optimization of current distribution in an applied-field MPD thruster N89-27743
THRUST MEASUREMENT
Experimental investigation on the characteristics of a low power dc arcjet thruster N89-27780
THRUST REVERSAL
Static internal performance of a nonaxisymmetric vaned thrust reverser with flow splay capability
[NASA-TP-2933] N89-27634
THRUST VECTOR CONTROL
Static internal performance of a nonaxisymmetric vaned thrust reverser with flow splay capability
[NASA-TP-2933] N89-27634
Controlling a stationary orbit using electric propulsion N89-27741
THUNDERSTORMS
Interpretation of F106B and CV580 in-flight lightning data and form factor determination
[NASA-CR-4250] N89-28115
TIDAL FLATS
Detection of short-term changes in tidal flat geomorphology N89-28070
TIMBER IDENTIFICATION
Forest classification with TM data in the area of Freiburg, Federal Republic of Germany N89-28081
TIME
Time variation of galactic cosmic rays N89-28469
TIME DEPENDENCE
Implicit time dependent methods for inviscid and viscous compressible flows, with a discussion of the concept of numerical dissipation N89-27990
Monte Carlo reliability analysis
[AD-A210052] N89-28024
TIME DIVISION MULTIPLE ACCESS
Proceedings of the Mobile Satellite System Architectures and Multiple Access Techniques Workshop
[NASA-CR-184564] N89-27907
Choice of FDMA/SCPC access technique for aeronautical satellite voice system N89-27909
Study on the applicability of Asynchronous Time Division (ATD) techniques to satellite communications systems
[ESA-CR(P)-2742] N89-27943
TIME DIVISION MULTIPLEXING
Choice of FDMA/SCPC access technique for aeronautical satellite voice system N89-27909
TIME LAG
Microwave time delays for the X/S-band feed system at X-band N89-27898
TIME OF FLIGHT SPECTROMETERS
Vibrational predissociation of shock-selected C2H4 and NH3 clusters
[MPIS-6/1988] N89-28373
CAMAC time-of-flight analyzer for molecular beam diagnostics N89-28377
TIME SERIES ANALYSIS
Time series modeling for structural response prediction
[AD-A208808] N89-28354
TIME SHARING
Load balancing in multiprocessor systems
[AD-A210144] N89-28327
TIRES
Nonlinear viscoelastic characteristics of polymeric materials
[DE89-012680] N89-27835
TITANIUM ALLOYS
Rapidly solidified titanium alloys by melt overflow
[NASA-CR-4253] N89-27818
Advanced tribological coatings for high specific strength alloys
[AD-A208504] N89-27825
Noncontacting laser diffraction strain extensometer for material properties characterization at high temperatures
[DE89-013551] N89-28393
TITANIUM COMPOUNDS
Fundamental magnetic studies of iron-rare-earth-metalloid alloys
[DE89-013803] N89-27820
TOKAMAK DEVICES
Development of high-current RF plasma sources for neutral particle injections N89-27785
Role of edge magnetic shear on the limiter H-mode transition of the JIPP T-IIU tokamak
[IPPJ-906] N89-28399
Experimental study on the deposition profile of the ICRF power and electron thermal diffusivity
[IPPJ-908] N89-28401

Review of effects of NBI (Neutral Beam Injection) and rotation on plasma transport in tokamaks
[DE89-014109] N89-28402

TOMOGRAPHY
Engineering research and development: Thrust area report FY 88
[DE89-014320] N89-28453

TOPOGRAPHY
European Coordinated Effort for Monitoring the Earth's Environment. A Pilot Project Campaign on LANDSAT Thematic Mapper Applications (1985-1987)
[ESA-SP-1102] N89-28055
Tests of topographic mapping with Thematic Mapper images N89-28091
Determination of local empirical covariance functions from residual terrain reduced altimeter data
[AD-A208678] N89-28095
Ocean topography experiment (TOPEX) radar altimeter N89-28119
Mars Observer Radar Altimeter Radiometer (MORAR) N89-28120
Advanced altimetry N89-28128
Earth Observing System (EOS) advanced altimetry N89-28129
Lunar observer laser altimeter N89-28134

TOPOLOGY
Topology of modified helical gears
[NASA-TM-102134] N89-28015
Automatic change in contour diagrams on the occasion of scale reduction using a material morphology
[INPE-4769-PRE/1438] N89-28049
Automatic construction of polyhedral surfaces from voxel representations
[AD-A210009] N89-28325
The topological structure of grain boundaries
[DE89-014676] N89-28415

TOROIDAL PLASMAS
Extension of stellarator approximation in magnetohydrodynamic equilibrium and stability of toroidal helical systems
[IPPJ-905] N89-28400

TORQUE
Implementation of a digital torque controller of a reaction wheel with an incremental computer
[INPE-4784-PRE/1447] N89-28333

TORSION
A data acquisition and control program for axial-torsional fatigue testing
[NASA-TM-102041] N89-28029
Differential geodesy of the Eotvos torsion balance
[AD-A208711] N89-28096

TORSIONAL STRESS
Anomalous stresses versus extent of cure in an epoxy composite specimen
[AD-A208523] N89-27798

TOUGHNESS
Novel methods for reinforcing elastomers
[AD-A210150] N89-27861
Dynamic fracture toughness testing
[AD-A209948] N89-28046

TOXICITY
The phototoxicity of blue light on the functional properties of the retinal pigment epithelium
[AD-A209834] N89-28204
United States Air Force Research Initiation Program for 1987, volume 4
[AD-A209729] N89-28438

TRACKING (POSITION)
The Telecommunications and Data Acquisition Report
[NASA-CR-185431] N89-27871
High-precision radiometric tracking for planetary approach and encounter in the inner solar system N89-27873
Fixed interval smoothing algorithm for an extended Kalman filter for over-the-horizon ship tracking
[AD-A208555] N89-28318

TRACKING NETWORKS
GPS (Global Positioning System) orbit determination: Bootstrapping to resolve carrier phase ambiguity
[AD-A209974] N89-27681

TRAJECTORIES
Quantum corrections for inelastic atom-surface scattering
[AD-A209850] N89-28387
Studies of the cosmic ray penumbra
[AD-A210109] N89-28484

TRANSIENT RESPONSE
A new method for analysis of limit cycle behavior of the NASA/JPL 70-meter antenna axis servos N89-27880

TRANSITION METALS
Transition metal activation and functionalization of carbon-hydrogen bonds
[DE89-012949] N89-27804
Superexchange coupling mechanisms for electron transfer processes
[DE89-013568] N89-28411
Preparation and characterization of several conduction transition metal oxides
[AD-A208895] N89-28424

TRANSITION TEMPERATURE
The influence of the polymer backbone flexibility on the phase transitions of side chain liquid crystal polymers containing
yl side groups
[AD-A208821] N89-27851

TRANSMISSION EFFICIENCY
MSAT signalling and network management architectures N89-27916
COMM-Q: A simulation model to determine saturation points in nodal type networks
[AD-A207294] N89-28329

TRANSMISSION LINES
Studies of phase-conjugate optical device concepts
[AD-A206219] N89-28391

TRANSMISSION LOSS
The use of interleaving for reducing radio loss in trellis-coded modulation systems N89-27889
Performance of concatenated codes using 8-bit and 10-bit Reed-Solomon codes N89-27890

TRANSMISSIONS (MACHINE ELEMENTS)
Topology of modified helical gears
[NASA-TM-102134] N89-28015

TRANSMITTERS
State-of-the-art fiber optics for short distance frequency reference distribution N89-27878
Thermal measurements of microwave transmitter feedhorn window N89-27885
Multipurpose exciter with low phase noise N89-27887

TRANSONIC FLOW
Computation of transonic potential flow past RAE-Wing-A and Body-B2 combination
[PD-CF-8921] N89-27637
Terminal shock response in ramjet inlets to abrupt downstream perturbations
[AD-A209788] N89-27640
Transonic and supersonic compressor blading design N89-27667
An evaluation of three experimental processes for two-dimensional transonic tests
[NASA-CR-181871] N89-27674

TRANSPORT AIRCRAFT
Investigation of transport airplane fuselage fuel tank installations under crash conditions
[DOT/FAA/CT-88/24] N89-27643
High-speed civil transport study. Summary
[NASA-CR-4234] N89-27647
High-speed civil transport study
[NASA-CR-4233] N89-27648

TRANSPORT PROPERTIES
United States Air Force Research Initiation Program for 1987, volume 3
[AD-A209728] N89-28437
The radial dependence of the solar energetic particle flux N89-28461

TRANSVERSE WAVES
Parametric study of electromagnetic waves propagating in absorbing curved S ducts
[NASA-TM-102024] N89-27923

TRAPPED MAGNETIC FIELDS
Detection of artificial sources of nuclear radiation in space, revision
[AD-A209720] N89-28480

TRIBOLOGY
Advanced tribological coatings for high specific strength alloys
[AD-A208504] N89-27825
Fundamental mechanisms of tribology and their implications
[AD-A209941] N89-28020

TROPICAL METEOROLOGY
Tropical Rainfall Measurement Mission N89-28126
Analyses of the wind-driven response of tropical oceans N89-28155

TROPOSPHERE
The effect of spatial and temporal wet-troposphere fluctuations on connected element interferometry N89-27874
Tropospheric nitric oxide measurements N89-28171

TUNGSTEN
Tungsten fiber reinforced copper matrix composites: A review
[NASA-TP-2924] N89-27796

TURBINE BLADES
Blading Design for Axial Turbomachines
[AGARD-LS-167] N89-27661
Review on turbomachinery blading design problems N89-27662
Overview on blading design methods N89-27664
Performance prediction for axial-flow compressor and turbine blading N89-27665
Blading design for cooled high-pressure turbines N89-27668

TURBINE ENGINES
Ceramic joining in the United States
[DE89-009323] N89-27834

TURBINE PUMPS
Space Shuttle Main Engine structural analysis and data reduction/evaluation. Volume 3A: High pressure oxidizer turbo-pump preburner pump housing stress analysis report
[NASA-CR-183665] N89-27694
Space Shuttle Main Engine structural analysis and data reduction/evaluation. Volume 4: High pressure fuel turbo-pump inlet housing analysis
[NASA-CR-183667] N89-27696
Probabilistic structural analysis methods of hot engine structures
[NASA-TM-102091] N89-28030

TURBOGENERATORS
Intermediate heat exchanger for a nuclear-powered space power system N89-28287

TURBOMACHINE BLADES
Probabilistic structural analysis methods of hot engine structures
[NASA-TM-102091] N89-28030

TURBOMACHINERY
Blading design for multi-stage HP compressors N89-27666

TURBULENCE MODELS
A critical comparison of turbulence models for homogeneous shear flows in a rotating frame
[NASA-CR-181864] N89-27977

TURBULENT BOUNDARY LAYER
Effects of an embedded vortex on a single film-cooling jet in a turbulent boundary layer
[AD-A207374] N89-27974
Three-dimensional vortex interactions in turbulent boundary layers
[AD-A208624] N89-27991

TURBULENT FLOW
A critical comparison of turbulence models for homogeneous shear flows in a rotating frame
[NASA-CR-181864] N89-27977
Wind-Wave-Current Tank Research Facility usage and status N89-28161

TURBULENT WAKES
Photogrammetric technique for in-flight ranging of trailing vortices using entrained balloons
[NASA-TM-4129] N89-27995

TWO DIMENSIONAL MODELS
Space Shuttle Main Engine structural analysis and data reduction/evaluation. Volume 4: High pressure fuel turbo-pump inlet housing analysis
[NASA-CR-183667] N89-27696

TWO PHASE FLOW
Further investigation of flow modeling during solid propellant processing
[AD-A209787] N89-27866
An experimental study to determine the relative influence of fluid-fluid interactions and media heterogeneities on the growth of immiscible viscous fingers
[DE89-013122] N89-27976
Interfacial area measurement methods
[DE89-013426] N89-27982
Subcooled boiling of downward flow in a vertical annulus
[DE89-005320] N89-27983
Development of a sensor for high-quality two-phase flow N89-28230

U

U.S.S.R.
Bibliography of Soviet laser developments: January - February 1988
[AD-A209802] N89-28011
International technology transfer: The rope to hang the west
[AD-A207347] N89-28452

U.S.S.R. SPACE PROGRAM
Recent progress in the USSR electric propulsion N89-27710

UH-60A HELICOPTER
Baseline performance verification of the 12th year production UH-60A Black Hawk helicopter
[AD-A208671] N89-27632

ULTRAHIGH FREQUENCIES
DSN 70-meter antenna X- and S-band calibration. Part 2: System noise temperature measurements and telecommunications link evaluation N89-27905

A comparative study of SHF (Super High Frequency) and EHF (Extremely High Frequency) satellite communications, volume 1
[AD-A208850] N89-27945
ULTRASONIC TESTS
Ultrasonic nondestructive evaluation of damage in continuous fiber composites
[AD-A208840] N89-27799
ULTRAVIOLET ASTRONOMY
Coronagraph observations and analyses of the ultraviolet solar corona
[NASA-CR-185830] N89-28476
ULTRAVIOLET SPECTRA
Coronagraph observations and analyses of the ultraviolet solar corona
[NASA-CR-185830] N89-28476
ULYSSES MISSION
Preparing Ulysses for launch N89-28260
UNDERWATER ACOUSTICS
Modeling of ocean surface spectrum and surface scattering. Applications to reverberation prediction in the AAUS program
[AD-A210127] N89-28197
UNITED STATES
The private sector economic and employment benefits to the nation and to each state of proposed FY 1990 NASA procurement expenditures
[NASA-CR-185894] N89-28448
International technology transfer: The rope to hang the west
[AD-A207347] N89-28452
UNIVERSE
Stochastic approach to chaotic inflation and the distribution of universes
[DE89-778051] N89-28473
UNSTEADY FLOW
Small scale model tests in small wind and water tunnels at high incidence and pitch rates. Volume 3: Water tunnel (HFF) data base
[AD-A208690] N89-27638
Studies of unsteady vortex flap aerodynamics
[AD-A209837] N89-27641
UPLINKING
The DSS-14 C-band exciter N89-27901
Geostar's system architectures N89-27911
UPPER ATMOSPHERE
Solar proton event forecasts N89-28462
USER MANUALS (COMPUTER PROGRAMS)
Missile Datcom. Volume 2: User's manual
[AD-A210128] N89-27685
User's guide for the Air Force surface-layer windflow model (AFWIND)
[AD-A208710] N89-28109
Ved editor for MC5600 computer system
[PD-SE-8907] N89-28306
Vi editor for MC56000 computer system
[PD-SE-8906] N89-28307
Image Algebra FORTRAN preprocessor: User's manual
[AD-A208612] N89-28349
USER REQUIREMENTS
Third International Satellite Direct Broadcast Services User's Conference N89-28176
An implementation of a data definition facility for the graphics language for database
[AD-A207380] N89-28442

V

VACUUM CHAMBERS
Xenon ion thruster test facility: Design and operation N89-27745
VACUUM DEPOSITION
Ion-assisted deposition of silver films on ceramics for friction and wear control
[DE89-014635] N89-27821
VALVES
A new method for analysis of limit cycle behavior of the NASA/JPL 70-meter antenna axis servos N89-27880
VAN DER WAAL FORCES
Infrared photodissociation and cluster-specific detection of internally cold (C2H4) van der Waals complexes N89-28375
Infrared photodissociation of van der Waals complexes selectively prepared by molecular beam scattering N89-28376
VANES
Space Shuttle Main Engine structural analysis and data reduction/evaluation. Volume 4: High pressure fuel turbo-pump inlet housing analysis
[NASA-CR-183667] N89-27696
VAPOR DEPOSITION
Nonpropulsive application of the RF-ion thruster for material processing with reactive gases N89-27786
Vapor phase deposition studies of phosphate esters on metal and ceramic surfaces
[PB89-148985] N89-27831
Equipment models for process optimization and control using smart response surfaces
[AD-A208321] N89-27838
Comparison of equipment modeling methods as applied to the LPCVD of in-situ P-doped polysilicon
[AD-A208373] N89-27839
Zinc telluride growth on InP
[AD-A209924] N89-28430
VAPOR PHASES
Vapor phase deposition studies of phosphate esters on metal and ceramic surfaces
[PB89-148985] N89-27831
VAPORS
ZPIMP: A zero-D Z-pinch implosion code
[AD-A208381] N89-27962
GMBU (Ground Mobile Breadboard Upgrade) lidar and bubbler correlation study at Dugway Proving Ground
[AD-A207297] N89-28002
VARIATIONS
The effect of spatial and temporal wet-troposphere fluctuations on connected element interferometry N89-27874
Time variation of galactic cosmic rays N89-28469
VAX COMPUTERS
The Laboratory for Oceans Computing Facility N89-28173
VEGETATIVE INDEX
Agricultural land-use classification in the Upper Rhine Valley using multitemporal TM data N89-28074
Mapping winter grazing areas for reindeer on Svalbard using LANDSAT Thematic Mapper data N89-28075
Agriculture Multiband Experiment Radiometer N89-28184
VELOCITY
Further investigation of flow modeling during solid propellant processing
[AD-A209787] N89-27866
VERBAL COMMUNICATION
Visualizing and rhyming cause differences in alpha suppression
[AD-A210005] N89-28210
VERTICAL DISTRIBUTION
Ozone measurements using balloon-borne ozonesondes N89-28165
VERY LARGE SCALE INTEGRATION
Average interconnection length and interconnection distribution for rectangular arrays
[AD-A209848] N89-27967
System theoretic models for high density VLSI structures
[AD-A209901] N89-27968
Hybrid wafer-scale processor
[AD-A209944] N89-27969
VERY LONG BASE INTERFEROMETRY
High-precision radiometric tracking for planetary approach and encounter in the inner solar system N89-27873
Operating and environmental characteristics of Sigma Tau hydrogen masers used in the Very Long Baseline Array (VLBA) N89-27877
VESTIBULAR TESTS
Age-related changes in human vestibulo-ocular reflexes: Sinusoidal rotation and caloric tests
[NASA-CR-185857] N89-28211
Age-related changes in human vestibulo-ocular and optokinetic reflexes: Pseudorandom rotation tests
[NASA-CR-185856] N89-28213
VIBRATION
The Shock and Vibration Digest, volume 21, no. 4 N89-28025
Damping in structural joints N89-28026
Recent advances on the dynamic behavior of stiffened plates N89-28027
Studies in stabilization and control of beams and plates
[AD-A208635] N89-28042
VIBRATION DAMPING
Model based damping of coupled horizontal and vertical oscillations in a flexible rod
[DE89-007034] N89-28039
VIBRATION TESTS
Shaking in cryogenic conditions N89-28277
VIBRATIONAL SPECTRA
Comparison of vacuum-annealed and electrochemically cycled electrodes in adsorption and electrocatalysis: Aromatic compounds at platinum (111) and polycrystalline platinum
[AD-A210011] N89-27814
Design considerations for an earth based flexible robotic system
[AD-A209635] N89-28018
Vibrational predissociation of shock-selected C2H4 and NH3 clusters, introduction N89-28374
Charge transfer and inelastic scattering in proton-molecule collisions
[MPIS-13/1988] N89-28378
Observation of vibrationally resolved charge transfer in H(+) + H2 at a collision energy Ecm = 20 eV N89-28382
A three-dimensional quantum mechanical study of vibrational inelastic and charge transfer processes in H(+) + H2 at a collision energy Ecm = 20 eV N89-28384
Charge transfer and structured vibrational distributions in H(+) + CH4 low-energy collisions N89-28385
VIBRATIONAL STRESS
Shaking in cryogenic conditions N89-28277
VIDEO SIGNALS
Digital CODEC for real-time processing of broadcast quality video signals at 1.8 bits/pixel
[NASA-TM-102325] N89-27927
VINYL COPOLYMERS
Piezoelectric polymer/ceramic composite
[AD-A208905] N89-27801
VINYL RADICAL
Poly(enaminonitriles): Novel materials for use in electronics
[AD-A208439] N89-27843
VISCOELASTICITY
Nonlinear viscoelastic characteristics of polymeric materials
[DE89-012680] N89-27835
Dynamic fracture and deformation of solid propellant
[AD-A208691] N89-27865
VISCOPLASTICITY
Refinements in a viscoplastic model
[NASA-TM-102338] N89-28036
Polycrystalline plastic deformation and texture evolution for crystals lacking five independent slip systems
[AD-A208902] N89-28425
VISCOUS FLOW
An experimental study to determine the relative influence of fluid-fluid interactions and media heterogeneities on the growth of immiscible viscous fingers
[DE89-013122] N89-27976
Implicit time dependent methods for inviscid and viscous compressible flows, with a discussion of the concept of numerical dissipation N89-27990
VISIBILITY
A visibility characterization program for optical communications through the atmosphere N89-27894
Options for daytime monitoring of atmospheric visibility in optical communications N89-27895
Site selection criteria for the optical atmospheric visibility monitoring telescopes N89-27896
Optimal three-dimensional path planning using visibility constraints
[AD-A207357] N89-28310
VISION
Pre-attentive and attentive visual information processing
[AD-A209884] N89-28206
Modulation of spontaneous brain activity during mental imagery
[AD-A209918] N89-28208
A survey of visual preprocessing and shape representation techniques
[NASA-CR-185418] N89-28309
VISUAL ACUITY
Higher order mechanisms of color vision
[AD-A209838] N89-28205
VISUAL FIELDS
Optimal three-dimensional path planning using visibility constraints
[AD-A207357] N89-28310
VISUAL FLIGHT
Effect of three-dimensional object type and density in simulated low-level flight
[AD-A209756] N89-27679
VISUAL PERCEPTION
Eye movements and visual information processing
[AD-A209817] N89-28203
Higher order mechanisms of color vision
[AD-A209838] N89-28205
Pre-attentive and attentive visual information processing
[AD-A209884] N89-28206
Visualizing and rhyming cause differences in alpha suppression
[AD-A210005] N89-28210
Age-related changes in human posture control: Sensory organization tests
[NASA-CR-185858] N89-28212
Age-related changes in human vestibulo-ocular and optokinetic reflexes: Pseudorandom rotation tests
[NASA-CR-185856] N89-28213
Perception of motion in statistically-defined displays
[AD-A208695] N89-28301

VISUAL SIGNALS
Eye movements and visual information processing
[AD-A209817] N89-28203
VISUAL STIMULI
Age-related changes in human vestibulo-ocular and optokinetic reflexes: Pseudorandom rotation tests
[NASA-CR-185856] N89-28213
VISUAL TASKS
Age-related changes in human vestibulo-ocular and optokinetic reflexes: Pseudorandom rotation tests
[NASA-CR-185856] N89-28213
VOICE COMMUNICATION
Choice of FDMA/SCPC access technique for aeronautical satellite voice system N89-27909
VORTEX FLAPS
Studies of unsteady vortex flap aerodynamics
[AD-A209837] N89-27641
VORTICES
Numerical simulation of control of supersonic shear layers
[AD-A209703] N89-27639
Effects of an embedded vortex on a single film-cooling jet in a turbulent boundary layer
[AD-A207374] N89-27974
VOYAGER PROJECT
DSN radio science system design and testing for Voyager-Neptune encounter N89-27899
VOYAGER 1 SPACECRAFT
Software package for performing experiments about the convolutionally encoded Voyager 1 link N89-27888

W

WAFERS
Equipment models for process optimization and control using smart response surfaces
[AD-A208321] N89-27838
Hybrid wafer-scale processor
[AD-A209944] N89-27969
WALKING
Analysis of articulated manikin based convective heat transfer during walking
[AD-A208299] N89-28298
Algorithmic control of walking
[AD-A210117] N89-28326
WALKING MACHINES
Algorithmic control of walking
[AD-A210117] N89-28326
WALLS
A new analysis of beam-waveguide antennas considering the presence of the enclosure N89-27886
WAR GAMES
Space asset modeling for wargame integration
[AD-A207350] N89-28365
WARFARE
Space asset modeling for wargame integration
[AD-A207350] N89-28365
WARNING SYSTEMS
Analysis of a system to prevent helicopter rotor blade-airframe strikes
[AD-A209804] N89-27649
Verification of the production safe flight instrument corporation OV/RV-1D stall warning system
[AD-A207392] N89-27659
Fiji South Pacific Severe Storm Detection and Warning System Project (SPSSD/WS) N89-28123
NASA follow-on on the Fiji South Pacific Severe Storm Warning System Project (SPSSD/WS) N89-28124
WASTE WATER
Analytical procedures for environmental quality control, volume 2
[PB89-158612] N89-28103
Test results on re-use of reclaimed shower water: Summary --- space stations N89-28262
WATER
Investigation of a liquid-fed water resistojet plume
[NASA-TM-102310] N89-27706
WATER COLOR
Oceanographic applications of laser technology N89-28141
Ocean Data Acquisition System N89-28144
Coastal Zone Color Scanner N89-28145
The Multichannel Ocean Color Sensor (MOCS) N89-28146
WATER DEPTH
Airborne in-situ spectral characterization and concentration estimates of fluorescent organics as a function of depth N89-28140
WATER MANAGEMENT
Use of satellite imagery for the investigation of pollution-related characteristics of Dublin Bay, Ireland N89-28063
LANDSAT-5 TM study of suspended sediments in a fjord system in western Norway N89-28064
MELISSA: A micro-organisms-based model for CELSS development N89-28222
WATER POLLUTION
Use of satellite imagery for the investigation of pollution-related characteristics of Dublin Bay, Ireland N89-28063
Analytical procedures for environmental quality control, volume 2
[PB89-158612] N89-28103
Analytical procedures for environmental quality control, volume 3
[PB89-158620] N89-28104
WATER QUALITY
Analytical procedures for environmental quality control, volume 2
[PB89-158612] N89-28103
Analytical procedures for environmental quality control, volume 3
[PB89-158620] N89-28104
The liquid management section of the Hermes ECLSS N89-28263
WATER RECLAMATION
Test results on re-use of reclaimed shower water: Summary --- space stations N89-28262
The liquid management section of the Hermes ECLSS N89-28263
WATER TREATMENT
Test results on re-use of reclaimed shower water: Summary --- space stations N89-28262
The liquid management section of the Hermes ECLSS N89-28263
WATER VAPOR
The effect of spatial and temporal wet-troposphere fluctuations on connected element interferometry N89-27874
Water vapor profiling using microwave radiometry N89-28163
Mobile lidar system for measurement of water vapor mixing ratio and ozone number density N89-28166
WATER WAVES
Microwave radar oceanographic investigations N89-28158
Surface Contour Radar (SCR) contributions to FASINEX N89-28159
Wind-Wave-Current Tank Research Facility usage and status N89-28161
The Surface Wave Dynamics Experiment (SWADE) N89-28162
WAVE ATTENUATION
Parametric study of electromagnetic waves propagating in absorbing curved S ducts
[NASA-TM-102024] N89-27923
WAVE DISPERSION
Investigation of instabilities in MPD thruster flows using a linear dispersion relation N89-27737
WAVE EQUATIONS
Reflection and refraction of finite amplitude acoustic waves at a fluid-fluid interface
[AD-A209800] N89-28371
WAVE EXCITATION
Nonlinear waves
[AD-A209822] N89-27993
WAVE FUNCTIONS
Superexchange coupling mechanisms for electron transfer processes
[DE89-013568] N89-28411
WAVE GENERATION
A two-stream plasma electron microwave source for high-power millimeter wave generation, phase 1
[AD-A209942] N89-28404
WAVE INTERACTION
Algebraic analysis of the electromagnetic wave interaction with the two-level system with two-fold degenerated states
[DE89-611932] N89-27926
Wave/current interaction model N89-28153
WAVE PROPAGATION
Propagation characteristics of electromagnetic waves in concrete
[AD-A207387] N89-27921
Parametric study of electromagnetic waves propagating in absorbing curved S ducts
[NASA-TM-102024] N89-27923
Nonlinear waves
[AD-A209822] N89-27993
Efficient second harmonic conversion of broadband high-peak-power Nd:glass laser radiation using large-aperture KDP crystals in quadrature
[DE89-012961] N89-28003
Reflection and refraction of finite amplitude acoustic waves at a fluid-fluid interface
[AD-A209800] N89-28371
WAVE REFLECTION
Analysis of maritime mobile satellite communication systems
[AD-A207358] N89-27920
WAVEGUIDE ANTENNAS
A new analysis of beam-waveguide antennas considering the presence of the enclosure N89-27886
WAVEGUIDES
A multiflare horn with 1-megawatt power handling capability N89-27884
Microwave time delays for the X/S-band feed system at X-band N89-27898
WEAPON SYSTEMS
A structured approach to weapon system design N89-27653
Integrated avionics: Conceptual design N89-27654
Critical technologies plan for the Committees on Armed Services, United States Congress, revision
[AD-A210170] N89-28439
WEAR RESISTANCE
Ion-assisted deposition of silver films on ceramics for friction and wear control
[DE89-014635] N89-27821
WEATHER
A visibility characterization program for optical communications through the atmosphere N89-27894
WEATHER FORECASTING
Adaptive grid methods for numerical weather prediction
[AD-A209950] N89-28117
Bangladesh Agro-Climatic Environmental Monitoring Project N89-28121
Solar proton event forecasts N89-28462
WEATHER STATIONS
NASA follow-on on the Fiji South Pacific Severe Storm Warning System Project (SPSSD/WS) N89-28124
WEIBULL DENSITY FUNCTIONS
Estimation of lower bound properties from material test data
[AD-A207378] N89-28361
WELDABILITY
The Sigmajig: An improved hot-cracking test
[DE89-013029] N89-28031
WHEAT
Report of the Project Estima, phase 2: LANDSAT-TM data and agrometeorology in crop yield estimation of wheat at the farm level
[INPE-4782-RPE/582-PHASE-2] N89-28051
WHITE NOISE
Capacity of discrete time Gaussian channel with and without feedback, 2
[AD-A207388] N89-27922
Discrete enforcement of uncertain oscillator Gaussian response
[DE89-005595] N89-28038
WIND EFFECTS
Wind-Wave-Current Tank Research Facility usage and status N89-28161
WIND MEASUREMENT
Zonal winds between 25 and 120 km retrieved from solar occultation spectra
[NASA-CR-180086] N89-28113
Rocket temperature soundings N89-28167
Electrodynamics, wind and temperature N89-28168
WIND PROFILES
User's guide for the Air Force surface-layer windflow model (AFWIND)
[AD-A208710] N89-28109
YAG aerosol lidar N89-28135
Analyses of the wind-driven response of tropical oceans N89-28155
Climatological aspects of Nimbus-7 SMMR data N89-28156
WIND TUNNEL MODELS
Small scale model tests in small wind and water tunnels at high incidence and pitch rates. Volume 3: Water tunnel (HFF) data base
[AD-A208690] N89-27638
An evaluation of three experimental processes for two-dimensional transonic tests
[NASA-CR-181871] N89-27674
Small scale model tests in small wind and water tunnels at high incidence and pitch rates. Volume 2: Small wind tunnel (ADF) data base
[AD-A208539] N89-27676
WIND TUNNEL TESTS
Static internal performance of a nonaxisymmetric vaned thrust reverser with flow splay capability
[NASA-TP-2933] N89-27634
Hypersonic prediction comparisons with experimental data for a cone-cylinder at mach 6.86
[AD-A207583] N89-27636
Small scale model tests in small wind and water tunnels at high incidence and pitch rates. Volume 3: Water tunnel (HFF) data base
[AD-A208690] N89-27638
Mach 5 inlet CFD and experimental results
[NASA-TM-102317] N89-27670

Small scale model tests in small wind and water tunnels at high incidence and pitch rates. Volume 2: Small wind tunnel (ADF) data base
[AD-A208539] N89-27676

WIND TUNNEL WALLS
An evaluation of three experimental processes for two-dimensional transonic tests
[NASA-CR-181871] N89-27674

WIND VELOCITY
User's guide for the Air Force surface-layer windflow model (AFWIND)
[AD-A208710] N89-28109
Rainfall on microwave return from the sea surface N89-28160
Analysis of articulated manikin based convective heat transfer during walking
[AD-A208299] N89-28298

WINDOWS (APERTURES)
Thermal measurements of microwave transmitter feedhorn window N89-27885

WINDOWS (INTERVALS)
Orthogonal sets of data windows constructed from trigonometric polynomials N89-27902

WING LOADING
Evaluation of a strain-gage load calibration on a low-aspect-ratio wing structure at elevated temperature
[NASA-TP-2921] N89-28034

WING TIP VORTICES
Photogrammetric technique for in-flight ranging of trailing vortices using entrained balloons
[NASA-TM-4129] N89-27995

WIRE
Composite ceramic superconducting wires for electric motor applications
[AD-A208598] N89-27847

X

X RAY DIFFRACTION
Martensitic phase transitions in nanocrystalline materials
[AD-A208804] N89-27827

X RAY FLUORESCENCE
Synchrotron X-ray fluorescence analyses of stratospheric cosmic dust: New results for chondritic and nickel-depleted particles
[DE89-014032] N89-28107

X RAY SCATTERING
Scattering from fractals
[DE89-013451] N89-27924
Evidence against the existence of strong diffuse X-ray scattering from gold twist boundaries at room temperature
[DE89-012726] N89-28407

XENON
Auxiliary propulsion RF engine RIT 15: Prototype design and performance N89-27731
Xenon ion thruster test facility: Design and operation N89-27745
Discharge performance of a 12 cm cusp xenon ion thruster N89-27746
A 30 cm diameter xenon ion thruster: Design and initial test results N89-27768
Propellant selection criteria for deep space electrically propelled missions N89-27769
Inert gas performance of the RIT 35 main propulsion unit N89-27770
Optical emission spectrum of the UK-10 ion thruster operating on xenon N89-27781
Performance research of xenon ion rocket engine N89-27788
Dynamics of H(+) + Kr and H(+) + Xe elastic and charge-transfer collisions: State-selected differential cross sections at low collision energies N89-28381

Y

YAG LASERS
A novel approach to a PPM-modulated frequency-doubled electro-optic cavity-dumped Nd:YAG laser N89-27897
New, efficient optically pumped solid state lasers
[AD-A209998] N89-28013
Diode-pumped laser research N89-28185

YAGI ANTENNAS
An experimental and computer modeling study of stepped radius monopole antennas
[AD-A207356] N89-27919

YIELD STRENGTH
The structure and properties of grain boundaries in B2 ordered alloys
[DE89-013266] N89-27817
Analysis and elimination of high temperature notch induced microcrack initiation in Inconel 718 nickel-based alloy
[AD-A209695] N89-27828

YTTRIUM
Composite ceramic superconducting wires for electric motor applications
[AD-A208598] N89-27847

YTTRIUM OXIDES
Superconductivity in the Ba(0.69)Y(0.46)CuO(3.15-delta) compound
[DE88-706000] N89-28406

Z

ZETA PINCH
ZPIMP: A zero-D Z-pinch implosion code
[AD-A208381] N89-27962
The stability of the High-Density Z-Pinch
[DE89-014276] N89-28403

ZINC
Preparation and characterization of colloidal ZnS particles
[AD-A210171] N89-27862

ZINC OXIDES
Growth and characterization of zinc sulfide films by conversion of zinc oxide films with H2S
[AD-A208727] N89-28423

ZINC SELENIDES
Zinc telluride growth on InP
[AD-A209924] N89-28430

ZINC SULFIDES
Growth and characterization of zinc sulfide films by conversion of zinc oxide films with H2S
[AD-A208727] N89-28423

ZINC TELLURIDES
Zinc telluride growth on InP
[AD-A209924] N89-28430

ZIRCONIUM OXIDES
High temp toughening and creep studies
[AD-A208714] N89-27826

ZONAL FLOW (METEOROLOGY)
Zonal winds between 25 and 120 km retrieved from solar occultation spectra
[NASA-CR-180086] N89-28113

Typical Personal Author Index Listing

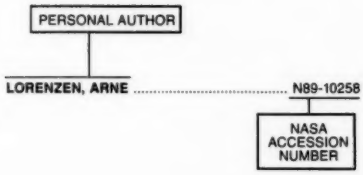

Listings in this index are arranged alphabetically by personal author. The NASA accession number denotes the number by which the citation is identified.

A

ABBOT, R. E. N89-27681
ABBOTT, W. H. N89-27686
ABD-ALLAH, MAHMOUD A. N89-27673
ABLOWITZ, MARK J. N89-27993
ABRAHAM, JACOB A. N89-27967
ACTIS, C. N89-28254
ADAMOVSKY, G. N89-27998
ADAMS, B. B. N89-28197
ADAMS, JAMES H., JR. N89-28455
N89-28456
N89-28458
AHZI, SAID N89-27852
N89-28425
AJAYI-MAJEBI, ABAYOMI J. N89-27673
AKINC, MUFIT N89-27862
AKIYAMA, R. N89-28401
ALBERTY, THOMAS N89-27938
ALBERTZ, JOERG N89-28089
ALBRECHTSEN, K. N89-27698
ALET, I. N89-28272
ALVAREZ, L. S. N89-27881
ALVIMDEOLIVEIRA, ENI N89-28048
AMIDIEU, M. N89-27689
N89-27690
N89-28235
N89-28265
AMMANN, K. N89-28239
AMSDEN, A. A. N89-27975
ANDERSON, E. M. N89-27945
ANDERSON, J. D., JR. N89-27986
ANDO, A. N89-28399
ANDO, R. N89-28401
ANDRE, M. N89-28223
ANDRE, S. N89-28282
ANDRENUCCI, M. N89-27714
ANDREWS, JOHN C. N89-27711
ANDREWS, T. M. N89-28281
ANGEL, S. M. N89-28000
ANNONI, ALESSANDRO N89-28088
ANTONENKO, J. N89-28296
ANZEL, BERNARD M. N89-27741
ANZURES, E. T. N89-27845
ARAKAWA, YOSHIHIRO N89-27743
N89-27760
ARCOZZI, RITA N89-28088
ARGON, ALI S. N89-27852
ARMSTRONG, T. P. N89-28459
ARNASON, K. N89-28068
ARNO, ROGER D. N89-28304
ARNOLDUS, HENK F. N89-28389
ASMUSSEN, JES N89-27773
ATWOOD, ALICE I. N89-27853
ATZEI, A. N89-27715
AUCEL, S. N89-28231
AUWETER-KURTZ, M. N89-27725
N89-27727
N89-27733
N89-27735
N89-27737
N89-27778
N89-27783
AVANZINI, P. G. N89-28287
N89-28290
AYERS, EVERETT N89-27945
AZZALI, S. N89-28060

B

BACON, L. D. N89-27957
BADRIPRASAD, N. S. N89-28306
BAER, MICHAEL N89-28381
N89-28383
N89-28384
BAESLACK, WILLIAM A., III N89-27818
BAGLIO, J. N89-28423
BAILEY, S. A. N89-28128
N89-28142
N89-28187
BAIN, COLIN D. N89-27824
N89-27840
BAIOCCHI, G. N89-27716
BAKER, I. N89-27817
BAKER, R. W. N89-27809
BALAAM, PHILIP N89-27771
BALES, KAY S. N89-28035
BALLUFFI, R. W. N89-28407
BANDARA, K. M. S. V. N89-27994
BANDERET, LOUIS E. N89-28201
BANGERT, LINDA S. N89-27634
BANKS, BRUCE A. N89-27836
BANNINGER, C. N89-28079
BARINAGA, C. J. N89-27806
BARRAQUAND, JEROME N89-28019
BARRERA, JUNIOR N89-28049
BARRIE, J. D. N89-27810
N89-27855
N89-27856
BARRINEAU, DRU N89-27684
BARTOLI, C N89-27792
BARTOLI, C. N89-27708
N89-27724
N89-27728
BASS, MICHAEL N89-28013
BASSNER, H. N89-27728
BATHKER, D. A. N89-27903
BATILL, STEPHEN M. N89-28354
BATISTA, GETULIO TEIXEIRA N89-28051
BAUER, H. N89-28242
BAUGHMAN, R. J. N89-28414
BAUMEISTER, KENNETH J. N89-27923
BEARDS, C. F. N89-28026
BEATTIE, JOHN R. N89-27761
BEAUCHAMP, EDWARD D. N89-27954
BECKER, LEE A. N89-28328
BEHEIM, GLENN N89-27999
BEHL, ERICH N89-27929
BEHRENS, B. N89-28216
N89-28232
BELL, C. M. N89-27809
BELL, KENNETH J. N89-27984
BELTON, MICHAEL J. S. N89-28474
BENNETT, GARY L. N89-27705
BENSMAN, D. N89-27870
BERARDI, F. N89-28233
BERARDI, L. N89-27657
BERCAW, ROBERT W. N89-27704
BERG, H.-P. N89-27728
BERGER, FRANZ H. N89-28086
BERNASCONI, M. C. N89-28236
BERNAYS, D. J. N89-28209
BERRY, DAVID M. N89-27693
BERRY, W. N89-27708
BERSHAD, NEIL J. N89-28319
BHATNAGAR, JAYANT N89-28328
BHATTI, R. S. N89-28225
N89-28294
BILES, JOHN A. N89-28334
BINDSCHADLER, R. N89-28152
N89-28186
BINOT, R. A. N89-28221
N89-28222
BIRKAN, MITAT N89-27749
BIRNBAUM, MILTON N89-28013
BIRNIE, R. W. N89-28047
BISANZ, R. N89-28247
N89-28261
BISHOP, MATT N89-28444
N89-28445
N89-28446
BISIAUX, P. N89-28217
BITTNER, ALVAH, JR. N89-28303
BLACHUT, TEODOR J. N89-28093
BLACK, F. O. N89-28211
N89-28212
N89-28213
BLASER, T. N89-28085
BLIVEN, L. F. N89-28160
N89-28161
BOCCHIOLA, C. N89-27722
BOEKER, F. N89-28070
BOERS, R. N89-28186
BOGAR, THOMAS J. N89-27640
BONACUSE, PETER J. N89-28029
BONATI, A. N89-27722
BOND, A. N89-27764
BOND, R. A. N89-27764
BORN, GEORGE N89-28195
BOYD, RONALD D. N89-27979
BRADSHAW, T. W. N89-28268
BRADY, DAVE N89-27966
BRAIG, A. N89-28275
BRANSTETTER, LINDA J. N89-28038
BRASMER, SUSAN E. N89-27818
BREZA, MICHAEL J. N89-27654
BRISTOWE, P. D. N89-28407
BROWN, R. L. N89-28052
BRUCE, THOMAS J., JR. N89-27818
BRY, P. F. N89-27668
BUCK, U. N89-28376
BUDD, WILLIAM F. N89-27677
BUFTON, J. L. N89-28134
N89-28185
N89-28186
BUGEAT, J. P. N89-27724
BULLE, C. N89-28276
BUNA, T. N89-28286
BUNKENBORG, C. N89-28232
BURKE, THOMAS J. N89-28300
BURKHARDT, RUDOLF N89-28094
BURKLE, P. H. N89-28255
BURNER, ALPHEUS W. N89-27995
BURNSIDE, W. D. N89-27870
BURSE, RICHARD L. N89-28201
BURSTON, STEWART A. N89-27762
BUSALACCHI, A. J. N89-28155
BUSHLOW, TODD N89-27638
N89-27676
BUTLER, P. BARRY N89-28432
BUTLER, T. D. N89-27975
BUTTRAM, M. T. N89-27955
BUTTRY, DANIEL A. N89-27811
N89-27812

C

CAIRD, R. S. N89-27960
CALABRESI, GIANNA N89-28055
CALHORDA, MARIA JOSE N89-27803
CALOZ, R. N89-28085
CAMBANIS, STAMATIS N89-28364
CAMPBELL, L. A. N89-27864
CANAVAN, GREGORY H. N89-28366
N89-28367
CANGAHUALA, LAUREANO A. N89-27692
CARHART, H. W. N89-27867
CARNEY, L. M. N89-27706
CARPENTER, STEVE H. N89-27816
CARRARA, VALDEMIR N89-27683
CARROLL, RAYMOND J. N89-28364
CARTER, GARY M. N89-28209
CARTWRIGHT, DAVID C. N89-28007
CASE, G. W. N89-28255
CASSANDRAS, CHRISTOS G. N89-28332
CATENA, J. N89-28125
CAVALIERI, D. J. N89-28147

CAVANAUGH, J. N89-28144
CEDERQUIST, J. N. N89-28397
CELIKKAYA, AHMET N89-27862
CEZZAR, RUKNET N89-28475
CHA, A. G. N89-27886
CHA, Y. S. N89-27866
CHADDHA, PARMEET SINGH N89-27839
CHAKRABARTTY, SUNIL KUMAR N89-27637
CHALMERS, D. R. N89-28255
CHAMIS, C. C. N89-27795
N89-28030
CHAN, K. N89-28185
CHANG-DIAZ, F. R. N89-27791
CHANG, STEPHEN KW. N89-28298
CHELOTTI, J. N. N89-28282
CHEN, C.-C. N89-27893
CHEN, J. N89-27898
CHEN, Y. D. N89-27788
CHENETTE, D. N89-28455
CHENG, C. C. N89-27821
CHENG, H. K. N89-27641
CHENG, U. N89-27888
CHEOUX-DAMAS, P. N89-28252
CHERNEK, PAUL J. N89-28369
CHEUNG, K.-M. N89-27890
N89-27892
CHIANG, K. T. N89-27829
CHIGER, H. D. N89-27687
CHIPAUX, C. N89-28222
N89-28223
CHIU, Y. N. N89-28385
CHIU, Y. T. N89-28479
CHOI, JIN-O N89-27842
CHOPRA, A. N89-27754
CHOUETRI, E. Y. N89-27736
CHOW, P. N89-27809
CHRISTENSEN, C. S. N89-27873
CHRISTIAN, ANDREW D. N89-28018
CHUDNOVSKY, D. V. N89-28348
CHUDNOVSKY, G. V. N89-28348
CHUPP, E. L. N89-28480
CHUVIECO, EMILIO N89-28084
CINLAR, ERHAN N89-28362
CLARK, G. N89-28044
CLARK, R. S. N89-27955
CLARK, S. K. N89-27835
CLEM, D. N89-28186
CLEM, T. D. N89-28178
CLINARD, J. A. N89-28308
COCHRAN, R. C. N89-27859
COLLAUDIN, B. N89-28269
COMISO, J. C. N89-28148
CONNELL, PETER S. N89-28108
CONROY, B. N89-27887
CONRY-MCDERMOTT, DYMPHNA N89-28063
COOKE, DAVID J. N89-28484
COON, DARRYL D. N89-27994
CORELLI, JOHN C. N89-27842
COSTAMAGNA, L. N89-28234
COTARAS, FREDERICK D. N89-28371
COTE, C. N89-28125
COTE, F. X. N89-28223
COTTLE, RICHARD W. N89-28352
COTTRELL, CHARLES J. N89-27636
COUNSELMAN, C. C., III N89-27681
COWLES, K. N89-27894
N89-27895
N89-27896
COY, J. J. N89-28015
CRANDALL, MICHAEL G. N89-28357
CREMER, JAMES F. N89-28326
CRESDEE, M. T. N89-27781
CRITCHLEY, M. F. N89-28065
CROWELL, CHARLES G. N89-27659
CRUCIANI, G. N89-27716
CUMMINGS, A. C. N89-28456
N89-28467
CUNNING, ROGER A. N89-28365
CUNNINGHAM, ATLEE M., JR. N89-27638
N89-27676
CUNNINGHAM, DIANE N89-28441
CURLANDER, J. N89-28097
CYCOWICZ, Y. N89-28210

D

DALLAS, ALLAN G. N89-28045
DAMMERMANN, C. N89-28265
DANDL, RAPHAEL A. N89-28101
N89-28404
DANTZIG, JONATHAN A. N89-27818
DAO-GIBNER, L. N89-28459
DARRAH, RODNEY C. N89-28436
N89-28437
N89-28438
DAS-GUPTA, D. K. N89-27801
DAS, PURNA C. N89-28390
DASGUPTA, PURNENDU K. N89-27805
DASHEFF, ANDREW N. N89-27844
N89-27854
DASILVA, ERIVALDO A. N89-28050
DAVIDSON, G. T. N89-28479
DAVIDSON, J. M. N89-27873
DAVIES, N. GEORGE N89-27915
DAYAL, VINAY N89-27799
DECKMAN, DOUGLAS E. N89-27831
DEGREZ, G. N89-27990
DEININGER, WILLIAM D. N89-27717
N89-27754
N89-27755
DEJNEKA, KATHERINE Y. N89-28303
DEKEERSMAECKER, M. L. N89-28073
DELIL, A. A. M. N89-28230
DELLIPRISCOLI, F. N89-27943
DELOREY, DENNIS E. N89-27691
DELTIN, G. N89-28287
DENUZZIO, J. D. N89-27813
DERBYSHIRE, K. N89-28297
DERYDER, D. D. N89-27687
DERYDER, L. J. N89-27687
DESA, L. N89-28269
DESJARDINS, M. N89-28122
DESSOUKY, KHALED N89-27907
N89-27910
DESTLER, WILLIAM W. N89-27944
DETHLEFSEN, ROLF N89-27790
DETWEILER, K. N. N89-27687
DEVADAS, SRINIVAS N89-28316
DEWEESE, MARY E. N89-28405
DEWULF, ROBERT R. N89-28080
DIAMOND, FRED I. N89-27651
DIANI, DAVID N89-27738
DICK, E. N89-27988
N89-27989
DICK, G. J. N89-27875
N89-27876
DICKINSON, BRADLEY W. N89-27968
DIDONATO, ARMIDO R. N89-28358
DIEHL, JOAO BENEDITO N89-28333
DILLMANN, A. N89-27731
DINENNO, P. J. N89-27867
DIVSALAR, D. N89-27889
DOBIAS, DAVID N89-27721
DOLAN, RAYMOND J. N89-28449
DOLCE, S. N89-28233
DOMANUS, H. M. N89-27866
DONNELLAN, T. M. N89-27859
DORNELLES, BEATRIZ CORREA PIRES N89-28114
DOTSON, NEIL N89-27857
DOUGLAS, A. S. N89-28046
DOVE, M. F. N89-27823
DRAVID, NARAYAN V. N89-27702
DRUEDING, THOMAS W. N89-28098
N89-28396
DUBERTRET, G. N89-28222
DUEREN, RUDOLF N89-28381
DUHAMEL, T. N89-27732
DUNCAN, J. H. N89-27996
DUNN, BRUCE N89-27810
N89-27855
N89-27856
DUPREE, R. L. N89-27687
DUPUY, A. N89-28276
DUTHIE, J. GRAEME N89-28001
DWIGHT, KIRBY N89-28423
N89-28424
DYER, M. J. N89-27807

E

EBELING, W.-D. N89-28232
N89-28295
N89-28296
EBERSOLE, JOHN F. N89-28098
N89-28396
ECKARDT, R. N89-28003
EDMONDS, C. G. N89-27806
EDWARDS, C. D. N89-27874
EGETH, H. E. N89-28206
EGGERS, M. D. N89-27946
EGUSA, SIGENORI N89-27794
EHLERS, J. N89-28070
EISELE, J. A. N89-28480
EISMANN, M. T. N89-28397
EL-HADY, NABIL M. N89-27978
EL-NEWEIHI, E. N89-28023
ELLIOTT, J. R. N89-28115
ELLIS, ARTHUR B. N89-27808
N89-28419
ELMS, T. N89-28262
ELPHIC, R. C. N89-28054
ELROD, J. N89-28122
N89-28138
ELVEBAKK, ARVE N89-28075
ENGLISH, CATHERINE N89-27956
ENNIS, JOEL N89-27790
EPPLE, J. N89-27783
ERCK, R. A. N89-27821
ERDEMIR, A. N89-27821
ERICKSON, D. N89-27895
ERIKSEN, F. J. N89-28115
ERLANDSON, A. C. N89-28006
ERSTFELD, THOMAS E. N89-28369
ESAIAS, W. N89-28137
N89-28144
ESCADAFAL, R. N89-28087
EUSTACE, J. G. N89-27998
EVENSON, PAUL N89-28456
N89-28469
EYSSELE, HELMUT N89-27937

F

FALKENHAINER, BRIAN CARL N89-28338
FARIS, G. W. N89-27807
FARRINGTON, G. C. N89-27813
FAZIO, M. V. N89-27958
FEARN, D. G. N89-27729
N89-27782
FENG, YU-CAI N89-27784
FENSKE, G. R. N89-27821
FERRO, C. N89-28234
FEYNMAN, JOAN N89-28454
N89-28455
N89-28459
FIENUP, J. R. N89-28397
FIGUEIRA, JOSEPH F. N89-28007
FILLIUS, W. N89-28456
FINGER, M. H. N89-27873
FIORE, JOSEPH V., JR. N89-28116
FLAISHER, HARVEY N89-27721
FLOOD, DENNIS J. N89-27705
FLYNN, G. J. N89-28107
FOKAS, ATHANASSIOS S. N89-27993
FOLKNER, W. M. N89-27873
FORET, J. L. N89-27689
N89-28235
FORSSELL, E. W. N89-27867
FOTTNER, L. N89-27662
FOWLER, C. M. N89-27958
N89-27960
N89-27961
FRANCHI, E. R. N89-28197
FRANCIS, W. E. N89-28479
FRANCISCO, GERSON N89-28472
FRANK, C. W. N89-27848
N89-27849
FREED, A. D. N89-28036
FREEMAN, B. L. N89-27961
FREISINGER, J. N89-27785
N89-27786
FRICK, F. A. N89-28006
FRIEDRICH, BRETISLAV N89-28381
N89-28385
FRIEDRICHS, BERND N89-27932
FRIEND, CYNTHIA M. N89-27803
FRY, R. J. M. N89-28478
FUJII, G. N89-28270
FUNKE, H. N89-28237

G

GABRIEL, STEPHEN N89-28454
GAIR, S. A. N89-27759
GAL-OR, L. N89-27800
GALINIS, WILLIAM J. N89-28318
GAMARRAROSADO, VICTOR ORLANDO N89-27680
GANGKOFNER, UTE N89-28057
GAO, Y-M. N89-28423
GARCIA, R. N89-28262
GARG, SANJAY N89-27672
GARLAND, PETER N89-27916
GARNER, JAMES M. N89-27682
GARVIN, J. N89-28186
GASPAR, THOMAS A. N89-27818
GATSKI, THOMAS B. N89-27977
GEORGE, THOMAS F. N89-28389
N89-28390
GERANIOTIS, EVAGGELOS N89-27914
GERSTLE, F. P., JR. N89-28032
GERVIN, J. N89-28122
GHONEM, H. N89-28043
GIANFIGLIO, G. N89-28234
GIANTURCO, F. A. N89-28380

GILBERT, E. N89-28121
GILHOUSEN, KLEIN S. N89-27912
GILLESPIE, V. P. N89-27687
GILLHAM, JOHN K. N89-27798
GINLEY, D. S. N89-28414
GIOVANANGELI, J.-P. N89-28160
GIULIANI, JOHN L. N89-27962
GLADDEN, HERBERT J. N89-27980
GLANZER, M. N89-28210
GLASER, S. F. N89-27735
GLASSER, A. H. N89-28403
GLASSGOLD, A. E. N89-28471
GLEITER, HERBERT N89-27827
GLICKER, S. N89-28190
GLOCKER, B. N89-27725
N89-27778
GLOERSEN, P. N89-28156
GOAD, WILLIAM K. N89-27995
GOECKLER, HEINZ N89-27937
GOFORTH, J. H. N89-27960
GOLDSTEIN, B. E. N89-28465
GOMBOS, FRANK J. N89-27702
GONZALEZ, RICHARD R. N89-28298
GONZALEZALONSO, FEDERICO N89-28077
GOODER, S. T. N89-27703
GOODFELLOW, K. D. N89-27753
GOODWIN, GENE M. N89-28031
GOOSSENS, ROLAND E. N89-28080
GORY, J. F. N89-28282
GOSWAMI, G. L. N89-27822
GOUREVITCH, S. A. N89-27681
GRALLERT, H. N89-28291
GREEN, CHARLES N89-27945
GREEN, D. L. N89-27955
GREEN, JOANNE N89-28299
GREEN, PETER G. N89-28328
GREENHALL, C. A. N89-27902
GREFF, P. N89-27732
GREGORY, DON A. N89-28001
GRIFFIN, D. N89-27791
GRIMSON, W. ERIC L. N89-28363
GRISSOM, WILLIAM A. N89-27673
GROH, K. H. N89-27731
N89-27770
N89-27786
GRONLIE, ARNE N89-28072
GROTEGUT, NEIL W. N89-28452
GRUNDMANN, R. N89-27987
GSCHWENDTNER, HANS N89-27928
GUENTHER, B. W. N89-28131
N89-28189
GUERRIERI, R. N89-27838
GUEST, GARETH E. N89-28101
N89-28404
GUI, JOHN Y. N89-27814
GUO, Z. Y. N89-27788
GUPTA, ROOP N. N89-27633
GURA, CAROL N89-27967
GUYENNE, T. DUC N89-28055
N89-28214

H

HAAG, THOMAS W. N89-27701
HABIGER, H. N89-27725
N89-27727
N89-27783
HACKMAN, LLOYD E. N89-27818
HADJIPANAYIS, GEORGE C. N89-27820
HALABE, UDAYA B. N89-27921
HALL, J. B. N89-27687
HALLORAN, JOHN W. N89-27847
HAM, N. C. N89-27899
HAMA, K. N89-28270
HAMADA, Y. N89-28399
N89-28401
HAMILTON, DOUGLAS C. N89-28455
N89-28461
HAMMER, PETER L. N89-28347
HAN, J. Z. N89-27788
HANAK, J. J. N89-27721
HANCOCK, D. W. N89-28119
N89-28120
N89-28174
HANDSCHUH, R. F. N89-28015
HARADA, H. N89-27739
HARRIS, DAVID B. N89-28007
HARRIS, J. M. N89-27815
HARRIS, JAMES S. N89-28429
HARRIS, P. T. N89-27759
HART, NICK N89-27917
HART, R. E., JR. N89-27868
HARTMANN, ROBERT A. N89-27972
HARTOOG, A. N89-28274
HARZ, PETER N89-27934
HASLER, A. N89-28123
N89-28124
HASTING, MICHAEL A. N89-27853
HASTINGS, DANIEL E. N89-27720
HASUI, T. N89-28270
HAUK, WALDEMAR N89-27928
HAUPT, S. N89-28238
HAUSER, G. N89-28241
HAUTH, WOLFGANG N89-27940
HAYAKAWA, Y. N89-27745
N89-27768
HAYASHI, T. N89-28289
HAYNE, G. S. N89-28119
N89-28120
HEATH, G. E. N89-28187
HECK, M. L. N89-27687
HECKMAN, G. R. N89-28455
N89-28462
HEDAYAT, A. S. N89-28023
HEEMSKERK, J. F. N89-28230
HELLMANN, H. N89-27785
HENNING, B. N89-28257
HENRY, THOMAS N89-27644
HERBER, N. N89-28243
N89-28246
HERBIG, PETER N89-27936
HERRICK, D. C. N89-27687
HERRINGTON, P. G. N89-27751
HERRMANN, GEORGE N89-27802
HERTEL, G. N89-27943
HESPELT, VOLKER N89-27933
N89-27938
HEWER, G. A. N89-28339
HIBSHOOSH, ELIPHAZ N89-27949
HIENERWADEL, K.-O. N89-28219
HIERMERDINGER, D. J. N89-27734
HIGUCHI, T. N89-27768
HILL, R. E. N89-27880
HILLENBRAND, JAMES N89-28334
HINES, D. E. N89-28126
HIROKURA, S. N89-28401
HIRSCHLER-MARCHAND, PATRICK R. N89-28356
HIXSON, R. S. N89-28435
HOBSON, D. O. N89-27837
HODSDON, DAVID M. N89-28209
HOEBERLING, R. F. N89-27958
HOETZL, H. N89-28069
HOFFMANN, MICHAEL H. W. N89-27935
HOFFMANN, ROALD N89-27803
HOGE, F. E. N89-28141
N89-28143
HOHLFELD, ROBERT G. N89-28098
N89-28396
HOLBEN, B. N89-28184
HOLDEN, KRITINA L. N89-28302
HOLLAND, PETER L. N89-28002
HOLLINGSWORTH, GARY N89-27810
HOLLKAMP, JOSEPH J. N89-28354
HONG, JOHN N89-27966
HONNEN, K. N89-28251
HOOTEN, PHILLIP M. N89-27945
HOOVER, DONALD R. N89-28353
HOPKINS, D. A. N89-27795
N89-28030
HOPKINS, WILLIAM E., JR. N89-27968
HOPPE, D. J. N89-27884
N89-27885
HOREMBALA, J. N89-28115
HORGAN, G. W. N89-28065
HORNET, D. N89-28245
HOURMOUZIADIS, J. N89-27669
HOVLAND, DOUGLAS LYLE N89-27793
HOWELL, LORA N89-28200
HOWELL, WILLIAM C. N89-28302
HOYDEM, A. N89-28071
HOYLE, C. E. N89-27845
HSIEH, ALEX J. N89-27833
HSU, STEPHEN M. N89-27831
HU, TONG N89-28033
HUANG, N. N89-28157
HUBBARD, DAVID C. N89-27679
HUDSON, JOHN B. N89-28420
HUDSON, SCOTT N89-27966
HUEGEL, F. G. N89-28183
HUESTIS, D. L. N89-27807
HUGHES, HUBERT G. N89-28110
HUGHSON, MONTGOMERY C. N89-27636
HUISKEN, FRIEDRICH N89-28375
N89-28376
N89-28377
HUMMEL, JOHN R. N89-28112
HUMPHRIES, R. N89-28215
HUNT, J. N89-28214
HUNTTENBACH, R. C. N89-28221
HURD, ALAN J. N89-27924
HURLEY, C. E. N89-28006
HYMAN, JAY, JR. N89-27761

I

IDA, K. N89-28399
IHARA, SHUNSUKE N89-27922
II, FERNANDO AUGUSTO MITSUO N89-28049
IJICHI, K. N89-27739
N89-27740
INTERRANTE, LEONARD N89-28420
IRISH, DALE N89-27917
IRONS, J. N89-28183
ITO, K. N89-28346
N89-28351
IZUTSU, N. N89-28228

J

JACKSON, F. C. N89-28158
JACOBI, WILLIAM J. N89-27969
JACOBS, IRWIN M. N89-27912
JAHN, R. G. N89-27736
N89-27756
JANCAITIS, K. S. N89-28006
JANDER, G. N89-28261
JAQUET, J.-M. N89-28062
JASKOLLA, F. N89-28068
JENEKHE, SAMSON A. N89-27832
JENNINGS, TOM N89-28200
JENSEN, DAVID W. N89-28369
JENSEN, DOUGLAS R. N89-28110
JENSEN, J. H. N89-28387
JEONG, GARRETT D. N89-28038
JEWELL, C. N89-28266
JOHNSON, B. N89-28144
N89-28145
JOHNSON, CATHERINE C. N89-28304
JOHNSON, G. L. N89-28308
JOHNSTON, B. S. N89-27983
JOHNSTONE, A. D. N89-27782
JOKIPII, J. R. N89-28456
N89-28470
JONES, EUGENE E. N89-27673
JONES, MARK T. N89-28341
JONES, W. H. N89-28184
JONES, WILLIAM D. N89-27804
JORGENSON, ROY E. N89-27953

K

KADRO, A. N89-28082
KAEPPLER, H. J. N89-27737
KAGAYA, Y. N89-27742
N89-27744
KAHN, BRUCE E. N89-27814
KAILATH, THOMAS N89-27952
KAISER, A. R. N89-28221
KAITA, KEIJI N89-27776
N89-27777
N89-27780
KAKO, E. N89-28401
KALLIANPUR, GOPINATH N89-28364
KALLURI, SREERAMESH N89-28029
KAMIYAMA, TAKAYUKI N89-27794
KAMOWSKI, J. N89-28121
N89-28123
N89-28124
N89-28176
KAMPER, ROBERT A. N89-28405
KANE, DENNIS L. N89-27635
KANEKO, K. N89-28289
KAO, R. N89-28173
N89-28175
KAPPEL, F. N89-28346
KAR, A. N89-27830
KARE, JORDIN N89-28009
KARSPECT, M. N89-28097
KARUNASIRI, R. P. G. N89-27994
KATIALAUS, J. J. N89-27859
KATZBERG, S. J. N89-27687
KAUFMAN, JONATHAN W. N89-28303
KAUFMAN, LLOYD N89-28207
N89-28208
N89-28210
KAUFMANN, H. N89-28067
N89-28069
N89-28071
KAUFMANN, M. N89-27785
KAUSEL, EDUARDO N89-27921
KAWAHATA, K. N89-28399
N89-28401
KAWASUMI, Y. N89-28401
KAWAUCHI, H. N89-27768
KEELTY, J. MALCOLM N89-27916

KELLER, K. N89-28291
KELLER, REINHARD N89-27941
KELLY, A. J. N89-27736
N89-27756
KENNEALY, JOHN P. N89-27951
KENNEDY, C. R. N89-27837
KENNEDY, LARRY Z. N89-28001
KENNEY, CHARLES N89-28339
KERBER, A. N89-28122
KESKINEN, M. J. N89-28111
KHOSIAINOV, V. T. N89-28416
KHOUN, T. S. N89-27946
KILIAN, JAMES C. N89-28098
KIM, SANG-YOUL N89-27842
KING, D. Q. N89-27754
KINNERSLEY, M. A. N89-27787
KINRA, VIKRAM K. N89-27799
KIPP, D. O. N89-28422
KIRK, M. T. N89-28361
KIRK, R. G. N89-28132
KIRSCHNER, G. N89-28284
KITAMURA, SHOJI N89-27745
N89-27746
N89-27768
KITAZAKI, KERRY S. N89-27972
KLABUNDE, RICHARD N89-28339
KLAUS, E. ERWIN N89-27831
KLEINAU, W. N89-27750
KLEISS, JAMES A. N89-27679
KNOX, JOSEPH B. N89-28105
KNUDSEN, PER N89-28095
KOBER, WOODY N89-28097
KOECK, C. N89-28249
N89-28252
KOEDINGER, M. N89-28256
KOELLE, D. E. N89-27750
KOERNER, M. A. N89-27900
KOESE, S. N89-28236
KOHL, JOHN L. N89-28478
KOHLBERG, IRA N89-27869
KOHN, W. N89-28367
KOLKA, MARGARET A. N89-28202
KOMVOPOULOS, KYRIAKOS N89-28020
KONRADI, A. N89-28455
KONZOK, H.-G. N89-28297
KOROTEEV, A. S. N89-27710
KORTE, ROSE M. N89-27951
KOSBAR, L. L. N89-27848
KOTANI, S. N89-27779
KOTHANDARAMAN, V. N89-28306
N89-28307
KOWLER, EILEEN N89-28203
KRABILL, W. B. N89-28179
KRASOWSKI, M. J. N89-27998
KRAUS, W. N89-27785
KRAUSKOPF, JOHN N89-28205
KREEB, H. N89-28224
KREMPEL-HESSE, J. N89-27786
KRING, G. N89-28219
KRIVEN, WALTRAUD M. N89-27826
KROLLER, M. N89-28351
KROUTIL, JOSEPH C. N89-27640
KRUEGER, W. A. N89-27791
KRUIDHOF, W. N89-28248
KRUMEICH, J. M. N89-27786
KUAN, S. W. N89-27848
N89-27849
KUANG, YUAN-ZHU N89-27784
KUHLEN, H. N89-27943
KUHN, P. N89-28240
KUKLA, GEORGE N89-28196
KUMAR, DILIP N89-27822
KUMAZAWA, R. N89-28399
KUNII, Y. N89-27739
N89-27740
KUNINAKA, H. N89-27719
KUNISCH, K. N89-28351
KUNKEL, BRUCE A. N89-28109
KURFESS, J. D. N89-28480
N89-28481
N89-28482
N89-28483
KURIKI, KYOICHI N89-27709
N89-27718
N89-27719
N89-27726
N89-27763
N89-27766
KUROSE, JAMES F. N89-28332
KURTZ, H. L. N89-27725
N89-27727
N89-27735
N89-27778
N89-27783
KVATERNIK, RAYMOND G. N89-28342
KWAK, J. F. N89-28414
KWONG, NORMAN N89-28012
KYOYA, M. N89-28270

L

LABRANDEROSANZ, JOSE LUIS N89-28076
LABUSCA, E. N89-28406
LACAZE, H. N89-28217
LADANY, I. N89-28004
LADD, J. W. N89-27681
LAFON, T. N89-27690
N89-28282
N89-28285
LAFRANCHI, E. N89-28453
LAGNESE, JOHN E. N89-28042
LAGUREN-DAVIDSON, LAARNI N89-27814
LAKIN, WILLIAM D. N89-28342
LANE, DAVID M. N89-28302
LANGER, WILLIAM D. N89-28471
LANTERI, A. N89-28257
LAPOINTE, MICHAEL R. N89-27700
LASSEUR, C. N89-28223
LATHAM, P. M. N89-27747
N89-27769
N89-27781
N89-27782
LATOMBE, JEAN-CLAUDE N89-28019
LAU, KAM Y. N89-28010
LAUENSTEIN, CH. N89-28376
LAUX, U. N89-28216
N89-28232
LAWSON, R. N89-28216
LE, D. N89-27687
LEADBETTER, M. R. N89-28364
LEAVITT, LAURENCE D. N89-27634
LEAVITT, WILLIAM E. N89-27945
LEBERL, FRANZ N89-28097
LEBRU, A. N89-28281
LECHI, G. N89-28091
LECHTE, H. G. N89-27713
LEE, MARTIN A. N89-28455
N89-28464
LEE, T. H. N89-27870
LEE, WEI N89-28420
LEFORT-TRAN, M. N89-28222
LEHMBERG, R. N89-28003
LENZ, KLAUS N89-28420
LENZ, TERRY G. N89-28433
LEONARD, J. T. N89-27867
LEPKOWSKI, RONALD J. N89-27911
LESTER, D. L. N89-28191
N89-28192
LEU, M. C. N89-28021
LEUNG, CHRISTOPHER K. N89-27858
LEUNG, LARRY K. N89-28419
LEVINE, D. M. N89-28181
N89-28182
LEVINE, HOWARD A. N89-28350
LEVY, R. N89-27906
LEWIS, C. A. N89-28267
LEWIS, DAVID H. N89-28310
LEWIS, ELMIR E. N89-28024
LEWIS, WILLIAM D. N89-27632
LI, VICTOR C. N89-27858
LI, VICTOR O. N89-28022
LIANG, EDISON P. N89-28477
LICHTEN, S. M. N89-27872
LIMADALGE, JULIO CESAR N89-28049
LIMOUZIN, G. N89-28250
LIN, C. S. N89-27950
LIN, CHIU-HSUN N89-27814
LINDEMUTH, I. R. N89-27959
N89-27960
LINDSAY, GEOFFREY A. N89-27853
LINEBERGER, ERNEST R., III N89-27973
LINNE, DORIS N89-28066
LINTON, A. T. N89-28262
LISENSKY, GEORGE C. N89-27808
N89-28419
LIST, FRANK K. N89-28066
LITVIN, F. L. N89-28015
LIU, A. K. N89-28153
LIU, K. C. N89-28393
LIUBOVICH, S. N89-27800
LOBANOV, A. D. N89-28229
LOBER, R. N89-27830
LOEB, H. W. N89-27731
N89-27770
N89-27785
N89-27786
LOEHMAN, RONALD E. N89-27834
LOESENER, O. N89-27783
LOESER, H. N89-28292
LOGAN, N. N89-27823
LONG, S. R. N89-28161
N89-28162
LONGTIN, DAVID R. N89-28112
LOO, J. A. N89-27606
LOSIER, PAUL W. N89-27632
LOUI, MICHAEL C. N89-28327
LOWE-MA, C. K. N89-28422
LOWE, BURKHARDT N89-27930
LU, FRANK N89-27814
LUNA, R. E. N89-27642
LUTES, G. F. N89-27878
N89-27879
LYLE, JOSEPH A. N89-27632
LYO, S. K. N89-28412
LYON, W. F. N89-27789

M

MACDONALD, DIGBY D. N89-27956
MACGIOLLAMHUIRIS, NESSAN N89-27977
MACHIDA, T. N89-28270
MACRAE, G. S. N89-27703
MAGILL, THOMAS N89-27918
MAINS, RICHARD N89-28304
MAJID, I. N89-28407
MAKSIMOVICH, W. N89-28121
N89-28123
N89-28124
MALANDRONE, M. N89-28287
MALEKI, L. N89-27875
MALLOVE, E. F. N89-27765
MALNIG, H. W. N89-28264
MANKA, C. N89-28003
MANNER, GERALD E. N89-27853
MANTENIEKS, MARIS A. N89-27701
MANZELLA, D. H. N89-27706
MARHEFKA, R. J. N89-27870
MARING, W. N89-28385
MARK, J. E. N89-27861
MARKL, G. N89-28058
MARLOW, K. W. N89-28480
MARSH, S. P. N89-27961
MARTIN, A. R. N89-27747
N89-27764
N89-27769
N89-27781
N89-27782
MARTIN, P. S. N89-27849
MARTINEZ-SANCHEZ, M. N89-27734
MASCARENHAS, NELSON D. A. N89-28050
MASER, KENNETH N89-27921
MASON, C. D. N89-28122
N89-28154
MASSIMINO, J. N89-28223
MASTERSON, BARTHOLOMEW N89-28063
MATHIAS, LON J. N89-27846
MATLOFF, G. L. N89-27765
MATSUMOTO, MANABU N89-27746
MATSUMOTO, T. N89-28270
MAUCK, LINDA S. N89-28330
MAUGER, J. P. N89-27823
MAUL, WILLIAM N89-27771
MAUNG, NICHOLAS N89-28430
MAURER, H. N89-28121
N89-28122
N89-28123
N89-28124
N89-28125
MAURER, M. N89-27737
MAUSER, WOLFRAM N89-28074
MAXWORTHY, T. N89-27641
MAYNARD, N. G. N89-28139
MAZUMDER, J. N89-27830
MCCLAIN, C. R. N89-28136
MCCLURE, J. D. N89-27642
MCCORMICK, B. W. N89-27649
MCDANELS, DAVID L. N89-27796
MCDONALD, THOMAS E. N89-28007
MCGARRIGLE, M. L. N89-28058
MCKIBBEN, R. B. N89-28456
N89-28468
MCLEAN, J. T. N89-28193
N89-28194
MCMICHAEL, I. C. N89-28391
MCWHORTER, ALAN L. N89-28426
N89-28431
MEAUZE, G. N89-27664
MECHERIKUNNEL, A. T. N89-28133
MEHLBREUER, ALFRED N89-28089
MEHTA, PARAG G. N89-27843
MEIER, G. H. N89-27829
MEISSNER, BERND N89-28066
MELFI, S. H. N89-28186
MELTON, R. G. N89-27649
MENEGHINI, R. N89-28127
MENENTI, M. N89-28060
MERCER, CAROLYN R. N89-27999

MERCER, JOHN R. N89-27638
N89-27676
MERGEAY, M. N89-28222
MERKE, W. D. N89-27725
N89-27727
N89-27778
MERKLE, CHARLES L. N89-28102
MERRI, M. N89-27943
MESSERSCHMID, E. N89-27783
MESSINA, D. C. N89-28481
N89-28482
N89-28483
MEWALDT, R. A. N89-28456
N89-28466
MEYER, GERALD J. N89-27808
N89-28419
MEYER, R. N89-28295
MEYER, RUDOLF X. N89-27992
MICCI, MICHAEL M. N89-27749
N89-27762
N89-27771
N89-27772
N89-28102
MICHELSEN, RANDY N89-28315
MIESS, JOSEPH C. N89-27659
MIHAI, I. N89-28406
MILLER, DEAN R. N89-27702
MILLER, DOUGLAS R. N89-27860
MILLER, R. A. N89-27829
MILLER, ROBERT L. N89-28101
MILLER, W. H. N89-28286
MIRTICH, MICHAEL J. N89-27836
MITTERAUER, J. N89-27723
MITTRA, RAJ N89-27953
MIYAZAKI, D. N89-27768
MIYAZAKI, KATSUHIRO N89-27745
N89-27746
N89-27768
MODESTINO, JAMES N89-28336
MOERZINGA, M. N89-27943
MOGOROVICH, P. N89-28090
MOHAN, MANOJ N89-27738
MOK, FAI N89-27966
MOLLO-CHRISTENSEN, E. N89-28122
MOMODA, L. A. N89-27855
N89-27856
MOORE, JAMES A. N89-27842
N89-27843
N89-27844
N89-27854
MOORE, JOHN, JR. N89-28053
MOORE, MARVIN E. N89-27685
MOORE, T. N89-28121
N89-28123
N89-28124
MOOSE, PAUL H. N89-27947
MOREY, B. E. N89-28394
MORGAN, D. REED N89-27655
MORIAI, T. N89-27739
N89-27740
MORIONDO, A. N89-28091
MORITA, S. N89-28399
N89-28401
MORIWAKI, MELVIN N89-27972
MOROSIN, B. N89-28414
MORRIS, ALFRED H., JR. N89-28358
MORRISSEY, STEPHEN N89-28303
MORTON, J. N89-28032
MOYZIS, ROBERT K. N89-28199
MUELLER, GEORGE P. N89-28028
MUELLER, JOERG-MARTIN N89-27939
MUELLER, JUERGEN N89-27772
MUELLER, R. N89-28226
MUELLER, W. N89-27750
MUKHERJEE, A. N89-28027
MUKHOPADHYAY, M. N89-28027
MULLIS, C. T. N89-27964
MULZER, D. N89-27783
MURA, JOSE CLAUDIO N89-28305
MURAKAMI, M. N89-28270
MURFEE, JAMES G. N89-27678
MURRAY, J. E. N89-28006
MURRAY, M. N89-27925
MURTHY, N. N. N89-28306
N89-28307
MURTHY, P. L. N. N89-27795
MURTHY, S. N. B. N89-27753
MYERS, ROGER M. N89-27701

N

NABORS, K. N89-28317
NACHTWEY, D. S. N89-28455
NADLER, MELVIN P. N89-27853
NAGATA, JOHN I. N89-27632
NAKAMURA, YOSHIHIRO N89-27709
N89-27745
N89-27746
N89-27768
NAKAO, TAKESHI N89-27794
NAKAYAMA, T. N89-27766
NAMBU, YASUSADA N89-28473
NASLUND, H. RICHARD N89-28047
NEBEL, R. A. N89-28403
NEIFELD, MARK N89-27966
NEILL, P. O. N89-28182
NEMEROFF, NORMAN N89-27859
NERHEIM, N. N89-27883
NERVEGNA, N. N89-28254
N89-28287
NEWTON, M. D. N89-28411
NGOC, T. D. N89-28197
NGUYEN, CHARLES C. N89-28016
N89-28017
NICKERSON, J. N89-27881
NIEDNER, GEREON N89-28378
N89-28379
N89-28380
N89-28381
N89-28382
N89-28383
N89-28384
N89-28385
NIEDRINGHAUS, WILLIAM P. N89-27645
N89-27646
NIGHTINGALE, R. W. N89-28479
NIJHAWAN, PREETISH N89-28307
NIKANPOUR, D. N89-28293
NILSEN, J. N89-28064
NILSEN, V. N89-28064
NISHIDA, EIJI N89-27726
NISHIDA, MICHIO N89-27776
N89-27777
N89-27780
NISHIKAWA, KEN-ICHI N89-28106
NISSAN, ROBIN A. N89-27853
NIXON, LAURENCE N89-28014
NOLL, MARTIN N89-28380
N89-28381
N89-28382
N89-28385
NOREEN, GARY K. N89-27908
NOVACU, A. N89-28406
NOZAKI, Y. N89-27719
NUNES, O. A. C. N89-28417

O

OBENSCHAIN, S. N89-28003
OBERHOLTZER, J. D. N89-28146
N89-28162
OBLER, H. N89-28121
OGAWA, Y. N89-28401
OHNISHI, A. N89-28289
OKA, Y. N89-28399
OKAMOTO, T. N89-28270
OKAMURA, T. N89-27739
N89-27740
OKUDA, H. N89-28270
OLIGER, JOSEPH N89-28117
N89-28355
OLSHAUSEN, BRUNO A. N89-28309
ONOE, K. N89-27774
N89-27779
ONWUMECHILI, C. A. N89-28343
ORLOWSKA, A. H. N89-28268
OROURKE, P. J. N89-27975
ORTIZCASAS, J. L. N89-28061
OSHIMA, K. N89-28228
OSTERYOUNG, JANET N89-27965
OSTGAARD, JOHN C. N89-27655
OTTKA, MANFRED N89-27934
OZOEMENA, P. C. N89-28343

P

PACCANI, GIORGI N89-27757
PADOVANI, ROBERTO N89-27912
PAI, DINESH K. N89-28021
PANDEY, BISHUN D. N89-27767
PARADISO, RICHARD A., JR. N89-28329
PARENTIEVA, A. A. N89-28229
PARFENTIEV, M. D. N89-28227
PARKER, S. L. N89-28115
PARKES, JAMES E. N89-27701
PARKINSON, C. L. N89-28151
PARKS, DAVID M. N89-27852
N89-28425
PARKS, V. J. N89-28032
PARR, J. T. N89-28047
PARSONS, C. L. N89-28128
N89-28129
N89-28164
PARSONS, CAROLYN M. N89-27691
PARTOM, YEHUDA N89-27863
PASKIN, HARVEY M. N89-27652
PASSMAN, J. N89-27698
PATE, VICKI M. N89-28025
PATRICK, MERRELL L. N89-28341
PATTERSON, ALEX G. N89-27702
PATTERSON, D. N89-28215
PAULTER, E. L. N89-28204
PAUS, LUDGER N89-28059
PAWLEY, C. N89-28003
PAWLOWSKI, P. N89-28275
PEASE, R. F. N89-27848
N89-27849
PENAMARTINEZ, R. N89-28061
PENG, S. N89-27791
PENN, LANNING M. N89-28116
PENNINGS, N. H. N89-28288
PERALA, R. A. N89-28115
PERCEC, VIRGIL N89-27850
N89-27851
PEREIRADOVALLE, A. N89-28345
PEREYDA, MARGARITA N89-28474
PEREZ, JUAN SUNE N89-28333
PEREZ, R. M. N89-27885
PERKINS, R. A. N89-27829
PERTSCH, THOMAS N89-28373
N89-28374
N89-28375
N89-28376
N89-28377
PETAGNA, C. N89-27792
PETERKA, R. J. N89-28211
N89-28212
N89-28213
PETERSEN, H. N89-28258
N89-28260
PETRASCU, H. N89-28406
PETRASCU, M. N89-28406
PETRUZZIELLO, M. N89-28293
PETTER, F. N89-28240
PETTERSON, B. J. N89-28039
PHILLIPS, J. T., JR. N89-28308
PHILLPOT, S. R. N89-28410
PIAZZA, C. R. N89-28142
N89-28187
PIERZGA, WAYNE N89-27918
PIH, H. N89-28393
PIOTROWSKI, JOSEPH L. N89-27632
PISZCZOR, MICHAEL, JR. N89-27705
PITMAN, E. BRUCE N89-28040
PIVIROTTO, THOMAS J. N89-27754
N89-27755
PLUMMER, MICHAEL D. N89-28359
POCO, J. F. N89-28000
POLIAKOFF, ERWIN D. N89-28372
POLK, J. E. N89-27756
POLLARA, F. N89-27890
PONZONI, FLAVIO JORGE N89-28048
POOL, KIRBY V. N89-27696
POROTNIKOV, A. A. N89-27710
POSNER, E. C. N89-27871
POST, D. N89-28032
POUGET, J. N89-28087
POULAIN, B. N89-28231
POWELL, DOUGLAS G. N89-27846
POWELL, H. T. N89-28006
POWELL, RONALD M. N89-28405
POWER, GLORIA B. N89-27695
POWERS, EDWARD J. N89-27970
PREISS, H. N89-28218
N89-28237
PRESTAGE, J. D. N89-27875
PREZELIN, BARBARA B. N89-28198
PRIMAS, L. E. N89-27878
N89-27879
PRONKO, M. N89-28003
PRUEGER, G. N89-27838
PRUNEAU, PAUL N. N89-27691
PSALTIS, DEMETRI N89-27966
PURI, ASHOK N89-28390

Q

QIN, J. M. N89-27788
QUINTANA, ROXANNE L. N89-27853

R

RADFORD, J. D. N89-28221

RAGONIDEMORAESCORREIA, VIRGINIA N89-28312
RAHE, JURGEN N89-28474
RAITANO, PAUL N89-27701
RAJAN, KRISHNA N89-28420
RAMAMOORTHY, P. N89-28313
RAMOS-IZQUIERDO, L. N89-28185
RAMPARIYAN, H. N89-28125
RASMUSSEN, GARY N89-28116
RATINO, DAVID N89-28200
RATNER, TODD G. N89-27675
REARDON, B. C. N89-28058
REARDON, LAWRENCE F. N89-28034
REBOLD, T. A. N89-27899
REDDY, D. R. N89-27670
REED, I. S. N89-27891
REED, RUSSELL N89-27853
REES, DAVID N89-27738
REICHERT, B. N89-28069
REIMERDES, H.-G N89-28296
REININGER, J. N89-28296
REINOVSKY, R. E. N89-27959
N89-27960
REMPFER, D. N89-27737
RENSHAW, KEN N89-27913
REUTER, J. N89-28215
REYSA, R. P. N89-28262
RHODY, HARVEY E. N89-28334
RIBAUDO, C. N89-27830
RICAUD, P. H. N89-27732
RICH, DAVID N89-28315
RICHINGS, J. F. N89-27823
RICHTER, P. H. N89-27904
N89-27905
RICKEL, D. G. N89-27961
RINALDI, M. A. N89-28479
RINDSTAD, BJORN N89-28072
RINEHART, L. R. N89-27955
RITTEL, MICHAEL N89-27929
RITTER, G. X. N89-28349
RIVIER, N. N89-28415
RIZA, NABEEL N89-27966
ROACH, PAUL D. N89-27984
ROBELLO, DOUGLAS R. N89-27843
ROBERTS, FRED S. N89-28347
ROBINETT, R. D. N89-28039
ROBINSON, D. L. N89-27897
ROBINSON, DAVID A. N89-28196
ROBINSON, J. J. N89-28308
ROBINSON, PAUL A., JR. N89-28456
N89-28457
ROCABOY, A. N89-28280
RODGERS, D. R. N89-27782
RODIERE, C. N89-28217
RODREVICH, B. B. N89-27710
RODRIGUES-COSTA, C. N89-28417
ROGERS, JAMES L. N89-28314
ROGERS, MARK E. N89-28389
ROGERSON, JOHN N89-27962
ROIG, P. B. N89-28271
ROJAS, R. N89-27870
ROSE, T. V. N89-28044
ROSSI, L. C. N89-28119
N89-28120
ROTHMEYER, M. N89-28283
ROTT, H. N89-28056
ROUST, LEAH M. N89-27660
ROVERI, A. N89-27943
ROWAN, D. R. N89-27901
ROWLEY, J. D. N89-27653
ROY, P. R. N89-27822
RUCHTI, RANDAL C. N89-27997
RUDOLPH, T. N89-28115
RUDORFF, BERNARDO FRIEDRICH THEODOR
..... N89-28051
RUPP, GEORGE D. N89-27670
RUSSELL-HEAD, DAVID S. N89-27677
RUSTAMOV, K. A. N89-27926
RYDEN, K. A. N89-27751
N89-27752
N89-27782

S

SACCHI, E. N89-28256
SACHS, E. N89-27838
SAGASER, MICHAEL B. N89-28331
SAHLING, S. N89-28418
SAJBEN, MIKLOS N89-27640
SAKA, NANNAJI N89-28020
SAKAKIBARA, TOSIO N89-27794
SAKAMOTO, M. N89-28399
SALOMONSON, V. N89-28125
SALUSTRI, CARLO N89-28208
SANKAR, L. N. N89-27639
SARRAZIN, DAVID B. N89-28392
SASAKI, H. N89-27739
SASAKI, MASAO N89-28473
SASOH, A. N89-27743
SASS, S. L. N89-28408
SASUGA, TSUNEO N89-27794
SATORI, S. N89-27719
SAUER, R. N89-28262
SAVAGE, C. J. N89-28225
SAWCHUK, A. A. N89-28395
SCHAEFER, R. N89-28220
SCHAEFER, T. N89-28275
SCHAPERY, R. A. N89-27865
SCHARDT, M. N89-28081
SCHARF, LOUIS L. N89-27964
SCHARMANN, A. N89-27785
N89-27786
SCHEID, R. E. N89-27882
SCHEUERMANN, HELMUT N89-27939
SCHILLING, DONALD L. N89-27949
SCHIRLE, PATRICK N89-27658
SCHLIER, CH. N89-28382
SCHMIDLIN, F. J. N89-28167
N89-28168
N89-28169
N89-28170
N89-28188
SCHMIDT, W. N89-27770
SCHMIDT, WAYNE M. N89-27711
SCHNEIDER, W. N89-28078
SCHOENHOFF, M. B. N89-28211
N89-28213
SCHRADE, H. O. N89-27725
N89-27727
N89-27733
N89-27735
N89-27775
N89-27778
SCHREIB, ROLLAND N89-27712
SCHRIMSHER, ROBERT H. N89-28300
SCHUENTZ, B. N89-27770
SCHUTT, J. N89-28184
SCHWANDER, THOMAS N89-27942
SCHWARTZ, ERIC L. N89-28325
SCHWARTZMAN, ALAN N89-28413
SCHWARZOTT, W. N89-28283
SCHWOERKE, STEVE N. N89-27638
N89-27676
SEAWORTH, JOHN N89-28200
SEERING, WARREN P. N89-28018
N89-28324
SEGUCHI, TADAO N89-27794
SEIDMAN, THOMAS I. N89-28335
SEIER, UDO N89-27934
SEKULER, ROBERT N89-28301
SELLMYER, DAVID J. N89-27820
SELSER, A. R. N89-28128
SELSETH, I. N89-28064
SEMPRINI, E. N89-28380
SEN, RANJAN K. N89-28475
SEROVY, GEORGE K. N89-27665
SESSLER, ANDREW M. N89-28005
SEYFERTH, DIETMAR N89-27841
SHA, W. T. N89-27866
SHALKHAUSER, MARY JO N89-27927
SHANER, J. W. N89-28434
SHANFIELD, ZEF N89-27972
SHANNON, ROBERT V., JR. N89-27694
SHARE, G. H. N89-28480
N89-28481
N89-28482
N89-28483
SHARPE, W. N., JR. N89-28046
SHAW, ALAN N89-28325
SHAW, JOHN H. N89-28113
SHEA, M. A. N89-28455
N89-28460
SHEN, EN LAI N89-28037
SHETTLE, ERIC P. N89-28112
SHIMIZU, YUKIO N89-27718
N89-27726
N89-27739
N89-27740
SHIN, DONG RYONG N89-28322
SHIRK, D. W. N89-28128
SHIRK, H. G. N89-28162
N89-28174
SHIUE, J. C. N89-28180
SHMITH, GARY N89-27917
SHREVE, STEVEN E. N89-28337
SHULER, JEAN N89-28447
SIBILO, G. N89-27689
N89-28235
SIEPMANN, R. N89-28224
SILVERMAN, S. N89-28459
SIMIONESCO, L. N89-28245
SIMON, M. K. N89-27889
SIMONS, JACK N89-28388
SIRCAR, S. N89-27830
SLEZIONA, P. C. N89-27733
N89-27735
N89-27775
SLOBIN, S. D. N89-27903
N89-27904
N89-27905
SMART, D. F. N89-28455
N89-28463
SMITH, ALVIN N89-27979
SMITH, C. R. N89-27991
SMITH, DANIEL R., JR. N89-27816
SMITH, G. K. N89-27909
SMITH, J. N89-28125
N89-28144
N89-28186
SMITH, L. SHELBERT N89-27673
SMITH, P. N89-27730
SMITH, PATRICK O. N89-27914
SMITH, R. D. N89-27806
SNOW, WALTER L. N89-27995
SOEFFKER, A. N89-28297
SOHONI, MILIND A. N89-28327
SOLEM, A. E. N89-27743
SOO, S. L. N89-27866
SOREM, MICHAEL E. N89-28007
SOTOMAYOR, J. L. N89-27998
SOVEY, JAMES S. N89-27701
SPEZIALE, CHARLES G. N89-27977
SPJELKAVIK, SIGMUND N89-28075
SROKA, R. N89-28376
SROUR, JOSEPH R. N89-27972
STACEY, WESTON M., JR. N89-28402
STAFSUDD, O. M. N89-27855
STANFORD, JOHN L. N89-27797
STANGERUP, P. N89-28253
STANSBERRY, MARK N89-27693
STARCHVILLE, M. D. N89-27867
STARK, J. P. W. N89-27787
STARKEN, HANS N89-27663
STEFANI, F. N89-28380
STEIER, W. H. N89-28395
STELLA, PAUL M. N89-27705
STELLRECHT, R. N89-28071
STEPHENSON, LOU A. N89-28202
STETINA, F. N89-28177
STEWART, A. J. N89-28326
STINE, WILLIAM B. N89-28100
STOELZEL, DANIEL M. N89-27976
STOJEK, ZBIGNIEW N89-27965
STONE, E. C. N89-28467
STOUT, WILLIAM F. N89-28360
STOW, P. N89-27666
STOY, STAN L. N89-27685
STRANGE, M. G. N89-28172
STRAYER, D. M. N89-27876
STREET, ROBERT L. N89-28117
STREIT, ULRICH N89-28059
STRIFFLER, CHARLES D. N89-27944
STRITTMATTER, R. N89-28263
STRONG, I. B. N89-28480
STROOM, C. N89-28278
STUEMPEL, D. N89-28297
STUFF, M. A. N89-28397
SUBRAMANIAN, DEVIKA N89-28340
SUGAHARA, NORIAKI N89-27794
SUH, NAM P. N89-28020
SUIT, WILLIAM T. N89-27671
SULLIVAN, PATRICK N89-27659
SULLIVAN, R. N89-28135
SUMIDA, M. N89-27739
N89-27740
SUTTON, S. R. N89-28107
SUZUKI, H. N89-27779
SVENSSON, B. N89-28244
N89-28246
SWANSON, ERIC A. N89-28209
SWARTZ, BARRY N89-28208
SWARTZ, C. K. N89-27868
SWEC, DIANE M. N89-27836
SWIFT, T. J. N89-28281
SYDNOR, R. L. N89-27879

T

TAHARA, H. N89-27742
N89-27744
N89-27774
TAI, A. M. N89-28397
TAKESHITA, Y. N89-27768
TALUKDER, MOSTAFA A. N89-27853
TALVACCHIO, J. N89-28409
TAMURA, NAOYUKI N89-27794
TAN, M. J. N89-27982

TANAKA, KEN-ICHI N89-27776
N89-27777
N89-27780
TANAKA, Y. N89-27774
TARIDE, S. N89-28277
TAYLOR, M. A. N89-27798
TEMKIN, S. N89-28370
THURMAN, S. W. N89-27873
TITTLE, R. A. N89-28140
TODOROKI, JIRO N89-28400
TOENNIES, J. PETER N89-28380
N89-28381
N89-28382
N89-28383
N89-28384
N89-28385
TOGLIATTI, G. N89-28091
TOI, K. N89-28399
TOKI, K. N89-27718
N89-27739
N89-27740
N89-27766
TOMAZOS, DIMITRIS N89-27850
N89-27851
TOMMERVIK, HANS N89-28083
TOOLE, JOSEPH E. N89-28369
TOOZE, M. J. N89-27656
TORRES, A. L. N89-28165
N89-28171
TORRESI, A. N89-28287
TOSTI, E. N89-27716
TOTH, R. P. N89-27957
TOWSLEY, DON N89-28332
TRAUTMAN, KRZYSZTOF N89-28344
TRICHILO, M. N89-28233
TRIPLETT, EDWARD L. N89-28198
TRIPP, LLOYD N89-28200
TRIPPI, A. N89-27708
N89-27714
N89-27728
TRIVELATO, GILBERTO DACUNHA N89-28333
TRUONG, T.-K. N89-27891
TSAI, M. Y. N89-28032
TSUCHIYA, KAZUO N89-27777
N89-27780
TSUI, D. C. N89-28428
TUCKER, T. K. N89-27877
TUNINETTI, G. N89-28290
TURKIEWICZ, J. M. N89-28130
TURKNETT, JERRY C. N89-27979
TURNER, J. R. N89-28281
TURNER, L. N89-28215
TWIDDY, NORMAN N89-28386
TZANOS, CONSTANTINE P. N89-27981

U

UDAGAWA, AKIRA N89-27794
UDSETH, H. R. N89-27806
UEMATSU, K. N89-27779
URBAHN, J. N89-27791
URENAFRANCES, JOSE MARIA N89-28077
URQUIDI-MACDONALD, MIRNA N89-27956
URSU, I. N89-28406
URY, I. N89-28010

V

VAETH, R. N89-28244
VALENTIAN, D. N89-27722
N89-27724
N89-27792
VALENTINI, S. N89-28290
VALLE, N. N89-28287
VANCLEEF, GARRETT WARREN N89-28113
VANDERAH, T. A. N89-28422
VANHOLTZ, L. C. N89-27713
VANOOST, S. N89-28225
N89-28294
VANSELOW, JANICE J. N89-27833
VAUGHAN, JOHN D. N89-28433
VAUGHN, C. R. N89-28146
VAUGHN, J. A. N89-27748
VELTEN, H. W. N89-27786
VENKAYYA, VIPPERLA B. N89-28321
VENTURINI, E. L. N89-28414
VERJOVSKY, A. N89-28345
VERMILLION, C. N89-28121
N89-28122
N89-28123
N89-28124
N89-28125
N89-28176
VERNUCCI, A. N89-27943
VEROSTKO, C. E. N89-28262
VERSTRAETE, W. N89-28222
VIEIRADIAS, LUIZ ALBERTO N89-28048
N89-28049
VIEIRADUTRA, LUCIANO N89-28311
N89-28312
VIOLETT, REBECA S. N89-27695
N89-27697
VOGT, L. N89-28246
VONDRA, ROBERT J. N89-27717
VONLONKHUYZEN, H. N89-28288
VONROHDEN, H. N89-27724
N89-27792
VORTHMAN, J. E. N89-27958
N89-27959
N89-27961
VUKELICH, STEVEN R. N89-27685

W

WALKER, J. D. A. N89-27991
WALKER, K. P. N89-28036
WALLACE, N. C. N89-27751
N89-27752
WALSH, E. J. N89-28129
N89-28159
WALTER, LEE N89-27721
WALTON, D. M. N89-27782
WALTON, J. R. N89-27865
WANG, CHARLES N89-27910
WANG, J. R. N89-28163
N89-28180
WANG, LAWRENCE K. N89-28103
N89-28104
WANG, MU HAO SUNG N89-28103
N89-28104
WANG, N. N89-27788
WANG, N. H. N89-27788
WANG, R. T. N89-27876
WANG, W. G. N89-27788
WARD, ALLEN C. N89-28324
WASA, T. N89-27742
WATARI, Y. N89-28399
N89-28401
WATSON, S. D. N89-27758
WEAMAN, EDWARD J. N89-27971
WEAVER, LINDSAY A. N89-27912
WEBER, F. N89-27731
WEESE, J. F. N89-27899
WEI, TANG N89-27639
WEI, XU N89-27816
WEIDMAN, PATRICK N89-28195
WEIGEL, H. S. N89-28115
WEINBERG, I. N89-27868
WEIR, LOIS J. N89-27670
WEISBRICH, W. N89-28071
WENNERSTROM, A. J. N89-27667
WEST, ROBERT A. N89-28474
WHITE, CARL L. N89-27673
WHITE, J. K. N89-28317
WHITEHAIR, STAN N89-27773
WHITELEY, STEPHEN R. N89-28421
WHITEMAN, D. N89-28166
WHITESIDES, GEORGE M. N89-27824
N89-27840
WHYTE, WAYNE A., JR. N89-27927
WIDMANN, FRITZ N89-27933
WIITALA, BRAD N89-27948
WILBUR, PAUL J. N89-27748
N89-27760
N89-27761
WILHEIT, T. T. N89-28126
N89-28163
WILLIAMS, J. G. N89-27859
WILLIAMS, J. O. N89-28430
WILLIAMS, M. N89-28121
N89-28122
N89-28123
N89-28124
WILLIAMS, WARREN W. N89-27974
WILLIAMSON, MICHAEL L. N89-28442
WILLIAMSON, S. J. N89-28210
WILLIAMSON, SAMUEL J. N89-28208
WILLINGHAM, REGINALD A. N89-27851
WILSON, D. CLAY N89-28349
WILSON, JOSEPH N. N89-28349
WILSON, R. J. N89-28250
N89-28273
N89-28279
WILSON, TIM A. N89-27638
N89-27676
WINES, MARIE N89-27917
WINKLER, M. A. N89-28435
WITT, J. N89-28244
WITTE, D. J. N89-28394
WITTLIN, GILL N89-27643
WOLD, A. N89-28423
WOLD, AARON N89-28424
WOLF, D. N89-28410
WONG, A. L. N89-27815
WONG, J. T. N89-27867
WOOD, J. D. N89-28032
WOODRUFF, E. M. N89-27837
WORCHESTER, KEVIN N89-28001
WRENN, G. L. N89-27782
WRIGHT, C. W. N89-28128
N89-28142
N89-28162
N89-28187
WRZESINSKY, RUDOLF N89-27931
WU, G. F. N89-27788
WU, P. N89-28423
WUEBBLES, DONALD J. N89-28108
WUERTZ, KENNETH L. N89-27954

Y

YAMAGIWA, Y. N89-27763
N89-27768
YAN, TSUN-YEE N89-27910
YANAGI, KENJIRO N89-27922
YANG, T. F. N89-27791
YANTIS, BONNIE N89-28315
YAO, X. N89-27791
YATES, JOHN T., JR. N89-28427
YEE, RENA Y. N89-27853
YEH, FREDERICK C. N89-27980
YEH, P. A. N89-28391
YIM, JAE YONG N89-27919
YIN, X. N89-27891
YOON, SANG I. N89-27699
YOSHIDA, H. N89-27768
N89-27779
YOSHIDA, T. N89-27740
YOSHIKAWA, T. N89-27742
N89-27744
N89-27774
N89-27779
YOSHIOA, YUJIRO N89-27794
YOSHIOKA, MASAKAZU N89-28008
YOUNG, CHRISTOPHER J. N89-27632
YOUNG, ROBERT J. N89-27797
YU, JEFF N89-27966
YU, JIM C. N89-28419

Z

ZAMBRA, A. N89-27943
ZAND, B. N89-28062
ZANINOTTI, S. N89-28259
ZAPATA, AUGUSTO J. N89-27920
ZARNITZ, E. N89-27770
ZAVESKY, R. J. N89-27703
ZENG, M. N89-28043
ZHANG, J. N89-28015
ZHOU, ZHEN-LEI N89-28016
N89-28017
ZHURIN, V. V. N89-27710
ZIELINSKI, ALEXANDER E. N89-27682
ZIKAN, KAREL N89-28320
ZILLY, F. N89-28247
N89-28261
ZINI, ENRICO N89-28088
ZINK, JEFFREY I. N89-27810
ZIPSER, DAVID N89-28323
ZUND, J. D. N89-28096
ZUPPARDI, GENNARO N89-27674
ZWALLY, J. N89-28149
N89-28150

Typical Corporate Source Index Listing

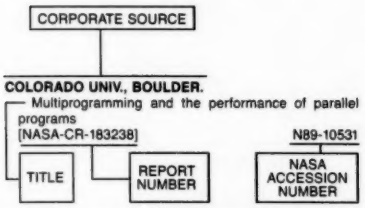

Listings in this index are arranged alphabetically by corporate source. The title of the document provides the user with a brief description of the subject matter. The report number helps to indicate the type of document cited (e.g., NASA report, translation, NASA contractor report). The NASA accession number denotes the number by which the citation is identified. The titles are arranged under each corporate source in ascending accession number order.

A

ACADEMIA SINICA, BEIJING (CHINA).
A 6 cm diameter ion source for assistant deposition N89-27784

ACADEMY OF SCIENCES (USSR), MOSCOW.
Recent progress in the USSR electric propulsion N89-27710

ACADEMY OF SPACE TECHNOLOGY, LANZHOU (CHINA).
Performance research of xenon ion rocket engine N89-27788

ADVISORY GROUP FOR AEROSPACE RESEARCH AND DEVELOPMENT, NEUILLY-SUR-SEINE (FRANCE).
Systems Engineering [AGARD-LS-164] N89-27650
Blading Design for Axial Turbomachines [AGARD-LS-167] N89-27661

AERITALIA S.P.A., CASELLE TORINESE (ITALY).
Rapid prototyping of complex avionics systems N89-27657

AERITALIA S.P.A., TURIN (ITALY).
Thermal control of Columbus pressurized modules N89-28233
Design concepts for Hermes thermal control N89-28234
An algorithm for calculating thermodynamic properties of simple fluids suitable for space thermal control N89-28254
The thermal control of EUTELSAT-2 N89-28256
Cyrogenic fluid sink device for thermal control of a spaceplane during ascent and re-entry phases N89-28293

AERONAUTICAL SYSTEMS DIV., WRIGHT-PATTERSON AFB, OH.
Integrated avionics: Conceptual design N89-27654

AEROSPACE CORP., EL SEGUNDO, CA.
A method for calculating asymmetric flow through nozzles [AD-A209689] N89-27992

AEROSPACE MEDICAL RESEARCH LABS., WRIGHT-PATTERSON AFB, OH.
The effect of various straining maneuvers on cardiac volumes at 1G and during +Gz acceleration [AD-A208846] N89-28200

AEROSPATIALE, CANNES LA BOCCA (FRANCE).
Radiators and heat exchangers for space applications [REPT-882-440-115] N89-27688
Radiator conceptual studies for the Hermes spaceplane N89-27689
Development of heat exchangers for hybrid radiators N89-27690
The two approaches for the thermal control of the Columbus resource module and polar platform N89-28231
Radiator conceptual studies for the Hermes spaceplane N89-28235
TELE-X antenna module thermal control N89-28257
The vegetation payload of the SPOT-4 spacecraft thermal design and analysis N89-28259
Thermal and cryogenic aspects of the ISO optical subsystem N89-28269
Shaking in cryogenic conditions N89-28277
Assembling the ISO thermal model with ESATAN N89-28280
The Fluidnet development and application to preliminary sizing of fluid-loop systems N89-28282
Development of heat exchangers for hybrid radiators N89-28285

AEROSPATIALE USINES DE TOULOUSE (FRANCE).
The Hermes spaceplane program: Status report on the thermal control, environment control and life support activities N89-28217

AIR FORCE ACADEMY, CO.
Symmetry in the basic sciences [AD-A207371] N89-28369

AIR FORCE ARMAMENT LAB., EGLIN AFB, FL.
Hypersonic prediction comparisons with experimental data for a cone-cylinder at mach 6.86 [AD-A207583] N89-27636

AIR FORCE ASTRONAUTICS LAB., EDWARDS AFB, CA.
Interests in electric propulsion N89-27711

AIR FORCE AVIONICS LAB., WRIGHT-PATTERSON AFB, OH.
The evolution of digital avionics architectures/systems N89-27655

AIR FORCE FLIGHT DYNAMICS LAB., WRIGHT-PATTERSON AFB, OH.
Aerospace structures design on computers [AD-A208811] N89-28321

AIR FORCE GEOPHYSICS LAB., HANSCOM AFB, MA.
User's guide for the Air Force surface-layer windflow model (AFWIND) [AD-A208710] N89-28109
Intensity/time profiles of solar particle events at one astronomical unit N89-28460
Predicting the arrival times of solar particles N89-28463

AIR FORCE LOGISTICS COMMAND, WRIGHT-PATTERSON AFB, OH.
Engineering drawing transfer test with Douglas Aircraft Company: MIL-D-28000 Class II (IGES) [DE89-012810] N89-28443

AIR FORCE OFFICE OF SCIENTIFIC RESEARCH, BOLLING AFB, WASHINGTON, DC.
Survey of electric propulsion thruster applicability to near earth space missions N89-27749

AIR FORCE WRIGHT AERONAUTICAL LABS., WRIGHT-PATTERSON AFB, OH.
Transonic and supersonic compressor blading design N89-27667

ALCALA DE HENARES UNIV., MADRID (SPAIN).
Multitemporal analysis of TM images: Application to forest fire mapping and inventory in a Mediterranean environment N89-28084

ALLIED-SIGNAL AEROSPACE CO., TORRANCE, CA.
Advanced motor and motor control development [AD-A207332] N89-27954

AMERICAN WATER WORKS ASSOCIATION, WASHINGTON, DC.
Analytical procedures for environmental quality control, volume 3 [PB89-158620] N89-28104

ANALYTICAL SERVICES AND MATERIALS, INC., HAMPTON, VA.
Spatial three-dimensional secondary instability compressible boundary-layer flows [NASA-CR-4251] N89-27978

ANALYTICS, INC., WILLOW GROVE, PA.
Evaluation of thermal stress induced by helicopter aircrew Chemical, Biological, Radiological (CBR) protective ensemble [AD-A210123] N89-28303

ANSALDO S.P.A., GENOA (ITALY).
A magnetically-driven droplet radiator concept N89-28290

ANT NACHRICHTENTECHNIK, BACKNANG (GERMANY, F.R.).
Communication engineering reports. Fundamental developments. Theoretical work [ETN-89-94623] N89-27928
Model and method for systems development N89-27929
Requirements for a technical data base N89-27930
Minimum shift keying. A modulation system with coding N89-27931
Analysis and dimensioning of a value-discrete adaptive compensation filter N89-27932
Synchronization of the receiver for the ISDN basic connection N89-27933
Receiver synchronization for spread spectrum transmission N89-27934
Carrier derivation in higher-stage QAM-signals N89-27935
Baseband equalizer for digital radio relay links N89-27936
Digital demultiplier for mobile satellite communication N89-27937
Digital demodulator for mobile satellite communication N89-27938
RELP: Speech coding using analysis by synthesis N89-27939
Field theory simulation of nonreciprocal microwave components N89-27940
The calculation of losses in waveguide networks N89-27941
Calculation of planar structures for optical wavelength multiplexers N89-27942

APPLIED MICROWAVE PLASMA CONCEPTS, CARLSBAD, CA.
Efficient energy storage and conversion using adiabatic compression of relativistic-electron plasmas [AD-A208657] N89-28101
A two-stream plasma electron microwave source for high-power millimeter wave generation, phase 1 [AD-A209942] N89-28404

ARGONNE NATIONAL LAB., IL.
Ion-assisted deposition of silver films on ceramics for friction and wear control [DE89-014635] N89-27821
Further investigation of flow modeling during solid propellant processing [AD-A209787] N89-27866
A central difference type approximation of convection in fluid flow [DE89-013282] N89-27981
Interfacial area measurement methods [DE89-013426] N89-27982
Analysis of pressure drop and heat transfer data from the reversing flow test facility [DE89-013907] N89-27984
Grain boundaries in silicon from zero temperature through melting [DE89-013186] N89-28410
The topological structure of grain boundaries [DE89-014676] N89-28415

ARINC RESEARCH CORP., WASHINGTON, DC.
A comparative study of SHF (Super High Frequency) and EHF (Extremely High Frequency) satellite communications, volume 1 [AD-A208850] N89-27945

ARIZONA UNIV., TUCSON.
Galactic cosmic rays in three dimensions N89-28470

ARMY AVIATION ENGINEERING FLIGHT ACTIVITY, EDWARDS AFB, CA.
Baseline performance verification of the 12th year production UH-60A Black Hawk helicopter [AD-A208671] N89-27632
Verification of the production safe flight instrument corporation OV/RV-1D stall warning system [AD-A207392] N89-27659

ARMY AVIATION SYSTEMS COMMAND, CLEVELAND, OH.
A data acquisition and control program for axial-torsional fatigue testing [NASA-TM-102041] N89-28029

ARMY LAB. COMMAND, WATERTOWN, MA.
Solvent assisted delamination crack growth behavior of amorphous thermoplastic materials
[AD-A207365] N89-27833
ARMY MISSILE COMMAND, REDSTONE ARSENAL, AL.
Computer generated matched filters with spatial frequency tailoring
[AD-A209786] N89-28001
ARMY RESEARCH INST. OF ENVIRONMENTAL MEDICINE, NATICK, MA.
Effects of high terrestrial altitude on military performance
[AD-A209614] N89-28201
Acetylcholinesterase inhibitor, pyridostigmine bromide, reduces skin blood flow in humans
[AD-A209615] N89-28202
Analysis of articulated manikin based convective heat transfer during walking
[AD-A208299] N89-28298
ARMY STATEGIC DEFENSE COMMAND, HUNTSVILLE, AL.
High Endoatmospheric Defense Interceptor (HEDI) technology testing program environmental assessment
[AD-A210006] N89-27684
ARMY WAR COLL., CARLISLE BARRACKS, PA.
Space asset modeling for wargame integration
[AD-A207350] N89-28365
Crisis decision-making: The impact of commercial satellites on the media, military and national leaders
[AD-A207334] N89-28449
International technology transfer: The rope to hang the west
[AD-A207347] N89-28452
AUBURN UNIV., AL.
A comparison of rutting behavior of asphalt concrete under the F-4C/G and F-15C/D aircraft
[AD-A208911] N89-27678
AUSSAT PROPRIETARY LTD., SYDNEY (AUSTRALIA).
A robust signalling system for land mobile satellite services N89-27917
AVIONS MARCEL DASSAULT-BREGUET AVIATION, SAINT-CLOUD (FRANCE).
Modeling functional specifications for onboard software N89-27658
Thermal modelling of the EVA-suited astronaut N89-28245

B

BALLISTIC RESEARCH LABS., ABERDEEN PROVING GROUND, MD.
Small scale testing of a mass-stabilized electromagnetic projectile
[AD-A206916] N89-27682
BATTELLE COLUMBUS LABS., RESEARCH TRIANGLE PARK, NC.
Solution of two-dimensional, two-region electromagnetic ground response
[AD-A206265] N89-27869
BATTELLE COLUMBUS LABS., OH.
Environmental effects of space shuttle exhaust on materials
[AD-A208813] N89-27686
BELL TELEPHONE LABS., INC., NEW YORK, NY.
Silicon chemistry in interstellar clouds
[NASA-CR-185862] N89-28471
BHABHA ATOMIC RESEARCH CENTRE, BOMBAY (INDIA).
Laser processing of metals and alloys
[DE89-613235] N89-27822
BODENKULTUR UNIV., VIENNA (AUSTRIA).
Forest damage mapping in Austria with the aid of LANDSAT TM image data N89-28078
BOEING COMMERCIAL AIRPLANE CO., SEATTLE, WA.
High-speed civil transport study. Summary
[NASA-CR-4234] N89-27647
High-speed civil transport study
[NASA-CR-4233] N89-27648
BOSTON COLL., CHESTNUT HILL, MA.
Database development for the DMSP (Defense Meteorological Satellite Program) SSIES experiment
[AD-A206712] N89-27691
BOSTON UNIV., MA.
Fluorescence probes of spectroscopic and dynamical aspects of molecular photoionization
[AD-A207185] N89-28372
BRASILIA UNIV. (BRAZIL).
Theory of photon-drag effect in bulk magnetic semiconductors
[DE89-612214] N89-28417
BRITISH AEROSPACE PUBLIC LTD. CO., BRISTOL (ENGLAND).
Long-life Stirling cycle coolers for applications in the 60 to 110 K range N89-28267
BRITISH AIRCRAFT CORP., PRESTON (ENGLAND).
A structured approach to weapon system design N89-27653
BROOKHAVEN NATIONAL LAB., UPTON, NY.
Synchrotron X-ray fluorescence analyses of stratospheric cosmic dust: New results for chondritic and nickel-depleted particles
[DE89-014032] N89-28107
Superexchange coupling mechanisms for electron transfer processes
[DE89-013568] N89-28411
BROWN UNIV., PROVIDENCE, RI.
A uniformly differentiable approximation scheme for delay systems using splines
[AD-A208567] N89-28346
A numerical study of an augmented Lagrangian method for the estimation of parameters in elliptic systems
[AD-A208658] N89-28351
Growth and characterization of zinc sulfide films by conversion of zinc oxide films with H2S
[AD-A208727] N89-28423
Preparation and characterization of several conduction transition metal oxides
[AD-A208895] N89-28424
BUNDESANSTALT FUER GEOWISSENSCHAFTEN UND ROHSTOFFE, HANNOVER (GERMANY, F.R.).
Detection of short-term changes in tidal flat geomorphology N89-28070

C

CALIFORNIA INST. OF TECH., PASADENA.
Acoustooptic processing of two dimensional signals using temporal and spatial integration
[AD-A208686] N89-27966
Elemental composition and energy spectra of galactic cosmic rays N89-28466
The anomalous cosmic-ray component N89-28467
CALIFORNIA UNIV., BERKELEY. LAWRENCE BERKELEY LAB.
Development of anodes for aluminum/air batteries: Solution phase inhibition of corrosion
[DE89-012839] N89-27956
High-power, high-efficiency FELs
[DE89-013002] N89-28005
Bibliography of high-T sub c superconducting films
[DE89-013395] N89-28409
CALIFORNIA UNIV., IRVINE.
Statistical analysis of the LMS and modified stochastic gradient algorithms
[AD-A208618] N89-28319
CALIFORNIA UNIV., LOS ANGELES.
Optical spectroscopy of copper (1) doped Na(+) beta-alumina
[AD-A209819] N89-27810
Energy transfer effects in beta-alumina
[AD-A209818] N89-27855
The use of multiple ion exchange to produce energy transfer in beta-aluminas
[AD-A209821] N89-27856
CALIFORNIA UNIV., SAN DIEGO.
The back propagation technique for modeling cortical computation
[AD-A209855] N89-28323
CALIFORNIA UNIV., SANTA BARBARA.
Molecular biology of the photoregulation of photosynthetic light-harvesting complexes in marine dinoflagellates
[AD-A209650] N89-28198
Quantum corrections for inelastic atom-surface scattering
[AD-A209850] N89-28387
CARNEGIE-MELLON UNIV., PITTSBURGH, PA.
Non-linear dynamics and chaotic motions in feedback controlled elastic system
[AD-A208628] N89-28041
Singular and bang-bang stochastic control
[AD-A208627] N89-28337
CASE WESTERN RESERVE UNIV., CLEVELAND, OH.
Transformation of a monotropic mesophase into an enantiotropic mesophase by copolymerization of the parent polymers' monomer pair containing constitutional isomeric mesogenic side groups
[AD-A208782] N89-27850
The influence of the polymer backbone flexibility on the phase transitions of side chain liquid crystal polymers containing
yl side groups
[AD-A208821] N89-27851
CATHOLIC UNIV. OF AMERICA, WASHINGTON, DC.
Joint-space adaptive control of a 6 DOF end-effector with closed-kinematic chain mechanism
[NASA-CR-185861] N89-28016
Design of an adaptive controller for a telerobot manipulator
[NASA-CR-185863] N89-28017
CENTRAL INST. OF PHYSICS, BUCHAREST (ROMANIA).
Superconductivity in the Ba(0.69)Y(0.46)CuO(3.15-delta) compound
[DE88-706000] N89-28406
CENTRAL STATE UNIV., WILBERFORCE, OH.
Theoretical model for stabilization of clay-silt airport pavement subgrade systems. Phase 1: Laboratory investigation. Phase 2: Rutting tests
[DOT/FAA/PM-87/20-PHASE-1/2] N89-27673
CENTRE D'ETUDE DE L'ENERGIE NUCLEAIRE, MOL (BELGIUM).
MELISSA: A micro-organisms-based model for CELSS development N89-28222
CENTRE DE VILLAROCHE, MOISSY (FRANCE).
Blading design for cooled high-pressure turbines N89-27668
CENTRE NATIONAL D'ETUDES SPATIALES, TOULOUSE (FRANCE).
Two years of in-orbit life of SPOT-1 heliosynchronous platform N89-28272
CENTRO DE ESTUDIOS Y EXPERIMENTACION DE OBRAS PUBLICAS, MADRID (SPAIN).
Remote sensing of limnological parameters in reservoirs N89-28061
CENTRO NAZIONALE UNIV. PER IL CALCOLO ELETTRONICO, PISA (ITALY).
Integrating TM and cartographic data N89-28090
CERAMIC PROCESS SYSTEMS CORP., MILFORD, MA.
Composite ceramic superconducting wires for electric motor applications
[AD-A208598] N89-27847
CHICAGO UNIV., IL.
Gradients of galactic cosmic rays and anomalous components N89-28468
CHUBU UNIV., KASUGAI (JAPAN).
Role of edge magnetic shear on the limiter H-mode transition of the JIPP T-IIU tokamak
[IPPJ-906] N89-28399
CINCINNATI UNIV., OH.
Comparison of vacuum-annealed and electrochemically cycled electrodes in adsorption and electrocatalysis: Aromatic compounds at platinum (111) and polycrystalline platinum
[AD-A210011] N89-27814
CITY COLL. OF THE CITY UNIV. OF NEW YORK, NY.
Novel methods for reinforcing elastomers
[AD-A210150] N89-27861
Communications using channels formed by meteor bursts
[AD-A209856] N89-27949
CITY UNIV. OF NEW YORK, NY.
Interstellar flight: Aspects of beamed electric propulsion N89-27765
CLARKSON UNIV., POTSDAM, NY.
Nonlinear waves
[AD-A209822] N89-27993
CLEMSON UNIV., SC.
COMM-Q: A simulation model to determine saturation points in nodal type networks
[AD-A207294] N89-28329
COLORADO SCHOOL OF MINES, GOLDEN.
An experimental study to determine the relative influence of fluid-fluid interactions and media heterogeneities on the growth of immiscible viscous fingers
[DE89-013122] N89-27976
COLORADO STATE UNIV., FORT COLLINS.
Ring cusp/hollow cathode discharge chamber performance studies N89-27748
An approach to the parametric design of ion thrusters N89-27761
The phototoxicity of blue light on the functional properties of the retinal pigment epithelium
[AD-A209834] N89-28204
Fiber-optic delay line storage in digital optical computers based on directional couplers
[PB89-185318] N89-28392
Study of improved methods for predicting chemical equilibria
[DE89-014535] N89-28433
COLORADO UNIV., BOULDER.
Quadratic estimators of the power spectrum
[AD-A208601] N89-27964
Ocean modelling and the use of altimetry data
[AD-A206841] N89-28195
Fiber-optic delay line storage in digital optical computers based on directional couplers
[PB89-185318] N89-28392
COLUMBIA UNIV., NEW YORK, NY.
Differential equations, related problems of Pade approximations and computer applications
[AD-A208590] N89-28348

COMMITTEE ON SCIENCE, SPACE AND TECHNOLOGY (U.S. HOUSE).
The 1990 National Aeronautics and Space Administration authorization
[GPO-99-550] N89-28450
COMMITTEE ON SCIENCE AND TECHNOLOGY (U.S. HOUSE).
National Aeronautics and Space Administration Multiyear Authorization Act of 1989
[H-REPT-101-226] N89-28451
CONNECTICUT DEPT. OF ENVIRONMENTAL PROTECTION, HARTFORD.
Analytical procedures for environmental quality control, volume 3
[PB89-158620] N89-28104
CONNECTICUT DEPT. OF HEALTH SERVICES, HARTFORD.
Analytical procedures for environmental quality control, volume 3
[PB89-158620] N89-28104
CONSTRUCCIONES AERONAUTICAS S.A., MADRID (SPAIN).
Thermal control of the GRASP detector section N89-28271
CONTRAVES CORP., ZURICH (SWITZERLAND).
The space-rigidised thermal shield for the ESA Far-Infrared Space Telescope (FIRST) N89-28236
CORNELL UNIV., ITHACA, NY.
Adsorption and reactions of cyclic sulfides on Mo(110)
[AD-A207324] N89-27803
Generic singularities of robot manipulators
[AD-A210116] N89-28021
Algorithmic control of walking
[AD-A210117] N89-28326
Experimental studies of the structure of grain boundaries
[DE89-012954] N89-28408
CREATIVE OPTICS, INC., BEDFORD, MA.
Novel methodology for application of adaptive systems techniques to DMSP (Defense Meteorological Satellite Program) remote temperature sensing
[AD-A209975] N89-28098
Application of optical measure theory to atmospheric temperature sounding from TOVS (TIROS Operational Vertical Sounder) radiances
[AD-A209955] N89-28396

D

DANISH RESEARCH CENTER FOR APPLIED ELECTRONICS, HOERSHOLM.
Efficient implementation of a description language for thermal simulators N89-28253
DARTMOUTH COLL., HANOVER, NH.
The structure and properties of grain boundaries in B2 ordered alloys
[DE89-013266] N89-27817
Theft of information in the take-grant protection model
[NASA-CR-185835] N89-28444
The sharing of rights and information in a capability-based protection system
[NASA-CR-185388] N89-28445
A model of security monitoring
[NASA-CR-185845] N89-28446
DAYTON UNIV., OH.
Effect of three-dimensional object type and density in simulated low-level flight
[AD-A209756] N89-27679
DEFENSE INTELLIGENCE AGENCY, WASHINGTON, DC.
Bibliography of Soviet laser developments: January - February 1988
[AD-A209802] N89-28011
DELAWARE UNIV., NEWARK.
Time variation of galactic cosmic rays N89-28469
DENVER UNIV., CO.
An acoustic emission investigation of the tensile failure of cathodically charged 304 stainless steel
[DE89-008752] N89-27816
DEPARTMENT OF DEFENSE, WASHINGTON, DC.
Critical technologies plan for the Committees on Armed Services, United States Congress, revision
[AD-A210170] N89-28439
DEPARTMENT OF ENERGY, WASHINGTON, DC.
MHD (Magnetohydrodynamics) Program Plan, FY 1989
[DE89-012232] N89-28398
DEUTSCHE FORSCHUNGS- UND VERSUCHSANSTALT FUER LUFT- UND RAUMFAHRT, COLOGNE (GERMANY, F.R.).
Design criteria for optimal blading design N89-27663
Come to flight rules: Rationale on environmental control and life support systems N89-28242
DEUTSCHE FORSCHUNGS- UND VERSUCHSANSTALT FUER LUFT- UND RAUMFAHRT, OBERPFAFFENHOFEN (WEST GERMANY).
Forest classification with TM data in the area of Freiburg, Federal Republic of Germany N89-28081
DEUTSCHE GESELLSCHAFT FUER LUFT- UND RAUMFAHRT, BONN (GERMANY, F.R.).
DGLR/AIAA/JSASS 20th International Electric Propulsion Conference: Proceedings
[DGLR-PAPER-88-02] N89-27707
DORNIER SYSTEM G.M.B.H., FRIEDRICHSHAFEN (GERMANY, F.R.).
European life support systems for space applications N89-28218
Environmental control and life support systems for pressurized modules: From Spacelab to Columbus N89-28219
The definition status of the environmental control and life support subsystems for Hermes N89-28220
Two-phase heat transport systems: Critical components N89-28224
Regenerative CO2-control N89-28237
The atmosphere pressure control section of the Hermes ECLSS N89-28241
The European space suit system N89-28243
Advanced modular software development in thermal engineering N89-28247
Thermal analysis of ROSAT in low-earth eclipse orbit employing steady-state calculations N89-28251
Thermal aspects of the ERS-1 SAR antenna deployment N89-28261
The liquid management section of the Hermes ECLSS N89-28263
Lessons learned from ROSAT thermal balance test: A combined solar simulation/infrared test N89-28275
Evolution of thermal analysis methods towards integrated system performance simulation N89-28283
ECLS simulation program N89-28284
DRAEGERWERK A.G., LUEBECK (GERMANY, F.R.).
Electrochemical removal and concentration of CO2 N89-28238
The catalytic oxiderzer: Description and first results of a breadboard model for a component of the Columbus ECLSS N89-28239
DU PONT DE NEMOURS (E. I.) AND CO., AIKEN, SC.
Subcooled boiling of downward flow in a vertical annulus
[DE89-005320] N89-27983

E

ECOLE POLYTECHNIQUE FEDERALE DE LAUSANNE (SWITZERLAND).
Large-scale forest management using LANDSAT Thematic Mapper data N89-28085
ELECTRO MAGNETIC APPLICATIONS, INC., LAKEWOOD, CO.
Interpretation of F106B and CV580 in-flight lightning data and form factor determination
[NASA-CR-4250] N89-28115
ENTWICKLUNGSRING NORD, BREMEN (GERMANY, F.R.).
System aspects of Columbus thermal control and life support N89-28216
Design and test of a two-phase coldplate N89-28226
ENVIRONMENTAL ASSOCIATES LTD., LIMESTONE, NY.
Analytical procedures for environmental quality control, volume 2
[PB89-158612] N89-28103
ENVIRONMENTAL PROTECTION AGENCY, WASHINGTON, DC.
Analytical procedures for environmental quality control, volume 2
[PB89-158612] N89-28103
Analytical procedures for environmental quality control, volume 3
[PB89-158620] N89-28104
ENVIRONMENTAL RESEARCH INST. OF MICHIGAN, ANN ARBOR.
Sensitivity analysis of reflection errors in infrared image simulation
[AD-A208600] N89-28394
Generalized beamforming with multiple computer originated holograms
[AD-A210175] N89-28397
ERNO RAUMFAHRTTECHNIK G.M.B.H. BREMEN (GERMANY, F.R.).
Redundancy concept for the Columbus man-tended free-flyer thermal control system N89-28232
Theoretical and experimental investigations on heat exchangers for Columbus hybrid radiators N89-28295
In-orbit degradation of thermo-optical properties on MARECS GEO-satellite N89-28297
EUROPEAN SPACE AGENCY, PARIS (FRANCE).
European Coordinated Effort for Monitoring the Earth's Environment. A Pilot Project Campaign on LANDSAT Thematic Mapper Applications (1985-1987)
[ESA-SP-1102] N89-28055
Third European Symposium on Space Thermal Control and Life Support Systems
[ESA-SP-288] N89-28214
EUROPEAN SPACE AGENCY. EUROPEAN SPACE RESEARCH AND TECHNOLOGY CENTER, ESTEC, NOORDWIJK (NETHERLANDS).
The ESA policy and program for the development of electric propulsion N89-27708
The role of electric propulsion in extending the economic life-cycle of commercial European telecommunication satellites N89-27713
The ROSETTA/CNSR mission: A possible application of electric propulsion to interplanetary missions N89-27715
Field Emission Electric Propulsion (FEEP): Experimental investigations on continuous and pulsed modes of operation N89-27792
Life support for EVA: The European system baseline N89-28244
EVA and human physiology N89-28246
Application of expert systems to the thermal configuration of Giotto N89-28250
Cryogenic activities at ESTEC N89-28266
Giotto: The thermal responses to its encounter with comet Halley N89-28273
Thermal software developments at ESTEC N89-28278
SOHO thermal modelling and analysis: The first application of ESATAN to a complete spacecraft N89-28279

F

FABRICA ITALIANA APPARECCHIATURE RADIOELETTRICHE S.P.A., MILAN.
FEEP power conditioning unit: Design and development status N89-27722
FEDERAL AVIATION ADMINISTRATION, WASHINGTON, DC.
Terminal area forecasts: FY 1989 - 2005
[AD-A209805] N89-27644
FLORIDA UNIV., GAINESVILLE.
Image Algebra FORTRAN preprocessor: User's manual
[AD-A208612] N89-28349
FOKKER B.V., AMSTERDAM (NETHERLANDS).
Lumping, a powerful design tool for thermal control N89-28248
A thermal control design for the Quasat spacecraft N89-28258
Preparing Ulysses for launch N89-28260
Thermal aspects of an extended mission for Giotto N89-28274
A 1-kW condenser for a two-phase heat rejection system N89-28288
FREIBURG UNIV. (GERMANY, F.R.).
Agricultural land-use classification in the Upper Rhine Valley using multitemporal TM data N89-28074
Use of LANDSAT TM data for forest damage inventory N89-28082
FREIE UNIV., BERLIN (GERMANY, F.R.).
LANDSAT TM study of sabkha surfaces in the Qattara Depression, northwestern Egypt N89-28066
Multitemporal analysis of forest areas in surroundings of Innsbruck, Austria N89-28086

G

GEC AVIONICS LTD., ROCHESTER (ENGLAND).
Avionic system design methodology N89-27656
GEC POWER ENGINEERING LTD., WHETSTONE (ENGLAND).
ESATAN FHTS: A piped fluid network capability N89-28281
GENERAL DYNAMICS CORP., FORT WORTH, TX.
Small scale model tests in small wind and water tunnels at high incidence and pitch rates. Volume 3: Water tunnel (HFF) data base
[AD-A208690] N89-27638
Small scale model tests in small wind and water tunnels at high incidence and pitch rates. Volume 2: Small wind tunnel (ADF) data base
[AD-A208539] N89-27676
GENERAL ELECTRIC CO., PRINCETON, NJ.
Design trends in communications satellite thermal subsystems N89-28255
GENEVA UNIV. (SWITZERLAND).
Color analysis of inland waters using LANDSAT TM data N89-28062

GEOLOGICAL SURVEY OF NORWAY, TRONDHEIM.
LANDSAT TM data used in the mapping of large-scale geological structures in coastal areas in Trondelag, central Norway N89-28072
GEORGE MASON UNIV., FAIRFAX, VA.
Hyperdimensional data analysis and structural inference
[AD-A210056] N89-27971
GEORGE WASHINGTON UNIV., WASHINGTON, DC.
Calculation of network parameters of crosslinked Markovian polymer chains
[AD-A210073] N89-27860
Data base development and research and editorial support
[NASA-CR-183249] N89-28440
GEORGETOWN UNIV., WASHINGTON, DC.
Studies in stabilization and control of beams and plates
[AD-A208635] N89-28042
GEORGIA INST. OF TECH., ATLANTA.
Numerical simulation of control of supersonic shear layers
[AD-A209703] N89-27639
Identification of variables determining intrahemispheric interference between processing demands
[AD-A208435] N89-28299
Review of effects of NBI (Neutral Beam Injection) and rotation on plasma transport in tokamaks
[DE89-014109] N89-28402
GEOSTAR MESSAGING CORP., WASHINGTON, DC.
Geostar's system architectures N89-27911
GESELLSCHAFT FUER ANGEWANDTE FERNERKUNDUNG, MUNICH (GERMANY, F.R.).
Multitemporal snow classification with TM data N89-28057
GEWERKSCHAFTEN BRIGITTA UND ELWERATH BETRIEBSFUEHRUNGSGESELLSCHAFT M.B.H., HANOVER (GERMANY, F.R.).
Classification of small-scale forests in Flanders using LANDSAT TM digital data: Preliminary results N89-28080
GHENT UNIV. (BELGIUM).
Introduction to finite element techniques in computational fluid dynamics N89-27988
Introduction to finite volume techniques in computational fluid dynamics N89-27989
GIESSEN UNIV. (GERMANY, F.R.).
Auxiliary propulsion RF engine RIT 15: Prototype design and performance N89-27731
Inert gas performance of the RIT 35 main propulsion unit N89-27770
Development of high-current RF plasma sources for neutral particle injections N89-27785
Nonpropulsive application of the RF-ion thruster for material processing with reactive gases N89-27786
GOOD SAMARITAN HOSPITAL AND MEDICAL CENTER, PORTLAND, OR.
Age-related changes in human vestibulo-ocular reflexes: Sinusoidal rotation and caloric tests
[NASA-CR-185857] N89-28211
Age-related changes in human posture control: Sensory organization tests
[NASA-CR-185858] N89-28212
Age-related changes in human vestibulo-ocular and optokinetic reflexes: Pseudorandom rotation tests
[NASA-CR-185856] N89-28213

H

HACH CO., LOVELAND, CO.
Analytical procedures for environmental quality control, volume 2
[PB89-158612] N89-28103
HAMPTON INST., VA.
Parallel Architectures for Planetary Exploration Requirements (PAPER)
[NASA-CR-185370] N89-28475
HARVARD UNIV., CAMBRIDGE, MA.
Formation of monolayers by the coadsorption of thiols on gold: Variation in the length of the alkyl chain
[AD-A208386] N89-27824
Modelling organic surfaces with self-assembled monolayers
[AD-A208385] N89-27840
HIROSHIMA UNIV., TAKEHARA (JAPAN).
Stochastic approach to chaotic inflation and the distribution of universes
[DE89-778051] N89-28473
HOCHSCHULE DER BUNDESWEHR, MUNICH (GERMANY, F.R.).
Review on turbomachinery blading design problems N89-27662
HONEYWELL, INC., BLOOMINGTON, MN.
Electronic properties of ordered ladder polymers
[AD-A207288] N89-27832
HUGHES COMMUNICATIONS, INC., LOS ANGELES, CA.
System level comparison of FDMA vs. CDMA (under conference guideline constraint) N89-27913
HUGHES SPACE AND COMMUNICATIONS GROUP, EL SEGUNDO, CA.
Controlling a stationary orbit using electric propulsion N89-27741
HYPRESS, INC., ELMSFORD, NY.
MM wavecomponents - SIS (Superconductor-Insulator-Superconductor) mixers
[AD-A208632] N89-28421

I

ILLINOIS UNIV. AT URBANA-CHAMPAIGN, SAVOY.
Average interconnection length and interconnection distribution for rectangular arrays
[AD-A209848] N89-27967
ILLINOIS UNIV., CHICAGO.
Design of experiments and reliability models
[AD-A209880] N89-28023
ILLINOIS UNIV., URBANA.
High temp toughening and creep studies
[AD-A208714] N89-27826
Laser cladding of Ni, Nb, Mg alloys for improved environmental resistance at high temperatures
[AD-A210134] N89-27830
Electromagnetic scattering from a structured slab comprised of periodically placed resistive cards
[AD-A210145] N89-27953
Load balancing in multiprocessor systems
[AD-A210144] N89-28327
Learning from physical analogies: A study in analogy and the explanation process
[AD-A208689] N89-28338
A new item response theory modeling approach with applications to unidimensionality assessment and ability estimation
[AD-A207301] N89-28360
IMPERIAL COLL. OF SCIENCE AND TECHNOLOGY, LONDON (ENGLAND).
Damping in structural joints N89-28026
INDIAN INST. OF TECH., KHARAGPUR.
Recent advances on the dynamic behavior of stiffened plates N89-28027
INNSBRUCK UNIV. (AUSTRIA).
Improved snow and glacier monitoring by the LANDSAT Thematic Mapper N89-28056
INSTITUT FUER ANGEWANDTE GEODAESIE, FRANKFURT AM MAIN (GERMANY, F.R.).
Reports on cartography and geodesy. Special issue: History of photogrammetry, number 1
[ISSN-0344-5879] N89-28092
The early period of photogrammetry till the invention of the aircraft N89-28093
Analog methods and instruments N89-28094
INSTITUT NATIONAL POLYTECHNIQUE, GRENOBLE (FRANCE).
Mechanical and physical study of the behavior under sequential loads of copper and steel plates
[ETN-89-94805] N89-28037
INSTITUTE FOR COMPUTER APPLICATIONS IN SCIENCE AND ENGINEERING, HAMPTON, VA.
Bunch-Kaufman factorization for real symmetric indefinite banded matrices
[NASA-CR-181860] N89-28341
An integrating matrix formulation for buckling of rotating beams including the effects of concentrated masses
[NASA-CR-181862] N89-28342
INSTITUTE FOR IMAGE PROCESSING COMPUTER MAPPING, GRAZ (AUSTRIA).
Discrimination of geobotanical anomalies in coniferous forests from LANDSAT TM data N89-28079
INSTITUTO DE EDAFOLOGIA Y FISIOLOGIA VEGETAL, MADRID (SPAIN).
Remote sensing of the Madrid area ecosystems N89-28076
INSTITUTO DE FISICA TEORICA, SAO PAULO (BRAZIL).
Information aspects of type 9 cosmological models
[DE89-612518] N89-28472
INSTITUTO DE PESQUISAS ESPACIAIS, SAO JOSE DOS CAMPOS (BRAZIL).
Optimization of maneuvers of a spin-stabilized satellite, using magnetic coils
[INPE-4778-TDL/350] N89-27680
Launch window for the Brazilian Data Collecting Satellite
[INPE-4773-PRE/1442] N89-27683
The use of digital elevation model for correcting the effects of projections in reforrestations of eucalyptus in mountainous regions
[INPE-4763-PRE/1432] N89-28048
Automatic change in contour diagrams on the occasion of scale reduction using a material morphology
[INPE-4769-PRE/1438] N89-28049
The use of edge detectors based on mathematical morphology in remote sensing imagery
[INPE-4777-PRE/1446] N89-28050
Report of the Project Estima, phase 2: LANDSAT-TM data and agrometeorology in crop yield estimation of wheat at the farm level
[INPE-4782-RPE/582-PHASE-2] N89-28051
Meteorology in the press
[INPE-4762-PRE/1432] N89-28114
Performance augmentation of SITIM-150 through a high performance numerical processor
[INPE-4770-PRE/1439] N89-28305
Preliminary statistical identification of radar imagery: Autoregressive-moving average (ARMA) models
[INPE-4771-PRE/1440] N89-28311
Mode filters and their applications
[INPE-4748-PRE/1421] N89-28312
Implementation of a digital torque controller of a reaction wheel with an incremental computer
[INPE-4784-PRE/1447] N89-28333
INSTITUTO NACIONAL DE INVESTIGACIONES AGRONOMICAS, MADRID (SPAIN).
Comparison of the classification results obtained with TM and MSS data in land uses identification of the Communidad Autonoma de Cantabria N89-28077
INSTITUUT VOOR CULTURRTECHNIEK EN WATERHUISHOUDING, WAGENINGEN (NETHERLANDS).
Application of remote sensing to irrigation water management in two Italian irrigation districts N89-28060
INTERNATIONAL CENTRE FOR THEORETICAL PHYSICS, TRIESTE (ITALY).
Algebraic analysis of the electromagnetic wave interaction with the two-level system with two-fold degenerated states
[DE89-611932] N89-27926
Soliton behaviour of crack propagation in brittle materials
[DE89-612190] N89-28033
Some basic theorems on the cross-sums of certain class of numbers (M-1) when the operations are done with different bases M of the arithmetic
[DE89-611892] N89-28343
Orbits which always have affine invariant neighbourhoods
[DE89-611895] N89-28344
Two examples of escaping harmonic maps
[DE89-611896] N89-28345
Differential geometric aspects of the theory of ferroelectricity
[DE89-612191] N89-28416
INTERNATIONAL MARITIME SATELLITE ORGANIZATION, LONDON (ENGLAND).
Choice of FDMA/SCPC access technique for aeronautical satellite voice system N89-27909
INTERNATIONAL TELECOMMUNICATIONS SATELLITE ORGANIZATION, WASHINGTON, DC.
Electric propulsion: Implementation issues N89-27712
IOWA STATE UNIV. OF SCIENCE AND TECHNOLOGY, AMES.
Performance prediction for axial-flow compressor and turbine blading N89-27665
Preparation and characterization of colloidal ZnS particles
[AD-A210171] N89-27862
Analysis and numerical analysis of some properly and improperly posed problems in applied mathematics
[AD-A208633] N89-28350
IOWA UNIV., IOWA CITY.
Particle simulations in magnetospheric plasmas
[AD-A206252] N89-28106
ISRAEL INST. OF METALS, HAIFA.
Coating and impregnation of carbon-carbon composites with ceramics by electrophoretic deposition
[AD-A208873] N89-27800

J

JAPAN ATOMIC ENERGY RESEARCH INST., TOKYO.
Irradiation effects on resistance of thermal impact of composite used in space
[DE89-778069] N89-27794
JET PROPULSION LAB., CALIFORNIA INST. OF TECH., PASADENA.
Spacecraft and mission design for the SP-100 flight experiment N89-27717
Thermal design improvements for 30kWe arcjet engine N89-27754
Electrode erosion in steady-state electric propulsion engines N89-27755

The Telecommunications and Data Acquisition Report [NASA-CR-185431] N89-27871
Estimation and filtering techniques for high-accuracy GPS applications N89-27872
High-precision radiometric tracking for planetary approach and encounter in the inner solar system N89-27873
The effect of spatial and temporal wet-troposphere fluctuations on connected element interferometry N89-27874
New ion trap for atomic frequency standard applications N89-27875
Operational parameters for the superconducting cavity maser N89-27876
Operating and environmental characteristics of Sigma Tau hydrogen masers used in the Very Long Baseline Array (VLBA) N89-27877
State-of-the-art fiber optics for short distance frequency reference distribution N89-27878
Stabilized fiber-optic frequency distribution system N89-27879
A new method for analysis of limit cycle behavior of the NASA/JPL 70-meter antenna axis servos N89-27880
Application of optimal control theory to the design of the NASA/JPL 70-meter antenna servos N89-27881
Precision pointing compensation for DSN antennas with optical distance measuring sensors N89-27882
The effects of atmospheric turbulence on precision optical measurements used for antenna-pointing compensation N89-27883
A multiflare horn with 1-megawatt power handling capability N89-27884
Thermal measurements of microwave transmitter feedhorn window N89-27885
A new analysis of beam-waveguide antennas considering the presence of the enclosure N89-27886
Multipurpose exciter with low phase noise N89-27887
Software package for performing experiments about the convolutionally encoded Voyager 1 link N89-27888
The use of interleaving for reducing radio loss in trellis-coded modulation systems N89-27889
Performance of concatenated codes using 8-bit and 10-bit Reed-Solomon codes N89-27890
Decoding of 1/2-rate (24,12) Golay codes N89-27891
The weight distribution and randomness of linear codes N89-27892
Effective amplifier noise for an optical receiver based on linear mode avalanche photodiodes N89-27893
A visibility characterization program for optical communications through the atmosphere N89-27894
Options for daytime monitoring of atmospheric visibility in optical communications N89-27895
Site selection criteria for the optical atmospheric visibility monitoring telescopes N89-27896
A novel approach to a PPM-modulated frequency-doubled electro-optic cavity-dumped Nd:YAG laser N89-27897
Microwave time delays for the X/S-band feed system at X-band N89-27898
DSN radio science system design and testing for Voyager-Neptune encounter N89-27899
Accuracy of telemetry signal power loss in a filter as an estimate for telemetry degradation N89-27900
The DSS-14 C-band exciter N89-27901
Orthogonal sets of data windows constructed from trigonometric polynomials N89-27902
DSN 70-meter antenna microwave optics design and performance improvements. Part 1: Design optimization N89-27903
DSN 70-meter antenna X- and S-band calibration. Part 1: Gain measurements N89-27904
DSN 70-meter antenna X- and S-band calibration. Part 2: System noise temperature measurements and telecommunications link evaluation N89-27905
Reanalysis, compatibility and correlation in analysis of modified antenna structures N89-27906
Proceedings of the Mobile Satellite System Architectures and Multiple Access Techniques Workshop [NASA-CR-184564] N89-27907
Performance of DA/FDMA architecture proposed for MSS N89-27910
Interplanetary Particle Environment. Proceedings of a Conference [NASA-CR-185461] N89-28454
Toward a descriptive model of solar particles in the heliosphere N89-28455
Toward a descriptive model of galactic cosmic rays in the heliosphere N89-28456
The effects of high energy particles on planetary missions N89-28457
A new proton fluence model for E greater than 10 MeV N89-28459
High-energy particles very near the sun N89-28465

JOHNS HOPKINS UNIV., BALTIMORE, MD.
Dynamic fracture toughness testing [AD-A209948] N89-28046
Pre-attentive and attentive visual information processing [AD-A209884] N89-28206

JOINT INST. FOR NUCLEAR RESEARCH, DUBNA (USSR).
Glassy behaviour of YBa2Cu3O7 [DE89-613399] N89-28418

K

KARLSRUHE UNIV. (GERMANY, F.R.).
Image processing strategies for mineral exploration in arid areas by use of TM data N89-28067
Karst drainage in the Peloponnesus area: A case study for application of TM data in hydrogeology N89-28069
Methodical and structural MSS and TM investigations in the Swabian Alb, SW Germany N89-28071

KOHLBERG ASSOCIATES, INC., ALEXANDRIA, VA.
Solution of two-dimensional, two-region electromagnetic ground response [AD-A206265] N89-27869

KYOTO UNIV. (JAPAN).
Numerical studies of the flow field in a dc arcjet thruster N89-27776

L

LAMONT-DOHERTY GEOLOGICAL OBSERVATORY, PALISADES, NY.
Cloud/cryosphere interactions [AD-A208377] N89-28196

LAWRENCE LIVERMORE NATIONAL LAB., CA.
High-temperature optical-fiber pH sensor [DE89-014103] N89-28000
Multi-segment Nd:glass disk amplifiers [DE89-014043] N89-28006
Pulsed laser propulsion for low cost, high volume launch to orbit [DE89-014049] N89-28009
Backgrounder contribution No. 18: Climate scenarios for the first UC/DOE workshop [DE89-014302] N89-28105
Evaluating CFC (Chlorofluorocarbon) alternatives from the atmospheric viewpoint, revision 1 [DE89-014268] N89-28108
Engineering drawing transfer test with Douglas Aircraft Company: MIL-D-28000 Class II (IGES) [DE89-012810] N89-28443
Problems and solutions in online documentation systems [DE89-014092] N89-28447
Engineering research and development: Thrust area report FY 88 [DE89-014320] N89-28453
Gamma ray bursts: Confrontation between theory and observational data [DE89-012936] N89-28477

LEHIGH UNIV., BETHLEHEM, PA.
Three-dimensional vortex interactions in turbulent boundary layers [AD-A208624] N89-27991

LENOX INST. FOR RESEARCH, INC., MA.
Analytical procedures for environmental quality control, volume 2 [PB89-158612] N89-28103
Analytical procedures for environmental quality control, volume 3 [PB89-158620] N89-28104

LOCKHEED AERONAUTICAL SYSTEMS CO., BURBANK, CA.
Investigation of transport airplane fuselage fuel tank installations under crash conditions [DOT/FAA/CT-88/24] N89-27643

LOCKHEED MISSILES AND SPACE CO., HUNTSVILLE, AL.
Space Shuttle Main Engine structural analysis and data reduction/evaluation. Volume 1: Aft Skirt analysis [NASA-CR-183663] N89-27693
Space Shuttle Main Engine structural analysis and data reduction/evaluation. Volume 3A: High pressure oxidizer turbo-pump preburner pump housing stress analysis report [NASA-CR-183665] N89-27694
Space Shuttle Main Engine structural analysis and data reduction/evaluation. Volume 3B: High pressure fuel turbo-pump preburner pump bearing assembly analysis [NASA-CR-183666] N89-27695
Space Shuttle Main Engine structural analysis and data reduction/evaluation. Volume 4: High pressure fuel turbo-pump inlet housing analysis [NASA-CR-183667] N89-27696
Space Shuttle Main Engine structural analysis and data reduction/evaluation. Volume 5: Main Injector LOX Inlet analysis [NASA-CR-183668] N89-27697

LOCKHEED MISSILES AND SPACE CO., PALO ALTO, CA.
Effect of alloying, rapid solidification, and surface kinetics on the high temperature environmental resistance of niobium [AD-A209934] N89-27829
A space radiation test model study [AD-A208760] N89-28479

LOS ALAMOS NATIONAL LAB., NM.
Shock initiation modeling of multicomponent explosives [DE89-012259] N89-27863
A battery-powered flux compression generator system [DE89-014230] N89-27958
High voltage power condition systems powered by flux compression generators [DE89-014259] N89-27959
High-performance, high-current fuses for flux compression generator driven inductive store power conditioning applications [DE89-014274] N89-27960
A simultaneous helical generator [DE89-014284] N89-27961
KIVA-2: A computer program for chemically reactive flows with sprays [DE89-012805] N89-27975
KrF lasers for inertial confinement fusion [DE89-014272] N89-28007
Magnetopause structure and dynamics: Issues for GEM [DE89-012620] N89-28054
The human telomere [DE89-014252] N89-28199
ParaGraph-RTS: A parallel reduction-based run-time system [DE89-005457] N89-28315
Goals for limited strategic defenses [DE89-012260] N89-28366
Constellation sizing for modest directed energy platforms [DE89-012826] N89-28367
The stability of the High-Density Z-Pinch [DE89-014276] N89-28403
Issues and future directions in subsecond thermophysics [DE89-014228] N89-28434
Thermophysical properties of liquid niobium [DE89-014288] N89-28435

M

MANAGEMENT INFORMATION SERVICES, INC., WASHINGTON, DC.
The private sector economic and employment benefits to the nation and to each state of proposed FY 1990 NASA procurement expenditures [NASA-CR-185894] N89-28448

MANCHESTER COLL. OF SCIENCE AND TECHNOLOGY (ENGLAND).
Zinc telluride growth on InP [AD-A209924] N89-28430

MANCHESTER UNIV. (ENGLAND).
High performance composites based on polyurethanes reinforced with polydiacetylenes [AD-A208436] N89-27797

MARCONI SPACE SYSTEMS LTD., PORTSMOUTH (ENGLAND).
Design and development of the UK-10 ion propulsion subsystem N89-27730
The Propellant Supply and Monitoring Equipment (PSME) for the UK-10 ion propulsion subsystem N89-27758

MARTIN MARIETTA AEROSPACE, DENVER, CO.
Development of a novel high-performance contact heat exchanger N89-28286

MARTIN MARIETTA AEROSPACE, WASHINGTON, DC.
A comparative study of SHF (Super High Frequency) and EHF (Extremely High Frequency) satellite communications, volume 1 [AD-A208850] N89-27945

MARYLAND UNIV., BALTIMORE.
Control and system theory, optimization, inverse and ill-posed problems [AD-A208570] N89-28335

MARYLAND UNIV., COLLEGE PARK.
Studies of the propagation of short burst, high power microwave radiation through neutral and ionized media [AD-A208664] N89-27944
Introduction N89-27986

The use of stereo optical flow fields in the determination of three-dimensional motion and stereo correspondence [DE89-012518] N89-27996
The radial dependence of the solar energetic particle flux N89-28461

MASSACHUSETTS DEPT. OF ENVIRONMENTAL QUALITY ENGINEERING, BOSTON.
Analytical procedures for environmental quality control, volume 2 [PB89-158612] N89-28103

MASSACHUSETTS INST. OF TECH., CAMBRIDGE.
GPS (Global Positioning System) orbit determination: Bootstrapping to resolve carrier phase ambiguity [AD-A209974] N89-27681
Feasibility of millimeter-accuracy geodetic positioning and vehicle tracking with repeater satellites [AD-A209958] N89-27692
The interaction between a positively biased conductor on a high voltage solar array and a plasma N89-27720
Fluid mechanics in a magnetoplasmadynamic thruster N89-27734
Equipment models for process optimization and control using smart response surfaces [AD-A208321] N89-27838
Comparison of equipment modeling methods as applied to the LPCVD of in-situ P-doped polysilicon [AD-A208373] N89-27839
Birth, death and transfiguration: The synthesis of preceramic polymers, their pyrolysis and their conversion to ceramics [AD-A208437] N89-27841
Simulation of deformation and texture evolution in semi-crystalline polymers [AD-A208854] N89-27852
Fiber reinforced structural ceramics for construction [AD-A209976] N89-27858
Propagation characteristics of electromagnetic waves in concrete [AD-A207387] N89-27921
Design considerations for an earth based flexible robotic system [AD-A209635] N89-28018
Fundamental mechanisms of tribology and their implications [AD-A209941] N89-28020
Satellite image analysis for marine applications [PB89-187330] N89-28053
Approaches to multi-level sequential logic synthesis [AD-A208322] N89-28316
A fast multipole algorithm for capacitance extraction of complex 3-D geometries [AD-A208374] N89-28317
Quantitative inference in a mechanical design compiler [AD-A209900] N89-28324
The combinatorics of heuristic search termination for object recognition in cluttered environments [AD-A209690] N89-28363
Evidence against the existence of strong diffuse X-ray scattering from gold twist boundaries at room temperature [DE89-012726] N89-28407
Polycrystalline plastic deformation and texture evolution for crystals lacking five independent slip systems [AD-A208902] N89-28425

MASSACHUSETTS INST. OF TECH., LEXINGTON.
Adaptive preprocessing of nonstationary signals [AD-A209646] N89-27946
Optical spatial tracking using coherent detection in the pupil plane [AD-A209970] N89-28209
Binary sequences of arbitrary length with near-ideal correlation [AD-A209956] N89-28356
Solid state research [AD-A209645] N89-28426
Solid state research [AD-A209969] N89-28431

MASSACHUSETTS UNIV., AMHERST.
Resource contention management in parallel systems [AD-A208809] N89-28332

MATERIALS RESEARCH LABS., ASCOT VALE (AUSTRALIA).
Stress intensity calibration of a ring specimen using a finite element technique [AD-A208678] N89-28044

MATRA ESPACE, PARIS-VELIZY (FRANCE).
Possible use of a gas monitoring system in space respirometry studies N89-28223

MATRA ESPACE, TOULOUSE (FRANCE).
Design and integration of an electric propulsion system on the Eurostar spacecraft N89-27732
Improved ray tracing technique for radiative heat transfer modelling N89-28249
Thermal effects of plume impingement N89-28252

MAX-PLANCK-INSTITUT FUER STROEMUNGSFORSCHUNG, GOETTINGEN (GERMANY, F.R.).
Vibrational predissociation of shock-selected C2H4 and NH3 clusters [MPIS-6/1988] N89-28373
Vibrational predissociation of shock-selected C2H4 and NH3 clusters, introduction N89-28374
Infrared photodissociation and cluster-specific detection of internally cold (C2H4) van der Waals complexes N89-28375
Infrared photodissociation of van der Waals complexes selectively prepared by molecular beam scattering N89-28376
CAMAC time-of-flight analyzer for molecular beam diagnostics N89-28377
Charge transfer and inelastic scattering in proton-molecule collisions [MPIS-13/1988] N89-28378
Charge transfer and inelastic scattering in proton-molecule collisions, introduction N89-28379
Potential energy curves for the (ArH(+)) and (NeH(+)) systems from the interplay of theory and experiments N89-28380
Dynamics of H(+) + Kr and H(+) + Xe elastic and charge-transfer collisions: State-selected differential cross sections at low collision energies N89-28381
Observation of vibrationally resolved charge transfer in H(+) + H2 at a collision energy Ecm = 20 eV N89-28382
A comparison between theoretical and experimental state-to-state charge transfer cross sections for H(+) + H2 at 20 eV: Evidence for quantum effects N89-28383
A three-dimensional quantum mechanical study of vibrational inelastic and charge transfer processes in H(+) + H2 at a collision energy Ecm = 20 eV N89-28384
Charge transfer and structured vibrational distributions in H(+) + CH4 low-energy collisions N89-28385

MAXWELL LABS., INC., SAN DIEGO, CA.
Capacitors for pulsed electric propulsion N89-27790

MCDONNELL-DOUGLAS ASTRONAUTICS CO., SAINT LOUIS, MO.
Missile Datcom. Volume 2: User's manual [AD-A210128] N89-27685

MCDONNELL-DOUGLAS RESEARCH LABS., SAINT LOUIS, MO.
Terminal shock response in ramjet inlets to abrupt downstream perturbations [AD-A209788] N89-27640

MELBOURNE UNIV., PARKVILLE (AUSTRALIA).
Compacted-snow runways: Guidelines for their design and construction in Antarctica [AD-A208910] N89-27677

MEMBRANE TECHNOLOGY AND RESEARCH, INC., MENLO PARK, CA.
Separation of oxygen from seawater by membrane permeation [AD-A208863] N89-27809

MESSERSCHMITT-BOELKOW-BLOHM G.M.B.H., BREMEN (GERMANY, F.R.).
Thermal protection concepts of recoverable capsules N89-28292
Development of the Hermes flexible external insulation N89-28296

MESSERSCHMITT-BOELKOW-BLOHM G.M.B.H., MUNICH (GERMANY, F.R.).
Electrical transfer vehicle analysis for future space operations (MESCATS) N89-27750
Study on the applicability of Asynchronous Time Division (ATD) techniques to satellite communications systems [ESA-CR(P)-2742] N89-27943
Thermal analysis of advanced heat protection systems N89-28291

MESSERSCHMITT-BOELKOW-BLOHM G.M.B.H., OTTOBRUNN (GERMANY, F.R.).
Status of the RITA experiment on EURECA N89-27728

MICHIGAN STATE UNIV., EAST LANSING.
Experiments and analysis of a compact electrothermal thruster N89-27773

MICHIGAN UNIV., ANN ARBOR.
Nonlinear viscoelastic characteristics of polymeric materials [DE89-012680] N89-27835

MICROTRONICS ASSOCIATES, PITTSBURGH, PA.
High dynamic range infrared radiometry and imaging [NASA-CR-183439] N89-27994

MIDWEST RESEARCH INST., GOLDEN, CO.
Photovoltaic Program Branch annual report, FY 1988 [DE89-000898] N89-28099
Progress in parabolic dish technology [DE89-009427] N89-28100

MINELECTROTECHPROM, MOSCOW (USSR).
Non-condensible gas effects on the low-temperature heat pipe characteristics N89-28227
Express-method investigation and its application for heat pipe quality control N89-28229

MINNESOTA UNIV., MINNEAPOLIS.
A statistical derivation of the average degree of polymerization in a stirred tank reactor [AD-A209873] N89-27857
Calculation of network parameters of crosslinked Markovian polymer chains [AD-A210073] N89-27860

MISSION RESEARCH CORP., NASHUA, NH.
Math and physics studies-multi-project support entropy-based image restoration: Modifications and additional results [AD-A209972] N89-27951

MITRE CORP., MCLEAN, VA.
Automated planning function for AERA 3: Maneuver option manager [DOT/FAA/DS-89/21] N89-27645
A mathematical formulation for planning automated aircraft separations for AERA 3 [DOT/FAA/DS-89/20] N89-27646

MITSUBISHI ELECTRIC CO., AMAGASAKI (JAPAN).
Computational investigation on the characteristics of a low power dc arcjet thruster N89-27777
Experimental investigation on the characteristics of a low power dc arcjet thruster N89-27780

MITSUBISHI ELECTRIC CORP., KANAGAWA (JAPAN).
Improved thrust generation mechanism for electrothermal/electromagnetic arcjet N89-27726
Verification of performance and endurance of capacitor bank for the electric propulsion experiment (EPEX) N89-27739
Verification of control sequence and algorithm for the electric propulsion experiment (EPEX) N89-27740

MONTANA STATE UNIV., BOZEMAN.
Evaluation of new thermomechanical constitutive theory for snow N89-28052

MORTON THIOKOL, BRIGHAM CITY, UT.
Flight set 360L001 (STS-26) insulation component. Volume 3: Final release [NASA-CR-183674] N89-27698
SRM propellant, friction/ESD testing [NASA-CR-183706] N89-27864

MOTOREN- UND TURBINEN-UNION MUENCHEN G.M.B.H. (GERMANY, F.R.).
Aerodynamic design of low pressure turbines N89-27669

MUENSTER UNIV. (GERMANY, F.R.).
Application of LANDSAT data to hydrological mapping N89-28059

N

NAGOYA UNIV. (JAPAN).
Role of edge magnetic shear on the limiter H-mode transition of the JIPP T-IIU tokamak [IPPJ-906] N89-28399
Extension of stellarator approximation in magnetohydrodynamic equilibrium and stability of toroidal helical systems [IPPJ-905] N89-28400
Experimental study on the deposition profile of the ICRF power and electron thermal diffusivity [IPPJ-908] N89-28401

NAPLES UNIV. (ITALY).
An evaluation of three experimental processes for two-dimensional transonic tests [NASA-CR-181871] N89-27674

NASA ALUMNI LEAGUE, WASHINGTON, DC.
The private sector economic and employment benefits to the nation and to each state of proposed FY 1990 NASA procurement expenditures [NASA-CR-185894] N89-28448

NATIONAL AERONAUTICAL LAB., BANGALORE (INDIA).
Computation of transonic potential flow past RAE-Wing-A and Body-B2 combination [PD-CF-8921] N89-27637
Ved editor for MC5600 computer system [PD-SE-8907] N89-28306
Vi editor for MC56000 computer system [PD-SE-8906] N89-28307
Extended Kalman Filter (EKF) algorithm [PD-CF-8922] N89-28313

NATIONAL AERONAUTICS AND SPACE ADMINISTRATION, WASHINGTON, DC.
Time-Variable Phenomena in the Jovian System [NASA-SP-494] N89-28474

NATIONAL AERONAUTICS AND SPACE ADMINISTRATION. AMES RESEARCH CENTER, MOFFETT FIELD, CA.
Evaluation of a strain-gage load calibration on a low-aspect-ratio wing structure at elevated temperature [NASA-TP-2921] N89-28034

Life science research objectives and representative experiments for the space station
[NASA-TM-89445] N89-28304

NATIONAL AERONAUTICS AND SPACE ADMINISTRATION. GODDARD SPACE FLIGHT CENTER, GREENBELT, MD.

Laboratory for Oceans
[NASA-TM-101257] N89-28118
Ocean topography experiment (TOPEX) radar altimeter N89-28119
Mars Observer Radar Altimeter Radiometer (MORAR) N89-28120
Bangladesh Agro-Climatic Environmental Monitoring Project N89-28121
NASA follow-on to the Bangladesh Agro-Climatic Environmental Monitoring Project N89-28122
Fiji South Pacific Severe Storm Detection and Warning System Project (SPSSD/WS) N89-28123
NASA follow-on on the Fiji South Pacific Severe Storm Warning System Project (SPSSD/WS) N89-28124
Monocular electro-optical stereo scanner N89-28125
Tropical Rainfall Measurement Mission N89-28126
Spaceborne meteorological radar studies N89-28127
Advanced altimetry N89-28128
Earth Observing System (EOS) advanced altimetry N89-28129
Wide band data collection system N89-28130
Calibration support for the Earth Observing System Project N89-28131
Oceanographic wide field sensor N89-28132
The Earth Radiation Budget Experiment N89-28133
Lunar observer laser altimeter N89-28134
YAG aerosol lidar N89-28135
Applications of the Coastal Zone Color Scanner in oceanography N89-28136
Ocean color observations of phytoplankton distributions and primary productivity N89-28137
Coastal Zone Color Scanner studies N89-28138
Remote sensing of ocean color in the Arctic N89-28139
Airborne in-situ spectral characterization and concentration estimates of fluorescent organics as a function of depth N89-28140
Oceanographic applications of laser technology N89-28141
NASA Charge Coupled Device (CCD) Spectrometer System (NCSS) N89-28142
Airborne Oceanographic Lidar (AOL) flight mission participation N89-28143
Ocean Data Acquisition System N89-28144
Coastal Zone Color Scanner N89-28145
The Multichannel Ocean Color Sensor (MOCS) N89-28146
Arctic Sea ice studies with passive microwave satellite observations N89-28147
Microwave remote sensing of sea ice N89-28148
Analysis of sea ice dynamics N89-28149
Ice sheet radar altimetry N89-28150
Sea ice/climate studies N89-28151
Ice sheet studies using synthetic aperture radar N89-28152
Wave/current interaction model N89-28153
Ocean Drifter Project N89-28154
Analyses of the wind-driven response of tropical oceans N89-28155
Climatological aspects of Nimbus-7 SMMR data N89-28156
Microscale ocean dynamics N89-28157
Microwave radar oceanographic investigations N89-28158
Surface Contour Radar (SCR) contributions to FASINEX N89-28159
Rainfall on microwave return from the sea surface N89-28160
Wind-Wave-Current Tank Research Facility usage and status N89-28161
The Surface Wave Dynamics Experiment (SWADE) N89-28162
Water vapor profiling using microwave radiometry N89-28163
Correlative Measurements Program N89-28164
Ozone measurements using balloon-borne ozonesondes N89-28165
Mobile lidar system for measurement of water vapor mixing ratio and ozone number density N89-28166
Rocket temperature soundings N89-28167
Electrodynamics, wind and temperature N89-28168
Radiosonde intercomparison N89-28169
Satellite/radiosonde comparison N89-28170
Tropospheric nitric oxide measurements N89-28171
Cloud absorption radiometer N89-28172
The Laboratory for Oceans Computing Facility N89-28173
Code 672 observational science branch computer networks N89-28174
Personal computers on Ethernet N89-28175
Third International Satellite Direct Broadcast Services User's Conference N89-28176
Low cost real time interactive analysis system N89-28177
Navigational and Environmental Measurement System (NEMS) N89-28178
Airborne lidar global positioning investigations N89-28179
Microwave remote sensing of soil moisture N89-28180
Synthetic aperture microwave radiometer N89-28181
Radar scattering and soil moisture N89-28182
Advanced Solidstate Array Spectroradiometer N89-28183
Agriculture Multiband Experiment Radiometer N89-28184
Diode-pumped laser research N89-28185
Large aperture scanning airborne lidar N89-28186
A multiprocessor airborne lidar data system N89-28187
Meteorological Sensor Calibration Facility N89-28188
NASA Aircraft-Satellite Instrument Calibration Project N89-28189
Flight calibration source development N89-28190
Radiance standards N89-28191
Environmental calibration chamber operations N89-28192
Calibration source maintenance, characterization and development N89-28193
Integrating sphere and hemisphere calibration update N89-28194

NATIONAL AERONAUTICS AND SPACE ADMINISTRATION. LYNDON B. JOHNSON SPACE CENTER, HOUSTON, TX.

A tandem mirror hybrid plume plasma propulsion facility N89-27791
Test results on re-use of reclaimed shower water: Summary N89-28262

NATIONAL AERONAUTICS AND SPACE ADMINISTRATION. LANGLEY RESEARCH CENTER, HAMPTON, VA.

Static internal performance of a nonaxisymmetric vaned thrust reverser with flow splay capability
[NASA-TP-2933] N89-27634
Summary of longitudinal stability and control parameters as determined from Space Shuttle Challenger flight test data
[NASA-TM-101605] N89-27671
NASA in-house Commercially Developed Space Facility (CDSF) study report. Volume 1: Concept configuration definition
[NASA-TM-101586-VOL-1] N89-27687
A critical comparison of turbulence models for homogeneous shear flows in a rotating frame
[NASA-CR-181864] N89-27977
Photogrammetric technique for in-flight ranging of trailing vortices using entrained balloons
[NASA-TM-4129] N89-27995
Research and technology plans for FY 1989 and accomplishments for FY 1988
[NASA-TM-101592] N89-28035
The potential application of the blackboard model of problem solving to multidisciplinary design
[NASA-TM-101633] N89-28314

NATIONAL AERONAUTICS AND SPACE ADMINISTRATION. LEWIS RESEARCH CENTER, CLEVELAND, OH.

Mach 5 inlet CFD and experimental results
[NASA-TM-102317] N89-27670
Performance of a 100 kW class applied field MPD thruster
[NASA-TM-102312] N89-27701
Development and refinement of test bed simulations
[NASA-TM-102335] N89-27702
Structural and thermal response of 30 cm diameter ion thruster optics
[NASA-TM-102124] N89-27703
Toward an electrical power utility for space exploration
[NASA-TM-102347] N89-27704
NASA advanced space photovoltaic technology-status, potential and future mission applications
[NASA-TM-102093] N89-27705
Investigation of a liquid-fed water resistojet plume
[NASA-TM-102310] N89-27706
Computational simulation of high temperature metal matrix composites cyclic behavior
[NASA-TM-102115] N89-27795
Tungsten fiber reinforced copper matrix composites: A review
[NASA-TP-2924] N89-27796
Ion beam and plasma methods of producing diamondlike carbon films
[NASA-TM-102301] N89-27836
Indium phosphide solar cell research in the US: Comparison with nonphotovoltaic sources
[NASA-TM-102103] N89-27868
Parametric study of electromagnetic waves propagating in absorbing curved S ducts
[NASA-TM-102024] N89-27923
Digital CODEC for real-time processing of broadcast quality video signals at 1.8 bits/pixel
[NASA-TM-102325] N89-27927
Experience with advanced instrumentation in a hot section cascade
[NASA-TM-102294] N89-27980
Compensation for effects of ambient temperature on rare-earth doped fiber optic thermometer
[NASA-TM-102282] N89-27998
Speckle interferometry using fiber optic phase stepping
[NASA-TM-102331] N89-27999
Topology of modified helical gears
[NASA-TM-102134] N89-28015
A data acquisition and control program for axial-torsional fatigue testing
[NASA-TM-102041] N89-28029
Probabilistic structural analysis methods of hot engine structures
[NASA-TM-102091] N89-28030
Refinements in a viscoplastic model
[NASA-TM-102338] N89-28036

NATIONAL AERONAUTICS AND SPACE ADMINISTRATION. MARSHALL SPACE FLIGHT CENTER, HUNTSVILLE, AL.

Status of the US Space Station ECLSS and internal TCS N89-28215

NATIONAL AEROSPACE LAB., EMMELOORD (NETHERLANDS).

Development of a sensor for high-quality two-phase flow N89-28230

NATIONAL AEROSPACE LAB., TOKYO (JAPAN).

Xenon ion thruster test facility: Design and operation N89-27745
Discharge performance of a 12 cm cusp xenon ion thruster N89-27746

NATIONAL INST. OF STANDARDS AND TECHNOLOGY, BOULDER, CO.

High-temperature superconductivity: Abstracts of NIST (National Institute of Standards and Technology) publications, 1987-1988
[PB89-148340] N89-28405

NATIONAL INST. OF STANDARDS AND TECHNOLOGY, GAITHERSBURG, MD.

Institute for Materials Science and Engineering: Metallurgy Division, technical activities 1988
[PB89-201321] N89-27819
Vapor phase deposition studies of phosphate esters on metal and ceramic surfaces
[PB89-148985] N89-27831
Data bases available at the National Institute of Standards and Technology Research Information Center
[PB89-160014] N89-28441

NATIONAL OCEANIC AND ATMOSPHERIC ADMINISTRATION, BOULDER, CO.

Solar proton event forecasts N89-28462

NATIONAL SANITATION FOUNDATION, ANN ARBOR, MI.

Analytical procedures for environmental quality control, volume 3
[PB89-158620] N89-28104

NAVAL AIR DEVELOPMENT CENTER, WARMINSTER, PA.

An adhesive for field repair of composites
[AD-A209992] N89-27859
Evaluation of thermal stress induced by helicopter aircrew Chemical, Biological, Radiological (CBR) protective ensemble
[AD-A210123] N89-28303

NAVAL CIVIL ENGINEERING LAB., PORT HUENEME, CA.

Development of a lightweight, high strength, collapsible hose
[AD-A207292] N89-28014

NAVAL OCEAN SYSTEMS CENTER, SAN DIEGO, CA.

DARPA (Defense Advanced Research Projects Agency) Review on EHF Devices
[AD-A208564] N89-27963
Aerosol model selection using surface measurements of IR horizon radiances and satellite detected visible radiances
[AD-A209638] N89-28110

NAVAL POSTGRADUATE SCHOOL, MONTEREY, CA.

Evaluation of head-up display formats for the F/A-18 hornet
[AD-A208651] N89-27660
Parametric study of the aerothermodynamics of a jet engine test facility
[AD-A208512] N89-27675
Definition study and model for a tethered sounding rocket
[AD-A207367] N89-27699

Particle sizing in solid rocket motors
[AD-A208740] N89-27793
An experimental and computer modeling study of stepped radius monopole antennas
[AD-A207356] N89-27919
Analysis of maritime mobile satellite communication systems
[AD-A207358] N89-27920
Theory of multi-frequency modulation (MFM) digital communications
[AD-A209737] N89-27947
Bubble detection using a dual frequency sound field
[AD-A207286] N89-27973
Effects of an embedded vortex on a single film-cooling jet in a turbulent boundary layer
[AD-A207374] N89-27974
Optimal three-dimensional path planning using visibility constraints
[AD-A207357] N89-28310
Fixed interval smoothing algorithm for an extended Kalman filter for over-the-horizon ship tracking
[AD-A208555] N89-28318
Parameter plane design method
[AD-A209845] N89-28322
Conversion of mass storage hierarchy in an IBM computer network
[AD-A208520] N89-28330
A computational comparison of the primal simplex and relaxation algorithms for solving minimum cost flow networks
[AD-A208534] N89-28331
An implementation of a data definition facility for the graphics language for database
[AD-A207380] N89-28442

NAVAL RESEARCH LAB., WASHINGTON, DC.
Tests of Halon 1301 test gas simulants
[AD-A207346] N89-27867
A comparative study of SHF (Super High Frequency) and EHF (Extremely High Frequency) satellite communications, volume 1
[AD-A208850] N89-27945
ZPIMP: A zero-D Z-pinch implosion code
[AD-A208381] N89-27962
Efficient second harmonic conversion of broadband high-peak-power Nd:glass laser radiation using large-aperture KDP crystals in quadrature
[DE89-012961] N89-28003
The inadequacies of damage energy as a measure of displacement damage
[AD-A207376] N89-28028
Analysis of a limiting-amplitude problem in acousto-elastic interactions, 1
[AD-A209741] N89-28045
Scaling laws for the spectrum of interchange instabilities in the high latitude ionosphere
[AD-A209993] N89-28111
Modeling of ocean surface spectrum and surface scattering. Applications to reverberation prediction in the AAUS program
[AD-A210127] N89-28197
Sound propagation in bubbly liquids: A review
[AD-A207377] N89-28370
Current models of the intensely ionizing particle environment in space N89-28458
Detection of artificial sources of nuclear radiation in space, revision
[AD-A209720] N89-28480
Monitoring sources of nuclear radiation in space. Part 1: Early 1984 observations, revision
[AD-A209721] N89-28481
Monitoring sources of nuclear radiation in space 1980-1984 observations, revision
[AD-A209722] N89-28482
Monitoring sources of nuclear radiation in space 1985-1987 observations, revision
[AD-A209723] N89-28483

NAVAL SHIP RESEARCH AND DEVELOPMENT CENTER, BETHESDA, MD.
Estimation of lower bound properties from material test data
[AD-A207378] N89-28361

NAVAL SURFACE WARFARE CENTER, DAHLGREN, VA.
Significant digit computation of the incomplete beta function ratios
[AD-A210118] N89-28358

NAVAL WEAPONS CENTER, CHINA LAKE, CA.
Energetic polyoxetane thermoplastic elastomers: Synthesis and characterization
[AD-A209612] N89-27853
Noise and false alarm rate characteristics for envelope detector systems preceded by RF amplification
[AD-A209789] N89-27948
State-space theory of structured uncertainty with examples
[AD-A209968] N89-28339
Crystal chemistry, synthesis, and characterization of infrared optical materials
[AD-A208723] N89-28422

NEBRASKA UNIV., LINCOLN.
Fundamental magnetic studies of iron-rare-earth-metalloid alloys
[DE89-013803] N89-27820

NELSON SPACE SERVICES LTD., LONDON (ENGLAND).
Physico-chemical atmosphere revitalisation: The qualitative and quantitative selection of regenerative designs N89-28221

NEW HAMPSHIRE UNIV., DURHAM.
Particles accelerated by shocks in the heliosphere N89-28464

NEW JERSEY INST. OF TECH., NEWARK.
Generic singularities of robot manipulators
[AD-A210116] N89-28021
Plastic deformation of granular materials
[AD-A208589] N89-28040

NEW MEXICO STATE UNIV., LAS CRUCES.
Differential geodesy of the Eotvos torsion balance
[AD-A208711] N89-28096

NEW YORK STATE DEPT. OF HEALTH, ALBANY.
Analytical procedures for environmental quality control, volume 3
[PB89-158620] N89-28104

NEW YORK UNIV., NEW YORK.
Higher order mechanisms of color vision
[AD-A209838] N89-28205
Attention, imagery and memory: A neuromagnetic investigation
[AD-A209917] N89-28207
Modulation of spontaneous brain activity during mental imagery
[AD-A209918] N89-28208
Visualizing and rhyming cause differences in alpha suppression
[AD-A210005] N89-28210
Automatic construction of polyhedral surfaces from voxel representations
[AD-A210009] N89-28325
Silicon chemistry in interstellar clouds
[NASA-CR-185862] N89-28471

NEW YORK UNIV. MEDICAL CENTER.
Automatic construction of polyhedral surfaces from voxel representations
[AD-A210009] N89-28325

NIPPON ELECTRIC CO. LTD., YOKOHAMA (JAPAN).
Thermal design of a superfluid helium dewar for infrared telescope on-board space flyer unit N89-28270

NORD-MICRO ELEKTRONIC FEINMECHANIK G.M.B.H., FRANKFORT (GERMANY, F.R.).
Condensing heat exchangers for European spacecraft ECLSS N89-28240

NORTH CAROLINA UNIV., CHAPEL HILL.
Capacity of discrete time Gaussian channel with and without feedback, 2
[AD-A207388] N89-27922
Research in stochastic processes
[AD-A209935] N89-28364

NORTHEAST ARTIFICIAL INTELLIGENCE CONSORTIUM, SYRACUSE, NY.
Northeast Artificial Intelligence Consortium annual report 1987. Volume 6: Artificial intelligence applications to speech recognition
[AD-A208380] N89-28334

NORTHROP RESEARCH AND TECHNOLOGY CENTER, PALOS VERDES PENINSULA, CA.
Investigation of radiation effects on semiconductor devices and integrated circuits
[AD-A210165] N89-27972

NORTHWESTERN UNIV., EVANSTON, IL.
Monte Carlo reliability analysis
[AD-A210052] N89-28024
Perception of motion in statistically-defined displays
[AD-A208695] N89-28301

NORWEGIAN HYDRODYNAMIC LABS., TRONDHEIM.
LANDSAT-5 TM study of suspended sediments in a fjord system in western Norway N89-28084

NOTRE DAME UNIV., IN.
Scintillating fiber detector development for the SSC
[DE89-013118] N89-27997
Time series modeling for structural response prediction
[AD-A208608] N89-28354

NOTTINGHAM UNIV. (ENGLAND).
Corrosion of aluminium alloys by IRFNA (Inhibited Red Fuming Nitric Acid)
[AD-A208326] N89-27823

O

OAK RIDGE NATIONAL LAB., TN.
The texture variation in extruded graphite
[DE89-014066] N89-27837
The Sigmajig: An improved hot-cracking test
[DE89-013029] N89-28031
Approaching distributed database applications using a programmable terminal emulator
[DE89-014831] N89-28308
Noncontacting laser diffraction strain extensometer for material properties characterization at high temperatures
[DE89-013551] N89-28393
Risk assessment and late effects of radiation in low-earth orbits
[DE89-013043] N89-28478

OFFICE DE LA RECHERCHE SCIENTIFIQUE ET TECHNIQUE, BONDY (FRANCE).
Comparison of MSS and TM LANDSAT data for cartography of surface structures in arid regions (southern Tunisia) N89-28087

OFFICE NATIONAL D'ETUDES ET DE RECHERCHES AERONAUTIQUES, PARIS (FRANCE).
Overview on blading design methods N89-27664

OHIO STATE UNIV., COLUMBUS.
Target signature modeling and bistatic scattering measurement studies
[NASA-CR-185434] N89-27870
Determination of local empirical covariance functions from residual terrain reduced altimeter data
[AD-A208678] N89-28095
Zonal winds between 25 and 120 km retrieved from solar occultation spectra
[NASA-CR-180086] N89-28113

OHIO STATE UNIV., MARION.
Analytical and numerical solutions for cylindrical blast waves in a plasma of varying density N89-27767

OPTIMETRICS, INC., BURLINGTON, MA.
A new background stratospheric aerosol model for use in atmospheric radiation models
[AD-A210110] N89-28112

ORTEL CORP., ALHAMBRA, CA.
Band structure engineering for ultra-low threshold laser diodes
[AD-A208629] N89-28010
Pigtailed single-mode diode lasers
[AD-A209913] N89-28012

OSAKA UNIV. (JAPAN).
Continuous operation of a quasi-steady MPD propulsion system with an external magnetic field N89-27742
Hybrid MPD thruster with axial and cusp magnetic fields N89-27744
Electrothermal thrusters utilizing electrodeless discharges N89-27774
Operating characteristics of 1 kW hydrazine arcjet thruster N89-27779

OSTERREICHISCHE RAUMFAHRT- UND SYSTEMTECHNIK G.M.B.H., VIENNA (AUSTRIA).
Hermes: Drink/food-water supply assembly N89-28264
Nutrition for short-duration space missions N89-28265

P

PACIFIC NORTHWEST LABS., RICHLAND, WA.
Electrospray ionization-mass spectrometry and tandem mass spectrometry
[DE89-014465] N89-27806

PACIFIC-SIERRA RESEARCH CORP., LOS ANGELES, CA.
Aerostat cold weather study
[AD-A207299] N89-27635

PARIS-SUD UNIV., ORSAY (FRANCE).
Vibrationally excited ions: Quenching, reaction and lifetimes
[AD-A208503] N89-28386

PENNSYLVANIA STATE UNIV., UNIVERSITY PARK.
Analysis of a system to prevent helicopter rotor blade-airframe strikes
[AD-A209804] N89-27649
Magnetic induction thruster with lithium propellant N89-27762
Characteristics of free-floating nitrogen and helium plasmas generated in a microwave resonant cavity N89-27771
Numerical and experimental investigations of a propagating microwave-heated plasma N89-27772
Coupling between radiation and gas dynamics
[AD-A209657] N89-28102

PENNSYLVANIA UNIV., PHILADELPHIA.
Protonic solid electrolytes: Thermal stability and conductivity of ammonium/hydronium beta'-alumina
[AD-A209911] N89-27813

PHILIPS COMPONENTS, MITCHAM (ENGLAND).
A review of the cathode construction for the RAE 10/25mN thruster N89-27759
PISA UNIV. (ITALY).
Electric propulsion for low earth orbit applications N89-27714
PITTSBURGH UNIV., PA.
The orientation of chemical bonds at surfaces: A key to understanding the structure and bonding of surface species
[AD-A209833] N89-28427
PLANNING RESEARCH CORP., HAMPTON, VA.
Approaches toward a blue semiconductor laser
[NASA-CR-4252] N89-28004
POLITECNICO DI MILANO (ITALY).
Tests of topographic mapping with Thematic Mapper images N89-28091
POLITECNICO DI TORINO (ITALY).
Intermediate heat exchanger for a nuclear-powered space power system N89-28287
PRAIRIE VIEW AGRICULTURAL AND MECHANICAL COLL., TX.
Flow boiling with enhancement devices for cold plate coolant channel design
[NASA-CR-185840] N89-27979
PRINCETON UNIV., NJ.
Current driven instabilities of an electromagnetically accelerated plasma N89-27736
Characterization of cold cathode erosion processes N89-27756
Anomalous stresses versus extent of cure in an epoxy composite specimen
[AD-A208523] N89-27798
System theoretic models for high density VLSI structures
[AD-A209901] N89-27968
Markov processes applied to control, reliability and replacement
[AD-A208634] N89-28362
Transport and submillimeter wave spectroscopy of GaAs/Al sub xGa sub 1-xAs heterostructures
[AD-A209836] N89-28428
PURDUE UNIV., WEST LAFAYETTE, IN.
Cathode processes in a MPD arcjet N89-27753

Q

QUADREX CORP., NEW HAVEN, CT.
Analytical procedures for environmental quality control, volume 3
[PB89-158620] N89-28104
QUALCOMM, INC., SAN DIEGO, CA.
Why is CDMA the solution for mobile satellite communication N89-27912

R

RENSSELAER POLYTECHNIC INST., TROY, NY.
Resist sensitivity enhancement by radiation-induced modification
[AD-A208438] N89-27842
Poly(enaminonitriles): Novel materials for use in electronics
[AD-A208439] N89-27843
Electron beam-positive polyimides
[AD-A208440] N89-27844
A soluble photosensitive polyimide
[AD-A209634] N89-27854
Northeast Artificial Intelligence Consortium annual report for 1987. Volume 4: Research in automated photointerpretation
[AD-A208610] N89-28336
Decomposition kinetics and film formation of an organometallic precursor to SiC on Si(100)
[AD-A208384] N89-28420
RESEARCH AND DATA SYSTEMS, INC., GREENBELT, MD.
Evaluation of the AFGL (Air Force Geophysics Laboratory) cloud simulation models using satellite data
[AD-A208713] N89-28116
RESEARCH INST. FOR ADVANCED COMPUTER SCIENCE, MOFFETT FIELD, CA.
A survey of visual preprocessing and shape representation techniques
[NASA-CR-185418] N89-28309
RHODE ISLAND UNIV., KINGSTON.
Probabilistic description of fatigue crack growth under constant-and variable-amplitude loading
[AD-A208717] N89-28043
RIBBON TECHNOLOGY CORP., GAHANNA, OH.
Rapidly solidified titanium alloys by melt overflow
[NASA-CR-4253] N89-27818
RICE UNIV., HOUSTON, TX.
Human cognition and information display in C3I system tasks
[AD-A210012] N89-28302
RIT RESEARCH CORP., ROCHESTER, NY.
Northeast Artificial Intelligence Consortium annual report 1987. Volume 6: Artificial intelligence applications to speech recognition
[AD-A208380] N89-28334
ROCHESTER UNIV., NY.
Transition metal activation and functionalization of carbon-hydrogen bonds
[DE89-012949] N89-27804
ROCKWELL INTERNATIONAL CORP., THOUSAND OAKS, CA.
Studies of phase-conjugate optical device concepts
[AD-A206219] N89-28391
ROLLS-ROYCE LTD., DERBY (ENGLAND).
Blading design for multi-stage HP compressors N89-27666
ROME AIR DEVELOPMENT CENTER, GRIFFISS AFB, NY.
Avionics system engineering: An introduction N89-27651
ROME UNIV. (ITALY).
Anode-nozzle experimental analysis in a coaxial non-steady solid propellant MPD thruster N89-27757
ROYAL AEROSPACE ESTABLISHMENT, FARNBOROUGH (ENGLAND).
The proposed demonstration of the UK-10 ion propulsion system on ESA's SAT-2 spacecraft N89-27729
Development of a flight standard power conditioning and control system for the T5 ion thruster N89-27738
A case study of a mission to the Kordylewski clouds using ion propulsion N89-27751
A small ion-propelled spacecraft for near earth experiments N89-27752
Diagnostic tools for an ion thruster in space N89-27782
RSDE S.R.L., MILAN (ITALY).
Processing and interpretation of Thematic Mapper images in the Province of Piacenza (Italy) N89-28088
RUTGERS - THE STATE UNIV., NEW BRUNSWICK, NJ.
Eye movements and visual information processing
[AD-A209817] N89-28203
A RUTCOR project on discrete applied mathematics
[AD-A208572] N89-28347
RUTHERFORD HIGH ENERGY LAB., CHILTON (ENGLAND).
A 4-K mechanical refrigerator for space applications N89-28268

S

SAARLAND UNIV., SAARBRUCKEN (GERMANY, F.R.).
Martensitic phase transitions in nanocrystalline materials
[AD-A208804] N89-27827
SAN ANTONIO AIR LOGISTICS CENTER, KELLY AFB., TX.
Analysis and elimination of high temperature notch induced microcrack initiation in Inconel 718 nickel-based alloy
[AD-A209695] N89-27828
SANDIA NATIONAL LABS., ALBUQUERQUE, NM.
An analysis of severe air transport accidents
[DE89-012642] N89-27642
Ceramic joining in the United States
[DE89-009323] N89-27834
Scattering from fractals
[DE89-013451] N89-27924
The effects of snow on landmarks in K(sub u) band SAR images
[DE89-014578] N89-27925
A one microsecond, thirty-five kilojoule, one hertz pulse generator
[DE89-013074] N89-27955
Line/Circuit Analysis Program: Cross-coupling on PC (Printed Circuit) board traces including discontinuities and circuit elements
[DE89-013884] N89-27957
Thermal strains in a bimaterial joint: Experimental and numerical analysis
[DE89-013935] N89-28032
Discrete enforcement of uncertain oscillator Gaussian response
[DE89-005595] N89-28038
Model based damping of coupled horizontal and vertical oscillations in a flexible rod
[DE89-007034] N89-28039
Phonon-drag thermoelectric power in high magnetic fields in heterojunctions
[DE89-013921] N89-28412
Diamagnetic shielding and flux creep in a Tl-Ba-Ca-Cu-O thin film
[DE89-014550] N89-28414
Real gas equations of state for CHEMKIN
[DE89-012794] N89-28432
SHERBROOKE UNIV. (QUEBEC).
Implicit time dependent methods for inviscid and viscous compressible flows, with a discussion of the concept of numerical dissipation N89-27990
SMITHSONIAN ASTROPHYSICAL OBSERVATORY, CAMBRIDGE, MA.
Coronagraph observations and analyses of the ultraviolet solar corona
[NASA-CR-185830] N89-28476
SNIA VISCOSA, COLLEFERRO (ITALY).
Plasma propulsion activites at SNIA BPD N89-27716
SOCIETE ANONYME BELGE DE CONSTRUCTIONS AERONAUTIQUES, BRUSSELS.
Feasibility demonstration model of a capillary pumping loop N89-28225
Qualification program on stainless steel A95 heatpipe for space application N89-28294
SOCIETE DES ACCUMULATEURS FIXES ET DE TRACTION, ROMAINVILLE (FRANCE).
Thermal control of Ni-H2 battery N89-28276
SOCIETE EUROPEENNE DE PROPULSION, VERNON (FRANCE).
Field Emission Electric Propulsion (FEEP) attitude control capabilities N89-27724
SOUTHAMPTON UNIV. (ENGLAND).
The use of electric propulsion techniques for LEO atomic oxygen simulation N89-27787
SOUTHWEST RESEARCH INST., SAN ANTONIO, TX.
A study of spacecraft electromagnetic contamination of artificial electron beams
[AD-A209954] N89-27950
SOVONICS SOLAR SYSTEMS, TROY, MI.
Deployable aerospace photovoltaic array based on amorphous silicon alloys N89-27721
SPACE COMPUTER CORP., SANTA MONICA, CA.
Hybrid wafer-scale processor
[AD-A209944] N89-27969
SPAR AEROSPACE LTD., STE-ANNE-DE-BELLEVUE (QUEBEC).
MSAT signalling and network management architectures N89-27916
SPREAD SPECTRUM SYSTEMS, INC., OLNEY, MD.
Alternative multiple-access techniques for mobile satellite systems N89-27914
SRI INTERNATIONAL CORP., MENLO PARK, CA.
Multiphoton detection techniques for F and F2
[AD-A208576] N89-27807
Development of anodes for aluminum/air batteries: Solution phase inhibition of corrosion
[DE89-012839] N89-27956
GMBU (Ground Mobile Breadboard Upgrade) lidar and bubbler correlation study at Dugway Proving Ground
[AD-A207297] N89-28002
STANFORD TELECOMMUNICATIONS, INC., SANTA CLARA, CA.
Aeronautical mobile TDMA/MCTDMA system N89-27918
STANFORD UNIV., CA.
Mechanical response of structural elements to dynamic loads
[AD-A209827] N89-27802
Characterization of structure in thin polymer resist films
[AD-A208677] N89-27848
Polymer chain configurations in constrained geometries: Ultrathin films for microlithography
[AD-A208692] N89-27849
Studies in statistical signal processing
[AD-A210054] N89-27952
Robot motion planning: A distributed representation approach
[AD-A209890] N89-28019
Adaptive grid methods for numerical weather prediction
[AD-A209950] N89-28117
An efficient exact algorithm for the least squares image registration problem
[AD-A208725] N89-28320
A theory of justified reformulations
[AD-A210153] N89-28340
The principal pivoting method revisited
[AD-A208796] N89-28352
Subset complement addition upper bounds: An improved inclusion/exclusion method
[AD-A208797] N89-28353
Computational methods and systems for problems in science and engineering
[AD-A209951] N89-28355
Application of quaternary phase diagrams to compound semiconductor processing
[DE89-014537] N89-28413

Development of superlattices for ultra high-speed electronic and optoelectronic devices
[AD-A209874] N89-28429

STATE UNIV. OF NEW YORK, BINGHAMTON.
Lithologic mapping of mafic intrusions in East Greenland using Landsat Thematic Mapper data
[NASA-CR-183440] N89-28047

STATE UNIV. OF NEW YORK, BUFFALO.
Experimental determination of the coefficient in the steady state current equation for spherical segment microelectrodes
[AD-A208662] N89-27965
Extraordinary behavior of atoms near a phase conjugator
[AD-A209946] N89-28389
Electromagnetic reaction to molecular relaxation and its effect on absorption near a rough surface
[AD-A210069] N89-28390

STRATEGIC DEFENSE INITIATIVE ORGANIZATION, WASHINGTON, DC.
The 1989 report to the Congress on the Strategic Defense Initiative
[PB89-196661] N89-28368

STUTTGART UNIV. (GERMANY, F.R.).
Cylindrical steady-state MPD thruster N89-27725
Nozzle type MPD thruster experimental investigations N89-27727
Numerical codes for cylindrical MPD thrusters N89-27733
An improved code for nozzle type steady state MPD thrusters N89-27735
Investigation of instabilities in MPD thruster flows using a linear diapersion relation N89-27737
Performance calculation of an H2 arcjet by means of a dual channel model N89-27775
A 15 kW experimental arcjet N89-27778
Steady state MPD devices for reentry simulation N89-27783

SVERDRUP TECHNOLOGY, INC., CLEVELAND, OH.
Stability robustness improvement of direct eigenspace assignment based feedback systems using singular value sensitivities
[NASA-CR-182302] N89-27672
Antiproton powered propulsion with magnetically confined plasma engines
[NASA-CR-185131] N89-27700

SYRACUSE UNIV., NY.
Northeast Artificial Intelligence Consortium annual report for 1987. Volume 4: Research in automated photointerpretation
[AD-A208610] N89-28336

T

TECHNISCHE UNIV., BERLIN (GERMANY, F.R.).
Production of satellite image maps from TM data N89-28089

TECHNISCHE UNIV., MUNICH (GERMANY, F.R.).
Applicability of LANDSAT TM data for geoscientific purposes in Iceland N89-28068

TECHNISCHE UNIV., VIENNA (AUSTRIA).
Field emission electric propulsion: Emission of slit-type liquid metal ion sources N89-27723

TELESAT MOBILE, INC., OTTAWA (ONTARIO).
Practical constraints on network architecture and signalling in the MSAT system N89-27915

TEXAS A&M UNIV., COLLEGE STATION.
KREM: A model for evaluating orbital transfer vehicles utilizing nuclear electric propulsion systems N89-27789
Ultrasonic nondestructive evaluation of damage in continuous fiber composites
[AD-A208840] N89-27799
Dynamic fracture and deformation of solid propellant
[AD-A208691] N89-27865

TEXAS TECHNOLOGICAL UNIV., LUBBOCK.
Novel approaches to ionic chromatography
[DE89-013942] N89-27805

TEXAS UNIV., AUSTIN.
Electronics research at the University of Texas at Austin
[AD-A209989] N89-27970
Reflection and refraction of finite amplitude acoustic waves at a fluid-fluid interface
[AD-A209800] N89-28371

TOKYO UNIV. (JAPAN).
Optimization of current distribution in an applied-field MPD thruster N89-27743
Discharge plasma calculations in cusped ion thrusters using the finite element method N89-27760
A very low reflectance diffuse surface for thermal design of spacecraft N89-28289

TOKYO UNIV., SAGAMIHARA (JAPAN).
Electric propulsion projects and research in Japan N89-27709
Development of an MPD propulsion system N89-27718
Interaction of high voltage solar array with ionospheric plasma N89-27719
Quantitative imaging of MPD flow fields N89-27766
Micro-fluid dynamical analysis of evaporating flows in heat pipes N89-28228

TOKYO UNIV., TANASHI (JAPAN).
Lasertron: A pulsed RF-source using laser triggered photocathode
[DE89-778130] N89-28008

TOSHIBA CORP., KAWASAKI (JAPAN).
Experimental study of double stage discharge Hall ion thruster N89-27763
A 30 cm diameter xenon ion thruster: Design and initial test results N89-27768

TRANSIT COMMUNICATIONS, INC., PASADENA, CA.
The AMSC mobile satellite system: Design summary and comparative analysis N89-27908

TRINITY COLL., DUBLIN (IRELAND).
The use of Thematic Mapper imagery for peatland mapping and mineral exploration in Ireland N89-28065

TROMSOE UNIV. (NORWAY).
Mapping winter grazing areas for reindeer on Svalbard using LANDSAT Thematic Mapper data N89-28075
Use of remote sensing in mapping of vegetation in the Dividalen area central Troms, northern Norway N89-28083

U

UNITED KINGDOM ATOMIC ENERGY AUTHORITY, CULHAM (ENGLAND).
High thrust operation of the UK-10 rare gas ion thruster (T4A) N89-27747
Ultimate performance limits and mission capabilities of advanced ion thrusters N89-27764
Propellant selection criteria for deep space electrically propelled missions N89-27769
Optical emission spectrum of the UK-10 ion thruster operating on xenon N89-27781

UNITED KINGDOM ATOMIC ENERGY AUTHORITY, RISLEY (ENGLAND).
Advanced tribological coatings for high specific strength alloys
[AD-A208504] N89-27825

UNIVERSAL ENERGY SYSTEMS, INC., DAYTON, OH.
Anthropometric measurements of aviators within the Aviation Epidemiology Data Register
[AD-A208609] N89-28300
United States Air Force Research Initiation Program for 1987, volume 1
[AD-A209726] N89-28436
United States Air Force Research Initiation Program for 1987, volume 3
[AD-A209728] N89-28437
United States Air Force Research Initiation Program for 1987, volume 4
[AD-A209729] N89-28438

UNIVERSITE CATHOLIQUE DE LOUVAIN (BELGIUM).
Evaluation of the LANDSAT TM satellite in urban media: Application to the case of Brussels, Belgium N89-28073

UNIVERSITY COLL., DUBLIN (IRELAND).
Utility of Thematic Mapper data for national survey of Irish lakes N89-28058
Use of satellite imagery for the investigation of pollution-related characteristics of Dublin Bay, Ireland N89-28063

UNIVERSITY COLL. OF NORTH WALES, BANGOR.
Piezoelectric polymer/ceramic composite
[AD-A208905] N89-27801

UNIVERSITY COLL. OF WALES, ABERYSTWYTH.
Vibrationally excited ions: Quenching, reaction and lifetimes
[AD-A208503] N89-28386

UNIVERSITY OF SOUTHERN CALIFORNIA, LOS ANGELES.
Studies of unsteady vortex flap aerodynamics
[AD-A209837] N89-27641
New, efficient optically pumped solid state lasers
[AD-A209998] N89-28013
Basic research in reliability for real systems
[AD-A209649] N89-28022
Integrated opto-electronic computing
[AD-A209936] N89-28395

UNIVERSITY OF SOUTHERN MISSISSIPPI, HATTIESBURG.
Photodegradation of polyimide 1. A spectral, viscometric, chromatographic and weight loss investigation of polyimides based on a perfluorinated dianhydride
[AD-A208507] N89-27845
Characterization of nylon 6 by 15N solid state NMR
[AD-A208508] N89-27846

UTAH UNIV., SALT LAKE CITY.
Quantitative estimation of component amplitude in multiexponential data: Application to time-resolved fluorescence spectroscopy
[AD-A210142] N89-27815
Modified rotationally adiabatic model for rotational autoionization of dipole-bound molecular anions
[AD-A209851] N89-28388
Studies of the cosmic ray penumbra
[AD-A210109] N89-28484

V

VANDERBILT UNIV., NASHVILLE, TN.
Claw-free maximal planar graphs
[AD-A210179] N89-28359

VEXCELL CORP., BOULDER, CO.
A smart, mapping, charting and geodesy control generator, phase 2
[AD-A208806] N89-28097

VIBRATION INST., CLARENDON HILLS, IL.
The Shock and Vibration Digest, volume 21, no. 4 N89-28025

VIGYAN RESEARCH ASSOCIATES, INC., HAMPTON, VA.
Low density flow effects for hypervelocity vehicles
[AD-A208218] N89-27633

VON KARMAN INST. FOR FLUID DYNAMICS, RHODE-SAINT-GENESE (BELGIUM).
An Introduction to Computational Fluid Dynamics
[VKI-LS-1989-02] N89-27985
Boundary layer equations and methods of solution N89-27987

W

WESTINGHOUSE ELECTRIC CORP., BALTIMORE, MD.
Avionic system requirements N89-27652

WESTINGHOUSE ELECTRIC CORP., PITTSBURGH, PA.
Bibliography of high-T sub c superconducting films
[DE89-013395] N89-28409

WISCONSIN UNIV., MADISON.
Selective detector for gas chromatography based on adduct-modulated semiconductor photoluminescence
[AD-A208616] N89-27808
Some problems in nonlinear analysis
[AD-A209991] N89-28357
Semiconductor-olefin adducts. Photoluminescent properties of cadmium sulfide and cadmium selenide in the presence of butenes
[AD-A208348] N89-28419

WORCESTER POLYTECHNIC INST., MA.
Evidence flow graph methods for validation and verification of expert systems
[NASA-CR-181810] N89-28328

WYOMING UNIV., LARAMIE.
The quartz crystal microbalance as an in situ tool in electrochemistry
[AD-A209852] N89-27811
Applications of the quartz crystal microbalance to electrochemistry
[AD-A209853] N89-27812

Typical Contract Number Index Listing

Listings in this index are arranged alphanumerically by contract number. Under each contract number the NASA accession numbers denoting documents that have been produced as a result of research done under that contract are arranged in ascending order. The NASA accession number denotes the number by which the citation is identified.

AF PROJ. 1900 ..... N89-27686
AF PROJ. 2068 ..... N89-28349
AF PROJ. 2104 ..... N89-27678
AF PROJ. 2301 ..... N89-27944
N89-28013
N89-28372
N89-28386
N89-28430
AF PROJ. 2302 ..... N89-28043
AF PROJ. 2303 ..... N89-27814
N89-28427
AF PROJ. 2304 ..... N89-27952
N89-27971
N89-28022
N89-28023
N89-28024
N89-28040
N89-28041
N89-28042
N89-28319
N89-28335
N89-28336
N89-28337
N89-28346
N89-28347
N89-28348
N89-28350
N89-28357
N89-28362
AF PROJ. 2305 ..... N89-27949
N89-27966
N89-28395
N89-28428
AF PROJ. 2306 ..... N89-27800
N89-27826
AF PROJ. 2307 ..... N89-27641
N89-27802
N89-27991
AF PROJ. 2308 ..... N89-27799
N89-27807
N89-28102
AF PROJ. 2310 ..... N89-28196
AF PROJ. 2312 ..... N89-28204
N89-28323
AF PROJ. 2313 ..... N89-28203
N89-28205
N89-28206
N89-28210
N89-28301
N89-28325
AF PROJ. 3005 ..... N89-28421
AF PROJ. 5581 ..... N89-28334
AF PROJ. 6670 ..... N89-28116
AF PROJ. 7601 ..... N89-27691
AF-AFOSR-0019-86 ..... N89-27734
AF-AFOSR-0031-88 ..... N89-28350
AF-AFOSR-0046-86 ..... N89-27944
AF-AFOSR-0048-84 ..... N89-27771
N89-27772
N89-28102
AF-AFOSR-0050-87 ..... N89-28362
AF-AFOSR-0051-84 ..... N89-28041
AF-AFOSR-0053-86 ..... N89-28196
AF-AFOSR-0062-86 ..... N89-28323
AF-AFOSR-0066-84 ..... N89-27799
AF-AFOSR-0093-86 ..... N89-28319
AF-AFOSR-0097-88 ..... N89-27800
AF-AFOSR-0107-86 ..... N89-28427
AF-AFOSR-0109-88 ..... N89-28430
AF-AFOSR-0117-87 ..... N89-28348
AF-AFOSR-0117-88 ..... N89-28341
AF-AFOSR-0122-88 ..... N89-28386
AF-AFOSR-0162-86 ..... N89-28042
AF-AFOSR-0171-88 ..... N89-28203
AF-AFOSR-0179-87 ..... N89-27971
AF-AFOSR-0180-87 ..... N89-28206
AF-AFOSR-0182-88 ..... N89-28040
AF-AFOSR-0189-87 ..... N89-28204
AF-AFOSR-0200-86 ..... N89-27814
AF-AFOSR-0202-87 ..... N89-28357
AF-AFOSR-0204-85 ..... N89-28428
AF-AFOSR-0211-88 ..... N89-28395
AF-AFOSR-0228-83 ..... N89-27952
AF-AFOSR-0234-85 ..... N89-27949
AF-AFOSR-0242-85 ..... N89-27826
AF-AFOSR-0261-84 ..... N89-28372
AF-AFOSR-0269-84 ..... N89-28022
AF-AFOSR-0271-85 ..... N89-28347
AF-AFOSR-0278-86 ..... N89-27753
AF-AFOSR-0318-85 ..... N89-27641
AF-AFOSR-0320-85 ..... N89-28023
AF-AFOSR-0332-85 ..... N89-27966
AF-AFOSR-0333-85 ..... N89-27830
AF-AFOSR-0334-86 ..... N89-28205
AF-AFOSR-0335-85 ..... N89-27753
AF-AFOSR-0337-86 ..... N89-27733
N89-27735
AF-AFOSR-0340-84 ..... N89-28024
AF-AFOSR-0341-85 ..... N89-28325
AF-AFOSR-0350-87 ..... N89-28335
AF-AFOSR-0360-85 ..... N89-28337
AF-AFOSR-0362-85 ..... N89-28043
AF-AFOSR-0370-85 ..... N89-28301
AF-AFOSR-0378-84 ..... N89-28013
AF-AFOSR-0398-84 ..... N89-28346
AF-AFOSR-3403-77 ..... N89-27802
AIRTASK-A540-5402 ..... N89-27948
AMD-BA-ROC-1/87(BEH-2001) N89-27783
BMWF-37.007/1-25/85 ..... N89-28078
CNES-87/CNES/3315 ..... N89-27783
DA PROJ. 1L1-61101-A-91-A N89-27866
DA PROJ. 1L1-61103-BH-57 ..... N89-27797
N89-27801
DA PROJ. 1L1-62120-AH-25 ..... N89-27869
DA PROJ. 1L1-62209-A-47-A N89-28015
DA PROJ. 3E1-62787-A-878 ..... N89-28298
N89-28300
DAAA01-88-C-0414 ..... N89-27809
DAAA21-89-C-0002 ..... N89-28019
DAAG29-85-K-0218 ..... N89-28046
DAAK11-82-C-0158 ..... N89-28002
DAAL03-86-D-0001 ..... N89-27869
DAAL03-86-K-0006 ..... N89-28397
DAAL03-86-K-0032 ..... N89-27861
DAAL03-87-K-0002 ..... N89-27649
DAAL03-87-K-0005 ..... N89-27858
N89-27921
DAAL03-88-C-0007 ..... N89-27969
DAAL03-88-K-0058 ..... N89-27964
DACA72-87-C-0011 ..... N89-28097
DACA76-85-C-0010 ..... N89-28363
DAJA45-86-C-0034 ..... N89-27801
DAJA45-86-C-0058 ..... N89-27797
DAJA45-87-C-0008 ..... N89-27827
DAJA45-87-C-0050 ..... N89-27823
DAJA45-89-C-0044 ..... N89-27825
DASG60-86-C-0075 ..... N89-27994
DE-AC02-76CH-00016 ..... N89-28107
N89-28411
DE-AC02-81EV-10665 ..... N89-28196
DE-AC02-83CH-10093 ..... N89-28099
N89-28100
DE-AC02-87ER-40372 ..... N89-27997
DE-AC03-76SF-00098 ..... N89-27956
N89-28005
N89-28409
DE-AC04-76DP-00789 ..... N89-27642
N89-27834
N89-27924
N89-27925
N89-27955
N89-27957
N89-28032
N89-28038
N89-28039
N89-28412
N89-28414
N89-28432
DE-AC05-84OR-21400 ..... N89-27837
N89-28031
N89-28393
N89-28478
DE-AC05-84OT-21400 ..... N89-28308
DE-AC06-76RL-01830 ..... N89-27806
DE-AC06-76RL-01857 ..... N89-27837
DE-AC09-76SR-00001 ..... N89-27983
DE-AI03-79DP-40092 ..... N89-28003
DE-AS05-78ET-52025 ..... N89-28402
DE-FG02-85ER-45182 ..... N89-27816
DE-FG02-85ER-45211 ..... N89-28408
DE-FG02-86ER-13569 ..... N89-27804
DE-FG02-86ER-13582 ..... N89-28433
DE-FG02-86ER-13599 ..... N89-27835
DE-FG02-86ER-45262 ..... N89-27820
DE-FG02-86ER-45263 ..... N89-27820
DE-FG02-87ER-45310 ..... N89-28407
DE-FG02-87ER-45311 ..... N89-27817
DE-FG03-84ER-45085 ..... N89-28413
DE-FG03-87ER-25028 ..... N89-28320
N89-28352
DE-FG05-84ER-13281 ..... N89-27805
DE-FG05-87ER-13782 ..... N89-27996
DE-FG22-87BC-14152 ..... N89-27976
DNA001-84-C-0196 ..... N89-27972
DTFA01-84-C-00023 ..... N89-27673
DTFA01-89-C-00001 ..... N89-27645
N89-27646
DTFA03-86-C-00005 ..... N89-27643
ESA-7300/87/F/RD(SC) N89-27943
ESTEC-5456/83/NL/DG N89-28297
ESTEC-6324/85/NL/PB(SC) N89-28236
ESTEC-6497/85 ..... N89-27937
N89-27938
ESTEC-6545/85 ..... N89-27723
ESTEC-6784/86/NL/PH(SC) N89-27775
FWF-P6005 ..... N89-28346
FWF-S3206 ..... N89-28346
F04611-88-X-0021 ..... N89-27793
F04701-88-C-0089 ..... N89-27992
F08635-84-C-0295 ..... N89-28349
F08635-85-C-0122 ..... N89-27686
F19628-81-K-0020 ..... N89-28484
F19628-85-C-0002 ..... N89-27946
N89-28209
N89-28356
N89-28426
N89-28431
F19628-85-C-0007 ..... N89-28116
F19628-85-C-0073 ..... N89-28479
F19628-85-C-0178 ..... N89-28112
F19628-85-K-0004 ..... N89-27950
F19628-86-K-0009 ..... N89-27681
N89-27692
F19628-86-K-0016 ..... N89-28095
F19628-86-K-0028. ..... N89-28096
F19628-87-C-0230 ..... N89-27951
F19628-87-K-0008 ..... N89-27691
F19628-88-C-0151 ..... N89-28098
N89-28396
F30602-81-C-0169 ..... N89-28332
F30602-85-C-0008 ..... N89-28334
N89-28336
F33615-81-C-3617 ..... N89-27685
F33615-82-C-2233 ..... N89-27954
F33615-84-C-0066 ..... N89-27679
F33615-85-C-3205 ..... N89-28354
F33615-85-C-5091 ..... N89-27832

F33615-86-C-3009 ..... N89-27633
F33615-87-C-0012 ..... N89-27679
F49620-85-C-0013 ..... N89-28436
N89-28437
N89-28438
F49620-85-C-0108 ..... N89-27991
F49620-85-C-0144 ..... N89-28364
F49620-86-C-0018 ..... N89-27829
F49620-86-C-0045 ..... N89-27970
F49620-86-C-0055 ..... N89-28101
F49620-86-C-0111 ..... N89-28346
N89-28351
F49620-86-C-0141 ..... N89-28210
F49620-87-C-0014 ..... N89-28421
F49620-88-C-0101 ..... N89-28404
F49620-88-K-0003 ..... N89-27807
F49620-88-K-0004 ..... N89-28207
N89-28208
N89-28210
MDA903-81-C-0443 ..... N89-28299
MDA903-85-C-0347 ..... N89-28302
MDA903-88-C-0020 ..... N89-27635
MDA908-87-C-3056 ..... N89-28394
MDA972-88-K-0008 ..... N89-27839
MIPR-88-526 ..... N89-28111
MOD-GR/E/07186 ..... N89-27787
NAGW-76 ..... N89-28464
NAGW-630 ..... N89-28471
NAGW-1129 ..... N89-28113
NAGW-1663 ..... N89-28054
NAG1-466 ..... N89-28341
NAG1-517 ..... N89-28346
NAG1-809 ..... N89-28328
NAG1-949 ..... N89-28475
NAG2-480 ..... N89-28444
N89-28445
N89-28446
NAG2-542 ..... N89-27870
NAG3-305 ..... N89-27773
NAG3-984 ..... N89-27998
NAG5-374 ..... N89-28469
NAG5-536 ..... N89-28054
NAG5-613 ..... N89-28476
NAG5-722 ..... N89-28466
NAG5-728 ..... N89-28464
NAG5-780 ..... N89-28016
NAG5-1124 ..... N89-28017
NAG9-106 ..... N89-28107
NAG9-117 ..... N89-28211
N89-28212
N89-28213
NAG9-257 ..... N89-28107
NAG9-310 ..... N89-27979
NASW-3165 ..... N89-28440
NAS1-17748 ..... N89-28115
NAS1-18000 ..... N89-28004
NAS1-18107 ..... N89-28341
N89-28342
NAS1-18288 ..... N89-27818
NAS1-18377 ..... N89-27647
N89-27648
NAS1-18599 ..... N89-27978
NAS1-18605 ..... N89-27977
N89-28341
N89-28342
NAS3-25266 ..... N89-27672
N89-27700
NAS5-28738 ..... N89-28047
NAS5-30282 ..... N89-27994
NAS7-918 ..... N89-27907
N89-28454
N89-28467
NAS8-30490 ..... N89-27698
N89-27864
NAS8-37282 ..... N89-27693
N89-27694
N89-27695
N89-27696
N89-27697
NAS9-54997 ..... N89-27736
NCC1-47 ..... N89-27674
NCC2-408 ..... N89-28309
NGR-05-002-160 ..... N89-28466
N89-28467
NGR-06-002-112 ..... N89-27748
N89-27761
NOAA-NA86AA-D-SG089 ..... N89-28053
NR PROJ. 042-267 ..... N89-28353
NR PROJ. 356-856 ..... N89-27824
N89-27840
NR PROJ. 372-160 ..... N89-28387
NR PROJ. 625-826 ..... N89-27843
N89-27844
NR PROJ. 625-856 ..... N89-27842
NR PROJ. 631-618 ..... N89-27841
NSF ATM-83-05537 ..... N89-28459
NSF ATM-83-18676 ..... N89-28196
NSF ATM-85-05558 ..... N89-28196
NSF ATM-85-13363 ..... N89-28464
NSF ATM-86-03192 ..... N89-28459
NSF ATM-87-12020 ..... N89-28196
NSF ATM-87-19865 ..... N89-28196
NSF CDR-86-22236 ..... N89-28392
NSF CHE-84-06078 ..... N89-28420
NSF CHE-88-14765 ..... N89-28388
NSF DMC-86-17355 ..... N89-28326
NSF DMR-88-03184 ..... N89-28423
NSF DMS-86-17355 ..... N89-28021
NSF DMS-88-00589 ..... N89-28320
N89-28352
NSF EAR-83-13683 ..... N89-28107
NSF MIP-87-17714 ..... N89-27964
NSF MSM-84-51074 ..... N89-28021
NSF UINT-85-21208 ..... N89-28346
N00014-81-K-0004 ..... N89-28340
N00014-81-K-0526 ..... N89-27813
N00014-82-K-0520 ..... N89-28020
N00014-82-K-0576 ..... N89-27803
N00014-83-K-0498 ..... N89-27810
N89-27855
N89-27856
N00014-83-K-0577 ..... N89-27968
N00014-84-C-0149 ..... N89-27953
N89-27967
N00014-84-C-0212 ..... N89-27922
N00014-84-K-0021 ..... N89-27798
N00014-84-K-0052 ..... N89-27965
N00014-84-K-0267 ..... N89-28117
N00014-84-K-0548 ..... N89-28387
N00014-84-K-0574 ..... N89-28371
N00014-85-C-0219 ..... N89-28391
N00014-85-C-0419 ..... N89-27638
N89-27676
N00014-85-K-0124 ..... N89-28363
N00014-85-K-0177 ..... N89-28423
N00014-85-K-0213 ..... N89-27838
N89-27839
N00014-85-K-0488 ..... N89-28359
N00014-85-K-0559 ..... N89-28338
N00014-85-K-0570 ..... N89-28327
N00014-85-K-0631 ..... N89-27808
N89-28419
N00014-85-K-0632 ..... N89-27842
N89-27843
N89-27844
N89-27854
N89-28420
N00014-85-K-0645 ..... N89-27841
N00014-85-K-0898 ..... N89-27824
N89-27840
N00014-86-K-0043 ..... N89-28389
N89-28390
N00014-86-K-0156 ..... N89-28353
N00014-86-K-0234 ..... N89-28424
N00014-86-K-0281 ..... N89-28021
N89-28326
N00014-86-K-0298 ..... N89-27865
N00014-86-K-0530 ..... N89-28429
N00014-86-K-0685 ..... N89-28018
N89-28324
N89-28363
N00014-86-K-0728 ..... N89-28195
N00014-86-K-0768 ..... N89-27852
N89-28425
N00014-86-K-0799 ..... N89-28032
N00014-87-G-0119 ..... N89-27725
N89-27733
N89-27735
N00014-87-K-0277 ..... N89-28360
N00014-87-K-0384 ..... N89-28355
N00014-87-K-0426 ..... N89-27848
N89-27849
N00014-87-K-0738 ..... N89-27862
N00014-87-K-0825 ..... N89-28316
N89-28317
N00014-87-M-0258 ..... N89-27945
N00014-88-C-0512 ..... N89-27847
N00014-88-C-0611 ..... N89-28010
N00014-88-C-2033 ..... N89-28012
N00014-88-F-0019 ..... N89-28410
N00014-88-K-0060 ..... N89-28198
N00014-88-K-0366 ..... N89-27857
N89-27860
N00014-88-K-0447 ..... N89-27993
N00014-88-K-0591 ..... N89-28021
N89-28326
N00014-88-K-0620 ..... N89-28019
N00014-88-K-2007 ..... N89-28106
N00014-89-J-1028 ..... N89-27845
N00014-89-J-1070 ..... N89-27964
N00014-89-J-1109 ..... N89-28371
N00014-89-J-1225 ..... N89-27846
N00014-89-J-1272 ..... N89-28338
N00014-89-J-1319 ..... N89-27639
N00014-89-J-1412 ..... N89-27815
N00014-89-J-1497 ..... N89-28388
N00014-89-J-1659 ..... N89-28320
N89-28352
N00014-89-J-1828 ..... N89-27850
N89-27851
N00014-89-K-0674 ..... N89-27811
N89-27812
N60530-83-C-0186 ..... N89-27640
PROJ. SE-0-135 ..... N89-28306
N89-28307
RR04024 ..... N89-28360
SNIA-BPD-DSR/DHG/74777/LS N89-27778
SNL-75-8962 ..... N89-28032
W-31-109-ENG-38 ..... N89-27821
N89-27866
N89-27981
N89-27982
N89-27984
N89-28410
N89-28415
W-7405-ENG-36 ..... N89-27863
N89-27958
N89-27959
N89-27960
N89-27961
N89-27975
N89-28007
N89-28054
N89-28199
N89-28315
N89-28366
N89-28367
N89-28403
N89-28434
N89-28435
W-7405-ENG-48 ..... N89-28000
N89-28006
N89-28009
N89-28105
N89-28108
N89-28443
N89-28447
N89-28453
N89-28477
199-80-02 ..... N89-28304
309-02-01-02 ..... N89-27979
324-02-00 ..... N89-27818
474-42-10 ..... N89-27702
505-60-21-06 ..... N89-27978
505-61-01-05 ..... N89-27995
505-62-01 ..... N89-27672
N89-27998
505-62-21 ..... N89-27923
N89-27980
505-62-71-01 ..... N89-27634
505-63-1B N89-28029
N89-28036
505-63-01-07 ..... N89-28314
505-63-11 ..... N89-27795
505-63-51 ..... N89-28015
505-66-21-01 ..... N89-28328
505-66-21-04 ..... N89-28115
505-69-01-01 ..... N89-27647
N89-27648
505-80-21 ..... N89-27670
505-90-21-01 ..... N89-27977
N89-28341
N89-28342
506-40-21-01 ..... N89-28035
506-41-11 ..... N89-27705
N89-27868
506-41-41 ..... N89-27704
506-41-42 ..... N89-27836
506-42-31 ..... N89-27701
N89-27703
N89-27706
506-42-41 ..... N89-27700
506-43-81 ..... N89-28034
506-44-21-01 ..... N89-28004
506-46-21-01 ..... N89-27671
553-13 ..... N89-28030
582-01-11 ..... N89-27999
586-01-11 ..... N89-27796
643-10-01 ..... N89-27927
650-60-15-01 ..... N89-27907
928-10-01 ..... N89-27687
992-15 ..... N89-27979

Typical Report Number Index Listing

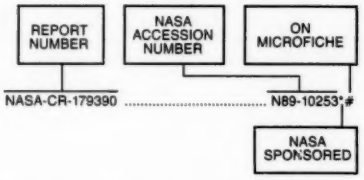

Listings in this index are arranged alphanumerically by report number. The NASA accession number denotes the number by which the citation is identified. An asterisk (*) indicates that the item is a NASA report. A pound sign (#) indicates that the item is available on microfiche.

A-87160 ..... N89-28304* #

AAMRL-TR-89-011 ..... N89-28200 #

ACT-107 ..... N89-28327 #

AD-A206218 ..... N89-27633 #
AD-A206219 ..... N89-28391 #
AD-A206252 ..... N89-28106 #
AD-A206265 ..... N89-27869 #
AD-A206841 ..... N89-28195 #
AD-A206916 ..... N89-27682 #
AD-A207185 ..... N89-28372 #
AD-A207286 ..... N89-27973 #
AD-A207288 ..... N89-27832 #
AD-A207292 ..... N89-28014 #
AD-A207294 ..... N89-28329 #
AD-A207297 ..... N89-28002 #
AD-A207299 ..... N89-27635 #
AD-A207301 ..... N89-28360 #
AD-A207324 ..... N89-27803 #
AD-A207332 ..... N89-27954 #
AD-A207334 ..... N89-28449 #
AD-A207346 ..... N89-27867 #
AD-A207347 ..... N89-28452 #
AD-A207350 ..... N89-28365 #
AD-A207356 ..... N89-27919 #
AD-A207357 ..... N89-28310 #
AD-A207358 ..... N89-27920 #
AD-A207365 ..... N89-27833 #
AD-A207367 ..... N89-27699 #
AD-A207371 ..... N89-28369 #
AD-A207374 ..... N89-27974 #
AD-A207376 ..... N89-28028 #
AD-A207377 ..... N89-28370 #
AD-A207378 ..... N89-28361 #
AD-A207380 ..... N89-28442 #
AD-A207387 ..... N89-27921 #
AD-A207388 ..... N89-27922 #
AD-A207392 ..... N89-27659 #
AD-A207583 ..... N89-27636 #
AD-A208299 ..... N89-28298 #
AD-A208321 ..... N89-27838 #
AD-A208322 ..... N89-28316 #
AD-A208326 ..... N89-27823 #
AD-A208348 ..... N89-28419 #
AD-A208373 ..... N89-27839 #
AD-A208374 ..... N89-28317 #
AD-A208377 ..... N89-28196 #
AD-A208380 ..... N89-28334 #
AD-A208381 ..... N89-27962 #
AD-A208384 ..... N89-28420 #
AD-A208385 ..... N89-27840 #
AD-A208386 ..... N89-27824 #
AD-A208435 ..... N89-28299 #
AD-A208436 ..... N89-27797 #
AD-A208437 ..... N89-27841 #
AD-A208438 ..... N89-27842 #
AD-A208439 ..... N89-27843 #
AD-A208440 ..... N89-27844 #
AD-A208503 ..... N89-28386 #
AD-A208504 ..... N89-27825 #
AD-A208507 ..... N89-27845 #
AD-A208508 ..... N89-27846 #
AD-A208512 ..... N89-27675 #
AD-A208520 ..... N89-28330 #
AD-A208523 ..... N89-27798 #
AD-A208534 ..... N89-28331 #
AD-A208539 ..... N89-27676 #
AD-A208555 ..... N89-28318 #
AD-A208564 ..... N89-27963 #
AD-A208567 ..... N89-28346 #
AD-A208570 ..... N89-28335 #
AD-A208572 ..... N89-28347 #
AD-A208576 ..... N89-27807 #
AD-A208589 ..... N89-28040 #
AD-A208590 ..... N89-28348 #
AD-A208598 ..... N89-27847 #
AD-A208600 ..... N89-28394 #
AD-A208601 ..... N89-27964 #
AD-A208609 ..... N89-28300 #
AD-A208610 ..... N89-28336 #
AD-A208612 ..... N89-28349 #
AD-A208616 ..... N89-27808 #
AD-A208618 ..... N89-28319 #
AD-A208624 ..... N89-27991 #
AD-A208627 ..... N89-28337 #
AD-A208628 ..... N89-28041 #
AD-A208629 ..... N89-28010 #
AD-A208632 ..... N89-28421 #
AD-A208633 ..... N89-28350 #
AD-A208634 ..... N89-28362 #
AD-A208635 ..... N89-28042 #
AD-A208651 ..... N89-27660 #
AD-A208657 ..... N89-28101 #
AD-A208658 ..... N89-28351 #
AD-A208662 ..... N89-27965 #
AD-A208664 ..... N89-27944 #
AD-A208671 ..... N89-27632 #
AD-A208677 ..... N89-27848 #
AD-A208678 ..... N89-28095 #
AD-A208686 ..... N89-27966 #
AD-A208689 ..... N89-28338 #
AD-A208690 ..... N89-27638 #
AD-A208691 ..... N89-27865 #
AD-A208692 ..... N89-27849 #
AD-A208695 ..... N89-28301 #
AD-A208710 ..... N89-28109 #
AD-A208711 ..... N89-28096 #
AD-A208712 ..... N89-27691 #
AD-A208713 ..... N89-28116 #
AD-A208714 ..... N89-27826 #
AD-A208717 ..... N89-28043 #
AD-A208723 ..... N89-28422 #
AD-A208725 ..... N89-28320 #
AD-A208727 ..... N89-28423 #
AD-A208740 ..... N89-27793 #
AD-A208760 ..... N89-28479 #
AD-A208782 ..... N89-27850 #
AD-A208796 ..... N89-28352 #
AD-A208797 ..... N89-28353 #
AD-A208804 ..... N89-27827 #
AD-A208806 ..... N89-28097 #
AD-A208808 ..... N89-28354 #
AD-A208809 ..... N89-28332 #
AD-A208811 ..... N89-28321 #
AD-A208813 ..... N89-27686 #
AD-A208821 ..... N89-27851 #
AD-A208840 ..... N89-27799 #
AD-A208846 ..... N89-28200 #
AD-A208850 ..... N89-27945 #
AD-A208854 ..... N89-27852 #
AD-A208863 ..... N89-27809 #
AD-A208873 ..... N89-27800 #
AD-A208878 ..... N89-28044 #
AD-A208895 ..... N89-28424 #
AD-A208902 ..... N89-28425 #
AD-A208905 ..... N89-27801 #
AD-A208910 ..... N89-27677 #
AD-A208911 ..... N89-27678 #
AD-A209612 ..... N89-27853 #
AD-A209614 ..... N89-28201 #
AD-A209615 ..... N89-28202 #
AD-A209634 ..... N89-27854 #
AD-A209635 ..... N89-28018 #
AD-A209638 ..... N89-28110 #
AD-A209645 ..... N89-28426 #
AD-A209646 ..... N89-27946 #
AD-A209649 ..... N89-28022 #
AD-A209650 ..... N89-28198 #
AD-A209657 ..... N89-28102 #
AD-A209689 ..... N89-27992 #
AD-A209690 ..... N89-28363 #
AD-A209695 ..... N89-27828 #
AD-A209703 ..... N89-27639 #
AD-A209720 ..... N89-28480 #
AD-A209721 ..... N89-28481 #
AD-A209722 ..... N89-28482 #
AD-A209723 ..... N89-28483 #
AD-A209726 ..... N89-28436 #
AD-A209728 ..... N89-28437 #
AD-A209729 ..... N89-28438 #
AD-A209737 ..... N89-27947 #
AD-A209741 ..... N89-28045 #
AD-A209756 ..... N89-27679 #
AD-A209786 ..... N89-28001 #
AD-A209787 ..... N89-27686 #
AD-A209788 ..... N89-27640 #
AD-A209789 ..... N89-27948 #
AD-A209800 ..... N89-28371 #
AD-A209802 ..... N89-28011 #
AD-A209804 ..... N89-27649 #
AD-A209805 ..... N89-27644 #
AD-A209817 ..... N89-28203 #
AD-A209818 ..... N89-27855 #
AD-A209819 ..... N89-27810 #
AD-A209821 ..... N89-27856 #
AD-A209822 ..... N89-27993 #
AD-A209827 ..... N89-27802 #
AD-A209833 ..... N89-28427 #
AD-A209834 ..... N89-28204 #
AD-A209836 ..... N89-28428 #
AD-A209837 ..... N89-27641 #
AD-A209838 ..... N89-28205 #
AD-A209845 ..... N89-28322 #
AD-A209848 ..... N89-27967 #
AD-A209850 ..... N89-28387 #
AD-A209851 ..... N89-28388 #
AD-A209852 ..... N89-27811 #
AD-A209853 ..... N89-27812 #
AD-A209855 ..... N89-28323 #
AD-A209856 ..... N89-27949 #
AD-A209873 ..... N89-27857 #
AD-A209874 ..... N89-28429 #
AD-A209880 ..... N89-28023 #
AD-A209884 ..... N89-28206 #
AD-A209890 ..... N89-28019 #
AD-A209900 ..... N89-28324 #
AD-A209901 ..... N89-27968 #
AD-A209911 ..... N89-27813 #
AD-A209913 ..... N89-28012 #
AD-A209917 ..... N89-28207 #
AD-A209918 ..... N89-28208 #
AD-A209924 ..... N89-28430 #
AD-A209934 ..... N89-27829 #
AD-A209935 ..... N89-28364 #
AD-A209936 ..... N89-28395 #
AD-A209941 ..... N89-28020 #
AD-A209942 ..... N89-28404 #
AD-A209944 ..... N89-27969 #
AD-A209946 ..... N89-28389 #
AD-A209948 ..... N89-28046 #
AD-A209950 ..... N89-28117 #
AD-A209951 ..... N89-28355 #
AD-A209954 ..... N89-27950 #
AD-A209955 ..... N89-28396 #
AD-A209956 ..... N89-28356 #
AD-A209958 ..... N89-27692 #
AD-A209968 ..... N89-28339 #
AD-A209969 ..... N89-28431 #
AD-A209970 ..... N89-28209 #
AD-A209972 ..... N89-27951 #
AD-A209974 ..... N89-27681 #
AD-A209975 ..... N89-28098 #
AD-A209976 ..... N89-27858 #
AD-A209989 ..... N89-27970 #
AD-A209991 ..... N89-28357 #

☆ U.S. GOVERNMENT PRINTING OFFICE: 1989— 261 - 275 / 00113

AD-A209992 ..... N89-27859 #
AD-A209993 ..... N89-28111 #
AD-A209998 ..... N89-28013 #
AD-A210005 ..... N89-28210 #
AD-A210006 ..... N89-27684 #
AD-A210009 ..... N89-28325 #
AD-A210011 ..... N89-27814 #
AD-A210012 ..... N89-28302 #
AD-A210052 ..... N89-28024 #
AD-A210054 ..... N89-27952 #
AD-A210056 ..... N89-27971 #
AD-A210069 ..... N89-28390 #
AD-A210073 ..... N89-27860 #
AD-A210109 ..... N89-28484 #
AD-A210110 ..... N89-28112 #
AD-A210116 ..... N89-28021 #
AD-A210117 ..... N89-28326 #
AD-A210118 ..... N89-28358 #
AD-A210123 ..... N89-28303 #
AD-A210127 ..... N89-28197 #
AD-A210128 ..... N89-27685 #
AD-A210134 ..... N89-27830 #
AD-A210142 ..... N89-27815 #
AD-A210144 ..... N89-28327 #
AD-A210145 ..... N89-27953 #
AD-A210150 ..... N89-27861 #
AD-A210153 ..... N89-28340 #
AD-A210165 ..... N89-27972 #
AD-A210170 ..... N89-28439 #
AD-A210171 ..... N89-27862 #
AD-A210175 ..... N89-28397 #
AD-A210179 ..... N89-28359 #

AD-E801892 ..... N89-28349 #
AD-E900851 ..... N89-27640 #
AD-E900865 ..... N89-27948 #
AD-E900879 ..... N89-27853 #
AD-E900902 ..... N89-28339 #
AD-E951363 ..... N89-28001 #
AD-E951367 ..... N89-27866 #

AFATL-TP-89-04 ..... N89-27636 #

AFATL-TR-88-156 ..... N89-28349 #

AFESC/ESL-TR-87-71 ..... N89-27686 #
AFESC/ESL-TR-88-48 ..... N89-27678 #

AFGL-ERP-1008 ..... N89-28109 #

AFGL-TR-88-0157 ..... N89-28109 #
AFGL-TR-88-0166 ..... N89-28112 #
AFGL-TR-88-0203 ..... N89-28484 #
AFGL-TR-88-0323 ..... N89-28098 #
AFGL-TR-88-0328 ..... N89-28116 #
AFGL-TR-88-0330 ..... N89-27951 #
AFGL-TR-89-0016 ..... N89-28095 #
AFGL-TR-89-0031 ..... N89-27692 #
AFGL-TR-89-0036 ..... N89-28479 #
AFGL-TR-89-0039 ..... N89-27681 #

AFHRL-TR-88-66 ..... N89-27679 #

AFOSR-87-2033TR ..... N89-27799 #
AFOSR-89-0329TR-VOL-1 ..... N89-28436 #
AFOSR-89-0473TR ..... N89-28372 #
AFOSR-89-0590TR ..... N89-28196 #
AFOSR-89-0618TR ..... N89-28335 #
AFOSR-89-0619TR ..... N89-28347 #
AFOSR-89-0620TR ..... N89-28421 #
AFOSR-89-0685TR ..... N89-27800 #
AFOSR-89-0688TR ..... N89-27826 #
AFOSR-89-0689TR ..... N89-27991 #
AFOSR-89-0697TR ..... N89-28351 #
AFOSR-89-0698TR ..... N89-28346 #
AFOSR-89-0700TR ..... N89-28362 #
AFOSR-89-0701TR ..... N89-28319 #
AFOSR-89-0702TR ..... N89-28350 #
AFOSR-89-0710TR ..... N89-27944 #
AFOSR-89-0711TR ..... N89-28101 #
AFOSR-89-0712TR ..... N89-27807 #
AFOSR-89-0716TR ..... N89-28043 #
AFOSR-89-0723TR ..... N89-28040 #
AFOSR-89-0724TR ..... N89-28337 #
AFOSR-89-0725TR ..... N89-28041 #
AFOSR-89-0726TR ..... N89-28042 #
AFOSR-89-0729TR ..... N89-28348 #
AFOSR-89-0730TR ..... N89-27966 #
AFOSR-89-0769TR ..... N89-28301 #
AFOSR-89-0772TR ..... N89-28023 #
AFOSR-89-0778TR ..... N89-27830 #
AFOSR-89-0783TR ..... N89-28022 #
AFOSR-89-0784TR ..... N89-28102 #
AFOSR-89-0800TR ..... N89-27970 #
AFOSR-89-0808TR ..... N89-28203 #
AFOSR-89-0815TR ..... N89-28206 #
AFOSR-89-0821TR ..... N89-27949 #
AFOSR-89-0831TR-VOL-3 ..... N89-28437 #
AFOSR-89-0832TR-VOL-4 ..... N89-28438 #
AFOSR-89-0840TR ..... N89-28404 #
AFOSR-89-0909TR ..... N89-27829 #
AFOSR-89-0910TR ..... N89-28395 #
AFOSR-89-0911TR ..... N89-28323 #
AFOSR-89-0913TR ..... N89-28364 #
AFOSR-89-0914TR ..... N89-27971 #
AFOSR-89-0915TR ..... N89-28024 #
AFOSR-89-0916TR ..... N89-27952 #
AFOSR-89-0918TR ..... N89-28357 #
AFOSR-89-0919TR ..... N89-28013 #
AFOSR-89-0925TR ..... N89-27814 #
AFOSR-89-0928TR ..... N89-28427 #
AFOSR-89-0930TR ..... N89-28204 #
AFOSR-89-0931TR ..... N89-28205 #
AFOSR-89-0933TR ..... N89-27641 #
AFOSR-89-0934TR ..... N89-28428 #
AFOSR-89-0956TR ..... N89-27802 #
AFOSR-89-0960TR ..... N89-28207 #
AFOSR-89-0961TR ..... N89-28208 #
AFOSR-89-0962TR ..... N89-28210 #
AFOSR-89-0978TR ..... N89-28325 #

AFWAL-TR-86-3091-VOL-2 ..... N89-27685 #
AFWAL-TR-88-2047 ..... N89-27954 #
AFWAL-TR-88-3114 ..... N89-28354 #
AFWAL-TR-88-4244 ..... N89-27832 #

AGARD-LS-164 ..... N89-27650 #
AGARD-LS-167 ..... N89-27661 #

AI-M-1062 ..... N89-28324 #
AI-M-1111 ..... N89-28363 #
AI-M-1115 ..... N89-28018 #

AIAA-89-2334 ..... N89-27700* #
AIAA-89-2355 ..... N89-27670* #
AIAA-89-2710 ..... N89-27701* #
AIAA-89-2719 ..... N89-27703* #
AIAA-89-2840 ..... N89-27706* #
AIAA-89-3071 ..... N89-28314* #

AMPC-028-036 ..... N89-28101 #
AMPC-033-038 ..... N89-28404 #

AMSMI/CR-RD-PR-89-1 ..... N89-27866 #

AMSMI/TR-RD-RE-89-2 ..... N89-28001 #

ANL/MCT-88/2 ..... N89-27984 #

ARI-RN-88-106 ..... N89-28302 #
ARI-RN-89-17 ..... N89-28299 #

ARL-TR-89-1 ..... N89-28371 #

ARO-22684.3-EG ..... N89-28046 #
ARO-23255.22-MS ..... N89-27861 #
ARO-23726.1-EG ..... N89-27649 #
ARO-24620.3-EG-UIR ..... N89-27921 #
ARO-24620.16-EG-UIR ..... N89-27858 #
ARO-26019.1-EL-SBI ..... N89-27969 #

ATC-HDQ/S/87-274 ..... N89-27945 #

AVSCOM-TR-89-C-002 ..... N89-28029* #
AVSCOM-TR-89-C-004 ..... N89-28015* #

BARC-1431 ..... N89-27822 #

BATT-TCN-87-116 ..... N89-27869 #

BC-SDAL-89-1 ..... N89-27691 #

BNL-42627 ..... N89-28107 #
BNL-42831 ..... N89-28411 #

BRL-MR-3740 ..... N89-27682 #

COI-SR-26 ..... N89-28098 #
COI-SR-31 ..... N89-28396 #

CONF-890423-11 ..... N89-28006 #
CONF-890604-12 ..... N89-27981 #
CONF-890627-2 ..... N89-27837 #
CONF-890631-23 ..... N89-27642 #
CONF-890665-7 ..... N89-27955 #
CONF-890665-29 ..... N89-27959 #
CONF-890692-13-REV-1 ..... N89-28108 #
CONF-890710-4 ..... N89-27961 #
CONF-890710-5 ..... N89-27958 #
CONF-890710-7 ..... N89-27960 #
CONF-890711-1 ..... N89-28007 #
CONF-890718-6 ..... N89-28414 #
CONF-890746-1 ..... N89-28412 #
CONF-890791-1 ..... N89-27924 #
CONF-890794-1 ..... N89-27982 #
CONF-890798-1-VUGRAPHS ..... N89-28435 #
CONF-890818-3 ..... N89-28039 #
CONF-890819-1 ..... N89-27983 #
CONF-890834-1 ..... N89-28315 #
CONF-890835-1 ..... N89-28038 #
CONF-8804256-1 ..... N89-27834 #
CONF-8810377-1 ..... N89-28410 #
CONF-8811188-1 ..... N89-27816 #
CONF-8902115-1 ..... N89-28054 #
CONF-8903111-4 ..... N89-28107 #
CONF-8903140-1 ..... N89-28415 #
CONF-8904107-7 ..... N89-28403 #
CONF-8904210-7 ..... N89-28447 #
CONF-8904216-3 ..... N89-28477 #
CONF-8904228-2 ..... N89-28005 #
CONF-8905107-4 ..... N89-28032 #
CONF-8905148-1 ..... N89-28411 #
CONF-8905157-1 ..... N89-28478 #
CONF-8905166-1 ..... N89-27806 #
CONF-8905168-1 ..... N89-27821 #
CONF-8906135-1 ..... N89-28031 #
CONF-8906147-1 ..... N89-28393 #
CONF-8906159-2 ..... N89-28199 #
CONF-8906164-1 ..... N89-28434 #
CONF-8906169-1 ..... N89-28009 #

CPS-89-007 ..... N89-27847 #

CRREL-SR-89-10 ..... N89-27677 #

CSG-101 ..... N89-27967 #

CU/ONR/2 ..... N89-27964 #

DE88-706000 ..... N89-28406 #
DE89-000898 ..... N89-28099 #
DE89-005320 ..... N89-27983 #
DE89-005457 ..... N89-28315 #
DE89-005595 ..... N89-28038 #
DE89-007034 ..... N89-28039 #
DE89-008752 ..... N89-27816 #
DE89-009323 ..... N89-27834 #
DE89-009427 ..... N89-28100 #
DE89-012232 ..... N89-28398 #
DE89-012259 ..... N89-27883 #
DE89-012260 ..... N89-28366 #
DE89-012518 ..... N89-27996 #
DE89-012620 ..... N89-28054 #
DE89-012642 ..... N89-27642 #
DE89-012680 ..... N89-27835 #
DE89-012726 ..... N89-28407 #
DE89-012794 ..... N89-28432 #
DE89-012805 ..... N89-27975 #
DE89-012810 ..... N89-28443 #
DE89-012826 ..... N89-28367 #
DE89-012839 ..... N89-27956 #
DE89-012936 ..... N89-28477 #
DE89-012949 ..... N89-27804 #
DE89-012954 ..... N89-28408 #
DE89-012961 ..... N89-28003 #
DE89-013002 ..... N89-28005 #
DE89-013029 ..... N89-28031 #
DE89-013043 ..... N89-28478 #
DE89-013074 ..... N89-27955 #
DE89-013118 ..... N89-27997 #
DE89-013122 ..... N89-27976 #
DE89-013186 ..... N89-28410 #
DE89-013266 ..... N89-27817 #
DE89-013282 ..... N89-27981 #
DE89-013395 ..... N89-28409 #
DE89-013426 ..... N89-27982 #
DE89-013451 ..... N89-27924 #
DE89-013551 ..... N89-28393 #
DE89-013568 ..... N89-28411 #
DE89-013803 ..... N89-27820 #
DE89-013884 ..... N89-27957 #
DE89-013907 ..... N89-27984 #
DE89-013921 ..... N89-28412 #
DE89-013935 ..... N89-28032 #
DE89-013942 ..... N89-27805 #
DE89-014032 ..... N89-28107 #
DE89-014043 ..... N89-28006 #
DE89-014049 ..... N89-28009 #
DE89-014086 ..... N89-27837 #
DE89-014092 ..... N89-28447 #
DE89-014103 ..... N89-28000 #
DE89-014109 ..... N89-28402 #
DE89-014228 ..... N89-28434 #
DE89-014230 ..... N89-27958 #
DE89-014252 ..... N89-28199 #
DE89-014259 ..... N89-27959 #
DE89-014268 ..... N89-28108 #
DE89-014272 ..... N89-28007 #

DE89-014274 ..... N89-27960 #
DE89-014276 ..... N89-28403 #
DE89-014284 ..... N89-27961 #
DE89-014286 ..... N89-28435 #
DE89-014302 ..... N89-28105 #
DE89-014320 ..... N89-28453 #
DE89-014465 ..... N89-27806 #
DE89-014535 ..... N89-28433 #
DE89-014537 ..... N89-28413 #
DE89-014550 ..... N89-28414 #
DE89-014578 ..... N89-27925 #
DE89-014635 ..... N89-27821 #
DE89-014676 ..... N89-28415 #
DE89-014831 ..... N89-28308 #
DE89-611892 ..... N89-28343 #
DE89-611895 ..... N89-28344 #
DE89-611896 ..... N89-28345 #
DE89-611932 ..... N89-27926 #
DE89-612190 ..... N89-28033 #
DE89-612191 ..... N89-28416 #
DE89-612214 ..... N89-28417 #
DE89-612518 ..... N89-28472 #
DE89-613235 ..... N89-27822 #
DE89-613399 ..... N89-28418 #
DE89-778051 ..... N89-28473 #
DE89-778069 ..... N89-27794 #
DE89-778130 ..... N89-28008 #

DGLR-PAPER-88-02 ..... N89-27707 #

DIA-DST-2700Z-007-89 ..... N89-28011 #

DNA-TR-88-221 ..... N89-27972 #

DODA-AR-005-679 ..... N89-28044 #

DOE/BC-14152/2 ..... N89-27976 #

DOE/ER-13281/5 ..... N89-27805 #
DOE/ER-13569/3 ..... N89-27804 #
DOE/ER-13582/T2 ..... N89-28433 #
DOE/ER-13599/T1 ..... N89-27835 #
DOE/ER-13782/3 ..... N89-27996 #
DOE/ER-40372/02 ..... N89-27997 #
DOE/ER-45085/T1 ..... N89-28413 #
DOE/ER-45211/13 ..... N89-28408 #
DOE/ER-45262/T1 ..... N89-27820 #
DOE/ER-45310/18 ..... N89-28407 #
DOE/ER-45311/2 ..... N89-27817 #

DOE/FE-0129 ..... N89-28398 #

DOT/FAA/CT-88/24 ..... N89-27643 #

DOT/FAA/DS-89/20 ..... N89-27646 #
DOT/FAA/DS-89/21 ..... N89-27645 #

DOT/FAA/PM-87/20-PHASE-1/2 ..... N89-27673 #

DP-MS-88-217 ..... N89-27983 #

DPG-FR-89-901 ..... N89-28002 #

DTRC/SME-88-63 ..... N89-28361 #

E-4054 ..... N89-28015* #
E-4318 ..... N89-27796* #
E-4761 ..... N89-27923* #
E-4790 ..... N89-28029* #
E-4853 ..... N89-27672* #
E-4855 ..... N89-28030* #
E-4856 ..... N89-27705* #
E-4869 ..... N89-27868* #
E-4888 ..... N89-27795* #
E-4904 ..... N89-27703* #
E-4946 ..... N89-27998* #
E-4962 ..... N89-27980* #
E-4980 ..... N89-27836* #
E-4988 ..... N89-28036* #
E-5005 ..... N89-27706* #
E-5006 ..... N89-27701* #
E-5011 ..... N89-27670* #
E-5025 ..... N89-27700* #
E-5026 ..... N89-27927* #
E-5040 ..... N89-27999* #
E-5043 ..... N89-27702* #
E-5055 ..... N89-27704* #

ECS-SS-0956 ..... N89-27698* #
ECS-SS-3059 ..... N89-27864* #

EMA-89-R-33 ..... N89-28115* #

EOARD-TR-89-07 ..... N89-28386 #
EOARD-TR-89-09 ..... N89-28430 #

EPRI-RP-2614-5 ..... N89-28000 #

ERIM-192400-13-F ..... N89-28397 #
ERIM-205200-12-T ..... N89-28394 #

ESA-CR(P)-2742 ..... N89-27943 #

ESA-SP-288 ..... N89-28214 #
ESA-SP-1102 ..... N89-28055 #

ESD-TR-88-209 ..... N89-28426 #
ESD-TR-88-250 ..... N89-28431 #
ESD-TR-88-329 ..... N89-27946 #
ESD-TR-89-107 ..... N89-28356 #

ESL-721432-1 ..... N89-27870* #
ESL-721446-1 ..... N89-27870* #
ESL-721447-1 ..... N89-27870* #
ESL-721711-1 ..... N89-27870* #

ETL-0523 ..... N89-28097 #

ETN-89-94383 ..... N89-28373 #
ETN-89-94464 ..... N89-27943 #
ETN-89-94508 ..... N89-27688 #
ETN-89-94569 ..... N89-28378 #
ETN-89-94623 ..... N89-27928
ETN-89-94678 ..... N89-28092 #
ETN-89-94805 ..... N89-28037 #
ETN-89-94967 ..... N89-27985 #
ETN-89-95006 ..... N89-27707 #
ETN-89-95009 ..... N89-28055 #
ETN-89-95012 ..... N89-28214 #

FAA-APO-89-5 ..... N89-27644 #

GL-TR-89-006 ..... N89-27691 #
GL-TR-89-0087 ..... N89-28096 #
GL-TR-89-0120 ..... N89-28396 #
GL-TR-89-0121 ..... N89-27950 #

GPO-99-550 ..... N89-28450 #

GTFR-91 ..... N89-28402 #

H-REPT-101-226 ..... N89-28451 #

H-1331 ..... N89-28034* #

HDL-CR-89-001-1 ..... N89-27869 #

IAF-88-328 ..... N89-27683 #

IC-88/350 ..... N89-28033 #
IC-88/358 ..... N89-27926 #
IC-88/365 ..... N89-28416 #
IC-88/374 ..... N89-28343 #
IC-88/393 ..... N89-28344 #
IC-88/408 ..... N89-28345 #

ICASE-89-37 ..... N89-28341* #
ICASE-89-39 ..... N89-28342* #
ICASE-89-43 ..... N89-27977* #

ICEFIZ-CS-12-1987 ..... N89-28406 #

IFT-P-03/87 ..... N89-28472 #

INPE-4748-PRE/1421 ..... N89-28312 #
INPE-4762-PRE/1432 ..... N89-28114 #
INPE-4763-PRE/1432 ..... N89-28048 #
INPE-4769-PRE/1438 ..... N89-28049 #
INPE-4770-PRE/1439 ..... N89-28305 #
INPE-4771-PRE/1440 ..... N89-28311 #
INPE-4773-PRE/1442 ..... N89-27683 #
INPE-4777-PRE/1446 ..... N89-28050 #
INPE-4778-TDL/350 ..... N89-27680 #
INPE-4782-RPE/582-PHASE-2 ..... N89-28051 #
INPE-4784-PRE/1447 ..... N89-28333 #

INS-726 ..... N89-28008 #

IPPJ-905 ..... N89-28400 #
IPPJ-906 ..... N89-28399 #
IPPJ-908 ..... N89-28401 #

ISBN-3-92-2010-40-7 ..... N89-27707 #
ISBN-9-29-092000-9 ..... N89-28055 #
ISBN-92-835-0512-3 ..... N89-27661 #
ISBN-92-835-0513-1 ..... N89-27650 #

ISSN-0344-5879 ..... N89-28092 #
ISSN-0377-8312 ..... N89-27985 #
ISSN-0379-6566 ..... N89-28214 #
ISSN-0436-1199 ..... N89-28373 #
ISSN-0436-1199 ..... N89-28378 #
ISSN-0469-4732 ..... N89-28399 #
ISSN-0469-4732 ..... N89-28401 #

JAERI-M-88-238 ..... N89-27794 #

JINR-E-8-88-638 ..... N89-28418 #

JPL-PUBL-88-28 ..... N89-28454* #
JPL-PUBL-89-13 ..... N89-27907* #

JPL-TDA-PR-42-97 ..... N89-27871* #

K/DSRD-80 ..... N89-28308 #

L-16551 ..... N89-27995* #
L-16552 ..... N89-27634* #

LA-UR-88-4110 ..... N89-28315 #
LA-UR-89-1595 ..... N89-28054 #
LA-UR-89-1941 ..... N89-27959 #
LA-UR-89-1989 ..... N89-28199 #
LA-UR-89-2097 ..... N89-27958 #
LA-UR-89-2105 ..... N89-28434 #
LA-UR-89-2150 ..... N89-28435 #
LA-UR-89-2163 ..... N89-27961 #
LA-UR-89-2188 ..... N89-28403 #
LA-UR-89-2194 ..... N89-27960 #
LA-UR-89-2205 ..... N89-28007 #

LA-10773-ADD ..... N89-27863 #
LA-11419-MS ..... N89-28366 #
LA-11560-MS ..... N89-27975 #
LA-11573-MS ..... N89-28367 #

LBL-26578 ..... N89-28409 #
LBL-26999 ..... N89-27956 #
LBL-27035 ..... N89-28005 #

LC-88-25450 ..... N89-28474* #
LC-88-600578 ..... N89-27831 #
LC-88-600602 ..... N89-28405 #
LC-88-600602 ..... N89-28441 #

LCDS/CCS-89-8 ..... N89-28346 #

LIR/01-89/332-VOL-2 ..... N89-28103 #
LIR/01-89/333-VOL-3 ..... N89-28104 #

LISS-26-2 ..... N89-27922 #

LMSC-HEC-TR-F268584-VOL-1 ..... N89-27693* #
LMSC-HEC-TR-F268584-VOL-3A ..... N89-27694* #
LMSC-HEC-TR-F268584-VOL-3B ..... N89-27695* #
LMSC-HEC-TR-F268584-VOL-4 ..... N89-27696* #
LMSC-HEC-TR-F268584-VOL-5 ..... N89-27697* #

LMSC/F297919 ..... N89-28479 #
LMSC/F352227 ..... N89-27829 #

LR-31443 ..... N89-27643 #

MDC-Q1285 ..... N89-27640 #

MITSG-89-3 ..... N89-28053 #

MM-5488-89-12 ..... N89-27865 #

MPIS-6/1988 ..... N89-28373 #
MPIS-13/1988 ..... N89-28378 #

MRC-NSH-R-88-0008 ..... N89-27951 #

MRL-TN-549 ..... N89-28044 #

MTL-TR-89-17 ..... N89-27833 #

MTR-88W00048 ..... N89-27645 #
MTR-88W00049 ..... N89-27646 #

NADC-88072-60 ..... N89-27859 #
NADC-89009-60 ..... N89-28303 #

NAS 1.15:4129 ..... N89-27995* #
NAS 1.15:89445 ..... N89-28304* #
NAS 1.15:101257 ..... N89-28118* #
NAS 1.15:101586-VOL-1 ..... N89-27687* #
NAS 1.15:101592 ..... N89-28035* #
NAS 1.15:101605 ..... N89-27671* #
NAS 1.15:101633 ..... N89-28314* #
NAS 1.15:102024 ..... N89-27923* #
NAS 1.15:102041 ..... N89-28029* #
NAS 1.15:102091 ..... N89-28030* #
NAS 1.15:102093 ..... N89-27705* #
NAS 1.15:102103 ..... N89-27868* #
NAS 1.15:102115 ..... N89-27795* #
NAS 1.15:102124 ..... N89-27703* #

NAS 1.15:102134 ..... N89-28015* #
NAS 1.15:102282 ..... N89-27998* #
NAS 1.15:102294 ..... N89-27980* #
NAS 1.15:102301 ..... N89-27836* #
NAS 1.15:102310 ..... N89-27706* #
NAS 1.15:102312 ..... N89-27701* #
NAS 1.15:102317 ..... N89-27670* #
NAS 1.15:102325 ..... N89-27927* #
NAS 1.15:102331 ..... N89-27999* #
NAS 1.15:102335 ..... N89-27702* #
NAS 1.15:102338 ..... N89-28036* #
NAS 1.15:102347 ..... N89-27704* #
NAS 1.21:494 ..... N89-28474* #
NAS 1.26:4233 ..... N89-27648* #
NAS 1.26:4234 ..... N89-27647* #
NAS 1.26:4250 ..... N89-28115* #
NAS 1.26:4251 ..... N89-27978* #
NAS 1.26:4252 ..... N89-28004* #
NAS 1.26:4253 ..... N89-27818* #
NAS 1.26:180086 ..... N89-28113* #
NAS 1.26:181810 ..... N89-28328* #
NAS 1.26:181860 ..... N89-28341* #
NAS 1.26:181862 ..... N89-28342* #
NAS 1.26:181864 ..... N89-27977* #
NAS 1.26:181871 ..... N89-27674* #
NAS 1.26:182302 ..... N89-27672* #
NAS 1.26:183249 ..... N89-28440* #
NAS 1.26:183439 ..... N89-27994* #
NAS 1.26:183440 ..... N89-28047* #
NAS 1.26:183663 ..... N89-27693* #
NAS 1.26:183665 ..... N89-27694* #
NAS 1.26:183666 ..... N89-27695* #
NAS 1.26:183667 ..... N89-27696* #
NAS 1.26:183668 ..... N89-27697* #
NAS 1.26:183674 ..... N89-27698* #
NAS 1.26:183706 ..... N89-27864* #
NAS 1.26:184564 ..... N89-27907* #
NAS 1.26:185131 ..... N89-27700* #
NAS 1.26:185370 ..... N89-28475* #
NAS 1.26:185388 ..... N89-28445* #
NAS 1.26:185418 ..... N89-28309* #
NAS 1.26:185431 ..... N89-27871* #
NAS 1.26:185434 ..... N89-27870* #
NAS 1.26:185461 ..... N89-28454* #
NAS 1.26:185830 ..... N89-28476* #
NAS 1.26:185835 ..... N89-28444* #
NAS 1.26:185840 ..... N89-27979* #
NAS 1.26:185845 ..... N89-28446* #
NAS 1.26:185856 ..... N89-28213* #
NAS 1.26:185857 ..... N89-28211* #
NAS 1.26:185858 ..... N89-28212* #
NAS 1.26:185861 ..... N89-28016* #
NAS 1.26:185862 ..... N89-28471* #
NAS 1.26:185863 ..... N89-28017* #
NAS 1.26:185894 ..... N89-28448* #
NAS 1.60:2921 ..... N89-28034* #
NAS 1.60:2924 ..... N89-27796* #
NAS 1.60:2933 ..... N89-27634* #

NASA-CR-4233 ..... N89-27648* #
NASA-CR-4234 ..... N89-27647* #
NASA-CR-4250 ..... N89-28115* #
NASA-CR-4251 ..... N89-27978* #
NASA-CR-4252 ..... N89-28004* #
NASA-CR-4253 ..... N89-27818* #
NASA-CR-180086 ..... N89-28113* #
NASA-CR-181810 ..... N89-28328* #
NASA-CR-181860 ..... N89-28341* #
NASA-CR-181862 ..... N89-28342* #
NASA-CR-181864 ..... N89-27977* #
NASA-CR-181871 ..... N89-27674* #
NASA-CR-182302 ..... N89-27672* #
NASA-CR-183249 ..... N89-28440* #
NASA-CR-183439 ..... N89-27994* #
NASA-CR-183440 ..... N89-28047* #
NASA-CR-183663 ..... N89-27693* #
NASA-CR-183665 ..... N89-27694* #
NASA-CR-183666 ..... N89-27695* #
NASA-CR-183667 ..... N89-27696* #
NASA-CR-183668 ..... N89-27697* #
NASA-CR-183674 ..... N89-27698* #
NASA-CR-183706 ..... N89-27864* #
NASA-CR-184564 ..... N89-27907* #
NASA-CR-185131 ..... N89-27700* #
NASA-CR-185370 ..... N89-28475* #
NASA-CR-185388 ..... N89-28445* #
NASA-CR-185418 ..... N89-28309* #
NASA-CR-185431 ..... N89-27871* #
NASA-CR-185434 ..... N89-27870* #
NASA-CR-185461 ..... N89-28454* #
NASA-CR-185830 ..... N89-28476* #
NASA-CR-185835 ..... N89-28444* #
NASA-CR-185840 ..... N89-27979* #
NASA-CR-185845 ..... N89-28446* #
NASA-CR-185856 ..... N89-28213* #
NASA-CR-185857 ..... N89-28211* #
NASA-CR-185858 ..... N89-28212* #
NASA-CR-185861 ..... N89-28016* #
NASA-CR-185862 ..... N89-28471* #
NASA-CR-185863 ..... N89-28017* #
NASA-CR-185894 ..... N89-28448* #

NASA-SP-494 ..... N89-28474* #

NASA-TM-4129 ..... N89-27995* #
NASA-TM-89445 ..... N89-28304* #
NASA-TM-101257 ..... N89-28118* #
NASA-TM-101586-VOL-1 ..... N89-27687* #
NASA-TM-101592 ..... N89-28035* #
NASA-TM-101605 ..... N89-27671* #
NASA-TM-101633 ..... N89-28314* #
NASA-TM-102024 ..... N89-27923* #
NASA-TM-102041 ..... N89-28029* #
NASA-TM-102091 ..... N89-28030* #
NASA-TM-102093 ..... N89-27705* #
NASA-TM-102103 ..... N89-27868* #
NASA-TM-102115 ..... N89-27795* #
NASA-TM-102124 ..... N89-27703* #
NASA-TM-102134 ..... N89-28015* #
NASA-TM-102282 ..... N89-27998* #
NASA-TM-102294 ..... N89-27980* #
NASA-TM-102301 ..... N89-27836* #
NASA-TM-102310 ..... N89-27706* #
NASA-TM-102312 ..... N89-27701* #
NASA-TM-102317 ..... N89-27670* #
NASA-TM-102325 ..... N89-27927* #
NASA-TM-102331 ..... N89-27999* #
NASA-TM-102335 ..... N89-27702* #
NASA-TM-102338 ..... N89-28036* #
NASA-TM-102347 ..... N89-27704* #

NASA-TP-2921 ..... N89-28034* #
NASA-TP-2924 ..... N89-27796* #
NASA-TP-2933 ..... N89-27634* #

NCEL-TN-1793 ..... N89-28014 #

NIST/SP-753 ..... N89-28441 #
NIST/SP-754 ..... N89-27831 #
NIST/SP-759 ..... N89-28405 #

NISTIR-88/3843 ..... N89-27819 #

NOSC/TD-1532 ..... N89-27963 #

NPS62-89-019 ..... N89-27947 #

NRL-MR-4596-REV ..... N89-28480 #
NRL-MR-5617-PT-1-REV ..... N89-28481 #
NRL-MR-5862-REV ..... N89-28482 #
NRL-MR-6205 ..... N89-28197 #
NRL-MR-6297-REV ..... N89-28483 #
NRL-MR-6403 ..... N89-28370 #
NRL-MR-6424 ..... N89-27867 #
NRL-MR-6443 ..... N89-28028 #
NRL-MR-6448 ..... N89-27962 #
NRL-MR-6453 ..... N89-28003 #
NRL-MR-6466 ..... N89-28480 #
NRL-MR-6467-PT-1 ..... N89-28481 #
NRL-MR-6468 ..... N89-28482 #
NRL-MR-6469 ..... N89-28483 #
NRL-MR-6481 ..... N89-28111 #

NRL-9172-1 ..... N89-28045 #

NRTC-88-22-R ..... N89-27972 #

NSWC/TR-88-365 ..... N89-28358 #

NWC-TP-6846 ..... N89-27640 #
NWC-TP-6945 ..... N89-27853 #
NWC-TP-6953 ..... N89-27948 #
NWC-TP-6971 ..... N89-28339 #

OCS-TR-89-04 ..... N89-28392 #

OMI-298 ..... N89-28112 #

OPPORTUNITY BRIEF-53 ..... N89-28053 #

OSU/DGSS-395 ..... N89-28095 #

PB89-148340 ..... N89-28405 #
PB89-148985 ..... N89-27831 #
PB89-158612 ..... N89-28103 #
PB89-158620 ..... N89-28104 #
PB89-160014 ..... N89-28441 #
PB89-185318 ..... N89-28392 #
PB89-187330 ..... N89-28053 #
PB89-196661 ..... N89-28368 #
PB89-201321 ..... N89-27819 #

PCS-TR88-136 ..... N89-28445* #
PCS-TR88-137 ..... N89-28444* #

PD-CF-8921 ..... N89-27637 #
PD-CF-8922 ..... N89-28313 #

PD-SE-8906 ..... N89-28307 #
PD-SE-8907 ..... N89-28306 #

PNL-SA-16621 ..... N89-27806 #

PSR-1925 ..... N89-27635 #

R/D-4858A-MS-01 ..... N89-27797 #
R/D-5496-MS-01 ..... N89-27801 #
R/D-5647-MS-01 ..... N89-27827 #
R/D-5876-MS-01-4 ..... N89-27825 #
R/D-5878-CH-01 ..... N89-27823 #

RADC-TR-88-324-VOL-4 ..... N89-28336 #
RADC-TR-88-324-VOL-6 ..... N89-28334 #
RADC-TR-89-48 ..... N89-28332 #

REPT-3 ..... N89-28426 #
REPT-53-4502-0337 ..... N89-28395 #
REPT-86-1 ..... N89-28302 #
REPT-88-4 ..... N89-28431 #
REPT-88-61112 ..... N89-27954 #
REPT-89-1-ONR ..... N89-28360 #
REPT-93 ..... N89-28011 #
REPT-882-440-115 ..... N89-27688 #
REPT-1988 ..... N89-28426 #
REPT-19176 ..... N89-27864* #

RIACS-TR-88.35 ..... N89-28309* #

RR-158 ..... N89-28325 #

RRK-88-35 ..... N89-28473 #

SAND-88-1112C ..... N89-27834 #
SAND-88-1304C ..... N89-28038 #
SAND-88-2876C ..... N89-28039 #
SAND-88-3118 ..... N89-28432 #
SAND-88-3153 ..... N89-27925 #
SAND-88-3475C ..... N89-27955 #
SAND-89-0037 ..... N89-27957 #
SAND-89-0506C ..... N89-28414 #
SAND-89-0542C ..... N89-28412 #
SAND-89-0815C ..... N89-28032 #
SAND-89-0922C ..... N89-27642 #
SAND-89-1346C ..... N89-27924 #

SASR-10 ..... N89-28476* #
SASR-11 ..... N89-28476* #
SASR-12 ..... N89-28476* #
SASR-13 ..... N89-28476* #

SCC-R-104-F ..... N89-27969 #

SC5424.FR ..... N89-28391 #

SD-TR-89-20 ..... N89-27992 #

SERI/PR-211-3483 ..... N89-28099 #

SERI/SP-220-3237 ..... N89-28100 #

SR-1 ..... N89-27691 #
SR-1 ..... N89-27951 #
SR-2 ..... N89-27692 #
SR-3 ..... N89-27681 #
SR-5 ..... N89-28095 #
SR-8 ..... N89-28112 #

SRI-MP-89-106 ..... N89-27807 #

SU-SOL-89-3 ..... N89-28352 #
SU-SOL-89-5 ..... N89-28320 #

SU-STAN-CS-89-1257 ..... N89-28019 #
SU-STAN-CS-89-1260 ..... N89-28340 #

SU-TR-18 ..... N89-27848 #
SU-TR-416 ..... N89-28353 #

TR-1 ..... N89-27860 #
TR-2 ..... N89-27857 #
TR-4 ..... N89-27862 #
TR-6 ..... N89-28420 #
TR-9 ..... N89-27842 #
TR-11 ..... N89-28423 #
TR-14 ..... N89-27844 #
TR-15 ..... N89-27843 #
TR-18 ..... N89-27824 #
TR-20 ..... N89-27798 #

TR-20 ..... N89-27840 #
TR-21 ..... N89-28424 #
TR-22 ..... N89-27965 #
TR-23 ..... N89-27850 #
TR-26 ..... N89-27851 #
TR-28 ..... N89-27841 #
TR-39 ..... N89-27970 #
TR-42 ..... N89-27803 #
TR-381 ..... N89-28325 #
TR-823 ..... N89-28209 #
TR-851 ..... N89-28356 #
TR-0088(4392-11)-1 ..... N89-27992 #

TWR-17272-VOL-3-REV-A ..... N89-27698* #

UBUFFALO/DC/TR-103 ..... N89-28389 #

UBUFFALO/DR/TR-102 ..... N89-28390 #

UCID-21634 ..... N89-28105 #
UCID-21677 ..... N89-28443 #

UCRL-21083 ..... N89-28000 #
UCRL-53868-88 ..... N89-28453 #
UCRL-99927-REV-1 ..... N89-28108 #
UCRL-101121 ..... N89-28477 #
UCRL-101139 ..... N89-28009 #
UCRL-101237 ..... N89-28447 #
UCRL-101266 ..... N89-28006 #

UILU-ENG-88-1785 ..... N89-28338 #
UILU-ENG-89-2212-CSG-101 ..... N89-27967 #
UILU-ENG-89-2218 ..... N89-27953 #
UILU-ENG-89-2219 ..... N89-28327 #

UIUCDCS-R-88-1479 ..... N89-28338 #

UNB-FIS-10/88 ..... N89-28417 #

URI-MSL-891 ..... N89-28043 #

USAAEFA-87-32 ..... N89-27632 #

USAARL-89-5 ..... N89-28300 #

USAFA-TR-89-3 ..... N89-28369 #

USARIEM-M-33-89 ..... N89-28201 #
USARIEM-M-49-89 ..... N89-28202 #

USARIEM-T-11-89 ..... N89-28298 #

UWIS/DC/TR-89/1 ..... N89-27808 #
UWIS/DC/TR-89/3 ..... N89-28419 #

VKI-LS-1989-02 ..... N89-27985 #

VLSI-MEMO-89-508 ..... N89-28317 #
VLSI-MEMO-89-509 ..... N89-28316 #
VLSI-MEMO-89-513 ..... N89-27838 #
VLSI-MEMO-89-517 ..... N89-27839 #

WRDC-TR-89-3034 ..... N89-27633 #
WRDC-TR-89-3045 ..... N89-28321 #

FEDERAL REGIONAL DEPOSITORY LIBRARIES

ALABAMA

AUBURN UNIV. AT MONTGOMERY LIBRARY
Documents Department
Montgomery, AL 36193
(205) 271-9650

UNIV. OF ALABAMA LIBRARY
Documents Dept.-Box S
University, AL 35486
(205) 348-6046

ARIZONA

DEPT. OF LIBRARY, ARCHIVES AND PUBLIC RECORDS
Third Floor—State Cap.
1700 West Washington
Phoenix, AZ 85007
(602) 255-4121

UNIVERSITY OF ARIZONA LIB.
Government Documents Dept.
Tucson, AZ 85721
(602) 621-6433

ARKANSAS

ARKANSAS STATE LIBRARY
One Capitol Mall
Little Rock, AR 72201
(501) 371-2326

CALIFORNIA

CALIFORNIA STATE LIBRARY
Govt. Publications Section
P.O. Box 2037
Sacramento, CA 95809
(916) 324-4863

COLORADO

UNIV OF COLORADO LIB.
Government Pub. Division
Campus Box 184
Boulder, CO 80309
(303) 492-8834

DENVER PUBLIC LIBRARY
Govt. Pub. Department
1357 Broadway
Denver, CO 80203
(303) 571-2131

CONNECTICUT

CONNECTICUT STATE LIBRARY
Government Documents Unit
231 Capitol Avenue
Hartford, CT 06106
(203) 566-7029

FLORIDA

UNIV. OF FLORIDA LIBRARIES
Library West
Documents Department
Gainesville, FL 32611
(904) 392-0367

GEORGIA

UNIV. OF GEORGIA LIBRARIES
Government Reference Dept.
Athens, GA 30602
(404) 542-8949

HAWAII

UNIV. OF HAWAII LIBRARY
Govt. Documents Collection
2550 The Mall
Honolulu, HI 96822
(808) 948-8230

IDAHO

UNIV. OF IDAHO LIBRARY
Documents Section
Moscow, ID 83843
(208) 885-6344

ILLINOIS

ILLINOIS STATE LIBRARY
Information Services Branch
Centennial Building
Springfield, IL 62756
(217) 782-5185

INDIANA

INDIANA STATE LIBRARY
Serials Documents Section
140 North Senate Avenue
Indianapolis, IN 46204
(317) 232-3686

IOWA

UNIV. OF IOWA LIBRARIES
Govt. Documents Department
Iowa City, IA 52242
(319) 353-3318

KANSAS

UNIVERSITY OF KANSAS
Doc. Collect—Spencer Lib.
Lawrence, KS 66045-2800
(913) 864-4662

KENTUCKY

UNIV. OF KENTUCKY LIBRARIES
Govt. Pub. Department
Lexington, KY 40506-0039
(606) 257-3139

LOUISIANA

LOUISIANA STATE UNIVERSITY
Middleton Library
Govt. Docs. Dept.
Baton Rouge, LA 70803
(504) 388-2570

LOUISIANA TECHNICAL UNIV. LIBRARY
Documents Department
Ruston, LA 71272-0046
(318) 257-4962

MAINE

UNIVERSITY OF MAINE
Raymond H. Fogler Library
Tri-State Regional Documents Depository
Orono, ME 04469
(207) 581-1680

MARYLAND

UNIVERSITY OF MARYLAND
McKeldin Lib.—Doc. Div.
College Park, MD 20742
(301) 454-3034

MASSACHUSETTS

BOSTON PUBLIC LIBRARY
Government Docs. Dept.
Boston, MA 02117
(617) 536-5400 ext.226

MICHIGAN

DETROIT PUBLIC LIBRARY
Sociology Department
5201 Woodward Avenue
Detroit, MI 48202-4093
(313) 833-1409

MICHIGAN STATE LIBRARY
P.O. Box 30007
Lansing, MI 48909
(517) 373-1593

MINNESOTA

UNIVERSITY OF MINNESOTA
Government Pubs. Division
409 Wilson Library
309 19th Avenue South
Minneapolis, MN 55455
(612) 373-7870

MISSISSIPPI

UNIV. OF MISSISSIPPI LIB.
Documents Department
University, MS 38677
(601) 232-5857

MONTANA

UNIV. OF MONTANA
Mansfield Library
Documents Division
Missoula, MT 59812
(406) 243-6700

NEBRASKA

UNIVERSITY OF NEBRASKA - LINCOLN
Love Library
Documents Department
Lincoln, NE 68588-0410
(402) 472-2562

NEVADA

UNIVERSITY OF NEVADA LIB.
Govt. Pub. Department
Reno, NV 89557-0044
(702) 784-6579

NEW JERSEY

NEWARK PUBLIC LIBRARY
5 Washington Street
Newark, NJ 07101-0630
(201) 733-7812

NEW MEXICO

UNIVERSITY OF NEW MEXICO
Zimmerman Library
Government Pub. Dept.
Albuquerque, NM 87131
(505) 277-5441

NEW MEXICO STATE LIBRARY
Reference Department
325 Don Gaspar Avenue
Santa Fe, NM 87503
(505) 827-3826

NEW YORK

NEW YORK STATE LIBRARY
Empire State Plaza
Albany, NY 12230
(518) 474-5563

NORTH CAROLINA

UNIVERSITY OF NORTH CAROLINA AT CHAPEL HILL
Davis Library
BA/SS Documents Division
Chapel Hill, NC 27515
(919) 962-1151

NORTH DAKOTA

UNIVERSITY OF NORTH DAKOTA
Chester Fritz Library
Documents Department
Grand Forks, ND 58202
(701) 777-4629
In cooperation with North Dakota State Univ. Library

OHIO

STATE LIBRARY OF OHIO
Documents Department
65 South Front Street
Columbus, OH 43266-0334
(614) 462-7051

OKLAHOMA

OKLAHOMA DEPT. OF LIB.
Government Documents
200 NE 18th Street
Oklahoma City, OK 73105
(405) 521-2502, ext. 252

OKLAHOMA STATE UNIV. LIB.
Documents Department
Stillwater, OK 74078
(405) 624-6546

OREGON

PORTLAND STATE UNIV. LIB.
Documents Department
P.O. Box 1151
Portland, OR 97207
(503) 229-3673

PENNSYLVANIA

STATE LIBRARY OF PENN.
Government Pub. Section
P.O. Box 1601
Harrisburg, PA 17105
(717) 787-3752

TEXAS

TEXAS STATE LIBRARY
Public Services Department
P.O. Box 12927—Cap. Sta.
Austin, TX 78711
(512) 475-2996

TEXAS TECH. UNIV. LIBRARY
Govt. Documents Department
Lubbock, TX 79409
(806) 742-2268

UTAH

UTAH STATE UNIVERSITY
Merrill Library, U.M.C. 30
Logan, UT 84322
(801) 750-2682

VIRGINIA

UNIVERSITY OF VIRGINIA
Alderman Lib.—Public Doc.
Charlottesville, VA 22903-2498
(804) 924-3133

WASHINGTON

WASHINGTON STATE LIBRARY
Documents Section
Olympia, WA 98504
(206) 753-4027

WEST VIRGINIA

WEST VIRGINIA UNIV. LIB.
Documents Department
Morgantown, WV 26506-6069
(304) 293-3640

WISCONSIN

MILWAUKEE PUBLIC LIBRARY
814 West Wisconsin Avenue
Milwaukee, WI 53233
(414) 278-3065

ST. HIST LIB. OF WISCONSIN
Government Pub. Section
816 State Street
Madison, WI 53706
(608) 262-4347

WYOMING

WYOMING STATE LIBRARY
Supreme Ct. & Library Bld.
Cheyenne, WY 82002
(307) 777-5919

National Aeronautics and
Space Administration
Code NTT-4
Washington, D.C.
20546

Official Business

Penalty for Private Use, $300

SPECIAL FOURTH-CLASS RATE
POSTAGE & FEES PAID
NASA
PERMIT No G-27

NASA

POSTMASTER If Undeliverable (Section 158
Postal Manual) Do Not Return